Biswanath Dinda *Editor*

Natural Products in Obesity and Diabetes

Therapeutic Potential and Role in Prevention and Treatment

Springer

Natural Products in Obesity and Diabetes

Biswanath Dinda
Editor

Natural Products in Obesity and Diabetes

Therapeutic Potential and Role in Prevention and Treatment

Springer

Editor
Biswanath Dinda
Department of Chemistry
Tripura University
Agartala, Tripura, India

ISBN 978-3-030-92195-8 ISBN 978-3-030-92196-5 (eBook)
https://doi.org/10.1007/978-3-030-92196-5

This Springer imprint is published by the registered company Springer Nature Switzerland AG
The registered company address is: Gewerbestrasse 11, 6330 Cham, Switzerland

• This book is dedicated to the people suffering from obesity and diabetes and the medical professionals who look after them.
• The editor also dedicates this book to Late Mrs. Chitralekha Dinda, wife of Biswanath Dinda, who lost her life in this corona pandemic, and whose constant sacrifice and encouragement helped the editor to finish the book.

Preface

The field of natural products science is immense, fascinating, and interesting because of structural diversity, versatile biological activities, and occurrence of natural molecules from various sources, as well as the specific metabolic origin, fate, and cellular biotransformation of these phytogenic compounds. These natural metabolites have defensive roles against harmful pathogens and environmental stress to protect parent organisms under various environments. Various herbal extracts have been used in the treatment of different diseases and ailments since the stone-age period. In many countries, these natural products have been used in their traditional folk medicine based on ethnobotanical knowledge. Various polyherbal formulations have been found to have potential efficacy in the treatment of obesity and diabetes. Most of these polyherbal formulations have poor scientific data on the composition and contents of bioactive phytochemicals and the mode of action in the treatment of diseases. As a result, the practitioners have no idea of the effective doses and treatment period of these phytomedicines. Most of currently prescribed synthetic oral drugs for the treatment of obesity and diabetes and their associated complications on their long-term use by the patients caused many adverse side effects. For this reason, most of leading pharmaceutical industries and research institutes have paid attention to the discovery of natural drugs as an alternative to currently used synthetic drugs. Recently, only a few natural and semi-natural molecules are in the global market for the treatment of these diseases. The major shortcomings of natural drugs in clinical trials in humans and in treatment are the lack of scientific data on the effective doses and the composition and contents of active phytochemicals and their active metabolites in disease-specific organs in humans, in addition to the requisite dose for a patient to cure the disease. Recently introduced "omics" technologies have been applied to evaluate the effective doses as "personalized medicine" for the treatment of the present global pandemic of obesity and diabetes.

The contributors of this monograph have highlighted the various aspects of natural products, particularly the impact of multi-omics biotechnology, gut microbiota dysbiosis, and cultivation and harvesting factors of plants and dietary vegetables and fruits on the composition and concentrations of anti-obese and antidiabetic phytochemicals present in them. Moreover, the contributors have elaborately discussed the different aspects of many natural molecules having potential

anti-obesity and antidiabetic activities, such as their major therapeutic targets, pharmacokinetics, metabolism, nanoformulations benefits and clinical progress. It will help for extensive studies of these natural molecules on toxicity and efficacy in future in human mimic animal models and humans and for large-scale application in global market as safe and low-cost drugs. In spite of sincere efforts for the publication of this monograph in correct form, any printing and other errors in this edition due to overlooking are regretted.

I hope this monograph will be useful for the practitioners in the field of traditional folk medicine, growers of fruits, vegetables, and crops, and students and researchers in the field of natural science and pharmaceutical chemistry.

I will appreciate valuable suggestions and comments from the readers of this book for its improvement in the next edition.

I am grateful to the publishers for their kind support and interest in the publication of this monograph. I am also grateful to Prof. A Basak, University of Ottawa, Canada, and Prof. G. H. Maity, Jadavpur University, India, for their kind help in providing some articles in the preparation of the manuscript of this monograph.

I wish to express my heartfelt thanks to all the contributors of this book including editorial and technical management staff for their sincere efforts in this endeavor.

Agartala, Tripura, India Biswanath Dinda
October, 2021

Contents

Contributors

Thais Cesar Department of Food and Nutrition, School of Pharmaceutical Sciences, São Paulo State University (UNESP), Araraquara, SP, Brazil

Ankita Chakraborty Department of Chemistry, ICFAI University, Agartala, Tripura, India

Mithun Chakraborty Department of Chemistry, University of Hyderabad, Hyderabad, Telangana, India

Biswanath Dinda Department of Chemistry, Tripura University, Suryamaninagar, Tripura, India

Manikarna Dinda Department of Biochemistry and Molecular Genetics, University of Virginia, School of Medicine, Charlottesville, USA

Subhajit Dinda Department of Chemistry, Government Degree College, Kamalpur, Tripura, India

Alexa K. Dowdell Earle A. Chiles Research Institute, Providence Health and Services, Portland, OR, USA

Brian D. Piening Earle A. Chiles Research Institute, Providence Health and Services, Portland, OR, USA

Fernanda Maria Manzini Ramos Department of Food and Nutrition, School of Pharmaceutical Sciences, São Paulo State University (UNESP), Araraquara, SP, Brazil

Shekhar Saha Department of Biochemistry and Molecular Genetics, University of Virginia, School of Medicine, Charlottesville, USA

Mateus Kawata Salgaço Department of Food and Nutrition, School of Pharmaceutical Sciences, São Paulo State University (UNESP), Araraquara, SP, Brazil

Katia Sivieri Department of Food and Nutrition, School of Pharmaceutical Sciences, São Paulo State University (UNESP), Araraquara, SP, Brazil

Michael P. Snyder Department of Genetics, Stanford University, Stanford, CA, USA

Abbreviations

ABCG5	ATP-binding cassette subfamily G member 5 protein
ACADM	Acyl-Coenzyme A dehydrogenase medium chain (C-4 to C-12)
ACADS	Acyl-CoA dehydrogenase short-chain
ACAT1	Acetoacetyl-CoA thiolase 1
ACC1	Acetyl-CoA carboxylase 1
ACE	Angiotensin-converting enzyme
Acly	ATP-citrate lyase
ACO	Acyl CoA oxidase
ACS	Acyl-CoA synthetase
ACSL3	Acyl-CoA synthetase long-chain family member 3
AgRP	Agouti-related protein
Akt	Protein kinase B
ALT	Alanine transaminase
AMPK	5′-Adenosine monophosphate (AMP)-activated protein kinase
Ang II	Angiotensin II
ANP	Atrial natriuretic peptide
AP-1	Activator protein-1
aP2	Adipocyte protein 2
ApoE	Apolipoprotein E
AS-160	Akt substrate of 160 kDa protein
AST	Aspartate transaminase
ATF4	Activating transcription factor 4
ATGL	Adipose triglyceride lipase
ATP5α	ATP synthase subunit alpha
BAECs	Bovine aortic endothelial cells
β-3-AR	Beta-3-adrenergic receptor
BAT	Brown adipose tissue
BBS-4	Bardet-Biedl syndrome 4
BCFAs	Branched-chain fatty acids
BDDE	Bis-(2,3-dibromo-4,5-dihydroxybenzyl)-ether
BDNF	Brain-derived neurotrophic factor
BGL	Blood glucose level
BK	Bradykinin

BMPR	Bone morphogenetic protein receptor
BNP	Brain natriuretic peptide
BUN	Blood urea nitrogen
BPN	3,4-Dibromo-5-(2-bromo-6-(ethoxymethyl)-3,4-dihydroxybenzyl)-benzene-1,2-diol
BSEP	Bile salt export pump
Bw	Body weight
CA	Cholic acid
CAD	Coronary artery disease
CaMKK	Calcium/calmodulin-dependent protein kinase kinase
CAT	Catalase
CB2R	Cannabinoid type 2 receptor
CCG	Cholecystokinin
CD2AP	CD2-associated protein
C/EBPα	CCAAT/enhancer-binding protein alpha
CD36	Cluster of differentiation 36
CD38	Cluster of differentiation 38
CDK4	Cyclin-dependent kinase 4
ChREBPα	Carbohydrate response element binding protein alpha
CHOP10	C/EBP homologous protein 10
Cidea	Cell death-inducing DFFA (DNA fragmentation factor-α)-like effector A
CITED1	Cbp/p300-interacting transactivator with Glu/Asp rich carboxy-terminal domain 1
CK-MB	Creatinine kinase - myocardial form present in heart and muscle
CNS	Central nervous system
Cox-2	Cyclooxygenase-2
CpG	Cytosine preceding guanosine
CPK	Creatinine phosphokinase
CPT-1	carnitine palmitoyltransferase 1
CREB	cAMP-response element binding protein
CREG1	Cellular repressor of adenovirus early region 1A-stimulated gene 1
CRP	C-reactive protein
CTGF	Connective tissue growth factor
CVD	Cardiovascular disease
CYP7A1	Cholesterol 7alpha-hydroxylase
CYP2E1	Cytochrome P4502E1
DCM	Diabetic cardiomyopathy
Defb2	Defensin beta 2
DGAT1	Diacylglycerol acyltransferase-1
DIO2	Deiodinase type II
DKK2	Dickkopf WNT signaling pathway inhibitor 2
DKO	Double knockout
DM	Diabetes mellitus
DMAPP	Dimethylallyl pyrophosphate

DN	Diabetic nephropathy
DPN	Diabetic peripheral neuropathy
DPP4	Dipeptidyl peptidase 4
DR	Diabetic retinopathy
DRP-1	Dynamin-related protein-1
dw	Dry weight
EAT	Epididymal adipose tissue
EGCG	(−)-Epigallocatechin-3-*O*-gallate
EGFR	Epidermal growth factor receptor
Elovl3	Elongation of very long chain fatty acids protein 3
EMT	Epithelial mesenchymal transition
eNOS	Endothelial nitric oxide synthase
ERDJ4	Endoplasmic reticulum (ER) localized-Dna J homolog 4
ERK	Extracellular signal-regulated kinase
ERRα	Estrogen-related receptor alpha
ET-1	Endothelin-1
EWAS	Epigenome-wide association study
FABP4	Fatty acid-binding protein 4
FADS1	Fatty acid desaturase-1
FAS	Fatty acid synthase
FBG	Fasting blood glucose
FPG	Fasting plasma glucose
FBPase	Fructose-1,6-bisphosphatase
FG	Fasting glucose
FGF21	Fibroblast growth factor 21
FoxO1	Forkhead box-containing protein O1
FTO	Fat mass and obesity-associated protein
FXR	Farnesoid X receptor
fw	Fresh weight
GABA	Gamma aminobutyric acid
GAD65	Glutamic acid decarboxylase 65
GADA	Glutamate decarboxylase alpha
GATA2	Zinc finger transcription factor-binding protein 2
GCK	Glucokinase
GDM	Gestational diabetes mellitus
GFAT	Glutamine:fructose 6-phosphate aminotransferase
GFR	Glomerular filtration rate
GGT	Gamma-glutamyl transferase
GI	Gastrointestinal
GIP	Glucose-dependent insulinotropic peptide
GK rats	Goto-Kakizaki rats
GLIS3	GLIS family zinc finger 3
GLP-1	Glucagon-like peptide-1
GLUT4	Glucose transporter type 4 protein

GlyK	Glycerol kinase
GOAT	Ghrelin-*O*-acyltransferase
GOT	Glutamic-oxaloacetic transaminase
G6Pase	Glucose-6-phosphatase
GP	Glycogen phosphorylase
GP_X	Glutathione peroxidase
G6PC	Glucose-6-phosphatase
G6PD	Glucose-6-phosphate dehydrogenase
GPDH	Glyceraldehyde 3-phosphate dehydrogenase
GPP	Geranyl pyrophosphate, also known as geranyl diphosphate
GPT	Glutamic pyruvic transaminase
GR	Glutathione reductase
GRP-43	G-protein-coupled receptor 43
GS	Glycogen synthase
GSH	Glutathione
GSK-3β	Glycogen synthase kinase 3 beta
GSR	Glutathione-disulfide reductase
GWAS	Genome-wide association study
HbA1c	Hemoglobin A1c, commonly known as glycosylated hemoglobin
HDACs	Histone deacetylases
HDL	High-density lipoproteins
HGMCs	Human glomerular mesangial cells
HIP	Hybrid insulin peptide
HK-2	Hexokinase-2
HLA	Human leukocyte antigen
HMGCS-1	3-Hydroxy-3-methylglutaryl-CoA synthase 1
HMGCR	3-Hydroxy-3-methylglutaryl-CoA reductase
HMTs	Histone methyltransferases
4-HNE	4-Hydroxynonenal
HNF4α	Hepatocyte nuclear factor 4 alpha
HO-1	Heme oxygenase-1
HOMA-IR	Homeostasis model assessment-estimated insulin resistance
hs-CRP	High-sensitive C-reactive protein
11β-HSD1	11beta-Hydroxysteroid dehydrogenase type 1
HSF1	Heat shock factor 1
HSL	Hormone-sensitive lipase
HSP72	Heat shock protein 72
IAPP	Islet amyloid polypeptide
ICAM-1	Intercellular adhesion molecule-1
IDDM	Insulin-dependent diabetes mellitus
IL-6	Interleukin-6
IPP	Isopentenyl pyrophosphate
JNK	c-Jun N-terminal kinase
KCNJ11	Potassium inwardly rectifying channel subfamily J, member 11

KCNQ1	Potassium voltage-gated channel subfamily Q member 1
Keap 1	Kelch-like ECH-associated protein 1
KLF4	Kruppel-like factor 4
KM mice	Kunming mice
L-NAME	N^G-nitro-L-arginine methyl ester
LBP	LPS-binding protein
LCAD	Very long-chain acyl CoA dehydrogenase
LCAT	Lecithin cholesterol acyltransferase
LDH	Lactate dehydrogenase
LDL	Low-density lipoproteins
LKB1	Liver kinase B 1
LPL	Lipoprotein lipase
LPO	Lipid peroxidase
LPS	Lipopolysaccharides
LSS	Lanosterol synthase
MAPK	Mitogen-activated protein kinase
MARCKS	Myristoylated alanine-rich C kinase substrate
MCAD	Medium-chain acyl CoA dehydrogenase
MC-4R	Melanocortin-4-receptor
MCP-1	Monocyte chemotactic protein-1
MDA	Malondialdehyde
MDA5	Melanoma differentiation-associated protein 5
MEST	Mesoderm-specific transcript
MGL	Monoacylglycerol lipase
MHC	Major histocompatibility complex
MMP-9	Matrix metalloproteinase-9
MODY	Maturity-onset diabetes of the young
MOGAT	Monoacylglycerol O-acyltransferase
MOR	(μ)-Opioid receptor
MPO	Myeloperoxidase
α-MSH	Alpha-melanocyte-stimulating hormone
MSI2	Musashi RNA binding protein 2
MTNR1B	Melatonin receptor type 1B
m-TOR	Mammalian target of rapamycin
MTP	Microsomal triglyceride transfer protein
Muc 2	Mucin 2
MUFA	Monounsaturated fatty acid
MyD88	Myeloid differentiation factor 88
NAFLD	Non-alcoholic fatty liver disease
NASH	Non-alcoholic steatohepatitis
NDUFS8	NADH: ubiquinone oxidoreductase core subunit 8
NEFAs	Non-esterified fatty acids
NEGR1	Neuronal growth regulator 1
NFAT	Nuclear factor of activated T-cells

NGAL	Neutrophil gelatinase-associated lipocalin
Nrf2	Nuclear factor (erythroid-derived 2)-like 2
NF-κB	Nuclear factor-kappa B
NIDDM	Non-insulin-dependent diabetes mellitus
NLRP3	Nucleotide-binding domain and leucine-rich repeat-containing-pyrin domain 3 inflammasome
NOD mice	Non-obese diabetic mice
NOX2	NADPH oxidase 2
NPPA	Natriuretic peptide A
NQO1	NAD(P)H quinone dehydrogenase 1
NRF-1	Nuclear respiratory factor-1
OGTT	Oral glucose tolerance test
ORAC	Oxygen radical absorbance capacity
PAI-1	Plasminogen activator inhibitor-1
PAP	Phosphatidate phosphatase
PARK2	Parkin 2
PARP	Poly(ADP-ribose) polymerase
PDE1	Pyruvate carboxylase E1
PDGF	Platelet-derived growth factor
PDI	Polymer density index
PDK1	Phosphoinositide-dependent kinase 1
PDK4	Pyruvate dehydrogenase kinase 4
PDX1	Pancreatic duodenal homeobox 1
PEPCK	Phosphoenolpyruvate carboxykinase
PERK	RNA-activated protein kinase -like ER kinase
PFK	Phosphofructo kinase
PGC1α	Peroxisome proliferator-activated receptor-gamma coactivator-1 alpha
PID1	Phosphotyrosine interaction domain containing 1
PK	Pyruvate kinase
PKCδ	Protein kinase C delta
PLs	Phospholipids
PLPP2	Phospholipid phosphatase 2
P-CO	Protein carbonyl
POMC	Pro-opiomelanocortin
PON	Paraoxonase
PPARD	Peroxisome proliferator activated receptor delta
PPARγ	Peroxisome proliferator-activated receptor gamma
PPBG	Postprandial blood glucose
PRDM-16	PR-domain containing zinc finger protein16
PS	Particle size
PTEN	Phosphatase and tensin homolog
PTP1B	Protein-tyrosine phosphatase 1B
PTPN2	Protein tyrosine phosphatase non-receptor type 2

PUFA	Polyunsaturated fatty acid
RAGE	Receptor for advanced glycation end product
RAS	Renin-angiotensin system
RBP-4	Retinol binding protein-4
ROS	Reactive oxygen species
RXR	Retinoid X receptor
s.c.	Subcutaneous injection
SCD1	Stearoyl-CoA desaturase 1
SCFAs	Short-chain fatty acids
scWAT	Subcutaneous white adipose tissue
SDHB	Succinate dehydrogenase complex iron sulfur subunit B
SFRP5	Secreted frizzled-related protein 5
SGLT2	Sodium-glucose co-transporter-2
SH2B1	Src homology 2B adapter protein 1
SHP	Small heterodimer partner
SHRs	Spontaneously hypertensive rats
SIRT1	Silent mating type information regulation 2 homolog-type 1
Smad7	Mothers against decapentaplegic homolog 7
SOCS3	Suppressor of cytokine signaling 3
S1P	Sphingosine 1-phosphate
SREBP-1c	Sterol regulatory element binding protein-1c
STAT	Signal transducer and activator of transcription
STZ	Streptozotocin
TAC	Total antioxidant capacity
TBARS	Thiobarbituric acid reactive substance
TBC1D1	TBC1 domain family member 1
TBC1D4	TBC1 domain family member 4, also known as AS160
TBX-1	T-box transcription factor-1
TC	Total cholesterol
TCF7L2	Transcription factor 7-like 2
T1DM	Type 1 diabetes mellitus
TFAM	Transcription factor A, mitochondrial
TG	Triglycerides
TGFβ1	Transforming growth factor beta1
TGR5	Transmembrane G-protein-coupled receptor 5
TLR4	Toll-like receptor 4
TMEM18	Transmembrane protein 18
TNF-α	Tumor necrosis factor-alpha
TRIF	Toll/interleukin-1 receptor (TIR)-domain containing adaptor protein inducing interferon beta
TrKB	Tropomyosin-receptor kinase B
TRPA1	Transient receptor potential ankyrin 1
TRPV1	Transient receptor potential vanilloid type 1
TXNIP	Thioredoxin interacting protein

TYK2	Tyrosine kinase 2
UCP-1	Uncoupling protein-1
USP18	Ubiquitin specific peptidase 18
UUO	Unilateral ureteral obstruction
VAT	Visceral adipose tissue
VEGF-A	Vascular endothelial growth factor-A
VLDL	Very low density lipoproteins
ZnT8	Zinc transporter 8 protein
ZP	Zeta potential

List of Figures

List of Schemes

List of Tables

Obesity and Diabetes

1

Biswanath Dinda and Shekhar Saha

1.1 Introduction

An increasing pandemic of obesity and diabetes (diabetes mellitus, DM) has become a serious health concern worldwide because these diseases contribute to the development of many chronic diseases including cardiovascular diseases, stroke, kidney diseases, ocular diseases, hypertension, non-alcoholic fatty liver disease (NAFLD), obstructive sleep apnea, osteoarthritis, and some types of cancer, among others. Obesity is a complex metabolic disease commonly accompanied by insulin resistance, increased oxidative stress, and low-grade inflammation and is characterized by accumulation of an excess fat mass in the body. Diabetes is a metabolic disorder characterized by destruction of pancreatic beta-cells or impaired insulin secretion and insulin action. The rise of obesity has been attributed to different potential factors including genetic predisposition, Western-type fast food diet, lack of physical activity, and social status. According to the report of the International Obesity Task Force, more than 600 million people are obese, and the number of obese-born children in developing countries is increasing at an alarming rate. One of three children born in this century is expected to develop obesity-related diabetes. Currently prescribed synthetic drugs for obesity and diabetes have several side effects on long-term use. A variety of natural products including antioxidant phytochemicals has emerged as promising potent herbal drugs for the treatment of obesity, diabetes, and their associated complications. Recent "omics" technologies (genomics, proteomics, transcriptomics, metabolomics, and microbiomics) have potentially improved our knowledge to identify the mechanism of action of these traditional natural

B. Dinda (✉)
Department of Chemistry, Tripura University, Suryamaninagar, Tripura, India

S. Saha
Department of Biochemistry and Molecular Genetics, School of Medicine, University of Virginia, Charlottesville, USA

B. Dinda (ed.), *Natural Products in Obesity and Diabetes*,
https://doi.org/10.1007/978-3-030-92196-5_1

medicines and the process of biosynthesis in nature and their efficient identification. Recent understanding on the diagnosis, clinical pathogenesis, epidemiology, risk factors, clinical treatments, and consequences of obesity and diabetes are summarized in this chapter.

1.2 Obesity and Its Diagnosis and Associated Complications

Obesity is the most common chronic metabolic disease worldwide, and its incidence is increasing at a high rate, generating enormous social cost. It is now reaching in pandemic shape worldwide, doubling its prevalence in more than that in 1980 in 70 countries, and over 600 million adults were found obese in 2015 (Afshin et al. 2017). The prevalence of overweight and obese people is extremely high in different parts of Europe, the USA, and Mexico. As it is a global phenomenon, it has been coined as "globesity" by WHO. If we search the history of the beginning of the epidemic obesity, we find that India had a leading role in the spread of obesity. In about 400 BC, Indian great physician Sushruta discovered sugarcane in the Ganges River Valley and reported that intake of sugary liquids could increase body weight. Subsequently, sugarcane was brought to China, Persia, and Egypt for cultivation and production of refined sugar (sucrose). At one time, sugar was so expensive that only kings and loyal families could afford it. Many kings in European countries became severely obese and were accused of being pregnant for this obesity. In 1907, Sir Richard Havelock Charles, a British physician stationed in India, observed that the reported type 2 diabetes cases were increased rapidly among the wealthy Bengali Indians living in Calcutta, whereas it was still rare among the poor Punjabi, and he linked this with an increasing intake of sugar. Later on, other world experts including Nobel laureate Sir Frederick Grant Banting, who received Nobel Prize for the discovery of insulin, pointed out that refined sugar might be a major cause of adult onset of obesity and diabetes. Later on, Prof Elliott Joslin coined the word "overnutrition" or high-calorie intake which was the cause of both obesity and diabetes (Bhishagranta 1911; Banting 1929; Joslin et al. 1934). Obesity is a complex metabolic disease characterized as an increased fat mass in the body, particularly from an increased mass of adipose tissue from sustained positive energy balance (energy intake > energy expenditure). In the body of obese individual, the increased fat mass, mainly as triglycerides, not only stored in the white adipose tissue but also stored in the liver and other tissues including skeletal muscle for utilization in the nutritionally deprived states such as in starvation. It is commonly accompanied by insulin resistance and enhanced inflammation.

Obesity is conventionally diagnosed by body mass index (BMI), which is the accurate approximation of obesity in obese individuals. Pre-obesity and obesity classes I, II, and III (extreme obesity) are defined as a BMI of 25–29.99 kg/m^2, 30–34.99 kg/m^2, 35–39.99 kg/m^2, and 40 kg/m^2 or greater, respectively. Pre-obese adult individuals are known as "overweight" individuals. For obese and overweight adult patients having a BMI > 25 mg/m^2 but <35 kg/m^2, clinicians also access their waist circumference (WC) to explore the risk factors of the patients. As per guide

line of the US Centre for Disease Control and Prevention, in USA, a WC >102 cm (40 inches) for men and > 88 cm (35 inches) for women indicate abdominal adiposity and have an increased risk of cardiometabolic diseases, whereas, in Southeast Asian and East Asian populations, a WC >80 cm (31 inches) for women and a WC > 85 cm (33 inches) for men indicate a higher risk factor on cardiometabolic diseases (Centre Dis Control Prevn, 2017).

The abnormal adiposity in obesity due to an increase mass of adipose tissue from increased adipocyte size (hypertrophy) and adipocyte number (hyperplasia or adipogenesis) leads to an excessive strain and a low-grade inflammation. In order to get relief from the strain, adipocytes release inflammatory adipokines such as tumor necrosis factor (TNF)-α, interleukin (IL)-1, and IL-6, as well as free fatty acids (FFAs) by enhanced lipolysis from their fat depots to the systemic circulation for storage in other diverse sites. Lipotoxicity from excessive FFAs and inflammatory adipokines results in the injury of pancreatic β-cells and leads to pancreatic β-cell dysfunction, which, in turn, decreases insulin synthesis and secretion. Moreover, FFAs also decrease the utilization of insulin-stimulated muscle glucose, contributing a hyperglycemic state. Furthermore, excessive FFAs in serum inhibit lipolysis of serum triacylglycerol levels and contribute to hypertriglyceridemia and consequently lead to insulin receptor dysfunction and insulin-resistant state. Lipotoxicity-induced insulin receptor dysfunction and hyperglycemia in adipose tissues are pathophysiologic basis of obesity which contribute to the conditions of insulin resistance and development of type 2 diabetes and other vascular complications (McKeigue et al. 1991; Unger 1995). Obesity-induced manifestations of inflammation in many tissues and organs lead to some forms of cancer, including breast, uterus, and ovarian cancer in women and prostate, kidney, colorectal, esophageal, pancreas, and liver cancer in men (Carroll 1998; Calle et al. 2003). Possibly, chronic adipokine-associated inflammation promotes cancers through the stimulation of cellular proliferation by modulation of the activities of insulin-like growth factor-1, several growth hormones and sex hormones, leptin, and others in different tissues/organs. Available evidence indicates that obesity accounts for 20–30% of the risk for breast, esophageal, and kidney cancers. Obesity-induced complications, also enhance degenerative joint diseases such as gut and osteoarthritis and result from increased weight-bearing load on joints from increased adiposity and injurious effects of inflammatory adipokines on joint synovial fluid and muscles (Schaffler et al. 2003). Obesity causes obstructive sleep apnea from the accumulation of extra adipose tissue on the upper respiratory tract and hypopharynx, which adversely affects ventilation and results in secondary hypoxia and hypercapnia. Excessive bronchial and peribronchial adipose cells secrete inflammatory adipokines that enhance bronchial mucosal inflammation, causing asthma in obese women (Bergeron et al. 2005). In overweight women of child-bearing age, obesity-associated cholesterol gallstone disease is occurred from enhanced mobilization of cholesterol from fat depots into the biliary ducts during fasting. This enhanced cholesterol level stimulates increased biliary cholesterol secretion and supersaturation of bile in the gallbladder, promoting gallstone formation (Bonfrate et al. 2014). Obesity-associated dyslipidemia, hypertension, and atherosclerosis are the risk

factors of many diseases, such as coronary artery disease, myocardial infarction, and stroke. All these diseases are originated from endothelial dysfunction by the secretion of diverse inflammatory adipokines, particularly from white adipose tissues (WAT) of visceral fat depots. Accumulating evidence demonstrates that perivascular fat tissues enhance endothelial vasomotor tone function by secreting rennin, angiotensinogen, and angiotensin II, to induce vasomotor dysfunction and cause hypertension and endothelial injury. These RAS proteins increase the expression of inflammatory vasoconstrictor, endothelin-1 (ET-1), in the aortic endothelium, which, in turn, mediates thromboxane A_2-dependent contraction in arteries for the induction of arterial hypertension (Engeli et al. 2003; Barton et al. 2012). Endothelial injury on the walls of arteries enhances the uptake of oxidized low-density lipoproteins, FFAs, and other lipid metabolites to form foam cells. These foam cells subsequently stimulate the macrophage and smooth muscle cell infiltration and secretion of inflammatory cytokines, MCP-1, macrophage migration inhibitory factor (MIF), and ET-1 to enhance the formation and stability of atherosclerotic plaques within the vascular walls. Other adipokines, such as plasminogen activator inhibitor 1 (PAI-1), IL-6, TNF-α, TNF-β, resistin, visfatin, and matrix metalloproteinases, MMP-9 and MMP-3, play an active role for thinning of atheroma cap, subsequently rupture of plaque, and release of the tissue factor and its coagulation and remodeling of plaque to cause thrombosis. Moreover, these MMPs along with troponin (C-reactive protein) participate in remodeling of cardiovascular tissue resulting in reduction of heart size, myocardial infarction, and heart failure (Rajala and Scherer 2005; Liu et al. 2006). Obesity is also a feature of polycystic ovarian syndrome, in which adipocyte secretagogues enhance metabolic abnormalities of hyperandrogenemia in obese women from insulin resistance and hyperinsulinemia and lead to a high risk of infertility, menstrual dysfunction, and pregnancy complications. Possibly, the secretion of sex hormone binding globulin, growth hormone, and insulin-like growth factor binding proteins is decreased significantly resulting in impaired ovulatory function (Dag and Dilbaz 2015). Obesity is a risk factor for pregnancy-specific disorder, preeclampsia, affecting 2–8% of all pregnancies and resulting in maternal or neonatal mortality. Adipocytes secrete several adipokines including RAS, prostaglandins, and others to induce hypertension and fluid retention in this syndrome. Endarteritis obliterans within the placenta induces toxicity by increasing the levels of inflammatory adipokines (Jeyabalan 2013). Obesity is associated with urinary incontinence (involuntary loss of urine) due to bladder to urethra stress in women. The common morbidities of obesity are depicted in Fig. 1.1 (Balaji et al. 2016).

1.3 Diabetes and Its Diagnosis and Classification

Diabetes mellitus (DM), commonly known as diabetes, is a chronic metabolic disorder, characterized by persistent hyperglycemia (high blood glucose levels) from impaired insulin secretion from pancreatic beta-cells or increased insulin resistance to insulin-responsive cells in peripheral tissues or both. The term, insulin

Fig. 1.1 Obesity and its associated morbidities. Adapted from Balaji et al. 2016 with permission of Elsevier. Copyright (2015) Elsevier

resistance, usually denotes resistance to action of insulin on glucose uptake from plasma and metabolism or storage of glucose as glycogen in the skeletal muscle and liver. Chronic hyperglycemia is associated with dyslipidemia, hypertension, and dysfunction or failure of different organs' functions, such as the heart, kidneys, eyes, nerves, and blood vessels, causing diabetic cardiovascular diseases, diabetic nephropathy, diabetic retinopathy, and diabetic peripheral neuropathy, which are responsible for morbidity, disability, and premature deaths of young adults. The global prevalence of diabetes among adults has increased from 4.7% on 1980 to about 8.5% in 2014. According to the report of WHO, about 422 million of adult are living with diabetes in 2014. More than half of these people are unaware of their disease status and even do not receive any treatment. The Asia-Pacific region is generally considered as the epicenter of diabetes (Chan 2016). As per the IDF Diabetes Atlas, the highest prevalence of diabetes was in North American and Caribbean region (11.5%) (International Diabetes Federation 2017). Over half of diabetic people are living in Southeast Asia and Western Pacific region (Ogurtsova et al. 2017).

Diagnosis

Currently, diabetes is usually diagnosed by blood or plasma glucose levels. A fasting plasma glucose level > or = 126 mg/dl or postprandial (2 h after an oral glucose

challenge of 75 g of glucose or a full meal) plasma glucose level, > or = 200 mg/dl, in an individual adult is sufficient evidence to diagnose DM. In addition to plasma glucose levels, glycosylated hemoglobin (HbA1c) levels are also considered to diagnose diabetes in individuals with risk factors. As per guidelines on diabetes by the American Diabetes Association, adult individuals with an HbA1c levels in the range of 5.7–6.4% are considered to have an increased risk of diabetes (pre-diabetes) and cardiovascular disease, and those with HbA1c > or = 6.5% are diagnosed as having diabetes. The most common symptoms of diabetes include thirst, polyuria (frequent urination), weight loss, and blurring of vision (American Diabetes Association 2014).

Classification

Diabetes mellitus (DM) is classified into four subtypes: type 1, type 2, MODY, and gestational diabetes. Type 1 diabetes (T1DM, previously known as insulin-dependent diabetes or IDDM) is an autoimmune disease that leads to destruction of pancreatic β-cells and depends on insulin supply. Type 2 diabetes (T2DM, previously known as non-insulin-dependent diabetes or NIDDM) is a progressive insulin resistance-related metabolic disease, leading to dysfunction of insulin secretion. The T1DM accounts for only 5–10% of the reported cases of diabetes, while T2DM accounts for 90–95% of reported cases of diabetes. In most of the type 1 diabetic patients, the insulin deficiency is found from destruction of pancreatic β-cells from autoimmune T-cell process. As per the estimate of the International Diabetes Federation (IDF), more than one million subjects of <20 years of age were affected by T1DM in 2017 worldwide. Major diagnostic criterion is the development of diabetic ketoacidosis (DKA), characterized by acidosis, ketonemia, ketonuria, and high HbA1c levels >6.5% (Durazzo et al. 2019). The third type is monogenic DM (because inherited from mutation of a single gene), known as maturity-onset diabetes of the young, MODY, characterized by defective pancreatic β-cell function and impaired insulin secretion. MODY is more like type 1 diabetes than type 2. Early symptoms of MODY include blurry vision, recurrent skin infections, fatigue, frequent urination, and high blood sugar levels. Up to 5% of all reported diabetes cases are diagnosed as MODY. Mutations of three genes, namely, hepatocyte nuclear factor 1 homeobox A (HNF1A) (MODY3), hepatocyte nuclear factor 4 homeobox A (HNF4A) (MODY1), and enzyme glucokinase (GCK) (MODY2), are the most common causes of MODY representing about 52%, 10%, and 32% of MODY cases, respectively, in the UK (Shields et al. 2010). The mutation of HNF1A has been reported as a common cause of MODY in other European countries, such as Sweden, Italy, Spain, and Germany. Mutations of other genes (with locus name), such as pancreas/duodenum homeobox 1 (PDX 1) (MODY 4), HNF-1B (MODY5), neurogenic differentiation 1 (NEUROD1) (MODY6), Krüppel-like factor 11 (KLF 11) (MODY 7), cholesteryl ester lipase (CEL) (MODY 8), paired homeobox 4 (PAX4) (MODY 9), INS (insulin) (MODY10), B-lymphoid tyrosine kinase (BLK) (MODY 11), ATP-binding cassette CB (ABCCB) (MODY12), inward rectifying potassium channel J11 (KCNJ11) (MODY13), adaptor protein, phosphotyrosine interaction, PH domain, and leucine zipper-containing-1 (APPL1)

(MODY 14), have been reported in a few cases. Serum low high-sensitive C-reactive protein (CRP) levels are considered as a biomarker in detection of HNF1A MODY cases (Gardner and Tai 2012; Naylor et al. 2018; Peixoto-Barbosa et al. 2020).

The fourth subtype of diabetes is gestational diabetes mellitus (GDM), developed among pregnant women from increased insulin resistance mainly in the skeletal muscle due to the increased level of insulin antagonist serum hormone and impairment of pancreatic β-cell function. GDM is associated with increased risk of T2DM in women later in their life (about 7.4-fold risk of T2DM, compared to with normoglycemic pregnant women). Exposure of the offspring to hyperglycemia in pregnancy period in untreated GDM-affected mothers has been found to have a high risk of childhood overweight and obesity from increased insulin resistance (Melmed et al. 2015).

1.4 Epidemiology of Obesity and Diabetes

According to the report of WHO, in 2016, more than 1.9 billion adults, 18 years and older, were overweight. Among them, over 650 million were obese. Moreover, it was estimated that about 13% of the world's adult population (11% of men and 15% of women) were obese in 2016. The prevalence of overweight and obesity among children and adolescents (5–19 years) has increased dramatically at an alarming rate from 4% in 1975 to over 18% in 2016. Furthermore, in 2019, 38.2 million children under the age of 5 were identified as overweight or obese (WHO fact sheets on obesity 2020). Another survey on the prevalence rate of overweight and obesity in different regions of the world between the period 1980 and 2015 reported that in low-income countries, obesity was generally higher from wealthy and urban families, whereas in high-income countries, it affected mostly in disadvantaged groups. In 2015, the prevalence of obesity in ten countries was much higher and in alarming rate, Egypt (35.3%), the USA (33.6%), Iraq (31.9%), South Africa (30.8%), Mexico (28.6%), Turkey (28.5%), the UK (24.3%), Russia (24%), Argentina (23.2%), and Brazil (22.6%), while in 1980, only two countries had the prevalence of obesity above 20%: Iraq (28.8%) and South Africa (22.6%). This increase in global obesity rate is mainly due to rapid changes in socioeconomic status, adoption of high-calorie fat-rich food, and sedentary lifestyle (Chooi et al. 2019).

According to the report of WHO, the number of people with diabetes had increased from 108 million in 1980 to 422 million in 2014, and diabetes was the seventh leading cause of death in 2016. The prevalence of diabetes rate in 2016 was in the following order: the USA and Caribbean (11.5%), the Middle East and North Africa (10.7%), South and Central America (9.6%), Southeast Asia (9.1%), Western Pacific (8.8%), Europe (7.3%), and Africa (3.8%). China, India, and the USA were the top three countries with the largest number of people with diabetes (WHO fact sheets on diabetes, 2020). Another survey reported that in 2017, 425 million individuals were affected in diabetes, and this number is expected to rise to 629 million by 2045. Among the reported cases of diabetes, more than 85% were T2DM.

Many of these diabetic patients had vascular complications including ischemic heart disease, stroke, nephropathy, retinopathy, and peripheral neuropathy (Forouhi and Wareham 2019). As per the IDF report on global diabetes, ninth edn, in 2019, the global diabetes prevalence was 9.3%, and about 463 million people were affected in diabetes worldwide (International Diabetes Federation 2019). Among them, 88 million people had diabetes from Southeast Asia region. Out of 88 million people, 77 million belonged to India. China had the highest number of people affected in diabetes in the world (116.4 million). The prevalence was higher in urban (10.8%) than in rural (7.2%) areas and in higher-income countries (10.4%). The IDF also estimated that 2.58 billion of children and adolescents (under the age of 19 years) were affected globally in type 1 diabetes and European countries were badly affected. India had the highest number of children and adolescents with type 1 diabetes (95.6 thousand), followed by the USA (94.2 thousand), Brazil (51.5 thousand), and China (28.7 thousand) (IDF diabetes atlas, International Diabetes Federation 2019). As per the US National Diabetes Statistics Report of 2020, in 2018, in the USA, about 34.2 million people of different ages (10.5% of US population) had diabetes (CDCP, US 2020).

1.5 Pathogenesis of Obesity and Diabetes

1.5.1 Pathogenesis of Obesity

The pathogenesis of obesity is a multifactorial process involving interactions among several genes, proteins, hormones, and inflammatory factors with environments. In an obese individual, the high levels of serum FFAs; glycerol; hormones such as ghrelin, neuropeptide NPY, melanocortin-4 receptor (MC4R), and beta-3-adrenergic receptor (β-3-AR); and pro-inflammatory adipokines such as leptin, TNF-α, IL-6, and PPAR-γ are found, which are possibly involved in the development of fat accumulation in the adipose tissue and liver and insulin resistance to skeletal muscle and other tissues in the development of obesity. Hence, these are considered as marker genes in the pathogenesis of obesity (Clement et al. 1995). Ghrelin, a gastric secreted peptide from the stomach, acts as an orexigenic (appetite-stimulating) hormone and stimulates feeding by its action on the growth hormone secretagogue receptor (GHSR), located in CNS of the brain. In a double-blind cross-over study, treatment of ghrelin into healthy volunteers leads to 30% increase of food intake. Ghrelin increases hypothalamic AMPK activity to increase both food intake and body weight. Moreover, it reduces glucose-stimulated insulin secretion and increases the mRNA levels of several fat storage-related (lipogenetic) proteins, SREBP1, ACC, FAS, and LPL, in the liver and adipose tissues. Plasma ghrelin levels inversely correlate with BMI (Wren et al. 2001; Zigman et al. 2006; Scerif et al. 2011).

Inflammatory adipokines, TNF-α and IL-6, on increased secretion from visceral fat of an obese individual, enhance insulin resistance through liberation of free fatty acids (FFAs) and reduce the levels of anti-inflammatory genes, adiponectin and IL-10, and impair insulin signaling in adipocytes. Both FFAs and TNF-α induce

JNK activation, which in turn increases serine phosphorylation of IRS-1 at ser307 and impairs insulin signaling and reduces GLUT4 protein expression to the cell membrane surface for glucose uptake in the cells of insulin-sensitive metabolic tissues such as the skeletal muscle, adipose tissue, and liver. Therefore, these FFAs and TNF-α are the key players of insulin resistance and potential biomarkers in the pathogenesis of obesity (Hotamisligil 1999; Hirosumi et al. 2002).

Another adipokine leptin is found in high concentrations in the serum of obese patients, and it correlates positively with fat mass of adipocytes. High serum leptin levels positively correlate with increased serum T_4, T_3, and TSH levels and leptin deficiency in the brain. Brain leptin-deficient mice have been shown to be hyperphagic and obese. High leptin level in the brain promotes the sensation of satiety and increases energy expenditure by stimulating anorexigenic (appetite-suppressing) pro-opiomelanocortin (POMC) neurons and inhibiting the activity of orexigenic (appetite-stimulating) NPY and GABA neurons. In vivo, hyperleptinemia (high leptin level in the brain), induced in normal rats, decreased TG content in the liver, skeletal muscle, and pancreas without increasing FFAs or ketones through increased intracellular fatty acid oxidation. Leptin in the brain stimulates the neurons in the arcuate nucleus of the hypothalamus to activate leptin signaling through binding of the leptin receptor LEPR to SH2B1. Activation of leptin receptor increases the phosphorylation of STAT3 and its translocation to the nucleus, where it activates POMC to stimulate the expression of melanocortin (MC) peptides. An elevated expression of MC peptides, it on binding to their receptor MC4R reduce food intake and increase energy expenditure, while antagonists of MC, agouti-related protein (AgRP) and neuropeptide Y (NPY) on upregulation, suppress the expression of POMC and activity of MC4R and lead to increased food intake and reduced energy expenditure to enhance fat mass and linear growth. Disruption of POMC expression in the brain from leptin deficiency results in hyperphagia (excessive eating) and early onset of obesity in humans. Central administration of NPY to rodents induces hyperphagia, decreases energy expenditure, activates lipogenic genes in the liver and adipose tissue, and contributes to the development of obesity. Moreover, Y1 receptor of NYP stimulates the proliferation of rat pre-adipocytes and 3T3-L1 pre-adipocytes in vitro (Shimabukuro et al. 1997; Cowley et al. 2001; Mizuno et al. 2003; Yulyaningsih et al. 2011; Farooqi and O'Rahilly 2014).

High levels of beta-3-adrenergic receptor (β-3-AR) in plasma are associated with increased plasma leptin and insulin levels and reduced insulin action in metabolic tissues in obese women. Therefore, β-3-AR is also a genetic marker of visceral obesity and insulin resistance for obese women (Sakane et al. 1997).

Expression levels of adipokine, adiponectin, are decreased in the adipose tissue of obese and diabetic patients. Adiponectin increases insulin-stimulated glucose uptake in the adipose tissue and liver through AMPK activation. Hence, low level of plasma adiponectin is a genetic marker in the pathogenesis of both obesity and diabetes (Oh et al. 2007).

Three serum microRNAs, miR-138, miR-376a, and miR-15b, have been identified as potential predictive biomarkers in obese patients. The serum levels of miR-138 and miR-376a were significantly lowered, and the serum levels of miR-15b

were higher in obese patients compared to that in non-obese healthy subjects or type 2 diabetic controls. miR-15b is a marker of NAFLD, whereas miR-138 is an enhancer of PPAR-γ2 activity, and miR-376a is a marker of hepatocellular carcinoma cells' apoptosis. The downregulation of miR-138 indicates its engagement in adipogenesis process (Pescador et al. 2012).

1.5.2 Pathogenesis of Type 2 Diabetes

Insulin resistance in muscle, liver, and pancreatic beta-cells represents the core pathophysiologic defects for chronic hyperglycemia in type 2 diabetic patients. The insulin resistance in the pancreas promotes impaired insulin secretion from beta-cells (De Fronzo in Lilly Lecture 1988). In addition to this triumvirate, another five players, namely, fat cells in the adipose tissue, gastrointestinal tract, pancreatic alpha-cells, kidney, and brain from impaired insulin action, play important roles in the development of glucose intolerance and chronic hyperglycemia in diabetic patients. Collectively, the eight players comprising the "ominous octet" from defective insulin secretion and insulin function in metabolic tissues regulate the development of impaired glucose tolerance and hyperglycemia in type 2 diabetic patients (Fig. 1.2) (De Fronzo Banting Lecture 2009).

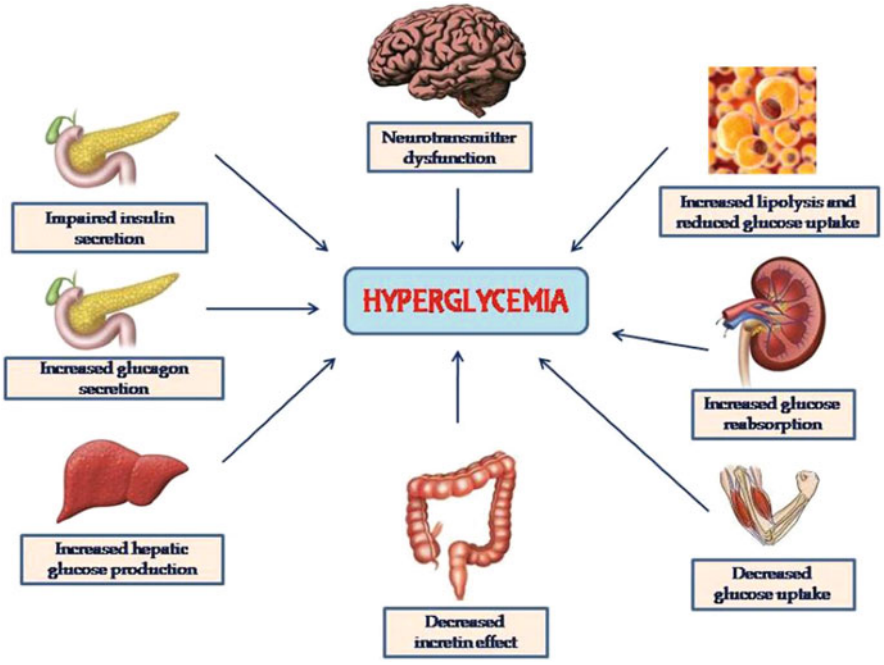

Fig. 1.2 Ominous octet for the development of hyperglycemia in type 2 diabetes. Insulin resistance in adipose tissue

Insulin resistance in fatty adipocytes stimulates lipolysis of stored triglycerides to produce high levels of non-esterified fatty acids (NEFAs), also called free fatty acids (FFAs), glycerol, diacylglycerol, ceramide, and fatty acid acyl esters and releases these lipolytic products into the systemic circulation and for their accumulation in other tissues such as the muscle, liver, pancreas, and brain to impair the action of insulin in these tissues (Reaven 1988). In adipose tissue of obese diabetic humans, a low-grade inflammation is observed due to macrophage infiltration and increased expression of pro-inflammatory cytokines including TNF-α, IL-6, and PAI-1 and chemokine, MCP-1. A significant amount of these inflammatory genes are released to the plasma and are accumulated in the pancreas, liver, and skeletal muscle and impair insulin action (Dandona et al. 2004). These pro-inflammatory genes oppose the activity of insulin signaling in adipose tissue and skeletal muscle in glucose uptake. Moreover, these inflammatory factors suppress the secretion of adiponectin, which mainly improves insulin-sensitizing effect and anti-inflammatory effect in the liver to decrease hepatic fat content (Weisberg et al. 2003; Di Gregorio et al. 2005).

Decreased Glucose Uptake in the Skeletal Muscle

Accumulation of FFAs as triglycerides in the skeletal muscle decreases the activity of insulin in glucose uptake by GLUT4 protein expression and glycogen synthesis by the enzyme glycogen synthase (GS) in the skeletal muscle and liver. Under postprandial conditions, approximately one-third of glucose is utilized in the skeletal muscle, one-third is oxidized in the brain, and the remaining one-third is stored in the liver (Kelley et al. 1988). Moreover, insulin resistance in the skeletal muscle reduces the expression levels of several genes, such as PGC-1α and PGC-1β, related to mitochondrial oxidative phosphorylation and biogenesis (Richardson et al. 2005).

Increased Glucose Production in the Liver

Hepatic insulin resistance from the accumulation of FFAs, LC-fatty acyl-CoAs, diacylglycerol, and ceramide as fat in the liver increases endogenous gluconeogenic glucose production, even after eating (Ferrannini et al. 1983). This persistent hepatic glucose production is the main reason of sustained postprandial hyperglycemia in diabetic patients. Possibly, impaired insulin-stimulated glucose uptake in the skeletal muscle and persistent hepatic glucose production are the main factors for chronic hyperglycemia in type 2 diabetic patients. Moreover, impaired insulin action in the liver decreases hepatic glucose uptake, glucose phosphorylation, glycolysis, and glycogen synthesis (Mitrakou et al. 1990; Dunning and Gerich 2007). Accumulating evidence demonstrates that in the liver insulin suppresses the production of VLDL, particularly VLDL1 apo B (apolipoprotein B) particles. The presence of high levels of FFAs in the liver suppresses the activity of insulin in the inhibition of VLDL production and results in the overproduction of VLDL and leads to increased serum triglyceride (TG) levels in diabetic patients. High serum TG levels reduce the serum HDL levels by increasing the activity of lipoprotein lipase (LPL) and cholesterol ester transfer protein (CETP) and increase the levels of serum LDL particles, which contribute to the development of atherogenic disorders, such as cardiovascular diseases, hypertension, and increased waist circumference in diabetic patients

(Lahdenpera et al. 1996; Eisenberg 1999; Austin et al. 2000; Adiels et al. 2007, 2008). A group of studies have shown that patients with type 2 diabetes frequently have elevated levels of plasma fibrinogen. High plasma fibrinogen levels of diabetic patients are correlated with hypertension and hypercholesterolemia. Plasma high fibrinogen concentrations have a key role in both early stages of plaque formation and late complications of cardiovascular diseases. Human plasma fibrinogen is mostly synthesized in the liver (about 98%) and the rest at the site of vascular injury. Hyperfibrinogenemia in diabetes is due to the production of high levels of LDL in the liver from impaired insulin action, which in turn inhibits the activity of plasminogen on fibrin binding (Tennent et al. 2007; Bembde 2012).

Impaired Insulin Secretion in Pancreatic Beta-cells

Increased levels of lipotoxic FFAs and inflammatory cytokines, such as nitric oxide (NO) and TNF-α in the pancreas, reduce pancreatic β-cell function and volume, resulting in impaired insulin secretion in type 2 diabetic patients (Butler et al. 2003; Kahn et al. 2008). Low levels of plasma arginine and insulin C peptide are found in most of the diabetic patients and provide an indication of impaired insulin secretion or insulin clearance. L-arginine was found to stimulate insulin secretion from β-cells by increasing intracellular Ca^{2+} ion concentrations and membrane depolarization in β-cells (Smith et al. 1997). Moreover, L-arginine protects the β-cells and islets from pro-inflammatory cytokines by increasing the levels of cellular GSH and glutamate and decreasing GSSG/GSH ratio and glutamate release (Krause et al. 2011). High FFA-loaded beta-cells markedly reduce the expression of insulin mRNA from β-cells and plasma insulin C-peptide level. A low level of plasma C-peptide indicates impaired insulin clearance or hyperinsulinemic condition of diabetic patients (Kotronen et al. 2008). Several lines of evidence demonstrate that a low C-peptide level in both type 1 and type 2 diabetic blood cells is responsible for low Na^+, K^+-ATPase activity and contributes to the development of diabetic complications such as diabetic cardiomyopathy and neuropathy (Vague et al. 2004). In diabetic islets, hypersecretion of islet amyloid polypeptide (IAPP) and islet amyloid (IA) deposits containing IAPP as the major constituent has been shown to develop in the progression of beta-cell failure. In more than 90% of type 2 diabetic patients, these IA deposits decrease islet beta-cell mass and thereby reduce the capacity of insulin release and play a significant role in the pathogenesis of this disease (Johnson et al. 1989; Eriksson et al. 1992; Wang et al. 2001). IA severity is associated with a decreased relative beta-cell volume and an increased alpha-cell volume in cultured islets and leads to hypersecretion of glucagon (hyperglucagonemia). An experimental study reported that when fasting plasma glucose (FPG) levels are above 90 mg/dl in diabetic patients, this deposition of IA is severe in both intracellular and extracellular spaces of beta-cells in the islets of type 2 diabetic baboons (Guardado-Mendoza et al. 2009). Moreover, several genes related to insulin secretion, such as transcription factor TCF7L2 on mutation in diabetic IA-accumulated islets, impair insulin secretion by reducing the responsiveness of beta-cells to GLP-1 (Lyssenko et al. 2007).

Increased Glucagon Secretion in Pancreatic Alpha-cells
In non-diabetic individuals, increased level of insulin in pancreatic alpha-cells decreases glucagon secretion from pancreatic alpha-cells and inhibits hepatic glucose production. But in type 2 diabetic patients, this suppression of glucagon secretion is incomplete because of insulin resistance and an increased relative volume of alpha-cells from IA deposit severity. An excessive plasma glucagon level from enhanced glucagon secretion from alpha-cells increases hepatic glucose production even after a meal and leads to postprandial hyperglycemia in diabetic patients (Dunning and Gerich 2007).

Decreased Incretin Secretion in the Gastrointestinal Tract (GI)
Incretin hormones GLP-1 and GIP, secreted from intestinal enteroendocrine L- and K-cells, increase insulin secretion, suppress glucagon secretion, inhibit gastric emptying, and reduce both appetite and meal size in non-diabetic healthy humans. This activity of incretins in insulin secretion is known as incretin effect. This incretin effect is significantly decreased (impaired) in type 2 diabetic patients due to enhanced activity of dipeptidyl peptidase-4 (DPP-4) enzymes from impaired insulin action in the GI tract (Holst et al. 2009). Insulin resistance in the gut increases gut microbiota dysbiosis and decreases endothelium cells' integrity and immunity and thereby increases the entry of several harmful pathogens in the systemic circulation and liver. These harmful pathogens increase inflammation in the liver and lungs and are associated with dysregulation of lipid and glucose metabolism.

Impaired Insulin Signaling in the Brain
In the fasting state, about 50% of whole-body glucose is utilized by the brain. Insulin resistance in the hypothalamus results in impaired insulin receptor function and leads to increased hepatic glucose production and reduced muscle glucose uptake in type 2 diabetic patients. Insulin signaling in the CNS regulates metabolic pathways in peripheral tissues such as in the liver and adipose tissue through the hypothalamus (Obici et al. 2002). Another study reported that in type 2 diabetic brain, glycogen synthesis in the hypothalamus is impaired (Soares et al. 2019). Moreover, impaired hypothalamic insulin action disrupts metabolic control and increases whole-body insulin resistance and brain dysfunction as well as promotes AGE formation in insulin-independent pathway and leads to the development of Alzheimer disease by increasing the deposition of amyloid-beta particles in brain neurons (Arnold et al. 2018).

Increased Glucose Reabsorption in the Kidney
Available evidence demonstrates that about 180 g of glucose are filtered daily by the kidney and enter the renal tubular system in a healthy non-diabetic human through the activity of SGLT-2 and SGLT-1. In both type 1 and type 2 diabetic kidney, the activity of renal SGLT-2 and SGLT-1 increases by 40–80% to reabsorb about >90% and about 3% of filtered glucose, respectively, due to impaired insulin action. SGLT-2 enzyme has the dominant role in the absorption of urinary glucose in renal proximal tubule. Application of selective SGLT-2 inhibitors increases the glucose

excretion to only 50–70%, and thus a part of reabsorbed glucose (about 30–50%) by SGLT-1 and SGLT-2 remains in the body (Rieg et al. 2014).

Therefore, impaired insulin secretion; decreased muscle glucose uptake, glucose oxidation, and glycogen synthesis; increased hepatic glucose production and decreased glucose uptake and glycogen synthesis; uncontrolled lipolysis in obese fat cells; increased glucose reabsorption in the kidney; and impaired insulin signaling in the brain are the major factors in the impaired insulin secretion and function and glucose tolerance and in the pathogenesis of type 2 diabetes in humans.

1.5.3 Pathogenesis of Type 1 Diabetes

Type 1 diabetes (T1DM) is an autoimmune disease, characterized by T-cell-mediated destruction of insulin-producing beta-cells in the pancreatic islets of diabetic patients. A decreased β-cell mass in association with insulitis (islet inflammation) is observed in the pancreas of NOD mice and human type 1 diabetes in the early stages of the disease. Moreover, destruction of more than 75% of β-cell mass in pancreatic islets was observed at the time of clinical diagnosis of type 1 diabetes. Several lines of studies in NOD mice and human type 1 diabetes patients have demonstrated that a breakdown in immune regulation in the pancreas from a synergistic effects of expanded autoreactive $CD4^+$ and $CD8^+$ T_{reg} cells, antibody-producing B-lymphocytes, and activation of innate immune system results in the destruction of β-cells (Bluestone et al. 2010). Most of the evidences demonstrate that autoreactive T-cells play a dominant role in disease initiation and progression. In NOD mice, $CD11c^+$ dendritic cells and ER-$MP23^+$ macrophages are the first cells to infiltrate in the insulitis region of the pancreas in NOD mice within 3 weeks period. Within a short time, pathogenic T-cells are detected in the islet insulitis region (Anderson and Bluestone 2005). Another study on the pancreata of human type 1 diabetic patients identified the presence of $CD8^+$ and $CD4^+$ T-lymphocytes, B-lymphocytes, and macrophages as infiltrates in the insulitis region of the pancreas, and $CD8^+$ T-cells were dominant in the infiltrates (In't Veld 2011). Another group reported that $CD8^+$ and $CD4^+$ T-cells and $CD11c^+$ cells were present in high numbers in the exocrine pancreas of autoantibody-positive (Ab^+) and type 1 diabetic patients. Possibly, dendritic cells ($CD11c^+$) provide critical antigenic stimulation to native $CD4^+$ T-cells, because both $CD4^+$ and $CD11c^+$ cell populations are elevated in the exocrine pancreas of T1D donors. Thus, $CD11c^+$ cells might play a critical role in immune activation and $CD4^+$ and $CD8^+$ T-cell infiltration in diabetic pancreas (Rodriguez-Calvo et al. 2014).

The most significant step in the discovery of biomarkers in the pathogenesis of T1D is the isolation of autoantigenic $CD4^+$ T-cell clone, BDC-5.2.9, known as islet amyloid polypeptide (IAPP), which is co-secreted along with insulin by injured β-cells in both NOD mice and human type 1 diabetic patients. These islet reactive $CD4^+$ T-cell clones are the representative of the memory effector $CD4^+$ T-cells and produce Th1-mediated inflammatory cytokines, especially interferon (IFN)-γ in disease induction and progression. IAPP is the major constituent of amyloid plaques

(deposits) found in the pancreatic islets of type 2 diabetic patients. This polypeptide stimulates HLA regions of islets for the production of inflammatory cytokines and for the accumulation of $CD8^+$ T-cells in type 1 diabetic HLA-A*0201 patients. Soluble oligomers of IAPP have been shown to activate NLRP3 inflammasome that leads to increased IL-β production in T2DM. Possibly, in type 1 diabetes, similar smaller aggregates of IAPP lead to the formation of neoantigenic epitopes (Delong et al. 2011). Another study by the same group reported the isolation and identification of peptide fusions, hybrid insulin peptides (HIPs), from the pancreas of non-obese diabetic (NOD) mice and found that these peptide fusions were highly antigenic to $CD4^+$ T-cells, isolated from the pancreatic islets of both type 1 diabetic patients and NOD mice. The autoreactive T-cells target these HIPs for the destruction of β-cells. These HIPs are formed by covalent cross-linking of proinsulin peptides to other peptides present in β-cell secretory granules in post-translational modifications by several environmental and genetic factors in the pancreas of type 1 diabetic patients. These HIPs have strong antigenic property (more than 1000 times higher) compared to other autoantigens, chromogranin A (chg A), IAPP, and WE14, a cleavage product of chg A. Moreover, these HIPs are also highly antigenic to $CD8^+$ T-cells. Two HIP clones formed by the fusion of proinsulin C-peptide with IAPP2, a fragment peptide of IAPP, were isolated and identified from the $CD4^+$ T-cell clones, from the pancreas of type 1 diabetic infant of 3 years old. Thus, these HIPs are the key antigens for the autoreactive T-cells and are responsible for the loss of self-tolerance in pancreatic islets and play a central role in the pathogenesis of type 1 diabetes in humans (Delong et al. 2016).

Several lines of evidence demonstrate that autoreactive $CD8^+$ T-cells play a central role in the destruction of pancreatic islet β-cells, because these cells are found in high concentrations in islet-centered leukocytic infiltrates (insulitis region) at the time of diagnosis in type 1 diabetic patients having inheritance of specific human leukocyte antigen (HLA) class I alleles. These $CD8^+$ T-cells directed islet antigens, such as preproinsulin (PPI), glutamic acid decarboxylase 65 (GAD 65), islet-specific glucose 6-phosphatase-catalytic subunit-related protein (IGRP), islet tyrosine phosphatase-like insulinoma antigen 2 (IA-2), zinc transporter 8 (ZnT8), and cytomegalovirus pp65 (CMV pp65), which are upregulated in the islets of many type 1 diabetic patients, for the activation of inflammatory Th 1 cells and production of inflammatory cytokines, as well as for the destruction of β-cells by initiation of pro-apoptotic cascades and, consequently, reduction of insulin-secreting function of β-cells in the secretion of insulin C-peptide, a marker of β-cell function (Skowera et al. 2015; Roep et al. 2013; Wenzlau et al. 2007; Ott et al. 2004).

Several classical inflammatory cytokines, such as IL-1, IL-6, IL-17, IL-21, TNF-α, IFN-α, and IFN-γ, promote the differentiation and function of diabetogenic immune cells, such as Th1, Th17, $CD8^+$ T-cells, $CD4^+$ T-cells, and NK cells, for the onset of type 1 diabetes and progression of destruction of pancreatic β-cells. By contrast, some anti-inflammatory cytokines, such as IL-10, TGF-β, and IL-33, are thought to restore immune tolerance and prevent β-cell damage. Overexpression of IL-6 in local pancreatic β-cells was shown to increase insulitis and infiltration of T-cells, β-cells, and macrophages. Overexpression of TNF-α was found to stimulate

the upregulation of dendritic cells (DC) maturation markers in the $CD11b^+$ and $CD11c^+$ subsets for the activation of T-cells via the upregulation of MHC-1 molecules. IFN-α also promotes the overexpression of HLA-1 (also called MHC-1) molecules and increases endoplasmic reticulum stress and apoptosis of β-cells. Similarly, IFN-γ induces the expression of MHC-I and MHC-II molecules in local pancreatic β-cells to enhance the inflammatory process for the destruction of β-cells (Lu et al. 2020).

Several viruses including coxsackievirus have been reported to involve in the initiation of type 1 diabetes. A low-grade enteroviral infection from enteroviral capsid protein 1 (VP 1) and enterovirus RNA in the pancreatic islets of type 1 diabetic patients has been observed to contribute in the progression of the disease (Krogvold et al. 2015).

A group of studies on gut microbiota of obese children demonstrate that gut microbiome dysbiosis in early childhood leads to loss of both maturation of self-immunity and self-tolerance by presentation of aberrant self-antigens and foreign antigens due to enhancement of systemic pro-inflammatory signals and entry of LPS and other harmful pathogens and deficiency of bacteria that produce short-chain fatty acids and mucus synthesis in the gut epithelium, thereby enhancing immune-mediated type 1 diabetes (Siljander et al. 2019; Vatanen et al. 2018). Gut microbiota dysbiosis increases the entry of harmful antigens through the intestinal gut epithelium. A comparative study on the gut microbial composition in the fecal samples of 16 Caucasian type 1 diabetic children of 7 years old and non-diabetic healthy children of the same age group reported that a significant decrease in the number of probiotic bacteria of the genera *Lactobacillus* and *Bifidobacterium* and levels of *Firmicutes* and an increase in the number of bacteria of the genera *Clostridium*, *Bacteroides*, and *Veillonella* were observed in the children with type 1 diabetes compared to non-diabetic children group. The bacteria of *Clostridium* and *Bacteroides* are not able to produce butyrate and induce mucus synthesis in the gut and thereby increase the permeability of harmful pathogens into systemic circulation in the children of type 1 diabetes (Murri et al. 2013). Several studies demonstrate that a prolonged deviation from optimal gut microbial homeostasis in children causes gut microbial dysbiosis, which results in the relative low abundance of bacteria of the genera *Bifidobacterium*, *Roseburia*, *Faecalibacterium*, *Lachnospira*, *Lactococcus*, *Akkermansia*, and *Lactobacillus* and the relative high abundance of bacteria of the genera *Bacteroides* (e.g., *Bacteroides dorei*), *Ruminococcus*, *Veillonella*, *Blautia*, and *Streptococcus*, and thereby leads to increased intestinal permeability of harmful toxic pathogens and aberrant presentation of foreign antigens and self-antigens, as well as spreading of local pro-inflammatory signals from the gut to the regional lymph nodes and pancreas, and contributes to the development of islet autoimmunity and type 1 diabetes (Fig. 1.3) (Siljander et al. 2019; Sprouse et al. 2019).

Several type 1 diabetic candidate genes such as PTPN2, TYK2, USP18, GLIS3, CD55, MDA5, STAT4, IFIH1, and SH2B3 are expressed in human pancreatic islets in high concentrations and possibly contribute to insulitis and β-cell destruction and in the progression of the disease. PTPN2 (protein tyrosine phosphatase N2) and MDA5 (melanoma differentiation-associated gene 5) have been shown to regulate

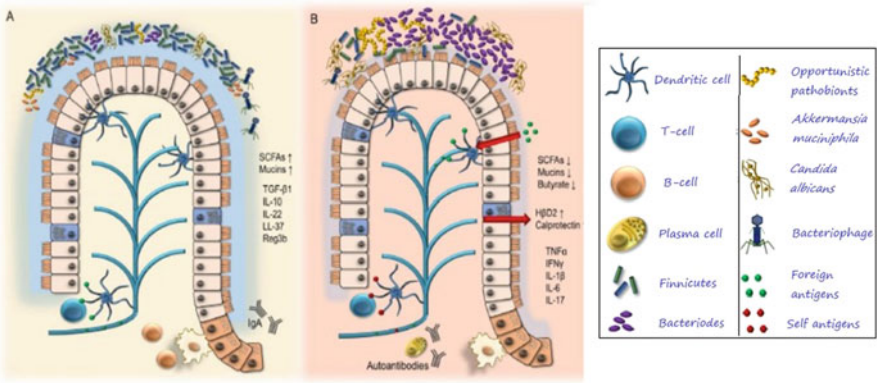

Fig. 1.3 (**a**) Healthy intestinal microbiome environment and (**b**) type 1 diabetic-related intestinal microbiome dysbiosis from the entry of pathogenic bacteria and consequent induction of intestinal inflammation and development of autoimmunity. Adapted from Siljander et al. 2019 with permission of Elsevier. Copyright (2019) Elsevier

pancreatic β-cell apoptosis through the generation of inflammatory signals in the presence of a viral infection (Colli et al. 2010; Eizirik et al. 2012; Santin and Eizirik 2013).

Some microRNAs are expressed in high levels in the pancreas of type 1 diabetic patients and contribute to the development of β-cell dysfunction and apoptosis. For instance, the expression levels of miR-21, miR-34a, and miR-146a are elevated in the pancreas of type 1 diabetic patients in the presence of IL-1β or a combination of IL-1β, TNF-α, and IFN-γ (Ventriglia et al. 2015).

1.6 Genetic, Epigenetic, and Environmental Risk Factors of Obesity and Diabetes

1.6.1 Genetic Risk Factors of Obesity

Obesity is a heritable trait disease influenced by the interactions of genetics, epigenetics, metagenomics, and several other environmental factors, including exercise, diet habits, and lifestyle. Numerous genes in metabolic tissues, such as the adipose tissue, skeletal muscle, pancreatic islets, liver, blood, and brain, are associated with the development of obesity and its associated type 2 diabetes and other vascular complications (Gesta et al. 2007).

Based on the involvement of gene or genes in the development of obesity, obesity is broadly classified into three types:

1. Monogenic obesity: Monogenic obesity is mainly caused by mutation of a single gene located in the leptin-melanocortin pathway.

2. Syndromic obesity: Obesity that are caused by mutation of several genes and associated with neuroabnormalities and malfunctions of other metabolic organs. The most frequent forms of syndromic obesity are Bardet-Biedl syndrome (BBS) in Northern European populations and Prader-Willi syndrome (PWS), characterized by severe neonatal hypotonia, eating disorders, and cognitive impairment.
3. Polygenic obesity: Several mutant genes work together in the development of this kind of obesity. This is the most common form of obesity.

Both monogenic and syndromic obesity are regulated by the central nervous system (CNS) through the modulation of signals in the brain-gut axis. The hypothalamic leptin-melanocortin pathway plays a key role in the regulation of energy homeostasis and body mass in humans (Morton et al. 2006). The hypothalamus integrates the signals received from metabolic tissues such as the gut, pancreas, and adipose tissue. The gut secretes ghrelin, peptide YY (PYY), cholecystokinin (CCK), glucagon-like peptide-1 (GLP-1), and diet-specific melanoreceptors, pancreas secretes insulin, and adipose tissue secretes leptin and adiponectin in response to food intake. The leptin-melanocortin pathway is activated by leptin receptor (LEPR) or insulin receptor (INSR) present in the neurons of arcuate nucleus. These LEPR and INSR signals are regulated by two sets of neurons in a feedback loop as per instruction from metabolic tissues. The pro-opiomelanocortin, cocaine, and amphetamine-related transcript (POMC/CART) neurons regulate LEPR signal for the production of anorexigenic (appetite-suppressing) peptide POMC, ghrelin, and PYY, while other sets of neurons regulate INSR signal for the production of orexigenic (appetite-stimulating) peptides, AgRP and NPY (Cowley et al. 2001). POMC upregulates its target peptides, α-, β-, and γ-melanocyte-stimulating hormone (MSH) and β-endorphin, to enhance its activity. Both β-MSH and AgRP bind in a competitive manner with melanocortin-4 receptor (MC-4R), expressed in the paraventricular nucleus of the hypothalamus to exhibit anorexigenic and orexigenic signals, respectively (Harrold and Williams 2006). Dominant signal for food intake from MC-4R is transmitted to higher cortical centers through a process involving brain-derived neurotrophic factor (BDNF) and neurotrophic tyrosine receptor kinase-2 (NTRK-2), known as tropomyosin receptor kinase B (TrKB). A group of evidence demonstrates that mutation of LEP, LEPR, POMC, MC-4R, BDNF, and SH2B1 (Src homology 2B adapter-1), a positive regulator of insulin sensitivity, disrupts the regulatory system of appetite and contributes to the development of obesity (Krude et al. 1998; Yeo et al. 2004; Han et al. 2008; Pearce et al. 2014; Saeed et al. 2015). To evaluate the genetic risk factor of obesity, a genome-wide association study (GWAS) and metabochip (MC, metabolic, and atherosclerotic/cardiovascular disease-related traits) meta-analysis of the genes of human tissues related to BMI of nearly 339,224 individuals were carried out and identified 97 BMI-associated loci, 56 of which were novel. These 97 loci accounted for about 2.7% variation of BMI. Most of these identified genes (64) are from CNS process in the hypothalamus and in relation to insulin secretion and action, energy metabolism, lipid biology and adipogenesis, and immune system. Among them, the obesity-related key genes

regulating insulin secretion and feeding behaviour, namely BDNF, MC4R, BBS4, and POMC are involved in hypothalamic function and body energy homeostasis processes, caused the formation of monogenic obesity syndrome, genes, namely, SH2B1 and NEGR1, that are involved in extreme/early onset of obesity in humans. In addition to these, some identified genes, such as, TCF7L2, GIPR, IRS1, FOXO3, ASB4, RPTOR, NCP1, CREB1, FAM57B, APOBR, HSD17B12, and MAPK3, are related to insulin secretion and action, energy metabolism, and lipid metabolism, and an immune-related gene, TLR4, is closely associated with the regulation of body mass. Possibly, TLR4 exhibits its influence on obesity through the gut microbiome (Locke et al. 2015).

1.6.2 Genetic Risk Factors of Diabetes

A group of evidence demonstrates that genetic variants have a crucial role in the development of both type 2 and type 1 diabetes in the next generations. Parents having type 2 diabetes affected their siblings at two- to threefold increased risk of diabetes compared to non-diabetic parents. It is observed that offsprings having one parent with diabetes increases the risk of diabetes (T2DM) by 30–40% and having both diabetic parents increases the risk of diabetes by 70% (Meigs et al. 2000). Trans-ancestry GWAS meta-analysis from diabetic Europeans, East and South Asians, and Mexican Americans identified three variant risk alleles, TCF7L2, PEPD, and KLF14, among these four ancestry groups (Mahajan et al. 2014). GWAS analysis on non-Europeans diabetes reported that a variant in KCNQ1 was significantly associated with type 2 diabetes in the diabetic parents of Japanese, Koreans, and Chinese (Unoki et al. 2008; Yasuda et al. 2008). Among the diabetic Mexicans and other Latin Americans, variants in SLC16A11 and SLC16A13 were associated with type 2 diabetes (Williams et al. 2014). Variants of melatonin receptor 1B, MTNR1B, are the risk factor of type 2 diabetes, as they impair melatonin secretion and inhibit insulin secretion from pancreatic β-cells at night (Bonnefond et al. 2012). GWAS meta-analysis from diabetic and non-diabetic South Asian ancestry originating from India, Pakistan, Sri Lanka, and Bangladesh identified common genetic variants at six loci, GRB14, ST6GAL1, HNF4A, HMG20A, AP3S2, and VPS26A, that were associated with T2DM. Among them, GRB14 is related to insulin action, and ST6GAL1 and HNF4A are related to pancreatic β-cell function (Kooner et al. 2011).

Type 1 diabetes is also a heritable risk factor for offspring from both maternal and paternal sides. Accumulating evidence indicates that the diabetic risk for the offspring of a father having type 1 diabetes is more than that of the mother with type 1 diabetes (6% and 1%, respectively). The dominant genetic drivers of this inheritance risk are class II HLA (human leukocyte antigen) DR and DQ genes, located in chromosome 6. The DR-DQ haplotypes conferring the highest risk are DRB1*03:01-DQA1*05-DQB1*02:01 (abbreviated DR3) and DRB1*04:01/02/04/05/08-DQA1*03:01-DQB1*03:02/04 (abbreviated DR4), and the former haplotypes are strongly associated with type 1 diabetes in European descent populations (Noble and

Valdes 2011). More than 90% of type 1 diabetic patients carry one or both of the haplotypes conferred by DR3-DQ2 and DR4-DQ8. These heterozygous genes have a high risk factor of type 1 diabetic patients because of their key role in antigen presentation and activation of helper T-cell-mediated immune response (Kelly et al. 2003). A cohort study among Japanese patients having type 1 diabetes reported that a combination of HLA class I and II alleles, HLA-A24, HLA-DQA1*03, and HLA-DR9 (DRB1*0901), contributes to the acute onset and early complete destruction of β-cells, whereas HLA-DR2 (HLA-DRB1*15 and HLA-DRB1*16) has a protective effect against complete β-cell loss in type 1 diabetic patients. Possibly, a combination of these alleles may have synergistic and complementary effects in various stages of immune response. The frequency of these three-allele combination was only 30% in acute onset of type 1 diabetes, so there remains a possibility of non-HLA genes and environmental factors that promote β-cell destruction in T1DM (Nakanishi and Inoko 2006). Another study reported that PTPN22 (protein tyrosine phosphatase non-receptor type 22) polymorphism was associated with type 1 diabetes among the population of Caucasian origin (in Greek children and adolescents) (Giza et al. 2013). Moreover, variants of MHC, INS, and CTLA-4 (cytotoxic T-lymphocyte antigen 4), ERBB3 (Erb-B2 receptor tyrosine kinase 3), STAT3, IFIH1 (interferon-induced helicase C domain 1), and insulin-VNTR (variable numbers of tandem repeats) are also the risk factors of human type 1 diabetes (Bottini et al. 2006; Nejentsev et al. 2009; Paschou et al. 2018). Available evidence indicates that HLA class II alleles confer about 50% of heritable risk in type 1 diabetes. These alleles are expressed in high concentrations in pancreatic β-cells and contribute to the progression of β-cell destruction. Immunohistological analysis of pancreata of type 1 diabetic patients revealed that both HLA and non-HLA alleles act on both pancreatic β-cells and immune B- and T-lymphocytes to induce islet inflammation and destruction of β-cells among the children of the age group of below 7 years, while B-lymphocytes are rare in the children of 13 years or above. Among HLA alleles, HLA class II heterozygous diplotype DR3-DQ2/DR4-DQ8 and HLA class I alleles A*24:02 and B*39:06 are the high-risk alleles as these are involved in the reduction of protective T regulatory cells and induction of strong autoantigen environment. Protective HLA class II haplotypes DRB1*15:01-DQB1*06:02 and DRB1*07:01-DQB1*03:03 are less prevalent among individuals of less than 7 years of age compared to those diagnosed at the age of 13 years or above. In addition to highly expressive HLA class II and I alleles in pancreatic beta cells, six non-HLA alleles, namely GLIS-3 which affect key T- and β-cells; and the remaining CTSH which acts on both immune and β-cells, have been identified as risk factors for type 1 diabetes (Inshaw et al. 2020).

GWAS meta-analysis of several gestational diabetes patients reported that several variants in genes related to β-cell function in insulin secretion and insulin action on glucose metabolism, such as KCNJ11 (potassium inwardly rectifying channel subfamily J, member 11), GCK (glucokinase), HNF1A (hepatocyte nuclear factor 1α), TCF7L2 (transcription factor 7 L2), CDKAL1 (CDK5 regulatory subunit-associated protein-1-like-1), SLC30A8 (solute carrier family 30, member 8), MTNR1B, PPARG, FTO (fat mass and obesity-associated protein), and IRS-1, are the risk factors of GDM (Rosik et al. 2020).

1.6.3 Epigenetic Risk Factors of Obesity

Epigenetics has been defined as heritable changes in gene function through DNA methylation, histone modifications, and non-coding RNA-mediated processes without any change in DNA sequence. These epigenetics processes disrupt lipid and carbohydrate metabolism in the offsprings and contribute to obesity and type 2 diabetes. The epigenetic alternations of gene expressions in human metabolic tissues, such as the skeletal muscle, adipose tissue, pancreatic islets, liver, and blood, lead to the development of obesity and its associated complications. In mammalian cells, DNA methylation takes place on a cytosine, mainly at cytosine (C) preceding guanosine (G), so-called CpG sites and to a less extent in non-CG content. Methyltransferases, such as DNA methyltransferase 1 (DNMT1), DNMT3A, and DNMT3B, are responsible for the attachment of methyl groups to DNA during replication and de novo methylation. These methyltransferases use S-adenosyl-L-methionine (SAM) as methyl donor. Sometimes passive demethylation occurs when the activity of DNMTs or the amount of methyl donors is low during replication, and active demethylation occurs by ten-eleven translocation (TET) enzymes, which can oxidize methyl groups to hydroxymethyl group followed by repair. The most widely studied post-translational histone modifications include methylation, acetylation, phosphorylation, and ubiquitination on amino terminus or tails of histones. A large number of enzymes are associated with histone modifications and contribute to epigenetic regulations. For instance, histone methyltransferases (HMT) promote histone methylation through the transfer of one, two, or three methyl groups from SAM to lysine or arginine residues of histone proteins. Histone acetylation occurs through the enzymatic addition of an acetyl group from acetyl coenzyme A by histone acetyltransferases (Kouzarides 2007; Keating and El-Osta 2015). Non-coding microRNAs on methylation and/or demethylation regulate gene expressions and are associated with human diseases including obesity and diabetes (Traube and Carell 2017).

These epigenetic modifications are observed in the offspring when their parents (particularly mother) are exposed in extreme environmental conditions of under- and over-nutritional diet. The maternal diet plays a crucial role in the development of fetus and progeny. The epidemiological studies of two large cohorts exposed to serious nutritional deficit during the Second World War in Dutch Hunger Winter cities (The Hague, Rotterdam, and Amsterdam) in 1944–1945 and in the Chinese famine in 1959–1961 revealed that the individuals prenatally exposed to famine were found to be overweight and to develop diabetes and cardiovascular diseases than those born the year before. Several indications on the epigenetic changes during the early development stage mediate the outcome in the later life. A lower degree of methylation in the imprinted IGF2 gene was found in blood cells of people born in famine-affected cities during the Dutch Hunger Winter compared to same-sex siblings that were born unexposed (Heijmans et al. 2008). Another study reported that altered DNA methylations in other genes related to metabolic disorders, such as INSIGF2 (hypomethylation), GNASAS1, MEG3, IL-10, and LEP (hypermethylation), were detected in the blood cells of the offspring of famine-

exposed mothers compared to unexposed same-sex siblings (Tobi et al. 2009). Neonatally overfed rats gained body weight rapidly and had hypermethylation of POMC gene (Plagemann et al. 2009). This alternation of DNA methylation of POMC gene was closely associated with BMI of offspring and related to paternal somatic methylation pattern (Kuhen et al. 2016). Another study reported that an elevated gestational weight gain of mother in early pregnancy was associated with increased DNA methylation of genes MMP7, KCNK4, TRPM5, and NFKB1 in offspring blood cells. These facts suggest that the association of maternal obesity to the offspring is stronger than that of paternal obesity and this effect is known as intrauterine influence of obesity (Sharp et al. 2017). Several majestic EWAS (epigenome-wide association study) analyses of blood-derived DNA samples of obese young adult individuals identified ten genes having 83 replicated CpG sites of differential methylation and altered gene expression and are related to metabolism, BMI and WC in obese adults. Among them, increased DNA methylations at CpG sites of HIF3A, CD38, CPT1A, MSI2 (Musashi RNA binding protein 2), LARS2 (leucyl-tRNA synthetase 2), ABCG1, and SREBF1 in leukocytes are associated with BMI, waist circumference, and eating behavior in young cohorts of ages 14–36 years; ABCG1, a cell membrane lipid transporter, increases cholesterol transport in obese rodents and humans. Hypermethylation of ABCG1 and SREBF1 (also known as SREBP1) is related to higher BMI and TG levels. Another obesity-related gene DHCR24 (24-dehydrocholesterol reductase) undergoes higher DNA methylation and is associated with only BMI, catalyzed the reduction of sterol intermediates in cholesterol biosynthesis, on hypermethylation, decreased its expression and increased high LDL level. MSI2 and LARS2 are associated with eating behaviour and bipolar disorder in obesity, respectively and on increased methylation and increased BMI and WC in obese adults. Epigenetic dysregulation of these genes promotes obesity and obesity-related morbidities (Demerath et al. 2015; Mendelson et al. 2017; Dhana et al. 2018). Dick et al. reported that an increased BMI in obese adults of European origin was associated with increased methylation of hypoxia-inducible transcription factor 3 alpha (HIF3A) in blood cells and adipose tissue. Possibly, hypermethylation at CpG sites in HIF3A reduces the gene expression, but increases the expression of angiopoietin-like-4 (ANGPTL-4) protein, which has a significant role in acquired obesity (Dick et al. 2014; Demerath et al. 2015). Another EWAS analysis of blood samples from obesity-related adults identified differential methylation pattern in SLC7A11 and MYLIP, which were associated with TG levels, and in SYNGAPI, which was associated with HDL cholesterol (Sayols-Baixeras et al. 2017). An EWAS meta-analysis of obesity-related African American young cohort under the ages of 14–36 years identified 29 novel CpG sites related to obesity, and these sites are replicated in leukocytes and are not driven by cell composition. This study identified five genes that have direct link between DNA methylation and gene expression in obesity. Among them, four genes, SOCS3, CISH (cytokine inducible src-homology 2 containing protein), PIM3 (pim-3 proto-oncogene), and KLF4, have decreased DNA methylation and increased expression levels in obesity. SOCS3 on upregulation induces both insulin and leptin resistance through the activation of inflammation-related JNK-STAT3 signaling pathway. PIM3 transcription factor on increased expression increases the risk of

obesity-related inflammation and is involved in the regulation of energy metabolism by burning of fats, while another gene HRASL2 was also associated with obesity with decreased DNA methylation and decreased gene expression. These genes are the risk factor of obesity-related disorders (Wang et al. 2018).

1.6.4 Epigenetic Risk Factors of Type 2 Diabetes

In type 2 diabetic patients, pancreatic islet function is decreased on long-term exposure to elevated glucose and lipid levels. The elevated glucose level is developed due to insulin resistance in target tissues, such as the skeletal muscle, liver, and adipose tissue. A group of studies in epigenetics of type 2 diabetic patients revealed that epigenetic alterations in DNA methylation patterns at the CpG sites of some candidate genes impair their activity in insulin secretion in pancreatic islet and in glucose and lipid metabolism in peripheral tissues.

Different groups reported that increased DNA methylation of the genes INS (encoding insulin), PDX1, PPARGC1A (encoding PGC1α), and GLP1R (encoding GLP-1 receptor) in pancreatic islets of type 2 diabetic patients, compared to non-diabetic controls, decreased the expression levels of these genes and leads to impaired insulin secretion. Possibly, elevated glucose and glycated hemoglobin (HbA1c) play a key role to increase the DNA methylation of these genes (Hall et al. 2013, 2018; Ling et al. 2008; Yang et al. 2011, 2012). Another study reported that the genes CDKN1A, PDE7B, and SEPT9, with decreased DNA methylation, increased their expression levels in the isolated pancreas from diabetic patients. These genes on overexpression in clonal β-cells decreased glucose-stimulated insulin secretion. CDKN1A, a potent inhibitor of cyclin-dependent kinase (CDK), decreases the proliferation of clonal β-cells by the suppression of cell cycle progression at G1 phase. PDE7B, a cAMP-specific phosphodiesterase, on hydrolyzing cAMP, reduces insulin secretion from β-cells. Moreover, overexpression of these genes in clonal α-cells increased glucagon secretion. Furthermore, altered DNA methylation of CpG sites of some other genes, ADCYs, IRS1, FTO, HHEX, KCNQ1, PPARG (encoding PPAR-γ), and TCF7L2, in diabetic pancreatic islets regulated the expression levels of the genes to impair insulin secretion (Dayeh et al. 2014). In high palmitate-exposed isolated human islets, the genes, TCF7L2 and GLIS3, increased DNA methylation and decreased expression levels and impaired insulin secretion (Hall et al. 2014). In obese diabetic patients and neonatal diabetes, the expression level of GLIS3 is reduced in the pancreas, causing an impaired insulin secretion. Possibly, an altered DNA methylation of GLIS3 in utero and in offspring at birth caused the decreased expression of the gene resulting in marked impairment of insulin production and culminating into permanent neonatal diabetes. An elevated expression of GLIS3 gene in pancreatic islets stimulates the expression of INS1 and INS2 and activation of PDX1 and MAFA genes for β-cell regeneration and function (Wen and Yang 2017). Whole-genome bisulfite sequencing (WGBS) analysis of human diabetic pancreatic tissues identified 457 genes having differentially methylated regions (DMRs) and expression changes in the islets. Among these

identified genes, three genes, NR4A3, PID1 (phosphotyrosine interaction domain containing 1), and SOCS2, were overexpressed, and another gene PARK2 (encoding Parkin 2) was silenced in cultured rat β-cells and induced the impairment of insulin secretion. Moreover, another identified gene SLC2A2 (encoding GLUT2) had increased DNA methylation and decreased expression in diabetic islets. NR4A3 gene on overexpression in the pancreas reduces insulin secretion by the suppression of PDX1 and NeuroD1 (ND1) activity. PID1 on overexpression impairs mitochondrial function in β-cells, and SOCS2 (suppressor of cytokine signaling 2) on overexpression decreases insulin secretion by decreasing the production of pro-hormone convertase-1 (PC1/3) and inhibiting the maturation of proinsulin. These results highlighted that epigenetic dysregulation of some key genes, related to insulin secretion in diabetic pancreatic islets, contributed to the impaired insulin secretion in type 2 diabetes (Volkov et al. 2017).

1.6.5 Epigenetic Post-transcriptional Risk Factors of Obesity and Diabetes

Post-transcriptional histone modifications of methylated DNA and non-coding microRNAs dysregulated the expression of several genes and are involved in the pathogenesis of many diseases including obesity and diabetes (Perera and Ray 2007).

The flexible N-terminal tails of the four histone proteins, namely, H2A, H2B, H3, and H4, in DNA may undergo post-translational modifications, including acetylation, deacetylation, methylation, phosphorylation, and ubiquitination, and alter their interactions with DNA and nuclear proteins, leading to changes of the genetic readout and thereby changes in the gene expression. These histone modifications are the indicators of active or repressed/silent regions of chromatin structure. For example, H3-K27me3 (trimethylation of histone 3 protein at lysine 27) represents a mark enriched inactive or silent promoter region of the genomic area throughout the chromatin structure. Similarly, H3-K9me (methylation of histone 3 protein at lysine 9) represents a hallmark of silenced genomic area throughout the chromatin structure, whereas H3-K4me denotes gain in activity and is found predominantly in the promoter area of the active genes. Similarly, H3K9ac (acetylation of histone 3 protein at lysine 9) represents an active gene promoter region, and its removal is associated with gene repression (Bernstein et al. 2002). Key enzyme families involved in histone modifications include histone deacetylases (HDACs), histone methyltransferases (HMTs), histone acetyltransferases (HATs), and methyl binding domain protein MECP2. Several methyl CpG binding proteins interact with histone deacetylases to regulate gene expression, suggesting that a mechanism of DNA methylation and histone modifications are held together (Fig. 1.4) (Klose and Bird 2006).

An overexpression of histone deacetylase-7, HDAC7 in pancreas has been found to reduce insulin secretion in pancreatic islets. It is upregulated in human diabetic islets and decreased DNA methylation in diabetic islets compared to non-diabetic donors. Its overexpression in rat islets and clonal INS1 beta-cells reduced insulin

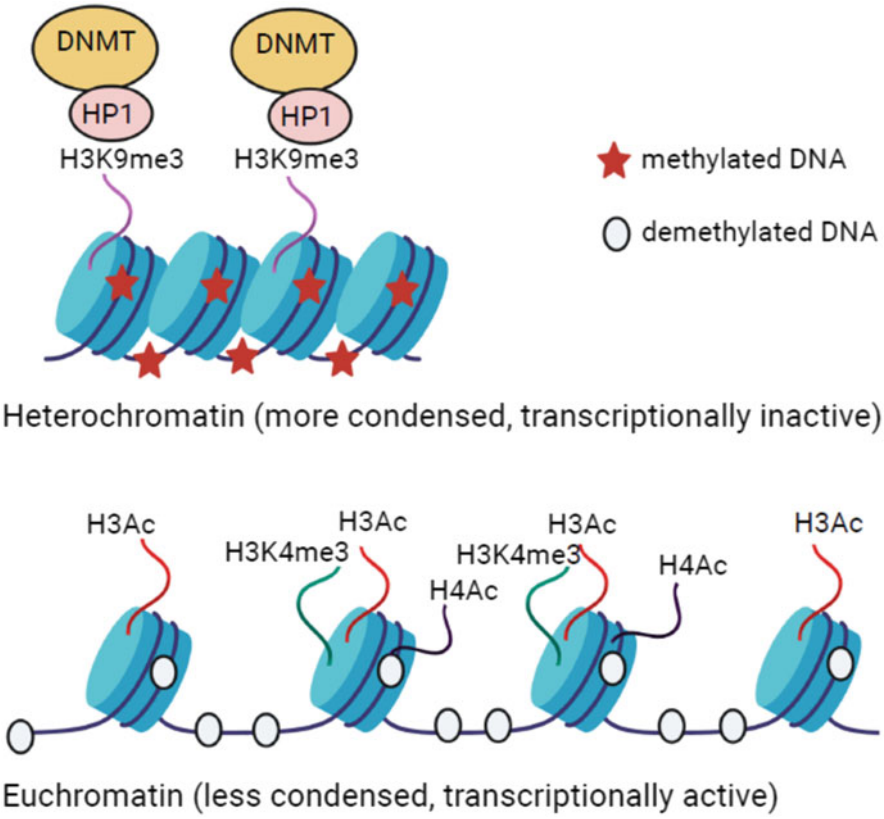

Fig. 1.4 Epigenetic modulation of transcriptional activity of genes related to diabetes

secretion and increased beta-cell apoptosis. In high glucose-exposed rat islets, HDAC7 decreased DNA methylation and increased the expression of diabetic marker gene TCF7L2 to reduce the mitochondrial function of beta-cells in ATP production in response to elevated glucose level and caused reduced insulin secretion. Possibly, HDAC7 increased the activity of HIF1α in mitochondria to reduce the activity of ATP production. Treatment of MC1568, a selective inhibitor of HDACs, restored insulin secretion in HDAC7 overexpressing rat pancreatic beta-cells (Daneshpajooh et al. 2017). It was observed in high-fat diet-fed obese mice, histone modification increased the interactions of chromatins and chromatin remodeling and the expression of stress-specific transcription factors, HNF-4α, C/EBPα, and FOXA1, and their target gene lipin-1 via JAK-STAT signaling pathway in the liver and led to increased hepatogenesis and the development of fatty liver disease (NAFLD) (Leung et al. 2014).

Non-coding microRNAs (miRNAs), having 21–25 nucleotides, represent one of the largest gene families accounting for about 2% of the whole genome and regulate the imprint of >90% of human genes. They function as key post-transcriptional regulatory mediators and are involved in the pathogenesis of a variety of diseases

including obesity and other metabolic diseases. These miRNAs repress the expression of the genes by binding to un-translated regions (such as DNA methylation regions) and coding sequences of the target mRNAs of the genes (Landrier et al. 2019).

Two groups demonstrated that pancreatic islet-specific miR-375 on overexpression in diabetic pancreas inhibited insulin secretion by suppressing the expression and activity of genes, myotrophin, and beta-cell growth regulatory kinase, 3′-phosphoinositide-dependent protein kinase-1 (PDK1), related to glucose-stimulated insulin secretion from beta-cells. PDK-1 increases the phosphorylation of PDX-1 to enhance insulin gene transcription (Poy et al. 2004; El Quaamari et al. 2008). miR-192 has been found in high concentrations in glomeruli of diabetic mice compared to non-diabetic mice. miR-192 was found to increase TGF–βinduced extracellular proteins collagen 1 and 2 expression and accumulation in diabetic glomeruli by the suppression of the activity of E-box repressors (Kato et al. 2007). Another study demonstrates that the expression levels of miR-221 are upregulated in the adipose tissue and liver of obese people. This miR-221 stimulates fat metabolism through the upregulation of the expression of lipogenesis-related genes, FAS, hydroxyacyl-CoA dehydrogenase alpha (HADHA), and aldo-keto reductase gene, AKRI4, via PPAR signaling pathway and downregulation of adiponectin receptor-1 (ADIPOR1). Both leptin and TNF-α suppress the expression of miR-221 in human pre-adipocytes (Meerson et al. 2013). MicroRNA-802 (miR-802) is expressed in high concentrations in the liver of obese mice and humans. Its overexpression in mice liver causes insulin resistance and suppression of insulin action via enhanced expression and activity of the gene, hepatocyte nuclear factor-1 homeobox B (Hnf1b), also known as transcription factor 2 (Tcf2). Moreover, suppression of hepatic Hnf1b downregulates miR-802 expression and increases hepatic insulin sensitivity and reduces hepatic gluconeogenesis (Kornfeld et al. 2013). In the fatty liver of obese humans and mice, the expression levels of miR-34 are upregulated. Its overexpression in the fatty liver of mice reduces the expression of sirtuin-1 (SIRT-1) and increases the expression levels of lipogenic genes, SREBP-1c, FAS, and ACC (Wu et al. 2014). The expression levels of miR-31-5p and miR-31-3p are increased in the adipose tissue of obese humans, and their overexpression reduces the expression levels of genes, IRS-1, GLUT-4, HK-2, and FOXO1, related to insulin-stimulated glucose uptake and utilization (Gottmann et al. 2018). miR-876-3p is expressed in high concentrations in the adipose tissue of obese humans and mice. Its overexpression in human adipocytes, isolated from human mesenchymal stem cells, decreases adiponectin secretion by binding in 3'-UTR site and increases insulin resistance (Rajan et al. 2018).

1.6.6 Effect of Physical Exercise on Epigenetics

Several studies discovered that long-term exercise altered the DNA methylation pattern of genes in the skeletal muscle of obese and type 2 diabetic patients. In men, a 6-month regular exercise altered the level of DNA methylation at numerous CpG

sites in more than 7000 genes throughout the genome. About one-third of the gene regions with absolute methylation changes and a simultaneous change in mRNA expression of the genes were observed. It was reported that after regular exercise for a period of 6 months, an increased DNA methylation and a corresponding decreased mRNA expression of the genes, HDAC4 (histone deacetylase 4) and NCOR2 (nuclear receptor co-receptor 2), were observed. In vitro, these two genes enhanced lipogenesis in adipocytes. These findings suggested that regular exercise might be effective in the prevention of epigenetics-related adipogenesis in obese white adipose tissue (Ronn et al. 2013). Another study reported that a single bout of exercise decreased promoter DNA methylation of metabolic genes, PPARGC1A (encoding PGC1α), PDK4, and PPARD, in human skeletal muscle and increased their activity (Barres et al. 2012).

1.6.7 Environmental Risk Factors of Type 1 Diabetes

A group of studies demonstrates that some environmental factors, such as infections, diet, intestinal microbiome, and drugs/food toxins, trigger the markers of islet autoimmunity to promote the progression of autoimmunity to expose type 1 diabetes. The autoimmunity has been defined as the presence of autoantibodies in pancreatic islet antigens since early childhood, i.e., in pre- and post-natal stages. The birth cohorts of children in European countries indicated that the presence of two or more islet autoantibodies, such as islet cell antibodies (ICA), insulin autoantibodies (IAA), glutamate decarboxylase alpha (GADA), insulinoma-associated 2 antigen antibodies (IA-2A), or zinc transporter 8 A (ZnT8A), promotes the progression to type 1 diabetes among 70% of children diagnosed as type 1 diabetes in a period of 15 years (Ziegler et al. 2013). In addition, hybrid insulin peptides (HIP), known as neo-antigens or neo-epitopes, formed by fusion with an insulin peptide, play an active role in the progression to type 1 diabetes in children. These HIPs are highly antigenic for autoreactive $CD4^+$ T-cells, which play a central role in β-cell destruction (Delong et al. 2016). An intriguing line of evidence indicates that enteroviral infections, particularly coxsackieviruses B3 and A16, during pregnancy may contribute to persistent infection and islet autoimmunity in both mother and offspring, as evident from matched type 1 diabetes-associated HLA-DQB1 genotypes and enterovirus-specific IgM (immunoglobulin) levels (Viskari et al. 2012). Moreover, enteroviral capsid protein VP1 was detected in high concentrations in the islets of type 1 diabetic patients. VP1 on overexpression in the pancreas upregulated the expression of immunodysfunctional marker, protein kinase R (PKR), in β-cells to enhance the apoptosis of β-cells through the inhibition of the activity of anti-apoptotic protein, myeloid cell leukemia sequence-1 (Mcl-1) (Richardson et al. 2013). Birth cohort studies of Finnish children have shown that cow's milk intake in children having HLA-DQB1 susceptibility is associated with an increased risk of islet autoimmunity and in the development of type 1 diabetes. Possibly, the proteins and fatty acids present in cow's milk regulate gut microbiome composition to decrease gut barrier integrity and to lead to the uncontrolled passage of pathogenic bacteria and food antigens into systemic circulation and thereby to activate beta-cell

autoimmunity in pancreatic lymph nodes and tissues for beta-cell damage and in the development of type 1 diabetes (Virtanen et al. 2012). Another study reported that infants of 3 months old, exposed to cow's milk or its relevant formula, have increased levels of IgG antibodies binding to bovine insulin and this immune response is converted into autoaggressive immunity against β-cells of the pancreas and subsequently contributes to the development of type 1 diabetes in infants, while in breastfeeding infants, breast milk having antibodies, immunoglobulin A, enhances the infant's immune response and increases β-cell proliferation and delays the induction of food antigens (Vaarala et al. 1999). Exposure of infant children to cereals, gluten-free (rice cereals) and gluten-containing oats, wheat, barley, or rye cereals, in the age of below 3 months compared to those exposed at 7 months of age has a high risk of islet autoimmunity risk, as evident from serum IA-2A-positive HLA-DRB1*03/04, DQB8 genotypes (Norris et al. 2003). Several studies on the role of breast milk in gut microbiota modulation reported that breastfeeding in infants transferred the maternal microbiota in infants. Specifically in breastfed infants, the bacteria of genera *Bifidobacterium* and *Lactobacillus* are transferred from the mother to child and are capable of breaking down of human milk oligosaccharides and production of short-chain fatty acids (SCFAs). These bacteria have been found to promote mucus production, alleviate diet-induced colonic mucus deterioration, and regulate intestinal immune system by the increased production of immunoglobulin A and β-cell function in the infant's body. Similarly, in virginally delived infants, the bacteria of genera *Bifidobacterium* and *Lactobacillus* were found in high abundances, whereas, in cow's milk-fed infants, low abundances of *Bifidobacterium* (<12%) and high abundance of *Bacteroidetes* are found, and these are directly correlated with increased levels of β-cell autoimmunity (Schroeder et al. 2018; Insel and Knip 2018). In a case-control study in Sweden, type 1 diabetes was found to be associated with children or their parents, who consumed high amounts of foods containing N-nitrosamines and nitrates (e.g., spinach, cabbage, processed meats, salted fish, beer, potatoes, and mushrooms). Possibly, nitrosamines exert toxic effect by the generation of superoxide and H_2O_2, which, in turn, increase lipid peroxidation and pro-inflammatory cytokine production in the pancreas and other tissues to impair insulin secretion and insulin action and thereby to increase insulin resistance. Streptozotocin, a nitrosamine-related compound, has been found to cause insulin resistance-related disorders, such as obesity, type 2 diabetes, and NASH (Dahlquist et al. 1990).

1.6.8 Environmental and Lifestyle Risk Factors of Type 2 Diabetes

Various types of environmental and lifestyle factors promote excessive stress and lead to the progression of T2DM. Long-term unemployment, low income, crime, social disorders, and unsafe neighborhood may incite social isolation and inhibit to do physical activity and promote adverse stress and mental depression. These mental strains accrued from the stress may stimulate the release of steroid hormone cortisol and many inflammatory cytokines, which can damage the immune system and the

normal functioning of the body and accelerate to increase blood sugar levels and the development of T2DM and other stress-related chronic diseases. Moreover, these excessive stresses motivate unhealthy eating, smoking, and drinking that affect sleep and mental health and consequently increase the risk of T2DM (Sunquist et al. 2015). Air pollution and constant road traffic noise adversely affect blood lipid levels and trigger inflammation and insulin resistance, which, in turn, may influence high blood pressure and the development of T2DM. The particulate matters and nitrogen oxides (NO_X) present in polluted air in high levels adversely affect the lungs and increase the expression levels of inflammatory cytokines that result in impaired glucose metabolism. Moreover, road traffic noise at night disturbs sound sleep and results in slow-wave sleep, which inhibits cortisol secretion and reduces insulin sensitivity. Slow-wave sleep elevates ghrelin levels resulting in the upregulation of appetite, which, in turn, increases BMI and the risk of obesity and T2DM (Sorensen et al. 2013; Teichert et al. 2013).

1.7 Diet and Physical Exercise in the Treatment of Obesity and Diabetes

The main cause of obesity is an imbalance between calories intake and calories expended. Therefore, maintenance of calorie restriction in dieting and physical exercise may be effective in weight loss for overweight and obese patients (Fock and Khoo 2013). The calorie-restriction strategies are one of the most dietary plans in the management of obesity and diabetes. A balanced healthy diet having low fat content and high protein and fiber-rich carbohydrates, antioxidant phytochemicals, vitamins, and minerals provides a calorie-restricted diet to overweight and obese patients. The dietary items include whole grains such as whole wheat, brown rice, and oats; whole fruits such as apples, oranges, and grapes; and different vegetables and legumes. Whole grains and fruits are rich in dietary fibers that promote satiation and satiety, prolong gastric emptying time, slow nutrient absorption, and affect gut hormone secretion and insulin action. Usually, a low-calorie diet (LCD) having a total dietary calorie intake of 800–1500 kcal/d is recommended for overweight and class I obese patients, whereas a very-low-calorie diet (VLCD) having a total dietary calorie intake of 800 or less kcal/d is recommended for class II and III obese patients. The dietary items need to be balanced in carbohydrate, protein, fat, antioxidant phytochemical, vitamin, and mineral content (NIH 1998). A meta-analysis of 16 trials in overweight and obese patients having low fat containing LCD with different whole grains, fruits, and vegetables in dietary items for a period of 2 to12 months showed a significant reduction in body weight gain (up to 3.2 kg), serum glucose, TG and LDL levels, and blood pressure and improved cardiovascular risk factors. However, its long-term use has adverse effects (Astrup et al. 2000).

Physical exercise is another plan for achieving weight loss in obesity. A meta-analysis showed that exercise alone exhibited very small weight loss. However, people who used both diet restriction and physical exercise rewarded better weight loss than those who relied on diet or exercise alone (Miller et al. 1997). A meta-analysis reported that an application of both calorie restriction and exercise for a

period of 6 months improved weight loss of 5–8.5 kg. Before starting of an exercise program, the patients should consult their physicians to get an advice on the types of exercises and its duration that will be more effective in weight loss. As per the recommendation of the American College of Sports Medicine, at least 200–300 min/week of moderate-intensity aerobic exercise, such as 60 min brisk-walking or bicycling or running or 35 min jogging per day for obese men and household food preparation, dish-washing, and laundry work for obese women, is required in preventing weight gain and in improving cardiovascular fitness and obesity-related health complications (Donelly et al. 2009). Available evidence demonstrates that exercise reduces food intake by increasing satiating efficiency in a meal. It also increases insulin sensitivity in peripheral tissues (King et al. 2009). For type 2 diabetic patients, adults >18 years old, an exercise of moderate intensity for at least 150 min/week such as walking for a 15–20 min in mile pace or vigorous physical activity for 75 min/week (namely, running, aerobics walking spread over in 3 days/week) is recommended. For patients <18 years old, a moderate physical activity of 60 min/day is adequate (American Diabetes Association 2016).

1.8 Impact of Gut Microbiota Dysbiosis on Obesity and Its Related Morbidities

Trillions of microorganisms including bacteria, viruses, fungi, and archaea inhabit in the human body, strongly colonizing the gastrointestinal (GI) tract maintaining a symbiotic relationship and outnumbering our own cells. Many of these guest gut microbiota play a significant role in the degradation of indigestible components of our diet, harvesting of energy and nutrients from diet, shaping of our immune system, and maintenance of integrity of gut mucosal barrier for the prevention of the entry of endotoxin-producing pathogens and metabolic functions of our body (Sonnenburg and Backhed 2016; Hooper et al. 2012). The commensal bacteria *Clostridium* clusters IV and XIVa and *Bacteroides fragilis* in the human gut improve immunity in the gut endothelium and systemic circulation of the host by the induction of induced T-regulatory (iTreg) cells to increase systemic anti-inflammatory potential via the upregulation of anti-inflammatory cytokine IL-10 for the prevention of autoimmune diseases (Hooper et al. 2012). An evolutionary pressure exerted by changes in lifestyle-related environmental and dietary effects of human beings, such as excessive sanitation, industrialized and abundant diet habits, sedentarism, and excessive antibiotic intake, resulted in the disruption of ecological harmony among the gut microbiota, thereby causing a dysbiosis of gut microbiota. As a consequence, this imbalanced or dysbiotic gut microbiota in modern civilized man is strongly associated with several complex diseases including obesity and its related morbidities. A group of metagenomic studies on gut microbial communities in humans using amplicon sequencing of 16S rDNA marker genes and whole metagenome shortgun (WMS) sequencing coupled with “multi-omics” data analysis revealed that an imbalance in relative abundance of some health-benefit bacterial families in gut microbial community plays a significant role in the pathogenesis of

obesity and its related type 2 diabetes and other vascular complications. A metagenome-wide association study (MGWAS) by DNA sequencing analysis of gut microbiota composition from Chinese diabetic patients identified about 60,000 type 2 diabetes-related marker genes and characterized a moderate degree of microbial dysbiosis from the low abundance of butyrate-producing bacteria and an increase level of various opportunistic pathogens and other bacteria related to sulfate reduction and oxidative stress production. A comparative study of distal gut microbiota of genetically obese mice and their lean littermates, as well as those of obese and lean humans, has revealed that obesity is associated with changes in the relative abundance of two bacterial divisions in phyla, *Firmicutes* and *Bacteroidetes*. In obesity, a division-wise increase in relative abundance of *Firmicutes* and a corresponding division-wise decrease of relative abundance of *Bacteroidetes* are found in the gut. An obese microbiome has an increased capacity to harvest energy from Western-type high-fat-rich diet due to the presence of some mollicutes, namely, *Eubacterium dolichum*, belonging to *Firmicutes* in a relative high abundance. *E. dolichum* is efficient in the fermentation of mono-, di-, and oligosaccharides present in Western diet to harvest energy as lactate and short-chain fatty acid (SCFA) end products (Turnbaugh et al. 2008). *Firmicutes* are distributed over four classes: *Bacilli*, *Clostridia*, *Erysipelotrichia*, and *Negativicutes*. In *Bacilli* class, the spp. of genera *Lactobacillus*, *Enterococcus*, and *Streptococcus* have a significant role in metabolic disorders. *Ruminococcaceae* and *Lachnospiraceae* are the important family members of *Clostridia*. Several spp. of *Lachnospiraceae*, such as *Anaerostipes* spp., *Butyrivibrio* spp., *Coprococcus* spp., *Roseburia* spp., and *Eubacterium* spp., are butyrate producers and have beneficial effects in glucose metabolism and are found in low levels in both type 1 and 2 diabetic patients (Qin et al. 2012). Several members of *Bacteroidetes* belonging to families *Bacteroidaceae*, *Prevotellaceae*, *Rikenellaceae*, and *Porphyromonadaceae* produce lactate, acetate, butyrate, and propionate as end products. Less abundance of some of these bacterial species in the gut was associated with adiposity, insulin resistance, dyslipidemia, and inflammatory phenotypes in obese and type 2 diabetic patients (Le Chatelier et al. 2013). A metagenome study on the gut microbiome of Swedish type 2 diabetic women indicated that the presence of butyrate-producing *Clostridia* class *Roseburia* and *Faecalibacterium prausnitzii* bacteria was found in less abundance compared to non-diabetic subjects (Karlsson et al. 2013). Another study on gut microbiota of pre-school normal and obese children revealed that the gram-negative bacterium *Akkermansia muciniphila* of *Verrucomicrobia* phylum was identified at low abundance in the gut of obese children (Karlsson et al. 2012). *A. muciniphila* has been found to reduce fat mass and metabolic endotoxemia by the secretion of endocannabinoids for the improvement of insulin sensitivity in obese adipose tissue and suppression of adipogenesis. Moreover, it suppressed the hepatic gluconeogenesis by decreasing the activity of gluconeogenic enzyme G6Pase (Everard et al. 2013). Several bacterial spp. of the genus *Bifidobacterium* have been identified in the gut and are found to improve insulin resistance and inflammation in obesity and diabetes through the improvement of gut barrier function. A significant relatively low abundance of *Lactobacillus* and *Bifidobacterium* was identified in the gut of

children with type 1 diabetes (Cani et al. 2009). An opportunist pathogen *Enterobacter cloacae*, a producer of endotoxin lipopolysaccharide (LPS), has been isolated from the gut of obese humans at relatively high levels. LPS was found to induce insulin resistance by increasing the expression of inflammatory factors, TNF-α, IL-β, IL-6, and TLR-4 (Fei and Zhao 2013). Therefore, manipulation of dysbiosis in gut microbiota by the use of prebiotic and probiotic dietary supplements is a promising approach for the treatment of obesity and its associated morbidities such as hyperglycemia, hypertension, dyslipidemia, atherosclerosis, and cardiovascular, ocular, and renal disorders (Anhe et al. 2015).

A large group of evidence demonstrates that short-chain fatty acids (SCFAs) are the main microbial end products from the bacterial fermentation of undigested diet containing complex polysaccharides, oligosaccharides, proteins, peptides, and glycoproteins in murine and human large intestine. In addition, some branched-chain fatty acids (BCFAs) and branched-chain amino acids (BCAAs) are also formed as side products. The major SCFAs derived from carbohydrates and proteins are acetate, propionate, and butyrate, while valerate, formate, and caproate are formed at a low extent (Macfarlane and Macfarlane 2003; Cummings and Macfarlane 1991). Obese humans and genetically obese mice have been found to excrete more SCFAs in the feces than that of lean subjects. These findings suggest that obese gut microbiota harvest more energy from diet through increased SCFA production and contribute to obese phenotype. It also demonstrates that high levels of SCFAs in feces may be due to decreased SCFA absorption and utilization (Fernandes et al. 2014; den Besten et al. 2013). Another study reported that SCFAs on diet supplementation in obese mice decreased body weight gain by preventing fat accumulation through enhanced energy metabolism in the skeletal muscle, gut barrier integrity, and anti-inflammatory responses in various metabolic tissues (Cox and Blaser 2013). SCFAs inhibited insulin-stimulated fat accumulation in adipose tissue of HFD-fed obese mice by the activation of short-chain fatty acid receptor, G-protein-coupled receptor GPR43, to suppress insulin signaling through decreasing Akt phosphorylation levels via promoting phosphorylation levels of PTEN (phosphatase and tensin homolog), a negative regulator of insulin/PI3K signaling. Moreover, activated GPR43 promote energy expenditure in muscle by increasing the expression of mitochondrial biogenesis and function-related genes PGC-1α, HK1/2, PKM2, CPT1B, and CPT2, to increase glycolysis and fatty acid beta-oxidation, and decreasing the expression of gluconeogenesis-related gene PEPCK in the liver. GPR43-deficient mice were found to be obese on a normal diet, whereas HFD-fed obese mice overexpressing GPR43 in adipose tissue remained lean (Kimura et al. 2013). Butyrate was found to increase mitochondrial function and biogenesis in the skeletal muscle and brown fat in obese mice by the upregulation of PGC-1α and increased the phosphorylation levels of AMPK and p38 proteins. In the liver of obese mice, it increased the insulin sensitivity by increasing the phosphorylation of Akt and IRS 1 proteins (Gao et al. 2009b). Another study reported that butyrate, propionate, and acetate protected against HFD-induced obesity and insulin resistance in obese mice. But, only butyrate and propionate induced the secretion of gut hormones, glucagon-like peptide-1 (GLP-1) and glucose-

dependent insulinotropic polypeptide (GIP), in a free fatty acid receptor 3 (FFAR3)-dependent and FFAR3-independent pathways and reduced food intake via the stimulation of the secretion of food-suppressing hormone, neuropeptide YY (NYY), from colonic L-cells in obese mice. Moreover, these SCFAs reduced plasma glucose, leptin, and insulin levels in obese mice. These effects of SCFAs were not altered significantly in FFAR3-deficient mice (Lin et al. 2012). Butyrate promoted intestinal gluconeogenesis (IGN) by the activation of GLP-1 through a cAMP-dependent pathway, while propionate activated IGN gene expression via a gut-brain neural circuit involving its receptor FFAR3 for body weight and glucose control in obesity (De Vadder et al. 2014). Butyrate also maintained intestinal epithelium integrity and decreased intestinal inflammatory macrophage nitric oxide (NO), IL-6, and IL-12 production via the inhibition of histone deacetylase activity (Bosi et al. 2006; Chang et al. 2014).

Serum branched-chain amino acids (BCAAs) such as valine (Val), leucine (Leu), and isoleucine (Ile) have been found to be in high concentrations in obese and diabetic humans, suggesting their contributions to the development of obesity-related insulin resistance, and are considered as a biopredictor for diabetes. Moreover, reduced serum BCAA levels are strongly correlated to increased insulin sensitivity and decreased body weight gain in obese humans. The reduced BCAAs are due to increased mitochondrial energy metabolism via their conversion into acetyl- and succinyl-CoAs (Newgard et al. 2009; Shah et al. 2012).

Several experimental studies demonstrate that obese gut microbiome is a transmissible trait from parents to offspring. It has been shown that in the marriage of gnotobiotic mouse models, transplanting both uncultured and cultured gut microbiota from human adult of opposite twin pairs, obese and lean, into germ-free mice transmitted the obesity-associated phenotype (increased body weight and fat mass) in mice receiving obese gut microbiota. In contrast, co-housing mice having an obese twin's microbiota with mice containing the lean twin's microbiota and provided high-fat diet, prevented the body weight gain and obesity-associated metabolic phenotypes (insulin resistance and levels of SCFA-producing bacteria in the gut) in obese cagemate mice. These findings suggested that gut microbiota configurations were transmissible and were influenced by an early environmental exposure and were more similar among the family members. In addition, gut microbiota was modified through diet and microbiota interactions (Ridaura et al. 2013; Turnbaugh et al. 2008). Another case report study indicated that transplantation of fecal microbiota to a non-obese woman for the treatment of *Clostridium difficile* infection from the stool of her healthy overweight daughter (BMI of 26.4 kg/m^2) developed new onset of obesity (Alang and Kelly 2015). The composition and development of infants's gut microbiota are influenced by BMI and weight gain of mothers during pregnancy. Higher BMI and weight gain of pregnant mothers are related to the presence of high abundance of *Bacteroides-Prevotella* spp., *Clostridium histolyticum*, and *Staphylococcus aureus* and low abundance of *Bifidobacterium* spp. in the feces of 6-month-old infants, whereas the presence of high abundance of *Bifidobacterium* spp. was identified in the feces of infants of the

same age from normal-weight mothers. These findings also suggested that high abundance of *Firmicutes* is correlated to obesity (Collado et al. 2010).

1.9 Currently Available Pharmacotherapy of Obesity

The National Institute for Health and Care Excellence (NICE) currently recommends pharmacological treatment in addition to dietary calorie restriction and optimal physical exercise for weight loss maintenance within a short period for obese diabetic patients. This pharmacotherapy has several risk factors on long-term use. The most common recommended drugs are orlistat, liraglutide, lorcaserin, and drug combinations, naltrexone/bupropion and phentermine/topiramate. In addition, many anti-obesity drug candidates are currently in clinical phase trials for obesity management (Budai et al. 2015).

Orlistat **46a**, an intestinal gastric and pancreatic lipase inhibitor, is the only recommended drug for long-term use in body weight reduction for overweight and obese diabetic patients in the USA. In a randomized, double-blind, placebo-controlled clinical trial, treatment of orlistat (120 mg, three times a day) or placebo, combined with a restricted low-fat diet in overweight and obese adults (BMI >28 kg/m^2) with type 2 diabetes and taking insulin or other oral drugs, related to glycemic control, for a period of 1 year, showed a weight loss of 3.89 kg versus 1.27 kg in placebo-controlled group. Moreover, orlistat treatment showed better improvement in the levels of serum glucose, HbA1c, TC, LDL-C, and LDL/HDL ratio compared to placebo group (Kelley et al. 2002). Another meta-analysis of orlistat therapy in obese patients showed that orlistat also improved the blood pressure of the patients. Orlistat prevented the absorption of dietary ingested fats (about 32%), which are excreted in the feces. Its long-term use results in adverse effects in patients including fecal urgency and incontinence, oily stool, abdominal cramps, increased flatulence, liver and kidney injury, and deposition of calcium oxalate crystals in tubular lumen (Singh et al. 2007; Sumithran and Proietto 2014; Sahebkar et al. 2017).

Liraglutide, a glucagon-like peptide-1 (GLP-1) receptor agonist, was recommended for weight loss in obese diabetic patients. Long-term treatment of liraglutide (3 mg daily) in obese type 2 diabetic patients for a period of 2 years showed an average reduction of weight of 7.8 kg and reduction of plasma glucose, HbA1c, TG and TC levels, and blood pressure (Astrup et al. 2012). A clinical trial by LEADER group reported that liraglutide on long-term treatment (42–60 months) at a lower dose (1.8 mg/d) in obese type 2 diabetic patients reduced major cardiovascular risk factors, such as myocardial infarction and stroke by the reduction of serum glucose and TG levels, but showed less effect in weight loss. The common side effects, such as gastrointestinal disorders, hypoglycemia, diabetic foot ulcer, gallstone, and pancreatitis, are found in some liraglutide-treated patients (Marso et al. 2016). Another study reported that long-term treatment (16 weeks) of liraglutide at the lower dose (1.8 mg/d) in type 2 diabetic patients improved hyperglycemia and hypertriglyceridemia in diabetic patients by the reduction of serum glucose, HbA1c,

TG, chylomicrons, and VLDL levels and suppression of postprandial apoCIII expression levels. Possibly, suppression of postprandial lipid profile improves cardiometabolic risk factors in diabetic patients (Matikainen et al. 2019).

A combination of naltrexone and bupropion was recommended by NICE as weight loss medication in addition to diet restriction and physical exercise to obese patients with BMI >30 kg/m^2 and in the presence of at least one weight-related comorbidity as a second choice for obesity management. Naltrexone is an opioid antagonist, whereas bupropion is an anti-convulsant drug. In a randomized, double-blind clinical trial, treatment of naltrexone-bupropion combination at an initial dose of 8 mg naltrexone plus 90 mg bupropion to a final dose of 32 mg naltrexone plus 360 mg bupropion per day in overweight and obese patients ($n = 9340$) for 56 weeks showed reduced food intake, a weight loss of 5% or more, and slight increased blood pressure in patients. Only half of the participants completed the treatment because of adverse side effects including nausea, headaches, dizziness, vomiting, and constipation during the treatment period (Greenway et al. 2010; Nissen et al. 2016).

A combination of phentermine and topiramate is recommended in obesity treatment for obese patients having BMI >27 kg/m^2 and at least one weight-related morbidity (e.g., hypertension, diabetes, or dyslipidemia) along with reduced dietary calorie intake and physical exercise. It is recommended to obese patients, who cannot tolerate liraglutide or orlistat and have binge eating disorder. Phentermine, an antagonist of α-adrenergic receptor, acts as an appetite suppressant through the regulation of serum leptin levels. Topiramate, an anti-convulsant drug, enhances the activity of GABA for lipid metabolism. Three groups, EQUIP, CONQUER, and SEQUEL, reported that treatment of this drug combination at a daily dose of 7.5 mg phentermine plus 46 mg controlled-release topiramate (7.5/46) or 15 mg phentermine plus 92 mg CR topiramate (15/92) in obese diabetic patients for a period of 56 weeks reduced the body weight by 9.3% or 10.5%, respectively, as well as improved serum BG, TG, TC, and LDL-C levels, blood pressure, and waist circumference in obese patients. The higher dose achieved a mean weight loss of 9.6 kg versus 2.1 kg in the placebo group after 108 weeks of treatment. The common side effects such as dry mouth, paresthesia, upper respiratory tract infection, back pain, dysgeusia, insomnia, constipation, and dizziness were reported by some patients (Allison et al. 2012; Garvey et al. 2012; Gadde et al. 2011).

Lorcaserin, a serotonin receptor agonist, was recommended for weight loss in pre-diabetic obese patients. It acts as an appetite suppressant and results in weight loss of 5.8 kg at a dose of 10 mg/twice daily on the treatment in obese type 2 diabetic patients for a period of 52 weeks. In addition, it reduces the cardiovascular risk markers, such as hypertension and serum fasting glucose, HbA1c, LDL-C, and C-reactive protein (CRP) levels, in obese patients. Several side effects including headache, upper respiratory tract infection, hypoglycemia, nausea, dizziness, and fatigue were observed during the treatment period (O'Neil et al. 2012). This drug has been withdrawn from the market in February 2020, by FDA after receiving a safety clinical trial data from about 12,000 patients that it showed an increase occurrence of various types of cancers compared to placebo group (7.7 versus 7.1% of patients),

the most common being pancreatic, colorectal, and lung cancers (Sombra and Anastasopoulou 2020).

1.10 Currently Available Pharmacotherapy of Diabetes

Algorithms for the treatment of type 2 diabetes highlight the need for a long-term glycemic control to reduce the risk of the development of diabetic complications, such as cardiovascular, renal, retinal, and neural disorders, in diabetic patients. To achieve good metabolic and glycemic controls, a combination of lifestyle changes, such as restricted low-calorie diet, physical activity and exercise, and sound long sleep at night (at least 7 h per night), and pharmacological treatment are prescribed by the concerned physicians of diabetic patients. The choice of oral antidiabetic and other injectable antidiabetic drugs in the pharmacological treatment of a diabetic patient depends on the clinical diagnosis of fasting and postprandial plasma glucose levels, plasma lipid profile and glycated hemoglobin levels, blood pressure, and other morbidities of the patient. A recent position statement by the American Diabetes Association (ADA) and the European Association for the Study of Diabetes (EASD) recommends that a patient-centered approach should be considered by the physicians for the treatment of type 2 diabetic patients. Pharmacological treatments are generally initiated along with dietary restriction and physical exercise, when the plasma HbA1c levels are 6.5% or above. If the plasma HbA1c levels of diabetic patients are 7.0% or above, a combination therapy with two or three oral antidiabetic drugs are prescribed to diabetic patients. Moreover, if the initial plasma HbA1c levels are 10.0% or above and plasma glucose levels are 300 mg/dl or above in diabetic patients, both oral antidiabetic drugs and injectable antidiabetic agents are prescribed. Several commonly used classic oral antidiabetic medications, such as biguanidines, sulfonylureas, glinides or meglitinides, thiazolidinediones (TZDs), dipeptidyl peptidase-4 inhibitors (DPP-4is), alpha-glucosidase inhibitors, and sodium-glucose co-transporter-2 inhibitors (SGLT-2is), and injectable antidiabetic agents such as receptor agonist of glucagon-like peptide-1 (RA-GLP-1) and insulins are available in the market. Some rarely used non-classic drugs, such as colesevelam, bromocriptine, and pramlintide, are also prescribed to diabetic patients, in addition to the commonly used drugs (Kahn et al. 2014; Inzucchi et al. 2015; Marin-Penalver et al. 2016).

Metformin **46b** (Fig. 4.1), a biguanidine, is prescribed as monotherapy for type 2 diabetic patients in the absence of any contraindications and prescribed in combination with other oral drugs in the presence of any contraindications. It activates mucosal AMPK to maintain integrity of intestinal epithelium barrier and reduces the levels of toxic LPS in the circulation and liver. Moreover, it inhibits the hepatic gluconeogenesis by enhanced LKB1-mediated AMPK activation and suppression of glycerol 3-phosphate dehydrogenase (GPDH) production in the liver. It decreases the serum fasting glucose level by about 20% and serum HbA1c level by 1.5%. It also reduces serum levels of FFAs and TG. Its major adverse effect is renal impairment. Hence, it is not prescribed to diabetic patients having serum creatinine

levels above 1.4 mg/dl and eGFR below 45 ml/min (Shin et al. 2014; Lalau et al. 2015; An and He 2016; Song 2016).

Sulfonylureas and glinides are second-line oral therapy for type 2 diabetic patients. These drugs stimulate pancreatic beta-cells to increase insulin secretion. The most commonly used second-generation sulfonylureas are glyburide (known as glibenclamide in Europe) **51a**, glipizide, gliclazide, and glimepiride (amaryl) **51b** (Fig. 4.1). These are the most cost-effective (low-cost) glucose-lowering drugs, particularly in the reduction of fasting blood glucose levels, and are widely utilized for their long-term efficacy and safety. Their long-term use results in hypoglycemia in many patients. Moreover, long-term use is associated with beta-cell apoptosis and in the development of type 1 diabetes (Krentz and Bailey 2005; Takahashi et al. 2007).

Glinides antidiabetic drugs, such as repaglinide **73b** (Fig. 4.1) and nateglinide, are prescribed along with metformin for the reduction of postprandial blood glucose levels in type 2 diabetic patients. These drugs are highly suitable for diabetic patients, who have irregular meal schedules. Their long-term use reduces their effectiveness on islet stimulation and results in beta-cell loss (Takahashi et al. 2007). In the consensus of ADA/EASD 2015, sulfonylureas and glinides are the alternative option to metformin, when metformin is not tolerated by the diabetic patients, whereas the American Association of Clinical Endocrinologists (AACE) in 2016 recommends that these sulfonylureas and glinides are the last alternative in both monotherapy and dual/triple therapy (Inzucchi et al. 2015; Garber et al. 2016).

Two thiazolidinediones (TZDs), namely, rosiglitazone **73a** (Fig. 4.1) and pioglitazone, are currently available in the USA. These drugs increase insulin sensitivity in the muscle, adipose tissue, and liver to improve glucose utilization and to decrease hepatic glucose production through the action of PPAR genes. Rosiglitazone is a purely PPAR-γ agonist, and PPAR-γ activation in CNS stimulates feeding and increases body weight gain; pioglitazone has both PPAR-γ and PPAR-α agonistic activity and improves lipid profile by the reduction of serum TG level. Rosiglitazone treatment in diabetic patients causes peripheral edema among 4–6% of patients and is the risk factor of heart failure in some patients. Hence, it was withdrawn from the market since 2010 in Europe as per recommendation by the European Medicines Agency. Pioglitazone has been shown to increase bladder cancer (14 versus 5) in the treatment group. It was also withdrawn from the market of Europe since 2011 as per recommendations of German and French Medicines Agencies (Nesto et al. 2003; Lewis et al. 2011; Schernthaner et al. 2013; Marin-Penalver et al. 2016).

DPP-4 inhibitors and alpha-glucosidase inhibitors mainly act on the gastrointestinal tract for the reduction of plasma glucose levels in type 2 diabetic patients. Five DPP-4 inhibitors, namely, sitagliptin, vildagliptin, saxagliptin, linagliptin, and alogliptin, are prescribed in many countries for the treatment of type 2 diabetes as single therapy or dual/triple therapy with metformin and sulfonylureas. These drugs increase incretins GLP-1 and GIP secretion from the intestinal L-cells and increase glucose-stimulated insulin secretion and inhibit postprandial glucagon response. These DPP-4 inhibitors significantly improve fasting blood glucose levels compared

to placebo group. Most common side effects include headache, nasopharyngitis, and upper respiratory tract infection. Sitagliptin also exhibits the risk of gastrointestinal infection (severe abdominal pain) and heart failure. These drugs should be discontinued, if the patients feel persistent abdominal pain during the treatment period (Goossen and Graber 2012; Bhatt and Cavender 2014).

Alpha-glucosidase inhibitors, namely, acarbose, miglitol, and voglibose, are prescribed to use just before meals for the reduction of postprandial hyperglycemia in diabetic patients having modest hyperglycemia. These drugs inhibit the activity of alpha-glucosidase in the small intestine in the hydrolysis of dietary carbohydrates. Elderly patients most often face diarrhea and flatulence during the treatment period (Johnston et al. 1998).

Three SGLT-2 inhibitors, namely, canagliflozin **174**, dapagliflozin **175**, and empagliflozin **176**, are used as antidiabetic agents for the treatment of hyperglycemia in type 2 diabetic patients. These drugs reduce both fasting and postprandial hyperglycemia by the reduction of renal glucose absorption in the proximal convoluted tubule by SGLT-2 enzyme in an insulin-independent mechanism. These drugs have been found to reduce body weight and blood pressure and improve beta-cell function, when used as monotherapy. Only canagliflozin has been shown to reduce serum TG levels and to increase serum HDL levels in diabetic patients. Major adverse effects, such as urinary tract infections and hypoglycemia, on long-term use of these drugs have been reported (Burki 2012; Riser Taylor and Harris 2013; Nisly et al. 2013).

Injectable GLP-1 receptor agonists (RA-GLP-1), namely, short-acting exenatide and lixisenatide and long-acting liraglutide, albiglutide, dulaglutide, and semaglutide, are frequently prescribed for the reduction of hyperglycemia in obese diabetic patients as an alternative to metformin. These drugs reduce plasma glucose levels through the stimulation of insulin secretion from pancreatic beta-cells, reduction of glucagon secretion, delaying gastric emptying, and increasing satiety. These drugs also contribute to weight loss through the reduction of food intake and promote both beta-cell regeneration and function. The common adverse effects of these drugs include hypoglycemia, acute pancreatitis, and gastrointestinal problems, such as nausea and vomiting (Gallwitz 2011; Nauck and Friedrich 2013).

Bromocriptine, an ergot derivative and a dopamine-2 receptor agonist, mainly acting in the brain, and traditionally used for the treatment of Parkinson's disease, is prescribed in type 2 diabetic patients for the treatment of hyperglycemia and dyslipidemia. Its exact mode of action is still unknown. However, it is believed that it reduces postprandial plasma glucose and hepatic glucose production through an increase of hypothalamic dopamine levels and inhibition of excess sympathetic tone in CNS via the inhibition of serotonin turnover and promotion of circadian neuroendocrine rhythms in early morning. It reduces the risk of cardiovascular disorders via the amelioration of serum lipid profile and hypertension. Some adverse effects, such as nausea, headache, vomiting, sleepiness, and hypoesthesia, are frequently reported by bromocriptine-treated patients. Detailed data on safety and efficacy on long-term use of this drug is not available (Scranton and Cincotta 2010; De Fronzo 2011; Gaziano et al. 2012).

Colesevelam, a bile acid binding resin primarily used for the treatment of hypercholesterolemia, is prescribed for the treatment of hyperglycemia and hypercholesterolemia in type 2 diabetic patients in combination with sulfonylureas. It reduces plasma and hepatic cholesterol levels through the activation of farnesoid X receptors (FXRs) in the liver and reduces both fasting and postprandial serum glucose concentrations by increasing insulin secretion in TGR5 signaling pathway. It also reduces the meal size by decreasing intestinal glucose absorption. This drug has been reported to increase serum TG level, and hence it increases the risk factor of cardiovascular diseases in hypertriglyceridemic patients. Another common adverse effect is constipation (Fonseca et al. 2008; Marina et al. 2012; Smushkin et al. 2013).

Pramlintide, an amylin analog mainly acting on the gastrointestinal tract, is prescribed for the treatment of hyperglycemia in type 2 diabetic patients. It slows gastric emptying, reduces postprandial glucagon release, promotes satiety, and delays intestinal glucose absorption from dietary carbohydrates (Ceriello et al. 2008; Younk et al. 2011).

Insulin therapy is prescribed for the treatment of hyperglycemia in both type 1 and severe type 2 diabetic patients. Human insulin and synthetic insulin analogs are utilized as injectable drugs, when oral drugs fail to reduce serum glucose concentrations in diabetic patients with high HbA1c levels (9% or above) and basal insulin levels are not enough. Different types of branded insulins, such as rapid- and short-acting insulins (regular insulin, insulin aspart, insulin glulisine, insulin lispro, insulin semilente), intermediate-acting insulins (NPH insulin, insulin lente), long-acting insulins (insulin detemir, insulin glargine), and ultra-long-acting insulins (insulin ultralente, insulin degludec, glargine U 300), are available in the global market. These insulins have flexibility in action and efficacy in diabetes management. Rapid- and short-acting insulins have shorter duration of action (10 min–4 h) and are mainly used before meals for meal coverage, while intermediate-acting insulins have action time up to 16 h, and long-acting analogs have longer duration of action, 24–36 h, and are used once in a day. Ultra-long-acting analogs have much longer duration of action compared with long-acting insulins, glargine and detemir. For example, insulin degludec has a greater half-life, more than 25 h, and acts more than 42 h and results in nocturnal hypoglycemias in many cases (Raccah 2008; Chen et al. 2008; Sanches et al. 2011; Ratner et al. 2013; Owens et al. 2014; Hollander et al. 2015).

1.11 Vascular Complications of Diabetes

Chronic diabetes is associated with a risk factor of several vascular diseases, including macrovascular cardiovascular diseases and microvascular diabetic nephropathy (DN), diabetic retinopathy (DR), and diabetic peripheral neuropathy (DPN). Among these vascular complications, DN and DR are the largest contributors of end-stage renal disease (ESRD) and blindness, respectively. In the USA, diabetes accounts for 30% to 50% of the incident cases of ESRD (Umanath and Lewis 2018). DR is common in both type 1 and type 2 diabetic patients. As per

the estimate of IDF, in 2015, the prevalence of DR and sight-threating (ST)-DR in the USA from type 1 diabetes was 36.5% to 93.6% and 6.7% to 34.9%, respectively, and from type 2 diabetes, 28.5% to 40.3% and 4.4% to 8.2%, respectively (Lee et al. 2015). Cardiovascular diseases (CVDs) are the prevalent causes of mortality and morbidity in diabetic patients. An estimate of WHO indicated that 17.9 million people died from cardiovascular diseases in 2016, representing 31% of global death. Moreover, 85% of these deaths were from heart attack and stroke (WHO 2017). All these vascular complications have similar etiologic characteristics, such as endothelial dysfunction from atherosclerosis in blood vessels (Rask-Madsen and King 2013).

Diabetic Nephropathy (DN)

Diabetic nephropathy (DN), a kidney disease, is characterized by microalbuminuria (increased albumin levels in urine), hematuria (blood in urine), increased serum levels of BUN and creatinine, and decreased urine volume from reduced glomerular filtration rate (GFR). Studies on the molecular mechanism of the disease demonstrate that insulin resistance in diabetic kidney increases de novo diacylglycerol (DAG) synthesis and AGE formation and accumulation and activation of protein kinase C (PKC) by the enhanced production of PGE2. PKC on activation increases the production of ROS from NADPH oxidase, the expression levels of endothelin 1 (ET-1), a biomarker of vasoconstriction and angiotensin II (Ang II) via AGE-RAGE-stimulated activation of rennin-angiotensin system (RAS) and subsequently reduces the expression of iNOS in glomeruli, which in turn reduces GFR. ET-1, a vasoconstrictor peptide, reduces the activity of iNOS in glomerular endothelium in NO production and thus decreases the vasodilation property. Moreover, it also enhances podocyte injury, mesangial proliferation, and matrix accumulation. Renin on overexpression converts angiotensinogen into angiotensin-1 (AT-1), which is converted into Ang II by angiotensin-converting enzyme (ACE). Ang II on binding to its receptor AT1 stimulates the expression of TGF-β1, CTGF, VEGF, and MCP-1 and activity of NF-κB for the expression of collagen types IV and VI, fibronectin, and other proteins and their accumulation as extracellular matrix (ECM) materials in glomerular basement membrane (fibrosis) and apoptosis of podocytes for the progression of glomerulosclerosis and DN. Therefore, ACE inhibitors and AT1 receptor blockers are considered as important therapeutic targets for the treatment of diabetic kidney disease (DKD) and DN (Noh and King 2007; Kanwar et al. 2011).

Diabetic Retinopathy (DR)

DR is the most common microvascular complication of diabetes in the eyes. Its development in type 2 diabetic patients is related to both severity of hyperglycemia and hypertension. Several factors such as high levels of aldose reductase and growth factors including VEGF and TGF-β have been postulated to play important roles in the pathogenesis of the disease in the diabetic retinas. DR is generally classified as either background (non-proliferative) or proliferative. Background retinopathy is characterized by small hemorrhages in the middle layers of the retina as red dots and

lipid deposition as hard exudates at the margins of the hemorrhages. Several microaneurysms (balloon-like sacs in vascular vessel walls) occur in the retinas. These microaneurysms in the retina are formed by microvascular leakage of the blood-retinal barrier membrane function due to local inside pressure. About 20% of reported eye diseases with macular edema have been reported to have serious vision loss within 2 years without proper treatment compared to 8% of treated eyes (Watkins 2003). In contrast, proliferative retinopathy is characterized by neovascularization (new blood vessel formation) as cotton wool spots and large dark blot hemorrhages on the surface of the retinas, either at the optic disc or elsewhere in the retinas. New blood vessels on the disc are particularly threatening to vision and often lead to vitreous hemorrhages and, if untreated, have a high risk of vision loss in about 26% of cases (Watkins 2003). As a consequence of neovascularization, two cellular components of retinal capillaries, pericytes, the vessel support cells, and endothelial cells, undergo a sequential loss and lead to constriction of blood flow through the capillaries. Among them, pericytes, the elongated contractile cells around the endothelium of capillary vessels, maintain the capillary tone (dilation and constriction), capillary growth, and protection, whereas endothelial cells maintain vasculature and survey of the retina for getting nutritional requirement and protection from potential pathogens through the maintenance of blood-retinal barrier function. The impairment of capillary blood flow in the retina by atherosclerotic plaques provokes the retinal cells, particularly neural and Müller cells, to initiate the repairing process by increasing the expression of numerous growth factors and cytokines, including VEGF, erythropoietin, PDGF, IGF-1, IL-1β, and TNF-α, which, in turn, accelerate the process of retinal pericyte and epithelial cell apoptosis and increase vascular permeability, occlusion, and neovascularization as well as impairment of vision. In neovascularization process, VEGFs play a key role for the stimulation of angiogenic sprouting formations from the pre-existing vasculature by increasing the expression levels of its receptors, VEGFR3 and VEGFR2, in the endothelial cells. Therefore, suppression of VEGF or VEGFR3 activity could be the potential therapeutic target for the prevention of angiogenesis process in diabetic retinopathy (Antonetti et al. 2006, 2012; Tammela et al. 2008). A vasoreactive plasma protein, plasma kallikrein (PK), has been found in high concentrations in the vitreous fluid in the subjects with advanced DR. PK on activation by Ang II increases the vascular permeability by generation of peptide, bradykinin (BK). BK on overexpression activates the receptors, BK2 and BK1, which in turn, on expression in vascular, glial, and neuronal cells, increase vasodilation and vascular permeability of plasma components. Therefore, inhibitors of PK decrease retinal vascular permeability (RVP) and improve this complication (Clermont et al. 2011).

Diabetic Peripheral Neuropathy (DPN)

Diabetic peripheral neuropathy (DPN), a neural pain disease in lower and upper limbs, is characterized by severe pain sensation like burning, tingling, or stabbing in the limbs and feet. More than 80% of amputations occur after foot ulceration or injury from DPN. DPN is the major cause of foot ulceration in patients with

peripheral arterial occlusive disease (PAOD). PAOD is a chronic atherosclerotic process that causes narrowing of the peripheral arterial vasculature mainly in the lower limb in the iliac and femoropopliteal arteries. PAOD increases the damage of somatic and autonomic nerve fibers and induces worsening of ischemic symptoms such as asymptomatic intermittent claudication, rest pain, and ulcer/gangrene and leads to ischemic tissue damage and limb amputation (Kim et al. 2014). Several studies demonstrated that poor glycemic control of chronic diabetes, hypertriglyceridemia, hypertension, elevated albuminuria, obesity, and smoking are the major risk factors for DPN. Microvascular disorders in epineural arteries and veins, such as basement membrane thickening, endothelial cell proliferation, hypertrophy, and reduced oxygen-induced atherosclerosis on the surface of sural nerves, impaired blood flow in epineural blood vessels and formation of new vessels, and reduced intra-epidermal nerve fiber density, are the major causes of DPN. N-Acetylaspartate (NAA) in white matter of the brain is the potential biomarker of central neuronal dysfunction, and its low levels are associated with low sural and tibial nerve amplitudes (short echo times), positively correlated to low recognition of pain and responsible for peripheral nerve damage. Some selective serotonin-norepinephrine reuptake inhibitor, duloxetine; anti-convulsant α-2-δ agonist, pregabalin; and opioids oxycodone and tapentadol are recommended for the treatment of pain in DPN (Tesfaye and Selvarajah 2012; Tesfaye et al. 2011; Yagihashi et al. 2011; Cameron et al. 2001).

Coronary Artery Disease (CAD)

Coronary artery disease, also known as coronary heart disease, is the most common cardiovascular complication of diabetes. Other cardiovascular complications of diabetes are peripheral artery disease, myocardial infarction, heart failure, and stroke. CAD is characterized by the impairment of both diastolic and systolic functions from the dysfunctions of cardiac endothelium and coronary arteries. Several factors, such as chronic severe hyperglycemia-induced increased atherosclerosis in the inner endothelial walls of the coronary arteries with increased NLRP3 inflammasome activation and high inflammatory infiltrates (macrophages and T-lymphocytes) and large necrotic core size in the endothelial walls, promote high constriction of blood flow into the heart and thereby increase the risk of both diastolic heart failure with preserved ejection fraction and systolic heart failure with reduced ejection fraction. Other important contributing factors include cardiomyocyte dysfunction (cardiomyopathy), impaired microvascular endothelial function, increased collagen deposition (fibrosis), and apoptosis of cardiomyocytes and maladaptive remodeling of the myocardium lead to both diastolic and systolic heart failure. Ventricular arrhythmias are the main cause of myocardial infarction mortality (Shah and Brownlee 2016). Different mechanisms have been suggested for atherosclerosis and cardiomyocyte dysfunction in diabetic hearts. In diabetic heart, elevated glucose and FFA levels increase mitochondrial ROS production in cardiomyocytes, which, in turn, increases intracellular Ca^{2+} concentrations and expression of calcineurin (Ca^{2+}/calmodulin-dependent serine/threonine phosphatase). Calcineurin on overexpression increases dephosphorylation of the

transcription factor, nuclear factor of activated T (NFAT)-cells, and facilitates NFAT translocation in nucleus and NFAT-stimulated poly ADP-ribose polymerase (PARP) activation to increase inflammation, and atherosclerosis, and subsequently increases cardiomyocyte hypertrophy, fibrosis, and apoptosis of cardiomyocytes for the induction of arterial vasoconstrictor activity and heart failure (Bourajjaj et al. 2008). Another group proposed that insulin resistance in diabetic hearts increased the levels of O-Glc-NAc via the formation of fructose 6-phosphate. Overexpression of O-Glc-NAc transferase significantly reduced the activity of sarco(endo)plasmic reticulum Ca^{2+}-ATPase-2 (SERCA2) pump, causing decreased Ca^{2+} reuptake (relaxation efficiency) by reducing the phosphorylation levels of phospholamban proteins and impaired diastolic relaxation. Cardial ventricular contraction and relaxation processes are regulated by SERCA2 pump. Thus, decreased cardiac contractibility increased fatal arrhythmias (abnormal heartbeats, too slow or too fast) through delayed after depolarizations (Clark et al. 2003). Another group proposed that in diabetic cardiomyocytes, elevated levels of increased fatty acid flux (lipotoxicity) from heart-specific LPL overexpression resulted in the increased synthesis of diacylglycerols, diglycerides, and ceramide. Aberrant accumulation of these signaling intermediates, particularly ceramide, enhanced cardiomyocyte architecture (hypertrophy), dilation of myocardial tissue, and impaired left ventricular systolic function (Yagyu et al. 2003).

1.12 Summary and Future Perspectives

Obesity is a global health problem affecting people in both the developed and the developing countries in the world. According to an estimate of the World Health Organization (WHO), in 2016, globally about 39% of adults aged 18 years and older were overweight or obese. The worldwide prevalence of overweight and obese among children and adolescents aged 5–19 years has risen dramatically from just 4% in 1975 to just over 18% in 2016. Several environmental factors including unhealthy diet and less physical activity as well as early life factors, such as diabetes exposure in mother's uterus, high birth weight, shorter breastfeeding duration, and more rapid infant weight gain, contribute synergistically in the development of childhood obesity (WHO 2018). Obesity is associated with several morbidities, including type 2 diabetes, cardiovascular disease, some cancers, kidney disease, obstructive sleep apnea, gout, osteoarthritis, and non-alcoholic fatty liver disease, and contributes to shortened lifespan. Several studies on the molecular basis of obesity demonstrate that a complex interaction among genetic, epigenetic, environmental, and behavioral factors, such as high-fat- and high-sugar-rich diet habit and sedentary lifestyle, influences the development of the disease. Family history of obesity demonstrates that genetic predisposition plays a significant role in childhood obesity. A cohort study of obese children in the UK demonstrates that the risk in a child is 2.5–4.0-fold higher if one of their parents is obese and 10-fold higher if both parents are obese, compared to both parents of normal weights (Reilly et al. 2005). Another GWAS analysis identified 17 rare copy number variant (CNV) loci that

were found only in obese children, but not in lean children of European ancestry. Out of these 17, 8 were also detected in obese children of African ancestry, but not in lean control of the same ethnicity (Glessner et al. 2010). Some genetic variants of the genes FTO, MC4R, TMEM18, SDCCAG8, and TNKS/MSRA were robustly associated with early onset of obesity in both extremely obese children and adolescents (Scherag et al. 2010).

Adipose tissue is considered as an energy storage organ in humans. It also controls the functions of endocrine organs by the secretion of various adipokines and cytokines. In obese humans, hypertrophic adipocytes in adipose tissue secrete various adipokines including leptin in high concentrations and adiponectin in low concentrations. Leptin and adiponectin, two well-characterized adipokines, are associated with insulin resistance and insulin action, respectively. Leptin concentration in serum correlates positively with the patient's adipose tissue reserve of energy and nutritional condition. High serum leptin concentration indicates a high energy reserve in adipocytes and leptin resistance in the brain and signifies hyperphagic condition of the patient, i.e., more food intake habit of the patient. A group of evidence advocates that leptin, leptin receptor, and melanocortin-4 receptor play central roles in the regulation of body fat in humans and rodents. Moreover, leptin has been identified as a potential mediator of cancer development through COX-2-mediated activation of signaling cascades in obese humans (Gao et al. 2009a), whereas adiponectin acts adversely to leptin and is inversely associated with obesity, insulin resistance, hyperinsulinemia, and inflammation and has potential anti-cancer effect through enhanced insulin action in the liver and insulin secretion from pancreatic beta-cells via AMPK activation in the liver and AMPK deactivation in the pancreas. Moreover, adiponectin-mediated AMPK activation in the skeletal muscle reduces muscle TG content and FFA level through increased fatty acid transport and oxidation and improves glucose uptake. Long-term calorie restriction in the diet has been found to improve weight loss in obese patients and to increase plasma adiponectin levels in obese patients. Furthermore, high adiponectin levels in plasma correlate with reduced chronic inflammation levels in bone-joint diseases such as gout and reduced the risk of obesity-associated malignancies (Dalamaga et al. 2012). Obese adipose tissue secretes several inflammatory cytokines, including IL-6 and TNF-α, which are associated with impaired insulin secretion and insulin resistance in different metabolic tissues. In addition, these pro-inflammatory cytokines stimulate lipolysis of triglycerides (TG) in adipocytes to release huge amount of FFAs and other lipid materials in plasma for the accumulation of these lipotoxic materials in different tissues, which in turn contribute to develop insulin resistance in these tissues. Therefore, the adipose tissue is the main organ for the initiation and progression of obesity in obese humans.

Various programs such as lifestyle modification programs, balanced low-calorie diets, commercial weight loss programs, exercise programs, medications, and bariatric surgery have been shown to be effective for weight loss to a great extent. Weight regain is resumed in all patients, especially when treatment is discontinued. Currently five synthetic drugs, orlistat, liraglutide, lorcaserin, combination of phentermine-topiramate, and bupropion-naltrexone, have been approved by FDA

for the long-term treatment of obesity. In February 2020, lorcaserin was withdrawn from the market because of serious adverse effects in patients. Moreover, the other recommended drugs are associated with several odd effects. Some herbal preparations are prescribed in the management of obesity. However, only poor data on the efficacy and safety of these herbal preparations are available. Most of the clinicians only consider the BMI of the patients in weight loss strategy, but not in body fat distribution. Moreover, they have a little knowledge on the exact amount of macro- and micro-nutrients that are required for a particular obese patient for the control fat mass.

Although several studies unanimously demonstrate that three genes, leptin, leptin receptor, and melanocortin-4 receptor, in combination play a key role in fat accumulation in the body of obese and overweight patients, studies on these obesity phenotype knockout mouse models are scanty. These studies in rabbits, mimic of human models, could be a powerful tool to get new insights on obesity-related human genes and proteins. Several antioxidant natural products and their parent extracts have been found to stimulate pancreatic beta-cell function by increasing beta-cell regeneration and insulin secretion, inhibit adipogenesis and oxidative stress, and improve insulin action in glucose uptake in the skeletal muscle, liver, and adipose tissue and in the suppression of hepatic glucose production. These natural products and their parent extracts could be utilized as a new approach in obesity management after extensive studies on their safety and dose-dependent optimum efficacy in different human mimic animal models. We need to apply the "omics technology" to evaluate the levels of obesity-related genes, other proteins, metabolites of used drugs, and their concentrations in the disease-affected metabolic tissues and gut microbiota composition of obese patients for the recommendation of "personalized medicine" to each patient to get maximum long-term benefits without odd adverse effects. Gut microbial composition has a significant role in the modulation of the inflammation in metabolic tissues and the activity of various genes-related to the suppression of fat metabolism and accumulation in the body. We need to explore this area to utilize these microbes by the use of dietary probiotic and prebiotic food as medicines in obesity management. We have to regulate the growth of the beneficial bacteria in the gut through the improvement of diet quality pattern in fruits, vegetables, and whole grain content and restrict food containing high levels of saturated and trans-fat and high sugar that are detrimental for the growth of health-benefit bacteria in gut. Moreover, both scientific and NGO communities should come forward in promoting sensible eating habits and regular physical activity for the management of obesity in different localities.

Diabetes (diabetes mellitus) is another global health problem affecting about 9.3% of adult population of the world in 2019, as per the IDF Diabetes Atlas report of ninth edn (International Diabetes Federation 2019). Diabetes mainly affected the low- and middle-income countries as about 77% of diabetic people of the world are living in those countries. Chronic hyperglycemia in type 2 diabetes leads to the progression of vascular complications including cardiovascular disease (cardiovascular artery disease, myocardial infarction, and stroke), kidney disease (diabetic nephropathy), eye disease (diabetic retinopathy), and neuronal disease (diabetic

peripheral neuropathy). Diabetes-accelerated atherosclerosis leads to endothelial dysfunction and constriction of blood flow in arteries, veins, and capillaries and contributes to the development of these vascular complications. Diabetes-specific microvascular complication is a leading cause of blindness, renal failure, and nerve damage, and macrovascular complication is a leading cause of heart failure, stroke, and limb amputation. The most common forms of diabetes are type 2 diabetes (T2DM) and type 1 diabetes (T1DM). Type 1 diabetes is caused by the autoimmune destruction of the pancreatic beta-cells and represents about 10% of all reported cases of diabetes, whereas type 2 diabetes is caused by impaired insulin secretion from pancreatic beta-cells and insulin resistance in insulin-sensitive metabolic tissues and is the most common form of the disease, accounting for about more than 85% of the reported diabetes cases. In addition to this, a modified form of type 2 diabetes, MODY, accounting for less than 5% of all type 2 diabetes cases, and gestational diabetes (GDM) among pregnant women, affecting about 10–15% of pregnant women, and is the risk factor for type 2 diabetes in mothers and offsprings. Exposure of the offspring to hyperglycemia in the mother's uterus has been reported to have a high risk of childhood overweight and obesity. A combination of various environmental, genetic, and epigenetic factors is considered responsible for the onset of all forms of diabetes. About 40% of type 2 diabetic patients have cardiovascular disease (CVD)-related complications. It indicates that type 2 diabetes is closely associated with CVD and they may be considered as opposite faces of a coin. As per the IDF report, diabetes or its complications account for about 50% of death of people worldwide under the age of 60 years. India has been projected to have the largest number of CVD patients. The main pathophysiological features of type 2 diabetes are impaired insulin secretion from pancreatic beta-cells and increased insulin resistance in insulin-sensitive metabolic tissues. It has been widely recognized that functional pancreatic beta-cell mass decreases over time and shows a progression of type 2 diabetes. A group of studies from different angles of the type 2 diabetes demonstrate that several genes related to insulin secretion and insulin action on mutation in the presence of various environmental factors exhibit abnormality in behavior and are considered responsible for the onset of the disease. The impaired insulin secretion is characterized by lowered glucose responsiveness in oral glucose tolerance test (OGTT). An over-response in OGTT is observed in diabetic patients with obesity and other associated morbidities. The decrease in insulin secretion at the early phase is the essential part of this disease. Chronic impaired insulin secretion on progression results in high glucose toxicity and shows an increase in both fasting and postprandial blood glucose levels in type 2 diabetic patients. When untreated for a long time, it causes permanent elevation of blood glucose levels in diabetic patients (Kaku 2010). The impairment of insulin action in major metabolic organs such as the liver and skeletal muscles is a common pathophysiological feature of type 2 diabetes. A group of evidence demonstrates that several genes related to insulin signaling, β_3-adrenergic receptor and fatty acid oxidation, and various environmental factors including hyperglycemia, high free fatty acids (FFAs) and pro-inflammatory cytokines, TNF-α, IL-6, leptin, resistin levels and gut microbiota dysbiosis-related endotoxemia promote insulin resistance

in these metabolic tissues. Insulin resistance in pancreatic islets increases high glucagon release from pancreatic α-cells and promotes glucagon-stimulated hepatic glucose production in neoglucogenic process. The microbiome communities in the gastrointestinal (GI) tract play an important role in the pathophysiology of both obesity and diabetes. However, the bacterial species that are involved in glucose and lipid metabolism have not yet clearly defined. Some of these gut bacteria promote incretin (GLP-1 and GIP) secretions, and secreted incretins act on pancreatic islets β- and α-cells to enhance insulin and suppress glucagon secretion, respectively. A recent proof-of-concept study demonstrates that infusion of intestinal microbiota (rich in butyrate-producing bacteria including *Roseburia intestinalis*) from lean individuals to the individuals with metabolic syndrome improves insulin sensitivity and reduces body fat mass (Vrieze et al. 2012). The hypothalamus in the brain also plays a significant role in beta-cell dysfunction and insulin resistance by the regulation of hepatic glucose production via the regulation of insulin action. Impaired insulin action at this site leads to increased fat metabolism and progression of obesity. Moreover, autonomous circadian clock in the brain composed of transcriptional activators, Clock and Bmal1, and their target genes, period and cryptochrome, maintain rhythmicity in day/night cycle and play an important role on maintenance of glucose homeostasis by regulation of insulin signaling in fasting and feeding behavioral cycle. Mutation of clock gene from environmental factors including sleep disturbance develops hyperglycemia, hypertriglyceridemia, and diet-induced obesity. Sound sleep at night improves oxidative metabolism of glucose and lipid in the skeletal muscle and gluconeogenesis in the liver (Bass and Takahashi 2010; Hanlon and Van Cauter 2011).

Currently various classes of oral and injectable medications are approved by FDA and other drug controlling agencies for the treatment of hyperglycemia in type 2 diabetes. Among the oral medications, metformin from biguanidine class; glibenclamide, glimepiride, and glipizide from sulfonylurea class; acarbose, miglitol, and voglibose from α-glucosidase inhibitor class; alogliptin, linagliptin, saxagliptin, sitagliptin, and vildagliptin from DPP-4 inhibitor class; canagliflozin and dapagliflozin from SGLT-2 inhibitor class; repaglinide and nateglinide from glinide class; pioglitazone and rosiglitazone from thiazolidinedione class; and bromocriptine, a dopamine receptor agonist, are available in the market. Some injectable medications including pramlintide (amylin analog), exenatide and liraglutide (GLP-1 receptor agonists), short-acting insulins (insulin regular, insulin aspart, insulin glulisine, and insulin lispro), intermediate-acting insulins (isophane insulin and insulin zinc), and long-acting insulins (ultralente, insulin detemir, and insulin glargine) are also prescribed for the control of severe hyperglycemia in both type 2 and type 1 diabetes. Most of the available oral drugs have various unwanted adverse effects in long-term use and have minimal therapeutic efficacy. Only a few are well accepted and utilized worldwide. Diabetic patients on treatment with insulin or insulin-secreting drugs showed a higher incidence of malignancies compared to those treated with metformin. Therefore, the development of metformin-type drugs in diabetes treatment is an essential requirement in the future (Dowling et al. 2012). In type 1 diabetes, lifelong insulin pump therapy is the most common treatment of

the disease. Recently introduced sensor-augmented insulin pump therapy, the bihormonal (insulin and glucagon) bionic artificial pancreas has been reported to be a superior device for glycemic control on long-term basis use (El-Khatib et al. 2017).

Current treatments in type 2 diabetes are largely based on industry-conducted studies. Hence, these medications are not effective in glycemic control of many patients. The main reason behind it is due to different tolerability and phenotype characteristics of different type 2 diabetic patients. Therefore, we need more personalized approach in the choice of drugs and their doses after evaluation of proteomics, genomics, lipidomics, and metabolomics levels in metabolic tissues and microbiome composition in the gut of both type 2 and type 1 diabetic individuals. Currently prescribed drugs do not prevent the loss of β-cell function, and hence we need new drugs that may affectively protect the function of β-cells under high glucose and lipid toxicities. Most of the research findings in the field of diabetes demonstrate that interactions between diabetes susceptible genes and environmental factors, including hyperglycemia, hypertension, and dyslipidemia, contribute to epigenetic modifications in DNA and histones, leading to modify the expression levels of genes related to β-cell function and insulin action in different metabolic organs and thereby play an active role in the onset and progression of type 2 and type 1 diabetes. However, the risk factor of each individual gene in the progression/pathogenesis of diabetes is not evaluated properly. Some branched-chain and aromatic amino acids have been found to be associated with the pathogenesis of obesity and type 2 diabetes. We need to explore whether these metabolites are the markers of some genetic determinants, dietary factors, or the actions of gut microbiomes. Further, we need to identify the genes and metabolic markers that act as mediators of the feedback loop, which interconnects the β-cell function with insulin-sensitive tissues (Kahn et al. 2014). As per WHO report, in 2014, about 50% of people with diabetes are unaware of their disease because of ignorance (Chan 2016). Hence, we need to set up healthcare policies in large scale in different countries to early identify the people having high risk of diabetes and provide the necessary diabetic therapy, for the suppression of diabetes-associated vascular complications and mortality (Standl et al. 2019). Several medicinal plants, seaweeds, microbial extracts, and isolated phytochemicals from them, which are used as folk medicine in diabetes treatment as well as in food supplements, have been found effective in the treatment of obesity and diabetes. These phytochemicals or their parent natural products (extracts) might be a new avenue for clinical trials in humans and animals for the management of diabetes as modern natural medicines (Sudhakar et al. 2020).

References

Adiels M, Westerbacka J, Soro-Paavonen A et al (2007) Acute suppression of VLDL-1 secretion rate by insulin is associated with hepatic fat content and insulin resistance. Diabetologia 50: 2356–2365

Adiels M, Olofsson SO, Taskinen MR et al (2008) Overproduction of very low-density lipoproteins is the hallmark of the dyslipidemia in the metabolic syndrome. Asterioscler Thromb Vasc Biol 28:1225–1236
Afshin A, Forouzanfar MH, Reitsma MB et al (2017) Health effects of overweight and obesity in 195 countries over 25 years. N Engl J Med 377:13–27
Alang N, Kelly CR (2015) Weight gain after fecal microbiota transplantation. Open Forum Infect Dis 2015:2
Allison DB, Gadde KM, Garvey WT et al (2012) Controlled-release phentermine/topiramate in severely obese adults: a randomized controlled trial (EQUIP). Obesity (Silver Spring) 20:330–342
American Diabetes Association (2014) Diagnosis and classification of diabetes mellitus. Diabetes Care 379(Suppl 1):S81–S90
American Diabetes Association (2016) Standards of medical care in diabetes-2016: summary of revisions. Diabetes Care 39(Suppl 1):S4–S5
An H, He L (2016) Current understanding of metformin effect on the control of hyperglycemia in diabetes. J Endocrinol 228:R97–R106
Anderson MS, Bluestone JA (2005) The NOD mouse: a model of immune dysregulation. Annu Rev Immunol 23:447–485
Anhe FF, Varin TV, Barz ML et al (2015) Gut microbiota dysbiosis in obesity-linked metabolic diseases and prebiotic potential of polyphenol-rich extracts. Curr Obes Rep 4:389–400
Antonetti DA, Barber AJ, Bronson SK, et al. On behalf of the JDRF Diabetic Retinopathy Center Group (2006) Diabetic retinopathy: seeing beyond glucose-induced microvascular disease. Diabetes 55: 2401–2411
Antonetti DA, Klein R, Gardner TW (2012) Diabetic retinopathy. N Engl J Med 366:1227–1239
Arnold SE, Arvanitakis Z, Macauley-Rambach SL et al (2018) Brain insulin resistance in type 2 diabetes and Alzheimer disease: concepts and conundrums. Nat Rev Neurol 14:168–181
Astrup A, Ryan L, Grunwald GK et al (2000) The role of dietary fat in body fatness: evidence from a preliminary meta-analysis of *ad libitum* low-fat dietary intervention studies. Br J Nutr 83 (Suppl 1):S25–S32
Astrup A, Carraro R, Finer N et al, NN8022 Investigators (2012) Safety, tolerability and sustained weight loss over 2 years with the once-daily human GLP-1 analog, liraglutide. Int J Obes 36: 843–854
Austin MA, Rodriguez BL, McKnight B et al (2000) Low-density lipoprotein particle size, triglycerides, and high-density lipoprotein cholesterol as risk factors for coronary heart disease in older Japanese-American men. Am J Cardiol 86:412–416
Balaji M, Ganjayi MS, Kumar GENH et al (2016) A review on possible therapeutic targets to contain obesity: the role of phytochemicals. Obes Res Clin Pract 10:363–380
Banting F (1929) The history of insulin. Edinburgh Med J 36:2
Barres R, Yan J, Egan B et al (2012) Acute exercise remodels promoter methylation in human skeletal muscle. Cell Metab 15:405–411
Barton M, Baretella O, Meyer MR (2012) Obesity and the risk of vascular disease: importance of endothelium-dependent vasoconstriction. Br J Pharmacol 165:591–602
Bass J, Takahashi JS (2010) Circadian integration of metabolism and energetic. Science 330:1349–1354
Bembde AS (2012) A study of plasma fibrinogen level in type 2 diabetes mellitus and its relation to glycemic control. Indian J Hematol Blood Transfus 28:105–108
Bergeron C, Boulet LP, Hamid Q (2005) Obesity, allergy and immunology. J Allergy Clin Immunol 115:1102–1104
Bernstein BE, Humphrey EL, Erlich RL et al (2002) Methylation of histone H3Lys4 in coding regions of active genes. Proc Natl Acad Sci U S A 99:8695–8700
Bhatt DL, Cavender MA (2014) Do dipeptidyl peptidase-4 inhibitors increase the risk of heart failure? JACC Heart Fail 2:583–585

Bhishagranta KL (1911) An English translation of the sushruta samhita: based on original Sanskrit text. Sutrasthanam, Calcutta, India
Bluestone JA, Herold K, Eisenbarth G (2010) Genetics, pathogenesis and clinical interventions in type 1 diabetes. Nature 464:1293–1300
Bonfrate L, Wang DQH, Garruti G et al (2014) Obesity and the risk and prognosis of gallstone disease and pancreatitis. Best Pract Res Clin Gastroenterol 28:623–635
Bonnefond A, Clement N, Fawcett K et al (2012) Rare MTNR1B variants impairing melatonin receptor 1B function contribute to type 2 diabetes. Nat Genet 44:297–301
Bosi E, Molteni L, Radaelli MG et al (2006) Increased intestinal permeability precedes clinical onset of type 1 diabetes. Diabetologia 49:2824–2827
Bottini N, Vang T, Cucca F et al (2006) Role of PTPN22 in type 1 diabetes and other autoimmune diseases. Semin Immunol 18:207–213
Bourajjaj M, Armand AS, Da Costa Martins PA et al (2008) NFATc2 is a necessary mediator of calcineurin-dependent cardiac hypertrophy and heart failure. J Biol Chem 283:22295–22303
Budai KA, Mirzahosseini A, Bela N et al (2015) The pharmacotherapy of obesity. Acta Pharm Hung 85:3–17
Burki T (2012) FDA rejects novel diabetes drug over safety fears. Lancet 379:507
Butler AE, Janson J, Bonner-Weir S et al (2003) Beta-cell deficit and increased beta-cell apoptosis in humans with type 2 diabetes. Diabetes 52:102–110
Calle EE, Rodriguez C, Walker-Thurmond K et al (2003) Overweight, obesity and mortality from cancer in a prospectively studied cohort of US adults. N Engl J Med 348:1625–1638
Cameron NA, Eaton SE, Cotter MA et al (2001) Vascular factors and metabolic interactions in the pathogenesis of diabetic neuropathy. Diabetologia 44:1973–1988
Cani PD, Possemiers S, de Wiele TV et al (2009) Changes in the gut microbiota control inflammation in obese mice through a mechanism involving GPL-2 driven improvement of gut permeability. Gut 58:1091–1103
Carroll KK (1998) Obesity as a risk factor for certain types of cancer. Lipids 33:1055–1059
CDCM (Centers for Disease Control and Prevention), US National Diabetes Statistics Report (2020). Available at: http://www.cdc.gov/diabetes/pdt/data
CDCM (Centers for Disease Control and Prevention), US National Health and Human Services (2017) Report on adult overweight and obesity. Available at: http://www.cdc.gov/obesity/adult/defining
Ceriello A, Lush CW, Darsow T et al (2008) Pramlintide reduced markers of oxidative stress in the postprandial period in patients with type 2 diabetes. Diabetes Metab Res Rev 24:103–108
Chan M Lecture at the 47th meeting of the National Academy of Medicine-2016 (2016) Obesity and diabetes: the slow-motion disaster. WHO-director-General's office, 17 October, 2016
Chang PV, Hao L, Offermanns S et al (2014) The microbial metabolite butyrate regulates intestinal macrophage function via histone deacetylase inhibition. Proc Natl Acad Sci U S A 111:2247–2252
Chen HS, Wu TE, Jap TS et al (2008) Beneficial effects of insulin on glycemic control and beta-cell function in newly diagnosed type 2 diabetes with severe hyperglycemia after short-term intensive insulin therapy. Diabetes Care 31:1927–1932
Chooi YC, Ding C, Magkos F (2019) The epidemiology of obesity. Metab Clin Exp 92:6–10
Clark RJ, McDonough PM, Swanson E et al (2003) Diabetes and the accompanying hyperglycemia impairs cardiomyocyte calcium cycling through increased nuclear O-Gle NAcylation. J Biol Chem 278:44230–44237
Clement K, Vaisse C, Manning BS et al (1995) Genetic variation in the beta 3-adrenergic receptor and an increased capacity to gain weight in patients with morbid obesity. N Engl J Med 333:352–354
Clermont A, Chilcote TJ, Kita T et al (2011) Plasma kallikrein mediates retinal vascular dysfunction and induces retinal thickening in diabetic rats. Diabetes 60:1590–1598

Collado MC, Isolauri E, Laitenen K et al (2010) Effect of mother's weight on infant's microbiota acquisition, composition and activity during early infancy: a perspective follow-up study initiated in early pregnancy. Am J Clin Nutr 92:1023–1030
Colli ML, Moore F, Gurzov EN et al (2010) MDA5 and PTPN2, two candidate genes for type 1 diabetes, modify pancreatic β-cell responses to the viral by-product double-stranded RNA. Hum Mol Genet 19:135–146
Cowley MA, Smart JL, Rubinstein M et al (2001) Leptin activates anorexigenic POMC neurons through a neural network in the arcuate nucleus. Nature 411:480–484
Cox LM, Blaser MJ (2013) Pathways in microbe-induced obesity. Cell Metab 17:883–894
Cummings JH, Macfarlane GT (1991) The control and consequences of bacterial fermentation in the human colon. J Appl Bacteriol 70:443–449
Dag ZO, Dilbaz B (2015) Impact of obesity on infertility in women. J Turk Ger Gynecol Assoc 16: 111–117
Dahlquist GG, Blom LG, Persson LA et al (1990) Dietary factors and the risk of developing insulin dependent diabetes in childhood. BMJ 300:1302–1306
Dalamaga M, Diakopoulos KN, Mantzoros CS (2012) The role of adiponectin in cancer: a review of current evidence. Endocr Rev 33:547–594
Dandona P, Aljada A, Bandyopadhyay A (2004) Inflammation: the link between insulin resistance, obesity and diabetes. Trends Immunol 25:4–7
Daneshpajooh M, Bacos K, Bysani M et al (2017) HDAC7 is overexpressed in human diabetic islets and impairs insulin secretion in rat islets and clonal beta cells. Diabetologia 60:116–125
Dayeh T, Volkov P, Salo S et al (2014) Genome-wide DNA methylation analysis of human pancreatic islets from type 2 diabetic and non-diabetic donors identifies candidate genes that influence insulin secretion. PLoS Genet 10:e1004160
De Fronzo RA (2011) Bromocriptine: a sympatholytic, D2-dopamine agonist for the treatment of type 2 diabetes. Diabetes Care 34:789–794
De Fronzo RA, Lilly Lecture (1988) The triumvirate: β-cell, muscle, liver: a collusion responsible for NIDDM. Diabetes 37:667–687
De Fronzo RA, Banting Lecture (2009) From the triumvirate to the ominous octet: a new paradigm for the treatment of type 2 diabetes mellitus. Diabetes 58:773–795
De Vadder F, Kovatcheva-Datehary P, Goncalves D et al (2014) Microbiota-generated metabolites promote metabolic benefits via gut-brain neural circuits. Cell 156:84–96
Delong T, Baker RL, Reisdorph N et al (2011) Islet amyloid polypeptide is a target antigen for diabetogenic $CD4^+$ T cells. Diabetes 60:2325–2330
Delong T, Wiles TA, Baker RL et al (2016) Pathogenic CD4T cells in type 1 diabetes recognize epitopes formed by peptide fusion. Science 351:711–714
Demerath EW, Guan W, Grove ML et al (2015) Epigenome-wide association study (EWAS) of BMI, BMI change and waist circumference in African American adults identifies multiple replicated loci. Hum Mol Genet 24:4464–4479
Den Besten G, van Eunen K, Groen AK et al (2013) The role of short-chain fatty acids in the interplay between diet, gut microbiota, and host energy metabolism. J Lipid Res 54:2325–2340
Dhana K, Braun KVE, Nano J et al (2018) An epigenome-wide study of obesity-related traits. Am J Epidemiol 187:1662–1669
Di Gregorio GB, Yao-Borengasser A, Rasouli N et al (2005) Expression of CD68 and macrophage chemoattractant protein-1 genes in human adipose and muscle tissues: association with cytokine expression, insulin resistance, and reduction by pioglitazone. Diabetes 54:2305–2313
Dick KJ, Nelson CP, Tsaprouni L et al (2014) DNA methylation and body mass index: a genome-wide analysis. Lancet 383:1990–1998
Donelly JE, Blair SN, Jackicic JM (2009) American College of Sports Medicine, ACSM position stand; appropriate physical activity intervention strategies for weight loss and prevention of weight gain in adults. Med Sci Sports Exerc 41:459–471
Dowling RJO, Niraula S, Stambolic V et al (2012) Metformin in cancer: translational challenges. J Mol Endocrinol 48:R31–R43

Dunning BE, Gerich JE (2007) The role of alpha-cell dysregulation in fasting and postprandial hyperglycemia in type 2 diabetes and therapeutic implications. Endocr Rev 28:253–283
Durazzo M, Ferro A, Gruden G (2019) Gastrointestinal microbiota and type 1 diabetes mellitus: the state of art. J Clin Med 8:1843
Eisenberg S (1999) High-density lipoprotein metabolism. In: Betteridge DJ, Illinfworth DR, Shepherd J (eds) Lipoproteins in health and disease, !St edn. Arnold, London, pp 71–85
Eizirik DL, Sammeth M, Bouckenooghe T et al (2012) The human pancreatic islet transcriptome: expression of candidate genes for type 1 diabetes and the impact of pro-inflammatory cytokines. PLoS Genet 8:e1002552
El Quaamari A, Baroukh N, Martens GA et al (2008) miR-375 targets 3′-phosphoinositide-dependent protein kinase-1 and regulates glucose-induced biological responses in pancreatic beta-cells. Diabetes 57:2708–2717
El-Khatib FH, Balliro C, Hillard MA et al (2017) Home use of a bihormonal bionic pancreas versus insulin pump therapy in adults with type 1 diabetes: a multicentre randomised crossover trial. Lancet 389:369–380
Engeli S, Schling P, Gorzelniak K et al (2003) The adipose tissue rennin-angiotensin-aldosterone system: role in the metabolic syndrome ? Int J Biochem Cell Biol 35:807–825
Eriksson J, Nakazato M, Miyazato M et al (1992) Islet amyloid polypeptide plasma concentrations in individuals at increased risk of developing type 2 (non-insulin-dependent) diabetes mellitus. Diabetologia 35:291–293
Everard A, Belzer C, Geurts L et al (2013) Cross-talk between *Akkermansia muciniphila* and intestinal epithelium controls diet-induced obesity. Proc Natl Acad Sci U S A 110:9066–9071
Farooqi IS, O'Rahilly S (2014) 20 years of leptin: human disorders of leptin action. J Endocrinol 223:163–170
Fei N, Zhao L (2013) An opportunistic pathogen isolated from the gut of an obese human causes obesity in germ-free mice. ISME J 7:880–884
Fernandes J, Su W, Rahat-Rozenbloom S et al (2014) Adiposity, gut microbiota and faecal short-chain fatty acids are linked in adult humans. Nutr Diabetes 4:e121
Ferrannini E, Barrett EJ, Bevilacqua S et al (1983) Effects of fatty acids on glucose production and utilization in man. J Clin Invest 72:1737–1747
Fock KM, Khoo J (2013) Diet and exercise in management of obesity and overweight. J Gastroenterol Hepatol 28(Suppl 4):59–63
Fonseca VA, Rosenstock J, Wang AC et al (2008) Colesevelam HCl improves glycemic control and reduces LDL cholesterol in patients with inadequately controlled type 2 diabetes on sulfonylurea-based therapy. Diabetes Care 31:1479–1484
Forouhi NG, Wareham NJ (2019) Epidemiology of diabetes. Medicine 47:22–27
Gadde KM, Allison DB, Ryan DH et al (2011) Effects of low dose, controlled release, phentermine plus topiramate combination on weight and associated comorbidities in overweight and obese adults (CONQUER): a randomised, placebo-controlled, phase 3 trial. Lancet 377:1341–1352
Gallwitz B (2011) Glucagon-like peptide-1 analogues for type 2 diabetes mellitus: current and emerging agents. Drugs 71:1675–1688
Gao J, Tian J, Lv Y et al (2009a) Leptin induces functional activation of cyclooxygenase-2 through JAK 2/STAT 3, MAPK/ERK, and PI3K/AKT pathways in human endometrial cancer cells. Cancer Sci 100:389–395
Gao Z, Yin J, Zhang J et al (2009b) Butyrate improves insulin sensitivity and increases energy expenditure in mice. Diabetes 58:1509–1517
Garber AJ, Abrahamson MJ, Barzilay JI et al (2016) Consensus statement by the American Association of Clinical Endocrinologists and American College of endocrinology on the comprehensive type 2 diabetes management algorithm-2016: executive summary. Endocr Pract 22:84–113
Gardner DSL, Tai ES (2012) Clinical features and treatment of maturity-onset diabetes of the young (MODY). Diab Metab Syndr Obes 5:101–108

Garvey WT, Ryan DH, Look M et al (2012) Two-year sustained weight loss and metabolic benefits with controlled-release phentermine/topiramate in obese and overweight adults (SEQUEL): a randomized, placebo-controlled, phase 3 extension study. Am J Clin Nutr 95:297–308

Gaziano JM, Cincotta AH, Vinik A et al (2012) Effect of bromocriptine-QR (a quick-release formulation of bromocriptine mesylate) on major adverse cardiovascular events in type 2 diabetic subjects. J Am Heart Assoc 1:e002279

Gesta S, Tseng YH, Kahn CR (2007) Developmental origin of fat: tracking obesity to its source. Cell 131:242–256

Giza S, Goulas A, Gbandi E et al (2013) The role of PTPN22.C1858T gene polymorphism in diabetes mellitus type 1: first evaluation in Greek children and adolescents. Biomed Res Int 2013:721604

Glessner JT, Bradfield JP, Wang K et al (2010) A genome-wide study reveals copy number variants exclusively to childhood obesity cases. Am J Hum Genet 87:661–666

Goossen K, Graber S (2012) Longer-term safety of dipeptidyl peptidase-4 inhibitors in patients with type 2 diabetes mellitus: systematic review and meta-analysis. Diabetes Obes Metab 14:1061–1072

Gottmann P, Ouni M, Saussenthaler S et al (2018) A computational biology approach of a genome-wide screen connected miRNAs to obesity and type 2 diabetes. Mol Metab 11:145–159

Greenway FL, Fujioka K, Plodkowski RA et al (2010) Effect of naltrexone plus bupropion on weight loss in overweight and obese adults (COR-1): a multicentre, randomized, double-blind, placebo-controlled, phase 3 trial. Lancet 376:595–605

Guardado-Mendoza R, Davalli AM, Chavez AO et al (2009) Pancreatic islet amyloidosis, β-cell apoptosis, and α-cell proliferation are determinants of islet remodelling in type 2 diabetic baboons. Proc Natl Acad Sci 106:13992–13997

Hall E, Dayeh T, Kirkpatrick CL et al (2013) DNA methylation of the glucagon-like peptide 1 receptor (GLP1R) in human pancreatic islets. BMC Med Genet 14:76

Hall E, Volkov P, Dayeh T et al (2014) Effects of palmitate on genome-wide mRNA expression and DNA methylation patterns in human pancreatic islets. BMC Med 12:103

Hall E, Nitert MD, Volkov P et al (2018) The effects of high glucose exposure on global gene expression and DNA methylation in human pancreatic islets. Mol Cell Endocrinol 472:57–67

Han JC, Liu QR, Jones M et al (2008) Brain-derived neurotrophic factor and obesity in the WAGR syndrome. N Engl J Med 359:918–927

Hanlon EC, Van Cauter E (2011) Quantification of sleep behaviour and its impact on the cross-talk between the brain and peripheral metabolism. Proc Natl Acad Sci U S A 108(Suppl 3):15609–15616

Harrold JA, Williams G (2006) Melanocortin-4 receptors, beta-MSH and leptin: key elements in the satiety pathway. Peptides 27:365–371

Heijmans BT, Tobi EW, Stein AD et al (2008) Persistent epigenetic differences associated with prenatal exposure to famine in humans. Proc Natl Acad Sci U S A 105:17046–17049

Hirosumi J, Tuncman G, Chang L et al (2002) A central role for JNK in obesity and insulin resistance. Nature 420:333–336

Hollander P, King AB, Del Prato S et al (2015) Insulin degludec improves long-term glycaemic control similarly to insulin glargine but with fewer hypoglycaemic episodes in patients with advanced type 2 diabetes on basal-bolus insulin therapy. Diabetes Obes Metab 17:202–206

Holst JJ, Vilsboll T, Deacon CF (2009) The incretin system and its role in type 2 diabetes mellitus. Mol Cell Endocrinol 297:127–136

Hooper LV, Littman DR, Macpherson AJ (2012) Interactions between the microbiota and the immune system. Science 336:1268–1273

Hotamisligil GS (1999) The role of TNF alpha and TNF receptors in obesity and insulin resistance. J Intern Med 245:621–625

In't Veld P (2011) Insulitis in human type 1 diabetes. Islets 3:131–138

Insel R, Knip M (2018) Prospects for primary prevention of type 1 diabetes by restoring a disappearing microbe. Pediatr Diabetes 19:1400–1406

Inshaw JRJ, Cutler AJ, Crouch DJM et al (2020) Genetic variants predisposing most strongly to type 1 diabetes diagnosed under age 7 years lie near candidate genes that function in the immune system and in pancreatic β-cells. Diabetes Care 43:169–177
International Diabetes Federation (2017) IDF diabetes atlas, 8th edn. Brussels, Netherland
International Diabetes Federation (2019) IDF diabetes atlas, 9th edn. Brussels, Netherland
Inzucchi SE, Bergenstal RM, Buse JB et al (2015) Management of hyperglycemia in type 2 diabetes, 2015: a patient-centered approach: update to a position statement of the American Diabetes Association and the European Association for the Study of diabetes. Diabetes Care 38:140–149
Jeyabalan A (2013) Epidemiology of preeclampsia: impact of obesity. Nutr Rev 71:S18–S25. https://doi.org/10.1111/nure.12055
Johnson KH, O'Brien TD, Betsholtz C et al (1989) Islet amyloid, islet-amyloid polypeptide, and diabetes mellitus. N Engl J Med 321:513–518
Johnston PS, Lebovitz HE, Conniff RF et al (1998) Advantages of α-glucosidase inhibition as monotherapy in elderly type 2 diabetic patients. J Clin Endocrinol Metab 183:1515–1522
Joslin EP, Dublin LI, Marks HH (1934) Studies in diabetes mellitus, II: its incidence and factors underlying its variations. Am J Med Sci 187:433–457
Kahn SE, Carr DB, Faulenbach MV et al (2008) An examination of beta-cell function measures and their potential use for estimating beta-cell mass. Diabetes Obes Metab 10(Suppl 4):63–76
Kahn S, Cooper ME, Prato SD (2014) Pathophysiology and treatment of type 2 diabetes: perspectives on the past, present, and future. Lancet 383:1068–1083
Kaku K (2010) Pathophysiology of type 2 diabetes and its treatment policy. JAAJ 53:41–46
Kanwar YS, Sun L, Xie P et al (2011) A glimpse of various pathogenic mechanisms of diabetic nephropathy. Annu Rev Pathol 6:395–423
Karlsson CLJ, Onnerfalt J, Xu J et al (2012) The microbiota of the gut in preschool children with normal and excessive body weight. Obesity 20:2257–2261
Karlsson FH, Tremaroli V, Nookaew I et al (2013) Gut metagenome in European women with normal, impaired and diabetic glucose control. Nature 498:99–103
Kato M, Zhang J, Wang M et al (2007) MicroRNA-192 in diabetic kidney glomeruli and its function in TGF-beta-induced collagen expression via inhibition of E-box repressors. Proc Natl Acad Sci U S A 104:3432–3437
Keating ST, El-Osta A (2015) Epigenetics and metabolism. Circ Res 116:715–736
Kelley D, Mitrakou A, Marsh H et al (1988) Skeletal muscle glycolysis, oxidation, and storage of an oral glucose load. J Clin Invest 81:1563–1571
Kelley DE, Bray GA, Pi-Sunyer FX et al (2002) Clinical efficacy of orlistat therapy in overweight and obese patients with insulin –treated type 2 diabetes: a 1-year randomized controlled trial. Diabetes Care 25:1033–1041
Kelly MA, Rayner ML, Mijovic CH et al (2003) Molecular aspects of type 1 diabetes. Mol Pathol 56:1–10
Kim YA, Kim ES, Hwang HK et al (2014) Prevalence and risk factors for the peripheral neuropathy in patients with peripheral arterial occlusive disease. Vasc Specialist Int 30:125–132
Kimura I, Ozawa K, Inoue D et al (2013) The gut microbiota suppresses insulin-mediated fat accumulation via the short-chain fatty acid receptor GPR43. Nat Commun 4:1829
King NA, Caudwell PP, Hopkins M et al (2009) Dual process action of exercise on appetite control: increase in orexigenic drive but improvement in meal-induced satiety. Am J Clin Nutr 90:921–927
Klose RJ, Bird AP (2006) Genomic DNA methylation: the mark and its mediators. Trends Biochem Sci 31:89–97
Kooner JS, Saleheen D, Sim X et al (2011) Genome-wide association study in people of south Asian ancestry identifies six novel susceptibility loci for type 2 diabetes. Nat Genet 43:984–989
Kornfeld JW, Baitzel C, Konner AC et al (2013) Obesity-induced overexpression of miR 802 impairs glucose metabolism through silencing of Hnf1b. Nature 494:111–115

Kotronen A, Juurinen L, Tiikainen M et al (2008) Increased liver fat, impaired insulin clearance, and hepatic and adipose tissue insulin resistance in type 2 diabetes. Gastroenterology 135:122–130

Kouzarides T (2007) Chromatin modifications and their function. Cell 128:693–705

Krause MS, McClenaghan NH, Flatt PR et al (2011) L-arginine is essential for pancreatic β-cell functional integrity, metabolism and defence from inflammatory challenge. J Endocrinol 211: 87–97

Krentz AJ, Bailey CJ (2005) Oral antidiabetic agents: current role in type 2 diabetes mellitus. Drugs 65:385–411

Krogvold L, Edwin B, Buanes T et al (2015) Detection of a low-grade enteroviral infection in the islets of Langerhans of living patients newly diagnosed with type 1 diabetes. Diabetes 64:1682–1687

Krude H, Biebermann H, Luck W et al (1998) Severe early-onset obesity, adrenal insufficiency and red hair pigmentation caused by POMC mutations in humans. Nat Genet 19:155–157

Kuhen P, Handke D, Waterland RA et al (2016) Interindividual variation in DNA methylation at a putative POMC metastable epiallele is associated with obesity. Cell Metab 24:502–509

Lahdenpera S, Syvanne M, Kahri J et al (1996) Regulation of low-density lipoprotein particle size distribution in NIDDM and coronary disease: importance of serum triglycerides. Diabetologia 39:453–461

Lalau JD, Arnouts P, Sharif A et al (2015) Metformin and other antidiabetic agents in renal failure patients. Kidney Int 87:308–322

Landrier JF, Derghal A, Mounien L (2019) MicroRNAs in obesity and related metabolic disorders. Cell 8:859

Le Chatelier E, Nielsen T, Qin J et al (2013) Richness of human gut microbiome correlates with metabolic markers. Nature 500:541–546

Lee R, Wong TY, Sabanayagam C (2015) Epidemiology of diabetic retinopathy, diabetic macular edema and related vision loss. Eye Vis (Lond) 2:17

Leung A, Parks BW, Du J et al (2014) Open chromatin profiling in mice livers reveals unique chromatin variations induced by high fat diet. J Biol Chem 289:23557–23567

Lewis JD, Ferrara A, Peng T et al (2011) Risk of bladder cancer among diabetic patients treated with pioglitazone; interim report of a longitudinal cohort study. Diabetes Care 34:916–922

Lin HV, Frassetto A, Kowalik EJ Jr, Nawrocki AR et al (2012) Butyrate and propionate protect against diet-induced obesity and regulate gut hormones via free fatty acid receptor 3-independent mechanisms. PLoS One 7:e35240

Ling C, Del Guerra S, Lupi R et al (2008) Epigenetic regulation of PPARGC1A in human type 2 diabetic islets and effect on insulin secretion. Diabetologia 51:615–622

Liu P, Sun M, Sader S (2006) Matrix metalloproteinases in cardiovascular disease. Can J Cardiol 22 (Suppl B):25B–30B

Locke AE, Kahali B, Berndt SI et al (2015) Genetic study of body mass index yield new insights for obesity biology. Nature 518:197–206

Lu J, Liu J, Li L et al (2020) Cytokines in type 1 diabetes: mechanisms of action and immunotherapeutic targets. Clin Transl Immunol 9:e1122

Lyssenko V, Lupi R, Marchetti P et al (2007) Mechanisms by which common variants in the TCF7L2 gene increase risk of type 2 diabetes. J Clin Invest 117:2155–2163

Macfarlane S, Macfarlane GT (2003) Regulation of short-chain fatty acid production. Proc Nutr Soc 62:67–72

Mahajan A, Go M, Zhang W et al (2014) Genome-wide trans-ancestry meta-analysis provides insight in to the genetic architecture of type 2 diabetes susceptibility. Nat Genet 46:234–244

Marina AL, Utzschneider KM, Wright LA et al (2012) Colesevelam improves oral but not intravenous glucose tolerance by a mechanism independent of insulin sensitivity and β-cell function. Diabetes Care 35:1119–1125

Marin-Penalver JJ, Martin-Timon I, Sevillano-Collantes C et al (2016) Update on the treatment of type 2 diabetes mellitus. World J Diabetes 7:354–395

Marso SP, Daniels GH, Brown-Frandsen K et al, LEADER Steering Committee on behalf of the LEADER Trial Investigators (2016) Liraglutide and cardiovascular outcomes in type 2 diabetes. N Engl J Med 375: 311–322

Matikainen N, Soderlund S, Bjomson E et al (2019) Liraglutide treatment improves postprandial lipid metabolism and cardiometabolic risk factors in humans with adequately controlled type 2 diabetes: a single-Centre randomized controlled study. Diabetes Obes Metab 21:84–94

McKeigue PM, Shah B, Marmot MG (1991) Relation of central obesity and insulin resistance with high diabetes prevalence and cardiovascular risk in south Asians. Lancet 337:382–386

Meerson A, Traurig M, Ossowski V et al (2013) Human adipose microRNA-221 is upregulated in obesity and affects fat metabolism downstream of leptin and TNF-α. Diabetologia 56:1971–1979

Meigs JB, Cupples LA, Wilson PW (2000) Parental transmission of type 2 diabetes: the Framingham offspring study. Diabetes 49:2201–2207

Melmed S, Polonsky K, Larsen P et al (2015) Williams textbook of endocrinology, 13th edn. Elsevier, Philadelphia

Mendelson MM, Marioni RE, Joehanes R et al (2017) Association of body mass index with DNA methylation and gene expression in blood cells and relation to cardiometabolic disease: a mendelian randomization approach. PLoS Med 14:e1002215

Miller WC, Koceja DM, Hamilton EJ (1997) A meta-analysis of the past 25 years of weight loss research using diet, exercise or diet plus exercise intervention. Int J Obes Relat Metab Disord 21: 941–947

Mitrakou A, Kelley D, Veneman T et al (1990) Contribution of abnormal muscle and liver metabolism to postprandial hyperglycemia in NIDDM. Diabetes 39:1381–1390

Mizuno TM, Kelley KA, Pasinetti GM et al (2003) Transgenic neuronal expression of proopiomelanocortin attenuates hyperphagic response to fasting and reverses metabolic impairments in leptin-deficient obese mice. Diabetes 52:2675–2683

Morton GJ, Cummings DE, Baskin DG et al (2006) Central nervous system control of food intake and body weight. Nature 443:289–295

Murri M, Leiva I, Gomez-Zumaquero JM et al (2013) Gut microbiota in children with type 1 diabetes differs from that in healthy children: a case-control study. BMC Med 11:46

Nakanishi K, Inoko H (2006) Combination of HLA-A24, -DQA1*03, and -DR9 contributes to acute onset and early complete beta-cell destruction in type 1 diabetes. Diabetes 55:1862–1868

National Institutes of Health (1998) Clinical guidelines on the identification, evaluation and treatment of overweight and obesity in adults-the evidence report. Obes Res 6(Suppl 2):51S–209S

Nauck MA, Friedrich N (2013) Do GLP-1 based therapies increase cancer risk ? Diabetes Care 36 (Suppl 2):S245–S252

Naylor R, Johnson AK, Gaudio DD (2018) Maturity-onset diabetes of the young overview. In: Adam MP et al (eds) Gene reviews (internet). University of Washington, Seattle, pp 1993–2020

Nejentsev S, Walker N, Riches D et al (2009) Rare variants of IFIH1, a gene implicated in antiviral responses, protect against type 1 diabetes. Science 324:387–389

Nesto RW, Bell D, Bonow RO et al (2003) Thiazolidinedione use, fluid retention, and congestive heart failure: a consensus statement from the American Heart Association and American Diabetes Association. Circulation 108:2941–2948

Newgard CB, An J, Bain JR et al (2009) A branched-chain amino-acid related metabolic signature that differentiates obese and lean humans and contributes to insulin resistance. Cell Metab 9: 311–326

Nisly SA, Kolanczyk DM, Walton AM (2013) Canagliflozin, a new sodium glucose cotransporter 2 inhibitor in the treatment of diabetes. Am J Health Syst Pharm 70:311–319

Nissen SE, Wolski KE, Prcela L et al (2016) Effect of naltrexone-bupropion on major adverse cardiovascular events in overweight and obese patients with cardiovascular risk factors: a randomized clinical trial. JAMA 315:990–1004

Noble JA, Valdes AM (2011) Genetics of HLA region in the prediction of type 1 diabetes. Curr Diab Rep 11:533–542
Noh H, King GL (2007) The role of protein kinase C activation in diabetic nephropathy. Kidney Int 72:S49–S53
Norris JM, Barriga K, Klingensmith G et al (2003) Timing of initial cereal exposure in infancy and risk of islet autoimmunity. JAMA 290:1713–1720
O'Neil PM, Smith SR, Weissman NJ et al (2012) Randomized placebo-controlled clinical trial of lorcaserin for weight loss in type 2 diabetes mellitus: the BLOOM-DM study. Obesity (Silver Spring) 20:1426–1436
Obici S, Feng Z, Karkanias G et al (2002) Decreasing hypothalamic insulin receptors causes hyperphagia and insulin resistance in rats. Nat Neurosci 5:566–572
Ogurtsova K, Fernandes JD, Huang Y et al (2017) IDF diabetes atlas: global estimates for the prevalence of diabetes for 2015 and 2040. Diabetes Res Clin Pract 128:40–50
Oh DK, Ciaraldi T, Henry RR (2007) Adiponectin in health and disease. Diabetes Obes Metab 9: 282–289
Ott PA, Dittrich MT, Herzog BA et al (2004) T cells recognize multiple GAD65 and proinsulin epitopes in human type 1 diabetes, suggesting determinant spreading. J Clin Immunol 24:327–339
Owens DR, Matfin G, Monnier L (2014) Basal insulin analogues in the management of diabetes mellitus: what progress have we made ? Diabetes Metab Res Rev 30:104–119
Paschou SA, Papadopoulou-Marketou N, Chrousos GP et al (2018) On type 1 diabetes mellitus pathogenesis. Endocr Connect 7:R38–R46
Pearce LR, Joe R, Doche ME et al (2014) Functional characterization of obesity-associated variants involving the alpha and beta isoforms of human SH2B1. Endocrinology 155:3219–3226
Peixoto-Barbosa R, Reis AF, Giuffrida FMA (2020) Update on clinical screening of maturity-onset diabetes of the young (MODY). Diabetol Metab Syndr 12:50
Perera RJ, Ray A (2007) MicroRNAs in the search for understanding human diseases. BioDrugs 21: 97–104
Pescador N, Perez-Barba M, Ibarra JM et al (2012) Serum circulating microRNA profiling for identification of potential type 2 diabetes and obesity biomarkers. PLoS One 8:e77251
Plagemann A, Harder T, Brunn M et al (2009) Hypothalamic proopiomelanocortin promoter methylation becomes altered by early overfeeding: an epigenetic model of obesity and the metabolic syndrome. J Physiol 587:4963–4976
Poy MN, Eliasson L, Krutzfeldt J et al (2004) A pancreatic islet-specific microRNA regulates insulin secretion. Nature 432:226–230
Qin J, Li Y, Cai Z et al (2012) A metagenome-wide association study of gut microbiota in type 2 diabetes. Nature 490:55–60
Raccah D (2008) Options for the intensification of insulin therapy when basal insulin is not enough in type 2 diabetes mellitus. Diabetes Obes Metab 10(Suppl 2):76–82
Rajala MW, Scherer PE (2005) Minireview: the adipocyte – at the cross roads of energy homeostasis, inflammation, and atherosclerosis. Endocrinology 144:3765–3773
Rajan S, Panzade G, Srivastava A et al (2018) miR-876-3p regulates glucose homeostasis and insulin sensitivity by targeting adiponectin. J Endocrinol 239:1–17
Rask-Madsen C, King GL (2013) Vascular complications of diabetes: mechanisms of injury and protective factors. Cell Metab 17:20–23
Ratner RE, Gough SC, Mathieu C et al (2013) Hypoglycaemia risk with insulin degludec compared with insulin glargine in type 2 and type 1 diabetes: a pre-planned meta-analysis of phase 3 trials. Diabetes Obes Metab 15:175–184
Reaven GM (1988) Banting lecture 1988. Role of insulin resistance in human disease. Diabetes 37: 1595–1607
Reilly JJ, Armstrong J, Dorosty AR et al (2005) Early life risk factors for obesity in childhood: cohort study. BMJ 330:1357

Richardson DK, Kashyap S, Bajaj M et al (2005) Lipid infusion induces an inflammatory/fibrotic response and decreases expression of nuclear encoded mitochondrial genes in human skeletal muscle. J Biol Chem 280:10290–10297

Richardson SJ, Leete P, Bone AJ et al (2013) Expression of the enteroviral capsid protein VP1 in the islet cells of patients with type 1 diabetes is associated with induction of protein kinase R and downregulation of Mcl-1. Diabetologia 56:185–193

Ridaura VK, Faith JJ, Rey FE et al (2013) Gut microbiota from twins discordant for obesity modulate metabolism in mice. Science 341:1241214

Rieg T, Mastuda T, Gerasimova M et al (2014) Increase in SGLT1-mediated transport explains renal glucose reabsorption during genetic and pharmacological SGLT2 inhibition in euglycemia. Am J Physiol Renal Physiol 306:F188–F193

Riser Taylor S, Harris KB (2013) The clinical efficacy and safety of sodium glucose cotransporter-2 inhibitors in adults with type 2 diabetes mellitus. Pharmacotherapy 33:984–999

Rodriguez-Calvo T, Ekwall O, Amirian N et al (2014) Increased immune cell infiltration of the exocrine pancreas: a possible contribution to the pathogenesis of type 1 diabetes. Diabetes 63: 3880–3890

Roep BO, Solvason N, Gottlieb PA et al (2013) Plasma-encoded proinsulin-specific $CD8^+$ T cells in type 1 diabetes. Sci Transl Med 5:191ra82

Ronn T, Volkov P, Davegardh C et al (2013) A six months exercise intervention influences the genome-wide DNA methylation pattern in human adipose tissue. PLoS Genet 9:e1003572

Rosik J, Szostak B, Machaj F et al (2020) The role of genetics and epigenetics in the pathogenesis of gestational diabetes mellitus. Ann Human Genet 84:114–124

Saeed S, Bonnefond A, Manzoor J et al (2015) Genetic variants in LEP, LEPR, and MC-4R explain 30% of severe obesity in children from a consanguineous population. Obesity (Silver Spring) 23:1687–1695

Sahebkar A, Simental-Mendia LE, Reiner Z et al (2017) Effect of orlistat on plasma lipids and body weight: a systematic review and meta-analysis of 33 randomized controlled trials. Pharmacol Res 122:53–65

Sakane N, Yoshida T, Umekawa T et al (1997) Beta 3-adrenergic receptor polymorphism: a genetic marker for visceral fat obesity and insulin resistance syndrome. Diabetologia 40:200–204

Sanches AC, Correr CJ, Venson R et al (2011) Revisiting the efficacy of long-acting insulin analogues on adults with type 1 diabetes using mixed-treatment comparisons. Diabetes Res Clin Pract 94:333–339

Santin I, Eizirik DL (2013) Candidate genes for type 1 diabetes modulate pancreatic islet inflammation and β-cell apoptosis. Diabetes Obes Metab 15(Suppl 3):71–81

Sayols-Baixeras S, Subirana I, Fernandez-Sanles A et al (2017) DNA methylation and obesity traits: an epigenome-wide association study. The REGICOR study. Epigenetics 12:909–916

Scerif M, Goldstone AP, Korbonits M (2011) Ghrelin in obesity and endocrine diseases. Mol Cell Endocr 340:15–25

Schaffler A, Ehling A, Neumann E et al (2003) Adipokines in synovial fluid. JAMA 290:1709–1710

Scherag A, Dina C, Hinney A et al (2010) Two new loci for body-weight regulation identified in a joint analysis of genome-wide association studies for early- onset extreme obesity in French and German study groups. PLoS Genet 6:e1000916

Schernthaner G, Currie CJ, Schernthaner GH (2013) Do we still need pioglitazone for the treatment of type 2 diabetes ? A risk-benefit critique in 2013. Diabetes Care 36(Suppl 2):S155–S161

Schroeder BO, Birchenough GMH, Stahlman M et al (2018) Bifidobacteria or fiber protects against diet-induced microbiota-mediated colonic mucus deterioration. Cell Host Microbe 23:27–40

Scranton R, Cincotta A (2010) Bromocriptine-unique formulation of a dopamine agonist for the treatment of type 2 diabetes. Expert Opin Pharmacother 11:269–279

Shah MS, Brownlee M (2016) Molecular and cellular mechanisms of cardiovascular disorders in diabetes. Circ Res 118:1808–1829

Shah SH, Crosslin DR, Haynes CS et al (2012) Branched-chain amino acid levels are associated with improvement in insulin resistance with weight loss. Diabetologia 55:321–330
Sharp GC, Salas LA, Monnereau C et al (2017) Maternal BMI at the start of pregnancy and offspring epigenome-wide DNA methylation: findings from the pregnancy and childhood epigenetics (PACE) consortium. Hum Mol Genet 26:4067–4085
Shields BM, Hicks S, Shepherd MH et al (2010) Maturity-onset diabetes of the young (MODY): how many cases are we missing? Diabetologia 53:2504–2508
Shimabukuro M, Koyama K, Chen X et al (1997) Direct antidiabetic effect of leptin through triglyceride depletion of tissues. Proc Natl Acad Sci U S A 94:4637–4641
Shin NR, Lee JL, Lee HY et al (2014) An increase in the *Akkermansia* spp. population induced by metformin treatment improves glucose homeostasis in diet-induced obese mice. Gut 63:727–735
Siljander H, Honkanen J, Knip M (2019) Microbiome and type 1 diabetes. EBioMedicine 46:512–521
Singh A, Sarkar SR, Gaber LW et al (2007) Acute oxalate nephropathy associated with orlistat, a gastrointestinal lipase inhibitor. Am J Kidney Dis 49:153–157
Skowera A, Ladell K, McLaren JE et al (2015) β-Cell-specific CD8 T cell phenotype in type 1 diabetes reflects chronic autoantigen exposure. Diabetes 64:916–925
Smith PA, Sakura H, Coles B et al (1997) Electrogenic arginine transport mediates stimulus-secretion coupling in mouse pancreatic beta-cells. J Physiol 499:625–635
Smushkin G, Sathananthan M, Piccinini F et al (2013) The effect of a bile acid sequestrant on glucose metabolism in subjects with type 2 diabetes. Diabetes 62:1094–1101
Soares AF, Nissen JB, Garcia-Serrano AM et al (2019) Glycogen metabolism is impaired in the brain of male type 2 diabetes Goto-Kakizaki rats. J Neurosci Res 97:1004–1017
Sombra LRS, Anastasopoulou C (2020) Pharmacologic therapy for obesity. Stat Pearls Publishing LLC [Internet] Last update: September 15, 2020 (http://creativecomments.org/licenses/by/4.0)
Song R (2016) Mechanism of metformin: a tale of two sites. Diabetes Care 39:187–189
Sonnenburg JL, Backhed F (2016) Diet-microbiota interactions as moderators of human metabolism. Nature 536:56–64
Sorensen M, Andersen ZJ, Nordsborg RB et al (2013) Long-term exposure to road traffic noise and incident diabetes: a cohort study. Environ Health Perspect 121:217–222
Sprouse ML, Bates NA, Felix KM et al (2019) Impact of gut microbiota on gut-distal autoimmunity: a focus on T cells. Immunology 156:305–318
Standl E, Khunti K, Hansen TB et al (2019) The global epidemics of diabetes in the 21st century: current situation and perspectives. Eur J Prev Cardiol 26(Suppl 2):7–14
Sudhakar CK, Mishra V, Hemani V et al (2020) Reverse pharmacology of phytoconstituents of food and plant in the management of diabetes: current status and perspectives. Trends Food Sci Technol 110:594–610. https://doi.org/10.1016/j.tifs.2020.10.024
Sumithran P, Proietto J (2014) Benefit-risk assessment of orlistat in the treatment of obesity. Drug Saf 37:597–608
Sunquist K, Eriksson U, Mezuk B et al (2015) Neighborhood walkability, deprivation and incidence of type 2 diabetes: a population-based study on 512,061 Swedish adults. Health Place 31:24–30
Takahashi A, Nagashima K, Hamasaki A et al (2007) Sulfonylurea and glinide reduce insulin content, functional expression of K(ATP) channels, and accelerate apoptotic beta-cell death in the chronic phase. Diabetes Res Clin Pract 77:343–350
Tammela T, Zarkada G, Wallgard E et al (2008) Blocking VEGFR-3 suppresses angiogenic sprouting and vascular network formation. Nature 454:656–660
Teichert T, Vossoughi M, Vierkotter A et al (2013) Association between traffic-related air pollution, subclinical inflammation and impaired glucose metabolism: results from the SALIA study. PLoS One 8:e83042
Tennent GA, Brennan SO, Stangou AJ et al (2007) Human plasma fibrinogen is synthesized in the liver. Blood 109:1971–1974

Tesfaye S, Selvarajah D (2012) Advances in the epidemiology, pathogenesis and management of diabetic peripheral neuropathy. Diabetes Metab Res Rev 28(Suppl 1):8–14
Tesfaye S, Vileikyte L, Raymon G et al (2011) Painful diabetic peripheral neuropathy: consensus recommendations on diagnosis, assessment and management. Diabetes Metab Res Rev 27:629–638
Williams AL, Jacobs SB, Moreno-Macias H, The SIGMA type 2 Diabetes Consortiums et al (2014) Sequence variants in SLC16A11 are a common risk factor for type 2 diabetes in Mexico. Nature 506:97–101
Tobi EW, Lumey LH, Talens RP et al (2009) DNA methylation differences after exposure to prenatal famine are common and timing-and sex-specific. Hum Mol Genet 18:4046–4053
Traube FR, Carell T (2017) The chemistries and the consequences of DNA and RNA methylation and demethylation. RNA Biol 14:1099–1107
Turnbaugh PJ, Backhed F, Fulton L et al (2008) Diet-induced obesity is linked to marked but reversible alternations in the mouse distal gut microbiome. Cell Host Microbe 3:213–223
Umanath K, Lewis JB (2018) Update on diabetic nephropathy: core curriculum-2018. Am J Kidney Res 71:884–895
Unger RH (1995) Lipotoxicity in the pathogenesis of obesity-dependent NIDDM: genetic and clinical implications. Diabetes 44:863–870
Unoki H, Takahashi A, Kawaguchi T et al (2008) SNPs in KCNQ1 are associated with susceptibility to type 2 diabetes in east Asian and European populations. Nat Genet 40:1098–1102
Vaarala O, Knip M, Paronen J et al (1999) Cow's milk formula feeding induces primary immunization to insulin in infants at genetic risk for type 1 diabetes. Diabetes 48:1389–1394
Vague P, Coste TC, Jannot MF et al (2004) C-peptide, $Na^{+\cdot}$, K^{+}-ATPase, and diabetes. Exp Diabesity Res 5:37–50
Vatanen T, Franzosa EA, Schwager R et al (2018) The human gut microbiome in early-onset type 1 diabetes from the TEDDY study. Nature 562:589–594
Ventriglia G, Nigi L, Sebastiani G et al (2015) MicroRNAs: novel players in the dialogue between pancreatic islets and immune system in autoimmune diabetes. Biomed Res Int 2015:749734
Virtanen SM, Nevalainen J, Kronberg-Kippila C et al (2012) Food consumption and advanced β-cell autoimmunity in young children with HLA-conferred susceptibility to type 1 diabetes: a nested case-control design. Am J Clin Nutr 95:471–478
Viskari H, Knip M, Tauriainen S et al (2012) Maternal enterovirus infection as a risk factor for type 1 diabetes in the exposed offspring. Diabetes Care 35:1328–1332
Volkov P, Bacos K, Ofori JK et al (2017) Whole-genome bisulfite sequencing of human pancreatic islets reveals novel differentially methylated regions in type 2 diabetes pathogenesis. Diabetes 66:1074–1085
Vrieze A, Van Wood E, Holleman F et al (2012) Transfer of intestinal microbiota from lean donors increases insulin sensitivity in individuals with metabolic syndrome. Gastroenterology 143: 913–916
Wang F, Hull RL, Vidal J et al (2001) Islet amyloid develops diffusely throughout the pancreas before becoming severe and replacing endocrine cells. Diabetes 50:2514–2520
Wang X, Pan Y, Zhu H et al (2018) An epigenome-wide study of obesity in African American youth and young adults: novel findings, replication in neutrophils, and relationship with gene expression. Clin Epigenetics 10:3
Watkins PJ (2003) Retinopathy. BMJ 326:924–926
Weisberg SP, Mc Cann D, Desai M et al (2003) Obesity is associated with macrophage accumulation in adipose tissue. J Clin Invest 112:1796–1808
Wen X, Yang Y (2017) Emerging roles of GLIS3 in neonatal diabetes, type 1 and type 2 diabetes. J Mol Endocrinol 58:873–885
Wenzlau JM, Juhl K, Yu L et al (2007) The cation efflux transporter ZnT8 (Slc30A8) is a major autoantigen in human type 1 diabetes. Proc Natl Acad Sci U S A 104:17040–17045
World Health Organization (2017) Fact sheets on cardiovascular diseases, 2017. Available at: http://www.who.int/news-room/fact-sheet/detal/cardiovasculardiseases

World Health Organization (2018) Fact sheets on obesity and overweight. Updated in February 2018
World Health Organization (2020) Fact sheets on obesity and diabetes. Available at: http://www.who.int/news-room/fact-sheets
Wren AM, Seal LJ, Cohen MA et al (2001) Ghrelin enhances appetite and increases food intake in humans. J Clin Endocrinol Metab 86:5992
Wu T, Liu YH, Fu YC et al (2014) Direct evidence of sirtuin downregulation in the liver of non-alcoholic fatty liver disease patients. Ann Clin Lab Sci 44:410–418
Yagihashi S, Mizukami H, Sugimoto K (2011) Mechanism of diabetic neuropathy: where are we now and where to go ? J Diabetes Investig 2:18–32
Yagyu H, Chen G, Yokoyama M et al (2003) Lipoprotein lipase (LpL) on the surface of cardiomyocytes increases lipid uptake and produces a cardiomyopathy. J Clin Invest 111: 419–426
Yang BT, Dayeh TA, Kirkpatrick CL et al (2011) Insulin promoter DNA methylation correlates negatively with insulin gene expression and positively with HbA1c levels in human pancreatic islets. Diabetologia 54:360–367
Yang BT, Dayeh TA, Volkov PA et al (2012) Increased DNA methylation and decreased expression of PDX-1 in pancreatic islets from patients of type 2 diabetes. Mol Endocrinol 26:1203–1212
Yasuda K, Miyake K, Horikawa Y et al (2008) Variants in KCNQ1 are associated with susceptibility to type 2 diabetes mellitus. Nat Genet 40:1092–1097
Yeo GSH, Connie Hung CC, Rochford J et al (2004) A de novo mutation affecting human TrKB associated with severe obesity and developmental delay. Nat Neurosci 7:1187–1189
Younk LM, Mikeladze M, Davis SM (2011) Pramlintide and the treatment of diabetes: a review of the data since its introduction. Expert Opin Pharmacother 12:1439–1451
Yulyaningsih E, Zhang L, Herzog H et al (2011) NPY receptors as potential targets for anti-obesity drug development. Br J Pharmacol 163:1170–1202
Ziegler AG, Rewers M, Simell O et al (2013) Seroconversion to multiple islet autoantibodies and risk of progression to diabetes in children. JAMA 309:2473–2479
Zigman JM, Jones JE, Lee CE et al (2006) Expression of ghrelin receptor mRNA in the rat and the mouse brain. J Comp Neurol 494:528–548

Elucidating Diversity in Obesity-Related Phenotypes Using Longitudinal and Multi-omic Approaches

2

Brian D. Piening, Alexa K. Dowdell, and Michael P. Snyder

2.1 Introduction

Precision medicine research in obesity hinges on the overarching concept that obesity is a condition that is phenotypically diverse and incredibly individualized. While obesity is often associated with a wide range of comorbidities including type 2 diabetes mellitus (T2DM), heart disease, high blood pressure, etc. that result in significant mortality, there are individuals who may spend a significant portion of their lives classified as obese but remain otherwise healthy. While this phenomenon has been known and reported back to the early days of modern medicine, only in the recent post-genome and multi-omic era do tools exist to deeply characterize a patient's genome and biomolecular physiology to elucidate the molecular underpinnings of patient-specific obesity phenotypes. As of 2021, these efforts are still nascent; current costs of whole genome sequencing and other 'omic profiling remain high enough that efforts are limited mainly to smaller cohorts and routine multi-omic profiling in the clinic remains an aspirational goal. Moreover, the tools and expertise to deeply integrate diverse types of biomolecular profiling data remain somewhat limited. All in all, while we can currently generate a massive amount of biomolecular data on a single individual, significant work remains in translating this information into novel and clinically actionable insights.

In this chapter, we seek to chronicle the journey from classical phenotyping of obesity and metabolic disease-related states to the application of modern high-throughput 'omic profiling for the better subclassification of obesity-related disease states, prediction of response to interventions and therapeutics, and prognostication

B. D. Piening (✉) · A. K. Dowdell
Earle A. Chiles Research Institute, Providence Health and Services, Portland, OR, USA
e-mail: brian.piening@providence.org

M. P. Snyder
Department of Genetics, Stanford University, Stanford, CA, USA
e-mail: mpsnyder@stanford.edu

B. Dinda (ed.), *Natural Products in Obesity and Diabetes*,
https://doi.org/10.1007/978-3-030-92196-5_2

for clinical outcome. We will discuss recent advances in both the molecular profiling technology and algorithmic methodologies that make these approaches possible and will highlight key early successes where multi-omics has advanced our understanding of these disease states. We will also discuss the future path where multi-omics may transform how we clinically diagnose, monitor, and treat obesity-related diseases.

2.2 Classical Phenotyping in Obesity and Metabolic Disease

Obesity remains one of the most widespread diseases in our modern era, with an estimated almost two billion individuals diagnosed worldwide. While it is one of the most prevalent human diseases in existence, it also remains one of the most complex. Although studies using mouse models have made significant contributions to our molecular understanding of obesity, these efforts fail to encapsulate the staggering diversity and complexity of obesity in humans. Across the human population, highly diverse genetics and the wide array of cultures, diets, environments, and lifestyles worldwide play a significant role in human health. Moreover, given that obesity typically develops over a prolonged period of years or decades of life, a microcosm of individualized events and choices ensure that no two individuals have the exact same health trajectory.

While measures such as body mass index (BMI) have significant utility in assessing generalized risk for adverse health events such as heart attack, stroke, or the development of T2DM, these metrics fail to encapsulate the diversity of underlying physiological states in obese individuals. Among a set of BMI-matched obese individuals, it is not well-understood why a subset will go on to develop significant obesity-associated morbidities such as T2DM, while others will not. Assays measuring fasting blood glucose or glycated hemoglobin are used in the diagnostic setting to assess prediabetic states or the diagnosis of T2DM; however, there still remains little in the way of early-stage biomarkers for predicting the subset of individuals that will eventually have an elevated result for one or more of these clinical biomarkers. This information is critical, as early intervention may be significantly more successful than later interventions when an individual presents to clinic with prediabetes or T2DM already.

2.3 The Genomic Revolution Gives Way to Multi-omics

As has been well-documented, the completion of the draft human genome ushered in a new era focused on the comprehensive evaluation of biomolecules (Lander et al. 2001; Wolfsberg et al. 2001). This has been accelerated by the rapid development and evolution of technologies for massively parallel sequencing of nucleic acids in a sample, currently dubbed next-generation sequencing (NGS) (Table 2.1). While the most common current approaches leverage sequencing-by-synthesis, there are a wide array of additional technologies for bulk sequencing, many that include unique

Table 2.1 Types of 'omics assays

Analyte	Detection method	Values assessed
Genome	Next generation sequencing	SNVs, indels, CNV, SV, others
Epigenome	Whole-genome bisulfite sequencing, others	DMRs
Chromatin Accessibility	ATAC-seq, DNAse-seq, others	Accessible regions
Transcriptome	RNA-seq, microarray	DEGs, differential splicing, others
Proteome	LC-MS, tagged multiplex antibodies, others	Protein abundance, PTMs
Metabolome	LC-MS	Metabolite abundance
Microbiome	Sequencing: 16S or shotgun metagenomics	Microbe abundance, OTUs, others

properties such as single-molecule sequencing or sequencing extended (10s to 100 s of kilobases) contiguous strands of DNA (Mardis 2011; van Dijk et al. 2018). Along with advances in wet-lab methodologies and instrumentation, a wide array of computational tools have been developed for rapidly assessing genomic alterations including single nucleotide variants (SNVs), insertions/deletions (indels), copy number variation (CV), and larger structural variation (SVs) (Li and Durbin 2009; Lam et al. 2010; McKenna et al. 2010; Fan et al. 2014; Mohiyuddin et al. 2015). These approaches have been utilized not just for human genomes, but for sequencing of collections of microbes from biological specimens. Generally these methods fall into two categories, targeted sequencing of variable and conserved regions in the 16S rRNA gene of microbial populations in a sample or untargeted shotgun metagenomic sequencing of all nucleic acid molecules in a specimen (Hamady and Knight 2009).

Beyond the assessment of genomic sequence, novel tools have also emerged for assessing RNA expression, collectively referred to as transcriptomics. Earlier technologies in this area focused on hybridization to probes printed on glass slides (microarrays); however, this has been largely supplanted by direct sequencing of RNA molecules (RNA-seq) (Schena et al. 1995; Brown and Botstein 1999; Stears et al. 2003; Nagalakshmi et al. 2008; Mortazavi et al. 2008; Wang et al. 2009). As with DNA-seq, gene expression software tools have evolved in parallel with wet-bench advances and now include a wide array of tools for transcriptome-wide clustering and other similarity approaches, differentially expressed gene (DEG) identification, assessment of differential splicing, and gene fusion detection (Kerr et al. 2008; Love et al. 2014; Kumar et al. 2016; Ding et al. 2017).

Sequencing technologies have also been applied to the large-scale quantification of additional layers of genome regulation. Genome-wide epigenetic methylation programming can be assessed by a variety of approaches including whole-genome bisulfite sequencing and methyl-capture sequencing, identifying differentially methylated regions (DMRs) of the genome across samples (Clark et al. 1994;

Schaefer et al. 2009; Pollex et al. 2010; Teh et al. 2016). Chromatin structure, binding, and accessibility can also be assessed by a wide array of different methods, including sequencing of DNAse hypersensitivity sites (DNAse-seq), assessment of transposase accessibility (ATAC-seq), and sequencing of transcription factor and other regulatory protein-bound sequences (ChIP-seq) (Lefrançois et al. 2009; Song and Crawford 2010; Buenrostro et al. 2015).

A number of current 'omics approaches do not involve sequencing. Proteomics is typically assessed using liquid chromatography mass spectrometry (LC-MS) instrumentation as is most common for metabolomics, though there exists a wide array of instrumentation and methodologies within these respective areas (Bain et al. 2009; Parker et al. 2010). Less common but still in significant use are collections of antibodies for proteomic assessment either with fluorescent detection in a pooled or array format or with oligo barcode tags (Zichi et al. 2002; Qi et al. 2019; Petrera et al. 2021).

While 'omics analyses have previously been performed mostly on bulk cells, tissues, or biological fluids, more recent advances leverage cell separation methods to perform 'omics analyses at the single cell level. Single-cell sequencing approaches enable researchers to generate complete transcriptomes or other 'omes for individual cells in a sample, a powerful approach for identifying cell type-specific phenotypes (Shapiro et al. 2013). Even more recent technologies combine microscopic imaging with sequencing or other technologies to generate 'omics profiles that are linked to spatial subregions of biological specimens (Fig. 2.1).

With the maturation and standardization of a variety of 'omics approaches, efforts in recent years have focused on combining multiple 'omics data types generated from the same specimen or individual, with the hypothesis that this would lead to the elucidation of novel biological mechanisms and get us closer to complete understanding of cellular regulation. Progress here has been relatively slow due to a number of factors. First, as individual 'omics assays require significant expertise to perform and analyze, it is still rare to have NGS-based sequencing and mass spectrometry-based proteomics or metabolomics performed in the same laboratory or facility. Second, the downstream data types, formats, and scales are highly diverse, making normalization across gene expression, proteomic abundance, etc. difficult. Third, single 'omics approaches already are of high complexity, making the construction and interpretation of multi-omics networks spanning thousands to millions of diverse analytes a significant challenge.

Still, key early studies have utilized integrative multi-omics approaches in a variety of ways to shed new light on various human disease conditions. For example, proteogenomics approaches that combine genomics, transcriptomics, and proteomics have been used to identify novel driver genes and pathways associated with a variety of tumor types (Zhang et al. 2014; Alfaro et al. 2014; Mertins et al. 2016). In recent years, groups have applied integrative multi-omics approaches to make novel discoveries across a wide variety of acute and chronic diseases (Ding et al. 2015; Higdon et al. 2015; Pavel et al. 2016; Sun and Hu 2016; Zierer et al. 2016; Hasin et al. 2017; Khan et al. 2019; Eddy et al. 2020). Beyond integrating multi-omic data for a single timepoint, there is significant promise in adding a longitudinal

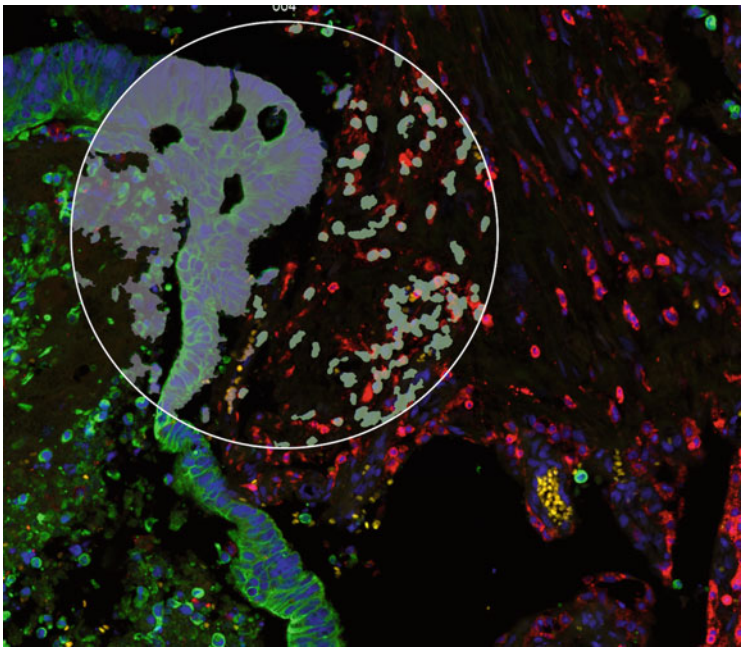

Fig. 2.1 Example tissue region of interest assessed for downstream profiling on the NanoString GeoMx Digital Spatial Profiler. The selected region of interest (ROI) is then subdivided into two masked regions for downstream spatial transcriptomic or proteomic comparisons

component: by tracking analytes over time in an individual, research may be able to uncover dynamic changes at different timeframes that might otherwise be invisible via an individual snapshot timepoint. Moreover, by tracking individuals over the course of healthy and disease states, an individual's own healthy baseline will likely provide a better control for detecting disease state changes versus typical cross-sectional studies. To this effect, our team pioneered integrative personal 'omics profiling (iPOP), an approach that utilizes dynamic multi-omic profiles generated across repeated blood and microbiome sampling over a number of years to identify analytes associated with the development of acute and chronic diseases (Chen et al. 2012). We and others have since applied these approaches across a variety of physiological states and disease conditions including T2DM, viral infection, aging, response to exercise, and changes during pregnancy and even during space exploration (Price et al. 2017; Garrett-Bakelman et al. 2019; Schussler-Fiorenza Rose et al. 2019; Zhou et al. 2019; Ahadi et al. 2020; Contrepois et al. 2020; Liang et al. 2020; Mars et al. 2020; Wilmanski et al. 2021; Zimmer et al. 2021). We expect these approaches to continue to become in widespread use across molecular biology including in the field of obesity and metabolic research.

2.4 Applying Multi-omics in Obese Cohorts

Despite the complex etiology of obesity spanning genetics and a wealth of environment and lifestyle factors, past genome-wide association studies have identified key loci associated with a predisposition to obesity. In 2007, two groups utilized genome-wide association studies (GWAS) across several large cohorts to identify a significant association between the *FTO* gene and adult and pediatric obesity (Frayling et al. 2007; Dina et al. 2007); this work has since been supplemented by significant functional characterization of FTO to determine molecular mechanisms (Fischer et al. 2009; Church et al. 2010). A variety of transcriptomic studies of blood, fat, and skeletal muscle tissues have elucidated mechanisms for obesity-mediated metabolic dysfunction, including dysregulation of adipogenesis pathways, induction of inflammatory cytokines, and other defects (Hotamisligil et al. 1993; van Harmelen et al. 2000; Nadler et al. 2000; Gómez-Ambrosi et al. 2004; You et al. 2005; Meugnier et al. 2007).

More recently, researchers have begun to integrate multiple 'omics strategies in their work, yielding novel perspectives on the biochemical processes that contribute to obesity and obesity-related phenotypes (Badoud et al. 2017; Sundekilde et al. 2020; Gomez-Llorente et al. 2020). Spector and colleagues have utilized a variety of cohorts including extensive studies of mono- and dizygotic twins to elucidate key links between obesity and aging-related molecular alterations including telomere lengths, multi-omics clusters associated with urate and oxytocin, as well as significant metabolomic perturbations (Valdes et al. 2005; Moayyeri et al. 2013; Zierer et al. 2016; Cirulli et al. 2019). Still other multi-omics studies have focused on obesity-related comorbidities, including cardiovascular effects and T2DM (Kretowski et al. 2016; Zhou et al. 2019; Regan and Shah 2020).

2.5 Longitudinal Profiling of Patients Undergoing Diet Modulation

Given that obesity is a chronic disease that develops over periods of months, years, and decades, it is important not only to characterize the steady-state biomolecular profiles of obese and lean humans but also to understand the changes that occur over time during the progression toward obesity. One way to do this is to track biomolecules longitudinally during experimental weight gain and loss using caloric excess or restriction or other diet modulations. As otherwise-matched individuals can exhibit a wide variety of physiological responses to weight gain and loss, it is important to understand from a biomolecular level what analyte changes are in common across individuals during weight gain and loss versus those that are unique to a particular subset of individuals, particularly in subsets that develop significant comorbidities such as T2DM, cardiovascular disease, and other ill effects.

For nearing a decade now, our group has been tracking a cohort of individuals with routine iPOP profiling to better understand the longitudinal multi-omic changes that occur during transitions between healthy and disease states. Over the course of

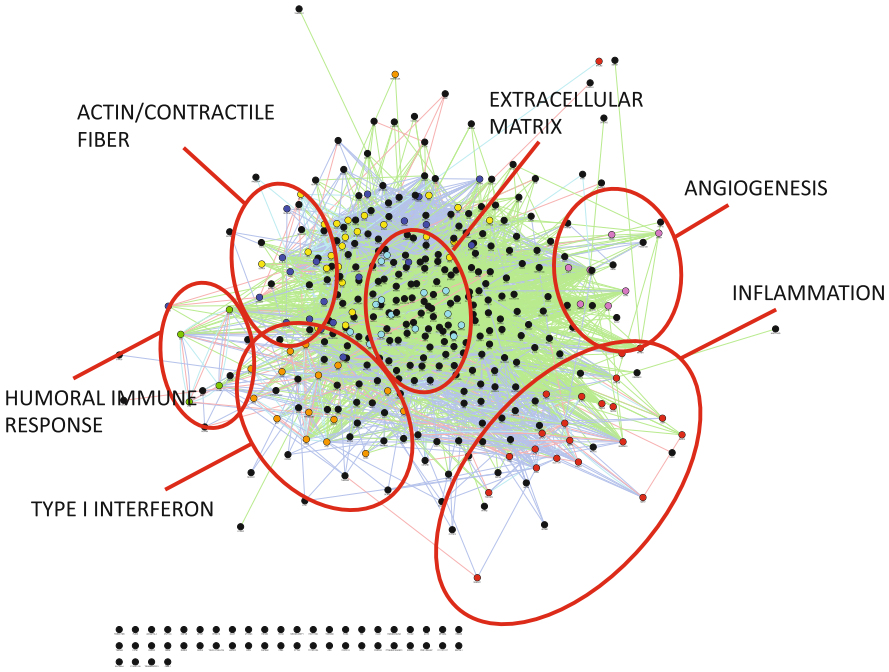

Fig. 2.2 Example Cytoscape gene expression network of weight gain-responsive genes. See Piening et al. 2018 for additional details on the dataset

these studies, a subcohort of individuals agreed to undergo a dietary perturbation, consisting of a period of controlled weight gain through caloric excess followed by a caloric restriction period back to their baseline weight (Piening et al. 2018). Multi-omics profiling was performed on blood and microbiome specimens taken over the course of this 90-day perturbation study, specifically at baseline, at peak weight, and after weight loss. Remarkably, despite the relatively modest weight gain achieved over the course of the study (2.8 kg per participant on average), a wealth of biomolecular changes were observed, including the upregulation of multiple inflammatory/immune pathways in the blood, activation of several pathways associated with cardiomyopathy, as well as remodeling of the gut microbiome (Fig. 2.2). Alleviating some of the concern associated with these results, we found that all changes reverted to baseline values when the patients subsequently returned to their baseline weight, suggesting that, at least in the short term, these biochemical alterations are entirely reversible. More recent multi-omics work using diet perturbations in mouse models has layered on additional information through profiling of diverse harvested tissues including the liver, fat, and muscle and has described novel 'omic associations with liver dysfunction and defects in lipogenesis (Badoud et al. 2017; Ægidius et al. 2020; Sundekilde et al. 2020). Still other studies have evaluated the impact of specific diet compositions including supplementation with compounds such as specific dietary fibers (Nieman et al. 2019; Chen et al. 2021;

Benítez-Páez et al. 2019). Overall, while longitudinal studies are still limited in this area and often confined to smaller cohorts, we expect this field to continue to expand leading to the identification of key biomarkers or signatures that predict negative responses to weight gain or which may be used to develop personalized interventions.

2.6 Microbiome-Host Interactions in Obesity

One area of key focus in diet and obesity research is the influence of the gut microbiome on obesity-related phenotypes. Given that host energy harvest and energy regulation are closely linked to microbial composition and function, it has become increasingly important not only to identify the specific microbial species that reside in the gut as well as their relative abundances but also to assess functional activity of these microbes through similar mechanisms (metatranscriptomics, metaproteomics, etc.) that we utilize for host 'omics.

Indeed, a large body of work has implicated microbiome function/dysfunction as a key factor in the development of obesity. Seminal work from Turnbaugh et al. linked microbiome composition differences to obese phenotypes, in particular the ratio of *Firmicutes* to *Bacteroidetes* was correlative with body fat percentage in mice, and transplantation of obesity-associated microbiota to lean mice would subsequently induce an obesity phenotype (Turnbaugh et al. 2006). This and other work elucidating links between the microbiome and obesity have led to proposals for novel strategies for treating microbiota directly as a way to treat overweight and obesity (Ridaura et al. 2013). Strategies for this include fecal transplantation (Allegretti et al. 2020; Mocanu et al. 2021) and supplementation with prebiotic fiber or probiotics (Arora et al. 2013; Everard et al. 2013; Aoun et al. 2020; Mocanu et al. 2021). Work by Sonnenburg, Gardner, and colleagues showed that while diet change could induce short-term shifts in gut microbiome composition, this was refractory, and the microbiome ultimately would revert back to its pre-perturbation state, identifying a significant challenge for microbiome-directed interventional therapy (Fragiadakis et al. 2020). An even bigger challenge remains that most microbiome studies have been conducted on Western cohorts, and given that obesity is a worldwide problem, the scope of microbiome research needs to be expanded significantly to include populations from diverse ancestries, geographies, diets, and cultures.

2.7 Summary and Future Perspectives

In summary, it is now possible to generate a comprehensive portrait of biological function spanning many levels of cellular regulation, from genomic and epigenomic programming, to transcriptomic gene expression, to large-scale proteomic profiling as well as characterization of the metabolic flux of biological systems (metabolome). Moreover, the diverse interplay between human physiology and our individualized

microbe residents (microbiome) can be deeply characterized as well (metagenome, metatranscriptome, etc.). As sequencing and other related 'omic technologies continue to decrease in cost and become more widely available, researchers will have the opportunity to expand this work to significantly larger cohorts as well as perform dense longitudinal profiling to generate dynamic multi-omic signatures associated with disease development and progression. While biomarker discovery work has traditionally focused on identifying single analytes with predictive and prognostic capability, it is reasonable to expect that larger multi-omic signatures may have better sensitivity and specificity to predict the onset of disease.

It is clear that the development and application of multi-omic approaches have significantly enhanced our understanding of the landscape of biomolecular changes associated with obesity. We can use multi-omics to stratify obese individuals based on levels of systemic inflammation, metabolic dysregulation, etc., and as these approaches become more refined, we expect that this information can be used to aid clinical decision-making in the future. Furthermore, we expect that multi-omic characterization of obese subjects will soon be an integral step in the evaluation of any novel therapeutic or interventional strategy. As discussed above, multi-omic efforts have already led to several novel treatment modalities, and there are likely many more in the pipeline.

There are still significant challenges to overcome. The field of integrative multi-omics is still in its relative infancy. As of 2021, there are still a limited number of approaches for integrating complex multi-omic data and still fewer that address longitudinal multi-omic analyses. Omics assays are generally still relatively expensive, limiting our ability to densely profile extensive cohorts of obese subjects, and in-human studies are typically limited to making inferences from non-invasive sampling of blood and/or biological fluids. Despite these challenges, integrative multi-omics clearly remains the next frontier in obesity research, with significant potential to yield translatable findings that will aid in the prevention and treatment of obesity.

References

Ægidius HM, Veidal SS, Feigh M et al (2020) Multi-omics characterization of a diet-induced obese model of non-alcoholic steatohepatitis. Sci Rep 10:1148. https://doi.org/10.1038/s41598-020-58059-7

Ahadi S, Zhou W, Schussler-Fiorenza Rose SM et al (2020) Personal aging markers and ageotypes revealed by deep longitudinal profiling. Nat Med 26:83–90. https://doi.org/10.1038/s41591-019-0719-5

Alfaro JA, Sinha A, Kislinger T, Boutros PC (2014) Onco-proteogenomics: cancer proteomics joins forces with genomics. Nat Methods 11:1107–1113. https://doi.org/10.1038/nmeth.3138

Allegretti JR, Kassam Z, Mullish BH et al (2020) Effects of fecal microbiota transplantation with Oral capsules in obese patients. Clin Gastroenterol Hepatol 18:855–863.e2. https://doi.org/10.1016/j.cgh.2019.07.006

Aoun A, Darwish F, Hamod N (2020) The influence of the gut microbiome on obesity in adults and the role of probiotics, prebiotics, and Synbiotics for weight loss. Prev Nutr Food Sci 25:113–123. https://doi.org/10.3746/pnf.2020.25.2.113

Arora T, Singh S, Sharma RK (2013) Probiotics: interaction with gut microbiome and antiobesity potential. Nutrition 29:591–596. https://doi.org/10.1016/j.nut.2012.07.017

Badoud F, Brewer D, Charchoglyan A et al (2017) Multi-omics integrative investigation of fatty acid metabolism in obese and lean subcutaneous tissue. OMICS 21:371–379. https://doi.org/10.1089/omi.2017.0049

Bain JR, Stevens RD, Wenner BR et al (2009) Metabolomics applied to diabetes research: moving from information to knowledge. Diabetes 58:2429–2443. https://doi.org/10.2337/db09-0580

Benítez-Páez A, Kjølbæk L, Gómez del Pulgar EM et al (2019) A multi-omics approach to unraveling the microbiome-mediated effects of arabinoxylan oligosaccharides in overweight humans. mSystems 4:e00209-19. https://doi.org/10.1128/mSystems.00209-19

Brown PO, Botstein D (1999) Exploring the new world of the genome with DNA microarrays. Nat Genet 21:33–37. https://doi.org/10.1038/4462

Buenrostro J, Wu B, Chang H, Greenleaf W (2015) ATAC-seq: a method for assaying chromatin accessibility genome-wide. Curr Protoc Mol Biol 109:21.29.1–21.29.9. https://doi.org/10.1002/0471142727.mb2129s109

Chen R, Mias GI, Li-Pook-Than J et al (2012) Personal omics profiling reveals dynamic molecular and medical phenotypes. Cell 148:1293–1307. https://doi.org/10.1016/j.cell.2012.02.009

Chen Y-S, Li J, Menon R et al (2021) Dietary spinach reshapes the gut microbiome in an Apc-mutant genetic background: mechanistic insights from integrated multi-omics. Gut Microbes 13:1972756. https://doi.org/10.1080/19490976.2021.1972756

Church C, Moir L, McMurray F et al (2010) Overexpression of Fto leads to increased food intake and results in obesity. Nat Genet 42:1086–1092. https://doi.org/10.1038/ng.713

Cirulli ET, Guo L, Leon Swisher C et al (2019) Profound perturbation of the metabolome in obesity is associated with health risk. Cell Metabol 29:488–500.e2. https://doi.org/10.1016/j.cmet.2018.09.022

Clark SJ, Harrison J, Paul CL, Frommer M (1994) High sensitivity mapping of methylated cytosines. Nucleic Acids Res 22:2990–2997

Contrepois K, Wu S, Moneghetti KJ et al (2020) Molecular choreography of acute exercise. Cell 181:1112–1130.e16. https://doi.org/10.1016/j.cell.2020.04.043

Dina C, Meyre D, Gallina S et al (2007) Variation in FTO contributes to childhood obesity and severe adult obesity. Nat Genet 39:724–726. https://doi.org/10.1038/ng2048

Ding K, Wu S, Ying W et al (2015) Leveraging a multi-omics strategy for prioritizing personalized candidate mutation-driver genes: a proof-of-concept study. Sci Rep 5:17564. https://doi.org/10.1038/srep17564

Ding L, Rath E, Bai Y (2017) Comparison of alternative splicing junction detection tools using RNASeq data. Curr Genomics 18:268–277

Eddy S, Mariani LH, Kretzler M (2020) Integrated multi-omics approaches to improve classification of chronic kidney disease. Nat Rev Nephrol 16:657–668. https://doi.org/10.1038/s41581-020-0286-5

Everard A, Belzer C, Geurts L et al (2013) Cross-talk between Akkermansia muciniphila and intestinal epithelium controls diet-induced obesity. Proc Natl Acad Sci U S A 110:9066–9071. https://doi.org/10.1073/pnas.1219451110

Fan X, Abbott TE, Larson D, Chen K (2014) BreakDancer - identification of genomic structural variation from paired-end read mapping. current protocols in bioinformatics/editorial board, Andreas D Baxevanis. https://doi.org/10.1002/0471250953.bi1506s45

Fischer J, Koch L, Emmerling C et al (2009) Inactivation of the Fto gene protects from obesity. Nature 458:894–898. https://doi.org/10.1038/nature07848

Fragiadakis GK, Wastyk HC, Robinson JL et al (2020) Long-term dietary intervention reveals resilience of the gut microbiota despite changes in diet and weight. Am J Clin Nutr 111:1127–1136. https://doi.org/10.1093/ajcn/nqaa046

Frayling TM, Timpson NJ, Weedon MN et al (2007) A common variant in the FTO gene is associated with body mass index and predisposes to childhood and adult obesity. Science 316:889–894

Garrett-Bakelman FE, Darshi M, Green SJ et al (2019) The NASA twins study: a multidimensional analysis of a year-long human spaceflight. Science 364(6436):eaau8650. https://doi.org/10.1126/science.aau8650

Gómez-Ambrosi J, Catalán V, Diez-Caballero A et al (2004) Gene expression profile of omental adipose tissue in human obesity. FASEB J 18:215–217. https://doi.org/10.1096/fj.03-0591fje

Gomez-Llorente MA, Martínez-Cañavate A, Chueca N et al (2020) A multi-omics approach reveals new signatures in obese allergic asthmatic children. Biomedicine 8:359. https://doi.org/10.3390/biomedicines8090359

Hamady M, Knight R (2009) Microbial community profiling for human microbiome projects: tools, techniques, and challenges. Genome Res 19:1141–1152. https://doi.org/10.1101/gr.085464.108

Hasin Y, Seldin M, Lusis A (2017) Multi-omics approaches to disease. Genome Biol 18:83. https://doi.org/10.1186/s13059-017-1215-1

Higdon R, Earl RK, Stanberry L et al (2015) The promise of multi-omics and clinical data integration to identify and target personalized healthcare approaches in autism spectrum disorders. Omics J Integr Biol 19:197–208. https://doi.org/10.1089/omi.2015.0020

Hotamisligil GS, Shargill NS, Spiegelman BM (1993) Adipose expression of tumor necrosis factor-alpha: direct role in obesity-linked insulin resistance. Science 259:87–91

Kerr G, Ruskin HJ, Crane M, Doolan P (2008) Techniques for clustering gene expression data. Comput Biol Med 38:283–293. https://doi.org/10.1016/j.compbiomed.2007.11.001

Khan MM, Ernst O, Manes NP et al (2019) Multi-omics strategies uncover host–pathogen interactions. ACS Infect Dis 5:493–505. https://doi.org/10.1021/acsinfecdis.9b00080

Kretowski A, Ruperez FJ, Ciborowski M (2016) Genomics and metabolomics in obesity and type 2 diabetes. J Diabetes Res 2016:9415645. https://doi.org/10.1155/2016/9415645

Kumar S, Vo AD, Qin F, Li H (2016) Comparative assessment of methods for the fusion transcripts detection from RNA-seq data. Sci Rep 6:21597. https://doi.org/10.1038/srep21597

Lam HY, Mu XJ, Stutz AM et al (2010) Nucleotide-resolution analysis of structural variants using BreakSeq and a breakpoint library. Nat Biotechnol 28:47–55. https://doi.org/10.1038/nbt.1600

Lander ES, Linton LM, Birren B et al (2001) Initial sequencing and analysis of the human genome. Nature 409:860–921. https://doi.org/10.1038/35057062

Lefrançois P, Euskirchen GM, Auerbach RK et al (2009) Efficient yeast ChIP-seq using multiplex short-read DNA sequencing. BMC Genomics 10:37. https://doi.org/10.1186/1471-2164-10-37

Li H, Durbin R (2009) Fast and accurate short read alignment with burrows-wheeler transform. Bioinformatics 25:1754–1760. https://doi.org/10.1093/bioinformatics/btp324

Liang L, Rasmussen MH, Piening B et al (2020) Metabolic dynamics and prediction of gestational age and time to delivery in pregnant women. Cell 181(1680–1692):e15. https://doi.org/10.1016/j.cell.2020.05.002

Love MI, Huber W, Anders S (2014) Moderated estimation of fold change and dispersion for RNA-seq data with DESeq2. Genome Biol 15:550. https://doi.org/10.1186/s13059-014-0550-8

Mardis ER (2011) A decade's perspective on DNA sequencing technology. Nature 470:198–203. https://doi.org/10.1038/nature09796

Mars RAT, Yang Y, Ward T et al (2020) Longitudinal multi-omics reveals subset-specific mechanisms underlying irritable bowel syndrome. Cell 182:1460–1473.e17. https://doi.org/10.1016/j.cell.2020.08.007

McKenna A, Hanna M, Banks E et al (2010) The genome analysis toolkit: a MapReduce framework for analyzing next-generation DNA sequencing data. Genome Res 20:1297–1303. https://doi.org/10.1101/gr.107524.110

Mertins P, Mani DR, Ruggles KV et al (2016) Proteogenomics connects somatic mutations to signalling in breast cancer. Nature 534:55–62. https://doi.org/10.1038/nature18003

Meugnier E, Bossu C, Oliel M et al (2007) Changes in gene expression in skeletal muscle in response to fat overfeeding in lean men. Obesity 15:2583–2594. https://doi.org/10.1038/oby.2007.310

Moayyeri A, Hammond CJ, Valdes AM, Spector TD (2013) Cohort profile: TwinsUK and healthy ageing twin study. Int J Epidemiol 42:76–85. https://doi.org/10.1093/ije/dyr207

Mocanu V, Zhang Z, Deehan EC et al (2021) Fecal microbial transplantation and fiber supplementation in patients with severe obesity and metabolic syndrome: a randomized double-blind, placebo-controlled phase 2 trial. Nat Med 27:1272–1279. https://doi.org/10.1038/s41591-021-01399-2

Mohiyuddin M, Mu JC, Li J et al (2015) MetaSV: an accurate and integrative structural-variant caller for next generation sequencing. Bioinformatics 31:2741–2744. https://doi.org/10.1093/bioinformatics/btv204

Mortazavi A, Williams BA, McCue K et al (2008) Mapping and quantifying mammalian transcriptomes by RNA-seq. Nat Methods 5:621–628. https://doi.org/10.1038/nmeth.1226

Nadler ST, Stoehr JP, Schueler KL et al (2000) The expression of adipogenic genes is decreased in obesity and diabetes mellitus. PNAS 97:11371–11376. https://doi.org/10.1073/pnas.97.21.11371

Nagalakshmi U, Wang Z, Waern K et al (2008) The transcriptional landscape of the yeast genome defined by RNA sequencing. Science 320:1344–1349. https://doi.org/10.1126/science.1158441

Nieman DC, Lila MA, Gillitt ND (2019) Immunometabolism: a multi-omics approach to interpreting the influence of exercise and diet on the immune system. Annu Rev Food Sci Technol 10:341–363. https://doi.org/10.1146/annurev-food-032818-121316

Parker CE, Pearson TW, Anderson NL, Borchers CH (2010) Mass-spectrometry-based clinical proteomics – a review and prospective. Analyst 135:1830–1838. https://doi.org/10.1039/C0AN00105H

Pavel AB, Sonkin D, Reddy A (2016) Integrative modeling of multi-omics data to identify cancer drivers and infer patient-specific gene activity. BMC Syst Biol 10:16. https://doi.org/10.1186/s12918-016-0260-9

Petrera A, von Toerne C, Behler J et al (2021) Multiplatform approach for plasma proteomics: complementarity of Olink proximity extension assay technology to mass spectrometry-based protein profiling. J Proteome Res 20:751–762. https://doi.org/10.1021/acs.jproteome.0c00641

Piening BD, Zhou W, Contrepois K et al (2018) Integrative personal omics profiles during periods of weight gain and loss. Cell Syst 6(157–170):e8. https://doi.org/10.1016/j.cels.2017.12.013

Pollex T, Hanna K, Schaefer M (2010) Detection of cytosine methylation in RNA using bisulfite sequencing. Cold Spring Harb Protoc 2010:pdb prot5505. https://doi.org/10.1101/pdb.prot5505

Price ND, Magis AT, Earls JC et al (2017) A wellness study of 108 individuals using personal, dense, dynamic data clouds. Nat Biotechnol 35:747–756. https://doi.org/10.1038/nbt.3870

Qi H, Wang F, Tao S (2019) Proteome microarray technology and application: higher, wider, and deeper. Expert Rev Proteomics 16:815–827. https://doi.org/10.1080/14789450.2019.1662303

Regan JA, Shah SH (2020) Obesity genomics and metabolomics: a nexus of cardiometabolic risk. Curr Cardiol Rep 22:174. https://doi.org/10.1007/s11886-020-01422-x

Ridaura VK, Faith JJ, Rey FE et al (2013) Gut microbiota from twins discordant for obesity modulate metabolism in mice. Science 341:1241214. https://doi.org/10.1126/science.1241214

Schaefer M, Pollex T, Hanna K, Lyko F (2009) RNA cytosine methylation analysis by bisulfite sequencing. Nucleic Acids Res 37:e12. https://doi.org/10.1093/nar/gkn954

Schena M, Shalon D, Davis RW, Brown PO (1995) Quantitative monitoring of gene expression patterns with a complementary DNA microarray. Science 270:467–470. https://doi.org/10.1126/science.270.5235.467

Schussler-Fiorenza Rose SM, Contrepois K, Moneghetti KJ et al (2019) A longitudinal big data approach for precision health. Nat Med 25:792–804. https://doi.org/10.1038/s41591-019-0414-6

Shapiro E, Biezuner T, Linnarsson S (2013) Single-cell sequencing-based technologies will revolutionize whole-organism science. Nat Rev Genet 14:618–630. https://doi.org/10.1038/nrg3542

Song L, Crawford GE (2010) DNase-seq: a high-resolution technique for mapping active gene regulatory elements across the genome from mammalian cells. Cold Spring Harb Protoc 2010:pdb.prot5384. https://doi.org/10.1101/pdb.prot5384

Stears RL, Martinsky T, Schena M (2003) Trends in microarray analysis. Nat Med 9:140–145. https://doi.org/10.1038/nm0103-140

Sun YV, Hu Y-J (2016) Chapter three - integrative analysis of multi-omics data for discovery and functional studies of complex human diseases. In: Friedmann T, Dunlap JC, Goodwin SF (eds) Advances in genetics. Academic Press, Cambridge, pp 147–190

Sundekilde UK, Yde CC, Honore AH et al (2020) An integrated multi-omics analysis defines key pathway alterations in a diet-induced obesity mouse model. Meta 10:80. https://doi.org/10.3390/metabo10030080

Teh AL, Pan H, Lin X et al (2016) Comparison of methyl-capture sequencing vs. Infinium 450K methylation array for methylome analysis in clinical samples. Epigenetics 11:36–48. https://doi.org/10.1080/15592294.2015.1132136

Turnbaugh PJ, Ley RE, Mahowald MA et al (2006) An obesity-associated gut microbiome with increased capacity for energy harvest. Nature 444:1027–1031. https://doi.org/10.1038/nature05414

Valdes A, Andrew T, Gardner J et al (2005) Obesity, cigarette smoking, and telomere length in women. Lancet 366:662–664. https://doi.org/10.1016/S0140-6736(05)66630-5

van Dijk EL, Jaszczyszyn Y, Naquin D, Thermes C (2018) The third revolution in sequencing technology. Trends Genet 34:666–681. https://doi.org/10.1016/j.tig.2018.05.008

van Harmelen V, Ariapart P, Hoffstedt J et al (2000) Increased adipose angiotensinogen gene expression in human obesity. Obes Res 8:337–341. https://doi.org/10.1038/oby.2000.40

Wang Z, Gerstein M, Snyder M (2009) RNA-seq: a revolutionary tool for transcriptomics. Nat Rev Genet 10:57–63. https://doi.org/10.1038/nrg2484

Wilmanski T, Diener C, Rappaport N et al (2021) Gut microbiome pattern reflects healthy ageing and predicts survival in humans. Nat Metab 3:274–286. https://doi.org/10.1038/s42255-021-00348-0

Wolfsberg TG, McEntyre J, Schuler GD (2001) Guide to the draft human genome. Nature 409:824–826. https://doi.org/10.1038/35057000

You T, Yang R, Lyles MF et al (2005) Abdominal adipose tissue cytokine gene expression: relationship to obesity and metabolic risk factors. Am J Physiol Endocrinol Metab 288:E741–E747. https://doi.org/10.1152/ajpendo.00419.2004

Zhang B, Wang J, Wang X et al (2014) Proteogenomic characterization of human colon and rectal cancer. Nature 513:382–387. https://doi.org/10.1038/nature13438

Zhou W, Sailani MR, Contrepois K et al (2019) Longitudinal multi-omics of host-microbe dynamics in prediabetes. Nature 569:663–671. https://doi.org/10.1038/s41586-019-1236-x

Zichi D, Koga T, Greef C et al (2002) Photoaptamer technology: development of multiplexed microarray protein assays. Clin Chem 48:1865–1868. https://doi.org/10.1093/clinchem/48.10.1865

Zierer J, Pallister T, Tsai PC et al (2016) Exploring the molecular basis of age-related disease comorbidities using a multi-omics graphical model. Sci Rep 6:37646. https://doi.org/10.1038/srep37646

Zimmer A, Korem Y, Rappaport N et al (2021) The geometry of clinical labs and wellness states from deeply phenotyped humans. Nat Commun 12:3578. https://doi.org/10.1038/s41467-021-23849-8

Impact of Probiotic and Prebiotic on Gut Microbiota in Pre-diabetes and Type 2 Diabetes

3

Fernanda Maria Manzini Ramos, Mateus Kawata Salgaço, Thais Cesar, and Katia Sivieri

3.1 Introduction

Pre-diabetes is a stage that usually precedes the onset of type 2 diabetes with a slight increase in fasting glucose, between 5.6 and 6.9 mmol/L; decreased glucose tolerance, between 7.8 and 11 mmol/L; and glycated hemoglobin, between 5.5 and 6.4% (ADA 2020). These biochemical abnormalities are usually caused by defects in insulin secretion from pancreatic cells, low insulin activity, or both (Unwin et al. 2002). Pre-diabetes can eventually lead to type 2 diabetes, which is characterized by hyperglycemia due to the inability of cells to respond fully to insulin, or to be resistant to insulin. Insulin resistance is characterized by insulin inefficiency in promoting glucose uptake by tissues and low intracellular glucose concentration signals for increased insulin production by the pancreas. Over time, depleted pancreatic beta cells reduce or stop insulin production, further elevating blood glucose levels (>6.9 mmol/L), characteristic of the diabetes condition. According to epidemiological data, type 2 diabetes is common in the elderly, but its frequency has increased in children and young adults due to high rates of obesity, sedentary lifestyle, and unbalanced diet, with excess fat and sugar. All of these factors indicate that both type 1 and type 2 diabetes result from a combination of genetic predisposition and environmental triggers (IDF 2020).

Type 2 diabetes symptoms are similar to those of type 1 diabetes, but they are difficult to be identified in the early stages due to the long pre-diagnosis process, and, therefore, up to one third of the population may not be diagnosed early (Bansal 2015; Kaur 2014; Buchanan et al. 2002). This can be detrimental for a favorable prognosis after a long period of latent disease, and complications such as retinopathy or ulcers in the lower limbs that do not heal may occur (Chiasson et al. 2002). Furthermore,

F. M. M. Ramos · M. K. Salgaço · T. Cesar (✉) · K. Sivieri
Department of Food and Nutrition, School of Pharmaceutical Sciences, São Paulo State University (UNESP), Araraquara, SP, Brazil
e-mail: thais.cesar@unesp.br

B. Dinda (ed.), *Natural Products in Obesity and Diabetes*,
https://doi.org/10.1007/978-3-030-92196-5_3

visceral obesity common in overweight and obese patients is related to the local and systemic inflammatory process, closely linked to the development of these comorbidities (ADA 2020). Regarding the healthy population, individuals with pre-diabetes and diabetes have a higher risk over the time of developing cardiovascular disease, metabolic syndrome, and polycystic ovaries, in addition to higher morbidity and mortality rates (Bansal 2015; Kaur 2014).

Considering the close relationship between pre-diabetes, obesity, and diet, it is important to examine the influence of intestinal microbiota in this context. Intestinal microbiota is characterized by a diverse community of bacteria responsible for influencing nutrient metabolism, immune responses, and resistance to infectious pathogens (Nicholson et al. 2012; Belkaid and Hand 2014; van Nood et al. 2013). In the diabetic population, the intestinal microbiota presents a pattern of dysbiosis, which can be the starting point for the evolution of pre-diabetes to type 2 diabetes and other chronic diseases (Pratley 2013; Ziemer et al. 2008; Tsui et al. 2008; Stefanakia et al. 2018). Current scientific evidence has shown that probiotics or prebiotics, including phenolic compounds, can play a widely recognized role in the regulation of the intestinal microbiota, altering microbial composition and the metabolism of the bacteria and host (Tsai et al. 2019; Wang et al. 2020). Based on these fundamentals, this chapter will address the intrinsic relationships between the consumption of probiotics and prebiotics in individuals with pre-diabetes and type 2 diabetes.

3.2 Gut Microbiota in Pre-diabetes and Type 2 Diabetes

The collection of Bacteria, Archaea, and Eukarya colonizing the gastrointestinal tract is termed the gut microbiota and has co-evolved with the host over thousands of years to form an intricate and mutually beneficial relationship. The number of microorganisms inhabiting the gastrointestinal tract has been estimated to exceed 10^{14}. Then, a result of the vast number of bacterial cells in the body, the host, and the microorganisms inhabiting it are often referred to as a "superorganism" (Thursby and Juge 2017).

Gut microbiota is composed mainly of five dominant phyla: *Bacteroidetes*, *Firmicutes*, *Actinobacteria*, *Proteobacteria*, and *Verrucomicrobia*, the first two being predominant, representing more than 90% of total gut bacteria (Qin et al. 2010; Huttenhower et al. 2012). Regarding species, the adult intestine harbors to approximately 500–1000 different bacterial genus, of which 300–500 are found in the colon and the most abundant of which are *Bacteroides*, *Clostridium*, *Prevotella*, *Eubacterium*, *Ruminococcus*, *Fusobacterium*, *Peptococcus*, *Peptostreptococcus*, and *Bifidobacterium* and the least present: *Escherichia*, *Enterococcus*, *Klebsiella*, *Lactobacillus*, and *Proteus* (Blaut and Clavel 2007; O'Hara and Shanahan 2006; Moore and Holdeman 1974; Suau et al. 1999).

Although the intestinal microbiota is unique for each individual, microbiota profiles are often similar among healthy individuals, and the diversity of the microbiota is directly related to the healthy profile of these individuals (Lozupone

et al. 2012; Zoetendal et al. 1998; Qin et al. 2010; Human 2012; Turnbaugh et al. 2009). In addition, the gut microbiota has been recognized to provide essential functions for host physiology, including metabolism, immunity, neuronal development, resistance to infectious pathogens, fermentation of non-digestible carbohydrates (fiber food) into short-chain fatty acids (SCFA), harvesting energy from food components, nutrient conversion, production of water-soluble vitamins and metabolites, and degradation of xenobiotics (Nicholson et al. 2012; Belkaid and Hand 2014; van Nood et al. 2013; Braune and Blaut 2016; Huang et al. 2016).

The increase of microbial diversity and microbial homeostasis is a key factor in health. A balanced microbial composition provides several benefits such as maintaining the healthy metabolic phenotype, having a direct influence on biochemistry, and protection against susceptibility to diseases (Chiva-Blanch and Visioli 2012; Zmora et al. 2019). Therefore, the increase in bacterial diversity is associated with better glucose regulation and less adiposity and inflammation. On the other hand, a low richness of the microbiota is associated with adiposity, insulin resistance, dyslipidemia, and inflammation (Marchesi et al. 2016; Le Chatelier et al. 2013).

Dysbiosis, which corresponds to changes in microbiota homeostasis, is characterized by a reduced microbial diversity, decreased abundance of butyrate-producing bacteria, increased opportunistic pathogens, and enriched mucin-degrading bacteria, among other characteristics such as changes in resistance, resilience, and stability (Lloyd-Price et al. 2016; Stefanakia et al. 2018). Studies show that low bacterial richness is associated with metabolic diseases, such as obesity, pre-diabetes, and type 2 diabetes (Mosca et al. 2016).

Among obese individuals, microbial dysbiosis is characterized by reduced proportions of members of the phylum *Bacteroidetes*, with an increased abundance of *Firmicutes*; however, a review by Bianchi (2018) on obesity and microbiota showed that the *Firmicutes*/*Bacteroidetes* ratio can change depending on the obese population studied; however, further studies including families, genera, and species are still needed to better identify the obese microbiota signature (Turnbaugh et al. 2009; Armougom et al. 2009; Bianchi et al. 2018).

Individuals with pre-diabetes and type 2 diabetes have lower abundance of SCFA and proliferation of non-butyrate-producing bacteria such as *Escherichia coli* and *Staphylococcus aureus*. Butyrate-producing bacteria can exert substantial beneficial metabolic and immune effects (Shen et al. 2013; Tilg and Moschen 2014). A Chinese clinical trial showed that diabetic individuals have less abundance of *Roseburia intestinalis* and *Faecalibacterium prausnitzii* (butyrate-producing bacteria) and greater abundance of *Lactobacillus gasseri*, *Streptococcus mutans*, *Proteobacteria*, and certain *Clostridiales*. Some studies highlight the reduced proportions of bacteria from the phylum *Bacteroidetes*, accompanied, in some cases, by increased proportions of phylum *Firmicutes*, like obese individuals (Turnbaugh et al. 2009; Armougom et al. 2009; Tilg and Moschen 2014).

Intestinal dysbiosis among pre-diabetic and obese individuals may be the trigger for the onset of type 2 diabetes, being a constant low-grade inflammatory stimulus that characterizes metabolic diseases in general (Stefanakia et al. 2018). Pre-diabetic

and type 2 diabetic patients usually exhibit an obese anthropometric profile, including altered BMI and increased waist circumference and waist-hip ratio, which closely correlates to the metabolic profile of these individuals' microbiota (Matos et al. 2011).

Type 2 diabetes is associated with increased bacterial expression of genes involved in oxidative stress, creating a pro-inflammatory signature in the intestinal microbiome (Turnbaugh et al. 2009; Armougom et al. 2009; Tilg and Moschen 2014).

Intestinal dysbiosis is related to metabolic diseases, such as diabetes and obesity, through increased permeability of the intestinal barrier that translocate bacterial endotoxins into the circulation. These endotoxins are derived from membrane components of gram-negative bacteria, such as lipopolysaccharides (LPS), which activate the host's innate immunity receptors, leading to metabolic endotoxemia (Neyrinck et al. 2016; Torres et al. 2018; Andreasen et al. 2010).

LPS can also be a trigger for the onset of insulin resistance, as it leads to the secretion of pro-inflammatory cytokines. The toll-like receptor 4 (TLR-4) is activated by LPS and this activation induces the nuclear inflammatory transcription factor kappa B (NF-kB) to trigger a systemic inflammatory process, with activation of the M1 macrophages and their infiltration in the visceral adipose tissue. This contributes to the increase of the inflammatory state, and the release of TNF alpha (TNFα) cytokines, interleukin-1 (IL1), interleukin-6 (IL6), leptin, resistin, and C-reactive protein (CRP), leading to insulin resistance (Neyrinck et al. 2016; Torres et al. 2018; Andreasen et al. 2010). Thus, the metabolic endotoxemia process is associated with changes in the intestinal microbiota, systemic inflammation, and metabolic dysfunctions (Torres et al. 2018; Ejtahed et al. 2012).

Therefore, modulation of the microbiota by diet can lead to changes in bacterial taxa, which may prevent the evolution from pre-diabetes to type 2 diabetes (Mohamadshahi et al. 2014).

The intestinal microbiota is responsible for the conversion of components of the diet, leading to the production of metabolites, which can have beneficial effects on human health (Blaut and Clavel 2007). As already mentioned, bacteria are responsible for the fermentation of complex polymers (such as carbohydrates and proteins), and the high diversity of bacteria, which is reduced in dysbiosis, is extremely important for this fermentation to occur, with the cooperative action of different microbial groups. The decomposition of carbohydrates and proteins gives rise to mono- and oligomeric compounds, which can undergo further decomposition, giving rise to SCFA (mainly acetate, propionate, and butyrate). The formation of SCFA is relevant because the host recovers part of the energy contained in the dietary fiber that would be lost if the substrate was not formed (Rajkumar et al. 2014).

The interrelationships between diet and the microbiota and their collective effect on the host, only now beginning to be deciphered, might reconcile some of the discrepancies that have been troubling nutrition researchers and could explain some of the previously unintelligible variability encountered in the response to diet. Therefore, one of the ways of modifying the microbiota through the diet may be

through the ingestion of probiotics, prebiotics, and symbiotics that will be widely discussed in the next section.

3.3 Probiotics

Live microorganisms, which must be administered in an adequate amount to benefit the health of the host, can act directly by their administration or by interacting with other organisms (Hill et al. 2014). These benefits occur through various mechanisms, such as the production of substances that inhibit the growth of pathogens (H_2O_2, bacteriocins, organic acids), blockage of the pathogenic bacteria adhesion sites, competition with pathogenic microorganisms for nutrients, degradation and blocking of receptors for toxins, and, finally, modulation of immune responses (Ostadrahimi et al. 2015).

Probiotics are non-invasive and can be an effective adjuvant therapy to pre-diabetes, leading to better glycemic control and possible interruption of type 2 diabetes development (Stefanakia et al. 2018). Probiotics can modify the profile of the intestinal microbiota, directly influencing metabolic parameters related to the glycemic profile, such as fasting glycemia and hemoglobin A1c and improving insulin sensitivity (Madjd et al. 2016; Sato et al. 2017; Sabico et al. 2017). They can also have positive effects on inflammatory markers such as interleukin-6 (IL-6) and interleukin-17 (IL-1β) (Razmpoosh et al. 2019).

For the control of type 2 diabetes, the probiotics normally used are strains of bacteria of the genus *Bifidobacterium*, to stabilize the microbiota of this group of individuals who tend to be dysbiosic. The use of this probiotic can decrease the permeability of the intestinal barrier, reducing the absorption of endotoxins and, thus, decreasing the inflammatory state directly related to insulin resistance (Szulińska et al. 2018). *Bifidobacterium* genus does not degrade glycoproteins in intestinal mucus, as do pathogenic bacteria, promoting a healthier environment and preventing bacterial permeability and translocation (Khalili et al. 2019; Depommier et al. 2019). Members of *Lactobacillaceae* family have been widely used as a probiotic to combat dysbiosis in the microbiota of individuals with pre-diabetes and type 2 diabetes (Rezazadeh et al. 2019).

As discussed before, most of the microorganisms considered as "probiotics" belong to the *Lactobacillaceae* family and *Bifidobacterium* genus. Nevertheless, this family or genera are not dominant in the intestinal microbiota in adults. This observation, combined with the increasing knowledge of the human microbiome, suggests that many potential novel probiotic candidates can be isolated from the dominant members of the adult microbiota. In this sense, the literature highlights the interest in several species such as *Faecalibacterium prausnitzii* and *Akkermansia muciniphila* as potential next-generation probiotics (NGPs) (Roediger 1980).

Akkermansia muciniphila, particularly, has low abundance among pre-diabetic and type 2 diabetic individuals, is characterized by anaerobiosis, and uses mucin as the only source to obtain elements of carbon and nitrogen, producing SCFA and being responsible for improving metabolic functions and the host's immune

response (Moore and Holdeman 1974). Increasing the abundance of *Akkermansia muciniphila* can be a strategy to improve glucose tolerance, act directly on the action of insulin, supply nutrients (acetate and propionate) for the growth of beneficial bacteria, and reduce intestinal permeability through regulation of mucin, which helps to improve metabolic endotoxemia, present in this group of individuals (Torres et al. 2018).

Table 3.1 described clinical trials with different probiotics and which had positive results in relation to the glycemic profile of obese, pre-diabetic, and type 2 diabetic individuals. It is important to note that the metabolic effects and the impact on the intestinal microbiota by probiotics will depend on the probiotic strain and daily dose (Razmpoosh et al. 2019). It is important to highlight that the dose of probiotics used in clinical studies ranged from 10^6 to 10^{10} cfu/g. However, there is a trend in more recent studies using doses greater than 10^9 cfu/g. The outcomes found in clinical trials showed improvement of fasting blood glucose (WHO 2018), decrease in HbA1c (Pandey et al. 2015; Vulevic et al. 2008), improvement of HOMA-IR (Wang 2009), reduction in bacterial translocation, and change in intestinal microbiota in type 2 diabetic volunteers; improvement in insulin sensitivity in overweight healthy adults (Kellow et al. 2014); and reduction in the level of blood glucose in volunteers with metabolic syndrome (Cui et al. 2017). The effects of treatment with probiotics appear after at least 4 weeks of supplementation. However, long-term studies (12 to 16 weeks) have shown interesting clinical results.

The main probiotic strains that have shown efficacy in the adjuvant treatment of type 2 diabetes were *L. acidophilus*, *L. casei* strain Shirota, and *B. lactis* Bb12. It is important to highlight a clinical trial that used a pasteurized *Akkermansia muciniphila* and showed improvement in insulin sensitivity and reduced insulinemia in overweight/obese insulin-resistant volunteers (Ouwehand et al. 2005).

3.4 Prebiotics

Prebiotic was described as "a non-digestible food ingredient that beneficially affects the host by selectively stimulating the growth and/or activity of one or a limited number of bacteria in the colon, and thus improves host health." In 2008, the 6th Meeting of the International Scientific Association of Probiotics and Prebiotics (ISAPP) defined "dietary prebiotics" as "a selectively fermented ingredient that results in specific changes in the composition and/or activity of the gastrointestinal microbiota, thus conferring benefit(s) upon host health" (Roediger 1980; WHO 2018; Pandey et al. 2015). The concept of prebiotics has been increasingly proposed as a modulator of ecology and microbial physiology in humans (Liu et al. 2017). It can be used as an alternative to probiotics or as an additional support for them (Markowiak and Slizewska 2017).

The effect of administering a prebiotic is usually due to an increase in the abundance of beneficial bacteria, mainly of the genus *Bifidobacterium* (Schiffrin et al. 2007; Vulevic et al. 2008). In general, prebiotics can regulate the relative abundance of bacteria, decreasing, for example, the abundance of bacteria in the

Table 3.1 Clinical trials with probiotics and respective effects on the glycemic profile of obese, pre-diabetic, and type 2 diabetic individuals

Effect	Probiotic(s)	Dose/duration	Authors
Insulin sensitivity was preserved in type 2 diabetic volunteers	Capsules with freeze-dried *L. acidophilus* NCFM	10^{10} cfu/g. 1× day/4 weeks	Andreasen et al. (2010)
Improved fasting blood glucose and antioxidant status in type 2 diabetic volunteers	300 g/d of probiotic yogurt with *L. acidophilus* La5 and *B. lactis* Bb12	*L. acidophilus* La5 (7.23×10^6 cfu/g); *B. lactis* Bb12 (6.04×10^6 cfu/g) 1× day/6 weeks	Ejtahed et al. (2012)
Decrease in HbA1c in type 2 diabetic volunteers	300 g/d of probiotic yogurt with *L. delbrueckii* subsp. bulgaricus, *S. thermophilus*, *B. animalis* subsp. lactis Bb12 (DSM 10140), and *L. acidophilus* La5	3.7×10^6 cfu/g 1× day/8 weeks	Mohamadshahi et al. (2014)
Improvement in insulin sensitivity in overweight healthy adults	Freeze-dried pharmaceutical probiotic with *B. longum*, *B. infantis*, *B. breve*, *L. acidophilus*, *L. paracasei*, *L. delbrueckii* subsp. bulgaricus, *L. plantarum*, *S. salivarius* subsp. thermophilus	112.5×10^9 cfu/ capsule 1× day/6 weeks	Rajkumar et al. (2014)
Reduction of glucose levels in postmenopausal women with metabolic syndrome	80 mL/d of fermented milk with *L. plantarum* (Lp 115)	1.25×10^7 cfu/g. 1× / 90 days	Barreto et al. (2014)
Reduction in HbA1C in type 2 diabetic volunteers	600 mL/d of probiotic fermented milk (kefir) with *L. casei*, *L. acidophilus*, and *B. lactis*	*L. casei* (2×10^6 cfu/ mL); *L. acidophilus* (3×10^6 cfu/mL); *B. lactis* (0.5×10^6 cfu/mL) 1× /8 weeks	Ostadrahimi et al. (2015)
Positive changes in insulin sensitivity, measured by HOMA-IR and 2 h postprandial glucose	200 g of probiotic yogurt with *S. thermophilus* and *L. bulgaricus*, enriched with *L. acidophilus* LA5 and *B. lactis* BB12	1×10^7 cfu/g 2× day/12 weeks	Madjd et al. (2016)
Reduction in bacterial translocation and change in intestinal	80 mL/d of fermented milk with *L. casei* strain Shirota	4×10^{10} cfu/g. 1× day/16 weeks	Sato et al. (2017)

(continued)

Table 3.1 (continued)

Effect	Probiotic(s)	Dose/duration	Authors
microbiota in type 2 diabetic volunteers			
Improved HOMA-IR status in type 2 diabetic volunteers	Sachets with 2 g freeze-dried powder of the probiotic mixture with *B. bifidum* W23, *B. lactis* W52, *L. acidophilus* W37, *L. brevis* W63, *L. casei* W56, *L. salivarius* W24, *L. lactis* W19, and *L. lactis* W58	2.5×10^9 cfu/g. 2× day/12 weeks	Sabico et al. (2017)
Decrease in the levels of fasting plasma glucose in type 2 diabetic volunteers	7 viable and freeze-dried strains: *L. acidophilus*, *L. casei*, *L. rhamnosus*, *L. bulgaricus*, *B. breve*, *B. longum*, *S. thermophilus*	*L. acidophilus* (2×10^9 cfu/g); *L. casei* (7×10^9 cfu/g); *L. rhamnosus* (1.5×10^9 cfu/g); *L. bulgaricus* (2×10^8 cfu/g); *B. breve* (3×10^{10} cfu/g); *B. longum* (7×10^9 cfu/g); *S. thermophilus* (1.5×10^9 cfu/g) 1× day/6 weeks	Razmpoosh et al. (2019)
Favorable modification of glucose metabolism in obese postmenopausal women	Sachets containing 2 g of freeze-dried powder of the probiotic mixture *B. bifidum* W23, *B. lactis* W51, *B. lactis* W52, *L. acidophilus* W37, *L. brevis* W63, *L. casei* W56, *L. salivarius* W24, *L. lactis* W19, *L. lactis* W58	1×10^{10} cfu/g. 2× day/12 weeks	Szulińska et al. (2018)
Improved glycemic response in type 2 diabetic patients	Capsule with *L. casei*	10^8 cfu/g. 1× day/8 weeks	Khalili et al. (2019)
Improved insulin sensitivity and reduced insulinemia in overweight/obese insulin-resistant volunteers	Pasteurized *Akkermansia muciniphila*	10^{10} cfu/g. 1× day/3 months	Depommier et al. (2019)
Reduction in the level of blood glucose in volunteers with metabolic syndrome	300 g/d of probiotic yogurt with *L. bulgaricus* and *S. thermophilus*	*L. acidophilus* La5 (6.45×10^6 cfu/g); *B. lactis* Bb12	Rezazadeh et al. (2019)

(continued)

Table 3.1 (continued)

Effect	Probiotic(s)	Dose/duration	Authors
	enriched with the probiotic culture of *L. acidophilus* La5 and *B. lactis* Bb12	(4.94×10^6 cfu/g) 1× day/8 weeks	

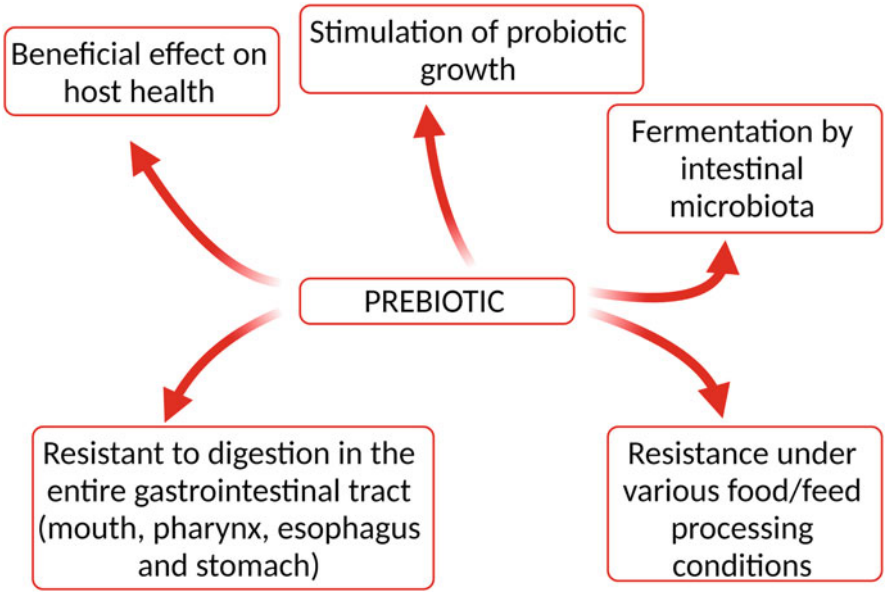

Fig. 3.1 Requirements for potential prebiotic

phylum *Firmicutes* and increasing the abundance of bacteria in the phylum *Bacteroidetes* (Barengolts 2016).

Supplementation with prebiotic such as inulin and fructooligosaccharides favors the proliferation of beneficial bacterial, such as *Bifidobacterium* and *Lactobacillus* genera (Kellow et al. 2014). Figure 3.1 shows the criteria for the selection of prebiotics (Wang 2009; Slizewska et al. 2013).

Mammals have limited capacity to hydrolyze polysaccharides, such as those found in vegetables, that reach the distal intestinal microbiota (Hooper et al. 2002). It is not necessary for mammals to develop an enzyme complex to disrupt the wide variety of bonds found in these polysaccharides, as the intestinal microbiota is responsible for this process, providing abundant and readily fermentable carbon sources that would be wasted by the host (Musso et al. 2011). Dietary fibers are widely known prebiotics and will be explained in the next topic.

3.4.1 Fibers

There are two types of fibers, prebiotic and dietary fibers, which are differentiated by the groups of microorganisms that act on them. Prebiotics are fermented by defined groups of microorganisms, while dietary ones are not restricted; most colon bacteria act in the fermentation of this type of fiber. Dietary fibers are cellulose, hemicellulose, pectin, gums, substances obtained from seaweed, as well as lactulose, soy oligosaccharides, inulin, fructooligosaccharides, galactooligosaccharides, xylooligosaccharides, and isomaltooligosaccharides (Markowiak and Slizewska 2017).

Regarding their structure, the fibers consist of polysaccharides composed of thousands of units of monosaccharides connected by glycosidic bonds. The fibers can be soluble (mainly pectin) or insoluble (mainly cellulose and hemicellulose), the soluble ones being generally more fermentable (Cui et al. 2017; Dhingra et al. 2012).

For the fermentation of fibers, the participation of different microbial groups is required, which first perform the depolymerization of these polymers, giving rise to smaller compounds (mono- and oligomeric), which can be decomposed into even smaller products, such as SCFA, carbon dioxide (CO_2), and hydrogen molecules (H_2) (Macfarlane and Macfarlane 1997).

The formation of SCFA is important for the host to recover part of the energy contained in the fibers that would be lost. As the human diet varies in the amount of fiber consumed, this directly affects the amount and type of SCFA produced, in addition to influencing the composition of the microbiota. The fermentation of 50–60 g of complex carbohydrates produces 0.5–0.6 mol of SCFA, with an energy value of 140–180 kcal, which corresponds to approximately 10% of the caloric maintenance requirement (Musso et al. 2011). In addition to the formation of SCFA, fibers (and prebiotics in general) can increase the thickness of the mucus layer in the intestine through bacterial fermentation, regulating it and consequently reducing the passage of LPS through this mucosa, leading to decreased development metabolic diseases, such as obesity, pre-diabetes, and type 2 diabetes (Burcelin et al. 2011). Butyrate also helps in this process by acting as an energetic substrate for colonocytes, with a trophic effect on the mucosa (Bartholome et al. 2004; Tappenden et al. 1998).

In vitro and in vivo studies have shown that structural differences in fibers are related to the most prevalent type of bacteria, that is, depending on the fiber structure, different bacteria are involved in its degradation, thus modulating the intestinal microbiota of its host (Reichardt et al. 2018; Yang et al. 2013; Baxter et al. 2019; Martınez et al. 2010; Davis et al. 2011; Flint et al. 2015).

In additional, beneficial mechanisms of the action of prebiotics are decreased systemic inflammation and improved glucose tolerance. Studies using in vitro and in vivo models have demonstrated the efficiency of prebiotics in energy and glucose homeostasis (Barengolts 2013; Roberfroid et al. 2010; Druart et al. 2014; Cani et al. 2007; Ciubotaru et al. 2015). Table 3.2 shows that different prebiotics have positive effects in reducing blood glucose, improving insulin in obese, pre-diabetic, and type 2 diabetic individuals.

Table 3.2 Clinical trials with prebiotics and their positive effects on the glycemic profile of obese, pre-diabetic, and type 2 diabetic individuals

Effect	Prebiotic(s)	Dose/duration	Authors
Reduction in insulin-mediated glucose metabolism in hyperinsulinemic non-insulin-dependent diabetic subjects	*Ginkgo biloba* extract with 24% ginkgo flavone glycosides	120 mg 1× day/3 months	Kudolo (2001)
Favorable change in insulin resistance and glycemic control in postmenopausal women with type 2 diabetes	Sachet containing soy phytoestrogen (isolated soy protein and isoflavones)	Isolated soy protein (30 g); isoflavones (132 mg) 1× day/12 weeks	Jayagopal et al. (2002)
Improved glycemic control in type 2 diabetes subjects	Arabinoxylan fiber-bread and muffins	50% whole wheat, 36% white flour, 14% arabinoxylan fiber 4–5 slices of bread. 1–2 muffins × day/ 5 weeks	Lu et al. (2004)
Improved postprandial metabolic responses (serum glucose and insulin) in obese and impaired glucose tolerance subjects	White bread rolls containing arabinoxylan supplement	20 g 1× day/18 weeks	Garcia et al. (2007)
Ameliorated insulin sensitivity and beta-cell function in patients with impaired glucose tolerance in hypertensive subjects	Flavanol-rich dark chocolate	100 g 1× day/15 weeks	Grassi et al. (2008)
Improved glucose regulation in overweight subjects	Oligofructose	7 g 3× day/12 weeks	Parnell and Reimer (2009)
Reduction in HOMA-IR and improvement in insulin sensitivity in postmenopausal women with type 2 diabetes	Epicatechin (flavan-3-ols) and isoflavones (aglycone equivalents)	Epicatechin (90 mg–850 mg flavan-3-ols); isoflavones (100 mg) 2× day/12 months	Curtis et al. (2002)
Improvement of some glycemic indexes (fasting plasma glucose and HbA1c) in women with type 2 diabetes	Inulin	5 g 2× day/2 months	Gargari et al. (2013)
Positive effects on plasma insulin concentration in	Galactooligosaccharide	5.5 g 1× day/12 weeks	Vulevic et al. (2013)

(continued)

Table 3.2 (continued)

Effect	Prebiotic(s)	Dose/duration	Authors
metabolic syndrome subjects			
Decrease in the levels of fasting plasma glucose and HbA1c in women with type 2 diabetes	Oligofructose-enriched inulin	10 g/d 1× day/8 weeks	Dehghan et al. (2014)
Improved insulin resistance in women with type 2 diabetes	Resistant dextrin	10 g 1× day/8 weeks	Aliasgharzadeh et al. (2015)
Reduction in blood glucose in volunteers with metabolic syndrome	Red wine and de-alcoholized red wine	272 mL 1× day/1 month	Moreno-Indias et al. (2016)
Improved glucose tolerance in overweight or obese subjects	Inulin, β-glucan, blueberry anthocyanins, and blueberry polyphenols	Inulin (4 g); blueberry extract (equivalent to two cups of whole blueberries without the sugar) β-Glucan (2.5 g of oat) 1× day/4 weeks	Rebello et al. (2015)
Improved insulin sensitivity	Flaxseed mucilage	10 g 1× day/6 weeks	Brahe et al. (2015)
Improved glycemic status in women with type 2 diabetes	Resistant starch	10 g 1× day/8 weeks	Gargari et al. (2015)
Reduction in areas under the curve for glucose and HbA1c in type 2 diabetic subjects	Dehydrated nopal, chia seeds, soy protein, and inulin	Dehydrated nopal (14 g); chia seeds (4 g); soy protein (30 g); inulin (4 g) 2× day/1 month	Medina-Vera et al. (2019)

Epidemiological and intervention studies have shown that insufficient fiber intake is directly related to the development of chronic non-communicable diseases, such as pre-diabetes and type 2 diabetes (Reynolds et al. 2019). For this, it is suggested that an adult should consume 20–35 g of fiber per day; some authors still suggest a higher consumption of 50 g/day to induce beneficial effects (Dhingra et al. 2012; Franz et al. 2003).

Among prebiotics, we can mention mainly fibers, which, as already explained, are complex carbohydrates digested only by the intestinal microbiota; however, polyphenols, as shown in Table 3.2, can also be considered prebiotics due to their mechanism of action.

3.4.2 Polyphenols

Polyphenols are substrates selectively metabolized by gut bacteria conferring health benefits. This metabolization can lead to the inactivation of a bioactive compound or even the activation of an originally inactive compound. When interacting with the microbiota, polyphenols can act by modulating it, through antimicrobial activity or favoring the growth of beneficial groups, thus exercising prebiotic activity (Faria et al. 2014; Cardona et al. 2013; Selma et al. 2009). They are found mostly in plants, including fruits, vegetables, and cereals, as well as derived beverages such as tea, coffee, and wine (Santino et al. 2017; Scalbert et al. 2005). The two main types of polyphenols include flavonoids (flavones, flavanols, flavan-3-ols, flavanones, isoflavones, anthocyanidins) and nonflavonoids (stilbenes, lignans, and phenolic acids) (Del Rio et al. 2013; Ozdal et al. 2016).

Polyphenols are usually found in glycosylated, acetylated, or conjugated rhamnosides. In the small intestine, most of these polyphenols undergo the first stage of their metabolism, in which intestinal enzymes, lactase-phlorizin hydrolase (LPH) or β-glucosidase (CBG), catalyze the breakdown of the sugar through oxidation or hydrolysis, thus releasing the glycoside aglycones (Santino et al. 2017; Day et al. 1998, 2000; Gee et al. 2000). Flavonoids linked to rhamnose directly reach the colon and are hydrolyzed by the enzyme α-rhamnosidase secreted by the colon microbiota (Bang et al. 2015). The aglycone produced by the microbiota is absorbed by the large intestine and transported to the circulation (Murota et al. 2018).

After absorption in the small intestine, these less complex polyphenolic compounds can undergo Phase I (oxidation, reduction, and hydrolysis) and Phase II (conjugation) biotransformation in enterocytes and then in hepatocytes, resulting in a series of biotransformation that make these water-soluble products, in addition to facilitating their excretion by bile and urine, the transport through the bloodstream, through the connection with plasma proteins (albumin), in order to reduce their toxicity (Bowey et al. 2003; Marín et al. 2015; Cassidy and Minihane 2017).

Through bile, polyphenols reach the small intestine again or pass directly to the large intestine, where they are metabolized by the microbiota, transforming into aglycones (those that have not yet been cleaved) or into simpler and more absorbable aromatic compounds. The metabolism of polyphenols by the microbiota involves the cleavage of glycosidic bonds and the breakdown of the heterocyclic structure (Fig. 3.2) (Aura et al. 2005).

Foods rich in polyphenols are protective against the development of chronic diseases, such as pre-diabetes and type 2 diabetes (Yang et al. 2014; Jumar and Schmieder 2016; Lee et al. 2016; Martin et al. 2016; Pang et al. 2016; Santos and Lima 2016).

In vitro studies have shown that polyphenols favor the growth of bacteria such as *Lactobacillaceae* family and *Bifidobacterium* spp., in addition to inhibiting the growth of harmful bacteria such as *Clostridiales* and *Enterobacteriales* family (Duda-Chodak et al. 2015). In a systematic review, which analyzed polyphenol supplementation, it identified a prebiotic effect of polyphenols, confirming its action on the *Lactobacillaceae* family and *Bifidobacterium* spp. (Ma and Chen 2020).

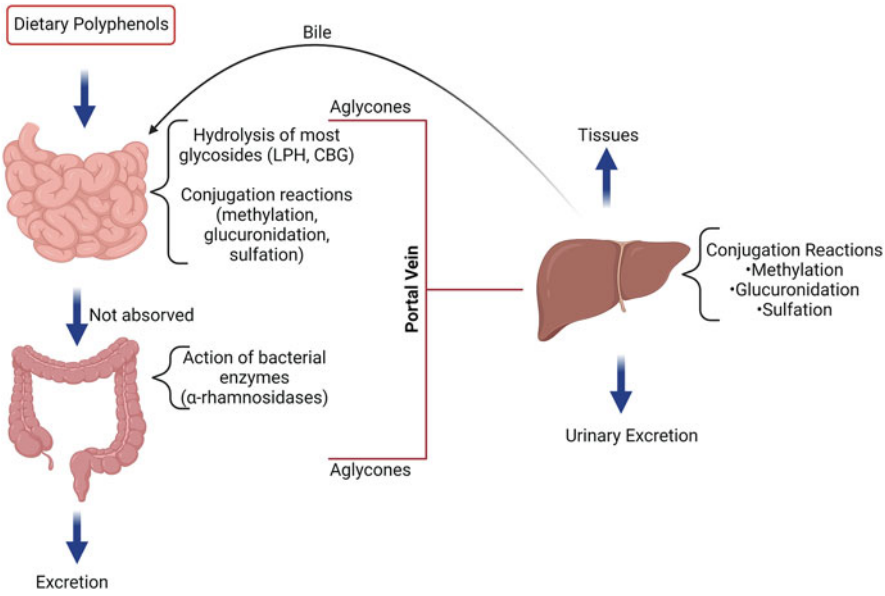

Fig. 3.2 Metabolism of polyphenols

Polyphenols from blueberries, for example, exert prebiotic effects by increasing the abundance of *Bifidobacterium* spp. (Aliasgharzadeh et al. 2015; Moreno-Indias et al. 2016).

Two meta-analyses evaluated the consumption of tea, a drink rich in polyphenols, and observed that regular consumption of this drink is associated with a lower risk of developing type 2 diabetes (Guglielmetti et al. 2013; Lacombe et al. 2013).

The consumption of polyphenols is generally associated with probiotics and other prebiotics, and the average consumption of polyphenols is 1 g/day (Marchesi et al. 2016; Oracz et al. 2019; Espín et al. 2017; Manach et al. 2005; Scalbert and Williamson 2000).

Although the literature presents several studies on the consumption of polyphenols and their action on the glycemic profile, most of them are in vitro or in animals; therefore, the mechanisms of action of polyphenols in humans are still unclear. Anti-diabetic activity is associated with reduced rates of digestion and absorption of nutrients, causing an attenuation in the postprandial glucose peak and activation of the AMP kinase protein, which leads to changes in energy metabolism and effects on the intestinal microbiota (Hara and Honda 1990; Williamson 2013; Yang et al. 2016).

3.5 Future Perspectives

Pre-diabetes and type 2 diabetes are important and widespread chronic diseases. This chapter shows that the consumption of probiotics and prebiotics is a promising strategy with a beneficial impact on gut microbiota and glycemic control (Fig. 3.3). Furthermore, several different probiotic strains, especially *L. acidophilus*, *L. casei* Shirota strain, and *B. lactis* Bb12, have demonstrated the ability to improve parameters related to pre-diabetes and type 2 diabetes. In addition, polyphenols are emerging as a new alternative in glycemic control through the production of SCFA, decreased LPS translocation leading to metabolic endotoxemia, and other mechanisms related to the intestinal microbiota. Finally, the ingestion of beneficial bacteria, foods rich in fiber and polyphenols, or a combination of them all is a good strategy for the control of pre-diabetes and type 2 diabetes, but more studies are still needed, mainly clinical trials, for these strategies to be improved and widely used.

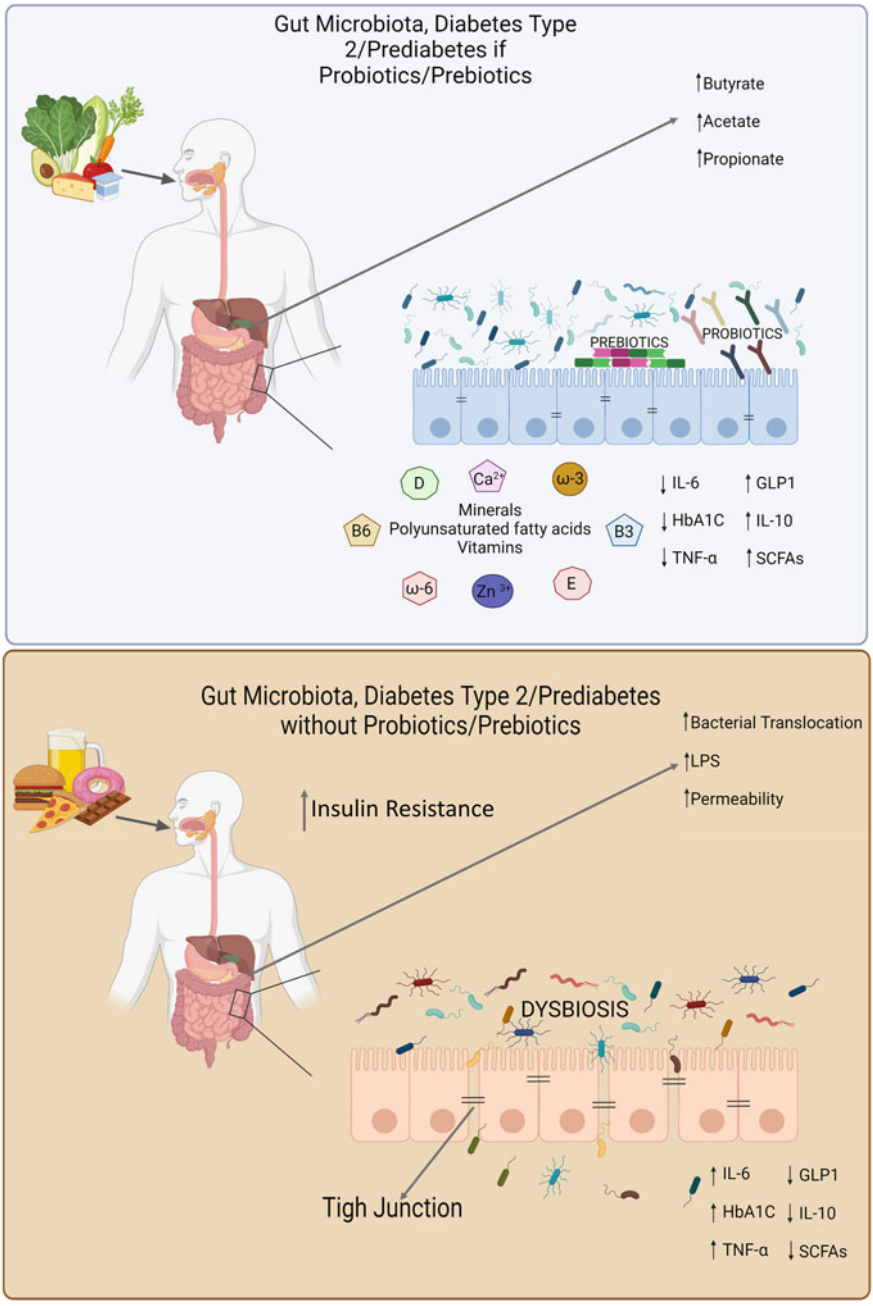

Fig. 3.3 Intestinal microbiota in homeostasis and dysbiosis promoted by diabetes/pre-diabetes and consequent impact on the development or prevention. Intake of probiotics/prebiotics can positively modulate the intestinal microbiota, resulting in increased production of intestinal metabolites such as short-chain fatty acids (SCFA) and improved function of the intestinal barrier

References

Aliasgharzadeh A, Dehghan P, Gargari BP, Asghari-Jafarabadi M (2015) Resistant dextrin, as a prebiotic, improves insulin resistance and inflammation in women with type 2 diabetes: a randomised controlled clinical trial. Br J Nutr 113(2):321–330. https://doi.org/10.1017/S0007114514003675

American Diabetes Association (ADA) (2020) 2. Classification and diagnosis of diabetes: standards of medical Care in Diabetes-2020. Diabetes Care 43(Suppl 1):S14–S31. https://doi.org/10.2337/dc20-S002

Andreasen AS, Larsen N, Pedersen-Skovsgaard T et al (2010) Effects of *lactobacillus acidophilus* NCFM on insulin sensitivity and the systemic inflammatory response in human subjects. Br J Nutr 104(12):1831–1838. https://doi.org/10.1017/S0007114510002874

Armougom F, Henry M, Vialettes B et al (2009) Monitoring bacterial community of human gut microbiota reveals an increase in lactobacillus in obese patients and methanogens in anorexic patients. PLoS One 4(9):e7125. https://doi.org/10.1371/journal.pone.0007125

Aura AM, Martin-Lopez P, O'Leary KA et al (2005) In vitro metabolism of anthocyanins by human gut microflora. Eur J Nutr 44(3):133–142. https://doi.org/10.1007/s00394-004-0502-2

Bang SH, Hyun YJ, Shim J et al (2015) Metabolism of rutin and poncirin by human intestinal microbiota and cloning of their metabolizing α-L-rhamnosidase from *Bifidobacterium dentium*. J Microbiol Biotechnol 25(1):18–25. https://doi.org/10.4014/jmb.1404.04060

Bansal N (2015) Prediabetes diagnosis and treatment: a review. World J Diabetes 15(6):296–303. https://doi.org/10.4239/wjd.v6.i2.296

Barengolts E (2013) Vitamin D and prebiotics may benefit the intestinal microbacteria and improve glucose homeostasis in prediabetes and type 2 diabetes. Endocr Pract 19(3):497–510. https://doi.org/10.4158/EP12263.RA

Barengolts E (2016) Gut microbiota, prebiotics, probiotics, and synbiotics in management of obesity and prediabetes: review of randomized controlled trials. Endocr Pract 22(10):1224–1234. https://doi.org/10.4158/EP151157.RA

Barreto FM, Colado Simão AN, Morimoto HK, Batisti Lozovoy MA, Dichi I, Helena da Silva Miglioranza L (2014) Beneficial effects of Lactobacillus plantarum on glycemia and homocysteine levels in postmenopausal women with metabolic syndrome. Nutrition 30(7–8):939–942. https://doi.org/10.1016/j.nut.2013.12.004

Bartholome AL, Albin DM, Baker DH et al (2004) Supplementation of total parenteral nutrition with butyrate acutely increases structural aspects of intestinal adaptation after an 80% jejunoileal resection in neonatal piglets. J Parenter Enter Nutr 28(4):210–222. https://doi.org/10.1177/0148607104028004210

Baxter NT, Schmidt AW, Venkataraman A et al (2019) Dynamics of human gut microbiota and short-chain fatty acids in response to dietary interventions with three fermentable fibers. MBio 10(1):e02566–e02518. https://doi.org/10.1128/mBio.02566-18

Belkaid Y, Hand T (2014) Role of the microbiota in immunity and inflammation. J Cell 157(1):121–114. https://doi.org/10.1016/j.cell.2014.03.011

Bianchi F, Duque ALRF, Saad SMI et al (2018) Gut microbiome approaches to treat obesity in humans. Appl Microbiol Biotechnol 103(3):1081–1094. https://doi.org/10.1007/s00253-018-9570-8

Blaut M, Clavel T (2007) Metabolic diversity of the intestinal microbiota: implications for health and disease. Nutr J 137(3):751S–755S. https://doi.org/10.1093/jn/137.3.751S

Bowey E, Adlercreutz H, Rowland I (2003) Metabolism of isoflavones and lignans by the gut microflora: a study in germ-free and human flora associated rats. Food Chem Toxicol 41(5):631–636. https://doi.org/10.1016/s0278-6915(02)00324-1

Brahe LK, Le Chatelier E, Prifti E et al (2015) Dietary modulation of the gut microbiota--a randomised controlled trial in obese postmenopausal women. Br J Nutr 114(3):406–417. https://doi.org/10.1017/S0007114515001786

Braune A, Blaut M (2016) Bacterial species involved in the conversion of dietary flavonoids in the human gut. Gut Microbes 7(3):216–234. https://doi.org/10.1080/19490976.2016.1158395

Buchanan TA, Xiang AH, Peters RK et al (2002) Preservation of pancreatic beta-cell function and prevention of type 2 diabetes by pharmacological treatment of insulin resistance in high-risk hispanic women. J Diabetes 51(9):2796–2803. https://doi.org/10.2337/diabetes.51.9.2796

Burcelin R, Serino M, Chabo C (2011) Gut microbiota and diabetes: from pathogenesis to therapeutic perspective. Acta Diabetol 48:257–273. https://doi.org/10.1007/s00592-011-0333-6

Cani PD, Amar J, Iglesias MA et al (2007) Metabolic endotoxemia initiates obesity and insulin resistance. J Diabetes 56(7):1761–1772. https://doi.org/10.2337/db06-1491

Cardona F, Andrés-Lacueva C, Tulipani S et al (2013) Benefits of polyphenols on gut microbiota and implications in human health. J Nutr Biochem 24(8):1415–1422. https://doi.org/10.1016/j.jnutbio.2013.05.001

Cassidy A, Minihane AM (2017) The role of metabolism (and the microbiome) in defining the clinical efficacy of dietary flavonoids. Am J Clin Nutr 105(1):10–22. https://doi.org/10.3945/ajcn.116.136051

Chiasson JL, Josse RG, Gomis R et al (2002) Acarbose for prevention of type 2 diabetes mellitus: the STOP-NIDDM randomised trial. Lancet 359(9323):2072–2077. https://doi.org/10.1016/S0140-6736(02)08905-5

Chiva-Blanch G, Visioli F (2012) Polyphenols and health: moving beyond antioxidants. J Berry Res 2:63–71. https://doi.org/10.3233/JBR-2012-028

Ciubotaru I, Green SJ, Kukreja S et al (2015) Significant differences in fecal microbiota are associated with various stages of glucose tolerance in African American male veterans. Transl Res 166(5):401–411. https://doi.org/10.1016/j.trsl.2015.06.015

Cui JF, Lian HY, Zhao CY et al (2017) Dietary fibers from fruits and vegetables and their health benefits via modulation of gut microbiota. Compr Rev Food Sci Food Saf 18(5):1514–1532. https://doi.org/10.1111/1541-4337.12489

Curtis PJ, Sampson M, Potter J et al (2002) Chronic ingestion of flavan-3-ols and isoflavones improves insulin sensitivity and lipoprotein status and attenuates estimated 10-year CVD risk in medicated postmenopausal women with type 2 diabetes: a 1-year, double-blind, randomized, controlled trial. Diabetes Care 35(2):226–232. https://doi.org/10.2337/dc11-1443

Davis LMG, Martınez I, Walter J et al (2011) Barcoded pyrosequencing reveals that consumption of galactooligosaccharides results in a highly specific bifidogenic response in humans. PLoS One 6(9):e25200. https://doi.org/10.1371/journal.pone.0025200

Day AJ, Dupont MS, Ridley S et al (1998) Deglycosylation of flavonoid and isoflavonoid glycosides by human small intestine and liver β-glucosidase activity. FEBS Lett 436(1):71–75. https://doi.org/10.1016/S0014-5793(98)01101-6

Day AJ, Canada FJ, Diaz JC et al (2000) Dietary flavonoid and isoflavone glycosides are hydrolysed by the lactase site of lactase phlorizin hydrolase. FEBS Lett 468(2–3):166–170. https://doi.org/10.1016/s0014-5793(00)01211-4

Dehghan P, Gargari BP, Jafar-abadi MA (2014) Oligofructose-enriched inulin improves some inflammatory markers and metabolic endotoxemia in women with type 2 diabetes mellitus: a randomized controlled clinical trial. Nutrition 30(4):418–423. https://doi.org/10.1016/j.nut.2013.09.005

Del Rio D, Rodriguez-Mateos A, Spencer JP et al (2013) Dietary (poly)phenolics in human health: structures, bioavailability, and evidence of protective effects against chronic diseases. Antioxid Redox Signal 18(14):1818–1892. https://doi.org/10.1089/ars.2012.4581

Depommier C, Everard A, Druart C et al (2019) Supplementation with *Akkermansia muciniphila* in overweight and obese human volunteers: a proof-of-concept exploratory study. Nat Med 25(7):1096–1103. https://doi.org/10.1038/s41591-019-0495-2

Dhingra D, Michael M, Rajput H et al (2012) Dietary fiber in foods: a review. J Food Sci Technol 9(3):255–266. https://doi.org/10.1007/s13197-011-0365-5

Druart C, Alligier M, Salazar N (2014) Modulation of the gut microbiota by nutrients with prebiotic and probiotic properties. Adv Nutr 5(5):S624–S633. https://doi.org/10.3945/an.114.005835

Duda-Chodak A, Tarko T, Satora P et al (2015) Interaction of dietary compounds, especially polyphenols, with the intestinal microbiota: a review. Eur J Nutr 54(3):325–341. https://doi.org/10.1007/s00394-015-0852-y

Ejtahed HS, Mohtadi-Nia J, Homayouni-Rad A et al (2012) Probiotic yogurt improves antioxidant status in type 2 diabetic patients. Nutrition 28(5):539–543. https://doi.org/10.1016/j.nut.2011.08.013

Espín JC, González-Sarrías A, Tomás-Barberán FA et al (2017) The gut microbiota: a key factor in the therapeutic effects of (poly) phenols. Biochem Pharmacol 139:82–93. https://doi.org/10.1016/j.bcp.2017.04.033

Faria A, Fernandes I, Norberto S et al (2014) Interplay between anthocyanins and gut microbiota. J Agric Food Chem 62(29):6898–6902. https://doi.org/10.1021/jf501808a

Flint HJ, Duncan SH, Scott KP et al (2015) Links between diet, gut microbiota composition and gut metabolism. Proc Nutr Soc 74(1):13–22. https://doi.org/10.1017/S0029665114001463

Franz MJ, Bantle JP, Beebe CA et al (2003) Evidence-based nutrition principles for the treatment and prevention of diabetes and related complications. Diabetes Care 26(Suppl1):S51–S61. https://doi.org/10.2337/diacare.26.2007.s51

Garcia AL, Otto B, Reich SC et al (2007) Arabinoxylan consumption decreases postprandial serum glucose, serum insulin and plasma total ghrelin response in subjects with impaired glucose tolerance. Eur J Nutr 61(3):334–341. https://doi.org/10.1038/sj.ejcn.1602525

Gargari BP, Dehghan P, Aliasgharzadeh A et al (2013) Effects of high performance inulin supplementation on glycemic control and antioxidant status in women with type 2 diabetes. Diabetes Metab J 37:140–148. pISSN 2233-6079 eISSN 2233-6087

Gargari BP, Namazi N, Khalili M et al (2015) Is there any place for resistant starch, as alimentary prebiotic, for patients with type 2 diabetes? Complement Ther Med 23(6):810–815. https://doi.org/10.1016/j.ctim.2015.09.005

Gee JM, DuPont MS, Day AJ et al (2000) Intestinal transport of quercetin glycosides in rats involves both deglycosylation and interaction with the hexose transport pathway. Nutr J 130(11):2765–2771. https://doi.org/10.1093/jn/130.11.2765

Grassi D, Desideri G, Necozione S et al (2008) Blood pressure is reduced and insulin sensitivity increased in glucose-intolerant, hypertensive subjects after 15 days of consuming high-polyphenol dark chocolate. Nutr J 138(9):1671–1676. https://doi.org/10.1093/jn/138.9.1671

Guglielmetti S, Fracassetti D, Taverniti V et al (2013) Differential modulation of human intestinal *bifidobacterium* populations after consumption of a wild blueberry (Vaccinium angustifolium) drink. J Agric Food Chem 61(34):8134–8140. https://doi.org/10.1021/jf402495k

Hara Y, Honda M (1990) The inhibition of alpha-amylase by tea polyphenols. Agr Biol Chem 54(88):1939–1945. https://doi.org/10.1080/00021369.1990.10870239

Hill C, Guarner F, Reid G et al (2014) Expert consensus document. The international scientific Association for Probiotics and Prebiotics consensus statement on the scope and appropriate use of the term probiotic. Nat Rev Gastroenterol Hepatol 11:506–144. https://doi.org/10.1038/nrgastro.2014.66

Hooper LV, Midtvedt T, Gordon JI (2002) How host-microbial interactions shape the nutrient environment of the mammalian intestine. Annu Rev Nutr 22:283–307. https://doi.org/10.1146/annurev.nutr.22.011602.092259

Huang J, Chen L, Xue B et al (2016) Different flavonoids can shape unique gut microbiota profile in vitro. J Food Sci 81(9):H2273–H2279. https://doi.org/10.1111/1750-3841.13411

Human - The Human Microbiome Project Consortium (2012) Structure, function and diversity of the healthy human microbiome. Nature 486(7402):207–214. https://doi.org/10.1038/nature11234

Huttenhower C, Gevers D, Knight R et al (2012) Structure, function and diversity of the healthy human microbiome. Nature 486(7402):207–214. https://doi.org/10.1038/nature11234

International Diabetes Federation (IDF) (2020) Diabetes Atlas, Nine Edition 2019. https://diabetesatlas.org/upload/resources/material/20200302_133351_IDFATLAS9e-final-web.pdf. Accessed 10 May 2020

Jayagopal V, Albertazzi P, Kilpatrick ES et al (2002) Beneficial effects of soy phytoestrogen intake in postmenopausal women with type 2 diabetes. Diabetes Care 25(10):1709–1714. https://doi.org/10.2337/diacare.25.10.1709

Jumar A, Schmieder RE (2016) Cocoa flavanol cardiovascular effects beyond blood pressure reduction. J Clin Hypertens 18(4):352–358. https://doi.org/10.1111/jch.12715

Kaur J (2014) A comprehensive review on metabolic syndrome. Cardiol Res Pract 2014:943162. https://doi.org/10.1155/2014/943162

Kellow NJ, Coughlan MT, Savige GS et al (2014) Effect of dietary prebiotic supplementation on advanced glycation, insulin resistance and inflammatory biomarkers in adults with pre-diabetes: a study protocol for a double-blind placebo-controlled randomised crossover clinical trial. BMC Endocr Disord 14:55. https://doi.org/10.1186/1472-6823-14-55

Khalili L, Alipour B, Asghari Jafar-Abadi M et al (2019) The effects of *lactobacillus casei* on glycemic response, serum Sirtuin1 and fetuin-a levels in patients with type 2 diabetes mellitus: a randomized controlled. Trial Iran Biomed J 23(1):68–77. https://doi.org/10.29252/.23.1.68

Kudolo GB (2001) The effect of 3-month ingestion of *Ginkgo biloba* extract (EGb 761) on pancreatic beta-cell function in response to glucose loading in individuals with non-insulin-dependent diabetes mellitus. J Clin Pharmacol 41(6):600–611. https://doi.org/10.1177/00912700122010483

Lacombe A, Tadepalli S, Hwang CA et al (2013) Phytochemicals in lowbush wild blueberry inactivate Escherichia coli O157:H7 by damaging its cell membrane. Foodborne Pathog Dis 10(11):944–950. https://doi.org/10.1089/fpd.2013.1504

Le Chatelier E, Nielsen T, Qin J et al (2013) Richness of human gut microbiome correlates with metabolic markers. Nature 500:541–546. https://doi.org/10.1038/nature12506

Lee AH, Tan L, Hiramatsu N et al (2016) Plasma concentrations of coffee polyphenols and plasma biomarkers of diabetes risk in healthy Japanese women. Nutr Diabetes 6:e212. https://doi.org/10.1038/nutd.2016.19

Liu F, Li P, Chen M et al (2017) Fructooligosaccharide (FOS) and Galactooligosaccharide (GOS) increase Bifidobacterium but reduce butyrate producing bacteria with adverse glycemic metabolism in healthy young population. Sci Rep 1:11789. https://doi.org/10.1038/s41598-017-10722-2

Lloyd-Price J, Abu-Ali G, Huttenhower C (2016) The healthy human microbiome. Genome Med 8(1):51. https://doi.org/10.1186/s13073-016-0307-y

Lozupone CA, Stombaugh JI, Gordon JI et al (2012) Diversity, stability and resilience of the human gut microbiota. Nature 489(7415):220–230. https://doi.org/10.1038/nature11550

Lu XZ, Walker KZ, Muir JG et al (2004) Arabinoxylan fibre improves metabolic control in people with type II diabetes. Eur J Clin Nutr 58(4):621–628. https://doi.org/10.1038/sj.ejcn.1601857

Ma G, Chen Y (2020) Polyphenol supplementation benefits human health via gut microbiota: a systematic review via meta-analysis. J Funct Foods 66:103829. https://doi.org/10.1016/j.jff.2020.103829

Macfarlane GT, Macfarlane S (1997) Human colonic microbiota: ecology, physiology and metabolic potential of intestinal bacteria. Scand J Gastroenterol Suppl 222:3–9. https://doi.org/10.1080/00365521.1997.11720708

Madjd A, Taylor MA, Mousavi N et al (2016) Comparison of the effect of daily consumption of probiotic compared with low-fat conventional yogurt on weight loss in healthy obese women following an energy-restricted diet: a randomized controlled trial. Am J Clin Nutr 103(2):323–329. https://doi.org/10.3945/ajcn.115.120170

Manach C, Williamson G, Morand C et al (2005) Bioavailability and bioefficacy of polyphenols in humans. I. Review of 97 bioavailability studies 1–3. Am J Clin Nutr 81(suppl 1):230–242. https://doi.org/10.1093/ajcn/81.1.230S

Marchesi JR, Adams DH, Fava F et al (2016) The gut microbiota and host health: a new clinical frontier. Gut 65(2):330–339. https://doi.org/10.1136/gutjnl-2015-309990

Marín L, Miguélez EM, Villar CJ et al (2015) Bioavailability of dietary polyphenols and gut microbiota metabolism: antimicrobial properties. Biomed Res Int 2015:905215. https://doi.org/10.1155/2015/905215

Markowiak P, Slizewska K (2017) Effects of probiotics, prebiotics, and Synbiotics on human health. Nutrients 9(9):1021. https://doi.org/10.3390/nu9091021

Martin MA, Goya L, Ramos S (2016) Antidiabetic actions of cocoa flavanols. Mol Nutr Food Res 60(8):1756–1769. https://doi.org/10.1002/mnfr.201500961

Martınez I, Kim J, Duffy PR et al (2010) Resistant starches types 2 and 4 have differential effects on the composition of the fecal microbiota in human subjects. PLoS One 5(11):e15046. https://doi.org/10.1371/journal.pone.0015046

Matos LN, Giorelli GV, Dias CB (2011) Correlation of anthropometric indicators for identifying insulin sensitivity and resistance. Sao Paulo Med J 129(1):30–35. https://doi.org/10.1590/s1516-31802011000100006

Medina-Vera I, Sanchez-Tapia M, Noriega-López L et al (2019) A dietary intervention with functional foods reduces metabolic endotoxaemia and attenuates biochemical abnormalities by modifying faecal microbiota in people with type 2 diabetes. Diabetes Metab J 45(2):122–131. https://doi.org/10.1016/j.diabet.2018.09.004

Mohamadshahi M, Veissi M, Haidari F et al (2014) Effects of probiotic yogurt consumption on inflammatory biomarkers in patients with type 2 diabetes. Bioimpacts 4(2):83–88. https://doi.org/10.5681/bi.2014.007

Moore WE, Holdeman LV (1974) Human fecal flora: the normal flora of 20 Japanese-Hawaiians. J Appl Microbiol 27(5):961–979. PMCID: PMC380185

Moreno-Indias I, Sánchez-Alcoholado L, Pérez-Martínez P, Andrés-Lacueva C, Cardona F, Tinahones F, Queipo-Ortuño MI (2016) Red wine polyphenols modulate fecal microbiota and reduce markers of the metabolic syndrome in obese patients. Food Funct 7(4):1775–1787. https://doi.org/10.1039/c5fo00886g

Mosca A, Leclerc M, Hugot JP (2016) Gut microbiota diversity and human diseases: should we reintroduce key predators in our ecosystem? Front Microbiol 31(7):455. https://doi.org/10.3389/fmicb.2016.00455

Murota K, Nakamura Y, Uehara M (2018) Flavonoid metabolism: the interaction of metabolites and gut microbiota. Biosci Biotechnol Biochem 82(4):600–610. https://doi.org/10.1080/09168451.2018.1444467

Musso G, Gambino R, Cassader M (2011) Interactions between gut microbiota and host metabolism predisposing to obesity and diabetes. Annu Rev Med 62:361–380. https://doi.org/10.1146/annurev-med-012510-175505

Neyrinck AM, Haller D, Delzenne NM et al (2016) Microbiome and metabolic disorders related to obesity: which lessons to learn from experimental models? Trends Food Sci Technol 57(8):256–264. https://doi.org/10.1016/j.tifs.2016.08.012

Nicholson JK, Holmes E, Kinross J et al (2012) Host-gut microbiota metabolic interactions. Science 336(6086):1262–1267. https://doi.org/10.1126/science.1223813

O'Hara AM, Shanahan F (2006) The gut flora as a forgotten organ. EMBO Rep 7(7):688–693. https://doi.org/10.1038/sj.embor.7400731

Oracz J, Nebesny E, Zyzelewicz D et al (2019) Bioavailability and metabolism of selected cocoa bioactive compounds: a comprehensive review. Crit Rev Food Sci Nutr 60(12):1947–1985. https://doi.org/10.1080/10408398.2019.1619160

Ostadrahimi A, Taghizadeh A, Mobasseri M et al (2015) Effect of probiotic fermented milk (kefir) on glycemic control and lipid profile in type 2 diabetic patients: a randomized double-blind placebo-controlled clinical trial. Iran J Public Health 44(2):228–237. PMCID: PMC4401881

Ouwehand A, Derrien M, de Vos W et al (2005) Prebiotics and other microbial substrates for gut functionality. Curr Biol 16(2):212–217. https://doi.org/10.1016/j.copbio.2005.01.007

Ozdal T, Sela DA, Xiao J et al (2016) The reciprocal interactions between polyphenols and gut microbiota and effects on bioaccessibility. Nutrients 8(2):78. https://doi.org/10.3390/nu8020078

Pandey KR, Naik SR, Vakil BV et al (2015) Probiotics, prebiotics and synbiotics- a review. J Food Sci Technol 52(12):7577–7587. https://doi.org/10.1007/s13197-015-1921-1

Pang J, Zhang Z, Zheng TZ et al (2016) Green tea consumption and risk of cardiovascular and ischemic related diseases: a meta-analysis. Int J Cardiol 202:967–974. https://doi.org/10.1016/j.ijcard.2014.12.176

Parnell JA, Reimer RA (2009) Weight loss during oligofructose supplementation is associated with decreased ghrelin and increased peptide YY in overweight and obese adults. Am J Clin Nutr 89(6):1751–1759. https://doi.org/10.3945/ajcn.2009.27465

Pratley RE (2013) The early treatment of type 2 diabetes. Am J Med 126(9 Suppl 1):S2–S9. https://doi.org/10.1016/j.amjmed.2013.06.007

Qin J, Li R, Raes J et al (2010) A human gut microbial gene catalogue established by metagenomic sequencing. Nature 464(7285):59–65. https://doi.org/10.1038/nature08821

Rajkumar H, Mahmood N, Kumar M et al (2014) Effect of probiotic (vsl#3) and omega-3 on lipid profile, insulin sensitivity, inflammatory markers, and gut colonization in overweight adults: a randomized, controlled trial. Mediators Inflamm 2014:348959. https://doi.org/10.1155/2014/348959

Razmpoosh E, Javadi A, Ejtahed HS, Mirmiran P, Javadi M, Yousefinejad A (2019) The effect of probiotic supplementation on glycemic control and lipid profile in patients with type 2 diabetes: a randomized placebocontrolled trial. Diabetes Metab Syndr 13(1):175–182. https://doi.org/10.1016/j.dsx.2018.08.008

Rebello CJ, Burton J, Heiman M (2015) Gastrointestinal microbiome modulator improves glucose tolerance in overweight and obese subjects: a randomized controlled pilot trial. J Diabetes Complicat 29(8):1272–1276. https://doi.org/10.1016/j.jdiacomp.2015.08.023

Reichardt N, Vollmer M, Holtrop G et al (2018) Specific substrate-driven changes in human faecal microbiota composition contrast with functional redundancy in short-chain fatty acid production. ISME J 12(2):610–622. https://doi.org/10.1038/ismej.2017.196

Reynolds A, Mann J, Cummings J et al (2019) Carbohydrate quality and human health: a series of systematic reviews and meta-analyses. Lancet 393(10170):434–445. https://doi.org/10.1016/S0140-6736(18)31809-9

Rezazadeh L, Gargari BP, Jafarabadi MA et al (2019) Effects of probiotic yogurt on glycemic indexes and endothelial dysfunction markers in patients with metabolic syndrome. Nutrition 62:162–168. https://doi.org/10.1016/j.nut.2018.12.011

Roberfroid M, Gibson GR, Hoyles L et al (2010) Prebiotic effects: metabolic and health benefits. Br J Nutr 104(Suppl 2):S1–S63. https://doi.org/10.1017/S0007114510003363

Roediger WE (1980) Role of anaerobic bacteria in the metabolic welfare of the colonic mucosa in man. Gut 21(9):793–798. https://doi.org/10.1136/gut.21.9.793

Sabico S, Al-Mashharawi A, Al-Daghri NM et al (2017) Effects of a multi-strain probiotic supplement for 12 weeks in circulating endotoxin levels and cardiometabolic profiles of medication naïve type 2 diabetes M patients: a randomized clinical trial. J Transl Med 15:249. https://doi.org/10.1186/s12967-017-1354-x

Santino A, Scarano A, De Santis S et al (2017) Gut microbiota modulation and anti-inflammatory properties of dietary polyphenols in ibd: new and consolidated perspectives. Cur Pharm Des 23(16):2344–2351. https://doi.org/10.2174/1381612823666170207145420

Santos RMM, Lima DRA (2016) Coffee consumption, obesity and type 2 diabetes: a mini-review. Eur J Nutr 55(4):1345–1358. https://doi.org/10.1007/s00394-016-1206-0

Sato J, Kanazawa A, Azuma K et al (2017) Probiotic reduces bacterial translocation in type 2 diabetes mellitus: a randomised controlled study. Sci Rep 7(1):12115. https://doi.org/10.1038/s41598-017-12535-9

Scalbert A, Williamson G (2000) Dietary intake and bioavailability of polyphenols. J Nutr 130-(8S Suppl):2073S–2085S. https://doi.org/10.1093/jn/130.8.2073S

Scalbert A, Manach C, Morand C et al (2005) Dietary polyphenols and the prevention of diseases. Crit Rev Food Sci Nutr 45(4):287–306. https://doi.org/10.1080/1040869059096

Schiffrin EJ, Thomas DR, Kumar VB et al (2007) Systemic inflammatory markers in older persons: the effect of oral nutritional supplementation with prebiotics. J Nutr Health Aging 11:475–479. PMID: 17985062

Selma M, Espín JC, Tomàs-Barberan FA (2009) Interaction between phenolics and gut microbiota: role in human health. J Agric Food Chem 57(15):6485–6501. https://doi.org/10.1021/jf902107d

Shen J, Obin MS, Zhao L (2013) The gut microbiota, obesity and insulin resistance. Mol Asp Med 34(1):39–58. https://doi.org/10.1016/j.mam.2012.11.001

Slizewska K, Nowak A, Barczynska R et al (2013) Prebiotyki Definicja, włas'ciwos'ci i zastosowanie w przemys'le. Z˙ ywnos'ć Nauka Technologia Jakosc 1(86):5–20

Stefanakia C, Bacopouloua F, Michosb A (2018) The impact of probiotics' administration on glycemic control, body composition, gut microbiome, mitochondria, and other hormonal signals in adolescents with prediabetes – a randomized, controlled trial study protocol. Contemp Clin Trials Commun 2(11):55–62. https://doi.org/10.1016/j.conctc.2018.06.002

Suau A, Bonnet R, Sutren M et al (1999) Direct analysis of genes encoding 16S rRNA from complex communities reveals many novel molecular species within the human gut. Appl Environ Microbiol 65(11):4799–4807. https://doi.org/10.1128/AEM.65.11.4799-4807.1999

Szulińska M, Łoniewski I, van Hemert S et al (2018) Dose-dependent effects of multispecies probiotic supplementation on the lipopolysaccharide (lps) level and cardiometabolic profile in obese postmenopausal women: a 12-week randomized. Clinical Trial Nutrients 10(6):773. https://doi.org/10.3390/nu10060773

Tappenden KA, Drozdowski LA, Thomson ABR et al (1998) Short-chain fatty acid supplemented total parenteral nutrition alters intestinal structure, glucose transporter 2 (GLUT2) mRNA and protein, and proglucagon mRNA abundance in normal rats. Am J Clin Nutr 68(1):118–125. https://doi.org/10.1093/ajcn/68.1.118

Thursby E, Juge N (2017) Introduction to the human gut microbiota. Biochem J 474(11): 1823–1836. https://doi.org/10.1042/BCJ20160510

Tilg H, Moschen AR (2014) Microbiota and diabetes: an evolving relationship. Gut 63(9): 1513–1521. https://doi.org/10.1136/gutjnl-2014-306928

Torres S, Fabersani E, Marquez A (2018) Adipose tissue inflammation and metabolic syndrome. The proactive role of probiotics. Eur J Nutr 58(1):27–43. https://doi.org/10.1007/s00394-018-1790-2

Tsai YL, Lin TL, Chang CJ et al (2019) Probiotics, prebiotics and amelioration of diseases. J Biomed Sci 26(1):3. https://doi.org/10.1186/s12929-018-0493-6

Tsui H, Winer S, Chan Y et al (2008) Islet glia, neurons, and beta cells. Ann N Y Acad Sci 1150:32–42. https://doi.org/10.1196/annals.1447.033

Turnbaugh PJ, Hamady M, Yatsunenko T et al (2009) A core gut microbiome in obese and lean twins. Nature 457(7228):480–484. https://doi.org/10.1038/nature07540

Unwin N, Shaw J, Zimmet P et al (2002) Impaired glucose tolerance and impaired fasting glycaemia: the current status on definition and intervention. Diabet Med 19(9):708–723. https://doi.org/10.1046/j.1464-5491.2002.00835.x

van Nood E, Vrieze A, Nieuwdorp M et al (2013) Duodenal infusion of donor feces for recurrent *Clostridium difficile*. N Engl J Med 368(5):407–415. https://doi.org/10.1056/NEJMoa1205037

Vulevic J, Drakoularakou A, Yaqoob P (2008) Modulation of the fecal microflora profile and immune function by a novel transgalactooligosaccharide mixture (B-GOS) in healthy elderly volunteers. Am J Clin Nutr 88(5):1438–1446. https://doi.org/10.3945/ajcn.2008.26242

Vulevic J, Juric A, Tzortzis G et al (2013) A mixture of trans-galactooligosaccharides reduces markers of metabolic syndrome and modulates the fecal microbiota and immune function of overweight adults. Nutr 143(3):324–331. https://doi.org/10.3945/jn.112.166132

Wang Y (2009) Prebiotics: present and future in food science and technology. Int Food Res J 42(1): 8–12. https://doi.org/10.1016/j.foodres.2008.09.001

Wang S, Xiao Y, Tian F et al (2020) Rational use of prebiotics for gut microbiota alterations: specific bacterial phylotypes and related mechanisms. J Funct Foods 66:103838. https://doi.org/10.1016/j.jff.2020.103838

Williamson G (2013) Possible effects of dietary polyphenols on sugar absorption and digestion. Mol Nutr Food Res 57(1):48–57. https://doi.org/10.1002/mnfr.201200511

World Health Organization (WHO) (2018) Obesity and overweight. Fact sheet No 311. Geneva, Switzerland

Yang J, Martınez I, Walter J et al (2013) In vitro characterization of the impact of selected dietary fibers on fecal microbiota composition and short chain fatty acid production. Anaerobe 23:74–81. https://doi.org/10.1016/j.anaerobe.2013.06.012

Yang J, Mao QX, Xu HX et al (2014) Tea consumption and risk of type 2 diabetes mellitus: a systematic review and meta-analysis update. BMJ Open 4(7):e005632. https://doi.org/10.1136/bmjopen-2014-005632

Yang CS, Zhang J, Zhang J et al (2016) Mechanisms of body weight reduction and metabolic syndrome alleviation by tea. Mol Nutr Food Res 60(1):160–174. https://doi.org/10.1002/mnfr.201500428

Ziemer DC, Kolm P, Foster JK et al (2008) Random plasma glucose in serendipitous screening for glucose intolerance: screening for impaired glucose tolerance study 2. J Gen Intern Med 23(5):528–535. https://doi.org/10.1007/s11606-008-0524-1

Zmora N, Suez J, Elinav E (2019) You are what you eat: diet, health and the gut microbiota. Nat Rev Gastroenterol Hepatol 16(1):35–56. https://doi.org/10.1038/s41575-018-0061-2

Zoetendal EG, Akkermans AD, De Vos WM (1998) Temperature gradient gel electrophoresis analysis of 16S rRNA from human fecal samples reveals stable and host-specific communities of active bacteria. Appl Environ Microbiol 64(10):3854–3859. https://doi.org/10.1128/AEM.64.10.3854-3859.1998

4 Natural Products, a Potential Source of New Drugs Discovery to Combat Obesity and Diabetes: Their Efficacy and Multi-targets Actions in Treatment of These Diseases

Biswanath Dinda and Manikarna Dinda

4.1 Introduction

Since the prehistoric times, at least 60,000 years back as per fossil records, humans have been using natural products, such as plants, animals, microorganisms, and marine organisms, in medicines to alleviate and treat diseases. The use of natural products as medicines must have a great challenge to early humans because when seeking food in forests and hills, early humans often consumed poisonous plants, which led them to vomiting, diarrhea, coma, or other toxic reaction-even death. Subsequently, they were able to develop knowledge about edible plant materials and to use many plants as natural medicines for treatment of diseases and ailments, which are the basis of traditional medicine. Such forms of traditional medicines, namely, traditional Chinese medicine (TCM), Indian Ayurveda, Greek-Arabic Unani, Japanese Kampo, and traditional Korean medicine, known as Sasang constitutional medicine (SCM) have been practiced worldwide for more than thousands of years and have blossomed into the present systems of modern medicines. The advancement of modern technology helped us to evaluate the pharmacology and mechanism of action of many medicinal herbs in treatment of diseases and to use them as cornerstones of modern medicine. In the historic year 1805, German pharmacist Friedrich Serturner isolated morphine from the opium plant, *Papaver somniferum* L., and laid the foundation of modern medicine. Subsequently, countless active natural molecules, known as phytochemicals have been separated from natural plant and microbial extracts, and many of them have potential anticancer, antihypertensive, hypolipidemic, antiobese, antidiabetic, antiviral, antileishmanial, and antimigraine

B. Dinda (✉)
Department of Chemistry, Tripura University, Suryamaninagar, Tripura, India

M. Dinda
Department of Biochemistry and Molecular Genetics, School of Medicine, University of Virginia, Charlottesville, USA

B. Dinda (ed.), *Natural Products in Obesity and Diabetes*,
https://doi.org/10.1007/978-3-030-92196-5_4

medicative properties. These phytochemicals, which have evolved over millions of years, have a unique chemical structural diversity, which results in the diversity of their biological actions to alleviate and treat critical human diseases. A group of evidence advocates that a "multidrugs" and "multi-targets" approach would be more effective compared to a "single-drug" and "single-target" approach in the treatment of complex diseases like obesity, diabetes, cardiovascular disease, and cancer. Phytochemicals present in a single herb or in a herbal formulation can function alone or synergistically with other phytochemicals in a "multi-targets" approach to produce desired pharmacological effect in prevention and cure of complex diseases. The optimal efficacy of the herbal/polyherbal extract depends on its correct dosage containing the optimal concentration of bioactive phytochemical (s) and the method of preparing and processing of the herbal/polyherbal composition and the appropriate time of collection of plant parts. Therefore, the research on natural products is a thrust area for future research in drug discovery (Yuan et al. 2016). This chapter summarizes the current progress in the study of the antiobesity and antidiabetic potentials of natural products and their main bioactive phytochemicals, major molecular mechanisms in preventing and treating obesity and diabetes, and their associated complications.

4.2 Natural Products in Human Health Care and Diseases

Natural products such as plants, animals, microorganisms, and marine organisms have been used by humans since the prehistoric times. As per records identified in the fossils, primitive humans have used some edible plants for treatment of diseases and minor illnesses from at least 60,000 years ago (Fabricant and Farnsworth 2001). Possibly, on eating these toxic plants as their diet, they experienced various adverse effects, such as vomiting, diarrhea, coma, and other toxic reactions, which led them to acquire knowledge on the medicinal properties of these edible plant materials. Subsequently, humans have made technological breakthroughs and developed methods of processing of these plant materials and to use them in traditional medicine for treatment of diseases and primary health care. As per literature evidence, natural products based traditional medicines, such as Indian Ayurveda, traditional Chinese medicine (TCM), Greek Unani in Greece and Islamic world, traditional Japanese medicine, Kampo, traditional Korean medicine known as Sasang constitutional medicine (SCM), traditional African medicine, traditional Aboriginal medicine of Australia, and Russian herbal medicine have been practiced all over the world for more than thousands of years and have blossomed into orderly regulated systems of natural medicines. In spite of certain defects on correct doses, safety, and efficacy of these medicines, these traditional medicines are in the backfoot of modern medicine (Alves and Rosa 2007). Natural products, namely, plants, marine algae and animals, microorganisms living in different habitable environments in both land and water mass, experienced many stresses, challenges, and attacks from harmful microbes and animals. To get rid off from these threats, these natural organisms have developed some tiny molecules, known as

phytochemicals, such as alkaloids, flavonoids, phenolic acids, glucosinolates, terpenoids, tannins, antibiotics, and others for their survival. These phytochemicals have reverse pharmacology of the diseases. Because of local availability and low cost, natural products have been playing a vital role in primary health care among unprivileged sections of people in the world. Over 70–95% of the population in Africa, Asia, Latin America, and Middle East use some form of traditional medicine as their first line of choice in primary health care. Several hospitals and clinics recommend herbal medicines for maintenance of good health, for alleviation of chronic diseases, and rarely for acute and life-threatening diseases (Robinson and Zhang 2011). About 40% of recent drugs in clinical practice have been developed from natural products. Several phytochemicals isolated from plants, animals, and microorganisms have made revolutions in modern medicine. Among them, pain killer alkaloid, morphine (**1**, Fig. 4.1) from opium plant, *Papaver somniferum*, anticancer diterpenoid taxol (**2**) from *Taxus brevifolia*, antileukemic alkaloids vincristine (**3**) and vinblastine (**4**) from *Catharanthus roseus* syn. *Vinca rosea*, anticancer alkaloid doxorubicin (**5**) from *Streptomyces peucetius*, antimalarial alkaloid quinine (**6**) from *Cinchona* spp., antimalarial sesquiterpene lactone, artemisinin (**7**) from *Artemisia annua*, antidiabetic flavonoid glycoside, puerarin (**8**) from *Pueraria lobata*, hypolipidemic polyphenolic curcumin (**9**) from *Curcumin longa*, anti-gastric-ulcer sesquiterpene lactone, costunolide (**10**) from *Saussurea lappa*, anti-hypercholesterolemic hexahydronaphthalene delta-lactone compound, lovastatin (**11**) from *Aspergillus terreus*, antibiotic tetracycline (**12**) from *Streptomyces aureofaciens*, pancreatic lipase inhibitor, a-four-membered-cyclic-beta-lactone lipstatin (**13**) from *Streptomyces toxytricini*, antibiotic cyclosporine (**14**) from *Tolypocladium inflatum*, antimuscarinic (anticholinergic) alkaloid, atropine (**15**) from *Atropa belladonna*, muscle-relaxant alkaloid, curare (**16**) from *Chondrodendron tomentosum*, antihypertensive L-proline derivative, captopril (**17**) from Brazilian viper, *Bothrops jararaca*, antidiabetic GLP-1 agonist peptide, exenatide (**18**) from lizard, *Heloderma suspectum* are significantly noted ones (Weibel et al. 1987; Dar et al. 2017; Thomford et al. 2018; Calixto 2019). It inspired the pharmaceutical industries for the discovery of bioactive natural products, and several natural molecules were reported as new drugs for treatment of life-risk diseases (Newman et al. 2003). However, at the beginning of the twenty-first century, several synthetic compounds related to the structures of natural products (natural molecules) were found to have better efficacy compared to natural molecules. As a result, most of the pharmaceutical industries and drug discovery-related research institutes have paid their attention for the development of synthetic drugs and reduced their efforts in the discovery of natural molecules (Li and Vederas 2009). After a couple of years, most of the synthetic drugs have been shown to exhibit many odd effects in patients and were withdrawn from the market. It provoked these pharmaceutical industries to search for discovery of natural molecules with minimum adverse effects in patients. A recent report on new drugs from natural resources demonstrated that about 40% of drugs were from natural products in the years 2000–2008, which dropped to about 20% in 2009, followed by

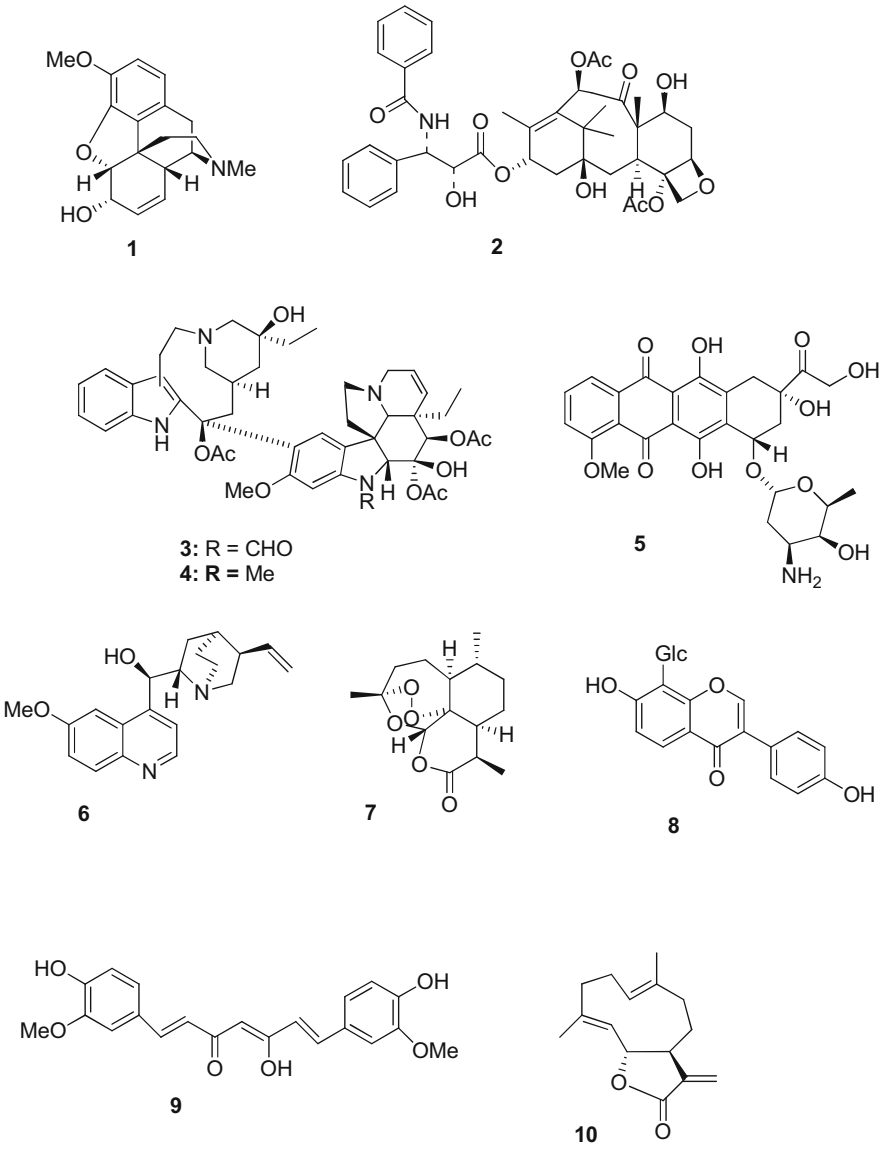

Fig. 4.1 Chemical structures of some natural products

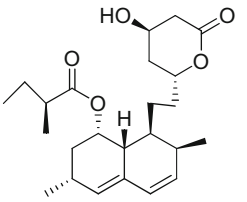

11

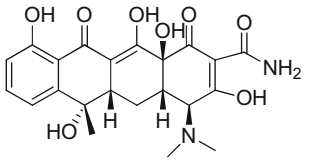

12

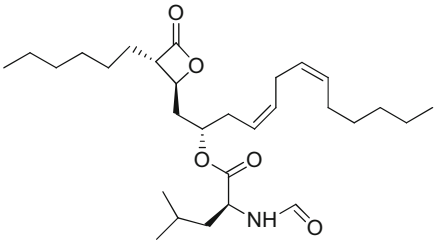

13

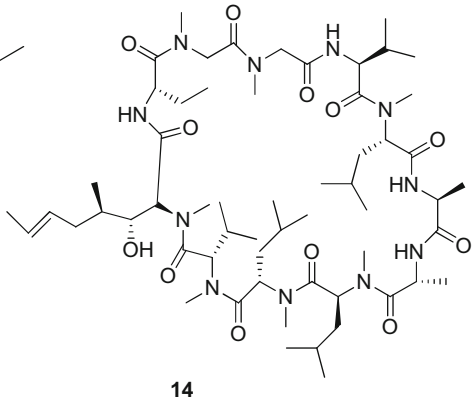

14

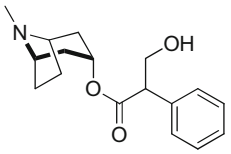

15

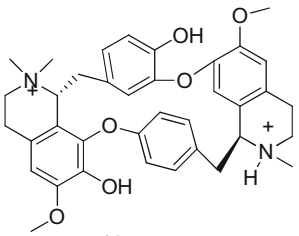

16

Fig. 4.1 (continued)

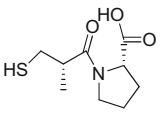

17

H-His-Gly-Glu-Gly-Thr-Phe-Thr-
-Ser-Asp-Leu-Ser-Lys-Glu-Met-
-Glu-Glu-Glu-Ala-Val-Arg-Leu-
-Phe-Ile-Glu-Try-Leu-Lys-Asn-
-Gly-Gly-Pro-Ser-Ser-Gly-Ala-
-Pro-Pro-Pro-Ser-NH_2

18

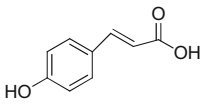

19

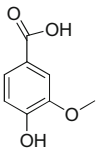

20

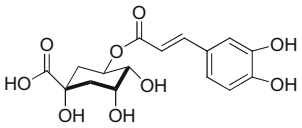

21

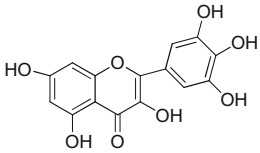

22

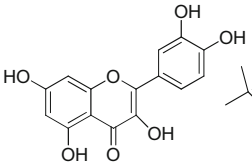

23

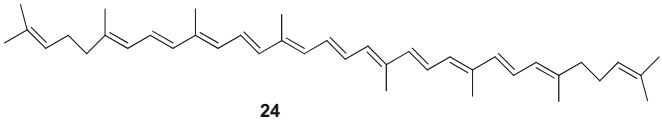

24

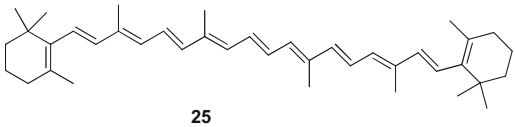

25

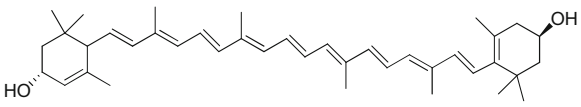

26

Fig. 4.1 (continued)

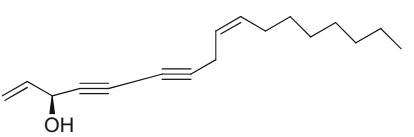

27

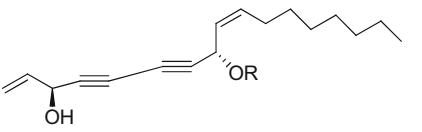

28: R = H
29: R = Ac

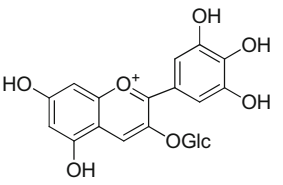

30

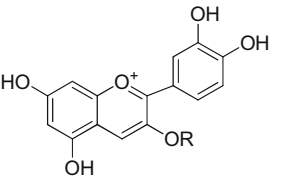

31: R = Glc
31a: R = Glc(6-1)-Rha

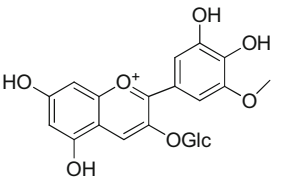

32

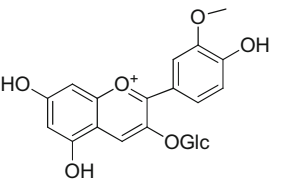

33

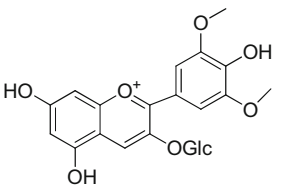

34

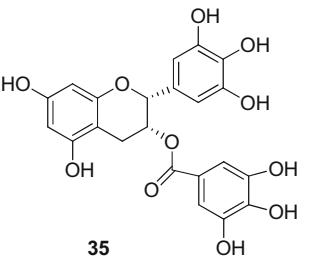

35

Fig. 4.1 (continued)

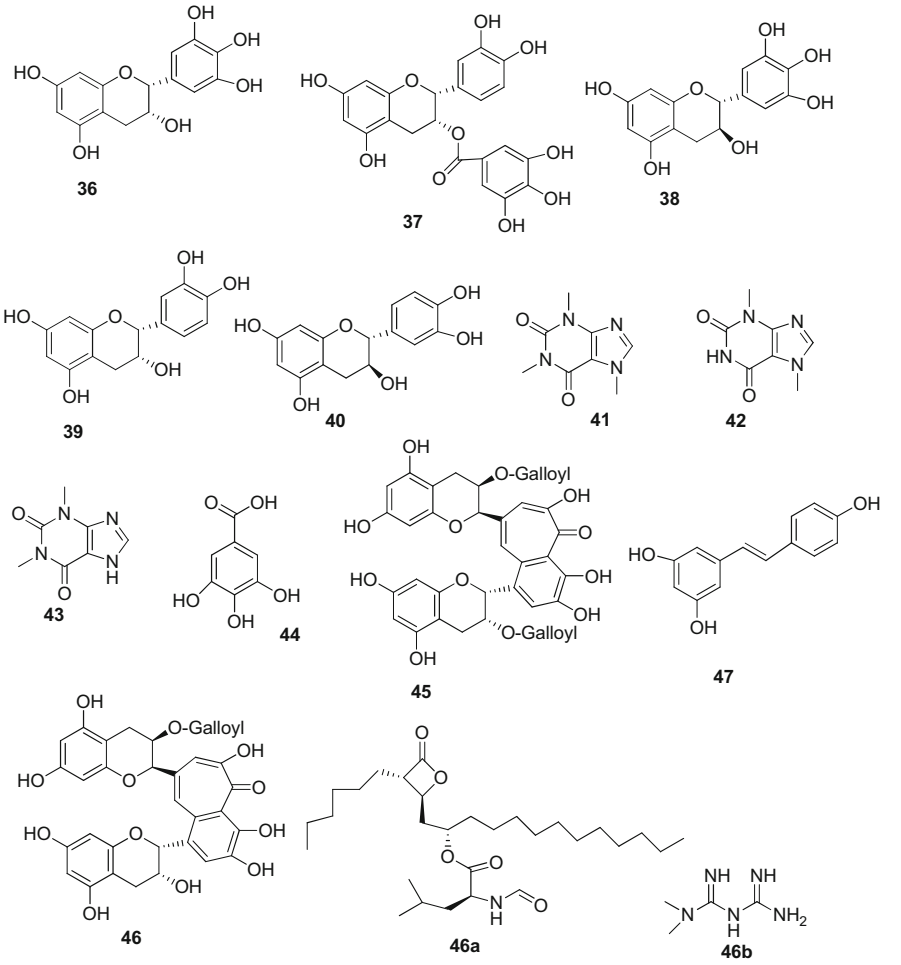

Fig. 4.1 (continued)

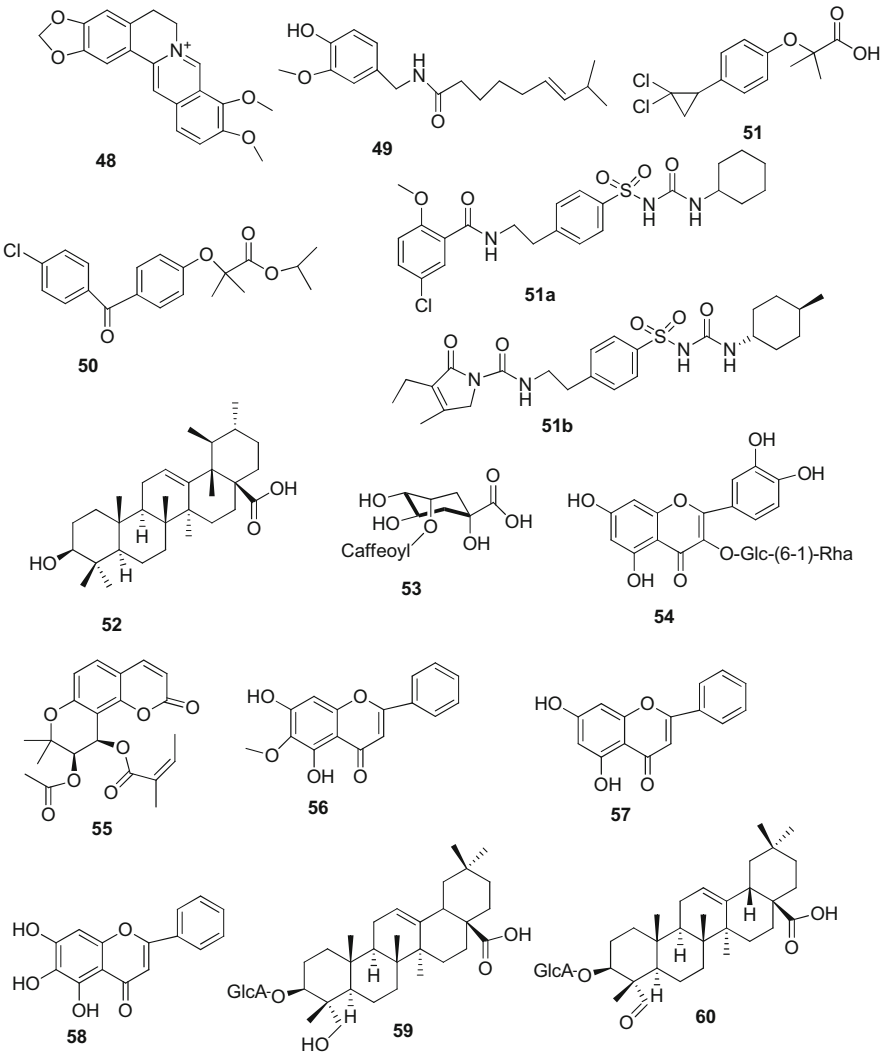

Fig. 4.1 (continued)

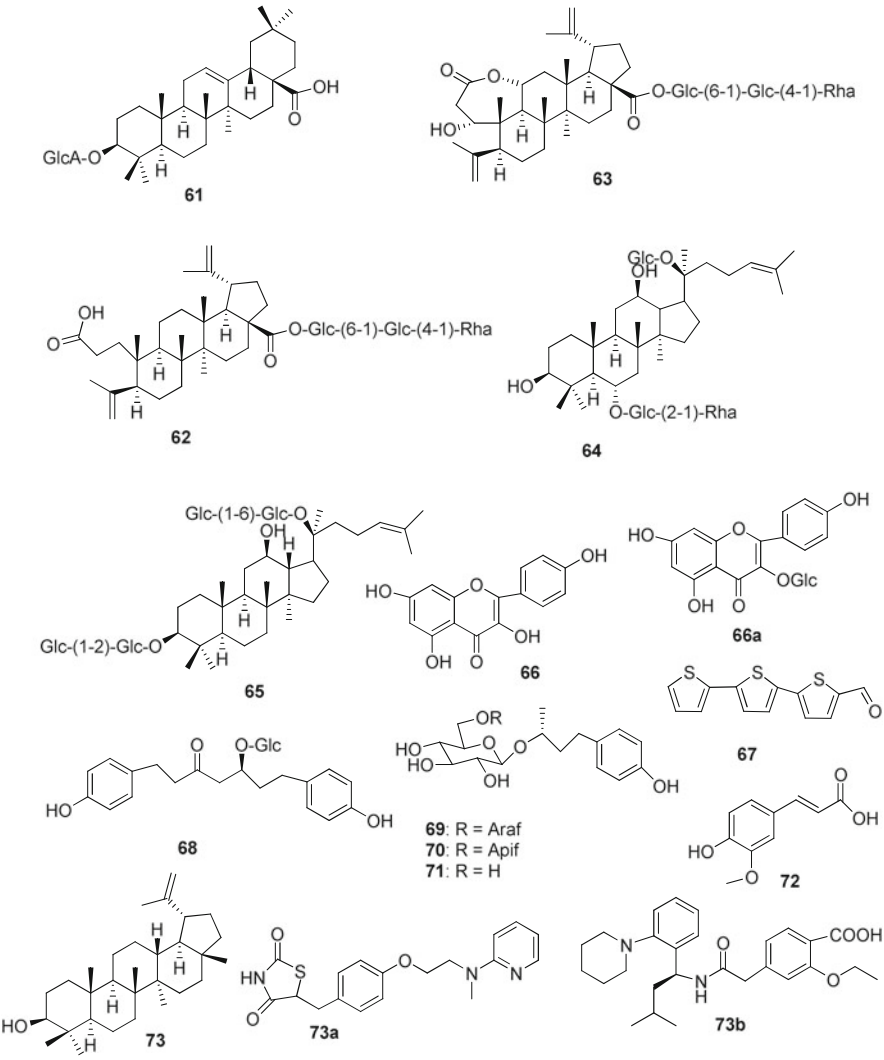

Fig. 4.1 (continued)

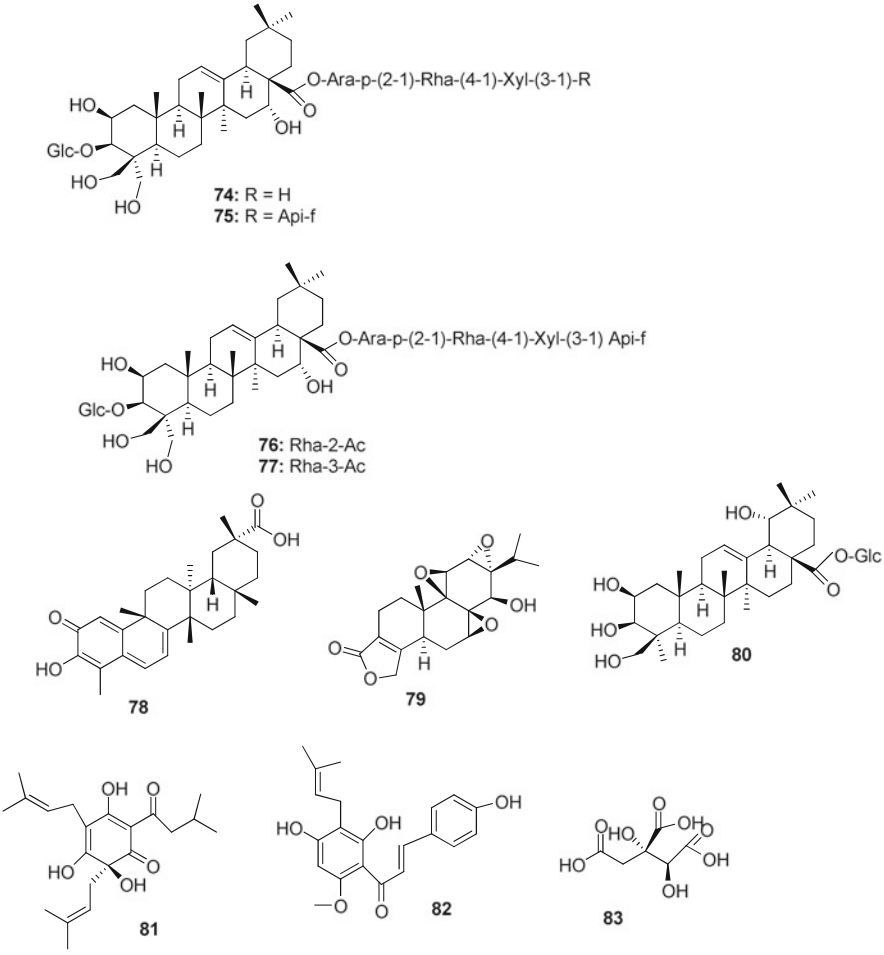

Fig. 4.1 (continued)

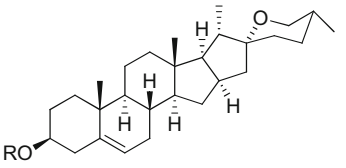

84: R = -Glc-(4-1)-Rha,-(2-1)-Rha
85: R = -Glc-(3-1)-Glc, -(2-1)-Rha
86: R = -Glc
87: R = -H
88: R = -Glc-(2-1)-Rha
89: R = -Glc

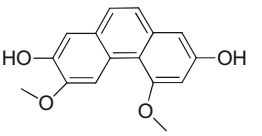

90

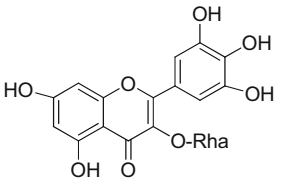

92

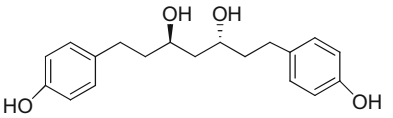

91

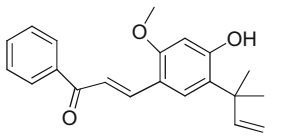

93

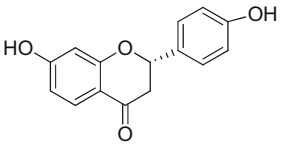

94

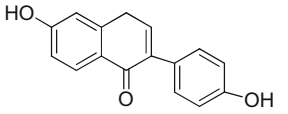

95

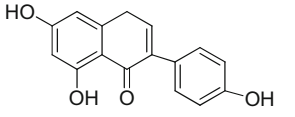

96

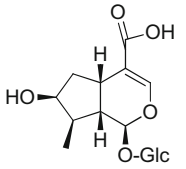

97

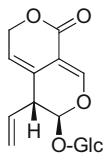

98

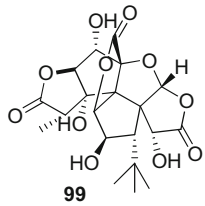

99

Fig. 4.1 (continued)

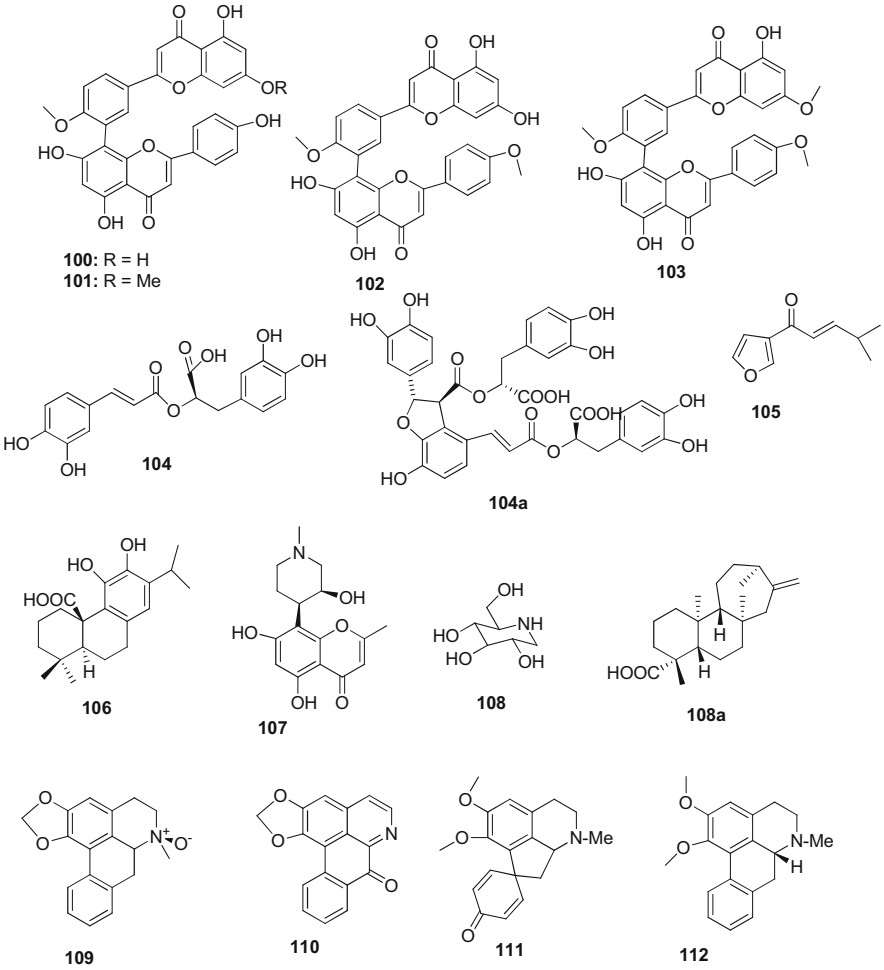

Fig. 4.1 (continued)

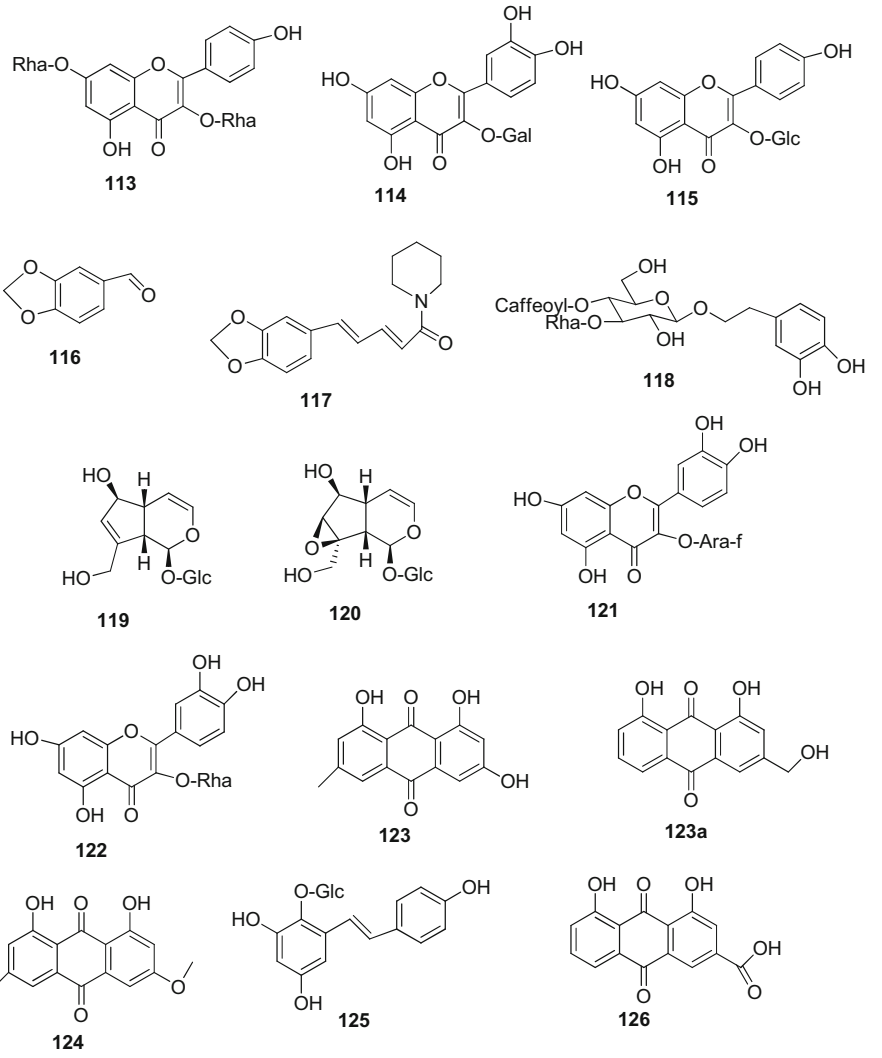

Fig. 4.1 (continued)

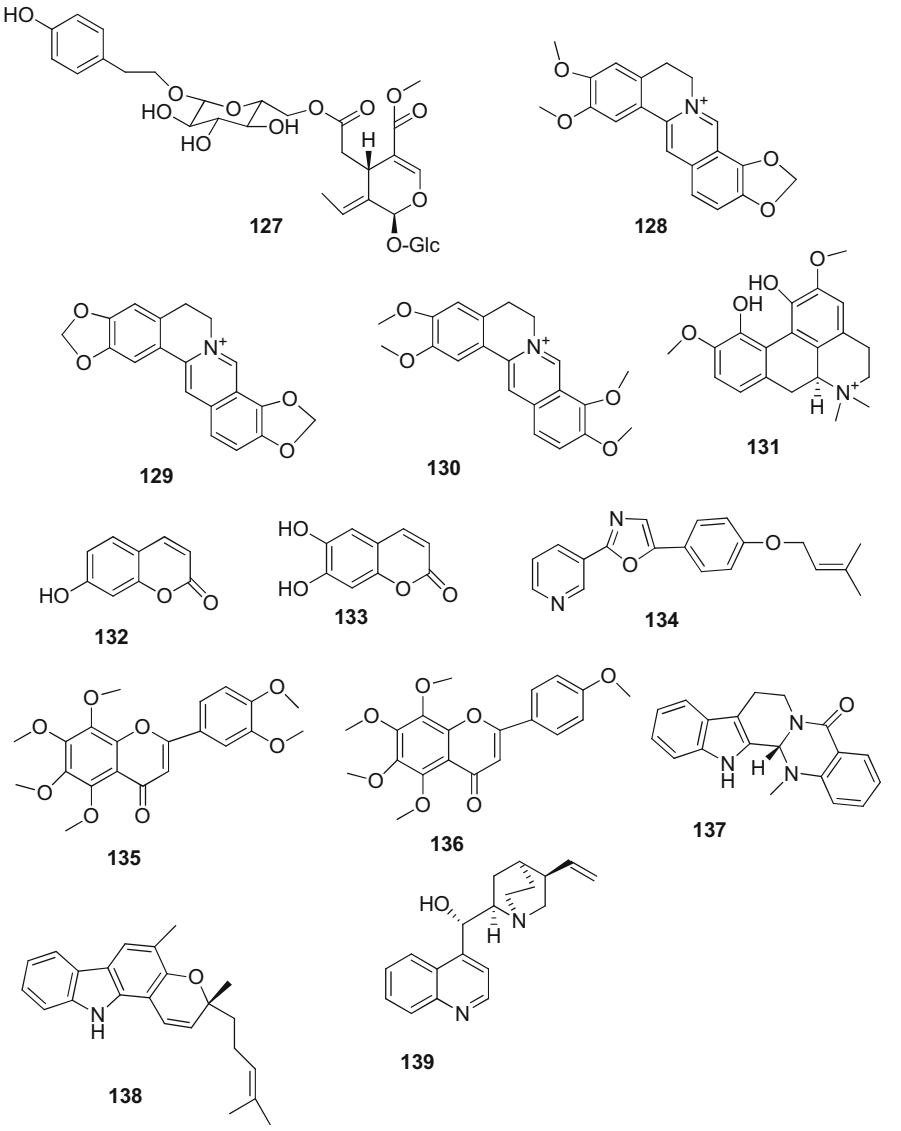

Fig. 4.1 (continued)

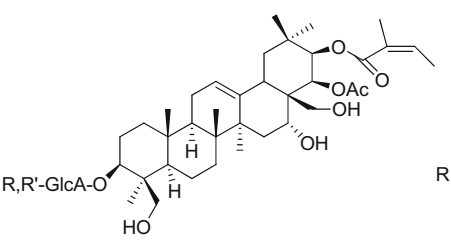

140: R = -(4-1)-Glc, R' = -(2-1)-Glc

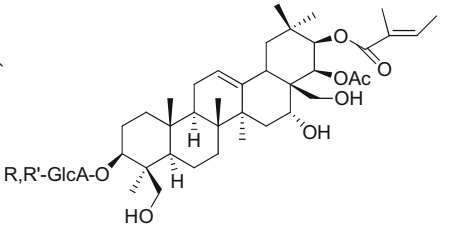

141: R = -(4-1)-Glc, R' = -(2-1)-Xyl

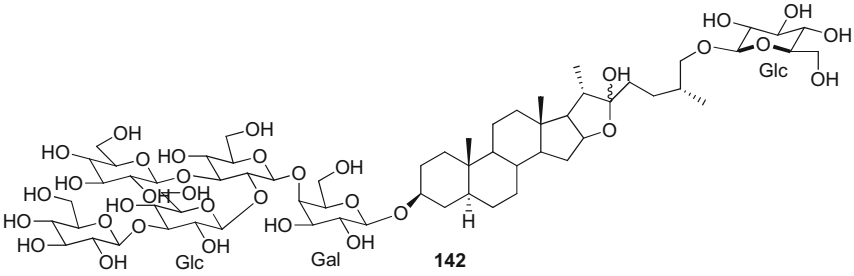

142

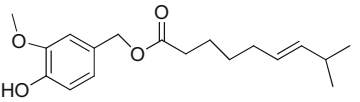

143

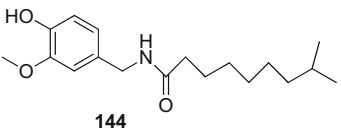

144

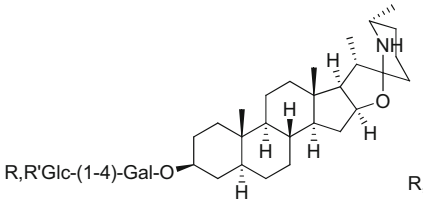

145: R = -(2-1)-Glc, R' = -(3-1)-Xyl

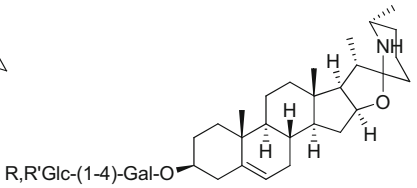

146: R =-(2-1)-Glc, R' = -(3-1)-Xyl

Fig. 4.1 (continued)

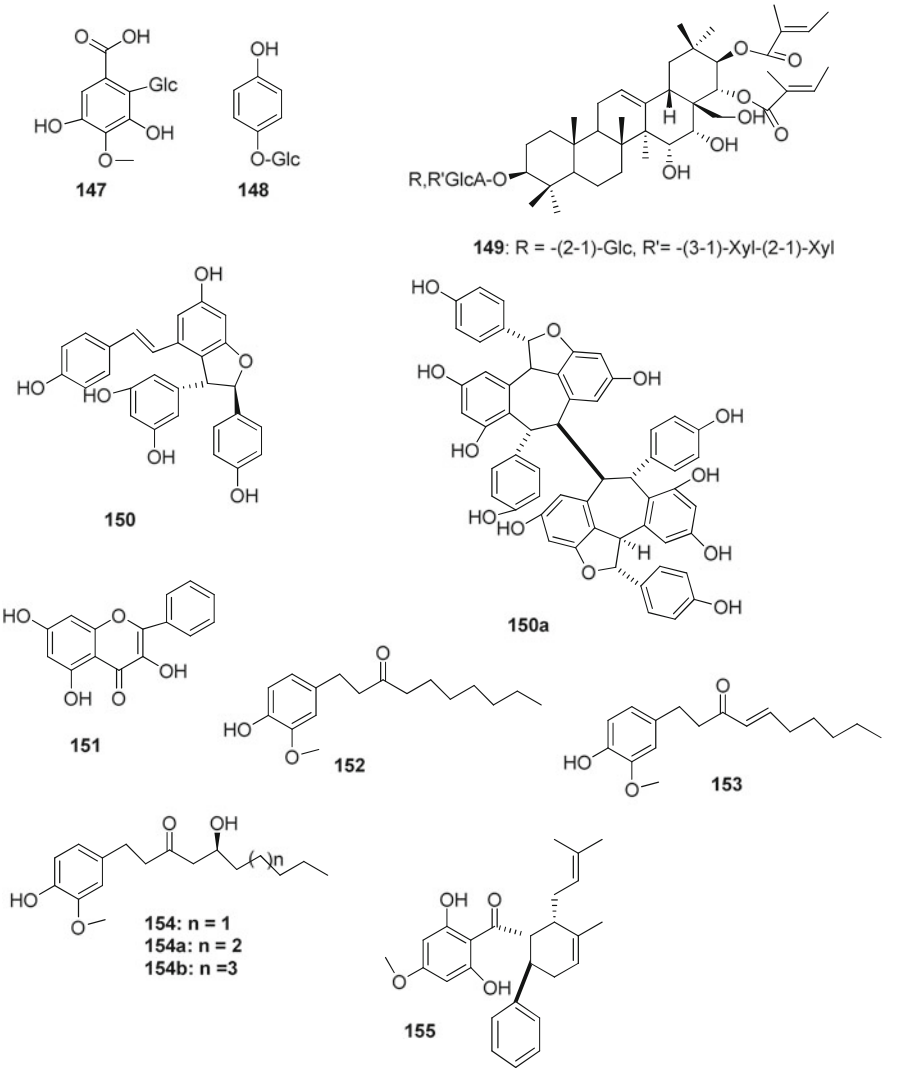

Fig. 4.1 (continued)

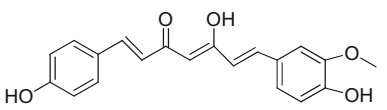

156

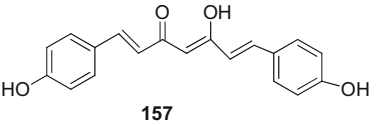

157

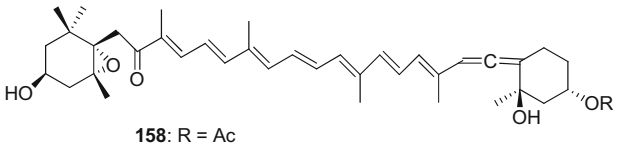

158: R = Ac
158a: R = H

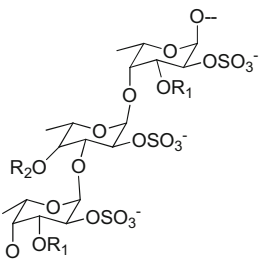

159: R_1 = SO_3- or H, R_2 = SO_3- or H

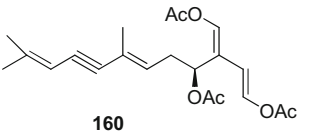

160

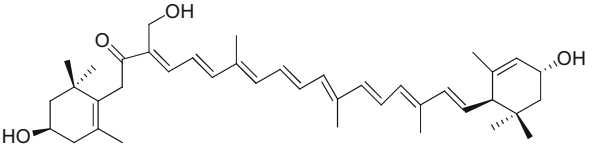

161

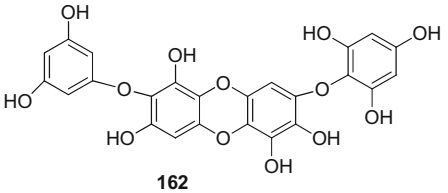

162

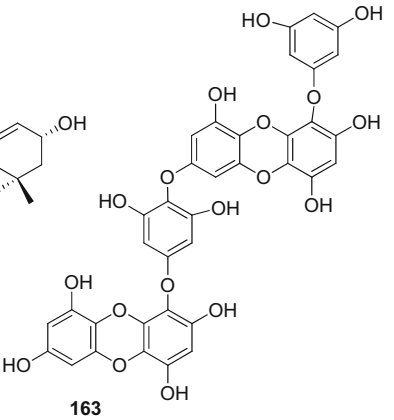

163

Fig. 4.1 (continued)

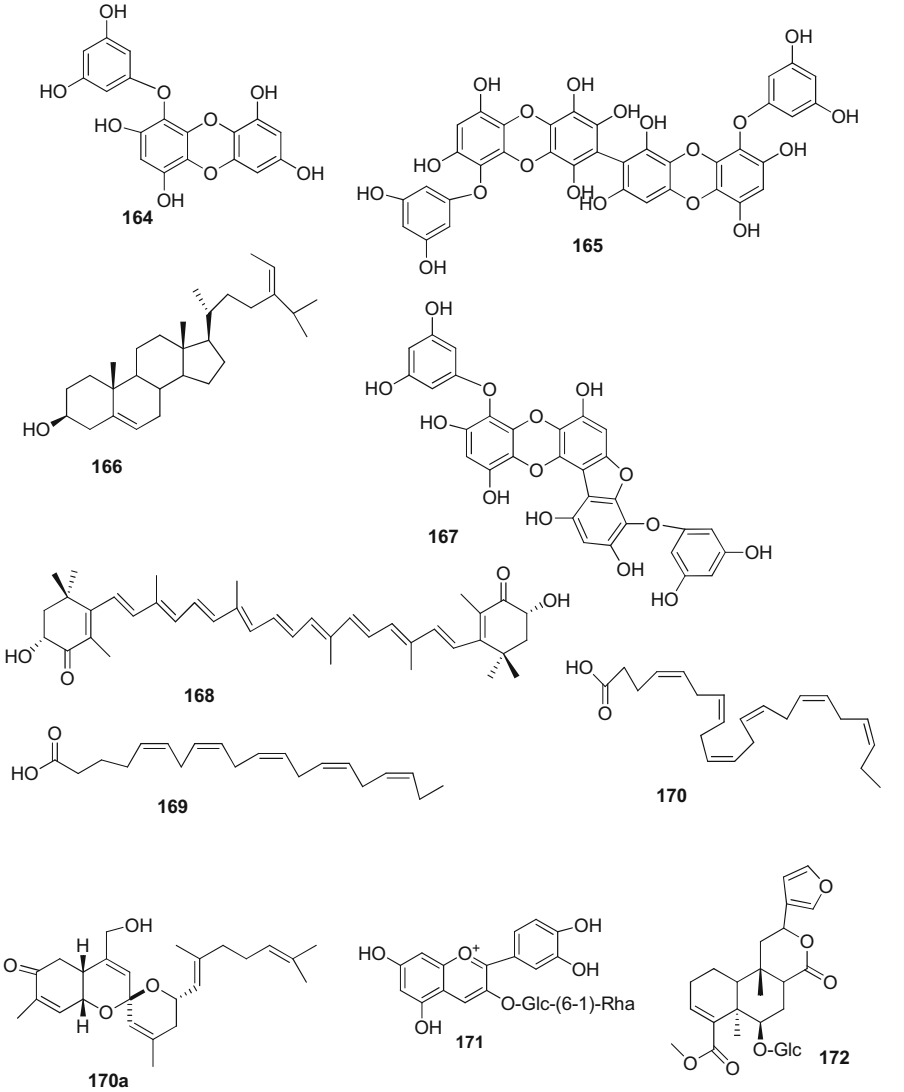

Fig. 4.1 (continued)

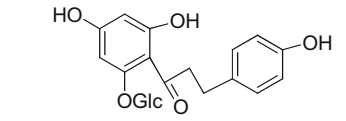

173

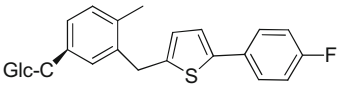

174

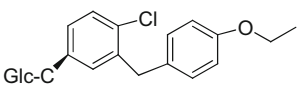

175

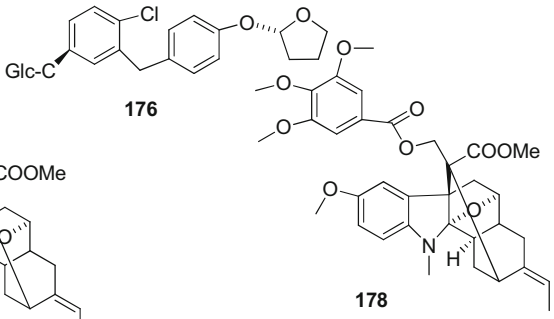

176

178

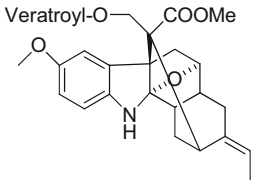

177

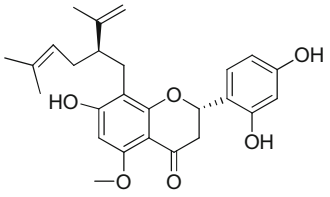

179

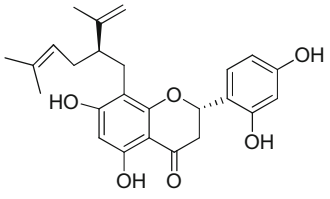

180

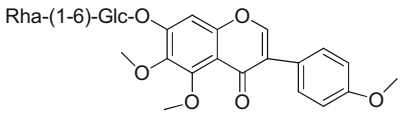

181

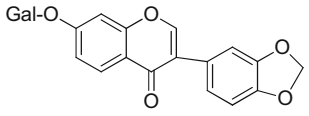

182

Fig. 4.1 (continued)

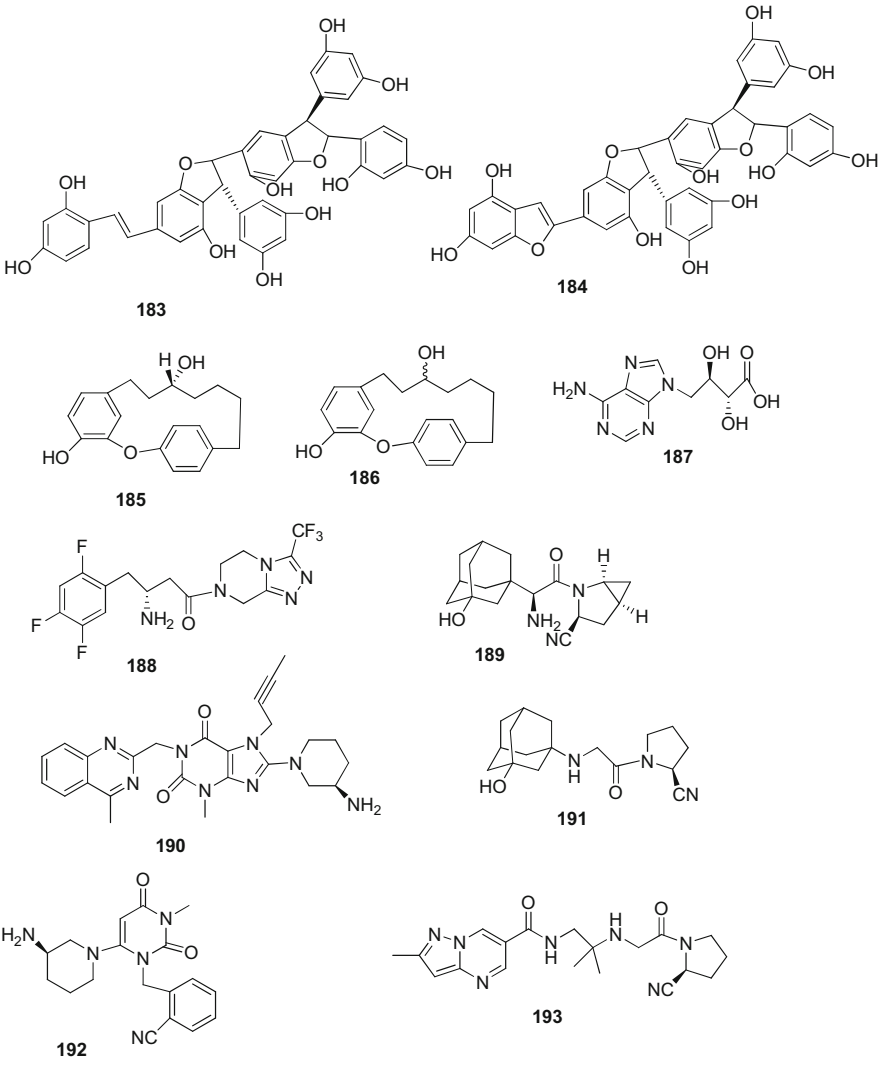

Fig. 4.1 (continued)

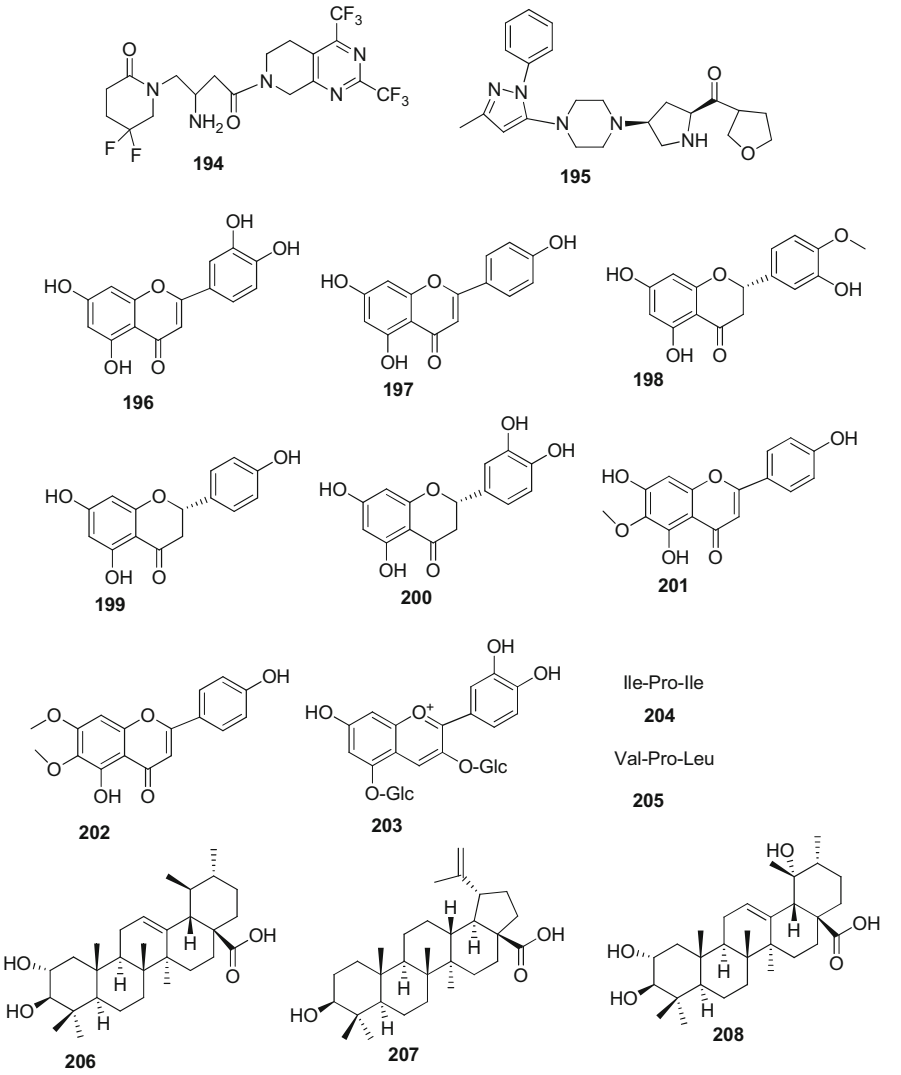

Fig. 4.1 (continued)

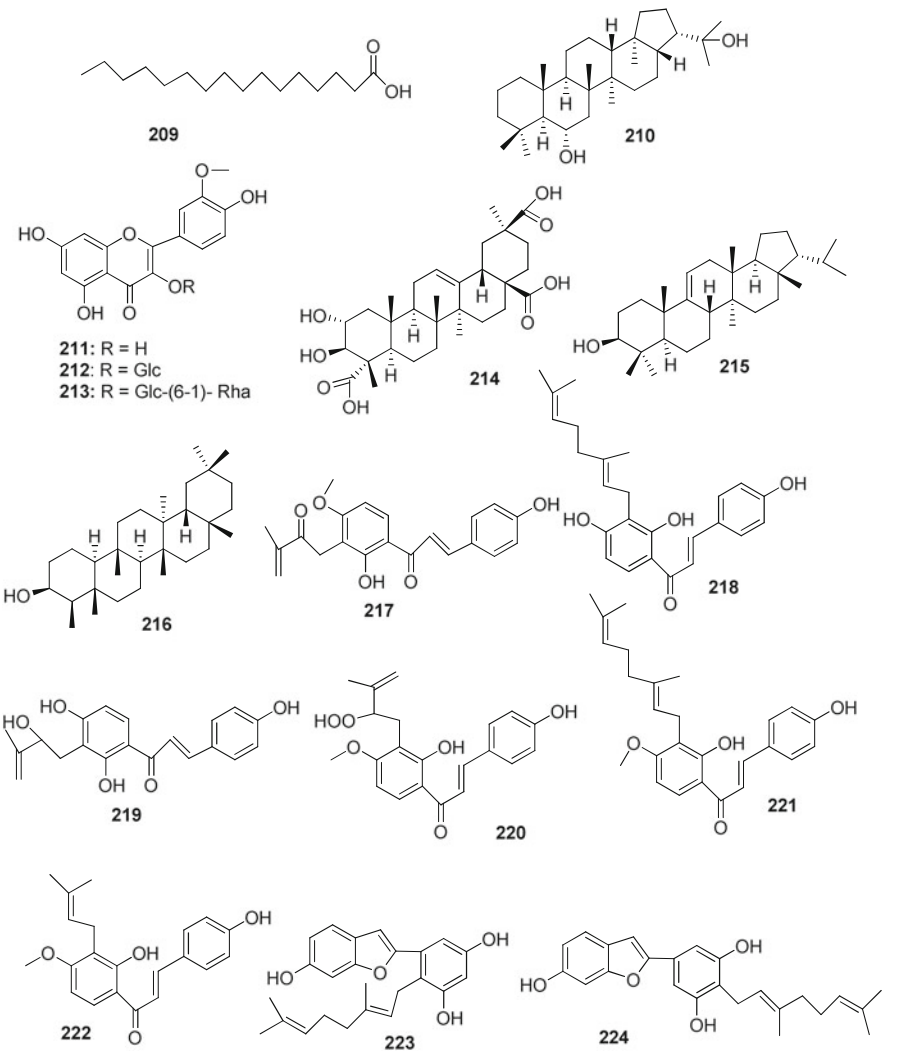

Fig. 4.1 (continued)

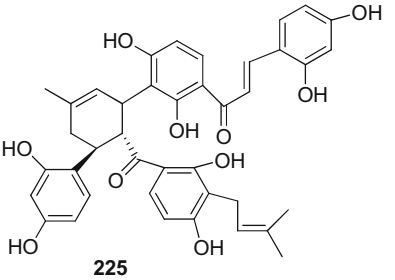

225

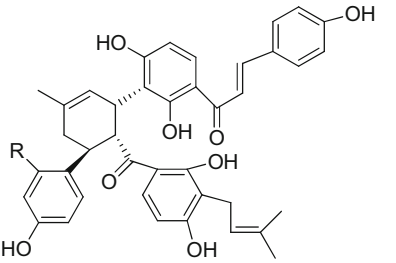

226: R = OH
227: R = H

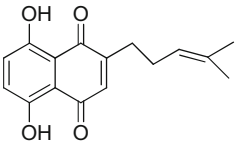

228

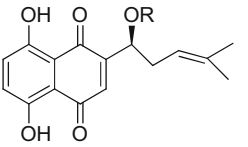

229: R = H
230: R = Ac

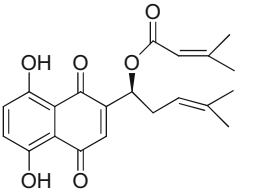

231

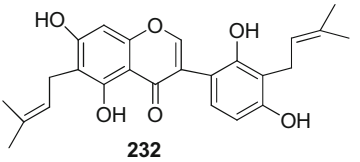

232

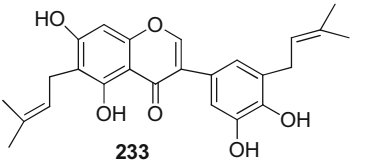

233

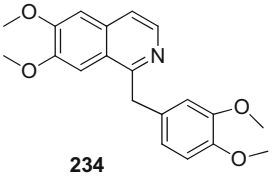

234

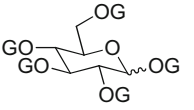

235: G = Galloyl

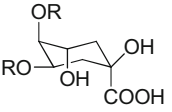

236: R = Caffeoyl

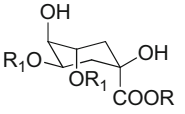

237: R = H, R_1 = Caffeoyl
238: R = Me, R_1 = Caffeoyl

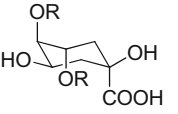

239: R = Caffeoyl

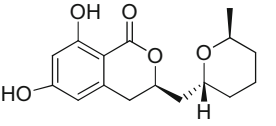

240

Fig. 4.1 (continued)

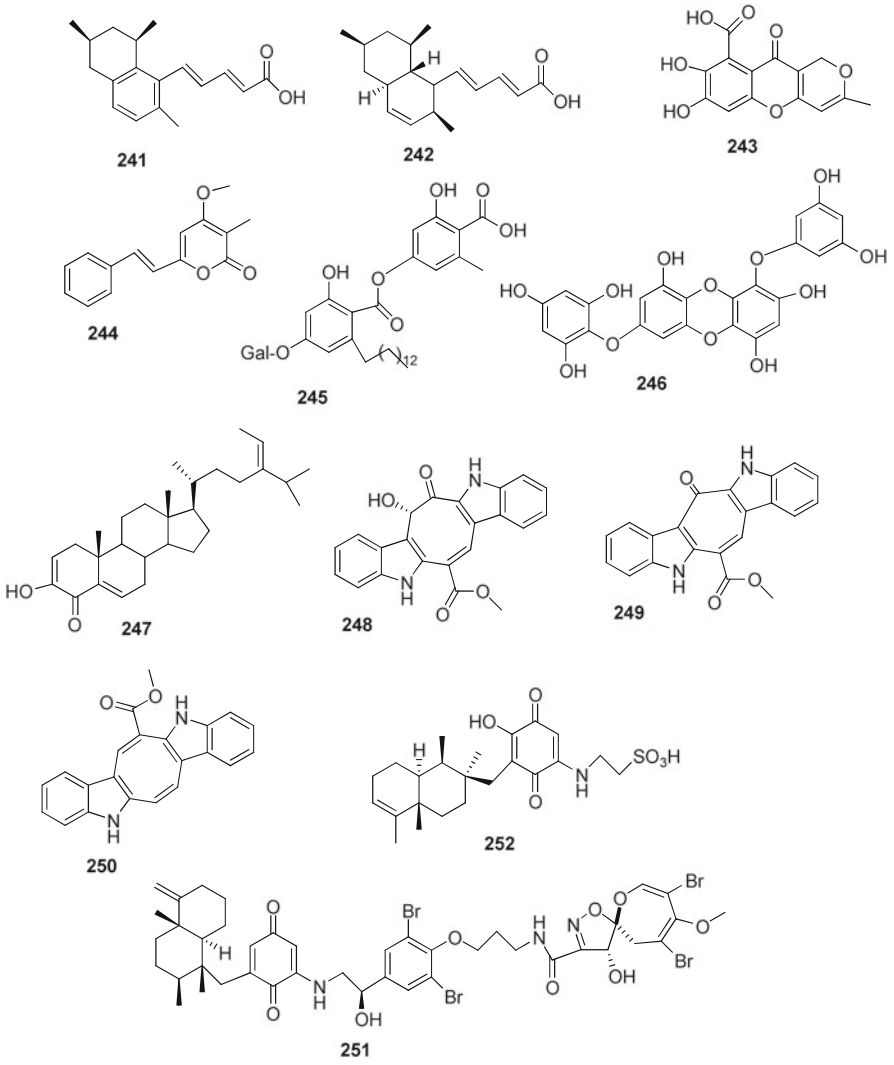

Fig. 4.1 (continued)

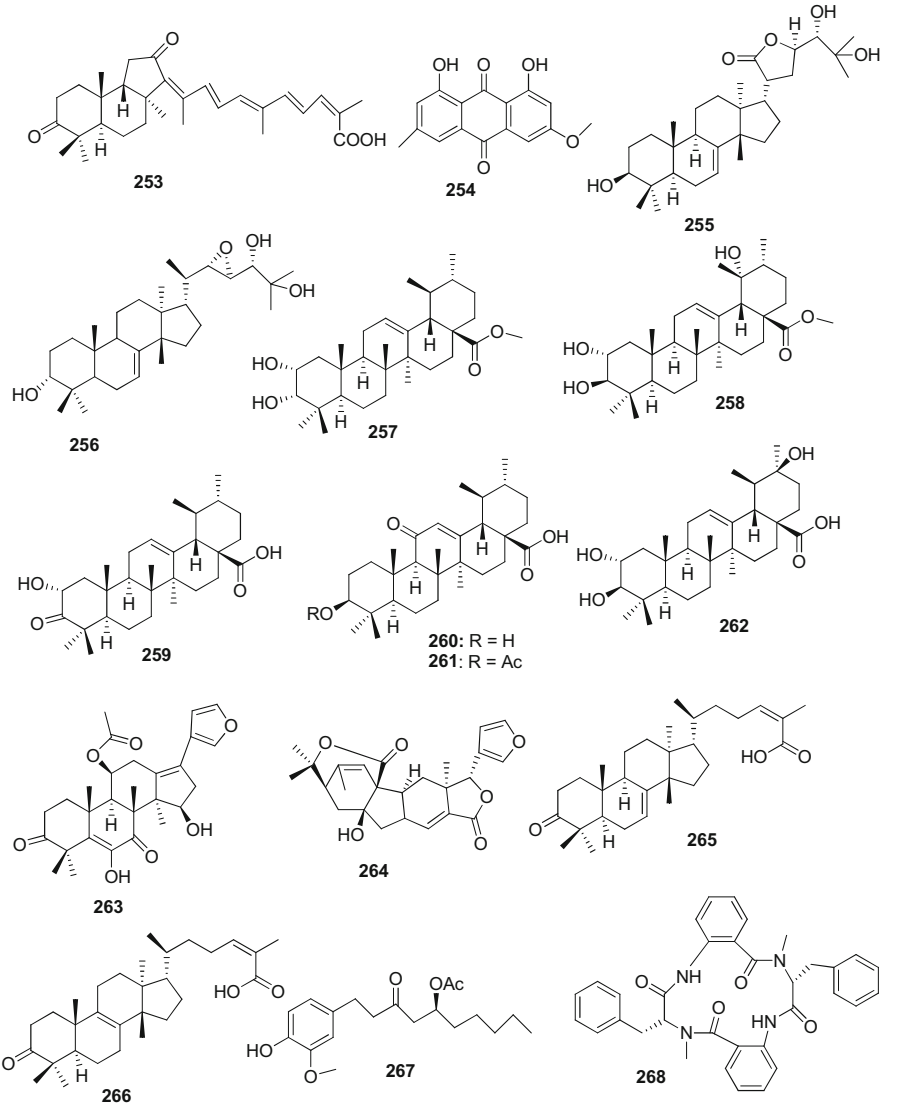

Fig. 4.1 (continued)

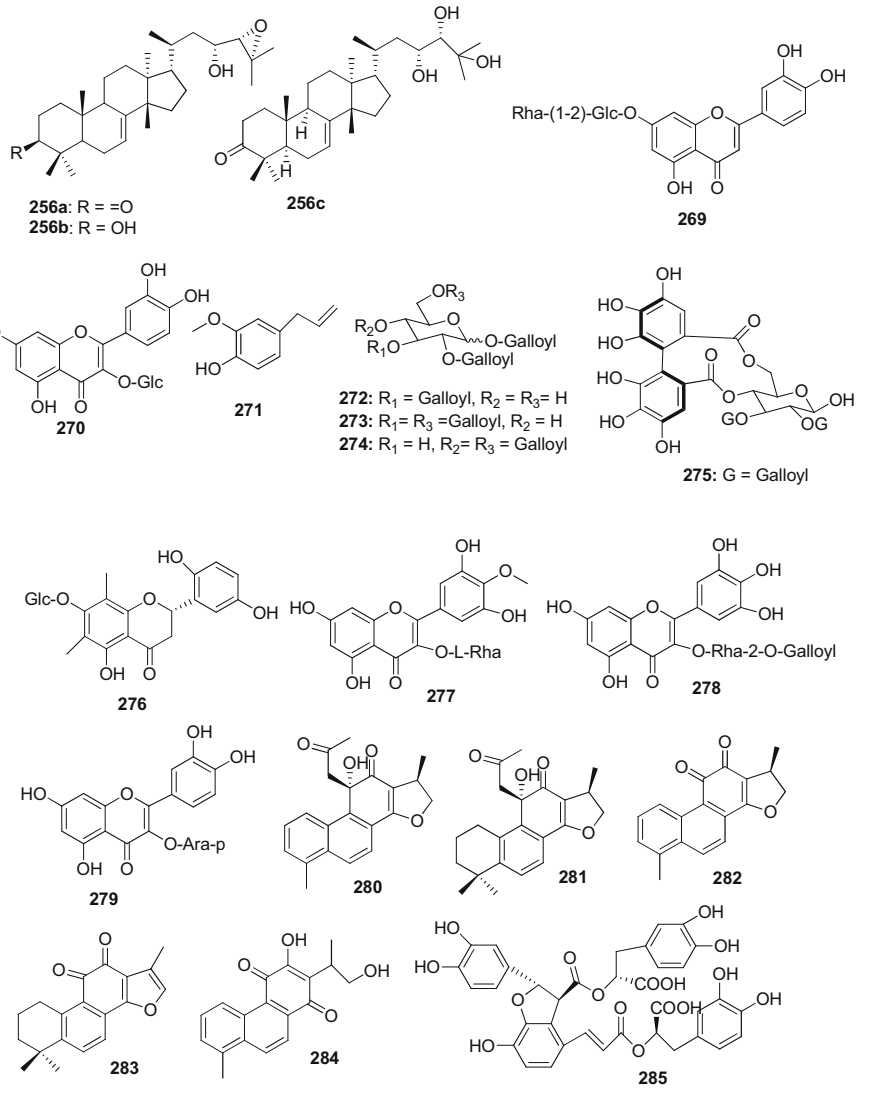

Fig. 4.1 (continued)

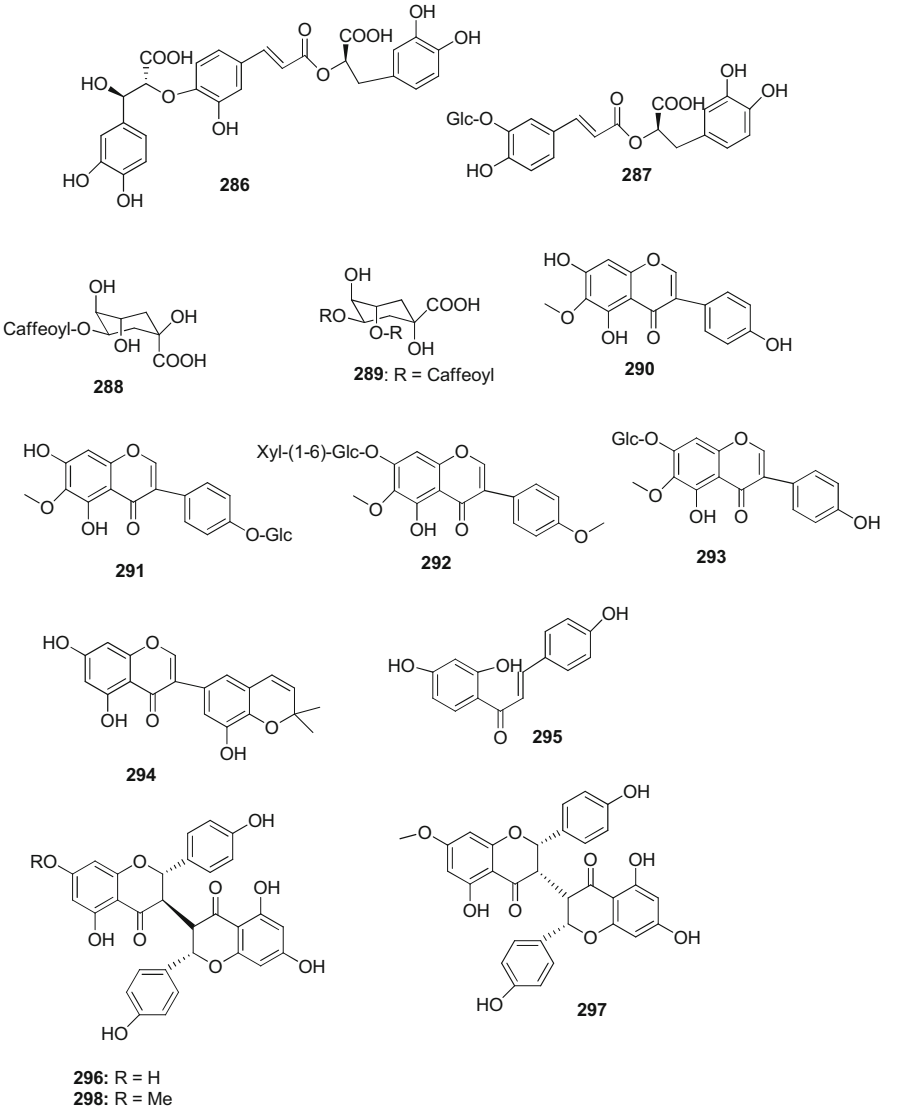

Fig. 4.1 (continued)

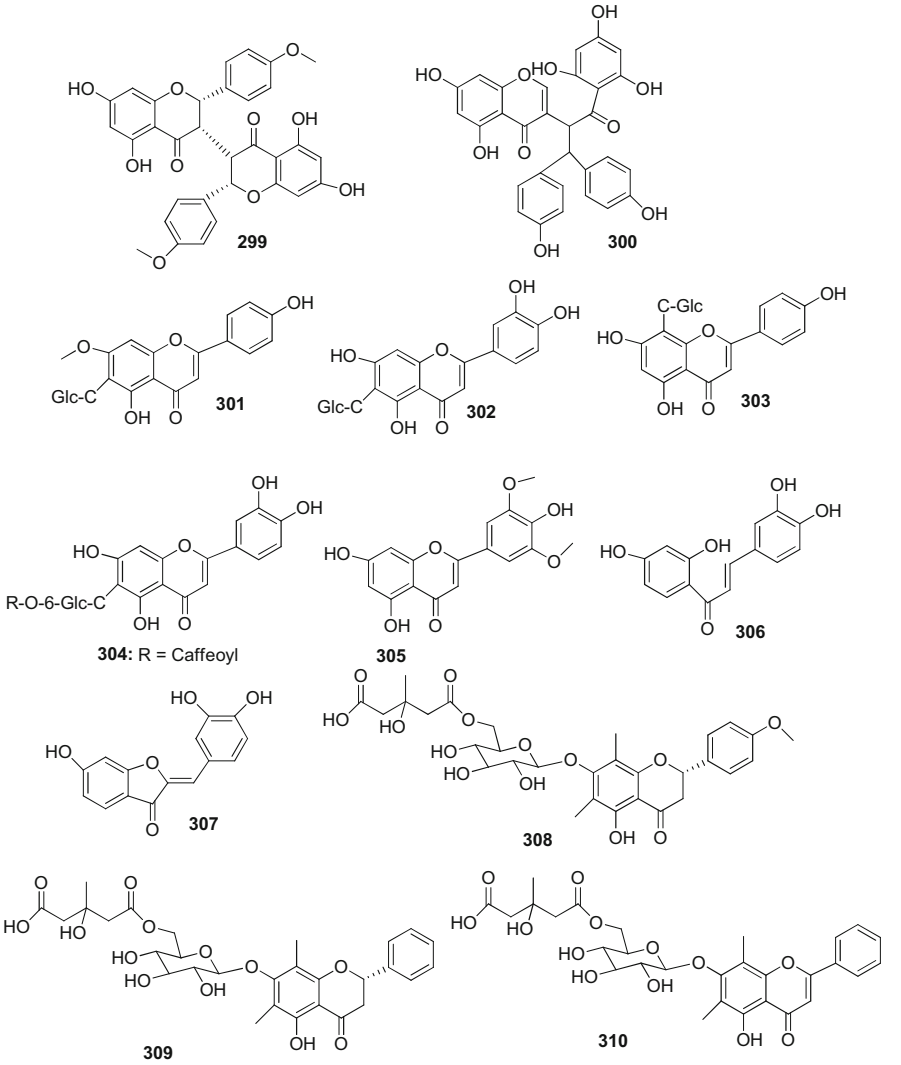

Fig. 4.1 (continued)

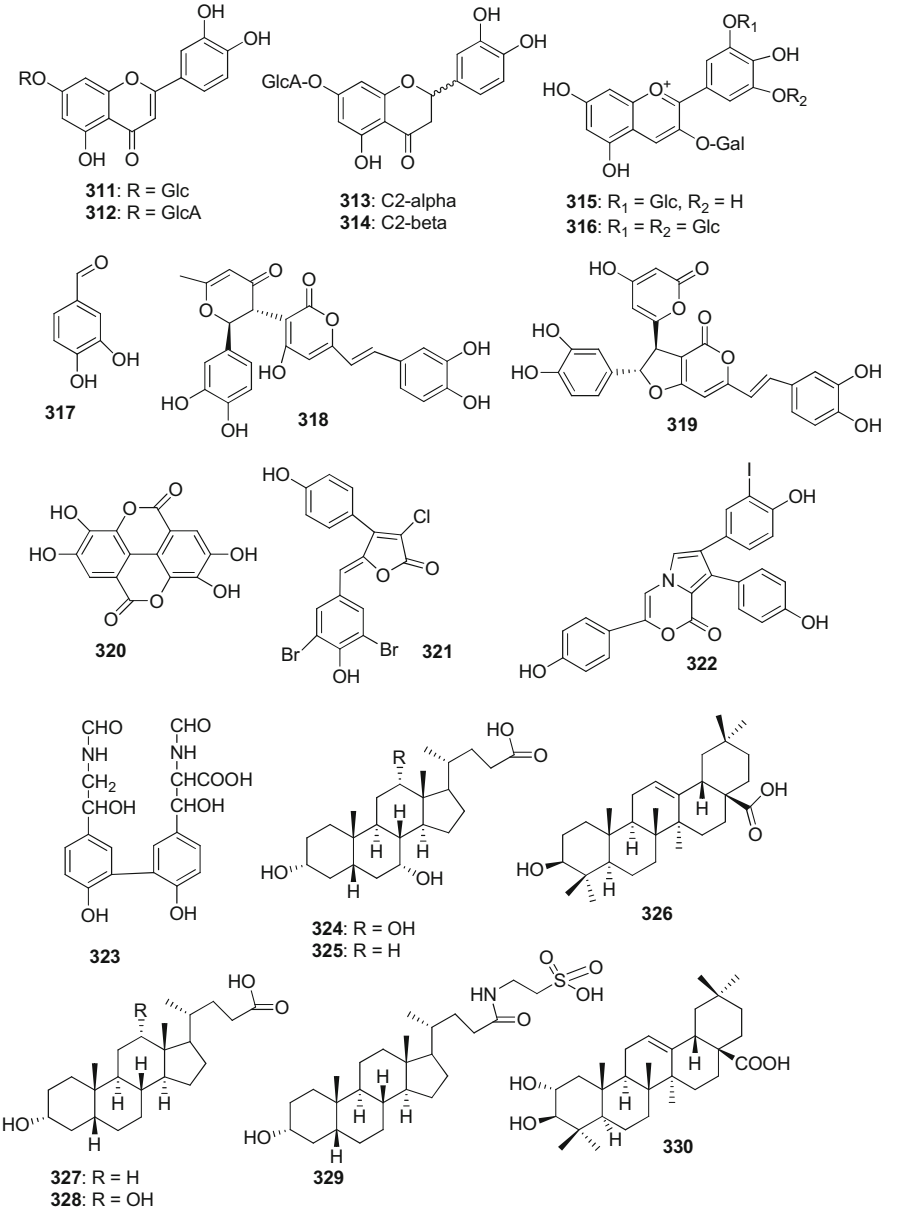

Fig. 4.1 (continued)

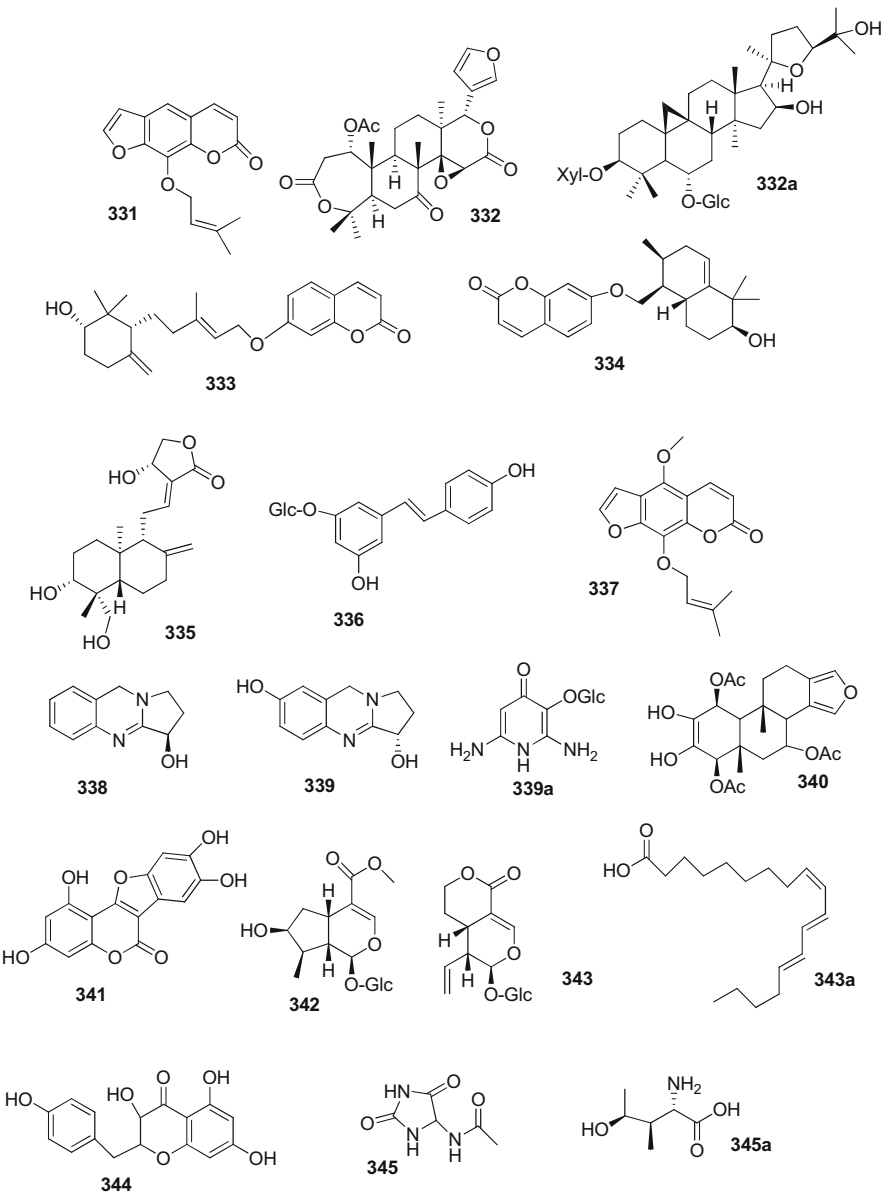

Fig. 4.1 (continued)

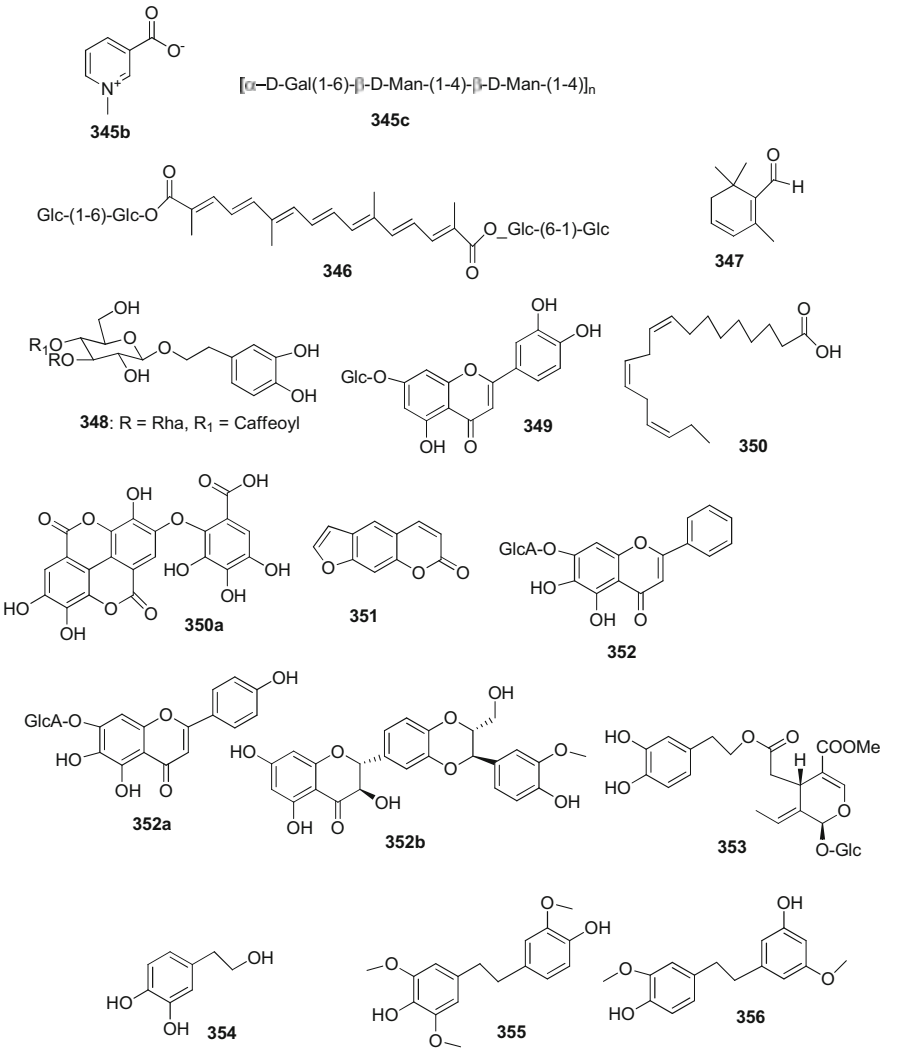

Fig. 4.1 (continued)

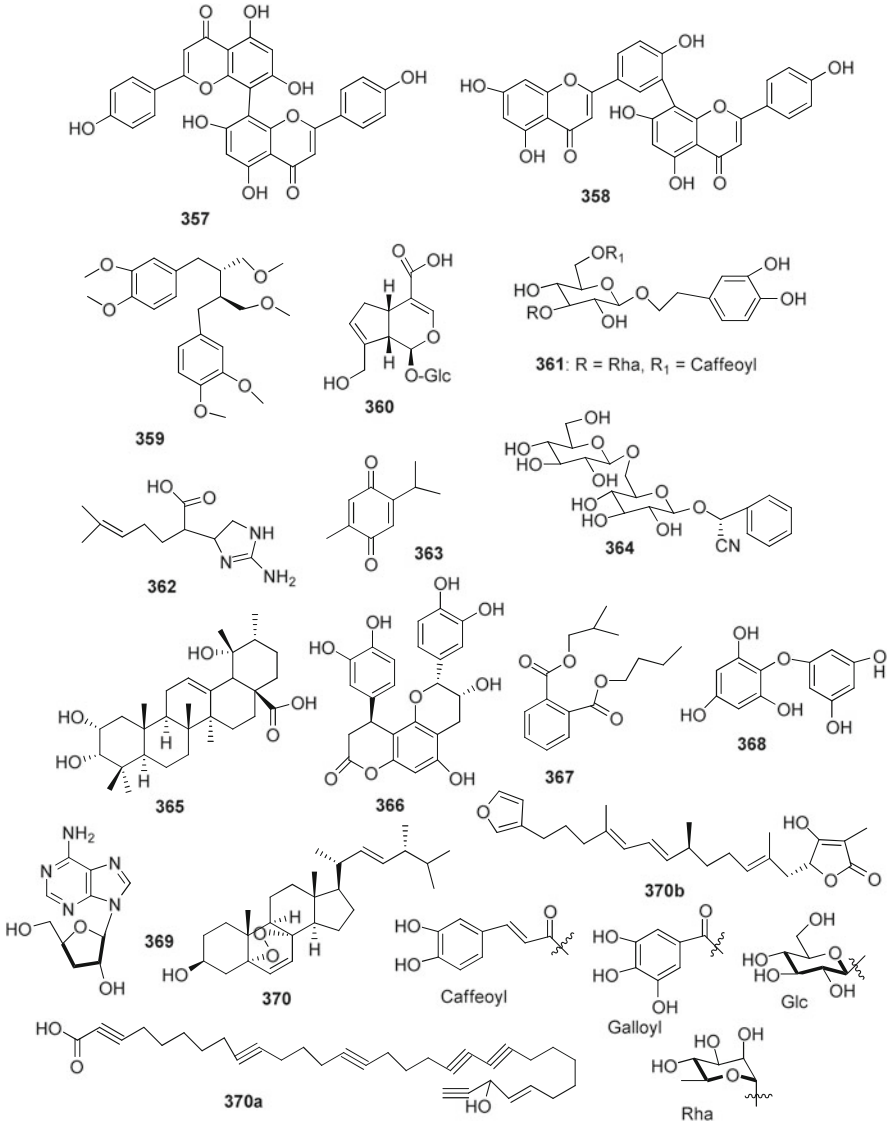

Fig. 4.1 (continued)

its rebound to 45% in 2010, then reduced to 13% in 2013, and increased again to 25% in 2015 and 33% in 2018 (Newman and Cragg 2020).

Among the existing 250,000–500,000 plant species, only a tiny proportion (about 5000 species) has been scientifically evaluated for bioactivities (Ngo et al. 2013; Payne et al. 1991). As per report of the International Union for Conservation of Nature and the World Wildlife Fund, about 50,000–80,000 flowering plants are being used for medicinal purpose worldwide. China and India have the highest numbers of medicinal plants used with 11,146 and 7500 species, respectively (Chen et al. 2016a). The WHO identified 21,000 medicinal plants from worldwide for evaluation of therapeutic potential, and out of them, 2500 species are of Indian origin, because of the location of India in a favorable climatic and geographical position for biodiversity (Modak et al. 2007). Therefore, a great proportion of untapped plants are remained to be explored in future research for identification of new natural products, which might offer huge potential information on their novel chemical structures and new types of biological actions related to new drug development. Recently introduced "multi-omics biotechnologies" are potential tools in the smart screening, robotic separation, and structural identification of bioactive metabolites and the proteins and genes involved in the biosynthesis of these metabolites. Moreover, these genomic, proteomic, transcriptomic, and metabolomic data analyses are greatly suitable for identification of plant species and microorganisms of therapeutic potential and their active metabolites by the use of instrumental facilities such as high-performance liquid chromatography, nuclear magnetic resonance spectroscopy, mass spectrometry, microfluidics, and computational algorithms. A recent report indicates that over 2,140,000 secondary metabolites from natural sources (plants, seaweeds, land and marine microorganisms, and marine animals) have been investigated and among them, over 35,000 are terpenoids and steroids (McMurry 2015). For example, the transcriptomic data of *Catharanthus roseus* helped us to find out the enzyme, iridoid synthase, responsible for conversion of linear monoterpene 10-oxo-geranial into bicyclic iridoids in medicinal plants by reduction and subsequent cyclization via a DA cycloaddition or a Michael addition (Geu-Flores et al. 2012). The genome analysis of medicinal plant, *Salvia miltiorrhiza* revealed the presence of 40 genes responsible for terpenoid biosynthesis, and out of them, 27 were novel, and 20 genes were involved in the biosynthesis of bioactive diterpenoids tanshinones (Ma et al. 2012). We have to pay our interest on herbal genomics and transcriptomics for the search of genes and enzymes that are used by medicinal plants and microorganisms for the synthesis of bioactive secondary metabolites and to use these genes and enzymes in biotechnical processes, such as in tissue culture, micropropagation, synthetic seed technology and molecular (SSRs) marker-based approaches for genome analysis, and plant breeding study to improve the yield and potency of medicinal plants as well as for large-scale production of these bioactive natural metabolites for their extensive clinical trials and commercial application (Chen et al. 2015, 2016a; Hao and Xiao 2015; Pandita et al. 2021; Sahu et al. 2014). Therefore, most of the pharmaceutical industries and research organizations related to drug

discovery have to rethink on their strategy for development of new drugs from untapped natural resources (Ngo et al. 2013; Zhu et al. 2012).

4.3 Factors Affecting the Composition and Contents of Phytochemicals in Processed Vegetative Foods

Phytochemicals are the important bioactive compounds of plant foods, such as fruits, vegetables, whole grains, and beverages, and are well recognized for their antioxidant, anti-inflammatory, and nutraceutical potentials, and their dietary consumption as plant foods is positively associated with health benefits, particularly in preventing the risks of a number of chronic diseases including obesity, diabetes, cardiovascular diseases, and cancers. Several studies demonstrate that the levels and composition of phytochemicals, such as phenolics (including flavonoids, catechins, anthocyanins, tannins and phenolic acids), terpenoids, carotenoids, saponins, alkaloids, and glucosinolates, depend on many factors, such as cultivar types, propagation types, environmental and agronomic conditions, harvest and food processing operations, and storage factors. Adequate knowledge on these areas might be useful to take suitable strategies in different stages of cultivation, harvesting, and post-storage of these dietary crops by the food producers to get maximum yields of better quality of fruits, vegetables, and other crops having high concentrations of bioactive phytochemicals (Tiwari and Cummins 2013; Li et al. 2012a).

4.3.1 Cultivar Effect

Fruits and vegetable growers need to select the cultivars or genotypes of a crop with high phenolic and carotenoids content. About 70–90% of the carotenoids consumed by humans are available from dietary fruits and vegetables. However, most of the fruits and vegetable growers prefer to cultivate a cultivar that provides high yield and large size of fruits and vegetables as per consumer's demand rather than considering the high quality of these fruits and vegetables in terms of health-benefit potential and concentration levels of bioactive phytochemicals. For instance, blueberry (*Vaccinium* spp.) fruits have health benefit effects due to presence of high content of polyphenolic compounds, particularly anthocyanins, flavonoids, chlorogenic acids, and other compounds, cellulose (about 3.5%), pectin (about 0.7%), and dietary fibers (about 1.5%), which have nutritional value. In New Zealand, two cultivars of blueberry, *Vaccinium corymbosum* and *V. virgatum*, are commercially cultivated. The highbush blueberry, *V. corymbosum*, is more acceptable to the consumers compared to rabbiteye blueberry *V. virgatum*, because of less seediness and better fruit size, although it has lower anthocyanins content (18–249 mg/100 g of fw) compared to rabbiteye seedy variety (12.7–410 mg/100 g of fw) (Scalzo et al. 2015). The delicious strawberry fruits (*Fragaria* × *ananassa* Duch) are consumed both as fresh and processed, because of the presence of health benefit polyphenolic compounds, anthocyanins, ellagitannins, flavonols, and polymeric flavan-3-ols. The

identification and quantification of the phenolic compounds in 27 cultivars of strawberry grown in Norway and harvested in 2009 revealed that total phenolic compounds content varied among the cultivars, from 57 to 133 mg/100 g of fw. Among the polyphenolic compounds, anthocyanins were most abundant (8.5–65.9 mg/100 g of fw), followed by flavan-3-ols (11–45 mg/100 g of fw), and ellagitannins (7.7–18.2 mg/100 g of fw). Among the common cultivars, Blink, Korona, Polka and Senga Sengana, among them, Senga Sengana is preferred for processing due to its low anthocyanins content (27.4 mg/100 g of fw), and Korona is preferred for fresh consumption due to high anthocyanins content (49.1 mg/100 g of fw) (Aaby et al. 2005, 2012). The contents of a variety of polyphenols (about 48) and triterpenes (mainly 3) at the ripening stage of three cranberry cultivars, Pilgrim, Stevens, and Ben Lear, grown in Poland are found different, although these polyphenols and triterpenes are identified in all these genotypes. The cultivar Stevens has highest concentrations of bioactive phenolic acids and antioxidant capacity compared to other tested cultivars (Oszmianski et al. 2018). Genotype (cultivar) variation in stone fruits, nectarines (*Prunus persica*), peaches (*Prunus persica vulgaris*), and plums (*Prunus salicina*) also reflects the variation of composition and contents of phenolic compounds, carotenoids, and vitamin C. A comparative study to the chemical composition of the stone fruits, from five cultivars, each of white-flesh nectarines, yellow-flesh nectarines, white-flesh peaches, and yellow-flesh peaches and plums, grown in California, revealed the ranges of total phenolics (in mg/100 g of fw) 14–102, 18–25. 28–111, 21–61, and 42–109; total carotenoids (mg/100 g of fw) 7–14, 80–186, 7–20, 71–210, and 70–260; and vitamin C (mg/100 g of fw) 5–14, 6–8, 6–9, 4–13, and 3–10, respectively. Major phenolic compounds in these fruits are hydroxycinnamic acids, flavan-3-ols, flavonols, and anthocyanins. In nectarines and peaches, both hydroxycinnamic acids and flavan-3-ols are strongly correlated with antioxidant activity of the fruits, whereas in case of plums, only flavan-3-ols are correlated to the antioxidant activity of fruits (Gil et al. 2002). A study on the phytochemicals levels and composition in the maturity stage of mulberry fruits in four cultivated mulberry cultivars, *Morus alba*, *M. laevigata*, *M. macroura*, and *M. nigra*, which are grown in Pakistan, reveals that the total phenolic content is highest in *M. nigra* (395–2287 mg GAE (gallic acid equivalent)/100 g of dw), while it is lowest in *M. laevigata* (201–1803 mg GAE/100 g of dw), whereas the total flavonoid content is highest in *M. nigra* (245–1021 mg catechin equivalent (CE)/100 g of dw), and it is lowest in *M. macroura* (145–249 mg CE/100 g of dw). Among the identified phenolic acids, p-coumaric acid (**19**) and vanillic acid (**20**) are major constituents in *M. nigra* and *M. laevigata*, while p-hydroxybenzoic acid and chlorogenic acid (**21**) are major phenolic acids in *M. alba* and *M. macroura*. Among the identified flavonoids, the content of myricetin (**22**) is high in *M. alba* (88 mg/100 g of dw) and the content of quercetin (**23**) is high in *M. laevigata* (145 mg/100 g of dw). It indicates that *M. nigra* cultivar fruits are rich in antioxidant phytochemicals (Mahmood et al. 2012).

A study on the contents and composition of phytochemicals in 20 cultivars of tomato (*Solanum lycopersicum* syn *Lycopersicon esculentum*) reveals that the levels of major phytochemicals, carotenoids (lycopene **24**, β-carotene **25**, all-*trans*-lutein

26, and their 22-*cis*-isomers) and phenolic compounds and their antioxidant activity are dependent on genetic background and maturity in the harvest stage (Li et al. 2012b). Among the two tomato cultivars, 'supersweet' cherry tomato and conventional 'counter' round tomato grown in a greenhouse, the cherry tomato has high content of lycopene (5.5–8.3 mg/100 g of fw) compared to round type (4.9–5.8 mg/100 g of fw), and high concentration is observed in autumn season (Krumbein et al. 2006).

4.3.2 Propagation Effect

The composition of phytochemicals, particularly phenolic compounds contents in berry fruits, depends on the propagation process of the berry plant, such as on seed germination process or clonal plantation through stem or rhizome cutting or in vitro microtissue culture process. Three varieties of blueberry crops, high-bush *Vaccinium corymbosum*, low-bush *V. angustifolium*, and rabbiteye *V. ashe* are commercially cultivated in many countries. Most of the nurseries or orchard farms prefer stem cutting (SC) and tissue culture (TC) process for propagation of blueberry plants rather than the conventional seed germination process. It is observed that in vitro TC-derived high bush and low bush blueberry plants grow faster with more shoots but with less flowers and smaller berries than SC-derived plants, while the berries from TC propagated plants have higher levels of polyphenols, flavonoids, and anthocyanins than that in the fruits from SC plants. Similar trends are also found in micro-propagated strawberry plants (Debnath and Goyali 2020).

4.3.3 Effects of Environmental Factors

Environmental factors, such as geographic location, soil type, soil nutritional status, temperature, precipitation, and sunlight, influence the concentrations and composition of phytochemicals in vegetable crops (Lumpkin 2005). Each vegetable crop requires a specific environmental setup that provides the crop plants to reach better growth and high concentrations of health-promoting phytochemicals. It has been observed that faster growth rate of crop plants reduces the concentrations of polyphenols and vitamins in crops by dilution effect (Davis et al. 2004). Soil-type and appropriate nutrient supply enhance the concentrations of antioxidant phytochemicals in vegetable crops. Available evidence demonstrates that muck soil rich in decomposed organic matters and nitrogen content is suitable for the growth of root crops, onions, carrots, radishes, lettuces, celery, etc. Cultivation of onions in raised beds (zone tillage) provides better size and yield of onions compared to conventional flat beds cultivation (Swanton et al. 2004). Soil moisture content also influences the concentrations of phytochemicals in vegetable crops. The bioactive polyacetylenes, falcarinol (**27**) and falcarindiol (**28**), present in carrots (*Daucus carota*) improve insulin stimulated glucose uptake in human adipocytes and myotubes and have antidiabetic property. In water stress conditions such as

insufficient water or excess soil moisture in carrot (cv 'Orlando Gold') grown in the green house reduce the concentrations of eight polyacetylenes including three known ones, falcarinol, falcarindiol, and falcarindiol-3-acetate (**29**) by about 30%, 37%, and 46%, respectively (Lund and White 1990). Tomato is the second largest group of vegetable crops cultivated in the world. It is rich in carotenoids (lycopene (**24**) of about 90% and β-carotene (**25**) of 6–8%), tocopherols, vitamin C, potassium, and iron. Consumption of tomatoes in diet significantly reduces the risk of atherosclerosis, cardiovascular diseases, and some types of cancer (Olson 1986). Lycopene content in tomatoes depends on water supply and temperature. The less-water supply and moderate temperature (12–32°C) favor high lycopene content. For this reason, higher lycopene content is observed in tomatoes harvested in greenhouse (83 mg/kg of fw) than in field-grown tomatoes (59.2 mg/kg of fw) at every harvesting time (Brandt et al. 2003). Another study reported that a temperature range (15–24°C) showed maximum concentration of lycopene, after which, lycopene biosynthesis was reduced sharply and completely inhibited at 32°C. For this reason, winter season is the best time for tomato cultivation in open fields (Krumbein et al. 2006). Agronomic practice of crop plants in extreme environmental stress situation influences the levels of phytochemicals in many vegetable crops. For example, application of rich sulfur fertilization (150 kg/ha) in the cultivation of eight broccoli cultivars in late spring season increases the total phenolic content (flavonoid content (about 3-fold) followed by total sinapic and feruloyl acid derivatives and total caffeoylquinic acid derivatives) and vitamin C content compared to those grown in poor sulfur fertilization (15 kg/ha) and conventional early winter season. Moreover, five commercially grown cultivars produced higher amounts of phenolic compounds and vitamin C than three experimental ones (Vallejo et al. 2003). Sowing season of agronomic practices has an impact on the levels of phytochemicals in crops. In Northwestern Spain, cabbages (*Brassica oleracea*) planted during the fall/winter season had 40% less of total glucosinolate content (13 μM/g of dw) than the same varieties planted during the spring/summer season (glucosinolate content, 22 μM/g of dw) (Cartea et al. 2008). Possibly higher day/night temperature (30/15°C) regime in spring favors healthy growth of sprouts compared to the lower fall day/night temperature (22/12°C) regime which improves glucosinolate levels in both cabbage and broccoli (*Brassica oleracea* var. *italica*). High day temperature-induced stress increases the expression levels of phase 2 chemoprotective enzymes (Pereira et al. 2002). Soil nutrients have a significant role in the concentrations of glucosinolates in cabbage. Low nitrogen and high sulfur applications during the growth of cabbage cultivars improve the total glucosinolate and glucobrassicin contents in cabbage (Rosen et al. 2005).

Climate condition in harvest season of fruits influences the concentrations of phytochemicals in fruits. Black chokeberry (*Aronia melanocarpa*) cultivars are cultivated in large scale in North America, Canada, and European countries because of high nutritional benefits of its fruits. The fruits are rich in anthocyanins (mainly cyanidin glycosides), proanthocyanidins (mainly oligomers and polymers of (-)-epicatechin linked by B-and A-type bonds), flavonoids and phenolic acids, vitamins, carbohydrates, PUFA, dietary fibers, and minerals, and fresh fruits are less

consumed due to their astringent taste, but these are used in food industry in large scale for production of juices, nectars, jams, jellies, wines, and other dietary supplements (Sidor and Gramza-Michalowska 2019). A comparative study on the total phenolic (TP) content and the total flavonoid (TF) content in the fruit juices from the fruits of black chokeberry collected in three harvest seasons, August 2012, August 2013, and August 2014 from an orchard in Donja Zelina, Croatia, revealed that both TP and TF were found high in the growing season 2012 (11093 mg GAE/l and 9710 mg GAE/l, respectively) and lowest in the season 2014 (8834 mg GAE/l and 6994 mg GAE/l, respectively). Possibly bright sunshine and dry climate with less seasonal rainfall during the growing season 2012 have a positive impact on the high concentrations of phenolic compounds including flavonoids in the fruits (Tolic et al. 2017). Sunlight has been found to regulate the gene expression related to increased synthesis of anthocyanins and flavonoids in plants. Solar UV radiation increases plasma membrane NADPH oxidase activity via ROS production in apple peel to increase anthocyanin synthesis by increasing the activity of dihydroflavonol 4-reductase (DFR) and UDP-glucose: flavonoid 3-*O*-glucosyltransferase (UFGT) (Zhang et al. 2014a). Another study on the role of light-induced expression of myeloblastosis-related protein B (MYB) genes in anthocyanin and flavonoid synthesis in wild red-fleshed apples (*Malus sieversii* f. *niedzwetzkyana*) reveals that two putative genes MYB12 and MYB 22 are expressed in high concentrations and their overexpression promotes the accumulation of proanthocyanidins and flavonols in apple callus through upregulating the activity of the genes, leucoanthocyanidin reductase (LAR), and flavonol synthase (FLS), respectively (Wang et al. 2017b). In diffused sunlight having low UV-B light, the ripening of apples is delayed, fruit size decreased, and both anthocyanins and flavonoids content are reduced (Henry-Kirk et al. 2018; Chen et al. 2019a). Similarly, exposure of grape berry (*Vitis vinifera* L) clusters to low-temperature sunlight in post-veraison (onset of ripening) stage increases anthocyanin accumulation in grape skin by upregulation of the expression of MYB 12 gene and its target genes related to anthocyanins and flavonols biosynthesis, whereas high-temperature sunlight increases the degradation of anthocyanins in grape skin as well as decreases the expression of flavonoid synthesis related genes. Thus, exposure of grape clusters to sunlight during the morning hours up to midday at the ripening stage is recommended to increase both anthocyanins and flavonols contents in ripe grapes. Sunlight exposure significantly increases the levels of delphinidin-, cyanidin-, petunidin-, peonidin-, and malvidin-3-*O*-glucosides (**30**–**34**) throughout the stages of berry ripening (Matus et al. 2009).

The maritime climate (mild summer) has a significant role to enhance the concentrations of phytochemicals in fruits and vegetables that are grown in summer in Southern Hemisphere, compared to those grown in Northern Hemisphere. The high levels of anthocyanins in cherries, nectarines, peaches, and plums as well as high levels of carotenoids in red bell peppers and nectarines and high levels of ascorbic acid in cherries, peaches, red bell peppers, and carrots are found in these crops that are grown in summer season in Otago, New Zealand, compared to those grown in summer in the US, Northern Greece, Spain, and Finland (Leong and Oey 2012).

The young and tender leaves of tea (*Camellia sinensis* L) are consumed as beverage to reduce the risk of various diseases including cardiovascular diseases, cancers, obesity, diabetes, and Alzheimer disease. The major constituents of green tea, such as phenolic compounds, including catechins (mainly epigallocatechin gallate (EGCG **35**), epigallocatechin (EGC **36**), epicatechin gallate (ECG **37**), gallocatechin (GC **38**), epicatechin (EC **39**), and catechin (C **40**)), flavonol glycosides, anthocyanidins, phenolic acids and caffeine, and their antioxidant property in tea are influenced by a variety of environmental factors, such as geographical location of cultivation, atmospheric temperature, rainfall, amount of sunlight, fertilization, soil type, and plucking standard and frequency. Green tea contains unoxidized polyphenols, whereas black tea contains both native unoxidized polyphenols and oxidized theaflavins (TFs) and thearubigins (TRs). The concentrations of flavonoids in fresh apical shoots of tea cultivated in cold season in Central Africa are high, whereas in Japan, the concentrations of EC and EGC are high in teas grown in spring season, and the concentrations of ECG and EGCG are high in teas grown in summer season. In China, the concentrations of EGC, C, GC, and EC are high in teas grown in spring season than those grown in autumn season. Tea cultivation in extreme rainfall in monsoon (summer) season compared to spring drought season reduces the functional quality of tea up to 50% by reducing the concentrations levels of catechins and methylxanthines (caffeine **41**, theobromine **42**, and theophylline **43**). Rapid growth of tea leaves in monsoon season decreases the concentrations of tea phenolic compounds including catechins and methylxanthines through a dilution effect. Hence, tea consumers prefer spring tea to get better flavor and functional quality (astringency, bitterness, and sweetness) of teas. Shade treatment of tea leaves during cultivation of tea plants improves the quality of tea beverage by reducing the levels of some flavonoids, particularly proanthocyanins and *O*-glycosylated flavonols by 53.4% and 43.3%, respectively, and astringency and increasing the concentrations of phenolic acids compared to sunlight exposed tea leaves (Ahmed et al. 2014; Wang et al. 2012a; Ku et al. 2010; Chen et al. 2010; Nakagawa and Torii 1964). Tea cultivation in high altitudes also influences the concentrations of phytochemicals in tea. Tea grown in high altitude has low levels of total polyphenols, particularly low levels of EGCG and ECG, and high levels of amino acids especially theanine, glutamic acid, arginine, serine, γ-aminobutyric acid, and aspartic acid, and thereby the tea possesses good flavor and taste (Han et al. 2017).

Both genotype and environmental effects have been shown to influence the composition and levels of phytochemicals in commercially cultivated coffee cultivars, *Coffea arabica* and *C. canephora*, mainly grown in Africa, Brazil, and India. The beverage quality of coffee depends on geographical origin and growth conditions, mainly shading and altitude in cultivation stage. Robusta coffee (*C. canephora*), mainly grown in India and Africa, has a higher caffeine content compared to Arabica (*C. arabica*), mainly grown in Brazil. The shade grown coffee improves the size of coffee beans and uniform ripening of berries and flavor by increasing the levels of caffeine and chlorogenic acids. High-altitude slope with morning sunlight in coffee cultivation increases the beverage quality of coffee by

increasing the levels of caffeine, trigonelline, and chlorogenic acids (Avelino et al. 2005; Vaast et al. 2006; Cheng et al. 2016).

4.3.4 Harvesting Effect

The total phenolic (TP) compounds and total anthocyanins (TA) contents of berry fruits at the time of harvest depend on the maturity stages. For example, the TP content of raspberries (*Rubus idaeus*) is decreased by 45% from green (unripe) to pink (semi-ripe) stage, while its TA content is increased by 129% from pink to ripe stage due to high anthocyanins content, whereas in blackberries (*Rubus fruticosus*) and strawberries (*Fragaria* × *ananassa*) fruits, the total phenolic content is decreased by 23% and 65%, respectively, from green to ripe stage (Wang and Lin 2000). In high bush blueberries (*Vaccinium corymbosum*), the TP content is decreased and TA content is increased by about 34% from green to ripe stage. Among the phenolic compounds, the contents of flavonols and hydroxycinnamic acids are decreased significantly from green to ripe stage due to their conversion into anthocyanins (Rodarte Castrejon et al. 2008). Hence, harvesting at the ripe stage of the berry fruits gives high levels of anthocyanins in fruits.

Harvested young tea twigs by plucking of one bud and three leaves (tri-leaves) and one bud and four leaves (quad-leaves) are better material for production of green tea or for production of fermented juice for black tea than the plucking of one bud and one leaf (mono-leaf) and one bud and two leaves (di-leaves) process. The former plucking process increases the levels of catechins and amino acids in green tea and the levels of theaflavins and thearubigins, amino acids, and soluble solids in black tea and thereby improves the sensory quality of tea. In black tea, theaflavins are mainly responsible for the astringency, brightness, color, and briskness of tea (Tang et al. 2018).

4.3.5 Postharvest Storage Effect

Postharvest storage of fruits and vegetables influences the concentrations of phytochemicals present in fruits and vegetables because of the decomposition of phytochemicals on storage condition and temperature induced lipid peroxidation and nonenzymatic browning processes in open atmosphere.

The storage of potato tubers (*Solanum tuberosum*) at low temperatures (near 4°C) increases sweetness of potatoes by breakdown of reserve starch into reducing sugars glucose and fructose. These high reducing sugar contents in potatoes negatively affect on the quality of processed products, such as chips and French fries. This cold-induced sweetening is also observed in ripe tomato (*Solanum lycopersicum*) storage because of similar genomes (Schreiber et al. 2014). However, the storage of potato tubers at 4°C prevents from the loss of its carotenoids and phenolics contents and antioxidant property (Blessington et al. 2010). Broccoli florets after packing in micro-perforated polypropylene bags and stored under open ambient condition at

15°C for a period of 144 h showed lower losses of chlorophyll, vitamin C, β-carotene, and total antioxidant contents than those stored under refrigerated condition (4°C) (Nath et al. 2011). Harvested broccoli on storage under controlled atmosphere (CA) or modified atmosphere packaging (MAP) prevents the loss of glucosinolate content (Jones et al. 2006). Small berries such as strawberries, red currants, and raspberries and cherries on storing at both room temperature (25°C) and refrigerating temperature (4°C) preserved the marketable qualities of fruits. Different cultivars of plums on storing in cold at 2°C for 35 d followed by shelf-life storage for 4 d at 20°C protected the fruits from the loss of phenolics, anthocyanins, and carotenoids contents as compared with freshly harvested fruits (Diaz-Mula et al. 2009).

4.3.6 Packaging Effect

Several studies demonstrate that CA or MAP packaging with low oxygen and high CO_2 concentrations or coating with edible chitosan on harvested fruits and vegetables is effective to maintain their freshness and prevents the loss of phytochemicals content by reducing the respiration rate of the enzymes. For instance, harvested carrots in both coating with chitosan and CA or MAP maintain the levels of carotenoids and phenolics in shelf-life storage (Simoes et al. 2009). Hot water treatment (46°C for 75 min) of harvested mangoes plus CA packaging prevents the loss of polyphenolic, such as gallic acid (**44**) and tannins content in mangoes (Kim et al. 2007). Harvested mushrooms on MAP with high oxygen concentrations (about 80%) improves shelf-life storage with freshness and antioxidant property up to 30 days (Wang et al. 2011a).

4.3.7 Chemical Treatment Effect

Plant growth hormone, 1-methylcyclopropene (1-MCP), is widely used in postharvest storage technologies to maintain freshness and prevent ripening of fruits and vegetables. It acts as ethylene antagonist and binds with the receptors of ethylene present in fruit tissues and blocks the ethylene-mediated processes of ripening, softening, and early senescence of fruits. Its efficiency depends on several factors, such as concentration, exposure duration, and maturity stage of harvested cultivars. Moreover, it enhances the antioxidant potential in fruits due to its ROS scavenging activity (Lata et al. 2017). Both 1-MCP treatment and CA storage condition of harvested matured mangoes maintain total phenolic and flavonoid contents and freshness and improve shelf-life storage of mangoes (Sivakumar et al. 2012). A similar combined 1-MCP treatment and CA storage condition at 0°C on 'Cripps Pink' apples maintain both phenolic content and total antioxidant property during long-term storage up to 160 days (Hoang et al. 2011). In case of sweet cherries (*Prunus avium* L), a treatment of both 1-MCP and hexanal enhances the quality and shelf-life of the cherries without significant loss of polyphenolics content. Hexanal, a

natural volatile aldehyde, inhibits the activity of phospholipase D enzyme in membrane degradation of fruit tissues during ripening and senescence processes (Sharma et al. 2010).

4.3.8 Processing Effect

Fruits and vegetables are processed to meet consumer's requirement and to increase their shelf-live for use in off-seasons. Major industrial processing of fruits and vegetables include blanching (heating), canning, sterilizing, and freezing as well as some cooking methods, such as boiling, steaming, and microwaving. Such processing normally reduces the content and alters the composition of nutrients including phytochemicals in processed foods. In conventional domestic cooking of red cabbage, only 32.7–64.5% of available 45.7–66.9% of total phenolics are retained in cooked food (Podsedek et al. 2008). The effects of food processing, such as blanching (98°C, 10 min), freezing (−20°C) and freeze-drying on the contents of anthocyanins, carotenoids, and vitamin C in some summer fruits (cherries, nectarines, apricots, peaches, plums) and vegetables (carrots and red bell peppers), have been reported. Blanching and freezing enhanced the contents of anthocyanins after processing compared to fresh commodities. Possibly, during processing stage, the plant cell membrane-bound anthocyanins are released to enhance their bioavailability. Moreover, the concentration of vitamin C was increased on heating process due to inactivation of ascorbic acid oxidase. Blanching also increased the anthocyanins content in cherries, peaches, and plums (Leong and Oey 2012). Blanching (95°C, 2 min) prior to pursee/juice processing of blueberries improves the phenolics and anthocyanins contents (Sablani et al. 2010). Only freezing of broccoli and carrots at 4°C for 7 days increased the total phenolics content but decreased ascorbic acid content, whereas both of their blanching (95°C, 3 min) and freezing retained both phenolic and ascorbic acid contents (Patras et al. 2011).

Fruiting bodies of several edible mushrooms are subjected to drying process in hot air or microovens at different temperatures for their storage for a longer time and to use all the year round. This drying process significantly affects the contents of phenolics, organic acids, polysaccharides, vitamins, and micronutrients, compared to fresh samples. Drying at air temperature for 7 days significantly increases the total phenolic (TP) content (8.77–119.8 mg GAE/g of dw) in the mushroom, *Amanita zambiana*, due to release of cell wall bound polyphenols as a result of cell wall destruction on drying (Reid et al. 2017). However, microoven drying at 43°C did not affect on TP or total flavonoid (TF) content in mushroom, *Pleurotus ostreatus* (Mutukwa et al. 2019). Microoven drying at higher temperature, 70°C, results 17% reduction in TP (3.79 to 3.14 mg GAE/g of dw) in *Hericium erinaceus*, and 40% reduction of TP (1.89 to 1.14 mg GAE/g of dw) in *Leccinum scabrum*, compared to fresh samples (Gasecka et al. 2020). Therefore, microoven drying at lower temperatures prevents the loss of phenolic contents in dried mushrooms.

The processing steps of both green and black teas play an important role to maintain their sensory quality and the content and composition of antioxidant phytochemicals, such as catechins in green tea and theaflavins, thearubigins, and flavonol glycosides in black tea.. The high content of catechins, EGCG, and ECG in green tea and high contents of theaflavins (TFs), particularly theaflavin 3,3′-di-*O*-gallate (TF-3,3′G **45**) and theaflavin 3-*O*-gallate (TF-3G **46**) in black tea, are the indicators of the quality of green and black teas. In green tea, the levels of EGCG and ECG are increased by about 2-fold in roasting process compared to that in fresh tea leaves. Possibly, high-temperature roasting process increases the epimerization of catechins to epicatechins, which on abstraction of gallate moiety from gallic acid/theogallin increases the yield of EGCG in roasted tea leaves. In the production of green tea, roasting (250–300°C, 10 min), rolling (10 min), and three consequent drying (150–200°C, 100–150°C, 90–100°C, 10 min each) steps provide high contents of EGCG (**35**) and ECG (**37**) in green tea, whereas in black tea, both fermentation and drying steps play positive roles for high contents of TFs through conversion of catechins into TFs by oxidation (catalyzed by polyphenol oxidase, PPO) and condensation processes. In black tea, there was no significant change in the content of kaempferol and quercetin glycosides between the fresh leaf and the final product in fermentation process, whereas the triglycosides of myricetin were completely decomposed and monoglycosides of myricetin were reduced to half (about 38%) during the fermentation process. Similarly, the content of methylxanthines, caffeine, and theobromine was decreased significantly in the fermentation step. However, the total TFs content was increased in both fermentation and drying steps in black tea compared to fresh leaf (Lee et al. 2019b). A study on fermentation process in the production of black tea reveals that fermentation conditions at 35°C and pH 5.1 for 75 min duration using tri-leaves and quad-leaves of tea twigs provide maximum concentrations of TFs in the fermented juices (Tang et al. 2018). Another study reports that in black tea production, withering (room temperature (rt) drying, 24 h), rolling (30 min), fermentation (rt, 3 h), and two consequent drying (110°C, 20 min; 90–100°C, 10 min) steps provide high contents of TFs in black tea (Lee et al. 2019b).

4.4 Inherent Properties of Natural Products in Prevention and Treatment of Human Diseases

Overexpression of oxidants, such as reactive oxygen species (ROS) and reactive nitrogen species (RNS) in human body from excessive oxidative stress under various environmental factors, is responsible for the pathogenesis of many chronic diseases including obesity, diabetes, cancers, cardiovascular diseases, and neurodegenerative diseases. The scavenging of these oxidants is thought to be an effective measure to reduce the level of oxidative stress and to exert a protective effect against the development of these chronic diseases. A growing piece of literature demonstrates that fruits, vegetables, and whole grains on dietary intake exert a protective effect against the development of these chronic diseases. Various classes of antioxidant

phytochemicals present in plant food (fruits, vegetables, and grains) and other medicinal plants, animals, and microorganisms are considered to be responsible to possess preventive roles against these chronic diseases and have health benefit effects. These phytochemicals reduce the oxidative stress through scavenging the free radicals and inducing anti-inflammatory action. These antioxidant phytochemicals are produced by the plants, animals, and microorganisms for their protection and survival under odd extreme environmental stress conditions in their habitats. The major identified antioxidant phytochemicals include polyphenolic compounds (e.g., flavonoids, phenolic acids, stilbenes, tannins, and coumarins), terpenoids, carotenoids, steroids, saponins, glucosinolates, and alkaloids. The flavonoids are subclassified into flavonols, flavones, flavanols, flavanones, anthocyanidins/anthocyanins, and isoflavonoids. The terpenoids are subclassified into monoterpenoids, sesquiterpenoids, diterpenoids, and triterpenoids (Zhang et al. 2015; Harborne and Mabry 1982; Finar 1995).

Metabolic inflammation, a low-grade chronic pro-inflammatory environment in metabolic tissues during nutrient excess, has emerged as an important event in the development of obesity, type 2 diabetes, and cardiovascular diseases (CVDs). Macrophages, endoplasmic reticulum stress, and NLRP3 inflammasome are the major inflammatory effectors that contribute to insulin resistance and atherosclerosis and are considered as precursors of obesity, type 2 diabetes, and CVDs. These antioxidant phytochemicals reduce metabolic inflammation in metabolic tissues by increasing insulin action and insulin secretion in pancreatic beta cells through AMPK activation and other signaling pathways. Moreover, these phytochemicals modulate gut microbiota composition to reduce metabolic inflammation, improve insulin secretion and insulin sensitivity in metabolic tissues, and improve immunity of the intestine for protection from the entry of toxic pathogens from the gut (Steinberg and Schertzer 2014).

Several phytochemicals isolated from plant food, herbs, animals, and microorganisms have been shown to possess antiobesity and antidiabetic effects equal to and even more potent than known antiobese drugs and oral hypoglycemic agents. These bioactive phytochemicals from nature might offer a key to unlock the nature's strategy in the synthesis of natural molecules of chemical structural diversity and new therapeutic targets in prevention of the development of obesity, diabetes, and their associated complications in humans (Karri et al. 2019; Fu et al. 2016; Qi et al. 2010; Jung et al. 2006).

4.5 Major Therapeutic Targets of Natural Products in Obesity Treatment

4.5.1 Lipase Inhibitory Effect

A growing body of evidence demonstrates that obesity can be prevented by reducing energy intake or by increasing energy expenditure through maintenance of energy homeostasis in the body. The energy intake can be reduced by either reducing

nutrient digestion and absorption of digested nutrients or reducing food intake. Dietary fat, one of the major sources of calorie intake, is absorbed in the intestine by the action of pancreatic lipase. Pancreatic lipase is a key enzyme for absorption of dietary triacylglycerols via hydrolysis to monoacylglycerols and fatty acids. A wide variety of plants and microorganisms extracts and their active phytochemicals have been reported to exhibit pancreatic lipase inhibitory effect. These phytochemicals and herbal/microbial extracts resemble the function of orlistat (**46a**), currently used lipase inhibitor for obesity treatment, but their inhibitory mechanisms are different from that of orlistat; some act as inhibitors in a reversible manner, while others as irreversible manner, similar to orlistat (Birari and Bhutani 2007).

4.5.2 Suppressive Effect on Appetite

A wealth of information indicates that the food intake in humans and rodents is regulated by a complicated central and peripheral neuroendocrine signaling pathways involving approximately 40 orexigenic (appetite stimulating) and anorexigenic (appetite suppressing) hormones, neuropeptides, enzymes, and other chemical signaling molecules and their receptors. Neuropeptide Y (NPY), agouti-related peptide (AgRP), and melanin-concentrating hormone (MCH) are orexigenic signaling molecules and are upregulated on fasting, whereas pro-opiomelanocortin (POMC), cocaine- and amphetamine-regulated transcript (CART), serotonin (5-HT), histamine, dopamine (DA), and noradrenaline (NE) are anorexigenic molecules, and their upregulation in brain increases satiety in the hypothalamus. Excessive nutrient intake-induced insulin resistance in obese brain, FoxO1 gene transcriptionally increases orexigenic neuropeptide AgRP via G-protein-coupled receptor 17 (GPR17) and decreases anorexigenic neuropeptide POMC via carboxypeptidase E (CPE) for increased food intake (Ren et al. 2012; Plum et al. 2009; Atkinson 2008). The gastrointestinal (GI) tract, the largest endocrine organ in humans, releases more than 20 peptide hormones to regulate appetite by inducing signals for a sense of starvation before a meal and satiety after a meal in healthy nonobese humans (Murphy and Bloom 2006). Ghrelin, an appetite-stimulating hormone, is secreted from the stomach on fasting, whereas GI tract secretes some anorexigenic peptide hormones including peptide YY (PYY), CCK, and GLP-1 to suppress appetite and to reduce food intake. Cholecystokinin (CCK) stimulates gallbladder contraction and pancreatic and gastric secretions to reduce energy intake. Glucagon-like peptide-1 (GLP-1) stimulates insulin release and reduces food intake (Yang et al. 2008; Naslund and Hellstrom 2007; Drucker 2006). Many phytochemicals and plant extracts reduce the food intake in animal models by reducing the expression of ghrelin or NPY or AgRP and increasing the expression of GLP-1 or CCK-8 in intestine or POMC in hypothalamus (Table 4.1).

Table 4.1 List of some natural products (extracts/active components isolated from various natural sources) having reported anti-obesity effects and their major molecular targets and actions

Family, Plant species	Active extract/active component	Experimental model	Major activity and molecular targets	References
A. Plant source				
1. Actinidaceae				
Actinidia arguta	Roots (EtOAc), ursolic acid **52** (Fig. 4.1)	Cellular, rat fat cells	Anti-lipase activity, lipolysis↑, AT mass↓	Kim et al. (2009)
Actinidia polygama	Fruits (70% EtOH)	HFD-fed obese mice	Serum TG, leptin↓	Sung et al. (2013a)
2. Apiaceae				
Ferula asafoetida	Gum (aqueous)	Obese diabetic rats	AT (abdominal) fat and adipocytes size↓, Serum leptin↓, Lipid metabolism↑	Azizian et al. (2012)
Angelica keiskei	Leaves, stems (90% EtOH)	Obese diabetic rats	Serum, liver G↓, liver ACOX, MCAD↑	Ohnogi et al. (2012)
Peucedanum japonicum	Leaves EtOH, 50% EtOH), neochlorogenic acid (**53**), chlorogenic acid (**21**), rutin (**54**), pteryxin (**55**)	Obese diabetic mice 3T3-L1 cells	Lipase activity↓, energy expenditure↑, lipid metabolism↑, UCP3, PPARα, CPT1α, GLUT4↑, Adipogenesis↓	Nukitrangsan et al. (2012), Nugara et al. (2016), Taira et al. (2017)
3. Amaranthaceae				
Amaranthus dubius	Leaves (MeOH)	Obese mice	AT mass, serum TG↓	Nderitu et al. (2017)
4. Apocynaceae				
Alstonia boonei	Stem bark (EtOH)	Obese rats	Food intake, AT mass↓ Serum TC, LDL, leptin↓	Onyeneke and Anyanwu (2014)
Oroxylum indicum	Bark (ethyl acetate), oroxylin A (**56**), chrysin (**57**), baicalein (**58**)	3T3-L1 cells, lipase inhibition assay	Adipogenesis, expression of PPARγ, C/EBPα, SREBP-1c in 3T3-L1 cells↓, Pancreatic lipase activity↓	Mangal et al. (2017)

(continued)

Table 4.1 (continued)

Family, Plant species	Active extract/active component	Experimental model	Major activity and molecular targets	References
Tabernaemontana divaricata	Aerial parts (MeOH)	HFD-fed obese rats	Serum lipids, liver, body mass↓	Kanthlal et al. (2012)
5. Amaryllidaceae				
Allium sativum	Stem (EtOH)	HFD-fed obese mice	Lipid metabolism, antioxidant status↑ Plasma lipid, leptin↓, liver TG, lipogenic genes↓ Lipid metabolism↑	Kim et al. (2013)
	Bulb oil	Obese mice	Hepatic lipid mass↓, PPARα↑	Lai et al. (2014)
6. Alismataceae				
Alisma orientale	Rhizomes (EtOH), triterpenoids	OP9 preadipocytes	Adipogenesis↓, PPARγ, C/EBPα, FAS, aP2, HSL↓	Park et al. (2014)
		Hyperlipidemic mice	Lipid metabolism↑ Serum lipids, lyso-PC↓	Li et al. (2016)
7. Araliaceae				
Acanthopanax senticosus	Fruits (EtOH), copteroside B (**59**), gypsogenin-3-O-Glc A (**60**), silphioside F (**61**)	HFD-fed obese mice	Lipid metabolism↑ Liver AMPK, PPARα↑ Hepatic lipid mass, lipogenesis↓	Saito et al. (2016)
		Enzyme assay	Pancreatic lipase activity↓	Li et al. (2007)
A. sessiliflorus	Leaves (EtOH) Sessiloside (**62**) Chiisanoside (**63**)	Enzyme assay	Pancreatic lipase activity↓	Yoshizumi et al. (2006)
Aralia elata	Shoots (70% EtOH), saponins	HepG2 cells, HFD-fed obese mice	Intracellular lipid mass↓, lipid metabolism↑, PPARα, CPT1, ACC2↑, SREBP1, FAS, ACC1↓, serum glucose, TG, hepatic fat↓	Huang et al. (2015)

Panax ginseng	Berry (75% EtOH), ginsenosides, ginsenoside Re (**64**)	Obese diabetic mice	Food intake, body weight, serum glucose, TC↓, energy expenditure↑ Adipogenesis↓	Attele et al. (2002)
	Dry leaves (aqueous), saponins	3T3-L1 cells, HFD-fed obese Rats	Food intake, AT mass, lipogenesis↓,PPARγ, C/EBPα, LPL, aP2↓	Lee et al. (2017b)
P. quinquefolius	Leaves, stems (aqueous) Saponins, ginsenoside Rb1 **65**	HFD-fed obese mice, enzyme assay	Food intake, body fat↓ Energy expenditure↑, central leptin signaling↑ Hopothalamic SOCS3, PTP1B↓, NPY, AgRP↓, PYY, POMC↑, pancreatic lipase activity↓	Liu et al. (2008), Liu et al. (2010b), Xiong et al. (2010), Wu et al. (2014b)
8. Asparagaceae				
Agave angustifolia, *A. potatorum*	Leaves (80% ethanol and water), agavins (oligofructosides)	Obese mice	Lipid metabolism↑ Food intake↓ Body fat mass, serum TG, TC, LDL-C, gastric ghrelin secretion↓ Serum HDL-C, GLP-1, colon SCFAs↑	Santiago-Garcia and Lopez (2014)
Liriope spicata var. *prolifera*	Tuberous roots (aqueous), polysaccharides fr	Obese diabetic mice	Lipid metabolism↑ Serum TC, TG, LDL, hepatic TG↓	Liu et al. (2013b)
Polygonatum falcatum	Rhizomes (EtOH), kaempferol **66**	3T3-L1 cells	Adipogenesis↓, PPARγ, SREBP1c, LXRβ↓	Park et al. (2012)

(continued)

Table 4.1 (continued)

Family, Plant species	Active extract/active component	Experimental model	Major activity and molecular targets	References
9. Asteraceae				
Eclipta alba	Whole plant (EtOAc fr), ecliptal (**67**)	3T3-L1 cells HFD-fed obese hamsters	Adipogenesis↓, Cell cycle proteins CDK2/4/6, cyclin D1/D3↓ Adipogenic genes PPARγ, C/EBPα, FAS, FABP4↓, serum lipids, hepatic lipid mass↓	Gupta et al. (2017, 2018)
Artemisia princeps	Aerial parts (EtOH), chlorogenic acid (**21**)	HFD-fed obese diabetic mice	Lipid synthesis↓, plasma lipids, leptin, hepatic lipid mass↓, hepatic FAS↓	Yamamoto et al. (2011)
A. vulgaris	Whole plant (70% MeOH)	Hypercholesterolemic rats	Lipid synthesis↓ Serum lipids, hepatic lipid mass↓, hepatic HMGCR↓	El-Tantawy (2015)
Taraxacum officinale	Leaves (60% EtOH)	3T3-L1 preadipocytes, enzyme inhibition assay	Adipogenesis↓, pancreatic lipase activity↓, serum lipids, hepatic lipid mass↓ Liver, muscle p-AMPK↑, lipid metabolism↑	Zhang et al. (2008), Davaatseren et al. (2013), Marta et al. (2014)
10. Asphodelaceae				
Aloe vera	Leaves (gel powder), phenolic acids	HFD-fed obese mice	Energy expenditure↑, WAT mass, serum glucose, TG, TC↓, adiponectin, AMPK↑	Pothuraju et al. (2016)
11. Basellaceae				
Boussingaultia gracilis var. *pseudobaselloides*	Leaves (EtOH)	HFD-fed obese rats, 3T3-L1 cells	Lipid metabolism, energy expenditure↑ Hepatic lipid mass, fat pad mass, serum lipids↓ Hepatic PPARγ, FAS, SREBP-1c↓, PPARα, CPT1, UCP2↑ Adipogenesis↓, p-AMPK↑	Wang et al. (2011b), Kim and Choung (2012)

12. Betulaceae				
Betula platyphylla var. *japonicum*	Bark (80% methanol, butanol fr) Phenylglycosides, platyphylloside (**68**), arylbutanoid glycosides (A-C **69–71**)	3T3-L1 cells	Adipogenesis, intracellular lipid content, expression of PPARγ, C/EBPα, SREBP-1c, SCD1, FAS, aP2, perilipin, LPL↓ Expression of lipolysis and insulin signaling-related genes HSL, ATGL, adiponectin, GLUT4↑	Lee and Sung (2016), Huh et al. (2018)
13. Bignoniaceae				
Tecomella undulata	Bark (EtOAc), ferulic acid (**72**), rutin (**54**)	3T3-L1 cells, HFD-fed obese mice	Adipogenesis↓, intracellular TG mass, PPARγ, C/EBPα, E2F1, leptin, LPL↓, body weight, plasma lipids↓, hepatic SIRT1, plasma adiponectin↑, lipid metabolism↑	Alvala et al. (2013), Kumar et al. (2012)
14. Bombacaceae				
Bombax ceiba	Stem-bark (MeOH), lupeol (**73**), flavonoids	HFD-fed obese rats	Thermogenesis, lipid metabolism↑, body fat mass, serum lipids, hepatic lipid mass, TBARS↓, hepatic FAS, PTP1B↓, AMPK↑	Gupta et al. (2013)
15. Brassicaceae				
Brassica juncea	Leaves (80% EtOH)	HF, HC-diet fed obese rats	Lipid metabolism, lipid excretion↑, liver, AT mass, serum lipids↓, hepatic PPARα, LDLR, CYP7α1, fecal lipid excretion↑, hepatic FAS, ACC, GPDH↓	Lee et al. (2018b)

(continued)

Table 4.1 (continued)

Family, Plant species	Active extract/active component	Experimental model	Major activity and molecular targets	References
Wasabia japonica	Leaves (water)	3T3-L1 cells, HFD-fed obese diabetic mice	Adipogenesis↓'Intracellular TG mass, PPARγ, C/EBPα, GPDH, aP2↓ Lipid metabolism↑, WAT, liver fat mass, serum TG, TC, leptin↓ Serum adiponectin, liver ACOX1, PPARα↑, liver PPARγ, SREBP1c, ACC, FAS, HMGCR↓	Ogawa et al. (2010), Yamasaki et al. (2013)
16. Campanulaceae				
Adenophora triphylla var. *japonica*	Roots (EtOH)	3T3-L1 cells, HFD-fed obese mice	Adipogenesis↓, intracellular TG, accumulation, PPARγ, FAS, aP2↓ Lipid metabolism↑ Oxidative stress↓ AT, liver fat mass, serum TG, LDL-C, glucose, insulin Liver TNFα, GPDH, PPARγ, SREBP-1c, LPL↓, adiponectin, AMPK, PPARα, CAT, SOD↑	Lee et al. (2013a, 2015)

Platycodon grandiflorus	Roots (EtOH), platycosides, platycodin D (**74**), deapioplatycodin D (**75**), platycodins A, C (**76**, **77**)	3T3-L1 cells, HepG2 cells, HFD-fed obese mice	Adipogenesis, pancreatic lipase activity, hepatogenesis↓, lipid metabolism, thermogenesis↑, body fat mass, plasma lipids, leptin, hepatic TG↓, thermogenesis-related genes AMPK, SIRT1, PPARα, PGC-1α, UCP1↑, lipogenesis genes FAS, SCD1, ME, PAP, G6PD↓, gluconeogenic genes PEPCK, G6Pase↓	Kim et al. (2016b), Hwang et al. (2013), Lee et al. (2012a), Xu et al. (2005)
17. Caprifoliaceae				
Lonicera caerulea var. *edulis*	Berries (powder), flavonoids, anthocyanins	HFD-fed obese mice	Lipid metabolism, hepatic antioxidant status↑, serum lipids, leptin, glucose, AST, ALP, LDH, body fat mass↓, hepatic AMPK, GSH, CAT, SOD↑, hepatic ACC, C/EBPα, SREBP-1c, G6Pase, PEPCK↓	Kim et al. (2018a)
18. Celastraceae				
Salacia oblonga	Roots (aqueous)	Zucker obese diabetic rats	Lipid metabolism↑, hepatic lipid mass, serum lipids, glucose↓, hepatic PPARα, CPT1, ACOX↑	Huang et al. (2006)
S. reticulata	Roots (hot water), catechins	Tsumura Suzuki obese diabetes (TSOD) mice, 3T3-L1 cells	Lipid synthesis↓, visceral and subcutaneous fat mass, serum lipids, liver TG content↓, serum adiponectin, liver HSL↑ Adipogenesis↓, PPARγ, C/EBPα, LPL, aP2, CD36, GPDH↓, p-AMPK, adiponectin, ATGL↑	Shimada et al. (2011, 2014), Akase et al. (2011)

(continued)

Table 4.1 (continued)

Family, Plant species	Active extract/active component	Experimental model	Major activity and molecular targets	References
Tripterygium wilfordii	Root-bark, celastrol **78**, triptolide **79**	3T3-L1 cells, HFD-fed ob/ob mice	Adipogenesis↓, intracellular lipid mass, PPARγ2, C/EBPα, ATGL, p53↓ Energy expenditure, glucose and lipid metabolism↑, central leptin sensitivity↑, food intake, body fat mass, serum TG, TC, LDL-C, central SOCS3↓, BAT, muscle HSF1, PGC-1α, UPC1, CPT1α, PRDM16↑	Wang et al. (2020b), Choi et al. (2016), Ma et al. (2015b), Liu et al. (2015a), Liu et al. (2011)
Euonymus alatus	Roots (50% EtOH)	HFD-fed obese mice	Food intake, lipogenesis↓, hepatic fat mass, lipogenic genes PPARγ, SREBP-1c, FAS, GAPT↓	Park et al. (2005)
19. Combretaceae				
Terminalia bellirica	Fruits (hot water), gallic acid	TSOD mice, lipase enzyme inhibition assay	Lipid metabolism↑, pancreatic lipase activity↓, plasma and hepatic TG content↓	Makihara et al. (2012)
T. paniculata	Bark (EtOH), triterpenoids, ellagic acids	HFD-fed obese rats	Lipid metabolism↑, AT and liver fat mass, serum lipids, leptin, AST, ALT, ALP, hepatic FAS, PPARγ, SREBP-1c↓, serum adiponectin, liver AMPK-1α↑	Mopuri et al. (2015)
T. sericea	Roots, leaves (aqueous), sericoside (**80**)	3T3-L1 cells, fructose-fed obese rats	Adipogenesis↓, lipolysis↑, visceral fat, serum and liver TG content↓	Lembede et al. (2019), Mochizuki and Hasegawa (2006)

20. Cannabaceae				
Humulus lupulus	Pomace (water), humulone (**81**), xanthohumol (**82**)	3T3-L1 cells, HFD-fed obese mice	Adipogenesis↓, lipid metabolism↑ AT mass, adipocyte size, plasma TC, liver TG, TC, PPARγ, SREBP-1c↓, PPARα↑	Takahashi and Osuda (2017), Sumiyoshi and Kimura (2013)
21. Clusiaceae				
Garcinia cambogia	Fruits (commercial ext.), (-)-hydroxycitric acid **83**	3T3-L1 cells, HFD-fed obese mice	Adipogenesis↓, food intake↓, lipid metabolism↑, visceral fat mass, serum TG, TC, glucose, leptin, TNFα, AT SREBP-1c, C/EBPα, aP2, PPARγ2, ATP citrate lyase↓, central serotonin↑	Chuah et al. (2013), Kim et al. (2008a), Sullivan et al. (1977)
22. Cornaceae				
Cornus mas	Fruits (methanol), ursolic acid (**52**), anthocyanins	HFD-fed obese mice	Lipid metabolism↑, serum glucose, TG, hepatic TG content↓, islet mass and function↑	Jayaprakasam et al. (2006)
23. Cucurbitaceae				
Coccinia grandis	Roots (ethanol, hexane fr)	3T3-L1 cells	Adipogenesis↓, intracellular lipid mass, PPARγ, C/EBPα, FAS, LPL, aP2, GLUT4↓	Bunkrongcheap et al. (2014)
Momordica charantia	Green fruits (fermented juice, both aq. and ethanol ext.), polysaccharides, saponins, triterpenes	HFD-fed obese rats and mice	Lipid metabolism and antioxidant status↑ AT fat mass, serum TG, TC, LDL-C, leptin, FFAs↓, serum HDL-C, adiponectin↑	Wen et al. (2019), Wang and Ryu (2015)

(continued)

Table 4.1 (continued)

Family, Plant species	Active extract/active component	Experimental model	Major activity and molecular targets	References
24. Cupressaceae				
Juniperus chinensis	Heartwood (hot water)	HFD-fed obese rats	Thermogenesis and lipid metabolism↑, visceral fat mass, plasma lipids (TG, TC, LDL-C, VLDL, FFAs), leptin, insulin↓, plasma HDL-C, AT p-AMPK, p-ACC2, UCP2, UCP3↑, AT ACC, PPARγ, SREBP-1c, FAS↓	Kim et al. (2008b)
25. Cynomoriaceae				
Cynomorium songaricum	Stem (ethanol), triterpenoids	HFD-fed obese mice	Thermogenesis and lipid metabolism↑, fat pad mass, serum glucose↓, muscle fatty acids oxidation, p-AMPK, PGC-1α, UCP2, UCP3, GLUT4↑	Chen et al. (2020)
26. Cyperaceae				
Cyperus rotundus	Rhizomes (hexane), sesquiterpenes	Zucker obese rats, 3T3-F442 cells	Thermogenesis and β3AR activity↑, adipogenesis↓	Lemaure et al. (2007)
27. Dioscoreaceae				
Dioscorea batatas	Tubers (50% ethanol)	HFD-fed obese mice	Lipogenesis and inflammation↓, viceral fat mass, serum and hepatic TG content, serum leptin, IL-6, TNFα, MCP-1, AT C/EBPα, CD36↓	Gil et al. (2015)

D. nipponica	Rhizomes (powder), saponins and sapogenins, dioscin (**84**), gracillin **85**, trillin (**86**), diosgenin **87**, prosapogenins A and C of dioscin (**88**, **89**)	HFD-fed obese rats, lipase enzyme inhibition assay	Lipid metabolism, antioxidant activity and fecal lipid excretion↑, pancreatic lipase activity and adipogenesis↓, fat mass of body, serum TG, VLDL-C, AT p-ERK1/2, SREBP-1c, C/EBPα, FAS, aP2↓, AT p-AMPK, p-ACC↑	Poudel et al. (2014), Wang et al. (2012a), Kwon et al. (2003)
D. oppositifolia	Tubers (ethanol ext., butanol fr or powder), polyphenolics, 3,5-dimethoxy-2,7-phenanthrenediol **90**, (3*R*,5*R*)-3,5-dihydroxy-1,7-*bis*(4-hydroxyphenyl)-3,5-heptanediol **91**	Lipase inhibition assay, HFD-fed obese mice	Pancreatic lipase activity, food intake↓, body weight gain, serum TG, TC, LDL-C, hepatic lipid content↓	Jeong et al. (2016), Yang et al. (2014b)
28. Elaeagnaceae				
Hippophae rhamnoides (seaberry)	Leaves (ethanol ext. or powder)	HFD-fed obese mice	Lipid and antioxidant metabolisms↑, epididymal fat mass, serum leptin, serum and hepatic TG, TC, hepatic ACC, CYP2E1↓, hepatic PPARα, CPT-1, SOD, CAT, fecal lipid excretion↑	Pichiah et al. (2012), Lee et al. (2011b)
29. Ericaceae				
Rhododendron groenlandicum (Labrador tea)	Leaves (80% ethanol), catechins, quercetin glycosides	HFD-fed obese mice	Lipid metabolism↑, serum glucose, liver TG content, SREBP-1c, p-IKK↓, muscle p-Akt, GLUT4, liver p-AMPK, PPARα↑	Ouchfoun et al. (2016)

(continued)

Table 4.1 (continued)

Family, Plant species	Active extract/active component	Experimental model	Major activity and molecular targets	References
30. Ebenaceae				
Diospyros lotus	Leaves (water), gallic acid (**44**), flavonoids, myricitrin (**92**)	3T3-L1 cells, HFD-fed obese mice	Adipogenesis, intracellular lipid accumulation↓, lipid metabolism↑, antioxidant activity↑, visceral fat mass, serum TG, TC, LDL-C, leptin, glucose, liver lipid content, MDA, AST, ALT↓, liver SOD, CAT, GP_x↑	Kim et al. (2019)
31. Fabaceae				
Acacia meansii	Bark (hot water), catechins	HFD-fed obese diabetic KK-Ay mice	Lipid metabolism and energy expenditure↑, WAT and liver lipid mass, plasma glucose, SGOT, SGPT, AT TNF-α, hepatic lipogenesis, SREBP-1c, ACC, FAS, PPARγ, LPL↓ Muscle PPARα, CPT1, ACOX, UCP3, GLUT4, AT adiponectin↑	Ikarashi et al. (2011)
Cassia tora	Seeds (ethanol)	HFD-fed obese rats	Lipid metabolism↑, WAT fat mass, plasma TG, TC, FFAs, AT FAS, ACC, SREBP-1c↓, AT p-AMPK, CPT1↑	Tzeng et al. (2013)
Glycyrrhiza uralensis	Roots (methanol ext., dichloromethane fr), licochalcone A (**93**), liquiritigenin (**94**)	HFD-fed obese mice, Lipase inhibition assay	Energy expenditure↑, inguinal fat pad mass, serum glucose, TC↓, WAT PGC-1α, UCP1, PRDM-16↑ Inhibition of pancreatic lipase activity by licochalcone A (IC_{50}, 35 μg/ml)	Lee et al. (2018a), Won et al. (2007)

Pueraria lobata	Roots (water ext. or powder), puerarin (**8**), daidzein (**95**), genistein (**96**)	HFD-fed obese mice	Energy expenditure and lipid metabolism↑, Serum glucose, LDL, AT ceramide↓, AT adiponectin↑	Buhlmann et al. (2019), Prasain et al. (2012)
Tamarindus indica	Fruits (aqueous pulp)	HFD-fed obese rats	Lipid synthesis↓ Anti-oxidant activity↑, serum TG, TC, LDL, leptin, MDA, liver fat mass↓, serum HDL, SOD, GP_x↑	Azman et al. (2012)
Glycine max	Seed-coat (ethanol), cyanidin-3-glucoside (**31**), delphinidin-3-glucoside (**30**), catechins, proanthocyanidins	HFD-fed obese mice, 3T3-L1 cells	Lipid metabolism and energy expenditure↑ Food intake↓, AT fat mass, plasma glucose, TNF-α, IL-6, MCP-1, AT ACC, C/EBPα↓, AT p-AMPK, LPL, HSL, UCP-1, UCP-2↑ Adipogenesis, intracellular lipid accumulation, PPARγ, LXRα, SREBP-1c, C/EBPα↓, PGC-1α, SIRT1↑	Kim et al. (2012b, 2015), Kanamoto et al. (2011)
32. Gentianaceae				
Gentiana lutea	Roots (30% ethanol), loganic acid (**97**), gentiopicroside (**98**)	3T3-L1 cells, HFD-fed obese mice	Adipogenesis, intracellular lipid mass, C/EBPα, adiponectin, GLUT4↓ AT and liver fat mass, serum leptin↓	Park et al. (2020a)
33. Geraniaceae				
Geranium thunbergii	Leaves (70% ethanol), flavonoids	HFD-fed obese mice	Lipid synthesis↓, AT mass, adipocyte size, serum TG, TC, LDL-C, leptin, AT SREBP-1c, PPARγ, FAS, aP2↓	Sung et al. (2011)

(continued)

Table 4.1 (continued)

Family, Plant species	Active extract/active component	Experimental model	Major activity and molecular targets	References
34. Ginkgoaceae				
Ginkgo biloba	Leaves (commercial ext.), ginkgolide C (**99**), bilobetin (**100**), ginkgetin (**101**), isoginkgetin (**102**), sciadopitysin (**103**)	3T3-L1 cells, Lipase inhibition assay, HFD-fed obese rats	Adipogenesis, intracellular lipid content, expression of C/EBPβ, C/EBPα, SREBP-1c, FAS, LPL, aP2↓, expression of ATGL, HSL, SIRT1, p-AMPK in 3T3-L1 cells↑ Pancreatic lipase activity↓, AT fat mass, plasma TG, TC, LDL-C, AT TNF-α, p-NFκB↓, AT and muscle insulin signaling, p-Akt, GLUT4, adipoR1, IL-10↑	Liu et al. (2018), Liou et al. (2015), Hirata et al. (2015)
35. Lamiaceae				
Clerodendron glandulosum	Leaves (aqueous)	3T3-L1 cells, HFD-fed obese mice	Adipogenesis, leptin release, TG accumulation, GPDH↓, glycerol release↑ Lipid metabolism↑, lipogenesis↓, WAT mass, adipocyte size, serum lipids, FFAs, glucose, leptin↓, AT CPT1↑, AT PPARγ2, SREBP-1c, FAS↓	Jadeja et al. (2011)
Orthosiphon stamineus	Leaves (70% ethanol) Rosmarinic acid **104**	HFD-fed obese mice, obese diabetic rats	Lipid metabolism↑ Anti-oxidant activity↑, food intake↓, serum TG, TC, LDL-C, glucose, visceral fat mass, hepatic lipid content↓, hypothalamic POMC, hepatic SOD↑, hypothalamic NPY↓	Seyedan et al. (2017), Son et al. (2011)

Melissa officinalis	Leaves (aqueous-ethanol ext., ethyl acetate fr, ALS-L1023, ethanol ext.)	HFD-fed obese mice, human adipocytes	Lipid metabolism↑, Lipogenesis↓, Visceral AT mass, adipocyte size, MMP9, MMP2↓, hepatic CPT1, ACOX, MCAD, VLCAD, SOD2↑, serum TG, TC, FFAs, LDL-C, VLDL-C, liver TG, PPARγ, FAS, SREBP-1c, CD68, TNFα, MCP1, ICAM1, VCAM1↓, Human adipocytes PPARα, LXRα, PDK4↑, aP2, SCD1↓	Kim et al. (2017), Park et al. (2015a), Weidner et al. (2014)
Perilla frutescens	Leaves (50% ethanol, 70% ethanol), rosmarinic acid (**104**), isoegomaketone (**105**)	3T3-L1 cells, HFD-fed obese mice	Adipogenesis, intracellular TG content, GPDH release↓ Lipid metabolism and energy expenditure↑, epididymal fat mass, serum TG, TC, LDL, GOT, GPT, AT PPARγ, ACC, GPDH↓, AT adiponectin, ATGL, AT and liver AMPK, CPT1, PPARα, ACOX, HSL, UCP2, UCP3↑	Thomas et al. (2018), So et al. (2015), Kim and Kim (2009)
Rosmarinus officinalis (rosemary)	Leaves (methanol, fr enriched with rosmarinic acid or carnosic acid (**106**))	HepG2 cells, HFD-fed obese mice	Glycolysis and fatty acid oxidation↑, p-AMPK, p-ACC, PGC-1α, SIRT1, PPARγ↑, G6Pase↓ Epididymal fat mass, serum glucose, TG, TC, pancreatic lipase activity↓, PPARγ, fecal lipid excretion↑	Tu et al. (2013), Ibarra et al. (2010, 2011)

(continued)

Table 4.1 (continued)

Family, Plant species	Active extract/active component	Experimental model	Major activity and molecular targets	References
36. Lauraceae				
Cinnamomum cassia	Cortex (water)	HFD-fed obese mice	Lipid metabolism and energy expenditure↑, food intake↓, hepatic, AT lipid mass, plasma lipids, glucose, adipocyte size↓, muscle MHC, PGC-1α, p-AMPK, p-ACC, NRF-1, Tfam↑	Song et al. (2017)
37. Lythraceae				
Lagerstroemia speciosa (banaba)	Leaves (hot water, ellagic acid rich fr)	3T3-L1 cells, Diabetic female KK-Ay mice	Adipogenesis, intracellular fat droplets, PPARγ, C/EBPα, SREBP-1c, FAS, HSL, ATGL, ACC↓ AT fat mass, hepatic TG content, serum glucose, HbA1c↓	Karsono et al. (2019), Suzuki et al. (1999)
Punica granatum (pomegranate)	Leaves	HFD-fed obese mice	Pancreatic lipase activity, food intake, AT fat mass, serum TG, TC, glucose↓	Lei et al. (2007)
38. Malvaceae				
Sida rhomboidea	Leaves (water)	3T3-L1 cells, HFD-fed obese mice	Adipogenesis, intracellular TG accumulation, leptin, GPDH↓, glycerol release↑ Epididymal fat mass, serum TG, TC, FFAs, and leptin, hepatic TG content, AT PPARγ2, SREBP-1c, FAS↓, AT CPT-1, lipid metabolism↑	Thounaojam et al. (2010, 2011)

39. Meliaceae				
Dysoxylum binectariferum	Stem-bark (ethanol ext., chloroform fr), rohitukine **107**	3T3-L1 cells, HFD-fed golden hamster	Adipogenesis, intracellular lipid accumulation, PPARγ, C/EBPα, aP2, FAS, GLUT4, p-Akt, MCE in adipocytes↓, Wnt3a, GATA2↑, hepatic lipogenesis↓, plasma TC, TG, LDL-C, hepatic TG content, expression of LDLR, HMGCR, SREBP2↓, hepatic LXRα↑	Varshney et al. (2014)
40. Moraceae				
Morus alba	Leaves (aqueous ethanol or fermented with *Cordyceps militaris*), 1-deoxynojirimycin (**108**), resveratrol (**47**)	HFD-fed obese mice	Lipid metabolism and energy expenditure↑, gut microbiota modulation, hepatic inflammation↓, serum TG, TC, LDL-C, hepatic TG content, inflammatory factors Nrf2, 4-HNE, HO-1, iNOS, COX2, p-JNK, lipogenic genes LXRα, SREBP-1c, C/EBPα, aP2, FAS, LPL↓, AT and liver PPARα, UCP1, UCP2, ATGL↑, Gut *Akkermansia*, *Bacteroidetes*↑, gut *Firmicutes*↓, fermented ext. autophagy genes beclin, LC3, Atg5↓, PI3K/Akt signaling↑	Lee et al. (2019c, 2020b), Sheng et al. (2019a), Ann et al. (2015)

(continued)

Table 4.1 (continued)

Family, Plant species	Active extract/active component	Experimental model	Major activity and molecular targets	References
41. Moringaceae				
Moringa oleifera	Leaves (70% ethanol)	HFD-fed obese rats	Energy expenditure, thyroid hormonal activity, and hepatic antioxidant activity↑, food intake↓, body fat mass, serum TG, TC, LDL-C, glucose, leptin, MDA, NO, protein carbonyls, GGT↓, Serum HDL-C, T3, T4, serum and hepatic GSH, GR, SOD, CAT↑, ghrelin secretion↓	Othman et al. (2019)
42. Nelumbonaceae				
Nelumbo nucifera	Leaves (ethanol), alkaloids, (6*R*, 6*aR*)-roemerine-N_{β}-oxide (**109**), liriodenine (**110**), pronuciferine (**111**), nuciferine (**112**); flavonoids, kaempferitrin (**113**), hyperoside (**114**), astragalin (**115**), quercetin (**23**)	Lipase enzyme inhibition assay, 3T3-L1 cells, HFD-fed obese mice	Pancreatic lipase activity, and adipogenesis↓, energy expenditure and lipid metabolism↑, hepatic inflammation↓, AT and liver fat mass, serum TG, TC, LDL-C, glucose, inflammatory cytokines IL-1β, IL-6, TNF-α, IFNγ↓, Serum HDL-C, hepatic AMPK, PPARα, CPT1, LPL, CYP7α1, IL-4, IL-10, muscle UCP3↑, hepatic PPARγ, C/EBPα↓	Wu et al. (2010, 2020b), Ma et al. (2015a), Ahn et al. (2013), Ono et al. (2006)
43. Pandanaceae				
Pandanus amaryllifolius (pandan)	Leaves (water)	HFD-fed obese mice	Central leptin sensitivity and insulin action in liver and muscle↑, plasma FG, leptin, TG, FFAs, hepatic lipid and TG content↓, plasma adiponectin, liver glycogen, muscle and AT GLUT4↑	Saenthaweesuk et al. (2016)

44. Piperaceae				
Piper nigrum	Seeds (water, ethyl acetate fr), piperonal (**116**)	HFD-fed obese rats	Lipid metabolism and thermogenesis↑, body fat mass, plasma glucose, insulin, TG, TC, LDL-C, leptin, MDA, TNFα, pancreatic lipase activity, expression of PPARγ, FAS, ACC, SREBP-1c, FAB4, HMGCR in liver and AT↓, AT adiponectin secretion, expression of hepatic GP_X, SOD, CAT, UCP2↑	Meriga et al. (2017), Parim et al. (2015)
P. nigrum and *P. longum*	Fruits (water), piperine (**117**)	HFD-fed obese rats	Lipid metabolism and energy expenditure↑, body fat mass, plasma TG, TC, LDL-C↓, plasma HDL-C, CNS MC-4R activity for energy expenditure↑	Shah et al. (2011)
45. Plantaginaceae				
Plantago lanceolata	Leaves (powder), acteoside (**118**), aucubin (**119**), catalpol (120)	HFD-fed obese mice	Lipid metabolism↑, visceral fat mass, serum glucose, TG, TC, FFAs, leptin, AT FAS↓, AT HSL, ADRD3, CPT2↑	Yoshida et al. (2013)

(continued)

Table 4.1 (continued)

Family, Plant species	Active extract/active component	Experimental model	Major activity and molecular targets	References
46. Poaceae				
Sasa quelpaertensis	Leaves (water), p-coumaric acid **19**	3T3-L1 cells, HFD-fed obese mice	Adipogenesis, intracellular lipid accumulation, SREBP-1c expression in 3T3-L1 cells↓, lipid metabolism and insulin action in mice↑, hepatic inflammation↓, liver and WAT fat mass, plasma TG, TC, GPT, GOT, LDH, expression of hepatic FAS, ACC, SCD1, TNFα↓, expression of adiponectin, p-AMPK, p-ACC, CPT-1α in AT, Nrf2, HO-1, PPARα, p-AMPK in liver↑	Park et al. (2020b), Kang et al. (2012a, 2013)
47. Polygonaceae				
Polygonum aviculare	Aerial parts (70% ethanol), myricitrin (**92**), avicularin (**121**), quercitrin (**122**), quercetin (**23**)	3T3-L1 cells, HFD-fed obese mice	Adipogenesis and intracellular lipid accumulation in adipocytes↓, WAT fat mass, adipocyte size, plasma TG, leptin, MDA, expression of lipogenic genes SREBP-1c, PPARγ, FAS, aP2 in WAT and 3T3-L1 cells↓	Sung et al. (2013b)
P. multiflorum	Roots (ethanol), emodin (**123**), physcion (**124**), 2,3,5,4'-tetrahydroxystilbene-2-glucoside **125**	3T3-L1 cells, hepatic steatosis LO2 cells, HFD-fed obese mice	Adipogenesis↓, Lipolysis and lipid metabolism↑ In LO2 cells, TC, TG, DGAT1, HMGCR↓, HTGL, CYP7α1↑. Visceral fat mass, serum glucose, leptin, AT PPARγ, DGAT2↓, AT PPARα, CPT1, CPT2, UCP1, HSL↑. In 3T3-L1 cells, C/EBPα, PPARγ, FAS↓	Choi et al. (2018), Wang et al. (2014)

Rheum palmatum	Rhizomes (methanol), rhein (**126**)	HFD-fed obese mice	Energy expenditure↑, lipogenesis↓, WAT fat mass, plasma TG, TC, LDL-C, expression of PPARγ, LPL, aP2, CD36 in WAT, expression of FAS, ACC, ACOX in liver↓, expression of UCP1, UCP3, D2 in BAT↑	Zhang et al. (2012)
48. Orobanchaceae				
Rehmannia glutinosa	Roots (hot water), polysaccharides, polyphenols	HFD-fed obese mice	Lipid and glucose metabolism↑, gut microbiota modulation, body fat mass, WAT aP2↓, gut *Actinobacteria*, *Bifidobacterium*↑	Park et al. (2017b), Han et al. (2015b)
49. Oleaceae				
Ligustrum lucidum	Fruits (80% ethanol), 8*E*-nuzhenide (**127**)	HFD-fed obese mice	Lipid metabolism↑, WAT fat mass, plasma TG, ALT, AST, ALP, liver lipid content↓	Liu et al. (2014)
L. robustum	Leaves (water), phenylpropanoid glycosides	HFD-fed obese mice and rats	Lipid and glucose metabolism via modulation of gut microbiota↑, body fat mass, plasma glucose, TC, TG, LDL-C, leptin, AT DGAT, adipocyte size↓, hepatic CYP7α1, central leptin signaling↑, gut *Lactobacillus*, *Bacteroides*, *Bacilli, Bacteroidaceae*↑, gut *Firmicutes to Bacteroidetes* ratio, *Enterococcus*, *Clostridia*, *Clostridiales*, *Lachnospiraceae*↓	Zhou et al. (2019), Xie et al. (2015), Yang et al. (2015b)

(continued)

Table 4.1 (continued)

Family, Plant species	Active extract/active component	Experimental model	Major activity and molecular targets	References
50. Ranunculaceae				
Coptis chinensis	Rhizomes (water, methanol ext., butanol fr), alkaloids, berberine (**48**), epiberberine (**128**), coptisine (**129**), palmatine (**130**), magnoflorine (**131**), polysaccharides	3T3-L1 cells, HFD-fed obese mice	Adipogenesis, intracellular lipid and TG accumulation, expression of PPARγ, C/EBPα in 3T3-L1 cells↓, lipid and glucose metabolism↑, plasma TG, TC, leptin, glucose, hepatic gluconeogenesis↓, muscle GLUT4, β-oxidation, glucose-oxidation, AMPK↑. Gut microbiota modulation Gut *Blautia*, *Allobaculum*, fecal SCFAs↑	Choi et al. (2014), Zhang et al. (2014b), Jiang et al. (2013)
51. Rutaceae				
Aegle marmelos (bael)	Leaves (methanol, dichloromethane fr), umbelliferone (**132**), esculetin (**133**), (3,3-dimethylallyl)-halfordinol (**134**)	3T3-L1 cells, HFFD-fed obese mice	Adipogenesis, intracellular lipid accumulation in 3T3-L1 cells↓, visceral fat mass, plasma glucose, insulin, TG, TC, expression of PPARγ, C/EBPα in WAT↓, plasma adiponectin, expression of PPARα, GLUT4 in WAT and muscle↑	Saravanan et al. (2014), Karmase et al. (2013a, 2013b)
Citrus depressa	Fruits (methanol), nobiletin (**135**), tangeritin (**136**)	HFD-fed obese mice	Lipid metabolism↑, inflammation↓, WAT fat mass, plasma TG, leptin, expression of SCD1, aP2, DGAT1, TNFα, MCP-1 in AT↓, expression of p-Akt, PPARα, CPT1, UCP2↑	Lee et al. (2011b, 2013b)

Citrus × *sinensis* (moro blood orange)	Fruit-juice, cyanidin-3-glucoside (**31**)	HFD-fed obese mice	Lipid metabolism↑, Hepatic lipid content, serum TG, TC, ALT, expression of hepatic LXRα, FAS, HMGCR, GPAT1↓, expression of hepatic PPARα, ACOX↑	Salamone et al. (2012)
Evodia rutaecarpa	Fruits (ethanol), evodiamine (**137**)	HFD-fed obese rats	Lipid metabolism↑, epididymal fat mass, serum FFAs, hepatic TG and lipids content↓	Kobayashi et al. (2001)
Murraya koenigii (curry leaves)	Leaves (ethanol, ethyl acetate fr), mahanimbine (**138**)	HFD-fed obese rats	Lipolysis↑, body fat mass, plasma glucose, TG, TC↓	Birari et al. (2010)
52. Rubiaceae				
Cinchona officinalis	Bark (methanol), cinchonine (**139**)	HFD-fed obese mice	Lipogenesis and inflammation↓, epididymal fat mass, plasma TG, TC, hepatic TG, TC, expression of TLR2, TLR4, MyD88, TNFα, IL-6, IFNα, GalR, C/EBPα, PPARγ2, SREBP-1c, aP2, LPL, leptin in AT, expression of FoxO1 in liver↓, AT Wnt signaling, Wnt10b↑	Jung et al. (2012c)
Morinda citrifolia (noni)	Fruit-juice, polysaccharides, iridoids, polyphenolics; leaves (60% ethanol)	HFCD-fed hamsters, HFD-fed obese mice	Lipid and glucose metabolism, antioxidant activity↑, plasma TG, TC, MDA, glucose, insulin, liver lipid mass, expression of hepatic SREBP-1c, FoxO1, PEPCK, G6Pase↓, expression of hepatic PPARα, UCP2, GSH, fecal lipid excretion↑	Lin et al. (2012), Nerurkar et al. (2012), Jambocus et al. (2016)

(continued)

Table 4.1 (continued)

Family, Plant species	Active extract/active component	Experimental model	Major activity and molecular targets	References
53. Sapindaceae				
Aesculus turbinata	Seeds (aqueous ethanol, butanol fr) escins, escin Ib (**140**), escin IIa (**141**), proanthocyanidins	Lipase inhibition assay, HFD-fed obese mice	Pancreatic lipase activity↓, WAT fat mass, serum TG, TC, glucose, hepatic TG, lipid content↓, fecal lipid excretion↑	Kimura et al. (2006, 2008, 2011), Hu et al. (2008)
54. Solanaceae				
Capsicum annuum, C. frutescens (hot peppers)	Seeds (methanol, capsicoside G (**142**) rich fr), capsaicin (**49**), dihydrocapsaicin (**144**)	3T3-L1 cells, HFD-fed obese mice	Adipogenesis, intracellular lipid content, expression of C/EBPα, PPARγ, SREBP-1c in 3T3-L1 cells↓, lipid metabolism and energy expenditure in mice↑, Inflammation↓, epididymal fat mass, serum lipids, hepatic TG, lipid content, expression of PPARγ, C/EBPα, SREBP-1c, FAS, FABP4, TNFα, IL-6, MCP-1, CD68 in AT and liver↓, expression of HSL, PPARα, PGC-1α, CPT-1α, adiponectin, UCP2 in AT and liver↑ Lipid metabolism↑	Sung et al. (2016), Lee et al. (2011a), Jeon et al. (2010), Kang et al. (2010b)
Solanum lycopersicum	Green fruits (water), α-tomatine (**145**), dehydrotomatine (**146**)	HFD-fed obese mice	Epididymal and live fat mass, serum TG, TC, LDL-C, hepatic TG, TC content, expression of HMGCR, C/EBPα, PPARγ, AT perlipin↓, liver p-AMPK, p-ACC↑	Choi et al. (2013)

55. Saxifragaceae				
Bergenia crassifolia	Leaves (fermented), bergenin (**147**), arbutin (**148**)	HFD-fed obese rats	Lipogenesis and food intake↓, body fat mass, serum TG, glucose↓	Shikov et al. (2012)
56. Theaceae				
Camellia sinensis	Leaves (water), flower-buds (methanol), EGCG **35**, chakasaponin-II **149**	HFD-fed obese rats, HFD-fed obese TSOD mice	Lipid metabolism, energy expenditure and food intake↓, visceral fat mass, plasma TG, TC, LDL-C, leptin, FFAs, AST, ALT, hypothalamic NPY expression↓, plasma HDL-C, hypothalamic serotonin expression, AT PGC-1α, PPARγ, CPT-1, adiponectin, UCP-1, CIDEA, PRDM-16 expression↑	Chen et al. (2017), Hamao et al. (2011)
57. Ulmaceae				
Holoptelea integrifolia	Bark (methanol)	HFD-fed obese rats	Lipogenesis↓, plasma lipids, apoB, hepatic HMGR↓, plasma HDL-C, apoA1, LCAT, fecal lipid excretion↑	Subash and Augustine (2013)
58. Vitaceae				
Vitis vinifera	Seeds (commercial ext.), proanthocyanidins, resveratrol (**47**)	HFD-fed obese mice	Lipid metabolism and energy expenditure↑, AT inflammation↓, epididymal and back fat mass, serum and hepatic TG, TC, ACC, AT iNOS, TNFα, IL-1β, IL-6, leptin↓, hepatic CPT-1, BAT UCP-1, serum HDL-C↑	Park et al. (2008), Mahanna et al. (2019)

(continued)

Table 4.1 (continued)

Family, Plant species	Active extract/active component	Experimental model	Major activity and molecular targets	References
Vitis thunbergii var. *taiwaniana*	Roots (aqueous ethanol or hot water), ε-viniferin **150**	3T3-L1 cells, HFD-fed obese mice	Adipogenesis, expression of HMGCR in 3T3-L1 cells↓, lipid and energy expenditure in mice↑ Epididymal and liver fat mass, serum leptin, glucose, insulin, TC, LDL-C, GOT, expression of hepatic SREBP-1, PPARγ↓, expression of hepatic p-AMPK, CPT1↑	Lu et al. (2017), Hsu et al. (2014)
59. Zingiberaceae				
Alpinia officinarum	Rhizomes (ethanol), galangin **151**	3T3-L1 cells, HFD-fed obese mice	Adipogenesis, intracellular lipid content, expression of PPARγ, C/EBPα, SREBP-1c in 3T3-L1 cells↓, lipogenesis, body fat mass, serum lipids, glucose, insulin, leptin, expression of FAS, C/EBPα, PPARγ, SREBP-1c in liver and AT of mice↓	Jung et al. (2012a)
Aframomum melegueta	Seeds (ethanol or methanol), 6-paradol (**152**), 6-shogaol (**153**), 6-gingerol (**154**)	HFD-fed obese mice, Obese men, Lipase inhibition assay	Energy expenditure and antioxidant activity↑, body fat mass, hepatic TG, TC, MDA↓, hepatic SOD, CAT, GP_X, GSH, BAT UCP-1, TRPV1 signaling↑, fecal lipid excretion↑ Pancreatic lipase activity↓	Hattori et al. (2017), Adigun et al. (2016), Sujita et al. (2013), Ekanem et al. (2007)

Boesenbergia pandurata	Rhizomes (ethanol), panduratin A **155**	3T3-L1 cells, HepG2 cells, L6 cells, HFD-fed obese mice	Adipogenesis, hepatogenesis↓, lipid metabolism↑, hepatic and AT fat mass, serum TC, TG, LDL-C, liver TG content↓, expression of ACC, FAS, PPARγ, SREBP-1c↓, expression of p-AMPK, PPARα, PGC-1α, CPT-1, UCP-1, UCP-2 in WAT, liver, 3T3-L1 and HepG2 cells↑, expression of p-AMPK, PGC-1α, SIRt1, NRF-1, Tfam, ERRα in L6 cells↑	Kim et al. (2012a, 2016a)
Curcuma longa	Rhizomes (ethanol ext., hexane and ethanol fr or 50% ethanol ext. fermented with *Aspergillus oryzae,* curcuminoids (curcumin (**9**), desmethoxycurcumin (**156**), bisdesmethoxycurcumin (**157**))	3T3-L1 cells, HFD-fed obese mice or rats, human subcutaneous AT (h-SAT) culture	Adipogenesis and lipogenesis↓, lipid and energy metabolism↑, body fat mass, plasma TG, TC, VLDL, hepatic TG, expression of ACC, PPARγ, C/EBPα, FAS, aP2, LPL in AT↓, expression of HSL, ATGL, adiponectin, CPT-1, p-AMPK in AT, ACOX in liver↑, leptin secretion in h-SAT↓	Al-Lahham et al. (2017), Kim et al. (2016), Ejaz et al. (2009), Asai and Miyazawa (2001)

(continued)

Table 4.1 (continued)

Family, Plant species	Active extract/active component	Experimental model	Major activity and molecular targets	References
Zingiber officinale	Rhizomes (95% ethanol or hot water), 6-gingerol (**154**), 6-shogaol (**153**)	3T3-L1 cells, human myotube culture, HFD-fed obese rats or mice, HFrucD-fed obese NAFLD rats	Adipogenesis, intracellular lipid content in 3T3-L1 cells↓, mitochondrial biogenesis in human myotubes↑, lipid metabolism in mice↑, lipid synthesis, oxidative stress and inflammation↓, body fat mass, hepatic TG content, plasma glucose, insulin, TG, TC, PL, LDL-C, FFAs↓, liver and AT TNF-α, MCP-1, IL-6, ACC, FAS, SCD1, aP2, PPARγ↓, hepatic HMGCR, CYP2E1, ChREBP, LPL, G6Pase↓, hepatic HO-1, SOD, GP_X, NRF1/2, FGF21, p-AMPK, CPT1, ACOX1, PGC1α↑, AMPK/PGC1α signaling in muscle, liver and BAT↑, expression of miR-21, miR-132, related to inflammation in WAT↓	Seo et al. (2021), Deng et al. (2019b), Kim et al. (2018b), Lai et al. (2016), Misawa et al. (2015), Li et al. (2014a), Gao et al. (2012), Nammi et al. (2009)
B. Dietary seaweeds (marine algae) (Brown/green/red algae family and species)				
1. Alariaceae				
Undaria pinnatifida (brown)	Ethanol ext. or dry powder, fucoxanthin (**158**), fucoidan (**159**) (sulfated polysaccharide)	3T3-L1 cells, HFD-fed obese rats	Adipogenesis, intracellular lipid content, expression of adipogenic and inflammation related genes PPARγ,	Grasa-Lopez et al. (2016), Kim and Lee (2012)

			C/EBPα, aP2, TNF-α, MCP-1, PAI-1 in 3T3-L1 cells↓, lipid metabolism and thermogenesis in rats↑, lipogenesis↓, WAT and liver fat mass, serum glucose, insulin, TG, TC, leptin, LDL/VLDL-C, CRP, hepatic ACC↓, expression of PPARα, PGC-1α, UCP-1 in WAT and liver↑	
2. Caulerpaceae				
Caulerpa okamurae (green)	Ethanol ext.	3T3-L1 cells, HFD-fed obese mice	Adipogenesis, intracellular lipid content, expression of PPARγ, C/EBPα, SREBP-1c in 3T3-L1 cells↓, lipogenesis in mice↓, plasma TG, TC, FFAs, WAT fat mass, expression of PPARγ, C/EBPα, SREBP-1c, FAS, ACC, CD36 in WAT↓	Sharma et al. (2017)
C. taxifolia	Methanol/ethyl acetate ext., caulerpenyne (**160**)	Lipase inhibition assay	Pancreatic lipase activity inhibited (IC_{50} of 13 μM against 4-MU oleate)	Bitou et al. (1999)
3. Codiaceae				
Codium cylindricum (green)	Powder, siphonaxanthin (**161**)	HFD-fed obese mice, HepG2 cells	Lipid metabolism in mice↑, lipogenesis↓, perirenal fat mass, expression of SREBP-1c, FAS, SCD1, PPARγ, GPDH in WAT↓, expression of CPT-1α, PGC-1α, ACOX1 in WAT↑, Nrf2 and its target genes in HepG2 cells↑	Li et al. (2018b), Zheng et al. (2020)

(continued)

Table 4.1 (continued)

Family, Plant species	Active extract/active component	Experimental model	Major activity and molecular targets	References
C. fragile	70% ethanol ext., sulfated polysaccharide	HFD-fed obese mice	Modulation of gut microbiota composition, relative abundance of bacteria of family, *Acetatifactor*, *Ruminococcaceae*, *Lachnospiraceae*, related to SCFA production↑	Kim et al. (2020)
4. Ishigeaceae				
Ishige okamurae (brown)	50% ethanol ext., fucoxanthin (**158**), diphlorethohydroxycarmalol (**162**)	3T3-L1 cells, HFD-fed obese mice	Adipogenesis, intracellular lipid droplets, expression of C/EBPα, PPARγ↓, p-HSL, ATGL, p-AMPK in 3T3-L1 cells↑, lipid metabolism↑, lipogenesis in mice↓, abdominal fat mass, serum FG ang PPG, TC, LDL-C, ALT, AST, LDH, expression of DGAT1, FAS, SREBP-1c in liver↓, expression of hepatic and WAT p-AMPKα, CPT-1, WAT ATGL, HSL↑	Ding et al. (2019), Seo et al. (2018)
5. Lessoniaceae				
Ecklonia cava (brown)	70% ethanol ext., ethyl acetate fr or water ext., dieckol (**163**) enriched fr, phlorotannins, phloroglucinol, eckol **164**, dieckol, 8,8'-bieckol **165**	HFD-fed obese male mice, Lipase inhibition assay	Lipid metabolism and antioxidant activity in mice↑, lipogenesis and inflammation in mice↓, Body fat mass, plasma leptin, TG, TC, LDL-C, 4-HNE, hepatic TG content, expression of SREBP-	Eo et al. (2015, 2017), Park et al. (2015b), Kim et al. (2012c)

			1c, FAS, ACC, LPL, NF-κB, IL-1β, TNF-α, MCP-1, FXR, SHP, MDA in liver↓, expression of hepatic CAT, GP_X, p-AMPK, SIRT1, CYP7α1, HNF-4α↑, expression of renal NLRP3 inflammasome, NF-κB, MCP-1, TNFα, CRP↓, pancreatic lipase activity↓	
E. stolonifera	Ethanol ext., ethyl acetate fr or methanol ext., dichloromethane fr, fucosterol (**166**) and phlorotannins, eckol, dieckol, phlorofucofuroeckol A **167**	3T3-L1 cells, HFD-fed obese mice	Adipogenesis, intracellular lipid content, expression of SREBP1, PPARγ, C/EBPα, lipin1, DGAT1 in 3T3-L1 cells↓, lipid catabolism, lipolysis and thermogenesis in mice↑, AT and hepatic lipid mass, serum TC, TG, LDL-C↓, expression of CPT1, UCP1, PRDM16, p-HSL, ATGL, MGL in WAT↑, expression of C/EBPα, PPARγ, FABP4 in WAT↓	Jin et al. (2020), Jung et al. (2014a, 2014b), Yoon et al. (2008)
6. Laminariaceae				
Laminaria japonica (brown)	Ethanol ext., fucoxanthin (**158**)	HFD-fed obese rats	Lipid metabolism and thermogenesis↑, lipogenesis↓, AT fat pad mass, adipocyte size, serum glucose, insulin, leptin, TG, TC, LDL-C, FFAs, TNF-α, GOT, expression of SREBP-1c, ACC, FAS, PPARγ, SCD1, GPAT,	Jang and Choung (2013)

(continued)

Table 4.1 (continued)

Family, Plant species	Active extract/active component	Experimental model	Major activity and molecular targets	References
			AGPAT, DGAT, LPL in WAT and liver↓, expression of hepatic p-AMPK, p-ACC, PPARα, CPT1↑, expression of ATGL, HSL, CPT1 in WAT↑, expression of PPARα, ACOX, CPT1, UCP2, UCP3 in muscle↑	
7. Halymeniaceae				
Grateloupia elliptica (red)	60% ethanol ext	3T3-L1 cells, HFD-fed obese mice	Adipogenesis, intracellular lipid content, expression of PPARγ, SREBP-1c, FABP4 in 3T3-L1 cells↓, thermogenesis↑, lipogenesis in mice↓, WAT fat mass, adipocyte size, serum TG, TC, leptin, expression of C/EBPα, SREBP-1c, PPARγ in WAT↓, expression of FGF21 in WAT, UCP1, UCP3 in BAT↑	Lee et al. (2020a)
8. Gelidiaceae				
Gelidium amansii (red)	Ethanol ext., hot water ext., sulfated polysaccharide	3T3-L1 cells, HFD-fed obese mice, HFD-fed hamsters	Adipogenesis, intracellular lipid content, expression of PPARγ, C/EBPα, SREBP-1c in 3T3-L1 cells↓, lipogenesis in mice↓, AT fat mass, adipocyte size, serum TG, TC, LDL-C, FFAs, expression of PPARγ, SREBP-1c, C/EBPα	Kang et al. (2016, 2017), Park et al. (2017a), Yang et al. (2017b)

			in WAT of mice↓, expression of hepatic SREBP1, SREBP2, FAS in hamsters↓, serum HDL-C, expression of adiponectin, HSL, p-AMPK in WAT↑, fecal lipids and bile acid excretion, hepatic p-AMPK expression in hamsters↑	
9. Plocamiaceae				
Plocamium telfairiae (red)	40% ethanol	3T3-L1 cells, HFD-fed obese mice	Adipogenesis, intracellular lipid droplets accumulation, expression of PPARγ, SREBP1, ACC, C/EBPα in 3T3-L1 cells↓, Thermogenesis in mice↑, WAT fat mass, serum TG, TC, insulin↓, expression of UCP1, UCP3 in BAT↑	Lu et al. (2020)
10. Sargassaceae				
Sargassum polycystum (brown)	Powder, fucoxanthin, fucoidan, high Ca content	HFD-fed obese rats	Thermogenesis, antioxidant activity, lipid metabolism and lipolysis↑, body fat mass, plasma TG, TC↓, plasma HDL-C, SOD, GP_X↑, fecal lipids excretion↑	Awang et al. (2014), Matanjun et al. (2010)

(continued)

Table 4.1 (continued)

Family, Plant species	Active extract/active component	Experimental model	Major activity and molecular targets	References
11. Scytosiphonaceae				
Petalonia binghamiae (brown)	Ethanol ext., fucoxanthin (**158**)	3T3-L1 cells, HFD-fed obese mice	Adipogenesis, intracellular lipid droplets, expression of C/EBPα, PPARγ, SREBP-1c, aP2 in 3T3-L1 cells↓, expression of p-AMPK, p-ACC in 3T3-L1 cells↑, lipid oxidation in mice↑, AT fat mass, liver lipid droplets, serum TG, GPT, GOT↓, expression of p-AMPK, p-ACC in WAT↑	Kang et al. (2010c, 2012b)
12. Hematococcaceae				
Haematococcus pluvialis (micro green alga)	Ethanol ext., astaxanthin (**168**)	HFD-fed obese mice, HF-HFrucD-fed obese mice, oerweight and obese adults	Lipid synthesis and oxidative stress↓, WAT and liver fat mass, plasma TG, TC, FFAs, MDA, ISP, hepatic TG content, AST, ALT, TGF-β1, CYP2E1, MPO↓, plasma and hepatic CAT, SOD, GP_X, GST, TAC↑	Bhuvaneswari et al. (2010), Ikeuchi et al. (2007), Choi et al. (2011)
C. Fungi (fruiting bodies or mycelia of macrofungi mushrooms and others microfungi). Family and species				
1. Auriculariaceae				
Auricularia polytricha (edible mushroom grows in trees)	Water ext., polysaccharides	HFD-fed NAFLD rats or STZ-diabetic mice	Lipogenesis, inflammation and oxidative stress↓, hepatic fat mass, plasma and hepatic TG, TC, FFAs, ALT, TNF-α, IL-6, MDA↓, plasma HDL-C, hepatic SOD, GP_X, GR↑	Chiu et al. (2014), Xiang et al. (2021)

A. auricular-judae (medicinal mushroom)	70% ethanol ext.	3T3-L1 cells, HFD-fed obese mice	Adipogenesis, intracellular TG content, expression of adipogenic genes, PPARγ, C/EBPα, FAS in 3T3-L1 cells↓, lipolysis and lipid metabolism in mice↑, lipogenesis↓, serum lipids, hepatic fat mass, expression of lipogenic genes↓	Reza et al. (2015)
2. Ganodermataceae				
Ganoderma lucidum (medicinal mushroom)	Water ext., polysaccharides	HFD-fed obese mice	Gut dysbiosis and inflammation in metabolic tissues↓, body fat mass, hepatic and WAT TNF-α, IL-6, IL-1β, PAI-1, MCP-1, p-JNK, serum LPS, TLR4↓, hepatic and WAT IL-10, p-Akt↑, relative abundance of gut bacterial spp. of *Eubacterium*, *Roseburia*, *Clostridium*↑, relative abundance of *Escherichia*, *Enterococcus*, *Lactococcus*, *Mucispirillum* spp. in gut↓	Chang et al. (2015)
3. Meripilaceae				
Grifola frondosa (edible mushroom grows on oak trees)	Ethanol ext. of mycelia, polysaccharides	HFD-fed obese mice, HFD-fed obese rats, C2C12 cells-exposed to high palmitate	Lipid and energy metabolism↑, Gut dysbiosis↓, body fat mass, plasma TC, TG, leptin, hepatic TG content, expression of SREBP-1c, LPL, FAS, C/EBPα, FABP4 in liver and WAT↓, expression of	Aoki et al. (2018), Li et al. (2019)

(continued)

Table 4.1 (continued)

Family, Plant species	Active extract/active component	Experimental model	Major activity and molecular targets	References
			PPARδ target genes, PDK4, CPT-1β, PGC-1α, ACSL3, UCP3, GLUT4 in muscle of mice↑, expression of PPARδ, PDK4, p-AMPK, p-Akt in C2C12 cells↑, expression of hepatic CYP7A1, BSEP in rats↑, relative abundance of gut bacterial spp. of *Clostridium* XVIII, *Butyricicoccus*, *Turicibacter*↓, bacterial spp of *Ruminococcus*, *Helicobacter*, *Barnesiella*, *Paraprevotella*, *Intestinimonas* in the gut↑	
4. Mycenaceae				
Panellus serotinus	Water ext.	Leptin-deficient obese diabetic mice	Lipid metabolism↑, serum TG, TC, LDL-C, AST, ALT, hepatic TG, TC content, FAS activity↓, serum adiponectin↑	Inoue et al. (2013)
5. Omphalotaceae				
Lentinus edodes (edible mushroom)	Powder, eritadenine (**187**), β-glucans	HFD-fed obese mice and rats	Lipid metabolism↑, abdominal fat mass, serum TC, TG, LDL-C↓, expression of hepatic CYP7A1↑	Yang et al. (2013), Handayani et al. (2011)

6. Physalacriaceae				
Flammulina velutipes (edible mushroom)	Water ext., polysaccharides fr	HFD-fed obese mice	Lipolysis↑, fat absorption↓, hepatic lipid content, serum TC, TG, LDL-C, GOT, GPT, LDH↓, serum HDL-C, fecal lipid excretion↑, gut *Firmicutes* to *Bacteroidetes* ratio↓, relative abundance of gut immunity improving bacteria, *Porphyromonadaceae*, *Bacteroidaceae* spp.↑, relative abundance of gut *Lactobacillaceae*, *Lachnospiraceae*↓	Miyazawa et al. (2018), Zhao et al. (2019)
7. Polyporaceae				
Pleurotus citrinopileatus	Water ext., polysaccharides, phenolics	HFD-fed obese mice	Lipogenesis and food intake↓, body fat mass, serum TG, TC, LDL-C, NEFAs, AST, LDH↓, serum HDL-C↑	Sheng et al. (2019b)
P. sajor-caju	Water ext., β-glycan rich fr	HFD-fed obese mice	Lipolysis and antioxidant activity↑, inflammation↓, WAT and liver fat mass, serum TG, TC, LDL-C, glucose, MDA, ALT, AST, ALP, expression of WAT NF-κB, TNF-α, IL-6, MCP-1, PPARγ, SREBP-1c, LPL↓, expression of adiponectin, HSL, ATGL in WAT, of SOD, CAT, GP_X in the liver and kidney↑	Kanagasabapathy et al. (2012, 2013)

(continued)

Table 4.1 (continued)

Family, Plant species	Active extract/active component	Experimental model	Major activity and molecular targets	References
P. ostreatus (edible mushroom)	DMSO ext., anthraquinones	3T3-L1 cells	Adipogenesis, intracellular lipid content, expression of C/EBPα, PPARγ, FAS, ACS, SREBP-1c, FABP4↓	Bindhu and Das (2019)
8. Tremellaceae				
Tremella fuciformis	Water ext., polysaccharides	3T3-L1 cells	Adipogenesis, intracellular TG content, expression of adipogenic-related genes, PPARγ, C/EBPα, leptin↓	Jeong et al. (2008)
D. Dietary marine fishes (family and species)				
1. Euphausiidae				
Euphausia superba (Antarctic krill)	Acetone-ethanol (1:1) ext., n-3-PUFA, eicosapentaenoic acid (**169**), docosahexaenoic acid (**170**)	HFD-fed obese mice	Lipid and glucose metabolism↑, insulin sensitivity↑, plasma TC, glucose, hepatic fat mass, TG, TC, expression of FAS, ACC, SCD1, MGL, SREBP-1c, SREBP2, HMGCR, LDL-R, HSL, TNF-α↓, plasma adiponectin↑	Gigliotti et al. (2011), Tandy et al. (2009)
E. Marine sponges (family and species)				
1. Hymedesmiidae				
Phorbas spp.	Phorbaketal A (sesterpenoid) (**170a**)	3T3-L1-adipocytes	Adipogenesis and adipogenic genes expression↓	Byun et al. (2013)

4.5.3 Stimulatory Effect on Energy Expenditure

White adipose tissue (WAT) is the main "storage site" of excess energy in obese humans, primarily in the form of triglycerides (TG) (fat). Therefore, stimulation of energy expenditure via lipolysis of TG into free fatty acids (FFAs) and glycerol and their mobilization to the energy-demanding tissues, liver, and skeletal muscles for FA oxidation is an important therapeutic target in prevention of obesity. The stimulation of energy expenditure may be regulated centrally via regulation of thermogenic markers, melanocortin receptor (MCR), melanin-concentrating hormone, and leptin signaling in suppression of food intake (Spiegelman and Flier 2001) and peripherally by promoting lipolysis and FA oxidation in the AT, liver, and skeletal muscle via upregulation of AMPK activation. Insulin acts as lipolytic inhibitor via its insulin receptors, while catecholamines (adrenaline and noradrenaline) and natriuretic peptide promote lipolysis by upregulation of the activity of two main lipolytic enzymes, hormone sensitive lipase (HSL), and adipose triglyceride lipase (ATGL) in human WAT. AMP-activated protein kinase (AMPK), a phosphorylating enzyme on activation (phosphorylation), stimulates the phosphorylation of HSL, which in turn increases the phosphorylation of ACC to suppress lipogenesis in metabolic tissues. Accumulating evidence demonstrates that activated AMPK stimulates hepatic FA oxidation (FAO) and ketogenesis; inhibits hepatic cholesterol and TG synthesis, and lipogenesis; stimulates FAO and glucose uptake in skeletal muscle; and stimulates thermogenesis and inhibits lipogenesis in BAT and WAT (Zimmermann et al. 2004; Sengenes et al. 2000; Langin 2006; Yuliana et al. 2014). Brown adipose tissue (BAT) within WAT, on activation is able to disperse stored energy as heat by non-shivering thermogenesis process. Brown adipocytes on activation by sirtuin-1 (SIRT-1) or AMPK or adrenergic receptor-beta 3 (ADRB3 or β3-AR) or heat shock factor-1 (HSF-1) upregulate the expression levels of heat producing mitochondrial membrane proteins, uncoupling protein-1 (UCP-1) and other proteins including Cidea, PR-domain containing protein 16 (PRDM-16), and Cox-7α1 through peroxisome proliferator-activated receptor gamma (PPARγ) deacetylation and PPARγ-coactivator 1α (PGC-1α) activation to produce heat and thermogenic "brown-like" cells (beige cells). Upregulation of deiodinase-2 (DIO2) increases the expression of thyroid hormone T3, which in turn activates β3-adrenergic receptor to increase UCP1 gene expression for browning of WAT. Stress kinase MEK promotes translocation of HSF-1 to nucleus for transcriptional activation of PGC-1α for energy expenditure. Therefore, promoting WAT browning and BAT activation is a potential therapeutic approach to combat obesity (Kurylowicz and Puzianowska-Kuznicka 2020; Volke and Krause 2020; Fischer et al. 2019; Wu et al. 2018; Tang et al. 2015; Qiang et al. 2012). Several phytochemicals including resveratrol (**47**) (Fig. 4.1), berberine (**48**), curcumin (**9**), capsaicin (**49**), cryptotanshinone (**452**) from *Salvia miltiorrhiza*, fucoxanthin (**158**) from seaweed *Undaria pinnatifida*, and green tea catechins, theaflavins, and caffeine **41** have been reported to stimulate lipolysis, FAO, and mitochondrial biogenesis and thermogenesis processes via activation of SIRT1, AMPK, β3-AR, and other pathways in treatment of obesity in animal models (Table 4.1).

4.5.4 Inhibition of Adipogenesis

Adipocytes play a central role in the maintenance of lipid homeostasis and energy balance in the body of humans by storing triglycerides or releasing free fatty acids (FFAs) in response to changes in energy demands. In obese humans, the adipose tissue is increased abnormally due to both hyperplasia (increased number of cells) and hypertrophy (increased size) of adipocytes by the process of maturation (cell growth) of preadipocytes and differentiation of mature adipocytes, known as adipogenesis. Therefore, inhibition of adipogenesis is considered as a promising therapeutic target for treatment of obesity and diabetes. In cellular model, mouse cell line, 3T3-L1 preadipocytes are commonly used for the study of obesity in vitro, because such cells accumulate triglycerides for differentiation in the maturity stage on culture under pro-differentiation cocktail stimulators, such as insulin, IBMX (3-isobutyl-1-methylxanthine), fetal bovine serum, dexamethasone, glucocorticoids, and thyroid hormone. A wealth of observations demonstrates that adipocyte differentiation of embryonic stem cells and 3T3-L1 preadipocytes occurs in four main stages, namely, growth arrest, mitotic clonal expansion (replication of DNA and duplication of cells), early differentiation, and terminal differentiation. At the growth arrest stage, preadipocytes induce the expression of early markers of differentiation, namely, C/EBPβ and C/EBPδ in response to hormonal stimulation. In mitotic clonal expansion (MCE) stage, C/EBPβ alone or in combination with C/EBPδ on activation induces the expression of adipocyte-specific genes, PPARγ, and CCAAT/enhancer binding protein-alpha (C/EBPα) and their target genes, sterol regulatory element binding protein-1c (SREBP-1c), fatty acid synthase (FAS), adipocyte binding protein 2 (aP2), stearoyl CoA desaturase-1 (SCD-1), acyl CoA oxidase (ACOX), phosphoenol pyruvate carboxykinase (PEPCK), glucose transporter-4 (GLUT-4), and lipoprotein lipase (LPL) via induction of MAPK cascade (increased phosphorylation of ERK1/2 and JNK kinases) by extracellular leukemia inhibitory factor (LIF) and its receptor (Wu et al. 1999). The MCE is considered as a prerequisite for differentiation of preadipocytes into adipocytes, because at this stage, preadipocytes increase DNA synthesis and double its cell number. Moreover, in this stage, C/EBPβ increases the expression of various cyclins, namely, cyclins A, B, D, and E, and cyclin-dependent kinases (CDKs), such as CDK-4, -2, and -1 for regulation of cell cycle process (Tang et al. 2003). Kruppel-like factor 4 (KLF-4) plays a significant role on directly binding to C/EBPβ promoter region and, in combination with early growth response protein (EGR2), also known as Krox20, induces the expression of PPARγ and C/EBPα, the main transcription factors of adipogenesis (Birsoy et al. 2008). A recent study demonstrates that C/EBPβ recruits epigenetic lysine methyltransferases, MLL3 and MLL4 for activation of bromodomain-containing protein 4 (BRD4), which induces Pol II for activation and upregulation of the expression of PPARγ and C/EBPα in obese mice (Lee et al. 2017a, 2019a). The cell cycle is closely associated with adipocyte cell growth and proliferation. A wide variety of phytochemicals (listed in Table 4.1) have been reported to inhibit adipogenesis of preadipocytes or to induce apoptosis of mature adipocytes by suppression of the expression of PPARγ and C/EBPα, key transcription factors for

adipogenesis by targeting different stages of adipocyte cell growth through cell cycle arrest in mitotic clonal expansion stages via suppression of MAPK/ERK phosphorylation, inhibition of FoxO1 signaling pathway, or induction of Wnt signaling and AMPK activation. AMPK activation induces G1 cell cycle arrest by decreasing the levels of cell growth proteins, cyclin A, cyclin D1, and phosphorylated-retinoblastoma (pRb) and increasing the expression of negative regulators of adipogenesis, CCAAT/enhancer-binding protein (C/EBP), homologous protein (CHOP), and Kruppel-like factor-2 (KLF-2). Some review articles highlighted the potentials of the phytochemicals in treatment of obesity via inhibition of adipogenesis at different stages of adipocyte cell growth and in mature adipocytes (Chang and Kim 2019; Rayalam et al. 2008; Kim et al. 2006; Rosen et al. 2000). However, a research finding demonstrates that the inhibition of adipogenesis or adipose tissue expansion is unhealthy because intracellular triglycerides removal rate from adipocytes is positively correlated with increased lipolysis (by mainly hormone-sensitive lipase (HSL)) leads to increased FFAs levels and development of dyslipidemia and insulin resistance in the body, which in turn, contribute to high risk factors for diabetes and cardiovascular complications (Arner et al. 2011).

4.5.5 Regulation of Lipid Metabolism via PPARα Activation

The reduction of fat stores by hydrolysis of accumulated triglycerides (TG) in the peripheral liver, adipose tissue, and skeletal muscle is one of the strategies to combat obesity. Obesity-related chronic inflammation increases the lipolytic release of free fatty acids (FFAs) from adipose tissue fat and raises plasma FFAs levels that are subsequently stored mainly in the liver as TGs and develops nonalcoholic fatty liver disease (NAFLD). In addition, accumulation of FFAs in other metabolic tissues, skeletal muscle, heart, and kidney causes insulin resistance. Moreover, obesity-related dyslipidemia results in the development of cardiovascular diseases (CVDs). Several studies demonstrate that in skeletal muscle of obese individuals, fatty acid oxidation is decreased due to low levels of CPT-1, citrate synthase, and cytochrome C oxidase because of intramuscular lipid accumulation, particularly in the cystol of skeletal muscle and thereby resulting in insulin resistance in myotubes. Peroxisome proliferator-activated receptor alpha (PPARα), a ligand-activated transcription factor of steroid hormone receptor subfamily and nuclear receptor, is highly expressed in the liver, skeletal muscle, brown adipose tissue, and heart for fatty acid oxidation in healthy nonobese humans. PPARα regulates the expression of a number of genes for lipid and lipoprotein metabolism for reduction of plasma and hepatic TGs levels and plasma small dense low-density lipoprotein (LDL) particles and enhancement of high-density lipoprotein cholesterol (HDL-C) levels. PPARα stimulates the transcription of genes critical for fatty acid oxidation (FAO) and ketogenesis in both humans and rodents and promotes gluconeogenesis only in rodents through upregulation of PGC-1α and HNF-α. Estrogen has been found to inhibit the actions of PPARα on obesity and lipid metabolism and hence PPARα is not effective in obese men and obese postmenopausal women in obesity management. Possibly,

17β-estradiol inhibits the activity of PPARα by inhibition of the recruitment of PPARα coactivator CREB-binding protein in premenopausal women because of ovarian factor. Synthetic PPARα agonists, such as fibrates, namely, fenofibrate (**50**) and ciprofibrate (**51**), used for treatment of dyslipidemia, have been shown to reduce the symptoms of obesity in animal models by both increasing hepatic fatty acid oxidation (FAO) and decreasing the levels of plasma and hepatic TGs levels by activation of PPARα gene in the liver. The transcription factor PPARα on activation recognizes the natural lipid ligands FA derivatives and binds them to PPAR response elements (PPREs) located in the regulatory regions of its target genes and upregulates the expression of peroxisomal β-oxidation related genes, such as acyl-CoA oxidase 1 (ACOX1) and mitochondrial β-oxidation-related genes, such as carnitine palmitoyltransferase 1 (CPT 1), CPT 2, medium-chain acyl-CoA dehydrogenase (MCAD), long-chain acyl-CoA dehydrogenase (LCAD), and very long-chain acyl-CoA dehydrogenase (VLCAD). The increased hepatic FAO increases the production of acetyl CoA, which on condensation with acetoacetyl CoA generates HMG-CoA and CoA as ketone bodies. Available evidence demonstrates that PPARα upregulates the expression of the gene fibroblast growth factor 21 (FGF-21) for upregulation of genes related to lipid and ketone metabolism in response to ketogenic diet (KD) (high fat, low carbohydrate diet)-fed obese mice. Moreover, PPARα activation markedly prevents hepatic inflammation by suppression of LPS-dependent production of inflammatory cytokines, IL-1, IL-6, and TNF-α, and adhesion molecules, ICAM-1 and VCAM-1 in the aorta. In suppression of inflammation, PPARα directly or indirectly interacts with the transcription factors to upregulate the expression of anti-inflammatory genes, interleukin-1 receptor antagonist (IL-1Ra), and IκBα, a cytoplasmic inhibitor of NF-κB, to block their activity. In addition, activated PPARα prevents hepatic fibrosis through upregulation of the expression of antioxidant enzyme, catalase (CAT), in the liver to reduce the levels of ROS-induced TGFβ and collagen production by hepatic stellate cells. The agonists of PPARα stimulate the activity of PPARα by increasing the expression of adiponectin for adiponectin-mediated activation of AMPK. Moreover, AMPK activation reduces FoxO1-dependent lipid synthesis by suppression of the expression of lipogenesis-related genes, LXRα, SREBP-1c, ACC, and FAS. AMPK on activation increases the phosphorylation of ACC to inhibit its action in the synthesis of malonyl-CoA, a potent inhibitor of CPT-1, which controls the entry of fatty acids into mitochondria for oxidation or conversion into ketone bodies in the liver. Therefore, the stimulation of lipid metabolism through AMPK-dependent PPARα activation in the liver, skeletal muscle, and WAT is a potential therapeutic approach in the treatment of obesity (Pawlak et al. 2015; Yoon 2009; Higuchi et al. 2008; Houmard 2008; Stienstra et al. 2007; Badman et al. 2007; Flier 2004). A variety of phytochemicals and extracts of plants and fungi have been reported to increase the expression levels of PPARα in the liver and skeletal muscle of obese animals for improvement of postprandial hyperlipidemia and hepatic steatosis through AMPK activation (Table 4.1).

4.5.6 Modulation of Gut Microbiota Composition

Gut microbiota (GM) present on the surface of the intestinal mucus membrane in humans plays a key role in the preservation of body homeostasis through maintenance of lipid and carbohydrate metabolism. Humans have two interacting genomes, their own and that of their host microbiome, the majority of them are colonized in the gut in the layer of mucin glycoproteins produced by a specific endothelial cells, called goblet cells (Zeng et al. 2012). The gut microbiome maintains a symbiotic relationship with the host and provides vitamins and other nutrients to the host cells and thereby establishes a beneficial ecosystem for the host's physiological functions and protects the host from the entry of harmful pathogens. Their symbiotic communication results in the accuracy of the mucosal barrier function by production of mucins and antimicrobial peptides and anti-inflammatory cytokines including IgA and IL-22 and maintenance of immune tolerance (Cani 2018; Vieira et al. 2016; Brown et al. 2013).

Several environmental factors, such as high fat and high carbohydrate diet, high dose of antibiotic intake, and excessive stress, result in the change of the relative abundance levels of different classes of health-promoting bacterial community, leading to an imbalance or dysbiosis of GM, and contribute to the progression of various diseases including gastrointestinal cancers, inflammatory bowel disease, obesity, and diabetes. Therefore, modulation of GM dysbiosis by intake of health promoting natural plant/algae/mushroom/marine animals extracts rich in antioxidant and anti-inflammatory phytochemicals including dietary fibers and proteins may be a potential therapeutic target for treatment of obesity and diabetes (Ortuno Sahagun et al. 2012; Wu et al. 2011). Various classes of phytochemicals including dietary proteins and fibers, nondigestible polysaccharides and digestible polyphenolics, carotenoids, and thiosulfides present in dietary fruits, vegetables, legumes, and beverages stimulate the growth of some beneficial bacterial species, such as bacterial spp. of genera, *Bifidobacterium*, *Lactobacillus*, yeast, *Prevotella*, and *Akkermansia*, which improve the insulin sensitivity in the metabolic tissues for metabolism of lipid and carbohydrate of the host through production of short-chain fatty acids (SCFAs) and branched-chain amino acids (BCAA) and increase innate immunity of the body for treatment of obesity and diabetes (Carrera-Quintanar et al. 2018). A good number of natural products have been reported to modulate GM dysbiosis for treatment of obesity and diabetes in animal models (see in the next section). The major therapeutic targets of natural products are presented in Fig. 4.2.

4.6 Natural Products Isolated from Various Natural Sources in Treatment of Obesity

A variety of natural products, including crude extracts of plants, mushrooms, marine algae, microorganisms, and animals and isolated phytochemicals from these extracts, have been reported to prevent obesity in cellular and animal models. Several review articles have highlighted antiobesity effects of natural products

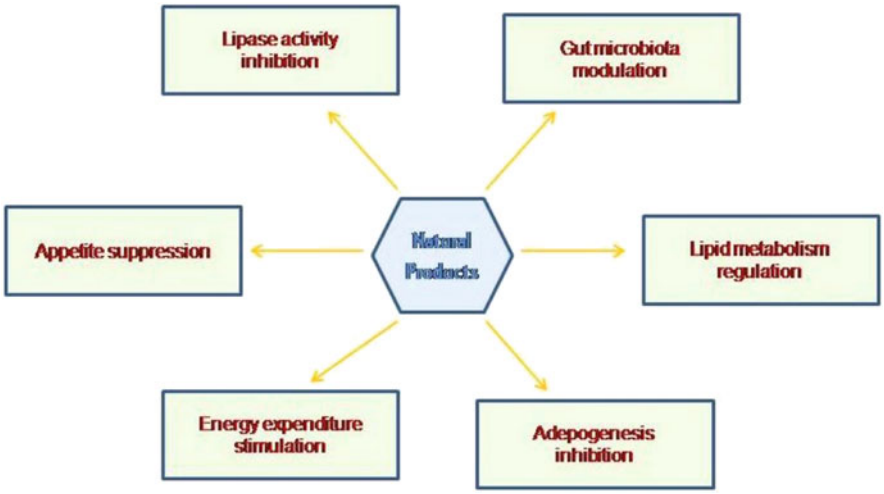

Fig. 4.2 Major therapeutic targets of natural products in obesity treatment

from diverse sources, but none of them provide the details of the mechanisms of action and active constituents of the bioactive extracts (Yun 2010; Fu et al. 2016; Mopuri and Islam 2017; Karri et al. 2019). Table 4.1 provides a comprehensive list of some natural products (extracts and bioactive components) in obesity treatment and their major modes of actions.

From the Table 4.1, it is evident that the plants from 59 families have been reported to possess antiobesity activity. Among these families, 10 families, namely, *Apiaceae*, *Araliaceae*, *Asteraceae*, *Celastraceae*, *Dioscoreaceae*, *Fabaceae, Lamiaceae*, *Solanaceae*, *Theaceae*, and *Zingiberaceae*, contribute a large number of plants and phytochemicals having antiobesity potentials. Most of the plants and their active phytochemicals reduce insulin resistance in obese animals by upregulation of lipid metabolism and energy expenditure through AMPK activation in the liver, adipose tissue, and skeletal muscle. Among the bioactive phytochemicals, flavonoids, and saponins have been shown to possess strong antiobesogenic potential for amelioration of the pathogenesis of obesity via multi-molecular targets in metabolic tissues including lipid and energy metabolism, modulation of gut dysbiosis composition, inhibition of pancreatic lipase activity, and suppression of appetite. Some edible and medicinal mushrooms including *Auricularia polytricha*, *Grifola frondosa*, *Ganoderma lucidum*, and *Pleurotus sajor-caju* have been found to have potential antiobesity effects via their polysaccharides and other phenolic and terpenoid phytochemicals. Marine algae, especially edible seaweeds, are a promising source of antiobesity agents. Four major classes of bioactive compounds, namely, carotenoids (fucoxanthin and astaxanthin), alginates (gelling-like polysaccharides), fucoidans (sulfated polysaccharides), and phlorotannins, present in these seaweeds are responsible for the antiobesity activity of these seaweeds. Usually, carotenoids and fucoidans inhibit lipid synthesis and

lipid absorption in the body, and alginates suppress appetite. Brown seaweeds, namely *Ecklonia cava*, *E. stolonifera*, *Undaria pinnatifida*, *Ishige okamurae*, and *Laminaria japonica* contain high concentrations of phlorotannins and carotenoids as bioactive components for inhibition of adipogenesis and lipogenesis and pancreatic lipase activity. Among these brown algae, *E. cava* contains the highest amounts of phlorotannins (Hu et al. 2016b). Polyunsaturated fatty acids, mainly eicosapentaenoic acid and docosahexaenoic acid isolated from Antarctic krill, have potential antioxidant, lipid catabolism, and insulin sensitivity effects. These natural products could be useful for clinical trials in humans for treatment of obesity after their extensive toxicological and pharmacokinetic studies.

4.7 Major Therapeutic Targets of Natural Products in Diabetes Treatment

4.7.1 Stimulatory Effect on AMPK Activation

In humans, the maintenance of normal glucose levels depends on the responsiveness of insulin in skeletal muscle and liver and insulin secretion from pancreatic beta cells. Both these factors are the main pathophysiological features of type 2 diabetes because of insulin resistance in the skeletal muscle and liver and impaired insulin secretion from pancreatic beta cells due to lipotoxicity and glucotoxicity in these metabolic tissues. AMP-activated protein kinase (AMPK) is a highly conserved sensor of cellular energy and its activation inhibits fat synthesis and fat accumulation by promoting lipolysis and fat oxidation and enhances mitochondrial function and biogenesis via phosphorylation of PGC-1α and induction of the expression of energy metabolism-related genes. Moreover, AMPK activation in skeletal muscle promotes glucose uptake via upregulation of GLUT4 expression and its translocation from intracellular storage vesicles to the plasma membrane for reduction of plasma glucose levels (Kelley et al. 2002; Lowell and Shulman 2005; Mcgee et al. 2008). In addition, activation of AMPK by its activator, 5-aminoimidazole-4-carboxamide riboside (AICAR), and other AMPK agonists downregulates the expression of gluconeogenic genes phosphoenolpyruvate carboxykinase (PEPCK) and glucose-6-phosphatase (G6Pase) in the liver to inhibit hepatic glucose production (Lochhead et al. 2000). Furthermore, phosphorylated AMPK inactivates two key enzymes of fatty acid and sterol synthesis, acetyl-CoA carboxylase-1 (ACC1) and 3-hydroxy-3-methylglutaryl-CoA reductase HMGCR), in the liver and adipose tissue (Hardie et al. 1989). In the brain, adipokine leptin sensitivity inhibits the activation of AMPKα2 to reduce both body weight and food intake, whereas adipokine adiponectin and stomach gastric peptide ghrelin promote its activation to increase food intake and energy expenditure (Minokoshi et al. 2004). Available evidence indicates that AMPK exists as heterotrimers composed of a catalytic α-subunit and regulatory β-and γ-subunits. Its α1 isoform predominates in the liver and adipose tissue, while its α2 isoform is mainly expressed in the muscle, brain, and heart (Hardie et al. 2012). AMPK activation depends on its phosphorylation of the

catalytic subunit α on threonine 172 by liver kinase B-1 (LKB1) or calcium-dependent calcium/calmodulin-dependent protein kinase kinase beta (CaMKKβ), and this is promoted by AMP or ADP binding to the γ-unit. Therefore, an increase of cellular AMP/ATP ratio or ADP/ATP ratio promotes AMPK activation (Oakhill et al. 2011; Xiao et al. 2011).

Several phytochemicals from natural products, namely, curcumin from *Curcuma longa*, resveratrol from *Vitis vinifera*, crytotanshinone from *Salvia miltiorrhiza*, berberine from *Coptis chinensis*, ginsenosides from *Panax ginseng*, epigallocatechin gallate from green tea, theaflavin from black tea, arctigenin from *Arctium lappa*, aspalathin from *Aspalathus linearis*, sophoricoside from *Sophora japonica*, p-coumaric acid from *Ganoderma lucidum*, and cyanidin-3-*O*-β-glucoside **31** from dietary fruits (Fig. 4.1) have been shown to activate AMPK for amelioration of hyperglycemia and insulin resistance in cellular and animal models of diabetes (Table 4.2) (Hardie 2013; Huang et al. 2012; Guo et al. 2012; Son et al. 2013; Wu et al. 2013; Yoon et al. 2013).

4.7.2 Stimulatory Effect on PI3K/Akt Signaling Pathway

The insulin-regulated PI3K/Akt signaling pathway plays a central role for regulation of many cellular processes including glucose homeostasis, lipid metabolism, carbohydrate metabolism, and protein synthesis in various insulin-responsive tissues such as the skeletal muscle, liver, adipose tissue, brain, and pancreas, in the body. The defect of this signaling pathway causes abnormalities in both glucose and lipid homeostasis and ultimately leads to the development of hyperglycemia and hyperlipidemia in both obese and type 2 diabetic patients. The Akt kinase, also known as protein kinase B (PKB), is serine/threonine kinase, mainly present in three isoforms, Akt1, Akt2, and Akt3, in humans. Akt2 is mainly expressed in the insulin-responsive tissues, brown fat, skeletal muscle, and liver, while Akt1 and Akt3 are ubiquitously expressed in different tissues. About 90% of insulin-stimulated glucose utilization occurs in skeletal muscle through PI3K/Akt signaling pathway by promoting GLUT4 proteins transport from inner cell to cell surface, glycogen synthesis, and protein synthesis (Abeyrathna and Su 2015; Ueki et al. 1998).

In skeletal muscle and adipose tissue, insulin promotes the activation of its receptor, IR by phosphorylation at tyrosine residues, and phosphorylated IR increases the expression and phosphorylation of insulin receptor substrate proteins, IRS1 and IRS2, which in turn activate phosphatidylinositol-3-kinase (PI3K) by its phosphorylation. The activated PI3K stimulates the phosphorylation of intracellular Akt via successive formation of phosphatidylinositol-3,4,5-triphosphate (PIP3) and phosphoinositide-dependent kinase 1 (PDK1). The activated Akt induces phosphorylation of its substrate AS160 protein at Thr and Ser sites for expression and translocation of glucose transporter protein GLUT4 from intracellular storage vesicle to the cell surface for plasma glucose uptake in an exocytosis process stimulated by ATP signal and participation of Ras-related protein Rab 8A (Osorio-Fuentealba et al. 2013). The expression of GagPKB, an active form of PKB (Akt), increases

Table 4.2 List of some natural products (extracts/active components isolated from various natural sources) having reported antidiabetic effects and their major molecular targets and actions

(family, species)	Active plant part and fraction, active phytochemical (s)	Model	Major molecular targets and actions	References
A. Plants				
1. Achariaceae				
Hydnocarpus laurifolia	Seeds, ethyl acetate ext.	STZ-diabetic rats	Serum glucose and lipid profile↓	Sailaja Rao and Krishna Mohan (2014)
2. Acoraceae				
Acorus calamus	Rhizomes, methanol ext., ethyl acetate fr	STZ-diabetic rats, obese diabetic mice, L6 cells, enzyme inhibition assay	Plasma glucose and lipid profile↓, insulin secretion and glycogen synthesis↑, glucose uptake in L6 cells↑, plasma adiponectin, GLP-1 expression, insulin secretion, insulin action in diabetic mice↑, α-glucosidase activity↓	Prisilla et al. (2012), Si et al. (2010), Liu et al. (2015b)
3. Actinidiaceae				
Actinidia deliciosa	Fruits, methanol ext.	Alloxan-diabetic rats	Plasma glucose, TG, TC, GOT, GPT↓, insulin secretion, plasma HDL-C↑	Soren et al. (2016)
4. Aizoaceae				
Zaleya decandra	Roots, ethanol ext.	Alloxan-diabetic rats	Plasma glucose, TG, TC, urea, creatinine↓, pancreatic and liver function↑	Meenakshi et al. (2010)
5. Amaranthaceae				
Amaranthus paniculatus	Leaves, ethanol ext.	Alloxan-diabetic rats	Plasma glucose, TG, TC, CRP, GPT, GOT↓, pancreatic islet mass↑	Nawale et al. (2017)

(continued)

Table 4.2 (continued)

(family, species)	Active plant part and fraction, active phytochemical (s)	Model	Major molecular targets and actions	References
A. spinosus, *A. viridis*	Leaves, methanol ext.	STZ-diabetic rats	Plasma glucose, TG, TC, LDL-C↓, body weight gain, plasma HDL-C, pancreatic β-cell mass↑	Krishnamurthy et al. (2011), Girija et al. (2011)
6. Amaryllidaceae				
Allium sativum	Bulb, ethanol ext.	STZ-diabetic rats	Plasma glucose, TG, TC, urea, creatinine, AST, ALT↓, insulin secretion, lipid metabolism↑	Eidi et al. (2006)
7. Anacardiaceae				
Anacardium occidentale	Leaves, ethanol ext.	STZ-diabetic rats	Plasma glucose, TG, TC, LDL-C↓, liver and kidney function↑	Jaiswal et al. (2017)
Mangifera indica (mango)	Leaves, water ext., mangiferin **336a**	STZ-diabetic rats	Plasma glucose, TC, TG, LDL-C, AI, MDA↓, Plasma HDL-C, insulin secretion, insulin action↑	Villas Boas et al. (2020), Muruganandan et al. (2005)
Pistacia lentiscus	Leaves and fruits, ethanol ext., flavonoids and tannins	STZ-diabetic rats, enzyme inhibition assay	Plasma postprandial glucose, AST, ALT, ALP, bilirubin↓, liver and kidney function↑, α-amylase activity↓	Mehenni et al. (2016)
Rhus coriaria	Fruits, water ext.	STZ-diabetic rats, enzyme inhibition assay	Plasma glucose, HbA1c, TG, TC, LDL-C↓, plasma HDL-C, liver and kidney function↑, α-glucosidase activity↓	Dogan and Celik (2016)
R. mysorensis	Leaves and rhizomes, aqueous ethanol ext., flavonoids	Enzyme inhibition assay, STZ-diabetic rats	α-Amylase, α-glucosidase activity↓, plasma glucose↓	Rani et al. (2017)

Spondias tuberosa	Inner stem-bark, aqueous ethanol ext	STZ-diabetic rats	Plasma glucose, TC, TG, VLDL↓, insulin action, liver function, antioxidant activity↑	Barbosa et al. (2018)
8. Apiaceae				
Angelica dahurica	Roots, methanol ext., n-hexane fr, phellopterin (**337**)	GLUTag cells, INS-1 cells, diabetic db/db mice	Insulin secretion in INS-1 cells↑, GLP-1 secretion in GLUTag cells↑, plasma glucose↓, GPR119 expression in pancreatic islet and GLUTag cells↑	Park et al. (2016)
A. sinensis	Roots, water ext., polysaccharide	STZ-diabetic rats	Plasma glucose, TG, TC, TNFα, IL-6↓, Insulin action, liver and muscle glycogen content↑	Wang et al. (2015a)
Centella asiatica	Leaves, 70% ethanol ext.	Obese diabetic rats	Plasma glucose, TG, TC↓, pancreatic insulin secretion↑	Maulidiani et al. (2016)
Ferula asafoetida	Oleo-gum, ethanol ext., ferulic acid **72**	STZ-diabetic rats	Serum FG, TC, LDL-C, GOT, GPT, creatinine, urea↓, serum HDL-C, pancreatic insulin secretion↑	Latifi et al. (2019)
Pimpinella anisum	Leaves, 80% methanol ext.	Enzyme inhibition assay, diabetic patients	α-Amylase, α-glucosidase, pancreatic lipase activity↓, plasma glucose, LDL-C, VLDL-C, MDA, LPO↓, plasma HDL-C↑	Shobha and Andallu (2018)
Pimpinella brachycarpa	Leaves, 70% ethanol ext.	HF-HS-fed diabetic mice, enzyme inhibition assay	Plasma glucose, insulin, HOMA-IR, TG, TC↓, plasma adiponectin, liver SOD, CAT, GP_X↑, activity of α-glucosidase↓	Lee et al. (2013)

(continued)

Table 4.2 (continued)

(family, species)	Active plant part and fraction, active phytochemical (s)	Model	Major molecular targets and actions	References
9. Apocynaceae				
Acanthus montanus	Leaves, methanol ext	Enzyme inhibition assay	α-Amylase and α-glucosidase activity↓	Ogundajo et al. (2016)
Adhatoda vasica	Leaves and roots, ethanol ext., vasicine (**338**), vasicinol (**339**)	Enzyme inhibition assay	α-Amylase, α-glucosidase activity↓	Gao et al. (2008)
Andrographis paniculata	Whole plant, 90% ethanol ext., andrographolide (**335**)	L6 myotubes, HF-Fruc-fed diabetic rats	GLUT4 expression in L6 myotubes↑, plasma glucose, TG, TC↓, glucose uptake in muscle and adipose tissue↑	Nugroho et al. (2012)
Barleria prionitis	Leaves and roots, ethanol ext.	Alloxan-diabetic rats	Plasma glucose↓, pancreatic insulin secretion, glycogen synthesis, glucose uptake in liver↑	Dheer and Bhatnagar (2010)
Catharanthus roseus	Leaves, powder or ethanol ext.	STZ-diabetic rats	Glucose metabolism↑, plasma glucose, TC, TG, LDL-C, VLDL-C↓, pancreatic insulin secretion, muscle and liver glycogen content, expression of GLUT4, GLUT2, GS, GCK, GPDH↑	Singh et al. (2001), Rasineni et al. (2010), Al-Shaqha et al. (2015)
Gymnema sylvestre	Leaves, acetone ext., dihydroxy-gymnemic triacetate (**340**)	STZ-diabetic rats	Serum glucose, HbA1c, TC, TG, LDL-C, AST↓, serum HDL-C, insulin, muscle and liver glycogen content↑	Daisy et al. (2009)
Holarrhena antidysenterica	Seeds, water ext.	STZ-diabetic rats	Plasma glucose, TG, TC, LDL-C, VLDL-C, plasma, liver and kidney GOT, GPT↓, plasma HDL-C, liver and muscle glycogen content, GCK, GPDH↑	Ali et al. (2011)

10. Asteraceae				
Artemisia amygdalina	Whole plant, aqueous-ethanol	STZ-diabetic rats	Plasma glucose, TC, TG, LDL-C, creatinine, hepatic GOT, GPT, food intake↓, pancreatic β-cell mass↑	Ghazanfar et al. (2014)
A. sphaerocephala	Seeds, water ext.	STZ-diabetic rats	Plasma FG, HbA1c, TC, TG↓, Plasma HDL-C, hepatic GCK expression, glycogen content↑, hepatic fat content, insulin resistance↓	Xing et al. (2009)
Cichorium intybus	Whole plant, 80% ethanol ext.	STZ-diabetic rats	Serum glucose, TG, TC↓, hepatic G6Pase expression↓, pancreatic insulin secretion↑	Pushparaj et al. (2007)
Elephantopus scaber	Roots, water ext.	Alloxan-diabetic rats	Serum glucose, HbA1c, TG, TC, creatinine, urea↓, pancreatic β-cell mass and function, liver glycogen content↑	Daisy et al. (2007)
Stevia rebaudiana	Leaves, ethanol ext., polyphenol-rich fr	STZ-diabetic rats	Serum glucose, ALT, AST, MDA↓, Hepatic insulin action, GSH, SOD, CAT, kidney GPDH↑, urine volume↓	Shivanna et al. (2013)
Wedelia calendulacea	Whole plant, methanol ext., wedelolactone **341**	STZ-diabetic rats, enzyme inhibition assay	Serum glucose, TG, Tc, LDL-C, VLDL-C, CRP, TNFα, IL-6↓, α-amylase, α-glucosidase, DPP-4 activity↓, pancreatic β-cell regeneration and function, serum HDL-C↑	Kumar et al. (2018)

(continued)

Table 4.2 (continued)

(family, species)	Active plant part and fraction, active phytochemical (s)	Model	Major molecular targets and actions	References
11. Begoniaceae				
Begonia malabarica	Stems, methanol ext.	STZ-diabetic rats	Serum glucose, urea, creatinine, GPT↓, hepatic glycogen content↑, kidney weight↓	Pandikumar et al. (2009)
12. Caprifoliaceae				
Lonicera japonica	Stems, 70% ethanol ext., loganin (**342**), sweroside (**343**)	HFD-fed STZ-diabetic rats	Serum FG, HOMA-IR↓, muscle PPARγ expression, hepatic IRS-1 expression, pancreatic β-cell mass and function↑	Han et al. (2015a)
13. Cistaceae				
Cistus laurifolius	Leaves, ethanol ext., flavonoids	STZ-diabetic rats, enzyme inhibition assay	Serum glucose↓, α-amylase, α-glucosidase activity↓	Orhan et al. (2013)
C. salviifolius	Aerial parts, water ext.	Enzyme inhibition assay, STZ-NA-diabetic rats	α-Amylase, α-glucosidase activity↓, plasma glucose, TG, creatinine↓, pancreatic islet mass↑	Sayah et al. (2017, 2020)
14. Combretaceae				
Anogeissus leiocarpus	Leaves, ethanol ext.	Alloxan-diabetic rats	Serum FG, TC, TG, LDL-C↓, hepatic glycogen content↑	Onoja et al. (2018)
15. Cornaceae				
Alangium lamarckii	Leaves, ethanol ext.	STZ plus NA-diabetic rats	Plasma glucose, TG, TC, LDL-C, TRABS↓, plasma HDL-C, hepatic glycogen content, SOD, CAT activity↑	Kumar et al. (2011)

16. Cucurbitaceae				
Citrullus lanatus	Fruit-juice, flavonoids	Alloxan-diabetic rats, SD-diabetic rats, enzyme inhibition assay	Plasma FG and PPG, TC, TG, LDL-C, VLDL-C, MDA, TNFα, IL-6, ALP↓, plasma HDL-C, hepatic glycogen content, expression of hepatic GK, GLUT2, GLUT4, GSH, SOD, CAT↑, expression of hepatic G6Pase, activity of α-amylase and α-glucosidase↓	Ajiboye et al. (2020), El-Razek and Sadeck (2011)
Cucumis sativus	Fruits, ethanol ext.	STZ-diabetic rats	Plasma FG, PPG, TG, TC, LDL-C, VLDL-C↓, Plasma HDL-C, pancreatic β-cell function↑	Karthiyayini et al. (2009)
Cucurbita ficifolia	Fruits, water ext.	STZ-diabetic rats	Plasma FG, MDA, food intake↓, hepatic, kidney and pancreas GSH, GP_X, GR, GSH/GSSG ratio↑	Diaz-Flores et al. (2012)
Cucurbita pepo (pumpkin)	Fruits, powder, polysaccharides	Alloxan-diabetic rats	Serum FG, TG, TC, LDL-C, CRP↓, Serum insulin, HDL-C, hepatic glycogen, pancreatic islets mass↑	Sedigheh et al. (2011), Wang et al. (2017c)
Luffa acutangula	Fresh fruits, aqueous-methanol ext., saponins, flavonoids	STZ plus NA-diabetic rats, enzyme inhibition assay	Serum FG, HbA1c, insulin, TC, TG, LDL-C, VLDL-C, AST, ALT↓, serum HDL-C, hepatic glycogen content↑, α-glucosidase activity↓	Pimple et al. (2011)

(continued)

Table 4.2 (continued)

(family, species)	Active plant part and fraction, active phytochemical (s)	Model	Major molecular targets and actions	References
Momordica charantia	Green fruits, ethanol ext., ethyl acetate fr, 9c,11t,13t-conjugated linolenic acid (**343a**), seed, chloroform ext., polypeptide k	Alloxan-diabetic rats, 4H11EC3 cells, enzyme inhibition assay	Plasma glucose, HbA1c, TC, TG, LDL-C, pancreatic necrosis↓, Plasma insulin, HDL-C, total proteins, liver glycogen content↑, Expression of PPARα, ACOX in H411EC3 cells↑, Activity of α-amylase and α-glucosidase↓	Fernandes et al. (2007), Chuang et al. (2006), Ahmad et al. (2012)
Trichosanthes cucumerina	Whole plant, water ext.	STZ-diabetic rats	Serum FG↓, Liver and muscle glycogen content↑	Kirana and Srinivasan (2008)
17. Dilleniaceae				
Dillenia indica	Leaves, ethanol ext., chromane derivative (3,5,7-trihydroxy-2 (4-hydroxybenzyl)-chroman-4-one) (**344**)	STZ-diabetic rats	Serum FG, TC, TG↓, Antioxidant enzyme activity in liver↑	Kaur et al. (2016)
18. Dioscoreaceae				
Dioscorea alata	Tubers, ethanol ext., flavonoids, anthocyanins	Alloxan-diabetic rats	Serum FG, TC, TG, LDL-C, VLDL-C, creatinine↓, serum proteins, HDL-C↑	Maithili et al. (2011)
D. batatas	Tubers, 50% ethanol ext., allantoin (**345**)	STZ-diabetic rats	Plasma FG, TC, TG, LDL-C, creatinine, CK, uric acid, MDA, LDH, ALT, AST↓, plasma insulin, C-peptide, proteins, GSH, SOD, tGSH↑, pancreatic β-cell mass and function↑	Go et al. (2015)

19. Ericaceae				
Vaccinium myrtillus (bilberry)	Fruits, powder, anthocyanins	Alloxan-diabetic rats	Serum glucose, TC, TG, LDL-C, VLDL-C↓, serum HDL-C, insulin, pancreatic islet size↑	Asgary et al. (2016)
V. vitis-idaea (lingonberry)	Berries, ethanol ext.	HFD-fed obese diabetic mice	Lipid metabolism and insulin sensitivity↑, serum glucose, insulin, TC, LDL-C, muscle acetyl p53↓, muscle and liver AMPK, Akt activation, muscle GLUT4, SIRT1 expression↑	Eid et al. (2014)
20. Ebenaceae				
Diospyros melanoxylon	Leaves, pet ether ext.	STZ-diabetic rats	Serum FG, TC, TG, food intake↓, serum HDL-C↑, lipogenesis↓	Rathore et al. (2014)
21. Elaeocarpaceae				
Aristotelia chilensis (maquiberry)	Fruits, 70% methanol ext., anthocyanin-rich fr, delphinidin glucoside	HFD plus STZ-obese diabetic mice, L6 cells, H411E cells	Plasma FG, insulin↓, glucose uptake in muscle and L6 cells↑, expression of G6Pase in liver and H411E cells↓	Rojo et al. (2012)
22. Euphorbiaceae				
Croton lobatus	Leaves, methanol ext.	Alloxan-diabetic rats	Plasma glucose, TC, TG, LDL-C, VLDL-C, MDA, NO↓, hepatic and plasma SOD, GSH activity↑, pancreatic islet cells integrity↑	Fasola et al. (2016)
23. Fabaceae				
Albizia lebbeck	Barks, methanol ext.	STZ plus NA-diabetic rats	Plasma FG, TC, TG, LDL-C, VLDL-C, urea, creatinine↓, plasma HDL-C↑	Patel et al. (2015)

(continued)

Table 4.2 (continued)

(family, species)	Active plant part and fraction, active phytochemical (s)	Model	Major molecular targets and actions	References
Astragalus membranaceus	Roots, hot water ext., polysaccharides	HFD-fed obese diabetic mice	Hepatic fat mass and TG content, plasma FG, insulin, HOMA-IR↓, Expression of hepatic PTP1B and XBP1↓	Mao et al. (2009)
Caesalpinia bonducella syn, *C. crista*, *C. bonduc*	Seeds, aqueous and ethanol ext.	STZ-diabetic rats	Plasma FG, TC, TG↓, pancreatic insulin secretion, liver glycogen content↑	Chakrabarti et al. (2005)
C. bonduc	Leaves, ethanol ext., polyphenolic fr rich in gallic-, caffeic-, p-coumaric-, and chlorogenic acids	Alloxan-diabetic rats	Plasma glucose, HbA1c, amylin, leptin, PYY↓, expression of hepatic G6Pase, FBPase, pancreatic p-MAPK-8↓, insulin secretion and sensitivity↑, hepatic glycogen content, expression of hepatic HK, GPDH, IRS-1, GLUT4, pancreatic Ins-1, Pdx-1, hepatic and pancreatic SOD, CAT, GSH, GP_X↑	Iftikhar et al. (2020)
Desmodium gangeticum	Aerial parts, 50% aqueous-ethanol ext.	STZ-diabetic rats, MIN6 cells	Plasma glucose, TG, TC↓, Plasma HDL-C↑, insulin secretion in MIN6 cells↑	Govindarajan et al. 2007)
Medicago sativa (alfalfa)	Aerial parts, water ext.	Alloxan-diabetic rats	Plasma glucose, TC, TG, LDL-C, VLDL-C, AST↓, liver and pancreatic injury↓, Plasma HDL-C↑	Farsani et al. (2016)
Mimosa pudica	Leaves, methanol ext.	STZ-diabetic rats	Plasma glucose, TC, TG, LDL-C, VLDL-C, ALT, urea, creatinine↓, plasma HDL-C↑, pancreas, liver and kidney injury↓	Parasuraman et al. (2019)

Pterocarpus marsupium	Bark, ethanol ext., butanol fr	Alloxan-diabetic rats	Plasma glucose, TC, TG, ALP, GOT, GPT↓, plasma proteins↑	Dhanabal et al. (2006)
Trigonella foenum-graecum (methi)	Seeds, aqueous-ethanol ext., 4-hydroxyisoleucine (**345a**), trigonelline (**345b**), diosgenin (**345c**), galactomannan (**345d**)	HFD-fed diabetic C57BL/6J mice, STZ-diabetic rats	Serum glucose, insulin, TG, HOMA-IR↓, serum HDL-C, liver CAT, hepatic, pancreatic and renal functions↑	Hamza et al. (2012), Baset et al. (2020)
24. Gentianaceae				
Enicostemma littorale	Whole plant, methanol ext.	Alloxan-diabetic rats	Serum glucose, LPO, expression of hepatic G6Pase↓, serum insulin, GSH↑	Maroo et al. (2003)
25. Hypoxidaceae				
Curculigo latifolia	Fruits and roots, water ext	HFD plus STZ-obese diabetic rats	Insulin-stimulated glucose and lipid metabolism↑, plasma glucose, TC, TG, LDL-C, ALT, urea, creatinine↓, plasma HDL-C, insulin, adiponectin, expression of IRS1, GLUT4, IGF1, PPARα, PPARγ, adipoR, LPL in muscle and AT↑	Ishak et al. (2013)
26. Iridaceae				
Crocus sativus	Stigma, ethanol ext., crocin (**346**), safranal (**347**)	Alloxan-diabetic rats, type 2 diabetic patients, STZ-diabetic rats	Serum FG, TG, TC, LDL-C in both diabetic rats and diabetic patients↓, serum insulin, HDL-C, GSH, SOD, CAT, pancreatic β-cell mass and function in diabetic rats↑	Mohajeri et al. (2009), Samarghandian et al. (2017), Aleali et al. (2019)
27. Lamiaceae				
Callicarpa nudiflora	Leaves, 80% ethanol ext., iridoids, phenyl propanoids	STZ plus HFD-type 2 diabetic rats	Insulin signaling and AMPK activation↑, plasma FG, TC, TG, LDL-C, HOMA-IR↓, Plasma HDL-C, expression of p-AMPK, p-ACC, GLUT4 in muscle, IRS-1 in liver↑	Ma et al. (2014)

(continued)

Table 4.2 (continued)

(family, species)	Active plant part and fraction, active phytochemical (s)	Model	Major molecular targets and actions	References
Marrubium vulgare	Aerial parts, aqueous and methanol ext., verbascoside **348**, luteolin-7-*O*-glucoside **349**	STZ-diabetic rats	Glucose utilization and insulin secretion↑, serum FG, TC, TG, LDL-C, MDA↓, serum insulin, HDL-C, muscle and hepatic glycogen content, expression of hepatic antioxidant enzymes GSH, GP_X, GR, GST↑	Elberry et al. (2015), Boudjelal et al. (2012)
Ocimum sanctum	Leaves, hexane ext., fixed oil, α-linolenic acid (**350**)	STZ-diabetic rats	Renal oxidative stress↓, serum glucose, TC, TG, LDL-C, creatinine, BUN, TBARS, kidney weight↓, serum insulin, HDL-C, activity of CAT, SOD, GP_X in renal tissue↑	Suanarunsawat et al. (2016)
Origanum majoranum	Leaves, hot water ext.	STZ plus diet-type 2 diabetic rats	Glucose and lipid metabolism↑, serum glucose, TC, TG, LDL-C, VLDL-C, insulin, leptin, hepatic and kidney lipid mass↓, serum HDL-C, expression of adiponectin, PPARγ, LPL in AT, GLUT2 in liver↑	Soliman et al. (2016)
Otostegia persica	Aerial parts, hot water ext.	STZ-diabetic rats	Serum FG, TG, HOMA-IR↓, serum HDL-C, pancreatic mass and insulin secretion↑	Akbarzadeh et al. (2012)
Phlomis persica	Aerial parts, 80% methanol ext., iridoid glycosides	STZ-diabetic rats	Hepatic oxidative stress↓, serum FG, hepatic TBARS↓, serum insulin, hepatic SOD, CAT, GP_X↑	Sarkhail et al. (2010)

Salvia officinalis	Leaves, ethanol and methanol ext.	STZ-diabetic rats	Serum glucose, TG, TC, urea, uric acid, creatinine, AST, ALT↓, Serum insulin↑	Eidi and Eidi (2009), Eidi et al. (2005)
28. Lythraceae				
Punica granatum (pomegranate)	Fruits, aqueous-methanol ext., ethyl acetate fr, or aqueous ext., gallic acid, ellagic acid, valoneic acid dilactone (**350a**)	Alloxan-diabetic rats, enzyme inhibition assay	Glucose and lipid metabolism, insulin secretion and action↑, serum FG, PPG, TG, FFAs↓, serum insulin, muscle and liver glycogen content, expression of IRS1, Akt, GLUT4, GLUT2, p-Akt↑, pancreatic β-cell function and regeneration↑, activity of α-amylase and PTP1B↓	Jain et al. (2012), Gharib and Kouhsari (2019)
29. Malvaceae				
Grewia asiatica	Fruits, ethanol ext.	STZ-diabetic rats	Insulin signaling↑, serum glucose, MDA, TNFα, IL-1β↓, liver glycogen content, hepatic SOD, GSH activity, pancreatic insulin secretion↑	Khattab et al. (2015)
Helicteres isora	Roots, aqueous-ethanol ext., butanol fr	Alloxan-diabetic rats	Serum glucose, TC, TG, urea↓, pancreas, liver, and kidney function↑	Venkatesh et al. (2010)
Hibiscus rosa-sinensis	Leaves, ethanol ext., chloroform fr	Non-obese diabetic mice	Serum glucose, HbA1c, TC, LDL-C, VLDL-C, urea↓, serum HDL-C, insulin↑	Moqbel et al. (2011)

(continued)

Table 4.2 (continued)

(family, species)	Active plant part and fraction, active phytochemical (s)	Model	Major molecular targets and actions	References
30. Menispermaceae				
Coscinium fenestratum	Stem, ethanol ext., berberine (**48**)	STZ plus NA-diabetic rats	Glucose utilization↑, glucose production↓, serum glucose, HbA1c, TG, TC, MDA, ALT, creatinine↓, Serum insulin, HDL-C, hepatic glycogen content, expression of hepatic HK, GPDH, CAT, SOD, GSH, GP_X↑, expression of G6Pase in liver and kidney↓	Shirwaikar et al. (2005), Punitha et al. (2005)
Tinospora cordifolia	Roots and stems, 70% ethanol, aqueous methanol ext., palmatine (**130**)	Alloxan-diabetic rats and STZ-diabetic rats, L6 myotubes	Carbohydrate metabolism and antioxidant status↑, serum glucose, HbA1c, ALP, LDH, MDA↓, serum insulin, C-peptide, expression of hepatic HK, PPARα, SOD, GSH, GP_X, hepatic and muscle glycogen content, pancreatic insulin secretion↑, expression of hepatic and kidney G6Pase, FBPase↓, expression of GLUT4 in L6 cells↑	Stanely et al. (2000), Rajalakshmi et al. (2009), Sangeetha et al. (2011, 2013)
31. Moraceae				
Ficus carica	Leaves, ethyl acetate ext., ficusin (**351**)	STZ-diabetic rats	Glucose utilization↑, serum FG, TC, TG↓, hepatic glycogen content, HK expression, pancreatic insulin secretion and β-cell regeneration↑, expression of hepatic G6Pase, FBPase↓	Irudayaraj et al. (2017)

F. lutea	Leaves, acetone ext., ethyl acetate fr	In vitro enzyme inhibition assay, cell line culture, high-calorie diet fed obese mice	Activity of α-amylase and α-glucosidase↓, insulin secretion in RIN-m5F cells↑, glucose uptake in C2C12 myotubes and H411E liver cells↑, plasma PPG↓	Olaokun et al. (2016)
F. racemosa	Stem-bark, ethanol ext., flavonoids fr rich in kaempferol (**66**), quercetin (**23**), baicalein (**352**)	Alloxan-diabetic rats and STZ-diabetic rats	Glucose metabolism and antioxidant status in liver and pancreas↑, serum FG, PLs, TC, TG, FFAs, LDL-C, VLDL-C, MDA, liver TG and TC content↓, hepatic glycogen content, body weight gain, activity of GSH, CAT, SOD in pancreas and liver↑	Sophia and Manoharan (2007), Keshari et al. (2016)
32. Musaceae				
Musa paradisiaca	Leaves and fruit peel, 70% ethanol ext.	STZ plus NA-diabetic rats	Insulin signaling↑, serum glucose, HOMA-IR, FFAs, TNFα, IL-6↓, serum insulin, C-proteins, QUICKI↑, expression of adiponectin, PPARγ, GLUT4, IRβ in AT↑	Aziz et al. (2020)
33. Myrtaceae				
Eugenia jambolana (Indian blackberry)	Fruit-pulp and seeds, ethanol, aqueous-methanol, ethyl acetate fr, gallic acid, unidentified sterol	Alloxan-diabetic rabbits, STZ-diabetic rats	Carbohydrate metabolism and pancreatic insulin secretion↑, serum FG, TC, TG, LDL-C, GOT, GPT↓, serum HDL-C, activity of SOD, CAT, GSH, GP_X in liver↑, glycogen content and expression of HK, GPDH in liver and muscle, pancreatic β-cell mass↑, expression of G6Pase, FBPase in liver↓	Mahajan et al. (2018), Chatterjee et al. (2012), Sharma et al. (2006, 2011)

(continued)

Table 4.2 (continued)

(family, species)	Active plant part and fraction, active phytochemical (s)	Model	Major molecular targets and actions	References
Eucalyptus tereticornis	Leaves, ethyl acetate ext., triterpenes-rich fr	STZ plus diet-diabetic rats, C2C12 cells	Carbohydrate metabolism and insulin action↑, serum FG, hepatic MCP-1, TNFα, IL-6↓, hepatic G6Pase expression↓ Glucose uptake in muscle and C2C12 cells↑	Guillen et al. (2015)
Myrtus communis	Fruits, 70% ethanol ext.	STZ-type 1 diabetic rats	Diabetic renoprotective effect↑, Serum glucose, TC, TG, BUN, MDA↓, urinary proteins excretion, urine volume↓	Talebianpoor et al. (2019)
Psidium guajava	Leaves, water ext.	STZ-diabetic rats	AMPK activation and insulin signaling↑, serum glucose, TG, TC, PLs, FFAs, LDL-C, AST, ALT↓, serum HDL-C, insulin, hepatic glycogen content, expression of IRS-1, p-Akt, p-AMPK, p-ACC, GLUT2↑, expression of G6Pase, FBPase in liver↓	Vinayagam et al. (2018)
34. Oleaceae				
Forsythia suspense	Fruits, methanol ext., ethyl acetate fr	STZ-diabetic mice, enzyme inhibition assay	Hepatic glucose metabolism and pancreatic insulin secretion↑, serum glucose, TG, TC, ACP, ALP, AST, creatinine↓, activity of α-amylase, HMGCR↓, expression of SOD, CAT, GP_X in liver and pancreas, PDX-1, INS-1, INS-2 in pancreas, GCK in liver↑, expression of G6Pase, PEPCK in liver↓	Zhang et al. (2016)

Olea europaea	Leaves, aqueous ethanol or hot water ext., oleuropein (**353**), hydroxytyrosol (**354**)	STZ-diabetic rats	Glucose metabolism and insulin signaling in liver↑, serum glucose, TC, TG, LDL-C, urea, uric acid, creatinine, CK, MDA, AST, ALT↓, serum HDL-C, insulin, hepatic glycogen content, SOD, CAT, GSH, IRS1, IRα↑	Eidi et al. (2009), Jemai et al. (2009), Al-Attar and Alsalmi (2019)
35. Orchidaceae				
Dendrobium loddigesii	Stems, aqueous-acetone ext., polyphenols-rich fr, moscatilin (**355**), gigantol (**356**)	Diabetic db/db mice	Gut microbiota dysbiosis↓, plasma glucose, LDL-C, Hepatic fat mass, TNFα↓, activity of SOD, CAT, GSH in liver, relative abundance of gut *Prevotella* and *Akkermansia*↑, relative abundance of gut *Escherichia coli* and *Rikenella* sp↓	Li et al. (2018a)
D. officinale	Roots, water ext., polysaccharides fr	STZ-diabetic rats, HepG2 cells	Insulin signaling and glucose utilization↑, serum FG, TG, TC, hepatic TG and fat content, PPARγ expression↓, activity of hepatic PEPCK, PTP1B, JNK↓, hepatic and muscle glycogen content, expression of HK, p-Akt, GLUT4↑, expression of p-IRβ, p-Akt in HepG2 cells↑	Wang et al. (2018)

(continued)

Table 4.2 (continued)

(family, species)	Active plant part and fraction, active phytochemical (s)	Model	Major molecular targets and actions	References
36. Oxalidaceae				
Averrhoa bilimbi	Fruits, ethyl acetate fr, quercetin	STZ-diabetic rats	Glucose metabolism↑, plasma FG, HbA1c, MDA↓, plasma insulin, hepatic antioxidant activity via CAT, GSH, GSR, GP_X↑, expression of hepatic glycolytic genes HK, PK↑, expression of hepatic gluconeogenic genes G6Pase, FBPase↓	Kurup and Mini (2017a, 2017b)
A. carambola	Fruits-juice	STZ-diabetic rats	Diabetic kidney injury↓, serum FG, TG, TC, BUN, creatinine, cAMP, MDA↓, serum insulin, SOD, sorbitol dehydrogenase↑, expression of TGFβ1, CTGF in kidney↓, pancreatic necrosis↓	Pham et al. (2017)
Biophytum sensitivum	Leaves, water ext., cupressuflavone (**357**), amentoflavone (**358**), isoorientin **302**	STZ plus NA-diabetic rats	Glucose metabolism↑, plasma glucose, HbA1c↓, plasma insulin, pancreatic insulin release, hepatic glycogen content, HK expression↑, expression of hepatic G6Pase, FBPase↓	Ananda et al. (2012)

37. Pandanaceae				
Pandanus tectorius	Fruits, ethanol ext., butanol fr rich in caffeoyl quinic acids	Diabetic db/db mice	Adiponectin-dependent AMPK activation and lipid and glucose metabolism ↑, serum FG, TG, TC, FFAs, insulin, HOMA-IR, LDL-C, leptin, TNFα, IL-6, MCP-1↓, serum adiponectin, expression of muscle GLUT4, p-AMPK, p-AS160, hepatic glycogen content, expression of HK, PPARα, CPT-1↑, hepatic fat content, expression of hepatic G6Pase, PEPCK, C/EBPα, FAS, ACC1↓	Wu et al. (2014a)
38. Phyllanthaceae				
Phyllanthus amarus	Whole plant and leaves, water ext.	STZ-diabetic rats and High-sucrose-fed diabetic rats	Oxidative stress↓, plasma FG, TG, TC, LDL-C↓, plasma HDL-C, expression of kidney CAT, SOD, GST, GR, GP_X, GSH↑	Karuna et al. (2011), Adeneye (2012)
P. niruri	Aerial parts, methanol ext., phyllanthin (**359**)	Alloxan-diabetic rats, HFD-fed obese mice, enzyme inhibition assay	Serum FG, PPG, HbA1c↓, hepatic glycogen content, expression of IRS-1/2, GLUT4, ACOX1, HSL, perilipin in liver and AT↑, expression of inflammatory genes TNFα, IL-6, NFκB, F4/80, lipogenesis-related genes PPARγ, C/EBPα, FAS, ACC in liver and AT↓, activity of α-amylase and α-glucosidase↓	Okoli et al. (2011), Jagtap et al. (2016)

(continued)

Table 4.2 (continued)

(family, species)	Active plant part and fraction, active phytochemical (s)	Model	Major molecular targets and actions	References
39. Plantaginaceae				
Plantago asiatica	Seeds, water ext., geniposidic acid (**360**), acteoside (**118**), isoacteoside (**361**), plantagoguanidinic acid (**362**), polysaccharides	HFD-fed obese mice, STZ plus HFD-fed diabetic rats	PPARs-dependent glucose and lipid metabolism↑, improvement of gut dysbiosis↑, serum FG, TG, TC, FFAs, MDA↓, serum HDL-C, antioxidant enzyme activity↑, hepatic fat mass and TG content, expression of aP2 in the liver↓, expression of PPARα, PPARγ, LPL, CD36, ACOX1 in liver, PGC-1α, GLUT4, Acacα in WAT, UCP1, UCP3, UCP2 in BAT of obese mice↑, relative abundance of SCFA-producing *Bacteroides vulgates*, *Lactobacillus fermentum*, *Prevotella loescheii* in gut of diabetic rats↑, rel. abundance of *Clostridium* sp., *Alistipes* sp. in gut↓	Yang et al. (2017a), Nie et al. (2019)

40. Ranunculaceae				
Nigella sativa	Seeds, ethanol ext., seed oil, thymoquinone (**363**)	STZ-diabetic rats, STZ plus HFD-fed diabetic rats, C2C12 cells, H411E cells	Glucose and lipid metabolism via insulin and AMPK activation↑, pancreatic insulin secretion↑, intestinal glucose absorption↓, plasma glucose, HOMA-IR, TG, TC, LDL-C, MDA, TNFα, NO↓, Plasma insulin, HDL-C↑, liver and muscle IRβ, PI3K, p-Akt, p-AMPK, muscle GLUT4↑, activity of SOD, CAT, GSH, GP_X in liver and kidney, SOD in pancreas↑, hepatic TIMP3↑, glucose uptake and Akt activation in C2C12 cells, H411E cells↑	Kaleem et al. (2006), Meddah et al. (2009), Abdelmeguid et al. (2010), Benhaddou-Andaloussi et al. (2011), Ali et al. (2008), Balbaa et al. (2016)
41. Rhamnaceae				
Ziziphus vulgaris syn, *Z. jujube*	Fruits, powder, kaempferol	STZ-diabetic rats, diabetic patients	Serum glucose, TC, TG, LDL-C, MDA, CRP↓, s erum insulin, HDL-C, antioxidant activity↑	Goli-malekadi et al. (2014), Yazdanpanah et al. (2017)
42. Rhizophoraceae				
Ceriops decandra	Leaves, ethanol ext.	Alloxan-diabetic rats	Glucose utilization↑, glucose production↓, plasma glucose, HbA1c↓, plasma insulin, liver glycogen content, expression of hepatic and renal HK↑, expression of hepatic and renal G6Pase, FBPase↓	Nabeel et al. (2010)

(continued)

Table 4.2 (continued)

(family, species)	Active plant part and fraction, active phytochemical (s)	Model	Major molecular targets and actions	References
Rhizophora mangle	Bark, acetone ext., catechins	STZ plus HFD-fed obese diabetic mice, enzyme inhibition assay	Serum FG, TC, LDL-C, insulin, leptin↓, hepatic TG content, expression of CD36, PPARγ, FAS in liver↓, activity of α-amylase, pancreatic lipase↓	Mesquita et al. (2018)
43. Rosaceae				
Amygdalus lycioides	Aerial parts, 50% ethanol ext., flavonoids	STZ-diabetic rats	Serum FG, TC, TG, LDL-C, ALP, creatinine↓, pancreatic β-cell mass and function↑	Moezi et al. (2018)
Eriobotrya japonica	Leaves and seeds, ethanol and hot water ext., flavonoids and triterpenoids including amygdalin (**364**), corosolic acid (**206**), euscaphic acid (**365**), cinchonain 1b (**366**), ursolic acid (**52**)	Alloxan-diabetic rats, HFD-fed obese mice, diabetic KK-Ay mice, INS-1 cells, enzyme inhibition assay	Insulin secretion, antioxidant activity, glucose and lipid metabolism↑, serum glucose, TG, TC↓, serum SOD, insulin↑, expression of leptin in WAT, SREBP-1c in liver↓, expression of PPARα, PPARγ in liver of obese mice↑, insulin secretion in pancreas and INS-1 cells↑, activity of 11β-HSD1↓	Tanaka et al. (2008), Chen et al. (2008), Qa'dan et al. (2009), Lu et al. (2009), Rollinger et al. (2010)
Prunus divaricata	Fruit-juice	STZ-diabetic rats	Serum FG, TC, TG, LDL-C↓, serum HDL-C↑	Minaiyan et al. (2014)
P. mume	Leaves, 70% ethanol ext., n-butanol fr, polyphenols including flavonoids	STZ plus HFD-fed diabetic rats, enzyme inhibition assay	Plasma glucose, TG↓, plasma adiponectin↑, activity of α-glucosidase↓, activity of PPARγ in AT↑	Lee et al. (2016)

44. Rubiaceae				
Paederia foetida	Leaves, methanol ext.	Alloxan-diabetic rats	Renal injury↓, plasma glucose, TG, TC, MDA, creatinine, BUN, bilirubin, AST, ALT, TNFα, IL-6↓, plasma SOD, CAT, GSH, proteins↑, expression of renal NFκBp-65↓	Borgohain et al. (2017)
45. Rutaceae				
Aegle marmelos	Fruits, water ext., eugenol (**366**), quercetin (**23**), rutin (**54**)	STZ-diabetic rats	Plasma FG, TC, TG, LDL-C, AGEs, HbA1c↓, plasma insulin, HDL-C, pancreatic mass and insulin secretion↑	Kamalakkannan and Prince (2005), Hafizur et al. (2017)
Murraya koenigii	Leaves, 70% ethanol ext., alkaloids	Enzyme inhibition assay, cell line culture	Activity of α-amylase and α-glucosidase↓, glucose uptake in L6 myotubes↑, lipid accumulation in 3T3-L1 cells↓	Parameswari et al. (2018)
Zanthoxylum aromatum	Bark, aqueous methanol ext.	STZ-diabetic rats	Serum glucose, TC, TG, LDL-C, VLDL-C, LPO↓, serum HDL-C, activity of CAT, SOD, GSH in the liver and kidney↑	Karki et al. (2014)
46. Sapotaceae				
Mimusops elengi	Leaves, ethanol ext.	STZ-diabetic rats	Serum glucose, HbA1c, TC, TG, LDL-C, PLs↓, serum insulin, HDL-C, TP, albumin, hepatic glycogen content, expression of HK, GPDH↑, expression of hepatic and renal G6Pase, FBPase↓	Jaffar et al. (2011)

(continued)

Table 4.2 (continued)

(family, species)	Active plant part and fraction, active phytochemical (s)	Model	Major molecular targets and actions	References
47. Solanaceae				
Lycium barbarum	Fruits, water ext., polysaccharides fr	STZ-diabetic rats	Serum glucose, insulin, leptin, AT fat mass↓, expression of melatonin and its receptor MT2 in AT↑, expression of pancreatic CLOCK, BMALI, islet growth↑	Zhao et al. (2016)
48. Urticaceae				
Urtica dioica	Leaves and aerial parts, water and 80% ethanol ext., cyclic peptide	Alloxan-diabetic rats, HFD-fed obese mice, cell line culture	Plasma FG, insulin, HOMA-IR↓, pancreatic insulin secretion, glucose uptake in muscle and C2C12 cells↑, muscle PP2A activity↓	Farzami et al. (2003), Domola et al. (2010), Obanda et al. (2016)
B. Seaweeds (Family, species)				
1. Ishigeaceae				
Ishige okamurae	50% Ethanol ext., fucoxanthin, diphlorethohydroxy-carmalol (**162**)	Diabetic db/db mice, enzyme inhibition assay	Carbohydrate metabolism↑, hepatic glucose production↓, plasma glucose, HbA1c↓, hepatic glycogen content, expression of GCK↑, expression of hepatic G6Pase, PEPCK↓, inhibited the activity of α-amylase and α-glucosidase by **162** with IC_{50} of 0.53 and 0.16 mM, respectively	Min et al. (2011), Heo et al. (2009)

2. Laminariaceae				
Laminaria japonica	Water ext., ethyl acetate fr, butyl-isobutyl-phthalate (**367**)	STZ-diabetic mice, enzyme inhibition assay	Plasma glucose↓, activity of α-glucosidase inhibited by **367** with IC_{50} of 38 μM	Bu et al. (2010)
3. Fucaceae				
Ascophyllum nodosum	Water ext., polysaccharide-rich fr, polyphenol-rich fr	STZ-diabetic mice	Plasma glucose, HbA1c, TC, TG↓, liver glycogen content, serum antioxidant activity↑, activity of α-glucosidase↓	Zhang et al. (2007)
4. Lessoniaceae				
Ecklonia cava	Water and methanol exts, dieckol-rich fr, dieckol **163**	Diabetic db/db mice, STZ-diabetic mice, enzyme inhibition assay	Plasma glucose, HbA1c, TG, TC, LDL-C, HOMA-IR↓, plasma insulin, HDL-C, hepatic glycogen content, expression of hepatic GCK, p-AMPK, p-Akt↑, plasma and hepatic SOD and CAT activity, pancreatic insulin secretion↑, expression of hepatic G6Pase, PEPCK↓, inhibited the activity of α-amylase and α-glucosidase by **163**	Lee et al. (2010a, 2012b), Kim and Kim (2012), Kang et al. (2010a)
5. Sargassaceae				
Sargassum patens	Ethanol ext., 2-(4-(3,5-dihydroxy-phenoxy)-3,5-dihydroxyphenoxy)-benzene-1,3,5-triol (**368**)	Enzyme inhibition assay	Inhibited the activity of human salivary and pancreatic α-amylase by 368 with IC_{50} of 3.2 μg/ml	Kawamura-Konishi et al. (2012)
S. ringgoldianum	80% methanol ext.	STZ-diabetic rats, enzyme inhibition assay	Plasma PPG↓, inhibited α-amylase and α-glucosidase activity with IC_{50} of 0.18 and 0.12 mg/ml, respectively	Lee and Han (2012)

(continued)

Table 4.2 (continued)

(family, species)	Active plant part and fraction, active phytochemical (s)	Model	Major molecular targets and actions	References
C. Macrofungi (mushrooms)				
1. Agaricaceae				
Agaricus bisporus	Mycelium powder or ethanol ext., lectin-like fiber rich in polysaccharides	STZ-diabetic rats and hypercholesterolemic rats	Glucose and lipid metabolism, insulin secretion↑, serum glucose, TG, AST, ALT, hepatic TG, TC in diabetic rats↓, serum HDL-C↑, Serum TC, TG, LDL-C in hypercholesterolemic rats↓	Jeong et al. (2010)
2. Cordycipitaceae				
Cordyceps militaris	Water ext. or acidic water ext., polysaccharides, cordycepin (**369**)	STZ-diabetic rats and mice, alloxan-diabetic rats	Glucose and lipid metabolism, antioxidant activity↑, plasma FG, TG, TC, BUN, creatinine, uric acid, urinary proteins excretion↓, plasma, pancreatic, renal and hepatic SOD, CAT, GP_X, hepatic glycogen content↑	Dong et al. 2014), Ma et al. (2015c), Zhao et al. (2018b)
3. Ganodermataceae				
Ganoderma atrum	Water ext., polysaccharide	HFD plus STZ-diabetic rats	Glucose and lipid metabolism↑, serum FG, insulin, TC, TG, LDL-C, FFAs↓, serum HDL-C, hepatic glycogen content, expression of hepatic PPARγ, GLUT4, PI3K, p-Akt, SCFAs, pancreatic Bcl-2, aortic NO, eNOS↑, pancreatic injury, Bax↓	Zhu et al. (2013, 2014, 2016)

4. Hericiaceae				
Hericium erinaceus (edible)	Water ext., polysaccharides	STZ-diabetic rats	Oxidative stress↓, glucose and lipid metabolism↑, serum glucose, TG, TC, LDL-C, MDA↓, serum insulin, HDL-C↑, serum and hepatic GSH, GP_X, SOD, CAT, activation of hepatic PI3K/Akt signaling↑	Liang et al. (2013), Cai et al. (2020)
5. Hymenochaetaceae				
Inonotus obliquus	Water ext., polysaccharides, ethyl acetate fr rich in triterpenoids and steroids	STZ-diabetic rats, alloxan-diabetic mice	Carbohydrate metabolism and antioxidant activity↑, plasma glucose, TG, TC, HbA1c, GSK-3↓, plasma insulin, HDL-C, PK, MMP-9, SOD, CAT, GP_X↑, hepatic and muscle glycogen content↑, kidney NF-κB expression↓, activity of α-amylase↓	Wang et al. (2017d), Lu et al. (2010)
Phellinus linteus	Hot water ext., polysaccharides	STZ-diabetic rats, alloxan-diabetic mice	Hepatic glucose and lipid metabolism↑, body weight gain, food intake, plasma glucose, insulin, HOMA-IR, TG, TC, LDL-C, FFAs, BUN, creatinine, uric acid, bilirubin↓, hepatic glycogen content, expression of GCK, GLUT2, LDLR, CPT1α, ACOX1↑, expression of hepatic HMGCR, FBPase, G6Pase↓	Liu et al. (2019), Zhao et al. (2014)

(continued)

Table 4.2 (continued)

(family, species)	Active plant part and fraction, active phytochemical (s)	Model	Major molecular targets and actions	References
6. Meripilaceae				
Grifola frondosa	Water ext., polysaccharides, ergosterol peroxide **370**	STZ-diabetic mice, KK-Ay diabetic mice, C2C12 cells	Hepatic glucose metabolism and antioxidant activity↑, gut microbiota dysbiosis↓, serum glucose, HbA1c, TG, TC, FFAs, MDA↓, Hepatic JNK1/2 activity↓, hepatic glycogen content, expression of IRS-1, PI3K, p-Akt, GLUT4, SOD, GSH, GP_X↑, rel. abundance of gut *Roseburia*, *Akkermansia*, *Lactobacillus*, *Bacteroides* spp.↑, expression of IRS-1, p-Akt, GLUT4 in high palmitate exposed C2C12 cells↑	Chen et al. (2019b), Wu et al. (2020a), Hong et al. (2007)
7. Pleurotaceae				
Pleurotus pulmonarius (edible)	Hot water ext., proteins and polysaccharides	STZ plus NA-diabetic mice, enzyme inhibition assay	Oxidative stress and dietary carbohydrate absorption↓, serum FG, PPG, TC, TG, LDL-C, VLDL-C, creatinine, BUN, MDA, LPO↓, serum HDL-C, insulin, CAT, GSSH↑, liver, kidney and pancreas necrosis↓, activity of α-amylase and α-glucosidase↓	Balaji et al. (2020), Waheb et al. (2014)

P. florida	Water ext., polysaccharides fr	STZ-diabetic rats	Oxidative stress↓, serum glucose, HbA1c, TC, TG, MDA, NO↓, excretion of urinary glucose, ketone bodies↓, serum SOD, CAT, GSH↑	Ganeshpurkar et al. (2014)
P. eryngii (edible)	Hot water ext., polysaccharides	KK-Ay diabetic mice, insulin resistant diabetic db/db mice	Glucose and lipid metabolism↑, serum glucose, HbA1c, HOMA-IR, TC, TG, LDL-C↓, serum HDL-C, liver glycogen↑	Chen et al. (2016b), Kim et al. (2010)
P. ostreatus (edible)	Methanol ext., ergosterol	KK-Ay diabetic mice, L6 myotubes	Serum FG↓, expression of p-Akt, p-PKC, GLUT4 in muscle and liver↑, expression and phosphorylation levels of AMPK, Akt, PKC, expression of GLUT4 in L6 cells↑	Xiong et al. (2018)
8. Tricholomataceae				
Catathelasma ventricosum	Water ext., polysaccharides fr (composed of mainly α-D-glucopyranose)	STZ-diabetic mice	Antioxidant activity↑, plasma glucose, TC, TG, LDL-C, MDA↓, plasma HDL-C, plasma, liver and kidney SOD, CAT, GP_X, vit C and E↑	Liu et al. (2013a)
D. Marine animals (class and species)				
1. Holothuroidea				
Cucumaria frondosa (edible sea cucumber)	Alkaline hydrolysis of freeze-dried body wall, fucoidan (polysaccharide), eicosapentaenoic acid-rich phosphatidylcholine	HF-HS-fed insulin resistant diabetic mice, STZ-diabetic rats	Serum glucose, resistin, leptin↓, serum adiponectin, hepatic glycogen↑, expression and p-levels of PI3K and Akt in muscle and AT↑, pancreatic apoptosis, expression of caspase-9 and -3↓, expression of pancreatic Bcl-xL, Bcl-2↑	Wang et al. (2016b), Hu et al. (2014, 2016a)

(continued)

Table 4.2 (continued)

(family, species)	Active plant part and fraction, active phytochemical (s)	Model	Major molecular targets and actions	References
Holothuria nobilis (sea cucumber)	Hydrolysates of water ext. with papain and protamix, peptides	STZ plus HFD-fed diabetic rats	Glucose and lipid metabolism, and insulin signaling↑, serum FG, insulin, HOMA-IR, TG, TC, LDL-C↓, expression of p-IRS1, PI3K, p-Akt in muscle 7 liver, GLUT4 in muscle, GLUT2 in liver, glycogen content in liver↑, activity of GSK-3β in liver↓	Wang et al. (2020a)
Callyspongia truncata (sponge)	Callyspongynic acid (**370a**)	Enzyme assay	α-Glucosidase activity↓	Nakao et al. (2002)
Ircinia dendroides and *I variabilis* (sponges)	Palinurin (sesquiterpene) (**370b**)	In vitro assay	GSK-3β activity↓	Bidon-Chanal et al. (2013)

glycogen synthesis in skeletal muscle L6 myotubes by increasing the activity of glycogen synthase (GS) and inhibiting the activity of glycogen synthase kinase 3β (GSK3β) via its phosphorylation in an independent of p-GSK3β pathway. This GagPKB also promotes protein synthesis in 3T3-L1 cells and L6 myotubes via phosphorylation of its substrate 4E-BP1 and p70S6K (Ueki et al. 1998; Wan et al. 2013). Moreover, Akt activation promotes the phosphorylation of forkhead O1 (FoxO1) protein for its exclusion from nucleus of hepatocytes for suppression of its activity on the expression of gluconeogenic enzymes G6Pase and PEPCK in the liver for inhibition of endogenous glucose production (Lin and Accili 2011). Akt activation in adipose tissue promotes fatty acid synthesis and cholesterol synthesis by upregulation of the expression of SREBP-1c and its target genes and inhibits lipolysis by suppression of the activity of ATGL (Chakrabarti and Kandror 2009). In pancreatic islets, PI3K/Akt signaling activation improves pancreatic β-cell mass, proliferation, and cell size and promotes insulin secretion (Bernal-Mizrachi et al. 2001).

Various phytochemicals and herbal extracts, such as 3β-taraxerol from *Mangifera indica*, catalpol and 7-hydroxyeucommiol from *Kigelia pinnata*, kaempferitrin from *Justicia spicigera*, puerarin from *Pueraria lobata*, alizarin from *Rubia cordifolia*, cyanidin-3-rutinoside **171** from *Morus nigra*, and polysaccharide from *Astragalus membranaceus*, exhibit insulin-like activity for activation of PI3K/Akt signaling pathway for improvement of hyperglycemia and hyperlipidemia in cellular and diabetic animal models (Table 4.2) (Sangeetha et al. 2010; Khan et al. 2012; Cazarolli et al. 2013; Li et al. 2014b; Xu et al. 2019; Choi et al. 2017; Liu et al. 2010a).

4.7.3 Inhibition of α-Amylase and α-Glucosidase Activity

Hydrolysis products of dietary carbohydrates (mainly starch and other related polysaccharides) are the major source of glucose in blood and main cause of postprandial high glucose levels in diabetic patients. Hydrolysis of dietary carbohydrates is carried out by a group of hydrolytic enzymes including pancreatic α-amylase and intestinal α-glucosidases. Pancreatic α-amylase hydrolyses starch into smaller oligosaccharides and disaccharides via cleavage of α-1,4-glycosidic bonds, and intestinal α-glucosidase hydrolyses these oligosaccharides and disaccharides into glucose and other monosaccharides. Therefore, the inhibition of the activity of these enzymes might be an important strategy for management of hyperglycemia in diabetic patients, wherein α-glucosidase inhibitors reduce the rapid utilization of dietary carbohydrates more effectively and thereby suppress the elevated glucose levels in postprandial hyperglycemia (Watanabe et al. 1997; Tundis et al. 2010). Currently used antihyperglycemic drugs, such as acarbose, voglibose, and miglitol, have been shown to reduce intestinal absorption of dietary sugars (Cheng and Fantus 2005). The main drawbacks of these currently used α-amylase and α-glucosidase inhibitors are their significant adverse side effects including bloating, abdominal discomfort, flatulence, and diarrhea (Derosa and Maffioli

2012; Aoki et al. 2010; Fujisawa et al. 2005). Possibly, such adverse effects might be caused by the excessive inhibition of pancreatic α-amylase activity resulting in abnormal bacterial fermentation of undigested carbohydrate diet in the colon. Some natural extracts from edible plants, seaweeds, and mushrooms and their active phytochemicals have been shown to have lower inhibitory effect against α-amylase activity and stronger α-glucosidase inhibitory activity and are therefore could be potentially effective for treatment of postprandial hyperglycemia in diabetic patients with minimal side effects (Tundis et al. 2010). For instance, proteins from bitter gourd fruit-pulp (*Momordica charantia* var. *charantia*, *M. charantia* var. *muricata*) inhibited the activity of α-amylase and α-glucosidase with IC_{50} of 0.267, 0.261, and 0.298, 0.292 mg/ml, respectively (Poovitha and Parani 2016). 6-Gingerol and oleanolic acid from *Aframomum melegueta* fruits inhibited the activity of α-amylase with IC_{50} of 81.78 and 91.72 μM and of α-glucosidase with IC_{50} of 21.55 and 17.35 μM, respectively (Mohammed et al. 2017). A 50% ethanol extract of *Orthosiphon stamineus* leaves and its active flavonoid sinensetin inhibited α-amylase and α-glucosidase activity of IC_{50} of 36.70, 1.13 mg/ml and 4.63, 0.66 mg/ml, respectively (Mohamed et al. 2012). An aqueous leaf extract of *Ocimum basilicum* (basil, tulsi) inhibited the activity of rat intestinal maltase and sucrase and porcine pancreatic α-amylase with IC_{50} of 21.31, 36.72, and 42.50 mg/mL, respectively (El-Beshbishy and Bahashwan 2012). Gamma-aminobutyric acid and ferulic acid, isolated from *Triticum aestivum* sprouts, inhibited the activity of α-amylase with IC_{50} of 5.4 and 9.5 mM/L and of α-glucosidase with IC_{50} of 1.4 and 4.9 mM/L, respectively (Jeong et al. 2012). Grape seed (*Vitis vinifera*) extract, green tea (*Camelia sinensis*) water extract and its active catechins, EGCG, GCG, and ECG, strongly inhibited the activity of α-amylase with IC_{50} of 8.7, 34.9, 24, 17, and 27 μg/ml, and of α-glucosidase with IC_{50} of 1.2, 0.5, 0.3,1.4, and 3.5 μg/ml, respectively (Yilmazer-Musa et al. 2012). Borapetoside C (**172**) from *Tinospora crispa* aqueous extract inhibited the activity of α-amylase and α-glucosidase with IC_{50} of 0.775 and 0.527 mg/ml, respectively (Hamid et al. 2015). Quercetin (**23**), found in various dietary fruits and vegetables and isolated from ethanol extract of *Callistephus chinensis*, showed strong α-glucosidase inhibitory activity with IC_{50} value of 2.04 μg/mL, similar to that of acarbose (IC_{50} of 2.24 μg/mL) (Zhang et al. 2013). A sulfated polysaccharide fucoidan from aqueous extract of marine brown alga *Ascophyllum nodosum* inhibited the activity of α-amylase and α-glucosidase with IC_{50} of 4.64 and 0.05 mg/ml, respectively (Kim et al. 2014). Moreover, a good number of extracts from plants, vegetables, seaweeds, and mushrooms and their active components having strong inhibitory effect against α-glucosidases enzymes are listed in Table 4.2.

4.7.4 Inhibition of SGLT2 Activity

Reabsorption of glucose in the kidney of humans is largely controlled by the membrane protein, sodium-glucose transporter protein 2, also known as sodium-glucose-co-transporter-2 (SGLT2). SGLT2 is expressed in high concentrations in the

proximal tubule of the kidney and is involved in glucose reabsorption and accounts for more than 90% of renal glucose reabsorption in normoglycemic conditions via an active transport of glucose through the Na^+ pump. Another SGLT enzyme, SGLT1, primarily localized in small intestine, has high affinity and low capacity for glucose reabsorption (Wright et al. 2011). Therefore, inhibition of SGLT2 activity by SGLT2 inhibitors increases urinary glucose excretion and lowers plasma glucose levels in type 2 diabetic patients in a non-insulin-dependent approach. SGLT2 inhibitors are highly effective for treatment of type 2 diabetic patients, who are failing to monotherapy and are not willing to take insulin therapy. Phlorizin (**173**) (Fig. 4.1), a dihydrochalcone glucoside, isolated from the bark of apple tree, *Malus pumila*, has been found to inhibit of human SGLT2 and SGLT1 enzyme activities with inhibitory constant Ki values of 18.6 and 151.0 nM, respectively. However, it was considered inappropriate for treatment of human diabetes because of its low oral bioavailability and poor selectivity on SGLT2 enzymes and many adverse effects including dehydration, diarrhea, and abnormal growth of muscle and bone (Takasu et al. 2019; Ehrenkranz et al. 2005). Currently prescribed synthetic SGLT2 inhibitors, canagliflozin (**174**), dapagliflozin (**175**), and empagliflozin (**176**) are used for treatment of type 2 diabetes in combination with other oral hypoglycemic drugs and effective in lowering of blood glucose, blood pressure, and body weight gain. However, the long-term use of these SGLT2 inhibitors in diabetic patients is associated with adverse side effects including female genital mycotic infections, urinary tract infections, increased urination, moderate to severe renal dysfunction, and diabetic ketoacidosis (DKA). The DKA develops extensively the states of low blood glucose levels (Hsia et al. 2017; Plodkowski et al. 2015; Halimi and Verges 2014). Some natural products have been reported to possess strong inhibitory effect against SGLT2 activity. These natural products could be utilized as an alternative to synthetic SGLT2 inhibitors for treatment of diabetes. For instance, two picraline-type alkaloids, 10-methoxy-N(1)-methylburnamine-17-O-veratrate (**177**) and alstiphyanine D (**178**) from antidiabetic plant, *Alstonia macrophylla*, strongly inhibited the activity of SGLT2 with IC_{50} of 0.5 and 2.0 μM and of SGLT1 with IC_{50} of 4.0 and 5.0 μM, respectively (Arai et al. 2010). Four flavonoids, (-)-kurarinone (**179**), sophoraflavanone G (**180**), isoflavone glycosides A (181) and B (**182**), from the roots of Chinese herb, *Sophora flavescens*, showed strong to moderate inhibitory effect on the activity of SGLT2 with IC_{50} of 1.7, 4.1, 2.6, and 15.3 μM, respectively (Sato et al. 2007b; Yang et al. 2015a). Two stilbene trimers, gneyulins A (**183**) and B (**184**) from *Gnetum gnemonoides*, showed moderate inhibitory effect against SGLT2 with IC_{50} of 25.0 and 18.0 μM and SGLT1 with IC_{50} of 27.0 and 37.0 μM, respectively (Shimokawa et al. 2010). Two cyclic diarylheptanoids, acerogenin-A (**185**) and B (**186**) from the bark of Japanese plant, *Acer nikoense*, showed moderate inhibitory effect against SGLT1 with IC_{50} of 20 and 26 μM and weak effect against SGLT2 with IC_{50} of 94 and 43 μM, respectively (Morita et al. 2010).

4.7.5 Inhibition of DPP4 Activity

Dipeptidyl peptidase-4 (DPP4), also known as cluster of differentiation-26 (CD26), is an exopeptidase glycoprotein, released from differentiated adipocytes and expressed in a variety of tissues including the pancreas, liver, and adrenal glands and exerts paracrine and endocrine effects in cell signaling and insulin action. It is expressed in high concentrations on plasma of obese and diabetic patients. DPP4 selectively cleaves N-terminal dipeptides from a variety of substrates including cytokines, growth factors, neuropeptides, and incretin hormones, GLP-1 and GIP. It is responsible for deactivation of incretin hormones and to reduce postprandial insulin secretion, resulting in decreased plasma insulin and elevated plasma glucose levels in obese and diabetic patients. It represents a molecular link between obesity and vascular dysfunction (Rohrborn et al. 2015; Drucker and Nauck 2006; Drucker 2006). A recent study reported that significantly high plasma DPP4 levels in obese and nonobese diabetic patients are positively correlated with fasting plasma insulin, HbA1c (above 9.0%), LDL-C levels, triceps skinfolds and intra-abdominal adiposity, and waist to hip ratio (Anoop et al. 2017). Incretin (insulin action potentiation) hormones, glucagon-like peptide-1 (GLP-1), and glucose-dependent insulinotropic polypeptide (GIP) are secreted from gut (small intestine) endocrine L- and K-cells after a meal intake to stimulate insulin secretion from pancreatic β-cells and to suppress glucagon secretion from pancreatic α-cells, to inhibit gastric emptying in stomach and reduce food intake and elevated serum glucose and HbA1c levels (Drucker 2006). Both GLP-1 and GIP exert their action through their G-protein coupled receptors, GLP-1R, GIPR, that are expressed in β-cells to increase the levels of cAMP and intracellular Ca^{2+} and insulin exocytosis in a glucose-dependent manner. Moreover, GLP-1R promotes insulin biosynthesis and β-cell proliferation and inhibits β-cell apoptosis (Drucker 2006). Therefore, inhibition of DPP4 activity is a promising therapeutic target for reduction of hyperglycemia in obese and diabetic patients. Currently some DPP4 inhibitors, namely, sitagliptin, saxagliptin, linagliptin, vildagliptin, alogliptin, anagliptin, gemigliptin, and teneligliptin (**188**–**195**), are widely prescribed in combination with other oral hypoglycemic agents for treatment of hyperglycemia in type 2 diabetic patients. Most of these DPP4 inhibitors (DPP4i) improve hyperglycemia, cardiovascular function, and aortic lesions in diabetic patients. However, about 5% or more of patients receiving these DPP4i have reported some adverse effects including upper respiratory tract infection, nasopharyngitis, headache, and skin lesions during the treatment period (Dicker 2011; Pathak and Bridgeman 2010). Various types of phytochemicals from fruits, vegetables, plants, edible seaweeds, and mushrooms have been reported to have potential inhibitory effect on DPP4 activity. These phytochemicals or their parent extracts could be useful for diabetes treatment as DPP4 inhibitors after clinical trials in humans. For example, resveratrol (**47**) from grape fruit, genistein (**96**) from soybean, flavonoids luteolin (**196**), apigenin (**197**), quercetin (**23**), kaempferol (**66**), hesperetin (**198**), naringenin (**199**) from citrus fruits, and anthocyanins cyanidin-3-glucoside (**31**), cyanidin, and malvidin from blueberry and blackberry showed strong inhibitory effect against DPP4 activity with IC_{50} of 0.0006, 0.048,

0.12, 0.14, 2.92, 0.49, 0.28, 0.24, 0.42, 1.41, and 1.41 μM, respectively (Fan et al. 2013). Emodin (**123**) from *Rheum palmatum*, eriodictyol (**200**), hispidulin (**201**) from Mexican oregano (*Lippia graveolens*), cirsimaritin (**202**), and rosmarinic acid **104** from rosemary (*Rosmarinus officinalis*) strongly inhibited the activity of DPP4 with an IC_{50} value of 5.76, 10.9, 0.49, 0.43, and 14.1 μM, respectively (Wang et al. 2017e; Bower et al. 2014). Cyanidin-3,5-diglucoside (**203**) from aronia berries (*Aronia melanocarpa*), berberine (**48**) from *Coptis chinensis*, aqueous leaf extract of tulsi (*Ocimum sanctum*), and tripeptides, diprotins A (**204**) and B (**205**) from bacterium *Bacillus cereus* BMF 673-RF1 showed strong inhibitory effect against the activity of DPP4 with IC_{50} of 5.5 μM, 13.3 μM, 0.38 μg/ml, 1.1 μg/ml, and 5.5 μg/ml, respectively (Kozuka et al. 2015; Al-Masri et al. 2009; De et al. 2015; Umezawa et al. 1984).

4.7.6 Inhibition of PTP1B Activity

Insulin resistance is a hallmark of type 2 diabetes and diet-induced obesity. The protein tyrosine phosphatase 1B of family protein tyrosine phosphatases and plays a key role as negative regulator of both insulin and leptin signaling for development of insulin and leptin resistance in obesity and type 2 diabetes. In insulin signaling, insulin on binding to its receptor IR promotes phosphorylation of IR, IRS, and Akt sequentially in peripheral tissues including the skeletal muscle, liver, and adipose tissue for glucose metabolism and utilization, while PTP1B negatively regulates the insulin signaling through dephosphorylation of phosphorylated IR and IRS. In HFD-fed obese mice, PTP1B on overexpressions in arcuate nucleus of hypothalamus in mice brain negatively regulates leptin signaling through dephosphorylation of Janus kinase 2 (JNK2) to increase the storage of fat mass in the body by increasing leptin resistance in the hypothalamus. PTP1B-deficient mice are more sensitive to insulin in the insulin-sensitive tissues, muscle, and liver and improve hyperglycemia in type 2 diabetes and fat metabolism in diet-induced obesity (Elchebly et al. 1999; Valverde and Gonzalez-Rodriguez 2011). In skeletal muscle of type 2 diabetic African Americans, overexpression of PTP1B proteins reduces the level of Akt phosphorylation and decreases insulin-stimulated glucose uptake and glucose metabolism. While, reduction of PTP1B expression by transfection with PTP1B siRNA vector increases the insulin-stimulated phosphorylation level of Akt in primary human skeletal muscle culture (HSMC), collected from the subjects with type 2 diabetes (Stull et al. 2012). Another study on PTP1B enzymes reported that in high-fat fed mice, the expression of PTP1B in the adipose tissue, muscle, liver, and arcuate nucleus of hypothalamus was increased by 1.5- to 7-folds and was positively correlated with increased expression of macrophage marker CD68 and TNFα in adipose tissue. Moreover, TNFα treatment in 3T3-L1 adipocyte and H4IIE hepatocyte culture increased the expression of PTP1B mRNA and protein levels by 2-to 5-folds. It suggested that overexpression of PTP1B enzymes in multiple tissues in obesity is regulated by inflammation (Zabolotny et al. 2008). It is also observed that the protein silent information regulator 1 (SIRT1) on overexpression or activation in

insulin resistant conditions reduces the expression levels of PTP1B mRNA and proteins and improves insulin sensitivity by increasing insulin stimulated phosphorylation of IR, IRs, and Akt by suppression of inflammation and improvement of antioxidant activity in the liver and skeletal muscle of obese mice (Sun et al. 2007). Therefore, inhibition or downregulation of PTP1B activity for improvement of insulin signaling pathway is a potential target for treatment of type 2 diabetes and diet-induced obesity. Various classes of phytochemicals from plants, seaweeds, fungi, and marine animals improved insulin resistance in obesity and type 2 diabetes by inhibition of PTP1B expression and activity (Table 4.2) (Wang et al. 2015b; Zhao et al. 2018a). These natural products could be utilized as diet supplement for treatment of both obesity and diabetes. For example, triterpenes ursolic acid (**52**) and corosolic acid (**206**) from *Symplocos paniculata* inhibited the activity of PTP1B in a competitive manner with IC_{50} of 3.8 and 7.2 μM, respectively (Na et al. 2006). Triterpenes, betulinic acid (**207**) from *Saussurea lappa*, tormentic acid (**208**) and palmitic acid (**209**) from *Agrimonia pilosa*, hopane-6α, 22-diol **210** from *Lecidella carpathica* inhibited the activity of PTP1B with IC_{50} of 0.70 μg/ml, 0.50 μM, 0.10 μm, and 3.7 μM, respectively (Choi et al. 2009; Na et al. 2016; Seo et al. 2011). Flavonols, isorhamnetin (**211**), isorhamnetin-3-*O*-β-D-glucoside (**212**), isorhamnetin-3-*O*-β-D-rutinoside (**213**) and quercetin (**23**) and three triterpenes, 2α, 3β-dihydroxy-olean-12-en-23, 28,30-trioic acid (**214**), sorghumol (**215**), and epifriedelanol (**216**) from *Anoectochilus chapaensis* exhibited strong inhibitory effect against hPTP1B protein with IC_{50} of 1,75, 1.16, 1.20, 5.63, 2.65, 3.50, and 3.75 μM, respectively (Cai et al. 2015). The chalcones, xanthoangelol K (**217**); xanthoangelol (**218**), xanthoangelols D (**219**), E (**220**), and F (**221**); 4-hydroxyderricin (**222**) from *Angelica keiskei* inhibited the activity of PTP1B with IC_{50} of 0.82, 1.97, 3.97, 1.43, 1.67, and 2.47 μg/ml, respectively (Li et al. 2015). Flavonoids, albafurans A (**223**) and B (**224**) from *Morus alba* var. *tatarica*, and kuwanons J (**225**), R (**226**), and V (**227**) from *Morus bombycis* inhibited the activity of PTP1B with IC_{50} of 7.9, 8.9, 2.7, 8.2, and 13.8 μM, respectively (Zhang et al. 2014a; Hoang et al. 2009). Naphthoquinones, deoxyshikonin (**228**), shikonin (**229**), acetylshikonin (**230**), and β,β′-dimethylacrylalkannin (**231**) from *Arnebia euchroma* strongly inhibited the activity of PTP1B with IC_{50} value of 0.80, 4.42, 1.02, and 0.36 μM, respectively (Wang et al. 2016a). Prenylated isoflavones, angustone A (**232**), isoangustone A (**233**) from *Glycyrrhiza uralensis*, alkaloid papaverine (**234**) from *Papaver somniferum*, and gallotannin, 1,2, 3,4,6-penta-*O*-galloyl-D-glucopyranose (**235**), from *Paeonia lactiflora* inhibited the activity of PTP1B with IC_{50} of 0.4, 3.0, 1.20, and 4.8 μM, respectively (Ji et al. 2016; Bustanji et al. 2009a; Baumgartner et al. 2010). Four quinic acid derivatives, 3,4-dicaffeoylquinic acid (**236**), 3,5-dicaffeoylquinic acid (**237**), 3,5-dicaffeoylquinic acid methyl ester (**238**), and 4,5-dicaffeoylquinic acid (**239**) from *Artemisia capillaris* showed strong inhibitory effect against PTP1B with IC_{50} value of 2.60, 2.02, 2.99, and 3.21 μM, respectively (Islam et al. 2013). Phytochemicals, asperentin B (**240**) from marine fungus, *Aspergillus sydowii*, tanzawaic acids A (**241**) and B (**242**) from fungus *Penicillium* sp. SF-6013, anhydrofulvic acid (**243**) and penstyrylpyrone (**244**) from *Penicillium* sp. JF-55,

and aquastatin A (**245**) from marine fungus *Cosmospora* sp. SF-5060, inhibited the activity of PTP1B with IC_{50} of 2.05, 8.2, 8.2, 1.90, 5.28, and 0.19 μM, respectively (Wiese et al. 2017; Quang et al. 2014; Lee et al. 2013a; Seo et al. 2009). Phlorotannins, eckol (**164**), dieckol (**163**), 7-phloroeckol (**246**), and phlorofurofucoeckol-A (**167**) from marine brown algae, *Ecklonia stolonifera* and *Eisenia bicyclis*; carotenoid fucoxanthin (**158**) from marine alga, *Undaria pinnatifida*; thunberol (**247**) from brown alga, *Sargassum thunbergii*; racemosin C (**248**) and caulersin (**249**) from marine green alga *Caulerpa racemosa*; and caulerpin (**250**) from *Caulerpa taxifolia* strongly inhibited the activity of PTP1B with an IC_{50} value of 2.64, 1.18, 2.09, 0.56, 4.80, 2.24, 5.86, 7.14, and 3.77 μM, respectively (Moon et al. 2011; Jung et al. 2012b; He et al. 2014; Yang et al. 2014a; Mao et al. 2006). Phytochemicals, such as sesquiterpene quinones, frondophysin A (**251**) from marine sponge *Dysidea frondosa*, dysidine (**252**) from *Dysidea villosa*, and stellettin G (**253**) from marine sponge *Stelleta* sp. exhibited inhibitory effect against PTP1B activity with IC_{50} of 0.39, 1.5, and 4.1 μM, respectively (Jiao et al. 2019; Zhang et al. 2009; Xue et al. 2013).

4.7.7 Inhibition of 11β-HSD1 Activity

The enzyme 11beta-hydroxysteroid dehydrogenase type 1 (11β-HSD1), a negative regulator of insulin signaling pathway, is overexpressed in the liver, adipose tissue, gonad, and brain in obese humans and rodents and actively regulates the function of glucocorticoids in these tissues by conversion of inactive cortisone into active cortisol in presence of NADPH. Emerging evidence demonstrates that high-fat-fed transgenic mice overexpressing 11β-HSD1 in adipose tissue increases visceral obesity, insulin resistance, hyperglycemia, hyperlipidemia, and hyperphagia. Moreover, overexpression of 11β-HSD1 in adipose tissue promotes adipocyte differentiation and upregulated the expression of leptin, LPL, and TNFα in adipocytes and increases lipid accumulation in abdominal lesion, and in the liver, it promotes gluconeogenesis through upregulation of the expression of PEPCK. It also reduces energy expenditure by decreasing the expression of thermogenic gene UCP1 in interscapular BAT (Masuzaki et al. 2001). 11β-HSD1-deficient mice markedly reduced hyperglycemia and hyperlipidemia by decreasing the levels of plasma TG, LDL-C, FFAs, and glucose and increased insulin sensitivity in the liver and adipose tissue by decreasing hepatic glucose production and increasing fat metabolism through downregulation of PEPCK and G6Pase and upregulation of CPT1, ACOX, PPARα, and UCP2 (Morton et al. 2001; Kotelevtsev et al. 1997). Moreover, high-dose cortisol administration maintaining pituitary-pancreatic (P-P) infusion protocol in humans increased plasma glucose, leucine, and phenylalanine levels by stimulating gluconeogenesis in the liver and proteolysis in skeletal muscle. These results suggest that cortisol reduces insulin action in liver and muscle in human subjects (Khani and Tayek 2001; Brillon et al. 1995). Therefore, inhibition of 11β-HSD1 activity is a potential strategy to improve insulin action in treatment of obesity and diabetes. Usually transfected HEK293 cells are used for the assay of

human and rodent 11β-HSD1 activity in cellular model. Various phytochemicals and plant extracts have been reported as potent inhibitors of 11β-HSD1 activity, and these natural products could be utilized in the development of natural antidiabetic medicines. Among these phytochemicals, emodin (**123**), aloe-emodin (**123a**), and rheochrysidin (**254**) from *Rheum palmatum* rhizomes inhibited the activity m (mouse)-11β-HSD1 with IC_{50} of 86, 98, and 81 nM and of human (h)-11β-HSD1 with IC_{50} of 186, 879, and 542 nM, respectively (Feng et al. 2010). Curcumin **9** from *Curcuma longa* rhizome strongly inhibited the activity of h-and m-11β-HSD1 with IC_{50} of 2.29 and 5.79 μM, respectively, in a competitive manner (Hu et al. 2013). Triterpene cochinchinoid K **255** from Vietnamese *Walsura cochinchinensis* herb showed strong inhibitory effect against m-11β-HSD1 with an IC_{50} of 0.82 μM (Han et al. 2013). Tirrucallane-type triterpene, 22*S*,23*R*-epoxytirrucalla-7-ene-3α,24,25-triol (**256**), from *Walsura robusta* leaves strongly inhibited the activity of human and mouse 11β-HSD1 with IC_{50} of 1.9 and 1.2 μM, respectively, while other three triterpenes from the same plant, niloticin (**256a**), dihydroniloticin (**256b**), and piscidinol A (**256c**) strongly inhibited the activity of mouse 11β-HSD1 with IC_{50} of 0.69, 3.8, and 0.88 μM, respectively (Wang et al. 2016). Ursane-type triterpenes, ursolic acid (**52**), corosolic acid (**206**), 3-epicorosolic acid methyl ester (**257**), tormentic acid methyl ester (**258**) and 2α-hydroxy-3-oxo-urs-12-en-28-oic acid (**259**), 11-keto-ursolic acid (**260**), and 3-acetyl-11-keto-ursolic acid (**261**) from an antidiabetic plant, *Eriobotrya japonica*, showed strong inhibitory effect against 11β-HSD1 with IC_{50} value of 1.9, 0.81, 5.2, 9.4, 17, 2.06, and 1.35 μM, respectively (Rollinger et al. 2010). Triterpene of ursane-type, isoyarumic acid (**262**) from Latin American *Cecropia telenitida* strongly inhibited the activity of 11β-HSD1 with IC_{50} of 0.95 μM (Mosquera et al. 2018). Limonoids, dysoxylumosin F (**263**) from *Dysoxylum mollissimum* twigs (red bean) and harperforin G (**264**) from Thai *Harrisonia perforata*, showed potent inhibitory effect against h-11β-HSD1 with an IC_{50} of 9.6 nM and 0.58 μM, respectively (Zhou et al. 2015; Yan et al. 2016). Two steroids, masticadienonic acid (**265**) and isomasticadienonic acid (**266**) from *Pistacia lentiscus* (mastic gum), exhibited strong inhibitory effect against 11β-HSD1 with IC_{50} of 2.51 and 1.94 μM, respectively (Assimopoulou et al. 2015). Phenolics, 6-paradol (**152**), 6-shogaol (**153**), and (5*R*)-acetoxy-6-gingerol (**267**) from white ginger, *Zingiber officinale*, rhizomes showed potent inhibitory effect against h-11β-HSD1 with IC_{50} in the range of 1.09–1.30 μM (Feng et al. 2011). A catechin derivative, EGCG (**35**), from green tea showed moderate inhibitory effect against h-11β-HSD1 with an IC_{50} of 57.99 μM (Hintzpeter et al. 2014). A cyclic tetrapeptide, penicopeptide A (**268**) isolated from the culture of endophytic fungus *Penicillium commune* of grape plant, *Vitis vinifera*, in rice, inhibited the activity of h-11β-HSD1 with an IC_{50} of 9.07 μM (Sun et al. 2016).

4.7.8 Inhibition of Aldose Reductase (AR) Activity

Aldose reductase (AR) (alditol: NADP oxidoreductase EC.1.1.1.21), an enzyme of aldo-keto reductase superfamily, catalyzes the conversion of glucose into sorbitol in

presence of NADPH in the polyol pathway under hyperglycemic condition in diabetes. Sorbitol is a membrane-impermeable substance, and its accumulation in cells increases osmotic stress. Sorbitol is further metabolized into fructose by sorbitol dehydrogenase (SDH), and fructose, in turn, is metabolized into dicarbonyl compounds, 3-deoxyglucosone (3-DG) and methyl glyoxal (MG), which are recognized as potent glycating agents and participate in the formation of advanced glycation end products (AGEs). Moreover, in the process of conversion of glucose into fructose under high glucose concentrations, in the first step, AR utilizes NADPH and consequently reduces GSH level, and in the second step, SDH utilizes cofactor NAD+ for conversion of sorbitol into fructose and thereby converts NAD+ into NADH, which is a substrate of NADH oxidase, leading to the production of superoxide anions. Further, AR on overexpression induces oxidative stress-induced inflammation via activation of PKC and NFκB in different tissues, particularly in the heart, retina, and kidney. Accumulation of sorbitol in different tissues under hyperglycemic conditions leads to secondary diabetic complications, such as diabetic cataractogenesis, retinopathy, neuropathy, myocardial infarction, and nephropathy (Brownlee 2001). Accumulating evidence demonstrates that human eye lens-specific overexpression of AR accelerates high-glucose-induced cataract via apoptosis of lens epithelial cells through stimulation of TNFα-induced activation of PKC and NFκB (Ramana et al. 2003). Treatment of AR inhibitor, tolrestat or sorbinil, or transfected AR siRNA in high-glucose exposed vascular smooth muscle cells (VSMCs) prevented the activation of PKC and formation of diacylglycerol (DAG) (Ramana et al. 2005). Moreover, inhibition of AR activity markedly protects both diabetic and nondiabetic rat hearts from ischemic injury via reduction of cystolic NADH/NAD+ ratio and creatine kinase production, and increased ATP production (Ramasamy et al. 1997). Various natural products have been shown strong in vitro inhibitory effects against rat lens AR (RLAR). These natural products could be useful in treatment of diabetic complications. The properties of RLAR are similar to those of human placental AR (HPAR), and these natural RLAR inhibitors would be effective against human AR. For example, flavonoids, quercetin (**23**) and luteolin **196** and its glycoside, scolymoside (**269**), apigenin (**197**), isoquercitrin (**270**), and hyperoside (**271**), and phenolic acids, chlorogenic acid (**21**) and 3,5-di-*O*-caffeoylquinic acid (**237**) from *Artemisia montana*, strongly inhibited the activity of RLAR with IC_{50} of 0.30, 0.19, 0.55, 0.67, 1.16, 1.85, 4.36, and 5.37 μM, respectively (Jung et al. 2011). Five gallotannins, 1,2,3-tri-*O*-galloyl-β-D-glucose (**272**), 1,2,3,6-tetra-*O*-galloyl-β-D-glucose (**273**), 1,2,4,6-tetra-*O*-galloyl-β-D-glucose (**274**), 1,2,3,4,6-penta-*O*-galloyl-β-D-glucose (**235**), and tellimagrandin (**275**) from *Cornus officinalis* seeds inhibited the activity of RLAR with IC_{50} values of 2.35, 0.70, 0.76, 1.93, and 0.90 μM, respectively (Lee et al. 2011c). Flavanone myrciacitrin I (**276**), flavonol glycosides myricitrin (**92**), mearnsitrin (**277**), quercitrin (**122**), desmanthin I (**278**), and guaijaverin (**279**) from *Myrcia multiflora* leaves inhibited the activity of RLAR with IC_{50} values of 3.2, 3.8, 1.4, 0.15, 0.082, and 0.18 μM, respectively (Yoshikawa et al. 1998). Diterpenes danshenols A (**280**) and B (**281**), dihydrotanshinone I (**282**), tanshinone IIA (**283**), and danshexinkun A (**284**) from *Salvia miltiorrhiza* root showed moderate to strong inhibitory effect

against RLAR with IC_{50} of 0.10, 1.75, 1.19, 1.14, and 0.87 μM, respectively (Tezuka et al. 1997). Phenolic acids, lithospermic acid B (**285**), salvianolic acid K (**286**), salviaflaside (**287**), and rosmarinic acid (**104**) from *Salvia deserta* showed moderate inhibitory effect against RLAR with IC_{50} of 2.63, 2.81, 3.15, and 3.91 μM, respectively (Kasimu et al. 1998). Three quinic acid derivatives, 3-caffeoylquinic acid (**288**), 3,5-di-*O*-caffeoylquinic acid (**237**), and 3,5-di-*O*-caffeoyl-*epi*-quinic acid (**289**) from *Erigeron annuus* inhibited the activity of RLAR with IC_{50} of 1.67, 0.79, and 0.44 μM, respectively (Jang et al. 2010). Isoflavonoids tectorigenin (**290**), tectoridin-4'-*O*-β-D-glucoside (**291**), and kakkalide (**292**), from *Viola hondoensis* and tectoridin (**293**) from *Belamcanda chinensis* inhibited the activity of RLAR with IC_{50} of 1.12 μM, 0.54 μM, 0.34 μg/ml and 1.08 μM, respectively (Moon et al. 2006; Chung et al. 2008; Jung et al. 2002). Isoflavonoids, semilicoisoflavone B (**294**), liquiritigenin (**94**), and isoliquiritigenin (**295**), from *Glycyrrhiza uralensis* roots inhibited the activity of RLAR and human recombinant (hr)-AR with IC_{50} of 1.8, 2.0, 3.4 μM, and 10.6, 21.9, 27.5 μM, respectively (Lee et al. 2010b). Four biflavonoids, chamaejasmin (**296**), 7-methoxyneochamaejasmin (**297**), 7-methoxychamaejasmin (**298**), and chamaejasmenin B (**299**), and a chromone, chamaechromone (**300**), from *Stellera chamaejasme* inhibited the activity of RLAR with IC_{50} of 1.8, 2.9, 4.1, 5.9, and 7.4 μM, respectively (Feng et al. 2005). A *C*-glycosidic flavonoid derivative, swertisin (**301**), from *Enicostemma hyssopifolium* inhibited the activity of RLAR with an IC_{50} of 1.6 μM (Patel and Mishra 2009). Flavonoids, isoorientin (**302**), vitexin (**303**), luteolin-6-*C*-(6"-*O*-*trans*-caffeoylglucoside) (**304**), tricin (**305**), and p-coumaric acid (**19**) from black bamboo, *Phyllostachys nigra*, leaves, showed strong to moderate inhibitory effect against the activity of RLAR with IC_{50} of 1.91, 2.03, 0.013, 2.03, and 0.14 μM, respectively (Jung et al. 2007). Flavonoid isorhamnetin-3-O-β-D-glucoside (**212**) from *Salicornia herbacea* inhibited the activity of RLAR with an IC_{50} of 1.4 μM (Lee et al. 2005b). Two flavonoids compounds, chalcone butein (**306**) and aurone sulfuretin (**307**), from Asian *Rhus verniciflua* bark showed strong inhibitory effect against RLAR with IC_{50} of 0.7 and 1.3 μM, respectively (Lee et al. 2008a). Three acylated flavanone glycosides, matteuorienates A (**308**), B (**309**), and C (**310**) from Chinese *Matteuccia orientalis* rhizomes, exhibited strong inhibitory effect against RLAR with IC_{50} values of 1.0, 1.0 and 2.3 μM, respectively (Kadota et al. 1994). Leuteolin and its glycosides, luteolin-7-O-β-D-glucopyranoside (**311**), luteolin-7-O-β-D-glucopyranosiduronic acid (**312**), (2*S*)-and (2*R*)-eriodictyol-7-O-β-D-glucopyranosiduronic acids (**313**), (**314**) from *Chrysanthemum indicum* flowers showed moderate inhibitory effect against RLAR with IC_{50} of 0.45, 0.99, 3.1, 2.1, and 1.5 μM, respectively (Yoshikawa et al. 1999; Matsuda et al. 2002). Two anthocyanins, delphinidin-3-*O*-β-galactopyranoside-3'-β-glucopyranoside (**315**) and delphinidin-3-*O*-β-galactopyranoside-3',5'-di-*O*-β-glucopyranoside (**316**) from *Litchi chinensis* fruits exhibited strong inhibitory effect against RLAR with IC_{50} of 0.23 and 1.23 μM, respectively (Lee et al. 2009). Phenolic aldehyde, protocatechualdehyde (**317**), from mushroom *Ganoderma applanatum* showed strong inhibitory effect against RLAR with IC_{50} of 0.7 μM (Lee et al. 2005a). Hispidin dimers, davallialactone (**318**), hypholomine B (**319**), and ellagic acid

(**320**), from medicinal mushroom *Phellinus linteus* showed potent inhibitory effect against both RLAR and hrAR with IC_{50} values of 0.33, 0.82, and 0.63 μM and of 0.56, 1.28, and 1.37 μM, respectively (Lee et al. 2008b). A bromophenol, rubrolide L (**321**), from marine tunicate *Ritterella rubra*, and lukianol B (**322**) from an unidentified Pacific tunicate, showed strong inhibitory effect against hAR2 with IC_{50} of 0.8 and 0.6 μM, respectively (Manzaro et al. 2006). A diphenyl aldostatin analog, WF-2421 (**323**), from fungus *Humicola grisea* showed strong inhibitory effect against rabbit lens AR with IC_{50} of 0.03 μM (Nishikawa et al. 1991).

4.7.9 Stimulatory Effect on TGR5 Activation

The membrane protein, Takeda G-protein receptor 5 (TGR5), also known as G-protein-coupled bile acid receptor 1 (GPBAR1) or membrane-type receptor for bile acid (M-BAR) mediates the physiological functions of bile acids. The membrane protein, TGR5 is expressed in the liver, brown adipose tissue, pancreas, intestine, and spleen and plays a key role in glucose and energy metabolism for maintenance of glucose and energy homeostasis in obesity and diabetes (Maruyama et al. 2006; Chen et al. 2011). Bile acids (BAs), such as cholic acid (CA **324**) and chenodeoxycholic acid (CDCA **325**) are the primary BAs that are synthesized in hepatocytes and transported into gallbladder for storage. BAs are secreted in small intestine in response to dietary intake for its emulsification as dietary lipids for absorption (Russell 2003). In vitro, TGR5 is endogenously expressed in enteroendocrine cells, such as human NCI-H716, mouse STC-1 and GLUTag cell lines, suggesting its potential role in intestine (Maruyama et al. 2002). TGR5 on activation by BAs increases energy expenditure in BAT through upregulation of intracellular cAMP and activation of the enzyme type 2 iodothyronine deiodinase (D2, also known as Dio2) for conversion of thyroxine (T4) to tri-iodothyronine (T3) and T3-induced upregulation of thermogenin gene, UCP1 via BAs/TGR5/cAMP/D2/T3/UCP1 signaling pathway (Watanabe et al. 2006). TGR5 activation increases the secretion of incretin GLP-1 from intestinal endocrine L-cells and promotes insulin action in the liver and muscle of obese mice and induces mitochondrial oxidative phosphorylation in amelioration of obesity-associated nonalcoholic steatohepatitis (NASH) (Thomas et al. 2009). TGR5 on activation protects high-glucose-induced cardiomyocyte injury by improving antioxidant status via upregulation of Nrf2 and HO-1 expression and improves diabetic retinopathy through upregulation of tight junction protein ZO-1 via suppression of TNF-α-induced RhoA/RhoA-associated coiled-coil containing protein kinase (ROCK) signaling pathway in human retinal microvascular endothelial cells (RMECs) (Deng et al. 2019a; Zhu et al. 2020). Therefore, the stimulation of TGR5 activity is a promising target for treatment of obesity and diabetes. Some natural products have been reported as potent TGR5 agonists. For example, oleanolic acid (**326**) from *Olea europaea* leaves acts as potential TGR5 agonist and improves insulin sensitivity in liver of HFD-fed obese mice by upregulation of IRS and suppression of FoxO1 activity and expression of gluconeogenic genes, PEPCK and G6Pase. Moreover, it

increases insulin secretion in pancreatic β-cells through promotion of stimulus-secretion coupling (SSC), activation of adenylyl cyclase (AC), increased accumulation of intracellular Ca^{2+} ions, cAMP production, and activation of protein kinase A (PKA) in a AC/cAMP/PKA pathway (Sato et al. 2007a; Maczewsky et al. 2019). In cellular model, the TGR5 agonistic activity of natural products is evaluated by measuring intracellular cAMP production in Chinese hamster ovary (CHO-K1) cells or human NCI-H716 cells or HEK293 cells transfected with human TGR5 cDNA plasmid (siRNA) gene in a cAMP response element (CRE)-luciferase assay using BAs as positive control (Lo et al. 2016). In addition to primary BAs, CA and CDCA, secondary BAs, lithocholic acid (LCA **327**), and deoxycholic acid (DCA **328**), formed by bacterial dehydroxylation in humans, are used as positive control. Two synthetic BAs, 6α-6-ethyl-23*S*-methyl-cholic acid (EMCA, INT-777) and taurolithocholic acid (TLCA **329**), are also used as positive control. Natural betulinic acid (**207**), oleanolic acid (**326**), and ursolic acid (**52**) exhibited strong TGR5 agonistic activity, similar to bile acids with EC_{50} of 1.04, 2.25 and 1.43 μM, respectively, in NCI-H716 cells. Moreover, betulinic acid in TGR5 receptor transfected CHO-K1 cells, increased glucose uptake and insulin secretion through increased intracellular cAMP level and PKA activity, and this effect was blocked on treatment of triamterene, an antagonist of PKA in the cell culture (Genet et al. 2010; Lo et al. 2016). Another study reported that four triterpene acids, oleanolic acid (**326**), maslinic acid (**330**), corosolic acid (**206**), and ursolic acid **52** from allspice (*Pimenta dioica*) unripe fruits and clove (*Syzygium aromaticum*) flower buds, showed TGR5 agonistic activity with EC_{50} of 2.2, 2.7, 0.5, and 1.1 μM, respectively in CRE-luciferase assay (Ladurner et al. 2017). Imperatorin (**331**), a furocoumarin present in many plants including *Angelica dahurica*, acts as TGR5 agonist by increasing glucose uptake in CHO-K1 cells transfected with TGR5 gene. In NCI-H716 cells, it increased intracellular Ca^{2+}-concentration and GLP-1 secretion, and these effects were blocked by triamterene treatment. Moreover, in type 2 diabetic rats, it increased plasma GLP-1 level (Wang et al. 2017a). Nomilin (**332**), present as a major limonoid constituent in many citrus seeds including *Citrus aurantium* and *C. reticulata*, showed strong TGR5 agonistic activity in h-TGR5-transfected HEK293 cell line culture with EC_{50} of 23.6 μM, compared to that of positive control, TLCA of EC_{50} of 1.37 μM, and weak activity for mTGR5 (EC_{50} of 46.2 μM). In silico docking study, it showed good binding interaction with h-TGR5 protein receptor through hydrogen bonding with three amino acid residues, Q77, R80, and Y89 via carbonyl oxygen and furan oxygen functions. Moreover, nomilin on treatment in HFD-fed obese mice reduced body weight gain and serum glucose and insulin levels and enhanced glucose tolerance in obese mice via upregulation of insulin secretion and lipid metabolism (Sasaki et al. 2017; Ono et al. 2011). Sesquiterpene coumarins, farnesiferol B (**333**) and microlobidene (**334**) from *Ferula assa-foetida*, showed TGR5 agonistic activity with EC_{50} of 13.53 and 13.88 μM, respectively, in HEK293 cells transfected with hTGR5 transmid gene (Kirchweger et al. 2018). Alkaloids coptisine (**129**), berberine (**48**), and palmatine (**130**) from *Rhizoma coptidis* enhanced the activity of BAs receptors, FXR and TGR5, in diet induced obese mice to ameliorate hyperlipidemia in mice by suppression of GOT-2

expression and upregulation of mitochondrial function in oxygen consumption and fatty acid oxidation (He et al. 2016).

4.7.10 Inhibition of GSK-3 Activity

Glycogen synthase kinase-3 (GSK-3) is a serine/threonine protein kinase and exists in two isoforms, GSK-3α and GSK-3β, with two distinct genes and both these genes have overlapping roles in the development of human diseases including obesity, type 2 diabetes, neurodegenerative disorders, such as Parkinson disease, Alzheimer disease, and bipolar disorders and cancers (Hansen et al. 1997; Eldar-Finkelman 2002). GSK-3 on overexpression in the skeletal muscle of type 2 diabetic humans promotes the phosphorylation of insulin receptor substrate-1 (IRS-1) at ser 332 site and inhibits the activity of insulin for tyrosine phosphorylation of IRS-1 and thereby causes insulin resistance in type 2 diabetes. The mutation of ser 332 site of IRS-1 enhances insulin-induced tyrosine phosphorylation of IRS-1 (Eldar-Finkelman and Krebs 1997; Liberman and Eldar-Finkelman 2005). Moreover, GSK-3, on overexpression in the skeletal muscle of obese rodents and type 2 diabetic humans impairs insulin stimulated glucose uptake and glycogen synthesis and in the liver increases the glucose production by upregulation of gluconeogenic gene PEPCK. In the skeletal muscle, GSK-3 phosphorylates glycogen synthase (GS) on three specific residues and thereby causes deactivation of GS and inhibits the activity of GS on glucose-6-phosphate in glycogen synthesis. Insulin-stimulated phosphorylated protein kinase B (PKB), also known as Akt or Rac, inhibits the activity of GSK-3 by promoting the phosphorylation at ser 21 in GSK-3α and ser 9 in GSK-3β to stimulate glucose uptake in skeletal muscle via upregulation of GLUT4 translocation into cell membrane and to increase glycogen synthesis via increasing the activity of GS by dephosphorylation and to reduce hepatic glucose production by decreasing the expression of gluconeogenic genes (Cross et al. 1995). Human muscle cell selective inhibitors of GSK-3, namely, lithium chloride and INHs (CHIR98014 and CHIR98023), in human diabetic muscle cells exhibit insulin-like effects on glucose metabolism by increasing glucose uptake and glycogen synthesis. In addition, these GSK-3 inhibitors in obese type 2 diabetic rodents and humans increase glycogen synthesis in skin and adipocytes and reduce hepatic glucose production and decrease hyperphosphorylation of tau proteins and neuronal apoptosis in the brain. Treatment of GSK-3β inhibitor, AR-AO14418 or TX14 (A), in diabetic mice improved the learning deficit in mice by upregulation of synaptophysin, a marker of hippocampal plasticity and preventing the activity of GSK-3β in the brain (Nikoulina et al. 2002; Henriksen and Dokken 2006; King et al. 2013). Therefore, inhibition of GSK-3 activity is a promising strategy in treatment of insulin resistance in obesity and type 2 diabetes. Some natural products have been found effective in the reduction of the activity of GSK-3β in cellular and diabetic animal models. For example, curcumin (**9**) strongly inhibited the activity of GSK-3β with IC_{50} value of 0.0663 μM in an in vitro assay. In vivo, it increased the liver glycogen content through suppression of GSK-3 activity in the liver (Bustanji et al. 2009b). Citrus flavonoids, luteolin (**196**),

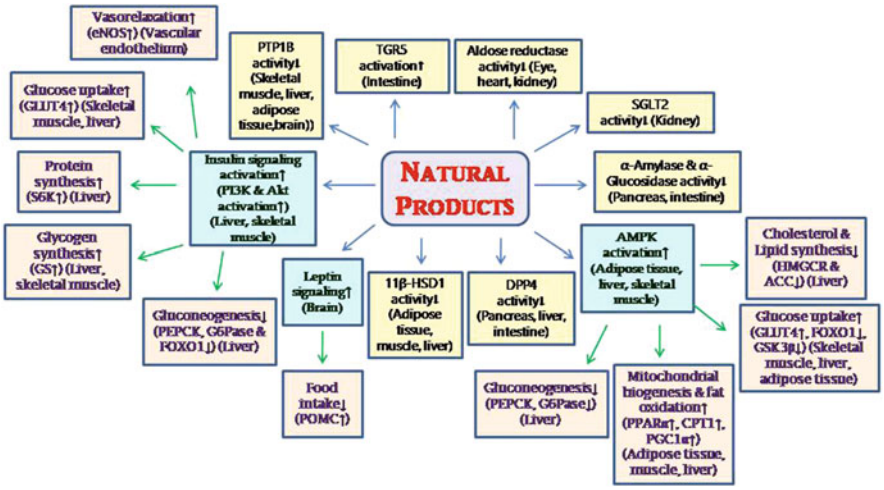

Fig. 4.3 Major therapeutic targets of natural products in diabetes treatment

apigenin (**197**), and quercetin (**23**) inhibited the activity of GSK-3β with IC_{50} of 1.5, 1.9, and 2.0 μM, respectively, in a luminescent kinase assay (Johnson et al. 2011). Accumulating evidence demonstrates that cAMP-dependent activation of PKA promotes the activity of GSK-3β in the upregulation of tyrosinase expression for melanogenesis in murine melanoma B16 cells and human melanocytes. Andrographolide (**335**), a labdane diterpenoid, from *Andrographis paniculata* decreased the melanin content and tyrosinase activity in B16F10 melanoma cells by increasing the phosphorylated level of GSK-3β and decreasing the expression of microphthalmia-associated transcription factor (MITF) in B16F10 cells (Khaled et al. 2002, 2009; Zhu et al. 2015). Polydatin (**336**), a glucoside of resveratrol, from *Polygonum cuspidatum* bark improved hyperglycemia and hyperlipidemia in diabetic rats by increasing the phosphorylation level of GSK-3β and decreasing the expression of G6Pase and SREBP-1c via insulin-dependent Akt activation in diabetic liver and HepG2 cells (Hao et al. 2014). A fraction from Chinese antidiabetic plant, *Sinocrassula indica*, inhibited the activity of GSK-3β and promoted glucose metabolism by upregulation of GLUT4 translocation in skeletal muscle of diabetic KK-Ay mice and in L6 myotubes and H411E hepatocytes via increasing the phosphorylation of GSK-3β (Yin et al. 2009). The major therapeutic targets of natural products against diabetes are presented in Fig. 4.3.

4.8 Natural Products Isolated from Various Natural Sources in Diabetes Treatment

Several natural products including the extracts from plants, dietary seaweeds, mushrooms, and various types of phytochemicals have been reported to exhibit antidiabetic activity in both cellular and animal models. These dietary natural

extracts and phytochemicals may provide a better and more efficient therapeutic approach to treat diabetes with minimal adverse effects. A few review articles highlighted the antidiabetic effect of some selected plants and phytochemicals. A list of plants, seaweeds, and mushrooms having antidiabetic efficacy and their main active components and mechanism of actions in treatment of diabetes is provided in Table 4.2.

Table 4.2 prepared on the basis of literature demonstrates that the plants belonging to 48 families, seaweeds from 5 families, and mushrooms from 8 families showed significant antidiabetic effects in cellular and animal models of diabetes. Among the plant families, the 14 families, namely, Apiaceae, Apocynaceae, Asteraceae, Cucurbitaceae, Dioscoreaceae, Fabaceae, Lamiaceae, Menispermaceae, Moraceae, Myrtaceae, Oleaceae, Oxalidaceae, Rhizophoraceae, and Rutaceae, contain large numbers of antidiabetic plants compared with other plant families. Moreover, some plants from other families, such as *Pandanus tectorius* from Pandanaceae, *Dendrobium officinale* from Orchidaceae, *Phyllanthus niruri* from Phyllanthaceae, *Plantago asiatica* from Plantaginaceae, *Nigella sativa* from Ranunculaceae, *Eriobotrya japonica* from Rosaceae, *Mimusops elengi* from Sapotaceae, and *Lycium barbarum* from Solaniaceae have potential antidiabetic effect. From these antidiabetic plants, the bioactive phytochemicals, namely, polysaccharides, flavonoids, terpenoids, alkaloids, and phenolic acids, modulate the activity of insulin via activation of AMPK and Akt in the skeletal muscle, liver, and adipose tissue for glucose uptake by upregulation of GLUT4 proteins in the skeletal muscle, liver, and adipose tissue and GLUT2 proteins in the liver and glucose utilization by glycogen synthesis by upregulation of GS enzyme activity in the liver. Moreover, insulin signaling inhibits hepatic glucose production through suppression of the expression of gluconeogenic genes, G6Pase and PEPCK. The AMPK activation in skeletal muscle, adipose tissue, and liver reduces dyslipidemia by increasing hydrolysis (lipolysis) of TG and fatty acid oxidation and decreasing the synthesis of fatty acids and cholesterol by regulation of related genes. These plant extracts and their active constituents improve insulin secretion from pancreatic β-cells and β-cell regeneration by suppression of oxidative stress, inflammation, and β-cell apoptosis through upregulation of the activity of antioxidant enzymes, SOD, CAT, and GP_X, and glucose-dependent insulin signaling pathway in pancreas. Moreover, the bioactive plant extracts/phytochemicals inhibit the activity of dietary carbohydrate digestive enzymes, α-amylase, and α-glucosidase. Some plant extracts inhibit the expression and activity of GSK-3β to promote glycogen synthesis in the liver and skeletal muscle. Various phlorotannins and polysaccharides from seaweeds, *Ecklonia cava*, *Ishige okamurae*, *Laminaria japonica*, and *Sargassum patens* reduce intestinal carbohydrates absorption by inhibition of the activity of α-amylase and α-glucosidase. Several identified and unidentified polysaccharides from mushrooms, *Agaricus bisporus*, *Cordyceps militaris*, *Ganoderma atrum*, *Hericium erinaceus*, *Grifola frondosa*, *Inonotus obliquus*, *Pleurotus pulmonarius*, and other *Pleurotus* spp., *P. florida* and *P. eryngii*, improve insulin secretion and insulin action for improvement of hyperglycemia and hyperlipidemia in diabetic animals. Possibly, these polysaccharides increase the fermentation process in gut by

gut microbiota for production of SCFAs to promote incretins secretion from intestinal L and K cells for insulin secretion from pancreas and insulin action in the metabolic tissues, liver, muscle, and adipose tissue. Fucoidans and proteins from marine animals, sea cucumbers, and terpenoids from marine sponges also exhibit potential insulin-like effect by activation of insulin signaling in diabetic rats and in in vitro assays. Therefore, these dietary plants, seaweeds, mushrooms, and marine animals could be utilized as nutraceuticals and diet supplements for treatment and prevention of diabetes.

4.9 Summary and Future Perspectives

Both obesity and its associated diabetes are complex metabolic disorders and caused by the interactions of genetic, epigenetic, dietary, lifestyle, and environmental factors. In the last three decades, the number of people with obesity and diabetes is increased rapidly in an alarming rate worldwide, about more than doubled, making these diseases as emergency health hazard to all nations. Currently, many synthetic drugs are being used for management of these diseases. Most of these drugs have harmful side effects and limit their utilization. The use of natural/herbal medicines for the treatment of various diseases has a long and extensive history. For this reason, the phytomedicines are considered to be used as a first choice of safe and low cost drugs as an alternative. Several polyherbal formulations prepared on the basis of traditional ethnobotanical and ethnopharmacological knowledge have been found potential antiobesity and antidiabetic effects. These polyherbal formulations contain various types of bioactive phytochemicals, which act in multiple targets for amelioration of these diseases. However, detail scientific knowledge on the composition and contents of phytochemicals present in them and their mode of actions is inadequate. As a result, the pharmacologists fail to prepare the formulations to get maximum efficacy from these herbal formulations. Several factors, such as cultivar effect, propagation effect, environmental factors (soil, climatic condition, geographical location, etc.), harvesting effect, postharvest storage effect, and packaging effect, are responsible for the composition and contents of the desired phytochemicals. Hence, adequate knowledge in these areas could be helpful for the farmers/growers to get maximum yields of these phytochemicals in their harvested crops. The extracts from various natural sources, namely, plants, seaweeds, mushrooms, marine animals, and microorganisms, have been reported to have potential antiobesity and antidiabetic effect. According to the literature, the plants from 59 families have been found antiobesity effect. The plant families Apiaceae, Apocynaceae, Araliaceae, Asteraceae, Celastraceae, Dioscoreaceae, Fabaceae, Lamiaceae, Solaniaceae, Theaceae, and Zingiberaceae contribute large number of plants having antiobesity efficacy and have a variety of phytochemicals. Dietary seaweeds from 12 families have significant antiobesity effect. Various sulfated polysaccharides and bromophenols from brown seaweeds/marine algae of families Alariaceae, Ishigaceae, Lessoniaceae, Laminariaceae, Sargassaceae, and Scytosiphonaceae have strong antiobesity effect. The extracts from the fruiting

bodies of edible and medicinal mushrooms from 8 families have significant antiobesity effect. Some dietary marine fishes and cucumbers have antiobesity activity. The extracts from these natural sources act through multiple targets against the pathogenesis of obesity for amelioration of the disease. The major targets are inhibition of the activity of dietary fat-digesting enzyme pancreatic lipase, suppressive effect on appetite, stimulatory effect on energy expenditure, inhibition of adipogenesis, regulation of lipid metabolism, and modulation of gut microbiota composition. These extracts from natural sources stimulate the activation of AMPK and insulin signaling pathway to increase insulin sensitivity in metabolic tissues for suppression of inflammation and synthesis of cholesterol and triglycerides and promotion of fat oxidation and mitochondrial biogenesis and glucose uptake in the liver, skeletal muscle, and adipose tissue, but deactivate AMPK in the hypothalamus in the brain to stimulate leptin signaling for suppression of food intake and in pancreas to stimulate insulin secretion. In addition, these natural polyphenols, polysaccharides and proteins increase the generation of pancreatic β-cells and secretion of insulin from β-cells by TGR5 activation as well as improve the integrity of gut barrier function for protection of the entry of harmful pathogens into systemic circulation and gut microbial activity for production of health-promoting bacteria to increase mucin synthesis, SCFAs production, and GLP-1 secretion from intestine by acting as probiotics and prebiotics.

The available literature on natural products reveal that plants belonging to 48 families, seaweeds from 5 families, and mushrooms from 8 families have been found to possess significant antidiabetic effect. Among them, the plants from families Anacardiaceae, Apiaceae, Apocynaceae, Asteraceae, Cucurbitaceae, Fabaceae, Lamiaceae, Moraceae, Myrtaceae, Oxalidaceae, Rosaceae, and Rutaceae and seaweeds from families Ishigeaceae, Lessoniaceae, and Sargassaceae, as well as mushrooms from families *Ganodermataceae*, *Hericiaceae*, *Hymenochaetaceae*, and *Pleurotaceae*, are in greater numbers compared to other families and have potential antidiabetic effect. The major bioactive phytochemicals of various classes, namely, flavonoids, anthocyanins, alkaloids, polyphenolic acids, tannins, terpenoids, saponins, organosulfur compounds, polyacetylenes, and saponins present in various bioactive natural extracts, act against the pathogenesis of diabetes through multiple targets. Their various bioactive major therapeutic targets include (a) the stimulation of AMPK activation and (b) PI3K/Akt insulin signaling pathway; (c) inhibition of the activity of dietary carbohydrate digesting enzymes α-amylase and α-glucosidase; (d) the inhibition of the activity of renal glucose reabsorption enzyme SGLT2; (e) inhibition of the the activity of DPP4 enzyme, a key enzyme responsible for deactivation of incretins that are secreted from intestinal K and L-cells; (f) inhibition of the activity of PTP1B enzyme, a negative regulator of insulin signaling pathway in peripheral tissues, and leptin signaling in hypothalamic brain; (g) inhibition of the activity of 11β-HSD1, a key regulator for induction of insulin resistance in metabolic tissues via formation of cortisol; (h) inhibition of the activity of GSK-3β, an inhibitor of the activity of the enzyme glycogen synthase (GS) in glycogen synthesis in the liver and muscle; (i) inhibition of the activity of aldose reductase (AR), a key enzyme in RAS activation and in development of diabetic vascular complications, renal

diseases, retinopathy, neuropathy, and myocardial infarction; and (j) activation of TGR5 protein, an agonist of bile acids, which on upregulation in enteroendocrine cells in intestine promotes energy expenditure in BAT to increase the expression of thermogenic genes, including UCP-1 and UCP3. These phytogenic chemicals increase glucose uptake in the liver, adipose tissue, and skeletal muscle by upregulation of GLUT4 expression; promote fat oxidation by upregulation of the expression of PPARα, CPT1, PGC-1α, and their target genes; promote lipolysis by upregulation of the expression of LPL and HSL; and suppress lipid and cholesterol synthesis by downregulation of the expression of ACC, PPARγ, C/EBPα, SREBP-1, SREBP2, FAS, HMGCR, and their target genes.

The most of the reported studies on antiobesity and antidiabetic activities of natural products isolated from various natural sources are not up to the mark for clinical trials in humans. Most of the studies are conducted in cellular and rodent models. The mutation of genes in humans and rodents is not similar and for this reason anomaly in antiobesity and antidiabetic efficacy of natural products in animal and human studies was found. These studies did not investigate the optimal doses, toxicities, and detailed pharmacokinetics of the extracts rich in phytochemicals and requisite maximum concentrations of phytochemicals to get optimum efficacy. Therefore, further research are required on the antiobesogenic and antidiabetic natural extracts and their active components to evaluate their optimum doses and long-term and short-term toxicities in animal models having mimic human genes related to obesity and diabetes. Only, a limited number of natural resources have been chemically and pharmaceutically investigated so far and hence further investigation is necessary for isolation of new drugs from unexplored plants and marine biosources.

References

Aaby K, Skrede G, Wrolstad RE (2005) Phenolic composition and antioxidant activities in fresh and achenes of strawberries (*Fragaria ananassa*). J Agric Food Chem 53:4032–4040

Aaby K, Mazur S, Nes A et al (2012) Phenolic compounds in strawberry (*Fragaria* × *ananassa* Duch.) fruits: composition in 27 cultivars and changes during ripening. Food Chem 132:86–97

Abdelmeguid NE, Fakhoury R, Kamal SM et al (2010) effects of *Nigella sativa* and thymoquinone on biochemical and subcellular changes in pancreatic β-cells of streptozotocin-induced diabetic rats. J Diabetes 2:256–266

Abeyrathna P, Su Y (2015) The critical role of Akt in cardiovascular function. Vascul Pharmacol 74:38–48

Adeneye AA (2012) The leaf and seed aqueous extract of *Phyllanthus amarus* improves insulin resistance diabetes in experimental animal studies. J Ethnopharmacol 144:705–711

Adigun NS, Oladiji AT, Ajiboye TO (2016) Anti-oxidant and anti-hyperlipidemic activity of hydroethanolic seed extract of *Aframomum melegueta* K. Schum in Triton X-100 induced hyperlipidemic rats. South Afr J Bot 105:324–332

Ahmad Z, Zamhuri KF, Yaacob A et al (2012) In vitro anti-diabetic activities and chemical analysis of polypeptide-k and oil isolated from seeds of *Momordica charantia* (bitter gourd). Molecules 17:9631–9640

Ahmed S, Stepp JR, Orians C et al (2014) Effects of extreme climate events on tea (*Camellia sinensis*) functional quality validate indigenous farmer knowledge and sensory preferences in tropical China. PLOS One 9:e109126

Ahn JH, Kim ES, Lee C et al (2013) Chemical constituents from *Nelumbo nucifera* leaves and their anti-obesity effects. Bioorg Med Chem Lett 23:3604–3608

Ajiboye BO, Shonibare MT, Oyinloye BE (2020) Antidiabetic activity of watermelon (*Citrullus lanatus*) juice in alloxan-induced diabetic rats. J Diabetes Metab Dis 19:343–352

Akase T, Shimada T, Harasawa Y et al (2011) Preventive effects of *Salacia reticulata* on obesity and metabolic disorders in TSOD mice. Evid Based Complement Altern Med 2011:484590

Akbarzadeh S, Bazzi P, Daneshi A et al (2012) Anti-diabetic effect of *Otostegia persica* extract on diabetic rats. J Med Plants Res 6:3176–3180

Al-Attar AM, Alsalmi FA (2019) Effect of *Olea europaea* leaves extract on streptozotocin induced diabetes in male albino rats. Soudi J Biol Sci 26:118–128

Aleali AM, Amani R, Shahbazian H et al (2019) The effect of the hydroalcoholic saffron (*Crocus sativus* L.) extract on fasting plasma glucose, HbA1c, lipid profile, liver, and renal function tests in patients with type 2 diabetes mellitus: a randomized double-blind clinical trial. Phytother Res 33:1648–1657

Ali B, Louis MC, Diane V et al (2008) Antidiabetic effects of *Nigella sativa* are mediated by activation of insulin and AMPK pathways, and by mitochondrial uncoupling. Can J Diabetes 32:333

Ali KM, Chatterjee K, De D et al (2011) Efficacy of aqueous extract of seed of *Holarrhena antidysenterica* for the management of diabetes in experimental model rat: a correlative study with antihyperlipidemic activity. Int J Appl Res Nat Prod 2:13–21

Al-Lahham S, Sawafta A, Jaradat N et al (2017) Polar *Curcuma longa* extract inhibits leptin release by adipose tissue derived from overweight and obese people. Eur J Inflamm 15:244–249

Al-Masri IM, Mohammad MK, Taha MO (2009) Inhibition of dipeptidyl peptidase IV (DPP IV) is one of the mechanisms explaining the hypoglycaemic effect of berberine. J Enzyme Inhib Med Chem 24:1061–1066

Al-Shaqha WM, Khan M, Salam N et al (2015) Antidiabetic potential of *Catharanthus roseus* Linn and its effect on the glucose transport gene (GLUT2 and GLUT4) in streptozotocin induced diabetic Wistar rats. BMC Complement Altern Med 15:379

Alvala R, Alvala M, Sama V et al (2013) Scientific evidence for traditional claim of anti-obesity activity of *Tecomella undulata* bark. J Ethnopharmacol 148:441–448

Alves RR, Rosa IM (2007) Biodiversity, traditional medicine and public health: where do they meet ? J Ethnobiol Ethnomed 3:14

Ananda PK, Kumarappan CT, Sunil C et al (2012) Effect of *Biophytum sensitivum* on streptozotocin and nicotinamide-induced diabetic rats. Asian Pac J Trop Biomed 2:31–35

Ann JY, Eo H, Lim Y (2015) Mulberry leaves (*Morus alba* L.) ameliorate obesity-induced hepatic lipogenesis, fibrosis, and oxidative stress in high-fat diet-fed mice. Genes Nutr 10:46

Anoop A, Misra A, Bhatt SP et al (2017) High circulating plasma dipeptidyl peptidase-4 levels in non-obese Asian Indians with type 2 diabetes correlate with fasting insulin and LDL-C levels, triceps skinfolds, total intra-abdominal adipose tissue volume and presence of diabetes: a case control study. BMJ Open Diab Res Care 5:e000393

Aoki K, Maraoka T, Ito Y et al (2010) Comparison of adverse gastrointestinal effects of acarbose and miglitol in healthy men: a crossover study. Inter Med 49:1085–1087

Aoki H, Hanayama M, Mori K et al (2018) *Grifola frondosa* (Maitake) extract activates PPARδ and improves glucose intolerance in high-fat diet-induced obese mice. Biosci Biotechnol Biochem 82:1550–1559

Arai H, Hirasawa Y, Rahman A et al (2010) Alstiphyllanines E-H, picraline and ajmaline-type alkaloids fron *Alstonia macrophylla* inhibiting sodium glucose cotransporter. Bioorg Med Chem 18:2152–2158

Arner A, Bernard S, Salehpour M et al (2011) Dynamics of human adipose lipid turnover in health and metabolic disease. Nature 478:110–113

Asai A, Miyazawa T (2001) Dietary curcuminoids prevent high-fat diet-induced lipid accumulation in rat liver and epididymal adipose tissue. J Nutr 131:2932–2935

Asgary S, Rafieiankopaei M, Sahebkar A et al (2016) Anti-hyperglycemic and anti-hyperlipidemic effects of *Vaccinium myrtillus* fruit in experimentally induced diabetes (antidiabetic effect of *Vaccinium myrtillus* fruit). J Sci Food Agric 96:764–768

Assimopoulou AN, Vuorinen A, Seibert J et al (2015) *Pistacia lentiscus* oleoresin: virtual screening and *in vitro* 11β-hydroxysteroid dehydrogenase 1 inhibition. Planta Med 81:525–532

Atkinson TJ (2008) Central and peripheral neuroendocrine peptides and signaling in appetite regulation: considerations for obesity pharmacotherapy. Obes Rev 9:108–120

Attele AS, Zhou YP, Xie JT et al (2002) Antidiabetic effects of *Panax ginseng* berry extract and the identification of an effective compound. Diabetes 51:1851–1858

Avelino J, Barboza B, Araya JC et al (2005) Effects of slope exposure, altitude and yield on coffee quality in two altitude terroirs of Costa Rica, Orosi and Santa Maria de Dota. J Sci Food Agric 85:1869–1876

Awang AN, Ng JL, Matanjun P et al (2014) Anti-obesity property of the brown seaweed, *Sargassum polycystum* using an in vivo animal model. J Appl Physol 26:1043–1048

Aziz SMA, Ahmed OM, El-Twab SMA et al (2020) Antihyperglycemic effects and mode of actions of *Musa paradisiaca* leaf and fruit peel hydroethanolic extracts in nicotinamide/streptozotocin-induced diabetic rats. Evid Based Complement Altern Med 2020:9276343

Azizian H, Rezvani ME, Esmacilidehaj M et al (2012) Anti-obesity, fat lowering and liver steatosis protective effects of *Ferula asafoetida* gum in type 2 diabetic rats: possible involment of leptin. Iran J Diabetes Obes 4:120–126

Azman KF, Amom Z, Azlan A et al (2012) Antiobesity effect of *Tamarindus indica* L. pulp aqueous extract in high-fat diet-induced obese rats. J Nat Med 66:333–342

Badman MK, Pissios P, Kennedy AR et al (2007) Hepatic fibroblast growth factor 21 is regulated by PPARα and is a key mediator of hepatic lipid metabolism in ketotic states. Cell Metab 5:426–437

Balaji P, Madhanraj R, Rameshkumar K et al (2020) Evaluation of antidiabetic activity of *Pleurotus pulmonarius* against streptozotocin-nicotinamide induced diabetic Wistar albino rats. Saudi J Biol Sci 27:913–924

Balbaa M, El-Zeftawy M, Ghareeb D et al (2016) *Nigella sativa* relieves the altered insulin receptor signaling in streptozotocin-induced diabetic rats fed with a high-fat diet. Oxid Med Cell Longev 2016:2492107

Barbosa HDM, Amaral D, do Nascimento JN et al (2018) *Spondias tuberosa* inner bark extract exerts antidiabetic effects in streptozotocin-induced diabetic rats. J Ethnopharmacol 227:248–257

Baset ME, Ali TI, Elshamy H et al (2020) Anti-diabetic effects of fenugreek (*Trigonella foenum-graecum*): a comparison between oral and intraperitoneal administration-an animal study. Int J Funct Nutr 1:1–8

Baumgartner RR, Steinmann D, Heiss EH et al (2010) Bioactivity-guided isolation of 1,2,3,4,6-penta-*O*-galloyl-D-glucopyranose from *Paeonia lactiflora* roots as a PTP1B inhibitor. J Nat Prod 73:1578–1581

Benhaddou-Andaloussi A, Martineau L, Vuong T et al (2011) The in vivo antidiabetic activity of *Nigella sativa* is mediated through activation of the AMPK pathway and increased muscle Glut4 content. Evid Based Complement Altern Med 2011:538671

Bernal-Mizrachi E, Wen W, Stahlhut S et al (2001) Islet β-cell expression of constitutively active Akt1/PKBα induces striking hypertrophy, hyperplasia and hyperinsulinemia. J Clin Invest 108: 1631–1638

Bhuvaneswari S, Arunkumar E, Viswanathan P et al (2010) Astaxanthin restricts weight gain, promotes insulin sensitivity and curtails fatty liver disease in mice fed a obesity-promoting diet. Process Biochem 45:1406–1414

Bidon-Chanal A, Fuertes A, Alonso D et al (2013) Evidence for a new binding mode to GSK-3β: allosteric regulation by the marine compound palinurin. Eur J Med Chem 60:479–489

Bindhu J, Das A (2019) An edible fungi *Pleurotus ostreatus* inhibits adipogenesis via suppressing expression of PPARγ and C/EBPα in 3T3-L1 cells: in vitro validation of gene knock out of RNAs in PPARγ using CRISPR spcas9. Biomed Pharmacother 116:109030

Birari RB, Bhutani KK (2007) Pancreatic lipase inhibitors from natural sources: unexplored potential. Drug Discovery Today 12:879–889

Birari R, Javia V, Bhutani KK (2010) Antiobesity and lipid lowering effects of *Murraya koenigii* (L.) Spreng leaves extract and mahanimbine on high fat diet induced obese rats. Fitoterapia 81: 1129–1133

Birsoy K, Chen Z, Friedman J (2008) Transcriptional regulation of adipogenesis by KLF4. Cell Metab 7:339–347

Bitou N, Ninomiya M, Tsujita T et al (1999) Screening of lipase inhibitors from marine algae. Lipids 34:441–445

Blessington T, Nzaramba MN, Scheuring DC et al (2010) Cooking methods and storage treatments of potato: effects of carotenoids, antioxidant activity and phenolics. Am J Potato Res 87:479–491

Borgohain MP, Chowdhury L, Ahmed S et al (2017) Renoprotective and antioxidative effects of methanolic *Paederia foetida* leaf extract on experimental diabetic nephropathy in rats. J Ethnopharmacol 198:451–459

Boudjelal A, Henchiri C, Siracusa L et al (2012) Compositional analysis and *in vivo* antidiabetic activity of wild Algerian *Marrubium vulgare* L. infusion. Fitoterapia 83:286–292

Bower AM, Hernandez LMR, Berhow MA et al (2014) Bioactive compounds from culinary herbs inhibit a molecular target for type 2 diabetes management, dipeptidyl peptidase IV. J Agric Food Chem 62:6147–6158

Brandt S, Lugasi A, Barna E et al (2003) Effects of the growing methods and conditions on the lycopene content of tomato fruits. Acta Alimentaria 32:269–278

Brillon DJ, Zheng B, Campbell RG et al (1995) Effect of cortisol on energy expenditure and amino acid metabolism in humans. Am J Physiol 268:E501–E513

Brown EM, Sadarangani M, Finlay BB (2013) The role of the immune system in governing host-microbe interactions in the intestine. Nat Immunol 14:660–667

Brownlee M (2001) Biochemistry and molecular cell biology of diabetic complications. Nature 414:813–820

Bu T, Liu M, Zheng L et al (2010) α-Glucosidase inhibition and the in vitro hypoglycaemic effect of butyl-isobutyl-phthalate derived from the *Laminaria japonica* rhizoid. Phytother Res 24:1588–1591

Buhlmann E, Horvath C, Houriet J et al (2019) *Puerariae lobatae* root extracts and the regulation of brown fat activity. Phytomedicine 64:153075

Bunkrongcheap R, Towatana NH, Noipha K et al (2014) Ivy gourd (*Coccinia grandis* L. Voigt) root suppresses adipocyte differentiation in 3T3-L1 cells. Lipids Health Dis 13:88

Bustanji Y, Taha MO, Al-Masri IM et al (2009a) Docking stimulations and *in vitro* assay unveil potent inhibitory action of papaverine against protein tyrosine phosphatase 1B. Biol Pharm Bull 32:640–645

Bustanji Y, Taha M, Almasri I et al (2009b) Inhibition of glycogen synthase kinase 3 by curcumin: investigation by stimulated molecular docking and subsequent in vitro/in vivo evaluation. J Enzyme Med Chem 24:771–778

Byun MR, Lee CH, Hwang JH et al (2013) Phorbaketal A inhibits adipogenic differentiation through the suppression of PPARγ-mediated gene transcription by TAZ. Eur J Pharmacol 718:181–187

Cai J, Zhao L, Tao W (2015) Potent protein tyrosine phosphatase 1B (PTP1B) inhibiting constituents from *Anoectochilus chapaensis* and molecular docking studies. Pharm Biol 53: 1030–1034

Cai WD, Ding ZC, Wang YY et al (2020) Hypoglycemic benefit and potential mechanism of a polysaccharide from *Hericium erinaceus* in streptozotocin-induced diabetic rats. Process Biochem 88:180–188

Calixto JB (2019) The role of natural products in modern drug discovery. An Acad Bras Cienc 91 (Suppl 3):e20190105

Cani PD (2018) Human gut microbiome: hopes, threats and promises. Gut 67:1716–1725

Carrera-Quintanar L, Lopez Roa RI, Quintero-Fabian S et al (2018) Phytochemicals that influence gut microbiota as prophylactics and for the treatment of obesity and inflammatory diseases. Mediators Inflam 2018:9734845

Cartea ME, Velasco P, Obregon S et al (2008) Seasonal variation in glucosinolate content in *Brassica oleracea* crops grown in northwestern Spain. Phytochemistry 69:403–410

Cazarolli LH, Pereira DF, Kappel VD et al (2013) Insulin signaling: a potential signaling pathway for the stimulatory effect of kaempferitrin on glucose uptake in skeletal muscle. Eur J Pharmacol 712:1–7

Chakrabarti P, Kandror KV (2009) FoxO1 controls insulin-dependent adipose triglyceride lipase (ATGL) expression and lipolysis in adipocytes. J Biol Chem 284:13296–13300

Chakrabarti S, Biswas TK, Seal T et al (2005) Antidiabetic activity of *Caesalpinia bonducella* F. in chronic type 2 diabetic model in long-evans rats and evaluation of insulin secretagogue property of its fractions on isolated islets. J Ethnopharmacol 97:117–122

Chang E, Kim CY (2019) Natural products and obesity: a focus on the regulation of mitotic clonal expansion during adipogenesis. Molecules 24:1157

Chang CJ, Lin CS, Lu CC et al (2015) *Ganoderma lucidum* reduces obesity in mice by modulating the composition of the gut microbiota. Nat Commun 6:7489

Chatterjee K, Ali KM, De D et al (2012) Antidiabetic and antioxidative potencies study of ethyl acetate fraction of hydromethanolic (40:60) extract of seed of *Eugenia jambolana* Linn and its chromatographic purification. J Pharm Res 5:696–703

Chen J, Li WL, Wu JL et al (2008) Euscaphic acid, a new hypoglycemic natural product from *Folium Eriobotryae*. Pharmazie 63:765–767

Chen Y, Jiang Y, Duan J et al (2010) Variation in catechin contents in relation to quality of 'Huang Zhi Xiang' Oolong tea (*Camellia sinensis*) at various growing altitudes and seasons. Food Chem 119:648–652

Chen X, Lou G, Meng Z et al (2011) TGR5: a novel target for weight maintenance and glucose metabolism. J Diabetes Res 2011:853501

Chen S, Song J, Sun C et al (2015) Herbal genomics: examining the biology of traditional medicines. Science 347:527–529

Chen SL, Yu H, Luo HM et al (2016a) Conservation and sustainable use of medicinal plants: problems, progress, and prospects. Chin Med 11:37

Chen L, Zhang Y, Sha O et al (2016b) Hypolipidemic and hypoglycemic activities of polysaccharide from *Pleurotus eryngii* in Kunming mice. Int J Biol Macromol 93:1206–1209

Chen LH, Chien YW, Liang CT et al (2017) Green tea extract induces genes related to browning of white adipose tissue and limits weight gain in high energy diet-fed rat. Food Nutr Res 61: 1347480

Chen W, Zhang N, Zhang G et al (2019a) Differential regulation of anthocyanin synthesis in apple peel under different sunlight intensities. Int J Mol Sci 20:6060

Chen Y, Liu D, Wang D et al (2019b) Hypoglycemic activity and gut microbiota regulation of a novel polysaccharide from *Grifola frondosa* in type 2 diabetic mice. Food Chem Toxicol 126: 295–302

Chen J, Leong PK, Leung HY et al (2020) 48 Biochemical mechanisms of the anti-obesity effect of a triterpenoid-enriched extract of *Cynomorium songaricum* in mice with high-fat-diet-induced obesity. Phytomedicine 73:153038

Cheng AY, Fantus IG (2005) Oral antihyperglycemic therapy for the type 2 diabetes mellitus. Can Med Assoc J 172:213–226

Cheng B, Furtado A, Smyth HE et al (2016) Influence of genotype and environment on coffee quality. Trends Food Sci Technol 57:20–30

Chiu WC, Yang HH, Chiang SC et al (2014) *Auricularia polytricha* aqueous extract supplementation decreases hepatic lipid accumulation and improves anti-oxidative status in animal model of non-alcoholic fatty liver. Biomedicine (Taipei) 4:12

Choi JY, Na M, Huang IH et al (2009) Isolation of betulinic acid, its methyl ester and guaiane sesquiterpenoids with protein tyrosine phosphatise 1B inhibitory activity from the roots of *Saussurea lappa* C B Clarke. Molecules 14:266–272

Choi HD, Kim JH, Chang MJ et al (2011) Effects of astaxanthin on oxidative stress in overweight and obese adults. Phytother Res 25:1813–1818

Choi KM, Lee YS, Shin DM et al (2013) Green tomato extract attenuates high-fat-diet-induced obesity through activation of the AMPK pathway in C57BL/6 mice. J Nutr Biochem 24:335–342

Choi JS, Kim JH, Ali MY et al (2014) *Coptis chinensis* alkaloids exert anti-adipogenic activity on 3T3-L1 adipocytes by downregulating C/EBP-α and PPAR-γ. Fitoterapia 98:199–208

Choi SK, Park S, Jang S et al (2016) Cascade regulation of PPARγ2 and C/EBP signaling pathways by celastrol impairs adipocyte differentiation and stimulates lipolysis in 3T3-L1 adipocytes. Metabolism 65:646–654

Choi KH, Lee HA, Park MH et al (2017) Cyanidin-3-rutinoside increases glucose uptake by activating PI3K/Akt pathway in 3T3-L1 adipocytes. Environ Toxicol Pharmacol 54:1–6

Choi RY, Lee HI, Ham JR et al (2018) Heshouwu (*Polygonum multiflorum* Thunb.) ethanol extract suppresses pre-adipocytes differentiation in 3T3-L1 cells and adipocity in obese mice. Biomed Pharmacother 106:355–362

Chuah LO, Ho WY, Beh BK et al (2013) Updates on antiobesity effect of *Garcinia* origin (-)-HCA. Evid Based Complement Altern Med 2013:751658

Chuang CY, Hsu C, Chao CY et al (2006) Fractionation and identification of 9c,11t,13t-conjugated linolenic acid as an activator of PPARα in bitter gourd (*Momordica charantia* L.). J Biomed Sci 13:763–772

Chung IM, Kim MY, Park WH et al (2008) Aldose reductase inhibitors from *Viola hondoensis* W. Baker et H Boss. Am J Chin Med 36:799–803

Cross DA, Alessi DR, Cohen P et al (1995) Inhibition of glycogen synthase kinase-3 by insulin mediated by protein kinase B. Nature 378:785–789

Daisy P, Rayan NA, Rajathi D (2007) Hypoglycemic and other related effects of *Elephantopus scaber* extracts on alloxan-induced diabetic rats. J Biol Sci 7:433–437

Daisy P, Eliza J, Farook KAMM (2009) A novel dihydroxygymnemic triacetate isolated from *Gymnema sylvestre* possessing normoglycemic and hypolipidemic activity on STZ-induced diabetic rats. J Ethnopharmacol 126:339–344

Dar RA, Shahnawaz M, Rasool S et al (2017) Natural product medicines: a literature update. J Phytopharmacol 6:340–342

Davaatseren M, Hur HJ, Yang HJ et al (2013) *Taraxacum official* (Dandelion) leaf extract alleviates high-fat diet-induced non-alcoholic fatty liver. Food Chem Toxicol 58:30–36

Davis DR, Epp MD, Riordan HD (2004) Changes in USDA food composition data for 43 garden crops, 1950 to 1999. J Am Coll Nutr 23:669–682

De B, Bhandari K, Singla RK et al (2015) Chemometrics optimized extraction procedures, phytosynergistic blending and in vitro screening of natural enzyme inhibitors amongst leaves of Tulsi, Banyan and Jamun. Pharmacogn Mag 11(Suppl 4):S522–S532

Debnath SC, Goyali JC (2020) In vitro propagation and variation of antioxidant properties in micropropagated *Vaccinium* berry plants-a review. Molecules 25:788

Deng L, Chen X, Zhong Y et al (2019a) Activation of TGR5 partially alleviates high-glucose-induced cardiomyocyte injury by inhibition of inflammatory responses and oxidative stress. Oxid Med Cell Longv 2019:6372786

Deng X, Zhang S, Wu J et al (2019b) Promotion of mitochondrial biogenesis via activation of AMPK-PGC1α signaling pathway by ginger (*Zingiber officinale* Roscoe) extract, and its major active component 6-gingerol. J Food Sci 84:2101–2111

Derosa G, Maffioli P (2012) Management of diabetic patients with hypoglycemic agents α-glucosidase inhibitors and their use in clinical practice. Arch Med Sci 8:899–906
Dhanabal SP, Kotake CK, Ramanathan M et al (2006) Hypoglycemic activity of *Pterocarpus marsupium* Roxb. Phytother Res 20:4–8
Dheer R, Bhatnagar P (2010) A study of the antidiabetic activity of *Barleria prionitis* Linn. Ind J Pharmacol 42:70–73
Diaz-Flores M, Angeles-Mejia S, Baize-Gutman LA et al (2012) Effect of an aqueous extract of *Cucurbita ficifolia* Bouche on the glutathione redox cycle in mice with STZ-induced diabetes. J Ethnopharmacol 144:101–108
Diaz-Mula HM, Zapata PJ, Guillen F et al (2009) Changes in hydrophilic and lipophilic antioxidant activity and related bioactive compounds during postharvest storage of yellow and purple plum cultivars. Postharvest Biol Technol 51:354–363
Dicker D (2011) Impact on glycemic control and cardiovascular risk factors. Diabetes Care 34 (Suppl 2):S276–S278
Ding Y, Wang L, Im ST et al (2019) Anti-obesity effect of diphlorethohydroxycarmalol isolated from brown alga *Ishige okamurae* in high-fat diet-induced obese mice. Mar Drugs 17:637
Dogan A, Celik I (2016) Healing effects of sumae (*Rhus coriaria*) in streptozotocin-induced diabetic rats. Pharm Biol 54:2092–2102
Domola MS, Vu V, Robson-Doucette CA et al (2010) Insulin mimetics in *Urtica dioica*: structural and computational analyses of *Urtica dioica* extracts. Phytother Res 24:S175–S182
Dong Y, Jing T, Meng Q et al (2014) Studies on the antidiabetic activities of *Cordyceps militaris* extract in diet-streptozotocin-induced diabetic Sprague-Dawley rats. Biomed Res Int 2014: 160980
Drucker DJ (2006) The biology of incretin hormones. Cell Metab 3:153–165
Drucker DJ, Nauck MA (2006) The incretin system: glucagon-like peptide-1 receptor agonists and dipeptidyl peptidase-4 inhibitors in type 2 diabetes. Lancet 368:1696–1705
Ehrenkranz RRL, Lewis NG, Kahn CR et al (2005) Phlorizin: a review. Diabetes Metab Res Rev 21:31–38
Eid HM, Quchfoun M, Brault A et al (2014) Lingonberry (*Vaccinium vitis-idaca* L.) exhibits antidiabetic activities in a mouse model of diet-induced obesity. Evid Based Complement Altern Med 2014:645812
Eidi A, Eidi M (2009) Antidiabetic effects of sage (*Salvia officinalis* L.) leaves in normal and streptozotocin-induced diabetic rats. Diabetes Metab Syndr: Chin Res Rev 3:40–44
Eidi M, Eidi A, Zamanizadeh H (2005) Effect of *Salvia officinalis* L. leaves on serum glucose and insulin in healthy and streptozotocin-induced diabetic rats. J Ethnopharmacol 100:300–310
Eidi A, Eidi M, Esmaeli E (2006) Antidiabetic effect of garlic (*Allium sativum* L.) in normal and streptozotocin-induced diabetic rats. Phytomedicine 13:624–629
Eidi A, Eidi M, Darzi R (2009) Antidiabetic effect of *Olea europaea* L. in normal and diabetic rats. Phytother Res 23:347–350
Ejaz A, Wu D, Kwan P et al (2009) Curcumin inhibits adipogenesis in 3T3-L1 adipocytes and angiogenesis and obesity in C57/BL mice. J Nutr 139:919–925
Ekanem AP, Wang M, Simon JE et al (2007) Antiobesity properties of two African plants (*Afromomum meleguetta* and *Spilanthes acmella*) by pancreatic lipase inhibition. Phytother Res 21:1253–1255
Elberry AA, Harraz FM, Ghareib SA et al (2015) Methanolic extract of *Marrubium vulgare* ameliorates hyperglycemia and dyslipidemia in streptozotocin-induced diabetic rats. Int J Diabetes Mellitus 3:37–44
El-Beshbishy H, Bahashwan S (2012) Hypoglycemic effect of basil (*Ocimum basilicum*) aqueous extract is mediated through inhibition of α-glucosidase and α-amylase activities: an in vitro study. Toxicol Ind Health 28:42–50
Elchebly M, Payette P, Michaliszyn E et al (1999) Increased insulin sensitivity and obesity resistance in mice lacking the protein tyrosine phosphatase-1B gene. Science 283:1544–1548

Eldar-Finkelman H (2002) Glycogen synthase kinase 3: an emerging therapeutic target. Trends Mol Med 8:126–132

Eldar-Finkelman H, Krebs EG (1997) Phosphorylation of insulin receptor substrate 1 by glycogen synthase kinase 3 impairs insulin action. Proc Natl Acad Sci USA 94:9660–9664

El-Razek FHA, Sadeck EA (2011) Dietary supplementation with watermelon (*Citrullus lanatus)* juice enhances arginine availability and modifies hyperglycemia, hyperlipidemia and oxidative stress in diabetic rats. Aust J Basic Appl Sci 5:1284–1295

El-Tantawy WH (2015) Biochemical effects, hypolipidemic and anti-inflammatory activities of *Artemisia vulgaris* extract in hypercholesterolemic rats. J Clin Biochem Nutr 57:33–38

Eo H, Jeon YJ, Lee M et al (2015) Brown alga *Ecklonia cava* polyphenol extract ameliorates hepatic lipogenesis, oxidative stress, and inflammation by activation of AMPK and SIRT1 in high-fat diet-induced obese mice. J Agric Food Chem 63:349–359

Eo H, Park JE, Jeon YJ et al (2017) Ameliorative effect of *Ecklonia cava* polyphenol extract on renal inflammation associated with aberrant energy metabolism and oxidative stress in high fat diet-induced obese mice. J Agric Food Chem 65:3811–3818

Fabricant DS, Farnsworth NR (2001) The value of plants used in traditional medicine for drug discovery. Environ Health Perspect 109:69–75

Fan J, Johnson MH, Lila MA et al (2013) Berry and citrus phenolic compounds inhibit dipeptidyl peptidase IV: implications in diabetes management. Evid Based Complement Altern Med 2013: 479505

Farsani MK, Amraie E, Kavian P et al (2016) Effects of aqueous extract of alfalfa on hyperglycemia and dyslipidemia in alloxan-induced Wistar rats. Interv Med Appl Sci 8:103–108

Farzami B, Ahmadvand D, Vardasbi S et al (2003) Induction of insulin secretion by a component of *Urtica dioica* leave extract in perifused islets of Langerhans and its in vivo effects in normal and streptozotocin diabetic rats. J Ethnopharmacol 89:47–53

Fasola TR, Ukwenya B, Oyagbemi AA et al (2016) Antidiabetic and antioxidant effects of *Croton lobatus* L. in alloxan-induced diabetic rats. J Intercult Ethnopharmacol 5:364–371

Feng B, Wang T, Zhang Y et al (2005) Aldose reductase inhibitors from *Stellera chamaejasme*. Pharm Biol 43:12–14

Feng Y, Huang SL, Dou W et al (2010) Emodin, a natural product, selectively inhibits 11-β-hydroxysteroid dehydrogenase type 1 and ameliorates metabolic disorder in diet-induced obese mice. Br J Pharmacol 161:113–126

Feng T, Su J, Ding ZH et al (2011) Chemical constituents and their bioactivities of "Tongling white ginger" (*Zingiber officinale*). J Agric Food Chem 59:11690–11695

Fernandes NPC, Lagishetty CV, Panda VS et al (2007) An experimental evaluation of the antidiabetic and antilipidemic properties of a standardized *Momordica charantia* fruit extract. BMC Complement Altern Med 7:29

Finar IL (1995) Organic chemistry, vol 2: stereochemistry and the chemistry of natural products, 5th edn. Longman, Singapore

Fischer AW, Schlein C, Cannon B et al (2019) Intact innervation is essential for diet-induced recruitment of brain adipose tissue. Am J Physiol Endocrinol Metab 316:E487–E503

Flier JS (2004) Obesity wars: molecular progress confronts an expanding epidemic. Cell 116:337–350

Fu C, Jiang Y, Guo J et al (2016) Natural products with anti-obesity effects and different mechanisms of action. J Agric Food Chem 64:9571–9585

Fujisawa T, Ikegami H, Inoue K et al (2005) Effect of two α-glucosidase inhibitors, voglibose and acarbose, on postprandial hyperglycemia correlates with subjective abdominal symptoms. Metabolism 54:387–390

Ganeshpurkar A, Kohli S, Rai G (2014) Antidiabetic potential of polysaccharides from the white oyster culinary-medicinal mushroom *Pleurotus florida* (higher Basidiomycetes). Int J Med Mushrooms 16:207–217

Gao H, Huang YN, Gao B et al (2008) Inhibitory effect on α-glucosidase by *Adhatoda vasica* Nees. Food Chem 108:965–972

Gao HT, Guan T, Li C et al (2012) Treatment of ginger ameliorates fructose-induced fatty liver and hypertriglyceridemia in rats: modulation of the hepatic carbohydrate response element-binding protein-mediated pathway. Evid Based Complement Alternat Med 2012:570948

Gasecka M, Siwulski M, Magdziak Z et al (2020) The effect of drying temperature on bioactive compounds and antioxidant activity of *Leccinum scabrum* (Bull.) Gray and *Hericium erinaceus* (Bull.) Pers. J Food Sci Technol 57:513–525

Genet C, Strehle A, Schmidt C et al (2010) Structure-activity relationship study of betulinic acid, a novel and selective TGR5 agonist and its synthetic derivatives: potential impact in diabetes. J Med Chem 53:178–190

Geu-Flores F, Sherden NH, Courdavault V et al (2012) An alternative route to cyclic terpenes by reductive cyclization in iridoid biosynthesis. Nature 492:138–142

Gharib E, Kouhsari SM (2019) Study of the antidiabetic activity of *Punica granatum* L. fruits aqueous extract on the alloxan-diabetic Wistar rats. Iran J Pharm Res 18:358–368

Ghazanfar K, Ganai BA, Akbar S et al (2014) Antidiabetic activity of *Artemisia amygdalina* Decne in streptozotocin induced diabetic rats. Biomed Res Int 2014:185676

Gigliotti JC, Davenport MP, Beamer SK et al (2011) Extraction and characterization of lipids from Antarctic krill (*Euphausia superba*). Food Chem 125:1028–1036

Gil MI, Tomas-Barberan FA, Hess-Pierce B et al (2002) Antioxidant capacities, phenolic compounds, carotenoids, and vitamin C contents of nectarine, peach, and plum cultivars from California. J Agric Food Chem 50:4976–4982

Gil HW, Lee EY, Lee JH et al (2015) *Dioscorea batatas* extract attenuates high-fat diet-induced obesity in mice by decreasing expression of inflammatory cytokines. Med Sci Monit 21:489–495

Girija K, Lakshman K, Chandrika U et al (2011) Antidiabetic and anticholesterolemic activity of three species of *Amaranthus*. Asian Pac J Trop Biomed 1:133–138

Go HK, Rahman MM, Kim GB et al (2015) Antidiabetic effect of yam (*Dioscorea batatas*) and its active constituent, allantoin, in rat model of streptozotocin-induced diabetes. Nutrients 7:8532–8544

Goli-malekadi N, Asgary S, Rashidi B et al (2014) The protective effects of *Ziziphus vulgaris* L. fruits on biochemical and histological abnormalities induced by diabetes in rats. J Complement Integr Med 11:171–177

Govindarajan R, Asare-Anane H, Persaud S et al (2007) Effect of *Desmodium gangeticum* extract on blood glucose in rats and on insulin secretion *in vitro*. Planta Med 73:427–432

Grasa-Lopez A, Miliar-Garcia A, Quevedo-Corona L et al (2016) *Undaria pinnatifida* and fucoxanthin ameliorate lipogenesis and markers of both inflammation and cardiovascular dysfunction in an animal model of diet-induced obesity. Mar Drugs 14:148

Guillen A, Granados S, Rivas KE et al (2015) Antihyperglycemic activity of *Eucalyptus tereticornis* in insulin-resistant cells and a nutritional model of diabetic mice. Adv Pharmacol Sci 2015:418673

Guo H, Liu G, Zhong R et al (2012) Cyanidin-3-*O*-β-glucoside regulates fatty acid metabolism via an AMP-activated protein kinase-dependent signaling pathway in human HepG2 cells. Lipids Health Dis 11:10

Gupta P, Goyal R, Chauhan Y et al (2013) Possible modulation of FAS and PTP-1B signaling in ameliorative potential of *Bombax ceiba* against high fat diet induced obesity. BMC Complement Altern Med 13:281

Gupta A, Kumar A, Kumar D et al (2017) Ethyl acetate fraction of *Eclipta alba*: a potential phytopharmaceutical targeting adipocyte differentiation. Biomed Pharmacother 96:572–583

Gupta A, Kumar A, Kumar D et al (2018) Ecliptal, a promising natural lead isolated from *Eclipta alba* modulates adipocyte function and ameliorates metabolic syndrome. Toxicol Appl Pharmacol 338:134–147

Hafizur RM, Momim S, Fatima N (2017) Prevention of advanced glycation end-products formation in diabetic rats through beta-cell modulation by *Aegle marmelos*. BMC Complement Altern Med 17:227

Halimi S, Verges B (2014) Adverse effects and safety of SGLT2 inhibitors. Diabetes Metab 40(6 Suppl 1):S28–S34

Hamao M, Matsuda H, Nakamura S et al (2011) Anti-obesity effects of the methanolic extract and chakasaponins from the flower buds of *Camellia sinensis* in mice. Bioorg Med Chem 19:6033–6041

Hamid HA, Yusoff MM, Liu M et al (2015) α-Glucosidase and α-amylase inhibitory constituents of *Tinospora crispa*: isolation and chemical profile confirmation by ultra-high performance liquid chromatography-quadrupole time-of-flight/mass spectrometry. J Funct Foods 16:74–80

Hamza N, Berke B, Cheze C et al (2012) Preventive and curative effect of *Trigonella foenum-graecum* L. seeds in C57BL/6J models of type 2 diabetes induced by high-fat diet. J Ethnopharmacol 142:516–522

Han ML, Shen Y, Wang GC et al (2013) 11β-HSD1 inhibitors from *Walsura cochinchinensis*. J Nat Prod 76:1319–1327

Han JM, Kim MH, Choi YY et al (2015a) Effects of *Lonicera japonica* Thunb on type 2 diabetes via PPAR-γ activation in rats. Phytother Res 29:1616–1621

Han K, Bose S, Kim Y et al (2015b) *Rehmannia glutinosa* reduced waist circumferences of Korean obese women possibly through modulation of gut microbiota. Food Funct 6:2684–2692

Han W, Huang JG, Li X et al (2017) Altitudinal effects on the quality of green tea in east China: a climate change perspective. Eur Food Res Technol 243:323–330

Handayani D, Chen J, Meyer BJ et al (2011) Dietary Shiitake mushroom (*Lentinus edodes*) prevents fat deposition and lowers triglycerides in rats fed a high-fat diet. J Obes 2011:258051

Hansen L, Arden KC, Rasmussen SB et al (1997) Chromosomal mapping and mutational analysis of the coding region of the glycogen synthase kinase-3α and 3β isoforms in patients with NIDDM. Diabetologia 40:940–946

Hao DC, Xiao PG (2015) Genomics and evolution in traditional medicinal plants: road to a healthier life. EBO 11:197–212

Hao J, Chen C, Huang K et al (2014) Polydatin improves glucose and lipid metabolism in experimental diabetes through activating the Akt signaling pathway. Eur J Pharmacol 745: 152–165

Harborne JB, Mabry TJ (1982) The flavonoids: advances in research. Chapman and Hall, London

Hardie DG (2013) AMPK: a target for drugs and natural products with effects on both diabetes and cancer. Diabetes 62:2164–2172

Hardie DG, Carling D, Sim ATR (1989) The AMP-activated protein kinase-a multisubstrate regulator of lipid metabolism. Trends Biochem Sci 14:20–23

Hardie DG, Ross FA, Hawley SA (2012) AMPK-a nutrient and energy sensor that maintains energy homeostasis. Nat Rev Mol Cell Biol 13:251–262

Hattori H, Yamauchi K, Onwona-Agyeman S et al (2017) Effects of the grains of paradise (GP) extract intake on obesity and sympathetic nerve activity. Am J Plant Sci 8:85–95

He WF, Yao LG, Liu HL et al (2014) Thunberol, a new sterol from the Chinese brown alga *Sargassum thunbergii*. J Asian Nat Prod Res 16:685–689

He K, Hu Y, Ma H et al (2016) *Rhizoma coptidis* alkaloids alleviate hyperlipidemia in B6 mice by modulating gut microbiota and bile acid pathways. Biochim Biophys Acta 1862:1696–1709

Henriksen EJ, Dokken BB (2006) Role of glycogen synthase kinase 3 in insulin resistance and type 2 diabetes. Curr Drug Targets 7:1435–1441

Henry-Kirk RA, Plunkett B, Hall M et al (2018) Solar UV light regulates flavonoid metabolism in apple (*Malus* × *domestica*). Plant Cell Environ 41:675–688

Heo SJ, Hwang JY, Choi JI et al (2009) Diphlorethohydroxycarmalol isolated from *Ishige okamurae*, a brown alga, a potent α-glucosidase and α-amylase inhibitor, alleviates postprandial hyperglycemia in diabetic mice. Eur J Pharmacol 615:252–256

Higuchi N, Kato M, Shundo Y et al (2008) Liver X receptor in cooperation with SREBP-1c is a major lipid synthesis regulator in non-alcoholic fatty liver disease. Hepatol Res 38:1122–1129

Hintzpeter J, Stapelfeld C, Loerz C et al (2014) Green tea and one of its constituents, epigallocatechin-3-gallate, are potent inhibitors of human 11β-hydroxysteroid dehydrogenase type 1. PLOS One 9:e84468

Hirata BKS, Banin RM, Dornellas APS et al (2015) *Ginkgo biloba* extract improves insulin signaling and attenuates inflammation in retroperitoneal adipose tissue depot of obese rats. Mediators Inflamm 2015:419106

Hoang DM, Ngoe TM, Dat NT et al (2009) Protein tyrosine phosphatase 1B inhibitors isolated from *Morus bombycis*. Bioorg Med Chem Lett 19:6759–6761

Hoang NTT, Golding JB, Wilkes MA (2011) The effect of postharvest 1-MCP treatment and storage atmosphere on Çripps Pink' apple phenolics and antioxidant activity. Food Chem 127: 1249–1256

Hong L, Xun M, Wutong W (2007) Antidiabetic effect of an α-glucan from fruit body of maitake (*Grifola frondosa*) on KK-Ay mice. J Pharm Pharmacol 59:575–582

Houmard JA (2008) Intramuscular lipid oxidation and obesity. Am J Physiol-Regulatory Integr Comp Physiol 294:R1111–R1116

Hsia DS, Grove O, Cefalu WT (2017) An update on SGLT2 inhibitors for the treatment of diabetes mellitus. Curr Opin Endocrinol Diabetes Obes 24:73–79

Hsu HM, Chen WY, Hu TK et al (2014) Supplementation of *Vitis thunbergii* root extract alleviated high-fat diet-induced obesity in C57BL/6J mice. Biosci Biotechnol Biochem 78:867–873

Hu J, Zhu X, Han L et al (2008) Anti-obesity effects of escins extracted from the seeds of *Aesculus turbinata* Blume (Hippocastanaceae). Chem Pharm Bull 56:12–16

Hu GX, Lin H, Lian QQ et al (2013) Curcumin as a potent and selective inhibitor of 11-β-hydroxysteroid dehydrogenase 1: improving lipid profiles in high-fat-diet-treated rats. PLOS One 8:e49976

Hu S, Xu L, Shi D et al (2014) Eicosapentaenoic acid-enriched phosphatidylcholine isolated from *Cucumaria frondosa* exhibits anti-hyperglycemic effects via activating phosphoinositide-3-kinase/protein kinase B signal pathway. J Biosci Bioeng 117:457–463

Hu S, Li S, Song W et al (2016a) Fucoidan from *Cucumaria frondosa* inhibits pancreatic islets apoptosis through mitochondrial signaling pathway in insulin resistant mice. Food Sci Technol Res 22:507–517

Hu X, Tao N, Wang X et al (2016b) Marine-derived bioactive compounds with anti-obesity effect: a review. J Funct Foods 21:372–387

Huang THW, Peng G, Li GQ et al (2006) *Salacia oblonga* root improves postprandial hyperlipidemia and hepatic steatosis in Zucker diabetic fatty rats: activation of PPAR-α. Toxicol Appl Pharmacol 210:225–235

Huang SL, Yu RT, Gong J et al (2012) Arctigenin, a natural compound, activates AMP-activated protein kinase via inhibition of mitochondria complex I and ameliorates metabolic disorders in ob/ob mice. Diabetologia 55:1469–1481

Huang KA, Huang YJ, Kim GR et al (2015) Extracts from *Aralia elata* (Miq.) Seem alleviate hepatosteatosis via improving hepatic insulin sensitivity. BMC Complement Altern Med 15:347

Huh JY, Lee S, Ma EB et al (2018) The effects of phenolic glycosides from *Betula platyphylla* var. *japonica* on adipocyte differentiation and mature adipocyte metabolism. J Enz Inhib Med Chem 33:1167–1173

Hwang YP, Choi JH, Kim HG et al (2013) Saponins from *Platycodon grandiflorum* inhibit hepatic lipogenesis through induction of SIRT1 and activation of AMP-activated protein kinase in high-glucose-induced HepG2 cells. Food Chem 140:115–123

Ibarra A, He K, Bily A et al (2010) Rosemary extract enriched in carnosic acid shows anti-obesity and anti-diabetic effects on *in vitro* and *in vivo* models. Planta Med 76:P565

Ibarra A, Cases J, Roller M et al (2011) Carnosic acid-rich rosemary (*Rosmarinus officinalis* L.) leaf extract limits weight gain and improves cholesterol levels and glycemia in mice on a high-fat diet. Br J Nutr 106:1182–1189

Iftikhar A, Aslam B, Iftikhar M et al (2020) Effect of *Caesalpinia bonduc* polyphenol extract on alloxan-induced diabetic rats in attenuating hyperglycemia by upregulating insulin secretion and inhibiting JNK signaling pathway. Oxid Med Cell Longev 2020:9020219

Ikarashi N, Toda T, Okaniwa T et al (2011) Anti-obesity and anti-diabetic effects of *Acacia* polyphenol in obese diabetic KK-Ay mice fed high-fat diet. Evid Based Complement Altern Med 2011:952031

Ikeuchi M, Koyama T, Takahashi J et al (2007) Effects of astaxanthin in obese mice fed a high-fat diet. Biosci Biotechnol Biochem 71:893–899

Inoue N, Inafaku M, Shirouchi B et al (2013) Effect of Mukitake mushroom (*Panellus serotinus*) on the pathogenesis of lipid abnormalities in obese diabetic ob/ob mice. Lipids Health Dis 12:18

Irudayaraj SS, Christudas S, Antony S et al (2017) Protective effects of *Ficus carica* leaves on glucose and lipid levels, carbohydrate metabolism enzymes and β-cells in type 2 diabetic rats. Pharm Biol 55:1074–1081

Ishak NA, Ismail M, Hamid M et al (2013) Antidiabetic and hypolipidemic activities of *Curculigo latifolia* fruit: root extract in high fat fed diet and low dose STZ induced diabetic rats. Evid based Complement Altern Med 2013:601838

Islam MN, Jung HA, Sohn HS et al (2013) Potent α-glucosidase and protein tyrosine phosphatase 1B inhibitors from *Artesimia capillaris*. Arch Pharm Res 36:542–552

Jadeja RN, Thounaojam MC, Ramani UV et al (2011) Anti-obesity potential of *Clerodendron glandulosum* Coleb leaf aqueous extract. J Ethnopharmacol 135:338–343

Jaffar SK, Khasim SM, Guru Prasad M et al (2011) Hypoglycemic activity of ethanolic leaf extract of *Mimusops elengi* Linn in streptozotocin induced diabetic rats. The Bioscan 6:673–679

Jagtap S, Khare P, Mangal P et al (2016) Protective effects of phyllanthin, a lignan from *Phyllanthus amarus* against progression of high fat diet induced metabolic disturbances in mice. RSC Adv 6:58343–58353

Jain V, Viswanatha GL, Manohar D et al (2012) Isolation of antidiabetic principle from fruit rinds of *Punica granatum*. Evid Based Complement Altern Med 2012:147202

Jaiswal YS, Tatke PA, Gabhe SY et al (2017) Antidiabetic activity of extracts of *Anacardium occidentale* Linn leaves on n-streptozotocin diabetic rats. J Tradit Complement Med 7:421–427

Jambocus NGS, Saari N, Ismail A et al (2016) An investivation into the anti-obesity effects of *Morinda citrifolia* L. leaf extract in high fat diet induced obese rats using a ^{1}H NMR metabolomic approach. J Diabetes Res 2016:2391592

Jang WS, Choung SY (2013) Antiobesity effects of the ethanol extract of *Laminaria japonica* Areshoung in high-fat diet-induced obese rats. Evid Based Complement Altern Med 2013: 492807

Jang DS, Yoo NH, Kim NH et al (2010) 3,5-Di-*O*-caffeoyl-*epi*-quinic acid from the leaves and stems of *Erigeron annuus* inhibits protein glycation, aldose reductase, and cataractogenesis. Biol Pharm Bull 33:329–333

Jayaprakasam B, Olson LK, Schutzi RE et al (2006) Amelioration of obesity and glucose intolerance in high-fat-fed C57BL/6 mice by anthocyanins and ursolic acid in cornelian cherry (*Cornus mas*). J Agric Food Chem 54:243–248

Jemai H, Feki AE, Sayadi S (2009) Antidiabetic and antioxidant effects of hydroxytyrosol and oleuropein from olive leaves in alloxan-diabetic rats. J Agric Food Chem 57:8798–8804

Jeon G, Choi Y, Lee SM et al (2010) Anti-obesity activity of methanol extract from hot pepper (*Capsicum annuum* L.) seeds in 3T3-L1 adipocyte. Food Sci Biotechnol 19:1123–1127

Jeong HJ, Yoon SJ, Pyun YR (2008) Polysaccharides from edible mushroom hinmogi (*Tremella fuciformis*) inhibit differentiation of 3T3-L1 adipocytes by reducing mRNA expression of PPARγ, C/EBPα, and leptin. Food Sci Biotechnol 17:267–273

Jeong SC, Jeong YT, Yang BK et al (2010) White buttom mushroom (*Agaricus bisporus*) lowers blood glucose and cholesterol levels in diabetic and hypercholesterolemic rats. Nutr Res 30:49–56

Jeong EY, Cho KS, Lee HS (2012) α-Amylase and α-glucosidase inhibitors isolated from *Tritium aestivum* L. sprouts. J Korean Soc Appl Biol Chem 55:47–51

Jeong EJ, Jegal J, Ahn J et al (2016) Antiobesity effect of *Dioscorea oppositifolia* extract in high-fat diet-induced obese mice and its chemical characterization. Biol Pharm Bull 39:409–414

Ji S, Li Z, Song W et al (2016) Bioactive constituents of *Glycyrrhiza uralensis* (Licorice): Discovery of the effective components of a traditional herbal medicine. J Nat Prod 79:281–292

Jiang S, Du P, An L et al (2013) Antidiabetic effect of *Coptis chinensis* polysaccharide in high-fat diet with STZ-induced diabetic mice. Int J Biol Macromol 55:118–122

Jiao WH, Li J, Zhang NM et al (2019) Frondophysins A and B, unprecedented terpenoid-alkaloid bioconjugates from *Dysidea frondosa*. Org Lett 21:6190–6193

Jin H, Lee K, Chei S et al (2020) *Ecklonia stolonifera* extract suppresses lipid accumulation by promoting lipolysis and adipose browning in high-fat diet-induced obese male mice. Cells 9:871

Johnson JL, Rupasinghe SG, Stefani F et al (2011) Citrus flavonoids luteolin, apigenin and quercetin inhibit glycogen synthase kinase-3β enzymatic activity by lowering the interaction energy within the binding cavity. J Med Food 14:325–333

Jones RB, Faragher JD, Winkler S (2006) A review of the influence of postharvest treatments on quality and glucosinolate content in broccoli (*Brassica oleracea* var. *italica*) heads. Postharvest Biol Technol 41:1–8

Jung SH, Lee YS, Lee S et al (2002) Isoflavonoids from the rhizomes of *Belamcanda chinensis* and their effects on aldose reductase and sorbitol accumulation in streptozotocin induced diabetic rat tissues. Arch Pharm Res 25:306–312

Jung M, Park M, Lee HC et al (2006) Antidiabetic agents from medicinal plants. Curr Med Chem 13:1203–1218

Jung SH, Lee JM, Lee HJ et al (2007) Aldose reductase and advanced glycation endproducts inhibitory effect of *Phyllostachys nigra*. Biol Pharm Bull 30:1569–1572

Jung HA, Islam MN, Kwon YS et al (2011) Extraction and identification of three major aldose reductase inhibitors from *Artemisia montana*. Food Chem Toxicol 49:376–384

Jung CH, Jang SJ, Ahn J et al (2012a) *Alpinia officinarum* inhibits adipocyte differentiation and high-fat diet-induced obesity in mice through regulation of adipogenesis and lipogenesis. J Med Food 15:959–967

Jung HA, Islam MN, Lee CM et al (2012b) Promising antidiabetic potential of fucoxanthin isolated from the edible brown algae *Eisenia bicyclis* and *Undaria pinnatifida*. Fish Sci 78:1321–1329

Jung SA, Choi M, Kim S et al (2012c) Cinchonine prevents high-fat-diet-induced obesity through downregulation of adipogenesis and adipose inflammation. PPAR Res 2012:541204

Jung HA, Jung HJ, Jeong HY et al (2014a) Anti-adipogenic activity of the edible brown alga *Ecklonia stolonifera* and its constituent fucosterol in 3T3-L1 adipocytes. Arch Pharm Res 37: 713–720

Jung HA, Jung HJ, Jeong HY et al (2014b) Phlorotannins isolated from the edible brown alga *Ecklonia stolonifera* exert anti-adipogenic activity on 3T3-L1 adipocytes by downregulating C/EBPα and PPARγ. Fitoterapia 92:260–269

Kadota S, Basnet P, Hase K et al (1994) Matteuorienate A and B, two new and potent aldose reductase inhibitors from *Matteuccia orientalis* (Hook.) Trev. Chem Pharm Bull 42:1712–1714

Kaleem M, Kirmani D, Asif M et al (2006) Biochemical effects of *Nigella sativa* L seeds in diabetic rats. Ind J Exp Biol 44:745–748

Kamalakkannan N, Prince PSM (2005) The effect of *Aegle marmelos* fruit extract in streptozotocin diabetes. J Herbal Pharmacother 5:87–96

Kanagasabapathy G, Kuppusamy UR, Malek SNA et al (2012) Glucan-rich polysaccharides from *Pleurotus sajor-caju* (fr.) Singer prevents glucose intolerance, insulin resistance and inflammation in C57BL/6J mice fed a high-fat diet. BMC Complement Alternat Med 12:261

Kanagasabapathy G, Malek SNA, Mahmood AA et al (2013) Beta-glucan-rich extract from *Pleurotus sajor-caju* (Fr.) Singer prevents obesity and oxidative stress in C57BL/6J mice fed on a high-fat diet. Evid Based Complement Alternat Med 2013:185259

Kanamoto Y, Yamashita Y, Nanba F et al (2011) A black soybean seed coat extract prevents obesity and glucose intolerance by up-regulating uncoupling proteins and down-regulating inflammatory cytokines in high-fat diet-fed mice. J Agric Food Chem 59:8985–8993

Kang C, Yin JB, Lee H et al (2010a) Brown alga *Ecklonia cava* attenuates type 1 diabetes by activating AMPK and Akt signaling pathways. Food Chem Toxicol 48:509–516

Kang JH, Tsuyoshi G, Han IS et al (2010b) Dietary capsaicin reduces obesity-induced insulin resistance and hepatic steatosis in obese mice fed a high-fat diet. Obesity (Silver Spring) 18: 780–787

Kang SI, Kim MH, Shin HS et al (2010c) a water-soluble extract of *Petalonia binghamiae* inhibits the expression of adipogenic regulators in 3T3-L1 preadipocytes and reduces adiposity and weight gain in rats fed a high-fat diet. J Nutr Biochem 21:1251–1257

Kang SI, Shin HS, Kim HM et al (2012a) Anti-obesity properties of a *Sasa quelpaertensis* extract in high-fat diet-induced obese mice. Biosci Biotechnol Biochem 76:755–761

Kang SI, Shin YS, Kim YM et al (2012b) *Petalonia kinghamiae* extract and its constituent fucoxanthin ameliorate high-fat diet-induced obesity by activating AMP-activated protein kinase. J Agric Food Chem 60:3389–3395

Kang SW, Kang SI, Shin HS et al (2013) *Sasa quelpaertensis* Nakai extract and its constituent p-coumaric acid inhibit adipogenesis in 3T3-L1 cells through activation of the AMPK pathway. Food Chem Toxicol 59:380–385

Kang MC, Kang N, Kim SY et al (2016) Popular edible seaweed, *Gelidium amansii* prevents against diet-induced obesity. Food Chem Toxicol 90:181–187

Kang JH, Ha L, Kim HJ et al (2017) *Gelidium amansii* ethanol extract suppresses fat accumulation by down-regulating adipogenic transcription factors in diet-induced obese mice. Nutr Res Pract 11:17–24

Kanthlal SK, Suresh V, Arunachalam G et al (2012) Anti-obesity and hypolipidemic activity of methanol extract of *Tabernaemontana divaricata* on atherogenetic diet induced obesity in rats. Int Res J Pharm 3:157–161

Karki H, Upadhayay K, Pal H et al (2014) Antidiabetic potential of *Zanthoxylum aromatum* bark extract on streptozotocin-induced diabetic rats. Int J Green Pharm 8:77–83

Karmase A, Birari R, Bhutani KK (2013a) Evaluation of anti-obesity effect of *Aegle marmelos* leaves. Phytomedicine 20:805–812

Karmase A, Jagtap S, Bhutani KK (2013b) Anti-adipogenic activity of *Aegle marmelos* Correa. Phytomedicine 20:1267–1271

Karri S, Sharma S, Hatware K et al (2019) Natural antiobesity agents and their therapeutic role in management of obesity: a future trend perspective. Biomed Pharmacother 110:224–238

Karsono AH, Tandrasasmita OM, Tjandrawinata RR (2019) Bioactive fraction from *Lagerstroemia speciosa* leaves (DLBS3733) reduces fat droplets by inhibiting adipogenesis and lipogenesis. J Exp Pharmacol 11:39–51

Karthiyayini T, Kumar R, Senthilkumar KL et al (2009) Evaluation of antidiabetic and hypolipidemic effect of *Cucumis sativus* fruit in streptozotocin-induced diabetic rats. Biomed Pharmacol J 2:351–355

Karuna R, Bharathi VG, Reddy SS et al (2011) Protective effects of *Phyllanthus amarus* aqueous extract against renal oxidative stress in streptozotocin-induced diabetic rats. Ind J Pharmacol 43: 414–418

Kasimu R, Tanaka K, Tezuka Y et al (1998) Comparative study of seventeen *Salvia* plants: aldose reductase inhibitory activity of water and MeOH extracts and liquid chromatography-mass spectrometry (LC-MS) analysis of water extracts. Chem Pharm Bull 46:500–504

Kaur N, Kishore L, Singh R (2016) Antidiabetic effect of new chromane isolated from *Dillenia indica* L. leaves in streptozotocin induced diabetic rats. J Funct Foods 22:547–555

Kawamura-Konishi Y, Watanabe N, Saito M et al (2012) Isolation of a new phlorotannin, a potent inhibitor of carbohydrate-hydrolyzing enzymes, from the brown alga *Sargassum patens*. J Agric Food Chem 60:5565–5570

Kelley DE, Goodpaster BH, Storlien L (2002) Muscle triglyceride and insulin resistance. Annu Rev Nutr 22:325–346

Keshari AK, Kumar G, Kushwaha PS et al (2016) Isolated flavonoids from *Ficus racemosa* stem bark possess antidiabetic, hypolipidemic and protective effects in albino Wistar rats. J Ethnopharmacol 181:252–262

Khaled M, Larribere L, Bille K et al (2002) Glycogen synthase kinase 3β is activated by cAMP and plays an active role in the regulation of melanogenesis. J Biol Chem 277:33690–33697

Khan MF, Dixit P, Jaiswal N et al (2012) Chemical constituents of *Kigelia pinnata* twigs and their GLUT4 translocation modulating effects in skeletal muscle cells. Fitoterapia 83:125–129

Khani S, Tayek JA (2001) Cortisol increases gluconeogenesis in humans: its role in the metabolic syndrome. Clin Sci 101:739–747

Khattab HAH, El-Shitany NA, Abdallah IZA et al (2015) Antihyperglycemic potential of *Grewia asiatica* fruit extract against streptozotocin-induced hyperglycemia in rats: anti-inflammatory and antioxidant mechanisms. Oxid Med Cell Longev 2015:549743

Kim H, Choung SY (2012) Anti-obesity effects of *Boussingaulti gracilis* Miers var. *pseudobaselloides* Bailey via activation of AMP-activated protein kinase in 3T3-L1 cells. J Med Food 15:811–817

Kim MJ, Kim HK (2009) *Perilla* leaf extract ameliorates obesity and dyslipidemia induced by high-fat diet. Phytother Res 23:1685–1690

Kim MJ, Kim HK (2012) Insulinotrophic and hypolipidemic effects of *Ecklonia cava* in streptozotocin-induced diabetic mice. Asian Pac J Trop Med 5:374–379

Kim KJ, Lee BY (2012) Fucoidan from the sporophyll of *Undaria pinnatifida* suppresses adipocyte differentiation by inhibition of inflammation-related cytokines in 3T3-L1 cells. Nutr Res 32: 439–442

Kim HK, Della-Fera MA, Lin J et al (2006) Docosahexaenoic acid inhibits adipocyte differentiation and induces apoptosis in 3T3-L1 preadipocytes. J Nutr 136:2965–2969

Kim Y, Brecht JK, Talcott ST (2007) Antioxidant phytochemical and fruit quality changes in mango (*Magnifera indica* L.) following hot water immersion and controlled atmosphere storage. Food Chem 105:1327–1334

Kim KY, Lee HN, Kim YJ et al (2008a) *Garcinia cambogia* extract ameliorates visceral adiposity in C57BL/6J mice fed on a high-fat diet. Biosci Biotechnol Biochem 72:1772–1780

Kim SJ, Jung JY, Kim HW et al (2008b) Antiobesity effects of *Juniperus chinensis* extract are associated with increased AMP-activated protein kinase expression and phosphorylation in the visceral adipose tissue of rats. Biol Pharm Bull 31:1415–1421

Kim J, Jang DS, Kim H et al (2009) Anti-lipase and lipolytic activities of ursolic acid isolated from the roots of *Actinidia arguta*. Arch Pharm Res 32:983–987

Kim JI, Kang MJ, Im J et al (2010) Effect of king oyster mushroom (*Pleurotus eryngii*) on insulin resistance and dyslipidemia in db/db mice. Food Sci Biotechnol 19:239–242

Kim DY, Kim MS, Sa BK et al (2012a) *Boesenbergia pandurata* attenuates diet-induced obesity by activating AMP-activated protein kinase and regulating lipid metabolism. Int J Mol Sci 13:994–1005

Kim HK, Kim JN, Han SN et al (2012b) Black soybean anthocyanins inhibit adipocyte differentiation in 3T3-L1 cells. Nutr Res 32:770–777

Kim KBWR, Jung JY, Cho JY et al (2012c) Lipase inhibitory activity of ethyl acetate fraction from *Ecklonia cava* extracts. Biotechnol Bioprocess Eng 17:739–745

Kim I, Kim HR, Kim JH et al (2013) Beneficial effects of *Allium sativum* L. stem extract on lipid metabolism and antioxidant status in obese mice fed a high-fat diet. J Sci Food Agric 93:2749–2757

Kim KT, Rious LE, Turgeon SL (2014) Alpha-amylase and alpha-glucosidase inhibition is differentially modulated by fucoidan obtained from *Ficus vesiculosus* and *Ascophyllum nodosum*. Phytochemistry 98:27–33

Kim SY, Wi HR, Choi S et al (2015) Inhibitory effect of anthocyanin-rich black soybean testa (*Glycine max* (L.) Merr.) on the inflammation-induced adipogenesis in a DIO mouse model. J Funct Foods 14:623–633

Kim JH, Kim OK, Yoon HG et al (2016) Anti-obesity effect of extract from fermented *Curcuma longa* L. through regulation of adipogenesis and lipolysis pathways in high-fat diet-induced obese rats. Food. Nutr Res 60:30428

Kim T, Kim MB, Kim C et al (2016a) Standardized *Boesenbergia pandurata* extract stimulates exercise endurance through increasing mitochondrial biogenesis. J Med Food 19:692–700

Kim YJ, Choi JY, Ryu R et al (2016b) *Platycodon grandiflorus* root extract attenuates body fat mass, hepatic steatosis, and insulin resistance through the interplay between the liver and adipose tissue. Nutrients 8:532

Kim J, Lee H, Lim J et al (2017) The angiogenesis inhibitor ALS-L1023 from lemon balm leaves attenuates high-fat diet-induced non-alcoholic fatty liver disease through regulating the visceral adipose tissue function. Int J Mol Sci 18:846

Kim JW, Lee YS, Seol DJ et al (2018a) Anti-obesity and fatty liver-preventing activities of *Lonicera caerulea* in high-fat diet-fed mice. Int J Mol Med 42:3047–3064

Kim S, Lee MS, Jung S et al (2018b) Ginger extract ameliorates obesity and inflammation via regulating microRNA-21/132 expression and AMPK activation in white adipose tissue. Nutrients 10:1567

Kim BM, Cho BO, Jang SI (2019) Anti-obesity effects of *Diospyros lotus* leaf extract in mice with high-fat diet-induced obesity. Int J Mol Med 43:603–613

Kim J, Choi JH, Oh T et al (2020) *Codium fragile* ameliorates high-fat diet-induced metabolism by modulating the gut microbiota in mice. Nutrients 12:1848

Kimura H, Ogawa S, Jisaka M et al (2006) Identification of novel saponins from edible seeds of Japanese horse chestnut (*Aesculus turbinata* Blume) after treatment with wooden ashes and their nutraceutical activity. J Pharm Biomed Anal 41:1657–1665

Kimura H, Ogawa S, Katsube T et al (2008) Anti-obese effects of novel saponins from edible seeds of Japanese horse chestnut (*Aesculus turbinata* BLUME) after treatment with wood ashes. J Agric Food Chem 56:4783–4788

Kimura H, Ogawa S, Sugiyama A et al (2011) Anti-obesity effects of highly polymeric proanthocyanidins from seed shells of Japanese horse chestnut (*Aesculus turbinata* Blume). Food Res Int 44:121–126

King MR, Anderson NJ, Guernsey LS et al (2013) GSK 3 inhibition prevents learning deficits in diabetic mice. J Neurosci Res 91:506–514

Kirana H, Srinivasan BP (2008) *Trichosanthes cucumerina* Linn improves glucose tolerance and tissue glycogen in non-insulin dependent diabetes mellitus induced rats. Ind J Pharmacol 40: 103–106

Kirchweger B, Kratz JM, Ladurner A et al (2018) In silico workflow for the discovery of natural products activating the G-protein-coupled bile acid receptor-1. Front Chem 6:242

Kobayashi Y, Nakano Y, Kizaki M et al (2001) Capsaicin-like anti-obese activities of evodiamine from fruits of *Evodia rutaecarpa*, a vanilloid receptor agonist. Planta Med 67:628–633

Kotelevtsev Y, Holmes MC, Burchell A et al (1997) 11beta-hydroxysteroid dehydrogenase type 1 knockout mice show attenuated glucocorticoid-inducible responses and resist hyperglycemia on obesity or stress. Proc Natl Acad Sci 94:14924–14929

Kozuka M, Yamane T, Kakano Y et al (2015) Identification and characterization of a dipeptidyl peptidase IV inhibitor from aronia juice. Biochem Biophys Res Commun 465:433–436

Krishnamurthy G, Lakshman K, Pruthvi N et al (2011) Antihyperglycemic and hypolipidemic activity of methanolic extract of *Amaranthus viridis* leaves in experimental diabetes. Ind J Pharmacol 43:450–454

Krumbein A, Schwarz D, Klaring HP (2006) Effects of environmental factors on carotenoid content in tomato (*Lycopersicon esculentum* (L.) Mill.) grown in a greenhouse. J Appl Bot Food Qual 80:160–164

Ku KM, Choi JN, Kim J et al (2010) Metabolomics analysis reveals the compositional differences of shade grown tea (*Camellia sinensis* L.). J Agric Food Chem 58:418–426

Kumar R, Pate DK, Prasad SK et al (2011) Antidiabetic activity of alcoholic leaves extract of *Alangium lamarckii* Thwaites on streptozotocin-nicotinamide induced type 2 diabetic rats. Asian Pac J Trop Med 4:904–909

Kumar S, Sharma S, Vasudeva N et al (2012) In vivo anti-hyperglycemic and antioxidant potentials of ethanolic extract from *Tecomella undulata*. Diabetol Metab Syndr 4:33

Kumar V, Sharma K, Ahmed B et al (2018) Deconvoluting the dual hypoglycaemic effect of wedelolactone isolated from *Wedelia calendulacea*: investigation via experimental validation and molecular docking. RSC Adv 8:18180

Kurup SB, Mini S (2017a) *Averrhoa bilimbi* fruits attenuate hyperglycemia-mediated oxidative stress in streptozotocin-induced diabetic rats. J Food Drug Anal 25:360–368

Kurup SB, Mini S (2017b) Protective potential of *Averrhoa bilimbi* fruits in ameliorating the hepatic key enzymes in streptozotocin-induced diabetic rats. Biomed Pharmacother 85:725–732

Kurylowicz A, Puzianowska-Kuznicka M (2020) Induction of adipose tissue browning as a strategy to combat obesity. Int J Mol Sci 21:6241

Kwon CS, Sohn HY, Kim SH et al (2003) Antiobesity effect of *Dioscorea nipponica* Makino with lipase inhibitory activity in rodents. Biosci Biotechnol Biochem 67:1451–1456

Ladurner A, Zehl M, Grienke U et al (2017) Allspice and clove as source of triterpene acids activating the G-protein-coupled bile acid receptor TGR5. Front Pharmacol 8:468

Lai Y, Chen W, Ho C et al (2014) Garlic essential oil protects against obesity-triggered non-alcoholic fatty liver disease through modulation of lipid metabolism and oxidative stress. J Agric Food Chem 62:5897–5906

Lai YS, Lee WC, Lin YE et al (2016) Ginger essential oil ameliorates hepatic injury and lipid accumulation in high fat diet-induced non-alcoholic fatty liver disease. J Agric Food Chem 64: 2062–2071

Langin D (2006) Adipose tissue lipolysis as a metabolic pathway to define pharmacological strategies against obesity and the metabolic syndrome. Pharmacol Res 53:482–491

Lata D, Kuchi VS, Nayik GA (2017) 1-Methyl cyclopropene (1-MCP) for quality preservation of fresh fruits and vegetables. J Postharvest Technol 5:9–15

Latifi E, Mohammadpour AA, Behrooz FH et al (2019) Antidiabetic and antihyperlipidemic effects of ethanolic *Ferula assa-foetida* oleo-gum-resin extract in streptozotocin-induced diabetic Wistar rats. Biomed Pharmacother 110:197–202

Lee CW, Han JS (2012) Hypoglycemic effect of *Sargassum ringgoldianum* extract in STZ-induced diabetic mice. Prev Nutr Food Sci 17:8–13

Lee M, Sung SH (2016) Platyphylloside isolated from *Betula platyphylla* inhibit adipocyte differentiation and induce lipolysis *via* regulating adipokines including PPARγ in 3T3-L1 cells. Pharmacog Mag 12:276–281

Lee S, Shim SH, Kim JS et al (2005a) Aldose reductase inhibitors from the fruiting bodies of *Ganoderma applanatum*. Biol Pharm Bull 28:1103–1105

Lee YS, Lee S, Lee HK et al (2005b) Inhibitory effects of isorhamnetin-3-*O*-β-D-glucoside from *Salicornia herbacea* on rat lens aldose reductase and sorbitol accumulation in streptozotocin-induced diabetic rat tissues. Biol Pharm Bull 28:916–918

Lee EH, Song DG, Lee JY et al (2008a) Inhibitory effect of the compounds isolated from *Rhus verniciflua* on aldose reductase and advanced glycation endproducts. Biol Pharm Bull 31:1626–1630

Lee YS, Kang YH, Jung JY et al (2008b) Inhibitory constituents of aldose reductase in the fruiting body of *Phellinus linteus*. Biol Pharm Bull 31:765–768

Lee SJ, Park WH, Park SD et al (2009) Aldose reductase inhibitors from *Litchi chinensis* Sonn. J Enzyme Inhib Med Chem 24:957–959

Lee SH, Park MH, Heo SJ et al (2010a) Dieckol isolated from *Ecklonia cava* inhibits α-glucosidase and α-amylase *in vitro* and alleviates post-prandial hyperglycemia in streptozotocin-induced diabetic mice. Food Chem Toxicol 48:2633–2637

Lee YS, Kim SH, Jung SH et al (2010b) Aldose reductase inhibitory compounds from *Glycyrrhiza uralensis*. Biol Pharm Bull 33:917–921

Lee MS, Kim CT, Kim IH et al (2011a) Effects of capsaicin on lipid metabolism in 3T3-L1 adipocytes. Phytother Res 25:935–939

Lee YS, Cha BY, Saito K et al (2011b) Effects of a *Citrus depressa* Hayata (shiikuwasa) extract on obesity in high-fat diet-induced obese mice. Phytomedicine 18:648–654

Lee EJ, Jang DS, Kim NH et al (2011c) Galloyl glucoses from the seeds of *Cornus officinalis* with inhibitory activity against protein glycation, aldose reductase, and cataractogenesis ex vivo. Biol Pharm Bull 34:443–446

Lee HI, Kim MS, Lee KM et al (2011d) Anti-visceral obesity and antioxidant effects of powdered sea buckthorn (*Hippophae rhamnoides* L.) leaf tea in diet-induced obese mice. Food Chem Toxicol 49:2370–2376

Lee EJ, Kang M, Kim YS (2012a) Platycodin D inhibits lipogenesis through AMPKα-PPARγ2 in 3T3-L1 cells and modulates fat accumulation in obese mice. Planta Med 78:1536–1542

Lee SH, Min KH, Han JS et al (2012b) Effects of brown algae, *Ecklonia cava* on glucose and lipid metabolism in C57BL/KsJ-db/db mice, a model of type 2 diabetes mellitus. Food Chem Toxicol 50:575–582

Lee DS, Jang JH, Ko W et al (2013a) PTP1B inhibitory and anti-inflammatory effects of secondary metabolites isolated from the marine-derived fungus *Penicillium* sp. JF-55. Mar Drugs 11:1409–1426

Lee SE, Lee EH, Lee TJ et al (2013b) Anti-obesity effect and action mechanism of *Adenophora triphylla* root ethanol extract in C57BL/6 obese mice fed a high-fat diet. Biosci Biotechnol Biochem 77:544–550

Lee SJ, Choi HN, Kang MJ et al (2013c) Chamnamul [*Pimpinella brachycarpa* (Kom) Nakai] ameliorates hyperglycemia and improves antioxidant status in mice fed a high-fat, high-sucrose diet. Nutr Res Pract 7:446–452

Lee YS, Cha BY, Choi SS et al (2013d) Nobiletin improves obesity and insulin resistance in high-fat diet-induced obese mice. J Nutr Biochem 24:156–162

Lee DR, Lee YS, Choi BK et al (2015) Roots extracts of *Adenophora triphylla* var. *japonica* improve obesity in 3T3-L1 adipocytes and high-fat diet-induced obese mice. Asian Pac J Trop Med 8:898–906

Lee MW, Kwon JE, Lee YJ et al (2016) *Prunus mume* leaf extract lowers blood glucose level in diabetic mice. Pharm Biol 54:2135–2140

Lee JE, Park YK, Park S et al (2017a) Brd4 binds to active enhancers to control cell identity gene induction in adipogenesis and myogenesis. Nat Commun 8:2217

Lee SG, Lee YJ, Jang MH et al (2017b) *Panax ginseng* leaf extract exerts anti-obesity effects in high-fat diet-induced obese rats. Nutrients 9:999

Lee HE, Yang G, Han SH et al (2018a) Anti-obesity potential of *Glycyrrhiza uralensis* and licochalcone A through induction of adipocyte browning. Biochem Biophys Res Commun 503:2117–2123

Lee JJ, Kim HA, Lee J (2018b) The effect of *Brassica juncea* l. leaf extract on obesity and lipid profiles of rats fed a high-fat/high cholesterol diet. Nutr Res Pract 12:298–306

Lee JE, Schmidt H, Lal B et al (2019a) Transcriptional and epigenomic regulation of adipogenesis. Mol Cell Biol 39:e00601–e00618

Lee MK, Kim HW, Lee SH et al (2019b) Characterization of catechins, theaflavins, and flavonols by leaf processing step in green and black teas (*Camellia sinensis*) using UPLC-DAD-QTOF/MS. Eur Food Res Technol 245:997–1010

Lee MR, Kim JE, Choi JY et al (2019c) Anti-obesity effect in high-fat-diet-induced obese C57BL/6 mice: study of a novel extract from mulberry (*Morus alba*) leaves fermented with *Cordyceps militaris*. Exp Ther Med 17:2185–2193

Lee HG, Lu YA, Li X et al (2020a) Anti-obesity effects of *Grateloupia elliptica*, a red seaweed, in mice with high-fat diet-induced obesity *via* suppression of adipogenic factors in white adipose tissue and increased thermogenic factors in brown adipose tissue. Nutrients 12:308

Lee MR, Kim JE, Park JW et al (2020b) Fermented mulberry (*Morus alba*) leaves suppress high fat diet-induced hepatic steatosis through amelioration of the inflammatory response and autophagy pathway. BMC Complement Med Ther 2020:283

Lei F, Zhang XN, Wang W et al (2007) Evidence of anti-obesity effects of the pomegranate leaf extract in high-fat diet induced obese mice. Int J Obes (Lond) 31:1023–1029

Lemaure B, Touche A, Zbinden I et al (2007) Administration of *Cyperus rotundus* tubers extract prevents weight gain in obese Zucker rats. Phytother Res 21:724–730

Lembede BW, Erlwanger KH, Chivandi E (2019) Effect of aqueous *Terminalia sericea* leaf extract on visceral obesity in fructose-fed Wistar rats. J Herbs Spicies Med Plants 25:428–440

Leong SY, Oey I (2012) Effects of processing on anthocyanins, carotenoids and vitamin C in summer fruits and vegetables. Food Chem 133:1577–1587

Li JW, Vederas JC (2009) Drug discovery and natural products: end of an era or an endless frontier ? Science 325:161–165

Li F, Li W, Fu H et al (2007) Pancreatic lipase-inhibiting triterpenoid saponins from the fruits of *Acanthopanax senticosus*. Chem Pharm Bull 55:1087–1089

Li H, Tsao R, Deng Z (2012a) Factors affecting the antioxidant potential and health benefits of plant foods. Can J Plant Sci 92:1101–1111

Li H, Deng Z, Liu R et al (2012b) Ultra-performance liquid chromatographic separation of geometrical isomers of carotenoids and antioxidant activities of 20 tomato cultivars and breeding lines. Food Chem 132:508–517

Li Y, Tran VH, Kota BP et al (2014a) Preventive effect of *Zingiber officinale* on insulin resistance in a high-fat high-carbohydrate diet-fed rat model and its mechanism of action. Basic Clin Pharmacol Toxicol 115:209

Li Z, Shangguan Z, Liu Y et al (2014b) Puerarin protects pancreatic β-cell survival via PI3K/Akt signaling pathway. J Mol Endocrinol 53:71–79

Li JI, Gao LX, Meng FW et al (2015) PTP1B inhibitors from the stems of *Angelica keiskei* (Ashitaba). Bioorg Med Chem Lett 25:2028–2032

Li S, Jina S, Songa C et al (2016) The metabolic change of serum lysophosphatidylcholines involved in the lipid lowering effect of triterpenes from Alismatis rhizome on high-fat diet induced hyperlipidemia mice. J Ethnopharmacol 177:10–18

Li XW, Chen HP, He YY et al (2018a) Effects of rich-polyphenols extract of *Dendrobium loddigesii* on anti-diabetic, anti-inflammatory, anti-oxidant, and gut microbiota modulation in db/db mice. Molecules 23:3245

Li ZS, Zheng JW, Manabe Y et al (2018b) Anti-obesity properties of the dietary green alga, *Codium cylindricum*, in high-fat diet-induced obese mice. J Nutr Sci Vitaminol (Tokyo) 64:347–356

Li L, Guo WL, Zhang W et al (2019) *Grifola frondosa* polysaccharides ameliorate lipid metabolic disorders and gut microbiota dysbiosis in high-fat diet-fed rats. Food Funct 10:2560–2572

Liang B, Guo Z, Xie F et al (2013) Antihyperglycemic and antihyperlipidemic activities of aqueous extract of *Hericium erinaceus* in experimental diabetic rats. BMC Complement Altern Med 13: 253

Liberman Z, Eldar-finkelman H (2005) Serine 332 phosphorylation of insulin receptor substrate-1 by glycogen synthase kinase 3 attenuates insulin signaling. J Biol Chem 280:4422–4428

Lin HV, Accili D (2011) Hormonal regulation of hepatic glucose production in health and disease. Cell Metab 14:9–19

Lin YL, Chou CH, Yang DJ et al (2012) Hypolipidemic and antioxidative effects of noni (*Morinda citrifolia* L.) juice on high-fat/cholesterol-dietary hamsters. Plant Foods Hum Nutr 67:294–302

Liou CJ, Lai XY, Chen YL et al (2015) Ginkgolide C suppresses adipogenesis in 3T3-L1 adipocytes via the AMPK signaling pathway. Evid Based Complement Alternat Med 2015: 298635

Liu M, Wu K, Mao X et al (2010a) Astragalus polysaccharide improves insulin sensitivity in KKAy mice: regulation of PKB/GLUT4 signaling in skeletal muscle. J Ethnopharmacol 127: 32–37

Liu W, Zheng Y, Han L et al (2010b) Saponins (ginsenosides) from stems and leaves of *Panax quinquefolium* prevented high fat diet induced obesity in mice. Phytomedicine 15:1140–1145
Liu Z, Ma L, Zhou GB (2011) The main anticancer bullets of the Chinese medicinal herb, Thunder God Vine. Molecules 16:5283–5289
Liu Y, Sun J, Rao S et al (2013a) Antihyperglycemic, antihyperlipidemic and antioxidant activities of polysaccharides from *Catathelasma ventricosum* in streptozotocin-induced diabetic mice. Food Chem Toxicol 57:39–45
Liu Y, Wan L, Xiao Z et al (2013b) Antidiabetic activity of polysaccharides from tuberous root of *Liriope spicata* var. *prolifera* in KK-Ay mice. Evid Based Complement Altern Med 2013: 349790
Liu Q, Kim SH, Kim SB et al (2014) Antiobesity effect of (8-*E*)-nuzhenide, a secoiridoid from *Ligustrum lucidum*, in high-fat diet-induced obese mice. Nat Prod Commun 9:1399–1401
Liu J, Lee J, Hernandez MAS et al (2015a) Treatment of obesity with celastrol. Cell 161:999–1011
Liu YX, Si MM, Lu W et al (2015b) Effects and molecular mechanisms of the antidiabetic fraction of *Acorus calamus* L on GLP-1 expression and secretion *in vivo* and *in vitro*. J Ethnopharmacol 166:168–175
Liu PK, Weng ZM, Ge GB et al (2018) Biflavones from *Ginkgo biloba* as novel pancreatic lipase inhibitors: inhibition potentials and mechanism. Int J Biol Macromol 118B:2216–2223
Liu Y, Wang C, Li J et al (2019) Hypoglycemic and hypolipidemic effects of *Phellinus linteus* mycelial extract from solid-state culture in a rat model of type 2 diabetes. Nutrients 11:296
LMDS M, CRP C, Santos PS et al (2018) Modulatory effect of polyphenolic compounds from the mangrove tree *Rhizophora mangle* L. on non-alcoholic fatty liver disease and insulin resistance in high-fat diet obese mice. Molecules 23:2114
Lo SH, Cheng KC, Li YX et al (2016) Development of betulinic acid as an agonist of TGR5 receptor using a new *in vitro* assay. Drug Des Devel Ther 10:2669–2676
Lochhead PA, Salt IP, Walker KS et al (2000) 5-Aminoimidazole-4-carboxamide riboside mimics the effects of insulin on the expression of the 2 key gluneogenic genes PEPCK and glucose-6-phosphatase. Diabetes 49:896–903
Lowell BB, Shulman GI (2005) Mitochondrial dysfunction and type 2 diabetes. Science 307:384–387
Lu H, Chen J, Li WL et al (2009) Hypoglycemic effect of the total flavonoid fraction from *Folium Eriobotryae*. Phytomedicine 16:967–971
Lu X, Chen H, Dong P et al (2010) Phytochemical characteristics and hypoglycaemic activity of fraction from mushroom *Inonotus obliquus*. J Sci Food Agric 90:276–280
Lu YL, Lin SY, Fang SU et al (2017) Hot water extracts from roots of *Vitis thunbergii* var. *taiwaniana* and identified ε-viniferin improve obesity in high-fat diet-induced mice. J Agric Food Chem 65:2521–2529
Lu YA, Lee YG, Li X et al (2020) Anti-obesity effects of red seaweed, *Plocamium telfairiae*, in C57BL/6 mice fed a high-fat diet. Food Funct 11:2299–2308
Lumpkin H (2005) A comparison of lycopene and other phytochemicals in tomatoes grown under conventional and organic management systems. Tech Bull 34, AVRDC publication number 05-623, Shanhua, Taiwan
Lund ED, White JM (1990) Polyacetylenes in normal and waterstressed Órlando Gold' carrots (*Daucus carota*). J Sci Food Agric 51:507–516
Ma Y, Yuan L, Wu B et al (2012) Genome-wide identification and characterization of novel genes involved in terpenoid biosynthesis in *Salvia miltiorrhiza*. J Exp Bot 63:2809–2823
Ma WY, Ma LP, Yi B et al (2014) Antidiabetic activity of *Callicarpa nudiflora* extract in type 2 diabetic rats via activation of the AMPK-ACC pathway. Asian Pac J Trop Biomed 9:456–466
Ma C, Li G, He Y et al (2015a) Pronuciferine and nuciferine inhibit lipogenesis in 3T3-L1 adipocytes by activating the AMPK signaling pathway. Life Sci 136:120–125
Ma X, Xu L, Alberobello AT et al (2015b) Celastrol protects against obesity and metabolic dysfunction through activation of a HSF1-PGC1α transcriptional axis. Cell Metab 22:1–14

Ma L, Zhang S, Du M (2015c) Cordycepin from *Cordyceps militaris* prevents hyperglycemia in alloxan-induced diabetic mice. Nutr Res 35:431–439

Maczewsky J, Kaiser J, Gresch A et al (2019) TGR5 activation promotes stimulus-secretion coupling of pancreatic β-cells via a PKA-dependent pathway. Diabetes 68:324–336

Mahajan S, Chauhan P, Mishra M et al (2018) Antidiabetic potential of *Eugenia jambolana* ethanolic seed extract: effect on antihyperlipidemic and antioxidant in experimental streptozotocin-induced diabetic rats. Adv Complement Altern Med 2:146–153

Mahanna M, Millan-Linares MC, Grao-Cruces E et al (2019) Resveratrol-enriched grape seed oil (*Vitis vinifera* L.) protects from white fat dysfunction in obese mice. J Funct Foods 62:103546

Mahmood T, Anwar F, Abbas M et al (2012) Effect of maturity on phenolics (phenolic acids and flavonoids) profile of strawberry cultivars and mulberry species. Int J Mol Sci 13:4591–4607

Maithili V, Dhanabal SP, Mahendran S et al (2011) Antidiabetic activity of ethanolic extract of tubers of *Dioscorea alata* in alloxan induced diabetic rats. Ind J Pharmacol 43:455–459

Makihara H, Shimada T, Machida E et al (2012) Preventive effect of *Terminalia bellirica* on obesity and metabolic disorders in spontaneously obese type 2 diabetic model mice. J Nat Med 66:459–467

Mangal P, Khare P, Jagtap S et al (2017) Screening of six Ayurvedic medicinal plants for anti-obesity potential: an investigation on bioactive constituents from *Oroxylum indicum* (L.) Kurz. bark. J Ethnopharmacol 197:138–146

Manzaro S, Salvia J, de la Fuente JA (2006) Phenolic marine natural products as aldose reductase inhibitors. J Nat Prod 69:1485–1487

Mao SC, Guo YW, Shen X (2006) Two novel aromatic valerenane-type sesquiterpenes from the Chinese green alga *Caulerpa taxifolia*. Bioorg Med Chem Lett 16:2947–2950

Mao XQ, Yu F, Wang N et al (2009) Hypoglycemic effect of polysaccharide enriched extract of *Astragalus membranaceus* in diet induced insulin resistant C57BL/6J mice and its potential mechanism. Phytomedicine 16:416–425

Maroo J, Ghosh A, Mathur R et al (2003) Antidiabetic efficacy of *Enicostemma littorale* methanol extract in alloxan-induced diabetic rats. Pharm Biol 41:388–391

Marta G, Belen G, Raquel F et al (2014) Reduction of adipogenesis and lipid accumulation by *Taraxacum officinale* (Dandelion) extracts in 3T3-L1 adipocytes: an in vitro study. Phytother Res 28:745–752

Maruyama T, Miyamoto Y, Nakamura T et al (2002) Identification of membrane-type receptor for bile acids (M-BAR). Biochem Biophys Res Commun 298:714–719

Maruyama T, Tanaka K, Sujuki J et al (2006) Targeted disruption of G-protein-coupled bile acid receptor 1 (Gpbar 1/M-Bar) in mice. J Endocrinol 191:197–205

Masuzaki H, Paterson J, Shinyama H et al (2001) A transgenic model of visceral obesity and metabolic syndrome. Science 294:2166–2170

Matanjun P, Mohamed S, Muhammad K et al (2010) Comparison of cardiovascular protective effects of tropical seaweeds, *Kappaphyens alvarezii*, *Caulerpa lentillifera*, and *Sargassum polycystum*, on high-cholesterol/high-fat diet in rats. J Med Food 13:792–800

Matsuda H, Morikawa T, Toguchida I et al (2002) Medicinal flowers. IV. Absolute streostructures of two new flavanone glycosides and a phenylbutanoid glycoside from the flowers of *Chrysanthemum indicum* L.: their inhibitory activities for rat lens aldose reductase. Chem Pharm Bull 50:972–975

Matus JT, Loyola R, Vega A et al (2009) Post-veraison sunlight exposure induces MYB-mediated transcriptional regulation of anthocyanin and flavonol synthesis in berry skins of *Vitis vinifera*. J Exp Bot 60:853–867

Maulidiani AF, Khatib A et al (2016) Metabolic alternation in obese diabetes rats upon treatment with *Centella asiatica* extract. J Ethnopharmacol 180:60–69

McGee SL, van Denderen BJ, Howlett KF et al (2008) AMP-activated protein kinase regulates GLUT4 transcription by phosphorylating histone deacetylase 5. Diabetes 57:860–867

McMurry JE (2015) Organic chemistry with biological applications. In: Secondary metabolites: an introduction to natural products chemistry. Cengage Learning Ltd, Stamford, pp 1016–1046

Meddah B, Ducroc R, Faouzi MEA et al (2009) *Nigella sativa* inhibits intestinal glucose absorption and improves glucose tolerance in rats. J Ethnopharmacol 121:419–424
Meenakshi P, Bhuvaneshwari R, Rathi MA et al (2010) Antidiabetic activity of ethanolic extract of *Zaleya decandra* in alloxan-induced diabetic rats. Appl Biochem Biotechnol 162:1153–1159
Mehenni C, Atmani-Kilani D, Dumarcay S et al (2016) Hepatoprotective and antidiabetic effects of *Pistacia lentiscus* leaf and fruit extracts. J Food Drug Anal 24:653–669
Meriga B, Parim B, Chunduri VR et al (2017) Antiobesity potential of piperonal: promising modulation of body composition, lipid profiles and obesogenic marker expression in HFD-induced obese rats. Nutr Metab (Lond) 14:72
Min KH, Kim HJ, Jeon YJ et al (2011) *Ishige okamurae* ameliorates hyperglycemia and insulin resistance in C57BL/KsJ-db/db mice. Diabetes Res Clin Pract 93:70–76
Minaiyan M, Ghannadi A, Movahedian A et al (2014) Effect of the hydroalcoholic extract and juice of *Prunus divaricata* fruit on blood glucose and serum lipids of normal and streptozotocin-induced diabetic rats. Res Pharm Sci 9:421–429
Minokoshi Y, Alquier T, Furukawa N et al (2004) AMP-kinase regulates food intake by responding to hormonal and nutrient signals in the hypothalamus. Nature 428:569–574
Misawa K, Hashizume K, Yamamoto M et al (2015) Ginger extract prevents high-fat diet-induced obesity in mice via activation of the peroxisome proliferator-activated receptor δ pathway. J Nutr Biochem 26:1058–1067
Miyazawa N, Yoshimoto H, Kurihara S et al (2018) Improvement of diet-induced obesity by ingestion of mushroom chitosan prepared from *Flammulina velutipes*. J Oleo Sci 67:245–254
Mochizuki M, Hasegawa N (2006) Acceleration of lipid degradation by sericoside of *Terminalia sericea* roots in fully differentiated 3T3-L1 cells. Phytother Res 20:1020–1021
Modak M, Dixit P, Londhe J et al (2007) Indian herbs and herbal drugs used for the treatment of diabetes. J Clin Biochem Nutr 40:163–173
Moezi L, Arshadi SS, Motazedian T et al (2018) Anti-diabetic effects of *Amygdalus lycioides* Spach in streptozotocin-induced diabetic rats. Iran J Pharm Res 17:353–364
Mohajeri D, Mousavi G, Doustar Y (2009) Antihyperglycemic and pancreas protective effects of *Crocus sativus* L. (saffron) stigma ethanolic extract on rats with alloxan-induced diabetes. J Biol Sci 9:302–310
Mohamed EAH, Siddiqui MJA, Ang LF et al (2012) Potent α-glucosidase and α-amylase inhibiting activities of standardized 50% ethanolic extracts and sinensetin from *Orthosiphon stamineus* Benth as anti-diabetic mechanism. BMC Complement Altern Med 12:176
Mohammed A, Gbonjubola VA, Koorbanally NA et al (2017) Inhibition of key enzymes linked to type 2 diabetes by compounds isolated from *Aframomum melegueta* fruit. Pharm Biol 55:1010–1016
Moon HI, Jung JC, Lee J (2006) Aldose reductase inhibitory effect of tectorigenin derivatives from *Viola hondoensis*. Bioorg Med Chem 14:7592–7594
Moon HE, Islam MN, Ahn BR et al (2011) Protein tyrosine phosphatase 1B and α-glucosidase inhibitory phlorotannins from edible brown algae, *Ecklonia stolonifera* and *Eisenia bicyclis*. Biosci Biotechnol Biochem 75:1472–1480
Mopuri R, Islam MS (2017) Medicinal plants and phytochemicals with anti-obesogenic potentials: a review. Biomed Pharmacother 89:1442–1452
Mopuri R, Ganjayi M, Banavathy KS et al (2015) Evaluation of anti-obesity activities of ehanolic extract of *Terminalia paniculata* bark on high-fat diet-induced obese rats. BMC Complement Altern Med 15:76
Moqbel FS, Naik PR, Najma Habeeb M et al (2011) Antidiabetic properties of *Hibiscus rosa sinensis* L. leaf extract fractions on non-obese diabetic (NOD) mouse. Ind J Exp Biol 49:24–29
Morita H, Deguchi J, Motegi Y et al (2010) Cyclic diarylheptanoids as Na^+-glucose cotransporter (SGLT) inhibitors from *Acer nikoense*. Bioorg Med Chem Lett 20:1070–1074
Morton NM, Holmes MC, Fievet C et al (2001) Improved lipid and lipoprotein profile, hepatic insulin sensitivity and glucose tolerance in 11beta-hydroxysteroid dehydrogenase type 1 null mice. J Biol Chem 276:41293–41300

Mosquera C, Panay AJ, Montoya G (2018) Pentacyclic triterpenes from *Cecropia telenitida* can function as inhibitors of 11β-hydroxysteroid dehydrogenase type 1. Molecules 23:1444

Murphy KG, Bloom SR (2006) Gut hormones and the regulation of energy homeostasis. Nature 444:854–859

Muruganandan S, Srinivasan K, Gupta S et al (2005) Effect of mangiferin on hyperglycemia and atherogenicity in streptozotocin diabetic rats. J Ethnopharmacol 97:497–501

Mutukwa IB, Hall CA III, Cihacek L et al (2019) Evaluation of drying method and pretreatment effects on the nutritional and antioxidant properties of oyster mushrooms (*Pleurotus ostreatus*). J Food Process Preserv 43:e13910

Na M, Yang S, He L et al (2006) Inhibition of protein tyrosine phosphatase 1B by ursane-type triterpenes isolated from *Symplocos paniculata*. Planta Med 72:261–263

Na B, Nguyen PH, Zhao BT et al (2016) Protein tyrosine phosphatase 1B (PTP1B) inhibitory activity and glucosidase inhibitory activity of compounds isolated from Argimonia pilosa. Pharm Biol 54:474–480

Nabeel MA, Kandasamy K, Manivannan S (2010) Antidiabetic activity of the mangrove species *Ceriops decandra* in alloxan-induced diabetic rats. J Diabetes 2:97–103

Nakagawa M, Torii H (1964) Studies on the flavonols in tea. Part II. Variation in the flavonolic constituents during the development of tea leaves. Agric Biol Chem 28:497–504

Nakao Y, Uehara T, Matunaga S et al (2002) Callyspongynic acid, a polyacetylenic acid, which inhibits alpha-glucosidase, from the marine sponge *Callyspongia truncata*. J Nat Prod 65:922–924

Nammi S, Sreemantula S, Roufogalis BD (2009) Protective effects of ethanolic extract of *Zingiber officinale* rhizome on the development of metabolic syndrome in high-fat diet-fed rats. Basic Clin Pharmacol Toxicol 104:366–373

Naslund E, Hellstrom PM (2007) Appetite signaling from gut peptides and enteric nerves to brain. Physiol Behav 92:256–262

Nath A, Bagchi B, Misra LK et al (2011) Changes in post-harvest phytochemical qualities of broccoli florets during ambient and refrigerated storage. Food Chem 127:1510–1514

Nawale RB, Mate GS, Wakure BS (2017) Ethanolic extract of *Amaranthus paniculatus* Linn. ameliorates diabetes-associated complications in alloxan-induced diabetic rats. Intg Med Res 6: 41–46

Nderitu KW, Mwenda NS, Macharia NJ et al (2017) Antiobesity activities of methanolic extracts of *Amaranthus dubius*, *Cucurbita pepo* and *Vigna unguiculata* in progesterone-induced obese mice. Evid Based Complement Altern Med 2017:4317321

Nerurkar PV, Nishioka A, Eck PO et al (2012) Regulation of glucose metabolism *via* hepatic forkhead transcription factor 1 (FoxO1) by *Morinda citrifolia* (noni) in high-fat diet-induced obese mice. Br J Nutr 108:218–228

Newman DJ, Cragg GM (2020) Natural products as sources of new drugs over the nearly four decades from 01/1981 to 09/2019. J Nat Prod 83:770–803

Newman DJ, Cragg GM, Snader KM (2003) Natural products as sources of new drugs over the period 1981–2002. J Nat Prod 66:1022–1037

Ngo LT, Okogun JI, Folk WR (2013) 21st century natural product research and drug development and traditional medicines. Nat Prod Rep 30:584–592

Nie Q, Hu J, Gao H et al (2019) Polysaccharide from *Plantago asiatica* L. attenuates hyperglycemia, hyperlipidemia and affects colon microbiota in type 2 diabetic rats. Food Hydrocolloids 86: 34–42

Nikoulina SE, Ciaraldi TP, Mudaliar S et al (2002) Inhibition of glycogen synthase kinase 3 improves insulin action and glucose metabolism in human skeletal muscle. Diabetes 51: 2190–2198

Nishikawa M, Tsurumi Y, Murai H et al (1991) WF-2421, a new aldose reductase inhibitor produced from a fungus, *Humicola grisea*. J Antibiot 44:130–135

Nugara RN, Inafuku M, Oku H (2016) *Peucedanum japonicum* Thunb and its antiobesity effects: evidence and related mechanisms. J Lipid Nutr 25:177–196

Nugroho AE, Andrie M, Warditani NK et al (2012) Antidiabetic and antihyperlipidemic effect of *Angrographis paniculata* (Burm. F.) Nees and andrographolide in high fructose-fed rats. Ind J Pharmacol 44:377–381

Nukitrangsan N, Okabe T, Toda T et al (2012) Effect of *Peucedanum japonicum* Thunb extract on high-fat diet-induced obesity and gene expression in mice. J Oleo Sci 61:89–101

Oakhill JS, Steel R, Chen ZP et al (2011) AMPK is a direct adenylate charge-regulated protein kinase. Science 332:1433–1435

Obanda DN, Ribnicky D, Yu Y et al (2016) An extract of *Urtica dioica* L. mitigates obesity induced insulin resistance in mice skeletal muscle via protein phosphatase 2A (PP2A). Sci Rep 6:22222

Ogawa T, Tabata H, Katsube T et al (2010) Suppressive effect of hot water extract of Wasabi (*Wasabia japonica* Matsum) leaves on the differentiation of 3T3-L1 preadipocytes. Food Chem 118:239–244

Ogundajo AL, Kazeem MI, Owoyele OA et al (2016) Inhibition of α-amylase and α-glucosidase by *Acanthus montanus* leaf extracts. Br J Pharm Res 9:1–8

Ohnogi H, Hayami S, Kudo Y et al (2012) *Angelica keiskei* extract improves insulin resistance and hypertriglyceridemia in rats fed a high fructose drink. Biosci Biotechnol Biochem 76:928–932

Okoli CO, Obidike IC, Ezike AC et al (2011) Studies on the possible mechanisms of antidiabetic activity of extract of aerial parts of *Phyllanthus niruri*. Pharm Biol 49:248–255

Olaokun OO, McGaw LJ, van Rensburg IJ et al (2016) Antidiabetic activity of the ethyl acetate fraction of *Ficus lutea* (Moraceae) leaf extract:comparison of an *in vitro* assay with an *in vivo* obese mouse model. BMC Complement Altern Med 16:110

Olson J (1986) Carotenoid, vitamin A and cancer. J Nutr 116:1127–1130

Ono Y, Hattori E, Fukaya Y et al (2006) Anti-obesity effect of *Nelumbo nucifera* leaves extract in mice and rats. J Ethnopharmacol 106:238–244

Ono E, Inoue J, Hashidume T et al (2011) Anti-obesity and anti-hyperglycemic effects of the dietary citrus limonoid nomilin in mice fed a high-fat diet. Biochem Biophys Res Commun 410:677–681

Onoja US, Ugwu CC, Uzor PF et al (2018) Effect of *Anogeissus leiocarpus* Guill and Perr leaf on hyperglycemia and associated dyslipidemia in alloxan-induced diabetic rats. Dhaka Univ J Pharm Sci 17:65–72

Onyeneke EC, Anyanwu GO (2014) Anti-obesity potential of the ethanolic extract of *Alstonia boonei* stem bark on high carbohydrate diet induced obesity in male Wistar rats. NISEB J 14: 46–50

Orhan N, Aslan M, Sukuroglu M et al (2013) *In vivo* and *in vitro* antidiabetic effect of *Cistus laurifolius* L. and detection of major phenolic compounds by UPLC-TOF-MS analysis. J Ethnopharmacol 146:859–865

Ortuno Sahagun D, Marquez-Aguirre AL, Quintero-Fabian S et al (2012) Modulation of PPAR-γ by nutraceutics as complementary treatment for obesity related disorders and inflammatory diseases. PPAR Res 2012:318613

Osorio-Fuentealba C, Contreras-Ferrat AE, Altamirano F et al (2013) Electrical stimuli release ATP to increase GLUT4 translocation and glucose uptake via PI3Kγ-Akt-AS160 in skeletal muscle cells. Diabetes 62:1519–1526

Oszmianski J, Lachowicz S, Gorzelany J et al (2018) The effect of different maturity stages on phytochemical composition and antioxidant capacity of cranberry cultivars. Eur Food Res Technol 244:705–719

Othman AI, Amer MA, Basos AS et al (2019) *Moringa oleifera* leaf extract ameliorated high-fat diet-induced obesity, oxidative stress and disrupted metabolic hormones. Clin Phytosci 5:48

Ouchfoun M, Eid HM, Musallam L et al (2016) Labrador tea (*Rhododendron groenlandicum*) attenuates insulin resistance in a diet-induced obesity mouse model. Eur J Nutr 55:941–954

Pandikumar P, Babu NP, Ignacimuthu S (2009) Hypoglycemic and antihyperglycemic effect of *Begonia malabarica* Lam in normal and streptozotocin induced diabetic rats. J Ethnopharmacol 124:111–115

Pandita D, Pandita A, Wani SH et al (2021) Crosstalk of multi-omics platforms with plants of therapeutic importance. Cells 10:1296

Parameswari RP, Janani M, Dinesh MG et al (2018) Hydroalcoholic and alkaloidal extracts of *Murraya koenigii* (L.) Spreng augments glucose uptake potential against insulin resistance condition in L6 myotubes and inhibits adipogenesis in 3T3-L1 adipocytes. Pharmacog J 10: 633–639

Parasuraman S, Ching TH, Leong CH et al (2019) Antidiabetic and antihyperlipidemic effects of a methanolic extract of *Mimosa pudica* (Fabaceae) in diabetic rats. Egypt J Basic Appl Sci 6:137–148

Parim B, Harishankar N, Balaji M et al (2015) Effects of *Piper nigrum* extracts: restorative perspectives of high-fat diet-induced changes on lipid profile, body composition, and hormones in Sprague-Dawley rats. Pharm Biol 53:1318–1328

Park SH, Ko SK, Chung SH (2005) *Euonymus alatus* prevents the hyperglycemia and hyperlipidemia induced by high-fat diet in ICR mice. J Ethnopharmacol 102:326–335

Park SH, Park TS, Cha YS (2008) Grape seed extract (*Vitis vinifera*) partially reverses high fat diet-induced obesity in C57BL/6J mice. Nutr Res Pract 2:227–233

Park U, Jeong J, Jang J et al (2012) Negative regulation of adipogenesis by kaempferol: a component of *Rhizoma Polygonati falcatum* in 3T3-L1 cells. Biol Pharm Bull 35:1525–1533

Park YJ, Kim MS, Kim HR et al (2014) EtOH extract of *Alismatis* rhizome inhibits adipocyte differentiation of OP9 cells. Evid Based Complement Altern Med 2014:415097

Park BY, Lee H, Woo S et al (2015a) Reduction of adipose tissue mass by the angiogenesis inhibitor ALS-L1023 from *Melissa officinalis*. PLOS One 10:e0141612

Park EY, Choi H, Yoon JY et al (2015b) Polyphenol-rich fraction of *Ecklonia cava* improves nonalcoholic fatty liver disease in high fat diet-fed mice. Mar Drugs 13:6866–6883

Park EY, Kim EH, Kim CY et al (2016) *Angelica dahurica* extracts improve glucose tolerance through the activation of GPR119. PLOS One 11:e0158796

Park MH, Kang JH, Kim HJ et al (2017a) *Gelidium amansii* ethanol extract suppresses fat accumulation by down-regulating adipogenic transcription factors in ob/ob mice model. Food Sci Biotechnol 26:207–212

Park MY, Lee HJ, Choi DH et al (2017b) Oral administration of *Rehmannia glutinosa* extract for obesity treatment *via* adipocity and fatty acid binding protein expression in obese rats. Toxicol Environ Health Sci 9:309–316

Park E, Lee CG, Kim J et al (2020a) Antiobesity effects of *Gentiana lutea* extract on 3T3-L1 preadipocytes and a high-fat diet-induced mouse model. Molecules 25:2453

Park JY, Jang MG, Oh JM et al (2020b) *Sasa quelpaertensis* leaf extract ameliorates dyslipidemia, insulin resistance, and hepatic lipid accumulation in high-fructose-diet-fed rats. Nutrients 12: 3762

Patel MB, Mishra SM (2009) Aldose reductase inhibitory activity of a C-glycosidic flavonoid derived from *Enicostemma hyssopifolium*. J Complement Integr Med 6:5

Patel PA, Parikh MP, Johari S et al (2015) Antihyperglycemic activity of *Albizzia lebbeck* bark extract in streptozotocin-nicotinamide induced type II diabetes mellitus rats. Ayu 36:335–340

Pathak R, Bridgeman MB (2010) Dipeptidyl peptidase-4 (DPP-4) inhibitors in the management of diabetes. PT 35:509–513

Patras A, Tiwari BK, Brunton NP (2011) Influence of blanching and low temperature preservation strategies on antioxidant activity and phytochemical content of carrots, green beans and broccoli. LWT-Food Sci Technol 44:299–306

Pawlak M, Lefebvre P, Staels B (2015) Molecular mechanism of PPARα action and its impact on lipid metabolism, inflammation and fibrosis in non-alcoholic fatty liver disease. J Hepatol 62: 720–733

Payne GF, Bringi V, Prince C et al (1991) The quest for commercial production of chemicals from plant cell culture. In: Payne GF et al (eds) Plant cell and tissue culture in liquid systems. Hanser, Munich, pp 1–10

Pereira FMV, Rosa E, Fahey JW et al (2002) Influence of temperature and ontogeny on the levels of glucosinolates in broccoli (*Brassica oleracea* var. *italica*) sprouts and their effect on the induction of mammalian phase 2 enzymes. J Agric Food Chem 50:6239–6244

Pham HTT, Huang W, Han C et al (2017) Effects of *Averrhoa carambola* L. (Oxalidaceae) juice mediated on hyperglycemia, hyperlipidemia, and its influence on regulatory protein expression in the injured kidneys of streptozotocin-induced diabetic mice. Am J Tranl Res 9:36–49

Pichiah PBT, Moon HJ, Park JE et al (2012) Ethanolic extract of seabuckthorn (*Hippophae rhamnoides* L.) prevents high-fat diet-induced obesity in mice through down-regulation of adipogenic and lipogenic gene expression. Nutr Res 32:856–864

Pimple BP, Kadam PV, Patil MJ (2011) Antidiabetic and antihyperlipidemic activity of *Luffa acutangula* fruit extracts in streptozotocin induced NIDDM rats. Asian J Pharm Clin Res 4:156–163

Plodkowski RA, McGarvey ME, Huribal HM et al (2015) SGLT2 inhibitors for type 2 diabetes mellitus treatment. Fed Pract 32(Suppl 11):8S–15S

Plum L, Lin HV, Dutia R et al (2009) The obesity susceptibility gene carboxypeptidase E links FoxO1 signaling in hypothalamic pro-opiomelanocortin neurons with regulation of food intake. Nat Med 15:1195–1201

Podsedek A, Sosnowska D, Redzynia M et al (2008) Effect of domestic cooking on the red cabbage hydrophilic antioxidants. Int J Food Sci Technol 43:1770–1777

Poovitha S, Parani M (2016) In vitro and in vivo α-amylase and α-glucosidase inhibiting activities of the protein extracts from two varieties of bitter gourd (*Momordica charantia* L.). BMC Complement Altern Med 16(Suppl 1):185

Pothuraju R, Sharma RK, Rather SA et al (2016) Comparative evaluation of anti-obesity effect of *Aloe vera* and *Gymnema sylvestre* supplementation in high-fat diet fed C57BL/6J mice. J Intercult Ethnopharmacol 5:403–407

Poudel B, Lim SW, Ki HH et al (2014) Dioscin inhibits adipogenesis through the AMPK/MAPK pathway in 3T3-L1 cells and modulates fat accumulation in obese mice. Int J Mol Med 34: 1401–1408

Prasain JK, Peng N, Rajbhandari R et al (2012) The Chinese *Pueraria* root extract (*Pueraria lobata)* ameliorates impaired glucose and lipid metabolism in obese mice. Phytomedicine 20:17–23

Prisilla DH, Balamurugan R, Shah HR (2012) Antidiabetic activity of methanol extract of *Acorus calamus* in STZ induced diabetic rats. Asian Pac J Trop Biomed 2(Suppl):S941–S946

Punitha ISR, Rajendran K, Shirwaikar A et al (2005) Alcoholic stem extract of *Coscinium fenestratum* regulates carbohydrate metabolism and improves antioxidant status in streptozotocin-nicotinamide induced diabetic rats. Evid Based Complement Altern Med 2: 825271

Pushparaj PN, Low HK, Manikandan J et al (2007) Anti-diabetic effects of *Cichorium intybus* in streptozotocin-induced diabetic rats. J Ethnopharmacol 111:430–434

Qa'dan F, Verspohl EJ, Nahrstedt A et al (2009) Cinchonain Ib isolated from *Eriobotrya japonica* induces insulin secretion. J Ethnopharmacol 124:224–227

Qi LW, Liu EH, Chu C et al (2010) Anti-diabetic agents from natural products-an update from 2004 to 2009. Curr Top Med Chem 10:434–457

Qiang L, Wang L, Kon N et al (2012) Brown remodelling of white adipose tissue by Sirt 1-dependent deacetylation of PPARγ. Cell 150:620–632

Quang TH, Ngan NTH, Ko W et al (2014) Tanzawaic acid derivatives from a marine isolate of *Penicillium* sp. (SF-6013) with anti-inflammatory and PTP1B inhibitory activities. Bioorg Med Chem Lett 24:5787–5791

Robinson M, Zhang X (2011) Traditional medicines: Global situation, issues and challenges, 3rd edn. WHO, Geneva

Rajalakshmi M, Eliza J, Priya C et al (2009) Antidiabetic properties of *Tinospora cordifolia* stem extracts on streptozotocin-induced diabetic rats. Afr J Pharm Pharmacol 3:171–180

Ramana KV, Friedrich B, Bhatnagar A et al (2003) Aldose reductase mediates cytotoxic signals of hyperglycemia and TNF-α in human lens epithelial cells. FASEB J 17:315–317

Ramana KV, Friedrich B, Tammali R et al (2005) Requirement of aldose reductase for the hyperglycaemic activation of protein kinase C and formation of diacylglycerol in vascular smooth muscle cells. Diabetes 54:818–829

Ramasamy R, Oates P, Schaefer S (1997) Aldose reductase inhibition protects diabetic and nondiabetic rat hearts from ischemic injury. Diabetes 46:292–300

Rani GR, Singara MAC, Viswanadham M et al (2017) Antidiabetic activity of the compounds isolated from *Rhus mysorensis* plant extract. IOSR-JBB 3:37–42

Rasineni K, Bellamkonda R, Singareddy SR et al (2010) Antihyperglycemic activity of *Catharanthus roseus* leaf powder in streptozotocin-induced diabetic rats. Phcog Res 2:195–201

Rathore K, Singh VK, Jain P et al (2014) In vitro and in vivo antiadipogenic, hypolipidemic and antidiabetic activity of *Diospyros melanoxylon* (Roxb). J Ethnopharmacol 155:1171–1176

Rayalam S, Della-Fera MA, Baile CA (2008) Phytochemicals and regulation of the adipocyte life cycle. J Nutr Biochem 19:717–726

Reid T, Merjury M, Takafira M (2017) Effect of cooking and preservation on nutritional and phytochemical composition of the mushroom *Amanita zambian*. Food Sci Nutr 5:538–544

Ren H, Orozeo IJ, Su Y et al (2012) FoxO1 target Gpr 17 activates AgRP neurons to regulate food intake. Cell 149:1314–1326

Reza MA, Hossain MA, Damte D et al (2015) Hypolipidemic and hepatic steatosis preventing activities of the wood ear medicinal mushroom *Auricularia auricular-judae* (higher basidiomycetes) ethanol extract *in vivo* and *in vitro*. Int J Med Mushrooms 17:723–734

Rodarte Castrejon AD, Eichholz I, Rohn S et al (2008) Phenolic profile and antioxidant activity of highbush blueberry (*Vaccinium corymbosum* L) during fruit maturation and ripening. Food Chem 109:564–572

Rohrborn D, Wronkowitz N, Eckel J (2015) DPP4 in diabetes. Front Immunol 6:386

Rojo LE, Ribnicky D, Logendra S et al (2012) *In vitro* and *in vivo* anti-diabetic effects of anthocyanins from maqui berry (*Aristotelia chinensis*). Food Chem 131:387–396

Rollinger JM, Kratschmar DV, Schuster D et al (2010) 11β-Hydroxysteroid dehydrogenase 1 inhibiting constituents from *Eriobotrya japonica* revealed by bioactivity-guided isolation and computational approaches. Bioorg Med Chem 18:1507–1515

Rosen ED, Walkey CJ, Puigserver P et al (2000) Transcriptional regulation of adipogenesis. Genes & Dev 14:1293–1307

Rosen CJ, Fritz VA, Gardner GM et al (2005) Cabbage yield and glucosinolate concentrations are affected by nitrogen and sulphur fertility. Hortiscience 40:1493–1498

Russell DW (2003) The enzymes, regulation, and genetics of bile acid synthesis. Annu Rev Biochem 72:137–174

Sablani SS, Andrews PK, Davies NM et al (2010) Effect of thermal treatments on phytochemicals in conventionally and organically grown berries. J Sci Food Agric 90:769–778

Saenthaweesuk S, Naowaboot J, Somparn N (2016) *Pandanus amaryllifolius* leaf extract increases insulin sensitivity in high-fat diet-induced obese mice. Asian Pac J Trop Biomed 6:866–871

Sahu J, Sen P, Choudhury MD et al (2014) Recovering medicinal plants' potential with OMICS: microsatellite survey in expressed sequence tags of eleven traditional plants with potent antidiabetic properties. Omics J Integr Biol 18:298–309

Sailaja Rao P, Krishna Mohan G (2014) Beneficial effects of *Hydnocarpus laurifolia* seed on lipid profile status in streptozotocin induced diabetic rats. J Pharm Res 8:1274–1278

Saito T, Nishida M, Saito M et al (2016) The fruit of *Acanthopanax senticosus* (Rupr. Et Maxim.) Harms improves insulin resistance and hepatic lipid accumulation by modulation of liver adenosine monophosphate-activated protein kinase activity and lipogenic gene expression in high-fat diet-fed obese mice. Nutr Res 36:1090–1097

Salamone F, Volti GL, Titta L et al (2012) Moro orange juice prevents fatty liver in mice. World J Gastroenterol 18:3862–3868

Samarghandian S, Azimi-Nezhad M, Farkhondeh T (2017) Immunomodulatory and antioxidant effects of saffron aqueous extract (*Crocus sativus* L.) on streptozotocin-induced diabetes in rats. Indian Heart J 69:151–159

Sangeetha KN, Sujatha S, Muthusamy VS et al (2010) 3β-Tarexerol of *Magnifera indica*, a PI3K-dependent dual activator of glucose transport and glycogen synthesis in 3T3-L1 adipocytes. Biochim Biophys Acta 1800:359–366

Sangeetha MK, Balaji Raghavendran HR, Gayathri V et al (2011) *Tinospora cordifolia* attenuates oxidative stress and distorted carbohydrate metabolism in experimentally induced type 2 diabetes in rats. J Nat Med 65:544–550

Sangeetha MK, Priya CD, Vasanthi HR (2013) Anti-diabetic property of *Tinospora cordifolia* and its active compound is mediated through the expression of Glut4 in L6 myotubes. Phytomedicine 20:246–248

Santiago-Garcia P, Lopez MG (2014) Agavins from *Agave angustifolia* and *Agave potatorum* affect food intake, body weight gain and satiety-related hormones (GLP-1 and ghrelin) in mice. Food Funct 5:3311–3319

Saravanan M, Pandikumar P, Saravanan S et al (2014) Lipolytic and antiadipogenic effects of (3,3-dimethylallyl)-halfordinol on 3T3-L1 adipocytes and high fat and fructose diet induced obese C57/BL6J mice. Eur J Pharmacol 740:714–721

Sarkhail P, Abdollahi M, Fadayevatan S et al (2010) Effect of *Phlomis persica* on glucose levels and hepatic enzymatic antioxidants in streptozotocin-induced diabetic rats. Pharmacogn Mag 6: 219–224

Sasaki T, Mita M, Ikari N et al (2017) Identification of key amino acid residues in the hTGR5-nomilin interaction and construction of its binding model. PLOS One 12:e0179226

Sato H, Genet C, Strehle A et al (2007a) Anti-hyperglycemic activity of a TGR5 agonist isolated from *Olea europaea*. Biochem Biophys Res Commun 362:793–798

Sato S, Takeo J, Aoyama C et al (2007b) Na^+-glucose cotransporter (SGLT) inhibitory flavonoids from the roots of *Sophora flavescens*. Bioorg Med Chem 15:3445–3449

Sayah K, Marmouzi I, Mrabti HN et al (2017) Antioxidant activity and inhibitory potential of *Cistus salviifolius* (L.) and *Cistus monspeliensis* (L.) aerial parts extracts against key enzymes linked to hyperglycemia. Biomed Res Int 2017:2789482

Sayah K, Mrabti HN, Belarj B et al (2020) Evaluation of antidiabetic effect of *Cistus salviifolius* L. (Cistaceae) in streptozotocin-nicotinamide induced diabetic mice. J Basic Chin Physiol pharmacol 2020:0044

Scalzo J, Stevenson D, Hedderley D (2015) Polyphenol compounds and other quality traits in blueberry cultivars. J Berry Res 5:117–130

Schreiber L, Nader-Nieto AC, Schonhals EM et al (2014) SNPs in genes functional in starch-sugar interconversion associate with natural variation of tuber starch and sugar content of potato (*Solanum tuberosum* L.). G3 (Bethesda) 4:1797–1811

Sedigheh A, Jamal MS, Mahbubeh S et al (2011) Hypoglycemic and hypolipidemic effects of pumpkin (*Cucurbita pepo* L.*)* on alloxan-induced diabetic rats. Afr J Pharm Pharmacol 5:2620–2626

Sengenes C, Berlan M, De Glisezinski L et al (2000) Natriuretic peptides: a new lipolytic pathway in human adipocytes. FASEB J 14:1345–1351

Seo C, Sohn JH, Oh H et al (2009) Isolation of the protein tyrosine phosphatase1B inhibitory metabolite from the marine-derived fungus *Cosmospora* sp. SF-506. Bioorg Med Chem Lett 19: 6095–6097

Seo C, Yim JH, Lee HK et al (2011) PTP1B inhibitory secondary metabolites from the Antarctic lichen *Locidella carpathica*. Mycology 2:18–23

Seo YJ, Lee K, Song JH et al (2018) *Ishige okamurae* extract suppresses obesity and hepatic steatosis in high fat diet-induced obese mice. Nutrients 10:1802

Seo SH, Fang F, Kang I (2021) Ginger (*Zingiber officinale*) attenuates obesity and adipose tissue remodeling in high-fat diet-fed C57BL/6 mice. Int J Environ Res Public Health 18:631

Seyedan A, Alshawsh MA, Alshagga MA et al (2017) Antiobesity and lipid lowering effects of *Orthosiphon stamineus* in high-fat diet-induced obese mice. Planta Med 83:684–692

Shah SS, Shah GB, Singh SD et al (2011) Effect of piperine in the regulation of obesity-induced dyslipidemia in high-fat diet rats. Ind J Pharmacol 43:296–299

Sharma SB, Nasir A, Prabhu KM et al (2006) Antihyperglycemic effect of the fruit-pulp of *Eugenia jambolana* in experimental diabetes mellitus. J Ethnopharmacol 104:367–373

Sharma M, Jacob JK, Subramanian J et al (2010) Hexanal and 1-MCP treatments for enhancing the shelf-life and quality of sweet cherry (*Prunus avium* L.). Sci Hortic 125:239–247

Sharma SB, Rajpoot R, Nasir A et al (2011) Ameliorative effect of active principle isolated from seeds of *Eugenia jambolana* on carbohydrate metabolism in experimental diabetes. Evid Based Complement Altern Med 2011:789871

Sharma BR, Kim HJ, Kim MS et al (2017) *Caulerpa okamurae* extract inhibits adipogenesis in 3T3-L1 adipocytes and prevents high-fat diet-induced obesity in C57BL/6 mice. Nutr Res 47: 44–52

Sheng Y, Liu J, Zheng S et al (2019a) Mulberry leaves ameliorate obesity through enhancing brown adipose tissue activity and modulating gut microbiota. Food Funct 10:4771–4778

Sheng Y, Zhao C, Zheng S et al (2019b) Anti-obesity and hypolipidemic effect of water extract from *Pleurotus citrinopileatus* in C57BL/6J mice. Food Sci Nutr 7:1295–1301

Shikov AN, Pozharitskaya ON, Makarova MN et al (2012) Effect of *Bergenia crassifolia* L. extracts on weight gain and feeding behaviour of rats with high carolic diet-induced obesity. Phytomedicine 19:1250–1255

Shimada T, Nagai E, Harasawa Y et al (2011) *Salacia reticulata* inhibits differentiation of 3T3-L1 adipocytes. J Ethnopharmacol 136:67–74

Shimada T, Nakayama Y, Harasawa Y et al (2014) *Salacia reticulata* has therapeutic effects on obesity. J Nat Med 68:668–676

Shimokawa Y, Akao Y, Hirasawa Y et al (2010) Gneyulins A and B, stilbene trimers, and noidesols A and B, dihydroflavonol-C-glucosides, from the bark of *Gnetum gnemonoides*. J Nat Prod 73: 763–767

Shirwaikar A, Rajendran K, Punitha ISR (2005) Antihyperglycemic activity of the aqueous stem extract of *Coscinium fenestratum* in non-insulin dependent diabetic rats. Pharm Biol 43:707–712

Shivanna N, Naika M, Khanum F et al (2013) Antioxidant, anti-diabetic and renal protective properties of *Stevia rebaudiana*. J Diabetes & Its Complications 27:103–113

Shobha R, Andallu B (2018) Antioxidant, antidiabetic and hypolipidemic effects of aniseeds (*Pimpinella anisum* L.): *in vitro* and *in vivo* studies. J Complement Med Alt Healthcare 5: 555656

Si MM, Lou SS, Zhou CX et al (2010) Insulin releasing and alpha-glucosidase inhibitory activity of ethyl acetate fraction of *Acorus calamus in vitro* and *in vivo*. J Ethnopharmacol 128:154–159

Sidor A, Gramza-Michalowska A (2019) Black chokeberry *Aronia melanocarpa* L.-a qualitative composition, phenolic profile and antioxidant potential. Molecules 24:3710

Simoes AND, Tudela JA, Allende A et al (2009) Edible coatings containing chitosan and moderate modified atmospheres maintain quality and enhance phytochemicals of carrot sticks. Postharvest Biol Technol 51:364–370

Singh SN, Vats P, Suri S et al (2001) Effect of an antidiabetic extract of *Catharanthus roseus* on enzymatic activities in streptozotocin induced diabetic rats. J Ethnopharmacol 76:269–277

Sivakumar D, Deventer FV, Terry LA et al (2012) Combination of 1-methylcyclopropene treatment and controlled atmosphere storage retains fruit quality and bioactive compounds in mango. J Sci Food Agric 92:821–830

So Y, Jo YH, Nam BM et al (2015) Anti-obesity effect of isoegomaketone isolated from *Perilla frutescens* (L.) Britt. cv. leaves. Kor J Pharmacogn 46:283–288

Soliman MM, Nassan MA, Ismail TA (2016) *Origanum majoranum* extract modulates gene expression, hepatic and renal changes in a rat model of type 2 diabetes. Iran. J Pharm Res 15 (S):45–54

Son JY, Park SY, Kim JY et al (2011) *Orthosiphon stamineus* reduces appetite and visceral fat in rats. J Korean Soc Appl Biol Chem 54:200–205

Son MJ, Minakawa M, Miura Y et al (2013) Aspalathin improves hyperglycemia and glucose intolerance in obese diabetic *ob/ob* mice. Eur J Nutr 52:1607–1619

Song MY, Kang SY, Kang A et al (2017) *Cinnamomum cassia* prevents high-fat diet-induced obesity in mice through the increase of muscle energy. Am J Chin Med 45:1017–1031
Sophia D, Manoharan S (2007) Hypolipidemic activities of *Ficus racemosa* Linn bark in alloxan induced diabetic rats. Afr J Trad CAM 4:279–288
Soren G, Sarita M, Prathyusha T (2016) Antidiabetic activity of *Actinidia deliciosa* fruit in alloxan induced diabetic rats. Pharma Innov J 5:31–34
Spiegelman BM, Flier JS (2001) Obesity and regulation of energy balance. Cell 104:531–543
Stanely P, Prince M, Menon VP (2000) Hypoglycemic and other related actions of *Tinospora cordifolia* roots in alloxan-induced diabetic rats. J Ethnopharmacol 70:9–15
Steinberg GR, Schertzer JD (2014) AMPK promotes macrophage fatty acid oxidative metabolism to mitigate inflammation: implications for diabetes and cardiovascular disease. Immunol Cell Biol 92:340–345
Stienstra R, Mandard S, Tan NS et al (2007) The interleukin-1 receptor antagonist is a direct target gene of PPARα in liver. J Hepatol 46:869–877
Stull AJ, Wang ZQ, Zhang XH et al (2012) Skeletal muscle protein tyrosine phosphatise 1B regulates insulin sensitivity in African Americans. Diabetes 61:1415–1422
Suanarunsawat T, Anantasomboon G, Piewbang C (2016) Anti-diabetic and anti-oxidative activity of fixed oil extracted from *Ocimum sanctum* L. leaves in diabetic rats. Exp Ther Med 11:832–840
Subash AK, Augustine A (2013) Hypolipidaemic effects of methanol extract of *Holoptelea integrifolia* (Roxb.) Planchon bark in diet-induced obese rats. Appl Biochem Biotechnol 169: 546–553
Sujita J, Yoneshiro T, Hatano T et al (2013) Grains of paradise (*Aframomum melegueta*) extract activates brown adipose tissue and increases whole-body energy expenditure in men. Br J Nutr 110:733–738
Sullivan AC, Triscari J, Spigel HE (1977) Metabolic regulation as a control for lipid disorders. II. Influence of (-)-hydroxycitrate on genetically and experimentally induced hypertriglyceridemia in the rat. Am J Clin Nutr 30:777–784
Sumiyoshi M, Kimura Y (2013) Hop (*Humulus lupulus* L.) extract inhibits obesity in mice fed a high-fat diet over the long term. Br J Nutr 109:162–172
Sun C, Zhang F, Ge X et al (2007) SIRT1 improves insulin sensitivity under insulin-resistant conditions by repressing PTP1B. Cell Metab 6:307–319
Sun W, Chen X, Tong Q et al (2016) Novel small molecule 11β-HSD1 inhibitor from the endophytic fungus *Penicillium commune*. Sci Rep 6:26418
Sung YY, Yoon T, Yang WK et al (2011) Anti-obesity effects of *Geranium thunbergii* extract via improvement of lipid metabolism in high-fat diet-induced obese mice. Mol Med Rep 4:1107–1113
Sung YY, Yoon T, Yang YK et al (2013a) Anti-obesity effects of *Actinidia polygama* extract in mice with high-fat diet-induced obesity. Mol Med Rep 7:396–400
Sung YY, Yoon T, Yang WK et al (2013b) The antiobesity effect of *Polygonum aviculare* L. ethanol extract in high-fat diet-induced obese mice. Evid Based Complement Alternat Med 2013:626397
Sung J, Jeong HS, Lee J (2016) Effect of the capsicoside G-rich fraction from pepper (*Capsicum annuum* L.) seeds on high-fat diet-induced obesity in mice. Phytother Res 30:1848–1855
Suzuki Y, Unno T, Ushitani M et al (1999) Antiobesity activity of extracts from *Lagerstroemia speciosa* L. leaves on female KK-Ay mice. J Nutr Sci Vitaminol 45:791–795
Swanton CJ, Janse S, Chandler K et al (2004) Zone tillage systems for onion and carrot production on muck soils. Can J Plant Sci 84:1167–1169
Taira N, Nugara RN, Inafuku M et al (2017) *In vivo* and *in vitro* anti-obesity activities of dihydropyranocoumarin derivatives from *Peucedanum japonicum* Thunb. J Funct Foods 29: 19–28

Takahashi K, Osuda K (2017) Effect of dietary purified xanthohumol from hop (*Humulus lupulus* L.) pomace on adipose tissue mass, fasting blood glucose level, and lipid metabolism in KK-Ay mice. J Oleo Sci 66:531–541

Takasu T, Yokono M, Tahara A et al (2019) *In vitro* pharmacological profile of ipragliflozin, a sodium glucose transporter 2 inhibitor. Biol Pharm Bull 42:507–511

Talebianpoor MS, Talebianpoor MS, Mansourian M et al (2019) Antidiabetic activity of hydroalcoholic extract of *Myrtus communis* (Myrtle) fruits in streptozotocin-induced and dexamethazone-induced diabetic rats. Phcog res 11:115–120

Tanaka K, Nishizono S, Makino N et al (2008) Hypoglycemic activity of *Eriobotrya japonica* seeds in type 2 diabetic rats and mice. Biosci Biotechnol Biochem 72:686–693

Tandy S, Chung RWS, Wat E et al (2009) Dietary krill oil supplementation reduces hepatic steatosis, glycemia, and hypercholesterolemia in high-fat-fed mice. J Agric Food Chem 57: 9339–9345

Tang QQ, Otto TC, Lane MD (2003) Mitotic clonal expansion: a synchronous process required for adipogenesis. PNAS 100:44–49

Tang Z, Dai S, He Y et al (2015) MEK guards proteome stability and inhibits tumor-suppressive amyloidogenesis via HSF1. Cell 160:729–744

Tang P, Shen DY, Xu YQ et al (2018) Effect of fermentation conditions and plucking standards of tea leaves on the chemical components and sensory quality of fermented juice. J Chem 2018: 4312875

Tezuka Y, Kasimu R, Basnet P et al (1997) Aldose reductase inhibitory constituents of the root of *Salvia miltiorhiza*. Chem Pharm Bull 45:1306–1311

Thomas C, Gioiello A, Noriega L et al (2009) TGR5-mediated bile acid sensing controls glucose homeostasis. Cell Metab 10:162–164

Thomas SS, Kim M, Lee SJ et al (2018) Antiobesity effects of purple perilla (*Perilla frutescens* var. *acuta*) on adipocyte differentiation and mice fed a high-fat diet. J Food Sci 83:2384–2393

Thomford NE, Senthebane DA, Rowe A et al (2018) Natural products for drug discovery in the 21st century: innovations for novel drug discovery. Int J Mol Sci 19:1578

Thounaojam MC, Jadeja RN, Ansarullah et al (2010) Prevention of high fat diet induced insulin resistance in C57BL/6J mice by *Sida rhomboidea* Roxb extract. J Health Sci 56:92–98

Thounaojam MC, Jadeja RN, Ramani UV et al (2011) *Sida rhomboidea* Roxb leaf extract down-regulates expression of PPARγ2 and leptin genes in high fat diet fed C57BL/6J mice and retards *in vitro* 3T3-L1 pre-adepocyte differentiation. Int J Mol Sci 12:4661–4677

Tiwari U, Cummins E (2013) Factors influencing levels of phytochemicals in selected fruit and vegetables during pre-and post-harvest food processing operations. Food Res Int 50:497–506

Tolic MT, Krbavcic IP, Vujevic P et al (2017) Effects of weather conditions on phenolic content and antioxidant capacity in juice of chokeberries (*Aronia melanocarpa* L.). Pol J Food Nutr Sci 67:67–74

Tu Z, Moss-Pierce T, Ford P et al (2013) Rosemary (*Rosmarinus officinalis* L.) extract regulates glucose and lipid metabolism by activating AMPK and PPAR pathways in HepG2 cells. J Agric Food Chem 61:2803–2810

Tundis R, Loizzo MR, Menichini F (2010) Natural products as α-amylase and α-glucosidase inhibitors and their hypoglycaemic potential in the treatment of diabetes: an update. Mini-Rev Med Chem 10:315–331

Tzeng T, Lu H, Liou S et al (2013) Reduction of lipid accumulation in white adipose tissues by *Cassia tora* (Leguminosae) seed extract is associated with AMPK activation. Food Chem 136: 1086–1094

Ueki K, Yamamoto-Honda R, Kaburagi Y et al (1998) Potential role of protein kinase B in insulin-induced glucose transport, glycogen synthesis, and protein synthesis. J Biol Chem 273:5315–5322

Umezawa H, Aoyagi T, Ogawa K et al (1984) Diproteins A and B, inhibitors of dipeptidyl peptidase IV, produced by bacteria. J Antibiot 37:422–425

Vaast P, Bertrand B, Perriot JJ et al (2006) Fruit thinning and shade improve bean characteristics and beverage quality of coffee (*Coffea arabica* L.) under optimal conditions. J Sci Food Agric 86:197–206

Vallejo F, Tomas-Barberan F, Garcia-Viguera C (2003) Effect of climatic sulphur fertilization conditions, on phenolic compounds and vitamin C, in the inflorescences of eight broccoli cultivars. Eur Food Res Technol 216:395–401

Valverde AM, Gonzalez-Rodriguez A (2011) IRS2 and PTP1B: two opposite modulators of hepatic insulin signalling. Arch Physiol Biochem 117:105–115

Varshney S, Shankar K, Beg M et al (2014) Rohitukine inhibits *in vitro* adipogenesis arresting mitotic clonal expansion and improves dyslipidemia *in vivo*. J Lipid Res 55:1019–1032

Venkatesh S, Reddy BM, Reddy CD et al (2010) Antihyperglycemic and hypolipidemic effects of *Helicteres isora* roots in alloxan-induced diabetic rats: a possible mechanism of action. J Nat Med 64:295–304

Vieira AT, Fukumori C, Ferreira CM (2016) New insights into therapeutic strategies for gut microbiota modulation in inflammatory diseases. Clin Transl Immunol 5:e87

Villas Boas GR, Rodrigues Lemons JM, de Oliveira MW et al (2020) Aqueous extract from *Magnifera indica* Linn (Anacardiaceae) leaves exerts long-term hypoglycaemic effect, increases insulin sensitivity and plasma insulin levels on diabetic Wistar rats. PLOS One 15:e0227105

Vinayagam R, Jayachandran M, Chung SSM et al (2018) Guava leaf inhibits hepatic gluconeogenesis, and increases glycogen synthesis via AMPK/ACC signaling pathways in streptozotocin-induced diabetic rats. Biomed Pharmacother 103:1012–1017

Volke L, Krause K (2020) Effect of thyroid hormones on adipose tissue flexibility. Eur Thyroid J 10(1):1–9. https://doi.org/10.1159/000508483

Waheb NAA, Abdullah N, Aminudin N (2014) Characterization of potential antidiabetic-related proteins from *Pleurotus pulmonarius* (Fr) Queb (Grey oyster mushroom) by MALDI-TOF/TOF mass spectrometry. Biomed Res Int 2014:131607

Wan M, Leavens KF, Hunter RW et al (2013) A noncanonical, GSK-3-independent pathway controls postprandial hepatic glycogen deposition. Cell Metab 18:99–105

Wang SY, Lin HS (2000) Antioxidant activity in fruits and leaves of blackberry, raspberry, and strawberry varies with cultivar and developmental stage. J Agric Food Chem 48:140–146

Wang J, Ryu HK (2015) The effects of *Momordica charantia* on obesity and lipid profiles of mice fed a high-fat diet. Nutr Res Pract 9:489–495

Wang CT, Wang CT, Cao YP et al (2011a) Effect of modified atmosphere packaging (MAP) with low and superatmospheric oxygen on the quality and antioxidant enzyme system of golden needle mushrooms (*Flammulina velutipes*) during post-harvest storage. Eur Food Res Technol 232:851

Wang L, Bang CY, Choung SY (2011b) Anti-obesity and hypolipidemic effects of *Boussingaultia gracilis* Miers. var. *pseudobaselloides* Bailey in obese rats. J Nat Med 14:17–25

Wang T, Choi RC, Li J et al (2012a) Trillin, a steroidal saponin isolated from the rhizomes of *Dioscorea nipponica*, exerts protective effects against hyperlipidemia and oxidative stress. J Ethnopharmacol 139:214–220

Wang YS, Gao LP, Shan Y et al (2012b) Influence of shade on flavonoid biosynthesis in tea (*Camellia sinensis* (L.) O. Kuntze). Sci Hortic 141:7–16

Wang W, He Y, Lin P et al (2014) *In vitro* effects of active components of *Polygonum multiflorum* radix on enzymes involved in the lipid metabolism. J Ethnopharmacol 153:763–770

Wang K, Cao P, Shui W et al (2015a) *Angelica sinensis* polysaccharide regulates glucose and lipid metabolism disorder in prediabetic and streptozotocin-induced diabetic mice through the elevation of glycogen levels and reduction of inflammatory factors. Food Funct 6:902–909

Wang LJ, Jiang B, Wu N et al (2015b) Natural and semisynthetic protein tyrosine phosphatise 1B inhibitors as anti-diabetic agents. RSC Adv 5:48822–48834

Wang GC, Yu JH, Shen Y et al (2016) Limonoids and triterpenoids as 11β-HSD1 inhibitors from *Walsura robusta*. J Nat Prod 79:899–906

Wang X, Tang ZS, Yang N et al (2016a) Protein tyrosine phosphatase 1B (PTP1B) inhibitors from *Arnebia euchroma*. Chin Pharm J 51:1120–1123

Wang Y, Wang J, Zhao Y et al (2016b) Fucoidan from sea cucumber *Cucumaria frondosa* exhibits antihyperglycemic effects in insulin resistant mice via activating the PI3K/PKB pathway and GLUT4. J Biosci Bioeng 121:36–42

Wang LY, Cheng KC, Li Y et al (2017a) The dietary furocoumarin imperatorin increases plasma GLP-1 levels in type-1-like diabetic rats. Nutrients 9:1192

Wang N, Xu H, Jiang S et al (2017b) MYB12 and MYB22 play essential roles in proanthocyanidin and flavonol synthesis in red-fleshed apple (*Malus sieversii* f. *niedzwetzkyana*). Plant J 90:276–292

Wang S, Lu A, Zhang L et al (2017c) Extraction and purification of pumpkin polysaccharides and their hypoglycaemic effect. Int J Biol Macromol 98:182–187

Wang J, Hu W, Li L et al (2017d) Antidiabetic activities of polysaccharides separated from *Inonotus obliquus* via the modulation of oxidative stress in mice with streptozotocin-induced diabetes. PLOS One 12:e0180476

Wang Z, Yang L, Fan H et al (2017e) Screening of a natural compound library identifies emodin, a natural compound from *Rheum palmatum* Linn that inhibits DPP4. Peer J 5:e3283

Wang K, Wang H, Liu Y et al (2018) *Dendrobium officinale* polysaccharide attenuates type 2 diabetes mellitus via the regulation of PI3K/Akt-mediated glycogen synthesis and glucose metabolism. J Funct Foods 40:261–271

Wang T, Zheng L, Zhao T et al (2020a) Anti-diabetic effects of sea cucumber (*Holothuria nobilis*) hydrohysates in streptozotocin and high-fat-diet induced diabetic rats via activating the PI3K/Akt pathway. J Funct Foods 75:104224

Wang X, Xu M, Peng Y et al (2020b) Triptolide enhances lipolysis of adipocytes by enhancing ATGL transcription via upregulation of p53. Phytother Res 34:3298–3310

Watanabe J, Kawabata J, Kurihara H et al (1997) Isolation and identification of α-glucosidase inhibitors from Tochu-cha (*Eucommia ulmoides*). Biosci Biotechnol Biochem 61:177–178

Watanabe M, Houten SM, Mataki C et al (2006) Bile acids induce energy expenditure by promoting intracellular thyroid hormone activation. Nature 439:484–489

Weibel EK, Hadvary P, Hochuli E et al (1987) Lipstatin, an inhibitor of pancreatic lipase, produced by *Streptomyces toxytricini*. 1. Producing organism, fermentation, isolation and biological activity. J Antibiot (Tokyo) 40:1081–1085

Weidner C, Wowro SJ, Freiwald A et al (2014) Lemon balm extract causes potent antihyperglycemic and antihyperlipidemic effects in insulin-resistant obese mice. Mol Nutr Food Res 58:903–907

Wen JJ, Gao H, Hu JL et al (2019) Polysaccharides from fermented *Momordica charantia* ameliorate obesity in high-fat-induced obese rats. Food Funct 10:448

Wiese J, Aldemir H, Schmaljohann R et al (2017) Asperentin B, a new inhibitor of the protein tyrosine phosphatase1B. Mar Drugs 15:191

Won SR, Kim SK, Kim YM et al (2007) Licochalcone A: a lipase inhibitor from the roots of *Glycyrrhiza uralensis*. Food Res Int 40:1046–1050

Wright EM, Loo DD, Hirayama BA (2011) Biology of human sodium glucose transporters. Physiol Rev 91:733–794

Wu GD, Chen J, Hoffmann C et al (2011) Linking long-term dietary patterns with gut microbial enterotypes. Science 334:105–108

Wu Z, Rosen ED, Brun R et al (1999) Cross regulation of C/EBPα and PPARγ controls the transcriptional pathway of adipogenesis and insulin sensitivity. Mol Cell 3:151–158

Wu CH, Yang MY, Chan KC et al (2010) Improvement in high-fat diet-induced obesity and body fat accumulation by a *Nelumbo nucifera* leaf flavonoid-rich extract in mice. J Agric Food Chem 58:7075–7081

Wu C, Luan H, Wang S et al (2013) Modulation of lipogenesis and glucose comsumption in HepG2 cells and C2C12 myotubes by sophoricoside. Molecules 18:15624–15635

Wu C, Zhang X, Zhang X et al (2014a) The caffeoylquinic acid-rich *Pandanus tectorius* fruit extract increases insulin sensitivity and regulates hepatic glucose and lipid metabolism in diabetic db/db mice. J Nutr Biochem 25:412–419

Wu Y, Yu Y, Szabo A et al (2014b) Central inflammation and leptin resistance are attenuated by ginsenoside Rb1 treatment in obese mice fed a high-fat diet. PLOS One 9:e92618

Wu L, Zhang L, Li B et al (2018) AMP-activated protein kinase (AMPK) regulates energy metabolism through modulating thermogenesis in adipose tissue. Front Pharmacol 9:122

Wu SJ, Tung YJ, Ng LT (2020a) Anti-diabetic effects of *Grifola frondosa* bioactive compound and its related molecular signaling pathways in palmitate-induced C2C12 cells. J Ethnopharmacol 260:112962

Wu Y, Tan F, Zhang T et al (2020b) The anti-obesity effect of lotus leaves on high-fat-diet-induced obesity by modulating lipid metabolism in C57BL/6J mice. Appl Biol Chem 2020:61

Xiang H, Sun-Waterhouse D, Cui C (2021) Hypoglycemic polysaccharides from *Auricularia auricula* and *Auricularia polytricha* inhibit oxidative stress, NF-κB signaling and proinflammatory cytokine production in streptozotocin-induced diabetic mice. Food Sci Hum Wellness 10:87–93

Xiao B, Sanders MJ, Underwood E et al (2011) Structure of mammalian AMPK and its regulation by ADP. Nature 472:230–233

Xie ZM, Zhou T, Liao HY et al (2015) Effects of *Ligutrum robustum* on gut microbes and obesity in rats. World J gastroenterol 21:13042–13054

Xing XH, Zhang ZM, Hu XZ et al (2009) Antidiabetic effects of *Artemisia sphaerocephala* Krasch gum, a novel food additive in China, on streptozotocin-induced type 2 diabetic rats. J Ethnopharmacol 125:410–416

Xiong Y, Shen L, Liu KJ et al (2010) Antiobesity and antihyperglycemic effects of ginsenoside Rb1 in rats. Diabetes 59:2505–2512

Xiong M, Huang Y, Liu Y et al (2018) Antidiabetic activity of ergosterol from *Pleurotus ostreatus* in KK-Ay mice with spontaneous type 2 diabetes mellitus. Mol Nutr Food Res 62:1700444

Xu BJ, Han LK, Zheng YN et al (2005) *In vitro* inhibitory effect of triterpenoidal saponins from *Platycodi Radix* on pancreatic lipase. Arch Pharm Res 28:180–185

Xu L, Xing M, Xu X et al (2019) Alizarin increase glucose uptake through PI3K/Akt signaling and improve alloxan-induced diabetic mice. Future Med Chem 11:395–406

Xue DQ, Mao SC, Yu XQ et al (2013) Isomalabaricane triterpenes with potent protein tyrosine phosphatase 1B (PTP1B) inhibition from the Hainan sponge *Stelletta* sp. Biochem Syst Ecol 49: 101–106

Yamamoto N, Kanemoto Y, Ueda M et al (2011) Anti-obesity and anti-diabetic effects of ethanol extract of *Artemisia princeps* in C57BL/6 mice fed a high-fat diet. Food Funct 2:45–52

Yamasaki M, Ogawa T, Wang L et al (2013) Anti-obesity effects of hot water extract from Wasabi (*Wasabia japonica* Matsum.) leaves in mice fed a high-fat diet. Nutr Res Pract 7:267–272

Yan XH, Yi P, Cao P et al (2016) 16-nor-Limonoids from *Harrisonia perforata* as promising selective 11β-HSD1 inhibitors. Sci Rep 6:36927

Yang J, Brown MS, Liang G (2008) Identification of the acyltransferase that octanoylates ghrelin, an appetite stimulating peptide hormone. Cell 132:387–396

Yang Y, Hwang I, Kim S et al (2013) *Lentinus edodes* promotes fat removal in hypercholesterolemic mice. Exp Ther Med 6:1409–1413

Yang H, Liu DQ, Liang TJ et al (2014a) Racemosin C, a novel minor bisindole alkaloid with protein tyrosine phosphatase 1B inhibitory activity from the green alga *Caulerpa racemosa*. J Asian Nat Prod Res 16:1158–1165

Yang MH, Chin YW, Yoon KD et al (2014b) Phenolic compounds with pancreatic lipase inhibitory activity from Korean yam (*Dioscorea oppositifolia*). J Enzyme Inhib Med Chem 29:1–6

Yang J, Yang X, Wang C et al (2015a) Sodium-glucose-linked transporter 2 inhibitors from *Sophora flavescens*. Med Chem Res 24:1265–1271

Yang RM, Liu F, He ZD et al (2015b) Anti-obesity effect of total phenylpropanoid glycosides from *Ligustrum robustum* Blume in fatty diet-fed mice *via* up-regulating leptin. J Ethnopharmacol 169:459–465

Yang Q, Qi M, Tong R et al (2017a) *Plantago asiatica* L. seed extract improves lipid accumulation and hyperglycemia in high-fat diet-induced obese mice. Int J Mol Sci 18:1393

Yang TH, Yao HT, Chiang MT (2017b) Red algae (*Gelidium amansii*) hot-water extract ameliorates lipid metabolism in hamsters fed a high-fat diet. J Food Drug Anal 25:931–938

Yazdanpanah Z, Ghadiri-Anari A, Mehrjardi AV et al (2017) Effect of *Ziziphus jujube* fruit infusion on lipid profiles, glycaemic index and antioxidant status in type 2 diabetic patients: a randomized controlled clinical trial. Phytother Res 31:755–762

Yilmazer-Musa M, Griffith AM, Michels AJ et al (2012) Grape seed and tea extracts and catechin-3-gallates are potent inhibitors of α-amylase and α-glucosidase activity. J Agric Food Chem 60: 8924–8929

Yin J, Zuberi A, Gao Z et al (2009) Shilianhua extract inhibits GSK-3β and promotes glucose metabolism. Am J Physiol Endocrinol Metab 296:E1275–E1280

Yoon M (2009) The role of PPARα in lipid metabolism and obesity: focusing on the effects of estrogen on PPARα action. Pharmacol Res 60:151–159

Yoon NY, Kim YR, Chung HY et al (2008) Anti-hyperlipidemic effect of an edible brown algae, *Ecklonia stolonifera*, and its constituents on poloxamer 407-induced hyperlipidemic and cholesterol-fed rats. Arch Pharm Res 31:1564–1571

Yoon SA, Kang SI, Shin YS et al (2013) p-Coumaric acid modulates glucose and lipid metabolism via AMP-activated protein kinase in L6 skeletal muscle cells. Biochem Biophys Res Commun 432:553–557

Yoshida T, Rikimaru K, Sakai M et al (2013) *Plantago lanceolata* leaves prevent obesity in C57BL/6J mice fed a high-fat diet. Nat Prod Res 27:982–987

Yoshikawa M, Shimada H, Nishida N et al (1998) Antidiabetic principles of natural medicines. II. Aldose reductase and α-glucosidase inhibitors from Brazilian natural medicine, the leaves of *Myrcia multiflora* DC (Myrtaceae): structures of myrciacitrins I and II and myrciaphenones A and B. Chem Pharm Bull 46:113–119

Yoshikawa M, Morikawa T, Murakami T et al (1999) Medicinal flowers. I. Aldose reductase inhibitors and three new cudesmane-type sesquiterpenes, kikkanols A, B and C, from the flowers of *Chrysanthemum indicum* L. Chem Pharm Bull 47:340–345

Yoshizumi K, Hirano K, Ando H et al (2006) Lupane-type saponins from leaves of *Acanthopanax sessiflorus* and their inhibitory activity on pancreatic lipase. J Agric Food Chem 54:335–341

Yuan H, Ma Q, Ye L et al (2016) Traditional medicine and modern medicine from natural products. Molecules 21:559

Yuliana ND, Korthout H, Wijaya CH et al (2014) Plant-derived food ingredients for stimulation of energy expenditure. Crit Rev Food Sci Nutr 54:373–388

Yun JW (2010) Possible anti-obesity therapeutics from nature-a review. Phytochemistry 71:1625–1641

Zabolotny JM, Kim YB, Welsh LA et al (2008) Protein-tyrosine phosphatise 1B expression is induced by inflammation in vivo. J Biol Chrm 283:14230–14241

Zeng T, Zhang CL, Song FY et al (2012) garlic oil alleviated ethanol-induced fat accumulation via modulation of SREBP-1, PPAR-α and CYP2E1. Food Chem Toxicol 50:485–491

Zhang J, Tiller C, Shen J et al (2007) Antidiabetic properties of polysaccharide-and polyphenolic-enriched fractions from the brown seaweed *Ascophyllum nodosum*. Can J Physiol Pharmacol 85: 1116–1123

Zhang J, Kang MJ, Kim MJ et al (2008) Pancreatic lipase inhibitory activity of *Taraxacum officinale in vitro* and *in vivo*. Nutr Res Pract 2:200–203

Zhang Y, Li Y, Guo YW et al (2009) A sesquiterpene quinone, dysidine, from the sponge *Dysidea villosa*, activates the insulin pathway through inhibition of PTPases. Acta Pharmacol Sin 30: 333–345

Zhang Y, Fan S, Hu N et al (2012) Rhein reduces fat weight in db/db mouse and prevents diet-induced obesity in C57BL/6 mouse through the inhibition of PPARγ signaling. PPAR Res 2012:374936

Zhang X, Liu Z, Bi X et al (2013) flavonoids and its derivatives from Callistephus chinensis flowers and their inhibitory activities against alpha-glucosidase. EXCLI J 12:956–966

Zhang J, Chen C, Zhang D et al (2014a) Reactive oxygen species produced via plasma membrane NADPH oxidase regulate anthocyanin synthesis in apple peel. Planta 240:1023–1035

Zhang X, Zhao Y, Zhang M et al (2014b) Structural changes of gut microbiota during berberine-mediated prevention of obesity and insulin resistance in high-fat diet-fed rats. PLOS One 7: e42529

Zhang YL, Luo JG, Wan CX et al (2014c) Geranylated 2-arylbenzofurans from *Morus alba* var. tatarica and their α-glucosidase and protein tyrosine phosphatase 1B inhibitory activities. Fitoterapia 92:116–126

Zhang YJ, Gan RY, Li S et al (2015) Antioxidant phytochemicals for the prevention and treatment of chronic diseases. Molecules 20:21138–21156

Zhang Y, Feng F, Chen T et al (2016) Antidiabetic and antihyperlipidemic activities of *Forsythia suspensa* (Thunb) Vahl (fruit) in streptozotocin-induced diabetic mice. J Ethnopharmacol 192: 256–263

Zhao C, Liao Z, Wu X et al (2014) Isolation, purification, and structural features of a polysaccharide from *Phellinus linteus* and its hypoglycaemic effect in alloxan-induced diabetic mice. J Food Sci 79:H1002–H1010

Zhao R, Gao X, Zhang T et al (2016) Effects of *Lycium barbarum* polysaccharide on type 2 diabetes mellitus rats by regulating biological rhythms. Iran J Basic Med Sci 19:1024–1030

Zhao BT, Nguyen DH, Le DD et al (2018a) Protein tyrosine phosphatise 1B inhibitors from natural sources. Arch Pharm Res 41:130–161

Zhao H, Lai Q, Zhang J et al (2018b) Antioxidant and hypoglycaemic effects of acidic-extractable polysaccharides from *Cordyceps militaris* on type 2 diabetes mice. Oxid Med Cell Longev 2018:9150807

Zhao R, Hu Q, Ma G et al (2019) Effects of *Flammulina velutipes* polysaccharide on immune response and intestinal microbiota in mice. J Funct Foods 56:255–264

Zheng J, Manabe Y, Sugawara T (2020) Siphonaxanthin, a carotenoid from green algae *Codium cylindricum*, protects ob/ob mice fed on a high-fat diet against lipotoxicity by ameliorating somatic stresses and restoring anti-oxidant capacity. Nutr Res 77:29–42

Zhou B, Shen Y, Wu Y et al (2015) Limonoids with 11β-hydroxysteroid dehydrogenase type 1 inhibitory activities from *Dysoxylum mollissimum*. J Nat Prod 78:2116–2122

Zhou T, Chen J, Chen Y et al (2019) *Ligustrum robustum* intake, weight loss, and gut microbiota: an intervention trial. Evid Based Complement Alternat Med 2019:4643074

Zhu F, Ma XH, Qin C et al (2012) Drug discovery prospect from untapped species: indications from approved natural product drugs. PLOS One 7:e39782

Zhu K, Nie S, Li C et al (2013) A newly identified polysaccharide from *Ganoderma atrum* attenuates hyperglycemia and hyperlipidemia. Int J Biol Macromol 57:142–150

Zhu K, Nie S, Li C et al (2014) *Ganoderma atrum* polysaccharide improves aortic relaxation in diabetic rats via PI3K/Akt pathway. Carbohydr Polym 103:520–527

Zhu PY, Yin WH, Wang MR et al (2015) Andrographolide suppresses melanin synthesis through Akt/GSK3β/ β-catenin signal pathway. J Dermatol Sci 79:74–83

Zhu K, Nie S, Tan L et al (2016) A polysaccharide from *Ganoderma atrum* improves liver function in type 2 diabetic rats via antioxidant action and short-chain fatty acids excretion. J Agric Food Chem 64:1938–1944

Zhu L, Wang W, Xie TH et al (2020) TGR5 receptor activation attenuates diabetic retinopathy through suppression of RhoA/ROCK signaling. FASEB J 34:4189–4203

Zimmermann R, Struss JS, Haemmerle G et al (2004) Fat mobilization in adipose tissue is promoted by adipose triglyceride lipase. Science 306:1383–1386

5 Pharmacology of Anti-obesity and Antidiabetic Phytochemicals Isolated from Various Natural Sources (Plants, Seaweeds, Mushrooms, Marine Animals, and Microorganisms)

Biswanath Dinda, Subhajit Dinda, and Mithun Chakraborty

5.1 Introduction

Recently available drugs of synthetic origin in management of obesity and diabetes are costly and not affordable by poor people and have potential adverse side effects, and thereby these cause serious other complications among many obese and diabetic patients. As a result, some of these drugs have been withdrawn from the market. For this reason, most of the leading pharmaceutical industries have paid their attention for discovery of potential natural compounds with low-cost and minimal adverse effects for treatment of obesity and diabetes as an alternative strategy. In the earlier chapter, we have discussed that a large variety of natural resources, namely, dietary fruits, vegetables, grains, plants, seaweeds, edible and medicinal mushrooms, marine fishes and cucumbers, and microorganisms, have potential anti-obesity and antidiabetic effects. Their bioactive phytochemicals having diverse skeletal structures and belonging to different chemical classes, such as flavonoids, simple phenolics, lignans, stilbenoids, curcuminoids, tannins, alkaloids, terpenoids, steroids, saponins, organosulfurs, thiosugars, and polysaccharides. A growing body of evidence demonstrates that these natural products have multiple targets of action for prevention and treatment of obesity and diabetes. Most of these natural components exhibit hypolipidemic, hypoglycemic, antioxidant, and anti-inflammatory activities for improvement of insulin resistance, insulin secretion, and insulin action in insulin-responsive tissues for amelioration of lipid and glucose metabolic disorders in cellular and vivo models of obesity and diabetes. In this

B. Dinda (✉)
Department of Chemistry, Tripura University, Suryamaninagar, Tripura, India

S. Dinda
Department of Chemistry, Government Degree College, Kamalpur, Dhalai, Tripura, India

M. Chakraborty
Department of Chemistry, University of Hyderabad, Gachibowli, Hyderabad, Telangana, India

B. Dinda (ed.), *Natural Products in Obesity and Diabetes*,
https://doi.org/10.1007/978-3-030-92196-5_5

chapter, we address the pharmacology of some phytochemicals having potent anti-obesity and antidiabetic activity and their major natural sources and molecular targets.

5.2 Pharmacology of Phytochemicals

5.2.1 Flavonoids

Flavonoids are the largest group of plant polyphenolics and found abundantly in our dietary fruits and vegetables, grains, spices, and beverages (tea, coffee, and wines). Numerous studies on these natural products in cellular and animal models revealed their potential therapeutic effects in various diseases including obesity, diabetes, cancer, cardiovascular diseases, and bone and neurodegenerative disorders (Chen et al. 2014; Hossain et al. 2016). Flavonoids are found in nature either as their glycosides or free aglycones. They have a common flavan nucleus of 15 carbon atoms, which are arranged in two aromatic (A and B) rings and a central oxygenated pyran ring (C) **371.** Flavonoids are broadly classified into eight sub-classes, flavonols **372**, flavones **373**, flavanones **374**, flavanols **375**, isoflavones **376**, anthocyanins **377**, chalcones **378**, and aurones **379**, according to the arrangements of aromatic rings to the central pyran ring and enzymatic transformation of pyran ring (Harborne and Mabry 1982) (Scheme 5.1). In obese patients and animals,

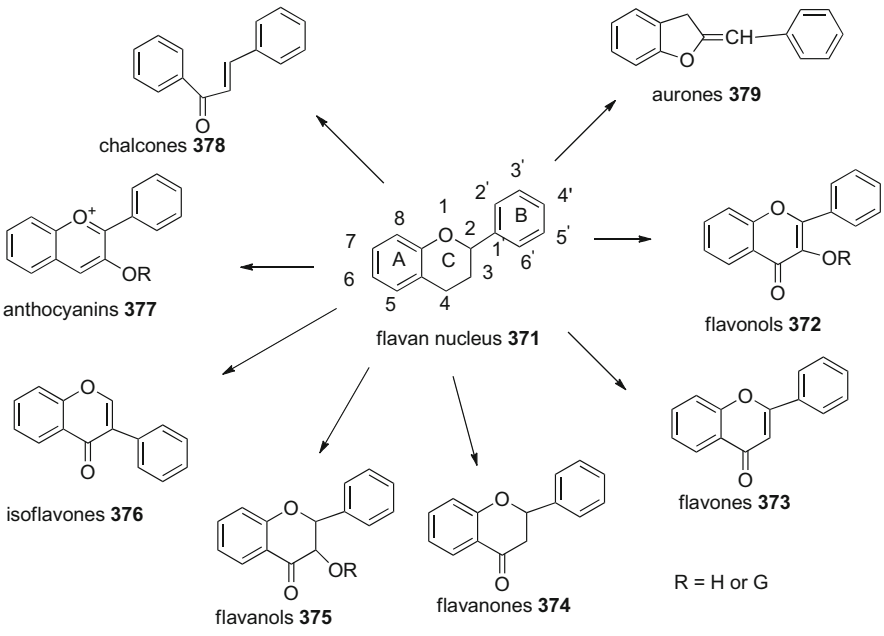

Scheme 5.1 Basic chemical structures of major sub-classes of flavonoids

flavonoids reduce the accumulation of excess body fat mass through regulation of dietary fat and carbohydrate digestion and metabolism in different metabolic tissues through different cell signaling pathways and inhibition of the activity of digestive enzymes in intestinal tissues.

5.2.1.1 Flavonols

Quercetin **23** is present abundantly in apples, red grapes, berries (cranberries, blueberries, cowberries, and raspberries), dark cherries, citrus fruits, mango, onions, and green leafy vegetables, such as broccoli. Among the fruits and vegetables, quercetin content is highest in onions (300 mg/kg) (Hollman and Arts 2000; Anand David et al. 2016). In 3T3-L1 adipocytes, quercetin decreased intracellular lipid accumulation by suppression of the expression of key adipogenic factors C/EBPα, C/EBPβ, PPARγ, and FABP4 and TG synthesis-related genes lipin 1, DGAT1, and lysophosphatidic acid acyltransferase, LPAAT-theta (LPAATθ), an activator of mTOR, through inhibition of the expression of inflammatory factors ERK1/2, JNK, and p38MAPK, MCP-1, IL-6, TNF-α, and NF-κB in MAPK signaling pathway. In DIO mice, quercetin reduced body weight by 40% and suppressed the expression of adipogenic and lipogenic-related genes and inflammatory cytokines in WAT of obese mice (Seo et al. 2015). Moreover, quercetin reduced obesity-induced hypothalamic inflammation by upregulation of the expression of heme oxygenase (HO-1), and suppression of the expression of heat shock proteins HSP72 and HSP70, and SOCS3 in hypothalamus for improvement of leptin signaling in DIO mice (Yang et al. 2017). In both STZ-diabetic rats and db/db diabetic mice, quercetin significantly reduced both fasting and postprandial glucose levels, and HbA1c levels by increasing insulin secretion and reducing the activity of intestinal maltase (α-glucosidase) in diabetic rodents (Kim et al. 2011). Quercetin and its glycosides, quercetin 3-*O*-glucoside **380** and quercetin 3-*O*-galactoside **381** (Fig. 5.1) from cowberries (*Vaccinium vitis-idaea*), increased glucose uptake in muscle C2C12 cells by upregulation of the expression and translocation of GLUT4 proteins into plasma membrane via activation of AMPK and Akt (Eid et al. 2010). In L6 myotubes, quercetin increased the activation of both AMPK and insulin signaling (PI3K/Akt), but the former pathway in a dominant manner (Dhanya et al. 2017).

Rutin **54**, also known as rutoside, quercetin-3-*O*-rutinoside, and sophorin, is widely distributed in fruits (citrus fruits, oranges, cherries, apple, aronia, grape seeds, cherries, and mulberry), vegetables (buckwheat, red hot chillis), and medicinal herbs (green tea and *Rheum* spp.). Among the fruits, rutin content is high in grape seeds (10.16% in dry extract) (Atanassova and Bagdassarian 2009). Rutin on dietary supplementation in both genetically obese (db/db) and diet-induced obesity (DIO) mice significantly reduced body weight, lipid content in adipose tissue (AT), and serum TG, TC levels, and increased energy expenditure in brown adipose tissue (BAT) by upregulation of the expression of thermogenic genes UCP1, PGC1α, PRDM16, nuclear respiratory factor 1 (NRF1), and NRF2 through enhanced expression and activation of SIRT1 via its deacetylation (Yuan et al. 2017). In 3T3-L1 adipocytes, rutin inhibited adipogenesis and reduced intracellular lipid and TG

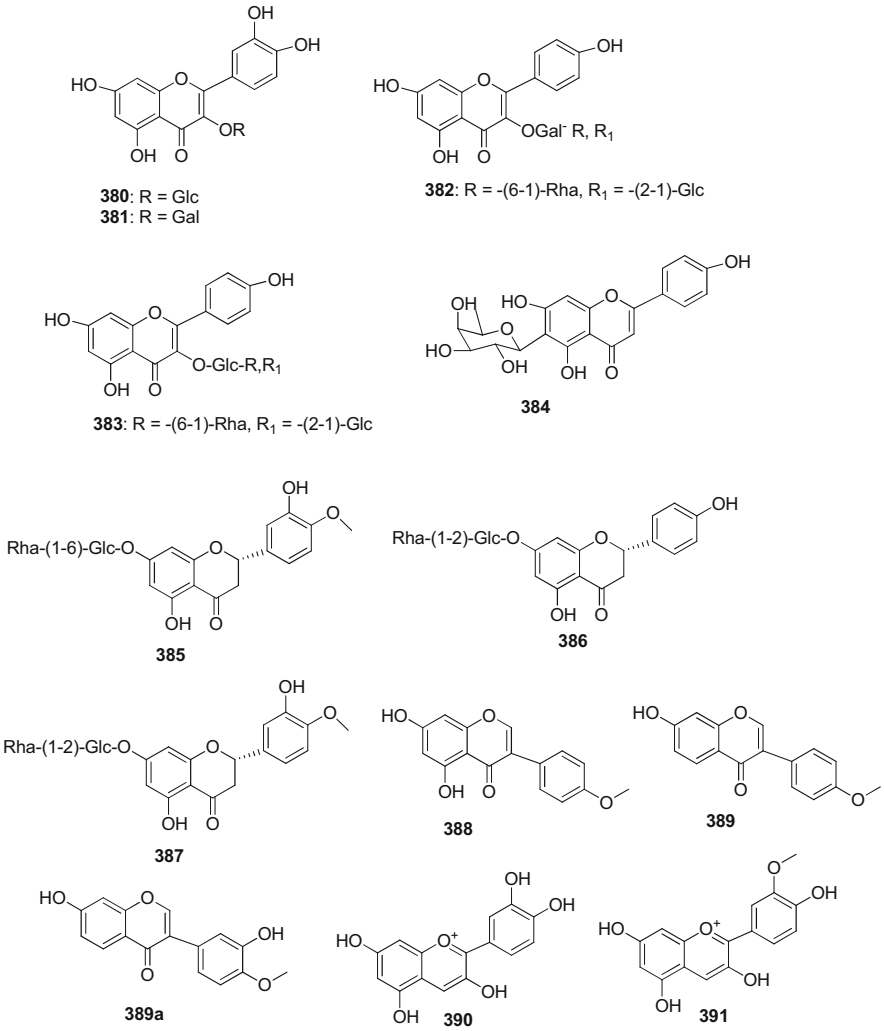

Fig. 5.1 Chemical structures of some natural products

accumulation by suppression of the expression of adipogenic genes C/EBPα, PPARγ and FABP4, and in palmitic acid-induced insulin resistance in muscle L6 cells, increased glucose uptake and translocation of GLUT4 proteins into cell membrane and insulin signaling through increased phosphorylation level of Akt. In animal model, rutin (25 mg/kg bw) in HFD-STZ-induced diabetic mice significantly decreased serum FG, TC, TG, LDL-C, and FFAs levels and increased insulin sensitivity in skeletal muscle of diabetic mice (Varshney et al. 2019). Rutin (500 mg/day) on supplementation in diet to diabetic patients for 60 days decreased the levels

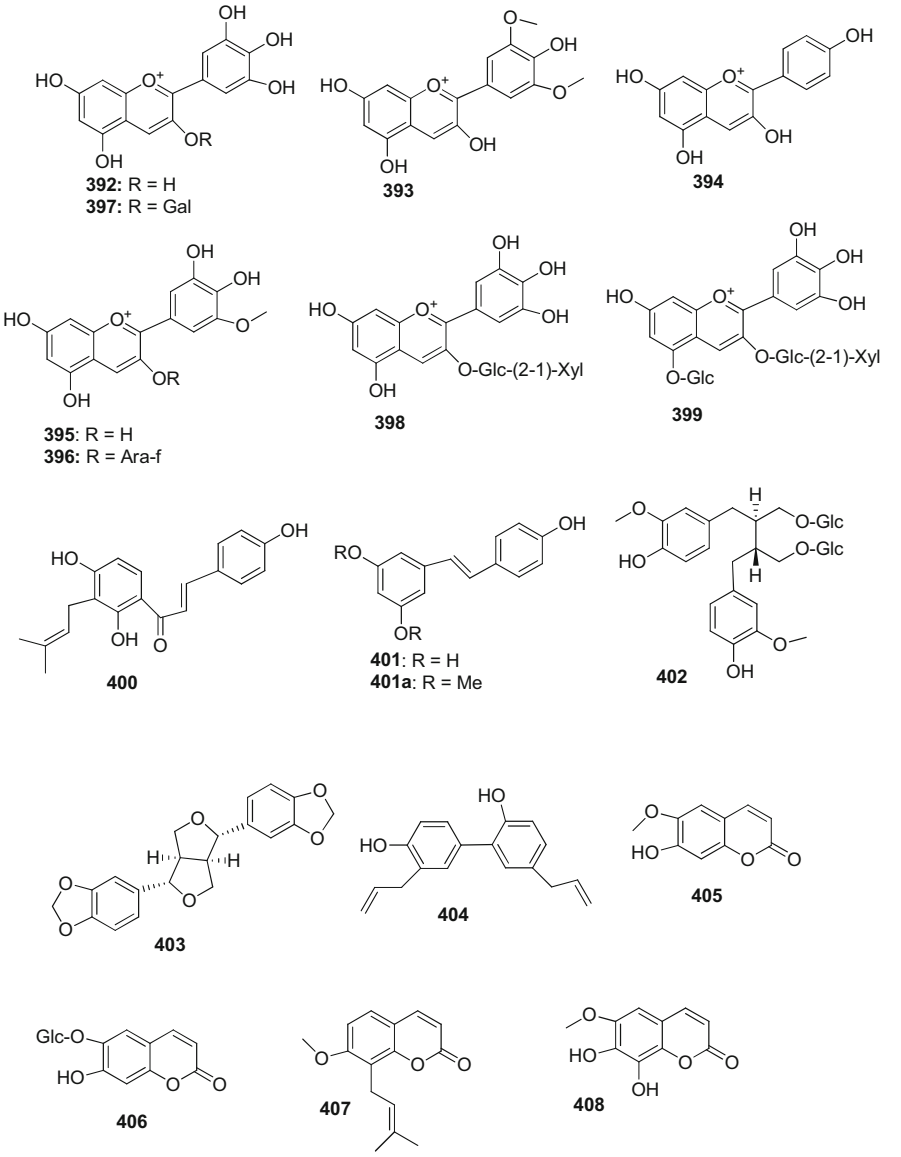

Fig. 5.1 (continued)

of FBG, systolic and diastolic blood pressure (BP), serum urea and creatinine, and increased serum HDL-C level (Sattanathan et al. 2011). Supplementation of rutin to healthy volunteers for 6 weeks resulted in the occurrence of quercetin, kaempferol, and isorhamnetin in different tissues of the volunteers, and no rutin was identified in

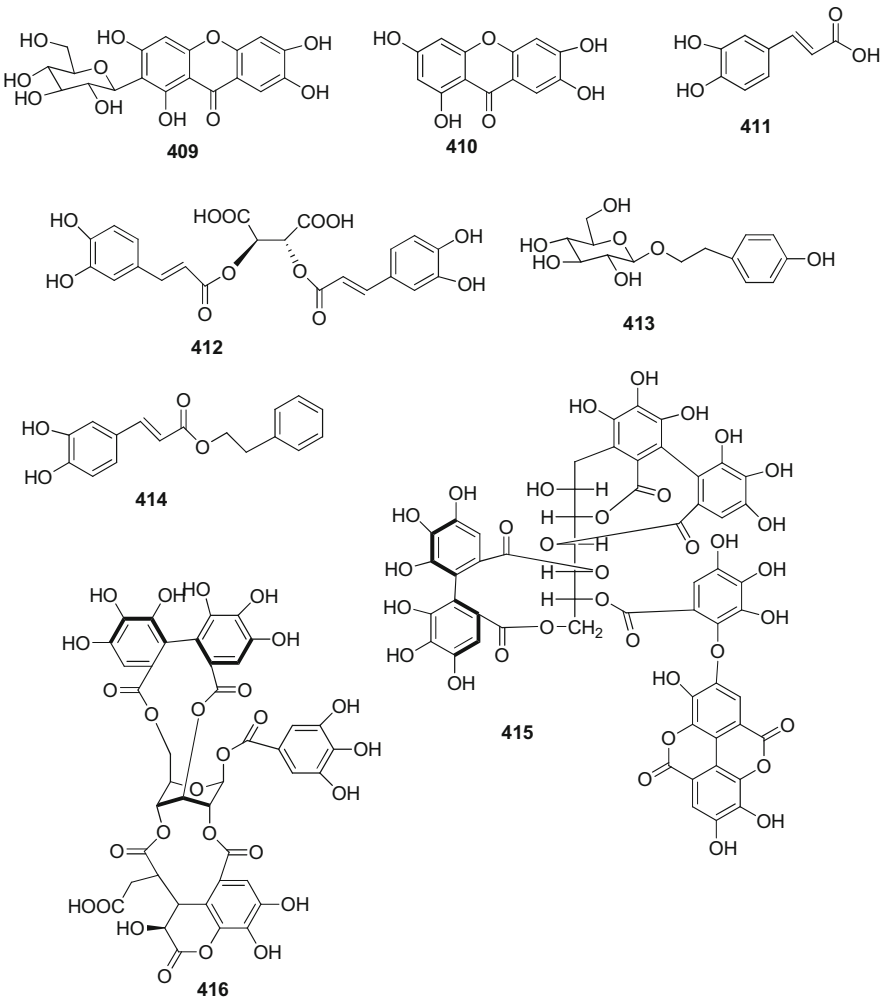

Fig. 5.1 (continued)

the tissues, suggesting that rutin was metabolized into its metabolites in humans and bioactivity of rutin was due to its metabolites (Boyle et al. 2000).

Kaempferol **66** is widely distributed in dietary fruits and vegetables, such as beans, broccoli, cabbage, gooseberries, strawberries, cherries, grapes, kale, and tomatoes, and medicinal plants including *Ginkgo biloba*, *Nelumbo nucifera*, soybean, and dill (*Anethum graveolens*) mainly as conjugates of carbohydrates (glycosides). The rich plant sources of kaempferol are green leafy vegetables, such as spinach and kale having kaempferol content of 55 mg and 47 mg/100 g of fw, respectively. Among fruits, kaempferol content is high in cherry (5.14 mg/100 g of

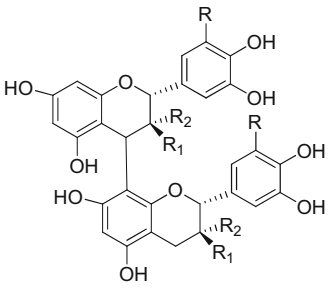

417

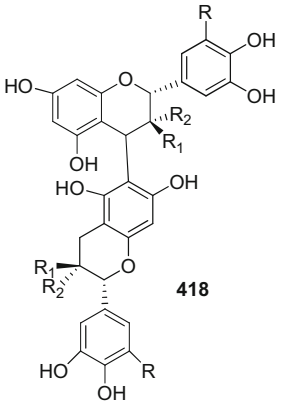

418

	R	R_1	R_2
(+)-catechin	H	OH	H
(-)-epicatechin	H	H	OH
(-)-epicatechin-3-gallate	H	H	OG
(+)-gallocatechin	OH	OH	H
(-)-epigallocatechin	OH	H	OH
(+)-gallocatechin-3-gallate	OH	H	OG
(-)-epigallocatechin 3-gallate	OH	OG	H

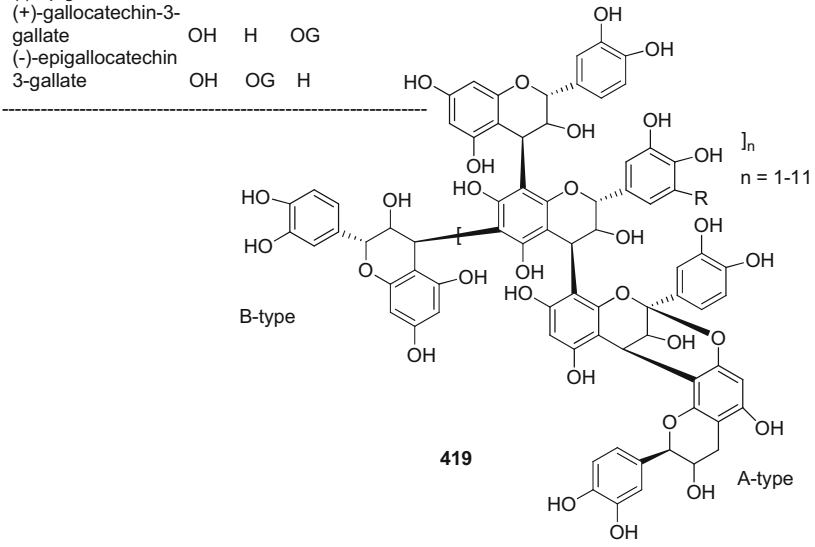

419

Fig. 5.1 (continued)

fw) (Dabeek and Marra 2019). In vitro, kaempferol in high palmitate and oleic acid-exposed insulin resistance muscle C2C12 myotubes increased glucose uptake, lipolysis, glycogen synthesis, AMPK activation, and GLUT4 expression and its translocation into plasma membrane. In animal models, kaempferol on supplementation in diet (0.05% of diet) in HFD-fed obese mice reduced body fat mass, serum

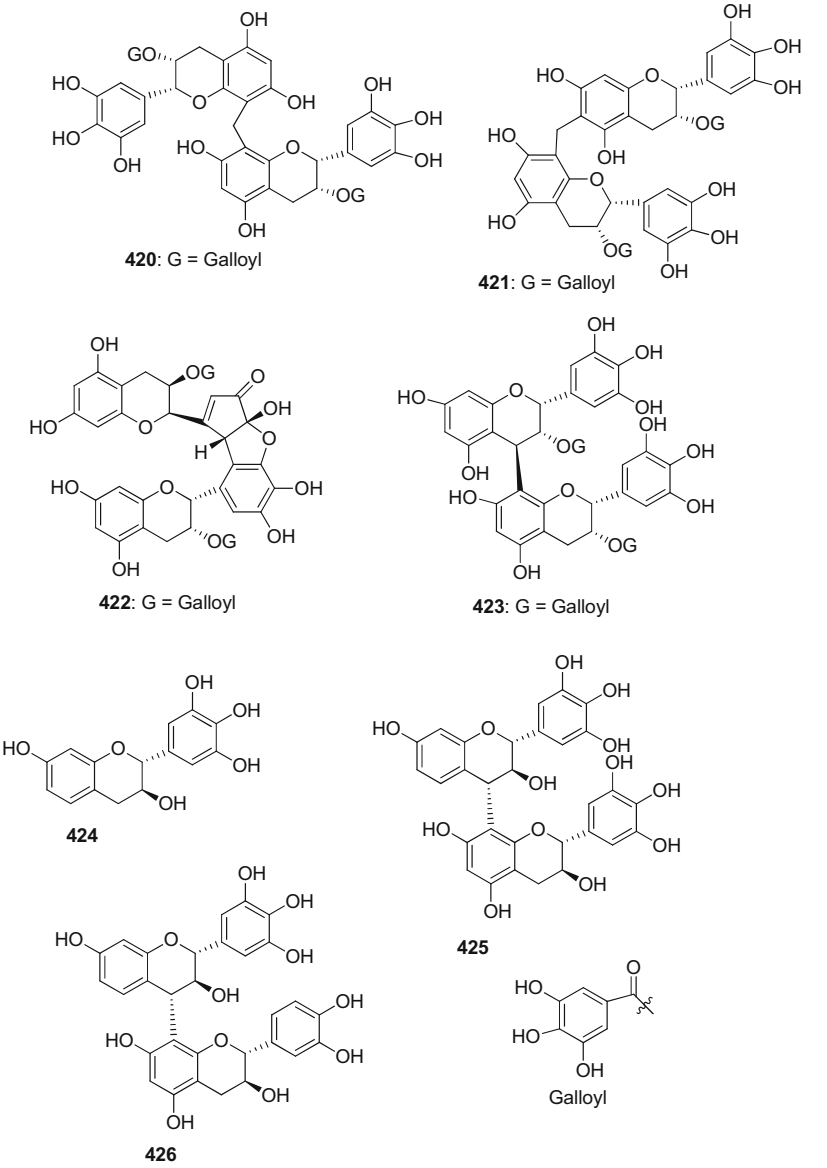

Fig. 5.1 (continued)

glucose, and TG, TC, and LDL-C levels and increased the levels of phosphorylated AMPK and expression of GLUT4 in skeletal muscle and AT of obese mice. In HFD and STZ-induced obese diabetic mice, kaempferol (0.05% of diet) treatment reduced serum glucose and increased serum insulin levels, and increased pancreatic β-cell

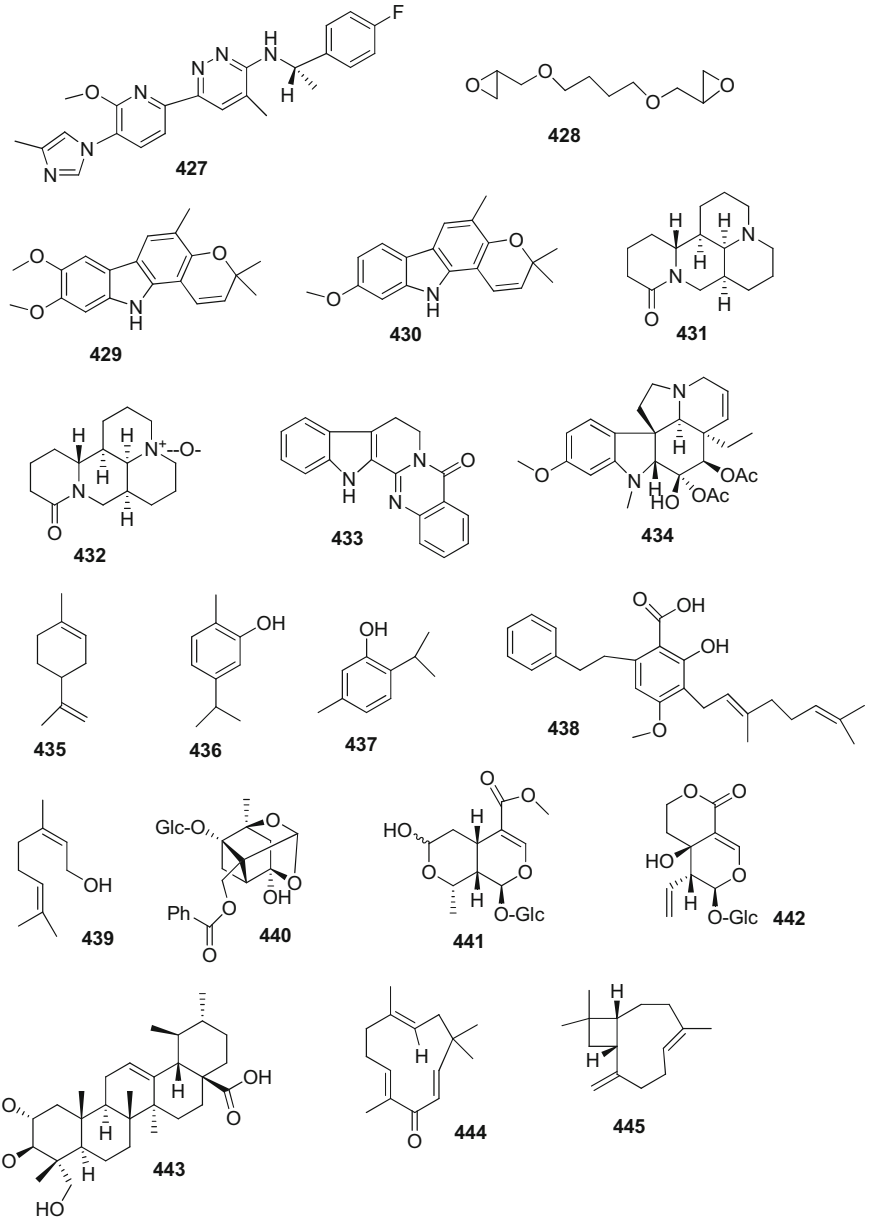

Fig. 5.1 (continued)

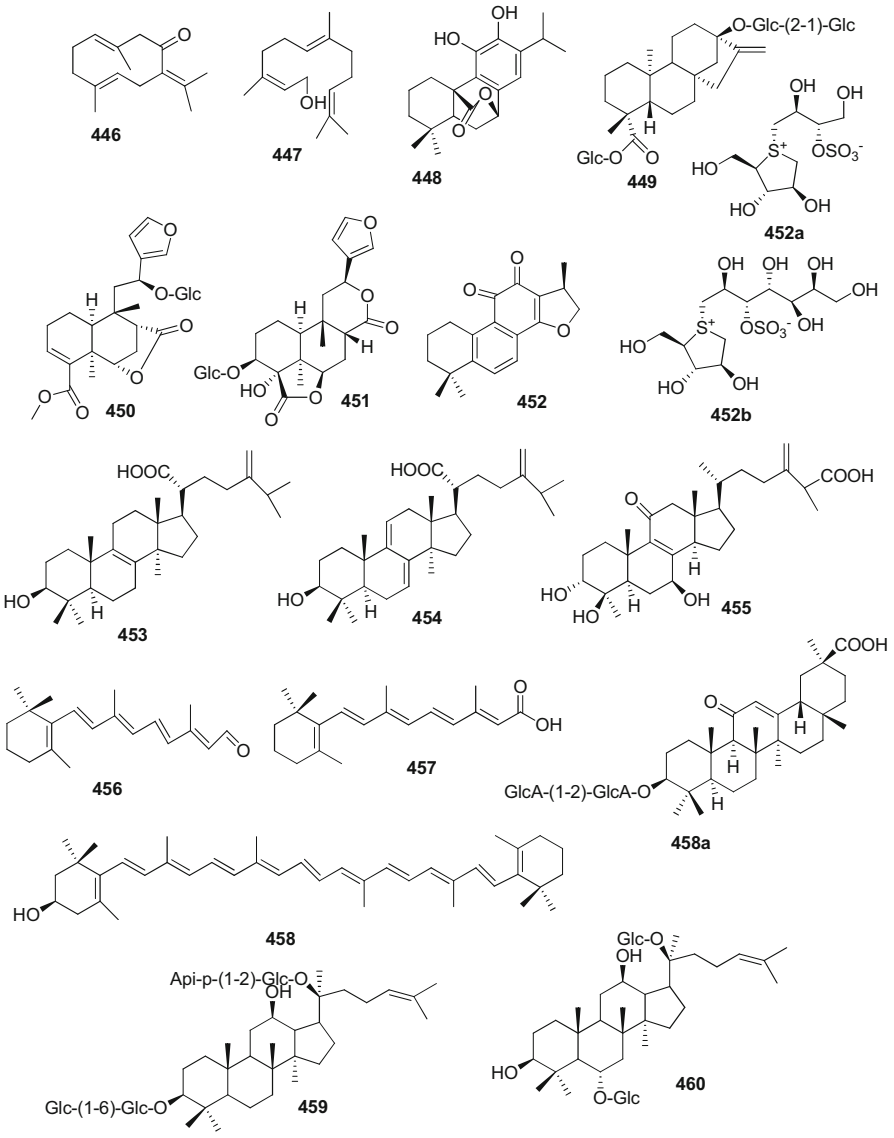

Fig. 5.1 (continued)

mass and insulin content in obese diabetic mice (Alkhalidy et al. 2015). In another animal model, oral administration of kaempferol (50 mg/kg/day) to HFD-fed obese mice increased hepatic glucose utilization and reduced hepatic glucose production by increased hepatic Akt and GCK activity and decreased pyruvate carboxylase (PC) and G6Pase activity. In HepG2 cells, kaempferol also decreased the activity of

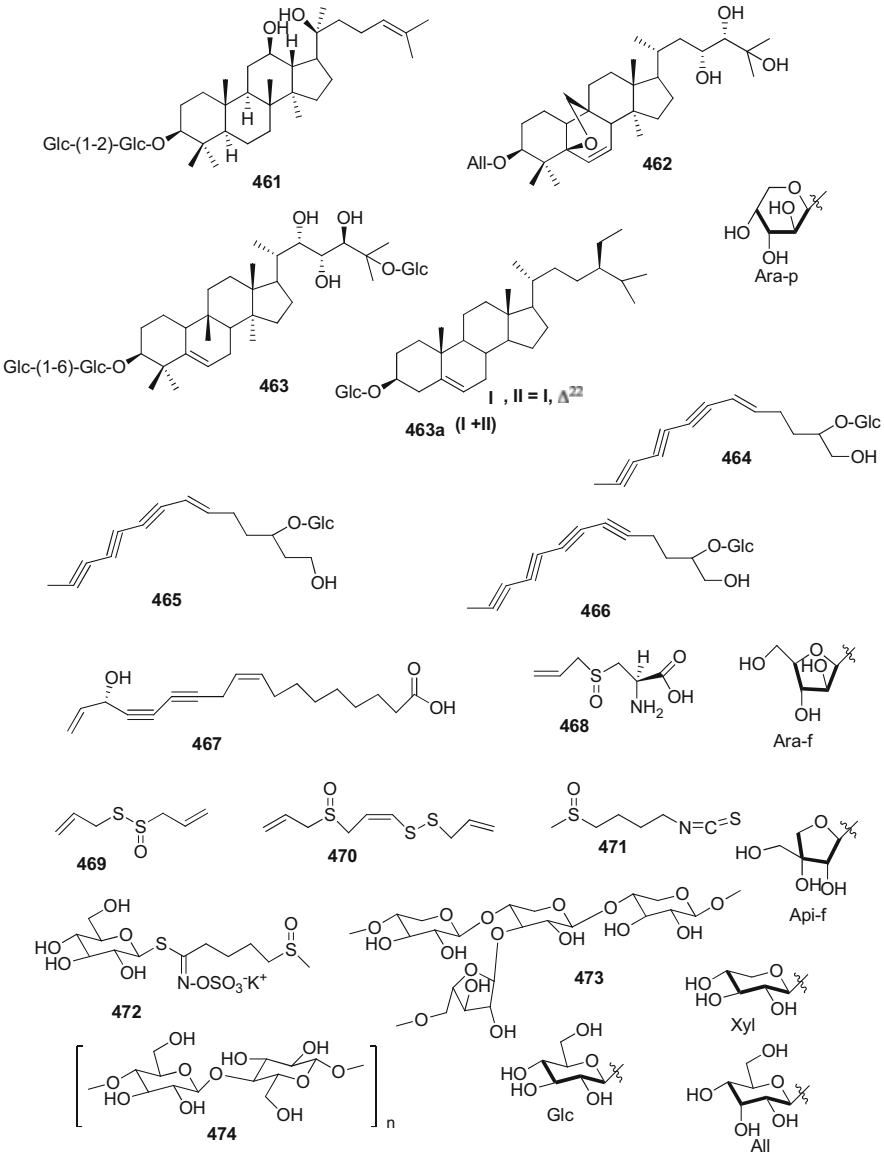

Fig. 5.1 (continued)

PC, the key enzyme responsible for gluconeogenesis in the first step (Alkhalidy et al. 2018). In 3T3-L1 adipocytes, kaempferol reduced cytoplasmic TG accumulation and adipocyte differentiation and increased fatty acid oxidation through upregulation of PPARα and its target genes (Lee et al. 2015). Moreover, kaempferol in STZ-diabetic

rats improved insulin resistance in liver by reducing hepatic inflammation via suppression of NF-κB activation and expression of IκB kinase β (IKKβ) proteins (Luo et al. 2015). Kaempferol glycosides (KG) fraction from unripe soybean (*Glycine max* L.) leaves on diet supplementation in STZ and HFD-fed obese diabetic mice reduced body weight, AT fat mass, serum FG, HbA1c, insulin, and leptin levels and improved insulin resistance in obese mice by down-regulation of lipogenesis-related genes PPARγ, FAS, and SREBP1c in the liver. Two major glycosides in KG fraction kaempferol-3-*O*-β-D-glucopyranoxy-(1→2)-*O*-[α-L-rhamnopyranosyl-(1→6)]-β-D-galactopyranoside **382** and kaempferol-3-*O*-β-D-glucopyranoxy-(1→2)-*O*-[α-L-rhamnosyl-(1→6)]-β-D-glucopyranoside **383** were found in 244 and 241 mg/g of dry weight extract, respectively (Zang et al. 2015). Therefore, kaempferol has potential anti-obesity and antidiabetic effects.

Myricetin **22** is mainly present as its *O*-glycosides in vegetables, fruits, nuts, berries, beverages, herbs, and medicinal plants. The content of myricetin in plant foods depends on several factors, such as genetic and environmental factors, ripeness degree of fruits and berries, storage, and processing conditions. Among fruits, myricetin is rich in cranberry (*Vaccinium oxycoccos*) (6600 mg/100 g of fw) (USDA 2020). Myricetin on diet supplementation (0.12% of diet) in HF-HS-fed obese mice for 12 weeks significantly improved obesity and insulin resistance by reduction of body weight, epididymal fat mass, serum glucose, insulin, TG, TC, leptin, TNF-α, and IL-6 levels and increased serum HDL-C and adiponectin levels in obese mice (Choi et al. 2014a). In another study, myricetin treatment in high-fructose-diet-fed insulin-resistant diabetic rats ameliorated impaired insulin action by increasing the secretion of β-endorphin to activate μ-opioid receptor (MOR) in the skeletal muscle for enhancement of glucose uptake via upregulation of GLUT4 translocation into plasma membrane and increased phosphorylation levels of IRS1, p85 subunit of PI3K, Akt and AS160 proteins. Moreover, co-treatment of β-funaltrexamine hydrochloride (β-FNA), an antagonist of MOR, inhibited the activity of myricetin in glucose uptake in skeletal muscle of diabetic rats. Therefore, myricetin possibly exhibits hypoglycemic effect in diabetic rats via MOR activation in skeletal muscle (Tzeng et al. 2011). Myricetin in DIO-mice increased hepatic GP_X and total antioxidant capacity (AOC) to reduce oxidative stress and down-regulated the expression levels of adipogenic genes PPARγ, C/EBPα, and SREBP1c in both liver and adipose tissues for reduction of whole body fat content (Su et al. 2016a). Furthermore, myricetin in STZ-diabetic rats improved cardiac function by protection of cardiomyocytes from oxidative stress, inflammation, apoptosis, and fibrosis through suppression of p-level of IκBα and inhibition of activation of IκBα/NF-κB/p65 and TGFβ/Smad3 signaling pathways, and enhanced the expression of anti-oxidant factors Nrf2 and its target genes HO-1, SOD1/2, and NQO1 in diabetic rats (Liao et al. 2017).

5.2.1.2 Flavones

Apigenin **197** (Fig. 4.1) is present in various dietary fruits and vegetables, such as grape fruits, oranges, chamomile, parsley, and onions as well as in medicinal plants including *Daphne genkwa* (Shukla and Gupta 2010). Apigenin in 3T3-L1 adipocytes

inhibited adipogenesis by suppression of the expression of adipogenic factors PPARγ and C/EBPα and their target genes through AMPK activation (Ono and Fujimori 2011). Moreover, apigenin suppressed the mitotic clonal expansion at the G0/G1 phase by down-regulation of the expression of cyclin D and cyclin-dependent kinase 4 (CDK4) and DNA-binding affinity of C/EBPβ in the adipocytes for inhibition of adipogenesis (Kim et al. 2014). In animal model, apigenin on supplementation in diet (0.005% of diet) to HFD-fed obese mice for 16 weeks significantly reduced obesity-related metabolic abnormalities by decreasing plasma FG, insulin, TC, FFAs, pro-inflammatory factors MCP-1, IFN-γ, TNF-α, IL-6 levels, and hepatic lipid droplets and gluconeogenic enzymes PEPCK and G6Pase activity in obese mice. Moreover, apigenin down-regulated the expression levels of lipolysis and lipogenesis-related genes LPL, PPARγ, SREBP1, ACAT, and PAP and upregulated the expression of fatty acid oxidation-related genes SCD1 and ACOX1 in the liver of obese mice (Jung et al. 2016). Another study reported that apigenin on acting as PPARγ agonist reduced obesity-related inflammation by reduction of the phosphorylation level of p65 proteins and inhibition of the translocation of PPARγ/p65 complex to the nucleus on binding to PPARγ, and inactivation of NF-κB/p65 signaling in adipose tissue and liver of obese mice (Feng et al. 2016). Apigenin in STZ-diabetic rats increased glucose uptake in skeletal muscle by upregulation of GLUT4 translocation into plasma membrane and increased insulin secretion from pancreatic β-cells. Moreover, apigenin improved glucose homeostasis in diabetic rats by suppression of CD38 expression (Hossain et al. 2014). Apigenin in HFD-fed obese mice reduced hepatic lipid content, increased hepatic NAD+ levels to increase insulin activity, and reduced CD38 activity, and promoted SIRT1 activation for fatty acid oxidation and deacetylation of several proteins including p53, p65, and histones for suppression of inflammation in liver. It increased the expression levels of fatty acid oxidation-related genes CPT1α, LACD, and MACD in the liver of obese mice (Escande et al. 2013). A glycoside of apigenin, apigenin-6-C-β-fucopyranoside **384** (Fig. 5.1) from *Averrhoa carambola* leaves, increased glucose uptake in rat soleus muscle through insulin-dependent Akt activation and GLUT4 expression and translocation into cell membrane. Moreover, this glycoside increased glycogen content in muscle and liver and reduced serum glucose level in high-glucose-fed hyperglycemic rats (Cazarolli et al. 2012).

The flavone luteolin **196** is present in high levels in many fruits and vegetables, such as carrot, pepper, parsley, celery, and spinach, and has various biological activities including antioxidant, anticancer, anti-inflammatory, and anti-obesity activities (Lopez-Lazaro 2009). Luteolin on supplementation in diet (0.0002 or 0.01%) to HFD-fed obese mice for 12 weeks reduced body weight and AT mass and epididymal adipocyte size and decreased the levels of serum glucose, insulin, and inflammation-related adipokines leptin, TNF-α, MCP-1, IL-6, and increased serum adiponectin level in obese mice. Moreover, luteolin increased glucose uptake in AT by increased translocation of GLUT4 proteins into plasma membrane and phosphorylation of Akt. In addition, luteolin suppressed the infiltration of mast cells and macrophages and production of inflammatory cytokines and cathepsin in epididymal adipose tissue (EAT) to inhibit adipogenesis and angiogenesis (Xu et al.

2014). In another study, luteolin on diet supplementation to HFD-fed obese mice reduced the metabolic macrophage activation (MM) in EAT through inhibition of macrophage polarization and increased phosphorylation of AMPKα1 (Zhang et al. 2016a). Both luteolin and luteolin-7-*O*-glucoside **311** in diabetic KKAy mice reduced serum glucose, HbA1c, insulin, and HOMA-IR levels and serum and hepatic TG levels and increased serum HDL-C level in the diabetic mice. Moreover, these flavonoids decreased the expression levels of hepatic lipid synthesis-related genes FAS and SREBP-1c, and inflammatory cytokine TNF-α and increased the expression of fatty acid oxidation-related gene CPT-1; the effects of luteolin were better than that of its glucoside (Zang et al. 2016).

Baicalein **58,** a major flavonoid constituent of many medicinal plants, such as *Oroxylum indicum* and *Scutellaria baicalensis*, possesses anti-obesity, antidiabetic, antioxidant, and anti-inflammatory activities (Dinda et al. 2017). Baicalein on long-term supplementation in diet (400 mg/kg bw/day) to HFD-fed obese mice for 29 weeks significantly reduced fatty liver mass, serum glucose, TG, TC, and LDL-C levels in obese mice. Moreover, baicalein decreased the expression levels of hepatic inflammatory cytokines TNF-α and MCP-1 (about 50%), and of hepatic lipid synthesis-related genes PPARγ, SREBP-1c, FAS, and aP2, and increased the expression of hepatic fatty acid oxidation-related genes PPARα, CPT-1, and UCP-2, and phosphorylation levels of AMPK and Akt. These findings indicate that baicalein ameliorates hepatic steatosis, hyperlipidemia, and hyperglycemia in obese mice through AMPKα_2 activation in liver (Pu et al. 2012a). Another study reported that baicalein treatment (20 mg/kg bw/day, *i.p.*) to HFD-fed obese mice for 21 days reduced plasma glucose, insulin, and HOMA-IR levels and adipocytes expression levels of p-p38MAPK, p-ERK, and PPARγ, related to inflammation and adipogenesis, and increased the expression levels of p-Akt, PGC-1α, and UCP-1 in adipocytes and both expression and translocation of GLUT4 into the plasma membrane of adipocytes to increase glucose uptake and FA oxidation in obese mice. These results indicate that baicalein improves glucose uptake in adipose tissues by activation of Akt/GLUT4 signaling pathway and suppression of inflammation through blocking of MAPKs signaling pathway (Min et al. 2018). Baicalein treatment in STZ and HFD-fed obese diabetic mice increased pancreatic β-cell mass and insulin content, and decreased the activity of pro-apoptotic enzyme caspase 3 in pancreas. Therefore, baicalein protected the diabetic pancreas from oxidative stress and injury (Fu et al. 2014). Baicalein treatment in obese diabetic rats reduced the levels of plasma endotoxin LPS, and inflammatory factors TNF-α, IL-6, and TLR-4, and increased the levels of SCFAs as well as increased relative abundance ratio of gut SCFA-producing bacteria *Bacteroidales* S24-7, *Bacteroides*, and *Akkermansia muciniphila* compared to *Firmicutes* in the intestinal gut of obese diabetic rats. These results suggest that baicalein improves insulin secretion and inflammatory disorders in obese diabetic rats through modulation of gut microbiota dysbiosis and improvement of intestinal gut barrier function via enhanced mucin synthesis and SCFAs production (Zhang et al. 2018a). Baicalein in STZ-NA-induced diabetic rats increased the expression and activity of antioxidant enzymes CAT, SOD, GSH, and GP_X in liver tissues. Therefore, suppression of oxidative stress in liver of

diabetic rats is also a mode of action of baicalein in amelioration of hyperglycemia and hyperlipidemia (Sarkar et al. 2019). Baicalin **352** (Fig. 4.1), a glycoside of baicalein, present in *Scutellaria baicalensis*, on treatment (50 mg/kg/day, *i.p.*) to DIO-mice for 21 days significantly decreased food intake, body weight, serum glucose, and HOMA-IR levels. Baicalin, in both skeletal muscle of obese mice and in vitro in muscle C2C12 cells, enhanced glucose uptake and increased the expression levels of p-Akt, GLUT4, p-AS160, and PGC-1α. Therefore, baicalin improves insulin resistance in obese mice by activation of Akt/ AS160/ GLUT4 signaling pathway (Fang et al. 2017). The same group also reported that baicalin in DIO mice increased glucose uptake in adipocytes by increasing the expression levels of p-Akt, GLUT4, and PGC-1α and decreasing the expression levels of p-p38MAPK and p-ERK (Fang et al. 2018).

Tangeretin **136**, a polymethoxylated flavone, found in the peels of many citrus fruits, such as mandarins, tangerines, grape fruits, and oranges, has potential bioactivities in prevention of cancer, obesity, and diabetes (Rouseff and Ting 1979). In C2C12 myotubes, tangeretin increased glucose uptake through upregulation of GLUT4 translocation from the cytosol to plasma membrane and enhanced phosphorylation of AMPK and AS160 proteins. Transfection of myotubes with AMPK siRNA prevented the activity of tangeretin in glucose uptake. In animal model, tangeretin on diet supplementation (200 mg/kg bw) to HFD-fed obese mice for 8 weeks decreased weight gain and serum levels of glucose, TC, leptin, resistin, IL-6, and MCP-1 and increased serum adiponectin level and glucose tolerance in obese mice. Moreover, tangeretin increased glucose uptake in skeletal muscle and decreased lipid synthesis in adipose tissue and liver by down-regulation of ACC expression and upregulation of p-AMPK and p-ACC levels (Kim et al. 2012b). Both tangeretin and nobiletin **135** increased glucose uptake in murine 3T3-F442A adipocytes and increased glucose uptake by increasing the activation of PI3K, Akt, and PKA (Onda et al. 2013). In another study, tangeretin on oral treatment (100 mg/kg/day) to STZ-diabetic rats for 30 days reduced food intake and serum glucose and HbA1c levels and increased body weight, serum insulin, and hemoglobin levels and hepatic glycogen content in diabetic rats. In addition, tangeretin decreased the activity of hepatic gluconeogenic enzymes G6Pase and FBPase, and increased the activity of glycolysis-related enzymes HK and PK (pyruvate kinase) and of glycogen synthesis enzyme GS as well as promoted pancreatic insulin secretion (Sundaram et al. 2014). In another study, tangeretin in STZ-diabetic rats improved cardiac dysfunction by decreasing plasma lipids (TC, TG, PLs, LDL-C, VLDL-C), lipid droplets in thoracic aorta and cardiac tissues, and increasing Ca^{2+}-ATPase activity in cardiac tissues of diabetic rats. Moreover, tangeretin reduced the oxidative stress and LPO levels in cardiac tissues by increasing the activities of antioxidant enzymes SOD, CAT, GP_X, and GR and reduction of both inflammatory cytokines and proteins TNF-α, IL-6, and NF-κBp65 and cardiac toxic marker enzymes AST, LDH, and creatine phosphokinase (CPK) in plasma and heart tissues. Furthermore, tangeretin increased insulin sensitivity in heart tissues by IRS-1 phosphorylation and increased glucose uptake through upregulation of GLUT4 translocation to plasma membrane. In addition, tangeretin decreased hepatic cholesterol

synthesis by down-regulation of HMGCR and increased HDL synthesis and TG hydrolysis by upregulation of the expression levels of lecithin cholesterol acyltransferase (LCAT) and LPL, respectively. These findings suggest that tangeretin protects diabetic heart from injury by suppression of oxidative stress and inflammatory factors through improvement of antioxidant status, glucose and lipid metabolism, and Ca^{2+}-ATPase activity (Sundaram et al. 2015). Tangeretin in diabetic db/db mice increased insulin sensitivity and glycogen content in liver by suppression of hepatic inflammation through down-regulation of p-p38MAPK and p-ERK1/2 (Guo et al. 2020a).

Nobiletin **135**, a hexamethoxylated flavone, found in the peels of citrus fruits such as *Citrus sinensis* (sweet oranges), *C. reticulata* (tangerines), *C. limon* (lemons), and *C. depressa* has health benefit properties, including neuroprotective, anti-carcinogenic, anti-inflammatory, anti-obesity, antidiabetic, and anti-atherogenic activities (Nakajima and Ohizumi 2019). In HepG2 cells, nobiletin reduced the secretion of apoB100-containing lipoproteins, decreased the expression of TG synthesis-related proteins DGAT1, DGAT2, and microsomal triglyceride transter protein (MTP), and increased the expression of LDLR and phosphorylation of ERK1/2. In animal model, nobiletin on supplementation in diet (0.3% of diet) to HFD-fed diabetic LDLR-silencing mice, a model of diet-induced insulin resistance and atherosclerosis, for 26 weeks, decreased body weight gain, adipocyte size, plasma glucose and lipid (TG, TC, FFAs, VLDL-TG) levels, and hepatic TG accumulation and VLDL-TG secretion in diabetic mice. Moreover, nobiletin increased the expression levels of hepatic fatty acid oxidation-related genes CPT-1α and PGC-1α, and decreased the expression of FA synthesis-related gene SREBP-1c. These results indicate that nobiletin reduces hepatic lipid storage through regulation of lipid metabolism (Mulvihill et al. 2011). Nobiletin in HepG2 cells and primary mouse hepatocytes increased the phosphorylation levels of AMPK and ACC and enhanced the expression of genes related to FA oxidation and decreased the expression of genes related to FA synthesis. Further, nobiletin supplementation in diet in both HF-HC diet-fed AMPK-β1-deficient (KO) mice and wild-type (WT) mice decreased body weight gain, plasma glucose, insulin levels, hepatic and plasma lipid levels, and insulin resistance, similar to the pharmacological activation of AMPK, while only increased UCP-1 expression was identified in WT mice. Possibly, AMPK-β1 deletion significantly reduces AMPK activity in hepatocytes and macrophages, while the residual AMPK in other tissues mediates the beneficial effects of nobiletin. These findings suggest that nobiletin possibly exerts its anti-obesity effect independent of AMPK activation in liver or adipose tissue (Morrow et al. 2020). In high-glucose exposed human glomerular mesangial (HM) cells, nobiletin decreased the expression levels of inflammatory cytokines IL-1β, IL-6, TNF-α, and MCP-1, and ECM accumulation-related proteins collagen type IV, and fibronectin through inhibition of p-STAT expression and NF-κBp65 activation (Liu et al. 2018d). In addition, nobiletin in STZ-induced diabetic cardiomyopathy (DCM) in mice ameliorated both diastolic and systolic myocardial dysfunction by suppression of the expression levels of TGF-β1, CTGF, fibronectin, and collagen 1α and activation of JNK, p38, and NF-κB signaling pathways (Zhang et al.

2016b). Therefore, nobiletin could be useful in treatment of obesity, diabetes, and their associated complications.

5.2.1.3 Flavanones

Eriodictyol **200**, a major bitter-masking flavanone present in citrus fruits, such as lemons, oranges, and grape fruits, and in many medicinal plants including *Eriodictyon californicum* (yerba santa), *E. angustifolium*, *Rosa canina*, *Rhus natalensis*, *Bauhinia ungulata*, and *Lyonia ovalifolia* has potential antidiabetic, anti-obesity, anticancer, anti-inflammatory, neuroprotective, cardioprotective, and hepatoprotective activities (Islam et al. 2020). Eriodictyol in isolated mouse islets and MIN6 cells increased glucose-dependent insulin secretion in presence of high-glucose concentrations via production of intracellular cAMP proteins. Moreover, pretreatment of diazoxide, a K-ATP channel opener, or verapamil, a Ca^{2+} channel blocker, or H89, an inhibitor of PKA, almost completely blocked the insulin secreting effect of eriodictyol, while treatment of SQ22536, an inhibitor of adenylate cyclase, partially inhibited the insulin secreting effect of eriodictyol. These findings suggest that eriodictyol stimulates glucose-dependent insulin secretion from pancreatic β-cells via production of adenylate cyclase (AC), cAMP, and PKA activation in a cAMP/PKA signaling cascade mainly dependent on K-ATP and Ca^{2+} channel pathways. Moreover, in type 2 diabetic rats, eriodictyol (10 mg/kg/day) significantly reduced serum fasting glucose levels on day 14 of treatment (191.7 vs. 238.8 mg/dl). Accumulating evidence demonstrates that activated protein kinase A (PKA) promotes insulin secretion by increasing the number of vesicles sensitive to Ca^{2+} and Ca^{2+}-dependent exocytosis via phosphorylation of proteins responsible for insulin secretion in β-cells (Hameed et al. 2018; Wan et al. 2004). Eriodictyol in diet supplementation (0.005% of diet) in HFD-fed obese mice for 16 weeks decreased body weight gain, WAT mass, adipocyte size, and plasma levels of glucose, insulin, HOMA-IR, TC, TG, apoB, FFAs, leptin, IFNγ, IL-1β, IL-6, and hepatic TG and FA content, and increased plasma HDL-C and gastric inhibitory polypeptide (GIP) levels and fecal lipid excretion content in obese mice. Moreover, eriodictyol down-regulated the expression levels of lipid uptake-related genes CD36 and LPL and lipogenesis-related genes SREBP1, ACC, SCD1, FAS, and PAP in adipose tissue and liver, and upregulated the expression of fatty acid oxidation-related genes PPARα, PGC-1α, CPT-1 in liver, and UCP-1 in adipose tissue. In addition, eriodictyol decreased the expression and activity of hepatic gluconeogenic genes G6Pase and PEPCK and upregulated the expression of GCK and IRS2 in liver. These results suggest that eriodictyol exerts its anti-obesity effect through upregulation of lipid and glucose metabolism via increasing insulin activity in liver and adipose tissue of obese mice (Kwon and Choi 2019). In high glucose-stimulated human mesangial cells (MCs), eriodictyol increased the antioxidant enzyme SOD activity and reduced the levels of ROS and MDA by suppression of the activity of NOX2 and NOX4 for protection of MCs from apoptosis and fibrosis. Moreover, eriodictyol suppressed the expression of extracellular matrix (ECM) proteins collagen IV and fibronectin and inflammatory cytokines TNF-α, IL-1β, and IL-6 through increased PI3K and Akt expression and inhibition of NF-κB

activation in MCs (Bai et al. 2019). Eriodictyol and other flavonoids including baicalein, baicalin, luteolin, and naringenin from *Scutellaria lateriflora* inhibited the activity of α-glucosidase (Kuroda et al. 2012).

Hesperidin **385** (Fig. 5.1), also known as hesperetin-7-rutinoside, is abundant in many citrus fruits, such as lemons, oranges, limes, and grapefruits. Generally, hesperidin content is high in citrus peel than in other parts of citrus fruits. But, in lemons, seeds methanol extract contains more hesperidin than peel. Hand-squeezed Florida orange juice contains 335–351 mg of hesperidin per liter of juice (Mouly et al. 1998). Several studies demonstrate that hesperidin and its aglycone hesperetin **198** have anti-obesity, antidiabetic, retinoprotective, and cardioprotective properties. Hesperetin stimulated the release of gastrointestinal hormone cholecystokinin (CCK), an appetite suppressing hormone from enteroendocrine STC-1 cells. Hesperetin strongly stimulated the secretion of CCK with an EC_{50} value of 0.05 mM, via increased expression of intracellular Ca^{2+} concentrations and activation of transient receptor potential (TRP) channel, TRP ankyrin 1 (TRPA1). In vivo, hesperidin on deglycosylation by mammalian β-glycosidases in small intestine is converted into hesperetin. Therefore, both hesperetin and its glycoside hesperidin are potential candidates for suppression of appetite and in treatment of obesity (Kim et al. 2012a). Hesperidin on supplementation in diet (0.2 g/kg of diet) to type 2 diabetic db/db C57BL/KsJ mice for 5 weeks decreased plasma glucose, TG, and TC levels and hepatic lipid content and increased plasma HDL-C level, and fecal lipid excretion content in diabetic mice. In addition, hesperidin decreased the expression levels of hepatic TG, cholesterol, and bile acid synthesis-related genes FAS, PAP, G6PD, HMGCR, and ACAT, and increased the expression of hepatic glycolysis-related gene GCK. Furthermore, hesperidin increased the expression of GLUT4 in adipocytes for glucose uptake, and the expression of PPARγ in both liver and adipocytes, and decreased the expression of hepatic glucose transporter protein GLUT2, and gluconeogenic enzyme PEPCK to reduce hepatic glucose uptake and hepatic endogenous glucose production, respectively. Moreover, hesperidin increased the level of antioxidant enzyme paraoxonase (PON) in serum to improve the activity of liver. These results suggest that hesperidin ameliorates hyperglycemia and hyperlipidemia through regulation of glucose and lipid metabolism (Jung et al. 2006a). Hesperidin on supplementation in diet (10 mg/kg of diet) to STZ-induced marginal type 1 diabetic rats for 4 weeks decreased hyperglycemia and hyperlipidemia by increasing serum adiponectin and insulin levels and decreasing hepatic G6Pase activity and increasing GCK activity. These findings suggest that hesperidin exhibits antidiabetic effect through improvement of insulin secretion and insulin action in liver of diabetic rats (Akiyama et al. 2010). Another study reported that hesperidin treatment (100 mg/kg/day) to Western diet-fed obese rats for 8 weeks prevented hepatic lipid accumulation by decreasing serum leptin level, and the expression of three key enzymes related to lipogenesis, SREBP1, FAS, and SCD1, and esterified lipid uptake gene LPL in liver and adipose tissue of obese rats (Mosqueda-Solis et al. 2018). In bovine aortic endothelial cells (BAECs), hesperetin increased the activity of endothelial NO synthase (eNOS) for nitric oxide production through stimulation of the phosphorylation of Akt, AMPK, and eNOS. Moreover, in

TNF-α-stimulated BAECs, herperetin reduced the expression of VCAM-1. In vivo, hesperidin treatment in obese, hypertensive, and insulin-resistant patients reduced the circulating inflammation by decreasing the levels of serum high-sensitive C-reative protein, amyloid A protein, and E-selectin. Therefore, both hesperidin and its active metabolite hesperetin have cardioprotective property through improvement of endothelial function via nitric oxide production (Rizza et al. 2011). Hesperidin in high-glucose-stimulated retinal ganglia cells (RGCs) protected the cells from mitochondrial-mediated apoptosis by suppression of oxidative stress through enhanced activities of antioxidant enzymes SOD, CAT, and GP_X and reduced the activities of pro-apoptotic proteins caspase 9, caspase 3, and Bax and the phosphorylation levels of the inflammatory kinases JNK and p38MAPK (Liu et al. 2017c). Bitter orange (*Citrus aurantium*) extract (CA) with 80% ethanol, rich in naringin **386** and neohesperidin **387** (Fig. 5.1) (20.13 and 14.44%, respectively) on diet supplementation (100 mg/kg of diet/day) to HFD-fed obese mice for 4 weeks, significantly reduced body weight, adipose tissue mass, and serum glucose and lipid levels. In vitro, CA in 3T3-L1 adipocytes decreased intracellular lipid droplets and suppressed the expression of adipogenic factors PPARγ and C/EBPα for inhibition of adipogenesis. Moreover, in primary brown adipocytes, CA increased the differentiation of the adipocytes by upregulation of the activity of thermogenic factors PGC-1α, UCP-1, PRDM-16, SIRT3, and Cidea in brown adipocytes. These effects of CA were abolished on co-treatment of compound C, an antagonist of AMPKα. These findings suggest that the anti-obesity effect of naringin and neohesperidin, major bioactive constituents of CA in inhibition of adipogenesis in white adipocytes, and induction of brown adipocyte thermogenesis is regulated via activation of AMPKα (Park et al. 2019).

Naringin **386** and its aglycone naringenin **199** are present in many citrus fruits, such as oranges, mandarins, and grapefruits and in acid citrus fruits, such as lemons, bergamots, and limes. Naringin content is high in sweet orange (*Citrus reticulata*) juice (3383.6 μg/ml), followed by *C. paradisi* juice (230 μg/ml) (Bilbao et al. 2007). Naringin on supplementation in diet (0.2 g/kg of diet) to diabetic db/db mice for 5 weeks significantly reduced blood glucose level and increased serum insulin, C-peptide, and leptin levels. In addition, naringin decreased the activity of hepatic gluconeogenic genes G6Pase and PEPCK and increased the hepatic glycogen content and activity of GCK in diabetic mice. Therefore, naringin ameliorates hyperglycemia, at least, in part, by increasing hepatic glycolysis and glycogen synthesis, and lowering hepatic endogenous glucose production in diabetic mice (Jung et al. 2004). Accumulating evidence demonstrates that hepatic overproduction of apolipoprotein B (apoB)-containing lipoproteins is one of the hallmarks of dyslipidemia in insulin-resistant obesity and is a risk factor of cardiovascular diseases. Naringenin **199** in human HepG2 cells decreased apoB secretion by activation of both PI3K and ERK1/2 signaling pathways with phosphorylation of IR and IRS-1. Possibly, naringenin potentiates the activity of insulin in inhibition of apoB secretion (Allister et al. 2008). Naringin (0.2 g/kg of diet) supplementation in HFD-fed obese diabetic mice for 10 weeks significantly ameliorated dyslipidemia

and fatty liver in mice by reduction of hepatic inflammation and lipogenesis and increased hepatic fatty acid oxidation through enhanced phosphorylation of AMPKα and IRS-1. Naringin decreased hepatic inflammation by inhibition of the activity of stress-related kinases ERK1/2, JNK, and p38MAPK and their transcription factors NF-κB and AP-1 proteins and decreased plasma lipotoxic FFAs levels by increasing the expression levels of FA oxidation-related genes PPARα, CPT-1α, and ACOX in liver and adipose tissues. In addition, AMPK activation down-regulated the expression levels of lipogenesis-related genes SREBP-1c, FAS, ACC1α, PPARγ, and SCD1 in liver and decreased the activity of gluconeogenic genes PEPCK and G6Pase through enhanced IRS-1 phosphorylation in liver. Moreover, naringin increased the activity of antioxidant enzymes SOD, CAT, GSH, and GP_X for normalization of liver function in maintenance of glucose and lipid homeostasis (Pu et al. 2012b). Naringin treatment in high-cholesterol-diet fed hypercholesterolemic rabbits showed hypocholestrolemic effect and significantly reduced plasma TC and LDL-C, and hepatic lipid levels, and increased plasma HDL-C/TC ratio and excretion of fecal lipids in the rabbits. In addition, naringin increased the expression of cholesterol synthesis-related enzyme HMGCR and decreased the expression of ACAT, marker of cholesterol reservoir, in the liver of hypercholesterolemic rabbits. The enzyme ACAT catalyzes the conversion of cholesterol into cholesteryl esters (CEs), and accumulation of CEs in macrophages causes the appearance of foamy cells in arteries, and is considered as a hallmark of atherosclerosis. Therefore, dietary supplementation of naringin is useful in prevention of atherogenic disorders (Jeon et al. 2004). Naringin supplementation (100 mg/kg of diet/day) to HF-HC-diet fed obese rats for 16 weeks improved ventricular and liver dysfunctions in obese rats. Naringin decreased systolic blood pressue, improved ventricular diastolic and systolic dysfunction and left-ventricular hypertrophy and fibrosis, and hepatic inflammation and steatosis. Naringin reduced aortic inner wall thickness by inhibition of inflammatory cell infiltration and fibrosis in cardiomyocytes by suppression of collagen deposition through enhanced mitochondrial activity (Alam et al. 2013). In high-palmitate exposed insulin-resistant L6 myotubes, naringenin significantly increased glucose uptake and GLUT4 translocation into plasma membrane and increased the phosphorylation of AMPK and expression levels of SIRT1 and PGC-1α (Krishnamoorthy and Venkatraman 2017). In human white adipocytes, naringenin treatment for 7–14 days promoted energy expenditure and thermogenesis by increasing the mRNA levels of fatty acid oxidation-related genes PGC-1α, PGC-1β, CPT-1β, UCP-1, and ATGL. In addition, naringenin increased insulin sensitivity by increasing adiponectin secretion and insulin-dependent GLUT4 proteins translocation into plasma membrane. Moreover, naringenin increased the phosphorylation of AMPK and the expression of carbohydrate response element binding protein (ChREBP). These results suggest that naringenin promotes thermogenesis and whole-body insulin sensitivity for conversion of WAT into BAT to prevent adiposity via AMPK activation (Rebello et al. 2019). In high-glucose exposed glucotoxic rat pancreatic INS-1E cells, naringenin enhanced glucose-stimulated insulin secretion by increasing the expression levels of β-cell survival and function-related genes Ins-1, Ins2, GCK, PDX1, IRS1, Akt1/2,

GLUT2, and HSP70/90, and protected the β-cells from apoptosis by down-regulation of the expression levels of pro-apoptotic marker genes caspase-3, Bax, and ACC1 (Bhattacharya et al. 2014a, b). Available evidence demonstrates that fibroblast growth factor 21 (FGF21) deficiency in mice potentiates HFD-induced obesity, greater muscle TG deposition, and hepatic steatosis and impaired glucose tolerance compared with wild-type (WT) mice. Naringenin in both HFD-fed WT obese mice and FGF21 null obese mice reduced hepatic lipid and TG accumulation by upregulation of the expression of FA oxidation-related genes PGC-1α and CPT-1α, and down-regulation of the expression of lipid synthesis-related gene SREBP-1c. These results suggest that naringenin promotes FA oxidation for reduction of hepatic fat accumulation in FGF21-independent path way (Assini et al. 2015).

5.2.1.4 Isoflavones

Isoflavones genistein **96** and daidzein **95** are found in many dietary legumes, such as soybeans (*Glycine max*), fava bean (*Vicia faba*), kudzu (*Pueraria lobata*), and psoralea (*Psoralea corylifolia*). Genistein is present in high concentrations in the leaves of psoralea (*P. corylifolia*) (2 g/kg of dw), while daidzein is found in high concentrations in the stems of *V. faba* (over 1 g/kg of dw) and in the roots of kudzu vine (0.95 g/kg of dw) (Kaufman et al. 1997). These isoflavones have potent estrogenic activity because of their structural similarity with human female 17-β-estradiol, and due to their mimic estrogen-like action, they have health-benefit properties in chemoprevention of breast and prostate cancers, cardiovascular diseases, osteoporosis, obesity, and diabetes (Vitale et al. 2013). Both genistein and daidzein on diet supplementation (0.02% of diet) to both type 2 diabetic db/db C57BL/KsJ mice and female non-obese diabetic (NOD) type 1 diabetic mice significantly decreased plasma glucose, TC, TG, FFAs, and hepatic TG levels, and increased pancreatic insulin secretion in both types of diabetic mice. Moreover, these isoflavones decreased the activity of hepatic gluconeogenic enzymes G6Pase and PEPCK, and the activity of hepatic lipogenesis-related gene FAS, and increased the activity of FA oxidation-related gene CPT, and glycolysis promoting gene GCK in the diabetic mice. These findings suggest that both genistein and daidzein exert their antidiabetic effect through enhancement of glucose and lipid metabolism (Park et al. 2006; Choi et al. 2008). In insulin secreting INS-1 and MIN6 cell lines and isolated mouse pancreatic islets, genistein increased glucose-stimulated insulin secretion through increased intracellular cAMP concentrations and activity of protein kinase A (PKA) (Liu et al. 2006). Genistein treatment (4 mg/kg bw/day) to HF-HS-diet fed obese mice for a period of 12 weeks reduced hepatic lipid mass and serum lipid profile through upregulation of the expression levels of FA oxidation-related genes PPARα, CPT-1, and ACOX and down-regulation of lipid synthesis-related genes FAS, GPAT, ACC, and SREBP-1 through increased phosphorylation of AMPK and ACC in the liver of obese mice (Liu et al. 2017a). Genistein treatment in HFD-fed obese female mice decreased the body weight, serum glucose, and lipid levels and hepatic lipid content through upregulation of the expression levels of hypothalamic circadian entrainment pathway genes, period 1 (Per-1) and c-Fos, and down-regulation of the expression of Grin-1 in obese mice (Zhou et al. 2019). Mounting

evidence suggests that the upregulation of the proteins Per-1 and c-Fos in hypothalamic molecular dark-light (DL) clock enhances the glucose and lipid metabolism through enhanced AMPK activation and the expression levels of PGC-1α and SIRT-1 and their target genes. AMPK activation promotes insulin secretion from pancreatic β-cells and BAT activation for maintenance of energy balance, and glucose and lipid homeostasis in the whole body (Cedernaes et al. 2019; Man et al. 2020). Genistein intake by obese patients (50 mg/day) for a period of 2 months reduced body weight and obesity-related dyslipidemia and hyperglycemia through improvement of insulin sensitivity via modulation of gut microbiota dysbiosis and upregulation of AMPK activation in skeletal muscle of obese patients. Genistein increased the relative abundance ratio of health-promoting bacteria *Akkermansia muciniphila*, *Paraprevotella* spp, and *Sutterella* spp in the intestinal gut to promote insulin secretion and insulin action and increased glucose utilization and FA oxidation in skeletal muscle, liver, and adipose tissue of obese patients (Guevara-Cruz et al. 2020).

Biochanin A **388** and fomononetin **389** (Fig. 5.1), natural isoflavones, present in legumes, such as red clover (*Trifolium pratense*), soybeans, alfalfa (*Medicago sativa*), chickpeas (*Cicer arietinum*), peanut, and cabbage, and in medicinal plants, such as *Astragalus membranaceus* and *A. mongholicus* roots, and have potential health-benefit activities in prevention of cancer, obesity, and diabetes and associated complications (Cassady et al. 1988; Tay et al. 2019). Biochanin A on treatment (10 or 20 or 40 mg/kg bw/day) to STZ and HFD-fed type 2 diabetic rats for 28 days decreased hyperglycemia and hyperlipidemia by reduction of serum glucose, HbA1c, TG, TC, and hepatic TG levels, glucose intolerance, and insulin resistance in diabetic rats. Moreover, biochanin A increased hepatic glycogen content and pancreatic insulin secretion by enhanced SIRT1 activity in pancreatic tissue and liver. Moreover, biochanin A increased AMPK activation in liver for improvement of insulin-dependent glucose utilization via upregulation of GCK enzyme activity and glycogen synthesis, and reduction of hepatic glucose production by suppression of the activity of gluconeogenic enzymes G6Pase and FBPase. In addition, biochanin A decreased hepatic lipid mass by upregulation of PPARγ activity and its target genes (Harini et al. 2012; Oza and Kulkarni 2018a). In STZ-type 1 diabetic rats, biochanin A on oral treatment (15 mg/kg bw/day) for 42 days decreased serum FG, adipokine resistin, and GGT levels and increased serum insulin, adiponectin, and GSH levels in diabetic rats. These findings suggest that biochanin A exerts antidiabetic effect through adiponectin-dependent insulin signaling in liver and suppression of hepatic oxidative stress (Salemi et al. 2018). Formononetin treatment (20 or 40 mg/kg bw/day) in STZ-HFD-fed type 2 diabetic rats for 28 days decreased plasma glucose, HbA1c, TG, TC, LDL-C, insulin, and HOMA-IR levels, and increased plasma HDL-C level, hepatic glycogen content, and pancreatic insulin secretion in diabetic rats. In addition, formononetin protected the pancreatic β-cells from apoptosis and improved the function of β-cells through increased activity and expression of SIRT1 proteins (Oza and Kulkarni 2018b). In another study, formononetin treatment in STZ-diabetic rats protected the rats from kidney dysfunction by reduction of serum glucose, creatinine, BUN levels, and urine volume and increased serum albumin level and urinary creatinine clearance level in diabetic rats.

Further, formononetin decreased interstitial fibrosis and the levels of inflammatory cytokines TNF-α, IL-6, and MDA levels by upregulation of the expression of SIRT1 in kidney tissue. Moreover, formononetin reduced the oxidative stress by increasing the activity of antioxidant enzymes SOD, CAT, and GSH in diabetic kidney. These findings suggest that formononetin ameliorates kidney dysfunction through upregulation of the activities of SIRT1 and antioxidant enzymes in kidney (Oza and Kulkarni 2019; Jain et al. 2020). Formononetin treatment at a high dose (40 mg/kg bw/day) to STZ-induced diabetic cardiomyopathy in rats for 16 weeks improved myocardial dysfunction, hypertrophy, and fibrosis by reduction of systolic and diastolic blood pressure, levels of serum glucose, lipid profile, and myocardial toxic marker factors CK-MB, LDH, and AST in diabetic rats. Moreover, formononetin decreased left ventricular end-diastolic volume and pressure, reduced collagen deposition, and increased heart rate and activity of antioxidant enzymes SOD, CAT, and GSH through upregulation of the activity of SIRT1 in heart tissue (Oza and Kulkarni 2020).

Puerarin (daidzein-8-C-glucoside) **8** is present in many plants and herbs including the roots of kudzu (*Pueraria lobata*), which has been used in traditional Chinese medicine for the treatment of diabetes, cardiovascular diseases, diarrhea, and dysentery (Wong et al. 2011). Puerarin treatment (100 mg/kg bw/day, i.p.) in STZ/HFD-fed type 2 diabetic rats for 4 weeks showed improvement of mitochondrial function and biogenesis by reduction of serum glucose, TG, FFAs, and MDA levels, and intramyocellular lipid (IMCL) accumulation in diabetic rats. Puerarin decreased IMCL accumulation by down-regulation of fatty acid trafficking protein CD36 expression and upregulation of mitochondrial biogenesis and FA oxidation-related genes and proteins, p-AMPK, p-ACC, SIRT1, SIRT3, PGC-1α, CPT-1β, TFAM, UCP2, UCP3, SOD2, ACOX1, LCAD, and PPARδ, in the skeletal muscle of the diabetic rats. Pre-treatment of naloxone, an antagonist of MOR, reduced the activity of puerarin in the enhancement of the expression levels of SIRT1 and PGC-1α, and the increased density of mitochondria in skeletal muscle of diabetic rats. These results suggest that puerarin stimulates MOR activity for improvement of mitochondrial oxidative phosphorylation activity in diabetic muscle. In vitro, in high-palmitate exposed insulin-resistant L6 myotubes, puerarin decreased the intracellular FFAs accumulation by increased the expression levels of FA oxidation-related factors, LCAD, p-AMPK, p-ACC, SIRT1, and CPT-1β, and decreased the expression of CD36. These findings suggest that puerarin improves insulin resistance in skeletal muscle of diabetic rats through enhanced mitochondrial function and biogenesis via activation of both AMPK and MOR (Chen et al. 2018b). Puerarin treatment (150 mg/kg/day) in HFD-fed obese diabetic mice for 35 days protected the pancreatic β-cells from apoptosis and increased β-cell mass and proliferation. Moreover, puerarin treatment in diabetic db/db mice reduced hyperlipidemia by decreasing serum TG, TC, and leptin levels and increased serum adiponectin level in the diabetic mice. In high-glucose-exposed isolated mouse islets and MIN6 cells, puerarin increased the β-cell mass and insulin secretion by upregulation of the expression levels of GLP-1R, Ins1, TCF7L2, PDX-1, and p-Akt, and decreased the expression of FoxO1 and caspase 3 proteins. Co-treatment of exendin (9-39), an

antagonist of GLP-1R, significantly suppressed the effect of puerarin in insulin secretion and β-cell proliferation, but co-treatment of exendin-4, an agonist of GLP-1R, significantly enhanced the effect of puerarin in insulin secretion and β-cell proliferation. These results suggest that puerarin exerts its insulin secreting effect on pancreatic β-cells by acting as GLP-1R agonist (Yang et al. 2016b). Puerarin treatment (100 mg/kg/day, *i.g.*) to type 2 diabetic rats for a period of 8 weeks attenuated hepatic steatosis by reduction of hepatic fat mass and TG content, body weight, serum levels of glucose, lipid (TG, TC, LDL-C) profile, MDA, and 8-hydroxy-2′-deoxyguanosine (8-HOdG), marker of oxidative DNA damage in diabetic rats. Moreover, puerarin decreased hepatic inflammation and fibrosis by reduction of the expression levels of inflammatory cytokines IL-1β,TNF-α, and chemokine MCP-1, and fibrosis-related factors α-SMA and TGF-β via inhibition of NF-κB activation and phosphorylation of Smad2/3 proteins in TGF-β/Smad signaling pathway. In addition, puerarin down-regulated the expression levels of lipogenic genes SREBP-1c and SCD1 and upregulated the expression levels of lipolysis-related gene hepatic lipase (HL) and FA oxidation-related genes ACOX and CPT-1α in liver tissues. Moreover, puerarin decreased the activity of hepatic gluconeogenic genes G6Pase and PEPCK mildly. Puerarin also increased serum SOD activity and hepatic CAT and total antioxidant capacity (TAC) for suppression of hepatic oxidative stress and restoration of normal function of liver. These findings suggest that puerarin prevents hepatic steatosis by suppression of hepatic inflammation, fibrosis, and lipogenesis and improvement of FA oxidation and antioxidant activity in diabetic liver (Hou et al. 2018). Puerarin treatment (100 mg/kg/day, i.p.) in HFD-fed obese mice improved insulin resistance, inflammation, and body weight gain by reshaping of gut microbiota composition in obese mice. Puerarin greatly increased the relative abundance of health-benefit bacteria *Akkermansia muciniphila* and proteobacteria and reduced the relative abundance of *Bacteroides* in intestinal gut for stabilization of host immunity and maintenance of integrity of barrier function in gut epithelial cells. Puerarin increased growth and function of goblet cells by upregulation of the expression of mucin-producing gene Muc2 and antimicrobial gene Reg 3 g in goblet cells. Moreover, puerarin increased the expression of tight junction proteins ZO-1 and occludin for improvement of gut barrier function and for suppression of entry of harmful pathogens into systemic circulation. In addition, puerarin increased the expression levels of Treg transcription factor Foxp3 and anti-inflammatory cytokine IL-10 and decreased the expression levels of pro-inflammatory cytokines IL-6 and MCP-1 for maintenance of host immune balance. Furthermore, puerarin decreased the activity of hepatic gluconeogenic genes G6Pase and PEPCK and hepatic toxic marker enzymes ALT and AST (Wang et al. 2019d).

5.2.1.5 Flavanols

Dietary natural flavan-3-ols, known as flavanols or catechins, are present in many fruits, such as apples, apricots, cherries, grapes, and beverages, such as teas and cocoa beans. These catechins have significant biological properties in prevention of cancer, obesity, diabetes, and cardiovascular diseases. The most common catechins

are (+)-catechin, (–)-catechin, (–)-epicatechin, (+)-gallocatechin, (–)-epigallocatechin, (–)-catechin gallate, and (–)-epigallocatechin gallate.

(–)-Epigallocatechin-3-*O*-gallate (EGCG) **35** is a major catechin constituent of green tea (*Camellia sinensis* L.) (7380 mg/100 g of dry leaves) and are present in small amounts in apple skin, plums, onions, and hazelnuts (109 mg/100 g of dw) (Bhagwat et al. 2011). EGCG on supplementation in diet (3.2 g/kg of diet) in HFD-fed obese mice for 16 weeks decreased body weight gain, body and visceral fat mass, the levels of plasma glucose, insulin, TC, and MCP-1, and hepatic fat mass and TG content in obese mice. Moreover, EGCG increased the excretion of fecal lipid content in obese mice (Bose et al. 2008). EGCG supplementation in diet (0.32% of diet) to HF-fed obese mice for 16 weeks significantly reduced body fat mass content by upregulation of the expression levels of FA oxidation-related genes PPARα, NRF-1, MCAD, and UCP-3 in the skeletal muscle of obese mice (Sae-Tan et al. 2011). In isolated primary rat hepatocytes, EGCG in low concentrations (< 1 μM) suppressed glucose production and expression levels of two key gluconeogenic enzymes PEPCK and G6Pase and increased the phosphorylation levels of AMPK, ACC, and CaMKK. Pre-treatment of LY294002, a PI3K inhibitor, did not alter the activity of EGCG in inhibition of glucose production and suppression of PEPCK and G6Pase expression, while co-treatment of compound C, an inhibitor of AMPK or AMPKα-siRNA, prevented the activity of EGCG in suppression of glucose production and on expression of PEPCK and G6Pase. Moreover, co-treatment of STO-609, a CaMKK inhibitor, blocked the activity of EGCG in the phosphorylation of both AMPK and CaMKK, and expression of PEPCK and G6Pase. Furthermore, co-treatment of a cell membrane permeable catalase (PEG-CAT) prevented the activity of EGCG in suppression of the activity of PEPCK and G6Pase. These findings demonstrate that EGCG at low concentrations (1 μM or less) inhibits hepatic gluconeogenesis via increased activation of AMPK mediated by CaMKK activation and ROS production (Collins et al. 2007). Another study reported that EGCG at high concentrations (>25 μM) in rat hepatoma H4IIE cells decreased the expression levels of gluconeogenic enzymes PEPCK and G6Pase and glucose production through insulin signaling pathway via increased phosphorylation of IRS-1 and IR-β (Waltner-Law et al. 2002). In dexamethasone-induced insulin-resistant L6 myotubes, EGCG increased glucose uptake by upregulation of GLUT4 translocation into plasma membrane via increasing the phosphorylation levels of AMPK, PI3K, and Akt. Pre-treatment of wortmannin, an inhibitor of PI3K, inhibited the glucose uptake activity of both EGCG and insulin, while genistein, an inhibitor of tyrosine kinase, failed to inhibit EGCG-dependent glucose uptake in L6 myotubes. These results indicate that EGCG increases glucose uptake in L6 myotubes via GLUT4 expression and activation of both AMPK and PI3K/Akt signaling pathways without phosphorylation of IRβ (Zhang et al. 2010b; Ueda et al. 2008). Accumulating evidence strongly demonstrates that the enzyme 11β-HSD1 is expressed in high concentrations in subcutaneous adipose tissues of obese and type 2 diabetic patients, and is the marker of insulin resistance and abdominal fat deposition. EGCG strongly inhibited the activity of human 11β-HSD1 activity with an IC_{50} value of 57.99 μM (reduction) and inhibition constant Ki of 22.68

and 18.74 μM for human liver microsomes and purified human 11β-HSD1, respectively (Hintzpeter et al. 2014). In diabetic vascular tissues, the elevated expression of vasoconstrictor factor, endothelin-1 (ET-1), causes restriction of vasorelaxation process of vascular endothelial cells in arteries by decreasing nitric oxide production from eNOS and leads to cardiovascular diseases. EGCG in both human aortic endothelial cells (HAECs) and bovine aortic endothelial cells (BAECs) reduced the expression and secretion of ET-1 by stimulating the phosphorylation of Akt, AMPK, and FoxO1 and increased the phosphorylation of endothelial nitric oxide synthase (eNOS) for NO production. Pre-treatment of compound C blunted the effect of EGCG in suppression of expression of ET-1 in both mRNA and protein levels. These findings suggest that EGCG suppresses the FoxO1-mediated expression of ET-1 by increasing the phosphorylation of FoxO1 and decreasing the activity of FoxO1 by its exclusion from nucleus via activation of AMPK and Akt (Reiter et al. 2010). In BAECs, the enhanced phosphorylation of eNOS by EGCG was prevented completely on pre-treatment of LY294002, a PI3K inhibitor. These findings suggest that EGCG-dependent Akt activation is essential for phosphorylation of eNOS. Thus, EGCG is a natural activator of eNOS in endothelial cells and has protective effect against cardiovascular disorders (Lorenz et al. 2004). EGCG supplementation (50 mg/kg/day) to a pressure-overload model of cardiac hypertrophy in (aortic banded) rats for 21 days improved cardiac hypertrophy by reduction of cardiomyocyte size, LV posterior wall thickness, LV end diastolic and systolic diameters, and systolic blood pressure and increased fractional shortening of ejection in the rats. To find out the molecular basis of EGCG in prevention of cardiac hypertrophy, EGCG was treated in angiotensin II (Ang II)-stimulated rat primary cardiomyocytes. Mounting evidence demonstrates that Ang II in cardiomyocytes promotes the expression of cardiac hypertrophy-related genes, atrial natriuretic peptide (ANP) and brain natriuretic peptide (BNP), via increasing the phosphorylation of epidermal growth factor receptor tyrosine kinase (EGFR), Akt, and ERK and ROS-dependent activation of NF-κB and AP-1. EGCG (50–100 μM) in Ang II-stimulated cardiomyocytes decreased the expression levels of ANP and BNP mRNA and proteins, suppressed ROS production, NF-κB and AP-1 activation, and p-levels of EGFR, PI3K, Akt and p38, JNK, and ERK. These findings suggest that EGCG prevents cardiac hypertrophy by inhibition of ROS-dependent phosphorylation of p38 and JNK and activation of NF-κB and AP-1 via suppression of EGFR phosphorylation and its downstream events ERK/PI3K/Akt signaling pathway (Li et al. 2006a). EGCG in diet supplementation (0.32% of diet) to HFD-fed obese mice for 8 weeks significantly decreased hepatic mass, fat droplets, and TG content by reshaping the gut microbiota composition, and the levels of serum bile acids (BAs) in obese mice. EGCG increased the relative abundance of bacteria of genera *Akkermansia*, *Adlercreutzia*, *Allobaculum*, and *Parabacteroides* and decreased the relative abundance of genera *Mucispirillum*, *Lactinospiraceae*, and *Desulfovibrionaceae* in the gut microbiota composition. Moreover, EGCG decreased the levels of serum conjugated-BAs, taurine-conjugated cholic acid (tauro-CA), taurine-conjugated deoxycholic acid (tauro-DCA), and taurine-conjugated β-muricholic acid (tauro-β-MCA), and increased the levels of CA,

chenodeoxycholic acid (CDCA), and ω-MCA for regulation of BA-mediated lipid and glucose metabolism in obese mice. *Akkermansia muciniphila* promoted the SCFAs production and insulin secretion by the release of GLP-1 from intestinal tract via the activation of TGR5. Moreover, increased abundance of *Akkermansia* and *Parabacteroides* reduces the levels of tauro-conjugated BAs by promoting their deconjugation. Tauro-BAs are the antagonist of farnesoid X receptor (FXR). CA is a dominant form of primary BAs (about 60% of primary BAs). Both CA and CDCA are the agonists of FXR and promote the activity of FXR in suppression of the activity of SREBP-1c and TG synthesis in liver. Desulfovibrionaceae has a positive correlation with tauro-conjugated BAs and plays a key role in the development of fatty liver in obese mice. Therefore, EGCG promotes the activity of BA-specific receptors, FXR and transmembrane G protein-coupled receptor (TGR)-5, in reshaping the gut microbiota composition and serum BAs composition in obese mice for prevention of hepatic steatosis (Ushiroda et al. 2019).

(–)-Epicatechin (EC) **39** is found in many dietary foods, such as green tea, grapes, and cocoa. EC has been reported to possess anti-obesity, antidiabetic, and anti-inflammatory activities. EC supplementation in diet (20 mg/kg bw/day) to HFD-fed obese type 2 diabetic mice for 15 weeks reduced plasma glucose, insulin, TG, and FFAs levels by increasing insulin sensitivity in obese mice. EC increased insulin signaling in the liver by increasing insulin-stimulated phosphorylation of IR, IRS-1, Akt, and ERK1/2 in adipose tissue of obese mice. Moreover, EC decreased the activity of PTP1B, a negative regulator of insulin signaling, and inflammation in metabolic tissues by inhibition of redox sensitive activation of NF-κB and JNK in adipose tissue (Cremonini et al. 2016). Furthermore, EC decreased the expression levels of inflammatory factors, macrophage marker F4/80, TNF-α, MCP-1, NOX4, and 4-hydroxynonenal (4-HNE), a marker of oxidative stress in visceral adipose tissue of obese mice for suppression of oxidative and ER stress via inhibition of NF-κB activity (Bettaieb et al. 2016).

5.2.1.6 Anthocyanins

Anthocyanins are a class of flavonoids having flavylium cation structures and present in a variety of dietary plant foods as glycosides and acylated forms. Both mono- and di-glycosides are the common glycosides, and coumaroylated, caffeoylated, and malonylated anthocyanins are common forms of acylated anthocyanins. Their aglycones are known as anthocyanidins. The most common anthocyanidins are cyanidin **390**, peonidin **391**, delphinidin **392**, malvidin **393,** pelargonidin **394,** and petunidin **395** (Fig. 5.1). Anthocyanins are abundant in colored fruits, such as berries (bilberry, blackberry, blackcurrant, blueberry, cranberry, mulberry, maquiberry, strawberry), cherries, red oranges, peaches, apples, grapes, and plums, and in colored vegetables, such as purple potatoes, red onions, red radish, purple turnip, purple cauliflower, black beans, red cabbage, and eggplant, as well as in pigmented grains including black rice, red sorghum, and purple maize (Wu et al. 2006; Zhang et al. 2019a). These are water-soluble plant pigments and have numerous health-benefit effects, such as antidiabetic, anti-obesity, cardioprotective, anti-inflammatory bowel disease and anti-cancer effects.

Cyanidin-3-glucoside (C3G) **31**, a constituent of many dietary foods, blueberry, black soybean, and red grapes, has potential antidiabetic effect. C3G on supplementation in diet (0.2% of diet) to type 2 diabetic KK-Ay mice for 5 weeks significantly reduced blood glucose levels and enhanced insulin sensitivity in WAT of diabetic mice. C3G increased glucose uptake in adipose tissue by upregulating the expression of GLUT4 in plasma membrane, and down-regulating the secretion of adipokine, retinol binding protein-4 (RBP-4), and pro-inflammatory adipokines MCP-1 and TNF-α. Accumulating evidence demonstrates that overexpression of RBP-4 in diabetic adipose tissue causes insulin resistance. Thus, these findings suggest that C3G exerts its antidiabetic effect by increasing insulin sensitivity via regulation of GLUT4-RBP4 system and related inflammatory factors in adipose tissue (Sasaki et al. 2007). Another study reported that anthocyanins-rich black soybean extract (BSAE) containing 72% of C3G on oral treatment (50 mg/kg/day) to STZ-diabetic rats for 30 days improved heart hemodynamic function (left ventricular (LV) end diastolic pressure and $\pm$ dp/dt parameters), reduced plasma glucose, and increased plasma insulin and activity of antioxidant enzymes SOD and CAT in plasma and pancreatic tissues in diabetic rats. Moreover, BSAE increased glucose uptake in both skeletal and hip muscle by upregulation of GLUT4 expression (about three- and fourfold, respectively, compared to control in these tissues), through increased phosphorylation levels of IR, PI3K, and Akt . In addition, BSAE protected the pancreatic islets from injury and apoptosis and improved β-cells mass and function by down-regulation of pro-apoptotic proteins caspase 3 and Bax, and upregulation of anti-apoptotic protein Bcl-2. Therefore, BSAE and its main constituent C3G have cardioprotective, pancreas protecting, and insulin signaling effects in diabetic rats (Nizamutdinova et al. 2009). In 3T3-L1 adipocytes, C3G increased differentiation of adipocytes through increased expression levels of adipogenic genes PPARγ and C/EBPα, increased adiponectin secretion, decreased TNF-α secretion, and increased GLUT4 expression and activation of insulin signaling. In C2C12 myotubes grown with media conditioned by 3T3-L1 cells, C3G (100 μM) increased mitochondrial biogenesis and function in thermogenesis and oxidative phosphorylation by upregulation of the expression of genes PGC-1α and SIRT1 and their target genes, UCP-1 and others. Moreover, black soybean seedcoat extract rich in C3G on supplementation in diet to type 2 diabetic db/db mice reduced body weight gain, mass, and size of adipocytes in WAT of diabetic mice. These results suggest that C3G exhibits browning of adipocytes via adipocyte differentiation and subsequent formation of smaller insulin-sensitive adipocytes and thermogenesis of these white and brown adipocytes in WAT for prevention of obesity (Matsukawa et al. 2015). Another study reported that C3G in 3T3-L1 adipocytes promoted adipocyte differentiation, thermogenesis, and mitochondrial biogenesis by elevation of intracellular cAMP levels, and upregulation of the expression of adipogenic factors C/EBPβ, C/EBPα, and PPARγ, and subsequent expression of mitochondrial beige adipocyte marker genes, PRDM-16, PGC-1α, UCP-1, UCP-2, TFAM, SOD2, and TBX1, through increased phosphorylation of AMPK. These findings suggest that C3G promotes beige adipocytes phenotypes through AMPK activation (Matsukawa et al. 2017).

Bilberry (*Vaccinium myrtillus*) extract (BBE) rich in anthocyanins (375 g/kg of extract) containing a mixture of cyanidin-, delphinidin-, petunidin-, peonidin-, and malvidin-glycosides in high concentrations, on supplementation in diet (27 g of BBE/kg of diet) to type 2 diabetic KK-Ay mice for 5 weeks, improved hyperglycemia by reduction of serum glucose and TG levels and hepatic TG content by enhancement of insulin sensitivity in WAT, skeletal muscle, and the liver of diabetic mice. BBE increased AMPK activation in liver, adipose tissue, and skeletal muscle for glucose uptake in WAT and muscle by upregulation of GLUT4 translocation into plasma membrane, and suppression of hepatic glucose production by decreasing the activity of gluconeogenic enzymes PEPCK and G6Pase in the liver. Moreover, BBE reduced the hepatic lipid content by down-regulation of the activity of FA synthesis gene ACC, and upregulation of the activity of FA oxidation-related genes PPARα, ACOX, and CPT-1 in the liver. Therefore, BBE improves hyperglycemia and hyperlipidemia by regulation of enzymes related to glucose and lipid metabolism through improvement of AMPK activation (Takikawa et al. 2010).

Blueberry powder rich in anthocyanins (BBA) on supplementation in diet (10% of diet) to HFD-fed obese rats for 8 weeks improved systemic inflammation and hepatic insulin sensitivity in obese rats by modulation of gut microbiota dysbiosis. BBA decreased the levels of serum glucose, MDA, and LPS-binding protein (LBP), the marker of circulating LPS in obese rats. Moreover, BBA increased the relative abundance of bacteria of genera *Actinobacillus* and *Aggregatibacter* from *Gammaproteobacteria* class in the gut and increased the growth and function of goblet cells by increasing the expression levels of mucin-producing gene Muc2 and antimicrobial gene Defb 2 in the ileum. Moreover, BBA increased the levels of serum SCFAs and the expression levels of GLP-1 and GRP-43 in ileum, and decreased the expression levels of pro-inflammatory adipokines TNF-α and IL-1β in visceral adipose tissue (VAT) and levels of IRS-1 Ser307 phosphorylation in the liver. In addition, BBA upregulated the expression of FA oxidation-related genes PPARα and PPARδ in VAT. These findings demonstrate that BBA increased the abundance of SCFAs producing bacteria in the gut to improve gut epithelial cells integrity for prevention of the entry of harmful pathogens and suppression of systemic inflammation and insulin resistance in obese rats (Lee et al. 2018b).

Blackcurrant extract rich in anthocyanins (BCA) containing delphinidin-3-glucoside **30**, delphinidin-3-rutinoside, cyanidin-3-glucoside **31**, and cyanidin-3-rutinoside as major constituents, on supplementation in diet (0.1% of diet) to HF/HC-diet fed obese mice for 12 weeks, decreased body weight gain and adipocyte size of epididymal fat through suppression of inflammation in epididymal adipose tissue (EAT). BCA decreased the inflammation in EAT by suppression of infiltration of inflammatory macrophage marker protein F4/80 and activation of NF-κBε. Moreover, BCA increased energy expenditure and mitochondrial biogenesis by upregulation of the expression levels of genes PPARα, PPARδ, UCP-2, and UCP-3 in skeletal muscle. Moreover, in LPS-stimulated splenocytes, isolated from obese mice, BCA decreased the expression levels of TNFα and IL-1β. These findings suggest that BCA exerts anti-obesity effect by modulation of energy

expenditure in skeletal muscle and suppression of inflammation in AT and splenocytes (Benn et al. 2014).

Mulberry (*Morus australis*) juice (MBJ) rich in anthocyanins content (21.86 mg/ml of juice) having cyanidin-3-glucoside **31** and cyanidin-3-rutinoside **31a** as major constituents (11.78 and 9.61 mg/ml, respectively), while blueberry (*Vaccinium ashei*) juice (BBJ) contains relatively less anthocyanins (4.09 mg/ml of juice) with petunidin-3-arabinoside **396** and delphinidin-3-galactoside **397** (Fig. 5.1) as major constituents (1.00 and 0.67 mg/ml of juice, respectively). Both MBJ and BBJ on supplementation in drinking water (4.56 and 4.83 ml of juice/day/mouse, respectively) to HFD-fed obese mice for 12 weeks significantly decreased body weight gain, adipocytes number and size, hepatic TG content and serum glucose, HOMA-IR and leptin levels, and increased serum adiponectin level in obese mice. Moreover, both MBJ and BBJ decreased the expression levels of hepatic inflammatory cytokines IL-6 and TNF-α, and expression of FA synthesis-related genes PPARγ and FAS, and increased the expression of FA oxidation-related genes ACOX and CPT-1 in liver; the effects of MBJ were better compared to that of BBJ. These results demonstrate that both MBJ and BBJ decrease lipid accumulation in liver and adipose tissue through improvement of lipid metabolism (Wu et al. 2013).

Anthocyanins-rich Maqui berry (*Aristotelia chilensis*) extract (MBA) containing delphinidin-3-*O*-sambubioside **398** and delphinidin-3-*O*-sambubioside-5-*O*-glucoside **399** (Fig. 5.1) as major constituents, on supplementation in drinking water (20 mg/ml of water/day/mouse) to HFD-fed obese mice for 16 weeks, decreased body weight gain, lipid droplets in subcutaneous WAT (scWAT), and serum FG and insulin levels in obese mice. MBA decreased the fat mass in scWAT by induction of brown like phenotype through fuel storage followed by thermogenesis via upregulation of the expression of fat-specific protein 27b (FSP27b) and upregulation of the activity of genes, carbohydrate response element binding proteins α and β (ChREBPα/β), GLUT4, fibroblast growth factor 21 (FGF21), and its receptors FGFR4 and FGFR1, PGC-1α, CPT-1α, UCP-1, ACOX3, DIO2, PRDM-16, CREG1, SREBP-1c, GyK, ACL, and FAS, related to lipogenesis, thermogenesis, and browning in scWAT. Mounting evidence demonstrates that FSP27 gene promotes lipolysis and insulin sensitivity in adipocytes, and its expression is down-regulated in association with visceral obesity. ChREBP promotes the activity of genes related to glucose metabolism (upregulation of GLUT4) and fat storage (upregulation of lipogenic genes SREBP-1c, FAS, GyK, and ACL) in the liver. Glycerol kinase (GyK) promotes the conversion of glycerol into glycerol-3-phosphate for glycolysis and lipid synthesis. ATP-citrate lyase (ACL) promotes mitochondrial function for increased oxygen function and ATP production. FGF21 has a key role in stimulation of fatty acid oxidation and in reduction of circulating FFAs and TG levels. Cellular repressor of adenovirus early antigen 1A-stimulated gene 1 (CREG1) stimulates brown adipocyte formation by induction of UCP-1. Deiodinase type II (DIO2) catalyzes the conversion of T4 into bioactive T3 for stimulation of thermogenic process and mitochondrial function. These findings suggest that MBA reduces fat mass in scWAT through regulation of genes related to de novo lipid synthesis, FA oxidation, thermogenesis, and browning phenotypes in obese mice (Sandoval et al. 2019).

Dietary purple sweet potato (*Ipomoea batatas*) (PSP) is rich in proteins and anthocyanins content and has potential antidiabetic and anti-obesity effects. Anthocyanins-rich fraction of PSP (PSP-AF) on supplementation in diet (200 mg/kg/day) to HFD-fed obese mice for 4 weeks reduced body weight gain, hepatic TG content, and serum lipid profile in obese mice. Moreover, PSP-AF increased the phosphorylation of AMPK and ACC, and down-regulated the expression of lipogenic genes SREBP-1 and FAS in both livers of obese mice and human HepG2 hepatocytes. Co-treatment of compound C, an inhibitor of AMPK, blocked the activity of PSP-AF in the expression levels of lipogenic genes. These findings suggest that PSP-AF ameliorates hepatic steatosis through regulation of lipid metabolism via AMPK activation (Hwang et al. 2011). Accumulating evidence demonstrates that obesity-induced oxidative stress in kidney promotes kidney damage by stimulating the over-production of AGEs, RAGE, TXNIP, and ROS and consequent activation of NF-κB and nucleotide-binding domain (NBD) and leucine-rich repeat (LRR)-containing a pyrin domain 3 (NLRP3) inflammasome. Both these activated NF-κB and NLRP3 inflammasome promote the expression of inflammatory cytokines and proteins including IL-1β and collagen IV via activation of caspase 1 for the development of kidney damage and fibrosis. PSP-color (PSPC) rich in anthocyanins having peonidin- and cyanidin-acyl glucosides as major constituents (> 90%), on supplementation in diet (700 mg/kg/day) to HFD-fed obese mice for 20 weeks, significantly improved kidney function by reduction of serum glucose and urine albumin content in obese mice. Moreover, PSPC decreased the expression levels of ROS, AGEs, RAGE, and TXNIP (thioredoxin interacting protein), markers of oxidative stress, and the expression levels of nuclear NF-κB, iNOS, COX-2, NLRP3, IL-1β, and collagen IV in kidney tissues. These results suggest that PSPC improves diabetic nephropathy through suppression of the activation of NF-κB and NLRP3 inflammasome signaling pathways (Shan et al. 2014). In another study, protein-bound anthocyanins of PSP (PSP-PBA) and free anthocyanins of PSP (PSP-FA) containing cyanidin-3-sophoroside-5-glucoside and peonidin-3-sophoroside-5-glucoside as major anthocyanins, on supplementation in diet (500 and 200 mg/kg, respectively) to STZ/HFD-induced diabetic mice, improved hyperglycemia and insulin resistance by reduction of serum FG,TG, and LDL-C levels in diabetic mice. Both PSP-PBA and PSP-FA increased the phosphorylation of hepatic AMPK and IRα and increased glucose uptake and glycolysis by upregulation of GLUT2, GCK, PFK, and PK expression levels, and decreased hepatic glucose production by down-regulation of the activity of G6Pase and PEPCK, and increased hepatic antioxidant activity by increasing the levels of total antioxidant capacity (T-AOC), SOD, and GP_X in the liver. These findings suggest that both PSP-PBA and PSP-FA exhibit hypoglycemic effects by regulation of hepatic glucose metabolism via AMPK activation and upregulation of hepatic antioxidant activity (Jiang et al. 2020).

5.2.1.7 Chalcones

4-Hydroxyderricin (4-HD) **222** and xanthoangelol (XA) **218**, two major chalcones from Japanese antidiabetic herb, "Ashitaba," *Angelica keiskei*, have insulin-like

activity in cellular and diabetic animal models. In 3T3-L1 adipocytes, 4-HD increased glucose uptake and adipogenesis acting as PPARγ agonist. Moreover, 4-HD showed strong hypoglycemic effect in genetically diabetic KK-Ay mice by decreasing plasma glucose and TG levels and increasing glucose uptake and GLUT4 translocation into plasma membrane in skeletal muscle and adipose tissue of diabetic mice (Enoki et al. 2007). In 3T3-L1 adipocytes, 4-HD promoted intracellular lipid accumulation, upregulated the expression levels of PPARγ, C/EBPα, aP2, and adiponectin, and increased Akt phosphorylation and GLUT4 expression and translocation into cell membrane. These findings suggest that 4-HD promotes insulin sensitivity acting as PPARγ agonist (Li et al. 2016b). Another study reported that both 4-HD and XA in 3T3-L1 adipocytes increased glucose uptake by increasing GLUT4 translocation to plasma membrane and increased the phosphorylation of AMPK and its downstream target gene ACC. Co-treatment of LKB1 siRNA prevented the activity of 4-HD and XA in AMPK phosphorylation and GLUT4 expression. These findings demonstrate that both 4-HD and XA stimulate GLUT4-dependent glucose uptake through activation of LKB1/AMPK signaling pathway in 3T3-L1 cells (Ohta et al. 2015). Both 4-HD and XA in high-FA exposed human HepG2 cells suppressed intracellular lipid accumulation by down-regulation of the expression of lipogenic gene SREBP-1 and upregulation of FA oxidation-related gene PPARα through increased phosphorylation of LKB1 and AMPK (Zhang et al. 2014a). In vitro, 4-HD inhibited the activity of DPP-4 with an IC_{50} value of 81.44 μM, compared to sitagliptin (IC_{50} of 0.87 μM), while docking analysis with DPP-4 enzyme revealed that 4-HD showed a strong inhibition to DPP-4 with Ki of 3.99 μM, compared with sitagliptin (Ki of 0.17 μM). Possibly, high polarity factor in 4-HD compared to sitagliptin plays a key role in weak activity in vitro study (Aulifa et al. 2019).

Another prenylated-chalcone, isobavachalcone (IBC) **400** isolated from *A. keiskei*, inhibited the differentiation of 3T3-L1 adipocytes by suppression of lipid accumulation and suppression of the expression levels of adipogenic factors PPARγ, C/EBPα, SREBP-1c, FAS, ACC1, and adiponectin through cell cycle arrest in G0/G1 stage and down-regulation of the expression of cell growth proteins cyclin D1, cdk-4, and cdk-6. In HC-diet-fed zebrafish larvae, IBC inhibited hepatic lipid accumulation by suppression of the expression levels of PPARγ and C/EBPα. Therefore, IBC exerts anti-adipogenic activity by suppression of mitotic clonal expansion in G0/G1 stage in 3T3-L1 adipocytes (Lee et al. 2018a).

5.2.2 Stilbenoids

Resveratrol (3,5,4′-trihydroxystilbene) (RSV) **47** is found in the skin of grapes, peanut, and berries and in processed food products, such as red wine, and in medicinal plants including *Polygonum cuspidatum*. RSV has been shown to combat a variety of diseases, such as type 2 diabetes, obesity, cardiovascular diseases, neurodegenerative disorders, and cancers. RSV on supplementation in diet (200 or 400 mg/kg/day) to HFD-fed obese mice for 15 weeks decreased body weight and

epididymal and inguinal WAT fat mass in obese mice. RSV increased both mitochondrial biogenesis and function for improvement of oxidative phosphorylation and ATP production by upregulation of the expression levels of thermogenic genes PGC-1α, PGC-1β, NRF-1, MCAD, and UCP3 in skeletal muscle, and the expression levels of FA oxidation-related genes PGC-1α, PPARα, and UCP1 in BAT through increased expression and activity of SIRT1 for reduction of fat mass in WAT (Lagouge et al. 2006). In another study, RSV supplementation in diet (0.04% of diet) to HFD-fed type 2 diabetic obese mice improved obesity-related abnormalities by reducing serum glucose and insulin levels, and increasing insulin sensitivity, mitochondrial number, and energy expenditure function through increased AMPK and PGC-1α activity in the muscle, adipose tissue, and liver of obese mice. These findings suggest that RSV promotes energy expenditure through AMPK activation (Baur et al. 2006). Moreover, RSV administration in CNS (79.2 ng/mouse/day) to HFD-fed type 2 diabetic mice for 5 weeks normalized hyperglycemia and hyperinsulinemia by reduction of serum glucose and insulin levels, and suppression of hypothalamic inflammation and NF-κB activation, and the activity of hepatic gluconeogenic enzyme PEPCK, and increased hepatic glycogen content through increased hypothalamic SIRT1 activity. Therefore, RSV stimulates hypothalamic SIRT1 activity for maintenance of glucose homeostasis in obese diabetic mice (Ramadori et al. 2009). Another study revealed that RSV supplementation in diet (400 mg/kg/day) in both HFD-fed wild-type (WT) mice and AMPKα null mice for 13 weeks increased metabolic rate and reduced body fat mass in WT mice, but not in AMPK null mice. In WT mice, RSV upregulated the expression levels of thermogenic genes UCP1, UCP2, and UCP3 and mitochondrial biogenesis and oxidative phosphorylation-related genes SIRT1, PGC-1α, PGC-1β, GLUT4, MCAD, NRF, and ERRα, and increased the ratio of NAD to NADH and deacetylation of PGC-α in WAT and BAT of WT mice. These findings demonstrate that RSV failed to increase insulin sensitivity, glucose tolerance, mitochondrial biogenesis, and function in AMPK-deficient mice. In C2C12 myotubes, RSV increased the phosphorylation of AMPK and ACC and increased NAD to NADH ratio without changing the levels of SIRT1. Accumulating evidence demonstrates that deacetylation of PGC-1α by SIRT1 promotes the activity of PGC-1α. In SIRT1 null mouse embryonic fibroblasts, RSV increased the activation of AMPK. Hence, SIRT1 is not essential for RSV in AMPK activation. Moreover, AMPK activates PGC-1α directly by its phosphorylation. Thus, SIRT1 plays a modulatory role on PGC-1α activation, but not a central role in response to RSV. Further, RSV in AMPKα2 null mice failed to increase insulin sensitivity and mitochondrial biogenesis and function. These results suggest that RSV stimulates mitochondrial biogenesis and activity by upregulation of PGC-1α activity via both AMPK and SIRT1 dependent pathways (Um et al. 2010). In neuro-2A (N2A) cells, RSV increased glucose uptake and increased phosphorylation of Akt, GSK-3β, and AMPK. Co-treatment of compound C abrogated the activity of RSV in the phosphorylation of Akt and GSK-3β and glucose uptake. These results demonstrate that RSV stimulates insulin signaling and glucose uptake via AMPK activation in N2A cells (Patel et al. 2011). RSV treatment (300 mg/day) to overweight and obese patients for a period of 3 months

decreased cardiovascular risk factors by decreasing the levels of serum FG, TC, and insulin and systolic and diastolic blood pressures (Huang et al. 2016a). Both RSV and its natural analog, piceatannol (PIC) **401**, increased nitric oxide (NO) bioavailability in bovine aortic endothelial cells (BAECs) under high-glucose-induced oxidative stress by increasing the activity of eNOS in NO production. They protected the activity of dimethylarginine dimethylaminohydrolase (DDAH) in protection of eNOS by inhibiting the activity of asymmetric dimethylarginine (ADMA), a natural inhibitor of eNOS, via its degradation into citrulline. In diabetic cardiovascular patients, over-expression of ADMA leads to the activation of NADPH oxidase and production of oxidative stress marker enzymes NOX1, NOX2, NOX4, etc. Both RSV and PIC restored DDAH activity even in presence of splitomicin, an inhibitor of SIRT1, and PIC was more effective. These findings suggest that both RSV and PIC improve eNOS activity in a mechanism independent of SIRT1 activation in high-glucose exposed BAECs (Frombaum et al. 2011; Bonnefont-Rousselot 2016). RSV supplementation in diet (50 or 100 mg/kg bw/day) to HFD-fed obese mice for 4 weeks reduced hepatic fat mass and TG content and decreased serum FG, insulin, HOMA-IR, TG, TC, LDL-C, ALT, and AST levels, and modulated gut microbiota composition for amelioration of hepatic steatosis in obese mice. In gut, RSV increased the relative abundance of SCFAs producing Actinobacteria of genera *Allobaculum*, *Olsenella*, and *Enterorhabdus* and decreased the relative abundance of pathogenic bacteria of genera *Oscillibacter*, *Anaerotruncus*, *Flavonifractor*, and *Clostridium* IV, which are positively correlated with hepatic fat accumulation. At the phylum level, RSV significantly increased *Firmicutes* and decreased *Bacteroides* in the gut of obese mice. In addition, RSV improved gut tight junction function by upregulation of ZO-1 and occludin and improved hepatic inflammation by reduction of inflammatory-related factors IL-1, TNF-α, TLR4, and MyD88 in the liver. Further, RSV decreased the expression of lipogenic related genes GPAT-1, MOGAT, PPARγ, and FAS and the expression of lipid uptake genes FABP2, FABP1, and CD36 in the liver. In vitro, RSV in fermented fecal microbiota of obese mice increased the abundance of *Olsenella* and decreased the abundance of *Bacteroides* and *Streptococcu*s spp. These findings suggest that RSV improves hepatic steatosis in obese mice by modulation of gut microbiota composition and hepatic lipid metabolism and inflammation (Du et al. 2021).

Piceatannol (PIC) **401**, an analog of resveratrol, is found in many fruits of dietary plants including grapes, berries, peanuts, seeds of passion (*Passiflora edulis*) fruits, and seeds of *Euphorbia lagascae*. PIC has health-benefit effects in prevention of many diseases including diabetes, obesity, and cancer. PIC on oral administration of a single dose of 50 mg/kg bw to genetically diabetic db/db mice reduced blood glucose level after 1 h of administration, but did not affect on body weight or visceral fat gain in mice (Uchida-Maruki et al. 2015). In insulin-resistant L6 myotubes, PIC increased glucose uptake, AMPK phosphorylation, and GLUT4 translocation into plasma membrane. In type 2 diabetic db/db mice, PIC decreased plasma glucose level by increasing glucose uptake in skeletal muscle (Minakawa et al. 2012). In 3T3-L1 preadipocytes, PIC inhibited adipogenesis of adipocytes in early phase of

differentiation process by suppression of the expression of pro-adipogenic transcription factors C/EBPβ, C/EBPα, and PPARγ for inhibition of cell cycle progression in mitotic clonal expansion stage and delaying of cell cycle entry into G2/M phase via inhibition of phosphorylation of IR and IRS-1 in insulin signaling pathway. PIC inhibited the activity of IR to ATP on direct binding to IR in a non-competitive manner (Kwon et al. 2012). In high-palmitic acid-induced insulin-resistant human umbilical vein endothelial cells (HUVECs), PIC increased eNOS activation and nitric oxide production by increasing insulin-mediated IRS-1 phosphorylation and increased expression of antioxidant enzyme heme oxygenase-1 (HO-1) via Nrf-2 activation. These findings suggest that PIC could be useful in prevention of endothelial dysfunction in diabetic patients (Jeong et al. 2015). In HFD-fed obese mice, PIC supplementation in diet (0.25% of diet) for 18 weeks significantly decreased body fat mass, liver weight, adipocyte size, and the levels of serum glucose, TC, and LDL-C by modulation of gut microbiota composition in obese mice. PIC increased the abundance of *Firmicutes* and pro-biotic *Lactobacillus* and decreased the abundance of *Bacteroidetes* in gut microbiota of obese mice compared with the HFD group. Moreover, PIC increased the phosphorylation levels of AMPK and ACC, and the expression levels of fat oxidation-related genes PPARα and CPT-1, and decreased the expression levels of lipid synthesis-related genes C/EBPα, PPARγ, and FAS in the adipose tissue and liver of obese mice. These results demonstrate that PIC exerts its anti-obesity effect by regulation of lipid metabolism via AMPK activation and reshaping of gut microbiota composition (Tung et al. 2016).

(+)-ε-Viniferin (VIN) **150**, a resveratrol dimer, found in grapes and grape plant (*Vitis thunbergii* var*, taiwaniana*) roots and shoots, has potential anti-obesity and antidiabetic effects. In 3T3-L1 preadipocytes, VIN at 15 μM concentration significantly suppressed intracellular lipid accumulation by reduction of the expression levels of adipogenic-transcription-related proteins PPARγ and FAS and increased expression of lipogenesis-related protein ATGL as well as increased secretion of adiponectin and expression of SIRT-1, phosphorylated AMPK, and FGF-21. Pre-treatment of EX527, an inhibitor of SIRT1, completely blocked the activity of VIN in suppression of lipid accumulation. These findings suggest that VIN exerts its lipid suppressive effect by increased expression of SIRT1. Moreover, resveratrol at 15 μM did not increase the expression of SIRT1 and p-AMPK, and did not exert any effect on the expression of ATGL, FAS, and adiponectin, and exhibited much less suppression of lipid accumulation in 3T3-L1 cells. These findings demonstrate that VIN is more effective in inhibition of adipocyte differentiation than resveratrol (RSV) (Hung et al. 2019; Ohara et al. 2015). Another study reported that VIN at high concentrations (120 or 160 μM) reduced the expression of HMGCR, a key enzyme for cholesterol biosynthesis, more efficiently than RSV in 3T3-L1 adipocytes. In HFD-fed obese mice, VIN on oral treatment (10 mg/kg/day for 38 days in the first stage, and 25 mg/kg/day for next day 39–day 58 in second stage) reduced body weight and the levels of serum glucose, TC, and LDL-C, compared to HFD group. Therefore, VIN exerts anti-obesity effect in obese mice (Lu et al. 2017). In HFD/STZ-induced type 2 diabetic rats, VIN supplementation in diet (30 or 60 mg/kg/day) for 8 weeks significantly improved hyperglycemia,

hyperlipidemia, and oral glucose tolerance, and liver and kidney functions by decreasing the levels of serum FG, TC, TG, LDL-C, creatinine, BUN, ALT, and AST in diabetic rats. Moreover, VIN increased the phosphorylation of AMPK in liver for suppression of hepatic steatosis and inflammation and endogenic glucose production by regulation of lipid metabolism (Liu et al. 2020). The renin-angiotensin system (RAS) plays a key role in the pathogenesis of hypertension and cardiac hypertrophy via vascular endothelial dysfunction. Under lipotoxic and glucotoxic conditions, RAS stimulates the production of excessive ROS, particularly superoxide and H_2O_2, which in turn impairs nitric oxide production from eNOS and contributes to impaired vasodilation process of arterial endothelial cells and leads to hypertension. Moreover, angiotensin-converting enzyme (ACE) in RAS catalyzes the formation of angiotensin II from angiotensin I and hydrolyzes and inactivates the vasodilator peptide bradykinin. Therefore, inhibition of ACE activity is an important therapeutic approach for treatment of hypertension and its associated coronary artery disease. In vascular endothelial cells (VECs) isolated from porcine pulmonary arteries, both VIN and its monomer RSV enhanced cell proliferation and cell functions via eNOS activation and nitric oxide production and protected the cells from intracellular ROS production by decreasing its expression levels and increasing the activity of antioxidant enzymes CAT and GP_X. VIN is more effective than RSV in most of these effects. Moreover, VIN, but not RSV, inhibited the activity of ACE in vitro. Further, VIN treatment (5 mg/kg/day) to spontaneously hypertensive rats (SHRs), a genetic model of hypertension and subsequent cardiac hypertrophy, for 3 weeks, reduced systolic blood pressure and improved whole cardiac mass and left ventricle mass indexes, while RSV (2.5 mg/kg/day) treatment to SHRs for the same period failed to lower the blood pressure and only improved these mass indexes. These findings suggest that VIN is more effective than RSV in improving the functions of VECs and hypertensive heart (Zghonda et al. 2012). In isolated rat thoracic aortas, VIN and RSV showed vasorelaxant effect, but VIN is more effective than RSV having a EC_{50} value of 2.4 μM. Pre-treatment of N^G-nitro-L-arginine methyl ester (L-NAME), an inhibitor of NOS, diminished the activity of VIN in vascular relaxant effect. These findings demonstrates that VIN exerts vascular relaxant effect via endothelial nitric oxide synthase (eNOS)-dependent NO signaling pathway (Yoo et al. 2007).

Resveratrol tetramer, (+)- and (–)-hopeaphenol **150a** and **150b**, isolated from Indian *Ampelocissus indica* (AI) syn. *Vitis indica* and *Vateria indica* (VI) acetone extract showed inhibitory effect against α-glucosidase enzyme with IC_{50} value of 21.21 and 9.47 μM, respectively, and against α-amylase enzyme with IC_{50} value of 68.75 and 71.63 μM, respectively, compared to acarbose of IC_{50} of 81.3 and 8.5 μM, respectively. In bovine serum albumin AGEs formation inhibitory assay, both (+)- and (–)-hopeaphenol showed strong antiglycation activity with IC_{50} value of 81.9 and 50.96 μM, respectively, compared to ascorbic acid of IC_{50} value of 158.23 μM. In L6 myotubes, both these enantiomers of hopeaphenol at 100 μM concentration increased glucose uptake by 31 and 26.4%, respectively, compared to rosiglitazone (35.9%) at the same concentration. These findings suggest that enantiomeric

hopeaphenols have potential antidiabetic effect in cellular models (Sasikumar et al. 2016).

5.2.3 Curcuminoids

Curcumin, a yellow pigment extracted from turmeric, the dried rhizome of the perennial herb *Curcuma longa*, is a popular dietary spice in Asian countries. Commercial curcumin, known as curcuminoids, consists of curcumin **9** (about 80%), desmethoxycurcumin **156** (about 10–20%), and bisdesmethoxycurcumin **157** (>5%), and is consumed by humans up to 12 g/day without any significant side effects (Lao et al. 2006). Curcumin has health-benefit effects including anti-inflammatory, anti-carcinogenic, anti-obesity, and antidiabetic effects. Curcumin on supplementation in diet (3% of diet) to both HFD-fed wild obese mice and genetically leptin-deficient obese ob/ob mice for 10 weeks significantly decreased body fat mass, serum glucose, and HbA1c levels and decreased inflammation responses in the adipose tissue and liver of both DIO- and ob/ob-mice. Curcumin decreased the expression of inflammatory macrophage marker gene F4/80 and increased adiponectin secretion and the expression levels of SIRT1, p-FoxO1, and HSP-70 in adipose tissue, and decreased the expression levels of inflammatory-related cytokines and proteins TNF-α, MCP-1, SOCS-3, IL-1β, and NF-κB p65 in the liver of both DIO mice and ob/ob mice. These findings suggest that curcumin ameliorates obesity-related fat mass and hyperglycemia by suppression of inflammatory-related macrophage infiltration in adipose tissue and cytokines expression in the liver via SIRT1 expression and inhibition of NF-κB activity (Weisberg et al. 2008). In another study, curcumin supplementation (4 g/kg of diet, 2 days/week for 28 weeks) to HFD-fed obese mice significantly decreased epididymal adipose tissue (EAT) fat mass, decreased serum glucose levels, and decreased the expression levels of F4/80, NF-κB, and p-JNK in EAT, and decreased the level of oxidative-stress-related protein TXNIP, and the expression of lipogenesis-related genes ChREBP and SREBP-1c in the liver of obese mice. Further, curcumin increased the insulin signaling in adipose tissue and liver by increasing the phosphorylation of Akt. In rat primary adipocytes, curcumin increased the expression of antioxidant enzyme HO-1. These findings demonstrate that curcumin improves insulin signaling in adipose tissue and liver for prevention of obesity-related body fat mass, oxidative stress, and inflammation in obese mice (Shao et al. 2012). Accumulating evidence demonstrates that farnesoid X receptor (FXR) and nuclear factor (erythroid-derived 2)-like 2 (Nrf2) play a critical defense role against hepatic lipid accumulation. Inactivation of FXR in obese liver is one of the leading factors for hepatic excessive fat accumulation in NAFLD and alcoholic liver disease (ALD). In ethanol-induced liver injury in ALD rats, curcumin treatment (200 or 400 mg/kg/day) for 4 weeks reduced the hepatic inflammation and MDA levels, number and size of lipid droplets in hepatic tissues, and hepatic TC and TG contents in ALD rats. Moreover, curcumin decreased the expression of lipogenesis-related genes SREBP-1c and FAS and increased the expression of FA oxidation-related genes PPARα and CPT-1, as

well as increased the expression of FXR and Nrf2 in the liver. In ethanol exposed human hepatocyte LO_2 cells, curcumin decreased intracellular lipid accumulation. Co-treatment of Z-guggulsterone, a FXR antagonist or transfection of hepatocytes with Nrf2 siRNA, reversed the effect of curcumin in lipid accumulation. These findings suggest that curcumin stimulates Nrf2 activity for increased expression of FXR for suppression of hepatic lipid accumulation (Lu et al. 2015). In another study, curcumin (75 and 150 mg/kg/day) to alcohol-exposed liver injury in Balb/c mice for 8 weeks promoted hepatic mitochondrial function by reducing the opening of mitochondrial permeability transition pore (MPTP) and thereby increasing mitochondrial membrane potential (MMP) and activity of antioxidant enzymes Na^{2+}/K^{+} ATPase, Ca^{2+}-ATPase, and Ca^{2+}/Mg^{2+}-ATPase and the expression levels of PGC-1α, NRF1, and Mn-SOD and suppressing the inflammation via inhibition of NF-κB-signaling pathway in mice liver. Thus, curcumin has potential activity in prevention of alcohol-induced hepatic injury (Wang et al. 2019a). Curcumin treatment (3 g/day in 6 capsules, each capsule contains 250 mg of curcumin) to prediabetic patients for 9 months significantly decreased the levels of FBG, serum HbA1c, HOMA-IR, and C-peptide and increased serum adiponectin level, and pancreatic β-cell function, and oral glucose tolerance in diabetic patients compared with the placebo group. Therefore, curcumin supplementation in diet has beneficial effect in diabetic patients (Cheungsamarn et al. 2012).

5.2.4 Lignans

Secoisolariciresinol diglucoside (SDG) **402**, a major lignan constituent of dietary flax seed or linseed (*Linum usitatissimum* L.), has various health-benefit effects in prevention of cancer, obesity, diabetes, and cardiovascular diseases. In HFD-fed obese mice, SDG treatment in diet (0.5 or 1.0% of diet) for 4 weeks significantly decreased visceral and liver fat mass, hyperlipidemia, hyperglycemia, and hyperinsulinemia by reducing serum glucose, TG, TC, leptin, insulin levels, and hepatic TG content. SDG also increased adiponectin secretion in adipose tissue, increased the expression levels of FA β-oxidation-related genes PPARα and CPT-1 in skeletal muscle, and decreased the expression levels of lipid synthesis-related genes SREBP-1c and FAS in liver for reduction of visceral and liver fat mass (Fukumitsu et al. 2008). Another study reported that in HFD-fed obese mice, SDG supplementation (1 g/kg/day) for 15 weeks improved hyperglycemia by decreasing FBG and serum insulin, FFAs, and TC levels, and improving oral glucose tolerance in obese mice. SDG increased glucose uptake and GLUT4 expression, increased Akt phosphorylation in skeletal muscle, and increased pancreatic insulin secretion for glycemic control in obese mice. These findings suggest that SDG improves hyperglycemia in obese mice through enhanced insulin signaling, insulin secretion, and GLUT4 expression (Wang et al. 2015a). In 3T3-L1 adipocytes, SDG inhibited adipocyte differentiation by suppressing intracellular lipid accumulation and the expression levels of adipogenic-related genes PPARγ, C/EBPα, FABP2, adiponectin, and resistin, and increasing the phosphorylation levels of AMPKα

and its upstream activator liver kinase B1 (LKB1). In HFD-fed DIO mice, SDG decreased body weight, adipose tissue mass, and adipocyte size and decreased the expression levels of adipogenic genes including PPARγ, C/EBPα, and their target genes for suppression of lipid synthesis in adipose tissue. These findings demonstrate that SDG improves obesity by suppression of lipid synthesis via AMPK signaling pathway (Kang et al. 2018a). In STZ-induced diabetic rats, SDG treatment (5 or 10 mg/kg bw/day) for 14 days improved hyperglycemia by reduction of serum glucose and lipid profile, increased serum insulin and C-peptide levels, and increased activity of antioxidant enzymes CAT, SOD, and GSH in plasma and pancreatic tissues. Moreover, SDG increased regeneration of β-cells in pancreas. These findings indicate that SDG improves hyperglycemia through enhanced pancreatic β-cells function by suppression of oxidative stress (Moree et al. 2013). SDG intake (100 mg/day) by moderately hypercholesterolemic subjects for a period of 12 weeks improves blood cholesterol and liver functions by decreasing the levels of serum TC, LDL-C, and liver toxic marker enzymes GPT and GGT (gamma-glutamyl transferase) (Fukumitsu et al. 2010).

Sesamin **403**, a lignan constituent of sesame seeds (*Sesamum indicum*), has potential health-benefit effects in obesity and diabetes. In high AGEs exposed pancreatic β-cell damage in mice, sesamin treatment (160 mg/kg bw/day) for 4 weeks improved β-cell function and apoptosis through reduction of oxidative stress and increased antioxidant activity (SOD and α-tocopherol activity). In AGEs-exposed MIN6 cells, sesamin reduced the formation of ROS production, the levels of NADPH oxidase, p22phox, and p67phox, and the expression of pro-apoptotic proteins caspase 3 and PARP (Kong et al. 2015). In HFD-fed NAFLD rats, sesamin treatment (80 or 160 mg/kg bw/day) for 5 weeks reduced hepatic steatosis by reduction of liver fat mass, TG, and TC levels and reduction of serum TC, TG, LDL-C, and FFAs levels and serum and hepatic tissue inflammation (IL-6 and TNF-α) levels. Moreover, sesamin decreased the expression levels of hepatic LXRα and its downstream target genes SREBP-1c and FAS, increased the expression levels of FA oxidation-related genes PPARα and ACOX1, and the activity of hepatic antioxidant enzymes SOD and GP_X, and reduced the expression of oxidative-stress related protein CYP2E1 in the liver. Therefore, sesamin improves hepatic steatosis by regulation of lipid metabolism and oxidative stress in obese rats (Zhang et al. 2016c). In spontaneously hypertensive rats (SHRs), sesamin treatment (80 or 160 mg/kg bw/day) for 12 weeks reduced LV hypertrophy, systolic blood pressue, LV mass index, and collagen deposition in cardiomyocytes by suppression of TGF-β1 expression and Smad3 phosphorylation and increased Smad 7 expression. Moreover, sesamin increased TAC level and the activity of SOD, and reduced the expression of p47phox and MDA in cardiac tissues. In rat cardiac myoblasts, sesamin reduced the expression of Ang II and p-Smad 3. Therefore, sesamin attenuates myocardial fibrosis by suppression of TGF-β1/Smad 3 signaling and upregulation of cardioprotective Smad 7 expression (Zhao et al. 2015). In HFD-fed hyperlipidemic rats, sesamin supplementation (80 or 160 mg/kg/day) for 7 weeks reduced hyperlipidemia and improved renal function by reduction of serum TC, TG, LDL-C, ox-LDL, apoB, creatinine, and BUN levels and reduction of

urinary albumin level, and increased the levels of serum HDL-C and apo A. Moreover, sesamin decreased mesangial cell proliferation, glomerular mesangial matrix index, and interstitial fibrosis in renal tubules by suppression of the expression of α-SMA and collagen-IV in kidney tissues. In addition, sesamin increased the SOD activity and reduced MDA level in renal tissues. These findings suggest that sesamin ameliorates hyperlipidemia and renal injury through suppression of oxidative stress and reduction of serum lipid profile (Zhang et al. 2016d).

Honokiol (HON) **404**, a neolignan, presents as a main constituent in different parts of *Magnolia officinalis*, a medicinal plant in Traditional Chinese and Japanese medicines for treatment of gastrointestinal disorders, thrombotic stroke, obesity, and other inflammatory disorders. In type 2 diabetic db/db mice, HON supplementation in diet (0.02% of diet) for 5 weeks significantly decreased adipose tissue mass and hepatic fat mass and TG content, levels of serum glucose, insulin, HbA1c, HOMA-IR, and leptin, and expression levels of inflammatory cytokines TNF-α and IL-6 in adipose tissue and liver. Moreover, HON decreased the expression of hepatic lipogenic genes FAS and ME (malic enzyme) and the expression of gluconeogenic enzymes PEPCK and G6Pase in liver. These findings suggest that HON ameliorates hepatic steatosis by improvement of both hepatic and systemic insulin resistance in diabetic db/db mice (Kim and Jung 2019). In vitro, HON inhibited the activity of PTP1B enzyme with an IC_{50} value of 63.43 μM in a competitive manner with inhibition constant Ki of 6.67 μM. In C2C12 myotubes, HON increased glucose uptake and GLUT4 translocation to the plasma membrane and increased insulin-stimulated IRβ and Akt phosphorylation. In STZ-induced type 2 diabetic mice, HON on oral treatment (200 mg/kg bw/day) for 8 weeks significantly decreased serum FG levels and increased phosphorylation levels of IRβ and Akt in the adipose tissue, skeletal muscle, and liver. These findings suggest that HON exerts hypoglycemic effect through improvement of insulin sensitivity and insulin signaling in diabetic mice (Sun et al. 2015). In HFD-fed obese male and female mice, HON supplementation in diet (400 or 800 mg/kg/day) for 8 weeks significantly reduced body weight gain, adipose tissue weight, adipocyte size, insulin resistance, serum FG, HOMA-IR, lipid profile, and inflammatory cytokines TNF-α, IL-6, IL-1β, IFN-γ, and LBP levels. Moreover, HON increased the abundances of gut *Akkermansia,* SCFAs producing *Bacteroides*, *Bilophila,* unclassified *Enterobacteriaceae*, and *Fusobacterium*, and decreased the abundance of obesity-related *Oscillospira* in the gut. In addition, HON reduced the abundance of gut *Clostridiales* in male mice and *Muribaculaceae* in female mice. These findings demonstrate that HON ameliorates insulin resistance in obese mice, partly by modulation of gut microbiota composition and suppression of LPS-induced inflammation (Ding et al. 2019).

5.2.5 Coumarins

Naturally occurring coumarins are chemically known as 1,2-benzopyrones and are found in many dietary fruits and medicinal plants. Some of these coumarins have

potential activities against obesity and diabetes. The most common natural coumarins are umbelliferone, scopoletin, esculetin, esculin, and osthole.

Umbelliferone (UMB) (7-hydroxycoumarin) **132** is found in many plants including the fruits of golden apple (*Aegle marmelos*) and bitter orange (*Citrus aurantium*) and in different parts of *Angelica decursiva*, asafoetida (*Ferula assafoetida*), coriander (*Coriandrum sativum*), *Edgeworthia chrysantha*, and *Justicia pectoralis* (Mazimba 2017). In STZ-induced diabetic rats, UMB treatment (30 mg/kg bw/day, *i.p.*) for 45 days improved hyperglycemia by reducing serum glucose and HbA1c levels, and increasing hepatic glycogen content. Moreover, UMB decreased hepatic glucose production by suppressing the activity of gluconeogenic enzymes G6Pase and FBPase and increased hepatic glycolysis by increasing the activity of GCK and G6PDH (Ramesh and Pugalendi 2006). In another study, in HFD/STZ-induced type 2 diabetic rats, UMB treatment for 8 weeks improved hyperglycemia by reduction of serum glucose and lipid levels, hepatic lipid droplets, and TG content and increased serum adiponectin and insulin levels and liver glycogen content, and upregulation of GLUT4, PPARγ, and PPARα expression in adipose tissue and the expression levels of FA oxidation related genes PPARα and its target genes in the liver. Moreover, UMB stimulated insulin secretion from pancreatic β-cells. These findings suggest that UMB promotes lipid and glucose metabolism via stimulation of insulin secretion and insulin action in metabolic tissues for glycemic control in diabetic rats (Naowaboot et al. 2015). In HFD-fed obese mice, UMB supplementation (0.02% of diet) for 12 weeks significantly decreased WAT mass and adipocyte size, hepatic fat content, and serum levels of glucose, TG, and FFAs by upregulation of FA oxidation and the activity of antioxidant enzymes SOD and GP_X in the liver and down-regulation of the activity of hepatic CYP2E1 enzyme, a marker of oxidative stress, inflammation, fibrosis, and lipid peroxidation. Moreover, UMB increased the secretion of adiponectin from adipose tissue. These findings suggest that UMB prevents hepatic steatosis by suppression of hepatic oxidative stress through adiponectin-dependent insulin sensitivity in the liver (Sim et al. 2014). In STZ-induced diabetic nephropathy (DN) in rats, UMB treatment (40 mg/kg/day) for 4 weeks improved renal injury by decreasing the levels of serum glucose, TG, TC, creatinine, BUN, and urinary protein excretion in DN rats. Moreover, UMB reduced the expression levels of inflammatory markers TLR2, TLR4, MyD88, and p-NF-κB and their downstream cytokines TNF-α, IL-6, and IL-1β in renal tissues. In addition, UMB increased the expression levels of epithelial to mesenchymal transition (EMT)-related proteins, podocin and CD2AP, in renal cortex tissues for restoration of podocytes normal function. CD2-associated protein (CD2AP) regulates glomerular filtration rate and decreases the excretion of proteins in urine. Both podocin and CD2AP proteins work together for maintenance of size-selective filtration barrier in glomerular filtration membrane to decrease the passage of relatively large protein molecules. These findings demonstrate that UMB mitigates hyperglycemia-induced inflammation and renal dysfunction in kidney by suppression of TLR/NF-κB signaling pathway (Wang et al. 2019b). Moreover, UMB decreased the expression levels of renal fibrosis-related proteins TGF-β1 and fibronectin in DN kidney (Naowaboot et al. 2020).

Scopoletin (7-hydroxy-6-methoxycoumarin) (SCL) **405** is found in many dietary fruits and plants, such as nani (*Morinda citrifolia*), *Scopolia japonica*, *Scopolia carniolica*, *Artemisia scoparia*, *Artemisia capillaris*, and *Polygala sabulosa*. SCL has been shown to possess antidiabetic and anti-obesity effects. In high-glucose induced insulin-resistant HepG2 cells, SCL increased the expression of PPARγ2 and phosphorylation of Akt. Co-treatment of LY294002, a PI3K inhibitor, blocked the activity of SCL in PPARγ2 expression and Akt phosphorylation. These findings suggest that SCL improves insulin resistance, at least in part, by upregulating PPARγ2 expression (Zhang et al. 2010a). In high-methylglyoxal (MG)-exposed mouse FL83B hepatocytes in presence of insulin, SCL increased the phosphorylation of Akt and the expression levels of PPARγ and GLUT2 proteins and decreased the expression of PTP1B enzyme, a negative regulator of insulin signaling. Several studies demonstrate that MG is found in high concentrations in the cerebrospinal fluid of diabetic individuals, and its accumulation in high levels in hepatic tissues results in the development of insulin resistance in the liver. In high-MG treated (300 mg/kg bw) diabetic rats, SCL administration (10 mg/kg bw/day, orally) for 12 weeks improved insulin resistance and decreased the levels of serum FG, TC, TG, LDL-C, and FFAs, and increased the levels of serum C-peptide, HDL-C, and D-lactic acid. Moreover, SCL increased the hepatic phosphorylated Nrf2 levels and decreased hepatic AGEs accumulation in diabetic rats. These antiglycation and insulin sensitivity effects of SCL were very similar to that of anti-glycation agent aminoguanidine treatment (30 mg/kg bw/day) in MG treated diabetic rats. These findings suggest that SCL improves insulin resistance and controls glycemia in MG-exposed diabetic rats through insulin-stimulated Akt activation and GLUT2 expression, and Nrf2-dependent MG degradation into D-lactic acid (Chang et al. 2015). In HFD/STZ-induced type 1 diabetic mice, SCL supplementation in diet (0.01% of diet) for 11 weeks significantly reduced hepatic lipid accumulation and levels of serum glucose, HbA1c, ALT, TNF-α, and IL-6 compared with diabetic control group. Moreover, SCL down-regulated the expression levels of hepatic TG and cholesterol biosynthesis-related genes PPARγ, DGAT2, FAS, and HMGCR and inflammation-related factors TLR-4, MyD88, NF-κB1, TNF-α, and IL-6, and upregulated the expression of hepatic CYP7α1 enzyme in diabetic mice. Accumulating evidence demonstrates that myeloid differentiation factor 88 (MyD88) on activation by TLR4 induces the expression of pro-inflammatory cytokines via induction of NF-κB activity in human hepatocytes. Hepatic cholesterol-7-alpha-hydroxylase-1 (CYP7α1) on over-expression in liver promotes bile acid pool size, that is, an increased biliary cholesterol and bile acid secretion, and leads to reduce blood and liver cholesterol levels. These findings suggest that SCL ameliorates hepatic steatosis and inflammation through suppression of lipid biosynthesis and TLR4/MyD88 signaling pathway (Choi et al. 2017). In 3T3-L1 adipocytes, SCL increased glucose uptake by upregulation of GLUT4 expression into plasma membrane and increased the phosphorylation of Akt, PI3K, and AMPK. Pre-treatment of each of wortmannin, a PI3K inhibitor, and compound C, an AMPK inhibitor, inhibited the activity of SCL in GLUT4 expression for glucose uptake.

These findings suggest that SCL stimulates GLUT4 expression via activation of PI3K and AMPK (Jang et al. 2020).

Esculetin (6,7-dihydroxycoumarin) **133** is isolated from many plants, including *Fraxinus chinensis*, *Euphorbia lathyris*, *Artemisia capillaris*, and *Citrus limonia*, and is the main constituent of *Cortex Fraxini*. It has potential benefit in prevention of various diseases including obesity, diabetes, cancers, and macro- and micro-vascular and neurological disorders. In HFD-fed obese mice, esculetin supplementation in diet (0.02% of diet) for 12 weeks decreased body weight gain, visceral fat mass, serum glucose and lipid profile, and increased plasma adiponectin level, compared to control group. Esculetin increased hepatic insulin sensitivity by increasing the levels of Adipo R2 protein and mRNA, phosphorylated AMPK, and upregulated the expression of FA oxidation-related genes PGC-1α, PPARα, CPT, and ACSII, and down-regulated the expression of lipogenesis-related genes SREBP-1c and FAS. In addition, esculetin increased hepatic glucose uptake and utilization by increasing the expression of GLUT2 and GCK, and decreased hepatic glucose production by suppressing the activity of G6Pase enzyme. Accumulating evidence demonstrates that adiponectin on binding to its receptor Adipo R2 increases the expression of LKB1, which in turn, stimulates the activation of AMPK and IRS2 expression for insulin signaling in the liver. These results suggest that esculetin reduces hepatosteatosis and insulin resistance, partly through AMPK activation (Sim et al. 2015; Combs and Marliss 2014). Esculetin was effective in protection of hepatic and renal tissues from hyperglycemia-induced oxidative stress in diabetic animals. In STZ-induced diabetic rats, esculetin on oral supplementation (40 mg/kg/day) for 45 days reduced serum glucose and TBARS levels and increased the activity of hepatic and kidney antioxidant enzymes SOD, CAT, GP_X, GST, and GSH and non-enzymatic antioxidants vitamin C and E, as well as reduced the necrosis in hepatic and renal tissues. These findings suggest that esculetin protects diabetic liver and kidney through improvement of antioxidant status (Prabakaran and Ashokkumar 2013). Several studies demonstrate that chronic hyperglycemia and hypertension in type 2 diabetic patients and animals stimulate the activation of RAS for induction of oxidative stress, inflammation, endothelial dysfunction, left ventricular stiffness, cardiomyocyte hypertrophy, cardiac fibrosis, and development of diabetic cardiomyopathy. Therefore, blockade of renin-angiotensin system (RAS) activity is a promising therapeutic target for reduction of cardiovascular risk in diabetic patients. A carboxypeptidase, angiotensin-converting enzyme 2(ACE2), inhibits the activity of RAS by degradation of angiotensin II (Ang II). Therefore, upregulation of ACE2 activity in diabetic heart improves cardiac dysfunction. A nuclear protein Ki-67 promotes cell proliferation in tumor growth in cancer and is found in high concentrations in diabetic heart. In diabetic heart, oxidative stress-induced Keap1 (kelch-like ECH-associated protein 1) is expressed in high levels. The over-expression of Keap1 reduces the expression of Nrf2 by Keap1-dependent ubiquitination of Nrf2. Therefore, suppression of Ki-67 and Keap1 in diabetic heart improves diabetic cardiomyopathy (Schmieder et al. 2007; Tikellis and Thomas 2012). In STZ-induced diabetic cardiomyopathy (DCM) in rats, esculetin supplementation (100 mg/kg bw/day) for 6 weeks improved cardiac function,

cardiomyocyte hypertrophy, and cardiac fibrosis through improvement of insulin resistance and oxidative stress and suppression of RAS activity in diabetic heart. Esculetin increased the expression of ACE2, reduced the expression of Keap1 and Ki-67, and decreased the elevated level of histone H2AK119Ub (ubiquitination) for suppression of Ang II-dependent NF-κB activation and cardiac inflammation, fibrosis, and cardiomyocyte apoptosis in heart tissues. An increased expression of H2AK119 and H2BK120 ubiquitination stimulates the expression of inflammatory protein TGF-β1 for induction of its target genes for cardiomyocyte hypertrophy and fibrosis. The reduced expression of H2AK119Ub and H2BK119Ub possibly decreases the expression of histone acetylation of H3K9ac and H3K27ac, phosphorylation of H3S10p and H3S28p, and methylation of H3Kme2, H3K79me2, and H3K36me2, which were elevated in insulin-resistant diabetic heart. In high-glucose exposed rat glomerular mesangial cells, an increased expression of histone H2AK119Ub was found. Moreover, an elevated expression of histone H2B ubiquitination promotes histone methylations (histone H3K4me2, H3K4me3, H3K79me2, and H3K79me3); the resultant methylated histones promote AGEs formation and cardiomyocyte hypertrophy. These findings suggest that esculetin improves DCM through suppression of RAS activity and histone ubiquitination expression (Kadakol et al. 2015; Gao et al. 2013). In another study, in STZ/HFD-fed type 2 diabetic nephropathy (DN) in rats, esculetin supplementation improved renal function by suppression of the expression of inflammation and fibrosis-related factors TGF-β1, MCP-1, fibronectin, histone acetylation, and histone H2AK119 monoubiquitination in renal tissues (Kadakol et al. 2017; Fontecha-Barriuso et al. 2018). In STZ/HFD-induced hepatic steatosis in mice, esculetin on supplementation in diet (100 mg/kg) for 11 weeks reduced liver hypertrophy and lipid accumulation through suppression of hepatic inflammation and regulation of lipid and glucose metabolism in obese mice. Esculetin decreased the levels of serum glucose, lipid profile, and inflammatory cytokines TNF-α , IL-6, and chemokine MCP-1, and increased the activity of serum antioxidant enzyme SOD, compared to diabetic control group. Moreover, esculetin down-regulated the expression of lipid synthesis-related genes FAS, DGAT2, PLPP2, and PAP, the expression of gluconeogenic gene G6Pase, and the expression levels of inflammatory factors TLR4, MyD88, NF-κB, TNF-α, and IL-6 in the liver of diabetic mice (Choi et al. 2016).

Esculin (esculetin-6-*O*-glucoside) **406**, present in many medicinal plants, such as horse chestnut (*Aesculus hippocastanum*), California buckeye (*Aesculus californica*), prickly box (*Bursaria spinosa*), and *Fraxinus rhynchophylla*, has health-benefit effects in various disorders including diabetes and diabetic complications. In STZ-induced diabetic rats, esculin supplementation (30 or 90 mg/kg/day) for 10 weeks significantly reduced hyperglycemia, dyslipidemia, inflammatory response in renal tissues, and renal injury by reduction of the elevated levels of serum glucose, lipid profile (TC, TG, LDL-C), and the levels of inflammatory markers cytokines and proteins IL-6, IL-1β, ICAM-1, NO, AGEs, and NGAL in both serum and renal tissues of diabetic rats. These effects of esculin were similar to that of aminoguanidine-treated diabetic rats. Neutrophil gelatinase-associated

lipocalin (NGAL) protein, a stress-related protein secreted by renal tubular epithelial cells, is expressed in high concentrations in plasma of aged diabetic patients having chronic kidney disease (CKD), and is related to impaired glomerular filtration rate, and considered as a biomarker of kidney injury and kidney function. Therefore, esculin protects the kidney injury through suppression of AGEs accumulation and inflammatory cytokines expression (Wang et al. 2015b; Guo et al. 2020b). Another study reported that in STZ-diabetic mice, esculin treatment (20 mg/kg/day) for 2 weeks improved renal injury by reduction of caspase-3 activation in kidney tissues, and serum glucose and creatinine levels, and enhanced insulin sensitivity in the liver and skeletal muscle. Moreover, esculin decreased hepatic glucose production by suppression of G6Pase activity in the liver. Possibly, esculin exhibits this renoprotective effect via its metabolite esculetin, as only esculetin was detected in blood of diabetic mice after 30 min of esculin administration (Kang et al. 2014).

Osthole (7-methoxy-8-prenylcoumarin) **407** is a major coumarin constituent of the fruits of *Cnidium monnieri* and *Angelica pubescens* and in other plants. It has been found health-promoting effects in prevention of obesity, diabetes, and cancers due to its potential antioxidant and anti-inflammatory properties. In both HFD and alcohol-fed fatty liver in rats and quails, osthole supplementation (10 or 20 mg/kg bw/day) for 6 weeks reduced hepatic fat accumulation, TG and TC content, and the levels of serum lipid profile (TC, FFAs, and LDL-C) and MDA, and increased serum HDL-C level, and the activity of hepatic antioxidant enzymes (SOD and GP_X). These findings suggest that osthole prevents hepatosteatosis by suppression of hepatic oxidative stress via improvement of antioxidant status (Song et al. 2006). In high oleic acid and H_2O_2-induced insulin-resistant mouse hepatic FL83B cells, osthole suppressed intracellular lipid accumulation, and decreased the expression levels of adipogenic genes PPARγ, C/EBPβ, C/EBPα, and SREBP-1c, and increased the expression levels of glycerol release and lipolysis-related genes ATGL and HSL, and the phosphorylation level of AMPK. Moreover, osthole reduced the oxidative stress promoted by H_2O_2 by reduction of MDA level and inhibition of the activity of NF-κB and p38MAPK kinases. Therefore, osthole decreases intracellular lipid accumulation by regulation of lipid metabolism and inflammatory response through AMPK activation (Huang et al. 2017b). In high glucose exposed insulin-resistant mouse skeletal myoblast C2C12 and L6 cells, osthole increased glucose uptake and GLUT4 translocation in plasma membrane and increased the phosphorylation of AMPK and ACC, and the AMP to ATP ratio. Moreover, osthole increased the phosphorylation levels of AMPK and ACC in human hepatocytes HepG2 cells to a lesser extent. Co-treatment of compound C, an inhibitor of AMPK, reversed the effect of osthole in glucose uptake and GLUT4 expression in Hep G2 cells. In STZ-diabetic mice, osthole significantly reduced hyperglycemia, and increased glucose uptake, GLUT4 expression, and AMPK activation in skeletal muscle. These findings demonstrate that osthole improves hyperglycemia, at least in part, by increasing GLUT4 expression via insulin-independent AMPK activation (Lee et al. 2011).

Fraxetin (7,8-dihydroxy-6-methoxycoumarin) **408**, present in plants, *Fraxinus rhynchophylla* and *Cortex Fraxini*, showed antidiabetic effect in animal model. In

STZ-induced diabetic rats, fraxetin on oral treatment (40 or 80 mg/kg bw/day) for 30 days reduced serum glucose and HbA1c levels and increased serum insulin level and hepatic glycogen content and body weight by regulation of key genes of carbohydrate metabolism. Fraxetin increased the activity of hepatic glycolysis-related genes GCK and G6PDH, and decreased the activity of hepatic gluconeogenic enzymes G6Pase and FBPase for suppression of glucose production. Therefore, fraxetin may be useful in treatment of diabetes (Murali et al. 2013).

5.2.6 Quinones

Emodin (1,6,8-trihydroxy-3-methylanthraquinone) **123** is a major anthraquinone derivative of hepatoprotective and anti-inflammatory plant, *Rheum palmatum*, and has been shown to possess potential anti-obesity and antidiabetic effects. In HFD-fed obese mice, emodin on oral treatment (100 mg/kg/day) for 35 days reduced visceral adiposity, serum FG levels, and activity of 11β-HSD1 enzyme in the liver and mesenteric adipose tissue and the activity of hepatic gluconeogenic enzymes PEPCK and G6Pase in the liver. In vitro, emodin strongly inhibited the activity of mouse and human 11β-HSD1 enzyme with IC_{50} value of 86 and 186 nM/l, respectively. These findings indicate that emodin exerts anti-obesity effect partly by suppression of the activity of 11β-HSD1 enzyme (Feng et al. 2010). In L6 myotubes, emodin increased glucose uptake and GLUT4 translocation and increased the phosphorylation of AMPK. Moreover, emodin increased cellular ROS and Ca^{2+} influx levels and CaMKK activity by suppression of NADH oxidation. Pre-treatment of LY-294002, a PI3K inhibitor, or SB20358, a p-38MAPK inhibitor, did not alter the glucose uptake activity of emodin. Pre-treatment of STO-609, a CaMKK inhibitor, decreased the activity of emodin in AMPK phosphorylation in L6 myotubes. In hepatocytes Hepa1c1c7 cells, emodin decreased the glucose production in hepatocytes by suppression of the activity of PEPCK and G6Pase, and increased the phosphorylation of AMPK. In HFD-fed diabetic mice, emodin treatment (3 mg/kg, *i.v.*) for 8 days decreased serum FG levels and increased glucose uptake and the phosphorylation levels of AMPK and ACC in skeletal muscle and liver, and decreased hepatic glucose production by suppression of the activity of PEPCK and G6Pase. Therefore, emodin improves glucose uptake in skeletal muscle and liver and reduces hepatic glucose production through AMPK activation (Song et al. 2013). In HFD-fed obese mice, emodin on oral treatment (80 mg/kg/day) for 6 weeks decreased body weight gain, size of white and brown adipocytes, hepatic lipid mass, TC and TG content, and the levels of serum glucose, insulin, and lipid profile. Emodin significantly decreased the expression levels of TG synthesis-related genes SREBP-1c, FAS, SCD-1, ACC1, GAPT, FADS1, and FADS2 and the expression of cholesterol synthesis-related genes SREBP2, HMGCR, and LSS, and increased the expression of lipolysis and cholesterol uptake related genes HL, SRB1 (Scavenger receptor class B type 1), and apoB in the liver. In addition, emodin increased the expression of energy expenditure-related genes UCP-1 and UCP-2, and adiponectin secretion, and decreased the expression of FAS and SCD-1 in WAT of obese mice. Accumulating evidence demonstrates that AMPK activation inhibits the expression

of SREBP-1 and SREBP2 by increasing their phosphorylation levels. These findings suggest that emodin improves lipid metabolism for suppression of hepatic steatosis through inhibition of SREBP pathway possibly via AMPK activation (Li et al. 2016a). In STZ-induced type 2 diabetic cardiomyopathy (DCM) in rats, emodin on oral treatment (50 or 100 mg/kg bw/day) for 16 weeks improved DCM by reduction of left atrial and left ventricular (LV) hypertrophy and improved cardiac systolic function through increased LV fractional shortening time, LV ejection volume fraction, and increased Akt phosphorylation, and reduced the activity of GSK-3β in cardiac tissues. These findings suggest that emodin improves DCM through activation of Akt/GSK-3β signaling pathway in diabetic rats (Wu et al. 2014c).

Rhein (4,5-dihydroxyanthraquinone-2-carboxylic acid) **126** is another major bioactive chemical constituent of *Rheum palmatum*, which is frequently used in weight reducing formulation of traditional Chinese medicine. Rhein has potential anti-obesity and antidiabetic effects. In diet-induced obese (DIO) mice, rhein on oral treatment (100 mg/kg/day) for 8 weeks decreased body fat mass, size of white and brown adipocytes, and the levels of serum FG, TC, and LDL-C. Moreover, rhein significantly suppressed the expression of adipogenesis-related genes PPARγ, aP2, CD36, and LPL in WAT, and the expression of lipid synthesis-related genes FAS, ACC, and CD36 in the liver of obese mice. In addition, rhein increased the expression levels of thermogenic genes UCP-1, UCP-3, and DIO2 in BAT of obese mice. In HEK293T cells, rhein suppressed PPARγ transactivity in presence of rosiglitazone, a PPARγ agonist. It indicates that rhein is a PPARγ antagonist. Thus, rhein ameliorates obesity through suppression of the activity of PPARγ and its target genes (Zhang et al. 2012). In high glucose exposed mouse pancreatic NIT-1-cells, rhein suppressed the expression of β-cell mitochondrial fission-related protein, dynamin-related protein-1(DRP-1), and protected the β-cells from apoptosis. In diabetic db/db mice, rhein treatment (120 mg/kg/day) for 8 weeks reduced serum FG, improved glucose tolerance, and protected pancreatic β-cells from apoptosis by suppression of DRP-1 expression in pancreas (Liu et al. 2013a). In high glucose exposed human kidney-2 (HK-2) cells, rhein reduced the expression levels of epithelial mesenchymal transition (EMT)-related proteins integrin-linked kinase (ILK) and MMP-9, and this effect of rhein was similar to that of ILK-siRNA in HK-2 cells. Mounting evidence demonstrates that TGF-β1-induced EMT in renal tubular epithelial cells promotes accumulation of extracellular matrix (ECM) proteins through overexpression of profibrotic proteins, including fibronectin, collagens, α-SMA, and matrix metalloproteinase-9 (MMP-9) in a Smad signaling pathway and leads to impairment of renal function in diabetic nephropathy. Therefore, rhein has renoprotective effect in diabetic kidney tissues (Peng et al. 2012). In high glucose exposed renal mesangial MCGT1 cells, rhein decreased the activity of glutamine:fructose 6 phosphate aminotransferase (GFAT) and the expression levels of TGF-β1 and p21 proteins, markers of renal injury via renal fibrosis. Several studies demonstrate that TGF-β1 stimulates the generation of Smad complex for upregulation of p21 protein, which plays a significant role in cell cycle growth arrest at G0/G1 phase of renal mesangial cells and leads to cell apoptosis. Therefore, rhein

inhibits the activity of GFAT in hexosamine pathway for protection of diabetic renal tissues from injury (Zheng et al. 2008).

Shikonin **229**, a naphthoquinone derivative, was isolated from koshikon, the roots of *Lithospermum erythrorhizon*. The roots of *L. erythrorhizon* has been used in traditional medicine for treatment of external injuries, cancer, and other inflammatory disorders. In HFD-fed obese mice, shikonin supplementation in diet (0.1% of diet) for 12 or 24 weeks reduced adipose tissue mass, adipocyte size, hepatic lipid mass, and TG content and the levels of serum FG, insulin, and lipid profile. Shikonin decreased the expression levels of hepatic lipogenic genes SREBP-1c and SCD1, and increased the expression levels of lipolysis-related genes ATGL and HSL, and FA oxidation-related gene CPT-1α. In addition, shikonin decreased the expression of hepatic gluconeogenic genes PEPCK and G6Pase, and increased the tyrosine phosphorylation of IR and IRS-1, and phosphorylation of Akt and ERK1/2. These findings suggest that shikonin prevents diet-induced adiposity and hepatic dyslipidemia through enhanced insulin sensitivity, insulin signaling, and regulation of lipid metabolism (Bettaieb et al. 2015). Another study reported that in HFD-fed obese mice, shikonin on supplementation in diet (0.2% of diet) for 8 weeks reduced fat mass in adipose tissue, hepatic lipid content, and serum lipid profile and leptin levels by down-regulation of the expression of lipogenesis-related genes C/EBPα, PPARγ, and CD36 in WAT, and of SREBP-1c, FAS, and SCD1 in the liver, and upregulation of the expression of β-oxidation-related genes PPARα, PGC-1α, and ACOX1 in the liver and skeletal muscle (Gwon et al. 2015). In L6 myotubes, shikonin increased glucose uptake and GLUT4 expression without increasing Akt phosphorylation. In non-obese diabetic Goto-Kakizaki rats, shikonin treatment (10 mg/kg/day, *i.p.*) for 4 days reduced plasma glucose levels and increased insulin sensitivity in rats (Oberg et al. 2011). In Hepa 1–6 cells, shikonin increased phosphorylation of AMPK and ACC. Co-treatment of compound C, an inhibitor of AMPK, prevented the activity of shikonin in AMPK phosphorylation. Moreover, in high oleic acid exposed Hepa 1–6 cells, shikonin decreased intracellular lipid accumulation and reduced the expression of lipogenic gene SREBP-1 and increased the expression of FA oxidation-related genes PPARα, CPT-1, and PGC-1α. In HFD-fed obese mice, shikonin treatment (30 mg/kg/day) for 4 weeks decreased body weight gain, WAT mass, adipocyte size, and hepatic fat mass through upregulation of FA oxidation and energy expenditure-related genes PPARα, CPT-1, PGC-1α, and UCP-2 , and increased phosphorylation of AMPK in the liver and skeletal muscle. Therefore, shikonin prevents hepatic steatosis by regulation of lipid catabolism and energy expenditure through AMPK pathway (Gwon et al. 2020).

Acetylshikonin **230**, another major naphthoquinone derivative isolated from Zicao root (*Lithospermum erythrorhizon*), has been shown to have anti-obesity effect. In HFD-fed genetically obese db/db mice, acetylshikonin on supplementation in diet (540 mg/kg/day) for 8 weeks decreased adiposity and hepatic steatosis by reduction of body weight gain, abdominal fat mass, adipocyte size, hepatic lipid content, food intake, serum levels of glucose, TG, FFAs, hepatic toxic marker enzymes choline esterase, AST, ALT, and pro-inflammatory cytokines TNF-α,

IL-6, and IL-1β. Moreover, acetylshikonin increased the expression levels of lipolysis-related genes ATGL, perilipin, and HSL in adipose tissue, and decreased the expression levels of lipid synthesis-related genes SREBP-1, FAS, and HMGCR in the liver of obese mice for maintenance of lipid homeostasis. These findings suggest that acetylshikonin improves obesity and its associated hepatic steatosis through regulation of lipid metabolism (Su et al. 2016b). In 3T3-L1 preadipocytes, acetylshikonin inhibited adipocyte differentiation by decreasing intracellular lipid accumulation via suppression of the expression levels of adipogenic factors PPARγ and C/EBPα (Su et al. 2016c). In L6 myotubes, acetylshikonin increased glucose uptake and translocation of GLUT4 into plasma membrane and increased the activation of PKCδ cascade, independent of insulin, AMPK, and ROS pathway. Pretreatment of rottlerin, a PKCδ inhibitor, in L6 myotubes significantly suppressed the glucose uptake activity of acetylshikonin (Huang et al. 2019). Shikonin increased glucose uptake through AMPK activation, while acetylshikonin increased glucose uptake through PKCδ activation in L6 myotubes. Further study is required to clarify this anomaly.

5.2.7 Xanthones

Mangiferin **409**, a xanthone-C-glucoside present in different parts of mango tree (*Mangifera indica*), exhibits several health-benefit effects against cancer, diabetes, obesity, cardiovascular diseases, and neurodisorders. In STZ-diabetic rats, mangiferin on treatment (10 or 20 mg/kg/day, *i.p.*) for 28 days showed significant antidiabetic and hypolipidemic effect by reduction of serum FG, TC, TG, LDL-C, atherogenic index levels, and increased serum HDL-C level. Possibly, mangiferin exhibits antidiabetic effect through improvement of both pancreatic and extrapancreatic functions (Muruganandan et al. 2005). In partial pancreatectomy (PP_X) induced in mice, mangiferin treatment (30 or 90 mg/kg/day) for 14 days improved pancreatic β-cells mass and function and protected the β-cells from apoptosis. Moreover, mangiferin increased the expression levels of cell cycle regulatory proteins cyclin D1, D2, and CDK4 and β-cell regeneration-related protein PDX1 in pancreas of PP_X mice (Wang et al. 2014a, b). In HFD-fed obese mice, mangiferin treatment in diet (0.5% of diet) for 18 weeks mitigated obesity-related hyperglycemia, hyperlipidemia, and insulin resistance. Mangiferin increased mitochondrial biogenesis and oxidative activity by upregulation of the expression levels of oxoglutarate dehydrogenase E1, CPT2, and fumarate hydratase 1(FH1), and down-regulated the expression of lipogenesis-related genes SCD1 and ACAT1 in the liver of obese mice (Lim et al. 2014). In STZ-induced diabetic nephropathy (DN) in rats, mangiferin treatment (30 or 60 mg/kg/day) for 9 weeks significantly improved renal function by decreasing serum BUN, urinary albumin excretion, glomerular extracellular matrix expansion, and glomerular basement membrane thickness and increasing the activity of glyoxalase1 (Glo1) for reduction of AGEs and RAGE accumulation in renal cortex (Liu et al. 2013c). In high oleic acid exposed HepG2 cells, mangiferin significantly decreased intracellular FFAs and

TG accumulation by increasing the expression of CD36 and CPT-1, and decreasing the expression of DGAT2 and ACC through increased phosphorylation of AMPK and ACC. Moreover, mangiferin increased the AMP/ATP ratio in HepG2 cells. In hyperlipidemic rats, mangiferin treatment (200 or 400 mg/kg/day) for 6 weeks decreased plasma and hepatic FFAs levels and hepatic TG accumulation by enhancing FFAs oxidation, lipolysis, and AMPK activation and suppressing lipogenesis in liver. Therefore, mangiferin promotes FFAs catabolism in liver through AMPK activation (Niu et al. 2012).

Norathyriol **410**, a metabolite of mangiferin, and isolated from mangosteen (*Garcinia mangostana*), in L6 myotubes, increased glucose uptake and AMPK activation. Possibly, antidiabetic effect of mangiferin is partly due to its metabolite norathyriol, produced in vivo by intestinal bacteria (Wang et al. 2014a). In vitro, norathyriol inhibited the activity of α-glucosidase in a non-competitive manner with an IC_{50} value of 3.12 μM, compared to mangiferin (IC_{50} of 358.54 μM) and acarbose (IC_{50} of 479.2 μM). Moreover, in alloxan-induced diabetic rats, norathyriol reduced FBG and PPBG levels at 2 hours after starch or glucose loaded diabetic rats (Shi et al. 2017). Norathyriol inhibited the activity of PTP1B in a competitive manner with an IC_{50} value of 9.59 μM. In mouse hepatocytes and myoblasts, norathyriol increased insulin-stimulated phosphorylation of IR and IRS-1 through suppression of PTP1B activity. In HFD-fed obese mice, norathyriol treatment (40 mg/kg/day) for 5 days decreased plasma glucose and lipid profile by down-regulation of lipogenesis-related genes SREBP-1c and HMGCS-1, and gluconeogenic gene G6Pase in liver. Cell permeability and oral bioavailability of norathyriol are better than mangiferin, and hence it could be a potential antidiabetic agent (Ding et al. 2014a). In fat-diet induced fatty liver in diabetic rats, norathyriol treatment decreased hepatic lipid accumulation, hepatic TG, and FFAs content by reducing lipogenesis by down-regulation of SREBP-1c and promoting lipolysis and FA oxidation by upregulation of ATGL and CPT-1 through increased AMPK phosphorylation and activation of SIRT1 and liver kinase B1 (LKB1). Moreover, norathyriol decreased the expression level of SREBP-1c in the liver. These findings suggest that norathyriol improves hepatic steatosis through activation of SIRT1/LKB1/AMPK/SREBP-1c signaling pathway (Li et al. 2018a).

5.2.8 Simple Phenolic Compounds

Ferulic acid (FA) **72** is found in many vegetable sources and present in high concentrations in popcorn and bamboo. FA has potential health-benefit effects against diabetes. IN HF and fructose-diet induced type 2 diabetic male rats, FA treatment (50 mg/kg/day) for 30 days reduced the serum glucose and insulin, and increased glucose tolerance and hepatic glycogen content in diabetic rats. FA increased the activity of glycogenesis-related genes GS and GCK, and reduced the activity of gluconeogenic enzymes PEPCK and G6Pase in the liver. Therefore, FA improves glucose homeostasis through improvement of insulin-dependent hepatic glycogenesis and inhibition of gluconeogenesis (Narasimhan et al. 2015). In

HFD-fed obese mice, FA on oral treatment (25 or 50 mg/kg/day) for 8 weeks reduced adipose tissue mass and adipocyte size, hepatic lipid droplets, TC and TG accumulation, and serum glucose, leptin, and lipid levels in obese mice. FA decreased the expression levels of hepatic lipogenesis-related genes SREBP-1c, FAS, and ACC, and increased the expression levels of FA oxidation-related genes PPARα and CPT-1α for suppression of hepatic lipid mass. Moreover, FA decreased the activity of hepatic gluconeogenic genes PEPCK and G6Pase for suppression of hepatic glucose production. Therefore, FA regulates lipid and glucose metabolism for maintenance of lipid and glucose homeostasis (Naowaboot et al. 2016).

Caffeic acid (3,4-dihydroxycinnamic acid) (CA) **411** is found in many dietary foods including apples, berries, pears, and coffee. It has health-promoting effects in prevention of diabetes and obesity. In diabetic db/db mice, CA on oral treatment (0.02% of diet) for 5 weeks significantly reduced serum glucose and HbA1c levels, and increased serum insulin, leptin, and C-peptide levels and hepatic glycogen content in diabetic mice. Moreover, CA increased glucose uptake and GLUT4 expression in adipose tissue, and increased hepatic GCK activity, and decreased the activity of hepatic gluconeogenic enzymes G6Pase and PEPCK. In addition, CA increased the activity of antioxidant enzymes SOD, CAT, and GP_X in serum and liver and improved pancreatic islet architecture. These results suggest that CA exerts antidiabetic effect through enhancement of adipocyte glucose uptake, pancreatic insulin secretion, and hepatic antioxidant activity and suppression of hepatic glucose production (Jung et al. 2006b). In another study, in HFD-fed obese mice, CA in supplementation in diet (0.02 or 0.08% of diet) for 6 weeks significantly decreased visceral fat mass, plasma, and liver TC and TG levels, plasma FG, FFAs, and GOT and GPT levels in obese mice. Moreover, CA decreased the expression levels of lipogenic genes SREBP-1c, FAS, HMGCR, and ACC, and increased the phosphorylation of AMPK and ACC in liver (Liao et al. 2013). In palmitate-exposed AML12 hepatocytes, CA reduced lipid accumulation, the expression levels of lipogenesis marker genes and ER stress, and increased the activity of autophagy marker genes. In diet-fed obese mice, CA treatment (50 mg/kg/day) for 10 weeks reduced hepatic steatosis by decreasing ER stress and increasing autophagy in liver (Kim et al. 2018a).

Chlorogenic acid (5-*O*-caffeoylquinic acid) (CGA) **21** is found in high concentrations in coffee and in many antidiabetic plants including *Cecropia obtusifolia*, *C. peltata*, and *Cichorium intybus*. In rat skeletal L6 myotubes, CGA stimulated glucose uptake by increasing the expression and translocation of GLUT4 into plasma membrane. CGA increased the expression of CaMKKβ and the phosphorylation of AMPK and Akt in L6 myotubes. Co-treatment of compound C, an inhibitor of AMPK, or transfection of myotubes with AMPKα1/2 siRNA significantly reduced the activity of CGA on glucose uptake and AMPK phosphorylation, while co-treatment of wortmannin, an inhibitor of PI3K, did not change the activity of CGA on glucose uptake. These findings suggest that CGA stimulates glucose uptake in L6 myotubes via insulin-independent AMPK activation and upregulation of the expression of its upstream target CaMKKβ. In diabetic db/db mice, CGA treatment (250 mg/kg, *i.p.*) decreased fasting BG at 10 minutes after the

administration of the drug (Ong et al. 2012). In HFD-fed obese mice, CGA on supplementation in diet (0.02% of diet) for 8 weeks reduced body weight, visceral fat mass, plasma leptin, insulin, TG and TC levels, and hepatic TG content, and increased plasma adiponectin level compared to the control group. Moreover, CGA reduced the expression levels of lipogenesis-related genes FAS, HMGCR, and ACAT for reduction of hepatic fat mass (Cho et al. 2010).

Chicoric acid, also known as cichoric acid (dicaffeoyltartaric acid) **412**, is found in many dietary plants including *Echinacea purpurea* roots, dandelion, basil, iceberg lettuce (*Lactuca sativa*), *Cichorium intybus*, and *Orthosiphon stamineus*, and is present in high concentrations in *Cichorium intybus* (about 64.2% in roots). Chicoric acid has been reported to improve insulin resistance in obesity and diabetes in animal models. In HFD-fed obese mice, chicoric acid on oral administration (15 or 60 mg/kg/day) for 8 weeks decreased body weight gain, adipose tissue fat mass, and serum lipids (TC, TG and LDL-C), leptin, and inflammatory cytokine (TNF-α, IL-6 and COX-2) levels, and increased serum adiponectin level in obese mice. Moreover, chicoric acid decreased the expression of lipogenesis-related genes C/EBPα and PPARγ and their target genes in liver and epididymal adipose tissue, and increased the activity of hepatic antioxidant enzymes SOD, CAT, and GP_X and decreased the levels of MDA, inflammatory cytokines, and p-JNK kinase for suppression of hepatic oxidative stress. Therefore, chicoric acid improves insulin sensitivity for suppression of fat accumulation in liver and adipose tissue (Xiao et al. 2013). In palmitate-induced insulin-resistant C2C12 myotubes, chicoric acid increased glucose uptake and GLUT4 translocation into plasma membrane, and increased the expression of PI3K and phosphorylation levels of Akt and p70S6K. Moreover, chicoric acid increased mitochondrial DNA content, mitochondrial membrane potential, and function in ATP production and oxidative phosphorylation. In HFD-fed obese mice, chicoric acid on supplementation in diet (0.03% of diet) for 6 weeks significantly reduced body weight, and serum levels of FG, TG, TC, NEFAs, insulin, HbA1c, and HOMA-IR, and increased the expression of hepatic and skeletal muscle mitochondrial biogenesis and oxidative phosphorylation-related genes PGC-1α, NRF-1, NRF-2, TFAM, NDUFS8, SDHB, and ATP5α1. In addition, chicoric acid increased insulin-dependent upregulation of the expression of hepatic glycolysis-related genes GCK and PFK, and down-regulated the expression of hepatic gluconeogenic genes G6Pase and PEPCK. Therefore, chicoric acid improves insulin sensitivity in liver for maintenance of glucose and lipid homeostasis through regulation of carbohydrate and lipid metabolism enzymes and mitochondrial thermogenesis function in the liver and skeletal muscle (Kim et al. 2018b). In glucosamine-induced HepG2 cells, chicoric acid increased glycogen synthesis and glucose uptake, and inhibited hepatic glucose production by increasing the phosphorylation of Akt, AMPK, and GSK-3β and the expression of SIRT1. Chicoric acid also activated Nrf-2-Keap1pathway for improvement of hepatic antioxidant response. Therefore, chicoric acid might be useful in prevention of obesity (Zhu et al. 2017).

Rosmarinic acid (α-*O*-caffeoyl-3,4-dihydroxyphenyllactic acid) (RA) **104**, a phenolic compound present in many culinary herbs of Lamiaceae family including

rosemary (*Rosmarinus officinalis*), Spanish sage (*Salvia lavandulifolia*), basil (*Ocimum tenuiflorum*), oregano (*Origanum vulgare*), and *Plectranthus amboinicus*, has health-benefit effects in prevention of obesity and diabetes. IN STZ/HFD-induced type 2 diabetic rats, RA on oral treatment (160 or 200 mg/kg/day) for 28 days reduced body weight, and the elevated levels of serum glucose, insulin, and HOMA-IR in diabetic rats. RA increased glucose uptake in skeletal muscle by upregulation of GLUT4 protein and its translocation into plasma membrane, and reduced hepatic glucose production by suppression of the activity of gluconeogenic enzyme PEPCK for maintenance of glucose homeostasis (Runtuwene et al. 2016). In high palmitate-exposed insulin-resistant C2C12 myotubes, RA increased glucose uptake and GLUT4 translocation into plasma membrane, and promoted FA oxidation through increased SIRT1 expression and PGC-1α activation by its deacetylation, and increased phosphorylation of CaMKK and AMPK. PGC-1α stimulates its downstream target genes LCAD and UCP-3 for energy expenditure. Pre-treatment of STO-609, a CaMKK inhibitor, suppressed the activity of RA in glucose uptake and FA oxidation. Therefore, RA improves glucose uptake and FA oxidation in skeletal muscle through activation of CaMKK/AMPK signaling pathway (Abe et al. 2016). In STZ and diet-induced type 2 diabetic rats, RA treatment (100 mg/kg/day, *i.g.)* for 30 days significantly reduced the levels of serum glucose, HbA1c, and glycoprotein components hexose, hexosamine, fucose, and sialic acid, and increased hepatic and muscle glycogen content in diabetic rats. Moreover, RA increased the activity of glycogen synthesis enzyme GS and decreased the activity of glycogen degrading enzyme GP (glycogen phosphorylase) for improvement of glycogen synthesis in liver and skeletal muscle and promoted insulin secretion from pancreatic β-cells. These effects of RA were comparable to that of metformin-treament group used as positive control (500 mg/kg bw/day) (Ramalingam et al. 2020).

Salvianolic acid B (Sal B) **104a**, a water-soluble dimer of rosmarinic acid, found in danshen (*Salvia miltiorrhiza* Bunge) roots and in other *Salvia* spp, has potential anti-obesity and cardioprotective effects. In traditional Chinese medicine danshen roots have been prescribed for treatment of cardiovascular disorders, hyperlipidemia and ischemic stroke via improvement of blood flow. In HFD-fed obese mice, Sal B on oral administration (100 mg/kg/day) for 8 weeks reduced body weight gain, WAT weight, adipocyte size of both visceral AT (VAT), and subcutaneous AT (ScAT), and the elevated levels of serum and liver TG and TC in obese mice. Moreover, Sal B improved both glucose and insulin tolerance in obese mice. In addition, Sal B decreased the expression levels of PPARγ and C/EBPα, and increased the expression levels of GATA2 and GATA3 in visceral fat tissues of obese mice. In pro-differentiation regimen exposed 3T3-L1 preadipocytes, Sal B inhibited adipogenesis by suppression of intracellular lipid accumulation and the expression levels of major adipogenic genes PPARγ and C/EBPα in mature adipocytes, and increased the expression levels of GATA2 and GATA3 in both differentiated and undifferentiated preadipocytes. Mounting evidence demonstrates that zinc finger transcription factors GATA2 and GATA3 on elevated expression in 3T3-L1 and 3T3-R442A preadipocytes suppress adipocyte differentiation either by direct

binding to PPARγ promoter to inhibit its basal activity or by formation of complexes of GATA2 or GATA3 proteins with C/EBPα and C/EBPβ for suppression of their activity in adipocyte differentiation (Tong et al. 2005; Wang et al. 2014c). Another study reported that Sal B in 3T3-L1 adipocytes promoted adipocyte differentiation and browning of WAT and increased glucose uptake and mitochondrial respiratory function and glycolytic function through increased expression of PGC-1α and its target genes UCP2, NRF1, NRF2, and PFKFB2. Possibly, PGC-1α promotes the expression of PPARγ, PPARα, and NRF1/2 for induction of mitochondrial respiratory function, and UCP2 expression promotes energy expenditure via enhanced glycolysis through phosphofructokinase 2/fructose-2,6-bisphosphatase (PFKFB2) expression (Pan et al. 2018). In type 2 diabetic db/db C57BL/KsJ mice, Sal B treatment (100 mg/kg) for 6 weeks significantly improved glucose intolerance, reduced the levels of serum FG, insulin, TG, and FFAs, and increased liver and muscle glycogen content in diabetic mice. Moreover, Sal B increased the activity of glycogen synthesis-related gene GS, and translocation of glucose uptake-related GLUT4 protein to the cell surface in skeletal muscle and the phosphorylation of AMPK in skeletal muscle and liver. Furthermore, Sal B decreased the activity of hepatic gluconeogenic genes PEPCK and G6Pase, and increased the expression levels of FA oxidation-related gene PPARα and glycolytic genes PK and GCK, and suppressed the activity of lipogenesis-related gene ACC by its increased phosphorylation in the liver of diabetic mice. In addition, Sal B protected pancreatic tissue from oxidative damage and increased insulin secretion from β-cells. The hypoglycemic, hypolipidemic, and pancreas protecting effects of Sal B were similar to that of metformin (positive drug, 300 mg/kg) treatment group. These findings suggest that Sal B ameliorates hyperglycemia, hyperlipidemia, and glucose intolerance by regulation of glucose and lipid metabolism in AMPK pathway (Huang et al. 2016b). Another study reported that Sal B regulated the expression levels of microRNA (mRNA) in obese adipose tissue of DIO mice for suppression of inflammation. Sal B increased the expression of anti-inflammatory mRNA, secreted frizzled-related protein 5 (Sfrp5), and decreased the expression of inflammation-related mRNA, serum amyloid A 3 (Saa3) in adipose tissue of obese mice. Sfrp5 on binding to Wnt5a inhibits the activation of its downstream target JNK kinase, and reduces the expression of inflammatory cytokines. Saa3 is over-expressed in diabetic adipocytes and promotes inflammation in adipocytes in presence of FFAs and high glucose. These findings suggest that Sal B exhibits its anti-obesity effect, partly by regulation of the expression of mRNAs (An et al. 2019).

Salidroside, a phenylethanoid glucoside **413**, is widely found in *Rhodiola* plants, *Rhodiola rosea*, *R. sachalinensis*, *R crenulata*, and *R. tibetica*, and in other plants, such as *Ligustrum lucidum, Salix triandra*, and willow bark. Salidroside has been found to possess antioxidant, antidiabetic, cardioprotective, renal protective, neuroprotective, and anticancer activities. In H_2O_2 or high glucose exposed MIN6 cells, salidroside protected the MIN6 cells from injury and apoptosis by suppression of the expression of NADPH oxidase 2 (NOX2) and the phosphorylation level of JNK kinase. Moreover, salidroside increased the p-levels of AMPK, Akt, and FoxO1 and increased the expression of PDX-1 in β-cells for improvement of regeneration

and functions of β-cells. Moreover, in high glucose exposed isolated mouse islets, salidroside increased β-cells proliferation. A growing body of evidence demonstrates that an elevated expression of NOX2 from glucotoxicity or peroxide toxicity in pancreatic β-cells stimulates the overproduction of ROS and activates the JNK-caspase 3-apoptotic cascade. In HFD-induced DIO mice and genetically obese diabetic db/db mice, salidroside on oral treatment (100 mg/kg/day) for 5 weeks improved β-cell function and glucose tolerance in both types of mice. Moreover, salidroside reduced serum glucose and LDL-C levels, and increased serum HDL-C and insulin levels, and increased the activity of antioxidant enzymes SOD, CAT, and GP_X in pancreas and adipose tissues. These findings suggest that salidroside protects pancreatic β-cells from apoptosis and dysfunction by AMPK-mediated suppression of NOX2 and FoxO1 activities (Ju et al. 2017). In another study, in obese mice, salidroside treatment (50 mg/kg/day) for 48 days improved both insulin signaling and insulin resistance by reduction of hepatic lipid accumulation and suppression of macrophage infiltration and pro-inflammatory cytokines (TNF-α, IL-1β and IL-6) in adipose tissues of obese mice. Moreover, salidroside decreased the expression levels of adipogenesis and lipogenesis-related genes PPARγ, C/EBPα, DGAT2, SCD-1, FABP4, RBP4, resistin, and leptin in white adipose tissue, and increased the phosphorylation levels of Akt and AMPK in the liver, skeletal muscle, and adipose tissue. In addition, salidrosise decreased hepatic glucose production by suppression of the expression of PGC-1α and G6Pase. PGC-1α promotes hepatic gluconeogenesis by inducing the expression of G6PC and PCK-1. Therefore, salidroside improves leptin sensitivity in hypothalamus to increase insulin sensitivity in peripheral tissues by suppression of inflammation and adipogenesis in adipose tissues through AMPK pathway (Wang et al. 2016a). In STZ and HFD-induced diabetic nephropathy (DN) in mice, salidroside on oral treatment (100 mg/kg/day) for 10 weeks mitigated DN in mice by reducing the levels of serum glucose, TG, BUN, creatinine, and glucose, and the levels of urinary albumin and renal fibrosis and increasing the expression of renal protective proteins nephrin and podocin in podocytes of renal cortex. Moreover, salidroside reduced the expression of renal fibrosis-related proteins TGF-β1, fibronectin, α-SMA, collagen 1, and myofibroblast activation, and enhanced the expression of SIRT1 and PGC-1α to increase mitochondrial biogenesis and function in kidney tissues (Xue et al. 2019). Another study reported that salidroside treatment (50 or 100 mg/kg/day) to type 2 diabetic db/db mice for 8 weeks reduced hepatic steatosis, muscle TG content by increasing the phosphorylation levels of Akt and GSK-3β in the liver, skeletal muscle, and adipose tissue, and increased the glucose uptake and GLUT4 expression in skeletal muscle and decreased lipogenesis by increasing the phosphorylation of AMPK and ACC in adipose tissue. Moreover, in liver, it reduced the activity of PEPCK and G6Pase (Zheng et al. 2015).

Eugenol (4-allyl-2-methoxyphenol) **271**, a major phenolic constituent of clove (*Syzygium aromaticum*) oil, betel (*Piper betle*) leaf (paan), basil (*Ocimum gratissimum*), and other *Ocimum* spp., and cinnamon, has potential hypoglycemic activity. In STZ-induced diabetic rats, eugenol on oral administration (10 mg/kg bw/day) for 30 days showed antidiabetic effect by reduction of the levels of serum

FG, HbA1c, and liver toxic marker enzymes AST, ALT, ALP, and kidney toxic marker factors CK and BUN, and increased serum insulin level and hepatic glycogen content in diabetic rats. Moreover, eugenol increased hepatic glucose utilization by upregulation of HK, PK, and G6PDH, and decreased hepatic glucose production by suppressing the activity of gluconeogenic genes G6Pase and FBPase for maintenance of glucose homeostasis. Therefore, eugenol regulates the activity of key carbohydrate metabolism-related enzymes in liver for its antidiabetic effect (Srinivasan et al. 2014). In L6 myotubes, eugenol increased glucose uptake by upregulation of the expression of GLUT4 and PI3K, and the phosphorylation level of Akt (Prabhakar and Doble 2011). Moreover, eugenol inhibited the activity of dietary carbohydrate and fat metabolizing enzymes pancreatic α-amylase and lipase with an IC_{50} value of 62.53 and 72.34 μg/ml, respectively, as well as the activity of hypertension-related enzyme, angiotensin converting enzyme (ACE), with an IC_{50} value of 130.67 μg/ml (Mnafgui et al. 2013). In STZ/HFD-induced obese type 2 diabetic rats, eugenol treatment (10 mg/kg/day) for 45 days significantly reduced the levels of serum glucose, TG, TC, LDL-C, MDA, and IL-6 and increased serum insulin and antioxidant GSH levels in diabetic rats. Moreover, eugenol increased glucose uptake in skeletal muscle by increasing the translocation of GLUT4 and the phosphorylation of AMPK, similar to that of metformin (Al-Trad et al. 2019). In triton WR-1339 induced hypercholesterolemic rats, eugenol treatment (5 mg/kg bw/day, *i.g.*) for 7 days significantly reduced serum lipid profile (TC, TG, LDL-C, VLDL-C) and increased serum HDL-C level in rats. These effects of eugenol were better than that of lovastatin (10 mg/kg bw/day) used as positive control. Moreover, eugenol increased the activity of enzymatic and non-enzymatic antioxidants GST, GP_X, and Vitamin E in hepatic tissues of hypercholesterolemic rats. Further, eugenol increased the expression of cholesterol metabolizing enzyme HMGCR and lipolysis enzyme LPL in hepatic tissues of atherogenic diet fed chronic hypercholesterolemic rats (Venkadeswaran et al. 2014, 2016).

Gallic acid (3,4,5-trihydroxybenzoic acid) (GA) **44**, a phenolic compound present in high concentrations in grapes, pomegranates, mulberry, blackcurrant, mango, and tea, has potential antidiabetic and anti-obesity effects. In HFD-fed NAFLD mice, GA supplementation in diet (50 or 100 mg/kg of diet/day) for 16 weeks significantly reduced hepatic steatosis and insulin resistance by regulation of glucose and lipid metabolism. GA significantly reduced body weight gain and hepatic vacuoles size and lipid droplets content, the levels of serum glucose, insulin, TG, TC, LDL-C, PLs, and hepatic TG, TC, FFAs, and hepatic toxic marker enzymes AST and ALT, and increased the levels of serum albumin and hepatic PUFA/MUFA ratio and insulin sensitivity in liver of NAFLD mice. Possibly GA regulated glucose metabolism by increasing glycolysis and decreasing gluconogenesis, amino acids and choline metabolism, and gut microbiota-related metabolism for suppression of hepatic fat accumulation (Chao et al. 2014). In HFD-fed obese mice, GA treatment (10 mg/kg/day) for 2 weeks reduced epididymal fat mass, adipocyte size, and hepatic and serum TG content by upregulation of PPARγ and its target genes and activation of Akt in WAT (Bak et al. 2013). In high oleic acid exposed HepG2 cells, GA reduced intracellular lipid accumulation, and increased the phosphorylation levels of

AMPK and ACC to increase the expression levels of autophagosomic protein LC3II and mitochondrial biogenesis and FA oxidation-related genes SIRT1, PGC-1α, PPARγ, SCD1, NRF-1, and UCP-1. Specific knockdown of SIRT1 in HepG2 hepatocytes markedly reduced the effect of GA in mitochondrial function and suppression of lipid accumulation. These findings suggest that GA stimulates AMPK-dependent autophagic process and mitochondrial energy expenditure process for suppression of lipid accumulation in hepatocytes. In DIO mice, GA treatment (10 mg/kg bw/day) for 9 weeks reduced body weight, hepatic and adipose tissue lipid mass, and hyperglycemia by increasing the phosphorylation of AMPK in the liver, skeletal muscle, and interscapular brown adipose tissue in obese mice. Moreover, GA increased the mitochondrial function in liver and brown adipose tissue by upregulation of the expression levels of relevant genes SIRT1, PGC-1α, CPT-1c, TFAM, UCP-1, NRF-1, NRF-2, GLUT4, GP_X-1, SOD-1, and SOD-2, and down-regulated the expression of lipogenic gene SREBP-1c in liver. In addition, GA increased hepatic Akt activation to reduce the expression levels of gluconeogenic genes PEPCK and G6Pase in the liver. These findings demonstrate that GA stimulates SIRT1 expression for promotion of glucose and lipid metabolism in obese mice (Doan et al. 2015). In STZ/HFD-induced type 2 diabetic rats, GA treatment (20 mg/kg bw/day) for 28 days reduced insulin resistance in adipose tissue by increasing PPARγ expression and glucose uptake via increased expression and translocation of GLUT4 into plasma membrane, and increased expression levels of PI3K and p-Akt in insulin signaling pathway. In addition, GA stimulated glucose-stumulated-insulin secretion from pancreatic β-cells. GA also increased PPARγ expression in the liver and skeletal muscle to a less extent (Gandhi et al. 2014).

Caffeic acid phenethyl ester (CAPE) **414** is found in propolis (honeybee hive) and in many *Populus* spp. including *Populus nigra* and has been shown to possess antidiabetic and anti-obesity effects. In STZ-induced diabetic rats, CAPE treatment (20 or 30 μM/kg/day) for 60 days improved hyperglycemia in rats by reduction of serum FG, TC, TG, and ALT levels and increased serum insulin level and hepatic glycogen content. CAPE enhanced the expression levels of glycolysis-related genes GCK and PK, and decreased the expression of gluconeogenic gene PEPCK and glucose uptake protein GLUT2 in the liver for maintenance of glucose homeostasis (Celik et al. 2009). In another animal model, in STZ and HFD-induced type 2 diabetic mice, CAPE on oral supplementation (30 mg/kg bw/day) for 5 weeks reduced the levels of serum glucose, lipids (TC, TG, LDL-C), and inflammatory cytokines (IL-6, TNF-α, and MCP-1) and increased serum HDL-C level, and the expression levels of FA oxidation-related gene PPARα and its downstream target genes in the liver and adipose tissue of diabetic mice. In vitro, in high glucose and high palmitic acid-exposed insulin-resistant HepG2 cells, CAPE increased glucose uptake and glycogen content, and increased the expression of phosphorylated IRS-1 and Akt, and decreased the expression levels of gluconeogenic gene G6Pase and inflammatory-related kinases p-JNK and p-NF-κBp65 in hepatocytes. These findings suggest that CAPE ameliorates insulin resistance in diabetic mice and HepG2 cells by suppression of inflammation via down-regulation of JNK/NF-κB signaling pathway and increased insulin sensitivity via activation of insulin signaling

pathway (Nie et al. 2017a). In STZ-induced type 1 diabetic rats, CAPE treatment (30 mg/kg bw/day) for 21 days improved hyperglycemia and insulin secretion by increasing antioxidant status in pancreatic β-cells. CAPE protected pancreatic tissues and β-cells from injury and β-cell apoptosis by promoting Nrf2 activation and Nrf2-dependent upregulated expression of antioxidant enzymes heme oxygenase-1 (HO-1), dimethylarginine dimethylaminohydroxylase-1 (DDAH-1), and gamma glutamyl cysteine ligase (GGCL) for suppression of excessive ROS production in pancreas. A group of evidence demonstrates that an elevated expression of ROS in diabetic pancreas stimulates the accumulation of asymmetric NG, NG-dimethyl-L-arginine (ADMA), and over-expression of iNOS and production of NO, lipid peroxide (LOOH), and NO_2^-/NO_3^- leading to injury of pancreatic tissues and impaired β-cell function. Accumulation of ADMA in the pancreas leads to pancreatic β-cell dysfunction and impaired insulin secretion. GGCL catalyzes the first and the limiting step in the synthesis of antioxidant enzyme GSH. An elevated expression of DDAH-1 in diabetic pancreas increases insulin secretion from β-cells by reducing the accumulation of ADMA in pancreas by its degradation. These findings indicate that CAPE protects pancreatic β-cells by upregulation of the expression levels of antioxidant enzymes via Nrf2 activation (Sorrenti et al. 2019).

6-Gingerol **154**, a phenolic constituent of ginger (rhizomes of *Zingiber officinale*), has significant antioxidant, antidiabetic, and anticancer effects. In L6 myotubes, 6-gingerol increased glucose uptake by increasing the expression and translocation of GLUT4 proteins into plasma membrane via increased phosphorylation of AMPK. 6-Gingerol elevated the expression of intracellular Ca^{2+} concentrations via upregulation of the expression of CaMKK for the phosphorylation of AMPK. Co-treatment of STO-609, a selective inhibitor of CaMKK, completely abolished the activity of 6-gingerol in glucose uptake and AMPK activation. These findings suggest that 6-gingerol increased glucose uptake in L6 myotubes in CaMKK/AMPK-dependent pathway. In synthetic AGE, AGE2-exposed rat pancreatic RIN-5F cells, 6-gingerol protected the pancreatic β-cells from injury by suppression of ROS production, and increased insulin secretion. In HFD-fed obese diabetic db/db mice, 6-gingerol on supplementation in diet (0.05% of diet) for 4 weeks reduced the levels of serum glucose, TG, TC, TBARS, and TNF-α, and increased hepatic glycogen content in diabetic mice. Moreover, 6-gingerol increased the expression levels of GLUT4 in skeletal muscle, hepatic glycogen synthase (GS), and reduced the expression of hepatic glycogen phosphorylase (GP), and the activity of gluconeogenic genes PEPCK and G6Pase. These findings suggest that 6-gingerol exerts antidiabetic effect via increasing insulin secretion, glucose uptake, and glycogen synthesis and decreasing hepatic glucose production (Li et al. 2013a; Son et al. 2015). In another study, in HFD-fed obese rats, 6-gingerol on oral treatment (50 or 75 mg/kg bw/day) for 30 days reduced body weight, and the levels of serum glucose, insulin, leptin, and plasma lipase and amylase activity, and plasma and liver lipid profile in obese rats (Saravanan et al. 2014). In isolated rat pancreatic islets, 6-gingerol increased insulin secretion by increasing the concentrations of cAMP and the expression of PKA and CREB protein levels. Co-treatment of H-89, an inhibitor of PKA, reduced the insulin

secreting effect of 6-gingerol. In type 2 diabetic LepR db/db mice, 6-gingerol treatment (200 mg/kg/day) for 4 weeks increased plasma GLP-1 level and increased glucose uptake and glycogen content in skeletal smooth muscle of diabetic mice. In skeletal muscle, 6-gingerol increased the expression of GLUT4 protein, Rab8, and Rab10 GTPases. These findings suggest that 6-gingerol increased GLUT4 translocation into plasma membrane by upregulation of vesicle membrane proteins and improved pancreatic insulin secretion by activation of GLP-1/cAMP/PKA/CREB pathway (Samad et al. 2017).

5.2.9 Tannins

Tannins are a group of polyphenolic compounds, in which galloyl or ellagic acid units are attached to a variety of polyols including glucopyranoses and catechins. These compounds are found in high concentrations in plant foods, such as fruits, legumes, vegetables, and beverages. These compounds are mainly classified into two major classes, hydrolyzable tannins, such as polyesters of gallic acid and hexahydroxydiphenic acid (gallotannins and ellagitannins, respectively), and non-hydrolyzable or condensed tannins (oligomers and polymers of flavan-3-ol moieties, such as condensed proanthocyanidins). Natural complex tannins are available, in which a catechin unit is attached glycosidically to a gallotannin or an ellagitannin unit. Hydrolyzable tannins are hydrolyzed into their basic components on treatment with hot water or with tannases. Tannins are used in pharmaceutical industry due to their potential biological activities including antimicrobial, antitumor, and antidiabetic activities. Several plant tannins have been reported to have potential antidiabetic effect due to their strong antioxidant and anti-inflammatory properties (Khanbabaee and Ree 2001).

Ellagic acid (EA) **320**, a natural polyphenolic compound commonly found in fruits, such as raspberries, pomegranates, grapes, blackcurrants, as well as in nuts, has been found effective in diabetic liver. In diabetic female Goto-Kakizaki (GK) rats, EA on oral treatment (50 mg/kg/day) for 45 days significantly reduced hepatic lipid accumulation and serum FG, HOMA-IR, and lipid profile levels by suppression of hepatic oxidative stress and improvement of hepatic insulin sensitivity. EA decreased hepatic oxidative stress by down-regulation of the expression of p47phox and HIF-α, key biomarkers for the development of NAFLD, and upregulation of antioxidant enzyme Nrf2 expression in the liver of diabetic rats. Nrf2 has been reported to increase FA oxidation and to suppress the activity of lipogenic gene SREBP-1c and inflammation levels in hepatocytes. Moreover, EA increased the phosphorylation level of Akt in the liver for activation of insulin signaling pathway. These findings suggest that EA improves Nrf2 expression and insulin sensitivity in liver for suppression of dyslipidemia and hyperglycemia in female diabetic rats (Polce et al. 2018). In HFD-fed obese rats, EA supplementation in diet (30 mg/kg of diet/day) for 24 weeks reduced hepatic steatosis, adipocyte hypertrophy, and adipocyte size of both WAT and BAT by increasing the expression levels of thermogenic brown adipocyte marker genes UCP-1, PGC-1α, PPARα,

PRDM-16, TFAM, CD-137, and Cidea in both WAT and BAT, and decreasing the expression levels of adipogenic genes PPARγ, C/EBPα, C/EBPβ, C2H2-zinc-finger protein-423 (Zfp-423), and retinaldehyde dehydrogenase 1α1 (Aldh1α1) in WAT of obese rats. In addition, EA reduced the level of serum resistin and increased the level of serum adiponectin for improvement of insulin signaling in adipocytes (Wang et al. 2019c). Another study reported that in obese diabetic KK-Ay mice, EA supplementation (0.1% of diet) for 68 days reduced hepatic steatosis, serum lipid profile, and resistin levels and upregulated the expression levels of FA oxidation and lipid uptake-related genes PPARα, CPT-1α, LDLR, and apoA1 in the liver of diabetic mice. These findings indicate that EA decreases lipid synthesis-related factor resistin for promotion of FA oxidation in the liver for mitigation of hepatic steatosis (Yoshimura et al. 2013).

A gallotannin, α- and β-anomeric mixture of penta-*O*-galloyl glucose (PGG) **235**, and an ellagitannin, lagerstroemin **415** isolated from South Asian plant, *Lagerstroemia speciosa* (banaba), showed significant glucose uptake by GLUT4 expression and anti-adipogenic activity in 3T3-L1 adipocytes (Klein et al. 2007). In 3T3-L1 adipocytes, PGG stimulated insulin-like GLUT4 translocation into plasma membrane by increasing the phosphorylation of IR and Akt for activation of insulin signaling pathway (Li et al. 2005). Another study reported that an ellagitannin casuarinin isolated from *Punica granatum*, *Lagerstroemia flos-reginae*, and *Syzygium aromaticum* increased glucose uptake and inhibited adipogenesis in 3T3-L1 adipocytes (Bai et al. 2008).

Chebulagic acid **416**, an ellagitannin isolated from *Terminalia chebula*, showed strong mammalian maltase (α-glucosidase) inhibitory activity in a reversible and non-competitive manner with a Ki value of 6.6 μM, and mild inhibitory activity against baker's yeast α-glucosidase 1, with an IC_{50} value of 50 μM (Gao et al. 2008).

Grape seed proanthocyanidins (GSP) contained a mixture of monomeric (21.3%), dimeric (17.4%), trimeric (16.3%), tetrameric (13.3%), and oligomeric (5-130 monomeric units, 31.7%) forms of (+)-catechin, (–)-epicatechin, (–)-epicatechin 3-gallate, and (–)-epigallocatechin-3-gallate via C4-C8 and C4-C6 bonds. The oligomers are known as procyanidins. GSP are essentially of B-type with C4-C8 linkages being much more abundant than C4-C6 linkages **417** and **418** (Monagas et al. 2010). In STZ-diabetic rats, GSP on oral administration of a single dose (250 mg/kg bw) significantly reduced serum glucose and insulin levels. In both L6E9 myotubes and 3T3-L1 adipocytes, GSP increased glucose uptake and GLUT4 translocation through increased PI3K and p38 mitogen-activated protein kinase (p38MAPK) activation. Co-treatment of wortmannin, an inhibitor of PI3K, or SB203580, an inhibitor of p38MAPK, inhibited the activity of GSP in glucose uptake in both L6E9 and 3T3-L1 cells (Pinent et al. 2004). In HFD-fed obese mice, GSP on oral administration of a single dose of 250 mg/kg bw reduced the serum TG levels by 40% in wild-type obese mice, but not in FXR-null mice. This fact indicates that FXR has an essential role in hypotriglyceridemic action of GSP in vivo. In the liver of WT-obese mice, GSP enhanced the transcriptional activity of bile acid-like hepatic FXR activity by down-regulation of the expression levels of lipogenesis-related gene SREBP-1c and its target genes ACSII and SCD1/2, and

upregulated the expression levels of TG-rich lipoproteins clearance gene ApoA5 for suppression of hepatic lipid and hypertriglyceridemia content. In both African green monkey fibroblasts (CV-1) and HeLa cells, exposed to bile acid chenodeoxycholic acid (CDCA), a natural FXR ligand, GSP increased the expression levels of FXR, cholesterol 7α-hydroxylase (CYP7A1), and orphan nuclear receptor, small heterodimer partner (SHP). These results suggest that GSP enhances the FXR activity for upregulation of SHP and subsequently down-regulates the expression levels of SREBP-1 and its target genes for reduction of FA and TG synthesis and suppression of elevated plasma TG levels in obese mice (Del Bas et al. 2009). Another study reported that GSP down-regulated the expression levels of lipid synthesis-related genes butyryl CoA synthetase 1 (BUCS-1) and acyl CoA thioesterase 2 (ACAT2) in the liver of obese rats for suppression of hepatic lipid synthesis (Baiges et al. 2010). In HF (cafeteria diet)-fed obese rats, GSP on supplementation in diet (25 mg/kg bw/day) for 3 weeks reduced the levels of plasma TG, TC, glucose, leptin, insulin, and IL-6, and reduced adipose tissue hypertrophy and hyperplagia, and increased the adipocyte number in WAT of obese rats. Moreover, GSP increased the expression levels of genes related to adipocyte differentiation and insulin signaling activation PPARγ, adiponectin, pre-adipocyte factor-1 (Pref-1), VEGF-A, UCP-1, and FABP-4 in adipose tissue for insulin-sensitive mitochondrial energy expenditure and FA uptake and oxidation for reduction of hypertrophy of WAT. These findings suggest that GSP increases insulin sensitivity in WAT by stimulation of lipolysis and subsequent fat mobilization and utilization for improved visceral adipocyte functionality (Pascual-Serrano et al. 2017). In HFD-fed obese hamsters, GSP treatment (25 mg/kg/day) for 15 days reduced retroperitoneal adipose tissue fat accumulation and plasma lipid profile through upregulation of the expression levels of genes acyl CoA dehydrogenase, very long-chain (ACADVL), CPT-1β, PPARα, HSL, ATGL, GyK, LPL, and FABP-4 related to FA oxidation, lipolysis, FA uptake, and transport in adipose tissue (Caimari et al. 2013). In HFD-fed obese mice, GSP supplementation in diet (300 mg/kg bw/day) for 7 weeks reduced epididymal and hepatic fat mass, levels of plasma inflammatory factors TNF-α, IL-6, and MCP-1, and suppressed macrophage infiltration in adipose tissue, and increased insulin sensitivity in the adipose tissue and liver of obese mice. Moreover, GSP modulated the gut microbiota composition by increasing the abundance of bacterial spp. in *Clostridium cluster XIVa*, *Roseburia*, and *Prevotella* to reduce the gut permeability by increasing the expression of tight junction proteins and proglucagon, precursor of GLP-2. These findings suggest that GSP reduces inflammation in the adipose tissue and liver by suppression of the entry of endotoxemia from the gut to increase insulin sensitivity in the adipose tissue and liver via modulation of gut microbiota dysbiosis in obese mice (Liu et al. 2017b). In STZ-induced diabetic nephropathy (DN) in rats, GSP treatment (250 or 500 mg/kg/day) for 24 weeks showed significant renoprotective effect by reduction of serum AGEs and HbA1c levels, urinary albumin excretion, systolic blood pressure, and deposition of ECM proteins in renal glomeruli. GSP decreased the activity of Ang II, and the expression levels of TGF-β1, CTGF, and RAGE, and increased the

expression of podocyte-protective protein, nephrin, in glomerular base membrane for protection of renal tissues from fibrosis and injury (Li et al. 2009, 2017).

Apple procyanidins (AP) are the main constituents of apple (*Malus pumila* cv. Fuji) polyphenols and consist of flavanols, (+)-catechin and (–)-epicatechin, and linked together B-type C4-C8 and C4-C6 bonds and have many isomeric forms **419**. The apple oligomeric procyanidins (AOP) consist of monomer- , dimer-, trimer-, and tetramers of 22.5, 30.4, 38.7, and 8.4%, respectively, while polymeric procyanidins (APP) consist of mainly penta-, hexa-, hepta-, and octamers of 27.1, 23.2, 17.5, and 8.8%, respectively. In obese diabetic ob/ob mice, apple procyanidins (AP) on administration in drinking water (0.5%, w/v/day) for 5 weeks reduced serum glucose and HOMA-IR levels and pancreatic islets hypertrophy and insulin resistance and increased pyruvate tolerance of diabetic mice. Moreover, AP decreased hepatic macrophage infiltration and the expression levels of pro-inflammatory cytokines TNF-α and IL-6 and the phosphorylation of JNK. In addition, AP suppressed hepatic gluconeogenesis by increasing the activation of insulin signaling pathway through increased Akt phosphorylation, but failed to alter hepatic fat accumulation. These findings indicate that AP improved hepatic insulin resistance by increasing insulin sensitivity, and suppressing pyruvate-induced gluconeogenesis and inflammation in liver (Ogura et al. 2016). In high fat/high-sucrose-diet fed obese mice, apple polymeric procyanidins (APP) on supplementation in diet (0.5% of diet) for 20 weeks significantly reduced body weight, liver and visceral fat mass, and the levels of serum glucose, TG, TC, TNF-α, IL-6, and LPS in obese mice. Moreover, APP modulated the gut microbiota composition by decreasing the *Firmicutes/Bacteroidetes* ratio, and increasing the abundance of the bacteria of *Akkermansia* (about eight times), *Adlerceitzia*, *Roseburia,* S24-7, *Bacteroides*, and *Anaerovorax*, and decreasing the abundance of *Clostridium*, *Lachnospiraceae*, and *Bifidobacterium* spp. In addition, APP increased the expression of phosphorylated AMPK, and the FA oxidation-related genes PPARα, CPT-1α, ACOX1, and decreased the expression of lipogenesis-related genes SREBP-1c, FAS, HMGCR, and of inflammatory factors LPS receptor TLR4 and CD14 in the liver. Furthermore, APP increased the expression levels of tight junction proteins ZO-1 and occludin in ileum of obese mice. Several studies demonstrate that gut *Akkermansia* reduces the levels of circulating LPS by reducing the gut permeability. These results suggest that APP prevent obesity-induced hepatic and visceral fat accumulation by modulation of gut microbiota composition and suppression of LPS-induced hepatic inflammation and lipogenesis, and upregulation of hepatic FA oxidation processes via AMPK activation. Apple oligomeric procyanidins (AOP) have similar anti-obesity effect (Masumoto et al. 2016).

Wild blueberries (*Vaccinium angustifolium*) are rich in polyphenolic compounds, such as flavonoids, anthocyanins, phenolic acids, and oligomeric- and polymeric proanthocyanidins, and have preventive activity against metabolic disorders including obesity and diabetes. A 70% hydro-ethanolic extract of wild blueberries rich in polyphenols (BBPE) was fractionated into three fractions, fraction 1 rich in anthocyanins and phenolic acids (BBPE-F1), fraction 2 rich in oligomeric proanthocyanidins (degree of polymerization <4) and flavanols (BBPE-F2), and

fraction 3 rich in polymeric proanthocyanidins (degree of polymerization >4) (BBPE-F3). In high fat-, high sucrose-fed obese mice, the parent BBPE and its fractions, F1, F2, and F3, on supplementation in diet (200 mg, 37 mg, 53 mg, and 37 mg/kg bw/day of BBPE, F1, F2, F3, respectively) for 8 weeks, improved insulin resistance by reducing serum glucose and insulin levels to different extent. BBPE and its F2 and F3 fractions modulated the composition of gut microbiota, but F1 did not show any significant change in the composition of gut microbiota. The BBPE, F2, and F3 improved the epithelial barrier function of the colon by increasing the expression of mucin-producing goblet cells, and increased the abundance of *Akkermansia muciniphila* and *Adlercreutzia equolifaciens* belonging to family Verrucomicrobiaceae and Coriobacteriaceae, respectively. The F3 fraction showed better effect in production of goblet cells in epithelium of colon tissues. Possibly mucin-secreting goblet cells produced by the proanthocyanidins present in F2 and F3 increase insulin sensitivity in the liver by suppression of the entry of endotoxic bacteria including LPS into circulatory system by increased production of *A. muniphila* and *A. equolifaciens* in the gut (Rodriguez-Daza et al. 2020). Blueberry proanthocyanidins consist of (+)-catechin and (–)-epicatechin as monomeric units, and these monomers are exclusively linked in B-type C4-C8 and C4-C6 bonds and to a less extent in A-type C2-O7 bonds (Prior et al. 2001).

Semi-fermented oolong tea prepared from leaves and twigs of tea (*Camellia sinensis*) is consumed for prevention of obesity by overweight and obese humans. Oolong tea consists of different types of polyphenols and alkaloids including flavonoids, caffeine, anthocyanins, monomeric, dimeric, and oligomeric flavan-3-ols. Many of them showed strong inhibitory effect against pancreatic lipase (PL) in vitro. Among the monomeric flavan-3-ols, only EGCG **35** showed strong inhibitory effect against PL with an IC_{50} value of 0.098 μM. Among the identified flavan-3-ols, four dimers, oolonghomobisflavans A and B and oolongtheanin 3′-*O*-gallate and prodelphinidin B-2 3,3′-di-*O*-gallate (**420**-**423**) showed strong inhibitory activity against pancreatic lipase (PL) isolated from porcine pancreas with IC_{50} values of 0.048, 0.108, 0.068, and 0.107 μM, respectively, while oolong tea polymerized polyphenols (OTPP) of average MW of 2017 showed stronger inhibitory effect against PL with IC_{50} value of 0.28 μg/ml, compared to that of hydrolyzable OTPP (IC_{50} of 1.38 μg/ml). These findings indicate that flavan-3-ols having galloyl moieties and polymerization of flavan-3-ols exhibit strong PL inhibitory effect (Nakai et al. 2005).

Black wattle tree, *Acacia mearnsii*, bark polyphenols are used to eliminate wine sedimentation and in food nutraceuticals for prevention of obesity. The polyphenols from hot water extract of *A. mearnsii* bark (AMP) showed in vitro inhibitory activity against pancreatic lipase (PL) and rat intestinal α-glucosidase enzymes, maltase and sucrase, with IC_{50} values of 0.95, 0.22, and 0.60 mg/ml, respectively. In ICR mice pretreated with olive oil and maltose, AMP significantly reduced plasma TG and glucose levels. These findings suggest that AMP inhibits intestinal absorption of lipids and carbohydrates in mice (Ikarashi et al. 2011a). Another study reported that AMP inhibited the activity of α-amylase by 88.4% at a concentration of 0.5 mg/ml. HPLC analysis of AMP revealed the presence of proanthocyanidin oligomers of B

types having (+)-catechin, (+)-gallocatechin, and robinetinidol **424** as monomeric units, and dimers, robinetinidol (4α-8)-gallocatechin/catechin **425** and **426** and oligomers of robinetinidol and gallocatechin/catechin were identified as major constituents (Matsuo et al. 2016).

The young leaves and beans of *Acacia mollissima* are consumed by Australian aborigines for health benefits. The catechin-like flavan-3-ols-rich polyphenols extracted from South African *A. mollissima* stem-bark with hot water (AMP) showed significant anti-obesity and antidiabetic effects in obese diabetic KK-Ay mice. AMP on supplementation in diet (5% of diet) to HFD-fed obese diabetic KK-Ay mice for 7 weeks reduced body weight, adipose tissue and liver mass, plasma glucose, insulin, and HOMA-IR levels in diabetic mice. AMP increased the expression levels of genes related to energy expenditure and glucose uptake, namely, PPARα, PPARδ, CPT-1, ACOX, UCP-3, and GLUT4, in the skeletal muscle, and reduced the expression levels of lipid synthesis-related genes SREBP-1c, ACC, and FAS, and fat intake-related genes PPARγ and LPL in the liver. Moreover, AMP increased the secretion of adiponectin and reduced the expression of TNF-α in white adipose tissue of obese mice. These findings suggest that AMP improves insulin resistance by modulation of glucose and lipid metabolism through upregulation of energy expenditure-related genes in skeletal muscle and down-regulation of lipid synthesis and fat intake-related genes in the liver, and upregulation of insulin-sensitive adiponectin in WAT of obese diabetic mice (Ikarashi et al. 2011b).

5.2.10 Bromophenols

3,4-Dibromo-5-(2-bromo-6-(ethoxymethyl)-3,4-dihydroxybenzyl)benzene-1,2-diol (BPN) **427**, a bromophenol isolated from marine alga *Rhodomela confervoides*, was found to exhibit antidiabetic effect. BPN inhibited the activity of PTP1B enzyme, a negative regulator of insulin signaling pathway, in a competitive manner with Ki of 0.54 μM. BPN binds directly to PTP1B enzyme with binding constant, K_D value of 3.3 μM. In PA-induced insulin-resistant HepG2 cells, BPN improved insulin resistance by increasing insulin-stimulated phosphorylation of IRβ, IRS-1, and Akt. Moreover, BPN promoted glucose uptake in HepG2 cells by increased translocation of GLUT1 to the plasma membrane and reduced ROS levels in DPPH radical scavenging assay in HepG2 cells. In STZ-induced diabetic rats, BPN on oral administration (20 mg/kg/day) for 21 days reduced serum glucose and FG levels. Moreover, it was non-toxic to diabetic rats (Guo et al. 2020c). In PA-induced insulin-resistant C2C12 myotubes, BPN increased glucose uptake and GLUT4 translocation to the plasma membrane and increased the expression and phosphorylation of IR, IRS-1, PI3K, and Akt. Therefore, BPN could be a lead compound in treatment of diabetes (Xu et al. 2018b).

Bis-(2,3-dibromo-4,5-dihydroxybenzyl) ether (BDDE) **428**, a bromophenol isolated from red alga *Odonthalia corymbifera*, showed antidiabetic effect both in vitro and in vivo models. In high glucose-induced insulin-resistant HepG2 cells, BDDE increased glucose uptake and the phosphorylation levels of IRβ, IRS-1,

PI3K, and Akt, and inhibited the activity of PTP1B enzyme. In diabetic db/db mice, BDDE treatment (40 mg/kg/day) for 28 days decreased serum glucose, HbA1c, and TG levels and increased serum insulin levels. The effects of BDDE were similar to those of metformin treated group (10 mg/kg/day). Moreover, BDDE decreased the expression of PTP1B enzyme and increased the expression of p-IRβ in skeletal muscle of diabetic mice. These findings suggest that BDDE exhibits antidiabetic effect by suppression of PTP1B activity and upregulation of p-IRβ expression and insulin signaling pathway (Xu et al. 2016). In vitro, BDDE inhibited the activity of α-glucosidase with IC_{50} value of 0.098 and 0.120 μM against yeast and *Bacillus stearothermophilus* α-glucosidases, respectively, and IC_{50} value of 1.00 and 1.20 mM against rat intestinal sucrase and maltase, respectively (Kim et al. 2010).

5.2.11 Alkaloids

1-Deoxynojirimycin (DNJ) **108**, a major piperidine alkaloid constituent of mulberry (*Morus alba*) leaves and a constituent of *Commelina communis*, and bacterial strains, *Bacillus* and *Streptomyces* spp., has significant antidiabetic and anti-obesity effects. In male SD rats, DNJ on oral administration (1 mg/kg bw/day) for 4 weeks reduced hepatic fat accumulation, hepatic PLs and hydroperoxides levels, and plasma TG level, and increased adiponectin secretion in WAT of the rats. Moreover, DNJ increased hepatic AMPK activation and the expression levels FA oxidation-related genes CPT and ACOX in the liver. These findings indicate that DNJ promotes FA β-oxidation for suppression of hepatic fat mass via adiponectin-dependent AMPK activation in liver of rats (Tsuduki et al. 2009). In STZ-induced diabetic mice, treatment of DNJ (50 mg/kg bw/twice daily) for 3 days reduced serum glucose level and increased hepatic glycogen content in diabetic mice. DNJ increased the expression levels of glycolysis-related enzymes GCK, PFK, PK, and pyruvate decarboxylase E1 (PDE1) and decreased the expression of gluconeogenic enzymes PEPCK and G6Pase in the liver of diabetic mice. PDE1 reduces the accumulation of pyruvate by its conversion into acetyl CoA to reduce the process of hepatic glucose production. Moreover, DNJ inhibited the intestinal glucose absorption by down-regulating the expression of SGLT1, Na^+/K^+ATPase, and GLUT2, the key enzymes involved in transepithelial glucose uptake in small intestine. These results suggest that DNJ promotes hepatic glucose metabolism by increasing glucose utilization and decreasing glucose production and reabsorption for maintenance of glucose homeostasis and suppression of hyperglycemia in diabetic mice (Li et al. 2013b). In diabetic db/db mice, DNJ administration (40 or 80 mg/kg/day, *i.v.)* for 4 weeks significantly reduced body weight, serum glucose, insulin, and HOMA-IR levels, and improved glucose and insulin tolerance in diabetic mice. In skeletal muscle of diabetic mice, DNJ increased glucose uptake, increased translocation of GLUT4 to the plasma membrane, and increased the phosphorylation levels of IRβ, IRS-1, PI3K, and Akt. These findings demonstrate that DNJ increases insulin sensitivity in skeletal muscle by activation of PI3K/Akt signaling pathway for reduction of hyperglycemia in diabetic mice (Liu et al. 2015c).

In HFD-fed obese diabetic db/db mice, DNJ treatment (40 or 80 mg/kg/day, *i.v.*) for 4 weeks significantly reduced the levels of serum TG, TC, LDL-C, ALT, and AST, and liver lipid mass, hepatic TG, TNF-α, IL-1, and IL-6 levels and increased hepatic glycogen content. DNJ increased the activity of glycolysis-related enzymes HK and PK, and reduced the activity of glycogen degrading enzyme GP and gluconeogenic enzymes G6Pase and PEPCK in liver tissues. In addition, DNJ increased hepatic insulin sensitivity by increasing the phosphorylation levels of p85-PI3K, Akt, and GSK-3β. The increased phosphorylation of GSK-3β inhibited its activity on the phosphorylation of GS, and thereby increased the activity of GS in glycogen synthesis. These findings suggest that DNJ improves hepatic glucose and lipid homeostasis to mitigate hepatic steatosis, inflammation, and fibrosis by activation of insulin-stimulated Akt/GSK-3β signaling pathway in diabetic mice (Liu et al. 2016b). In HFD-fed obese mice, DNJ on intracerebroventricular (*i.c.v.*) administration (50 μg/ml,1 μL) significantly reduced body weight and food intake by increasing the expression of anorexigenic (appetite suppressing) hormone POMC and suppressing hypothalamic ER stress in obese mice. DNJ reduced hypothalamic ER stress by increasing leptin-related signaling through increasing the phosphorylation levels of JNK2 and STAT3 and decreasing the phosphorylation of AMPK in the hypothalamus. In hypothalamic neuronal GTI-7 cells, DNJ (50 μg/ml) reduced the ER stress-related expression levels of proteins, GRP78, CHOP, spliced X-box binding protein-1 (XBP-1s), activating transcription factor 4 (ATF4), and ER DnaJ homolog 4(ERDJ4) by increasing leptin signaling in GTI-7 cells. These findings suggest that DNJ on central administration increases leptin signaling in the hypothalamus for suppression of body weight and food intake via inhibition of hypothalamic AMPK activation in obese mice (Kim et al. 2017b). In 3T3-L1 white preadipocytes, DNJ inhibited adipogenesis by suppression of intracellular lipid accumulation through upregulation of energy expenditure-related genes UCP1, PRDM16, and TMEM26, and down-regulation of the expression levels of adipogenic genes aP2, PPARγ, and Pref-1 via increased phosphorylation of AMPK (Li et al. 2019a).

Piperine (N-acyl piperidine) **117**, a major alkaloid constituent of Indian spice, black pepper (*Piper nigrum*) and long pepper (*Piper longum*) fruits, has hepatoprotective, cardioprotective, anti-obesity, and antidiabetic effects. In HFD-fed obese rats, piperine treatment in a suspension of 0.5% carboxymethyl cellulose (40 mg/kg/day) for 3 weeks significantly reduced body weight, epididymal and interscapular fat mass, and serum TG, TC, LDL, and VLDL levels and increased serum HDL level in obese rats. Piperine being a piperidine derivative, possibly acting as MC-4 agonistic agent, mitigates dyslipidemia in obese rats (Shah et al. 2011). In high carbohydrate and high fat-fed obese rats, piperine supplementation (30 mg/kg bw/day) for last 8 weeks of 16 weeks period of experiment significantly reduced elevated blood pressure, oxidative stress, and inflammation-induced cardiac and hepatic fibrosis in obese rats. Piperine decreased plasma NEFAs, ALT, ALP, CRP, and ROS levels, and increased plasma antioxidant GP_X levels, and reduced the collagen deposition in aortic rings and in walls of the left ventricle in obese rats. In addition, piperine reduced the infiltration of mast cells and its degranulation in aortic

rings for improvement of blood flow and both systolic and diastolic functions of the heart (Diwan et al. 2013). Another study reported that piperine increased resting metabolic rate of muscle by increasing the ATPase activity of fast twitch skeletal muscle skinned relaxed myocin fibers by 66 ± 15% with K_D of 2 μM through stimulation of myosin fibers from super-relaxed (SRX) state to disordered-relaxed (DRX) state or active state. This increased ATPase activity improves adaptive thermogenesis through upregulation of UCP-1 and other genes in skeletal muscle. These findings demonstrate that piperine ameliorates obesity and diabetes through increased resting muscle metabolic rate for fat and glucose metabolism (Nogara et al. 2016). In HFD-fed DIO mice, piperine treatment (30 mg/kg bw/day) for 12 weeks significantly reduced body weight, visceral adipose tissue (VAT), and subcutaneous adipose tissue (SAT) fat mass, serum FG (to a less extent), insulin, HOMA-IR, TG, TC, and LDL-C levels in DIO mice. Piperine down-regulated the expression levels of adipose tissue expansion (ATE)-related genes polymerase 1 and transcript release factor (PTRF), mesoderm-specific transcript (MEST), and secreted frizzled-related protein 5 (Sfrp 5), and lipogenesis-related genes FAS, SREBP-1c, C/EBPα, and FABP-4, and upregulated the expression levels of lipolysis-related genes ATGL, HSL, and LPL in adipose tissue of DIO mice. These findings indicate that piperine ameliorates obesity-related body fat mass by regulation of lipid metabolism through down-regulation of ATE and lipogenesis-related genes and upregulation of lipolysis-related genes in VAT and SAT of DIO mice (Du et al. 2020).

Trigonelline **345b**, a pyridine alkaloid and a major constituent of the seeds of fenugreek (*Trigonella foenum-graecum* L.), pumpkin, and *Mirabilis jalapa*, exhibited significant anti-obesity and antidiabetic effects. In STZ/HFD-fed type 2 diabetic rats, trigonelline on oral treatment (40 mg/kg bw/day) for 4 weeks significantly reduced serum glucose, HOMA-IR, FFA, TNF-α, and IL-6 levels and increased serum insulin and leptin levels in diabetic rats. Moreover, trigonelline increased the expression of PPARγ in adipose tissue, acting as PPARγ agonist to improve insulin sensitivity and glucose uptake via GLUT4 expression. In addition, trogonelline protected the pancreas by increasing the activity of antioxidant enzymes SOD, CAT, GSH, and GP_X, and decreasing the expression levels of ER-stress-related proapoptotic proteins CHOP, caspase 12, and caspase 3 in the pancreas of diabetic rats. These results suggest that trigonelline improves hyperglycemia by increasing insulin sensitivity in adipose tissue and insulin secretion from pancreatic β-cells (Tharaheswari et al. 2014). In STZ-induced type 1 diabetic mice, trigonelline treatment (70 mg/kg bw/day, *i.g.*) for 4 weeks significantly reduced the levels of serum glucose, inflammatory cytokines TNF-α, IL-6, and IL-1β, and increased the levels of serum insulin and adiponectin in diabetic rats. Trigonelline protected the pancreatic β-cells from apoptosis by decreasing the expression of proapoptotic protein caspase 3, and the level of MDA, and increasing the activity of antioxidant enzymes GSH, CAT, and SOD. Moreover, trigonelline increased β-cells mass and insulin secretion. Therefore, trigonelline exerts hypoglycemic effect in type 1 diabetic mice by increasing insulin secretion and insulin sensitivity in metabolic tissues via adiponectin secretion (Liu et al. 2018c). In STZ/HFD-induced obese diabetic rats, trigonelline supplementation (40 mg/kg bw/day) for 48 weeks significantly

improved diabetic peripheral neuropathy in rats by decreasing serum glucose, HbA1c, TC, and TG levels and increasing serum and sciatic nerves GLP-1R and SOD levels. In addition, trigonelline decreased the levels of phosphorylated p38MAPK proteins and MDA content in sciatic nerves, and increased tail flick latency in both cold and hot immersion tests, and both motor and sensory nerve conduction velocity (49.74 vs. 35.04 m/s, 51.76 vs. 40.17 m/s, respectively) compared to diabetic control group to improve motor nerve function. The effects of trigonelline in sciatic nerves were similar to sitagliptin (4 mg/kg bw/day) treated group. These findings suggest that trigonelline improves peripheral neuropathy through upregulation of the expression of GLP-1R proteins and down-regulation of p-p38MAPK kinases in sciatic nerves (Zhou and Zhou 2012). In STZ-induced diabetic nephropathy (DN) in type 2 diabetic rats, trigonelline treatment (40 mg/kg/day) for 8 weeks improved DN in rats by reduction of serum glucose, BUN, creatinine, and urinary albumin excretion levels. Moreover, trigonelline increased the activity of antioxidant enzymes SOD, GSH, and GP_X and reduced the levels of MDA and inflammatory cytokines IL-1β, IL-6, and IL-18 and the expression of pro-apoptotic proteins p53, Bax, caspase 3, and caspase 9 in kidney tissues. In addition, trigonelline suppressed the secretion of leptin and TNF-α, and increased the expression of GLUT4 and PPARγ in adipose tissue. These findings suggest that trigonelline improves DN by suppression of oxidative stress, inflammation, and expression of pro-apoptotic proteins in kidney and adipose tissues via PPAR-γ-dependent insulin sensitivity in kidney and adipose tissues (Li et al. 2019a, b).

Capsaicin **49**, a major pungent alkaloid constituent of hot chili peppers (*Capsicum frutescens*, *C. annuum*, *C. chinense*), has significant anti-obesity and antidiabetic effects. In vitro, capsaicin in obese mice adipocytes inhibited the expression levels of inflammatory cytokines IL-6 and MCP-1, and enhanced the expression of anti-inflammatory adiponectin via inactivation of NF-κB and activation of PPARγ. Moreover, capsaicin suppressed macrophage migration and activation in mesenteric adipose tissue culture-conditioned medium containing MCP-1 and RAW 264.7 macrophages. Thus, capsaicin attenuates obesity-induced inflammation and macrophage infiltration and activation in adipose tissue (Kang et al. 2007). In HFD-fed obese mice, capsaicin on supplementation in diet (0.015%) for 10 weeks reduced obesity-induced glucose intolerance and hepatic steatosis by reduction of serum FG, insulin, and leptin levels and inflammatory cytokines TNF-α, MCP-1, and IL-6 in the adipose tissue (AT) and liver, and increased adiponectin secretion in AT. Moreover, capsaicin decreased hepatic macrophage infiltration and TG levels, and increased transient receptor potential vanilloid type 1(TRPV1) expression in AT and PPARα expression in the liver. Accumulating evidence demonstrates that TRPV-1, a non-selective cation channel receptor of capsaicin, is highly expressed in neurons, pancreas, and intestinal tissues and cells, and associated with various functions of capsaicin including suppression of inflammatory adipokines from obese adipocytes and secretion of incretin-like hormones (GLP-1) from intestinal tissues. In vitro, capsazepine, an antagonist of TRPV-1, blocked the inhibitory effect of capsaicin on obesity-induced adipocyte inflammation. In addition, capsaicin increased FA oxidation in the liver by promoting the expression of PGC-1α, and

reduced insulin resistance in AT by increasing the expression of IRS-1 and GLUT4. These findings suggest that capsaicin improves insulin resistance in the AT and liver of obese mice, acting as TRPV-1 and PPARα agonist (Kang et al. 2010). The same group in another study reported that in genetically obese diabetic KK-Ay mice, capsaicin on supplementation in diet (0.015% of diet) for 3 weeks reduced both hyperglycemia and hyperlipidemia by increasing the expression of adiponectin and its receptor, AdipoR2, in the AT, which in turn, increased the phosphorylation of AMPK in the liver for enhanced FA oxidation. Activated AMPK increased the expression of PPARα and its target genes including CPT-1, and decreased the activity of hepatic lipid synthesis-related genes ACC and FAS. Therefore, capsaicin ameliorates obesity-related hepatic steatosis via AMPK activation (Kang et al. 2011a). The mechanism of anti-obesity effect of capsaicin via activation of TRPV-1 channel was studied in detail by Baskaran et al. (2016). In HFD-fed obese wild-type mice, capsaicin on supplementation in diet (0.01% of diet) for 32 weeks induced browning of white adipose tissue (WAT) via promoting energy expenditure, while such capsaicin supplementation in TRPV-1 null mice did not show any anti-obesity effect. This fact demonstrates that TRPV-1 activation of capsaicin plays a key role in its anti-obesity effect. In WT obese mice, capsaicin promoted thermogenesis in WAT by upregulation of the expression of thermogenic genes UCP-1 and bone morphogenetic protein 8b (BMP8b) via SIRT1 expression and activity and TRPV-1-dependent elevation of intracellular Ca^{2+} ions and phosphorylation of CaMKIIα and AMPKα. SIRT1 expression increased deacetylation of PPARγ and its transcription factor PRDM-16 to increase their interaction and enhanced expression of PGC-1α. PGC-1α plays a pivotal role in cellular energy metabolism and energy expenditure. Co-treatment of capsazepine, an antagonist of TRPV-1, decreased capsaicin-stimulated Ca^{2+} influx in the adipocytes of WAT. These findings suggest that capsaicin stimulates TRPV-1-dependent SIRT1 expression and deacetylation of PPARγ to promote thermogenesis and browning of WAT in obese WT mice (Baskaran et al. 2016). In both WT mice and TRPV1 knockout mice, dietary capsaicin on long-term treatment (0.01% of diet) for 24 weeks ameliorated hyperglycemia only in WT mice through insulin secretion, but not in TRPV1 knockout mice. In WT mice, capsaicin promoted TRPV1-mediated GLP-1 production from both intestinal enteroendocrine L-cells and gastrointestinal tract secretin tumor cell 1(STC-1) cells. Moreover, capsaicin treatment (0.01% of diet) in HFD-fed obese db/db mice for 14 weeks ameliorated hyperglycemia by increasing GLP-1 levels in plasma and ileum. In vitro, in STC-1 cells, co-treatment of intracellular Ca^{2+} ions channel blocker, BAPTA or EGTA, or TRPV1 blocker, capsazepine, inhibited the effect of capsaicin in GLP-1 secretion. These findings suggest that capsaicin-mediated TRPV1-activated GLP-1 secretion could be a promising approach in treatment of diabetes (Wang et al. 2012a). Capsaicin supplementation in diet to both WT mice (0.01% of diet) and spontaneously hypertensive rats (SHR) (0.02% of diet) for 6 months reduced elevated blood pressure (both systolic and diastolic) in both WT mice and SHR, while capsaicin treatment in TRPV1 null mice failed to reduce the blood pressue. In both WT mice and SHR, capsaicin increased the expression and activation of TRPV1 cation channel, and increased PKA

activation, eNOS phosphorylation, and NO production in mesenteric arteries for improvement of vasorelaxation process. In vitro, in isolated endothelium endothelial cells (ECs) from aortas of WT mice, co-treatment of Ca-channel blocker, BAPTA or EGTA, or TRPV1 blocker, 5′-iodo-resiniferatoxin (iRTX), inhibited the effect of capsaicin in eNOS phosphorylation. These findings indicate that TRPV1 activation increases intracellular Ca^{2+} influx for phosphorylation of eNOS. Moreover, significant increase of plasma levels of sensory nerve calcitonin gene-related peptide (CGRP) was found in SHR. Such effects of capsaicin were not found in TRPV1 null mice. Therefore, capsaicin-mediated endothelial TRPV1 activation is considered as a potential target for management of hypertension (Yang et al. 2010). In WT diet-induced obese mice, capsaicin supplementation in diet (0.01% of diet) for 12 weeks reduced metabolic endotoxemia by modulation of gut microbiota composition. Capsaicin increased the production of butyrate producing bacteria of Ruminococcaceae and Lachnospiraceae families, and decreased the Gram-negative LPS producing bacteria of S24-7 family, Bacteroidetes, for inhibition of LPS synthesis and chronic low-grade inflammation in adipose tissue (AT). Moreover, capsaicin reduced the expression of cannabinoid receptor type 1 (CBR1) proteins in the gut to improve gut-barrier integrity for reduction of permeability of endotoxic bacteria into blood. Therefore, capsaicin prevents the production and entry of metabolic endotoxemia for suppression of inflammation in AT in treatment of obesity (Kang et al. 2017).

Dihydrocapsaicin **144**, another pungent constituent of hot chili peppers, has been found to increase energy metabolism and thermogenesis in animal models. In SD rats, dihydrocapsaicin on treatment (3 mg/kg bw/day, *s.c.*) for 10 days decreased plasma glucose, FFAs, and glycerol levels by enhancement of energy metabolism and thermogenesis through activation of glycogen synthesis via secretion of β-adrenoreceptor in the liver and lipolytic action of β-adrenoreceptor in adipose tissues and visceral organs in rats through activation of sympathetic nerve systems, while capsaicin has no significant effect on plasma glucose level in rats (Imaizumi et al. 2011).

Capsiate **143**, a non-pungent chemical analogue of capsaicin having an ester bond instead of amide bond between vanillyl moiety and fatty acid chain, is found in high concentrations in sweet red pepper (*Capsicum annum* L.) fruits. Commercially available capsiate contains 63% capsiate, 30% dihydrocapsiate, and 7% nordihydrocapsiate. In SD rats, capsiate on oral administration (100 mg/kg bw/day) for 14 days reduced body weight and abdominal fat content by increasing mitochondrial aerobic ATP production and energy metabolism by suppressing UCP3 gene expression in both resting and exercise states and increasing the expression of thermogenic gene UCP1 in skeletal muscle. Possibly, capsiate increased the secretion of catecholamine to enhance energy metabolism and the activity of lipase and HSL in WAT for reduction of fat volume. Thus, capsiate regulates the expression of UCP3 and UCP1 in skeletal muscle of rats for the control of energy metabolism and reduction of fat accumulation (Faraut et al. 2009).

Mahanimbine **138**, a carbazole alkaloid isolated from the leaves of "meetineem," *Murraya koenigii*, has potential antidiabetic effect. The leaves of *M. koenigii*, locally

known as "curry patta," are traditionally used in India for treatment of diabetes. In STZ-induced diabetic rats, mahanimbine on administration (50 or 100 mg/kg bw/day, *i.p.*) for 30 days reduced elevated FBG and levels of serum lipids TG, TC, LDL, and VLDL, and increased serum HDL level in diabetic rats. In vitro, mahanimbine significantly inhibited the activity of dietary carbohydrate digesting enzymes, α-amylase with an IC_{50} value of 83.72 μg/ml, similar to that of acarbose (IC_{50} of 83.33 μg/ml), and weakly inhibited the activity of α-glucosidase with IC_{50} value of 99.89 μg/ml. These findings indicate that mahanimbine might be a candidate for treatment of both fasting and postprandial hyperglycemia and dyslipidemia in diabetes (Dineshkumar et al. 2010).

Koenidine **429**, another carbazole alkaloid constituent of *M. koenigii* leaves, exhibited antidiabetic effect in animal models. In STZ-induced diabetic rats, koenidine at a dose of 100 mg/kg bw reduced FBG by 30% after 24 h, compared to that of metformin (100 mg/kg bw) of 36% after 24 h. In leptin receptor-deficient db/db mice, koenidine treatment (30 mg/kg bw/day) for 15 days decreased postprandial BG and insulin levels by 40.5% and 17.3%, respectively, and these effects were comparable to that of pioglitazone (10 mg/kg bw/day) of 62.4% and 32.3%, respectively, used as positive control. In vitro, in L6 myotubes, koenidine increased glucose uptake and GLUT4 translocation to the plasma membrane, and increased the phosphorylation of Akt. Therefore, koenidine improves hyperglycemia by increasing glucose uptake in skeletal muscle of diabetic rats or mice. Another carbazole alkaloid *O*-methylmurrayamine A **430**, isolated from *M. koenigii* leaves, exhibited antidiabetic effect in animal model to a less extent because of less metabolic stability (Patel et al. 2016a).

Matrine **431**, a tetracycloquinolizidine alkaloid, is a major constituent of *Sophora flavescens* radix and other *Sophora* spp. In traditional Chinese medicine (TCM), *Sophora* radix has been used for treatment of viral hepatitis and hepatitis tumors. In HFD-fed obese mice, matrine on oral treatment (100 mg/kg bw/day, *i.g.*) for 4 weeks reduced glucose intolerance, plasma FG and insulin levels, and hepatic TG content and lipid mass in obese mice. Metformin (250 mg/kg bw) used as positive control showed less effect in improvement of fatty liver. In contrast to metformin, matrine neither suppressed mitochondrial respiration nor activated AMPK in the liver, but increased the expression and activation of hepatic heat shock protein 72 (HSP72), and inhibited the expression of inflammatory cytokine TNF-α in the liver. Moreover, matrine decreased the elevated expression of hepatic lipogenic genes ACC, FAS, SREBP-1, and SCD-1, and increased the expression of energy expenditure and FA oxidation-related genes UCP2 in the liver and UCP1 in the epididymal adipose tissue. Accumulating evidence demonstrates that HSP72 protects against obesity-induced hyperglycemia, glucose intolerance, and insulin resistance by suppression of inflammation and JNK phosphorylation and NF-κB activation in the liver and skeletal muscle, and prevents hepatic lipid accumulation by increasing mitochondrial health and function. Docking study revealed that matrine has a greater affinity with HSP90, a negative regulator of HSP72. These findings suggest that matrine upregulated the expression of HSP72 via inhibition of HSP90 expression for suppression of hepatic lipid accumulation. Matrine did not change the expression level

of hepatic ACOX1, a downstream target of PPARα, suggesting that PPARα pathway was not activated in liver of obese mice. Therefore, HSP72 is the key molecular target of matrine in suppression of hepatic steatosis and hyperglycemia in obese mice (Zeng et al. 2015). Matrine on pre-treatment (200 mg/kg bw/day, *p.o.*) to STZ-induced diabetic cardiomyopathy (DCM) rats for 10 days before STZ injection, and 8 weeks after STZ injection, improved cardiac function in left ventricular tissues by reducing left ventricular end diastolic pressure (LVEDP), and improving left ventricular systolic pressure (LVSP), maximum rate of increased pressure (+LVdP/dt_{max}), and maximum rate of decreased pressure (–LVdP/dt_{max}) via suppression of ROS/TLR-4/MyD88 signaling pathway in cardiac tissues. In vitro, in high glucose exposed myocytes, matrine decreased the intracellular ROS levels and expression levels of TLR-4, MyD88, cleaved caspase 8, and cleaved caspase 3, and increased antioxidant enzyme GP_X activity. These findings suggest that matrine protects diabetic (hyperglycaemic) myocytes from apoptosis by suppression of ROS/TLR-4/MyD88/caspase signaling pathway (Liu et al. 2015d). In HFD-induced obese mice, matrine on oral treatment (10 mg/kg of diet) for 12 weeks improved vascular endothelial function by reduction of the thickness of blood vessels inner walls via increased phosphorylation of Akt and eNOS and increased NO production. Moreover, matrine reduced the levels of serum lipid profile (TC, TG, and LDL) and inflammatory cytokines (TNF-α, IL-6, and others), and increased the levels of serum HDL and anti-inflammatory cytokine IL-10 in obese mice. In vitro, in ox-LDL exposed human umbilical vein endothelial cells (HUVECs), matrine reduced intracellular ROS accumulation and expression of LDH levels, inhibited the activity of PKCα and increased the phosphorylation of PI3K, Akt, and eNOS (ser1177 site), and increased NO production. Co-treatment of L-NAME, an eNOS inhibitor, or LY-294002, a PI3K inhibitor, inhibited the activity of matrine in eNOS phosphorylation and NO production, while co-treatment of GO6976, a PKCα inhibitor, did not alter the effect of matrine in eNOS phosphorylation. These findings suggest that matrine inhibits the activity of ox-LDL in PKCα activation and suppression of NO production via activation of PI3K/Akt/eNOS pathway. Therefore, matrine improves vasorelaxation of blood vessels by reduction of thickening of blood vessel walls and vascular injury via activated PI3K/Akt-dependent phosphorylation of eNOS (Zhang et al. 2019b).

Oxymatrine **432**, another quinolizidine alkaloid constituent of *Sophora flavescens*, has been shown to exhibit hypolipidemic effect in NAFLD (non-alcoholic fatty liver disease) rats. In HFD-fed NAFLD rats, oxymatrine on oral treatment (80 mg/kg/day) for 4 weeks reduced hepatic steatosis by reduction of body weight, visceral fat mass, liver TG content, and the levels of serum TC, TG, FFAs, and insulin, and enhanced glucose infusion rate (GIR). Oxymatrine increased the expression of PPARα as an agonist, and its target genes CPT-1α and microsomal triglyceride transfer protein (MTTP) in the liver to increase FA β-oxidation and export of lipoproteins VLDL and LDL from the liver for suppression of hepatic lipid content. The anti-hypertriglyceridemic effect of oxymatrine was better than that of fenofibrate, a PPARα agonist, treatment group (30 mg/kg/day), used as positive control. A group of evidence demonstrates that an increased expression of MTTP in

the liver reduces hepatic fat accumulation via increasing the export of lipoproteins from the liver. Therefore, hepatic mitochondrial PPARα activation is the key molecular target of oxymatrine in attenuation of NAFLD in rats (Shi et al. 2013).

Rutaecarpine **433**, a major indolopyridoquinazolinone alkaloid constituent of *Evodia rutaecarpa* fruits, has significant anti-obesity and antidiabetic effects. In 3T3-L1 adipocytes, rutaecarpine and its analogue reduced intracellular lipid accumulation by suppression of the expression levels of both adipogenic and lipogenic genes PPARγ, C/EBPα, SREBP-1c, ACC, FAS, and SCD-1 during adipocyte differentiation process via activation of AMPK (Chen et al. 2013). In both HFD-fed obese mice and leptin-deficient genetically obese ob/ob mice, rutaecarpine on treatment (20 mg/kg/day) for 4 weeks reduced food intake and body weight and serum glucose, TC, TG, insulin, and leptin levels and increased serum HDL-C levels. Moreover, rutaecarpine suppressed the expression levels of orexigenic (appetite stimulating) neuropeptides NPY and AgRP in the arcuate nucleus of hypothalamus in mice brain compared with the control group. In mouse neuroblastoma N29-4 cells, rutaecarpine significantly down-regulated the expression of NPY and AgRP compared with the control. These findings indicate that rutaecarpine ameliorates obesity-induced food intake in obese mice via suppression of the expression of orexigenic neuropeptides NPY and AgRP in hypothalamic brain of mice (Kim et al. 2009). In STZ/HFD-induced obese type 2 diabetic rats, rutaecarpine on oral treatment (25 mg/kg/day, *i.g.*) for 7 weeks significantly decreased visceral fat accumulation, and the elevated levels of serum TC, TG, and LDL-C and inflammatory factors TNF-α, IL-6, CRP, and MCP-1 in obese rats. These effects of rutaecarpine were similar to those of metformin treatment group (250 mg/kg/day). Both rutaecarpine and metformin increased insulin sensitivity in the liver by increasing the phosphorylation levels of PI3K and Akt, and decreasing the expression levels of inflammatory-related protein NF-κB in liver tissues. In rat skeletal muscle cells, both rutaecarpine and metformin increased glucose uptake and GLUT4 translocation to the plasma membrane, and increased the phosphorylation of AMPK and ACC2. Therefore, rutaecarpine ameliorates obesity-induced hyperlipidemia and hyperglycemia by increasing insulin sensitivity via activation of both PI3K/Akt and AMPK/ACC2 signaling pathways and might be effective for treatment obesity and diabetes (Nie et al. 2016).

Evodiamine **137**, another major alkaloid constituent of the fruits of *Evodia rutaecarpa* Benth, syn. *E. fructus*, has significant anti-obesity and antidiabetic effects. In HFD-fed UCP1 knockout obese mice, evodiamine on supplementation in diet (0.03% of diet, w/w) for 2 months reduced body weight gain, hepatic TG content, serum leptin level, and fat accumulation in the WAT, BAT, and liver of obese mice. Evodiamine increased ERK phosphorylation and inhibited insulin-stimulated Akt phosphorylation in the WAT of obese mice. In HepG2 cells, evodiamine increased ERK phosphorylation and decreased intracellular lipid accumulation. Therefore, evodiamine exhibits anti-obesity effect via ERK activation and suppression of adipocyte transcription factors and insulin-stimulated Akt activation in UCP1-independent pathway in adipocytes and liver (Wang et al. 2008). In 3T3-L1 preadipocytes, evodiamine inhibited adipogenesis by suppression of the activity of

PPARγ and its target genes via increasing the phosphorylation levels of epidermal growth factor receptor (EGFR), protein kinase C alpha (PKCα), and extracellular signal-regulated kinases (ERK). Co-treatment of AG1478, an EGFR inhibitor, or chelerythrine chloride, a PKCα inhibitor, inhibited the anti-adipogenesis activity of evodiamine, while co-treatment of capsazepine, an antagonist of TRPV-1, did not block the anti-adipogenic activity of evodiamine in 3T3-L1 cells. Thus, evodiamine being an agonist of TRPV-1 does not involve TRPV-1 gene in inhibition of adipogenesis. These findings suggest that evodiamine inhibits adipogenesis of 3T3-L1 adipocytes via activation of EGFR/PKCα/ERK signaling pathway (Wang et al. 2009a). In obese diabetic KK-Ay mice, evodiamine on treatment (3 mg/kg/day, *i.p.*) for 7 days improved glucose tolerance, and insulin sensitivity through stimulation of the phosphorylation of AMPK in the WAT, liver, and skeletal muscle and suppression of insulin stimulated phosphorylation of mammalian target of rapamycin (mTOR), ribosomal S6 protein kinase (S6K), and insulin receptor substrate 1 (IRS1) serine phosphorylation in the WAT and liver of diabetic mice. In vitro, in 3T3-L1 adipocytes, evodiamine suppressed the phosphorylation of mTOR, S6K, and IRS1 and Akt via AMPK activation. Therefore, evodiamine increases insulin sensitivity and glucose and lipid metabolism via AMPK signaling pathway in obese diabetic mice (Wang et al. 2013a).

Rohitukine **107**, a major chromone alkaloid constituent of Indian *Amoora rohituka* and *Dysoxylum binectariferum*, has been shown to exhibit various biological activities including anticancer, anti-inflammatory, and anti-obesity activities. In both 3T3-L1 and C3H10T1/2 adipocytes, rohitukine inhibited adipogenesis by suppression of intracellular lipid accumulation, and the expression levels of adipogenic and lipogenic genes PPARγ, C/EBPα, aP2, FAS, GLUT4, LPL, and SREBP-1c via inhibition of insulin-dependent Akt-mTOR phosphorylation. Moreover, rohitukine arrested the cell cycle process in S phase during mitotic clonal expansion by down-regulating the expression of cell growth-related proteins cyclin-D and E, CDK4, and CDK2, and increasing the expression of anti-adipogenic factors GATA2 and Wnt3a in adipocytes. In HFD-fed obese Syrian golden hamsters, rohitukine on treatment (50 mg/kg/day) for 7 days reduced body weight gain, hepatic lipid droplets, and the levels of serum lipid profile (TG, TC, and LDL-C) in obese hamsters. Rohitukine increased the expression of hepatic LXRα gene and decreased the expression of hepatic cholesterol synthesis-related gene SREPB2 and its target genes HMGCR and LDLR, and the expression levels of TG synthesis-related genes PPARγ, FAS, aP2, and GLUT4 in adipose tissues. These findings suggest that rohitukine prevents dyslipidemia in obese hamsters by suppression of the expression levels of fatty acid synthesis and cholesterol synthesis-related genes in liver and adipose tissues (Varshney et al. 2014).

Berberine **48**, a major quaternary isoquinoline alkaloid constituent of *Coptis chinensis* rhizomes, has been used in TCM for treatment of diabetes. In rat skeletal muscle L6 cells, berberine increased glucose uptake by weakly stimulating insulin-dependent phosphorylation of Akt and strongly stimulating insulin-independent phosphorylation of AMPK and p38 MAPK. Co-treatment of wortmannin, a PI3K inhibitor, reduced the glucose uptake effect of berberine to a small extent, while

co-treatment of compound C, a AMPK inhibitor, or SB202190, a p38 MAPK inhibitor, significantly reduced the activity of berberine in glucose uptake. These findings indicate that berberine improves glucose uptake in L6 myotubes, by both insulin-dependent Akt activation and insulin-independent AMPK and p38 MAPK activation, the latter pathway being the dominant one (Cheng et al. 2006). In 3T3-L1 adipocytes, berberine inhibited adipocyte differentiation by suppression of intracellular lipid accumulation, and the expression levels of lipogenic genes, PPARγ, C/EBPα, FAS, SREBP-1c, aP2, 11β-HSD1, and GLUT4, and increased the phosphorylation of AMPK, ACC, and p38 MAPK. These findings indicate that berberine blocks adipocyte differentiation via activated AMPK and p38 MAPK-mediated phosphorylation of PPARγ and suppression of PPARγ activity in adipocytes. In rat hepatoma FAO cells, berberine increased glucose uptake and phosphorylation of both AMPK and p38 MAPK. In L6 myotubes, berberine increased glucose uptake, GLUT4 translocation to the plasma membrane, and AMPK phosphorylation. In diabetic db/db mice, berberine on oral treatment (560 mg/kg/day) for 7 days reduced body weight and improved glucose tolerance in diabetic mice. In HFD-fed obese rats, berberine on oral treatment (380 mg/kg/day, *i.g.*) for 2 weeks reduced body weight, visceral fat mass, and serum glucose, insulin, and TG levels. Moreover, berberine decreased the expression levels of adipogenic and lipogenic genes FAS, PPARγ, SREBP-1c, 11β-HSD1, and aP2 in adipose tissues, and increased the expression of FA oxidation and thermogenesis and glucose uptake-related genes PPARα, UCP2, PGC-1α, and GLUT4 in skeletal muscle as well as increased the phosphorylation of AMPK in the adipose tissue, liver, and muscle. The activity of berberine is different from that of metformin, which activates AMPK mainly in the liver. Therefore, berberine ameliorates diabetes and obesity via AMPK activation (Lee et al. 2006). Another study reported that berberine increased insulin sensitivity in both cellular and animal models by upregulation of the expression of insulin receptor (InsR) gene via activation of protein kinase C (PKC). In human HepG2 cells, berberine increased the expression of InsR and LDLR, and increased the activity of PKC. Co-treatment of calphostin C, a PKC inhibitor, reduced the effect of berberine in InsR expression, while co-treatment of UO126, a ERK inhibitor, completely abolished the effect of berberine in LDLR expression in HepG2 cells. Moreover, PKC inhibitors abrogated AMPK activation. Therefore, PKC activation is an upstream event of AMPK activation. Possibly, berberine increases Akt activation via activation of the cascade PKC-InsR-PI3K-Akt pathway. In STZ/HF-fed type 2 diabetic rats, berberine treatment (75 or 150 mg/kg/day) for 15 days reduced insulin resistance by reduction of serum FBG and insulin levels and upregulation of InsR expression and PKC activity in diabetic rats. Moreover, berberine increased insulin sensitivity in the liver by increasing the expression of InsR and LDLR and activity of PKC. This effect of berberine was also found in KK-Ay type 2 diabetic mice, but not in insulin-deficient type 1 diabetic mice. These findings suggest that berberine improves insulin resistance in type 2 diabetic rats/mice via increasing both InsR and LDLR expression through Akt and AMPK activation (Kong et al. 2009). In HFD-fed obese mice, both berberine and its parent *Rhizoma coptidis* ethanol extract (RC) on treatment (200 mg/kg/day) significantly reduced hyperglycemia and

hyperlipidemia by modulation of the composition of gut microbiota. Both berberine and RC decreased the degradation of dietary polysaccharides, and reduced the proportions of fecal Firmicutes and Bacteroidetes and intestinal microbe levels. Moreover, both berberine and RC increased the expression of fasting-induced adipose factor (Fiaf) for reduction of adipose tissue mass, and of the expression levels of mitochondrial β-oxidation, lipolysis, and energy metabolism-related genes AMPK, PGC-1α, UCP2, CPT-1α, ACOX, hydroxyacyl-CoA-dehydrogenase (Hadhb), and LPL in visceral adipose tissues. In vitro, both RC and berberine inhibited the growth of *Lactobacillus*, an important genus of Firmicutes under anaerobic conditions. Possibly, both RC and berberine exhibit anti-obesity effect, at least in part, through regulation of gut microbes in obese mice (Xie et al. 2011). In STZ-induced DN mice, berberine treatment (200 mg/kg bw/day) for 8 weeks attenuated kidney dysfunction by reduction of serum BUN and creatinine levels and urinary albumin excretion and increased urinary creatinine clearance through increased phosphorylation of AMPK in kidney tissues. Activated AMPK increased the antioxidant status in glomerular mesangial cells (GMCs) to reduce fibrosis and dysfunction of GMCs in DN mice. In human glomerular mesangial cells (HGMCs), berberine increased the phosphorylation of AMPK and the expression levels of LKB1 for suppression of fibrosis. HGMCs infected with LKB1 siRNA prevented berberine-induced AMPK activation. Therefore, berberine ameliorated kidney dysfunction in diabetic mice via LKB1-mediated AMPK activation (Zhao et al. 2014). In another study, in high glucose exposed GMCs, berberine decreased the levels of fibrosis by increasing the activation of G-protein-coupled bile acid receptor 5 (TGR5) for suppression of the activity of sphingosine 1 phosphate (S1P) and its receptor 2 (S1PR2), and the phosphorylation levels of c-Jun (JNK)/ c-Fos (a member of p38 MAPK family) in GMCs. Deactivation of c-Jun/c-Fos suppressed the expression levels of pro-fibrogenic proteins fibronectin (FN), ICAM-1, and TGF-β1 in GMCs. Accumulating evidence demonstrates that S1P is a regulator of many pathophysiological processes, including cancer and diabetes via NF-κB activation and inflammation generation through binding to its receptor S1PR2. TGR5 controls the expression levels of S1P and its receptor. Infection of GMCs with TGR5 siRNA blocked the activity of berberine in S1PR2 degradation, while co-treatment of INT-777, a TGR5 agonist, increased the activity of berberine in suppression of FN, ICAM-1, and TGF-β1 proteins content in GMCs. Therefore, renoprotective effect of berberine depends on TGR5 activation (Yang et al. 2016c). In human umbilical vein endothelial cells (HUVECs), berberine increased nitric oxide (NO) production through enhanced phosphorylation of endothelial nitric oxide synthase (eNOS) and its interaction with heat shock protein 90 (HSP90) via AMPK phosphorylation. Pre-treatment of compound C, a specific inhibitor of AMPK, or L-NAME, an inhibitor of eNOS, blocked berberine-induced phosphorylation of eNOS at Ser1177, and its interaction with HSP90, leading to markedly reduced NO production. In high glucose exposed HUVECs, berberine reduced cellular apoptosis, NF-κB activation, and expression of inflammatory adhesion molecules VCAM-1 and ICAM-1 for suppression of the attachment of monocytes THP1 to endothelial cells. Moreover, berberine reduced intracellular ROS

accumulation, and increased the phosphorylation of AMPK and eNOS, and the expression of antioxidant enzymes GP_X, SOD, and CAT in HUVECs. In high glucose exposed isolated rat aorta, berberine stimulated vasodilation, and prevented vascular injury through increased phosphorylation of AMPK and eNOS. Therefore, berberine could be useful in treatment of diabetes-related endothelial dysfunction and cardiovascular diseases (Wang et al. 2009b).

Vindoline **434**, an indole alkaloid constituent of the leaves of traditional antidiabetic herb, *Catharanthus roseus*, syn. *Vinca rosea*, also known as Madagascar periwinkle, has been reported to possess significant antidiabetic effect in animal models. In insulinoma MIN6 cells and isolated rat pancreatic islets, vindoline increased glucose-stimulated insulin secretion with an EC_{50} value of 50 μM. It also protected pancreatic β-cells from inflammatory cytokines-induced apoptosis and increased intracellular Ca^{2+} influx through L-type Ca-channel and suppressed the voltage-dependent outward K-currents for improvement of insulin secretion. In STZ/HFD-induced type 2 diabetic rats, vindoline treatment (20 mg/kg/day) for 4 weeks decreased hyperglycemia by reduction of serum FG, HbA1c, and TG levels and increased serum insulin level, as well as increased oral glucose tolerance in diabetic rats. In addition, vindoline increased β-cells mass and function (Yao et al. 2013). Another study reported that vindoline improved both hepatic and pancreatic function for amelioration of hyperglycemia and hypertriglyceridemia in diabetic rats. In STZ-induced diabetic male Wistar rats, vindoline on oral treatment (20 mg/kg/day) for 6 weeks reduced serum glucose and TG levels, hepatic TG content, inflammatory cytokines TNF-α and IL-6, hepatic injury marker enzymes ALT, AST, and ALP, and serum insulin level in diabetic rats. Moreover, vindoline suppressed the expression of hepatic pro-apoptotic enzyme caspase 9, and reduced the MDA level, and increased the activity of antioxidant enzymes SOD, CAT, and GSR and ORAC levels for protection of hepatic tissues from injury. Vindoline also increased insulin secretion from pancreatic β-cells and protected the pancreas from injury by increasing the activity of antioxidant enzymes including SOD. These effects of vindoline were comparable to that of glibenclamide-treated diabetic rats (5 mg/kg/day). These findings suggest that vindoline improves hyperglycemia by protection of hepatic and pancreatic tissues from inflammation and oxidative stress (Goboza et al. 2019). In STZ-induced diabetic kidney and cardiovascular hypertrophy in rats, vindoline treatment (20 mg/kg/day) for 6 weeks improved both kidney and cardiac functions by reduction of serum glucose, lipid profile (TG, TC, LDL-C, VLDL-C), urea and creatinine levels, and atherogenic index, and increased serum HDL-C level in diabetic rats. Vindoline reduced the level of inflammatory cytokine TNF-α in both kidney and hearts, and increased the activity of antioxidant enzyme SOD and ORAC level, and decreased the expression of caspase 9 and MDA levels, and glomerular space area in kidney tissues for protection of kidney from injury. Therefore, vindoline is effective in treatment of diabetes and its associated complications (Oguntibeju et al. 2019).

Cinchonine **139**, a quinoline alkaloid constituent of cinchona bark (*Cinchona officinalis*), has potential anti-obesity effect in animal model. In HFD-fed obese C57BL/6N mice, cinchonine on supplementation in diet (0.05% of diet) for

10 weeks reduced body weight by 38%, visceral fat-pad mass by 26%, and levels of plasma glucose, TG, TC, FFAs, and hepatic TC and TG contents compared to HFD-fed control group. Cinchonine significantly suppressed adipogenesis by down-regulation of the expression levels of key adipogenic genes, PPARγ2, C/EBPα, SREBP1c, and FoxO1, and their target genes leptin, aP2, and LPL in epididymal adipose tissue (EAT) of obese mice via upregulation of the expression of Wingless-type MMTV integration site, family member 10b (Wnt10b) and β-catenin, and down-regulation of the expression of galanin (Gal) and its receptors GalR1 and GalR2, and their target proteins PKCδ, cyclin D, and others, related to adipogenesis. Further, cinchonine reduced the inflammation levels by decreasing the expression levels of pro-inflammatory transcription factors IRF5 and their downstream target cytokines TNFα, IFNα, and IL-6 via suppression of the expression of TLR2, TLR4, MyD88, TNF receptor associated factor 6 (TRAF6), and TIR-domain-containing adapter-inducing interferon β (TRIF) in EAT. A group of evidence demonstrates that an elevated expression of Wnt10b stimulates the expression of β-catenin to block the expression of PPARγ and C/EBPα and their target genes for inhibition of adipogenesis in AT, while an elevated expression of Gal and its receptors GalR1 and GalR2 promotes PKCδ activation for stimulation of ERK phosphorylation, leading to an increased expression of adipogenic regulators PPARγ and C/EBPα and their target genes. An increased expression of TLR2 and TLR4 promotes inflammatory signaling pathways through MyD88-dependent and MyD88-independent pathways for increased expression of TRAF6 and TRIF, leading to NF-κB activation and induction of inflammatory cytokines production. Therefore, cinchonine promotes Wnt signaling cascades for suppression of galanin signaling-dependent adipogenesis, and TLR2- and TLR4-mediated pro-inflammatory signaling pathways for suppression of inflammation in EAT of obese mice (Jung et al. 2012).

5.2.12 Terpenoids

Natural terpenoids are known as isoprenoids because these compounds are biosynthesized in plants by condensation of isoprene units, isopentenyl pyrophosphate (IPP) and dimethylallyl pyrophosphate (DMAPP). Condensation of these two isoprene units produces 10-carbon-skeleton geranyl pyrophosphate (GPP), an intermediate precursor of all monoterpenes. Sequential addition of further isoprene units to GPP leads to sesquiterpenes (C_{15}), diterpenes (C_{20}), triterpenes (C_{30}), and tetraterpenes (C_{40}), respectively. Several terpenoids have been reported to possess significant anti-obesity and antidiabetic effects through regulation of key pathopharmacological targets of obesity and diabetes including PPARs pathways, NF-κB signaling pathway, insulin, and AMPK signaling pathways for maintenance of glucose and lipid homeostasis in both in vitro and in vivo models.

5.2.12.1 Monoterperpenoids

Most of the monoterpenoids exist in acyclic or cyclic forms as hydrocarbons, phenols, acids, esters, or glycosides.

D-Limonene **435**, a monoterpene, found in high concentrations in citrus fruits including grapes, oranges, and lemons, has significant anti-obesity and antidiabetic effects. In HFD-fed obese mice, D-limonene on supplementation in diet (0.5% of diet) for 4 weeks reduced the size of both white and brown adipocytes, hepatic lipid accumulation, and the levels of serum glucose, TC, TG, LDL-C, and increased serum HDL-C in obese mice. D-Limonene suppressed the expression levels of lipid synthesis-related genes, LXRβ, and its target genes SREBP-1c, ApoE, HMGCR, and ABCA1, and increased the expression of FA β-oxidation-related genes PPARα, PGC-1α, and UCP2 in the liver for suppression of hepatic lipid mass. Apolipoprotein E (ApoE) plays a key role in catabolism of TG-rich lipoproteins in both adipocytes and hepatocytes. Therefore, D-limonene improves insulin resistance and lipid metabolism through activation of LXRβ and PPARα signaling pathways (Jing et al. 2013). In STZ-induced diabetic rats, D-limonene on oral treatment (100 or 200 mg/kg bw/day) for 45 days reduced plasma glucose and HbA1c levels, and increased liver glycogen content in diabetic rats. Moreover, D-limonene increased the expression of glycolysis-related enzyme GCK, and decreased the expression and activity of gluconeogenic enzymes G6Pase and FBPase in the liver of diabetic rats. The lower dose (100 mg/kg) was more effective. The antidiabetic effect of D-limonene was comparable with glibenclamide (600 μg/kg bw) treated diabetic group. Therefore, D-limonene mitigates hyperglycemia through regulation of carbohydrate metabolism-related genes in diabetic rats (Murari and Saravanan 2012).

Carvacrol **436**, a monoterpene phenolic constituent found as a major active constituent in essential oil of many aromatic plants in high concentrations, such as in *Lavandula multifida*, *Coridothymus capitatus*, *Origanum syriacum*, and other *Origanum* spp., and *Thymus eigii* and *T. vulgaris*, has potential anti-obesity and antidiabetic effects. In HFD-fed obese mice, carvacrol supplementation in diet (0.1% of diet) for 10 weeks reduced body weight gain, visceral fat-pad mass, and plasma and hepatic TG and TC levels in obese mice. Carvacrol decreased the expression levels of adipogenesis-related genes SREBP-1c, PPARγ2, C/EBPα, LXR, leptin, aP2, LPL, bone morphogenetic protein receptor (BMPR), fibroblast growth factor receptor 1(FGFR1), cathepsin S, galanin receptor 1(GalR1), GalR2, and PKCδ in epididymal adipose tissue (EAT), and increased the expression levels of thermogenesis and FA oxidation-related genes SIRT1, PGC-1α, RXR, UCP1, and UCP3 in retroperitoneal AT (RAT) of obese mice. In addition, carvacrol suppressed the expression levels of inflammation-related genes TLR2, TLR4, MyD88, TRIF, TRAF6, IRF5, and TNFα and phosphorylation levels of ERK1/2 in EAT. A group of evidence demonstrates that elevated expressions of BMPR, FGFR1, GalR1, and GalR2 in AT promote adipogenesis in adipocytes by induction of adipogenic factors. Moreover, an elevated expression of TLR2 and TLR4 stimulates the activation of NF-κB in both MyD88-dependent and MyD88-independent pathways for generation of inflammatory cytokines. Therefore, carvacrol prevents obesity by suppression of

adipogenesis and inflammation in AT of obese mice (Cho et al. 2012). In STZ-induced type 1 diabetic mice, carvacrol treatment (20 mg/kg bw/day. *i.p.*) for 6 weeks reduced hyperglycemia by reduction of serum FG, PG, LDH, and TG levels and increased serum insulin level in diabetic mice. Carvacrol upregulated the expression of hepatic glucose metabolism (glycolysis and oxidation)-related genes HK, 6-phosphofructokinase (PFK) and citrate synthase (CS) in diabetic mice. Therefore, carvacrol ameliorates hyperglycemia through regulation of hepatic glucose utilization enzyme activities (Li et al. 2020). In both STZ-induced type 1 diabetic (T1DM) mice and db/db type 2 diabetic (T2DM) mice, carvacrol treatment (20 mg/kg/day) for 6 weeks delayed the progression of diabetic cardiomyopathy (DCM) in mice by reduction of cardiac hypertrophy and fibrosis, the levels of natriuretic peptide A (NPPA), and myosin heavy chain-beta (MYH7), cardiac hypertrophic markers, and serum glucose and TC levels in both types of diabetic mice. NPPA is secreted in cardiac atria and increases stretching of atrial wall by increasing atrial blood volume, while MYH-7 plays a key role in cardiac muscle contraction due to obstructive blood flow from septum hypertrophy. Moreover, carvacrol increased the chamber size of LV (left ventricle) and RV, decreased both systolic and diastolic pressure, and reduced the thickness of both LV anterior wall (LVAW) and LV posterior wall (LVPW), and increased the ratio of E/A, LV vasorelaxation filling velocity (E) (diastolic filling) and atrial contraction flow velocity (A) (atrial filling) in T2DM mice. In both T1DM and T2DM mice, carvacrol increased the phosphorylation of PI3K, PKD1, Akt, and AS160, and translocation of GLUT4 into plasma membrane, and decreased the phosphorylation of PTEN, a negative regulator of Akt signaling pathway. These findings suggest that carvacrol protects diabetic hearts from DCM via activation of PI3K/Akt/GLUT4 signaling pathway in cardiomyocytes (Hou et al. 2019). Transient receptor potential melastatin related 7 (TRPM-7) proteins are major Ca^{2+} permeable channels and are expressed in kidneys, brain, and hearts and act as biological sensors against oxidative stress. Its overexpression in human atrial myofibroblast promotes upregulation of currents and Ca^{2+} influx, proliferation, and differentiation of myofibroblasts and expression of TGF-β1, leading to fibrogenesis and apoptosis of cells. In human embryonic kidney (HEK)-293 cells, carvacrol inhibited the activity of TRPM-7 by suppression of both inward and outward current with an IC_{50} value of 306 μM. Carvacrol also inhibited the activity of TRPM7 in brain hippocampal CA3-CA1 neuron cells. Possibly, carvacrol protects renal tubular cells, brain neuron cells, and cardiomyocytes from apoptosis by suppression of TRPM-7 activity and reduction of hypertension (Parnas et al. 2009; Du et al. 2010).

Thymol **437**, a monoterpene phenol found in many aromatic plants, including thyme (*Thymus vulgaris*) and other *Thymus* spp., *Ocimum gratissimum*, and *Nigella sativa*, has significant anti-obesity and antidiabetic effects. In HFD-fed type 2 diabetic mice, thymol on oral treatment (20 or 40 mg/kg bw/day) for 5 weeks reduced body weight gain, food intake, levels of plasma glucose, HbA1c, insulin, TG, TC, FFAs, PLs, LDL-C, and leptin, and increased plasma HDL-C and adiponectin levels in diabetic mice. Thymol reduced hepatic lipid content by down-regulation of the expression levels of lipid synthesis-related genes FAS, HMGCR, and G6PD, and

upregulation of the expression levels of lipolysis-related genes LCAT and LPL, and FA β-oxidation-related genes CPT1, malic enzyme (ME), and PAP in the liver of diabetic mice. Therefore, thymol ameliorates hyperglycemia and hyperlipidemia by regulation of lipid and glucose metabolism-related enzyme activities in liver via adiponectin-dependent insulin sensitivity (Saravanan and Pari 2015). Another study by the same group reported that in HFD-fed obese diabetic nephropathy (DN) mice, thymol on treatment (40 mg/kg bw/day, *i.g.*) for 5 weeks reduced kidney weight, levels of serum glucose, insulin, BUN, and creatinine, and levels of urinary proteins and urea, and increased serum proteins, serum and kidney antioxidant enzymes SOD, CAT, GP_X, and GSR, and non-enzymatic antioxidants Vit E, C, and GSH levels and urinary creatinine clearance in DN mice. Moreover, thymol decreased kidney lipid accumulation by reduction of the levels of TG, TC, FFAs, and PLs and suppression of the activity of lipogenesis-related genes SREBP-1c and its target genes, and fibrosis in renal tissues by reduction of expression levels of fibrogenic proteins TGF-β1 and VEGF in DN mice. Therefore, thymol exhibits nephroprotective effect by suppression of renal lipogenesis, fibrosis, and improved insulin resistance and oxidative stress (Saravanan and Pari 2016). In HF and high cholesterol-fed hyperlipidemic rabbits, thymol on treatment (3 or 6 mg/kg/day, *i.g.*) for 8 weeks improved aortic atherosclerotic lesions by reduction of aortic intimal thickening areas, and the levels of serum lipids (TG, TC, LDL-C), CRP, MDA, and inflammation-related cytokines, chemokines, adhesion molecules, and proteins TNFα, IL-1β, IL-6, TNFβ, VCAM-1, MCP-1, and MMP-9 in hyperlipidemic rabbits. These findings suggest that thymol improves atherosclerotic lesions in aortic walls by suppression of inflammation-related cytokines, chemokines, and adhesion molecules in aortic endothelium cells (Yu et al. 2016).

Amorfrutin B **438**, a monoterpene from liquorice (*Glycyrrhiza foetida*), has been reported to possess PPARs agonistic activity and antidiabetic property. Amorfrutin B strongly induced the transcriptional activity of PPARγ with binding affinity constant Ki of 19 nM and EC_{50} value of 73 nM, compared to that of rosiglitazone, Ki and EC_{50} of 7 and 4 nM, respectively, in reporter gene assay. Amorfrutin B also possessed weak binding affinity with PPARα and PPARβ/δ having binding affinity constant Ki, 2624 and 1782 nM, respectively. In HFD-fed DIO mice, amorfrutin B on supplementation in diet (100 mg/kg/day) for 4 weeks improved insulin resistance by reduction of serum glucose, insulin, TG, and NEFA levels in DIO mice. Moreover, amorfrutin B increased the expression levels of mitochondrial biogenesis and FA oxidation-related genes PPARα, PGC-1α, PGC-1β, and UCP3 in adipose tissue and reduced the expression of lipid uptake gene FABP4 and proinflammatory cytokine TNFα in the liver and adipose tissue. But amorfrutin B had no effect on plasma bone osteocalcin and endocrine hormones T3 and T4 levels. In human primary adipocytes, amorfrutin B induced the expression of adipogenic genes C/EBPα, C/EBPβ, FABP4, adiponectin, and FGF21. In FGF21 knockout mice, amorfrutin B increased insulin sensitizing effect. These findings suggest that amorfrutin B improves insulin sensitivity in a FGF21-independent PPARγ activation pathway (Weidner et al. 2013).

Geraniol **439**, an acyclic monoterpene alcohol present in high concentrations in essential oil of rose and lemon, has significant antidiabetic and anti-obesity effects. In STZ-induced diabetic rats, geraniol on oral treatment (200 mg/kg bw) for 45 days significantly improved hyperglycemia in diabetic rats by decreasing serum glucose and HbA1c levels, and increasing pancreatic insulin secretion, serum insulin level, and hepatic glycogen content. Moreover, geraniol increased the activity of glycolysis-related enzymes HK and G6PDH, decreased the activity of gluconeogenic enzymes G6Pase and FBPase in the liver and kidney, and protected pancreatic β-cells and increased insulin secretion in diabetic rats. These findings suggest that geraniol promotes insulin secretion and regulation of the activity of glucose metabolic genes in the liver and kidney for amelioration of hyperglycemia (Babukumar et al. 2017). In atherogenic diet (coconut oil, cholesterol, and cholic acid)-fed hyperlipidemic hamsters, geraniol treatment (100 or 200 mg/kg bw) for 12 weeks significantly decreased hyperlipidemia in hamsters by reduction of serum, liver, heart, and aortic TC, TG, FFAs, and PLs levels, and serum LDL-C, VLDL-C, and CRP levels, and increased serum HDL-C and LCAT levels. Moreover, geraniol decreased the expression of cholesterol synthesis-related gene HMGCR, and increased the expression of free cholesterol esterification enzyme LCAT and TG hydrolysis gene LPL in liver of hamsters. Therefore, geraniol regulates the expression of lipid metabolism-related genes for improvement of hyperlipidemia in hyperlepidemic hamsters (Jayachandran et al. 2015). In HFD-fed obese mice, geraniol treatment (20 mg/kg bw, *i.p.*), for 6 weeks improved endothelial dysfunction by reduction of oxidative stress-induced elevated expression of NOX2 proteins, ROS generation, and adhesion molecules VCAM-1 and ICAM-1 in aortic tissues for restoration of acetylcholine-induced vasorelaxation of aorta in obese mice (Wang et al. 2016b).

Paeoniflorin **440**, a monoterpene glucoside found as a major constituent in many medicinal plants, including *Paeonia lactiflora* and *Salvinia molesta*, showed a variety of pharmacological activities, including antioxidant, hepatoprotective, hypolipidemic, and hypoglycemic properties. In high fructose-fed hepatic steatosis rats, paeoniflorin on oral treatment (40 mg/kg, *i.g.*) for 8 weeks reduced hepatic lipid accumulation and AST levels and levels of serum glucose, insulin, HOMA-IR, glucagon, TG, TC, LDL-C, and NEFAs, and increased hepatic glycogen content in rats. Moreover, paeoniflorin decreased the expression levels of hepatic lipogenesis-related genes SREBP-1c, FAS, and SCD-1, and increased the expression levels of FA oxidation-related gene CPT-1 and others, and the phosphorylation levels of Akt, AMPK, and ACC1, and the expression of LKB1 proteins, an upstream of AMPK phosphorylation in the liver of fructose-fed diabetic hepatic steatosis in rats. The inhibitory effect of paeoniflorin on hepatic steatosis was similar to that of insulin-resistant pioglitazone-treated diabetic rats (20 mg/kg).These findings suggest that paeoniflorin reduces hepatic fat mass and improves hepatic glycogen synthesis via activation of LKB1/AMPK and insulin signaling pathways (Li et al. 2018c). In STZ-induced DN mice, paeoniflorin treatment (30 or 60 mg/kg bw, *i.p.*) for 10 weeks improved kidney function by reduction of urinary albumin excretion rate, increased urinary creatinine clearance rate, and inhibition of macrophage

infiltration via down-regulation of the expression levels of TLR2 and TLR4, and their downstream signaling molecules, MyD88, phosphorylated interleukin 1 receptor associated kinase 1 (p-IRAK1), TRIF, phospho-interferon regulating factor 3 (p-IRF3), and NF-κB-p-p65 in kidneys of diabetic mice. Moreover, paeoniflorin reduced the expression level of macrophage accumulation marker CD68 positive cells in the kidney tissues. In vitro, in AGEs-stimulated RAW 264.7 macrophage cells, paeoniflorin decreased the elevated expression levels of TLR2, TLR4, MyD88, p-IRAK1, TRIF, p-IRF3, NF-κBp-p65, and iNOS proteins. These findings indicate that paeoniflorin protects the kidneys in DN mice by suppression of macrophage infiltration and activation via suppression of TLR2/TLR4-mediated inflammation in renal tissues (Zhang et al. 2017).

Catalpol **120**, a monoterpene iridoid glucoside present in high concentrations in the roots of *Rehmannia glutinosa*, has been used in TCM for treatment of diabetes disorders for thousands of years. Catalpol has been reported to possess significant properties in prevention of diabetes and diabetic complications. In diabetic db/db mice, catalpol on oral treatment (80 or 160 mg/kg bw, *i.g.*) for 4 weeks improved insulin resistance by reduction of serum FG, HbA1c, TG, TC, insulin, and HOMA-IR levels, and increased serum adiponectin level in diabetic mice. Catalpol increased glucose uptake via GLUT4 translocation into plasma cell membrane in skeletal muscle and adipose tissue and increased the phosphorylation levels of AMPKα1/2 in liver, skeletal muscle, and adipose tissues. Moreover, catalpol decreased the expression levels of lipid synthesis-related genes ACC and HMGCR in the liver of diabetic mice. A group of evidence demonstrates that adiponectin improves glucose and lipid metabolism by activating its downstream factor AMPK. These findings suggest that catalpol ameliorates hyperglycemia and hyperlipidemia by improvement of insulin resistance via adiponectin-dependent AMPK activation in diabetic mice (Bao et al. 2016). In HFD-fed obese type 2 diabetic mice, catalpol on oral treatment (100 mg/kg) for 4 weeks reduced body weight gain, epididymal adipose tissue mass, and serum levels of FG and HOMA-IR, and suppressed the macrophage infiltration and expression levels of macrophage M1-related pro-inflammatory cytokines TNFα, IL-6, IL-1β, MCP-1, iNOS, and CD11c in adipose tissues. Moreover, catalpol increased the expression levels of M2-related anti-inflammatory genes arginase 1, IL-10, macrophage galactose-type lectin 1 (MGL1), and macrophage mannose receptor (MMR) in adipose tissues of obese mice. In addition, catalpol decreased the phosphorylation levels of JNK and IKKβ in epididdymal adipose tissues. These findings indicate that catalpol improves insulin resistance by suppression of inflammation in adipose tissues via inhibition of JNK and NF-κB signaling pathways (Zhou et al. 2015). In alloxan and diet-induced hyperlipidemic diabetic rabbits, catalpol treatment (5 mg/kg/day) for 12 weeks reduced atherosclerotic lesions (plaque) content in VSMCs of thoracic aorta by suppression of ECM deposition via down-regulation of the expression of TGF-β1 and collagen IV proteins and macrophage infiltration in neointimal vascular walls of aorta in diabetic rabbits. Moreover, catalpol reduced plasma glucose, insulin, HOMA-IR, lipids (TC, TG), inflammatory cytokines (TNFα, MCP-1, VCAM-1, and TGF-β1), and AGEs and MDA levels, and increased plasma antioxidant enzymes SOD and GSH-P_X

levels in diabetic rabbits. These antiatherosclerotic effects of catalpol were similar to that of metformin-treated (50 mg/kg/day) diabetic rabbits (Liu et al. 2016a).

Aucubin **119**, an iridoid glucoside, is present in high concentrations in the leaves of *Eucommia ulmoides*. *E. ulmoides* is consumed in Japan and China as teas for prevention of various diseases, including hypertension, osteoporosis, diabetes, and diabetic complications. In diabetic rats, aucubin on oral treatment (20 mg/kg) for 15 days improved hyperglycemia by reduction of serum glucose and increased insulin secretion from pancreatic β-cells. Aucubin protected the pancreatic β-cells from high glucose-induced oxidative stress by upregulation of the activity of antioxidant enzymes CAT, GP_X, and SOD, and reduction of MDA levels, and increased pancreatic β-cells mass and insulin secretion (Jin et al. 2008). In vitro, aucubin inhibited the formation of methylglyoxal (MGO) modified AGE-bovine serum albumin with IC_{50} of 0.57 mM and its cross-links to collagen with IC_{50} of 0.55 mM. In vivo, in MGO-injected rats, aucubin treatment (20 mg/kg) reduced AGEs burden in the blood, kidney, heart, and retina. These findings suggest that dietary consumption of aucubin delayed the progression of AGEs-related diabetic complications (Jung et al. 2019). In STZ and HFD-induced diabetic mice, aucubin on oral treatment (40 or 80 mg/kg/day) for 10 weeks improved renal function and renal injury by reduction of urinary albumin excretion, serum levels of glucose, BUN, creatinine, glomerular extracellular matrix expansion, and renal fibrosis in diabetic mice. Moreover, aucubin promoted antioxidant defenses in kidney tissues by increasing nuclear translocation of Nrf2 and FoxO3a for upregulation of the expression levels of antioxidant genes NQO1, HO-1, Mn-SOD, CAT, and GSH/T-GSH via induction of SIRT1 and SIRT3 activities. Aucubin increased deacetylation of FoxO3a by stimulating the expression of SIRT1 and SIRT3 for translocation of FoxO3a in nucleus for prevention of its damaging effect on kidney tissues. In addition, aucubin reduced the expression levels of pro-inflammatory cytokines TNFα, IL-1β, and IL-6 and nuclear accumulation level and phosphorylation of NF-κB-p65 proteins in kidney tissues for suppression of NF-κB activation. These findings suggest that aucubin ameliorates oxidative stress and inflammation in kidney tissues by upregulation of SIRT1 and SIRT3-mediated nuclear translocation of FoxO3a and Nrf2 proteins, and down-regulation of NF-κB activation (Ma et al. 2020).

Loganin **342**, an iridoid glucoside present in the fruits of *Cornus officinalis*, and other *Cornus* spp., and *Strychnos nux-vomica*, has significant antidiabetic and hepatoprotective effects. *Corni Fructus* (fruits of *C. officinalis*) are frequently prescribed in traditional Chinese, Japanese, and Korean medicines for treatment of diabetes and hepatic and kidney disorders. In high glucose and FoxO1-stimulating deoxycycline-exposed rat islet INS-1 cells, loganin markedly increased insulin secretion and Akt phosphorylation as well as increased phosphorylation of FoxO1 and its nuclear exclusion. Co-treatment of LY294002, a PI3K inhibitor, blocked the activity of loganin on insulin secretion and phosphorylation of FoxO1 and its nuclear exclusion. Accumulating evidence demonstrates that in pancreatic β-cells, forkhead box-containing protein O1 (FoxO1) on nuclear translocation by deacetylation under oxidative stress promotes β-cells apoptosis, and inhibits cell growth and insulin

secretion. Therefore, loganin improves impaired insulin secretion in diabetic pancreas by increasing Akt-dependent phosphorylation of FoxO1 and nuclear exclusion of FoxO1 in PI3K/Akt/FoxO1 signaling pathway (Mo et al. 2019). In type 2 diabetic db/db mice, loganin on oral treatment (100 mg/kg bw/day) for 8 weeks protected the hepatic tissues from oxidative stress, inflammation, and cell apoptosis by reduction of serum glucose, insulin, and oxidative stress-related elevated ROS and TBARS levels, increased serum leptin level, and the expression levels of hepatic antioxidant factors Nrf2 and HO-1 in diabetic mice. Moreover, loganin reduced the expression levels of inflammation-related factors MCP-1, NOX-4, p22phox, COX2, iNOS, and NF-κB-p65, and pro-apoptotic proteins Bax and cytochrome C, and increased the expression of anti-apoptotic proteins Bcl-2 in hepatic tissues of diabetic mice. Therefore, loganin exhibits hepatoprotective effect in diabetic mice through regulation of key protein expressions related to oxidative stress, inflammation, and apoptosis (Park et al. 2011a).

Morroniside **441**, another iridoid glucoside of *Corni Fructus*, exhibited significant hepatoprotective effect in diabetic liver in animal model study. In type 2 diabetic db/db mice, morroniside treatment (100 mg/kg bw/day, *p.o.*) for 8 weeks protected the hepatic tissues from injury by suppression of oxidative stress, inflammation, and apoptosis in the liver. Morroniside decreased the elevated levels of serum glucose and hepatic oxidative stress markers ROS, TBARS, and Nox-4, hepatic inflammatory genes and proteins Cox-2, iNOS, MCP-1, ICAM-1, and NF-κB-p65, and apoptosis-related proteins Bax and cytochrome C, and increased the expression levels of antioxidant proteins Nrf2 and HO-1 in liver tissues of diabetic mice (Park et al. 2011b).

Swertiamarin **442**, a major secoiridoid constituent of Asian herb, *Enicostemma littorale* Blume, and in other plants, has significant bioactivities against obesity and diabetes. In Indian traditional medicine, *E. littorale* has been prescribed for treatment of diabetes, swelling, rheumatism, and abdominal ulcers. In STZ-induced type 1 diabetic rats, both ELE (*E. littorale* aqueous ext) and swertiamarin on oral treatment (1.0 g and 50 mg/kg, respectively, *p.o.*, daily) for 3 weeks showed significant nephroprotective effect by improvement of kidney function by reduction of serum glucose, urea, creatinine, lipid profile, GPT, GOT levels, and glomerular hypertrophy and injury in diabetic rats (Sonawane et al. 2010). In high oleic acid exposed insulin-resistant and steatosis HepG2 cells, swertiamarin reduced intracellular TG accumulation, and the levels of LDH, and apoptosis-related proteins caspase 3 and PARP1 in HepG2 cells. Moreover, swertiamarin increased the expression levels of IR, PI3K, p-Akt, and p-AMPK and FA oxidation-related gene PPARα, and decreased the expression of gluconeogenic enzyme PEPCK and lipid synthesis-related genes PPARγ, SREBP-1c, ACC-1, and FAS in hepatocytes. Therefore, swertiamarin improves both glycemic burden and fat accumulation through activation of AMPK and insulin signaling pathways (Patel et al. 2016b). In nematode *Caenorhabditis elegans*, swertiamarin reduced hepatic fat accumulation. In *C. elegans*, swertiamarin reduced the fat accumulation by suppression of the expression level of fat storage-related gene 3-ketoacyl-CoA-thiolase-1 (Kat-1) in the intestine, the major fat storage tissue in *C. elegans*, for reduction of fat accumulation

in the intestine. Co-treatment of mutant Kat-1 RNAi or compound C, an antagonist of AMPK, significantly blocked the effect of swertiamarin in fat mass suppression in the intestine. Kat-1 is very similar to mammalian enzyme acetoacetyl CoA thiolase, encoded by ACAT1. ACAT1 on overexpression promotes uptake of intracellular free cholesterol and formation of cholesteryl esters for storage as lipid droplets and formation of atherosclerotic lesion area in aortas of hyperlipidemic mice. In HFD-fed obese mice, swertiamarin treatment (30 or 60 mg/kg) for 6 weeks reduced serum TG, TC, and LDL-C and hepatic TC and TG content and increased serum HDL-C level and hepatic glycogen content. Therefore, suppression of Kat-1 or ACAT1 could be a potential target for obesity treatment (Wang and He 2019).

Oleuropein **353**, a secoiridoid constituent in dietary olives (*Olea europaea*) and in other *Olea* spp., has been reported to possess various biological activities in prevention of obesity, diabetes, and cancers. In both basic and high palmitic acid exposed insulin-resistant skeletal muscle C2C12 cells, oleuropein enhanced glucose uptake and GLUT4 protein translocation to the plasma membrane, and increased phosphorylation of AMPK, but not Akt. In HFD-fed obese mice, oleuropein supplementation in diet (0.038% of diet) for 12 weeks reduced the weight of WAT and BAT, and the levels of serum FG, insulin, HOMA-IR, and NEFAs, and increased glucose uptake in skeletal muscle via increased GLUT4 translocation to plasma membrane in obese mice. These findings suggest that oleuropein improves insulin resistance in skeletal muscle through enhanced glucose uptake and upregulation of GLUT4 translocation in insulin-independent AMPK activation (Fujiwara et al. 2017). Another study reported that in high H_2O_2 exposed C2C12 muscle cells, oleuropein reduced the expression levels of oxidative stress markers ROS and TBARS, and increased the phosphorylation levels of AMPK and its downstream targets ACC and ERK to increase insulin sensitivity in C2C12 cells. These results suggest that oleuropein stimulates AMPK activation for suppression of oxidative stress and to increase insulin sensitivity in C2C12 cells (Hadrich et al. 2016). In HFD-fed DIO mice, oleuropein supplementation in diet (0.03% of diet, w/w) for 10 weeks significantly ameliorated hepatic steatosis by reduction of hepatic lipid mass, and inflammation as well as suppression of both hepatic and plasma TG, TC, and FFAs levels. Oleuropein reduced the hepatic lipid content by down-regulation of the expression levels of lipogenesis-related genes PPARγ2, C/EBPα, LXR, LPL, aP2, cyclin D, cathepsin S, SFRP5, E2F1, and DKK2 via suppression of the expression levels of their regulatory genes FGFR1 and p-ERK1/2, and upregulation of the expression levels of Wnt10b and β-catenin in the liver. Moreover, oleuropein reduced hepatic inflammation by suppression of the expression levels of pro-inflammatory cytokines TNFα, IL-1β, and IFNγ by down-regulation of the expression levels of TLR2, TLR4, and MyD88 for inhibition of TLR/MyD88 signaling pathway in the liver. A group of evidence demonstrates that suppression of the expression of SFRP5 and DKK2, negative regulators of Wnt10b activity, increases Wnt10b activation and β-catenin expression for reduction of the expression of adipogenic key gene PPARγ2. Moreover, reduced FGFR1 expression decreases p-levels of ERK for suppression of PPARγ expression via down-regulation of cyclin D and E2F1 protein expressions. These findings suggest that oleuropein improves hepatic steatosis in

DIO mice by suppression of hepatic lipogenesis and inflammation via regulation of Wnt10b, FGFR1, and TLR2/TLR4-dependent signaling pathways (Park et al. 2011c). Another study reported that in DIO mice, oleuropein treatment in diet (0.03% of diet) for 8 weeks reduced hepatic injury by suppression of oxidative stress and inflammation through upregulation of the activity of antioxidant enzymes SOD1 and SOD2 via increased expression of SIRT1 and SIRT3 in the liver of DIO mice (Santini et al. 2020).

5.2.12.2 Sesquiterpenoids

Zerumbone **444**, a sesquiterpene ketone, is found as a major constituent of *Zingiber zerumbet* Smith. In Southeast Asian countries, this plant has been used in folk medicine for treatment of ulcers, diabetes, and other inflammatory disorders. In HFD-fed obese hamsters, zerumbone treatment (300 mg/kg/day) for 8 weeks improved hepatic insulin resistance, steatosis, and inflammation by reduction of hepatic lipid accumulation and levels of inflammatory cytokines TNFα and IL-1β, plasma and hepatic TC and TG levels, plasma LDL-C, FFAs, and HOMA-IR levels, and increased plasma HDL-C level in obese hamsters. Zerumbone induced the expression levels of FA oxidation-related genes PPARα, CPT-1, ACO, and ACOX1, and decreased the expression levels of lipogenesis-related genes SREBP-1c, ACC1, FAS, and SCD1 in the liver of hamsters for suppression of hepatic lipid mass. These findings suggest that zerumbone improves hepatic insulin resistance and steatosis by regulation of the expression of lipid metabolism-related genes (Tzeng et al. 2013).

β-Caryophyllene (BCP), also known as *trans*-caryophyllene **445**, a bicyclic sesquiterpene present in the essential oil of several Asian plants, including oregano (*Origanum vulgare*), thyme (*Thymus vulgaris*), cloves (*Syzygium aromaticum*), black pepper (*Piper nigrum*), and cinnamon (*Cinnamomum cassia* syn. *C. tamala*), has been reported to possess various biological activities, including antidiabetic and anti-obesity effects. In STZ-induced diabetic rats, BCP on treatment (200 mg/kg bw/day) for 45 days significantly reduced elevated plasma glucose and HbA1c levels, and increased plasma insulin level and hepatic and muscle glycogen content in diabetic rats. Moreover, BCP increased the activity of glycogen synthesis-related gene GS, and down-regulated the expression of glycogen degrading gene GP (glycogen phosphorylase) in the liver and skeletal muscle for improvement of glycogen synthesis. In addition, BCP increased the activity of glycolysis-related genes HK, PC, and PK , and decreased the activity of gluconeogenic gene PEPCK in the liver of diabetic rats. Therefore, BCP improves glycemic control by regulation of the expression of genes related to carbohydrate metabolism (Basha and Sankaranarayanan 2014). In another study, in STZ-induced diabetic rats, BCP treatment reduced the elevated levels of glycoproteins fucose, sialic acid, hexose, and hexosamine in plasma, and of fucose, hexose, and hexosamine in hepatic and renal tissues, and increased the level of sialic acid in hepatic and renal tissues of diabetic rats. These glycoproteins are the markers of AGEs accumulation in diabetic tissues, and their elevated levels lead to the development of diabetic complications in the relevant tissues (Basha and Sankaranarayanan 2015). In high palmitate exposed

steatosis HepG2 cells, BCP prevented intracellular lipid accumulation, and increased the phosphorylation of AMPK and ACC1, decreased the expression levels of lipid synthesis-related genes SREBP-1c, FoxO1, and FAS, and increased the expression of TG hydrolysis-related gene ATGL in HepG2 cells. Moreover, BCP promoted the activity of cannabinoid type 2 receptor (CB2R)-dependent Ca^{2+} signaling pathway for activation of AMPK (Kamikubo et al. 2016). In HF and high fructose-diet fed obese Wistar rats, BCP treatment (30 mg/kg/day) for 4 weeks improved hyperglycemia, hyperlipidemia, and vascular oxidative stress and inflammation in obese rats. BCP significantly reduced the elevated levels of serum glucose, insulin, TC, TG, LDL-C, VLDL-C, and HOMA-IR, and increased serum HDL-C level, and suppressed the expression levels of inflammatory genes and proteins TNFα, VCAM-1, and NF-κB in vascular tissues of aorta in obese rats. Furthermore, BCP improved aortic vascular function by increasing the expression of eNOS and decreasing the expression of iNOS. BCP on binding to CB2R, and PPARγR, promoted the transcriptional activity of PGC-1α by increasing its deacetylation and to increase the expression of PPARα and its target genes for FA oxidation in liver via SIRT1 expression (Youssef et al. 2019). In mouse myoblast C2C12 cells, BCP increased glucose uptake, glycolysis, TCA cycle oxidative pathways, and mitochondrial ATP production by upregulation of the activity of glycolytic enzyme PDH, TCA cycle enzymes citrate synthase, aconitase, isocitrate dehydrogenase, succinate dehydrogenase, and electron transport chain through CB2R-dependent pathway. Co-treatment of AM630 or SR114528, antagonist of CB2R, significantly blocked the activity of BCP in glucose uptake, glycolysis, aerobic oxidation in TCA cycle and ATP production. Possibly, CB2R activation promoted AMPK activation for insulin-like activity of BCP in C2C12 cells (Geddo et al. 2021).

Germacrone (GM) **446**, a sesquiterpene ketone, present in high concentrations in Zedoary oil (*Curcuma zedoaria* Roscoe), and in other plants, including *Aster spathulifolius* Makim and *Garcinia cambogia*, has significant anti-obesity and antidiabetic effects. In HFD-fed obese mice, GM on oral administration (20 mg/kg/day) for 30 days reduced body weight gain, visceral fat-pad weight, elevated levels of plasma FG, insulin, leptin, TG, and TC, and hepatic lipid content, and increased the levels of serum adiponectin and HDL-C in obese mice. Moreover, GM decreased the expression levels of lipid synthesis-related genes SREBP-1c, PPARγ, ACC1, FAS, and SCD1 in adipose tissue, and increased the expression levels of FA oxidation-related genes PPARα, CPT-1β, ACOX1, UCP2, and UCP3 in skeletal muscle of obese mice. Further, GM increased the expression levels of p-AMPK, p-ACC, PPARα, and CPT-1α, and decreased the expression levels of lipogenesis and TG hydrolysis-related genes SREBP-1c, ACC1, FAS, SCD1, GPAT, and DGAT in the liver of obese mice. These findings suggest that GM attenuates hyperlipidemia by regulation of the expression of genes related to lipid metabolism via AMPK activation (Guo and Choung 2017a). In 3T3-L1 preadipocytes, GM inhibited intracellular lipid accumulation and adipogenic differentiation by down-regulation of the expression levels of adipogenesis-related genes C/EBPα, C/EBPβ, C/EBPδ, PPARγ, KLF4, and KLF5, and upregulation of the expression of lipolysis-related genes, p-AMPK, and its target genes including CPT-1 in 3T3-L1 cells.

Kruppel-like factor 4 and 5 (KLF4 and KLF5) are involved in the initial stages of adipogenesis (Guo and Choung 2017b).

Costunolide **10**, a sesquiterpene lactone, found in high concentrations in the rhizomes of *Costus speciosus* and *Saussurea lappa*, has significant antidiabetic and anticancer effects. The rhizomes of *C. speciosus* has been prescribed in traditional medicine in South Asian countries for treatment of diabetes, bronchitis, jaundice, syphilis, and chicken-pox. In STZ-induced diabetic rats, costunolide on oral treatment (20 mg/kg) for 30 days markedly reduced the elevated levels of serum FG, HbA1c, TC, TG, and LDL-C, and increased serum insulin, HDL-C, and protein levels, and glycogen content in skeletal muscle and liver of diabetic rats. Moreover, costunolide reduced plasma AST, ALT, ALP, and LDH levels near normal. These findings suggest that costunolide ameliorates hyperglycemia through improvement of insulin secretion and insulin action in peripheral tissues (Eliza et al. 2009). Another study reported that in high fructose-fed insulin-resistant rats, costunolide treatment (20 mg/kg) for 4 weeks improved liver and kidney function in insulin-resistant rats by increasing the activity of antioxidant enzymes SOD and GSH in the liver, and reducing the levels of serum creatinine and uric acid (Rashwan et al. 2019).

Farnesol **447**, an acyclic sesquiterpene alcohol, present in many dietary fruits and berries, including apricots, peaches, plums, blueberries, cranberries, raspberries, and strawberries, in vegetables, such as tomatoes, and in many plants including citronella (*Cymbopogon citratus*) and tuberose (*Polyanthus tuberosa* L.), has been reported to have anti-obesity and antidiabetic effects. In HFD-fed obese diabetic KK-Ay mice, farnesol on supplementation in diet (0.5% of diet) for 35 days significantly reduced hyperlipidemia, hyperglycemia, and hepatic steatosis by reduction of serum and liver TG and TC levels, hepatic lipid content, and serum glucose level in obese diabetic mice. Moreover, farnesol upregulated the expression levels of FA β-oxidation-related gene PPARα, and its target genes CPT1, ACO, ACS, and UCP2, and down-regulated the expression levels of lipid synthesis-related genes SREBP-1c and FAS in the liver of obese mice. In both wild-type and PPARα-deficient hepatocytes isolated from wild-type and PPARα knockout mice, farnesol stimulated the activity of farnesoid X-receptor (FXR) to increase the expression of small heterodimer partner (SHP) for suppression of the expression of SREBP-1c and FAS. These findings suggest that farnesol prevents hepatic steatosis and hyperlipidemia via activation of both PPARα and FXR signaling pathways (Goto et al. 2011). In both 3T3-L1 adipocytes and human adipose tissue-derived mesenchymal stem cells (hAMSCs), farnesol inhibited adipogenesis by suppression of intracellular lipid accumulation and the expression levels of key genes related to adipogenesis, namely, PPARγ and C/EBPα, and their target genes FABP4, adiponectin, resistin, and lipin1 through upregulation of the phosphorylation levels of AMPK and ACC. Moreover, farnesol increased the expression levels of UCP1 and PGC-1α in hAMSCs. Pre-treatment of compound C, an inhibitor of AMPK, reversed the effect of farnesol in suppression of PPARγ and C/EBPα expression. In HFD-fed obese mice, farnesol on oral treatment (5 mg/kg/day) for 12 weeks reduced adipose tissue weight and size of adipocytes in inguinal WAT (iWAT) and epididymal WAT (eWAT) in obese mice. In addition, farnesol decreased the expression levels of

adipogenesis-related genes PPARγ, C/EBPα, and lipin 1, and increased the expression levels of thermogenesis- and beige adipocyte-specific genes UCP-1, TMEM-26, TBX-1, and CD137, and the phosphorylation level of AMPK in both iWAT and eWAT of obese mice. These findings suggest that farnesol exerts anti-obesity effect by inhibition of adipogenesis and stimulation of browning process in WAT through AMPK signaling pathway (Kim et al. 2017a).

5.2.12.3 Diterpenoids

Carnosic acid (CA) **106**, a major abietane diterpene constituent of rosemary (*Rosmarinus officinalis*) and sage (*Salvia officinalis* L.), has potential activity in prevention of obesity and obesity-related hepatic steatosis. In palmitate-exposed steatosis HepG2 cells, CA suppressed intracellular lipid accumulation and the expression level and transcriptional activity of key adipogenic gene PPARγ, and expression levels of inflammatory cytokines IL-1β, IL-12, IL-17, IFN-γ, and MCP-1, and increased the phosphorylation levels of EGFR, MAPK(ERK1/2), and AMPKα. Pretreatment of AG1478, an inhibitor of EGFR, or U0126, an inhibitor of MEK/ERK, markedly abolished the effects of CA in lipid accumulation and expression and activity of PPARγ in HepG2 cells. Possibly, an increased phosphorylated-MAPK increased the phosphorylation of PPARγ to inhibit its expression and activity. In HFD-fed obese diabetic db/db mice, CA on supplementation in diet (0.05% of diet) for 5 weeks reduced hepatic lipid content, and increased the phosphorylation levels of AMPK, ACC, MAPK, and EGFR in the liver of obese diabetic mice. These findings suggest that CA prevents PPARγ-mediated hepatic steatosis by regulation of both AMPK and EGFR/MAPK signaling pathways (Wang et al. 2012b). In another study, in HFD-fed obese mice, CA supplementation in diet (0.02% of diet, w/w) for 12 weeks reduced body weight gain, weight of the WAT and liver, adipocyte size, and the levels of serum glucose, insulin, and lipid profile, and increased serum HDL-C level in obese mice. Moreover, CA decreased the expression levels of hepatic lipid synthesis-related genes SREBP-1c, liver-FABP, SCD1, and FAS, and increased the expression levels of hepatic β-oxidation-related genes PPARα, CPT1, and ACO, and reduced the contents of palmitic acid, palmitoleic acid, and oleic acid in liver tissues for suppression of hepatic lipid and FFAs content in obese mice. These findings suggest that CA improves diet-induced hepatic steatosis through regulation of fat metabolism via suppression of lipogenesis, and FA elongation, and increased fat oxidation in obese mice (Park and Mun 2013). A large body of evidence demonstrates that the expression level of myristoylated alanine-rich C kinase substrate (MARCKS), a major protein kinase C (PKC) substrate, is reduced significantly in hepatic steatosis and leads to an increased fat accumulation and inflammation in obese liver. It was substantiated by the fact that MARCKS-knockout mice fed a HF diet had high levels of pro-inflammatory cytokines and lipid accumulation in serum and liver tissues, compared to wild-type mice fed a HF diet. In HFD-fed obese NAFLD mice, CA on oral treatment (15 or 30 mg/kg bw/day) for 8 weeks reduced hepatic lipid accumulation, serum glucose, insulin, and lipid (TG, TC, NEFAs) levels, and the levels of pro-inflammatory cytokines (TNF-α, IL-2, IL-4, IL-6, IL-12, and IFN-γ) in the

serum and liver of obese mice. CA increased the expression level of MARCKS, and the level of FA oxidation-related gene PPARα, and decreased the expression levels of lipogenesis-related genes SREBP-1c, ACCα, FAS, and SCD1 in the liver of obese mice. Moreover, CA decreased the expression of PI3K, p-Akt, NLRP3 inflammasome, and p-NF-κB in the liver of obese mice. These findings indicate that CA prevents hepatic steatosis by upregulation of MARCKS expression, and MARCKS-dependent suppression of lipogenesis and inflammation via inhibition of PI3K/Akt, NLRP3/NF-κB, and SREBP-1c signaling pathways activation (Song et al. 2018).

Carnosol **448**, another phenolic abietane diterpene constituent of rosemary and sage, has potential antidiabetic and anti-obesity effects. Carnosol strongly inhibited the activity of pancreatic lipase (PL) with an IC_{50} value of 13 μM, while carnosic acid (CA) had relatively weak inhibitory effect against PL with IC_{50} value of 36 μM (Ninomiya et al. 2004). In HepG2 cells, carnosol inhibited intracellular TG synthesis by suppression of the activity of diacylglycerol acyltransferase (DGAT), a key enzyme that catalyzes the synthesis of TG from acetyl CoA and diacylglycerol, with an IC_{50} value of 39.5 μM (Cui et al. 2012). In STZ-induced diabetic rats, carnosol treatment (10 mg/kg/day, *i.p.*) for 4 weeks reduced the elevated levels of serum glucose, TG, TC, LDL-C, MDA, IL-6, and TNF-α, and increased the levels of serum HDL-C, and antioxidant enzymes GST, SOD, and CAT in diabetic rats. These findings suggest that carnosol ameliorates hyperglycemia by suppression of oxidative stress and inflammation (Samarghandian et al. 2017). In skeletal muscle L6 cells, carnosol increased glucose uptake and GLUT4 translocation to the plasma membrane and increased AMPK phosphorylation, but not Akt phosphorylation. Pre-treatment of compound C, an inhibitor of AMPK, significantly suppressed the activity of carnosol in GLUT4 translocation, while co-treatment of STO-609, an inhibitor of CaMKK, or 5z-oxozeaenone, an inhibitor of TAK-1, did not alter the effect of carnosol in glucose uptake and GLUT4 translocation. Moreover, carnosol did not alter the phosphorylation of LKB1 and Akt in L6 cells. These findings suggest that carnosol improves glucose uptake in L6 myotubes through an insulin-independent AMPK-dependent pathway (Vlavcheski et al. 2018).

Andrographolide (AGL) **335**, a labdane diterpenoid from South Asian herb *Andrographis paniculata* (Burm. F.) Nees (locally known as kalmegh), has potential anti-obesity effects. *A. paniculata* has been used in Indian Ayurvedic medicine for treatment of endocrine and liver disorders, colic pains, and hypertension. In high glucose exposed human HepG2 cells, AGL significantly reduced intracellular TC and TG accumulation. In HFD-fed obese mice, AGL on oral treatment (100 mg/kg/day, *i.g.*) for 4 weeks reduced body weight gain, weight of AT, adipocyte size of both WAT and BAT, levels of TC and TG in the serum and liver, and the levels of serum glucose, insulin, and LDL-C in obese mice. Moreover, AGL suppressed the expression levels of cholesterol synthesis-related gene SREBP2 and its target genes HMGCR, farnesyl diphosphate synthase (FDPS), farnesyl diphosphate farnesyltransterase-1 (FDFT-1), 24-dehydrocholesterol reductase (DHCR24), DHCR7, lanosterol synthase (LSS), and LDLR, as well as suppressed the expression levels of FA and TG synthesis-related gene SREBP-1c and its target genes ACC1,

FAS, SCD1, ACL, ACS, fatty acid desaturase 1 (FADS1), and FADS2 in the liver of obese mice. But AGL did not alter the expression levels of hepatic LXR and its target gene ABCG5-related to efflux and clearance of cholesterol. In addition, AGL increased the expression level of thermogenic gene UCP2 in BAT of obese mice. The hypolipidemic effect of AGL was similar to that of lovastatin (positive drug, 30 mg/kg/day) treated obese group. These findings suggest that AGL improves obesity via suppression of lipid synthesis and enhanced insulin sensitivity (Ding et al. 2014b). In 3T3-L1 preadipocytes, AGL inhibited adipogenesis by suppression of intracellular lipid accumulation and the expression levels of adipogenic genes C/EBPα, C/EBPβ, and PPARγ, and their target genes FAS and SCD via inhibition of PKA phosphorylation and CREB activation. Moreover, AGL suppressed the mitotic clonal expansion (MCE) by decreasing the expression of cell growth-related proteins cyclin A and E, and CDK2, and cell cycle arrest at G0/G1 phase (Chen et al. 2016a). In STZ/HFD-induced DN mice, AGL treatment (2 mg/kg, twice a week) for 8 weeks improved kidney function by reduction of kidney weight, glomerular hypertrophy, mesangial matrix expansion, urinary albumin excretion, levels of serum BUN, creatinine, glucose, and TG, and inflammation and ECM accumulation in renal tissues of DN mice. Moreover, AGL reduced the expression levels of oxidative stress-related markers NOX1, ROS, 4-hydroxynonenal (4-HNE), and inflammatory marker genes and proteins TNF-α, TGF-β1, fibronectin, F4/80, and NF-κB-p-p65, and increased Akt phosphorylation in renal tissues. These findings suggest that AGL ameliorates DN by suppression of oxidative stress and inflammation via Akt-mediated inactivation of NF-κB proteins in renal tissues (Ji et al. 2016).

Stevioside **449**, a diterpene glycoside from Latin American shrub *Stevia rebaudiana* Bertoni, has potential antidiabetic effect. In Southern Brazil and Northern Paraguay, the leaves of this plant have heen used commercially as a natural non-calorie sweetener, which are about 200–300 times sweeter than sucrose, and diterpene glycosides present in the leaves are responsible for this activity. In type 2 diabetic Goto-Kakizaki rats, stevioside on oral treatment (0.025 g/kg/day) for 6 weeks significantly reduced serum glucose (985 vs. 1575 in control mM/l after 3 h of administration) level and increased serum insulin (343 vs. 136 (control) μU/ml after 30 min of administration) and decreased serum glucagon levels, as well as reduced both systolic and diastolic blood pressures in diabetic rats. In INS-1 cells, stevioside increased insulin secretion. These findings suggest that stevioside ameliorates hyperglycemia and hypertension via increased insulin secretion and insulin action (Jeppesen et al. 2003). Another study reported that in both type 1 and type 2 diabetic rats, stevioside treatment (0.5 mg/kg, twice daily) for 15 days decreased serum glucose levels and the expression levels of hepatic gluconeogenic enzyme PEPCK in the liver of both types of diabetic rats (Chen et al. 2005). In double knockout (DKO) obese mice, stevioside on oral treatment (10 mg/kg/day) for 12 weeks showed significant antiatherosclerotic effect by reduction of serum glucose, insulin, and inflammatory cytokines TNF-α and IL-6 levels and plaque volume in aortic arch of obese mice. Stevioside decreased the levels of inflammatory factors MCP-1 and its receptor MCP-1R, macrophage, lipid content, and ox-LDL, and increased the expression levels of IRS1 and IRS2, adiponectin, and

antioxidant enzymes SOD1, SOD2, and SOD3 in vascular walls of aorta and increased insulin sensitivity in both vascular walls and adipose tissues. Moreover, stevioside increased glucose uptake via GLUT4 translocation to the plasma membrane, and the expression levels of lipogenesis-related genes PPARγ, FABP4, and LXRα in visceral adipose tissue and inhibited the inflammatory factor, activation of NF-κB. Possibly, an increased expression of LXRα promoted the expression of ABCA1 gene for clearance of cholesterol from the plaque area. These findings suggest that stevioside reduces aortic plaque area through increased insulin signaling in vascular walls of aorta and adipose tissue and suppression of oxidative stress and inflammation (Geeraert et al. 2010). In chronic thioacetamide (TAA)-induced liver injury in rats, stevioside treatment (20 mg/kg, twice daily along with TAA (200 mg/kg) for 8 weeks protected the liver from fibrosis by suppression of oxidative stress and inflammation. Stevioside suppressed the expression levels of pro-inflammatory cytokines IL-1β, IL-6, IL-17, and TNF-α, and protein kinase NF-κBp-65 and LPO, and increased the expression levels of antioxidant enzymes Nrf2, GSH, and GP_X in rat liver. In LPS or ethanol exposed hHSC and VL-17A cells, stevioside reduced the expression levels of inflammation-related genes and proteins TNF-α, IL-6, and NF-κB. In silico analysis, stevioside showed a strong interaction with TLR4-MD2 complex. Accumulating evidence indicates that TLR4 on binding to cell membrane protein, myeloid differentiation protein 2 (MD2) forms a fusion complex to inhibit the activity of LPS in pro-inflammatory signaling via NF-κB activation in liver. These findings suggest that stevioside prevents hepatic inflammation via inhibition of TLR4/MD2-mediated NF-κB activation (Casas-Grajales et al. 2019).

Borapetoside E (BE) **450**, a clerodane diterpenoid from *Tinospora crispa*, has significant antidiabetic and hypolipidemic effects. In Indian traditional medicine, *T. crispa* has been used in treatment of various disorders including diabetes. In STZ/HFD-fed type 2 diabetic mice, BE treatment (40 mg/kg, twice daily for 3 days and then once daily for 12 days) reduced insulin resistance and hepatic steatosis by reduction of hepatic lipid accumulation and TG content, and elevated levels of serum glucose, insulin, TG, TC, LDL-C, FFAs, CK (creatine kinase), and creatinine in diabetic mice. Moreover, BE down-regulated the expression levels of FA, TG, and cholesterol-synthesis-related genes SREBP-1 and SREBP2, and their downstream target genes FAS, ATP citrate lyase 1 (ACL1), HMGCR, and HMGCS in the liver and adipose tissue, and the expression of LXRα and its target genes ABCG5/8 in the liver of diabetic mice. Furthermore, BE promoted insulin signaling in the liver and skeletal muscle by increasing the phosphorylation levels of Akt and GSK-3β, and glucose uptake in skeletal muscle (Xu et al. 2017).

Borapetoside A (BA) **451**, and borapetoside C (BC) **172**, two more clerodane diterpenoids, isolated from *Tinospora crispa*, exhibited hypoglycemic effect; BA has stronger activity than BC. In STZ-induced type 2 diabetic mice, both BA and BC on oral treatment (5 mg/kg/day) for 7 days significantly reduced the elevated levels of serum glucose and increased serum insulin levels and glycogen content in skeletal muscle of diabetic mice. Moreover, both BA and BC increased the phosphorylation levels of IR and Akt, and the expression of GLUT2, and decreased the expression of gluconeogenic enzyme PEPCK in the liver of diabetic mice. These findings suggest

that both BA and BC ameliorate hyperglycemia by increasing insulin sensitivity in the liver and regulation of genes expression related to glucose metabolism (Ruan et al. 2012, 2013). BC strongly inhibited the activity of α-glucosidase with an IC_{50} value of 0.0527 mg/ml, and moderately inhibited the activity of α-amylase with an IC_{50} value of 0.775 mg/ml. Therefore, BC is more effective for suppression of postprandial hyperglycemia (Hamid et al. 2015).

Cryptotanshinone (CT) **452**, a major quinonoid diterpenoid of *Salvia miltiorrhiza* roots, has potential antidiabetic and anti-obesity effects. The root extracts of *S. miltiorrhiza* has been used in traditional medicine in Asian countries for treatment of several pathogenesis including cardiovascular diseases, hepatotitis, and hyperlipidemia. CT in C2C12 myotubes increased glucose uptake and GLUT4 translocation to the plasma membrane, and increased the phosphorylation level of AMPK. CT is a more rapid and active AMPK activator than metformin; only at 20 μM concentration, it increases AMPK activation within 30 mins, while metformin, at 2 mM concentration, increases AMPK activation after 12 h in C2C12 cells. Moreover, CT in both C2C12 cells and 3T3-L1 adipocytes increased glucose uptake in presence of insulin by increasing the phosphorylation levels of Akt and AMPKα, but not of PI3K, while this effect of CT on Akt and AMPK phosphorylation was markedly reduced on co-treatment of compound C, an inhibitor of AMPK. These findings suggest that CT increases glucose uptake in insulin-independent AMPK activation in both C2C12 myotubes and 3T3-L1 cells. Furthermore, long-term treatment of CT (6-12 h) in C2C12 cells reduced the expression levels of FA synthesis-related genes ACC1 and ACC2, and increased the expression levels of FA oxidation and thermogenesis-related genes PGC-1α, CPT-1, and UCP-2. In HFD-fed obese ob/ob (leptin-deficient) mice, CT on oral treatment (600 mg/kg/day) for 28 days reduced body weight gain, food intake, AT weight, hepatic lipid and TG content, and the levels of serum TG, TC, and glucose in obese mice. Oral treatment of CT (600 mg/kg/day) in diabetic db/db mice for 28 days reduced serum glucose level significantly. Moreover, CT increased the phosphorylation levels of AMPKα in AT of both obese and diabetic mice. These findings suggest that CT modulates the expression levels of genes related to glucose and lipid metabolism via AMPK activation for amelioration of obesity and diabetes (Kim et al. 2007). Another study reported that in 3T3-L1 pre-adipocytes, CT inhibited adipogenesis by markedly reducing intracellular lipid accumulation, and suppressing the expression of key adipogenic genes C/EBPβ, C/EBPα, and PPARγ, and their target genes aP2, adiponectin, and GLUT4, as well as by increasing the expression levels of anti-adipogenic genes GATA2 and CHOP10. Moreover, CT reduced the phosphorylation of STAT3 in the early phase of adipogenesis. Accumulating evidence demonstrates that both GATA2 and CHOP10, an ER stress response protein, reduce the DNA-binding activity of C/EBPβ and suppress its transcriptional activity in PPARγ and C/EBPα expression in 3T3-L1 cells. These results suggest that CT inhibits adipogenesis by suppression of the expression of adipogenic genes via suppression of STAT3 signaling pathway (Rahman et al. 2016).

5.2.12.4 Triterpenoids

Celastrol **78**, a pentacyclic triterpene constituent of the roots of thunder god vine, *Tripterygium wilfordii*, has potential anti-obesity and antidiabetic effects. In traditional Chinese medicine, the roots of *T. wilfordii*, has been prescribed for treatment of various disorders, including rheumatoid arthritis, fever, heavy menstrual flows, swelling, and psoriasis. In PGC-1α expressing mesenchymal 10T1/2 cell line, celastrol increased the activity of heat-shock factor-1 (HSF-1), and the expression levels of mitochondrial thermogenesis-related gene PGC-1α and its target genes UCP-1, CPT-1, PRDM-16, Cox4β, HSP70, and MCAD in 10T1/2 cells. Transfection of 10T1/2 cells with siRNA of HSF-1 markedly reduced the effect of celastrol in the expression of PGC-1α and its target genes. The majority of HSF-1, a circadian transcription factor gene, exists in a repressed state in association with molecular chaperones HSP90, HSP70, and HSP40, and distributed in peripheral metabolic tissues, such as in the adipose tissue, muscle, and liver. HSF-1 on activation in the adipose tissue, liver, and muscle binds to DNA and regulates mitochondrial function in fat oxidation and energy production by upregulation of the expression of its downstream gene PGC-1α and its target genes for reduction of insulin resistance and suppression of hepatic steatosis in obesity. In HFD-fed obese wild-type (WT) mice, celastrol treatment (3 mg/kg/day, *i.p.*) for 4 weeks reduced body weight gain, body fat mass, WAT and liver weights, and the levels of serum glucose, TC, and LDL-C in obese mice, but these effects of celastrol were not observed in HSF-1 knockout (KO) mice. Moreover, celastrol increased the expression levels of PGC-1α, UCP-1, MCAD, HSP70, Cidea, and PRDM16 in inguinal WAT (iWAT) and BAT of WT-obese mice. These findings suggest that celastrol ameliorates metabolic dysfunction in obesity by activation of HSF1/PGC-1α signaling pathway (Ma et al. 2015). Celastrol in human HeLA cells transfected with GAL4-HSF1 increased the activation of HSF1, on binding to HSF1 and forming a covalent adduct to activate HSF1 and increased the levels of HSF1-DNA binding to the heat shock element in the HSP70 promoter region for activation of HSP70 and other genes in vitro. Possibly, celastrol used its quinone methide chromophore to react with the thiol group of cysteine residues of HSF1 for binding (Westerheide et al. 2004). In HFD-fed DIO mice, celastrol administration (100 μg/kg/day, *i.p.* or *i.g.*) for 3 weeks reduced body weight and food intake up to 45%, by increasing leptin sensitivity in the hypothalamus, but it was ineffective in both leptin-deficient ob/ob mice and leptin receptor-deficient db/db mice models . Moreover, celastrol reduced fat mass and serum levels of glucose, insulin,TG,TC, and thyroid hormone T3 in obese mice compared to control group. Further, administration of a bolus dose of leptin along with celastrol in ob/ob mice led to a greater reduction of body weight compared to leptin plus celastrol treated DIO mice. Moreover, celastrol reduced hypothalamic ER stress by reduction of phosphorylation of protein kinase R (PKR)-like ER kinase (PERK) and the expression of sarco (endo) plasmic reticulum Ca^{2+} ATPase2B (SERCA2B). In addition, celastrol increased hypothalamic leptin sensitivity by increasing the phosphorylation of STAT3 in the hypothalamus of obese mice. These findings suggest that celastrol ameliorates obesity by increasing leptin sensitivity in the hypothalamus via activation of LepR-STAT3 signaling pathway (Liu

et al. 2015a). Celastrol on systemic administration (0.5 mg/kg) for 5 consecutive days in three different mouse models, DIO mice, genetically obese LepR null mice, and MC4R null mice, significantly reduced body weight, gonodal WAT mass, and food intake in both DIO and MC4R null mice, but relatively mild in LepR null mice. Celastrol steadily increased sympathetic nerve activity in brown fat and kidney tissue and consequently increased resting metabolic rate and atrial pressure for improvement of metabolic functions and cardiovascular disorders. Moreover, celastrol increased the expression of thermogenesis-related genes β3-adrenergic receptor (β3AR), PGC-1α, and PRDM16 in BAT and kidney of both DIO and MC4R null mice, and down-regulated the expression of vasoconstrictive marker gene, regulator of G-protein signaling 2 (RGS2) in MC4R null mice, but not in DIO mice. In addition, no significant changes in the expression levels of p-PERK and SERCA2 in the hypothalamus of DIO mice was observed, but decreased the expression levels of leptin resistance-related genes SOCS3 and PTP1B in DIO mice. These findings suggest that celastrol exhibits anti-obesity effect in a MC4R-independent pathway in addition to leptin receptor signaling for reduction of body weight (Saito et al. 2019). Another study reported that in HFD-fed obese mice, celastrol treatment (100 μg/kg/day, *i.p.*) for 21 days reduced both hyperglycemia and hyperlipidemia by improvement of insulin sensitivity and reduction of serum FG, insulin, HOMA-IR, fat- and food intake-related genes galanin (GAL) and galanin-like peptide (GALP) levels, and the expression levels of fat and food intake-related genes GAL, and its receptors GALR1/3, GALP, and NYP in the hypothalamus of obese mice. Moreover, celastrol increased glucose uptake and energy expenditure by increasing the expression levels of GLUT4, PGC-1α, and UCP-1 in adipose tissue and skeletal muscle, and decreased hepatic glucose production by suppression of the expression of gluconeogenic genes G6Pase and PEPCK in liver of obese mice. Furthermore, celastrol increased the phosphorylation of Akt and decreased the phosphorylation of ERK in adipose tissue, and increased the phosphorylation of p38MAPK and activating transcription factor 2 (ATF2) in skeletal muscle, and decreased the expression levels of p-CREB and PGC-1α in the liver of obese mice. These findings suggest that celastrol increased GLUT4 and PGC-1α activity via activation of Akt/ERK signaling pathway in adipose tissue and p38MAPK/ATF2-signaling in skeletal muscle, and decreased hepatic gluconeogenesis via suppression of p-CREB/PGC1α signaling pathway for amelioration of obesity (Fang et al. 2019).

Corosolic acid **206**, an ursane-type pentacyclic triterpene, isolated from the leaves of banaba (*Lagerstroemia speciosa* Linn), *Eriobotrya japonica*, *Vaccinium macrocarpon*, and *Rubus biflorus*, and from other plants, has potential antidiabetic, anti-obesity, and anti-inflammatory effects. Banaba leaves tea and its extracts have been used in traditional medicine in Southeast Asian countries for treatment of diabetes and kidney disorders. In L6 myotubes, corosolic acid increased insulin-stimulated glucose uptake and GLUT4 translocation to the plasma membrane by increasing the phosphorylation levels of IRS-1 and Akt, and inhibited the activity of PTP1B and T-cell PTP, negative regulators of insulin signaling. Co-treatment of wortmannin, a PI3K inhibitor, blocked the activity of corosolic acid in glucose

uptake, GLUT4 expression, and Akt phosphorylation in L6 cells (Shi et al. 2008). In HFD-fed genetically obese diabetic KK-Ay mice, corosolic acid on supplementation in diet (0.023% of diet) for 9 weeks reduced obesity and hepatic steatosis in obese mice by reduction of body weight by 10%, visceral and subcutaneous fat mass by 15%, and plasma levels of glucose, insulin, and TG by 23, 41, and 22%, respectively, and enhanced plasma adiponectin level by 16%. Moreover, corosolic acid increased the expression level of FA oxidation-related gene PPARα in the liver and the expression of PPARγ and AdipoR1 in WAT of diabetic mice. These findings suggest that corosolic acid improves hepatic steatosis by increasing insulin sensitivity in the liver and adipose tissue through adiponectin/AdipoR1-mediated pathway (Yamada et al. 2008). In HFD-fed obese mice, corosolic acid treatment (20 mg/kg/day) for 8 weeks reduced adipose tissue mass and adipocyte size, the levels of plasma FG, TG, TC, LDL-C, and FFAs, and inflammation in adipose tissue by suppression of the macrophage infiltration (F4/80 positive cells) and inflammatory cytokines TNF-α, IL-6, MCP-1, and p-IKKβ protein expression, and by increasing the phosphorylation levels of IRS at tyrosine sites and Akt and AMPK in adipose tissue of obese mice. In 3T3-L1 adipocytes, corosolic acid decreased the expression levels of inflammatory cytokines and p-Ikkβ, and increased the expression of LKB1 and p-AMPK. These results suggest that corosolic acid improves adipose tissue inflammation and insulin resistance via LKB1-dependent AMPK activation (Yang et al. 2016a). In STZ-induced type 2 diabetic rats, corosolic acid treatment (50 or 100 mg/kg) for 6 weeks reduced hyperglycemia and hyperlipidemia in diabetic rats by reduction of the elevated levels of serum FG, TC, TG, LDL-C, and FFAs, and increased levels of serum HDL-C and antioxidant enzyme SOD. In insulin-resistant HepG2 cells, corosolic acid increased glycogen content and reduced the expression of gluconeogenic enzyme PEPCK. These effects of corosolic acid in type 2 diabetic rats were similar to that of metformin (160 mg/kg) treatment group of diabetic rats. In cAMP and DEX-induced type 2 zebrafish model, corosolic acid increased the expression of glycolytic genes glycogen synthase 1(GS1) and PFKFB3, and decreased the expression of gluconeogenic gene PEPCK in the liver. These findings suggest that corosolic acid ameliorates hyperglycemia in diabetic rats by regulation of the expression of genes related to glucose metabolism (Xu et al. 2019).

Ursolic acid (UA) **52**, a pentacyclic triterpenoid present in high concentrations in many fruits and plants, such as rosemary (2.95 g/100 g of dry matter), basil (*Ocimum sanctum*) (9 g/100 g of dry acetone extract), cranberries (*Vaccinium macrocarpon*), blueberries (*Vaccinium* spp.), cherries (*Cornus* spp.), apples, pears (*Pyrus pyrifolia*), lavender, peppermint, and thyme, has potential biological activities, including anti-obesity and antidiabetic effects. In HFD-fed obese mice, UA on supplementation in diet (0.14% of diet) for 6 weeks reduced obesity and hepatic steatosis, and increased skeletal muscle and brown fat growth and energy expenditure by reduction of hepatic TG and lipid content, weight of WAT and liver, and the elevated levels of serum FG, hepatic toxic marker enzymes AST and ALT in obese mice. UA increased skeletal muscle growth and exercise capacity by increasing the phosphorylation of Akt and upregulation of its target genes HKII, VEGFA, and IGF-1 in muscle, and expression of thermogenic gene UCP-1 in BAT. In addition, UA

decreased the expression level of FA synthesis-related gene SREBP-1c and its downstream target genes FAS, ACC1, and SCD1 in liver of obese mice. These findings suggest that UA ameliorates obesity and hepatic steatosis by improvement of insulin signaling and lipid metabolism (Kunkel et al. 2012). In 3T3-L1 adipocytes, UA inhibited adipogenesis by suppression of intracellular lipid accumulation, and down-regulation of the expression levels of adipogenic genes C/EBPβ, C/EBPα, PPARγ, and SREBP-1c and their target genes FAS, FABP4, and ACC, and enhanced lipolysis and upregulation of the expression levels of FA oxidation-related proteins LKB1, SIRT-1, and CPT-1 and the phosphorylation levels of AMPK and ACC. Co-treatment of AMPK siRNA reversed the anti-adipogenic effect of UA, and co-treatment of LKB1 siRNA or radicicol, an inhibitor of LKB1, suppressed the effect of UA in AMPK activation. These findings suggest that UA inhibits adipogenesis in 3T3-L1 cells via LKB1-dependent AMPK activation (He et al. 2013). In primary rat adipocytes, UA increased lipolysis by upregulation of the genes HSL and ATGL, and down-regulation of perilipin A expression as well as increased cAMP expression and PKA activation. Co-treatment of H89, an inhibitor of PKA, blocked the activity of UA on the expression of HSL and perilipin A, but not in ATGL expression. These findings suggest that UA promotes lipolysis via both PKA-dependent and -independent pathways (Li et al. 2010). In HFD-fed obese mice, UA on oral supplementation in distilled water (50 mg/kg/day, *p.o.*) for 9 weeks improved insulin resistance, hyperinsulinemia, and inflammation by reduction of visceral adipose tissue (VAT) mass, adipocyte size, body weight gain, and the elevated levels of serum glucose, insulin, TG, TC, HOMA-IR, inflammatory cytokines MCP-1, IL-1β, and IL-6, and increased level of serum adiponectin in obese mice (Gonzalez-Garibay et al. 2020). In STZ-induced DCM rats, UA treatment (35 mg/kg, *i.g.*) for 8 weeks improved cardiac function by reduction of the elevated levels of serum FG, lipid profile, CK and LDH (markers of myocardial damage), and the levels of inflammatory cytokines TNF-α, TGF-β1, and MCP-1, fibrosis, and MDA in myocardial tissues of DCM rats. Moreover, UA reduced the oxidative stress in myocardium by increasing the activity of antioxidant enzyme SOD, and upregulated the expression of MMP-2 for remodelling of LV for restoration of its normal function. In addition, UA improved both systolic and diastolic function of LV by decreasing LV end diastolic pressure (LVEDP) by 63.6%, and increasing LV beat rate (Wang et al. 2018).

Oleanolic acid (OA) **326**, a pentacyclic triterpenoid constituent present in many dietary fruits and vegetables, including grapes (*Vitis vinifera*), pomegranate (*Punica granatum*), olives (*Olea europaea*), cloves (*Syzygium aromaticum*), *Viscum album*, and other *Viscum* spp., has potential anti-obesity and antidiabetic effects. In HFdiet-induced obese mice, OA treatment (10 mg/kg/day) for 15 weeks significantly decreased body weight gain, visceral fat mass, and the levels of plasma glucose, TG, TC, and orexigenic hormone ghrelin, and α-amylase activity by 32%, and increased plasma leptin level in obese mice. OA treatment in normal mice reduced plasma glucose and improved glucose tolerance. Moreover, OA decreased the activity of PPARγ and increased energy expenditure in adipose tissue of obese mice. These findings suggest that OA reduces visceral fat mass by regulation of

fat metabolism (de Melo et al. 2010). In high sodium oleate exposed insulin-resistant HepG2 cells, OA reduced insulin resistance by increasing glucose uptake, and the expression levels of GLUT4 and IRS1, and decreasing the expression levels of inflammatory cytokines TNF-α and IL-6 and protein NF-κB in hepatocytes. These findings suggest that OA improves insulin sensitivity in HepG2 cells by inhibition of inflammation via NF-κB inactivation (Li et al. 2015). In type 2 diabetic db/db mice, OA treatment (20 mg/kg/day, *i.p.*) for 2 weeks reduced hepatic insulin resistance, and fat accumulation, and the elevated levels of serum FG, TG, TC, LDL-C, and FFAs, and increased serum HDL-C level in diabetic db/db mice. Moreover, OA increased insulin sensitivity in liver by suppression of inflammation via decreasing the elevated levels of serum and liver pro-inflammatory cytokines IL-1β, IL-6, and TNF-α, and down-regulating the expression levels of gluconeogenic genes G6Pase and PEPCK in the liver, as well as increasing the activity of antioxidant enzyme Nrf2 and its target genes GSH, SOD2, and CAT and the phosphorylation of AMPK in the liver. Therefore, OA improves hepatic insulin resistance via suppression of oxidative stress, inflammation, and gluconeogenesis in AMPK activation pathway (Wang et al. 2013b). In HFD-fed hyperlipidemic mice, OA treatment (20 mg/kg/day, *i.p.*) for 4 weeks showed hypolipidemic effect by reduction of serum levels of TG, TC, and LDL-C, and down-regulation of the expression levels of hepatic TG synthesis-related gene PGC-1β and its downstream target genes FAS and SCD1, and upregulation of the expression of micro RNA , miR-98-5p protein. In cultured mouse primary hepatocytes exposed to high oleic and palmitic acids, OA increased the expression of miR-98-5p protein and decreased the expression of PGC-1β gene. Transfection of mouse hepatocytes with miR98-5p siRNA reversed the inhibitory effect of OA on PGC-1β expression. Accumulating evidence demonstrates that an elevated expression of miR98-5p protein decreases the expression level of LOX-1 and inhibits foam cells formation and lipid accumulation by suppression of the activity of PGC-1β and its target genes related to lipogenesis SREBP-1c, LXR, and Foxa2 and activity in secretion of apoC3 lipoprotein. These findings suggest that OA exerts hypolipidemic effect, at least in part, by regulation of miR98-5p/PGC-1β pathway (Chen et al. 2017). In ox-LDL-exposed human umbilical vein endothelial cells (HUVECs), OA reduced the elevated expression of oxidized-LDL-receptor-1 (LOX-1) and NADPH-oxidase (NOX) and ROS production, and increased the expression of Nrf2 and HO-1 in HUVECs. Several lines of evidence support that LOX-1 is a key player in the development of atherosclerosis. An elevated expression of LOX-1 in atrial vascular tissue promotes vascular smooth muscle cells proliferation and foam cells formation in macrophages and accelerates atherosclerosis by increased expression of NF-κB and CD68, and p38MAPK activation. In vivo, OA treatment in HFD-fed obese quails improved lipid profile and antioxidant status, and reduced atherosclerotic lesions in aortic rings of quails. Thus, OA exerts antiatherosclerotic effect through improvement of antioxidant activity and suppression of LOX-1 activity in vascular tissue of aorta in obese quails (Jiang et al. 2015). In both atherogenic-diet fed rabbits and LDLR-knockout mice, OA treatment (10 mg/kg and 25 mg/kg, respectively) for 5 weeks significantly reduced serum TG, TC, and LDL-C, and increased serum HDL-C level, reduced intima thickness of

artery, increased AdipoR1, and decreased AdipoR2 in the liver of rabbits, while in LDLR-null mice, reduced serum LDL-C level and intima thickness of artery, and increased hepatic AdipoR1 and PPARγ expression and decreased hepatic AdipoR2 expression. Accumulating evidence demonstrates that AdipoR2 plays a key role in the development of atherosclerosis, and AdipoR1 and PPARγ activity reduces atherosclerosis by suppression of inflammation and insulin resistance. Therefore, OA delays the progression of atherosclerosis by down-regulation of AdipoR2 and upregulation of AdipoR1 and PPARγ expression and activity in the liver (Luo et al. 2017). Ghrelin-*O*-acyltransferase (GOAT), an octanoylated derivative of ghrelin, is essential for orexigenic effect of ghrelin. OA on oral administration (20 or 40 mg/kg) for 7 days in standard-diet, high-fat-diet, and high-glucose-diet-fed mice reduced plasma ghrelin (GOAT) levels and body weight gain in standard-diet fed mice, but not in other two diet-fed mice. Possibly the inhibitory effect of OA in GOAT production is masked by glucose and FAs in high glucose and high fat-fed mice. The reduction of plasma GOAT levels by OA may be a prospective target for its anti-obesity effect (Nakajima et al. 2019). OA on oral administration (6 mg/kg/day) after unilateral ureteral obstruction (UUO) surgery in rats, a model of impaired renal function, for 21 days improved kidney function by reduction of kidney index, serum creatinine, and BUN levels, urinary levels of total microalbumin, α1-microalbumin, and *N*-acetyl-β-glucosaminidase, and the deposition levels of collagen I, collagen III, fibronectin, and α-SMA in renal tissues. Moreover, OA decreased the expression levels of TGFβ, and its receptors, TGFβR1 and TGFβR2, and phosphorylated Smad2 in renal tissues of UUO rats. Accumulating evidence indicates that TGF-β-mediated epithelial mesenchymal transition (EMT) promotes the expression of extracellular matrix proteins, fibronectin, collagens, and other proteins for the progression of kidney interstitial fibrosis. TGFβ on binding to its receptors increases the phosphorylation of Smad2 to initiate the process. Therefore, OA ameliorates renal fibrosis in UUO rats through suppression of TGFβ/ Smad2 signaling pathway (Zhao and Luan 2020).

Maslinic acid (MA) **330**, a pentacyclic triterpenoid present in olives, cloves, basil, and mustard seeds, has various pharmacological activities, including antidiabetic and anti-obesity activities. In genetically diabetic KK-Ay mice, MA on oral treatment (10 or 30 mg/kg bw/day) for 2 weeks showed significant reduction of food intake, plasma glucose, and insulin levels, and enhancement of plasma adiponectin level and hepatic glycogen content in diabetic mice. Moreover, MA decreased the activity of glycogen degrading enzyme GP in the liver for improvement of glycogen content. These findings suggest that MA exhibits hypoglycemic effect by increasing hepatic insulin sensitivity (Liu et al. 2007). In HepG2 cells, MA increased glycogen content and the phosphorylation levels of IRβ, Akt, and GSK-3β, and inhibited the activity of glycogen-degrading enzyme glycogen phosphorylase a. Co-treatment of wortmannin, a PI3K inhibitor, suppressed the activity of MA in Akt phosphorylation. These findings suggest that in HepG2 cells, MA promotes glycogen synthesis via stimulation of insulin signaling pathway (Liu et al. 2014). In high oleic acid exposed insulin-resistant HepG2 cells, MA suppressed intracellular lipid accumulation, and down-regulated the expression levels of lipid synthesis-related genes

C/EBPβ, PPARγ, and SREBP-1c, and upregulated the expression levels of lipolysis genes ATGL, HSL, and SIRT1, and phosphorylation levels of AMPK and ACC. In HFD-fed obese mice, MA treatment (20 mg/kg/day) for 12 weeks reduced obesity-induced hepatic steatosis by reduction of body and liver weights, EAT mass, hepatic lipid accumulation, and the elevated levels of serum glucose, insulin, HOMA-IR, TC, TG, LDL-C, leptin, serum, and liver TNF-α levels, and increased serum HDL-C and adiponectin levels, and hepatic glycogen content in obese mice. Moreover, MA decreased macrophage infiltration and the expression levels of lipid synthesis-related genes C/EBPβ, PPARγ, SREBP-1c, and FAS, and increased the expression levels of lipolysis-related genes ATGL and HSL, and FA oxidation-related genes SIRT1, CPT1, and CPT2, as well as phosphorylation level of AMPK in the liver of obese mice. These findings suggest that MA prevents hepatic steatosis and dyslipidemia by regulation of lipid metabolism in the SIRT1/AMPK pathway (Liou et al. 2019).

Betulinic acid (BA) **207**, a pentacyclic triterpene acid, present in many plants, including *Diospyros peregrina*, *Morus alba*, and *Vitex nedundo*, has potential antidiabetic ad anti-obesity effects. In STZ/NA-induced type 2 diabetic mice, BA on oral treatment (20 or 40 mg/kg/day) for 2 weeks significantly reduced elevated levels of plasma glucose, insulin, HOMA-IR index, and α-amylase activity in diabetic mice. Moreover, BA increased insulin secretion and the number of β-cells in pancreas by improvement of pancreatic islet regeneration, and this effect of BA in pancreas is stronger than that of metformin-treated group (200 mg/kg). Therefore, BA reduces hyperglycemia by increasing insulin secretion and decreasing the activity of carbohydrate digesting enzyme α-amylase (Birgani et al. 2018). In HFD-fed obese mice, BA on oral treatment (150 mg/kg/day) for 11 weeks reduced obesity and hepatic steatosis by reduction of body weight gain, weight of inguinal-, perigonadal-, and mesenteric-WAT, adipocyte size, and the levels of serum glucose, insulin, leptin, TC, and TG in obese mice. Moreover, BA promoted mitochondrial thermogenesis, energy expenditure, and FA oxidation by upregulation of the expression levels of their related genes PGC-1α, CPT-1α, UCP-1 , UCP-2, MCAD, and FABP, and the phosphorylation levels of AMPK and ACC in BAT and skeletal muscle, and of GLUT4 expression in skeletal muscle of obese mice. Furthermore, BA decreased the expression levels of inflammatory factors IL-1β, IL-6, TNF-α, and F4/80 (macrophage infiltration marker), and the expression levels of lipogenesis-related genes SREBP-1c, ApoC2, RBP4, FAS, and SCD-1 in the liver of obese mice. In 3T3-L1 cells, BA suppressed intracellular lipid accumulation, and down-regulated the expression levels of adipogenesis and TG synthesis-related genes PPARγ, FAS, GPAT, DGAT1, and DGAT2, and upregulated the expression levels of FA oxidation and glucose uptake-related genes and proteins CPT-1, MCAD, FABP, ACOX1, GLUT4, and p-AMPK in differentiated 3T3-L1 cells. Therefore, BA prevents obesity-associated adiposity and hepatic steatosis by stimulation of energy expenditure, lipid oxidation and thermogenesis, and suppression of lipogenesis processes via AMPK-dependent pathway (Kim et al. 2019). BA is a potent activator of TGR5 receptor protein with an EC_{50} value of 1.04 μM and efficacy of 83%, compared to bile acid lithocholic acid, of EC_{50} of 5.60 μM, and efficacy of 100%. Available evidence demonstrates that TGR5 agonist activates FXR in the

liver for suppression of the expression of genes related to FA synthesis, lipogenesis, and gluconeogenesis. Therefore, BA could be a potential TGR5 agonistic drug in prevention of obesity and insulin resistance (Genet et al. 2010; Cipriani et al. 2010). ApoE KO (knockout) mice model has been used in the study of atherosclerosis, because this type of mice develops hypercholesterolemia and atherosclerosis spontaneously in a reproducible manner similar to that occurring in humans. In diabetic apoE KO mice, BA treatment reduced the levels of serum glucose, TG, TC, insulin, BUN, HOMA-IR, and systolic blood pressure, vascular inflammation, and atherosclerotic lesions in inner endothelial layers of aorta, by increasing eNOS expression and subsequent decreasing the expression of adhesion molecules ICAM-1 and endothelin-1 (ET-1) in vascular tissues of aorta. Therefore, BA could be useful in treatment of atherosclerosis (Yoon et al. 2017).

Tormentic acid (TA) **208**, a pentacyclic triterpenoid, present in many plants, such as in cell culture of *Eriobotrya japonica*, *Rosa rugosa*, and *Argimonia pilosa*, has potential antidiabetic and anti-obesity effects. In Korea, the roots of *R. rugosa* have been used in traditional medicine for treatment of diabetes. In vitro, TA strongly inhibited the activity of PTP1B enzyme with an IC_{50} value of 0.50 μM in a mixed competitive manner, and of the activity of α-glucosidase with an IC_{50} value of 23.8 μM, compared to positive control acarbose of IC_{50} of 124.2 μM. PTP1B enzyme acts as a negative regulator of insulin sensitivity via dephosphorylation of phosphotyrosine residue of IRS1. Carbohydrate digesting enzyme α-glucosidase, present in intestine, plays an active role for postprandial hyperglycemia in diabetic patients. Therefore, TA may be a prospective drug for reduction of PPBG in diabetes (Na et al. 2015). In HFD-fed hyperlipidemic type 2 diabetic mice, TA on supplementation in diet (0.12 g/kg of diet) for 4 weeks reduced visceral fat mass, hepatic TG content, adipocyte and hepatocyte size, and the levels of serum glucose, insulin, TC, FFAs, and leptin in diabetic mice. Moreover, TA increased glucose uptake, GLUT4 protein translocation to the plasma membrane, and the phosphorylation levels of AMPK and Akt in skeletal muscle, and decreased the expression levels of hepatic gluconeogenic enzymes PEPCK and G6Pase, and of lipogenesis-related genes SREBP-1c, FAS, DGAT2, 11β-HSD1, and apoCIII, and increased the expression levels of FA oxidation-related proteins PPARα and p-AMPK in the liver of diabetic mice. These findings demonstrate that TA improves hyperglycemia and hyperlipidemia in diabetic mice by regulation of the expression of genes related to glucose and lipid metabolism through AMPK and Akt activation (Wu et al. 2014a).

Asiatic acid (AA) **443**, a major pentacyclic triterpenoid constituent of Asian hepatoprotective creeper plant *Centella asiatica*, has significant anti-obesity and antidiabetic effects. In high FA exposed hepatoma H4IIE cells, AA reduced intracellular lipid content, and suppressed the expression levels of lipid synthesis-related genes SREBP-1c and FAS, and increased the expression levels of FA oxidation-related genes SIRT1, PGC-1α, PPARα, and CPT-1α, as well as increased the phosphorylation levels of AMPK and ACC. In HFD-fed diabetic db/db mice, AA on oral treatment (50 mg/kg bw/day) for 4 weeks reduced hepatic steatosis by upregulation of the expression levels of FA oxidation-related genes PGC-1α, PPARα, SIRT1, CPT-1α, and p-AMPK and down-regulation of lipogenesis-related

genes SREBP-1c, FAS, and ACC1 in the liver of db/db mice. These findings suggest that AA promotes AMPK-dependent expression of genes related to FA oxidation and lipogenesis for suppression of hepatic steatosis in diabetic db/db mice (Xu et al. 2018a). Another group reported that in HFD-fed obese SD rats, AA on oral treatment (20 mg/kg bw/day) for 45 days reduced body weight gain, hepatic lipid content, and TBARS level, and the levels of plasma glucose, insulin, leptin, TG, TC, PLs, LDL-C, FFAs, and the activity of pancreatic lipase and amylase in obese rats. Moreover, AA increased the activity of hepatic antioxidant enzymes GSH, SOD, CAT, and GP_X, and the expression of fat oxidation-related genes CPT1 and UCP2, and decreased the expression levels of lipogenic genes FAS, aP2, PPARγ, and ACC1, and of inflammatory cytokine TNFα I liver of obese rats. These findings also support that AA ameliorates hyperlipidemia and hyperglycemia in obesity through reduction of insulin resistance, oxidative stress, and inflammation and regulation of lipid metabolism in the liver and inhibition of the activity of pancreatic lipase and amylase activity (Rameshreddy et al. 2018; Sathibabu Uddandrao et al. 2020). AA treatment (25 mg/kg/day) for 4 weeks in genetically type 2 diabetic GK rats reduced serum glucose levels and increased insulin secretion from pancreatic islets by suppression of islet fibrosis (Wang et al. 2015c). In high-carbohydrate, high-fat diet-fed metabolic syndrome (MS) rats, AA treatment (20 mg/kg bw/day) for 3 weeks reduced hypertension and heart beat by reduction of the expression level of inducible nitric oxide synthase (iNOS) in vascular tissue and increased expression of endothelial nitric oxide synthase (eNOS) in aortic tissues. Moreover, AA reduced the expression levels of elevated plasma angiotensin II (AngII), angiotensin converting ezyme (ACE), and norepinephrine (NE) and of AngII receptor type-1 (AT1R) in thoracic aorta of MS rats. In addition, AA reduced the wall thickness of both thoracic aorta and mesenteric arteries, and increased their luminal diameters and reduced the expression of inflammatory cytokines TNF-α, IL-1β, and p-NF-κB in aortic vascular tissues. Accumulating evidence demonstrates that hyperglycemia-induced Ang II activation in renin-angiotensin system promotes the expression of AT1R in thoracic aorta for induction of vasoconstriction, leading to high blood pressure. Moreover, an elevated expression of NE induces vasoconstriction through binding to its α_3 receptors. These findings suggest that AA prevents vascular dysfunction by regulation of eNOS/iNOS expression and suppression of Ang II and NF-κB activation in aortic tissues (Pakdeechote et al. 2014; Maneesai et al. 2016).

Eburicoic acid (EA) **453**, an ergostane-type triterpene, isolated from the fruiting bodies of Taiwanese medicinal mushroom *Antrodia camphorata* syn. *A. cinnamomea*, grown in endemic trees, has significant hypolipidemic and hypoglycemic effects. In Taiwan, the mycelium of *A. camphorata* has been used in traditional medicine for treatment of dyslipidemia and diabetic problems. In chronic STZ-induced type 1 diabetic mice, EA on oral treatment (20 or 40 mg/kg/day) for 14 days ameliorated hyperglycemia and hyperlipidemia by reduction of FBG, serum HbA1c, TC, and TG levels, visceral fat mass, and hepatic lipid droplets content, and increased serum insulin, leptin, and adiponectin levels in diabetic mice. Moreover, EA increased pancreatic β-cells mass and insulin secretion by reduction of ROS

production. In addition, EA increased glucose uptake and GLUT4 protein translocation to the plasma membrane, and increased the phosphorylation levels of Akt and AMPK in skeletal muscle, and increased the expression levels of phospho (p)-Akt, p-FoxO1, and p-AMPK in the liver and reduced the expression levels of hepatic gluconeogenic genes PEPCK and G6Pase. An elevated level of p-FoxO1 in the liver inhibits the activity of gluconeogenic enzymes in glucose production. Furthermore, EA increased the expression of FA oxidation-related gene PPARα and decreased the expression levels of FA synthesis-related genes FAS and PPARγ, and expression levels of TG and cholesterol synthesis-related genes SREBP-1c and SREBP2, respectively, in the liver of diabetic mice. In C2C12 myotubes, EA increased the phosphorylation of Akt. Moreover, in high palmitate exposed insulin-resistant C2C12 cells, it increased glucose uptake and the expression of GLUT4 proteins, and the phosphorylation of Akt and AMPK. These findings suggest that EA prevents hyperglycemia and dyslipidemia by increasing insulin secretion from the pancreas, glucose uptake in skeletal muscle, and decreasing hepatic glucose production and lipogenesis via increased phosphorylation of Akt, FoxO1, and AMPK in the liver and Akt phosphorylation in skeletal muscle (Lin et al. 2017, 2018).

Dehydroeburicoic acid (DEA) **454**, another ergostane-type triterpenoid isolated from mushroom *A. camphorata* and *Poria cocos*, has significant hypoglycemic and hypolipidemic effects. In C2C12 myoblast cells, DEA increased glucose uptake, GLUT4 expression, and the phosphorylation level of Akt. In HFD-fed obese mice, DEA treatment (20 or 40 mg/kg/day, *i.g.*) for 4 weeks reduced hyperglycemia and hyperlipidemia by reduction of visceral fat mass and hepatic lipid and TG content, serum glucose by 39.7 or 43.4%, respectively, and serum insulin, leptin, TG, and TC levels in obese mice. Moreover, DEA decreased the expression of hepatic gluconeogenic enzyme G6Pase and expression levels of lipogenic genes FAS, PPARγ, aP2, GPAT, SREBP-1c, and SREBP2, and of insulin signaling suppressor gene 11β-HSD1, and increased the expression levels of fat oxidation-related genes PPARα, CPT-1α, and UCP-3, and phosphorylation of AMPK in the liver. Furthermore, DEA increased the expression of GLUT4 and phosphorylation of AMPK in skeletal muscle, and decreased the expression levels of lipogenic genes PPARγ and FAS in adipose tissue of obese mice. The TC lowering effect of DEA was comparable to fenofibrate (250 mg/kg/day) treated group. These results suggest that DEA improves insulin sensitivity for mitigation of hyperglycemia and dyslipidemia via AMPK activation (Kuo et al. 2016a).

Antcin K (AnK) **455**, the major ergostane-type triterpenoid constituent of Taiwanese mushroom *A. camphorata*, exhibited potential antidiabetic and hypolipidemic effects. In C2C12 myotubes, AnK increased GLUT4 expression and the phosphorylation levels of Akt and AMPK. In HFD-fed type 2 diabetic obese mice, AnK on oral supplementation (40 mg/kg bw/day) for 28 days showed hypoglycemic and hypolipidemic effects by reduction of body weight gain, visceral fat mass, hepatic lipid, and TG content and the levels of serum glucose, insulin, leptin, TG, TC, and FFAs, and increased serum adiponectin level in diabetic mice. In addition, AnK increased the expression of PPARα and phosphorylation levels of Akt and AMPK, and decreased the expression levels of FA and cholesterol synthesis-

related genes FAS, aP2, DGAT2, SREBP-1c, SREBP2, and apoCIII, and of gluconeogenic gene G6Pase in the liver, and decreased the expression levels of genes PPARγ and FAS in adipose tissue, and increased the expression levels of glucose uptake-related proteins GLUT4 and p-Akt and p-AMPK in skeletal muscle of diabetic mice. The antihyperglycemic effect of AnK was comparable to metformin (300 mg/kg) treated group, and the antihypertriglyceridemic effect of AnK was comparable to fenofibrate (250 mg/kg) treated group. These findings suggest that AnK mitigates hyperglycemia and dyslipidemia through regulation of genes expression related to glucose and lipid metabolism via increased phosphorylation of Akt and AMPK in metabolic tissues of diabetic mice (Kuo et al. 2016b).

5.2.12.5 Carotenoids

Carotenoids are isoprenoids belonging to tetraterpene group and are produced by plants, fungi, and bacteria as yellow to red colored pigments. In plants, these compounds are found in fruits, flowers, and rhizomes. These compounds are classified into two subgroups, carotenes, which are hydrocarbons, and xanthophylls, which are the oxygenated derivatives of hydrocarbons. More than 600 carotenoids have been identified, and many of them have significant role in health promoting effects in prevention of obesity and other metabolic disorders. Carotenoids containing an unsubstituted β-ionone ring are called provitamin A, because they are cleaved by animal intestinal and liver enzymes to release retinal, which is converted into retinol. Several dietary carotenoids from plants and marine algae, such as lycopene, β-carotene, β-cryptoxanthin, astaxanthin, and fucoxanthin have potential role in prevention of obesity and diabetes by inhibition of adipogenesis, regulation of fat metabolism, and intestinal lipid absorption, as well as have nutritional value (Von Lintig 2010).

Lycopene **24**, a lipophilic red colored non-provitamin A carotenoid, present in various fruits and vegetables such as tomato, water melon, guava, and grape fruits, has significant effects in suppression of cardiovascular disorders, obesity, and its associated metabolic disorders. In HFD-fed obese mice, lycopene supplementation in diet (10 mg/kg food/day) for 12 weeks significantly decreased the weights of liver and epididymal adipose tissue (EAT), the levels of serum TG, NEFAs, 8-iso-$PGF_{2\alpha}$, glucose, insulin, and HOMA-IR, and the levels of proinflammatory cytokines, adipokines, and chemokines in the liver and EAT of obese mice. In addition, lycopene decreased the expression levels of lipogenic genes ACC1, FAS, SREBP-1c, PPARγ, and its target genes aP2, LPL, and CD36, and increased the expression levels of FA oxidation-related genes CPT1, ACOX, and PPARα in the liver for suppression of hepatic lipid content and decreased the expression levels of inflammatory cytokines and proteins IL-6, MCP-1, MMP9, MMP3, leptin, resistin, visfatin, p-p65, and p-IκB in EAT, and TNF-α in the liver, and increased the expression of anti-inflammatory protein IL-10 in EAT for suppression of inflammation in obese mice. These findings suggest that lycopene reduces adiposity and hepatic steatosis by regulation of genes expression related to lipid metabolism and suppression of inflammation in the liver and EAT in obese mice. Supplementation of tomato powder containing equivalent amount of lycopene in diet of obese mice also

exhibited similar effect, but the presence of other carotenoids in tomato powder might have synergistic effect (Fenni et al. 2017). Another group reported that lycopene supplementation in diet to HFD-fed obese mice for 8 weeks improved insulin resistance, glucose intolerance, and hyperinsulinemia by reduction of M1 macrophage infiltration and increased anti-inflammatory M2 macrophage polarization in the liver and EAT of obese mice. In RAW 264.7 macrophages, lycopene increased IL-4-mediated M2 macrophage polarization via increasing the phosphorylation levels of STAT6 and Akt. These results suggest that lycopene increases insulin sensitivity in the liver and EAT for mitigation of inflammation-mediated adiposity and hepatic steatosis (Chen et al. 2019). In STZ-induced type 2 diabetic rats, lycopene treatment (10 or 15 mg/kg bw/day) for 10 weeks reduced FBG and the levels of serum oxidative stress biomarker factors HbA1c, LDL-C, ox-LDL, and MDA and inflammatory factors TNF-α and CRP, and increased the levels of serum antioxidant enzymes SOD, CAT, and GP_X in diabetic rats. These findings suggest that lycopene reduces oxidative stress and inflammation for protection against diabetes (Zheng et al. 2019). Another group reported that lycopene reduces serum cortisol level and increases antioxidant capacity in diabetic rats for improvement of hyperglycemia in diabetic rats (Eze et al. 2018).

Beta (β)-carotene **25**, a major provitamin A carotenoid having two cyclic β-ionone rings, present in high concentrations in dietary vegetables and spices such as carrots, peppers, chili powder, paprika, and sweet potatoes, has potential health benefit effects in prevention of some types of cancer, obesity, eye, and cardiovascular diseases. Beta-carotene is the preferential food source of vitamin A in mammals, because its two β-ionone rings on enzymatic cleavage provide two vitamin A molecules. Two proteins, namely, β-carotene-15,15′-oxygenase 1 (BCO1) and β-carotene-9,10′-oxygenase 2 (BCO2) mainly expressed in high levels in the intestine and liver of mammals promote the cleavage of β-carotene. Beta-carotene by cleavage with BCO 1 protein is converted into retinal **456**, which is rapidly converted into its transcriptionally active form retinoic acid (RA) **457** (Wang et al. 2017a). While the cleavage of β-carotene by BCO2 enzyme produces β-ionone and apo-10′-carotenal, the latter is subsequently converted to retinal by BCO1 enzyme. Therefore, BCO1 protein is the main player for conversion of β-carotene to RA in mammal tissues (Dela Sena et al. 2013). In 3T3-L1 adipocytes, RA on binding to its receptor (RAR) blocks the transcriptional activity of C/EBPβ in the expression of PPARγ and C/EBPα, and thereby inhibits their activity in the expression levels of other adipogenic genes including aP2 and PEPCK. Therefore, β-carotene inhibited adipogenesis via suppression of the transcriptional activity of C/EBPβ via formation of RA in 3T3-L1 cells (Schwarz et al. 1997). In obese mice, RA treatment (10 mg/kg bw) for 1 week reduced the levels of serum glucose, TG, and FFAs, and increased the expression levels of angiogenic genes VEGFA, VEGF1, VEGF2, PDGFRα$^+$ in adipocytes, and the expression levels of thermogenic genes PRDM16, UCP1, PPARγ, Cidea, and Cox7α1 , and the phosphorylation level of p38MAPK in EAT of obese mice, while this effect of RA on proliferation of PDGFRα$^+$ cells was not observed in PDGFRα-VEGFR2-knockout mice. These findings indicate that RA promotes browning of WAT via VEGFA/VEGF2 signaling pathway through

upregulation of PDGFRα$^+$ cells expression in adipose tissue and p38MAPK activation. RA on interaction with VEGFA increased the phosphorylation level of p38MAPK to increase the binding activity of RAR on the promoter region of PRDM16 for induction of transcriptional activity of PRDM16 on its target genes related to browning of WAT (Wang et al. 2017a).

Beta-cryptoxanthin (β-CRX) **458**, a yellow to orange coloured carotenoid provitamin A, found in fruits and vegetables such as tangerines, satsuma mandarin oranges (*Citrus unshiu* Marc), peaches, red peppers, butternut squash, sweet oranges, pumpkin, and papaya, has several health-benefit effects in preventing the risk factors of some cancers, degenerative diseases, osteoporosis, and obesity. In mammalian enterocytes, β-CRX-rich foods have greater bioavailability than β-carotene-rich foods. The enzymes BCO1 and BCO2 that cleave β-carotene also cleave β-CRX into retinal. Several studies have shown that β-CRX is a poorer substrate for BCO1 than is β-carotene (Von Lintig 2010; Mein et al. 2011; Dela Sena et al. 2013). In Tsumura Suzuki obese, diabetes (TSOD) mice, β-CRX on oral administration in the form of enzyme-processed Satsuma mandarin (EPSM) powder (400 mg/kg/day, equivalent to 0.8 mg β-CRX/kg/day) for 8 weeks reduced visceral fat mass, liver weight, and the levels of serum TG, TC, and NEFAs in TSOD mice. Moreover, β-CRX increased the expression levels of FA oxidation-related gene PPARα in adipocytes and muscle, and decreased the expression levels of inflammatory cytokines TNFα and IL-1β, and increased the expression of anti-inflammatory cytokine IL-10 and adiponectin in adipose tissue. In addition, β-CRX decreased the expression levels of lipid transport genes ABCA-1, high-density lipoprotein binding protein (HDLBP), Apo A and ApoC, and lipid synthesis-related genes FAS and SCD1 and elongation of very long-chain fatty acids protein 6(ELOVL6) in the liver and adipose tissue, and the expression levels of proteins related to adipocyte cell cycle process and proliferation, and the expression levels of circadian rhythm-related gene, brain and muscle Arnt-like protein-1 (Bmal-1) in adipocytes. Accumulating evidence demonstrates that overexpression of Bmal 1 in adipocytes stimulates adipogenesis and several other factors related to lipid synthesis. Moreover, it inhibits brown fat formation and thermogenic function through regulation of TGF-β and BMP signaling pathways via increasing the activity of TGF-β and decreasing the activity of bone morphogenetic protein (BMP) in WAT. These findings suggest that β-CRX reduces visceral and hepatic fat mass by regulation of the expression of genes PPARα and Bmal1, and suppression of inflammation in TSOD mice (Takayanagi 2011; Nam et al. 2015; Shimba et al. 2005). Daily intake of β-CRX containing beverage (2 mg of β-CRX/day) for 12 weeks by pre-obese men significantly reduced body mass index (BMI) and visceral fat area, as well as serum TG and PAI-1 levels compared to placebo group. Therefore, consumption of β-CRX containing food can mitigate obesity-related complications (Iwata et al. 2018).

Astaxanthin (ASX) **168**, a pink colored xanthophyll carotenoid found in many marine organisms, including shrimp, salmon, crustaceans, and algae such as *Haematococcus pluvialis*, has potential antioxidant and anti-obesity activities (Ambati et al. 2014). In high-cholesterol, high-fat-fed DIO mice and genetically

obese (ob/ob) mice, ASX supplementation in diet (0.02% of diet) for 12 weeks significantly reduced steatohepatitis and insulin resistance by reduction of hepatic lipid accumulation, inflammation, and TBARS levels, and the levels of plasma glucose, insulin, AST, and ALT in both types of obese mice. Moreover, ASX increased hepatic insulin sensitivity by increasing insulin-stimulated phosphorylation of IRβ and Akt, and reduced hepatic inflammation by suppression of macrophage ($F4/80^+$ cells) infiltration, expression levels of pro-inflammatory cytokines TNF-α, IL-6, and IL-1β, and phosphorylation of JNK, p38MAPK, and NF-κBp-65, as well as by increasing M2-type macrophage recruitment and subsequent reducing $CD4^+$ and $CD8^+$ T cells recruitment in the liver of mice. Further, ASX reduced hepatic fibrosis by suppression of fibrogenic genes TGF-β1, collagen I, α-SMA, PAI-1, and hydroxyproline. In addition, ASX reduced the expression levels of hepatic lipogenic genes SREBP-1c, LXRα, ChREBP, FAS, SCD1, and lipid uptake gene CD36 for suppression of lipid accumulation. The effects of ASX in suppression of hepatic lipid accumulation, inflammation, and whole body insulin resistance were superior than vitamin E (0.02% of diet) treated mice. These findings indicate that ASX improves whole body insulin resistance, hepatic steatosis, and inflammation by regulation of M1/M2 macrophage accumulation and lipid metabolism in liver (Ni et al. 2015). ASX administration (5 and 20 mg/once, daily) to Korean overweight and obese adults (n = 30) for 3 weeks significantly reduced the levels of plasma oxidative stress markers MDA and iosprostane by 34.6 and 64.9%; 35.2 and 64.7%, respectively and increased the levels of plasma SOD and TAC by 193 and 121%; 194 and 125%, for 5 and 20 mg doses respectively. These results suggest that ASX has potential antioxidant efficacy for suppression of oxidative stress in overweight and obese adults (Choi et al. 2011).

Fucoxanthin (FXN) **158**, a yellow colored carotenoid present in edible brown algae such as *Undaria pinnatifida*, *Hijikia fusiformis*, and *Petalonia binghamiae*, and in some microalgae such as *Phaeodactylum tricornutum* and *Cylindrotheca closterium*, has significant health promoting effects in prevention of obesity, diabetes, cancer, and other inflammatory disorders. In 3T3-L1 adipocytes, FXN promoted adipocyte differentiation in the early stage (D0-D2) of differentiation by increasing the expression of PPARγ, C/EBPα, SREBP-1c, and aP2, but it suppressed differentiation of adipocytes in the intermediate (D2-D4) and last stages (D4-D7) by suppression of the expression of PPARγ and SREBP-1c. Moreover, it inhibited glucose uptake by reducing the phosphorylation of IRS-1 in mature adipocytes (Kang et al. 2011b). In HFD-fed obese mice, FXN on supplementation in diet (0.2% of diet) for 4 weeks mitigated hyperglycemia and hyperlipidemia by reduction of serum glucose, HbA1c, insulin, resistin, TG, andTC levels, hepatic lipid content, and increased serum HDL-C level in obese mice. Moreover, FXN decreased the expression levels of hepatic lipogenic genes FAS, PPARγ, G6PDH, ME, PAP, and of cholesterol synthesis-related genes HMGCR and ACAT, and increased the expression of hepatic FA oxidation-related genes PPARα, CPT-1, and ACOX1. These findings suggest that FXN regulates hepatic lipid and glucose metabolism by enhancing insulin sensitivity in the liver of obese mice (Woo et al. 2010). In mature

3T3-L1 adipocytes, FXN increased the phosphorylation levels of AMPK and ACC via increasing LKB1 phosphorylation, and increased the expression of FA oxidation-related gene CPT-1α, and decreased the expression of lipogenic gene SREBP-1c. Moreover, *Petalonia binghamiae* extract rich in FXN on supplementation in diet (150 mg/kg/day) to HFD-fed mice for 70 days reduced body weight gain, AT weight, hepatic lipid accumulation, and serum TG, GPT, and GOT levels in obese mice. These findings suggest that FXN improves diet-induced obesity by promoting fat oxidation and suppressing lipogenesis via LKB1-mediated AMPK activation in the liver and adipose tissue (Kang et al. 2012).

5.2.12.6 Saponins

Saponins are naturally occurring surface-active glycosides, mainly produced by plants, and their chemical structure consists of a sugar moiety (glucose, galactose, rhamnose, glucuronic acid, or xylose) linked to a hydrophobic aglycone called sapogenin, a steroid or a triterpene. These phytochemicals are called saponins because of their ability to form stable soap-like foams in aqueous solutions. Steroidal saponins are mainly found in monocotyledons, while triterpenoid saponins are predominantly found in dicotyledons. These compounds have many pharmacological activities, including anti-inflammatory, immunostimulant, hypoglycemic, hypolipidemic, antifungal, and cytotoxic activities.

Dioscin (**84**), a steroidal saponin present in many medicinal plants, such as in rhizomes of *Dioscorea nipponica*, *D. alata*, *D. bulbifera*, *D. pentaphylla*, *D. oppositifolia*, and *D. zingiberensis*, has potential anti-obesity effect. In traditional Indian, Chinese, and African medicines, the tubers of *Dioscorea* spp. have been used for treatment of piles, birth control, abdominal pain, gastritis, tumor, asthma, rheumatic swelling, diabetes, and obesity (Kumar et al. 2017). In 3T3-L1 adipocytes, dioscin inhibited adipogenesis by suppression of intracellular lipid accumulation, and the expression levels of adipogenic genes PPARγ, C/EBPα, and C/EBPβ/δ, and their target genes FAS, SREBP-1c, aP2, leptin, and GLUT4 in 3T3-L1 cells. In addition, dioscin decreased MCE in adipocytes by cell cycle arrest at G0/G1 phase, and decreased phosphorylation levels of ERK1/2 and p38MAPK kinases, and increased the phosphorylation of AMPK and ACC. In HFD-fed obese mice, dioscin treatment (100 mg/kg/day) for 7 weeks reduced abdominal fat mass and serum lipids levels significantly in obese mice. These findings suggest that dioscin exerts hypolipidemic effect by regulation of lipid metabolism via AMPK/MAPK pathway (Poudel et al. 2014). Another study reported that in both diet-induced obese (DIO) mice and genetically obese (ob/ob) mice, dioscin supplementation in diet (80 mg/kg/day) for 10 weeks showed anti-obesity effect by reduction of body weight gain, hepatic lipid accumulation, levels of serum glucose, insulin, TC, TG, FFAs, AST, ALT, and MDA, and increased the activity of hepatic antioxidant enzymes Nrf2, HO-1, GSS, and SOD2 in both DIO and ob/ob mice. In addition, dioscin decreased the expression of inflammation-related factors TNF-α, IL-1, IL-6, AP-1, CYP2E1, COX-2, NF-κB, p-p38, p-JNK, and p-ERK, and the expression of lipogenic and TG synthesis genes SREBP-1c, FAS, ACC1 and SCD1, GPAT, DGAT1, and DGAT2 and increased the expression of FA oxidation-related genes PPARα, CPT-1,

ACADM, ACADS, and ACO in the livers of both DIO and ob/ob mice. Furthermore, dioscin upregulated the expression of autophagy-related proteins including LC3-II, beclin, and Atg5 by increasing the level of p-mTOR and of cholesterol synthesis-related genes HMGCR, HMGCS1, and SREBP2 in livers of both DIO and ob/ob mice. These findings suggest that dioscin mitigates hyperglycemia and hyperlipidemia by regulation of genes expression related to lipogenesis, fat oxidation, and autophagy via suppression of oxidative stress and inflammation in livers of obese mice (Liu et al. 2015b). A recent study reported that in both STZ-induced type 2 diabetic rats and genetically diabetic KK-Ay mice, dioscin treatment reduced hyperglycemia and hyperlipidemia by reduction of serum glucose, TG, and TC levels and hepatic lipid content, and increased hepatic glycogen content via upregulation of micro RNA miR-125a-5p and the phosphorylation levels of PI3K, Akt, GSK-3β, and FoxO1 in livers of diabetic rats and mice and decreased the phosphorylation of STAT3 and the expression levels of gluconeogenic genes PEPCK and G6Pase, and of lipognic genes SREBP-1c, FAS, ACC, and SCD1 in diabetic livers. A growing number of studies demonstrate that an increased phosphorylation of STAT3 by inflammatory cytokine IL-6 increases the activity of SOCS-3 to increase the activity of GSK-3β by reducing its p-level for suppression of insulin sensitivity in liver. Moreover, an increased p-level of FoxO1 decreases the activity of FoxO1 for induction of the expression of gluconeogenic enzymes PEPCK and G6Pase in diabetic livers. These facts suggest that dioscin stimulates the expression of miR-125a-5p in diabetic livers for improvement of insulin sensitivity and insulin-dependent suppression of hepatic glucose production and lipogenesis, and improvement of hepatic glycogen content (Xu et al. 2020a). Diosgenin **87**, the aglycone of dioscin and present as a major constituent in Chinese yam sanyaku (dried powder of *Dioscorea batatas*), on oral treatment (0.05% of diet) to HFD-fed obese diabetic KK-Ay mice for 8 weeks significantly decreased serum fasting and postprandial TG and hepatic TG content and FBG and increased serum HDL-C level by upregulation of hepatic lipolysis and fat oxidation-related genes LPL, PPARγ, and PGC-1α in diabetic mice. Possibly, hepatic TG-rich VLDL-C is hydrolyzed by LPL to reduce hepatic TG content. In HepG2 cells, diosgenin decreased intracellular TG accumulation by decreasing the expression levels of lipogenic gene LXRα and its target genes FAS, SREBP-1c, ACOX, and SCD1. These findings suggest that possibly dioscin by conversion to its metabolite diosgenin in vivo ameliorates hyperlipidemia and hyperglycemia on obese diabetic animals (Hashidume et al. 2018; Uemura et al. 2011).

Capsicoside G **142**, a furostanol saponin from pepper (*Capsicum annum* L.) seeds, exhibited significant anti-obesity effect in animal model. In HFD-fed obese mice, oral treatment of a capsicoside G rich fraction isolated from pepper seeds containing 13.35% of capsicoside G (10 and 100 mg/kg bw) for 4 weeks reduced epididymal adipose tissue weight and adipocyte hypertrophy by suppression of the expression of adipogenic factor related genes in adipocytes. In 3T3-L1 adipocytes, capsicoside G inhibited adipogenesis by suppression of intracellular lipid accumulation and down-regulation of the expression levels of adipogenic-related genes C/EBPα, PPARγ, SREBP-1c, FAS, FABP4, and GPAT-1 via increasing the

phosphorylation levels of AMPK and ACC, and the expression of the target gene of AMPK, CPT-1. Co-treatment of compound C, an inhibitor of AMPK, significantly suppressed the anti-adipogenic effect of capsicoside G. These findings suggested that capsicoside G exhibited anti-obesity effect by regulation of AMPK signaling pathways (Sung et al. 2016; Sung and Lee 2016).

Gensinoside Rb1 **65**, a major bioactive triterpenoid saponin present in different parts of *Panax ginseng*, *P. quinquefolius*, and *P. notoginseng*, and in high concentrations in the roots of these plants, has potential hypoglycemic and hypolipidemic effects in obesity-related disorders. In HFD-fed obese rats, Rb1 treatment (10 mg/kg/day, *i.p.*) for 4 weeks reduced food intake, body weight gain, epididymal and inguinal fat mass, and the levels of plasma FG, TC, TG, and leptin in obese rats. Moreover, Rb1 improved glucose tolerance and energy expenditure, and increased the insulin sensitivity in the hypothalamus via increased phosphorylation of Akt, and reduced the expression of orexigenic gene NPY in the hypothalamus. Further, Rb1 increased the expression of c-Fos in brain nucleus of solitary tract (NTS), arcuate (ARC), and ventromedial (VMH) areas. Accumulating evidence demonstrates that an elevated expression of c-Fos stimulates a satiation signal from abdominal viscera to NTS and ARC regions of brain through vagus nerve for suppression of food intake. In addition, Rb1 increased glucose uptake in both 3T3-L1 adipocytes and C2C12 myotubes by increasing GLUT4 expression and Akt phosphorylation, and promoted insulin secretion in mouse MIN6 cells. These findings suggest that Rb1 improves obesity-related hyperglycemia and hyperlipidemia through increased insulin secretion and insulin-dependent glucose uptake and suppression of food intake in obese rats (Xiong et al. 2010). In HFD-fed obese rats, Rb1 treatment (10 mg/kg/day) for 4 weeks reduced hepatic lipid accumulation and TG content. Moreover, Rb1 increased the expression of FA oxidation-related genes PGC-1α, PPARα, and ACOX1, and decreased the expression of lipid synthesis-related genes SREBP-1c, FAS, ACC, and SCD1 in the liver of obese rats. In high-palmitate exposed rat hepatocytes, Rb1 reduced intracellular lipid accumulation, and increased the expression of FA oxidation-related gene CPT-1α, and the phosphorylation of AMPK and ACC, and decreased the expression of lipid synthesis-related genes SREBP-1c, FAS, ACC, and SCD1. Co-treatment of compound C, an inhibitor of AMPK, reversed the effects of Rb1on AMPK phosphorylation and lipogenesis-related genes expression in hepatocytes. Moreover, Rb1 significantly increased the AMP levels and AMP to ATP ratio in hepatocytes compared with vehicle treatment. These findings suggest that Rb1 reduces hepatic lipid mass and TG level by regulation of genes expression on lipid metabolism through AMP-dependent AMPK activation (Shen et al. 2013). In HFD-fed severe chronic obese mice for 16 weeks, Rb1 treatment (14 mg/kg/day, *i.p.*) for 21 days reduced visceral and inguinal fat accumulation, and improved serum adiponectin level, glucose, and insulin tolerance in obese mice. Moreover, Rb1 decreased inflammation in the adipose tissue, liver, and hypothalamus, and decreased the hypothalamic inflammation by suppression of the expression levels of inflammatory factors IL-6, IL-1β, and p-IKK and of negative regulators of leptin signaling SOCS-3 and PTP1B and increased the activation of Akt. The activation of PI3K/Akt signaling in hypothalamus reduced the activity of

FoxO1 by increasing its phosphorylation. The increased p-FoxO1 promoted p-STAT3 level to restore leptin signaling for enhanced activity of anorexigenic gene POMC, and decreased the activity of orexigenic gene AgRP in hypothalamus. Therefore, Rb1 mediated insulin signaling in hypothalamus decreases hypothalamic inflammation and the expression levels of SOCS3 and PTP1B to restore central leptin signaling and sensitivity for suppression of food intake in obese mice (Wu et al. 2014b). Another study reported that Rb1 treatment (10 mg/kg/day) to HFD-fed obese rats for 5 days significantly reduced hepatic glucose production by suppression of the expression and activity of gluconeogenic enzymes PEPCK and G6Pase, and increased glucose uptake in skeletal muscle, and increased glycogen content in the liver and skeletal muscle through increased phosphorylation of AMPK and its downstream target gene TBC1D4 (AS160) in skeletal muscle. TBC1D4 activation improves GLUT4 translocation to the plasma membrane for glucose uptake in response to both Akt and AMPK activation. Therefore, Rb1 improves insulin sensitivity in the liver and skeletal muscle for maintenance of whole body glucose homeostasis (Shen et al. 2015).

Ginsenoside Rb2 **459**, another major triterpenoid saponin constituent of *Panax ginseng* and other *Panax* spp., has potential anti-obesity effect. In genetically obese (LepR deficient) type 2 diabetic mice, Rb2 treatment (10 mg/kg/day, *i.p.*) for 4 weeks significantly alleviated hepatic steatosis by reduction of hepatic lipid accumulation, TG and AST levels, and the levels of serum glucose, insulin, TG, and TC in obese mice through improvement of hepatic autophagy process. Rb2 increased the expression of autophagy-related gene LC-3II, the expression level of Sirt1 and phosphorylation of AMPK, and decreased the expression of the genes related to negative regulators of autophagy p62, p-mTOR, and p-ULK1 in the liver of obese mice. An increased phosphorylation of mammalian target of rapamycin (mTOR) promotes the expression and phosphorylation of UNC-51 like kinase 1 (ULK1) for protein synthesis by suppression of autophagy, and polyubiquitin-binding protein p62 promotes lipid accumulation in liver on overexpression. In high oleic acid exposed HepG2 cells and mouse hepatocytes, Rb2 decreased intracellular lipid accumulation, increased the expression of LC-3II, Sirt1, and p-AMPK, and decreased the expression of p62, p-mTOR, and p-ULK1. Co-treatment of Ex-528, a Sirt1 inhibitor, or compound C, an inhibitor of AMPK, partly blocked the effect of Rb2 in suppression of lipid accumulation and regulatory effect in the expression of LC-3II and p62 in HepG2 and rat hepatocytes. These findings indicate that Rb2 attenuates hepatic steatosis through improvement of impaired hepatic autophagy via both Sirt1 and AMPK pathways (Huang et al. 2017a). In DIO mice, Rb2 supplementation (40 mg/kg/day) for 10 days improved insulin resistance and reduced body weight gain and lipid droplets in WAT through increased energy expenditure and mitochondrial function in WAT. Rb2 increased mitochondrial oxygen consumption and the expression levels of thermogenesis and biogenesis-related genes including PGC-1α and UCP1 in BAT and WAT of DIO mice. In adipose tissue and 3T3-L1 cells, Rb2 increased the expression levels of thermogenic genes PRDM-16, Cidea, Elovl3, DIO2, FGF21, and Cox8β along with PGC-1α and UCP1. These findings

suggest that ginsenoside Rb2 prevents obesity by regulation of genes expression related to browning of white adipose tissues (Hong et al. 2019).

Ginsenoside Rg1 **460**, another major triterpene saponin constituent of the leaves of *Panax ginseng* and *P. quinquefolius*, exhibited significant antidiabetic and anti-obesity effects. In HFD-fed obese mice, Rg1 on oral treatment (20 mg/kg/day) for 4 weeks improved diet-induced obesity by reduction of body fat accumulation, epididymal-white adipose tissue mass, and the levels of serum glucose, TG, TC, and FFAs in obese mice. Rg1 in both adipose tissue and 3T3-L1 adipocytes decreased the expression of adipogenic genes C/EBPα, PPARγ, and SREBP-1c, and their target genes ACC, FAS, and FABP4, and increased the expression of lipolysis-related gene HSL and the phosphorylation levels of AMPK and ACC. These findings suggest that Rg1 reduces fat accumulation in WAT by regulation of genes expression related to lipid metabolism via AMPK activation (Liu et al. 2018b). Another study reported that Rg1 in skeletal muscle C2C12 cells increased glucose uptake and GLUT4 translocation to the plasma membrane and increased phosphorylation of AMPK. In DIO mice, Rg1 treatment (300 or 500 mg/kg/day) for 2 months reduced fat accumulation in WAT, and serum FG and PPG, and insulin levels and increased the phosphorylation of IR and AMPK in the liver and skeletal muscle of DIO mice. These findings suggest that Rg1 ameliorates diet-induced obesity by increasing insulin sensitivity via both Akt and AMPK activation (Li et al. 2018b).

Ginsenoside Rg2 **460a,** another major triterpene saponin constituent of *Panax ginseng* roots, exhibited significant anti-obesity effect in cellular and animal models. In high oleic acid and palmitic acid-induced mouse primary hepatocytes, Rg2 significantly decreased intracellular lipid accumulation and oxidative stress by upregulation of the activity of SIRT1 proteins. In HFD-fed obese hepatic steatosis in mice, Rg2 significantly decreased body weight gain, hepatic lipid content, serum glucose, and lipid levels by suppression of hepatic lipogenesis and oxidative stress via upregulation of the activity of SIRT1 proteins and antioxidant enzymes SOD and CAT in the liver of obese mice (Cheng et al. 2020).

Ginsenoside Rg3 **461**, another triterpenoid saponin constituent of Korean red ginseng, *Panax ginseng*, has potential antidiabetic and anti-obesity effects. In human enteroendocrine NCI-H716 cells, collected from diabetic patient, Rg3 stimulated glucagon-like peptide-1(GLP-1) secretion through its protopanaxadiol (PPD)-type aglycone by induction of the activity of sweet-taste specific G-protein receptor, Gα-gustducin (Gα-gust), and expression of sweet sensing taste receptors T1R2 and T1R3. Rg3 induced the activity of Gα-gust via intracellular cAMP accumulation, and increased phosphorylation of PKA, cAMP response element binding protein (CREB), and ERK1/2 kinase in NCI-H716 cells. Co-treatment of lactisole, an inhibitor of T1R3, inhibited the GLP-1 secreting activity of Rg3 in NCI-H716 cells. Among the isolated ginsenosides from different *Panax* spp., Rg3 had strongest GLP-1 secreting effect in NCI-H716 cells. In type 2 diabetic db/db mice, Rg3 treatment (0.5 g/kg) increased plasma GLP-1 and insulin levels and decreased plasma glucose level on oral glucose tolerance test. However, these effects of Rg3 were abolished in Gα-gust deficient mice. These findings indicate that ginsenoside Rg3 exhibits hypoglycemic effect by increasing glucose-stimulated insulin secretion

from pancreatic β-cells via enhanced GLP-1 secretion from endocrine L-cells by activation of Gα-gust (Kim et al. 2015). In high palmitate exposed skeletal muscle C2C12 cells, Rg3 increased the activation of insulin signaling pathway by increasing the phosphorylation of IRS-1 and Akt, and increased the mitochondrial function in ATP production and oxygen consumption rate, as well as increased mitochondrial biogenesis by upregulation of the expression levels of genes PGC-1α, NRF-1, and mitochondrial transcription factor (Tfam) in myotubes. Even in pre-treatment of antimycin A, an inhibitor of oxidative complex III, Rg3 increased the phosphorylation levels of IRS-1 and Akt in C2C12 cells. These findings suggest that ginsenoside Rg3 improves insulin sensitivity and mitochondrial function in C2C12 myotubes for its glucose uptake (Kim et al. 2016). In HFD-fed obese and hepatic steatosis mice, Rg3 treatment (1 mg/kg/day, *i.p.*) for 8 weeks reduced epididymal white AT (eWAT) size and hepatic steatosis, and TG contents in both eWAT and liver of obese mice. In both e-WAT and 3T3-L1 adipocytes, Rg3 decreased the expression levels of adipogenic genes PPARγ, FABP4, and SCD1, and the phosphorylation level of STAT5, as well as in e-WAT, the expression of inflammatory cytokines TNF-α and IL-1β, and increased the expression of anti-inflammatory cytokine IL-10. These findings suggest that ginsenoside Rg3 reduces lipid accumulation in eWAT and liver by suppression of STAT5 activation and inhibition of STAT5-induced PPARγ activity in obese mice (Lee et al. 2017).

Karaviloside XI **462**, and momordicoside S **463**, two triterpenoid saponins isolated from dietary green fruits of bitter melon or bitter gourd (*Momordica charantia*) have significant antidiabetic effects. In Asian countries, the green fruits of bitter gourd have been used in traditional medicine for treatment of diabetes and related inflammatory disorders. Both karaviloside XI and momordicoside S and their aglycones in L6 myotubes and 3T3-L1 adipocytes increased glucose uptake and GLUT4 translocation to plasma membrane, and increased the phosphorylation level of AMPK. These compounds at much lower concentrations (at 0.1 μM) stimulated GLUT4 translocation compared to AMPK agonist AICAR (at 1-2 mM). Moreover, these compounds increased AMPK activation via increased expression of LKB1, an upstream of AMPK, similar to metformin. These compounds failed to activate AMPK in LKB1 knockout HeLa cells. Momordicoside S improved glucose tolerance in normal mice. These compounds could be useful in treatment of diabetes and obesity, because activated AMPK improves insulin sensitivity by stimulation of fat oxidation and suppression of lipid synthesis in adipose tissue and muscle (Tan et al. 2008).

Glycyrrhizic acid (GA), also known as glycyrrhizin **458a**, a major saponin constituent of licorice (*Glycyrrhiza glabra*) roots, an important ingredient of Kampo medicine of Korea for diabetes treatment, has significant hypoglycemic effect in animal models. Oral treatment of GA in diet (0.41% of diet) in HFD-fed genetically type 2 diabetic mice for 9 weeks significantly reduced serum glucose (256.7 vs. 394.6 mg/dl in control) and insulin (29.9 vs. 64.8 μU/ml) levels compared to the control group (Takii et al. 2001). In another study, GA on oral treatment (100 mg/kg/day) to HFD-fed obese rats for 28 days significantly reduced the elevated levels of serum glucose, FFAs, TC, and LDL-C, and abdominal fat mass,

and increased insulin sensitivity and LPL enzyme expression levels in non-hepatic tissues, kidney, heart, abdominal muscle, and visceral and subcutaneous adipose tissues of obese rats. Possibly, GA increased the activity of PPARα and its target genes for FA oxidation via AMPK activation for reduction of fat mass (Eu et al. 2010). These findings suggest that GA has both hypoglycemic and hypolipidemic effects.

5.2.13 Polyacetylenes

Two polyacetylenic glucosides, 3β-D-glucopyranosyloxy-1-hydroxy-6(*E*)-tetradecene-8,10,12-triyne (BP-1) **464** and 2β-D-glucopyranosyloxy-1-hydroxy-5(*E*)-tridecene-7, 9,11-triyne (BP-2) **465**, isolated from antidiabetic butanol fraction of *Bidens pilosa*, have significant antidiabetic effect. In Asian and South American countries, the extracts of *B. pilosa* have been used in traditional medicine for treatment of diabetes and liver and stomach disorders. A butanol fraction of *B. pilosa* (BE) on treatment in NOD mice suppressed the development of type 1 diabetes by reduction of serum glucose level and increased serum insulin and IgE levels in NOD mice. Moreover, BE decreased the differentiation of native $CD4^+$ helper T (Th0) cells into Th1 cells, and increased the transition of Th0 cells into Th2 cells for production of IgE proteins and anti-inflammatory cytokine IL-4 for protection of pancreatic β-cells from injury and apoptosis. A group of evidence demonstrates that infiltration of Th-1 ($CD4^+$ type 1T) cells in pancreatic islets plays a pivotal role in the progression of type 1 diabetes in NOD mice by destruction of β-cells via inflammatory cytokine IFNγ-mediated IgG2α production, while Th2 cells promote β-cells growth and function via production of IgE from IL-4 cytokine. In isolated pancreatic islets of NOD mouse, compound BP-1 promoted the differentiation of Th0 cells into Th2 cells by 34%, and inhibited the differentiation of Th0 cells into Th1 cells by 40% at a dose of 15 μg/ml concentration, while at the same dose, BP-2 inhibited the differentiation of Th0 into Th1 cells by 10%, and increased the differentiation of Th0 cells to Th2 cells by 8%. Moreover, a mixture of BP-1 and BP-2 on treatment in type 2 diabetic db/db mice reduced blood glucose levels, partly by their anorexigenic effect (Chang et al. 2004). Another polyacetylene, cytopiloyne **466**, a major polyacetylenic compound of *B. pilosa*, in isolated pancreatic islets from NOD mouse, significantly promoted the differentiation of Th0 cells to Th2 cells and inhibited the differentiation of Th0 cells to Th1 cells substantially in a low concentration, 5 μg/ml. Moreover, cytopiloyne on *i.p.* treatment (25 μg/kg bw, 3 times/week) for 27 weeks completely prevented the development of type 1 diabetes in NOD mice. These findings suggest that cytopiloyne suppressed adaptive immunity in pancreatic islets of NOD mice via regulation of Th0 cells differentiation processes for prevention of type 1 diabetes (Chang et al. 2007; Chiang et al. 2007). In another study, an aqueous extract of *B. pilosa* containing cytopiloyne as a major constituent on treatment (250 mg/kg bw/day) for 4 weeks in type 2 diabetic db/db mice showed hypoglycemic effect by reduction of serum glucose and HbA1c levels and increased

serum insulin level via protection of pancreatic β-cells and stimulation of insulin secretion (Hsu et al. 2009).

(9*Z*,16*S*)-16-Hydroxy-9,17-octadecadiene-12,14-diynoic acid (HODA) **467**, a polyacetylene compound isolated from methanolic extract of *Dendropanax morbifera* leaves (DME), showed significant anti-obesity effect. The leaves of *D. morbifera* are consumed by Korean people as tea for prevention of various health disorders including headache, obesity, diabetes, and infectious diseases. In high oleic acid (OA) exposed HepG2 cells, HODA reduced intracellular TG accumulation, and increased the phosphorylation of LKB1, AMPK, and ACC. Co-treatment of compound C reversed the effect of HODA in TG accumulation and AMPK activation. Moreover, in OA and MDI exposed 3T3-L1 adipocytes, HODA inhibited adipogenesis by suppressing the intracellular lipid accumulation and increasing the phosphorylation levels of AMPK and ACC. These findings suggest that HODA prevents lipid accumulation in hepatocytes and adipogenesis in adipocytes through AMPK-dependent pathway (Kang et al. 2018a). In HFD-fed obese mice, an DME rich in HODA content on oral treatment (250 or 500 mg/kg/day) for 8 weeks significantly reduced body weight gain, AT fat mass, adipocyte size of subcutaneous AT, hepatic lipid accumulation, hepatic GOT and GPT levels, and serum TG and leptin levels in obese mice. The effects of higher dose (500 mg/kg) were very similar to those in orlistat treated (50 mg/kg) group. These results suggest that DME and its active constituent HODA have preventive effect against obesity and its associated hepatic steatosis in DIO mice via AMPK activation (Kang et al. 2018b).

Falcarinol **27**, a polyacetylene compound present in carrots (*Daucus carota*) and other vegetables, has antidiabetic effect. In insulin-resistant porcine myotubes, falcarinol increased glucose uptake and GLUT4 translocation to plasma membrane, and increased the phosphorylation of TBC1D1, a downstream target of Akt and AMPK to reduce the activity of this protein in GLUT4 translocation process. Co-treatment of wortmannin, an inhibitor of PI3K, significantly decreased the effect of falcarinol on GLUT4 expression and TBC1D1 phosphorylation, while co-treatment of dorsomorphin, an inhibitor of AMPK, did not alter the effect of falcarinol on GLUT4 expression and TBC1D1 phosphorylation. Accumulating evidence demonstrates that TBC1D1 activation promotes the activation of Rab-GTPases and leads to cytoskeleton reorganization, which in turn, triggers the translocation of GLUT4 protein from intracellular vesicles to the plasma membrane. These findings indicate that falcarinol stimulates insulin-dependent glucose uptake via GLUT4 expression and TBC1D1 activation (Bhattacharya et al. 2014b).

5.2.14 Organosulfur Compounds

Alliin (S-allyl cysteine sulfoxide) **468**, an organosulfur compound present in high concentration on fresh garlic bulbs (*Allium sativum* L.), has potential hypoglycemic and hypolipidemic effects in diabetes and obesity. The bulbs of garlic, a dietary vegetable, have been used in traditional medicine in many countries for treatment of various health disorders including atherosclerosis, cardiovascular diseases, obesity, diabetes, hypertension, and some types of cancer. On crushing the bulbs of garlic, a

major part of alliin is converted to allicin **469** by the enzyme allinase. In HFD-fed DIO mice, alliin on oral treatment (0.1 mg/ml of drinking water/day) for 8 weeks reduced obesity by reduction of FBG and the levels of serum insulin, lipid profile (TG, LDL-C, and FFAs), AST, ALP, TP, and albumin in DIO mice. Moreover, alliin improved both glucose and insulin tolerance in DIO mice. In addition, alliin modulated the composition of gut microbiota by decreasing the abundance of bacteria of family Lachnospiraceae and increasing the abundance of bacteria of family Ruminococcaceae. In Ruminococcaceae, the high abundance of the butyrate producing bacteria of genus *Oscillospira* and *Ruminococcus* was detected. Several studies indicate that Lachnospiraceae is closely associated with the development of obesity and diabetes in db/db mice by induction of inflammation and insulin resistance in combination with Gram-negative bacteria *Enterobacter* spp. and *Escherichia coli.* Ruminococcaceae bacteria act as negative regulators of fat accumulation in obesity by improvement of SCFAs production and energy expenditure in adipose tissues. Alliin was almost non-toxic to animal tissues. These findings indicate that alliin improves obesity by increasing insulin sensitivity and SCFAs production and energy expenditure through modulation of gut microbiota dysbiosis (Zhai et al. 2018).

Allicin **469**, another organosulfur constituent of garlic, has potential activity in prevention of obesity and cardiovascular diseases. In HFD-fed obese mice, allicin on oral administration (100 mg/kg/day) for 6 weeks reduced body weight gain, AT fat deposition, hepatic lipid accumulation, and serum LDL-C level, and increased serum HDL-C level in obese mice. Moreover, allicin decreased the expression levels of hepatic lipid transport gene FABP4 and of hepatic lipogenic genes SREBP-1c, FAS, SCD1, and PPARγ, and increased the expression levels of lipolytic genes LPL, ATGL, and HSL in epididymal-adipose tissue. In addition, allicin increased the expression of insulin signaling-related genes IRS-1, IRS-2, and IRS-3, and the expression of mitochondrial thermogenesis and biogenesis-related genes PGC-1α, UCP-1, PRDM-16, Cidea, and Cox7A in eWAT and BAT, and decreased the expression of fat metabolism-related genes leptin and resistin in adipose tissues. Furthermore, allicin modulated the composition of gut microbiota by increasing the abundance of Bacteroidetes and Clostridiates, and reducing the abundance of Firmicutes and *Lactobacillus* spp. At the genus level, allicin increased the abundance of SCFAs producing bacteria *Akkermansia* and cholesterol-lowering bacteria *Eubacterium* spp. in the gut of obese mice. Some *Clostridium* spp. have been reported to increase glycolysis process in adipose tissue by increasing the production of glyceraldehydes-3-phosphate dehydrogenase. These results suggest that allicin reduces obesity and hepatic steatosis by regulation of insulin-dependent lipid metabolism and amelioration of gut microbiota dysbiosis in obese mice (Shi et al. 2019). In both differentiated mouse embryonic fibroblast 3T3-L1 cells and differentiated inguinal WAT-derived stromal vascular cells (SVCs), allicin induced brown-like adipogenesis by increasing the expression of kruppel-like factor 15 (KLF15) and UCP-1, and such effects of allicin were not found in KLF15 knockout cells. These findings indicate that allicin stimulates KLF15 signal cascade to enhance the expression of thermogenic gene UCP-1 during brown like adipogenesis (Lee et al. 2019).

In STZ-induced diabetic rats, allicin treatment (8 or 16 mg/kg/day, *i.p.*) for 4 weeks mitigated myocardial injury by decreasing cardiac hypertrophy and fibrosis, serum glucose level, and increasing LV systolic pressure and maximum rate of LV pressure rise (+d*p*/d*t* max) and decreasing the maximum rate of LV pressure fall (–d*p*/d*t* max) toward normal levels in diabetic rats. In addition, allicin suppressed the expression of fibrogenic proteins TGF-β1 and CTGF, and the expression of pro-apoptotic protein Fas, and increased the expression of anti-apoptotic protein Bcl-2 in cardiomyocytes for suppression of myocardial fibrosis and apoptosis in diabetic rats. These findings suggest that allicin protects cardiomyocytes from injury against fibrosis and apoptosis by regulation of related genes expression (Liu et al. 2012).

Ajoene, [(E,Z)-4,5,9-trithiadodeca-1,6,11-triene-9-oxide], **470**, a by-product of garlic, produced from allicin during processing of garlic, has potential anti-obesity effect. In diet-induced DIO mice, ajoene on oral treatment (30 mg/kg/day) for 4 weeks significantly reduced hepatic steatosis by reduction of hepatic fat and TG content, and the levels of FBG, and plasma insulin in DIO mice. In molecular level, ajoene suppressed the activity of hepatic LXRα gene and the expression levels of its target lipogenic genes SREBP-1c, FAS, ACC, and SCD1. Moreover, ajoene decreased the hepatic oxidative stress by reducing the levels of TBARS and inflammatory cytokines TNF-α and COX-2, and increased the activity of hepatic antioxidant enzymes GSH, GP_X, and CAT, as well as increased the phosphorylation of AMPK and decreased the phosphorylation of S6K1 in the liver of DIO mice. In LXRα agonist T0901317 exposed HepG2 cells, ajoene decreased the expression levels of LXRα and SREBP-1c and its downstream target genes and increased the expression of Sirt1, deacetylation of LKB1, and the phosphorylation level of AMPK. Co-treatment of sirtinol, an inhibitor of Sirt1, or transfection of HepG2 cells with LKB1 siRNA, abolished the effect of ajoene on AMPK phosphorylation. These findings suggest that ajoene stimulates the activity of AMPK via LKB1 and Sirt1 and decreases the phosphorylation of S6K1 for suppression of the activity of LXRα and its target genes in the liver of DIO mice. The activated AMPK inhibited the activity of p70-ribosomal S6 kinase 1(S6K1) for suppression of LXRα-mediated mTOR/S6K1/SREBP-1c signaling pathway in lipogenesis in hepatocytes (Han et al. 2011).

Sulforaphane (SFN) **471**, an isothiocyanate organosulfur compound present in many cruciferous vegetables, such as broccoli and cabbage, has potential anti-obesity effect. In DIO mice, sulforaphane on oral treatment (0.1% of diet) for 6 weeks reduced body weight gain, perirenal and epididymal AT mass, adipocyte hypertrophy, hepatic fat, and TG content, and the levels of serum glucose, TC, and leptin, and increased serum adiponectin level in DIO mice. Moreover, SFN decreased the adipogenesis, and the expression levels of lipogenesis-related genes PPARγ, C/EBPα, ACC, and HMGCR, and increased the phosphorylation levels of AMPK and ACC in adipose tissues. These findings suggest that SFN prevents obesity by suppression of lipid synthesis via AMPK pathway in adipose tissues (Choi et al. 2014b). In STZ-induced type 2 diabetic mice, SFN on oral treatment (0.5 mg/kg/day, 5 days/week) for 4 months improved cardiac function by reduction of lipid accumulation, inflammation, oxidative stress, and fibrosis in myocardial

tissues of diabetic mice. SFN down-regulated the expression levels of inflammatory cytokines TNF-α and PAI-1, oxidative marker genes 3-NT and 4-HNE, and fibrosis-related proteins TGF-β1 and CTGF, and upregulated the expression levels of antioxidant enzymes Nrf2, NQO1, and HO-1, and the expression of LKB1 and phosphorylated levels of AMPK and ACC, as well as the expression of the downstream target genes of AMPK related to fat oxidation and autophagy, including Sirt1, PGC-1α, CPT-1, ULK-1, and LC-3II in myocardial tissues in the heart of diabetic mice. 4-Hydroxy-2-nonenal (4-HNE), a secondary product of LPO, on elevated expression in cardiomyocytes reduces mitochondrial ATPase activity, and promotes apoptosis of cardiomyocytes by activation of JNK and caspase 3 proteins. 3-Nitrotyrosine (3-NT) is formed by nitration of tyrosine with toxic peroxynitrite and impairs myocardial function by induction of cardiomyocyte apoptosis via activation of caspase-cascade pathway. Therefore, SFN protects myocardial tissues from oxidative stress-induced apoptosis and fibrosis by improvement of antioxidant status and suppression of lipotoxicity through upregulation of FA β-oxidation and autophagy in cardiomyocytes via LKB1-mediated AMPK activation (Zhang et al. 2014b). In C3H10T1/2 preadipocytes, SFN inhibited differentiation of adipocytes by suppression of intracellular lipid accumulation and the expression levels of core adipogenic genes PPARγ, C/EBPβ, C/EBPα, FAS, and SCD1, but induced trans-differentiation of mature adipocytes into beige cells by increasing the expression levels of genes UCP-1, PGC-1α, PRDM-16, Chop, Tmem-26 (transmembrane protein 26), HSL, and CPT-1α, related to browning of adipocytes. Moreover, SFN increased the expression levels of Nrf2, p-Akt, p-JNK, and p-p38MAPK in adipocytes. IN HFD-fed obese mice, SFN treatment (10 mg/kg/day, *i.p.*) for 36 days substantially decreased the volume and weight of inguinal fat, and improved glucose and insulin tolerance in obese mice. Moreover, SFN increased the mitochondrial biogenesis and function by increasing the expression of browning genes UCP-1, PGC-1α, PRDM-16, HSL, Tmem-26, and others in inguinal and visceral WAT and BAT in obese mice. These findings suggest that SFN reduces fat mass in obesity by promoting insulin sensitivity for glucose metabolism and browning of white fat through enhanced mitochondrial biogenesis and function and suppression of mitochondrial oxidative stress through activation of Nrf2/PGC-1α and MAPK pathways (Liu et al. 2021).

Glucoraphanin **472**, a glucosinolate (β-thioglucoside-*N*-hydroxysulfate) present in several cruciferous vegetables, such as broccoli (*Brassica oleracea* L.) and broccoli sprouts, cauliflower, and mustard seeds, is hydrolyzed by gut microbiota-derived myrosinase (thioglucoside glucohydrolase) into bioactive metabolite sulforaphane before intestinal absorption in humans and other herbivores, and has potential anti-obesity effect. In high-fat diet-induced DIO mice, broccoli extract powder supplementation in diet (2.2% of extract powder containing 0.3% of glucoraphanin in diet) for 14 weeks significantly reduced body weight gain, hepatic lipid accumulation, plasma LPS, and plasma and hepatic LBP levels and improved glucose and insulin tolerance in wild-type (WT) obese mice, but not in HFD-fed Nrf2 knockout mice. Possibly, glucoraphanin decreased the relative abundance of Gram-negative toxic bacteria producing proteobacteria of family

Desulfovibrionaceae in gut microbes for suppression of hepatic inflammatory LBP levels. Moreover, glucoraphanin increased the expression of antioxidant genes Nrf2 and NQO1, and of thermogenic genes UCP-1, Cidea, and PRDM-16 in inguinal and epididymal adipose tissues, and decreased the expression levels of inflammatory cytokines TNF-α, MCP-1, M1 macrophage (F4/80), Cd11b, and CD68, and kinases p-JNK and p-ERK, and of lipogenic genes SREBP-1c, FAS, and PPARγ in the liver of obese WT mice. In addition, glucoraphanin increased the expression of FA oxidation-related genes PPARα, and CPT-1α, and of antioxidant enzymes CAT, GP_X, and SOD1 in the liver of obese WT mice. However, glucoraphanin did not increase the p-levels of AMPK and ACC in the liver and adipose tissue. These findings suggest that glucoraphanin probably ameliorates obesity and hepatic steatosis through Nrf2-mediated antioxidant, anti-inflammatory, lipid metabolic, and browning activity in the liver and adipose tissue independent of AMPK pathway (Nagata et al. 2017). In another study, in HFD-fed obese mice, glucoraphanin treatment (2.64 g of broccoli seeds extract powder containing 150 μM glucoraphanin/kg bw/day) for 8 weeks reduced the weight of epididymal and mesenteric fat, liver fat, the levels of serum FG, fasting insulin, HOMA-IR, inflammatory factors, and hepatic oxidative stress and increased hepatic lipid oxidation, and decreased the Firmicutes/Bacteroidetes ratio in gut microbiota of obese mice. Glucoraphanin decreased the abundance of bacteria of family Lachnospiraceae and Desulfovibrionaceae, and increased the abundance of bacteria of family Bacteroidaceae of genus *Akkermansia* and *Alloprevotella* in gut microbiomes of obese mice. The bacteria of genus *Akkermansia* and *Alloprevotella* improve carbohydrate and lipid metabolism via improvement of insulin sensitivity in liver and adipose tissue. These findings suggest that glucoraphanin prevents obesity at least in part, by modulation of gut microbiota dysbiosis for regulation of genes expression related to glucose and lipid metabolism in obese mice (Xu et al. 2020b).

5.2.15 Polysaccharides

Dietary polysaccharides from natural sources, namely, plants, grains, fruits, vegetables, and dietary mushrooms, medicinal mushrooms, dietary seaweeds, marine animals, and bacteria, have potential antidiabetic and anti-obesity effects. So far more than 120 types of polysaccharides from natural sources have been reported. These polysaccharides alleviate pancreatic β-cells dysfunction through suppression of inflammation and oxidative stress and increase insulin secretion. Some polysaccharides inhibit the activity of dietary starch and carbohydrate digesting enzymes α-amylase and α-glucosidase. These polysaccharides on partial or complete fermentation by intestinal microbiota produce SCFAs, increase pancreatic β-cells mass and insulin secretion, and increase insulin signaling in the liver, adipose tissue, and skeletal muscle for improving glucose uptake, glycolysis, and glycogen synthesis and suppression of hepatic gluconeogenesis, inflammation, and oxidative stress through activation of AMPK/PGC-1α signaling pathway. Various dietary sulfated polysaccharides (SPs), such as amylopectin, pectin, xylan, fucoidan,

ulvan, and laminarin, isolated from seafoods (algae and animals) are degraded by some bacterial strains of *Bifidobacterium*, *Peptostreptococcus*, and *Ruminococcus* to increase the abundance of beneficial bacteria of genus *Lactobacillus*, *Akkermansia*, and *Bifidobacterium*. Some SPs reduce the abundance of *Proteobacteria* in the gut, which include many pathogenic bacteria, such as *Escherichia coli, Vibrio cholerae*, *Salmonella*, and *Heliobacter pylori* for suppression of inflammation. Therefore, dietary consumption of polysaccharides might be a suitable choice for management of diabetes and obesity (Wu et al. 2016; Hu et al. 2018; Ganesan and Xu 2019; Zhu et al. 2021).Several common dietary grains, namely, wheat, rice, barley, rye, and oat, are rich sources of carbohydrates, including monosaccharides, disaccharides, oligosaccharides, starch, and non-starch polysaccharides (NSP) (mainly cellulose, arabinoxylan (AX), and β-glucans). Beta-glucans are the major dietary fibers (DF) and have potential role in regulation of insulin sensitivity. Starch is composed of glucan polymers, amylopectin, and amylase in a 3:1 ratio, and both are composed of α-D-glucose with different levels of branching. Most of the starch are not digestable by human enzymes, but have a significant role in production of health-benefit bacteria by fermentation of gut microbiota. AX **473** comprises of several β-D-xylopyranosyl residues linked through (1→4) glycosidic linkages, with some residues being substituted α-L-arabinofuranosyl residues either in position 3 or in positions 2 and 3. In many cases, arabinose residue is substituted in position 3 by ferulic acid or its derivative. Cellulose **474** consists of (1→4) β-D-glucopyranosyl residues. Similarly, β-glucan comprises of only glucose residues, which are linked by (1→4) and (1→3) bonds. In general, single (1→3) linkages are separated by 2 or 3 (1→4) linkages, and the ratio of (1→4) and (1→3) linkages depends on their sources of cereals. Such variation in linkage pattern determines their properties, such as solubility, viscosity, and biological activity (Lafiandra et al. 2014; Stone and Morell 2009; Li et al. 2006b). Accumulating evidence demonstrates that AX and β-glucans account for about 70% and 20%, respectively, of total cell wall polysaccharides in starchy endosperm of wheat, with small amount of cellulose (about 2%) and glucomannan (about 7%), while barley and oats have higher contents of β-glucans than of AX. Both NSP and undigested starch increase dietary food viscosity to reduce the digestion of carbohydrate diet, and thereby reduce the absorption of dietary sugars, and reduce postprandial glucose and insulin response. Moreover, high viscosity of digested food inhibits the mixing of diet with intestinal tract and delays gastric emptying. Furthermore, it decreases enzyme diffusion and decreases glucose transport to enterocytes (De Natale et al. 2012). A significant portion of DF and starch enters the large bowel, and partly or completely fermented by colon bacteria, and produces SCFAs, acetate, propionate, and butyrate together with methane, hydrogen, carbon dioxide, and lactate. Particularly butyrate reduces hepatic glucose production and plasma glucose concentrations by increased insulin sensitivity via increased levels of plasma GLP-1 and food intake suppressant gene PYY. Moreover, butyrate protects colorectal cells from DNA damage and prevents colorectal cancer. Therefore, improvement of high DF producing grain varieties is a prospective target in treatment of obesity and diabetes (Slavin 2013).

Asian rice (*Oryza sativa* L.) bran polysaccharide (RBP) composed of Xyl, Rha, Man, Gal, Ara, and Glc as sugar units, on oral treatment (500 mg/kg/day, *i.g.*) to HFD-fed obese mice for 10 weeks, showed hypolipidemic effect by reduction of the levels of plasma TC, TG, LDL-C, and hepatic lipid droplets in obese mice. Moreover, RBP decreased the expression levels of hepatic lipogenic genes SREBP-1c, FAS, ACC, and CD36, and increased the expression levels of FA oxidation-related genes PPARα, PGC-1α, and Sirt1, and decreased the expression of inflammatory protein NF-κB in the liver of obese mice. These findings suggest that RBP ameliorates hyperlipidemia by regulation of the genes expression related to lipid metabolism and suppression of hepatic inflammation in obese mice (Nie et al. 2017b).

The polysaccharide from wolfberry (*Lycium barbarum*) (LBP) has potential anti-obesity effect. In HFD-fed obese mice, LBP treatment (100 or 200 mg/kg/day) for 12 weeks decreased hepatic steatosis by reduction of liver weight, hepatic lipid accumulation, and serum and liver TG content in obese mice. Moreover, LBP decreased the expression of hepatic lipogenic genes FAS, ACC1, Elovl 6, and DGAT, and increased the expression of lipolysis gene ATGL, and expression of FA oxidation-related gene CPT-1α and Sirt1, and the phosphorylation levels of AMPK and ACC. In palmitic acid exposed insulin-resistant HepG2 cells, LBP decreased TG accumulation, and the expression of lipogenic gene FAS, and increased the expression of Sirt1, and the NAD^+ and NAD^+/NADH ratio, and LKB1 deacetylation and the phosphorylation levels of AMPK and ACC. Transfection of HepG2 with Sirt1 siRNA decreased LBP-mediated LKB1 deacetylation and AMPK phosphorylation. These findings indicate that LBP reduces hepatic steatosis and TG accumulation in the liver and HepG2 cells by stimulation of Sirt1/LKB1/AMPK pathway (Jia et al. 2016).

Total polysaccharide fraction from tuberous roots of *Liriope spicata* (LSTP), and two polysaccharides (LSP1 and LSP2) isolated from LSTP, on oral administration (100 or 200 mg/kg/day) to HFD-fed obese diabetic KK-Ay mice for 4 weeks reduced hyperglycemia, hepatic steatosis, and hepatocyte hypertrophy by reduction of hepatic lipid accumulation, plasma lipid profile (TC, TG, and LDL-C), and plasma FG, fasting insulin, HOMA-IR, and increased plasma HDL-C levels and hepatic glycogen content in diabetic mice. Moreover, LSTP, LSP1, and LSP2 decreased hepatic gluconeogenic process by suppression of the activity of G6Pase enzyme, and increased hepatic glycolysis by upregulation of the expression of GCK enzyme, and increased hepatic insulin sensitivity by increasing the expression of IRα, IRS-1, and PI3K. LSTP was more effective than LSP1 and LSP2. In Chinese traditional medicine, the tuberous roots of *L. spicata* have been used in treatment of diabetes (Liu et al. 2013b).

Two polysaccharide fractions from the fruits of white mulberry (*Morus alba* L.) MFP50 and MFP90 showed significant antidiabetic effect. The fruits of *M. alba* have been used in traditional Chinese medicine for treatment of diabetes, dizziness, insomias, and hepatic and kidney disorders. In STZ and HFD-induced type 2 diabetic rats, MFP50 and MFP90 on oral treatment (100 mg/kg/day) for 7 weeks reduced hyperglycemia and hyperlipidemia by reduction of serum FG, fasting insulin,

HbA1c, HOMA-IR, TG levels and increased serum HDL-C level and glucose tolerance in diabetic rats. Moreover, both MFP50 and MFP90 increased pancreatic insulin secretion, and increased glucose uptake in skeletal muscle by upregulation of the expression of IR, IRS-2, phosphorylated Akt, and GLUT4 translocation to the plasma membrane. The hypoglycemic effect of MFP50 was better than that of MFP90, while hypolipidemic effect of MFP90 was better than that of MFP50 (Jiao et al. 2017). In another study, polysaccharides of *M. alba* fruits (MFP) on treatment (800 mg/kg/day) for 8 weeks in obese diabetic db/db mice increased the activity of antioxidant enzymes SOD, CAT, and GSH-P_X in the liver and pancreas, and modulated the composition of gut microbiota for amelioration of hyperglycemia, hyperlipidemia, and body weight gain in obese diabetic mice. MFP significantly increased the abundance of bacteria of genus *Lactobacillus*, *Allobaculum*, and *Akkermansia* in gut microbiota for improvement of insulin sensitivity in the liver, adipose tissue, and muscle (Chen et al. 2018a).

A polysaccharide from *Momordica charantia* L. fruits (MCPIIa) of MW 13,029 Da, contained L-Rha, D-Gal A, D-Gal, D-Xyl, and L-Ara in a molar ratio of 12:3.05:19.89:5.95:56, which are linked via β-glycosidic bonds to a large number of arabinofuranose, glucuronic acid, and xylopyranosyl residues. In STZ-induced diabetic mice, MCPIIa on oral treatment (200 or 300 mg/kg/day) for 28 days showed significant antidiabetic effect by reduction of serum glucose level and increased serum insulin level in diabetic mice. Moreover, MCPIIa protected the pancreatic tissue from injury and improved insulin secretion (Zhang et al. 2018b). Another study reported that polysaccharides from *M. charantia* fruits (MCP) on oral treatment (500 mg/kg/day) for 35 days to STZ-induced type 2 diabetic mice significantly decreased hyperglycemia and hyperlipidemia by reduction of serum glucose, TG, LDL-C, creatinine, and uric acid levels, pancreatic β-cells injury, and increased serum insulin and HDL-C levels, and increased hepatic SOD activity and decreased hepatic MDA level toward normal in diabetic mice. The hypoglycemic effect of MCP was comparable to that of *M. charantia* saponins (MCS) treated group (40 mg/kg). Moreover, MCS significantly increased the phosphorylation level of AMPK in the liver, but such effect was not observed in MCP treated group. These findings suggest that MCPexert hypoglycemic effect mainly by repairing pancreatic damaged β-cells and promoting antioxidant capacity, while MCS exert hypoglycemic effect mainly via activation of AMPK (Wang et al. 2019e).

The polysaccharides isolated from pumpkin (*Cucurbita moschata* Duch.) (PPs) on oral treatment (1 g/kg/day) to HFD-fed obese diabetic rats for 4 weeks alleviated diabetes by reduction of serum glucose, TC, and LDL-C, and increased serum HDL-C level (Wang et al. 2017b). Moreover, PPs modulated the composition of gut microbiota by increasing the abundance of SCFAs producing bacteria of *Bacteroidetes*, *Prevotella,* *Deltaproteobacteria*, *Oscillospira*, *Sutterella*, Veillonellaceae, and *Bilophila* for improvement of insulin action and insulin tolerance in diabetic rats. Therefore, PPs exhibit antidiabetic effect by modulation of gut microbiota composition (Liu et al. 2018a). In another study, the PPs on oral treatment in alloxan-induced diabetic ICR mice showed hypoglycemic effect by reduction of serum FG, and increased serum insulin and hepatic glycogen content, as

well as enhanced pancreatic islet proliferation in diabetic mice. Chemically, PPs composed of Rha, Ara, Glc, Gal, and a small amount of inositol (Wang et al. 2017b).

The polysaccharides extracted from common edible oyster mushroom *Pleurotus ostreatus* (POP) on oral administration (200 or 400 mg/kg/day) to STZ plus HFD-induced type 2 diabetic rats for 4 weeks showed significant hypoglycemic and hypolipidemic effects by reduction of serum glucose, insulin, TG, and TC levels and reduction of hepatic oxidative stress marker MDA level, and increased the activity of serum and hepatic antioxidant enzymes SOD, CAT, and GSH-P_X. Moreover, POP increased hepatic and muscle glycogen content by increasing glucose uptake and glycogen synthesis via upregulation of GLUT4 translocation to plasma membrane and increased phosphorylation of GSK-3β in skeletal muscle and liver of diabetic rats (Zhang et al. 2016e). *P. ostreatus* have health-benefit effects against diabetes, cancer, and viral and bacterial infections.

Beta-glucan-rich polysaccharides extract from edible Malaysian gray oyster mushroom *Pleurotus sajor-caju* syn *Lentinus sajor-caju* (PSP) on diet supplementation (240 mg/kg bw/day) to HFD-fed obese mice for 16 weeks prevented obesity and obesity-associated oxidative stress by reduction of body weight gain and levels of serum TG, TC, LDL-C, MDA, AST, ALT, and ALP, and increased serum HDL-C level and the activity of hepatic and kidney antioxidant enzymes CAT, SOD, and GP_X in obese mice. Moreover, PSP down-regulated the expression levels of lipogenic genes PPARγ, SREBP-1c, and LPL, and upregulated the expression of lipolysis (TG hydrolysis)-related genes HSL and ATGL in adipose tissue of obese mice. These findings suggest that PSP prevents obesity via improvement of antioxidant capacity and regulation of genes expression related to lipid metabolism (Kanagasabapathy et al. 2013).

A polysaccharide isolated from edible mushroom *Lentinus edodes* mycelia (LMP) inhibited the activity of α-glucosidase by 34.38% at the concentration of 2.7 mM in a mixed-type manner. Moreover, LMP inhibited the formation of AGEs in high glucose exposed HUVECs by suppression of ROS production and activation of MAPK signaling pathway. Therefore, LMP could be a potential candidate in treatment of diabetes and its related complications (Cao et al. 2020).

The polysaccharides isolated from medicinal mushroom *Ganoderma lucidum* (GLPs) on oral administration (50 or 100 mg/kg/day) to STZ-induced type 2 diabetic mice for 7 days showed significant antidiabetic effect by reduction of body weight gain, epididymal fat mass, and levels of serum FG and insulin and increased hepatic glycogen content in diabetic mice. GLPs decreased hepatic glucose production by down-regulation of the expression levels of gluconeonegic genes PEPCK, FBPase, and G6Pase, and increased hepatic glycogen content by down-regulation of the expression of glycogen-degrading gene GP in the liver. These results suggest that GLPs ameliorate hyperglycemia by regulation of genes expression related to glucose metabolism in liver (Xiao et al. 2012).

The polysaccharides fraction H1 containing high molecular weight polysaccharides (>300 kDa) isolated from medicinal mushroom *Hirsutella sinensis* mycelium water extract (HSM) showed potential anti-obesity effect by modulation of gut microbiota composition. In HFD-fed obese mice, both HSM and H1 on oral

treatment (20 mg/kg of each) for 12 weeks reduced body weight, visceral fat and hepatic lipid content, and the levels of serum FG, fasting insulin, IL-1β, and TNF-α in obese mice. Moreover, both HSM and H1 increased hepatic β-oxidation, and the expression of UCP-1 in BAT and WAT, decreased hepatic lipogenesis, and increased gut barrier integrity by upregulation of the expression of zonula occludens (ZO-1) for suppression of the entry of LPS into blood, and thereby reduction of inflammation and insulin resistance in metabolic tissues. In addition, both HSM and H1 modulated the composition of gut microbiota by increasing the abundance of health-benefit bacteria including *Parabacteroides goldsteinii*, *Clostridium cocleatum*, and *Anaerotruncus colihominis,* and decreased the abundance of endotoxic-bearing bacteria *Pseudomonas aeruginosa*, *E. Coli*, and *Shewanella algae*. *P. goldsteinii* is negatively correlated with obesity because treatment of *P. goldsteinii* to HFD-fed obese mice for 8 weeks significantly reduced body weight, liver fat content, and serum IL-1β level, and increased the expression of UCP-1 in BAT and WAT, and increased the expression of anti-inflammatory cytokine IL-10 and ZO-1 in colon tissue. The effect of H1 in upregulation of *P. goldsteinii* expression in the gut was suppressed by co-treatment of neomycin in HFD-fed obese mice. These findings suggest that H1 prevents obesity mainly by upregulation of the expression of *P. goldsteinii* in the gut. Although the polysaccharides in H1 have not yet been identified, the presence of β-glucans has been identified in another medicinal fungus *Ophiocordyceps sinensis*, which is an anamorph of *H. sinensis*. These findings also suggest that *P. goldsteinii* could be a potential probiotic bacterium for treatment of obesity (Wu et al. 2019).

The polysaccharide isolated from dietary mushroom *Pleurotus eryngii* (PEP) on oral treatment (100 or 200 mg/kg/day) to diabetic KM mice for 6 weeks showed antidiabetic effect by decreasing the body weight gain, and reducing the elevated levels of serum FG, insulin, TG, TC, and LDL-C, and increasing serum HDL-C level and hepatic glycogen content in diabetic mice (Chen et al. 2016b).

The polysaccharides rich in alginate, fucoidan, and laminarin, isolated from dietary marine alga *Laminaria japonica* (LJP) on oral treatment (150 and 300 mg/kg/day) to alloxan-induced diabetic mice for 4 weeks showed hypoglycemic and hypolipidemic effects by reduction of body weight loss, serum levels of FG, TC, TG, and LDL-C, and increased serum insulin and HDL-C levels in diabetic mice (Jia et al. 2014). Another study reported that LJP treatment in normal mice increased hepatic glycogen content, and activity of antioxidant enzymes SOD, CAT, and GP_X and decreased MDA level in the serum, liver, and skeletal muscle of mice (Yan and Hao 2016). In TCM, the extracts of *L. japonica* have been used for treatment of weight loss and phlegm elimination.

Sulfated polysaccharides, composed of agarose and agaropectin, isolated from large-scale cultivation of Chinese marine red seaweed *Gracilaria lemaneiformis* (GLP), having MW, 121.89 KDa, and its degradation products GLP1 and GLP2 of respective MW of 57.02 and 14.29 kDa, on oral treatment (200 mg/kg bw/day) in alloxan-induced diabetic mice for 21 days showed significant hypoglycemic effect by reduction of serum glucose level and increased both antioxidant enzymes SOD and GSH-P_X activity and T-AOC levels, and decreased MDA levels in the serum,

liver, kidney, and pancreas of diabetic mice. GLP1 had more hypoglycemic effect than GLP and GLP2 at the same dose. In vitro, GLP, GLP1, and GLP2 inhibited the activity of α-glucosidase, and GLP1 had the strongest inhibitory activity. Natural agarose has been reported to have many other beneficial activities, including antitumor, antiviral, immunomodulatory, and antioxidant activities (Liao et al. 2015). Another study reported that GLP isolated from *G. lemaneiformis* by citric acid extraction process of MW of 21.2 kDa had strong inhibitory effect against α-amylase with IC_{50} value of 3.94 μg/ml compared to that of acarbose of IC_{50} of 22.94 μg/ml. In STZ-induced diabetic Kunming (KM) mice, GLP on oral treatment (60, 120, and 225 mg/kg bw/day) for 6 weeks showed significant hypoglycemic effect by reduction of serum FG, improvement of oral glucose tolerance, increased the levels of serum C-peptide, HDL-C, and liver glycogen, and decreased the levels of serum TC, TG, LDL-C, and BUN in diabetic mice. Moreover, GLP increased hepatic glucose utilization and glycogen synthesis by upregulation of the expression levels of glycolysis-related genes GCK and G6PD, and decreased hepatic glucose production by down-regulation of the activity of gluconeogenic gene G6Pase, and improved hepatic function by lowering the levels of hepatic toxic marker enzymes AST and ALT and oxidative stress toxic marker MDA level in the serum and liver of diabetic mice. In addition, GLP increased the activity of hepatic antioxidant enzymes SOD, GSH-P_X, and CAT for suppression of oxidative stress and protected pancreatic β-cells from injury and insulin secretion. GLP-treated diabetic group was more effective in regulation of insulin secretion, lipidemic parameters, and BUN levels than metformin treatment (300 mg/kg bw) group in prevention of diabetes. These findings indicate that GLP exerts its antidiabetic effect by reduction of oxidative stress, regulation of genes expression related to glucose metabolism, increased insulin secretion, and inhibition of the activity of carbohydrate digesting enzyme in diabetic mice (Wen et al. 2017).

The sulfated polysaccharides isolated from edible green sea lettuce *Ulva lectuca* (ULP) on oral treatment (180 mg/kg bw/day) in alloxan-induced diabetic rats for 30 days significantly showed hypoglycemic and hypolipidemic effects by reduction of the elevated levels of plasma glucose, TC, TG, LDL-C, and liver and kidney toxic marker factors AST, ALT, GGT, LDH, creatinine, urea, and albumin, and increased plasma HDL-C level in diabetic rats. Moreover, ULP significantly inhibited the activity of dietary starch digesting enzymes α-amylase and maltase, and of fat digesting enzyme lipase in plasma and small intestine of diabetic rats. These findings suggest that ULP exerts its hypoglycemic and hypolipidemic effects mainly by suppression of the activity of key enzymes related to starch and fat digestion, α-amylase, maltase, and lipase, and improvement of liver and kidney dysfunction. In traditional medicine, *U. lectuca* has been used in treatment of hyperlipidemia, sunstroke, and urinary disorders (BelHadj et al. 2013).

The polysaccharide ulvan isolated from alga *Ulva pertusa* of MW 151.6 kDa, and its degradation products U1 and U2, on oral treatment to hypercholesterolemic rats for 21 days, significantly reduced hypercholesterolemia and hypertriglyceridemia in rats by reduction of the elevated levels of serum TC, TG, and LDL-C, and increased serum HDL-C levels. In addition, these sulfated polysaccharides increased fecal bile acid excretion in rats (Pengzhan et al. 2003).

The sulfated polysaccharide from sea cucumber *Stichopus japonicus* (SCSP) and its depolymerized product (d-SCSP) on treatment to HFD-fed obese mice for 8 weeks prevented obesity by reduction of body weight gain, adipose tissue, and liver hypertrophy, and the levels of serum lipids, inflammatory cytokines, and LPS in obese mice. Moreover, both SCSP and d-SCSP modulated the gut microbiota dysbiosis by increasing the abundance of SCFAs producing bacteria of genus *Akkermansia* and decreasing the abundance of endotoxin-bearing bacteria of family Proteobacteria in gut of obese mice. The depolymerized polysaccharide product, d-SCSP, was more effective in suppression of fat accumulation than that of SCSP (Zhu et al. 2018).

The sulfated polysaccharides of black sea cucumber *Holothuria leucospilota* (HLP) of MW 52.80 kDa, composed of monosaccharides Fuc, Rha, and Glc-A, on oral administration (100 or 200 mg/kg bw) to HFD-fed obese rats for 4 weeks decreased hyperlipidemia by reduction of the elevated levels of serum TC, TG, LDL-C, and leptin, and increased the levels of serum HDL-C and adiponectin in obese rats. Moreover, HLP decreased the expression of inflammatory cytokines TNF-α, IL-6, and IL-12, and increased the expression of anti-inflammatory cytokine IL-10 in adipose tissue, and decreased the expression levels of lipogenic genes ACC and CD36, and of inflammatory-related factors TNF-α and NF-κB, and of fat lesions in the liver of obese rats. In addition, HLP modulated the gut microbiota composition by increasing the abundance of SCFAs producing bacteria of genus *Oscillospira*, *Prevotella*, and *Dorea,* and decreasing the abundance of bacteria of genus *Ruminococcus* in the gut of obese rats. Several studies demonstrate that the bacteria of *Prevotella* enterotype promote the production of SCFAs in high levels with propionate as a major product. These findings suggest that HLP reduces hyperlipidemia mainly by modulation of gut microbiota composition and regulation of lipid metabolism (Yuan et al. 2019). Figure 5.2 represents the major therapeutic targets of phytochemicals via stimulation of AMPK activation or AMPK deactivation and insulin signaling pathways in different metabolic tissues for maintenance of carbohydrate and lipid homeostasis in obese and diabetic animals (Table 5.1).

5.3 Summary and Future Perspectives

Both obesity and its associated type 2 diabetes mellitus (T2DM) are the most common diseases and are endemic worldwide and becoming a serious public health threat to all countries. Obesity is characterized by an excessive fat accumulation in the body from an imbalance of energy intake and energy expenditure. The insulin resistance, hyperlipidemia, hypertension, hyperglycemia, and inflammation in different organs are the major symptoms of this disease. T2DM is a severe endocrine metabolic disorder and is characterized by chronic hyperglycemia from impaired insulin secretion from pancreas and insulin resistance in different metabolic tissues resulting in the dysregulation of carbohydrates, lipid, and protein metabolism. Obesity and inflammation are closely associated to T2DM (Fig. 5.3). Therefore, suppression of the major pathogenic factors of obesity and inflammation are important therapeutic targets of T2DM. Moreover, both obesity and T2DM are associated

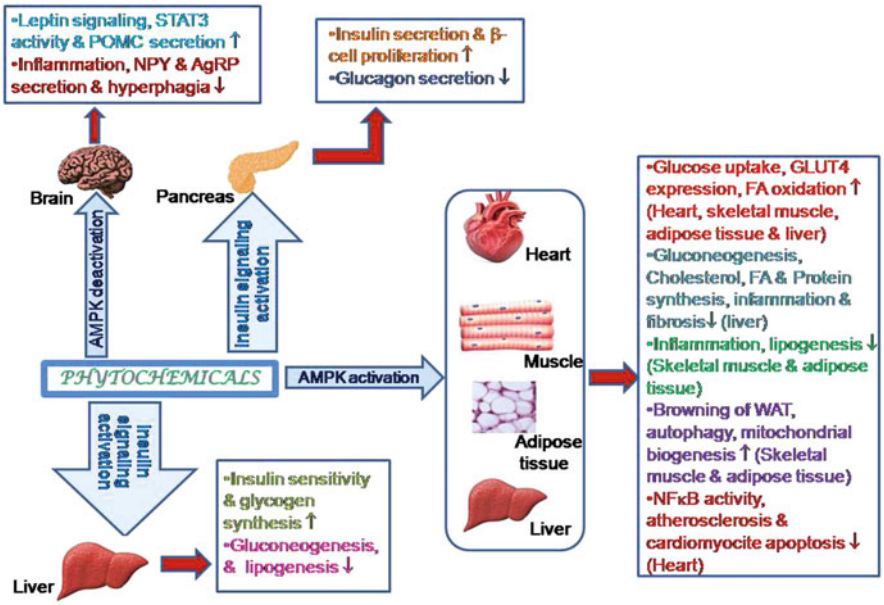

Fig. 5.2 Phytochemicals stimulate AMPK activation or AMPK deactivation and insulin signaling pathways in different metabolic tissues for maintenance of carbohydrate and lipid homeostasis in obese and diabetic animals

with gut microbial dysbiosis, that is, characterized by low levels of health-benefit short-chain fatty acids (SCFAs)-producing bacteria, namely, of genera *Eubacterium*, *Roseburia*, *Faecalbacterium*, etc., and high levels of opportunist pathogens including *Clostridium* spp. A group of evidence demonstrates that SCFAs play a significant role in the maintenance of glucose homeostasis through multiple targets: (1) regulation of insulinotropic and satiety effects; (2) promoting secretion of GLP-1 and PYY hormones from the gut; (3) protecting pancreatic β-cells from injury and insulin secretion; (4) decreasing the levels of pro-inflammatory cytokines in different organs; and (5) increasing insulin sensitivity and GLUT4 expression via upregulation of AMPK activation. Moreover, *Akkermansia muciniphila* reduces the levels of tauro-conjugated bile acids to improve the activation of FXR for suppression of the expression levels of genes related to TG synthesis. Therefore, modulation of gut microbial composition by the use of probiotic and prebiotic natural products is one of the important therapeutic strategies for treatment of obesity.

Natural products have been used in traditional medicines in the treatment of various diseases including obesity, diabetes, and their associated vascular complications including cardiovascular diseases, renal diseases, retinopathy, and neuropathy. A variety of natural products, namely, flavonoids (flavonols, flavones, flavanones, flavanols, isoflavones, anthocyanins, chalcones), terpenoids (monoterpenoids, sesquiterpenoids, diterpenoids, triterpenoids, carotenoids),

Table 5.1 Summary of major therapeutic targets of some phytochemicals that are discussed here in obesity and diabetes treatment

Phytochemicals	Experimental models	Major therapeutic targets	References
1. Flavonoids			
Quercetin **23**	3T3-L1 adipocytes	Adipogenesis and inflammation↓	Seo et al. (2015)
	L6 and C2C12 myotubes	GLUT4 expression and activation of AMPK and Akt↑	Dhanya et al. (2017); Eid et al. (2010)
	DIO mice	Hypothalamic leptin signaling↑	Yang et al. (2017)
Rutin **54**	3T3-L1 adipocytes L6 myotubes	Adipogenesis↓ GLUT4 expression and Akt activation↑	Varshney et al. (2019)
	DIO mice	Energy expenditure and thermogenesis in WAT↑	Yuan et al. (2017)
Kaempferol **66**	DIO mice	Glucose uptake, GLUT4 expression, and AMPK activation in skeletal muscle↑ Hepatic inflammation and gluconeogenesis↓	Alkhalidy et al. (2015, 2018); Luo et al. (2015)
Kaempferol glycosides **382** and **383**	DIO mice	Lipogenesis in the liver and AT↓	Zang et al. (2015)
Myricetin **22**	STZ-diabetic rats	Hypoglycemic effect via MOR activation in skeletal muscle↑ Inflammation and NF-κB activation in AT↓	Tzeng et al. (2011); Liao et al. (2017)
	DIO mice	Lipogenesis in the liver and AT↓	Su et al. (2016a)
Apigenin **197**	3T3-L1 adipocytes	Adipogenesis↓, AMPK activation↑	Ono and Fujimori (2011)
	STZ-diabetic rats	Glucose uptake, GLUT4 expression, and insulin signaling in skeletal muscle↑, pancreatic insulin secretion↑	Hossain et al. (2014)
	DIO mice	Hepatic inflammation, lipogenesis, and gluconeogenesis↓, SIRT1 expression in the liver↑	Jung et al. (2016); Escande et al. (2013)

(continued)

Table 5.1 (continued)

Phytochemicals	Experimental models	Major therapeutic targets	References
Luteolin **196**	DIO mice	Inflammation and lipogenesis in AT and the liver↓, Akt and AMPK activation in AT and the liver↑	Xu et al. (2014); Zang et al. (2016)
Baicalein **58**	DIO mice	Hepatic and AT inflammation and lipogenesis↓, hepatic and AT-FA oxidation, energy expenditure, activation of Akt and AMPK↑. Pancreatic insulin secretion↑, gut microbial dysbiosis↓	Pu et al. (2012a); Min et al. (2018); Zhang et al. (2018a)
Baicalin **352**	C2C12 cells and DIO mice	Glucose uptake, GLUT4 expression, and Akt activation in C2C12 cells and skeletal muscle↑, Inflammation in AT and the liver↓	Fang et al. (2017, 2018)
Tangeretin **136**	C2C12 myotubes and DIO mice	Glucose uptake, GLUT4 expression 7 AMPK activation in C2C12 cells, and skeletal muscle↑, Hepatic and AT lipogenesis↓, hepatic AMPK activation↑	Kim et al. (2012b)
	STZ-diabetic rats	Hepatic glycogen synthesis↑, hepatic inflammation, and gluconeogenesis↓	Sundaram et al. (2014); Guo et al. (2020a)
Nobiletin **135**	3T3-F442A cells	Adipogenesis↓	Onda et al. (2013)
	STZ-diabetic rats	Fibrosis, inflammation, and NF-κB signaling in myocardial tissues↓	Zhang et al. (2016b)
	DIO mice	Energy expenditure and AMPK activation in WAT and BAT↑	Marrow et al. (2020)
Eriodictyol **200**	MIN6 cells	Insulin secretion↑	Hameed et al. (2018)
	MC cells	Inflammation↓, PI3K and Akt phosphorylation↑	Bai et al. (2019)

(continued)

Table 5.1 (continued)

Phytochemicals	Experimental models	Major therapeutic targets	References
	DIO mice	Lipogenesis in the liver and AT↓, FA oxidation in the liver and AT↑	Kwon and Choi (2019)
Hesperidin **385**	DIO mice	Hepatic cholesterol and fat synthesis, gluconeogenesis↓, antioxidant PON activity in the liver↑	Jung et al. (2006a)
	BAECs	Endothelial vasorelaxation process and p-levels of Akt, AMPK, and eNOS↑	Rizza et al. (2011)
Naringin **386** and neohesperidin **387**	DIO mice	Energy expenditure and AMPK activation in WAT↑, lipogenesis, inflammation in the liver and AT↓, gluconeogenesis in liver↓	Park et al. (2019); Pu et al. (2012b)
Naringenin **199**	Human white adipocytes	Energy expenditure, thermogenesis, ChREBP expression, and AMPK activation↑	Rebello et al. (2019)
	DIO mice	Hepatic FA oxidation↑, hepatic lipogenesis↓	Assini et al. (2015)
Genistein **96** and daidzein **95**	NOD-T1DM mice and T2DM mice	AT and hepatic FA oxidation and glycolysis↑, hepatic gluconeogenesis↓, pancreatic insulin secretion↑	Park et al. (2006); Choi et al. (2008)
Genistein	DIO mice	AMPK activation in the liver, AT, and skeletal muscle↑, Lipogenesis in the liver and AT↓	Liu et al. (2017a)
	Obese patients	Glucose uptake and FA oxidation in skeletal muscle, the liver, and AT↑, gut microbial dysbiosis↓	Guevara-Cruz et al. (2020)

(continued)

Table 5.1 (continued)

Phytochemicals	Experimental models	Major therapeutic targets	References
Biochanin A **388**	Obese diabetic rats	Hepatic and muscle glycogen synthesis, SIRT1 expression, and AMPK activation↑, hepatic lipid synthesis, and gluconeogenesis↓	Harini et al. (2012); Oza and Kulkarni (2018a)
Formononetin **389**	STZ-DCM rats	Myocardial hypertrophy, inflammation, and fibrosis↓, myocardial antioxidant status↑	Oza and Kulkarni (2020)
Puerarin **8**	Mouse islets and MIN6 cells	β-cells mass, insulin secretion, and Akt activation↑	Yang et al. (2016b)
	T2DM rats	Hepatic inflammation, fibrosis, NF-κB activation, and lipogenesis↓, hepatic FA oxidation↑	Hou et al. (2018)
	Obese diabetic rats and DIO mice	Glucose uptake, mitochondrial biogenesis, FA oxidation, and activation of AMPK and MOR in skeletal muscle↑, gut microbial dysbiosis↓, abundance of *Akkermansia* in gut↑	Chen et al. (2018b); Wang et al. (2019d)
EGCG **35**	Rat hepatocytes and L6 myotubes	Glucose uptake and activation of Akt and AMPK↑	Collins et al. (2007); Zhang et al. (2010b)
	HAECs	Aortic endothelial function and p-levels of Akt, AMPK, and FoxO1↑	Reiter et al. (2010)
	In vitro enzyme assay	11β-HSD1 activity↓, pancreatic lipase activity↓	Hintzpeter et al. (2014); Nakai et al. (2005)
	DIO mice	FA oxidation in skeletal muscle↑, gut microbial dysbiosis↓, abundance of	Sae-Tan et al. (2011); Ushiroda et al. (2019)

(continued)

Table 5.1 (continued)

Phytochemicals	Experimental models	Major therapeutic targets	References
		Akkermansia, *Adlercreutzia*, *Allobaculum*, and Parabacteroides in gut↑	
EC **39**	DIO mice	Hepatic inflammation↓, Hepatic insulin signaling↑	Cremonini et al. (2016)
Cyanidin-3-*O*-glucoside **31**	Diabetic KK-Ay mice and STZ-diabetic rats	Glucose uptake, GLUT4 expression, and Akt activation in skeletal muscle↑, RBP4 expression in AT↓	Sasaki et al. (2007); Nizamutdinova et al. (2009)
	C2C12 myotubes and DIO mice	Mitochondrial biogenesis, glucose uptake in C2C12 cells, and skeletal muscle↑	Matsukawa et al. (2015)
	3T3-L1 adipocytes	Adipogenesis↓, AMPK activation↑	Matsukawa et al. (2017)
Bilberry anthocyanins	Diabetic KK-Ay mice	Glucose uptake, FA oxidation, and AMPK activation in AT, skeletal muscle, and the liver↑	Takikawa et al. (2010)
	DIO mice	Gut microbial dysbiosis↓, abundance of *Actinobacillus*, and *Aggregatibacter* in gut↑	Lee et al. (2018b)
Mulberry and blueberry anthocyanins	DIO mice	Hepatic inflammation↓, hepatic FA oxidation↑	Wu et al. (2013)
Maquiberry anthocyanins	DIO mice	Thermogenesis and browning of WAT and BAT↑	Sandoval et al. (2019)
Purple sweet potato anthocyanins	DIO mice	Hepatic lipogenesis↓, hepatic AMPK activation↑, fibrosis, RAGE expression, and necrosis in kidney tissues↓	Hwang et al. (2011); Shan et al. (2014)

(continued)

Table 5.1 (continued)

Phytochemicals	Experimental models	Major therapeutic targets	References
Isobavachalcone **400**	3T3-L1 adipocytes	Adipogenesis↓	Lee et al. (2018a)
4-Hydroxyderricin **222** and xanthoangelol **218**	3T3-L1 adipocytes	Adipogenesis↓, glucose uptake, GLUT4 expression, and AMPK activation↑	Li et al. (2016b); Ohta et al. (2015)
	HepG2 cells	Lipogenesis↓, FA oxidation, and phosphorylation of LKB1 and AMPK↑	Zhang et al. (2014a)
	Diabetic KK-Ay mice	Glucose uptake, GLUT4 expression, and AMPK activation in skeletal muscle and AT↑	Enoki et al. (2007)
2. Stilbenoids			
Resveratrol **47**	DIO mice	Thermogenesis, FA oxidation, SIRT1 expression, and AMPK activation in WAT and BAT↑, hypothalamic SIRT1 expression and insulin signaling↑, hepatic inflammation and lipogenesis↓, gut microbial dysbiosis↓	Lagouge et al. (2006); Baur et al. (2006); Ramadori et al. (2009); Patel et al. (2011); Du et al. (2021)
	BAECs	Vascular tissue relaxation process and activation of Akt and eNOS↑	Frombaum et al. (2011); Bonnefont-Rousselot (2016)
Piceatannol **401**	3T3-L1 adipocytes	Adipogenesis↓	Kwon et al. (2012)
	DIO mice	FA oxidation and AMPK activation in WAT and the liver↑, gut microbial dysbiosis↓, abundance of Firmicutes and *Lactobacillus* in gut↑	Tung et al. (2016)
ε-Viniferin **150**	3T3-L1 adipocytes	Adipogenesis↓, SIRT1 expression and AMPK activation↑	Hung et al. (2019); Ohara et al. (2015)
	DIO mice	Hepatic FA oxidation and AMPK activation↑, hepatic inflammation, lipogenesis, and gluconeogenesis↓	Liu et al. (2020)

(continued)

Table 5.1 (continued)

Phytochemicals	Experimental models	Major therapeutic targets	References
	VECs	Endothelial function and eNOS activation↑	Zghonda et al. (2012)
Hopeaphenols **150a** and **150b**	In vitro enzyme assay and L6 myotubes	α-Amylase and α-glucosidase activity↓, glucose uptake, GLUT4 expression, and insulin signaling↑	Sasikumar et al. (2016)
3. Curcuminoids			
Curcumin **9**	DIO mice	Hepatic and AT inflammation, NF-κB activation, and lipogenesis↓, adiponectin secretion in AT, SIRT1 expression, and insulin signaling in liver↑	Weisberg et al. (2008); Shao et al. (2012)
	Alcohol-induced liver injury in mice	Mitochondrial function and antioxidant activity in hepatocytes↑	Lu et al. (2015); Wang et al. (2019a)
4. Lignans			
Secoisolariciresinol **402**	3T3-L1 adipocytes	Adipogenesis↓, LKB1 expression, and AMPK activation↑	Kang et al. (2018b)
	DIO mice	FA oxidation, glucose uptake, GLUT4 expression, and activation of Akt and AMPK in the liver, AT, and skeletal muscle↑, Lipogenesis in the liver and AT↓, pancreatic insulin secretion↑	Wang et al. (2015a); Moree et al. (2013)
Sesamin **403**	DIO mice	LXRα and its target genes expression↓, hepatic FA oxidation↑	Zhang et al. (2016c)
	SH rats	Myocardial inflammation, fibrosis, and TGFβ1/Smad3 signaling↓	Zhao et al. (2015)

(continued)

Table 5.1 (continued)

Phytochemicals	Experimental models	Major therapeutic targets	References
Honokiol **404**	C2C12 myotubes	Glucose uptake, GLUT4 expression, and Akt activation↑	Sun et al. (2015)
	STZ-diabetic mice	Hepatic lipogenesis and gluconeogenesis↓	Kim and Jung (2019)
	DIO mice	Gut microbial dysbiosis↓, abundance of health-benefit bacteria of genus *Akkermansia*, *Bacteroides, Bilophila*, and *Fusobacterium* in gut↑	Ding et al. (2019)
5. Coumarins			
Umbelliferone **132**	STZ-diabetic rats	Hepatic lipogenesis↓, hepatic glycolysis, FA oxidation, glycogen synthesis, and insulin signaling, AT adiponectin secretion↑, AGEs accumulation, and necrosis in renal tissues↓	Ramesh and Pugalendi (2006); Naowaboot et al. (2015, 2020); Sim et al. (2014); Wang et al. (2019b)
Scopoletin **405**	HepG2 cells	FA oxidation and insulin signaling↑, Lipogenesis↓	Zhang et al. (2010a)
	3T3-L1 adipocytes	Adipogenesis↓, glucose uptake, and activation of Akt and AMPK↑	Jang et al. (2020)
	STZ-diabetic rats	Hepatic inflammation, lipogenesis, and AGEs accumulation↓, hepatic antioxidant activity↑	Choi et al. (2017)
Esculetin **133**	STZ-diabetic rats	Inflammation, fibrosis, and RAS activation in the heart and kidney tissues↓, lipogenesis and gluconeogenesis in the liver↓, antioxidant status in the heart, liver, and kidney↑	Prabakaran and Ashokkumar (2013); Kadakol et al. (2015, 2017); Gao et al. (2013); Choi et al. (2016)

(continued)

Table 5.1 (continued)

Phytochemicals	Experimental models	Major therapeutic targets	References
	DIO mice	Hepatic lipogenesis↓, hepatic and AT FA oxidation and AMPK activation↑	Sim et al. (2015); Combs and Marliss (2014)
Esculin **406**	STZ-diabetic rats	Glucose uptake and insulin sensitivity in the liver and skeletal muscle↑, hepatic gluconeogenesis and inflammation ↓, inflammation and AGEs accumulation in renal tissues↓	Wang et al. (2015b); Kang et al. (2014); Guo et al. (2020b)
Osthole **407**	Hepatic FL83B cells	Lipogenesis↓, lipolysis, FA oxidation, and AMPK activation↑	Huang et al. (2017b)
	C2C12 myotubes, L6 myotubes, and STZ-diabetic mice	Glucose uptake, GLUT4 expression and AMPK activation in myotubes and skeletal muscle↑	Lee et al. (2011)
	DIO rats	Hepatic antioxidant status and FA oxidation↑	Song et al. (2006)
Fraxetin **408**	STZ-diabetic rats	Hepatic glycolysis, FA oxidation, insulin sensitivity, and glycogen synthesis↑, hepatic gluconeogenesis↓	Murali et al. (2013)
6. Quinones			
Emodin **123**	L6 myotubes	Glucose uptake, GLUT4 expression, and AMPK activation↑	Song et al. (2013)
	Hepa1c1c7 cells	Gluconeogenesis↓, AMPK activation↑	Li et al. (2016a)
	DIO mice	11β-HSD1 activity in the liver and AT↓, hepatic lipogenesis, and gluconeogenesis↓, hepatic AMPK signaling pathway↑	Feng et al. (2010)

(continued)

Table 5.1 (continued)

Phytochemicals	Experimental models	Major therapeutic targets	References
	DCM rats	Myocardial injury and fibrosis, 11β-HSD1 activity↓, Akt activation in myocardial tissues↑	Wu et al. (2014c)
Rhein **126**	DIO mice	Lipogenesis in the liver and AT↓, thermogenesis in WAT and the liver↑	Zhang et al. (2012)
	HK-2 cells	Inflammation, fibrosis, and TGFβ1/Smad signaling↓	Peng et al. (2012); Zheng et al. (2008)
Shikonin **229**	Diabetic GK rats	Glucose uptake, GLUT4 expression, and insulin sensitivity in skeletal muscle, the liver, and AT↑	Oberg et al. (2011)
	HepG2 cells and DIO mice	Lipogenesis↓, hepatic gluconeogenesis↓, hepatic FA oxidation, thermogenesis, insulin signaling, and AMPK activation↑	Bettaieb et al. (2015); Gwon et al. (2020)
Acetylshikonin **230**	3T3-L1 adipocytes	Adipogenesis↓	Su et al. (2016c)
	L6 myotubes	Glucose uptake, GLUT4 expression, and AMPK activation↑	Huang et al. (2019)
	Obese db/db mice	Inflammation and lipogenesis in the liver and AT↓, lipolysis and FA oxidation in the liver and AT↑	Su et al. (2016b)
7. Xanthones			
Mangiferin **409**	STZ-diabetic rats	Hepatic lipogenesis and oxidative stress↓, hepatic FA oxidation and AMPK activation↑, pancreatic β-cells mass and function↑	Muruganandan et al. (2005); Niu et al. (2012); Wang et al. (2014a)
	DIO mice	AGEs accumulation and fibrosis in renal tissues↓	Liu et al. (2013c)
Norathyriol **410**	In vitro enzyme assay	α-Glucosidase activity and PTP1B activity↓	Shi et al. (2017)

(continued)

Table 5.1 (continued)

Phytochemicals	Experimental models	Major therapeutic targets	References
	L6 myotubes	Glucose uptake, GLUT4 expression, and AMPK activation↑	Wang et al. (2014a)
	DIO mice	Hepatic lipogenesis↓, hepatic FA oxidation, SIRT1 and LKB1 expression, and AMPK activation↑	Li et al. (2018a)
8. Phenolic compounds			
Ferulic acid **72**	STZ-diabetic rats	Hepatic glycogen content and insulin sensitivity↑, hepatic gluconeogenesis↓	Narasimhan et al. (2015)
	DIO mice	Hepatic lipogenesis and gluconeogenesis↓, hepatic FA oxidation↑	Naowaboot et al. (2016)
Caffeic acid **411**	Diabetic db/db mice	Hepatic glycogen synthesis, glycolysis, FA oxidation, autophagy, insulin sensitivity and AMPK activation↑, hepatic lipogenesis, gluconeogenesis, ER stress↓, pancreatic insulin secretion↑	Jung et al. (2006b); Liao et al. (2013); Kim et al. (2018a)
Chlorogenic acid **21**	L6 myotubes	Glucose uptake, GLUT4 and CaMKKβ expression, and activation of Akt and AMPK↑	Ong et al. (2012)
	DIO mice	Hepatic lipogenesis↓, adiponectin secretion in AT↑	Cho et al. (2010)
Chicoric acid **412**	HepG2 cells	Glucose uptake, glycogen synthesis, Nrf2 and SIRT1 expression, and p-levels of AMPK, Akt, and GSK-3β↑	Zhu et al. (2017)
	C2C12 myotubes	Glucose uptake, GLUT4 expression, and Akt phosphorylation↑	Kim et al. (2018b)

(continued)

Table 5.1 (continued)

Phytochemicals	Experimental models	Major therapeutic targets	References
	DIO mice	Inflammation and lipogenesis in the liver and AT↓, antioxidant activity, mitochondrial biogenesis and function in the liver and WAT↑, hepatic gluconeogenesis↓	Xiao et al. (2013); Kim et al. (2018b)
Rosmarinic acid **104**	C2C12 myotubes	Glucose uptake, GLUT4 and SIRT1 expression, p-levels of CaMKK and AMPK↑	Abe et al. (2016)
	STZ-diabetic rats	Glucose uptake and GLUT4 expression in skeletal muscle↑, glycogen synthesis, GS enzyme activity in skeletal muscle, and the liver↑, hepatic gluconeogenesis↓, pancreatic insulin secretion↑	Runtuwene et al. (2016); Ramalingam et al. (2020)
Salvianolic acid B **104a**	3T3-L1 adipocytes	Adipocyte differentiation and browning of WAT, mitochondrial function, glucose uptake, and glycolysis↑	Pan et al. (2018)
	Diabetic db/db mice	Glucose uptake, glycogen synthesis, GLUT4 expression, and AMPK activation in skeletal muscle and the liver↑, hepatic lipogenesis, and gluconeogenesis↓	Huang et al. (2016b)
	DIO mice	Inflammation and inflammatory gene Saa3 activity, lipogenesis in AT↓, GATA2 and GATA3 activity in AT↑	Tong et al. (2005); An et al. (2019)
Salidroside **413**	DIO mice	Antioxidant activity and AMPK activation in the pancreas and AT↑,	Wang et al. (2016a); Xue et al. (2019)

(continued)

Table 5.1 (continued)

Phytochemicals	Experimental models	Major therapeutic targets	References
		lipogenesis in AT and the liver, fibrosis in renal tissues↓	
	Diabetic db/db mice	Glucose uptake, GLUT4 expression, and AMPK activation in skeletal muscle↑	Zheng et al. (2015)
Eugenol **271**	In vitro enzyme assay	α-Amylase, pancreatic lipase, and ACE activity↓	Mnafgui et al. (2013)
	STZ-diabetic rats	Glucose uptake, GLUT4 expression, and Akt activation in skeletal muscle and the liver↑	Prabhakar and Doble (2011)
	Hypercholesterolemic diabetic rats	Hypocholesterolemic effect, LPL and HMGCR activity↑	Venkadeswaran et al. (2014, 2016)
Gallic acid **44**	HepG2 cells	FA oxidation, energy expenditure, autophagy, and AMPK activation↑	Chao et al. (2014)
	DIO mice	Hepatic lipogenesis, gluconeogenesis, and amino acid metabolism↓, hepatic glycolysis, FA oxidation, SIRT1 expression, and activation of AMPK and Akt↑, pancreatic insulin secretion↑	Chao et al. (2014); Doan et al. (2015); Gandhi et al. (2014)
CAPE **414**	STZ-diabetic rats	Glucose uptake and glycolysis in the liver↑, inflammation and lipogenesis in the liver↓, pancreatic insulin secretion↑	Celik et al. (2009); Nie et al. (2017a); Sorrenti et al. (2019)
6-Gingerol **154**	L6 myotubes	Glucose uptake, GLUT4 and CaMKK expression, and AMPK activation↑	Li et al. (2013a)
	DIO mice	Glucose uptake and glycogen synthesis in skeletal muscle and the liver↑, hepatic gluconeogenesis↓,	Son et al. (2015); Saravanan et al. (2014); Samad et al. (2017)

(continued)

Table 5.1 (continued)

Phytochemicals	Experimental models	Major therapeutic targets	References
		pancreatic lipase and α-amylase activity↓	
9. Tannins			
Ellagic acid **320**	Diabetic GK rats	Hepatic inflammation, oxidative stress and lipogenesis↓, thermogenesis and FA oxidation in WAT and BAT↑	Wang et al. (2019c); Yoshimura et al. (2013)
Pentagalloylglucose **235** and lagerstroemin **415**	3T3-L1 adipocytes	Adipogenesis↓	Klein et al. (2007)
Chebulagic acid **416**	In vitro enzyme assay	α-Glucosidase activity↓	Gao et al. (2008)
Grapeseed proanthocyanidins **417** and **418**	STZ-diabetic rats	Glucose uptake, GLUT4 expression and Akt activation in skeletal muscle and the liver↑, renal fibrosis↓	Pinent et al. (2004); Li et al. (2009, 2017)
	DIO mice	FA oxidation and FXR activity↑, lipogenesis↓, gut microbiota dysbiosis↓, abundance of bacteria of genus *Roseburia* and *Prevotella* in the gut↑	Del Bas et al. (2009); Caimari et al. (2013); Liu et al. (2017b)
Apple procyanidins **419**	DIO mice	AT and liver inflammation and JNK activation↓, activation of Akt and AMPK in AT and the liver↑, gut microbiota dysbiosis↓, abundance of bacteria of genus *Akkermansia*, *Roseburia*, and *Bacteroides* in the gut↑, abundance of bacteria of genus *Clostridium* and *Lachnospiraceae* in the gut↓	Ogura et al. (2016); Masumoto et al. (2016)

(continued)

Table 5.1 (continued)

Phytochemicals	Experimental models	Major therapeutic targets	References
Blueberry anthocyanins	DIO mice	Gut microbial dysbiosis↓, abundance of bacteria of genus *Akkermansia* and *Adlercreutzia* in the gut↑	Rodriguez-Daza et al. (2020)
Oolonghornobisflavans A and B, oolongtheanin-3′-*O*-gallate, prodelphnidin B2-3,3′-di-*O*-gallate **420–423**	In vitro enzyme assay	Pancreatic lipase activity↓	Nakai et al. (2005)
Acacia meansii bark polyphenols	In vitro enzyme assay	Pancreatic lipase activity↓	Matsuo et al. (2016)
Acacia mollissima polyphenols	Diabetic KK-Ay mice	Glucose uptake and FA oxidation in AT, skeletal muscle, and the liver↑, lipogenesis and fat intake in liver↓	Ikarashi et al. (2011b)
10. Bromophenols			
BPN **427**	In vitro enzyme assay	PTP1B activity↓ Hypoglycemic effect↑	Guo et al. (2020c)
	STZ-diabetic rats C2C12 myotubes	Glucose uptake, GLUT4 expression and Akt activation↑	Xu et al. (2018b)
BDDE **428**	STZ-diabetic mice	PTP1B activity in skeletal muscle↓, glucose uptake and insulin signaling in skeletal muscle↑	Xu et al. (2016)
11. Alkaloids			
1-Deoxynojirimycin **108**	STZ-diabetic mice and diabetic db/db mice	Adiponectin secretion in AT, FA oxidation, and AMPK activation in the liver↑, hepatic gluconeogenesis and kidney SGLT1 activity↓, glucose uptake, GLUT4 expression and activation of PI3K/Akt signaling in skeletal muscle↑	Tsuduki et al. (2009); Li et al. (2013b); Liu et al. (2015c)
	DIO mice	Hepatic glycogen content and insulin signaling↑, hepatic	Liu et al. (2016b); Kim et al. (2017b); Li et al. (2019a)

(continued)

Table 5.1 (continued)

Phytochemicals	Experimental models	Major therapeutic targets	References
		inflammation, lipogenesis, fibrosis and gluconeogenesis↓, hypothalamic ER stress and AMPK activation, appetite intake and adipogenesis↓, hypothalamic leptin signaling and p-levels of JNK2 and STAT3↑	
Piperine **117**	DIO mice	Myocardial fibrosis and collagen deposition in aortic rings in the heart↓, resting metabolic rate, expression of PTRF and MEST in AT↑, lipogenesis in VAT↓, lipolysis in AT↑	Diwan et al. (2013); Nogara et al. (2016); Du et al. (2020)
Trigonelline **345b**	STZ-type 2 diabetic rats	Glucose uptake, GLUT4 expression and insulin signaling in AT↑, antioxidant activity, β-cells mass and insulin secretion in the pancreas↑, peripheral neuropathy and p-p38MAPK in sciatic nerves↓, inflammation, oxidative stress, and apoptosis in kidney cells↓	Tharaheswari et al. (2014); Liu et al. (2018c); Zhou and Zhou (2012); Li et al. (2019b)
Capsaicin **49**	DIO mice	Inflammation in AT and the liver↓, adiponectin, AdipoR2 and TRPV1 expression in adipocytes↑, insulin signaling in AT and the liver↑, AMPK activation, FA oxidation and energy expenditure in the liver↑, gut microbial dysbiosis↓,	Kang et al. (2010, 2011a, 2017); Wang et al. (2012a); Baskaran et al. (2016)

(continued)

Table 5.1 (continued)

Phytochemicals	Experimental models	Major therapeutic targets	References
		abundance of bacteria of Ruminococcaceae and Lachnospiraceae in gut↑, abundance of LPS producing bacteria of S24-7 family, Bacteroidetes in gut↓	
Dihydrocapsaicin **144**	SD rats	Thermogenesis, lipolysis and glycogen synthesis in the liver↑	Imaizumi et al. (2011)
Capsiate **143**	SD rats	Energy expenditure and lipolysis in skeletal muscle↑	Faraut et al. (2009)
Mahanimbine **138**	STZ-diabetic rats	α-Amylase and α-glucosidase activity↓, hypoglycemic effect↑	Dineshkumar et al. (2010)
Koenidine **429**	Diabetic db/db mice and L6 myotubes	Glucose uptake, GLUT4 expression and Akt activation in skeletal muscle and L6 cells↑	Patel et al. (2016a)
Matrine **431**	DIO mice	Hepatic HSP72 protein activity, FA oxidation and energy expenditure↑, hepatic inflammation and lipogenesis↓	Zeng et al. (2015)
	STZ-DCM rats	Myocardial inflammation, apoptosis and ROS/TLR4/MyD88 signaling pathway↓, vascular endothelial function, insulin signaling and p-levels of Akt and eNOS in cardiac tissues↑	Liu et al. (2015d); Zhang et al. (2019b)
Oxymatrine **432**	NAFLD rats	PPARα and MTTP activity, FA oxidation in AT↑	Shi et al. (2013)
Rutaecarpine **433**	3T3-L1 adipocytes	Adipogenesis↓, AMPK activation↑	Chen et al. (2013)
	DIO mice	Hypothalamic leptin signaling↑, NPY and AgRP expression↓	Kim et al. (2009)

(continued)

Table 5.1 (continued)

Phytochemicals	Experimental models	Major therapeutic targets	References
	STZ/HFD-type 2 diabetic rats	Hepatic inflammation↓, glucose uptake, GLUT4 expression and activation of Akt and AMPK in skeletal muscle and the liver↑	Nie et al. (2016)
Evodiamine **137**	DIO mice	ERK phosphorylation in WAT and the liver↑	Wang et al. (2008)
	3T3-L1 adipocytes	Adipogenesis↓, p-levels of EGFR, PKCα and ERK↑	Wang et al. (2009a)
	Diabetic KK-Ay mice	Glucose uptake, GLUT4 expression, lipid metabolism, insulin sensitivity and AMPK activation in WAT, the liver, and skeletal muscle↑	Wang et al. (2013a)
Rohitukine **107**	3T3-L1 adipocytes	Adipogenesis and p-mTOR↓, GATA2 and Wnt3a expression↑	Varshney et al. (2014)
	DIO hamsters	Hepatic and AT cholesterol and TG synthesis↓, hepatic LXRα expression↑	
Berberine **48**	L6 myotubes	Glucose uptake, GLUT4 expression and p-levels of AMPK, Akt, and p38MAPK↑	Cheng et al. (2006)
	3T3-L1 adipocytes	Adipogenesis and 11β-HSD1 activity↓, activation (p-levels) of AMPK, p38MAPK, and PPARγ↑	
	DIO mice	Lipogenesis in the liver and AT↓, FA oxidation, thermogenesis and AMPK activation in skeletal muscle, AT, and the liver↑	Lee et al. (2006)

(continued)

Table 5.1 (continued)

Phytochemicals	Experimental models	Major therapeutic targets	References
	HepG2 cells STZ-diabetic rats	InsR and LDLR expression, PKC activity and AMPK activation↑	Kong et al. (2009)
	DIO mice	InsR and LDLR expression and PKC activity in the liver↑	Xie et al. (2011)
	DN mice	Mitochondrial β-oxidation, lipolysis, and energy metabolism in VAT↑, gut microbial dysbiosis↓, abundance of *Lactobacillus* in the gut↓	Zhao et al. (2014)
	GMCs	Inflammation and fibrosis in kidney tissues↓, LKB1 expression and AMPK activation in GMCs of the kidney↑	Yang et al. (2016c)
	HUVECs	TGR5 activation↑, inflammation, fibrosis, p-JNK level and NF-κB activity↓ Cells apoptosis and inflammation↓, expression of antioxidant enzymes, p-levels of AMPK and eNOS↑	Wang et al. (2009b)
Vindoline **434**	Pancreatic islets	Insulin secretion, intracellular Ca^{2+} influx↑	Yao et al. (2013); Goboza et al. (2019); Oguntibeju et al. (2019)
	STZ-diabetic rats	Inflammation and oxidative stress in the liver, pancreas, and kidney↓, hypoglycemic effect and insulin secretion↑	
Cinchonine **139**	DIO mice	Inflammation and lipogenesis in EAT↓, Wnt10b and β-catenin expression in AT↑	Jung et al. (2012)

(continued)

Table 5.1 (continued)

Phytochemicals	Experimental models	Major therapeutic targets	References
12. Terpenoids			
D-Limonene **435**	DIO mice	Lipogenesis via LXRβ in the liver↓, FA oxidation in the liver↑	Jing et al. (2013)
	STZ-diabetic rats	Hepatic glycolysis and FA oxidation↑, hepatic gluconeogenesis↓	Murari and Saravanan (2012)
Carvacrol **436**	DIO mice T1DM mice	Inflammation and lipogenesis in EAT↓, FA oxidation and thermogenesis in EAT↑	Cho et al. (2012) Li et al. (2020)
	DCM mice	Glycolysis and glycogen synthesis in the liver↑ Myocardial inflammation, hypertrophy and fibrosis↓, glucose uptake, GLUT4 expression and Akt activation in cardiomyocytes↑, TRPM7 expression in the heart, kidney, and brain↑	Hou et al. (2019); Parnas et al. (2009); Du et al. (2010)
Thymol **437**	Type 2 diabetic mice	Hepatic lipid synthesis↓, hepatic lipolysis and FA oxidation↑	Saravanan and Pari (2015)
	Obese DN mice	Inflammation, lipogenesis, and fibrosis in kidney tissues↓, antioxidant activity in kidney tissues↑	Saravanan and Pari (2016)
	Hypercholesterolemic rabbits	Aortic atherosclerotic lesions↓	Yu et al. (2016)
Amorfrutin B **438**	DIO mice	Mitochondrial biogenesis and FA oxidation in AT↑, lipid uptake and inflammation in the liver and AT↓, insulin sensitivity via PPARγ agonistic activity in AT and the liver↑	Weidner et al. (2013)

(continued)

Table 5.1 (continued)

Phytochemicals	Experimental models	Major therapeutic targets	References
Geraniol **439**	STZ-diabetic rats	Hepatic glycolysis↑, hepatic gluconeogenesis↓, pancreatic insulin secretion↑	Babukumar et al. (2017)
	Hyperlipidemic hamsters	Cholesterol synthesis↓, cholesterol esterification and lipolysis↑	Jayachandran et al. (2015)
	DIO mice	Aortic vasorelaxation process↑	Wang et al. (2016b)
Paeoniflorin **440**	Hepatic steatosis rats	Hepatic lipogenesis↓, hepatic FA oxidation, LKB1 expression, and activation of Akt and AMPK↑	Li et al. (2018c)
	STZ-DN mice	Inflammation, fibrosis, and necrosis in kidney tissues↓	Zhang et al. (2017)
Catalpol **120**	Diabetic db/db mice	Inflammation and lipogenesis in AT and the liver↓, glucose uptake, GLUT4 expression, and AMPKα1/2 activation in the liver, skeletal muscle, and AT↑	Bao et al. (2016); Zhou et al. (2015)
	Diabetic hyperlipidemic rabbits	Atherosclerotic lesions in aortic rings↓	Liu et al. (2016a)
Aucubin **119**	STZ-diabetic rats	Antioxidant activity, β-cells mass, and insulin secretion in pancreas↑	Jin et al. (2008)
	STZ-HFD-DN mice	Inflammation, fibrosis, and NF-κB activation in renal tissues↓, SIRT1 and SIRT3 activity in renal tissues↑	Ma et al. (2020)
Loganin **342**	Glucotoxic INS1 cells	Insulin secretion and Akt activation in β-cells↑, activity of FoxO1↓	Mo et al. (2019)

(continued)

Table 5.1 (continued)

Phytochemicals	Experimental models	Major therapeutic targets	References
	Type 2 diabetic mice	Hepatic inflammation↓, hepatic antioxidant enzymes (Nrf2 and HO-1) activity↑	Park et al. (2011a)
Morroniside **441**	Diabetic db/db mice	Hepatic oxidative stress and inflammation↓, hepatic antioxidant enzymes Nrf2 and HO-1 activity↑	Park et al. (2011b)
Swertiamarin **442**	HepG2 cells	FA oxidation and activation of Akt and AMPK↑, lipogenesis and gluconeogenesis↓	Patel et al. (2016b)
	STZ-type 1 diabetic rats	Kidney function↑, inflammation, fibrosis, and necrosis in kidney tissues↓	Sonawane et al. (2010)
	DIO mice	Hepatic lipid accumulation and ACAT1 enzyme activity↓, hepatic glycogen content and plasma HDL-C level↑	Wang and He (2019)
	C. elegans	Intestinal fat deposit and Kat-1 enzyme activity↓	
Oleuropein **353**	C2C12 myotubes	Glucose uptake, GLUT4 expression and AMPK activation↑	Fujiwara et al. (2017)
	DIO mice	Glucose uptake, GLUT4 expression and AMPK activation in skeletal muscle↑, hepatic inflammation, lipogenesis and FGFR1 activity↓, hepatic Wnt10b activity and expression of SIRT1 and SIRT3↑	Park et al. (2011c); Santini et al. (2020)
Zerumbone **444**	DIO hamsters	FA oxidation in AT and the liver↑, lipogenesis in the liver and AT↓	Tzeng et al. (2013)

(continued)

Table 5.1 (continued)

Phytochemicals	Experimental models	Major therapeutic targets	References
Beta-caryophyllene **445**	HepG2 cells	CB2R expression, lipolysis and AMPK activation↑, lipogenesis↓	Kamikubo et al. (2016)
	C2C12 myotubes	Glucose uptake, glycolysis, mitochondrial function,TCA cycle process, CB2R expression and AMPK activation↑	Geddo et al. (2021)
	STZ-diabetic rats	Hepatic glycolysis↑, hepatic gluconeogenesis↓, glycoproteins expression in plasma, liver, and kidney tissues↓	Basha and Sankaranarayanan (2014, 2015)
	DIO rats	Aortic vascular tissue inflammation↓, hepatic FA oxidation and SIRT1 expression↑	Youssef et al. (2019)
Germacrone **446**	DIO mice	FA oxidation, energy expenditure and AMPK activation in skeletal muscle↑, lipogenesis and inflammation in the liver↓	Guo and Choung (2017a)
	3T3-L1 adipocytes	Adipogenesis and KLF4 activity↓, lipolysis and AMPK activation↑	Guo and Choung (2017b)
Costunolide **10**	STZ-diabetic rats	Insulin sensitivity and glycogen contents in the liver and skeletal muscle↑	Eliza et al. (2009)
Farnesol **447**	Diabetic KK-Ay mice	Hepatic lipogenesis↓, hepatic FXR activity and FA oxidation↑	Goto et al. (2011)
	DIO mice	Adipogenesis/ lipogenesis in WAT↓, FA oxidation, thermogenesis, and AMPK activation in WAT↑	Kim et al. (2017a)

(continued)

Table 5.1 (continued)

Phytochemicals	Experimental models	Major therapeutic targets	References
Carnosic acid **106**	HepG2 cells	Inflammation and lipogenesis↓, p-levels of EGFR, ERK1/2, and AMPK↑	Wang et al. (2012b); Park and Mun (2013)
	Obese diabetic db/db mice	Hepatic inflammation and lipid synthesis↓, hepatic FA oxidation, and activation of AMPK, EGFR, and ERK1/2 via p-levels↑	Song et al. (2018)
Carnosol **448**	HepG2 cells	TG synthesis and DGAT activity↓	Cui et al. (2012)
	L6 myotubes	Glucose uptake, GLUT4 expression and AMPK activation↑	Vlavcheski et al. (2018)
	STZ-diabetic rats	Glucose uptake in skeletal muscle↑, inflammation and oxidative stress in the liver and AT↓	Samarghandian et al. (2017)
Andrographolide **335**	DIO mice	Cholesterol and TG synthesis, activity of SREBP2 and SREBP-1c in the liver↓, FA oxidation and thermogenesis in BAT↑	Ding et al. (2014b)
	STZ-DN mice	Inflammation, fibrosis, and necrosis in renal tissues↓, Akt activation in renal tissues↑	Ji et al. (2016)
Stevioside **449**	Diabetic GK rats	Hypoglycemic effect and insulin secretion↑, pancreatic glucagon secretion↓	Jeppesen et al. (2003)
	DKO obese mice	Inflammation and aortic plaque formation in aortic tissues↓, glucose uptake GLUT4 expression and LXRα activity in AT↑	Geeraert et al. (2010)
	TAA-induced liver injury in rats	Hepatic inflammation and NF-κB activation↓	Casas-Grajales et al. (2019)

(continued)

Table 5.1 (continued)

Phytochemicals	Experimental models	Major therapeutic targets	References
Borapetoside E **450**	STZ-type 2 diabetic rats	Hepatic cholesterol and TG synthesis↓, glucose uptake, GLUT4 expression and p-levels of Akt and GSK-3β in skeletal muscle↑	Xu et al. (2017)
Borapetosides A and C **451** and **172**	STZ-diabetic rats	Glycogen contents and Akt activation in the liver and skeletal muscle↑, hepatic gluconeogenesis and α-glucosidase activity↓	Ruan et al. (2012, 2013); Hamid et al. (2015)
Cryptotanshinone **452**	C2C12 myotubes	Glucose uptake, GLUT4 expression, and activation of Akt and AMPK↑	Kim et al. (2007)
	3T3-L1 adipocytes	Adipogenesis and STAT3 activation↓, FA oxidation, thermogenesis, expression of GATA2 and CHOP10 and activation of AMPK↑	Kim et al. (2007); Rahman et al. (2016)
	Diabetic db/db mice	Glucose and lipid metabolism and AMPK activation in liver and AT↑	Kim et al. (2007)
Celastrol **78**	Mesenchymal 10T1/2 cells	HSF1 activity and mitochondrial thermogenesis↑	Ma et al. (2015)
	DIO mice	HSF1 and PGC-1α expression, thermogenesis in WAT and BAT↑, leptin signaling and p-STAT3 level in hypothalamus↑, p-p38MAPK/ATF2 signaling in skeletal muscle↑, Akt/ERK signaling in AT↑	Liu et al. (2015a); Fang et al. (2019)
Corosolic acid **206**	L6 myotubes	Glucose uptake, GLUT4 expression and Akt activation↑	Shi et al. (2008)

(continued)

Table 5.1 (continued)

Phytochemicals	Experimental models	Major therapeutic targets	References
	Diabetic KK-Ay mice	Glucose uptake, FA oxidation, adiponectin secretion and AdipoR1 expression in AT, glucose uptake in skeletal muscle↑	Yamada et al. (2008)
	STZ-diabetic rats	Insulin signaling and glycogen content in the liver↑, hepatic gluconeogenesis↓	Xu et al. (2019)
	3T3-L1 adipocytes	Adipogenesis and inflammation↓, LKB1 expression and AMPK activation↑	Yang et al. (2016a)
	DIO mice	Macrophage infiltration and inflammation in AT↓, p-levels of IRS, Akt and AMPK in AT↑	Yang et al. (2016a)
Ursolic acid **52**	3T3-L1 adipocytes	Adipogenesis↓, Lipolysis, FA oxidation, LKB1 expression and AMPK activation↑	He et al. (2013)
	DIO mice	Lipogenesis in the liver, inflammation in VAT↓, FA oxidation and thermogenesis in BAT↑	Kunkel et al. (2012); Gonzalez-Garibay et al. (2020)
	DCM rats		
		Myocardial inflammation and fibrosis↓	Wang et al. (2018)
Oleanolic acid **326**	HepG2 cells	Glucose uptake, GLUT4 expression in cell membrane and insulin signaling↑, inflammation↓	Li et al. (2015)
	Type 2 diabetic db/db mice	Hepatic insulin sensitivity, antioxidant Nrf2 activity and AMPK activation↑, hepatic inflammation and gluconeogenesis↓	Wang et al. (2013b)

(continued)

Table 5.1 (continued)

Phytochemicals	Experimental models	Major therapeutic targets	References
	Hypolipidemic mice	Hepatic lipid synthesis↓, Hepatic miR-98-5p protein expression↑	Chen et al. (2017)
	DIO mice	Ghrelin and plasma GOAT expression, α-amylase activity, PPARγ activity in AT↓, energy expenditure in AT↑	De Melo et al. (2010); Nakajima et al. (2019)
	DIO quails		Jiang et al. (2015)
	DIO rabbits	Atherosclerotic lesions in aorta and LOX-1 activity in epithelial tissue↓	Luo et al. (2017)
	UUO rats	Hepatic lipogenesis, AdipoR2 expression↓, hepatic AdipoR1 and PPARγ expression↑ Inflammation, fibrosis and TGFβ1/Smad2 signaling in renal tissues↓	Zhao and Luan (2020)
Maslinic acid **330**	Diabetic KK-Ay mice	Hepatic insulin sensitivity, glycogen content and p-levels of Akt and GSK-3β↑, hepatic GP enzyme activity↓	Liu et al. (2007, 2014)
	DIO mice	Hepatic lipid synthesis↓, hepatic lipolysis, FA oxidation, SIRT1 expression and AMPK activation↑	Liou et al. (2019)
Betulinic acid **207**	DIO mice	Mitochondrial thermogenesis, FA oxidation and AMPK activation in BAT and skeletal muscle↑, hepatic inflammation and lipogenesis↓, hepatic TGR5 and FXR activation↑	Kim et al. (2019); Genet et al. (2010)
	ApoE-KO mice	Inflammation and atherosclerotic lesions in endothelial tissue of aorta↓	Yoon et al. (2017)

(continued)

Table 5.1 (continued)

Phytochemicals	Experimental models	Major therapeutic targets	References
Tormentic acid **208**	In vitro enzyme assay	α-Glucosidase and PTP1B enzymes activity↓	Na et al. (2015) Wu et al. (2014a)
	Type 2 diabetic mice	Glucose uptake, GLUT4 expression and activation of AMPK and Akt↑, hepatic gluconeogenesis and lipogenesis↓, hepatic FA oxidation and AMPK activation↑	
Asiatic acid **443**	Hepatoma H411E cells	FA oxidation, SIRT1 and PGC-1α expression and AMPK activation↑, lipid synthesis↓	Xu et al. (2018a)
	Diabetic db/db mice	Hepatic FA oxidation, SIRT1 expression and AMPK activation↑, hepatic lipogenesis↓	Xu et al. (2018a)
	DIO rats	Hepatic FA oxidation and antioxidant enzymes activity↑, hepatic inflammation and lipogenesis↓, PL and α-amylase activity↓	Rameshreddy et al. (2018); Sathibabu Uddandrao et al. (2020)
	MS rats	iNOS, Ang II, ACE, and NE expression in vascular tissues of aorta↓, eNOS expression and insulin signaling in aortic vascular tissue↑	Pakdeechote et al. (2014); Maneesai et al. (2016)
Eburicoic acid **453**	STZ-type 1 diabetic mice	Pancreatic β-cells mass and function↑, glucose uptake, GLUT4 expression and activation of Akt and AMPK in skeletal muscle↑, hepatic FA oxidation↑, hepatic lipogenesis↓	Lin et al. (2017, 2018)
Dehydroeburicoic acid **454**	C2C12 myotubes	Glucose uptake, GLUT4 expression and Akt activation↑	Kuo et al. (2016a)

(continued)

Table 5.1 (continued)

Phytochemicals	Experimental models	Major therapeutic targets	References
	DIO mice	Hepatic gluconeogenesis, 11β-HSD1 activity and lipogenesis↓, hepatic FA oxidation and AMPK activation and skeletal muscle glucose uptake, GLUT4 expression and AMPK activation↑	Kuo et al. (2016a)
Antcin K **455**	C2C12 myotubes	Glucose uptake, GLUT4 expression and activation of Akt and AMPK↑	Kuo et al. (2016b)
	Type 2 diabetic mice	Glucose uptake, GLUT4 expression and activation of Akt and AMPK in skeletal muscle↑, FA and cholesterol synthesis and gluconeogenesis in the liver↓	Kuo et al. (2016b)
Lycopene **24**	DIO mice	Inflammation in EAT and the liver, lipogenesis in the liver↓, hepatic FA oxidation and p-levels of STAT6 and Akt↑	Fenni et al. (2017); Chen et al. (2019)
	STZ-diabetic rats	Hypoglycemic effect and antioxidant activity↑	Zheng et al. (2019)
Beta-carotene **25**	3T3-L1 adipocytes DIO mice	Adipogenesis↓ Thermogenesis and browning of WAT and BAT, PDGFRα^{+} cells expression in EAT↑	Schwarz et al. (1997) Wang et al. (2017a)
Beta-cryptoxanthin **458**	TSOD mice	Inflammation, lipogenesis, lipid transport activity, and Bmal1 expression in AT↓, FA oxidation and AMPK activation in AT↑	Takayanagi (2011)

(continued)

Table 5.1 (continued)

Phytochemicals	Experimental models	Major therapeutic targets	References
Astaxanthin **168**	DIO mice	Hepatic inflammation, lipogenesis and lipid uptake activity↓, M2 macrophage recruitment in the liver↑	Ni et al. (2015)
Fucoxanthin **158**	3T3-L1 adipocytes	Lipid accumulation and adipogenesis↓, FA oxidation and AMPK activation↑	Kang et al. (2011b, 2012)
	DIO mice	Hepatic lipogenesis↓, hepatic FA oxidation and insulin sensitivity↑	Woo et al. (2010)
13. Saponins			
Dioscin **84**	3T3-L1 adipocytes	Adipogenesis↓, MCE and p-levels of ERK1/2 and p38MAPK↓, AMPK activation↑	Poudel et al. (2014)
	DIO mice	Hepatic inflammation and lipogenesis↓, hepatic FA oxidation, autophagy and AMPK activation in liver↑	Liu et al. (2015a)
	Diabetic KK-Ay mice	Hepatic glycogen content, miR125a-5p expression and insulin signaling↑, hepatic gluconeogenesis, lipogenesis, FoxO1, and GSK-3β-expression↓	Xu et al. (2020a)
Diosgenin **87**	Diabetic KK-Ay mice	Hepatic inflammation and lipogenesis↓, hepatic lipolysis and FA oxidation↑	Hashidume et al. (2018); Uemura et al. (2011)
Capsicoside G **142**	3T3-L1 adipocytes	Adipogenesis↓, AMPK activation and FA oxidation↑	Sung et al. (2016)
	DIO mice	Lipogenesis in the liver and AT↓, FA oxidation and AMPK activation in the liver↑	Sung and Lee (2016)

(continued)

Table 5.1 (continued)

Phytochemicals	Experimental models	Major therapeutic targets	References
Ginsenoside Rb1 **65**	C2C12 myotubes	Glucose uptake, GLUT4 expression and Akt activation↑	Shen et al. (2013)
	DIO mice	Lipid synthesis in the liver and AT, inflammation in the liver, AT, and hypothalamus↓, hypothalamic insulin sensitivity, Akt activation, c-Fos expression↑, glucose uptake, GLUT4 expression and activation of AMPK in skeletal muscle↑, hepatic and AT FA oxidation and AMPK activation↑	Xiong et al. (2010); Wu et al. (2014b); Shen et al. (2015)
Ginsenoside Rb2 **459**	Obese diabetic db/db mice	Hepatic autophagy, FA oxidation, SIRT1 expression and AMPK activation↑	Huang et al. (2017a)
	DIO mice	Mitochondrial biogenesis and thermogenesis in BAT and WAT↑	Hong et al. (2019)
Ginsenoside Rg1 **460**	DIO mice	Adipogenesis in AT↓, lipolysis, FA oxidation and AMPK activation in AT↑, glucose uptake, GLUT4 expression and activation of Akt and AMPK in the liver and skeletal muscle↑	Liu et al. (2018b); Li et al. (2018b)
Ginsenoside Rg2 **460a**	DIO mice	Hepatic lipogenesis↓, hepatic FA oxidation, antioxidant activity and SIRT 1 activity↑	Cheng et al. (2020)
Ginsenoside Rg3 **461**	Endocrine NCIH716 cells	GLP-1 secretion and Gα-gust expression↑	Kim et al. (2015, 2016)
	C2C12 myotubes	Glucose uptake, insulin signaling and p-levels of IRS-1 and Akt↑	Kim et al. (2016)

(continued)

Table 5.1 (continued)

Phytochemicals	Experimental models	Major therapeutic targets	References
	DIO mice	Adipogenesis and inflammation, p-levels of STAT5 in EAT↓	Lee et al. (2017)
Karaviloside XI **462** and momordicoside S **463**	L6 myotubes and 3T3-L1 adipocytes	Glucose uptake, GLUT4 expression and AMPK activation↑	Tan et al. (2008)
14. Polyacetylenes			
3β-Glucopyranosyloxy-1-hydroxy-6E-tetradecene-8,10,12-triyne **464** and 2β-glucopyranosyloxy-1-hydroxy-5E-tridecene-7,9,11-triyne **465** and cytopiloyne **466**	NOD-type 1 diabetic mice	Insulin secretion and Th2 cells expression in the pancreas↑, pancreatic Th1 cells expression↓	Chang et al. (2004, 2007); Chiang et al. (2007)
(9Z, 16S)-16-Hydroxy-9,17-octadecadiene-12,14-diynoic acid **467**	HepG2 cells and 3T3-L1 adipocytes	TG accumulation and synthesis↓, FA oxidation, LKB1 expression and AMPK activation↑	Kang et al. (2018a)
	DIO mice	Lipid accumulation and synthesis in the liver and AT↓, AMPK activation in the liver and AT↑	Kang et al. (2018b)
Falcarinol **27**	Porcine myocells	Glucose uptake, GLUT4 expression and p-levels of Akt and AS160↑	Bhattacharya et al. (2014b)
15. Organosulphur compounds			
Alliin **468**	DIO mice	Gut microbial dysbiosis↓, abundance of bacteria of genus *Oscillospira* and *Ruminococcus* in the gut↑	Zhai et al. (2018)
Allicin **469**	DIO mice	Hepatic lipogenesis↓, lipolysis, FA oxidation, mitochondrial biogenesis and thermogenesis in AT and liver↑, gut microbial dysbiosis↓, abundance of health-	Shi et al. (2019)
	STZ-diabetic rats		Liu et al. (2012)

(continued)

Table 5.1 (continued)

Phytochemicals	Experimental models	Major therapeutic targets	References
		benefit bacteria of genus *Akkermansia* and *Eubacterium* in the gut↑	
	SVCs	Myocardial fibrosis and apoptosis of cardiomyocytes↓ Brown-like adipogenesis and KLF-15 expression↑	Lee et al. (2019)
Ajoene **470**	DIO mice	Hepatic lipogenesis↓, hepatic FA oxidation, SIRT1 and LKB1 expression and AMPK activation↑,	Han et al. (2011)
Sulforaphane **471**	DIO mice	lipogenesis in AT↓, FA oxidation and AMPK activation in AT↑, mitochondrial biogenesis and browning-like activity in WAT and BAT↑	Choi et al. (2014b); Liu et al. (2021)
	STZ-DCM mice	Myocardial inflammation and fibrosis↓, antioxidant activity, FA oxidation, SIRT1 and LKB1 expression and AMPK activation in myocardial tissues↑	Zhang et al. (2014b)
Glucoraphanin **472**	DIO mice	Hepatic inflammation and lipogenesis↓, antioxidant activity, FA oxidation, thermogenesis and AMPK activation in the liver and AT↑, abundance of bacteria of genus *Akkermansia* and *Alloprevotella* in the gut↑	Nagata et al. (2017); Xu et al. (2020b)
16. Polysaccharides			
Rice bran polysaccharides	DIO mice	Hepatic inflammation and lipogenesis↓, hepatic FA oxidation and SIRT1 expression↑	Nie et al. (2017b)

(continued)

Table 5.1 (continued)

Phytochemicals	Experimental models	Major therapeutic targets	References
Wolfberry polysaccharides	DIO mice	Hepatic lipogenesis↓, hepatic lipolysis, FA oxidation, SIRT1 expression and AMPK action↑	Jia et al. (2016)
Mulberry polysaccharides	STZ-diabetic rats	Glucose uptake, GLUT4 expression and Akt phosphorylation in skeletal muscle↑, pancreatic insulin secretion↑, abundance of bacteria of genus *Lactobacillus*, *Allobaculum*, and *Akkermansia* in the gut↑	Chen et al. (2018a)
Momordica charantia polysaccharides	STZ-diabetic rats	Hepatic gluconeogenesis↓, hepatic AMPK activation↑	Wang et al. (2019e)
Pumpkin polysaccharides	DIO mice	Gut microbial dysbiosis↓, Abundance of bacterial spp. of *Bacteroidetes*, *Prevotella*, *Oscillospira*, *Sutterella*, and *Bilophila* in the gut↑	Wang et al. (2017b)
Pleurotus ostreatus polysaccharides	Type 2 diabetic rats	Hepatic antioxidant activity and glycogen content↑, glucose uptake, GLUT4 expression and Akt phosphorylation in the liver and skeletal muscle↑	Zhang et al. (2016e)
Pleurotus sajor-caju polysaccharides	DIO mice	Lipogenesis in AT↓, lipolysis and antioxidant activity in AT↑	Kanagasabapathy et al. (2013)
Ganoderma lucidum polysaccharides	STZ-diabetic rats	Hepatic glycogen content and insulin sensitivity↑, hepatic gluconeogenesis↓	Xiao et al. (2012)

(continued)

Table 5.1 (continued)

Phytochemicals	Experimental models	Major therapeutic targets	References
Hirsutella sinensis polysaccharides	DIO mice	Hepatic lipogenesis↓, hepatic FA β-oxidation and energy expenditure in BAT and WAT↑, abundance of health-benefit bacteria, *Parabacteroides goldsteinii*, *Clostridium cocleatum*, and *Anaerotruncus colihominis* in the gut↑, abundance of *E. coli* in the gut↓	Wu et al. (2019)
Gracilaria lemaneiformis sulfated polysaccharides	Diabetic mice	Insulin secretion and hepatic glycogen content↑, hepatic gluconeogenesis↓	Liao et al. (2015); Wen et al. (2017)
Holothuria leucospilota sulfated polysaccharides	DIO mice	Hepatic nflammation and lipogenesis↓, abundance of bacteria of genus *Oscillospira*, *Prevotella*, and *Dorea* in the gut↑	Yuan et al. (2019)

saponins, alkaloids, phenolic acids, tannins, stilbenoids, coumarins, xanthones, lignans, curcuminoids, polyacetylenes, organosulfur compounds, bromophenols, and polysaccharides isolated from various natural sources (plants, seaweeds, mushrooms, marine animals, and microorganisms), have been found to possess significant anti-obesity and antidiabetic effects in both cellular and animals models. These natural products could be considered as a first choice for development of new drugs for obesity and diabetes treatment having minimum adverse side effects and of low cost and easy availability. These natural phytochemicals reduce the severity of the pathogenic factors of these diseases, obesity, diabetes, and their associated vascular complications by their multitarget approaches. Their major targets include (1) suppression of the activity of fat digesting enzyme pancreatic lipase, and dietary carbohydrates digesting enzymes α-amylase and α-glucosidase; (2) stimulation of the activation of AMPK and insulin signaling pathway via PI3K/Akt activation; (3) stimulation of energy expenditure and lipolysis; (4) suppression of lipid synthesis and inflammation; (5) inhibition of adipogenesis; (6) inhibition of the activity of PTP1B enzyme, a negative regulator of insulin signaling pathway, and of the activity of 11β-HSD1 enzyme, a key enzyme for conversion of inactive cortisone to active cortisol, a negative regulator of insulin sensitivity in metabolic tissues; (7) activation

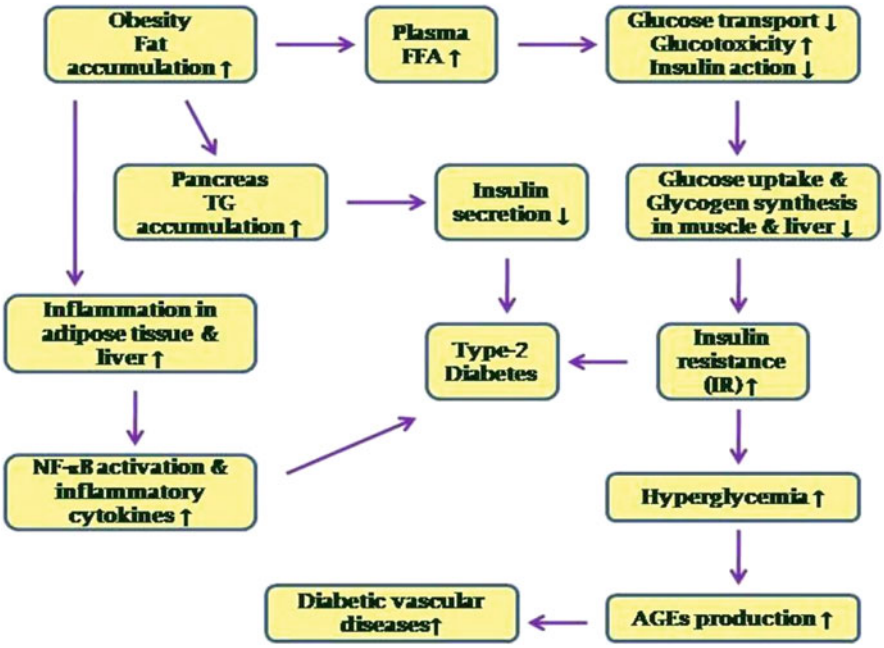

Fig. 5.3 Inter-relationship of obesity, type 2 diabetes, and inflammation

of MOR; (8) inhibition of the activity of aldose reductase (AR), a key enzyme for accumulation AGEs and consequently stimulation for deposition of ECM particles in different organs for progression of vascular diseases; and (9) modulation of gut microbiota dysbiosis. Among the natural molecules, dietary fibers, polysaccharides, and polyphenols modulate the composition of gut microbiota dysbiosis. A growing piece of evidence demonstrates that intestinal microbiome dysbiosis has a key role in development of inflammation and metabolic dysregulation in metabolic organs, resulting in hyperglycemia and dyslipidemia in both genetically obese ob/ob, db/db mice, and in DIO mice. On the other hand, Intestinal healthy microbiota is a key factor in the physiological functions of dietary polyphenols via catabolism of various dietary tannins, and other polyphenols for activation of SCFAs secretion, GLP-1 secretion, and improvement of intestinal inflammation and immune function (Tilg et al. 2020; Kawabata et al. 2019). Available evidence demonstrates that polysaccharides mitigate both obesity and T2DM by multiple targets, namely, reducing the digestion of carbohydrates via inhibition of the activities of alpha-amylase and alpha-glucosidase in the intestine, scavenging free radicals from systemic circulation, reducing pancreatic glucagon secretion, suppressing inflammatory cytokines expression by suppression of activation of ERK/JNK/MARK signaling pathway, increasing hepatic glycogen synthesis and pancreatic insulin secretion, and modulating gut microbiota composition by acting as prebiotic for the growth of health promoting bacteria via fermentation to produce diverse metabolites including

SCFAs as an additional energy source for the host. In most cases, these natural molecules increase the abundance of phylum Bacteroidetes and genus levels of *Akkermansia*, *Bifidobacterium*, *Lactobacillus*, *Allobaculum*, *Olsenella*, *Bacteroides*, and *Prevotella*, and reduce the abundance of phylum Firmicutes and Firmicutes/Bacteroidetes ratio in the gut. A large number of phytochemicals, including resveratrol, quercetin, apigenin, naringenin, scopoletin, osthole, emodin, shikonin, mangiferin, berberine, stevioside, corosolic acid, ursolic acid, betulinic acid, asiatic acid, eburicoic acid, chlorogenic acid, chicoric acid, catalpol, loganin, oleuropein, swertiamarin, rosmarinic acid, fucoxanthin, capsaicin, ginsenosides Rb1 and Rg1, karaviloside XI, sulporaphane, eugenol, caffeic acid, salvianolic acid B, salidroside, and thymoquinone, improved hyperglycemia by promoting glucose uptake and GLUT4 expression and its translocation to plasma membrane in skeletal muscle, and down-regulating hepatic gluconeogenic enzymes PEPCK and G6Pase via activation of IRS-1/PI3K/Akt/AMPK signaling pathway. Many of them, such as resveratrol, baicalin, quercetin, myricitrin, curcumin, rosmarinic acid, anthocyanins, tannins, etc., improved postprandial glucose levels by suppression of the activity of intestinal carbohydrate digesting enzymes α-amylase and α-glucosidase in diabetic animals.

Although a good number of natural products have been reported to have potential efficacy in obesity and diabetes treatment, only a few of them are used directly in clinical application because of low aqueous solubility, stability, poor oral bioavailability, lack of information on target specificity, toxicity at high doses, and availability in low quantity from natural sources. Moreover, the results in clinical trials in humans are not promising. The reason behind this shortcoming in results from clinical trials in humans is due to defects in design of in vivo studies in animal models. Most of the reported in vivo studies on bioactive phytochemicals were conducted in normal obese and diabetic rodents, but not in transgenic rodents. The transgenic mice have lipoproteins and genetic profile very similar to that in humans. Structural modifications of these bioactive natural products are required to get potent molecules of high efficacy at low concentrations and of minimal adverse effects on long term use. Encapsulation of these phytochemicals into nanoparticles may increase their bioavailability and protect them from premature degradation by the host bacterial species mainly present in the intestine, liver, and kidney before their entry to the disease-affected target tissues/cells and thus enhance their efficacy. Moreover, biotechnology can be developed for biosynthesis of phytochemical-like derivatives for their isolation in large quantities and clinical applications and study on toxicity and adverse side effects on long-term treatment in obese and diabetic patients. For example, canagliflozin, a modified compound of natural phlorizin, has potential antidiabetic effect in clinical trials and has been used for treatment of T2DM as per approval of the FDA. Further, systematic studies on these bioactive phytochemicals in transgenic mice or human-like animals are required to evaluate their optimal doses and minimal adverse side effects on prolonged intake. Therefore, synthetic approaches are required for synthesis of these bioactive phytochemicals to get in large quantity for extensive clinical studies before their entry in global market. Meanwhile, we have learnt the technology of the nature in natural products

biosynthesis, biochemistry and bioengineering, we may design new potent bioactive natural metabolites from the existing natural products by the use of plant and microbial gene clusters, interspecies cross talk genes and optimal fermentation conditions to get high dividend in our inputs. Both pharmaceutical industries and academic institutes should emphasize their attention jointly to fulfil this venture.

References

Abe D, Saito T, Nagata Y (2016) Rosmarinic acid regulates fatty acid and glucose utilization by activating the CaMKK/AMPK pathway in C2C12 myotubes. Food Sci Technol Res 22:779–785

Akiyama S, Katsumata SI, Suzuki K et al (2010) Dietary hesperidin exerts hypoglycaemic and hypolipidemic effects in streptozotocin-induced marginal type 1 diabetic rats. J Clin Biochem Nutr 46:87–92

Alam MA, Kauter K, Brown L (2013) Naringin improves diet-induced cardiovascular dysfunction and obesity in high carbohydrate, high fat diet-fed rats. Nutrients 5:637–650

Alkhalidy H, Moore W, Zhang Y et al (2015) Small molecule kaempferol promotes insulin sensitivity and preserved pancreatic β-cell mass in middle-aged obese diabetic mice. J Diabetes Res 2015:532984

Alkhalidy H, Moore W, Zhang Y et al (2018) Kaempferol ameliorates hyperglycemia through suppressing hepatic gluconeogenesis and enhancing hepatic insulin sensitivity in diet-induced obese mice. J Nutr Biochem 58:90–101

Allister EM, Mulvihill EE, Barrett PHR et al (2008) Inhibition of apo B secretion from HepG2 cells by insulin is amplified by naringenin, independent of the insulin receptor. J Lipid Res 49:2218–2229

Al-Trad B, Alkhateeb H, Alsmadi W et al (2019) Eugenol ameliorates insulin resistance, oxidative stress and inflammation in high fat-diet/streptozotocin-induced diabetic rats. Life Sci 216:183–188

Ambati RR, Phang SM, Ravi S et al (2014) Astaxanthin: sources, extraction, stability, biological activities and its commercial applications-a review. Mar Drugs 12:128–152

An T, Zhang J, Lv B et al (2019) Salvianolic acid B plays an anti-obesity role in high fat diet-induced obese mice by regulating the expression of mRNA, circRNA and lncRNA. Peer J 7: e6506

Anand David AV, Arulmoli R, Parasuram S (2016) Overviews of biological importance of quercetin: a bioactive flavonoid. Pharmacogn Rev 10:84–89

Assini JM, Mulvihill EE, Burke AC et al (2015) Naringenin prevents obesity, hepatic steatosis, and glucose intolerance in male mice independent of fibroblast growth factor 21. Endocrinology 156:2087–2102

Atanassova M, Bagdassarian V (2009) Rutin content in plant products. J Univ Chem Technol Metallur 44:201–203

Aulifa DL, Adnyana IK, Levita J et al (2019) 4-Hydroxyderricin isolated from the sap of *Angelica keiskei* Koidzumi: evaluation of its inhibitory activity towards dipeptidyl peptidase-IV. Sci Pharm 87:30

Babukumar S, Vinothkumar V, Sankaranarayanan C et al (2017) Geraniol, a natural monoterpene, ameliorates hyperglycemia by attenuating the key enzymes of carbohydrate metabolism in streptozotocin-induced diabetic rats. Pharm Biol 55:1442–1449

Bai N, He K, Roller M et al (2008) Active compounds from *Lagerstroemia speciosa*, insulin-like glucose uptake-stimulatory/inhibitory and adipocyte differentiation-inhibitory activities in 3T3-L1 cells. J Agric Food Chem 56:11668–11674

Bai J, Wang Y, Zhu X et al (2019) Eriodictyol inhibits high glucose-induced extracellular matrix accumulation, oxidative stress, and inflammation in human glomerular mesangial cells. Phytother Res 33:2775–2782

Baiges I, Palmfeldt J, Blade C et al (2010) Lipogenesis is decreased by grape seed proanthocyanidins according to liver proteomics of rats fed a high fat diet. Mol Cell Proteomics 9:1499–1513

Bak EJ, Kim J, Jang S et al (2013) Gallic acid improves glucose tolerance and triglyceride concentration in diet-induced obesity mice. Scand J Clin Lab Invest 73:607–614

Bao Q, Shen X, Qian L et al (2016) Anti-diabetic activities of catalpol in db/db mice. Korean J Physiol Pharmacol 20:153–160

Basha RH, Sankaranarayanan C (2014) β-Caryophyllene, a natural sesquiterpene, modulates carbohydrate metabolism in streptozotocin-induced diabetic rats. Acta Histochem 116:1469–1479

Basha RH, Sankaranarayanan C (2015) Protective effect of β-caryophyllene, a sesquiterpene lactone on plasma and tissue glycoprotein components in streptozotocin-induced hyperglycaemic rats. J Acute Med 5:9–14

Baskaran P, Krishnan V, Ren J et al (2016) Capsaicin induces browning of white adipose tissue and counters obesity by activating TRPV-1 channel-dependent mechanisms. Br J Pharmacol 173: 2369–2389

Baur JA, Pearson KJ, Price NL et al (2006) Resveratrol improves health and survival of mice on a high-calorie diet. Nature 444:337–342

BelHadj S, Hentati O, Elfeki A et al (2013) Inhibitory activities of *Ulva lactuca* polysaccharides on digestive enzymes related to diabetes and obesity. Arch Physiol Biochem 119:81–87

Benn T, Kim B, Park YK et al (2014) Polyphenol-rich blackcurrant extract prevents inflammation in diet-induced obese mice. J Nutr Biochem 25:1019–1025

Bettaieb A, Hosein E, Chahed S et al (2015) Decreased adiposity and enhanced glucose tolerance in shikonin treated mice. Obesity (Silver Spring) 23:2269–2277

Bettaieb A, Cremonini E, Kang H et al (2016) Anti-inflammatory actions of (-)-epicatechin in the adipose tissue of obese mice. Int J Biochem Cell Biol 81(Pt B):383–392

Bhagwat S, Haytowitz DB, Holden JM (2011) USDA database for the flavonoid content of selected foods: release 3, US Department of Agriculture, Washington. USA. 2011:1–156

Bhattacharya S, Oksbjerg N, Young JF et al (2014a) Caffeic acid, naringenin and quercetin enhance glucose-stimulated insulin secretion and glucose sensitivity in INS-1E cells. Diabetes Obes Metab 16:602–612

Bhattacharya S, Rasmussen MK, Christensen LP et al (2014b) Naringenin and falcarinol stimulate glucose uptake and TBC1D1 phosphorylation in porcine myotube cultures. J Biochem Pharmacol Res 2:91–98

Bilbao LMM, Andres-Lacueva C, Jauregui O et al (2007) Determination of flavonoids in a citrus fruit extract by LC-DAD and LC-MS. Food Chem 101:1742–1747

Birgani GA, Ahangarpour A, Khorsandi L et al (2018) Anti-diabetic effect of betulinic acid on streptozotocin-nicotinamide induced diabetic male mouse model. Braz J Pharm Sci 54:e17171

Bonnefont-Rousselot D (2016) Resveratrol and cardiovascular diseases. Nutrients 8:250

Bose M, Lambert JD, Ju J et al (2008) The major green tea polyphenol, (-)-epigallocatechin-3-gallate, inhibits obesity, metabolic syndrome, and fatty liver disease in high-fat-fed mice. J Nutr 138:1677–1683

Boyle SP, Dobson VL, Duthie SJ et al (2000) Bioavailability and efficiency of rutin as an antioxidant: a human supplementation study. Eur J Clin Nutr 54:774–782

Caimari A, Del Bas JM, Crescenti A et al (2013) Low doses of grape seed procyanidins reduce adiposity and improve the plasma lipid profile in hamsters. Int J Obes 37:576–583

Cao X, Xia Y, Liu D et al (2020) Inhibitory effects of *Lentinus edodes* mycelia polysaccharide on α-glucosidase, glycation activity and high-glucose-induced cell damage. Carbohydr Polymers 246:116659

Casas-Grajales S, Ramos-Tovar E, Chavez-Estrada E et al (2019) Antioxidant and immunomodulatory activity induced by stevioside in liver damage: in vivo, in vitro and in silico assays. Life Sci 224:187–196

Cassady JM, Zennie TM, Chae YH et al (1988) Use of a mammalian cell culture benzo(a) pyrene metabolism assay for the detection of potential anticarcinogens from natural products: inhibition of metabolism by biochanin A, an isoflavone from *Trifolium pratense* L. Cancer Res 48:6257–6261

Cazarolli LH, Kappel VD, Pereira DF et al (2012) Antihyperglycemic action of apigenin-6-C-β-fucopyranoside from *Averrhoa carambola*. Fitoterapia 83:1176–1183

Cedernaes J, Waldeck N, Bass J (2019) Neurogenetic basis for circadian regulation of metabolism by the hypothalamus. Genes Dev 33:1136–1158

Celik S, Erdogan S, Tuzcu M (2009) Caffeic acid phenethyl ester (CAPE) exhibits significant potential as an antidiabetic and liver protective agent in streptozotocin-induced diabetic rats. Pharmacol Res 60:270–276

Chang SL, Chang CLT, Chiang YM et al (2004) Polyacetylenic compounds and butanol fraction from *Bidens pilosa* can modulate the differentiation of helper T cells and prevent autoimmune diabetes in non-obese diabetic mice. Planta Med 70:1045–1051

Chang CLT, Chang SL, Lee YM et al (2007) Cytopiloyne, a polyacetylenic glucoside, prevents type 1 diabetes in nonobese diabetic mice. J Immunol 178:6984–6993

Chang WC, Wu SC, Xu KD et al (2015) Scopoletin protects against methylglyoxal-induced hyperglycemia and insulin resistance mediated by suppression of advanced glycation endproducts (AGEs) generation and anti-glycation. Molecules 20:2786–2801

Chao J, Huo TI, Cheng HY et al (2014) Gallic acid ameliorated impaired glucose and lipid homeostasis in high fat diet-induced NAFLD mice. PLoS One 9:e96969

Chen TH, Chen SC, Chan P et al (2005) Mechanism of the hypoglycemic effect of stevioside, a glycoside of *Stevia rebaudiana*. Planta Med 71:108–113

Chen YC, Zeng XY, He Y et al (2013) Rutaecarpine analogues reduce lipid accumulation in adipocytes via inhibiting adipogenesis/lipogenesis with AMPK activation and UPR suppression. ACS Chem Biol 8:2301–2311

Chen Z, Zheng S, Li L et al (2014) Metabolism of flavonoids in humans: a comprehensive review. Curr Drug Metab 15:48–61

Chen CC, Chuang WT, Lin AH et al (2016a) Andrographolide inhibits adipogenesis of 3T3-L1 cells by suppressing C/EBPβ expression and activation. Toxicol Appl Pharmacol 307:115–122

Chen L, Zhang Y, Sha O et al (2016b) Hypolipidaemic and hypoglycaemic activities of polysaccharide from *Pleurotus eryngii* in Kunming mice. Int J Biol Macromol 93(Pt A):1206–1209

Chen S, Wen X, Zhang W et al (2017) Hypolipidemic effect of oleanolic acid is mediated by the miR-98-5p/PGC-1β axis in high-fat diet-induced hyperlipidemic mice. FASEB J 31:1085–1096

Chen C, You LJ, Huang Q et al (2018a) Modulation of gut microbiota by mulberry fruit polysaccharide treatment of obese diabetic *db/db* mice. Food Funct 9:3732–3742

Chen XF, Wang L, Wu YZ et al (2018b) Effect of puerarin in promoting fatty acid oxidation by increasing mitochondrial oxidative capacity and biogenesis in skeletal muscle in diabetic rats. Nutr Diabetes 8:1

Chen G, Ni Y, Nagata N et al (2019) Lycopene alleviates obesity-induced inflammation and insulin resistance by regulating M1/M2 status of macrophages. Mol Nutr Food Res 63:1900602

Cheng Z, Pang T, Gu M et al (2006) Berberine-stimulated glucose uptake in L6 myotubes involves both AMPK and p38 MAPK. Biochim Biophys Acta 1760:1682–1689

Cheng B, Gao W, Wu X et al (2020) Ginsenoside Rg2 ameliorates high-fat diet-induced metabolic disease through SIRT 1. J Agric Food Chem 68:4215–4226

Cheungsamarn S, Rattanamongkolgul S, Luechapudiporn R et al (2012) Curcumin extract for prevention of type 2 diabetes. Diabetes Care 35:2121–2127

Chiang YM, Chang CLT, Chang SL et al (2007) Cytopiloyne, a novel polyacetylenic glucoside from *Bidens pilosa*, functions as a T helper cell modulator. J Ethnopharmacol 110:532–538

Cho AS, Jeon SM, Kim MJ et al (2010) Chlorogenic acid exhibits anti-obesity property and improves lipid metabolism in high-fat diet-induced obese mice. Food Chem Toxicol 48:937–943

Cho S, Choi Y, Park S et al (2012) Carvacrol prevents diet-induced obesity by modulating gene expressions involved in adipogenesis and inflammation in mice fed with high-fat diet. J Nutr Biochem 23:192–201

Choi MS, Jung UJ, Yeo J et al (2008) Genistein and daidzein prevent diabetes onset by elevating insulin level and altering hepatic gluconeogenic and lipogenic enzyme activities in non-obese diabetic (NOD) mice. Diabetes Metab Res Rev 24:74–81

Choi HD, Kim JH, Chang MJ et al (2011) Effects of astaxanthin on oxidative stress in overweight and obese adults. Phytother Res 25:1813–1818

Choi HN, Kang MJ, Lee SJ et al (2014a) Ameliorative effect of myricetin on insulin resistance in mice fed a high-fat, high-sucrose diet. Nutr Res Pract 8:544–549

Choi KM, Lee YS, Kim W et al (2014b) Sulforaphane attenuates obesity by inhibiting adipogenesis and activating the AMPK pathway in obese mice. J Nutr Biochem 25:201–207

Choi RY, Ham JR, Lee MK (2016) Esculetin prevents non-alcoholic fatty liver in diabetic mice fed high-fat diet. Chem Biol Interact 260:13–21

Choi RY, Ham JR, Lee HI et al (2017) Scopoletin supplementation ameliorates steatosis and inflammation in diabetic mice. Phytother Res 31:1795–1804

Cipriani S, Mencarelli A, Palladino G et al (2010) FXR activation reverses insulin resistance and lipid abnormalities and protects against liver steatosis in Zucker (fa/fa) obese rats. J Lipid Res 51:771–784

Collins QF, Liu HY, Pi J et al (2007) Epigallocatechin-3-gallate (EGCG), a green tea polyphenol, suppresses hepatic gluconeogenesis through 5′-AMP-activated protein kinase. J Biol Chem 282: 30143–30149

Combs TR, Marliss EB (2014) Adiponectin signaling in liver. Rev Endocr Metab Disord 15:137–147

Cremonini E, Bettaieb A, Haj FG et al (2016) (-)-Epicatechin improves insulin sensitivity in high fat diet-fed mice. Arch Biochem Biophys 599:13–21

Cui L, Kim MO, Seo JH et al (2012) Abietane diterpenoids of *Rosmarinus officinalis* and their diacylglycerol acyltransferase inhibitory activity. Food Chem 132:1775–1780

Dabeek WM, Marra MV (2019) Dietary quercetin and kaempferol: bioavailability and potential cardiovascular-related bioactivity in humans. Nutrients 11:2288

Dela Sena C, Narayanasamy S, Riedi KM et al (2013) Substrate specificity of purified recombinant human β-carotene-15,15′-oxygenase (BCO1). J Biol Chem 288:37094–37103

Del Bas JM, Ricketts ML, Vague M et al (2009) Dietary procyanidins enhance transcriptional activity of bile acid-activated FXR in vitro and reduce triglyceridemia in vivo in a FXR-dependent manner. Mol Nutr Food Res 53:805–814

De Melo CL, Queiroz MGR, Fonseca SGC et al (2010) Oleanolic acid, a natural triterpenoid improves blood glucose tolerance in normal mice and ameliorates visceral obesity in mice fed a high-fat diet. Chem Biol Interact 185:59–65

De Natale C, Minerva V, Patti L et al (2012) Effects of baked products enriched with n-3 fatty acids, folates, β-glucans, and tocopherol in patients with mild mixed hyperlipidemia. J Am Col Nutr 31:211–319

Dhanya R, Arya AD, Nisha P et al (2017) Quercetin, a lead compound against type 2 diabetes, ameliorates glucose uptake via AMPK pathway in skeletal muscle cell line. Front Pharmacol 8: 336

Dinda B, Dinda S, DasSharma S et al (2017) Therapeutic potentials of baicalin and its aglycone, baicalein against inflammatory disorders. Eur J Med Chem 131:68–80

Dineshkumar B, Mitra A, Mahadevappa M (2010) Antidiabetic and hypolipidemic effects of mahanimbine (carbazole alkaloid) from *Murraya koenigii* (Rutaceae) leaves. Int J Phytomed 2:22–30

Ding H, Zhang Y, Xu C et al (2014a) Norathyriol reverses obesity- and high-fat-diet-induced insulin resistance in mice through inhibition of PTP1B. Diabetologia 57:2145–2154
Ding L, Li J, Song B et al (2014b) Andrographolide prevents high-fat diet-induced obesity in C57BL/6 mice by suppressing the sterol regulatory element-binding protein pathway. J Pharmacol Exp Ther 351:474–483
Ding Y, Song Z, Li H et al (2019) Honokiol ameliorates high-fat-diet-induced obesity of different sexes of mice by modulating the composition of the gut microbiota. Front Immunol 10:2800
Diwan V, Poudyal H, Brown L (2013) Piperine attenuates cardiovascular, liver and metabolic changes in high carbohydrate, high fat-fed rats. Cell Biochem Biophys 67:297–304
Doan KV, Ko CM, Kinyua AW et al (2015) Gallic acid regulates body weight and glucose homeostasis through AMPK activation. Endocrinology 156:157–168
Du J, Xie J, Zhang Z et al (2010) TRPM7-mediated Ca^{2+} signals confer fibrogenesis in human atrial fibrillation. Circ Res 106:992–1003
Du Y, Chen Y, Fu X et al (2020) Effects of piperine on lipid metabolism in high-fat diet induced obese mice. J Funct Foods 71:104011
Du F, Huang R, Lin D et al (2021) Resveratrol improves liver steatosis and insulin resistance in non-alcoholic fatty liver disease in association with the gut microbiota. Front Pharmacol 12: 611323
Eid HM, Martineau LC, Saleem A et al (2010) Stimulation of AMP-activated protein kinase and enhancement of basal glucose uptake in muscle cells by quercetin and quercetin glycosides, active principles of the antidiabetic medicinal plant *Vaccinium vitis-idaea*. Mol Nutr Food Res 54:991–1003
Eliza J, Daisy P, Ignacimuthu S et al (2009) Normo-glycemic and hypolipidemic effect of costunolide isolated from *Costus speciosus* (Koen ex. Retz.)Sm. in streptozotocin-induced diabetic rats. Chem Biol Interact 179:329–334
Enoki T, Ohnogi H, Nagamine K et al (2007) Antidiabetic activities of chalcones isolated from a Japanese herb, *Angelica keiskei*. J Agric Food Chem 55:6013–6017
Escande C, Nin V, Price NL et al (2013) Flavonoid apigenin is an inhibitor of the NAD+ ase CD38. Diabetes 62:1084–1093
Eu CHA, Lim WYA, Ton SH et al (2010) Glycyrrhizic acid improved lipoprotein lipase expression, insulin sensitivity, serum lipid and lipid deposition in high-fat-diet-induced obese rats. Lipids Health Dis 9:81
Eze ED, Afodun AM, Sulaiman SO et al (2018) Lycopene attenuates diabetes-induced oxidative stress in Wistar rats. J Diabetes Endocrinol 9:11–19
Fang P, Yu M, Zhang L et al (2017) Baicalin against obesity and insulin resistance through activation of AKT/AS160/GLUT4 pathway. Mol Cell Endocrinol 448:77–86
Fang P, Yu M, Min W et al (2018) Beneficial effect of baicalin on insulin sensitivity in adipocytes of diet-induced obese mice. Diabetes Res Clin Pract 139:262–271
Fang P, He B, Yu M et al (2019) Treatment with celastrol protects against obesity through suppression of galanin-induced fat intake and activation of PGC-1α/GLUT4 axis-mediated glucose consumption. Biochim Biophys Acta 1865:1341–1350
Faraut B, Giannesini B, Matarazzo V et al (2009) Capsiate administration results in an uncoupling protein 3 downregulation, an enhanced muscle oxidative capacity and a decreased abdominal fat content in vivo. Int J Obes 33:1348–1355
Feng Y, Huang SL, Dou W et al (2010) Emodin, a natural product, selectively inhibits 11-β-hydroxysteroid dehydrogenase type 1 and ameliorates metabolic disorder in diet-induced obese mice. Br J Pharmacol 161:113–126
Feng X, Weng D, Zhou F et al (2016) Activation of PPARγ by a natural flavonoid modulator, apigenin ameliorates obesity-related inflammation via regulation of macrophage polarization. EBioMedicine 9:61–76
Fenni S, Hammou H, Astier J et al (2017) Lycopene and tomato powder supplementation similarly inhibit high-fat diet induced obesity, inflammatory response and associated metabolic disorders. Mol Nutr Food Res 61:1601083

Fontecha-Barriuso M, Martin-Sanchez D, Ruiz-Andres O et al (2018) Targeting epigenetic DNA and histone modifications to treat kidney disease. Nephol Dial Transplant 33:1875–1886

Frombaum M, Therond P, Djelidi R et al (2011) Piceatannol is more effective than resveratrol in endothelial cell dimethylarginine dimethylaminohydrolase expression and activity after high-glucose oxidative stress. Free Radic Res 45:293–302

Fu Y, Luo J, Jia Z et al (2014) Baicalein protects against type 2 diabetes via promoting islet β-cell function in obese diabetic mice. Int J Endocrinol 2014:846742

Fujiwara Y, Tsukahara C, Ikeda N et al (2017) Oleuropein improves insulin resistance in skeletal muscle by promoting the translocation of GLUT4. J Clin Biochem Nutr 61:196–202

Fukumitsu S, Aida K, Ueno N et al (2008) Flaxseed lignan attenuates high-fat diet-induced fat accumulation and induces adiponectin expression in mice. Br J Nutr 100:669–676

Fukumitsu S, Aida K, Shimizu H et al (2010) Flaxseed lignan lowers blood cholesterol and decreases liver disease risk factors in moderately hypercholesterolemic men. Nutr Res 30: 441–446

Gandhi GR, Jothi G, Antony PJ et al (2014) Gallic acid attenuates high-fat diet fed-streptozotocin-induced insulin resistance via partial agonism of PPARγ in experimental type 2 diabetic rats and enhances glucose uptake through translocation and activation of GLUT4 in PI3K/p-Akt signaling pathway. Eur J Pharmacol 745:201–216

Ganesan K, Xu B (2019) Anti-diabetic effects and mechanisms of dietary polysaccharides. Molecules 24:2556

Gao H, Huang YN, Gao B et al (2008) Chebulagic acid is a potent α-glucosidase inhibitor. Biosci Biotechnol Biochem 72:601–603

Gao C, Chen G, Liu L et al (2013) Impact of high glucose and proteasome inhibitor MG132 on histone H2A and H2B ubiquitination in rat glomerular mesangial cells. J Diabetes Res 2013: 589474

Geddo F, Antoniotti S, Querio G et al (2021) Plant-derived *trans*-β-caryophyllene boosts glucose metabolism and ATP synthesis in skeletal muscle cells through cannabinoid type 2 receptor stimulation. Nutrients 13:916

Geeraert B, Crombe F, Hulsmans M et al (2010) Stevioside inhibits atherosclerosis by improving insulin signaling and antioxidant defense in obese insulin-resistant mice. Int J Obes 34:569–577

Genet C, Strehle A, Schmidt C et al (2010) Structure-activity relationship study of betulinic acid, a novel and selective TGR5 agonist and its synthetic derivatives: potential impact in diabetes. J Med Chem 53:178–190

Goboza M, Aboua YG, Chegou N et al (2019) Vindoline efficiently ameliorated diabetes-induced hepatotoxicity by docking oxidative stress, inflammation and hypertriglyceridemia in type 2 diabetes-induced male Wistar rats. Biomed Pharmacother 112:108638

Gonzalez-Garibay AS, Lopez-Vazquez A, Garcia-Banuelos J et al (2020) Effect of ursolic acid on insulin resistance and hyperinsulinemia in rats with diet-induced obesity: role of adipokines expression. J Med Food 23:297–304

Goto T, Kim Y-II, Funakoshi K et al (2011) Farnesol, an isoprenoid, improves metabolic abnormalities in mice via both PPARα-dependent and -independent pathways. Am J Physiol Endocrinol Metab 301:E1022–E1032

Guevara-Cruz M, Godinez-Salas ET, Sanchez-Tapia M et al (2020) Genistein stimulates insulin sensitivity through gut microbiota reshaping and skeletal muscle AMPK activation in obese subjects. BMJ Open Diab Res Cure 8:e000948

Guo YR, Choung SY (2017a) Germacrone attenuates hyperlipidemia and improves lipid metabolism in high-fat diet-induced obese C57BL/6J mice. J Med Food 20:46–55

Guo YR, Choung SY (2017b) Germacrone inhibits adipogenesis and stimulates lipolysis via AMP-activated protein kinase signalling pathway in 3T3-L1 preadipocytes. J Pharm Pharmacol 69:202–212

Guo J, Chen J, Ren W et al (2020a) Citrus flavone tangeretin is a potential insulin sensitizer targeting hepatocytes through suppressing MEK-ERK1/2 pathway. Biochem Biophys Res Commun 529:277–282

Guo L, Zhu B, Yuan H et al (2020b) Evaluation of serum neutrophil gelatinase-associated lipocalin in older patients with chronic kidney disease. Aging Med (Milton) 3:32–39
Guo S, Wang L, Chen D et al (2020c) Effects of a natural PTP1B inhibitor from Rhodomela confervoides on the amelioration of fatty acid-induced insulin resistance in hepatocytes and hyperglycemia in STZ-induced diabetic rats. RSC Adv 10:3429–3437
Gwon SY, Choi WH, Lee DH et al (2015) Shikonin protects against obesity through the modulation of adipogenesis, lipogenesis and β-oxidation in vivo. J Funct Foods 16:484–493
Gwon SY, Ahn J, Jung CH et al (2020) Shikonin attenuates hepatic steatosis by enhancing beta oxidation and energy expenditure via AMPK activation. Nutrients 12:1133
Hadrich F, Garcia M, Maalej A et al (2016) Oleuropein activated AMPK and induced insulin sensitivity in C2C12 muscle cells. Life Sci 151:167–173
Hameed A, Hafizur RM, Hussain N et al (2018) Eriodictyol stimulates insulin secretion through cAMP/PKA signalling pathway in mice islets. Eur J Pharmacol 820:245–255
Hamid HA, Yusoff MM, Liu M et al (2015) α-Glucosidase and α-amylase inhibitory constituents of *Tinospora crispa*: isolation and chemical profile confirmation by ultra-high performance liquid chromatography-quadrupole time-of-flight/mass spectrometry. J Funct Foods 16:74–80
Han CY, Ki SH, Kim YW et al (2011) Ajoene, a stable garlic by-product, inhibits high fat diet-induced hepatic steatosis and oxidative injury through LKB1-dependent AMPK activation. Antioxid Redox Signal 14:187–202
Harborne JB, Mabry TJ (1982) The flavonoids: advances in research, 1st edn. Chapman & Hall, New York
Harini R, Ezhumalai M, Pugalendi KV (2012) Antihyperglycemic effect of biochanin A, a soy isoflavone, on streptozotocin-diabetic rats. Eur J Pharmacol 676:89–94
Hashidume T, Sasaki K, Hirata J et al (2018) Effects of sanyaku and its constituent diosgenin on the fasted and postprandial hypertriacylglycerolemia in high-fat-diet-fed KK-Ay mice. J Agric Food Chem 66:9968–9975
He Y, Li Y, Zhao T et al (2013) Ursolic acid inhibits adipogenesis in 3T3-L1 adipocytes through LKB1/AMPK pathway. PLoS One 8:e70135
Hintzpeter J, Stapelfeld C, Loerz C et al (2014) Green tea and one of its constituents, epigallocatechin-3-gallate, are potent inhibitors of human 11β-hydroxysteroid dehydrogenase type 1. PLoS One 9:e84468
Hollman PCH, Arts ICW (2000) Flavonols, flavones and flavanols-nature, occurrence and dietary burdens. J Sci Food Agric 80:1081–1093
Hong Y, Lin Y, Si Q et al (2019) Ginsenoside Rb2 alleviates obesity by activation of brown fat and induction of browning of white fat. Front Endocrinol (Lausanne) 10:153
Hossain CM, Ghosh MK, Satapathy BS et al (2014) Apigenin causes biochemical modulation, GLUT4 and CD38 alternations to improve diabetes and to protect damages of some vital organs in experimental diabetes. Am J Pharmacol Toxicol 9:39–52
Hossain MK, Dayem AA, Han J et al (2016) Molecular mechanism of the anti-obesity and anti-diabetic properties of flavonoids. Int J Mol Sci 17:569
Hou B, Zhao Y, Qiang G et al (2018) Puerarin mitigates diabetic hepatic steatosis and fibrosis by inhibiting TGF-β signaling pathway activation in type 2 diabetic rats. Oxid Med Cell Longev 2018:4545321
Hou N, Mai Y, Qiu X et al (2019) Carvacrol attenuates diabetic cardiomyopathy by modulating the PI3K/Akt/GLUT4 pathway in diabetic mice. Front Pharmacol 10:998
Hsu YJ, Lee TH, Chang CLT et al (2009) Anti-hyperglycemic effects and mechanism of *Bidens pilosa* water extract. J Ethnopharmacol 122:379–383
Hu JL, Nie SP, Xie MY (2018) Antidiabetic mechanism of dietary polysaccharides based on their gastrointestinal functions. J Agric Food Chem 66:4781–4786
Huang H, Chen G, Liao D et al (2016a) The effects of resveratrol intervention on risk markers of cardiovascular health in overweight and obese subjects: a pooled analysis of randomized controlled trials. Obes Rev 17:1329–1340

Huang MQ, Zhou CJ, Zhang YP et al (2016b) Salvianolic acid B ameliorates hyperglycemia and dyslipidemia in *db/db* mice through the AMPK pathway. Cell Physiol Biochem 40:933–943

Huang Q, Want T, Yang L et al (2017a) Ginsenoside Rb2 alleviates hepatic lipid accumulation by restoring autophagy via induction of Sirt1 and activation of AMPK. Int J Mol Sci 18:1063

Huang WC, Liao PC, Huang CH et al (2017b) Osthole attenuates lipid accumulation, regulates the expression of inflammatory mediators, and increases antioxidants in FL83B cells. Biomed Pharmacother 91:78–87

Huang W, Zeng J, Liu Z et al (2019) Acetylshikonin stimulates glucose uptake in L6 myotubes via a PLC-β3/PKCδ-dependent pathway. Biomed Pharmacother 112:108588

Hung MW, Wu CW, Kokubu D et al (2019) ε-Viniferin is more effective than resveratrol in promoting adipocyte differentiation with enhanced adiponectin expression and decreased lipid accumulation. Food Sci Technol Res 25:817–826

Hwang YP, Choi JH, Han EH et al (2011) Purple sweet potato anthocyanins attenuate hepatic lipid accumulation through activating adenosine monophosphate-activated protein kinase in human HepG2 cells and obese mice. Nutr Res 31:896–906

Ikarashi N, Takeda R, Ito K et al (2011a) The inhibition of lipase and glucosidase activities by acacia polyphenol. Evid Based Complement Altern Med 2011:272075

Ikarashi N, Toda T, Okaniwa T et al (2011b) Anti-obesity and anti-diabetic effects of acacia polyphenol in obese diabetic KK-Ay mice fed high-fat diet. Evid Based Complement Altern Med 2011:952031

Imaizumi K, Sato S, Kumazawa M et al (2011) Capsaicinoids-induced changes of plasma glucose, free fatty acid and glycerol concentrations in rats. J Toxicol Sci 36:109–116

Islam A, Islam MS, Rahman MK et al (2020) The pharmacological and biological roles of eriodictyol. Arch Pharm Res 43:582–592

Iwata A, Matsubara S, Miyazaki K (2018) Beneficial effects of a β-cryptoxanthin-containing beverage on body mass index and visceral fat in pre-obese men: double-blind, placebo-controlled parallel trials. J Funct Foods 41:250–257

Jain PG, Nayse PG, Patil DJ et al (2020) The possible antioxidant capabilities of formononetin in guarding against streptozotocin-induced diabetic nephropathy in rats. Future J Pharm Sci 6:53

Jang JH, Park JE, Han JS (2020) Scopoletin increases glucose uptake through activation of PI3K and AMPK signaling pathway and improves insulin sensitivity in 3T3-L1 cells. Nutr Res 74:52–61

Jayachandran M, Chandrasekaran B, Namasivayam N (2015) Effect of geraniol, a plant derived monoterpene on lipids and lipid metabolizing enzymes in experimental hyperlipidemic hamsters. Mol Cell Biochem 398:39–53

Jeon SM, Park YB, Choi MS (2004) Antihypercholesterolemic property of naringin alters plasma and tissue lipids, cholesterol-regulating enzymes, fecal sterol and tissue morphology in rabbits. Clin Nutr 23:1025–1034

Jeong SO, Son Y, Lee JH et al (2015) Resveratrol analog piceatannol restores the palmitic acid-induced impairment of insulin signaling and production of endothelial nitric oxide via activation of anti-inflammatory and antioxidative heme oxygenase-1 in human endothelial cells. Mol Med Rep 12:937–944

Jeppesen PB, Gregersen S, Rolfsen SED et al (2003) Antihyperglycemic and blood pressure-reducing effects of stevioside in the diabetic Goto-Kakizaki rat. Metabolism 52:372–378

Ji X, Li C, Qu Y et al (2016) Andrographolide ameliorates diabetic nephropathy by attenuating hyperglycemia-mediated renal oxidative stress and inflammation via Akt/NF-κB pathway. Mol Cell Endocrinol 437:268–279

Jia X, Yang J, Wang Z et al (2014) Polysaccharides from *Laminaria japonica* show hypoglycemic and hypolipidemic activities in mice with experimentally induced diabetes. Exp Biol Med 239:1663–1670

Jia L, Li W, Li J et al (2016) *Lycium barbarum* polysaccharide attenuates high-fat diet-induced hepatic steatosis by up-regulating SIRT1 expression and deacetylase activity. Sci Rep 6:36209

Jiang Q, Wang D, Han Y et al (2015) Modulation of oxidized-LDL-receptor-1 (LOX-1) contributes to the antiatherosclerosis effect of oleanolic acid. Int J Biochem Cell Biol 69:142–152
Jiang T, Shuai X, Li J et al (2020) Protein-bound anthocyanin compounds of purple sweet potato ameliorate hyperglycemia by regulating hepatic glucose metabolism in high-fat-diet/streptozotocin-induced diabetic mice. J Agric Food Chem 68:1596–1608
Jiao Y, Wang X, Jiang X et al (2017) Antidiabetic effects of *Morus alba* fruit polysaccharides on high-fat diet- and streptozotocin-induced type 2 diabetes in rats. J Ethnopharmacol 199:119–127
Jin L, Xue HY, Jin LJ et al (2008) Antioxidant and pancreas-protective effect of aucubin on rats with streptozotocin-induced diabetes. Eur J Pharmacol 582:162–167
Jing L, Zhang Y, Fan S et al (2013) Preventing and ameliorating effects of citrus D-limonene on dyslipidemia and hyperglycemia in mice with high-fat-diet-induced obesity. Eur J Pharmacol 715:46–55
Ju L, Wen X, Wang C et al (2017) Salidroside, a natural antioxidant, improves β-cell survival and function via activating AMPK pathway. Front Pharmacol 8:749
Jung UJ, Lee MK, Jeong KS et al (2004) The hypoglycemic effect of hesperidin and naringin are partly mediated by hepatic glucose-regulating enzymes in C57BL/ksJ-db/db mice. J Nutr 134: 2499–2503
Jung UJ, Lee MK, Park YB et al (2006a) Effects of citrus flavonoids on lipid metabolism and glucose-regulating enzyme mRNA levels in type 2 diabetic mice. Int J Biochem Cell Biol 38: 1134–1145
Jung UJ, Lee MK, Park YB et al (2006b) Antihyperglycemic and antioxidant properties of caffeic acid in db/db mice. J Pharmacol Exp Ther 318:476–483
Jung SA, Choi M, Kim S et al (2012) Cinchonine prevents high-fat-diet-induced obesity through downregulation of adipogenesis and adipose inflammation. PPAR Res 2012:541204
Jung UJ, Cho YY, Choi MS (2016) Apigenin ameliorates dyslipidemia, hepatic steatosis and insulin resistance by modulating metabolic and transcriptional profiles in the liver of high-fat diet-induced obese mice. Nutrients 8:305
Jung E, Park SB, Jung WK et al (2019) Antiglycation activity of aucubin in vitro and in exogenous methylglyoxal injected rats. Molecules 24:3653
Kadakol A, Malek V, Goru SK et al (2015) Esculetin reverses histone 2A/2B ubiquitination, H3 dimethylation, acetylation and phosphorylation in preventing type 2 diabetic cardiomyopathy. J Funct Foods 17:127–136
Kadakol A, Malek V, Goru SK et al (2017) Esculetin ameliorates insulin resistance and type 2 diabetic nephropathy through reversal of histone H3 acetylation and H2A lysine119 monoubiquitination. J Funct Foods 35:256–266
Kamikubo R, Kai K, Tsuji-Naito K et al (2016) β-Caryophyllene attenuates palmitate-induced lipid accumulation through AMPK signaling by activating CB2 receptor in human HepG2 hepatocytes. Mol Nutr Food Res 60:2228–2242
Kanagasabapathy G, Malek SNA, Mahmood AA et al (2013) Beta-glucan-rich extract from *Pleurotus sajor-caju* (Fr) Singer prevents obesity and oxidative stress in C57BL/6J mice fed on a high-fat diet. Evid Based Complement Alternat Med 2013:185259
Kang JH, Kim CS, Han IS et al (2007) Capsaicin, a spicy component of hot peppers, modulates adipokine gene expression and protein release from obese mouse adipose tissues and isolated adipocytes, and suppresses the inflammatory responses of adopose tissue macrophages. FEBS Lett 581:4389–4396
Kang JH, Goto T, Han IS et al (2010) Dietary capsaicin reduces obesity-induced insulin resistance and hepatic steatosis in obese mice fed a high-fat diet. Obesity 18:780–787
Kang JH, Tsuyoshi G, Ngoc HL et al (2011a) Dietary capsaicin attenuates metabolic dysregulation in genetically obese diabetic mice. J Med Food 14:310–315
Kang SI, Ko HC, Shin HS et al (2011b) Fucoxanthin exerts differing effects on 3T3-L1 cells according to differentiation stage and inhibits glucose uptake in mature adipocytes. Biochem Biophys Res Commun 409:769–777

Kang SI, Shin HS, Kim HM et al (2012) *Petalonia binghamiae* extract and its constituent fucoxanthin ameliorate high-fat diet-induced obesity by activating AMP-activated protein kinase. J Agric Food Chem 60:3389–3395

Kang KS, Lee W, Jung Y et al (2014) Protective effect of esculin on streptozotocin-induced diabetic renal damage in mice. J Agric Food Chem 62:2069–2076

Kang C, Wang B, Kaliannan K et al (2017) Gut microbiota mediates the protective effects of dietary capsaicin against chronic low-grade inflammation and associated obesity induced by high-fat diet. mBio 8:e00470-17

Kang JW, Park J, Kim HL et al (2018a) Secoisolariciresinol diglucoside inhibits adipogenesis through the AMPK pathway. Eur J Pharmacol 820:235–244

Kang MJ, Kwon EB, Ryu HW et al (2018b) Polyacetylene from *Dendropanax morbifera* alleviates diet-induced obesity and hepatic steatosis by activating AMPK signaling pathway. Front Pharmacol 9:537

Kaufman PB, Duke JA, Brielmann H et al (1997) A comparative survey of leguminous plants as sources of the isoflavones, genistein and daidzein: implications for human nutrition and health. J Altern Complement Med 3:7–12

Kawabata K, Yoshioka Y, Terao J (2019) Role of intestinal microbiota in the bioavailability and physiological functions of dietary polyphenols. Molecules 24:370

Khanbabaee K, Ree TV (2001) Tannins: classification and definition. Nat Prod Rep 18:641–649

Kim YJ, Jung UJ (2019) Honokiol improves insulin resistance, hepatic steatosis, and inflammation in type 2 diabetic db/db mice. Int J Mol Sci 20:2303

Kim EJ, Jung SN, Son KH et al (2007) Antidiabetes and antiobesity effect of cryptotanshinone via activation of AMP-activated protein kinase. Mol Pharmacol 72:62–72

Kim SJ, Lee SJ, Lee S et al (2009) Rutecarpine ameliorates body weight gain through the inhibition of orexigenic neuropeptides NPY and AgRP in mice. Biochem Biophys Res Commun 389:437–442

Kim KY, Nguyen TH, Kurihara H et al (2010) α-Glucosidase inhibitory activity of bromophenol purified from the red alga *Polyopes lancifolia*. J Food Sci 75:H145–H150

Kim JH, Kang MJ, Choi HN et al (2011) Quercetin attenuates fasting and postprandial hyperglycemia in animal models of diabetes mellitus. Nutr Res Pract 5:107–111

Kim HY, Park M, Kim K et al (2012a) Hesperetin stimulates cholecystokinin secretion in enteroendocrine STC-1 cells. Biomed Ther (Seoul) 21:121–125

Kim MS, Hur HJ, Kwon DY et al (2012b) Tangeretin stimulates glucose uptake via regulation of AMPK signaling pathways in C2C12 myotubes and improves glucose tolerance in high-fat diet-induced obese mice. Mol Cell Endocrinol 358:127–134

Kim MA, Kang K, Lee HJ et al (2014) Apigenin isolated from *Daphne genkwa* Siebold et Zucc. inhibits 3T3-L1 preadipocyte differentiation through a modulation of mitotic clonal expansion. Life Sci 101:64–72

Kim KS, Yang HJ, Lee IS et al (2015) The aglycone of ginsenoside Rg3 enables glucagon-like peptide-1 secretion in enteroendocrine cells and alleviates hyperglycemia in type 2 diabetic mice. Sci Rep 5:18325

Kim MJ, Koo YD, Kim M et al (2016) Rg3 improves mitochondrial function and the expression of key genes involved in mitochondrial biogenesis in C2C12 myotubes. Diabetes Metab J 40:406–413

Kim HL, Jung Y, Park J et al (2017a) Farnesol has an anti-obesity effect in high-fat diet-induced obese mice and induces the development of beige adipocytes in human adipose tissue derived-mesenchymal stem cells. Front Pharmacol 8:654

Kim J, Yun EY, Quan FS et al (2017b) Central administration of 1-deoxynojirimycin attenuates hypothalamic endoplasmic reticulum stress and regulates food intake and body weight in mice with high-fat diet-induced obesity. Evid Based Complement Altern Med 2017:3607089

Kim HM, Kim Y, Lee ES et al (2018a) Caffeic acid ameliorates hepatic steatosis and reduces ER stress in high fat diet-induced obese mice by regulating autophagy. Nutrition 55-56:63–70

Kim JS, Lee H, Jung CH et al (2018b) Chicoric acid mitigates impaired insulin sensitivity by improving mitochondrial function. Biosci Biotechnol Biochem 82:1197–1206
Kim KD, Jung HY, Ryu HG et al (2019) Betulinic acid inhibits high-fat diet-induced obesity and improves energy balance by activating AMPK. Nutr Metab Cardiovasc Dis 29:409–420
Klein G, Kim J, Himmeldirk K et al (2007) Antidiabetes and anti-obesity activity of *Lagerstroemia speciosa*. eCAM 4:401–407
Kong WJ, Zhang H, Song DQ et al (2009) Berberine reduces insulin resistance through protein kinase C-dependent up-regulation of insulin receptor expression. Metabolism 58:109–119
Kong X, Wang GD, Ma MZ et al (2015) Sesamin ameliorates advanced glycation endproducts-induced pancreatic β-cell dysfunction and apoptosis. Nutrients 7:4689–4704
Krishnamoorthy RM, Venkatraman AC (2017) Polyphenols activate energy sensing network in insulin resistant models. Chem Biol Interact 275:95–107
Kumar S, Ds G, Shin HS et al (2017) *Dioscorea* spp. (a wild edible tuber): a study of its ethnopharmacological potential and traditional use by the people of similipal biosphere reserve, India. Front Pharmacol 2017:00052
Kunkel SD, Elmore CJ, Bongers KS et al (2012) Ursolic acid increases skeletal muscle and brown fat and decreases diet-induced obesity, glucose intolerance and fatty liver disease. PLoS One 7: e39332
Kuo YH, Lin CH, Shih CC (2016a) Dehydroeburicoic acid from *Antrodia camphorata* prevents the diabetic and dyslipidemic state via modulation of glucose transporter 4, peroxisome proliferator-activated receptor α expression and AMP-activated protein kinase phosphorylation in high-fat-fed mice. Int J Mol Sci 17:872
Kuo YH, Lin CH, Shih CC et al (2016b) Antcin K, a triterpenoid compound from *Antrodia camphorata*, displays antidiabetic and antihyperlipidemic effects via glucose transporter 4 and AMP-activated protein kinase phosphorylation in muscles. Evid Based Complement Altern Med 2016:4867092
Kuroda M, Iwabuchi K, Mimaki Y (2012) Chemical constituents of *Scutellaria lateriflora* and their alpha-glucosidase inhibitory activities. Nat Prod Commun 7:471–474
Kwon EY, Choi MS (2019) Dietary eriodictyol alleviates adiposity, hepatic steatosis, insulin resistance, and inflammation in diet-induced obese mice. Int j Mol Sci 20:1227
Kwon JY, Seo SG, Heo YS et al (2012) Piceatannol, a natural polyphenolic stilbene, inhibits adipogenesis via modulation of mitotic clonal expansion and insulin receptor-dependent insulin signaling in early phase of differentiation. J Biol Chem 287:11566–11578
Lafiandra D, Riccardi G, Shewry PR (2014) Improving cereal grain carbohydrates for diet and health. J Cereal Sci 59:312–326
Lagouge M, Argmann C, Gerhart-Hines Z et al (2006) Resveratrol improves mitochondrial function and protects against metabolic disease by activating SIRT1 and PGC-1alpha. Cell 127:1109–1122
Lao CD, Ruffin MT IV, Normolle D et al (2006) Dose escalation of a curcuminoid formulation. BMC Complement Altern Med 6:10
Lee YS, Kim WS, Kim KH et al (2006) Berberine, a natural plant product, activates AMP-activated protein kinase with beneficial metabolic effects in diabetic and insulin-resistant states. Diabetes 55:2256–2264
Lee WH, Lin RJ, Lin SY et al (2011) Osthole enhances glucose uptake through activation of AMP-activated protein kinase in skeletal muscle cells. J Agric Food Chem 59:12874–12881
Lee B, Kwon M, Choi JS et al (2015) Kaempferol isolated from *Nelumbo nucifera* inhibits lipid accumulation and increases fatty acid oxidation signaling in adipocytes. J Med Food 18:1363–1370
Lee JB, Yoon SJ, Lee SH et al (2017) Ginsenoside Rg3 ameliorated HFD-induced hepatic steatosis through downregulation of STAT5-PPARγ. J Endocrinol 235:223–235
Lee H, Li H, Kweon M et al (2018a) Isobavachalcone from *Angelica keiskei* inhibits adipogenesis and prevents lipid accumulation. Int J Mol Sci 19:1693

Lee S, Keirsey KI, Kirkland R et al (2018b) Blueberry supplementation influences the gut microbiota, inflammation, and insulin resistance in high-fat-diet-fed rats. J Nutr 148:209–219

Lee CG, Rhee DK, Kim BO et al (2019) Allicin induces beige-like adipocytes *via* KLF-15 signal cascade. J Nutr Biochem 64:13–24

Li Y, Kim J, Li J et al (2005) Natural antidiabetic compound 1,2,3,4,6-penta-*O*-galloyl-D-glucopyranoside binds to insulin receptor and activates insulin-mediated glucose transport signaling pathway. Biochem Biophys Res Commun 336:430–437

Li HL, Huang Y, Zhang CN et al (2006a) Epigallocatechin-3-gallate inhibits cardiac hypertrophy through blocking reactive oxidative species-dependent and -independent signal pathways. Free Radic Biol Med 40:1756–1775

Li W, Cui SW, Kakuda Y (2006b) Extraction, fractionation, structural and physical characterization of wheat β-D-glucans. Carbohydr Polym 63:408–416

Li X, Xiao Y, Gao H et al (2009) Grape seed proanthocyanidins ameliorate diabetic nephropathy via modulation of levels of AGE, RAGE and CTGF. Nephron Exp Nephrol 111:e31

Li Y, Kang Z, Li S et al (2010) Ursolic acid stimulates lipolysis in primary-cultured rat adipocytes. Mol Nutr Food Res 54:1609–1617

Li Y, Tran VH, Koolaji N et al (2013a) (S)-[6]-Gingerol enhances glucose uptake in L6 myotubes by activation of AMPK in response to $[Ca^{2+}]i$. J Pharm Pharm Sci 16:304–312

Li YG, Ji DF, Zhong S et al (2013b) 1-Deoxynojirimycin inhibits glucose absorption and accelerates glucose metabolism in streptozotocin-induced diabetic mice. Sci Rep 3:1377

Li M, Han Z, Bei W et al (2015) Oleanolic acid attenuates insulin resistance via NF-κB to regulate the IRS1-GLUT4 pathway in HepG2 cells. Evid Based Complement Altern Med 2015:643102

Li J, Ding L, Song B et al (2016a) Emodin improves lipid and glucose metabolism in high fat diet-induced obese mice through regulating SREBP pathway. Eur J Pharmacol 770:99–109

Li Y, Goto T, Yamakuni K et al (2016b) 4-Hydroxyderricin, as a PPARγ agonist, promotes adipogenesis, adiponectin secretion, and glucose uptake in 3T3-L1 cells. Lipids 51:787–795

Li X, Gao Z, Gao H et al (2017) Nephrin loss is reduced by grape seed proanthocyanidins in the experimental diabetic nephropathy rat model. Mol Med Rep 16:9393–9400

Li J, Liu M, Yu H et al (2018a) Mangiferin improves hepatic lipid metabolism mainly through its metabolite-norathyriol by modulating SIRT1/AMPK/SREBP-1c signaling. Front Pharmacol 9:201

Li JB, Zhang R, Han X et al (2018b) Ginsenoside Rg1 inhibits dietary-induced obesity and improves obesity-related glucose metabolic disorders. Braz J Med Biol Res 51:e7139

Li YC, Qiao JY, Wang BY et al (2018c) Paeoniflorin ameliorates fructose-induced insulin resistance and hepatic steatosis by activating LKB1/AMPK and AKT pathways. Nutrients 10:1024

Li AN, Chen JJ, Li QQ et al (2019a) Alpha glucosidase inhibitor 1-deoxynojirimycin promotes beige remodeling of 3T3-L1 preadipocytes via activating AMPK. Biochem Biophys Res Commun 509:1001–1007

Li Y, Li Q, Wang C et al (2019b) Trigonelline reduced diabetic nephropathy and insulin resistance in type 2 diabetic rats through peroxisome proliferator-activated receptor-γ. Exp Ther Med 18:1331–1337

Li Y, Mai Y, Qiu X et al (2020) Effect of long-term treatment of carvacrol on glucose metabolism in streptozotocin-induced diabetic mice. BMC Complement Med Ther 20:142

Liao CC, Ou TT, Wu CH et al (2013) Prevention of diet-induced hyperlipidemia and obesity by caffeic acid in C57BL/6 mice through regulation of hepatic lipogenesis gene expression. J Agric Food Chem 61:11082–11088

Liao X, Yang L, Chen M et al (2015) The hypoglycemic effect of a polysaccharide (GLP) from *Gracilaria lemaneiformis* and its degradation products in diabetic mice. Food Funct 6:2542–2549

Liao HH, Zhu JX, Feng H et al (2017) Myricetin possesses potential effects on diabetic cardiomyopathy through inhibiting IκBα/NF-κB and enhancing Nrf2/HO-1. Oxid Med Cell Longev 2017:8370593

Lim J, Liu Z, Apontes P et al (2014) Dual mode of action of mangiferin in mouse liver under high fat diet. PLoS One 9:e90137

Lin CH, Kuo YH, Shih CC (2017) Eburicoic acid, a triterpene compound from *Antrodia camphorata*, displays antidiabetic and antihyperlipidemic effects in palmitate treated C2C12 myotubes and in high-fat diet-fed mice. Int J Mol Sci 18:2314

Lin CH, Kuo YH, Shih CC (2018) Antidiabetic and hypolipidemic activities of eburicoic acid, a triterpenoid compound from *Antrodia camphorata*, by regulation of Akt phosphorylation, gluconeogenesis and PPARα in streptozotocin-induced diabetic mice. RSC Adv 8:20462–20476

Liou CJ, Dai YW, Wang CL et al (2019) Maslinic acid protects against obesity-induced non-alcoholic fatty liver disease in mice through regulation of the Sirt1/AMPK signaling pathway. FASEB J 33:11791–11803

Liu D, Zhen W, Yang Z et al (2006) Genistein acutely stimulates insulin secretion in pancreatic β-cells through a cAMP-dependent protein kinase pathway. Diabetes 55:1043–1050

Liu J, Sun H, Duan W et al (2007) Maslinic acid reduces blood glucose in KK-Ay mice. Biol Pharm Bull 30:2075–2078

Liu Y, Qi H, Wang Y et al (2012) Allicin protects against myocardial apoptosis and fibrosis in streptozotocin-induced diabetic rats. Phytomedicine 19:693–698

Liu J, Chen Z, Zhang Y et al (2013a) Rhein protects pancreatic β-cells from dynamin-related protein 1-mediated mitochondrial fission and cell apoptosis under hyperglycemia. Diabetes 62:3927–3935

Liu Y, Wan L, Xiao Z et al (2013b) Antidiabetic activity of polysaccharides from tuberous root of *Liriope spicata* var. *prolifera* in KK-Ay mice. Evid Based Complement Alternat Med 2013:349790

Liu YW, Zhu X, Zhang L et al (2013c) Upregulation of glyoxalase 1 by mangiferin prevents diabetic nephropathy progression in streptozotocin-induced diabetic rats. Eur J Pharmacol 721:355–364

Liu J, Wang X, Chen YP et al (2014) Maslinic acid modulates glycogen metabolism by enhancing the insulin signaling pathway and inhibiting glycogen phosphorylase. Chin J Nat Med 12:259–265

Liu J, Lee J, Hernandez MAS et al (2015a) Treatment of obesity with celastrol. Cell 161:999–1011

Liu M, Xu L, Yin L et al (2015b) Potent effects of dioscin against obesity in mice. Sci Rep 5:7973

Liu Q, Li X, Li C et al (2015c) 1-Deoxynojirimycin alleviates insulin resistance via activation of insulin signaling PI3K/Akt pathway in skeletal muscle of db/db mice. Molecules 20:21700–21714

Liu ZW, Wang JK, Qiu C et al (2015d) Matrine pretreatment improves cardiac function in rats with diabetic cardiomyopathy via suppressing ROS/TLR-4 signaling pathway. Acta Pharmacol Sin 36:323–333

Liu JY, Zheng CZ, Hao XP et al (2016a) Catalpol ameliorates diabetic atherosclerosis in diabetic rabbits. Am J Transl Res 8:4278–4288

Liu Q, Li X, Li C et al (2016b) 1-Deoxynojirimycin alleviates liver injury and improves hepatic glucose metabolism in db/db mice. Molecules 21:279

Liu H, Zhong H, Yin Y et al (2017a) Genistein has beneficial effects on hepatic steatosis in high fat-high sucrose diet-treated rats. Biomed Pharmacother 91:964–969

Liu W, Zhao S, Wang J et al (2017b) Grape seed proanthocyanidin extract ameliorates inflammation and adiposity by modulating gut microbiota in high-fat diet mice. Mol Nutr Food Res 61:1601082

Liu WY, Liou SS, Hong TY et al (2017c) Protective effects of hesperidin (citrus flavanone) on high glucose induced oxidative stress and apoptosis in a cellular model for diabetic retinopathy. Nutrients 9:1312

Liu G, Liang L, Yu G et al (2018a) Pumpkin polysaccharide modifies the gut microbiota during alleviation of type 2 diabetes in rats. Int J Biol Macromol 115:711–717

Liu H, Wang J, Liu M et al (2018b) Antiobesity effects of ginsenoside Rg1 on 3T3-L1 preadipocytes and high fat diet-induced obese mice mediated by AMPK. Nutrients 10:830
Liu L, Du X, Zhang Z et al (2018c) Trigonelline inhibits caspase 3 to protect β-cells apoptosis in streptozotocin-induced type 1 diabetic mice. Eur J Pharmacol 836:115–121
Liu Z, Han Y, Zhao F et al (2018d) Nobiletin suppresses high-glucose-induced inflammation and ECM accumulation in human mesangial cells through STAT3/NF-κB pathway. J Cell Biochem 2018:1–7
Liu R, Zhang Y, Yao X et al (2020) ε-Viniferin, a promising natural oligostilbene, ameliorates hyperglycemia and hyperlipidemia by activating AMPK *in vivo*. Food Funct 11:10084–10093
Liu Y, Fu X, Chen Z et al (2021) The protective effects of sulforaphane on high-fat diet-induced obesity in mice through browning of white fat. Front Pharmacol 12:665894
Lopez-Lazaro M (2009) Distribution and biological activities of the flavonoid luteolin. Mini Rev Med Chem 9:31–59
Lorenz M, Wessler S, Follmann E et al (2004) A constituent of green tea, epigallocatechin-3-gallate, activates endothelial nitric oxide synthase by a phosphatidylinositol-3-OH-kinase-, cAMP-dependent protein kinase-, and Akt-dependent pathway and leads to endothelial-dependent vasorelaxation. J Biol Chem 279:6190–6195
Lu C, Zhang F, Xu W et al (2015) Curcumin attenuates ethanol-induced hepatic steatosis through modulating Nrf2/FXR signaling in hepatocytes. IUBMB Life 67:645–658
Lu YL, Lin SY, Fang SU et al (2017) Hot-water extracts from roots of *Vitis thunbergii* var. *taiwaniana* and identified ε-viniferin improve obesity in high-fat diet-induced mice. J Agric Food Chem 65:2521–2529
Luo C, Yang H, Tang C et al (2015) Kaempferol alleviates insulin resistance via hepatic IKK/NF-κB signal in type 2 diabetic rats. Int Immunopharmacol 28:744–750
Luo H, Liu J, Ouyang Q et al (2017) The effects of oleanolic acid on atherosclerosis in different animal models. Acta Biochim Biophys Sin 49:349–354
Ma X, Xu L, Alberobello AT et al (2015) Celastrol protects against obesity and metabolic dysfunction through activation of a HSF1-PGC1α transcriptional axis. Cell Metab 22:695–708
Ma B, Zhu Z, Zhang J et al (2020) Aucubin alleviates diabetic nephropathy by inhibiting NF-κB activation and inducing SIRT1/SIRT3-FoxO3a signaling pathway in high-fat diet/streptozotocin-induced diabetic mice. J Funct Foods 64:103702
Man AWC, Xia N, Li H (2020) Circadian rhythm in adipose tissue: novel antioxidant target for metabolic and cardiovascular diseases. Antioxidants 9:968
Maneesai P, Bunbupha S, Kukongviriyapan U et al (2016) Asiatic acid attenuates renin-angiotensin system activation and improves vascular function in high-carbohydrate, high-fat diet fed rats. BMC Complement Altern Med 16:123
Masumoto S, Terao A, Yamamoto Y et al (2016) Non-absorbable apple polycyanidins prevent obesity associated with gut microbial and metabolomic changes. Sci Rep 6:31208
Matsukawa T, Inaguma T, Han J et al (2015) Cyanidin-3-glucoside derived from black soybeans ameliorate type 2 diabetes through induction of differentiation of preadipocytes into smaller and insulin-sensitive adipocytes. J Nutr Biochem 26:860–867
Matsukawa T, Villareal MO, Motojima H et al (2017) Increasing cAMP levels of preadipocytes by cyanidin-3-glucoside treatment induces the formation of beige phenotypes in 3T3-L1 adipocytes. J Nutr Biochem 40:77–85
Matsuo Y, Kusano R, Ogawa S et al (2016) Characterization of the α-amylase inhibitory activity of oligomeric proanthocyanidins from *Acacia mearnsii* bark extract. Nat Prod Commun 11:1851–1854
Mazimba O (2017) Umbelliferone: sources, chemistry and bioactivities review. Bull Fac Pharm, Cairo Univ 55:223–232
Mein JR, Dolnikowski GG,Ernst H et al (2011) Enzymatic formation of apo-carotenoids from xanthophylls carotenoids lutein, zeaxanthin and β-cryptoxanthin by ferret carotene-9′-10-′-monooxygenase. Arch Biochem Biophys 506:109–121

Min W, Wu M, Fang P et al (2018) Effect of baicalein on GLUT4 translocation in adipocytes of diet-induced obese mice. Cell Physiol Biochem 50:426–436
Minakawa M, Miura Y, Yagasaki K (2012) Piceatannol, a resveratrol derivative, promotes glucose uptake through glucose transporter 4 translocation to plasma membrane in L6 myotubes and suppresses blood glucose levels in type 2 diabetic model db/db mice. Biochem Biophys Res Commun 422:469–475
Mnafgui K, Kaanich F, Derbali A et al (2013) Inhibition of key enzymes related to diabetes and hypertension by eugenol in vitro and in alloxan-induced diabetic rats. Arch Physiol Biochem 119:225–233
Mo FF, Liu HX, Zhang Y et al (2019) Anti-diabetic effect of loganin by inhibiting FOXO1 nuclear translocation via PI3K/Akt signaling pathway in INS-1 cell. Iran J Basic Med Sci 22:262–266
Monagas M, Quintanilla-Lopez JE, Gomez-Cordoves C et al (2010) MALDI-TOF MS analysis of plant proanthocyanidins. J Pharm Biomed Anal 51:358–372
Moree SS, Kavishankar GB, Rajesha J (2013) Antidiabetic effect of secoisolariciresinol diglucoside in streptozotocin-induced diabetic rats. Phytomedicine 20:237–245
Morrow NM, Burke AC, Samsoondar JP et al (2020) The citrus flavonoid nobiletin confers protection from metabolic dysregulation in high-fat-fed mice independent of AMPK. J Lipid Res 61:387–402
Mosqueda-Solis A, Sanchez J, Reynes B et al (2018) Hesperidin and capsaicin, but not the combination, prevent hepatic steatosis and other metabolic syndrome-related alternations in Western diet-fed rats. Sci Rep 8:15100
Mouly P, Gaydou EM, Auffray A (1998) Simultaneous separation of flavanone glycosides and polymethoxylated flavones in citrus juices using liquid chromatography. J Chromatogr A 800: 171–179
Mulvihill EE, Assini JM, Lee JK et al (2011) Nobiletin attenuates VLDL overproduction, dyslipidemia, and atherosclerosis in mice with diet-induced insulin resistance. Diabetes 60: 1446–1457
Murali R, Srinivasan S, Ashokkumar N (2013) Antihyperglycemic effect of fraxetin on hepatic key enzymes of carbohydrate metabolism in streptozotocin-induced diabetic rats. Biochimie 95: 1848–1854
Murari R, Saravanan R (2012) Antidiabetic effect of D-limonene, a monoterpene in streptozotocin-induced diabetic rats. Biomed Prev Nutr 2:269–275
Muruganandan S, Srinivasan K, Gupta S et al (2005) Effect of mangiferin on hyperglycemia and atherogenicity in streptozotocin diabetic rats. J Ethnopharmacol 97:497–501
Na B, Nguyen PH, Zhao BT et al (2015) Protein tyrosine phosphatase 1B (PTP1B) inhibitory activity and glucosidase inhibitory activity of compounds isolated from *Agrimonia pilosa*. Pharm Biol 54:474–480
Nagata N, Xu L, Kohno S et al (2017) Glucoraphanin ameliorates obesity and insulin resistance through adipose tissue browning and reduction of metabolic endotoxemia in mice. Diabetes 66: 1222–1236
Nakai M, Fukui Y, Asami S et al (2005) Inhibitory effects of oolong tea polyphenols on pancreatic lipase in vitro. J Agric Food Chem 53:4593–4598
Nakajima A, Ohizumi Y (2019) Potential benefits of nobiletin, a citrus flavonoid, against Alzheimer's disease and Parkinson's disease. Int J Mol Sci 20:3380
Nakajima K, Maeda N, Oiso S et al (2019) Decreased plasma octanoylated ghrelin levels in mice by oleanolic acid. J Oleo Sci 68:103–109
Nam D, Guo B, Chatterjee S et al (2015) The adipocyte clock controls brown adipogenesis through the TGF-β and BMP signaling pathways. J Cell Sci 128:1835–1847
Naowaboot J, Somparn N, Saenthaweesuk S et al (2015) Umbelliferone improves an impaired glucose and lipid metabolism in high-fat diet/streptozotocin-induced type 2 diabetic rats. Phytother Res 29:1388–1395
Naowaboot J, Piyabhan P, Munkong N et al (2016) Ferulic acid improves lipid and glucose homeostasis in high-fat diet-induced obese mice. Clin Exp Pharmacol Physiol 43:242–250

Naowaboot J, Somparn N, Saenthaweesuk S (2020) Renoprotective effect of umbelliferone in high-fat diet/streptozotocin-induced type 2 diabetic rats. Asian Pac J Trop Med 10:11–17
Narasimhan A, Chinnaiyan M, Kurundevi B (2015) Ferulic acid exerts its antidiabetic effect by modulating insulin-signaling molecules in the liver of high-fat diet and fructose-induced type 2 diabetic adult male rats. Appl Physiol Nutr Metab 40:769–781
Ni Y, Nagashimada M, Zhuge F et al (2015) Astaxanthin prevents and reverses diet-induced insulin resistance and steatohepatitis in mice: a comparison with vitamin E. Sci Rep 5:17192
Nie XQ, Chen HH, Zhang JY et al (2016) Rutaecarpine ameliorates hyperlipidemia and hyperglycemia in fat-fed, streptozotocin-treated rats via regulating the IRS-1/PI3K/Akt and AMPK/ACC2 signaling pathways. Acta Pharmacol Sin 37:483–496
Nie J, Chang Y, Li Y et al (2017a) Caffeic acid phenethyl ester (Propolis extract) ameliorates insulin resistance by inhibiting JNK and NF-κB inflammatory pathways in diabetic mice and HepG2 cell models. J Agric Food Chem 65:9041–9053
Nie Y, Luo F, Wang L et al (2017b) Anti-hyperlipidemic effect of rice bran polysaccharide and its potential mechanism in high-fat diet mice. Food Funct 8:4028–4041
Ninomiya K, Matsuda H, Shimoda H et al (2004) Carnosic acid, a new class of lipid absorption inhibitor from sage. Bioorg Med Chem Lett 14:1943–1946
Niu Y, Li S, Na L et al (2012) Mangiferin decreases plasma free fatty acids through promoting its catabolism in liver by activation of AMPK. PLoS One 7:e30782
Nizamutdinova IT, Jin YC, Chung JI et al (2009) The anti-diabetic effect of anthocyanins in streptozotocin-induced diabetic rats through glucose transporter 4 regulation and prevention of insulin resistance and pancreatic apoptosis. Mol Nutr Food Res 53:1419–1429
Nogara L, Naber N, Pate E et al (2016) Piperine's mitigation of obesity and diabetes can be explained by its up-regulation of the metabolic rate of resting muscle. Proc Natl Acad Sci USA 113:13009–13014
Oberg AI, Yassin K, Csikasz RI et al (2011) Shikonin increases glucose uptake in skeletal muscle cells and improves plasma glucose levels in diabetic Goto-Kakizaki rats. PLOS One 6:e22510
Oguntibeju OO, Aboua Y, Goboza M (2019) Vindoline-a natural product from *Catharanthus roseus* reduces hyperlipidemia and renal pathophysiology in experimental type 2 diabetes. Biomedicines 7:59
Ogura K, Ogura M, Shoji T et al (2016) Oral administration of apple procyanidins ameliorates insulin resistance via suppression of pro-inflammatory cytokines expression in liver of diabetic ob/ob mice. J Agric Food Chem 64:8857–8865
Ohara K, Kusano K, Kitao S et al (2015) ε-Viniferin, a resveratrol dimer, prevents diet-induced obesity in mice. Biochem Biophys Res Commun 468:877–882
Ohta M, Fujinami A, Kobayashi N et al (2015) Two chalcones, 4-hydroxyderricin and xanthoangelol, stimulate GLUT4-dependent glucose uptake through the LKB1/AMP-activated protein kinase signaling pathway in 3T3-L1 adipocytes. Nutr Res 35:618–625
Onda K, Horike N, Suzuki TI et al (2013) Polymethoxyflavonoids tangeretin and nobiletin increase glucose uptake in murine adipocytes. Phytother Res 27:312–316
Ong KW, Hsu A, Tan BKH (2012) Chlorogenic acid stimulates glucose transport in skeletal muscle via AMPK activation: a contributor to the beneficial effects of coffee on diabetes. PLOS One 7:e32718
Ono M, Fujimori K (2011) Antiadipogenic effect of dietary apigenin through activation of AMPK in 3T3-L1 cells. J Agric Food Chem 59:13346–13352
Oza MJ, Kulkarni YA (2018a) Biochanin A improves insulin sensitivity and controls hyperglycemia in type 2 diabetes. Biomed Pharmacother 107:1119–1127
Oza MJ, Kulkarni YA (2018b) Formononetin treatment in type 2 diabetic rats reduces insulin resistance and hyperglycemia. Front Pharmacol 9:739
Oza MJ, Kulkarni YA (2019) Formononetin attenuates kidney damage in type 2 diabetic rats. Life Sci 219:109–121
Oza MJ, Kulkarni YA (2020) Formononetin alleviates diabetic cardiomyopathy by inhibiting oxidative stress and upregulating SIRT1 in rats. Asian Pac J Trop Biomed 10:254–262

Pakdeechote P, Bunbupha S, Kukongviriyapan U et al (2014) Asiatic acid alleviates hemodynamic and metabolic alternations via restoring eNOS/iNOS expression, oxidative stress, and inflammation in diet-induced metabolic syndrome rats. Nutrients 6:355–370

Pan Y, Zhao W, Zhao D et al (2018) Salvianolic acid B improves mitochondrial function in 3T3-L1 adipocytes through a pathway involving PPARγ coactivator-1α (PGC-1α). Front Pharmacol 9: 671

Park MY, Mun ST (2013) Dietary carnosic acid suppresses hepatic steatosis formation via regulation of hepatic fatty acid metabolism in high-fat diet-fed mice. Nutr Res Pract 7:294–301

Park SA, Choi MS, Cho SY et al (2006) Genistein and daidzein modulate hepatic glucose and lipid regulating enzyme activities in C57BL/KsJ-db/db mice. Life Sci 79:1207–1213

Park CH, Tanaka T, Kim JH et al (2011a) Hepatoprotective effects of loganin, iridoid glucoside from Corni Fructus, against hyperglycemia-activated signaling pathway in liver of type 2 diabetic db/db mice. Toxicology 290:14–21

Park CH, Noh JS, Kim JH et al (2011b) Evaluation of morroniside, iridoid glucoside from *Corni Fructus*, on diabetes-induced alternations such as oxidative stress, inflammation, and apoptosis in the liver of type 2 diabetic *db/db* mice. Biol Pharm Bull 34:1559–1565

Park S, Choi Y, Um SJ et al (2011c) Oleuropein attenuates hepatic steatosis induced by high-fat diet in mice. J Hepatol 54:984–993

Park J, Kim HL, Jung Y et al (2019) Bitter orange (*Citrus aurantium* Linn) improves obesity by regulating adipogenesis and thermogenesis through AMPK activation. Nutrients 11:1988

Parnas M, Peters M, Dadon D et al (2009) Carvacrol is a novel inhibitor of *Drosophila* TRPL and mammalian TRPM 7 channels. Cell Calcium 45:300–309

Pascual-Serrano A, Arola-Arnal A, Suarez-Garcia S et al (2017) Grape seed proanthocyanidin supplementation reduces adipocyte size and increases adipocyte number in obese rats. Int J Obes 41:1246–1255

Patel MI, Gupta A, Dey CS (2011) Potentiation of neuronal insulin signaling and glucose uptake by resveratrol: the involement of AMPK. Pharmacol Rep 63:1162–1168

Patel OPS, Mishra A, Maurya R et al (2016a) Naturally occurring carbazole alkaloids from *Murraya koenigii* as potential antidiabetic agents. J Nat Prod 79:1276–1284

Patel TP, Rawal K, Soni S et al (2016b) Swertiamarin ameliorates oleic acid induced lipid accumulation and oxidative stress by attenuating gluconeogenesis and lipogenesis in hepatic steatosis. Biomed Pharmacother 83:785–791

Peng L, Yang J, Ning C et al (2012) Rhein inhibits integrin-linked kinase expression and regulates matrix metalloproteinase-9/tissue inhibitor of metalloproteinase-1 ratio in high glucose-induced epithelial-mesenchymal transition of renal tubular cell. Biol Pharm Bull 35:1676–1685

Pengzhan Y, Ning L, Xiguang L et al (2003) Antihyperlipidemic effects of different molecular weight sulphated polysaccharides from *Ulva pertusa* (Chlorophyta). Pharmacol Res 48:543–549

Pinent M, Blay M, Blade MC et al (2004) Grape seed-derived procyanidins have an antihyperglycemic effect in streptozotocin-induced diabetic rats and insulinomimetic activity in insulin-sensitive cell lines. Endocrinology 145:4985–4990

Polce SA, Burke C, Franca LM et al (2018) Ellagic acid alleviates hepatic oxidative stress and insulin resistance in diabetic female rats. Nutrients 10:531

Poudel B, Lim SW, Ki HH et al (2014) Dioscin inhibits adipogenesis through the AMPK/MAPK pathway in 3T3-L1 cells and modulates fat accumulation in obese mice. Int J Mol Med 43: 1401–1408

Prabakaran D, Ashokkumar N (2013) Protective effect of esculetin on hyperglycemia-mediated oxidative damage in the hepatic and renal tissues of experimental diabetic rats. Biochimie 95: 366–373

Prabhakar PK, Doble M (2011) Interaction of phytochemicals with hypoglycemic drugs on glucose uptake in L6 myotubes. Phytomedicine 18:285–291

Prior RL, Lazarus SA, Cao G et al (2001) Identification of procyanidins and anthocyanins in blueberries and cranberries (*Vaccinium* spp) using high-performance liquid chromatography/mass spectrometry. J Agric Food Chem 49:1270–1276

Pu P, Wang XA, Salim M et al (2012a) Baicalein, a natural product, selectively activating AMPKα_2 and ameliorates metabolic disorder in diet-induced mice. Mol Cell Endocrinol 236:128–138

Pu P, Gao DM, Mohamed S et al (2012b) Naringin ameliorates metabolic syndrome by activating AMP-activated protein kinase in mice fed a high-fat diet. Arch Biochem Biophys 518:61–70

Rahman N, Jeon M, Song HY et al (2016) Cryptotanshinone, a compound of *Salvia miltiorrhiza* inhibits pre-adipocytes differentiation by regulation of adipogenesis-related genes expression via STAT3 signaling. Phytomedicine 23:58–67

Ramadori G, Gautron L, Fujikawa T et al (2009) Central administration of resveratrol improves diet-induced diabetes. Endocrinology 150:5326–5333

Ramalingam S, Karuppiah M, Thiruppathi M (2020) Antihyperglycaemic potential of rosmarinic acid attenuates glycoprotein moiety in high-fat diet and streptozotocin-induced diabetic rats. Front Life Sci 13:120–130

Ramesh B, Pugalendi KV (2006) Antihyperglycemic effect of umbelliferone in streptozotocin-diabetic rats. J Med Food 9:562–566

Rameshreddy P, Sathibabu Uddandrao VV, Brahmnaidu P et al (2018) Obesity-alleviating potential of asiatic acid and its effects on ACC1, UCP2, and CPT1 mRNA expression in high fat diet-induced obese Sprague-Dawley rats. Mol Cell Biochem 442:143–154

Rashwan AS, El-Beltagy MA, Saleh SY et al (2019) Potential role of cinnamaldehyde and costunolide to counteract metabolic syndrome induced by excessive fructose consumption. Beni-Suef Univ J Basic Appl Sci 8:17

Rebello C, Greenway FL, Lau FH et al (2019) Naringenin promotes thermogenic gene expression in human white adipose tissue. Obesity 27:103–111

Reiter CEN, Kim J, Quon MJ (2010) Green tea polyphenol epigallocatechin gallate reduces endothelin-1 expression and secretion in vascular endothelial cells: roles for AMP-activated protein kinase, Akt, and FoxO1. Endocrinology 151:103–114

Rizza S, Muniyappa R, Lantorno M et al (2011) Citrus polyphenol hesperidin stimulates production of nitric oxide in endothelial cells while improving endothelial function and reducing inflammatory markers in patients with metabolic syndrome. J Clin Endocrinol Metab 96:E782–E792

Rodriguez-Daza MC, Daoust L, Boutkrabt L et al (2020) Wild blueberry proanthocyanidins shape distinct gut microbiota profile and influence glucose homeostasis and intestinal phenotypes in high-fat high-sucrose fed mice. Sci Rep 10:2217

Rouseff R, Ting S (1979) Tangeretin content of Florida citrus peel as determined by HPLC. Proc Fla State Hort Soc 92:145–148

Ruan CT, Lam SH, Chi TC et al (2012) Borapetoside C from *Tinospora crispa* improves insulin sensitivity in diabetic mice. Phytomedicine 19:719–724

Ruan CT, Lam SH, Lee SS et al (2013) Hypoglycemic action of borapetoside A from the plant *Tinospora crispa* in mice. Phytomedicine 20:667–675

Runtuwene J, Cheng KC, Asakawa A et al (2016) Rosmarinic acid ameliorates hyperglycemia and insulin sensitivity in diabetic rats, potentially by modulating the expression of PEPCK and GLUT4. Drug Des Devel Ther 10:2193–2202

Sae-Tan S, Grove KA, Kennett MJ et al (2011) (-)-Epigallocatechin-3-gallate increases the expression of genes related to fat oxidation in the skeletal muscle of high fat-fed mice. Food Funct 2:111–116

Saito K, Davis KC, Morgan DA et al (2019) Celastrol reduces obesity in MC4R deficiency and stimulates sympathetic nerve activity affecting metabolic and cardiovascular functions. Diabetes 68:1210–1220

Salemi Z, Ghasemi H, Morovati A et al (2018) Effects of biochanin A on resistin, adiponectin and some stress oxidative markers in normal and STZ-induced diabetic rats. Arch Med Lab Sci 4:9–16

Samad MB, Mohsin MNAB, Razu BA et al (2017) [6]-Gingerol, from Zingiber officinale, potentiates GLP-1 mediated glucose-stimulated insulin secretion pathway in pancreatic β-cells and increases RAB8/RAB10-regulated membrane presentation of GLUT4 transporters in skeletal muscle to improve hyperglycemia in Lepr db/db type 2 diabetic mice. BMC Complement Altern Med 17:395

Samarghandian S, Borji A, Farkhondeh T (2017) Evaluation of antidiabetic activity of carnosol (phenolic diterpene in rosemary) in streptozotocin-induced diabetic rats. Cardiovasc Hematol Disord Drug Targets 17:11–17

Sandoval V, Femenias A, Martinez-Garza U et al (2019) Lyophilized maqui (*Aristotelia chilensis*) berry induces browning in the subcutaneous white adipose tissue and ameliorates the insulin resistance in high fat diet-induced obese mice. Antioxidants 8:360

Santini SJ, Porcu C, Tarantino G et al (2020) Oleuropein overrides liver damage in steatotic mice. J Funct Foods 65:103756

Saravanan S, Pari L (2015) Role of thymol on hyperglycemia and hyperlipidemia in high fat diet induced type 2 diabetic C57BL/6J mice. Eur J Pharmacol 761:279–287

Saravanan S, Pari L (2016) Protective effect of thymol on high fat diet-induced diabetic nephropathy in C57BL/6J mice. Chem Biol Interact 245:1–11

Saravanan G, Ponmurugan P, Deepa MA et al (2014) Anti-obesity action of gingerol: effect on lipid profile, insulin, leptin, amylase and lipase in male obese rats induced by a high-fat diet. J Sci Food Agric 94:2972–2977

Sarkar P, Nath K, Banu S (2019) Modulatory effect of baicalein on gene expression and activity of antioxidant enzymes in streptozotocin-nicotinamide induced diabetic rats. Braz J Pharm Sci 55: e18201

Sasaki R, Nishimura N, Hoshino H et al (2007) Cyanidin-3-glucoside ameliorates hyperglycemia and insulin sensitivity due to downregulation of retinol binding protein 4 expression in diabetic mice. Biochem Pharmacol 74:1619–1627

Sasikumar P, Prabha B, Reshmitha TR et al (2016) Comparison of antidiabetic potential of (+)- and (-)-hopeaphenol, a pair of enantiomers isolated from *Ampelocissus indica* (L.) and *Vateria indica* Linn., with respect to inhibition of digestive enzymes and induction of glucose uptake in L6 myotubes. RSC Adv 6:77075–77082

Sathibabu Uddandrao VV, Rameshreddy P, Brahmanaidu P et al (2020) Antiobesity efficacy of asiatic acid: down-regulation of adipogenic and inflammatory processes in high fat diet induced obese rats. Arch Physiol Biochem 126:453–462

Sattanathan K, Dhanapal CK, Umarani R et al (2011) Beneficial health effects of rutin supplementation in patients with diabetes mellitus. J Appl Pharm Sci 1:227–231

Schmieder RE, Hilgers KF, Schlaich MP et al (2007) Renin-angiotensin system and cardiovascular risk. Lancet 369:1208–1219

Schwarz EJ, Reginato MJ, Shao D et al (1997) Retinoic acid blocks adipogenesis by inhibiting C/EBPβ-mediated transcription. Mol Cell Biol 17:1552–1561

Seo MJ, Lee YJ, Hwang JH et al (2015) The inhibitory effects of quercetin on obesity and obesity-induced inflammation by regulation of MAPK signaling. J Nutr Biochem 26:1308–1316

Shah SS, Shah GB, Singh SD et al (2011) Effect of piperine in the regulation of obesity-induced dyslipidemia in high-fat diet rats. Ind J Pharmacol 43:296–299

Shan Q, Zheng Y, Lu J et al (2014) Purple sweet potato color ameliorates kidney damage via inhibiting oxidative stress mediated NLRP3 inflammasome activation in high fat diet mice. Food Chem Toxicol 69:339–346

Shao W, Yu Z, Chiang Y et al (2012) Curcumin prevents high fat diet induced insulin resistance and obesity via attenuating lipogenesis in liver and inflammatory pathway in adipocytes. PLoS One 7:e28784

Shen L, Xiong Y, Wang DQH et al (2013) Ginsenoside Rb1 reduces fatty liver by activating AMP-activated protein kinase in obese rats. J Lipid Res 54:1430–1438

Shen L, Haas M, Wang DQH et al (2015) Ginsenoside Rb1 increases insulin sensitivity by activating AMP-activated protein kinase in male rats. Physiol Rep 3:e12543

Shi L, Zhang W, Zhou YY et al (2008) Corosolic acid stimulates glucose uptake via enhancing insulin receptor phosphorylation. Eur J Pharmacol 584:21–29
Shi L, Shi L, Zhang H et al (2013) Oxymatrine ameliorates non-alcoholic fatty liver disease in rats through peroxisome proliferator-activated receptor-α activation. Mol Med Rep 8:439–445
Shi ZL, Liu YD, Yuan YY et al (2017) In vitro and in vivo effects of norathyriol and mangiferin on α-glucosidase. Biochem Res Int 2017:1206015
Shi X, Zhou X, Chu X et al (2019) Allicin improves metabolism in high-fat diet-induced obese mice by modulating the gut microbiota. Nutrients 11:2909
Shimba S, Ishii N, Ohta Y et al (2005) Brain and muscle Arnt-like protein-1 (Bmal1), a component of the molecular clock, regulates adipogenesis. PNAS 102:12071–12076
Shukla S, Gupta S (2010) Apigenin: a promising molecule for cancer prevention. Pharm Res 27: 962–978
Sim MO, Ham JR, Lee HI et al (2014) Long-term supplementation of umbelliferone and 4-methylumbelliferone alleviates high-fat diet induced hypertriglyceridemia and hyperglycemia in mice. Chem Biol Interact 216:9–16
Sim MO, Lee HI, Ham JR et al (2015) Long-term supplementation of esculetin ameliorates hepatosteatosis and insulin resistance partly by activating Adipo R2-AMPK pathway in diet-induced obese mice. J Funct Foods 15:160–171
Slavin J (2013) Fiber and prebiotics: mechanisms and health benefits. Nutrients 5:1417–1435
Son MJ, Miura Y, Yagasaki K (2015) Mechanisms for antidiabetic effect of gingerol in cultured cells and obese diabetic model mice. Cytotechnology 67:641–652
Sonawane RD, Vishwakarma SL, Lakshmi S et al (2010) Amelioration of STZ-induced type 1 diabetic nephropathy by aqueous extract of *Enicostemma littorale* Blume and swertiamarin in rats. Mol Cell Biochem 340:1–6
Song F, Xie ML, Zhu LJ et al (2006) Experimental study of osthole on treatment of hyperlipidemic and alcoholic fatty liver in animals. World J Gastroenterol 12:4359–4363
Song P, Kim JH, Ghim J et al (2013) Emodin regulates glucose utilization by activating AMP-activated protein kinase. J Biol Chem 288:5732–5742
Song HM, Li X, Liu YY et al (2018) Carnosic acid protects mice from high-fat diet-induced NAFLD by regulating MARCKS. Int J Mol Med 42:193–207
Sorrenti V, Raffaele M, Vanella L et al (2019) Protective effect of caffeic acid phenethyl ester (CAPE) and novel cape analogue as inducers of heme oxygenase-1 in streptozotocin- induced type 1 diabetic rats. Int J Mol Sci 20:2441
Srinivasan S, Sathish G, Jayanthi M et al (2014) Ameliorating effect of eugenol on hyperglycemia by attenuating the key enzymes of glucose metabolism in streptozotocin-induced diabetic rats. Mol Cell Biochem 385:159–168
Stone B, Morell MK (2009) Carbohydrates. In: Khan K, Shewry PR (eds) Wheat: chemistry and technology, 4th edn. American Association of Cereal Chemists, St Paul, MN, pp 299–362
Su HM, Feng LN, Zheng XD et al (2016a) Myricetin protects against diet-induced obesity and ameliorates oxidative stress in C57BL/6 mice. Biomed Biotechnol 17:437–446
Su ML, He Y, Li QS et al (2016b) Efficacy of acetylshikonin in preventing obesity and hepatic steatosis in db/db mice. Molecules 21:976
Su M, Huang W, Zhu B (2016c) Acetylshikonin from Zicao prevents obesity in rats on a high-fat diet by inhibiting lipid accumulation and inducing lipolysis. PLoS One 11:e0146884
Sun J, Fu X, Liu Y et al (2015) Hypoglycemic effect and mechanism of honokiol on type 2 diabetic mice. Drug Des Devel Ther 9:6327–6342
Sundaram R, Shanthi P, Sachdanandan P (2014) Effect of tangeretin, a polymethoxylated flavones on glucose metabolism in streptozotocin-induced diabetic rats. Phytomedicine 21:793–799
Sundaram R, Shanthi P, Sachdanandan P (2015) Tangeretin, a polymethoxylated flavone, modulates lipid homeostasis and decreases oxidative stress by inhibiting NF-κB activation and proinflammatory cytokines in cardiac tissues of streptozotocin-induced diabetic rats. J Funct Foods 16:315–333

Sung J, Lee J (2016) Capsicoside G, a furostanol saponin from pepper (*Capsicum annum* L.) seeds, suppresses adipogenesis through activation of AMP-activated protein kinase in 3T3-L1 cells. J Funct Foods 20:148–158

Sung J, Jeong HS, Lee J (2016) Effect of the capsicoside G-rich fraction from pepper (*Capsicum annuum* L.) seeds on high-fat diet-induced obesity in mice. Phytother Res 30:1848–1855

Takayanagi K (2011) Prevention of adiposity by the oral administration of β-cryptoxanthin. Front Neurol 2:67

Takii H, Kometani T, Nishimura T et al (2001) Antidiabetic effect of glycyrrhizin in genetically diabetic KK-Ay mice. Biol Pharm Bull 24:484–487

Takikawa M, Inoue S, Horio F et al (2010) Dietary anthocyanin-rich bilberry extract ameliorates hyperglycemia and insulin sensitivity via activation of AMP-activated protein kinase in diabetic mice. J Nutr 140:527–533

Tan MJ, Ye JM, Turner N et al (2008) Antidiabetic activities of triterpenoids isolated from bitter melon associated with activation of the AMPK pathway. Chem Biol 15:263–273

Tay KC, Tan LTH, Chan CK et al (2019) Formononetin: a review of its anticancer potentials and mechanisms. Front Pharmacol 10:820

Tharaheswari M, Jayachandra Reddy N, Kumar R et al (2014) Trigonelline and diosgenin attenuate ER stress, oxidative stress-mediated damage in pancreas and enhance adipose tissue PPARγ activity in type 2 diabetic rats. Mol Cell Biochem 396:161–174

Tikellis C, Thomas MC (2012) Angiotensin-converting enzyme 2(ACE2) is a key modulator of the rennin angiotensin system in health and disease. Int J Peptides 2012:256294

Tilg H, Zmora N, Adolph TE et al (2020) The intestinal microbiota fuelling metabolic inflammation. Nat Rev Immunol 20:40–54

Tong Q, Tsai J, Tan G et al (2005) Interaction between GATA and the C/EBP family of transcription factors is critical for GATA-mediated suppression of adipocyte differentiation. Mol Cell Biol 25:706–715

Tsuduki T, Nakamura Y, Honma T et al (2009) Intake of 1-deoxynojirimycin suppresses lipid accumulation through activation of the β-oxidation system in rat liver. J Agric Food Chem 57: 11024–11029

Tung YC, Lin YH, Chen HJ et al (2016) Piceatannol exerts anti-obesity effects in C57BL/6 mice through modulating adipogenic proteins and gut microbiota. Molecules 21:1419

Tzeng TF, Liou SS, Liu IM (2011) Myricetin ameliorates defective post-receptor insulin signalling via β-endorphin signalling in skeletal muscles of fructose-fed rats. Evid Based Complement Altern Med 2011:150752

Tzeng TF, Liou SS, Chang CJ et al (2013) Zerumbone, a natural cyclic sesquiterpene of *Zingiber zerumbet* Smith, attenuates non-alcoholic fatty liver disease in hamsters fed on high-fat diet. Evid Based Complement Altern Med 2013:303061

Uchida-Maruki H, Inagaki H, Ito R et al (2015) Piceatannol lowers the blood glucose level in diabetic mice. Biol Pharm Bull 38:629–633

Ueda M, Nishiumi S, Nagayasu H et al (2008) Epigallocatechin gallate promotes GLUT4 translocation in skeletal muscle. Biochem Biophys Res Commun 377:286–290

Uemura T, Goto T, Kang MS et al (2011) Diosgenin, the main aglycone of fenugreek, inhibits LXRα activity in HepG2 cells and decreases plasma and hepatic triglycerides in obese diabetic mice. J Nutr 141:17–23

Um JH, Park SJ, Kang H et al (2010) AMP-activated protein kinase-deficient mice are resistant to the metabolic effects of resveratrol. Diabetes 59:554–563

USDA (2020) US, Department of Agriculture, Food database-2020

Ushiroda C, Naito Y, Takagi T et al (2019) Green tea polyphenol (epigallocatechin-3-gallate) improves gut dysbiosis and serum bile acids dysregulation in high-fat diet-fed mice. J Clin Biochem Nutr 65:34–46

Varshney S, Shankar K, Beg M et al (2014) Rohitukine inhibits in vitro adipogenesis arresting mitotic clonal expansion and improves dyslipidemia in vivo. J Lipid Res 55:1019–1032

Varshney R, Mishra R, Das N et al (2019) A comparative analysis of various flavonoids in the regulation of obesity and diabetes: an *in vitro* and *in vivo* study. J Funct Foods 59:194–205

Venkadeswaran K, Muralidharan AR, Annadurai T et al (2014) Antihypercholesterolemic and antioxidant potential of an extract of the plant, *Piper betle*, and its active constituent eugenol, in triton WR-1339-induced hypercholesterolemia in experimental rats. Evid Based Complement Altern Med 2014:478973

Venkadeswaran K, Thomas PA, Geraldine P (2016) An experimental evaluation of the anti-atherogenic potential of the plant, *Piper betle*, and its active constituent, eugenol, in rats fed on atherogenic diet. Biomed Pharmacother 80:276–288

Vitale DC, Piazza C, Melilli B et al (2013) Isoflavones: estrogenic activity, biological effect and bioavailability. Eur J Drug Metab Pharmacokinet 38:15–25

Vlavcheski F, Baron D, Vlachogiannis IA et al (2018) Carnosol increases skeletal muscle cell glucose uptake via AMPK-dependent GLUT4 glucose transporter translocation. Int J Mol Sci 19:1321

Von Lintig J (2010) Colors with functions: elucidating the biochemical and molecular basis of carotenoid mechanism. Annu Rev Nutr 30:35–56

Waltner-Law ME, Wang XL, Law BK et al (2002) Epigallocatechin gallate, a constituent of green tea, represses hepatic glucose production. J Biol Chem 277:34933–34940

Wan QF, Dong Y, Yang H et al (2004) Protein kinase activation increases insulin secretion by sensitizing the secretory machinery to Ca^{2+}. J Gen Physiol 124:653–662

Wang J, He J (2019) Swertiamarin decreases lipid accumulation dependent on 3-ketoacyl-CoA-thiolase. Biomed Pharmacother 112:108668

Wang T, Wang Y, Kontani Y et al (2008) Evodiamine improves diet-induced obesity in a uncoupling protein-1-independent manner: involvement of antiadipogenic mechanism and extracellularly regulated kinase/mitogen activated protein kinase signaling. Endocrinology 149:358–366

Wang T, Wang Y, Yamashita H (2009a) Evodiamine inhibits adipogenesis via the EGFR-PKCalpha-ERK signalling pathway. FEBS Lett 583:3655–3659

Wang Y, Huang Y, Lam KSL et al (2009b) Berberine prevents hyperglycemia-induced endothelial injury and enhances vasodilation via adenosine monophosphate-activated protein kinase and endothelial nitric oxide synthase. Cardiovasc Res 82:484–492

Wang P, Yan Z, Zhong J et al (2012a) Transient receptor potential vanilloid 1 activation enhances gut glucagon-like peptide-1 secretion and glucose homeostasis. Diabetes 61:2155–2165

Wang T, Takikawa Y, Tabuchi T et al (2012b) Carnosic acid (CA) prevents lipid accumulation in hepatocytes through the EGFR/MAPK pathway. J Gastroenterol 47:805–813

Wang T, Kusado T, Takeuchi T et al (2013a) Evodiamine inhibits insulin-stimulated mTOR-S6K activation and IRS1 serine phosphorylation in adipocytes and improves glucose tolerance in obese/diabetic mice. PLoS One 8:e83264

Wang X, Liu R, Zhang W et al (2013b) Oleanolic acid improves hepatic insulin resistance via antioxidant, hypolipidemic and anti-inflammatory effects. Mol Cell Endocrinol 376:70–80

Wang F, Yan J, Niu Y et al (2014a) Mangiferin and its aglycone, norathyriol, improve glucose metabolism by activation of AMP-activated protein kinase. Pharm Biol 52:68–73

Wang HL, Li CY, Zhang B et al (2014b) Mangiferin facilitates islet regeneration and β-cell proliferation through upregulation of cell cycle and β-cell regeneration regulators. Int J Mol Sci 15:9016–9035

Wang P, Xu S, Li W et al (2014c) Salvianolic acid B inhibited PPARγ expression and attenuated weight gain in mice with high-fat diet-induced obesity. Cell Physiol Biochem 34:288–298

Wang Y, Fofana B, Roy M et al (2015a) Flaxseed lignan secoisolariciresinol diglucoside improves insulin sensitivity through upregulation of GLUT4 expression in diet-induced obese mice. J Funct Foods 18A:1–9

Wang YH, Liu YH, He GR et al (2015b) Esculin improves dyslipidemia, inflammation, and renal damage in streptozotocin-induced diabetic rats. BMC Complement Altern Med 15:402

Wang X, Lu Q, Yu DS et al (2015c) Asiatic acid mitigates hyperglycemia and reduces islet fibrosis in Goto-Kakizaki rat, a spontaneous type 2 diabetic animal model. Chin J Nat Med 13:529–534
Wang M, Luo L, Yao L et al (2016a) Salidroside improves glucose homeostasis in obese mice by repressing inflammation in white adipose tissues and improving leptin sensitivity in hypothalamus. Sci Rep 6:25399
Wang X, Zhao S, Su M et al (2016b) Geraniol improves endothelial function by inhibiting NOX-2 derived oxidative stress in high fat diet fed mice. Biochem Biophys Res Commun 474:182–187
Wang B, Fu X, Liang X et al (2017a) Retinoic acid induces white adipose tissue browning by increasing adipose vascularity and inducing beige adipogenesis of PDGFRα^{+} adipose progenitors. Cell Discov 3:17036
Wang S, Lu A, Zhang L et al (2017b) Extraction and purification of pumpkin polysaccharides and their hypoglycemic effect. Int J Biol Macromol 98:182–187
Wang XT, Gong Y, Zhou B et al (2018) Ursolic acid ameliorates oxidative stress, inflammation and fibrosis in diabetic cardiomyopathy rats. Biomed Pharmacother 97:1461–1467
Wang B, Gao X, Liu B et al (2019a) Protective effects of curcumin against chronic alcohol-induced liver injury in mice through modulating mitochondrial dysfunction and inhibiting endoplasmic reticulum stress. Food Nutr Res 63:3567
Wang HQ, Wang SS, Chiufai K et al (2019b) Umbelliferone ameliorates renal function in diabetic nephropathy rats through regulating inflammation and TLR/NF-κB pathway. Chin J Nat Med 17:346–354
Wang L, Wei Y, Ning C et al (2019c) Ellagic acid promotes browning of white adipose tissues in high-fat diet-induced obesity in rats through suppressing white adipocyte maintaining genes. Endocrine J 66:923–936
Wang L, Wu Y, Zhuang L et al (2019d) Puerarin prevents high-fat diet-induced obesity by enriching *Akkermansia muciniphila* in the gut microbiota of mice. PLoS One 14:e0218490
Wang Q, Wu X, Shi F et al (2019e) Comparison of antidiabetic effects of saponins and polysaccharides from *Momordica charantia* L. in STZ-induced type 2 diabetic mice. Biomed Pharmacother 109:744–750
Weidner C, Wowro SJ, Freiwald A et al (2013) Amorfrutin B is an efficient natural peroxisome proliferator-activated receptor gamma (PPARγ) agonist with potent glucose lowering properties. Diabetologia 56:1802–1812
Weisberg SP, Leibel R, Tortoriello DV (2008) Dietary curcumin significantly improves obesity-associated inflammation and diabetes in mouse models of diabesity. Endocrinology 149:3549–3558
Wen L, Zhang Y, Sun-Waterhouse D et al (2017) Advantages of the polysaccharides from *Gracilaria lemaneiformis* over metformin in antidiabetic effects on streptozotocin-induced diabetic mice. RSC Adv 7:9141–9151
Westerheide SD, Bosman JD, Mbadugha BNA et al (2004) Celastrols as inducers of the heat shock response and cytoprotection. J Biol Chem 279:56053–56060
Wong KH, Li GQ, Li KM et al (2011) Kudzu root: traditional uses and potential medicinal benefits in diabetes and cardiovascular diseases. J Ethnopharmacol 134:584–607
Woo MN, Jeon SM, Kim HJ et al (2010) Fucoxanthin supplementation improves plasma and hepatic lipid metabolism and blood glucose concentration in high-fat fed C57BL/6N mice. Chem Biol Interact 186:316–322
Wu X, Beecher GR, Holden JM et al (2006) Concentrations of anthocyanins in common foods in the United States and estimation of normal consumption. J Agric Food Chem 54:4069–4075
Wu T, Tang Q, Gao Z et al (2013) Blueberry and mulberry juice prevent obesity development in C57BL/6 mice. PLoS One 8:e77585
Wu JB, Kuo YH, Lin CH et al (2014a) Tormetic acid, a major component of suspension cells of *Eriobotrya japonica*, suppresses high-fat diet-induced diabetes and hyperlipidemia by glucose transporter 4 and AMP-activated protein kinase phosphorylation. J Agric Food Chem 62:10717–10726

Wu Y, Yu Y, Szabo A et al (2014b) Central inflammation and leptin resistance are attenuated by ginsenoside Rb1 treatment in obese mice fed a high-fat diet. PLoS One 9:e92618

Wu Z, Chen Q, Ke D et al (2014c) Emodin protects against diabetic cardiomyopathy by regulating the Akt/GSK-3β signaling pathway in the rat model. Molecules 19:14782–14793

Wu J, Shi S, Wang H et al (2016) Mechanisms underlying the effect of polysaccharides in the treatment of type 2 diabetes: a review. Carbohydr Polym 144:474–494

Wu TR, Lin CS, Chang CJ et al (2019) Gut commensal *Parabacteroides goldsteinii* plays a predominant role in the anti-obesity effects of polysaccharides isolated from *Hirsutella sinensis*. Gut 68:248–262

Xiao C, Wu QP, Cai W et al (2012) Hypoglycemic effects of *Ganoderma lucidum* polysaccharides in type 2 diabetic mice. Arch Pharm Res 35:1793–1801

Xiao H, Xie G, Wang J et al (2013) Chicoric acid prevents obesity by attenuating hepatic steatosis, inflammation and oxidative stress in high-fat diet-fed mice. Food Res Int 54:345–353

Xie W, Gu D, Li J et al (2011) Effects and action mechanisms of berberine and *Rhizoma coptidis* on gut microbes and obesity in high-fat diet-fed C57BL/6J mice. PLoS One 6:e24520

Xiong Y, Shen L, Liu KJ et al (2010) Antiobesity and antihyperglycemic effects of ginsenoside Rb1 in rats. Diabetes 59:2505–2512

Xu N, Zhang L, Deng J et al (2014) Low-dose diet supplementation of a natural flavonoid, luteolin, ameliorates diet-induced obesity and insulin resistance in mice. Mol Nutr Food Res 58:1258–1268

Xu F, Wang F, Wang Z et al (2016) Glucose uptake activities of bis (2,3-dibromo-4,5-dihydroxybenzyl) ether, a novel marine natural product from red alga *Odonthalia corymbifera* with protein tyrosine phosphatase 1B inhibition, in vitro and in vivo. PLoS One 11:e0147748

Xu Y, Niu Y, Gao Y et al (2017) Borapetoside E, a clerodane diterpenoid extracted from *Tinospora crispa*, improves hyperglycemia and hyperlipidemia in high-fat-diet-induced type 2 diabetes mice. J Nat Prod 80:2319–2327

Xu G, Sun W, Guo X et al (2018a) Asiatic acid promotes liver fatty acid metabolism in diabetic models. Int J Clin Exp Med 11:11837–11845

Xu Q, Luo J, Wu N et al (2018b) BPN, a marine-derived PTP1B inhibitor, activates insulin signaling and improves insulin resistance in C2C12 myotubes. Int J Biol Macromol 106:379–386

Xu S, Wang G, Peng W et al (2019) Corosolic acid isolated from *Eriobotrya japonica* leaves reduces glucose level in human hepatocellular carcinoma cells, zebrafish and rats. Sci Rep 9:4388

Xu LN, Yin LH, Jin Y et al (2020a) Effect and possible mechanisms of dioscin on ameliorating metabolic glycolipid metabolic disorder in type 2 diabetes. Phytomedicine 67:153139

Xu X, Dai M, Lao F et al (2020b) Effect of glucoraphanin from broccoli seeds on lipid levels and gut microbiota in high-fat diet-fed mice. J Funct Foods 68:103858

Xue H, Li P, Luo Y et al (2019) Salidroside stimulates the Sirt1/PGC-1α axis and ameliorates diabetic nephropathy in mice. Phytomedicine 54:240–247

Yamada K, Hosokawa M, Yamada C et al (2008) Dietary corosolic acid ameliorates obesity and hepatic steatosis in KK-Ay mice. Biol Pharm Bull 31:651–655

Yan F, Hao H (2016) Effects of *Laminaria japonica* polysaccharides on exercise endurance and oxidative stress in forced swimming mouse model. J Biol Res (Thessalon) 23:7

Yang D, Luo Z, Ma S et al (2010) Activation of TRPV-1 by dietary capsaicin improves endothelium-dependent vasorelaxation and prevents hypertension. Cell Metab 12:130–141

Yang J, Leng J, Li JJ et al (2016a) Corosolic acid inhibits adipose tissue inflammation and ameliorates insulin resistance *via* AMPK activation in high-fat fed mice. Phytomedicine 23:181–190

Yang L, Yao D, Yang H et al (2016b) Puerarin protects pancreatic β-cells in obese diabetic mice via activation of GLP-1R signaling. Mol Endocrinol 30:361–371

Yang Z, Li J, Xiong F et al (2016c) Berberine attenuates high glucose-induced fibrosis by activating the G-protein-coupled bile acid receptor TGR5 and repressing the S1P2/MAPK signaling pathway in glomerular mesangial cells. Exp Cell Res 346:241–247

Yang J, Kim CS, Tu TH et al (2017) Quercetin protects obesity-induced hypothalamic inflammation by reducing microglia-mediated inflammatory responses via HO-1 induction. Nutrients 9:650

Yao XG, Chen F, Li P et al (2013) Natural product vindoline stimulates insulin secretion and efficiently ameliorates glucose homeostasis in diabetic murine models. J Ethnopharmacol 150: 285–297

Yoo MY, Oh KS, Lee JW et al (2007) Vasorelaxant effect of stilbenes from rhizome extract of rhubarb (*Rheum undulatum*) on the contractility of rat aorta. Phytother Res 21:186–189

Yoon JJ, Lee YJ, Han BH et al (2017) Protective effect of betulinic acid on early atherosclerosis in diabetic apolipoprotein E gene knockout mice. Eur J Pharmacol 796:224–232

Yoshimura Y, Nishii S, Zaima N et al (2013) Ellagic acid improves hepatic steatosis and serum lipid composition through reduction of serum resistin levels and transcriptional activation of hepatic PPARα in obese, diabetic KK-Ay mice. Biochem Biophys Res Commun 434:486–491

Youssef DA, El-Fayoumi HM, Mahmoud MF (2019) Beta-caryophyllene protects against diet-induced dyslipidemia and vascular inflammation in rats: involvement of CB2 and PPARγ receptors. Chem Biol Interact 297:16–24

Yu YM, Chao TY, Chang WC et al (2016) Thymol reduces oxidative stress, aortic intimal thickening, and inflammation-related gene expression in hyperlipidemic rabbits. J Food Drug Anal 24:556–563

Yuan X, Wei G, You Y et al (2017) Rutin ameliorates obesity through brown fat activation. FASEB J 31:333–345

Yuan Y, Liu Q, Zhao F et al (2019) *Holothuria leucospilota* polysaccharides ameliorate hyperlipidemia in high-fat diet-induced rats via short-chain fatty acids production and lipid metabolism regulation. Int j Mol Sci 20:4738

Zang Y, Zhang L, Igarashi K et al (2015) The anti-obesity and anti-diabetic effects of kaempferol glycosides from unripe soybean leaves in high-fat-diet mice. Food Funct 6:834–841

Zang Y, Igarashi K, Li Y (2016) Anti-diabetic effects of luteolin and luteolin-7-*O*-glucoside on KK-Ay mice. Biosci Biotechnol Biochem 80:1580–1586

Zeng XY, Wang H, Bai F et al (2015) Identification of matrine as a promising novel drug for hepatic steatosis and glucose intolerance with HSP72 as an upstream target. Br J Pharmacol 172:4303–4318

Zghonda N, Yoshida S, Ezaki S et al (2012) ε-Viniferin is more efficient than its monomer resveratrol in improving the functions of vascular endothelial cells and the heart. Biosci Biotechnol Biochem 76:954–960

Zhai B, Zhang C, Sheng Y et al (2018) Hypoglycemic and hypolipidemic effect of S-allyl-cysteine-sulfoxide (alliin) in DIO mice. Sci Rep 8:3527

Zhang WY, Lee JJ, Kim Y et al (2010a) Amelioration of insulin resistance by scopoletin in high-glucose induced, insulin resistant HepG2 cells. Horm Metab Res 42:930–935

Zhang ZF, Li Q, Liang J et al (2010b) Epigallocatechin-3-*O*-gallate (EGCG) protects insulin sensitivity in rat L6 muscle cells exposed to dexamethasone condition. Phytomedicine 17:14–18

Zhang Y, Fan S, Hu N et al (2012) Rhein reduces fat weight in db/db mouse and prevents diet-induced obesity in C57Bl/6 mouse through inhibition of PPARγ signalling. PPAR Res 2012: 374936

Zhang T, Yamamoto N, Ashida H (2014a) Chalcones suppress fatty acid-induced lipid accumulation through a LKB1/AMPK signaling pathway in HepG2 cells. Food Funct 5:1134–1141

Zhang Z, Wang S, Zhou S et al (2014b) Sulforaphane prevents the development of cardiomyopathy in type 2 diabetic mice probably by reversing oxidative stress-induced inhibition of LKB1/AMPK pathway. J Mol Cell Cardiol 77:42–52

Zhang L, Han YJ, Zhang X et al (2016a) Luteolin reduces obesity-associated insulin resistance in mice by activating AMPKα1 signaling in adipose tissue macrophages. Diabetologia 59:2219–2228

Zhang N, Yang Z, Xiang SZ et al (2016b) Nobiletin attenuates cardiac dysfunction, oxidative stress, and inflammatory in streptozotocin: induced diabetic cardiomyopathy. Mol Cell Biochem 417: 87–96

Zhang R, Yu Y, Deng J et al (2016c) Sesamin ameliorates high-fat diet-induced dyslipidemia and kidney injury by reducing oxidative stress. Nutrients 8:276

Zhang R, Yu Y, Hu S et al (2016d) Sesamin ameliorates hepatic steatosis and inflammation in rats on a high-fat diet via LXRα and PPARα. Nutr Res 36:1022–1030

Zhang Y, Hu T, Zhou H et al (2016e) Antidiabetic effect of polysaccharides from *Pleurotus ostreatus* in streptozotocin induced diabetic rats. Int J Biol Macromol 83:126–132

Zhang T, Zhu Q, Shao Y et al (2017) Paeoniflorin prevents TLR2/4-mediated inflammation in type 2 diabetic nephropathy. Biosci Trends 11:308–318

Zhang B, Sun W, Yu N et al (2018a) Anti-diabetic effect of baicalein is associated with the modulation of gut microbiota in streptozotocin and high-fat-diet induced diabetic rats. J Funct Foods 46:256–267

Zhang C, Chen H, Bai W (2018b) Characterization of *Momordica charantia* L. polysaccharide and its protective effects on pancreatic cells injury in STZ-induced diabetic mice. Int J Biol Macromol 115:45–52

Zhang J, Celli GB, Brooks MS (2019a) Natural sources of anthocyanins. In: Brooks MS, Celli GB (eds) Anthocyanins from natural sources: exploiting targeted delivery for improved health, 1st edn. Royal Soc Chem, Cambridge, UK, pp 154–196

Zhang S, Guo S, Gao XB et al (2019b) Matrine attenuates high-fat diet-induced in vivo and ox-LDL-induced in vitro vascular injury by regulating the PKCα/eNOS and PI3K/Akt/eNOS pathways. J Cell Mol Med 23:2731–2743

Zhao D, Luan Z (2020) Oleanolic acid attenuates renal fibrosis through TGF-β/Smad pathway in a rat model of unilateral ureteral obstruction. Evid Based Complement Altern Med 2020:2085303

Zhao L, Sun LN, Nie HB et al (2014) Berberine improves kidney function in diabetic mice via AMPK activation. PLoS One 9: e113398; Idem. PLoS One 12:e0190562

Zhao M, Zheng S, Yang J et al (2015) Suppression of TGF-β1/Smad signalling pathway by sesamin contributes to the attenuation of myocardial fibrosis in spontaneously hypertensive rats. PLoS One 10:e0121312

Zheng JM, Zhu JM, Li LS et al (2008) Rhein reverses the diabetic phenotype of mesangial cells over-expressing the glucose transporter (GLUT1) by inhibiting the hexosamine pathway. Br J Pharmacol 153:1456–1464

Zheng T, Yang X, Wu D et al (2015) Salidroside ameliorates insulin resistance through activation of a mitochondria-associated AMPK/PI3K/akt/GSK-3β pathway. Br J Pharmacol 172:3284–3301

Zheng Z, Yin Y, Lu R et al (2019) Lycopene ameliorated oxidative stress and inflammation in type 2 diabetic rats. J Food Sci 84:1194–1200

Zhou JY, Zhou SW (2012) Protection of trigonelline on experimental diabetic peripheral neuropathy. Evid Based Complement Altern Med 2012:164219

Zhou J, Xu G, Ma S et al (2015) Catalpol ameliorates high-fat diet-induced insulin resistance and adipose tissue inflammation by suppressing the JNK and NF-κB pathways. Biochem Biophys Res Commun 467:853–858

Zhou L, Xiao X, Zhang Q et al (2019) Dietary genistein could modulate hypothalamic circadian entrainment, reduce body weight, and improve glucose and lipid metabolism in female mice. Int J Endocrinol 2019:2163838

Zhu D, Zhang N, Zhou X et al (2017) Cichoric acid regulates the hepatic glucose homeostasis via AMPK pathway and activates the antioxidant response in high glucose-induced hepatocyte injury. RSC Adv 7:1363–1375

Zhu Z, Zhu B, Sun Y et al (2018) Sulfated polysaccharide from sea cucumber and its depolymerised derivative prevent obesity in association with modification of gut microbiota in high-fat diet-fed mice. Mol Nutr Food Res 62:e1800446

Zhu Z, Han Y, Ding Y et al (2021) Health effects of dietary sulphated polysaccharides from seafoods and their interaction with gut microbiota. Compr Rev Food Sci Food Saf 20:2882–2913

Pharmacokinetics and Metabolism of Phytochemicals Having Anti-obesity and Antidiabetic Activity

6

Biswanath Dinda and Ankita Chakraborty

6.1 Introduction

The pharmacokinetics and metabolic knowledge of natural medicine (phytochemicals and herbal formulations) are highly beneficial for clinical dose adjustment and in the development of personalized medicine. A variety of natural bioactive compounds with low lipid membrane permeability undergo a series of metabolic reactions, including phase I reactions (oxidation, hydrolysis, and reduction reactions) and phase II reactions, known as binding reactions (methylation, glucuronidation, and sulfation reactions) in different tissues, such as the liver, gastrointestinal tract, and kidney. The first-pass effect, also known as first-pass metabolism of natural medicines in the gastrointestinal tract and liver, results in the reduction of the concentrations of natural medicines to a great extent because of metabolism before they reach the systemic circulation. Several metabolic enzymes and bacteria present in the gastrointestinal tract and liver, namely, β-glucosidase, uridine-5′-diphosphate glucuronosyl transferases (UGTs), sulfotransferases (SULTs), and other *O*-methyl transfer enzymes, actively participate in the formation of glucuronide, sulfate, and methylated conjugates of natural medicine (Fig. 6.1). The conjugation reactions with glucuronic acid and/or sulfate are the most common type of metabolic pathways for flavonoids, terpenoids, and alkaloids. UGTs catalyze glucuronidation of a large number of functional groups, such as, –OH, –COOH, –NH_2, –SH, etc. Sulfonation and methylation occur in the cystol by SULTs and catechol-*O*-methyltransferases (Viskupicova et al. 2008; Meech and Mackenzie 1997). Therefore, the bioactive potential of anti-obesity and antidiabetic phytochemicals depends on their bioavailability and stability as well as

B. Dinda (✉)
Department of Chemistry, Tripura University, Suryamaninagar, Tripura, India

A. Chakraborty
Department of Chemistry, ICFAI University, Mohanpur, Agartala, Tripura, India

B. Dinda (ed.), *Natural Products in Obesity and Diabetes*,
https://doi.org/10.1007/978-3-030-92196-5_6

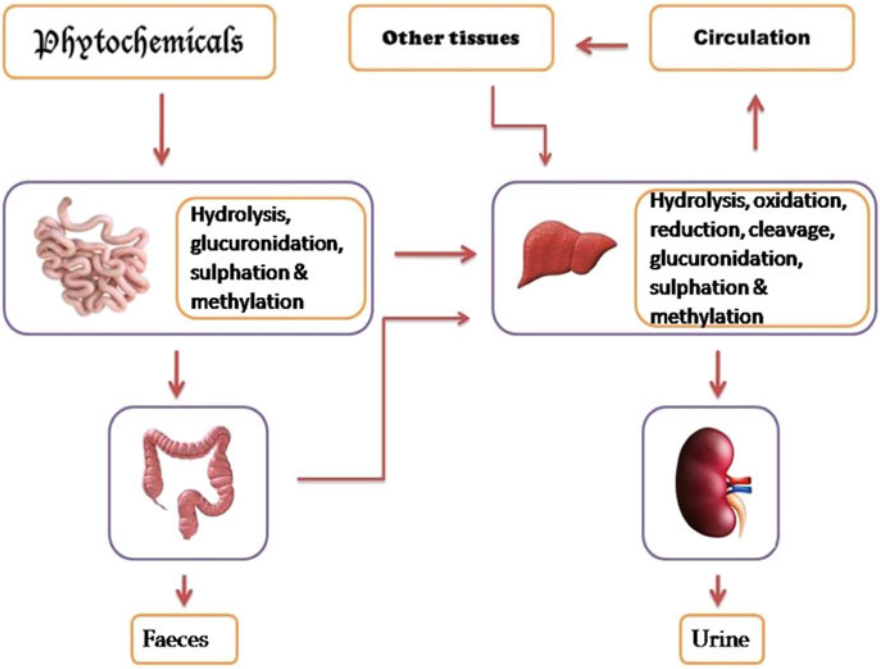

Fig. 6.1 In vivo metabolism of phytochemicals

bioavailability of active metabolites in metabolic tissues and cells. Dietary phytochemicals are absorbed in the small intestine, particularly in the jejunum and ileum through epithelial cells membrane. A major part of absorbed phytochemicals are metabolized by the enzymes and commensal microbiota present in colon tissues, and both parent and metabolized phytochemicals are transported to the liver for further biotransformations via portal veins. After absorption and intestinal/hepatic metabolism of phytochemicals, the major metabolic products and unmetabolized phytochemicals are transported through the blood into different tissues and cells for their biological actions. The bioavailability of these metabolites and unmetabolized phytochemicals depends on their solubility and ability to cross the biological lipid membranes. The major pharmacokinetic parameters of natural medicine in plasma are the area under plasma concentration-time curve (AUC), maximum concentration in plasma (C_{max}), the corresponding time when maximum concentration is reached (T_{max}), the steady-state volume of distribution (V_d), the mean residence time (MRT), whole-body clearance (CL), the mean absorption time (MAT), the absorption constant (K_a), the elimination constant (K_{el}), the half-life of absorption ($t_{1/2\ ka}$), the half-life of distribution ($t_{1/2\alpha}$), and the half-life of elimination ($t_{1/2\beta}$) (Zeng et al. 2017).

6.2 Pharmacokinetics and Metabolism of Phytochemicals

6.2.1 Flavonoids

Flavonol aglycone quercetin **23** and its glycoside rutin **54** are widely distributed in many dietary fruits and vegetables and have potential health benefit in obesity, diabetes, cancer, and other inflammatory disorders. The pharmacokinetic study on quercetin revealed that after intravenous (i.v.) administration of quercetin in rats, about 93.8% of the applied dose was circulated in the bloodstream as its sulfates and glucuronides, while after oral administration of quercetin in rats, the sulfates and glucuronides of quercetin were exclusively found in the bloodstream, and parent form of aglycone was not detected. The oral absorption rate of quercetin was 53% compared to i.v. administration. After oral administration of rutin in rats, the sulfates and glucuronides of quercetin were detected in the bloodstream, but rutin and quercetin were not detected. The following pharmacokinetic parameters of quercetin and its metabolites sulfates and glucuronides in serum after i.v. administration of quercetin in rats ($n = 6$) at a dose of 10 mg/kg (33 μM/kg) were observed: $AUC_{0–60\text{-}min}$ of 114.1, 1606.8, and 311.2 nM min/ml; AUC_{0_t} of 450.1, 6662.3, and 1931.8 nM min/ml; $T_{1/2}$ of 20.7, 371.2, and 560.7 min; and MRT (mean residence time) of 223.4, 473.4, and 716.8 min, for free quercetin, quercetin sulfates, and quercetin glucuronides, respectively. The following pharmacokinetic parameters of quercetin sulfates and glucuronides in serum after oral administration of quercetin at a single dose of 50 mg/kg (165 μM/kg) in rats ($n = 6$) were found: C_{max} 27.3 and 11.9 nM/ml, AUC_{0_t} 17,756.4 and 6803.8 nm min/ml, and MRT 1265.1 and 1063.7 min for quercetin sulfates and quercetin glucuronides, respectively. These findings suggest that quercetin sulfates and glucuronides are the major metabolites of both quercetin and rutin in rats that actively participate in the biological activities of quercetin and rutin in animal models (Yang et al. 2005). In another study, after oral administration of quercetin and rutin in healthy volunteers ($n = 16$) in three different doses of 8, 20, and 50 mg for a period of 32 h, in plasma, the glucuronides and sulfates of quercetin and quercetin aglycone were detected, but rutin was not detected. The maximum plasma concentration (C_{max}) values of the two treatments were similar, but the time to reach the C_{max} (T_{max}) was shorter after quercetin treatment than after rutin treatment (1.9, 2.7, and 4.8 vs. 6.5, 7.4, and 7.5 h for the doses of 8, 20, and 50 mg, respectively). These findings suggest that glucuronides and sulfates of quercetin are the major bioactive metabolites of quercetin and rutin in humans (Erlund et al. 2000).

Naringin **386**, a dietary flavanone glycoside (naringenin 7-*O*-rhamnoglucoside) present in many citrus fruits, has various beneficial effects in diabetes and other age-related chronic cardiovascular, kidney, and neurodegenerative diseases. Pharmacokinetic study of naringin in aged rats revealed that naringin and its major metabolite naringenin **199** were mostly distributed in rat plasma and in other tissues. Moreover, a total of 39 flavonoid metabolites mainly glucuronides and sulfates and 46 microbial-derived phenolic catabolites have been detected in tissues, urine, and feces. The following pharmacokinetic parameters of serum naringin and naringenin

after administration of a single dose of 42 mg/kg naringin in aged rats ($n = 12$) were observed: AUC_{0-t} 459.6 and 33,115.2 μg/l h, $AUC_{0-\infty}$ 601.2 and 33,438.2 μg/l h, $t_{1/2}$ 9.52 and 3.18 h, C_{max} 179.6 and 3520.6 μg/l, and T_{max} 5.20 and 8.83 h for naringin and naringenin, respectively. The highest concentrations of naringin and naringenin in the tested tissues appeared within 3 h and 6 h, respectively. The accumulation of naringin in different tissues was in the following descending order – lung > trachea > liver > kidney > muscle > fat > spleen > heart > brain – while of total naringenin in order: liver > kidney > lung > trachea > heart > fat > spleen > muscle > brain. In urine and feces, naringin and its main metabolites naringenin, hesperetin, apigenin, hippuric acid, 4-hydroxybenzoic acid, and 3(4-′-hydroxyphenyl) propionic acid were detected. The urinary excretion of naringenin in female aged rats was remarkably higher (25.3%) than that in male rats (12.7%). These findings suggest that naringin exhibits its bioactivity through mainly its naringenin and flavonoid metabolites as their glucuronides and sulfates in animal models (Zeng et al. 2019).

Hesperidin **385**, a major flavanone glycoside of orange juice, has several health effects including in the prevention of obesity, diabetes, and other chronic disorders. The bioavailability of this flavanone glycoside in humans was studied. After oral intake of orange juice at a dose of 0.5 or 1.0 l containing 444 mg/l hesperidin by overnight fasted healthy volunteers ($n = 5$) along with a polyphenol-free breakfast, the major pharmacokinetics index of plasma hesperetin (aglycone of hesperidin) observed were: C_{max} 0.46 and 1.28 μM/l, T_{max} 5.4 and 5.8 h, $AUC_{0-24\ h}$ 4.19 and 9.28 μM h/l, and urinary excretion at 24 h after ingestion of 4.54 and 14.10 mg for the dose 0.5 l and 1.0 l, respectively. The plasma circulating hesperetin were glucuronides (87%) and sulfoglucuronides (13%). The flavanone metabolites appeared in plasma at 3 h after juice intake, reached the maximum concentration between 5 and 7 h, and then returned to the baseline at 24 h. The bioavailability of hesperetin in human plasma was better than that of quercetin (0.30–0.74 μM/l) (Manach et al. 2003).

Tangeretin **136**, a polymethoxyflavone present in high concentrations in citrus fruits, particularly in the peels of sweet oranges and mandarins, has several health-promoting effects, such as anti-obesity, antidiabetes, anti-inflammatory, and neuroprotective effects. To find out the bioavailability and tissue distributions of tangeretin in vivo, a study on its pharmacokinetics, bioavailability, tissue distribution, and excretion in rats was undertaken. After oral administration of a single dose of 50 mg/kg bw and after intravenous administration of a single dose of 5 mg/kg bw in rats ($n = 6$), the following pharmacokinetic parameters of plasma tangeretin were observed: C_{max} 0.87 and 1.07 μg/ml, T_{max} 340.0 and – min, $t_{1/2\beta}$ 342.4 and 69.8 min, and $AUC_{0-24\ h}$ 213.8 and 78.8 min μg/ml, for oral and intravenous dose, respectively. Based on the AUC data, the absolute oral bioavailability of tangeretin was calculated as 27.11%. The maximum concentrations of tangeretin in vital tissues such as the kidney, liver, lung, spleen, heart, and stomach occurred at 4 and 8 h after oral administration. Tangeretin was detected in high concentrations in the kidney, liver, and lung. Only 24% of tangeretin was detected in the organs and digestive tract at 4 h after oral administration, and the remaining 76% of tangeretin retained in the

lumen of the digestive tract as metabolites, such as dimethylated derivatives and glucuronides and sulfates. In urine and fecal samples, less than 8% of unchanged tangeretin was detected, and this fact indicated that the major amount of tangeretin (about 92%) was either absorbed or excreted in the form of its metabolites (Hung et al. 2018).

Puerarin **8**, an isoflavone glucoside, present in many *Pueraria* spp., including *P. lobata*, *P. candollei* var. *mirifica*, and *P. phaseoloides*, has many beneficial effects in the prevention of diabetes, osteoporosis, and cardiovascular and neurodegenerative diseases. The pharmacokinetic study, tissue distribution, metabolism, and excretion of puerarin in rats have been reported. After intravenous administration of 1 mg/kg puerarin, and oral administration of 5 and 10 mg/kg puerarin in rats ($n = 16$), the main pharmacokinetic parameters of plasma puerarin observed were as follows: C_{max} 621.96, 145.47, and 228.0 μg/l; T_{max} N/A, 0.19, and 0.33 h; $t_{1/2\beta}$ 0.21, 0.88, and 0.86 h; AUC_{0-t} 291.47, 109.45, and 212.20 μg h/l; V_d 1.16, 101.59, and 90.17 l/kg; and MRT 0.24, 0.67, and 0.88 h for 1 mg, 5 mg, and 10 mg dose, respectively. Puerarin reached a maximum concentration of 140–230 μg/l in plasma within 1–3 h after oral dosing. A major part of puerarin was converted into its glucuronide, and both puerarin and its glucuronide were detected at 2 h in plasma and different tissues/organs, such as in the heart, lung, stomach, liver, kidney, spleen, mammary gland, femur, and tibia, with highest concentrations in the kidney, followed by the lung, stomach, and liver. Puerarin was excreted mainly as puerarin glucuronide, and about 50% of intravenously administered dose of 1 mg/kg was detected in urine, while 1–10% of administered oral dose was excreted in urine as glucuronide. The absolute oral bioavailability of puerarin was about 7% at the tested oral doses of 5 and 10 mg/kg (Anukunwithaya et al. 2018). Oral bioavailability of puerarin was improved by nanoformulation with polybutylcyanoacrylate nanoparticles (PBCN). Oral administration of a single dose of puerarin-PBCN containing 25 mg/kg puerarin and puerarin suspension in CMC (30 mg/kg puerarin) in rats showed $AUC_{0-\infty}$ 6.76 and 1.22 mg/l h, C_{max} 0.90 and 0.36 mg/l, $t_{1/2}$ 3.94 and 2.41 h, and *CL* (total clearance) 4.94 and 25.04 l/h. kg for puerarin-PBCN and puerarin suspension dose, respectively. These findings indicate that PBCN enhances oral bioavailability of puerarin by more than 5.5-fold than that of puerarin suspension. Possibly, PBCN formulation increases permeability of puerarin through the GI tract and decreases degradation and clearance of puerarin. Therefore, nanodelivery is a promising approach for improvement of oral bioavailability of puerarin and other flavonoids (Zhao et al. 2011).

Tea catechins have several health benefits, such as in the prevention of obesity, diabetes, cancers, and cardiovascular and neurodegenerative diseases, among others. 1.0 g of decaffeinated green tea (DGT) powder contains EGCG, EGC, ECG, and EC of 73, 68, 22, and 25 mg, respectively. The tea catechins on oral ingestion undergo extensive biotransformation reactions via intestinal microbiota into methylated, sulfated, and glucuronide conjugated forms in humans. After oral ingestion of DGT or green tea (GT) by humans, glucuronide and sulfate conjugates of EGCG, EGC, and EC were detected in plasma in high concentrations, and glucuronides and sulfates of EGC and EC were identified in urine (Lee et al. 1995). Pharmacokinetic

study of three major GT catechins, EGCG, EGC, and EC, in humans has been reported. After oral intake of three different doses (1.5, 3.0, and 4.5 g) of GT preparation (dissolved in 500 ml water) by human volunteers ($n = 18$), the following pharmacokinetic parameters of plasma EGCG, EGC, and EC were observed: C_{max} 119, 148, and 55 ng/h/ml; T_{max} 1.6, 1.4, and 1.4 h; $t_{1/2}$ 5.5, 2.7, and 5.7 h; AUC 897, 617, and 279 ng/l/ml; and MRT 5.9, 3.5, and 5.1 h for EGCG, EGC, and EC, respectively, for 1.5 g dose; C_{max} 326, 508, and 189 ng/ml; T_{max} 2.4, 1.8, and 1.8 h; $t_{1/2}$ 5.0, 2.8, and 3.4 h; AUC 2223, 2493, and 1059 ng/h/ml; and MRT 5.8, 4.0, and 4.5 h for EGCG, EGC, and EC, respectively, for 3.0 g dose; and C_{max} 321, 550, and 190 ng/ml; T_{max} 2.7, 1.3, and 1.8 h; $t_{1/2}$ 4.9, 2.5, and 3.2 h; AUC 2462, 3281, and 1199 ng/h/ml; and MRT 5.5, 3.9, and 4.3 h for EGCG, EGC, and EC, respectively, for 4.5 g dose. The observed data indicates that on increasing the dose from 1.5 to 3.0 g, the C_{max} values increase 2.7- to 3.4-fold, but further increasing the dose to 4.5 g does not increase the C_{max} values significantly. The T_{max} value of EGCG is longer than that of EGC and EC. The half-life of EGCG was higher than that of EGC and EC. The AUC values indicate that the extent of absorption increases 2.5-fold for EGCG, 4.0-fold for EGC, and 3.8-fold for EC on increasing the dose from 1.5 to 4.5 g. The C_{max} values were observed at 1.4–2.4 h after intake of tea preparation. Both EGC and EC were excreted in urine, but not EGCG. Over 90% of total urinary EGC and EC were excreted within 8 h of tea intake (Yang et al. 1998). In another study, tissue distribution, elimination, and bioavailability of DGT catechins in rat model were evaluated. After i.v. administration of DGT at a dose of 25 mg/kg in rats ($n = 4$), the highest level of EGCG was found in the intestine, followed by the lung, kidney, and liver (AUC 1707.9, 410.6, 325.5, and 104.8 μg min/g, respectively), while the concentration of EGC was highest in the kidney, followed by the lung, intestine, and liver (AUC 1427.4, 1209.7, 864.4, and 85.6 μg min/g, respectively), and for EC, the highest concentration was found in the intestine, followed by the kidney, lung, and liver (AUC 373.4, 335.7, 87.0, and 26.3 μg min/g, respectively). These results suggest that EGCG is excreted mainly through the bile, while EGC and EC are most likely excreted through the urine and bile because similar AUC values of EGC and EC were obtained in the kidney and intestine. After an i.g. administration of DGT at a dose of 200 mg/kg in rats ($n = 4$), the Ka values were 5.0, 11.6, and 12.7 for EGCG, EGC, and EC, respectively; the C_{max} were 16.3, 1432.8, and 685.4 ng/ml, respectively; and the fractions of absorption (F) of these polyphenols were 0.1, 13.7, and 31.2%, respectively. These results suggest that EGC and EC are absorbed faster (larger Ka) than EGCG, and EGCG has much lower bioavailability in terms of F values (Chen et al. 1997). The tissue distribution of pure EGCG was determined in rats. After administration of a single oral dose of EGCG (500 mg/kg) in rats, at 1 h, the highest level of unchanged EGCG was found in the small intestinal mucosa (565 μM), followed by the colon mucosa (69 μM), liver (48 μM), plasma (12 μM), and brain (0.5 μM). These findings suggest that availability of EGCG in the intestine in high concentration supports the significant effect of EGCG in the prevention of intestinal carcinogenesis (Nakagawa and Miyazawa 1997).

The absorption and metabolism of antidiabetic chalcones 4-hydroxyderricin (4-HD) **222** and xanthoangelol (XAN) **218**, major constituents of ashitaba (*Angelica keiskei*) extract (AE), were studied in rats. After oral administration of AE at a dose of 500 mg/kg bw in mice, both 4-HD and XAN were absorbed quickly in plasma and achieved maximum concentrations in plasma at 2 and 0.5 h, respectively. The total plasma concentration (C_{max}) of 4-HD and its metabolites were about fourfold higher than that of XAN and its metabolites at 24 h of AE administration. Both 4-HD and XAN have aglycone and glucuronide and sulfate conjugates of aglycone as major metabolites. Both 4-HD and XAN were mostly excreted as their metabolites in urine between 2 and 4 h of AE administration, but only aglycones were excreted in feces. Both 4-HD and XAN were detected in different tissues, namely, the liver, kidney, spleen, and muscle, at 2 h after AE administration mainly as their metabolites (Nakamura et al. 2012).

6.2.2 Stilbenoids

Resveratrol **47** and its 3,5-dimethylether analog pterostilbene **401a** are naturally occurring polyphenols having a broad spectrum of health benefits against cancer, diabetes, viral infections, and neurodegenerative and cardiovascular diseases. Pharmacokinetics, oral bioavailability, and metabolism of these polyphenols were evaluated in rats using single and multiple oral doses. The main pharmacokinetic parameters of resveratrol and pterostilbene after a single i.v. dose of 10 mg/kg resveratrol and 11.2 mg/kg pterostilbene in rats were C_0 3450 and 7340 ng/ml, $t_{1/2}$ NC and 2.9 h, $AUC_{0-\infty}$ 906 and 4000 ng h/ml, and *CL* 11.0 and 2.7 l/h/kg, respectively, while after administration of a single oral dose of 50 mg/kg resveratrol and 56 mg/kg pterostilbene in rats, the pharmacokinetic profile were T_{max} 1 and 2 h, C_{max} 76.7 and 2830 ng/ml, $AUC_{0-\infty}$ 1350 and 13,700 ng h/ml, $t_{1/2}$ 11.8 and 1.5 h, and *F* (fraction absorbed) 29.8% and 66.9%, respectively, and after multiple dosing of 50 mg/kg resveratrol and 56 mg/kg pterostilbene in rats for 14 days, main pharmacokinetic parameters were T_{max} 0.25 and 2.0 h, C_{max} 176 and 2550 ng/ml, $AUC_{0-\infty}$ 902 and 15,000 ng/ml, $t_{1/2}$ 5.5 and 1.6 h, and *F* 19.9% and 73.2%, respectively. Similarly, pharmacokinetic parameters after a single oral dosing of 150 mg/kg resveratrol and 168 mg/kg pterostilbene and after multiple dosing of 150 mg/kg resveratrol and 168 mg/kg pterostilbene in rats for 14 days were evaluated. The findings indicate that the oral bioavailability of resveratrol and pterostilbene were about 20% and 80%, respectively. Both resveratrol and pterostilbene have glucuronide and sulfate conjugates as their primary metabolites. After oral dosing, the plasma concentration levels of pterostilbene and pterostilbene sulfate were remarkably higher than the plasma levels of resveratrol and resveratrol sulfate, while the plasma resveratrol glucuronide levels were higher than the plasma pterostilbene glucuronide levels. Moreover, the AUC of resveratrol sulfate was 9–24-fold higher than that of resveratrol, but only 2–4-fold higher than the levels of resveratrol glucuronide following high dose exposure. Meanwhile, the AUC of pterostilbene glucuronide were much lower than the AUC of both the parent and its

sulfate. Possibly, these stilbenoids exhibit their bioactivities through their metabolites (Kapetanovic et al. 2011). In another study, the tissue distribution of resveratrol in rats was determined using radioactive [^{3}H]-resveratrol. After oral administration of a single dose of 50 mg/kg bw [^{3}H]-resveratrol in rats ($n = 6$), the concentration of resveratrol in the plasma, liver, and kidney were 1.7%, 0.98%, and 0.59%, respectively, of administered dose at 2 h after resveratrol administration, while the concentrations of resveratrol in the brain, lung, heart, and spleen were in trace amounts (< 0.1%). At 18 h, only 0.5% and 0.35% of administered dose was detected in the plasma and in all tissues, respectively. Resveratrol glucuronide was identified as major metabolite in the plasma with a concentration of 7 μM at 2 h of drug administration. About 5.1% of administered dose was detected in the GI tract, 3.3% was eliminated in the urine, and about 1.55% was eliminated in feces at 18 h. Phenolic degradation products of resveratrol were not detected in urine and tissues. This fact suggested that possibly resveratrol was not degraded by large intestinal microbiota (Abd El-Mohsen et al. 2006). To evaluate the safety of short-term multiple dosing and higher dosing of resveratrol in humans, a pharmacokinetic study was undertaken. Administration of a single oral dose of resveratrol at different doses of 25, 50, 100, and 150 mg in adult healthy humans ($n = 8$) showed C_{max} of 1.48, 6.59, 21.4, and 24.8 ng/ml; T_{max} of 1.0, 0.9, 1.3, and 1.3 h; AUC_{0-t} of 0.814, 4.27, 19.5, and 32.0 ng h/ml; and $t_{1/2}$ of 2.0, 1.8, 1.1, and 1.9 h for the dose 25, 50, 100, and 150 mg, respectively. Meanwhile, repeated oral administration of the doses of 25, 50, 100, and 150 mg six times a day and a total of 13 doses in adult healthy humans ($n = 8$) showed C_{max} of 3.89, 7.39, 23.1, and 63.8 ng/ml; T_{max} of 1.5, 0.8, 1.1, and 0.8 h; AUC_{0-t} of 3.1, 11.2, 33.0, and 78.9 ng h/ml; and $t_{1/2}$ of NA, 3.2, 2.4, and 1.9 h, for the dose 25, 50, 100, and 150 mg, respectively. These findings indicate that the repeated administration of resveratrol was well tolerated and produced relatively low plasma concentration, despite the high dosing material. Hence, multiple dosing of resveratrol is safe in human use for clinical trials (Almeida et al. 2009).

ε-Viniferin **150**, a *trans*-resveratrol dehydrodimer, present in grapevine (*Vitis vinifera* L.) has numerous pharmacological properties, including anti-obesity, antidiabetic, and cardioprotective activities. Due to low oral bioavailability (0.77%), and high i.p. bioavailability (above 85%) of ε-viniferin, the tissue distribution of this compound was evaluated by i.p. administration of ε-viniferin in rat model. A major part of ε-viniferin underwent metabolism in liver rapidly and converted mostly into its glucuronides and to a lesser extent to sulfate conjugates. LC-HRMS study revealed that ε-viniferin and its metabolites were present in the plasma, liver, kidneys, adipose tissues, feces, and urine after i.p. administration of a single dose of 50 mg/kg ε-viniferin in rats ($n = 6$). At 24 h, about 7.7%, 0.6%, and 1.4% of ε-viniferin, ε-viniferin glucuronate, and ε-viniferin sulfate, respectively, of administered dose were eliminated in feces, and less than 0.0001% of ε-viniferin and its metabolites were excreted in urine. These findings indicate that biliary excretion was the main elimination pathway. The highest glucuronide concentrations were found in the liver followed by the plasma and kidneys, and only trace amounts were detected in adipose tissues, while the high AUC and MRT values of ε-viniferin were found in the epididymal (E)-WAT and retroperitoneal (R)-WAT. Moreover,

ε-viniferin concentrations in the plasma, liver, and kidneys decreased rapidly within 4 h of administered i.p. dose, while high concentrations of ε-viniferin still remained in both E-WAT and R-WAT. The AUC_{0-t} values of ε-viniferin glucuronides in the liver were 8.4- and 10.1-fold higher than those in the plasma and kidneys, respectively. Plasma and tissue concentrations of ε-viniferin increased rapidly and reached a maximum concentration between 15 and 60 min after i.p. administration. The high accumulation of ε-viniferin in WATs suggests that these tissues serve as reservoir of parent form of ε-viniferin and allow its slow release and a sustained presence in rats. The major pharmacokinetic parameters of ε-viniferin and its metabolites ε-viniferin glucuronide and ε-viniferin sulfate in the plasma and tissues after i.p. administration of a single dose of 50 mg/kg ε-viniferin in rats ($n = 6$) were as follows: for ε-viniferin, C_{max} of 6.80, 13.41, 12.30, 47.78, and 48.32 nM/ml; AUC_{0-t} of 12.52, 20.05, 15.86, 84.16, and 109.02 nM/ml h and nM/g h; and MRT of 1.53, 1.24, 1.62, 3.86, and 4.13 h for the plasma, liver, kidney, e-WAT, and R-WAT, respectively; for ε-viniferin glucuronides, C_{max} of 8.20, 58.17, 3.30, and 0.52 nM/ml; AUC_{0-t} of 10.14, 85.01, 8.42, and 1.61 nM/ml h or nM/g h; and MRT of 1.66, 1.52, 2.03, and 8.81 h for the plasma, liver, kidney, and R-WAT, respectively; and for ε-viniferin sulfates, C_{max} of 0.38, 3.82, and 0.74 nM/ml; AUC_{0-t} of 0.44, 5.31, and 1.50 nM/ml h; and MRT of 1.22, 1.37, and 1.69 h for the plasma, liver, and kidney, respectively (Courtois et al. 2018).

6.2.3 Curcuminoids

Curcumin (diferuloylmethane) **9**, a polyphenolic yellow pigment of Asian spice turmeric (*Curcuma longa* L.), has several health-promoting activities, such as in the prevention of cancer and obesity. Pharmacokinetic study, tissue distribution, and metabolism in rat were evaluated. After i.p. administration of a single dose of 0.1 g/kg curcumin in mice, curcumin appeared in plasma quickly, about 2.25 μg/ml of plasma curcumin was found at 15 min, and at 1 h after drug administration, curcumin was found in different tissues with levels of curcumin in the intestines, spleen, liver, and kidneys at 177.04, 26.06, 26.90, and 7.51 μg/g, respectively. However, after administration of a single oral dose of curcumin (1.0 g/kg) in mice, at 15 min, only 0.13 μg/ml of curcumin in plasma was detected, and curcumin reached the maximum concentration (0.22 μg/ml) at 1 h and declined rapidly within 6 h. HPLC analysis of tissue distribution of curcumin and its metabolites revealed that a major part of curcumin was metabolized into dihydrocurcumin (DHC) **475** and tetrahydrocurcumin (THC) **476** (Fig. 6.2), which were subsequently converted to monoglucuronide conjugates as major metabolite and to a lesser extent to sulfate conjugates in the liver and were distributed in plasma and different tissues. About 99% of curcumin and more than 85% of THC as glucuronides were identified in the plasma. These findings suggest that THC, the major metabolite of curcumin, plays an important role in the biological activities of curcumin (Pan et al. 1999). In another study, oral administration of a single dose of curcumin (500 mg/kg) and a single i.v. dose of curcumin (10 mg/kg) in STZ-induced diabetic rats showed the following

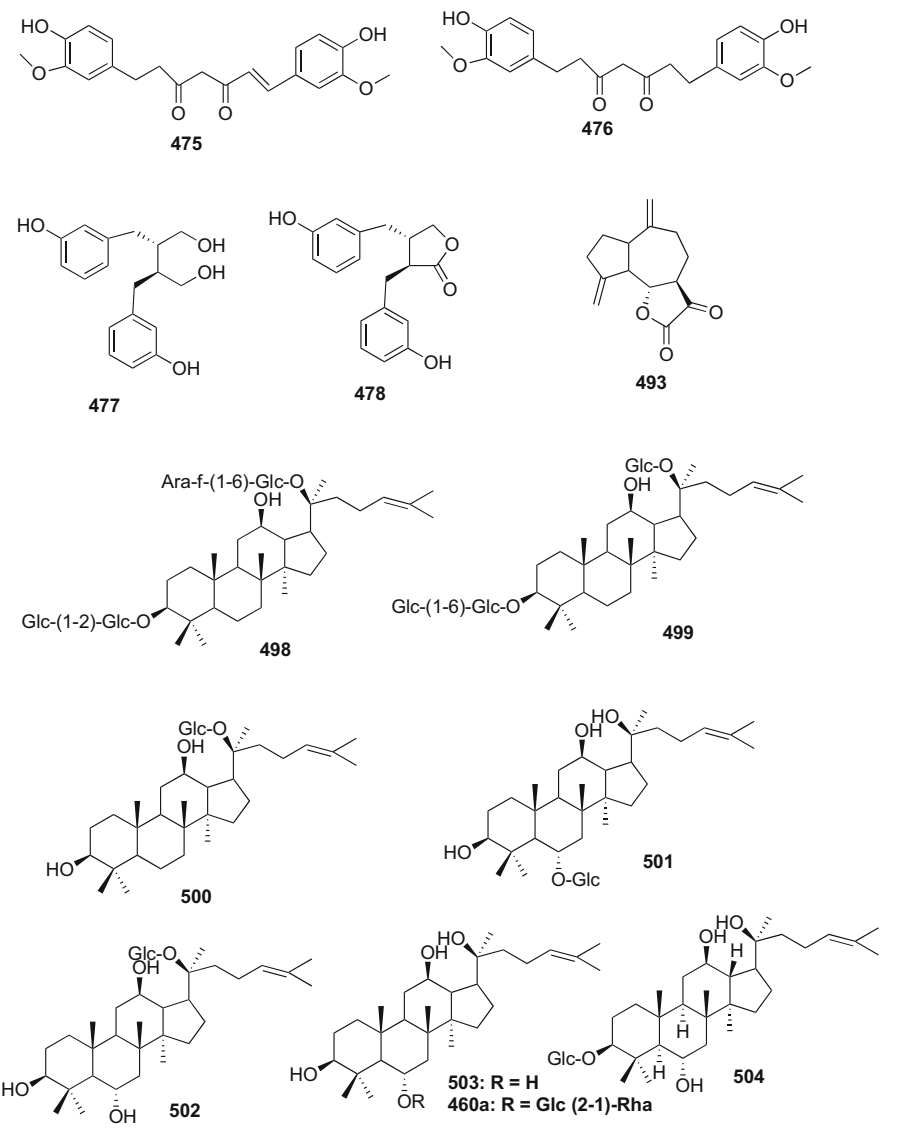

Fig. 6.2 Chemical structures of some natural products and their metabolites that are discussed in this chapter and in other chapters

pharmacokinetic parameters: C_{max} of 0.06 and 3.14 μg/ml, T_{max} of 15 and 5 min, $T_{1/2}$ of 32.70 and 8.64 min, $AUC_{0-\infty}$ of 2.97 and 12.45 μg/ml/min, MRT of 55.41 and 12.46 min, V_d of 37.49 and 10.63 l/kg, and F (bioavailability %) of 0.47 and 100 for oral and i.v. dose, respectively. These results suggest that curcumin could not be available after 5.45 h because of short half-life (32.70 min). Moreover, treatment of curcumin (90 mg/kg) and piperine (40 mg/kg) in yoghurt in STZ-diabetic rats for

45 days did not exhibit antidiabetic and antioxidant activities of curcumin. While treatment of curcumin (90 mg/kg/day) in yoghurt (1 ml) to STZ-diabetic rats for 15 days showed significant hypoglycemic effect by increasing GLUT4 translocation to plasma membrane and Akt phosphorylation to skeletal muscle of diabetic rats. Further, treatment of tetrahydrocurcumin (THC) (80 mg/kg/day) to STZ-/NA-diabetic rats for 45 days showed significant hypoglycemic effect by reduction of serum glucose levels in diabetic rats. These findings suggest that THC is the active metabolite of curcumin in the prevention of hyperglycemia. Possibly, metabolism of curcumin by hepatic enzymes is inhibited by piperine, because piperine on coadministration with curcumin increased the bioavailability of curcumin 20 times in humans and 1.56 times in rats by inhibiting the activity of hepatic P-glycoprotein (P-gp) and CYP3A4 and thereby increased the absorption and C_{max} of curcumin (Gutierres et al. 2015; Han et al. 2008).

6.2.4 Lignans

Secoisolariciresinol-diglucoside (SDG) **402**, a major lignan constituent of dietary flaxseeds, has been used extensively in dietary supplements for its various health benefits in the prevention of estrogen-related breast and prostate cancers and diabetes and other inflammatory-related chronic diseases. Pharmacokinetics and metabolism of SDG in healthy postmenopausal women were reported. SDG rapidly hydrolyzed and subsequently metabolized to secoisolariciresinol (SECO), enterodiol **477**, and enterolactone **478** (Fig. 6.2) by intestinal microbiota and circulated to plasma and tissues, and SDG was not detected in plasma. After intake of a single bolus oral dose containing 86 mg and 172 mg of pure SDG in SDG extract by healthy postmenopausal women ($n = 5$), the main serum pharmacokinetic parameters of SECO, enterodiol, and enterolactone were as follows: after intake of 86 mg dose, C_{max} of 247, 35.3, and 38.7 ng/ml; T_{max} of 6.8, 13.2, and 27.6 h; $t_{1/2}$ of 4.8, 10.2, and 13.2 h; $AUC_{0-\infty}$ of 2675, 622, and 1033 h mg/ml; and V_d of 132.5, -and, - L and after 172 mg dose, C_{max} of 544, 75.6, and 49.1 ng/ml; T_{max} 7.6, 25.2, and 25.5 h; $t_{1/2}$ of 3.7, 7.7, and 9.6 h; $AUC_{0-\infty}$ of 5609, 1949, and 1303 h ng/ml; and V_d of 90.5, -, and - L, respectively. The key findings indicate that mean half-life of enterodiol and enterolactone was 9.0 and 11.6 h, respectively among male and female volunteers. The maximum serum concentrations of enterodiol and enterolactone reached after 12–24 h and 24–36 h, respectively. SECO appeared in urine rapidly and mostly excreted within 24 h, while enterodiol and enterolactone appeared in delay and mostly excreted in urine after 2 and 5 days, respectively. The total recovery of SECO and sum of enterodiol and enterolactone in urine were 74.6% and 68.2%, respectively. The phytoestrogens enterodiol and enterolactone produced by the colon bacteria have antiestrogenic activities of type II estrogen receptor (E2) to protect against the growth of breast cancer and prostate cancer cells (Setchell et al. 2014).

Honokiol (HK) **404**, a major bioactive lignan of *Magnolia officinalis* bark, has potential bioactivity in the treatment of anxiety, depression, diabetes, and brain

disorders. The pharmacokinetics and tissue distribution of HK and its metabolites HK glucuronide and HK sulfate were reported after administration of an oral dose of HK (40 mg/kg) in Wistar rats. The results showed that HK was distributed in the plasma, liver, kidney, and brain; HK glucuronide in the plasma, liver, and kidney; and HK sulfate in the plasma only. The elimination rate of HK from the liver, kidney, and brain and of HK monoglucuronide from the liver and kidney were more rapid than that in plasma. Moreover, HK monoglucuronide was the major compound in the liver and plasma. These findings suggest that HK monoglucuronide has an active role in the pharmacological activities of HK (Wang et al. 2016a).

6.2.5 Coumarins

Esculetin **133**, a major bioactive coumarin of *Artemisia montana* (Nakai) Pamp and *Euphorbia lathyris* L., has many health benefits in the prevention of diabetes, obesity, some types of cancers, and other chronic diseases. The pharmacokinetics and oral bioavailability of esculetin were investigated after intravenous and oral administration of a single dose of esculetin (10 mg/kg) in rats. The results showed that the mean oral bioavailability of esculetin was 19%. The half-life, steady-state volume of distribution, and clearance of esculetin after i.v. dosing were 2.08 h, 1.81 l/kg, and 1.27 l/h/kg, respectively. In a two-compartment pharmacokinetic model, the first-order absorption and elimination rate constants of esculetin were 0.98/h and 2.47/h, respectively (Kwak et al. 2021). In another study, distribution of esculetin in the plasma and tissues in rats was investigated. After administration of a single oral dose of esculetin (25 mg/kg bw) in rats ($n = 6$), the following pharmacokinetic parameters were observed: T_{max} of 5 min, C_{max} of 173.3 ng/ml, $t_{1/2}$ of 45 min, and $AUC_{0–180\ min}$ of 5167.5 ng min/ml. At 180 min post-administration of esculetin, esculetin was detected in the liver (31.87 ng/g) and kidney (20.19 ng/g).These findings indicate that orally administered esculetin is rapidly absorbed and eliminated from the plasma, liver, and kidney, and not detected in other tissues (Kim et al. 2014).

6.2.6 Quinones

Anthraquinones rhein **126**, emodin **123**, aloe-emodin **123a**, physcion **124**, and chrysophanol **124a** are the major quinone constituents of *Rhei Rhizoma*, rhizome of *Rheum palmatum* L. (RP), which have several health benefits including the prevention of diabetes and other chronic diseases. These anthraquinones exist as free forms and glycosides in RP. The pharmacokinetics and tissue distribution of these anthraquinones were investigated after administration of seven consecutive oral doses of RP decoction (2 g/kg, twice daily) to rats. A major part of these anthraquinones was converted to their glucuronide (G) and sulfate (S) conjugates by intestinal microbiota, and both free forms and G/S forms are found in serum and tissues to different extent. The pharmacokinetic parameters of the anthraquinones

and their G/S forms and G form after oral administration of seventh dose of RP (2 g/kg) in rats ($n = 6$) were as follows: for rhein, C_{max} of 5.8, 17.1, and 9.3 nM/ml; $AUC_{0–72\ min}$ of 1250.2, 3209.4, and 1725.1 nM min/ml; and $MRT_{0–720\ min}$ of 243.1, 236.8, and 215.5 min, for free form, G/S, and G, respectively; for emodin, C_{max} of 3.7 and 2.1 nM/ml, $AUC_{0–720\ min}$ of 717.0 and 391.5 nM min/ml, and $MRT_{0–720\ min}$ of 235.9 and 203.6 min, for G/S and G, respectively; for aloe-emodin, C_{max} of 2.1 and 1.5 nM/ml, $AUC_{0–720\ min}$ of 288.0 and 151.7 nM min/ml, and $MRT_{0–720\ min}$ of 147.5 and 105.5 min, for G/S and G, respectively; and for chrysophanol, C_{max} of 1.8 and 1.4 nM/ml, $AUC_{0–720\ min}$ of 161.6 and 117.6 nM min/ml, and $MRT_{0–720\ min}$ of 93.5 and 136.5 min, for G/S and G, respectively. The results indicate that the AUC of the anthraquinones are in the following descending order: rhein G/S > rhein > emodin G/S > aloe-emodin G/S > chrysophanol G/S. Moreover, these anthraquinones were present in serum as glucuronides/sulfates (G/S) and contained higher ratio of sulfates compared to single dose administration of RP. The free form of rhein was found in the serum, kidney, liver, and lung, while free form of aloe-emodin was found in the liver, kidney, and lung and emodin in the liver and lung and trace amount of chrysophanol in the kidney and liver. The anthraquinone G/S were predominant in the plasma, while free forms were predominant in the kidney and lung (Shia et al. 2011).

6.2.7 Xanthones

Mangiferin **409**, a xanthone glucoside present in high levels in *Mangifera indica* bark, different *Salacia* spp. including *S. oblonga* and *S. roxburghii*, and *Swertia chirata*, has potential efficacy in the treatment of diabetes and its complications. A polyherbal formulation composed of *Salacia oblonga*, *S. roxburghii*, *Garcinia indica*, and *Lagerstroemia parviflora* was developed by Dubay et al. and patented in the USA for the management of type 2 diabetes and its vascular complications. The comparative pharmacokinetics and bioavailability of pure mangiferin and mangiferin from the polyherbal formulation were reported. After oral administration of pure mangiferin and the polyherbal formulation at a dose of 30 mg/kg mangiferin in rats ($n = 6$), the following pharmacokinetic parameters for free mangiferin and mangiferin in polyherbal formulation were observed: C_{max} of 15.23 and 44.16 μg/ml, T_{max} of 0.67 and 3.00 h, $t_{1/2}$ of 1.06 and 1.89 h, $AUC_{0-\infty}$ of 155.03 and 187.53 μg h/ml, K_a of 0.56 and 0.36 h, K_e of 0.41 and 0.50 h, CL of 1.59 and 6.35 μg/ml/h, V_d of 7.21 and 1.86 ml, and MRT of 3.21 and 3.65 h, for pure mangiferin and polyherbal formulation dose, respectively. Moreover, after oral administration of polyherbal formulation, mangiferin was distributed in various tissues, such as in the small intestine, heart, kidney, and liver, and at 180 min, the concentration of mangiferin was 754, 321.5, 143.3, and 128.5 ng/g, in these tissues, respectively, and a small amount was detected in the stomach, spleen, and lung. These results indicate that polyherbal formulation increases the C_{max} and AUC value of mangiferin compared to that of pure mangiferin. The higher value of volume of distribution (V_d) suggests the greater binding capacity of mangiferin with plasma and

tissue proteins. This higher binding capacity reduces the rate of elimination and total body clearance. Possibly, the presence of other phytoconstituents in polyherbal formulation, such as ellagic acid and others, reduces the activity of intestinal and hepatic metabolic enzymes on mangiferin and thereby promotes the absorption of mangiferin to increase its plasma C_{max} and AUC values. Therefore, polyherbal formulation improves the efficacy of mangiferin in diabetes treatment (Kammalla et al. 2015).

6.2.8 Phenolic Acids

Rosmarinic acid (RA) **104**, an ester of caffeic acid and 3,4-dihydroxyphenyllactic acid, is widely distributed in the culinary herbs of Lamiaceae family, such as in rosemary (*Rosmarinus officinalis*), *Salvia officinalis*, *S. miltiorrhiza*, *Perilla frutescens*, and *Thymus vulgaris* and has a wide spectrum of pharmacological properties, including antidiabetic and anticancer activities. The pharmacokinetics of RA was reported by several groups. After oral administration of RA in rats, a major part of RA was metabolized to its glucuronide and sulfate conjugates, caffeic acid (CA), ferulic acid (FA) and meta-coumaric acid (m-COA), and others by the intestinal microbiota and hepatic enzymes, leading to poor absorption by intestinal epithelial membrane and low availability in plasma and tissues. After oral administration of a single dose of RA (50 mg/kg) to rats, RA and its glucuronide and sulfate were mainly found in the plasma and tissues, and in urine these metabolites and other metabolites, namely, conjugated forms of CA, FA, and m-COA, were identified. About 83% of the total amount of these metabolites was excreted in urine within 8–18 h after oral administration of RA in rats (Baba et al. 2004). Another group reported the pharmacokinetic results of RA and its two bioactive metabolites CA and FA after oral and intravenous (i.v.) administration of RA in rats. Only CA and FA were identified in plasma after oral administration, but not in i.v. administration. After administration of a single dose of RA (50 mg/kg) to rats ($n = 6$), the following pharmacokinetic parameters of plasma RA, CA, and FA were observed: C_{max} of 1087.64, 30.62, and 25.95 ng/ml; T_{max} of 0.19, 0.19, and 0.36 h; $t_{1/2}$ of 1.34, 0.78, and 0.46 h; $AUC_{0-\infty}$ of 972.36, 33.08, and 24.61 ng h/ml; $MRT_{0-\infty}$ of 1.57, 1.17, and 0.78 h; and F (bioavailability, %) of 4.13, N/A and N/A for RA, CA and FA, respectively. While after administration of a single intravenous dose of RA (2 mg/kg) in rats ($n = 6$), the following pharmacokinetic parameters of plasma RA were observed: C_{max} of 3416.95 ng/ml, $t_{1/2}$ of 0.67 h, $AUC_{0-\infty}$ of 999.70 ng h/ml, and $MRT_{0-\infty}$ of 0.22 h. These findings suggest that both CA and FA had low plasma C_{max} and short half-lives compared to RA. The poor absolute bioavailability of R (4.13%) suggests that a major part of RA undergoes hydrolysis in the gastrointestinal tract and its poor permeability through the intestinal epithelial cell membrane and the first-pass effect of the liver decrease its availability in plasma (Wang et al. 2021). Another group reported the tissue distribution of RA in rats. Administration of a single dose of *Salvia miltiorrhiza* depside (Mg) salts (60 mg/kg) containing 10.1%

RA and lithospermic acids A and B as major constituents, in rats, showed the distribution of RA in different tissues in the following descending order: kidney > lung > heart > liver > spleen > brain having $AUC_{0-\infty}$ of 10.84, 1.68, 0.34, 0.04, 0.01, and 0.01 ng h/kg, respectively. Moreover, the maximum concentrations of RA in these tissues were found within 5 min of dosing, and these concentrations declined within 30 min and almost cleared completely from the tissues at 4 h, with half-life less than 2 h for RA (Li et al. 2007).

Salidroside **413**, a glucoside of p-tyrosol, found in many *Rhodiola* spp., has various biological activities, including anticancer, antidiabetic, and neuro-, hepato-, and cardioprotective activities. The pharmacokinetics, excretion, and tissue distribution of salidroside in rat model were reported. After intravenous administration of a single dose of salidroside (7.5, 15, and 30 mg/kg) in rats, the following pharmacokinetic parameters were observed: AUC of 300.48, 514.51, and 1,036.64 mg min/l; *CL* of 0.025, 0.031, and 0.029 l/min/kg; and V_d of 2.02, 2.47, and 2.58 l/kg, for 7.5, 15, and 30 mg dose, respectively. The concentration of salidroside in plasma declined rapidly due to short half-life of about 1 h. At 15 mg/kg dosing, about 54% of administered dosage was eliminated in urine within 48 h, but only 0.09% and 0.18% of the administered dose were excreted in bile and feces, respectively. Moreover, the concentrations of salidroside in 12 tissues and plasma were measured at 15, 40, and 120 min after dosing, and at all time points, no higher concentration of salidroside in different tissues was detected than that in plasma. A better distribution of salidroside in the ovary and testis followed by the kidney and spleen was observed, and its low concentrations in the liver, adipose tissue, and muscle were detected. These findings suggest that salidroside maintains a dose-dependent linear absorption and AUC value and is cleared from the body via kidney pathway (Zhang et al. 2013). Another study reported the tissue distribution and metabolism of salidroside in rats in details. A major part of salidroside was hydrolyzed to its aglycone p-tyrosol by intestinal bacteria, and both salidroside and p-tyrosol were distributed in different tissues after both intravenous and oral (i.g.) administration of salidroside in rats. After i.v. administration of a single dose of salidroside (50 mg/kg) in rats, the maximum concentrations of salidroside were observed in the liver (15,713.30 ng/g) followed by the kidney (1480.54 ng/g) and heart (170.34 ng/g), whereas the maximum concentrations of p-tyrosol were detected in the heart (7497.17 ng/g) followed by the spleen (4421.92 ng/g), kidney (3857.97 ng/g), liver (3190.49 ng/g), lung (1742.90 ng/g), and brain (1118.38 ng/g). At 0.17 h after administered dose of salidroside, the concentrations of p-tyrosol declined rapidly in these tissues and were almost non-detectable after 4 h of administration of salidroside. In an oral administration of a single i.g. dose of salidroside (100 mg/kg) in rats, the maximum concentrations of salidroside in rat plasma were 1113.07 and 1088.87 ng/ml at 1 h and 2 h, respectively after administered dose of salidroside. In contrast, p-tyrosol was detected in most of the tissues except in the brain, and in the kidney, and the maximum concentration in the plasma (4568.0 ng/ml) was found at 1 h after administration of salidroside. In addition, salidroside was excreted mainly through urine (64% of total i.v. dose and 23.8% of total i.g. dose), whereas p-tyrosol was excreted through urine to a lesser extent (0.19% and 2.25% of i.v. and i.g. doses,

respectively). These findings suggest that salidroside undergoes extensive metabolism in i.g. administration compared to i.v. administration in rats (Guo et al. 2014). Another group also reported the metabolic profile of salidroside in rats and identified the presence of eight metabolites of salidroside in urine. Moreover, both salidroside and p-tyrosol remained as glucuronide and sulfate conjugates in different tissues, and the sulfate conjugates of p-tyrosol underwent further hydroxylation, dehydroxylation, and methylation on phenyl ring to form hydroxylated and methylated conjugates (Hu et al. 2015).

Chlorogenic acid (3-*O*-caffeoylquinic acid) (ChA) **21**, a major bioactive constituent in many medicinal plants, including *Solanum lyratum* and *Lonicera japonica*, has a variety of biological activities, such as antidiabetic, hypotensive, cardio- and hepato-protective, and antiviral activities. A comparative pharmacokinetic study of pure ChA and ChA in *Solanum lyratum* ethanol extract (SLE) was reported. After oral administration of a single dose of ChA (50 mg/kg) and a single dose of SLE (3.31 g/kg containing 50 mg/kg ChA) in rats ($n = 6$), the following pharmacokinetic parameter of plasma ChA were observed: C_{max} of 0.55 and 0.37 mg/l, T_{max} of 0.48 and 0.36 h, $t_{1/2}$ of 1.70 and 1.70 h, $AUC_{0-\infty}$ of 1.61 and 0.83 mg h/l, *CL* of 39 and 65 l/h kg, V_d of 97.5 and 154 l/kg, and K_e of 0.41 and 0.41/h, for pure ChA and SLE dose, respectively. These findings indicate that SLE due to the presence of other constituent prohibits absorption of ChA and accelerates the elimination of ChA. Moreover, low plasma availability of ChA suggests that a major part of ChA is metabolized in the intestine into its active metabolites benzoic acid, benzene propionic acid, and cinnamic acid (Qi et al. 2011). Another study reported the tissue distribution of ChA after oral administration of Lonicerae Japonicae Flos (LJF) extract containing ChA as major constituent in rats. After administration of an oral dose of LJF extract (400 g/kg containing 16.7% ChA) in rats ($n = 6$), the analysis of tissue distribution of ChA revealed that ChA was detected in high concentrations in the liver followed by the kidney, lung, heart, and spleen. The low concentrations of ChA in the tissues suggested that ChA quickly metabolized and was not detected in tissues after 4 h of LJF administration (Zhou et al. 2014).

6-Gingerol **154**, a major phenolic constituent of Asian spice ginger, the rhizome of *Zingiber officinale* Roscoe, has a variety of health benefits, such as in the prevention of skin carcinogenesis, diabetes, and hepatic disorders. The pharmacokinetics, tissue distribution, and excretion studies of 6-gingerol in rats were reported using LC-TOF/MS technology. In rats, and humans, 6-gingerol is rapidly metabolized to its glucuronide, and both 6-gingerol and its glucuronide are found in plasma and tissues. After oral (i.g.) administration of a single high dose (120 mg/kg) of 6-gingerol, and intraperitoneal (i.p.) administration of a single low dose (30 mg/kg) of 6-gingerol in rats ($n = 6$), the following plasma pharmacokinetic parameters of 6-gingerol were observed: AUC_{0-tn} of 1.33 and 4.06 μg h/ml, C_{max} of 1.90 and 5.96 μg/ml, T_{max} of 0.083 and 0.083 h, and $t_{1/2}$ of 0.766 and 0.381 h, for 120 mg/kg oral dose and 30 mg/kg i.p. dose, respectively. Meanwhile, after oral administration of a single dose of 6-gingerol (30 and 120 mg/kg) and i.p. administration of a single dose of 6-gingerol (30 mg/kg) in rats ($n = 6$), the following pharmacokinetic parameters of plasma 6-gingerol glucuronide were

observed: AUC_{0-tn} of 23.49, 76.62, and 30.96 μg h/ml; $C_{max\ 1}$ of 15.14, 51.99, and 18.88 μg/ml; $T_{max\ 1}$ of 0.083, 0.25, and 0.083 h; $C_{max\ 2}$ of 2.88, 3.83, and 1.63 μg/ml; $T_{max\ 2}$ of 3, 6, and 4 h; and $t_{1/2}$ of 0.495, 0.923, and 0.645 h, for oral 30 and 120 mg/kg doses and i.p. 30 mg/kg dose, respectively. These findings indicated that 6-gingerol was not found in plasma at low oral dose (30 mg/kg), but its glucuronide was found in plasma, suggesting its first-pass metabolism, while at high oral dose of 6-gingerol (120 mg/kg), both C_{max} and AUC values of 6-gingerol glucuronide were substantially higher than that of 6-gingerol. After i.p. administration of 6-gingerol (30 mg/kg), it was rapidly absorbed and cleared from plasma. At 0.5 h after administration of 6-gingerol (30 mg/kg), 6-gingerol glucuronide appeared at highest concentration in the liver followed by the lung, spleen, and kidney. Possibly the liver and kidney are responsible for excretion of 6-gingerol. 6-Gingerol was excreted as its glucuronide in urine, and about 5.4% of administered dose was excreted as glucuronide in urine within 24 h (Wang et al. 2009).

Chicoric acid (2,3-*O*-dicaffeoyltartaric acid) **412**, mainly found in nature in L-form in many plants, such as chicory (*Cichorium intybus*), purple coneflower (*Echinacea purpurea*), and basil, has a variety of health benefits, including amelioration of diabetes, obesity, viral infection, and inflammatory disorders. The pharmacokinetics, tissue distribution, and plasma protein binding (PPB) activity of chicoric acid in rat were investigated. After oral administration of a single dose of chicoric acid (50 mg/kg) in rats ($n = 6$), the following plasma pharmacokinetic parameters of chicoric acid were observed: AUC of 26.14 mg h/l, MRT of 18.58 h, and $t_{1/2}$ of 4.53 h. The tissue distribution analysis of chicoric acid in rats after oral administration of a single dose of chicoric acid (50 mg/kg) showed that chicoric acid was distributed in many tissues, and the highest concentration was found in the liver, followed by the lung, kidney, heart, spleen, and brain. Moreover, chicoric acid has high PPB capacity with rat plasma, human plasma, and bovine serum albumin having PPB rates of 98.3, 96.9, and 96.6%, respectively (Wang et al. 2016a, b).

6.2.9 Tannins

Ellagic acid (EA) **320**, an ellagitannin constituent found in many fruits and plants, is the main active constituent of pomegranate (*Punica granatum*) leaves and has several health benefits, including antitumor and antidiabetic effects. The pharmacokinetics of EA in rat was investigated after oral administration of pomegranate leaf extract (PLE). After oral administration of a single dose of PLE (0.8 g/kg containing 85.3 mg/kg EA) in rats ($n = 5$), the following pharmacokinetic parameters of EA in rat plasma were observed: C_{max} of 203 ng/ml, T_{max} of 0.541 h, $t_{1/2\alpha}$ of 0.770 h, $t_{1/2\beta}$ of 5.0 h, AUC of 0.838 μg h/ml, *CL* of 102.32 l/(h kg), V_d of 334.07 l/kg, and K_a of 5.91/h. These findings suggested that EA had a maximum concentration of 203 ng/ml in plasma at 0.54 h of post dosing and this concentration declined rapidly and half of it was out of plasma at 40 min after oral dosing of the extract. The poor adsorption and rapid distribution and elimination of EA prevent the tissues to achieve sufficient high concentration of EA for its bioactivity (Lei et al. 2003).

Grape seed extract (GSE) containing (+)-catechin, (–)-epicatechin, and their dimers, trimers, tetramers, and polymeric procyanidins **417** and **418** has potential health benefits in the prevention of cancer, cardiovascular diseases, obesity, diabetes, and its associated vascular complications. The absorption, metabolism, and excretion of GSE were investigated in rat. Administration of a single dose of GSE (1 g/kg) by dissolving in water (6 ml) in rats ($n = 24$) showed the presence of glucuronides of (+)-catechin, (–)-epicatechin, methyl-(+)-catechin, and methyl-(-)-epicatechin in rat plasma, liver, kidney, and urine, but no free (+)-catechin and (–)-epicatechin were detected in urine samples. In urine samples, the presence of sulfates and methylsulfates of the monomers (+)-catechin and (–)-epicatechin was also detected. The majority of oligomeric procyanidins were detected in the GI tract at 6 h, declined at 24 h, and disappeared after 24 h. There was no indication that these procyanidin oligomers were depolymerized to monomers to any extent. Only trace amounts of these procyanidins were excreted in feces. These findings suggested that these oligomeric procyanidins of GSE might be converted to low molecular weight phenolic acids including 3-hydroxyphenylpropionic acid by intestinal microbiota, and these phenolic acids have significant role in glucose and lipid metabolism and insulin sensitivity in metabolic tissues (Tsang et al. 2005).

6.2.10 Alkaloids

Berberine (BBR) **48**, an isoquinoline alkaloid present in many plants, is a major alkaloid constituent of *Coptis chinensis* rhizomes and has several beneficial effects in humans, including cholesterol lowering, hypoglycemic, cardioprotective, and anti-inflammatory activities. The pharmacokinetics and tissue distribution of BBR in rat were investigated. After oral administration of a single dose of BBR (200 mg/kg) in rats ($n = 6$), the following pharmacokinetic parameters were observed in non-compartmental methods: AUC_{0-t} of 75.83 ng h/ml, $AUC_{0-\infty}$ of 86.37 ng h/ml, C_{max} of 25.85 μg/l, T_{max} of 1.33 h, and $t_{1/2}$ of 14.73 h. Analysis of the distribution of BBR in different tissues revealed that BBR reached the tissues within 0.25 h and its level in most of investigated tissues was higher than that in plasma at 4 h after administration. The maximum concentration of BBR was highest in the liver, followed by the kidneys, muscle, lungs, brain, heart, pancreas, and fat tissue as evident from their respective AUC_{0-t} value of 728.6, 362.7, 84.2, 66.0, 47.8, 47.4, 12.0, and 6.8 ng h/ml, while the metabolites were in high concentration in the liver (AUC_{0-t} 2103.5 ng h/ml). BBR reached the maximum concentration in the tissues in 2–24 h; 2 h in the pancreas and fat; 4 h in the lungs; 12 h in kidneys, muscle, and brain; and 24 h in the heart. Three metabolites of BBR, namely, thalifendine (M1) **479**, berberrubine (M2) **480**, and jatrorrhizine (M3) **481** (Fig. 6.2), were detected in high concentrations in the liver and kidney. In the liver, the metabolites M2 and M1 were found at very high concentrations, about 65.1% and 33.3%, respectively. Moreover, the total AUC_{0-t} for BBR and its metabolites in the liver and kidney was about 40 and 7 times higher than that in plasma. These metabolites were also detected in other tissues. Available evidence demonstrates that both

thalifendine and berberrubine upregulate the expression levels of IR and LDLR and increase the phosphorylation of AMPK in the liver and other metabolic tissues. The high levels of BBR and its metabolites in the liver suggest that BBR and its metabolites stimulate the activity of the liver to take a key role for the regulation of lipid and carbohydrate metabolism in obesity and diabetes. Moreover, the high distribution of BBR in the brain and heart supports the neuro- and cardioprotective activity of BBR on CNS and cardiovascular systems. These findings suggest that the metabolites of BBR are partly responsible for the activities of BBR (Tan et al. 2013). A recent study reported the pharmacokinetics, metabolism, and excretion of BBR and its metabolites in rat. The absolute bioavailability of BBR was 0.37%. BBR in the intestine and liver underwent extensive phase I and phase II metabolism, and nine metabolites of BBR were identified and detected in rat plasma in both after intravenous and oral administration of BBR in rats. These metabolites are as follows: phase I-, berberrubine (M1) **480**, demethyleneberberine (M2) **482**, jatrorrhizine (M3) **481**, phase II-, jatrorrhizine-3-*O*-β-D-glucuronide (M4) **483**, jatrorrhizine-3-*O*-sulfate (M5) **484**, thalfendine-10-*O*-β-D-glucuronide (M6) **485**, berberrubine-9-*O*-β-D-glucuronide (M7) **486**, demethyleneberberine-2-*O*-sulfate (M8) **487**, and demethyleneberberine-2-*O*-β-D-glucuronide (M9) **488** (Scheme 6.1). It was evident from the $AUC_{0–48\ h}$ values that the phase II metabolites were much higher concentrations than those of phase I metabolites and BBR, suggesting that phase II metabolites were dominant metabolites in rat blood. Three phase II metabolites, namely, M7, M9, and M6, had much higher $AUC_{0–48\ h}$ values compared to that of BBR and their $AUC_{0–48\ h}$ values after a single oral dose of BBR (240 mg/kg) were 13,362.0, 4417.0, and 1621.0 mg/l h, respectively, compared to BBR (166.0 mg/l h). About 18.6% of BBR was excreted in feces as berberrubine (M1). The total recovery of BBR and its nine metabolites from urine, bile, and feces was 41.2% within 48 h. The main pharmacokinetic parameters of plasma BBR after administration of a single i.v. dose of BBR (4 mg/kg) and a single oral dose of BBR (120 mg/kg) in rats ($n = 6$) were as follows: $AUC_{0–48\ h}$ of 839.0 and 81.30 mg/l h, C_{max} of 963.0 and 32.60 ng/ml, T_{max} of N/D and 1.88 h, $t_{1/2\alpha}$ of 23.60 and 21.20 h, *CL* of 0.021 and 1.23 l/h/kg, V_d of 0.71 and 38.70 l/kg, and $MRT_{0–48\ h}$ of 9.95 and 12.30 h, for i.v. (4 mg/kg) and oral (120 mg/kg) doses, respectively. Available evidence indicates that phase II M7 metabolite shows better glucose lowering effect than that of phase I M1 metabolite. These findings suggest that the metabolites of BBR play a significant role in the activity of BBR in vivo models (Feng et al. 2021). The absolute bioavailability of BBR can be improved by using the organic acid salt of BBR. In a study, after oral administration of a single dose of BBR hydrochloride and BBR fumarate (500 mg/kg) in type II diabetic rats ($n = 5$), the following pharmacokinetic parameters were observed: C_{max} of 4.22 and 5.47 μg/ml, $AUC_{0-\infty}$ of 8.29 and 10.60 μg/ml h, and *F* (absolute bioavailability, %) of 0.708% and 0.970%, respectively. These findings suggest that organic acid salt of BBR improves the permeability of BBR through intestinal epithelial cells to increase the absorption of BBR (Cui et al. 2019).

Capsaicin **49**, a pungent amide constituent of spice red pepper (*Capsicum annuum*), has beneficial effects, such as hypolipidemic, hypoglycemic, anti-

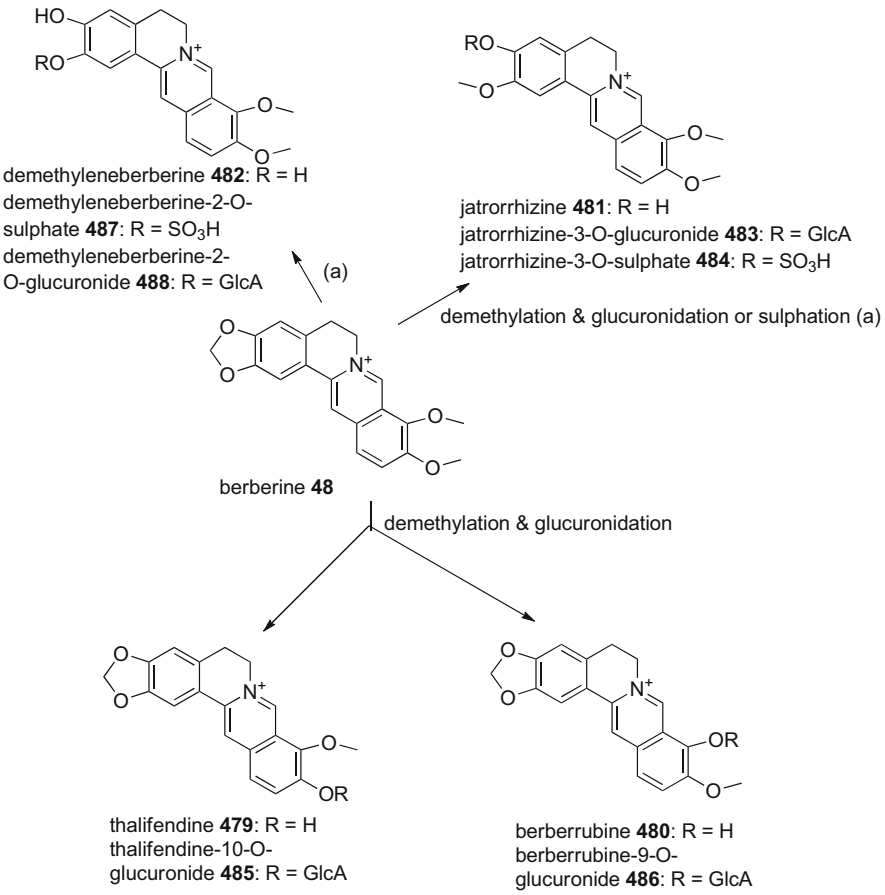

Scheme 6.1 Metabolism of berberine in rats

inflammatory, and abdominal pain relieving effects. The pharmacokinetics, tissue distribution, and excretion of capsaicin in rats were investigated. Administration of a single oral dose of capsaicin (30 mg/kg) in rats showed the following main pharmacokinetic parameters: AUC of 15.6 μg h/ml, C_{max} of 1.90 μg/ml, and $t_{1/2}$ of 7.88 h. The highest concentration of capsaicin in plasma (1.90 μg/ml) was detected at 1 h; it declined rapidly to less than half (0.83 μg/ml) at 6 h and further decreased to 2.5% (0.05 μg/ml) at 24 h after dosing. The maximum distribution of capsaicin (24.2%) of administered dose was detected in different tissues, namely, the blood, liver, kidney, and intestine at 1 h, while no capsaicin was detected after 96 h. The absorption of capsaicin was about 94%. In liver, the highest concentration of capsaicin (44.7 μg/whole tissue) was observed at 3 h and then reduced to 8.7 μg/whole tissue at 24 h. While in the kidney, the highest concentration of capsaicin (6.73 μg/whole kidney tissue) was found at 6 h and decreased to 0.48 μg/whole tissue at 48 h. In the intestine, the highest concentration of capsaicin (1057.0 μg/whole tissue) was observed at 1 h and declined to 1.14 μg/whole tissue at 48 h. About 6.3% of

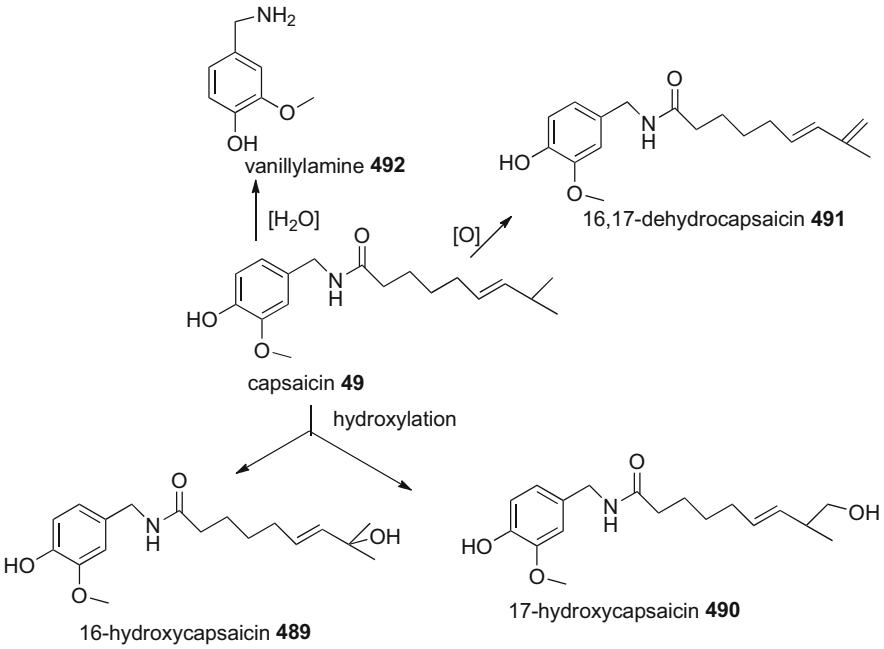

Scheme 6.2 Metabolism of capsaicin in rat hepatic microsomes

administered dose was excreted in feces within 96 h, and only a trace amount (0.095%) was excreted in urine (Suresh and Srinivasan 2010). The in vitro study on the metabolism of capsaicin in rat, dog, and human hepatic microsomes revealed the presence of three major metabolites: 16-hydroxycapsaicin **489**, 17-hydroxycapsaicin **490,** and 16,17-dehydrocapsaicin **491** (Scheme 6.2). In addition, in rat liver microsomes, two more metabolites, vanillylamine **492** and vanillin, were identified (Chanda et al. 2008).

Piperine (*trans-trans* isomer of 1-piperoylpiperidine) **117**, a major piperidine alkaloid constituent of Asian spice, black pepper (*Piper nigrum*), and long pepper (*Piper longum*), has several health benefits. The pharmacokinetic study of piperine in rats was reported. After administration of a single intravenous (i.v.) dose of piperine (10 mg/kg) and a single oral dose of piperine (20 mg/kg) to rats, the following pharmacokinetic parameters of plasma piperine were observed: $AUC_{0–24\ h}$ of 15.6 and 7.48 μg h/ml, C_{max} of N/D and 0.983 μg/ml, T_{max} of N/D and 2.0 h, $t_{1/2\beta}$ of 7.99 and 1.22 h, V_d of 7.046 and 4.692 l/kg, and *CL* of 0.642 and 2.656 l/h/kg, for i.v. dose and oral dose, respectively. The absolute oral bioavailability was 24.1%. The results indicate that piperine has poor absorption and extensive distribution and reaches the maximum plasma concentration at 2 h after orally administered dose. Moreover, piperine undergoes extensive first-pass metabolism after absorption in plasma due to short half-life period (1.22 h) after oral dose (Sahu et al. 2014). The tissue distribution and excretion of piperine in rat were investigated

by another group. Oral administration of a single dose of piperine (170 mg/kg) in rats showed that piperine was distributed in the blood, liver, kidney, and intestine, and a maximum of 10.8% of administered piperine was found in these tissues at 6 h. The maximum concentrations of piperine in the blood, liver, kidney, and intestine at 6 h were 64.71 μg/whole blood, 96.62 μg/whole liver tissue, 91.75 μg/whole kidney tissue, and 2450.3 μg/whole intestine tissue, respectively. The concentrations of piperine in these tissues gradually reduced to 0.30% after 48 h and were not found after 96 h. About 3.64% of administered piperine was excreted in feces within 96 h, but no detectable amount of piperine was found in urine. The absorption of administered piperine was 96%. These findings suggest that the liver plays a key role in excretion of piperine (Suresh and Srinivasan 2010).

6.2.11 Terpenoids

6.2.11.1 Monoterpenoids

Catalpol **120**, an iridoid glucoside constituent of many *Catalpa* spp. and Chinese antidiabetic plant, *Rehmannia glutinosa*, has been found to have promising beneficial effects in protection against diabetes and its associated complications. The pharmacokinetics of catalpol in rat was investigated. After administration of a single oral dose of catalpol (50 mg/kg) in Wistar rats, the main pharmacokinetic parameters of plasma catalpol were as follows: $AUC_{0-\infty}$ of 69,520 ng h/ml, C_{max} of 23,318 ng/ml, T_{max} of 1.33 h, $t_{1/2}$ of 1.21 h, $MRT_{0-\infty}$ of 3.273 h, and $V_{d\ (1/F)}$ of 1.43 l/kg. The absolute bioavailability of catalpol was 66.7%. These results suggest that catalpol is quickly absorbed in plasma after oral administration (Lu et al. 2009). Another study reported the distribution of catalpol in the brain. After administration of a single intravenous dose of catalpol (6 mg/kg) in rats, catalpol was found to enter the brain through the blood-brain barrier (BBB) and absorbed in cerebrospinal fluid (CSF) and showed the ratio of AUC_{CSF}/AUC_{plasma} of 5.8%, $t_{1/2}$ of 1.5 h, and $MRT_{0-\infty}$ for CSF and plasma of 2.12 and 0.70 h, respectively. These findings suggest that catalpol exhibits neuroprotective effect by its distribution in the CSF of the brain (Wang et al. 2012). Another comparative pharmacokinetic study of catalpol in STZ-induced diabetic CKD (chronic kidney disease) rats and normal rats was reported. Administration of a single oral dose of *Rehmannia glutinosa* extract containing 37.3 mg/kg catalpol in both STZ-CKD rats and normal rats showed AUC_{0-t} of 1627.83 and 439.71 μg min/ml, C_{max} of 2.14 and 7.94 μg/ml, T_{max} of 54 and 60.5 min, and $t_{1/2}$ of 118.3 and 84 min, respectively. These findings support the renoprotective effect of catalpol in diabetic CKD rats (Zhao et al. 2015).

6.2.11.2 Sesquiterpenoids

Costunolide **10** and dehydrocostus lactone **493** are the main active constituents of Radix Aucklandiae (RA), the dried roots of *Aucklandia lappa* (Decen.). In Asian countries, RA has been widely used for the treatment of various digestive disorders, including loss of appetite, indigestion, diarrhea, and gastric ulcer-related abdominal pain. The active constituent costunolide has significant anti-ulcer, anticancer, and

antidiabetic activities. A comparative pharmacokinetic study of pure costunolide, a mixture of costunolide and dehydrocostus lactone, and RA extract in normal rats and RA extract in gastric ulcer rats was reported. After oral administration of a single dose of pure costunolide (84.4 mg/kg), a mixture of costunolide and dehydrocostus lactone (containing 84.4 mg/kg costunolide), RA extract (650 mg/kg containing 84.4 mg/kg costunolide) in normal rats ($n = 5$), and RA extract containing 84.4 mg/kg costunolide in gastric ulcer rats ($n = 5$), the following pharmacokinetic parameters of costunolide in plasma were observed: $C_{\max\ 1}$ of 0.052, 0.055, 1.30, and 0.75 μg/ml; $T_{\max\ 1}$ of 0.75, 0.25, 0.27, and 0.35 h; $t_{1/2}$ of 14.62, 11.74, 12.63, and 13.99 h; $C_{\max\ 2}$ of 0.106, 0.116, 1.15, and 0.95 μg/ml; $T_{\max\ 2}$ of 8.0, 6.0, 4.20, and 8.40 h; AUC_{0-t} of 1.23, 1.57, 14.80, and 19.84 μg/h/ml; MRT_{0-t} of 13.33, 12.51, 12.86, and 14.85 h; V_d of 1667.41, 1022.22, 95.26, and 84.46 l/kg; and CL of 78.88, 60.34, 5.26, and 4.45 l/h/kg, respectively. These findings suggest that compared to normal rats, the relative costunolide bioavailability in RA extract has changed significantly with respect to increased $t_{1/2}$, MRT_{0-t}, $T_{\max\ 2}$, and AUC_{0-t} and decreased V_d, *CL*, $C_{\max\ 1}$, and $C_{\max\ 2}$ values. Moreover, the presence of other constituents in RA extract alters the pharmacokinetic parameters of costunolide in plasma (Dong et al. 2018). Another study reported a comparative pharmacokinetic study of costunolide and dehydrocostus lactone in rats after intravenous administration. After administration of a single intravenous (i.v.) dose of costunolide and dehydrocostus lactone mixture (20 mg/kg each) in rats ($n = 6$), the pharmacokinetic parameters of costunolide and dehydrocostus lactone in rat plasma were: AUC_{0-t} of 3.11 and 1.37 μg h/ml, MRT_{0-t} of 1.49 and 1.26 h, $C_{\max}$ of 12.29 and 5.79 μg/ml, $t_{1/2z}$ of 1.16 and 2.33 h, V_d of 10.71 and 35.55 l/kg, and *CL* of 6.39 and 10.85 l/h/kg, respectively. Moreover, four metabolites of costunolide and six metabolites of dehydrocostus lactone were identified in plasma, urine, and feces of rats. These metabolites are S-cysteine conjugation, S-glutathione conjugation, *N*-acetylcysteine conjugation, and metabolites of two step sequential desaturation. These findings suggested that costunolide has higher bioavailability ($C_{\max}$ and AUC_{0-t} values) compared to that of dehydrocostus lactone. But the clearance and volume of distribution (V_d) of dehydrocostus lactone were much larger than that of costunolide. The short half-life of both costunolide and dehydrocostus lactone suggests their rapid elimination. The poor absorption of costunolide after oral administration is due to poor water solubility. The higher bioavailability of both costunolide and dehydrocostus lactone after i.v. administration suggests the i.v. administration of these sesquiterpenoid lactones is a better route for clinical use (Peng et al. 2014).

6.2.11.3 Diterpenoids

Andrographolide (AG) **335** is a major diterpenoid lactone constituent of *Andrographis paniculata*, which has been widely used in Chinese and Indian Ayurvedic medicine, for the treatment of various disorders, including gastric disorders, colds, influenza, cardiovascular diseases, and diabetes. AG has significant antidiabetic and cardioprotective effects. The pharmacokinetics of AG in rats and humans were investigated after oral and intravenous administration of an ethanolic *A. paniculata* extract (APE). After administration of a single dose of an 60% ethanolic APE (20 and 200 mg/kg bw containing 1 and 10 mg/kg AG) in rats

($n = 6$), the following pharmacokinetic parameters of AG in rat plasma were observed: $AUC_{0-\infty}$ of 7.09 and 15.07 μg h/ml, T_{max} of 2.41 and 1.67 h, C_{max} of 1.27 and 3.00 μg/ml, *CL* of 0.29 and 0.35 ml/min, $t_{1/2}$ of 2.4 and 2.9 h, K_{el} of 0.34 and 0.31/h, MRT of 4.71 and 4.78 h, and *F* (bioavailability, %) of 0.91 and 0.214, respectively. Meanwhile, intravenous administration of a single dose of APE (20 mg/kg containing 1 mg/kg AG) in rats ($n = 30$) showed the following pharmacokinetic parameters of AG in rat plasma: $AUC_{0-\infty}$ of 7.92 μg h/ml, $t_{1/2}$ of 1.31 h, MRT of 2.9 h, V_d of 0.27 l/kg, and *CL* of 0.24 ml/min. These findings suggested that AG was quickly and almost completely absorbed in blood after an oral dose of APE (20 mg/kg). But its bioavailability decreased fourfold on increasing a ten times higher dose of APE (250 mg/kg). Most probably, AG was metabolized extensively and the metabolism of AG was increased on increasing the dosing. At higher dose, a larger part of AG (about 55%) was bound to plasma proteins, and only a limited amount entered the cells causing poor bioavailability. AG reached the maximum concentration in plasma at 2 h and eliminated at the same rate at 3 h. The renal elimination of AG was less than 10% in both doses within 72 h. In humans, oral administration of a single dose of four Kan Jang tablets prepared from APE, equal to 20 mg of AG/human volunteer to human healthy volunteers ($n = 16$), showed maximum plasma AG level of 393 ng/ml, reached after 1.5–2 h, and half-life and mean residence time of 6.6 and 10.0 h, respectively. These comparative pharmacokinetic results of AG in both rats and humans are similar (Panossian et al. 2000). Another study reported the tissue distribution and pharmacokinetics of AG in rats after oral administration for 4 weeks. Oral administration of AG at a dose of 100 mg/kg/day to rats ($n = 8$) for 4 weeks showed the distribution of AG in different tissues. The highest concentration of AG was found in the kidney (156.12 ng/g of tissue) at 1 h, followed by the liver, spleen, and brain (21.26 ng/g), while the same concentration of AG was found in the heart and lung. The maximum concentration of156.12 ng/g of AG in the kidney at 1 h was gradually declined to 23.65 ng/g at 8 h and not found after 24 h, and similar trend was also observed in other tissues. Meanwhile, oral administration of APE at a dose of 133.33 mg/kg/day to rats for 4 weeks showed C_{max}, T_{max}, $t_{1/2\ el}$, K_{el}, and $AUC_{0-\infty}$ of 115.81 ng/ml, 0.75 h, 2.45 h, 0.29/h, and 278.44 ng h/ml, respectively (Bera et al. 2014).

Carnosic acid (CA) **106**, a diterpene constituent of rosemary (*Rosmarinus officinalis*), has several pharmacological activities, including antioxidant and antidiabetic activities. The pharmacokinetics of CA in rats was reported after administration of *R. officinalis* extract (ROE). Administration of a single intravenous dose of ROE containing 20.5 mg/kg CA in rats ($n = 4$) showed $AUC_{0-\infty}$ and $t_{1/2\ el}$ of 6.12 mg min/ml and 93 min, respectively. Meanwhile, administration of a single oral dose of ROE containing 64.3 mg/kg CA in rats ($n = 9$) showed $AUC_{0–6\ h}$, C_{max}, and T_{max} of 7.05 mg min/ml, 0.035 mg/ml, and 136.6 min, respectively, and bioavailability of 40.1% at 6 h. The recovery of CA in feces was 15.6% within 24 h after oral dosing. At 4 h of i.v. administration, the plasma CA was below the detection limit. These findings indicate that CA has poor absorption and rapid elimination in rats, possibly due to metabolism (Doolaege et al. 2011). Another study reported that after oral administration of CA at a dose of 90 mg/kg/twice a day

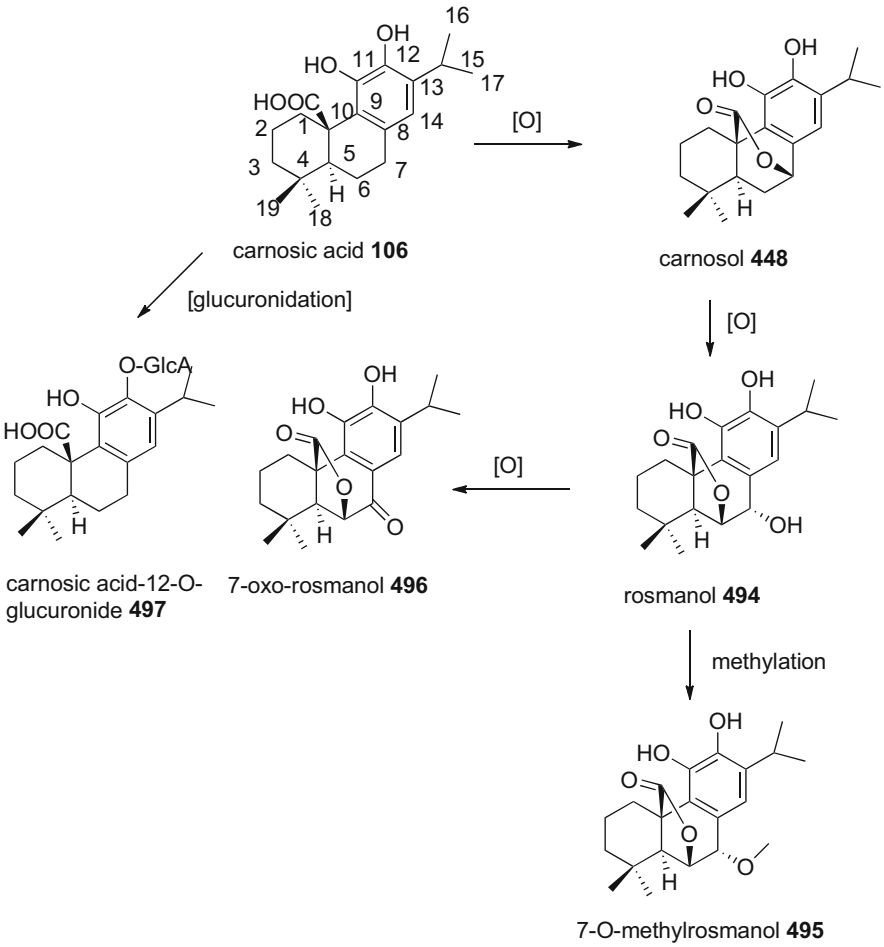

Scheme 6.3 Metabolism of carnosic acid in rats

to rats for 1 week, CA was metabolized to 18 metabolites. Among these metabolites, 12 were detected in urine and 6 in feces of rats. Out of 18 metabolites, 5 were identified as carnosol **448**, rosmanol **494**, 7-methylrosmanol **495**, 7-oxorosmanol **496**, and carnosic acid-12-*O*-β-D-glucurono-pyranoside **497** (Scheme 6.3). A large amount of CA glucuronide was found along with CA in rat plasma. Possibly, the presence of CA glucuronide in high concentration in rat plasma along with CA increases the bioavailability of CA after oral administration (Song et al. 2014).

6.2.11.4 Triterpenoids

Celastrol **78**, a pentacyclic triterpene constituent of Chinese medicinal herb, Thunder God vine (TGV) (*Trypterygium wilfordii* Hook F), has been shown to have potential anti-inflammatory, antitumor, and anti-obesity effects and a candidate for clinical

use. The pharmacokinetics of pure celastrol and TGV extract in gender-related female and male rats was reported. Administration of a single oral dose of celastrol (1000 μg/kg) and a single intravenous dose of celastrol (100 μg/kg) in female rats ($n = 6$) showed the pharmacokinetic parameters of celastrol as follows: C_{max} of 13.75 and 38.83 μg/ml, T_{max} of 3.00 and 0.083 h, $AUC_{0-\infty}$ of 135.50 and 79.35 μg h/l, $MRT_{0-\infty}$ of 14.11 and 9.46 h, $t_{1/2\ el}$ of 10.20 and 8.33 h, and *CL* of 11.29 and 0.45 l/h for oral and i.v. doses, respectively. Meanwhile, oral administration of a single dose of TGV tablets (1.5 tablets containing 534 μg/kg celastrol) in both female and male rats ($n = 7$) showed the following pharmacokinetic parameters of celastrol in rat plasma: C_{max} of 32.03 and 14.31 μg/l, T_{max} of 6.71 and 5.14 h, AUC_{0-t} of 379.49 and 188.17 μg h/l, $AUC_{0-\infty}$ of 443.52 and 221.87 μg h/l, MRT_{0-t} of 13.87 and 14.19 h, $MRT_{0-\infty}$ of 16.72 and 16.96 h, $t_{1/2\ el}$ of 10.02 and 8.38 h, and *CL* of 0.96 and 2.58 l/h, respectively. These findings indicated that the orally administered celastrol in rats was poorly absorbed into the systemic circulation, but its absorption could be increased by using celastrol containing TGV tablets. The absolute bioavailability of pure celastrol was 17.06%, which was increased to 94.19% on using TGV tablets containing the equivalent amount of celastrol. Moreover, female rats showed better absorption of celastrol than male rats. Possibly, the other constituents present in TGV tablets improve the bioavailability of celastrol by their synergistic effects (Zhang et al. 2012).

Ursolic acid (UA) **52**, an α-amyrin-type triterpene constituent, present in many plants, fruits, and vegetables, including *Eriobotyra japonica*, *Eugenia jambolana*, *Psidium guajava*, and *Rosmarinus officinalis*, as well as in apples, plums, pears, and other fruits, has a wide spectrum of biological activities, such as antiviral, anti-inflammatory, anticancer particularly breast cancer, anti-obesity, antiprotozoal (anti-trypanosomiasis), and antimicrobial activities. The pharmacokinetics of UA in rats was reported. After administration of a single intravenous dose of UA (1 mg/kg) and two oral doses of UA (20 and 50 mg/kg) in male rats ($n = 5$), the following pharmacokinetic parameters of UA in rat plasma were observed: C_{max} of 0.76, 0.33, and 0.50 μg/ml; T_{max} of N/A, 1.05, and 1.18 h; $t_{1/2\ el}$ of 2.61, 2.88, and 2.70 h; K_{el} of 0.28, 0.24, and 0.26/h; AUC_{0-t} of 2.83, 1.44, and 2.08 μg h/ml; $AUC_{0-\infty}$ of 2.99, 1.68, and 2.33 μg h/ml; V_d of 1279.46, 1488.35, and 1426.55 ml/kg; MRT of 4.05, 3.7, and 2.98 h; *CL* of 357.69, 357.14, and 368.29 ml/h/kg; $t_{1/2a}$ of -, 0.27, and 0.39 h; K_a of -, 4.12, and 1.96/h; *F* (bioavailability,%) of -, 2.80, and 1.55, for i.v. and two oral doses, respectively. These findings suggested that UA has poor oral bioavailability due to its poor aqueous solubility. The values for K_a and $t_{1/2a}$ suggested that UA was absorbed rapidly and linearly. The higher oral dose had lower bioavailability than that of lower oral dose. These results suggested that a new pharmaceutical formulation of UA is needed for improvement of its bioavailability (Alzate et al. 2018). Another study reported the metabolism of UA in mice. After administration of a single oral dose of UA (30 mg/kg) in male Kunming mice ($n = 6$), seven metabolites of UA were identified by the use of UPLC-Q/TOF method. Among these metabolites, two phase-I metabolites, α- and β-epoxides, of UA along with UA were identified in plasma, and five phase-II metabolites of UA, namely, glucuronide, glycine (Gly), and glutathione (GSH) conjugates of UA, were

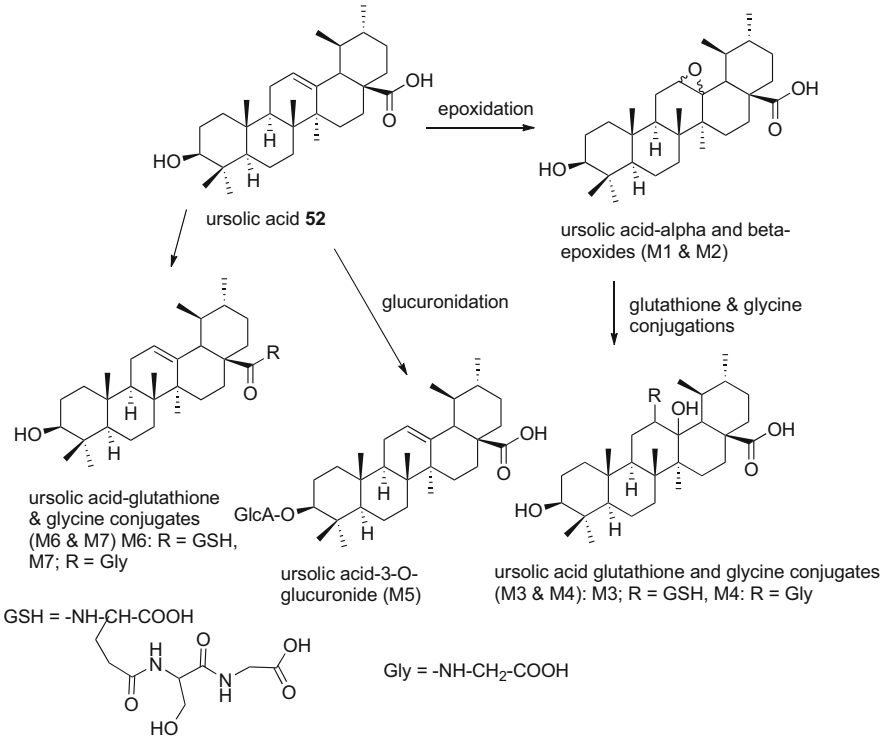

Scheme 6.4 Metabolism of ursolic acid in mice

identified in urine of mice. These metabolites were generated via olefin oxidation and conjugation with glucuronic acid, glycine, and glutathione (Scheme 6.4) (Hu et al. 2018). The tissue distribution of UA in rats was reported. After oral administration of a single dose of UA (10 mg/kg) in rats ($n = 5$), a wide tissue distribution of UA was observed at 1 h after oral dosing. The concentration of UA was highest in the lung followed by the spleen, liver, cerebrum, heart, and kidney. These findings suggested that the distribution of UA was in high concentrations in blood supply tissues such as the lung, spleen, and liver, and possibly, its distribution was dependent on blood flow and perfusion rate of the organ. The high distribution of UA in the lung and liver supports the curative effects of UA in respiratory and liver disorders. The lowest level of UA in the kidney demonstrates that the kidney does not play the key role in the excretion of UA (Chen et al. 2011).

Oleanolic acid (OA) **326** and maslinic acid (MA) **330** are major triterpene constituents of functional dietary olive (*Olea europaea*) oil (FOO) (about 40 mg/kg). Both OA and MA have anticancer, antioxidant, anti-inflammatory, antidiabetic, and cardioprotective activities. The pharmacokinetics of OA and MA in humans was reported. After oral intake of a single dose of 30 ml of FOO containing 4.7 mg of OA and 6.0 mg of MA along with 80 g of bread by healthy human male and female

volunteers ($n = 12$), the following pharmacokinetic parameters of OA and MA in human plasma were observed in a non-compartmental analysis method: C_{max} of 5.1 and 32.8 ng/ml, T_{max} of 4.0 and 3.0 h, $t_{1/2el}$ of 1.41 and 2.26 h, K_{el} of 0.50 and 0.37/h, $AUC_{0–10\ h}$ of 28.2 and 185.1 ng h/ml, and cumulative excretion fraction in urine, $f_{c0–10\ h}$ of 0.15 and 0.38%, for OA and MA, respectively. Meanwhile, after oral intake of the same dose of FOO (30 ml) by healthy human volunteers ($n = 12$), the pharmacokinetic parameters of MA observed in a bi-compartmental method were C_{max} of 32.8 ng/ml, T_{max} of 4 h, $t_{1/2a}$ of 0.7 h, K_a of 1.5/h, $t_{1/2el}$ of 16.3 h, K_{el} of 0.06/h, MAT of 1.1 h, $AUC_{0-\infty}$ of 387 ng h/ml, $V_{d(central)}$ of 97.8 l, and *CL* of 18.6 l/h, and amount of MA excreted in urine within 10 h was 3322 ng. These findings suggested that compartmental pharmacokinetic study of MA provided more accurate information on absorption, distribution, and elimination of MA. Moreover, the bioavailability of MA was about 7-fold higher than that of OA, despite only a difference of 1.3-fold higher in administered doses (De La Torre et al. 2020). The absolute bioavailability of OA and MA was 0.7% and 5.13%, respectively, as determined after administration of a single dose of OA and MA (50 mg/kg) in rats (Jeong et al. 2007; Sanchez-Gonzalez et al. 2014). The microemulsion formulation of OA in a self-microemulsifying drug delivery system (SMEDDS), composed of cremophor EL, ethanol, and ethyl oleate (50:35:15) mixture, was found to improve the oral bioavailability of OA by 5.07-fold compared to free form after oral administration of a single dose of 50 mg/kg in rats. The main pharmacokinetic parameters of OA were as follows: C_{max} of 209.80 and 77.60 ng/ml, T_{max} of 2 and 2.75 h, AUC_{0-t} of 1740.06 and 308.19 ng h/ml, and $AUC_{0-\infty}$ of 1775.26 and 350.13 ng h/ml, for SMEDDS-loaded OA and free OA dose, respectively (Yang et al. 2013).

Betulinic acid (BA) **207**, a lupane-type triterpene, present in many plants, including *Diospyros peregrina*, has various health benefits, including in the prevention of some cancers and diabetes. The pharmacokinetics and tissue distribution of BA in mice were reported. After administration of a single intraperitoneal dose of BA (500 mg/kg) in the skin of CD-1 mice, the following pharmacokinetic parameters of BA in mouse skin were observed: T_{max} of 3.90 h, C_{max} of 300.9 μg/ml, AUC of 3504 μg h/ml, $t_{1/2a}$ of 2.63 h, $t_{1/2\beta}$ of 20.2 h, and V_d of 0.61 l/kg. The distribution of BA in different tissues at 24 h after administration of BA (500 mg/kg) in mice was found with highest concentration of BA in perirenal fat tissue, and the concentrations of BA in other tissues were in the following descending order: ovary > spleen > mammary gland > uterus > liver > small intestine > lung > kidney > skin > heart > brain (Udeani et al. 1999).

6.2.12 Saponins

Dioscin (diosgenyl-2,4-di-*O*-α-L-rhamnopyranosyl-β-D-glucopyranoside) **84**, a steroid saponin constituent of many *Dioscorea* spp., has several health-promoting pharmacological activities, including antitumor, neuroprotective, antiviral, and antidiabetic activities. The dose-dependent pharmacokinetics of dioscin was investigated in rats. After administration of single intravenous doses of dioscin

(0.064 and 1.0 mg/kg) in rats, the following pharmacokinetic parameters of dioscin in rat plasma were observed: $AUC_{0-\infty}$ of 270 and 5194 ng h/ml, $t_{1/2a}$ of 0.37 and 0.38 h, $t_{1/2\beta}$ of 8.96 and 22.5 h, MRT of 12.5 and 31.5 h, *CL* of 4.67 and 3.49 ml/min/kg, and V_d of 3.75 and 6.60 l/kg, for 0.064 and 1.0 mg/kg doses, respectively. These results indicated that a significant decrease in clearance and a longer half-life elimination ($t_{1/2\beta}$) at higher dose of dioscin occurred for its removal from plasma because of a certain degree of saturation. After administration of single oral dose of dioscin (45 and 90 mg/kg) in rats, the following pharmacokinetic parameters of dioscin in rat plasma were found: C_{max} of 9.30 and 16.5 ng/ml, T_{max} of 19.4 and 16.1 h, $t_{1/2\beta}$ of 15.2 and 26.6 h, $AUC_{0-\infty}$ of 536 and 1002 ng h/ml, MRT of 40.1 and 47.0 h, CL of 1,500 and 1576 ml/min/kg, and V_d of 2.056 and 3632 l/kg, for 45 and 90 mg/kg doses, respectively. The absolute oral bioavailability for oral dose of 45 and 90 mg/kg of dioscin was 0.23% and 0.21%, respectively. These findings indicated that both C_{max} and AUC values of dioscin were increased at higher dose. In the analysis of tissue distribution of dioscin after i.v. dose of 1.0 mg/kg in rats, at 3 h, the higher concentrations of dioscin were found in the intestine and liver, followed by the lungs, stomach, and kidneys. After single oral dose of dioscin (90 mg/kg) in rats, at 3 h after administered dosing, the higher concentration of dioscin was observed in the stomach (2335 ng/g), followed by the liver and lungs (82.9 and 30.8 ng/g respectively). Possibly, dioscin underwent a prolonged absorption in the intestinal tract and a slow elimination from the organs, and only a small amount of dioscin was recovered in the bile. Dioscin and its aglycone diosgenin **87** are mainly excreted in feces. About 36.9% of i.v. dose and 25.8% of oral dose of dioscin are excreted in feces and urine within 24 h (Li et al. 2005). The study of metabolite profile in rats revealed that dioscin was metabolized rapidly by intestinal bacteria and hepatic enzymes, and eight metabolites of dioscin were identified in plasma, feces, and urine by application of UPLC-Q-TOF-MS. These metabolites were produced in phase I and phase II processes through oxidation, deglycosylation, and glucuronidation (Scheme 6.5) (Zhu et al. 2015).

Ginsenoside Rb1 **65**, a dammarane-type triterpene saponin, present in high concentrations in different parts, particularly in roots of Korean red ginseng (*Panax ginseng*) and American ginseng (*Panax quinquefolius*), has various health benefits, such as in the prevention of some forms of cancer and diabetes. A group of studies demonstrates that after oral intake of ginsenosides Rb1, Rb2 **459**, Rc **498,** and Rd **499**, compound K (20-*O*-β-D-glucopyranosyl-20(*S*)-protopanaxadiol) **500** (Fig. 6.2) was identified as major metabolite in human plasma. The pharmacokinetics of ginsenoside Rb1 and compound K in humans was investigated. After oral intake of a single dose of Korean red ginseng extract (KRGE) (9 g by each male Korean healthy adult subject containing 45.81 mg of Rb1), the following pharmacokinetic parameters of Rb1 and compound K in human plasma were observed: $AUC_{0-36\ h}$ of 102.3 and 110.7 ng h/ml, $AUC_{0-\infty}$ of 307.7 and 123.9 ng h/ml, C_{max} of 3.94 and 8.35 ng/ml, T_{max} of 8.70 and 12.20 h, and $t_{1/2\beta}$ of 58.47 and 7.82 h, for Rb1 and compound K, respectively. The compound K was detected in human plasma between 4 and 9 h after oral administration of KRGE. These results indicated that both C_{max} and $AUC_{0-36\ h}$ values of compound K were higher than that of Rb1.

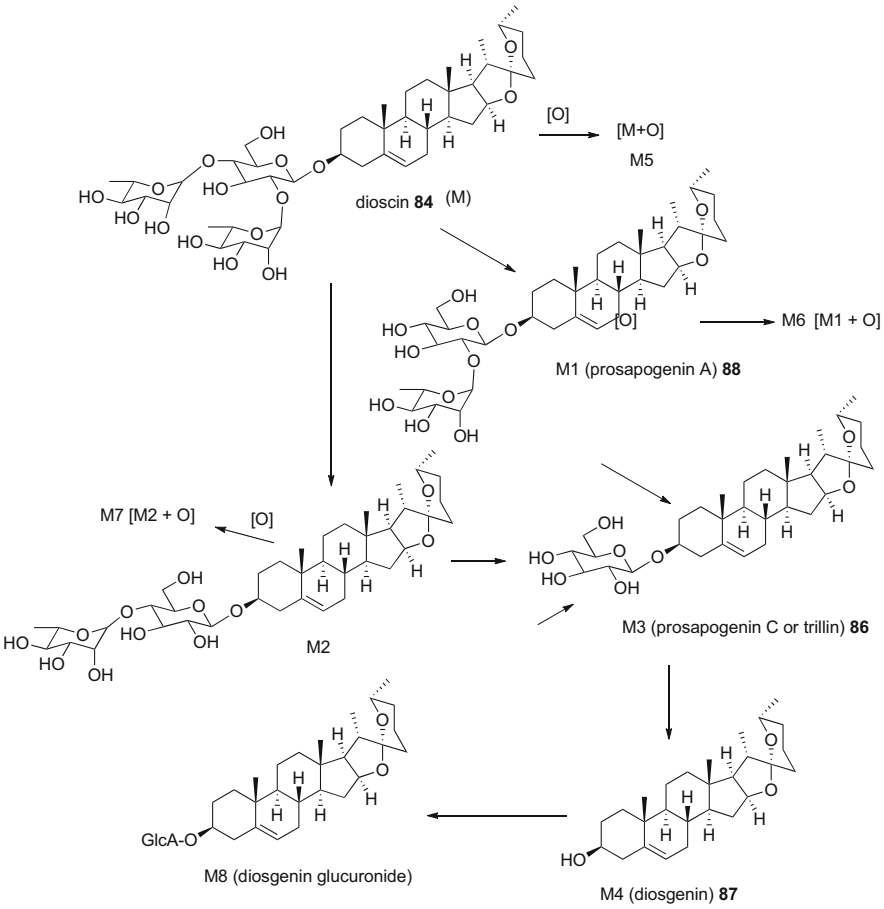

Scheme 6.5 Metabolism of dioscin in rats

Moreover, the elimination half-life ($t_{1/2\beta}$) of compound K was 7 times shorter than that of Rb1, and T_{max} of compound K was higher than that of Rb1. It suggested that the absorption of compound K in plasma is delayed because of its biotransformation by intestinal bacteria (Kim 2013). The tissue distribution of Rb1 analysis after administration of a single intravenous dose of Rb1 (5 mg/kg) in rats revealed that the concentrations of Rb1 in the kidney, heart, and liver were relatively high at 5 min and were 9.0, 5.3, and 2.9 μg/g, respectively, and declined gradually similar to that in serum. The concentration of Rb1 in the lung was maximum (5.0 μg/g) at 30 min to 1 h after administration of Rb1 and declined slowly. The detected concentrations of Rb1 in the brain and spleen were only less than 0.5 μg/g of tissue at 5 min after Rb1 administration but were not detectable at any time after that period (Odani et al. 1983).

Ginsenoside Rg1 **460**, a main triterpenoid saponin constituent of *Panax ginseng* roots, has been used frequently in many Asian countries for treatment of CNS, cardiovascular, endocrine, and immune systems disorders. The pharmacokinetics, tissue distribution, metabolism, and excretion of ginsenoside Rg1 in Wistar rats were investigated. After intravenous (i.v.) and oral dosing in rats, three metabolites of Rg1, namely, ginsenoside Rh1 **501**, 6-*O*-deglucosylated Rg1 (F1) **502**, and (20*S*)-protopanaxatriol (PPT) **503** (Fig. 6.2), were detected in rat plasma, bile, urine, and feces. After i.v. administration of a single dose of Rg1 (10 mg/kg) in rats ($n = 6$), the following pharmacokinetic parameters of Rg1, Rh1, and F1 were observed: C_{max} of N/D, 55.7, and 71.4 ng/ml; T_{max} of N/D, 5.32, and 6.88 h; $t_{1/2\alpha}$ of 0.37, 0.30, and 0.23 h; $t_{1/2\beta}$ of 1.82, 5.87, and 6.87 h; V_c of 0.021, 0.028, and 0.035 l/kg; *CL* of 0.037, 0.009, and 0.016 ml/h/kg; AUC_{0-t} of 1595.7, 597.5, and 805.6 ng h/ml; and MRT of 1.92, 5.99, and 7.13 h, for Rg1, Rh1, and F1, respectively. After oral administration of a single dose of Rg1 (150 mg/kg) in rats ($n = 6$), the following pharmacokinetic parameters of Rg1, Rh1, F1, and PPT in rat plasma were observed: C_{max} of 1,134.4, 584.6, 522.2, and 38.3 ng/ml; T_{max} of 0.92, 3.64, 5.17, and 7.30 h; $t_{1/2\alpha}$ of 0.14, 0.29, 0.22, and 0.20 h; $t_{1/2\beta}$ of 2.25, 6.73, 5.44, and 5.06 h; V_c/F of 0.008, 0.015, 0.020, and 0.027 l/kg; AUC_{0-t} of 2363.5, 4185.5, 3774.3, and 396.2 ng h/ml; and MRT of 2.68, 5.06, 6.65, and 5.33 h, for Rg1, Rh1, F1, and PPT, respectively. The maximum concentration of Rg1 in blood was reached at 5 min of post i.v. dosing of Rg1, and the concentration decreased rapidly and completely cleared within 4 h, while the maximum concentration of the metabolites in blood was detected at 1 h and decreased rapidly and cleared completely within 24 h. After oral dosing of Rg1, it was detected in the blood at 15 min, and mean C_{max} was observed at 1 h, and the concentration decreased very fast and cleared completely within 8 h, while after oral dosing of Rg1, its metabolites were detected in the blood at 3 h, and maximum concentrations were found within 8 h of post dosing and were still found after 24 h. After oral administration of Rg1, the AUC_{0-t} values of Rh1 and F1 were about 77% and 60% larger than that of Rg1, suggesting that the metabolites Rh1 and F1 were the dominant compounds in the blood after Rg1 dosing. Moreover, the $t_{1/2\beta}$ values of Rh1 and F1 in blood were more than 5 h in both i.v. and oral dosing of Rg1 and were larger than that of Rg1, indicating that both Rh1 and F1 were eliminated from the blood slowly. Analysis of the tissue distribution of Rg1 and its metabolites revealed that they were distributed in most of the tissues and their maximum concentrations were reached in the tissues between 4 and 6 h after i.v. dosing of Rg1. The maximum concentration of Rg1 was found in the liver (1134.7 ng/g) followed by the kidney (977.9 ng/g), spleen (523.0 ng/g), heart (424.0 ng/g), pancreas (367.6 ng/g), and lung (300.9 ng/g) and only a little amount in the brain (90.5 ng/g). Meanwhile, the maximum concentration of Rh1 was found in the liver (46.6 ng/g) followed by the kidney (43.5 ng/g), lung (38.4 ng/g), and heart (32.6 ng/g). The maximum concentration of F1 was found in the liver (73.6 ng/g), followed by the kidney (61.5 ng/g) and heart (36.4 ng/g). The total recovery of Rg1 and its metabolites in urine and feces were 51.31% and 47.46%, respectively. After i.v. dosing, the mean recovery of Rg1 in bile, urine, and feces were 60.77%, 27.95%,

and 7.64%, respectively. These findings indicated that both the liver and kidney played key roles in the elimination of Rg1 and its metabolites (Feng et al. 2010).

Ginsenoside Rg3 **461**, another major bioactive dammarane-type triterpenoid saponin constituent of *Panax ginseng* roots, has potential activity against breast cancer, obesity, and diabetes. A comparative pharmacokinetics of ginsenoside Rg3 and its major metabolite ginsenoside Rh2 **504** (Fig. 6.2) in rat was reported. After oral administration of a single dose of ginsenoside Rg3 (50 mg/kg) to normal Wistar rats ($n = 6$), the following pharmacokinetic parameters of ginsenoside Rg3 and ginsenoside Rh2 in rat plasma were observed: $AUC_{0–12\ h}$ of 219 and 11.5 mg h/l, $AUC_{0-\infty}$ of 326 and 14.9 mg h/l, C_{max} of 81.6 and 6.17 mg/l, T_{max} of 2.33 and 1.72 h, $t_{1/2\ ter}$ of 4.27 and 3.25 h, and *CL* of 67.3 and 1344 l/h/kg, for Rg3 and Rh2, respectively. These findings suggested that Rg3 has better absorption than Rh2, as evident from much higher C_{max} and $AUC_{0-\infty}$ values of Rg3 compared to that of Rh2. It indicates that Rg3 plays a major role in its pharmacological effects than its metabolite Rh2 (He et al. 2016).

6.2.13 Organosulfur Compounds

The organosulfur compounds of garlic (*Allium sativum*), namely, alliin **468**, allicin **469**, diallyl disulfide (DADS), and diallyl trisulfide (DATS), have several health benefits. In traditional medicine, garlic has been used for the treatment of various health disorders, such as in treatment of hypertension, hyperlipidemia, hypercholesterolemia, diabetes, thrombosis, and hepatic disorders (Gao et al. 2013). The pharmacokinetics of alliin, allicin, and vinyldithiines (2-vinyl-[4H]-1,3-dithiine and 3-vinyl-[4H]-1,2-dithiine) was reported. Oral administration of a single doses of ^{35}S-alliin, ^{35}S-allicin, and labeled vinyldithiines (8 mg/kg) in rats ($n = 3$) showed different pharmacokinetic behaviors in rat plasma. ^{35}S-alliin reached the maximum concentration in blood plasma within 10 min and eliminated from the blood almost completely after 6 h of administration. ^{35}S-Allicin and labeled vinyldithiines reached the maximum concentration in blood between 30 and 60 min and 120 min, respectively, and their concentrations in blood were still detected after 72 h. The mean total urinary and fecal excretion for ^{35}S-allicin and labeled vinyldithiines was 85.5% and 92.3%, of administered dose, respectively, after 72 h of administration (Lachmann et al. 1994).

Sulforaphane **471**, an organosulfur constituent of many cruciferous vegetables like broccoli, Brussels sprouts, and cabbage, exists as inactive form, glucosinolate, glucoraphanin. It has various health-promoting effects, including antitumor and antidiabetic effects. The absolute bioavailability and pharmacokinetics of sulforaphane in rat were determined. After administration of a single intravenous(i.v.) dose of sulforaphane (2.8 μM/kg equal to 0.5 mg/kg) and single oral doses (0.5 and 5.0 mg/kg) in rats ($n = 4$), the following pharmacokinetic parameters of sulforaphane in rat plasma were observed: $AUC_{0-24\ h}$ of 476, 392, and 1001 ng h/ml; C_{max} of N/D, 46.4, and 211.3 ng/ml; T_{max} of N/D, 0.5, and 1.0 h; K_{ab} of -, 5.78, and 2.57/h; K_{el} of 0.011, 0.012, and 0.028/h; $t_{1/2}$ of 65.6, 62.2, and 27.3 h; *CL* of 265, 264, and 263 ml/

h; V_d of 102, 95, and 42 l/kg; and F (bioavailability,%) of 100, 82.4, and 21.0, for i.v. and oral doses, respectively. These findings indicated that sulforaphane was absorbed rapidly at low doses, and its oral absolute bioavailability was dose-dependent and was high (82.4%) at low dose and low (21.0%) at high dose. Possibly, at high dose, sulforaphane underwent modest first-pass metabolism to glutathione and mercapturate metabolites by intestinal and hepatic enzymes. Moreover, the C_{max} value did not rise proportionately to the increased dose. The values of K_{ab}, $t_{1/2}$, and V_d were decreased at higher oral dose. The plasma concentration of sulforaphane almost remained unaltered between 6 and 24 h following i.v. and oral administration at low doses. Possibly the high protein binding of sulforaphane rendered its unavailability for elimination from plasma through metabolism and excretion. These results demonstrate that at dietary low oral doses, sulforaphane achieves rapid absorption and high absolute bioavailability compared to high oral doses (Hanlon et al. 2008).

6.3 Summary and Future Perspectives

A variety of natural products from different classes, isolated from various natural sources, such as plants, marine seaweeds and animals, mushrooms, and microorganisms, have been shown to have positive impact on human health. Many of these phytochemicals/phytogenic compounds, namely, flavonoids, tannins, phenolic acids, alkaloids, terpenoids, saponins, polysaccharides, organosulfur compounds, have been found effective in the treatment of obesity, diabetes, and associated complications like vascular diseases and other chronic diseases. In literature, most of their pharmacokinetic studies and metabolic transformations have been focused in animal models, and only a little information on their bioavailability, biotransformations, and bioactivity in humans is available. These phytochemicals are mainly absorbed in the gastrointestinal tract, and the process of absorption in the small intestine depends on several factors including polarity and nature of skeletal structure and substitution pattern of the phytochemicals. In case of flavonoids, the highest bioavailability was found for isoflavones, followed by flavonols, flavanones, and flavonol glycosides. Flavonoid glycosides and terpenoid glycosides (saponins) are deglycosylated by intestinal microbiota prior to intestinal absorption, whereas aglycones can freely penetrate through epithelial cell membrane. The absorbed phytochemicals are transported to the liver, where they undergo extensive phase I and phase II metabolism to generate different types of oxidation, reduction, and hydrolysis and skeletal rings-cleavage products and conjugates, such as glucuronides, sulfates, and methylated derivatives. Many of these metabolites have better biological activities than the parent phytochemicals. The liver is the crucial organ responsible for the first-pass metabolic process. The intestinal mucosa and microbiota, kidney, and other tissues are also involved in the metabolic process. In most cases, the conjugation reactions with glucuronic acid and/or sulfate are the main types of metabolic pathways of the phytochemicals. Uridine-5′-phosphate glucuronosyl transferases (UGTs) catalyze glucuronidation of a variety of functional groups, including –OH, –COOH, $–NH_2$, and –SH groups. Sulfation occurred by

sulfotransferases, SULTs, namely, SULT1A1, SULT1A2, and others. Most of the pharmacokinetic and metabolic studies of phytochemicals have been reported in animal models without determining the concentrations of the metabolites in different metabolic tissues. These insufficient scientific data on pharmacokinetic and metabolite study greatly hamper in evaluating the effective doses of these phytochemicals in humans for the treatment of obesity and diabetes. Possibly, multi-omics technology will be useful to get the relevant information for the formulation of personalized medicine for effective treatment.

For application of herbal medicine in commercial scale for the treatment of obesity, diabetes, and other associated complications, it is necessary to pay more attention in studies on the activity and effective doses of these phytochemicals and the concentrations of their active metabolites in disease-affected tissues in humans.

References

Abd El-Mohsen M, Bayele H, Kuhnle G et al (2006) Distribution of [^{3}H]-*trans*-resveratrol in rat tissues following oral administration. Br J Nutr 96:62–70

Almeida L, Vaz-da-Silva M, Falcao A et al (2009) Pharmacokinetic and safety profile of *trans*-resveratrol in a rising multiple-dose study in healthy volunteers. Mol Nutr Food Res 53:S7–S15

Alzate MAH, Filho MAFN, Franchin TB et al (2018) Kinetic disposition of ursolic acid in rats. Pharm Biomed Res 4:25–31

Anukunwithaya T, Poo P, Hunsakunachai N et al (2018) Absolute oral bioavailability and disposition kinetics of puerarin in female rats. BMC Pharmacol Toxicol 19:25

Baba S, Osakabe N, Natsume M et al (2004) Orally administered rosmarinic acid is present as the conjugated and/or methylated forms in plasma, and is degraded and metabolized to conjugated forms of caffeic acid, ferulic acid and m-coumaric acid. Life Sci 75:165–178

Bera R, Milan Ahmed SK, Sarkar L et al (2014) Pharmacokinetic analysis and tissue distribution of andrographolide in rat by a validated LC-MS/MS method. Pharm Biol 52:321–329

Chanda S, Bashir M, Babbar S et al (2008) In vitro hepatic and skin metabolism of capsaicin. Drug Metab Dispos 36:670–675

Chen L, Lee MJ, Li H et al (1997) Absorption, distribution and elimination of tea polyphenols in rats. Drug Metab Dispos 25:1045–1050

Chen Q, Luo S, Zhang Y et al (2011) Development of a liquid chromatography-mass spectrometry method for the determination of ursolic acid in rat plasma and tissue: application to the pharmacokinetic and tissue distribution study. Anal Bioanal Chem 399:2877–2884

Courtois A, Atgie C, Marchal A et al (2018) Tissular distribution and metabolism of *trans*-ε-viniferin after intraperitoneal injection in rat. Nutrients 10:1660

Cui HX, Hu YN, Li JW et al (2019) Preparation and evaluation of antidiabetic agents of berberine organic acid salts for enhancing the bioavailability. Molecules 24:103

De La Torre R, Carbo M, Pujadas M et al (2020) Pharmacokinetics of maslinic and oleanolic acids from olive oil-effects on endothelial function in healthy adults: a randomized, controlled, dose-response study. Food Chem 322:126676

Dong S, Ma LY, Liu YT et al (2018) Pharmacokinetics of costunolide and dehydrocostus lactone after oral administration of *Radix aucklandiae* extract in normal and gastric ulcer rats. J Asian Nat Prod Res 20:1055–1063

Doolaege EHA, Raes K, De Vos F et al (2011) Absorption, distribution and elimination of carnosic acid, a natural antioxidant from *Rosmarinus officinalis*, in rats. Plant Foods Hum Nutr 66:196–202

Erlund I, Kosonen T, Alfthan G et al (2000) Pharmacokinetics of quercetin from quercetin aglycone and rutin in healthy volunteers. Eur J Clin Pharmacol 56:545–553
Feng L, Wang L, Hu C et al (2010) Pharmacokinetics, tissue distribution, metabolism, and excretion of ginsenoside Rg1 in rats. Arch Pharm Res 33:1975–1984
Feng X, Wang K, Cao S et al (2021) Pharmacokinetics and excretion of berberine and its nine metabolites in rats. Front Pharmacol 11:594852
Gao C, Jiang X, Wang H et al (2013) Drug metabolism and pharmacokinetics of organosulfur compounds from garlic. J Drug Metab Toxicol 4:159
Guo N, Zhu M, Han X et al (2014) The metabolism of salidroside to its aglycone *p*-tyrosol in rats following the administration of salidroside. PLOS One 9:e103648
Gutierres VO, Campos ML, Arcado CA et al (2015) Curcumin pharmacokinetic nd pharmacodynamic evidences in streptozotocin-diabetic rats support the antidiabetic activity to be via metabolite (s). Evid Based Complement Alternat Med 2015:678218
Han Y, Tan TMC, Lim L (2008) In vitro and in vivo evaluation of the effects of piperine on P-gp function and expression. Toxicol Appl Pharm 230:283–289
Hanlon N, Coldham N, Gielbert A et al (2008) Absolute bioavailability and dose-dependent pharmacokinetic behaviour of dietary doss of the chemopreventive isothiocyanate sulforaphane in rat. Br J Nutr 99:559–564
He F, Sun XL, Su Y et al (2016) Comparative pharmacokinetics of ginsenoside Rg3 and ginsenoside Rh2 after oral administration of ginsenoside Rg3 in normal and Walker 256 tumor-bearing rats. Pharmacogn Mag 12:21–24
Hu Z, Wang Z, Liu Y et al (2015) Metabolic profile of salidroside in rats by ultraperformance liquid chromatography coupled with quadrupole time of flight mass spectrometry and high-performance liquid chromatography coupled with quadrupole-linear ion trap mass spectrometry. J Agric Food Chem 63:8999–9005
Hu X, Shen Y, Yang S et al (2018) Metabolite identification of ursolic acid in mouse plasma and urine after oral administration by ultra-high performance liquid chromatography/quadrupole time-of-flight mass spectrometry. RSC Adv 8:6532–6539
Hung WL, Chang WS, Lu WC et al (2018) Pharmacokinetics, bioavailability, tissue distribution and excretion of tangeretin in rat. J Food Drug Anal 26:849–857
Jeong DW, Kim YH, Kim HH et al (2007) Dose-linear pharmacokinetics of oleanolic acid after intravenous and oral administration in rats. Biopharm Drug Dispos 28:51–57
Kammalla AK, Ramasamy MK, Inampudi J et al (2015) Comparative pharmacokinetic study of mangiferin after oral administration of pure mangiferin and US patented polyherbal formulation to rats. AAPS PharmSciTech 16:250–258
Kapetanovic IM, Muzzio M, Huang Z et al (2011) Pharmacokinetics, oral bioavailability, and metabolic profile of resveratrol and its dimethylether analog, pterostilbene, in rats. Cancer Chemother Pharmacol 68:593–601
Kim HK (2013) Pharmacokinetics of ginsenoside Rb1 and its metabolite compound K after oral administration of Korean red ginseng extract. J Ginseng Res 37:451–456
Kim JS, Ha TY, Ahn J et al (2014) Analysis and distribution of esculetin in plasma and tissues of rats after oral administration. Prev Nutr Food Sci 19:321–326
Kwak JH, Kim Y, Staatz CE et al (2021) Oral bioavailability and pharmacokinetics of esculetin following intravenous and oral administration in rats. Xenobiotica 51:811–817
Lachmann G, Lorenz D, Radeck W et al (1994) The pharmacokinetics of the S35 labeled labeled garlic constituents alliin, allicin and vinyldithiine. Arzneimittel-forschung 44:734–743
Lee MJ, Wang ZY, Li H et al (1995) Analysis of plasma and urinary tea polyphenols in human subjects. Cancer Epidemiol Biomarkers Prev 4:393–399
Lei F, Xing DM, Xiang L et al (2003) Pharmacokinetic study of ellagic acid in rat after oral administration of pomegranate leaf extract. J Chromatogr B 796:189–194
Li K, Tang Y, Fawcett JP et al (2005) Characterization of the pharmacokinetics of dioscin in rat. Steroids 70:525–530

Li X, Yu C, Lu Y et al (2007) Pharmacokinetics, tissue distribution, metabolism, and excretion of depside salts from *Salvia miltiorrhiza* in rats. Drug Metab Dispos 35:234–239

Lu R, Gu Y, Si D et al (2009) Quantification of catalpol in rat plasma by liquid chromatography/electrospray ionization tandem mass spectrometry and its pharmacokinetic study. J Chromatogr B 877:3589–3594

Manach C, Morand C, Gil-Izquierdo A et al (2003) Bioavailability in humans of the flavanones hesperidin and narirutin after ingestion of two doses of orange juice. Eur J Clin Nutr 57:235–242

Meech R, Mackenzie PI (1997) Structure and function of uridine diphosphate glucuronosyltransferases. Clin Exp Pharmacol 24:907–915

Nakagawa K, Miyazawa T (1997) Absorption and distribution of tea catechin, (-)-epigallocatechin-3-gallate, in the rat. J Nutr Sci Vitaminol 43:679–684

Nakamura T, Tokushima T, Kawabata K et al (2012) Absorption and metabolism of 4-hydroxyderricin and xanthoangelol after oral administration of *Angelica keiskei* (Ashitaba) extract in mice. Arch Biochem Biophys 521:71–76

Odani T, Tanizawa H, Takino Y (1983) Studies on the absorption, distribution, excretion and metabolism of ginseng saponins. III. The absorption, distribution and excretion of ginsenoside Rb1 in the rat. Chem Pharm Bull 31:1059–1066

Pan MH, Huang TM, Lin JK (1999) Biotransformation of curcumin through reduction and glucuronidation in mice. Drug Metab Dispos 27:486–494

Panossian A, Horhannisyan A, Mamikonyan G et al (2000) Pharmacokinetic and oral bioavailability of andrographolide from *Andrographis paniculata* fixed combination Kan Jang in rats and human. Phytomedicine 7:351–364

Peng Z, Wang Y, Gu X et al (2014) Study on the pharmacokinetics and metabolism of costunolide and dehydrocostus lactone in rats by HPLC-UV and UPLC-Q-TOF/MS. Biomed Chromatogr 28:1325–1334

Qi W, Zhao T, Yang WW et al (2011) Comparative pharmacokinetics of chlorogenic acid after oral administration in rats. J Pharm Anal 1:270–274

Sahu PK, Sharma A, Rayees S et al (2014) Pharmacokinetic study of piperine in Wistar rats after oral and intravenous administration. Int J Drug Deliv 6:82–87

Sanchez-Gonzalez M, Colom H, Lozano-Mena G et al (2014) Population pharmacokinetics of maslinic acid, a triterpene from olives, after intravenous and oral administration in rats. Mol Nutr Food Res 58:1970–1979

Setchell KDR, Brown NM, Zimmer-Nechemias L et al (2014) Metabolism of secoisolariciresinol-diglucoside the dietary precursor to the intestinally derived lignan enterolactone in humans. Food Funct 5:491–501

Shia CS, Tsai SY, Lin JC et al (2011) Steady-state pharmacokinetics and tissue distribution of anthraquinones of Rhei Rhizoma in rats. J Ethnopharmacol 137:1388–1394

Song Y, Yan H, Chen J et al (2014) Characterization of *in vitro* and *in vivo* metabolites of carnosic acid, a natural antioxidant, by high performance liquid chromatography coupled with tandem mass spectrometry. J Pharm Biomed Anal 89:183–196

Suresh D, Srinivasan K (2010) Tissue distribution & elimination of capsaicin, piperine & curcumin following oral intake in rats. Ind J Med Res 131:682–691

Tan XS, Ma JY, Feng R et al (2013) Tissue distribution of berberine and its metabolites after oral administration in rats. PLoS One 8:e77969

Tsang C, Auger C, Mullen W et al (2005) The absorption, metabolism and excretion of flavan-3-ols and procyanidins following the ingestion of a grape seed extract by rats. Br J Nutr 94:170–181

Udeani GO, Zhao GM, Shin YG et al (1999) Pharmacokinetics and tissue distribution of betulinic acid in CD-1 mice. Biopharm Drug Dispos 20:379–383

Viskupicova J, Ondrejovic M, Sturdik E (2008) Bioavailability and metabolism of flavonoids. J Food Nutr Res 47:151–162

Wang W, Li CY, Wen XD et al (2009) Plasma pharmacokinetics, tissue distribution and excretion study of 6-gingerol in rat by liquid chromatography-electrospray ionization time-of –flight mass spectrometry. J Pharm Biomed Anal 49:1070–1074

Wang Q, Xing M, Chen W et al (2012) HPLC-APCI-MS/MS method for the determination of catalpol in rat plasma and cerebrospinal fluid: application to an in vivo pharmacokinetic study. J Pharm Biomed Anal 70:337–343

Wang JJ, Miao XL, Chen JY et al (2016a) The pharmacokinetics and tissue distribution of honokiol and its metabolites in rats. Eur J Drug Metab Pharmacokinet 41:587–594

Wang Y, Xie G, Liu Q et al (2016b) Pharmacokinetics, tissue distribution, and plasma protein binding study of chicoric acid by HPLC-MS/MS. J Chromatogr B 1031:139–145

Wang X, Qian Y, Li X et al (2021) Rapid determination of rosmarinic acid and its two bioactive metabolites in the plasma of rats by LC-MS/MS and application to a pharmacokinetic study. Biomed Chromatogr 35:e4984

Yang CS, Chen L, Lee MJ et al (1998) Blood and urine levels of tea catechins after ingestion of different amounts of green tea by human volunteers. Cancer Epidemiol Biomarkers Prev 7:351–354

Yang CY, Hsiu SL, Wen KC et al (2005) Bioavailability and metabolic pharmacokinetics of rutin and quercetin in rats. J Food Drug Anal 13:244–250

Yang R, Huang X, Dou J et al (2013) Self-microemulsifying drug delivery system for improved oral bioavailability of oleanolic acid: design and evaluation. Int J Nanomed 8:2917–2926

Zeng M, Yang L, He D et al (2017) Metabolic pathways and pharmacokinetics of natural medicines with low permeability. Drug Metab Rev 49:464–476

Zeng X, Su W, Zheng Y et al (2019) Pharmacokinetics, tissue distribution, metabolism, and excretion of naringin in aged rats. Front Pharmacol 10:34

Zhang J, Li CY, Xu MJ et al (2012) Oral bioavailability and gender-related pharmacokinetics of celastrol following administration of pure celastrol and its related tablets in rats. J Ethnopharmacol 144:195–200

Zhang Y, Li L, Lin L et al (2013) Pharmacokinetics, tissue distribution, and excretion of salidroside in rats. Planta Med 79:1429–1433

Zhao L, Liu A, Sun M et al (2011) Enhancement of oral bioavailability of puerarin by polybutylcyanoacrylate nanoparticles. J Nanomater 2011:126562

Zhao M, Qian D, Liu P et al (2015) Comparative pharmacokinetics of catalpol and acteoside in normal and chronic kidney disease rats after oral administration of *Rehmannia glutinosa* extract. Biomed Chromatogr 29:1842–1848

Zhou Y, Zhou T, Pei Q et al (2014) Pharmacokinetics and tissue distribution study of chlorogenic acid from Lonicerae Japonicae Flos following oral administration in rats. Evid Based Complement Alternat Med 2014:979414

Zhu H, Xu JD, Mao Q et al (2015) Metabolic profiles of dioscin in rats revealed by ultra-performance liquid chromatography quadrupole time-of-flight mass spectrometry. Biomed Chromatogr 29:1415–1421

7 Advances in Nanoencapsulated Phytomedicines (Phytochemicals and Their Extracts) for the Treatment of Obesity, Diabetes, and Their Associated Complications

Biswanath Dinda and Subhajit Dinda

7.1 Introduction

In traditional medicine of different countries, several herbal formulations are prescribed for the treatment of obesity, diabetes, and its associated complications including cardiovascular diseases, diabetic nephropathy, diabetic retinopathy, and diabetic neuropathy. In the prescribed herbal formulations, a variety of antioxidant phytochemicals have been found to reduce fat mass and body weight by suppressing adipogenesis and lipid accumulation; increasing lipolysis, thermogenesis, and energy expenditure via fatty acid oxidation; and reducing oxidative stress and inflammation in major metabolic tissues, such as the adipose tissue, skeletal muscle, and liver of obese humans and rodents. In addition, these phytochemicals reduce hyperglycemia in diabetic humans and rodents through improvement of glucose uptake from the plasma, glycogen synthesis in the liver and skeletal muscle, suppression of hepatic glucose production, and enhanced insulin secretion from pancreatic beta cells and insulin action in major metabolic tissues. Usually, these herbal medicines are prescribed at high doses for long-term consumption for the amelioration of these metabolic disorders because of low efficacy, poor aqueous solubility, stability, bioavailability, and target specificity of the phytochemicals present in herbal medicines. Long-term use of herbal medicines at high doses results in unpleasant adverse effects and toxicity in patients. All these factors have restricted the clinical applications of these herbal medicines. To overcome the problems of phytochemicals in clinical applications, these phytochemicals and plant extracts have been encapsulated into biocompatible and biodegradable nanoparticles/nanocarriers to increase their solubility and stability, enhance their bioavailability,

B. Dinda (✉)
Department of Chemistry, Tripura University, Suryamaninagar, Tripura, India

S. Dinda
Department of Chemistry, Government Degree College, Kamalpur, Dhalai, Tripura, India

B. Dinda (ed.), *Natural Products in Obesity and Diabetes*,
https://doi.org/10.1007/978-3-030-92196-5_7

protect them from metabolic degradation in the body, prolong their systemic circulation time, and thereby enhance their anti-obesity and antidiabetic efficacy at relatively lower doses compared to free phytochemicals and plant extracts. In this context, the existing research findings on the efficacy of some phytochemicals and plant extracts in nanoencapsulated forms in combating obesity, diabetes, and its comorbidities are summarized in this chapter.

7.2 Nanocarriers Used in the Delivery of Phytomedicines

In the last two decades, different fabricated nanoparticles have been applied as carriers of phytochemicals and plant extracts to improve their aqueous solubility, stability, bioavailability, circulation time, and target specificity to disease tissues and thereby to increase their therapeutic efficacy in treatment of obesity, diabetes, and its comorbidities at low doses. Major characteristics of nanoparticles are their size, zeta potential (surface charge), polydispersity index (homogeneity size), physical and chemical stabilities, encapsulation efficiency, and loading capacity. These characteristics of nanoparticles in phytomedicines regulate their stability, bioavailability, and metabolism in in vivo system (Blanco et al. 2015). The most common types of nanocarriers, such as lipid-based nanocarriers (nanoliposomes, solid-lipid nanoparticles, nanostructured lipid carriers) and polymeric-based nanocarriers (polymeric nanoparticles, micelles, nanoemulsions) (Fig. 7.1) (Goktas et al. 2020), are widely used for delivery of bioactive phytochemicals and dietary nutrients.

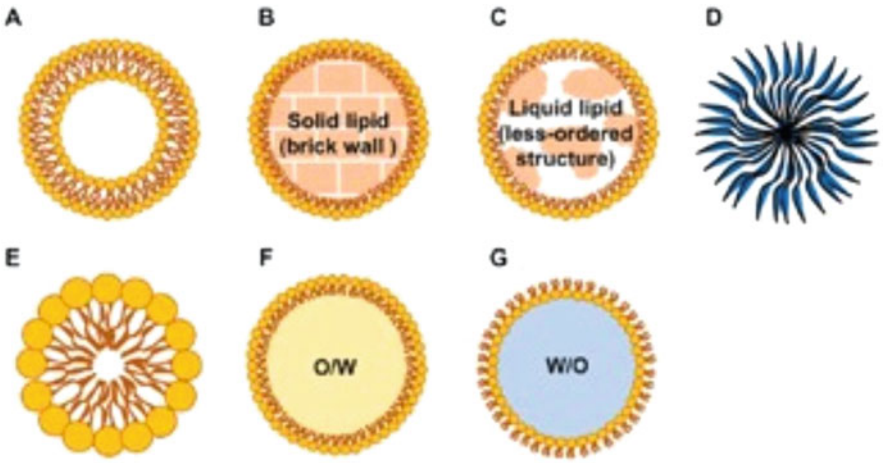

Fig. 7.1 Schematic structures of biodegradable and biocompatible nanoparticles: (**a**) liposome, (**b**) solid-lipid nanoparticle (SLN), (**c**) nanostructured lipid carriers (NLC), (**d**) polymeric nanoparticle, (**e**) micelle, (**f**) nanoemulsion, oil in water (O/W), and (**g**) nanoemulsion, water in oil (W/O). Adapted from Goktas et al. (2020) with permission of American Chemical Society. Copyright (2020) American Chemical Society

(a) **Nanoliposomes**
Nanoliposomes are nanosized vesicles composed of phospholipid (e.g., phosphatidylcholine) bilayers entrapping aqueous compartments. The word liposome derives from Greek words *lipos* (fat) and *soma* (structure), meaning a fatty envelope encapsules internal aqueous compartment. The phospholipids (PCs) with a hydrophilic head and two fatty acid tails self-organize in a lipid bilayer structure in an aqueous solution. These nanoliposomes are synthesized by sonication, extrusion, freeze-thawing, ether injection, and multifluidization (using high force technology). Due to presence of both lipid and aqueous phases in the structure of lipid vesicles, these liposomes can be utilized in entrapment, delivery, and release of water-soluble, lipid-soluble, and amphiphilic compounds. Stability of liposomes can be improved by coating the surface of vesicles with some polymers, such as polyethylene glycol (PEG) or chitosan, or using cationic or anionic ingredients in the structure of liposomes, or employing a stabilizing agent, cholesterol, or glycol. The application of charged ingredients in liposome structure reduces aggregation and precipitation of the vesicles and results in increased stability of the liposomal suspension. In general, liposomal particles having zeta potential values greater than +30 mV or lower than –30 mV possess prolong electrostatic stability. Moreover, phase transition temperature (T_c) of the liposome vesicles affects the pharmacokinetics of the encapsulated drugs. Hence, liposome preparations are carried out at 10 °C higher than the T_c of PC (Reza Mozafari et al. 2008; Mozafari 2010).

(b) **Solid-lipid nanoparticles (SLNs)**
Solid-lipid nanoparticles (SLNs) contain a solid hydrophobic lipid core matrix having hydrophobic tails of phospholipids, and the active pharmaceuticals remain in the matrix. The key ingredients of SLNs are lipids, emulsifier, drug, and an adequate solvent system. The lipids used in SLNs are surfactant stabilized and are solid at both physiological and room temperature. Lipids are mainly fatty acids, fatty esters, fatty alcohols, triglycerides, and partial glycerides. Ionic and nonionic polymers (e.g., pluronic F-68 and F-127), surfactants, and organic salts are used as emulsifiers. SLNs are spherical in shape with diameter range of 50–1000 nm. These nanoparticles are a good choice for hydrophobic drugs. SLNs are more stable than liposomes and are less toxic than polymeric nanoparticles. The major advantage of SLNs is that it provides increased stability of the drugs. The major potential disadvantage of SLNs is the poor drug loading capacity due to limited solubility of drugs in lipid melt (Duan et al. 2020).

(c) **Nanostructured lipid carriers (NLCs)**
Nanostructured lipid carriers (NLCs) are lipid-based nanoparticles containing an unsaturated solid-lipid core that improves the loading of highly lipophilic drugs, protects them from degradation, and enhances their stability. The unsaturated solid-lipid matrix core is made up with a mixture of blended solid and liquid lipid and an aqueous phase containing a surfactant or a mixture of surfactants. Typically, solid lipids are mixed with liquid lipids in a ratio of 70:30 to 99.1: 0.1 and the surfactant content in the range 1.5–5.0% (w/v). The high-pressure

homogenization process is the preferred method for preparation of NLCs. In this process, hot surfactant solution is added to the blended and melted lipids containing the drug (at about 10 °C above the melting temperature of the drug), and the resulting microemulsion is subsequently homogenized under high pressure and cooled. Most commonly long-chain fatty acids or their esters are used as solid lipid, triglycerides or lecithins are used as liquid lipid, and polysorbates or polyoxyethylene stearate are used as surfactants. The average particle size of NLCs is in the range less than 300 nm. NLC encapsulation of drugs is mainly used for oral, dermal, and intravenous administration of drugs. Encapsulation of quercetin in NLCs increased the aqueous solubility of quercetin by 1000-fold compared to free quercetin (Sun et al. 2014; Beloqui et al. 2016).

(d) **Polymeric nanoparticles**

Several polymers in the form of solid colloidal nanoparticles of size range 10–100 nm serve as an excellent vehicle for delivery of both hydrophilic and hydrophobic drugs to the site of interest. Polymeric nanoparticles (PLNs) not only deliver the drug to a particular site but also deliver the drug at a controlled rate to the disease cell. They have longer clearance time, which means a small amount of drug is sufficient to show better therapeutic efficacy. The drugs are encapsulated within the polymeric matrix or adsorbed or conjugated to the surface by covalent bonds. The most commonly used synthetic biodegradable polymers include polylactic acid (PLA), polyethylene glycol (PEG), poly-lactic-co-glycolic acid (PLGA), poly-cyanoacrylate (PCA), and poly-ε-caprolactone (PCL), and natural polymers include gelatin (emulsifying agent), alginate, chitosan, and agarose. The PLNs are usually prepared by emulsification-diffusion, nanoprecipitation, and solvent-evaporation methods (Reis et al. 2006; Sur et al. 2019).

(e) **Micelles**

Micelles are colloidal amphiphilic phospholipid monolayers in which the head group faces the outside and the hydrophobic tails form the micelle core. Micelles are used as nanocarriers for water-insoluble drugs. Usually, amphiphilic copolymers, i.e., polymers having both hydrophobic block and hydrophilic block, are commonly used as micelle-forming polymers. Conjugates of soluble copolymers, such as polyethylene glycol-phosphatidyl ethanolamine conjugate (PEG-PE) are frequently used as micelle-forming polymers. Specific targeting ligands can be grafted on the micelle surface to generate "targeting micelles" for increased uptake of disease cells. Major advantages of micelles are ease of synthesizing and long circulation time and stability, and disadvantages include low encapsulation efficiency and loading capacity of drugs (Torchilin 2007).

(f) **Nanoemulsions**

Nanoemulsions are lipid-biopolymer-based colloidal mixture of two immiscible liquids, oil and water, stabilized by surfactants and cosurfactants. When oil is dispersed into droplets through the aqueous phase, it is referred to as oil-in-water (O/W) emulsions. On the contrary, if an aqueous solution is dispersed in oil phase, it is referred as water-in-oil (W/O) emulsions. Most of the O/W-type

nanoemulsions are selected for oral administration of hydrophobic phytochemicals. In these nanoemulsions, the oil droplets exhibit sizes in the range of 10–300 nm. These nanoemulsions are prepared by high-energy emulsification methods (high-energy stirring, ultrasonic emulsification, high-pressure homogenization, and membrane emulsification) and low-energy emulsification methods (phase inversion temperature, emulsion inversion point, and spontaneous emulsification) (Anton and Vandamme 2011; Jaiswal et al. 2015).

(g) **Metallic nanoparticles**
Different types of metallic nanoparticles, such as gold, silver, copper, selenium, zinc and titanium nanoparticles, and carbon nanotubes, are also used for active or passive delivery of phytochemicals.

7.3 Nanoencapsulated Phytochemicals

7.3.1 Flavonoids

Quercetin (Q) **23**, a flavonoid constituent of many fruits and vegetables, has been found to exhibit different pharmacological activities including antioxidant, anticancer, antidiabetic, and diabetic nephroprotective activities. However, poor aqueous solubility, low bioavailability, and short half-life of quercetin restricted its clinical applications. To overcome these problems, quercetin-loaded polymeric nanoparticles (QPNs) were prepared using polymer, poly(ethylene glycol)-*block*-(poly(ethylenediamine-1-glutamate)-*graft*-poly-(ε-benzyloxy carbonyl-1-lysine)) (PEG-*b*-(PEGL-*g*-PZLL)). In vitro, QPNs released quercetin 15.23% at 4 h, 71.15% after 3 days, and 85.43% after 5 days, showing biphase release of quercetin. Pharmacokinetic study of QPNs in rats after oral administration of a single dose (10 mg/kg) showed maximum concentration of quercetin in plasma (C_{max} 17.85 μg/ml), at T_{max} of 8 h, and decreased to baseline after 5 days, whereas oral administration of a single dose of free quercetin (10 mg/kg) in rats showed maximum quercetin concentration in plasma, C_{max} 26.78 μg/ml, at T_{max} of 2 h, and decreased to baseline at 10 h, suggesting that the release of quercetin from QPNs was substantially sustained for longer period compared to free quercetin administration. Both QPNs and free quercetin on administration (10 mg/kg, every 5 days in a week, and 10 mg/kg/day, respectively, abdominal subcutaneous injection) to STZ-induced diabetic nephropathy (DN) in rats for 8 weeks improved renal function by reduction of the levels of serum glucose, lipid profile, urea nitrogen, and creatinine and suppression of the expression levels of inflammatory factor ICAM-1 and inflammatory cell infiltration marker protein $CD11b^+$ in renal tissues of diabetic rats, but the effects of QPN-treated group were better than free quercetin-treated diabetic rats. For instance, QPN-treated group reduced serum creatinine level to 178.93 μM/l compared to 213.56 and 289.16 μM/l in free quercetin-treated group and diabetic control group, respectively. Similarly, QPN group decreased urinary protein excretion remarkably to 15.79 mg/24 h, compared to 28.15 mg/24 h in free quercetin-treated group. These findings indicate that QPNs improve renal function more efficiently

compared to free quercetin in diabetic rats through increased bioavailability of quercetin (Tong et al. 2017). In another study, encapsulation of quercetin in alginate and succinyl chitosan core-shell nanoparticles improved both bioavailability and hypoglycemic effect of quercetin compared to free quercetin treatment in diabetic rats. The quercetin-loaded succinyl chitosan(SCS)/alginate (ALG) nanoparticles (Q-SCS/ALGNs) have an average particle size of 91.6 nm, zeta potential in the range of –19.83 to –35.55 mV, polydispersity index (PI) of 0.436–0.671, and encapsulation efficiency (EE) of 95%. In vitro, in stimulated gastric fluid (SGF), these nanoparticles released 16–27% of quercetin at pH 1.2 after 2 h of administration, whereas in pH 6.8 of SGF, it released 88–95% of quercetin, but at intestinal pH 7.4, it released quercetin at moderate rate due to electrostatic repulsion between the ionized acid groups. In diabetic rats, both free quercetin and Q-SCS/ALGNs on oral administration at the dose of 100 mg/kg bw reduced blood glucose level (BGL) and the levels of serum TC, TG, ALT, AST, and ALP, compared to diabetic control group, but the effects of Q-SCS/ALGNs were better than that of free quercetin-treated group. These core-shell corona nanoparticles are biodegradable and nontoxic to humans. Hence, these nanoparticles could be useful in clinical trials for diabetes (Mukhopadhyay et al. 2018). Quercetin-loaded Soluplus micelles (QSMs) increased the bioavailability and antidiabetic effect of quercetin. Soluplus is a triblock copolymer consisting of polyvinylcaprolactam (PCL)-polyvinyl acetate (PVAc)-polyethylene glycol (PEG) units and is capable to encapsulate the hydrophobic drugs. QSMs have particle size in the range of 85–108 nm, EE of 70.7%, PDI of 0.271, zeta potential of –12.30 mV, and drug loading capacity of 8.33%. In vitro, these micelles released quercetin slowly, 6.8% at initial 8 h and 28.75% within 24 h, compared to release of quercetin of 49.84% from free quercetin solution at 8 h. These results indicate that QSMs exhibit sustained release property of quercetin. Pharmacokinetic study of QSMs in rats showed higher bioavailability of quercetin (about 10.7 times higher) compared to free quercetin solution (plasma C_{max} 4.83 vs. 0.45 μg/ml). For evaluation of anti-diabetic efficacy of QSMs in diabetic rats, oral treatment of QSMs and free quercetin (50 mg/kg/day, for 14 days), QSMs treated group reduced serum glucose level and increased insulin secretion and the activity of antioxidant enzymes SOD and CAT in pancreas and kidney, more efficiently compared to free quercetin-treated diabetic rats (Singh et al. 2018).

Naringenin **199**, a major flavanone constituent of grapes and many citrus fruits including oranges, lemons, and tangerines, has anti-inflammatory, anticancer, hepatoprotective, and antidiabetic activities. However, its poor aqueous solubility and low bioavailability restrict its clinical applications. Naringenin (N)-loaded chitosan (CS)/alginate (ALG) core-shell polymeric nanoparticles (NCS-ALGNs) exhibited naringenin entrapment of 91.4% with loading capacity of 15.9% and pH-dependent slow and sustained release of naringenin. In vitro, these nanoparticles released maximum 15% of naringenin at pH 1.2 after 2 h of incubation, whereas at pH 7.4, more than 90% of naringenin was released in a slow sustained fashion. These NCS-ALGNs have an average particle size in the range of 150–300 nm and zeta potential of –26.3 to –38.2 mV. This higher negative surface charge supported

higher stability of these nanoparticles. Both NCS-ALGNs and free naringenin on oral treatment at a daily dose of 50 mg/kg bw of naringenin to STZ-induced type 1 diabetic rats for 19 days reduced blood glucose and the levels of serum TC and TG in diabetic rats. However, the effects of NCS-ALGN-treated group were better than free naringenin-treated diabetic rats. Moreover, NCS-ALGN treatment reduced the blood glucose level toward normal up to 27 days after the treatment, whereas free naringenin treatment reduced the blood glucose level up to 21 days of treatment. Furthermore, NCS-ALGNs protected the pancreatic β-cells and liver tissues and reduced the free iron content in hemoglobin, more efficiently compared to free naringenin treatment. These findings indicate that NCS-ALGNs improve both hypoglycemic and hypolipidemic effects of naringenin in diabetic animals through long-acting release of naringenin (Maity et al. 2017). Liposomal nanoformulation of naringenin enhanced the bioavailability of naringenin by 13.44-fold compared to free naringenin after oral administration in rats and increased distribution of naringenin in the liver. However, the efficacy of these nanoliposomes of naringenin has not yet explored (Wang et al. 2017b).

Myricitrin (myricetin 3-*O*-rhamnoside) **92**, a flavonol glycoside, present in many plants including *Myrica rubra*, *M. esculenta, Manikara zapota*, and *Eugenia uniflora*, has been reported to possess hepatoprotective, antidiabetic, antinociceptive, anxiolytic, and antioxidant activities. However, its poor bioavailability due to extensive metabolism and hydrolysis by intestinal and hepatic enzymes and bacteria hampers its clinical applications. Encapsulation of myricitrin (M) in solid-lipid nanoparticles (MSLNs) improved bioavailability and antioxidant and hypoglycemic potentials of myricitrin in both animal and cellular models of diabetes. These MSLNs were prepared by mixing an aqueous solution of myricitrin in a melting lipid phase of a mixture of campritol and oleic acid. These MSLNs have an average particle size of 76.1 nm, zeta potential of –5.51 mV, EE of 56.2%, and encapsulation capacity (EC) of 5.62%. In vitro, these nanoparticles released myricitrin of 1.44%, 8.32%, 27.18%, and 50.34% at 1 h, 4 h, 8 h, and 24 h, respectively. MSLNs on oral treatment (10 mg/kg of myricitrin/day) to STZ-NA-induced diabetic mice for 4 weeks showed significant hypoglycemic effect in diabetic mice by reduction of plasma glucose and HOMA-IR levels and increased plasma insulin level. Moreover, these MSLNs increased glycogen content and GLUT4 protein expression in the skeletal muscle of diabetic mice. In addition, these MSLNs increased the pancreatic β-cell mass and protected β-cells from apoptosis by increasing the activity of CAT and the level of total antioxidant capacity (TAC) in the pancreas. In high glucose exposed C2C12 myotubes, these MSLNs protected the cells from apoptosis by increasing the expression of antiapoptotic gene Bcl2 and decreasing the expression of proapoptotic gene Bax and increasing the activities of antioxidant enzymes, SOD and CAT. This antidiabetic effect of MSLNs was similar to that of metformin-treated (200 mg/kg) diabetic mice. These findings indicate that myricitrin in nanoencapsulation exhibits hypoglycemic effect at a low dose (Ahangarpour et al. 2018).

Baicalin **352**, a major flavonoid glycoside of *Scutellaria baicalensis* rhizome, has several pharmacological activities including anticancer and antidiabetic activities.

Despite these pharmacological functions, the poor bioavailability of baicalin has restricted its clinical applications. To overcome this problem, baicalin is encapsulated in biodegradable and biocompatible nanostructured lipid carriers to enhance its bioavailability and antidiabetic efficacy. Baicalin (B)-loaded nanostructured lipid carriers (BNLCs) were prepared by using baicalin, precirol ATO5 (glyceryl palmitosterate), miglyol 812 (medium-chain triglycerides), and pluronic F68 surfactant (polyoxyethylene-polyoxypropylene block polymer) in high-speed stirring method. These nanostructured lipid carriers have an average particle size of 92 nm, zeta potential of –31.35 mV, and an EE of 85.4% of baicalin. In vitro in dialysis diffusion method, BNLCs released 65% of baicalin at 4 h and almost complete drug (80%) at 12 h, whereas more than 90% of baicalin was released at 4 h from free baicalin solution. Both free baicalin and BLNCs on oral treatment (200 mg baicalin/kg bw/day, i.g.) to STZ plus HFD-induced diabetic rats for 4 weeks showed antidiabetic effect by reduction of FBG and the levels of plasma HbA1c, TC, and TG in diabetic rats. However, the effects of BNLCs were much better than that of free baicalin-treated diabetic rats. For instance, BNLCs reduced FBG (7.03 mM/l against 9.7 mM/l of free baicalin-treated group) and reduced plasma HbA1c level (15.26 absorbance/10 g protein against 19.92 absorbance/10 g protein of free baicalin-treated group) (Shi et al. 2016).

Scutellarin **352a**, a flavonoid glycoside constituent of Chinese herb *Erigeron breviscapus*, has been extensively used for treatment of retinal diseases. However, low oral bioavailability and low aqueous solubility of scutellarin restrict its therapeutic applications. To improve oral bioavailability of scutellarin (S), its nanomicelles (NMs) were prepared using biocompatible amphiphilic polymer, chitosan-deoxycholic acid derivative, and vitamin B12 (CS-DC-VB12). These S-CS-DC-VB12NMs have an average particle size of 182 nm, zeta potential of +16.5 mV, and drug loading capacity of 13%. Pharmacokinetic study of these nanomicelles in rats showed an increased bioavailability of scutellarin by two- to threefold compared to free scutellarin solution, as evident from plasma $AUC_{0-\infty}$ 22.096 ng/ml h against 6.419 ng/ml h from free scutellarin solution. Moreover, elimination half-life of scutellarin was also increased by 44.31% compared to free scutellarin solution. These scutellarin nanomicelles on oral treatment (40 mg scutellarin/kg/day) to diabetic retinopathy (DR) in rats for 8 weeks improved retinal function by inhibiting retinal neovascularization through increased retinal blood flow velocity and downregulation of the expression of angiogenesis proteins, VEGF, VEGFR2, and von Willebrand factor (vWF) in retinas compared to free scutellarin treatment group (40 mg/kg/day). Accumulating evidence demonstrates that vWF proteins regulate angiogenesis and inflammation for leukocyte adhesion to endothelial cells in retinas, whereas VEGF and its receptor 2, VEGFR2, promote endothelial proliferation, migration, and sprouting in retinal neovascularization. Hence, nanomicelles of scutellarin have potential application in treatment DR (Wang et al. 2017a).

Epigallocatechin 3-*O*-gallate (EGCG) **35**, a major bioactive catechin constituent of green tea and other teas as well as present in many fruits and nut including apples, blueberries, grapes, and peanut, has several health benefits in cancer, heart diseases,

obesity, and diabetes, among others. Available evidence demonstrates that EGCG is a more efficient radical scavenger compared to vitamins E and C. However, poor bioavailability, 0.1% in humans and less than 1.0% in research animals, hampers its bioefficacy. To improve the bioavailability, stability, and shelf life of EGCG, encapsulation of EGCG (E) in nanoliposomes (NLipos) was prepared using synthetic phospholipid component, (*N*-carbonyl-methoxypolyethylene glycol)-2000-(1,2-distearoyl-sn-glycero-3-phosphoethanolamine-Na-salt) (MPEG-2000-DSPE), cholesterol, and an aqueous EGCG solution. These ENLipos and free EGCG on oral administration at a dose of 25 mg/kg bw/day to rats for two consecutive days before STZ administration in diabetic rats improved both liver and kidney functions by the reduction of the levels of plasma glucose, MDA, NO_x, AST, ALT, MMP-2, and MMP-9 and enhanced activity of antioxidant enzymes, CAT, GSH, and TOC level in plasma of diabetic rats. The effects of EGCGNLipos were much better than the free EGCG-treated diabetic rats. Accumulating evidence demonstrates that both MMP-2 and MMP-9 proteins play key roles in deposition of atherosclerotic plaque and endothelial dysfunction and diabetic macrovascular complications. Therefore, ENlipos could be useful in management of diabetic complications (Bulboaca et al. 2020). Several research results indicate that more than 50% of cardiovascular disease (CVD)-related death is caused by deposition of atherosclerotic plaques in arteries from diabetic complications. Inflammatory chemokine MCP-1 stimulates the migration of inflammatory monocytes to the intimal layer of arteries, and these monocytes in the intimal layer of arteries, on activation, express the receptor CD36 for uptake of cholesterol-rich oxLDL and receiving excess oxLDL form foam cells, which are the hallmark of atherosclerosis. A phospholipid, 1-(palmitoyl)-2-(5-keto-6-octene-dioyl)-phosphatidylcholine (KOdiA-PC), a CD36-targeted ligand, has been identified in oxLDL, and it had a high binding affinity to CD36 receptor and is actively involved in CD36-mediated uptake of oxLDL from the intimal macrophage colony in the injury site to reduce lesion severity in atherosclerosis in arteries. Therefore, uptake of oxLDL from intimal macrophage colony through CD36 receptor binding ligand is a promising avenue for treatment of atherosclerosis and CVD. An EGCG-loaded CD36-targeted ligand-bound (LB) nanoliposomes (NLipos) were synthesized using soy phosphatidylcholine, kolliphor HS15 surfactant, alpha-tocopheryl acetate, KOdiA-PC, and EGCG. These E-LB-NLipos have an average particle diameter of 108 nm, ZP of –20.3 mV, PDI of 0.18, loading capacity of 12%, and EF of 96%. In vitro, these nanoliposomes showed sustained EGCG release property, released EGCG of 200 μg, 100 μg, 50 μg, 40 μg, and 30 μg at the first, second, third, fourth, and fifth 2-h period, respectively, whereas free EGCG exhibited a complete release (100%) in the initial 2-h period and no EGCG was detected in the dialysis bag after 2 h. In vitro, in LPS-treated human monocytic THP-1 cells, these E-LB-NLipos at the concentration of 40 μg/ml significantly reduced MCP-1 secretion from the cells, compared to free EGCG treatment, but failed to reduce the cholesterol content of THP-1 cells derived from macrophages. Moreover, these nanoliposomes in phorbol myristate acetate (PMA)-induced differentiated THP-1 cells decreased the macrophage level through increased binding with macrophages. Therefore, specific CD36 receptor-ligand-bound EGCG

nanoliposomes could be effective to enhance the activity of EGCG in treatment of diabetic-related atherosclerosis (Zhang et al. 2016a). Encapsulation of EGCG in natural polymeric nanoparticles consisting of chitosan and polyaspartic acid improved bioavailability of EGCG and exhibited pH-dependent EGCG release profile in stimulated GI tract. These polymeric nanoparticles, E-CS-PAANs on oral administration to rabbits, reduced foam cell deposition in the arteries more efficiently compared to free EGCG treatment. These E-CS-PAANs decreased the deposition area to 16.9% compared to 42.1 and 65.3% in free EGCG and blank nanoparticle-treated rabbits, respectively (Hong et al. 2014). A group of evidence demonstrates that in diabetic retinas, several integrins including $\alpha_v\beta_3$ are expressed in high levels in retinal endothelial cells to stimulate ocular angiogenesis process for the development of neovascularization (NV) in the cornea. Synthetic arginine-glycine-aspartic acid (RGD) peptides have strong binding affinity to $\alpha_v\beta_3$ and block $\alpha_v\beta_3$-mediated reduction of blood flow in vascular area through cellular uptake and thereby prevent NV formation in cornea. EGCG loaded in RGD-ligand-bound polymeric nanoparticles consists of natural polymer gelatin (G), EGCG (E), and conjugate of hyaluronic acid (H) with RGD peptide ligand. These RGD-ligand-bound polymeric nanoparticles of EGCG (GEH-LBNs) were used as eye drops to evaluate the efficacy of EGCG in treatment of corneal NV in mouse model. These GEH-LBNs have particle size of average diameter of 168.9 nm, ZP of +19.7 mV, PDI of 0.25, and EF of 95%. In vitro, these nanoparticles exhibited a slow release pattern, released about 30% of EGCG after 30 h. In vitro, in HUVECs, these GEH-LBNs in low concentration (20 μg/ml) more effectively inhibited the proliferation and migration of HUVECs, compared to GEH and free EGCG solution. Moreover, surface plasmon resonance (SPR) assay showed a stronger SPR signal due to a high number of surface particles compared to GEH and free EGCG solution, suggesting strong binding of the ligand with $\alpha_v\beta_3$ integrin in HUVECs. Application of these ligand-bound nanoparticles as eye drops twice daily on alkali-burned cornea in mice for 7 days showed less and thinner vessel formation in the cornea of mice compared to free EGCG-treated group. Therefore, these vascular endothelial cell-integrin-target-specific ligand-bound nanoparticles could be used in treatment of NV in the cornea (Chang et al. 2017). Nanoemulsions of tea polyphenols (TPNE) in corn oil and polysorbate 8 increased the bioaccessibility of EGCG, whereas it greatly decreased the bioaccessibilities of EGC, EC, and GCG after oral administration in rats. Pharmacokinetic study of TPNE after oral administration in rats revealed that maximum plasma concentration of EGCG was lowered (C_{max} 166.7 μg/l against 258.8 μg/l of free EGCG solution), but the area under plasma concentration-time curve (AUC_{0-t}) of EGCG was increased (17.1 mg/l against 13.3 mg/l of free EGCG solution) (Peng et al. 2018).

Silybin **352b**, major flavonolignan constituent of silymarin, has been used in the treatment of diabetes and hepatic disorders. Poor water solubility (0.4 mg/ml) and low bioavailability restrict its clinical applications. Natural chitosan (CS)-coated silybin (Sb)-loaded polymeric PLGA nanoparticles (CS-Sb-PNs) were prepared using triblock copolymer pluronic F-127 as stabilizer in solvent diffusion method. These CS-Sb-PNs have an average PS of 229.7 nm, ZP of +21 mV, PDI of 0.124,

and EF of 92.11% of Sb. In vitro, these PNs released Sb in pH-dependent manner. At pH 7.4, these PNs released Sb initially in fast rate up to 8 h and then in a steady and sustained manner over a period of 120 h releasing 31% of Sb. CS-Sb-PNs and free Sb on intraperitoneal treatments (50 mg/kg/day of Sb) to STZ-induced diabetic rats for 28 days exhibited significant antidiabetic, antioxidant, and hypolipidemic effects by reduction of FBG level and the levels of serum HbA1c, fructosamine, TC, TG, and MDA and increased the levels of serum insulin, hepatic glycogen content and antioxidant enzymes, SOD, CAT, and GSH in diabetic rats, while the effects of CS-Sb-PNs were better than that of free Sb-treated group. Moreover, CS-Sb-PNs improved pancreatic β-cell regeneration more effectively compared to free Sb-treated group. Therefore, these polymeric nanoparticles of Sb have better antidiabetic, antioxidant, and hypolipidemic effects compared to free Sb because of enhanced bioavailability (Das et al. 2014).

7.3.2 Stilbenoids

Trans-Resveratrol **47**, a polyphenolic stilbenoid constituent of various berries, red grapes, and other plant foods, has several health benefits against obesity, obesity-related insulin resistance, inflammation, and hyperlipidemia. It exhibits anti-obesity effect in diabetic obese animals by inhibition of lipogenesis and increased lipolysis, fatty acid oxidation, mitochondrial biogenesis, and energy expenditure through AMPK activation and enhanced expression of SIRT1, UCP1, and PGC1α. However, its low aqueous solubility (<0.1 mg/ml), low trivial bioavailability (plasma peak concentration, $C_{max} < 10$ μM after oral administration of *t*-resveratrol at high dose), low chemical stability, and anti-obesity bioefficacy restrict its clinical trials in humans. To overcome these problems, *t*-resveratrol-loaded nanolipid carriers (R-NLCs) were synthesized using *t*-resveratrol (R) and a mixture of soy L-α-phosphatidylcholine (PC), kolliphor HS15, and α-tocopherol acetate in sonication method. Moreover, *t*-resveratrol-loaded nanoliposomes (R-NLipos) were also synthesized by using a mixture of t-resveratrol, soy PC, and cholesterol in membrane extrusion method. Among these nanos, R-NLipos were relatively more stable than R-LNCs. These R-NLCs and R-NLipos have an average particle size of 140 nm and 100 nm, PDI of 0.084 and 0.140, and ZP of –19 mV and –28 mV, respectively. In vitro, native R showed rapid release behavior, while R-NLCs and R-NLipos exhibited steady slow release behavior for a long time. After 1 h, about 0.17 mg, 0.05 mg, and 0.02 mg of R were released from dialysis bags containing native R, R-NLipos, and R-NLCs, respectively. After 2 h, accumulative release of native R reached a plateau, while R was continuously released from R-NLipos and R-NLCs in 10-h period. In 3T3-L1 white adipocytes, at low concentration (5 μM), free t-resveratrol (native R), R-NLCs, and R-NLipos decreased the expression of white marker gene, and insulin-like growth factor-binding protein 3 (IGFBP3) and increased the expression of browning marker genes, PPARγ, UCP1, PRDM16, and PGC1α in both basal and isoproterenol (ISO)-stimulated conditions, while these three forms of R only increased the expression of beige marker gene CD137

under ISO-stimulated conditions. However, both R-NLCs and R-NLipos showed better anti-obesity effects by suppression of IGFBP3 expression and higher expression of browning marker genes in 3T3-L1 cells compared to that of native R. Possibly, these nanoparticles of *t*-resveratrol improved bioavailability of *t*-resveratrol to increase their bioefficacy (Zu et al. 2018). Resveratrol-loaded nanoencapsulation in polymer, poly-(d,l-lactide co-glycolic acid) (PLGA) (R-PNs), exhibited remarkably high EF of 97.25% and drug loading capacity of 14.9% and has an average particle size of 176 nm and ZP of –22.6 mV. These R-PNs enhanced stability, aqueous solubility, and bioactivity of R compared to native R in reduction of cellular proliferation and intracellular lipid accumulation in high oleic acid exposed steatosis in HepG2 cells (Wan et al. 2018). *T*-Resveratrol-loaded solid-lipid nanoparticles (R-SLNs) were prepared using *t*-resveratrol (R) and a molten lipid matrix of sorbitol, S100 (hydrogenated soybean lecithin) and S154 (hydrogenated palm oil). These R-SLNs have an average particle size of 248 nm, ZP of –16.5 mV, PDI of 0.42, and EF of 79.9% of R. In vitro, these R-SLNs released about 70% of R after 6 and 1 h in neutral and acidic pH conditions. Afterward, a sustained slow release behavior was observed up to 10 h. In STZ-NA-induced diabetic rats, both native R and R-SLNs on oral treatment (10 mg R/kg/day) for 1 month showed antidiabetic effect by reduction of FBG, levels of serum insulin, HOMA-IR, and MDA and increased TAC and reduced TOS (total oxidant status) levels in adipose and muscle tissues of diabetic rats compared to diabetic control group. But the effects of R-SLNs were better than native R-treated group. Moreover, both native R and R-SLNs increased GLUT4 expression and the expression of SNARE proteins, SNAP23, STX4, and VAMP2, in adipose and muscle tissues of diabetic rats, but the effects of R-SLNs in the skeletal muscle were much higher than those of native R-group. Emerging evidence demonstrates that SNARE proteins, synaptosomal-associated protein 23 (SNAP23), syntaxin 4 (STX4), and vesicle-associated membrane protein 2 (VAMP2) play an important role in membrane trafficking of GLUT4 into the cell membrane in both adipose and muscle tissues. In diabetic humans and animals, their expression levels are decreased causing insulin resistance. These results indicate that nanoformulated R-SLNs improve antidiabetic effect of R through improvement of insulin resistance in adipose and muscle tissues via regulating the expression of SNAP23, STX4, and VAMP2 proteins (Mohseni et al. 2019).

7.3.3 Curcuminoids

Curcumin **9**, a major polyphenolic yellow pigment of Asian spice, turmeric (*Curcuma longa*) rhizomes, has a variety of pharmacological activities in prevention of inflammatory-related diseases, such as cardiovascular diseases, diabetes, rheumatoid arthritis, Alzheimer disease, multiple sclerosis, and cancer. However, very low aqueous solubility (0.6 μg/ml) and rapid metabolism of curcumin by hepatic enzymes result in poor bioavailability in plasma and restrict clinical applications of curcumin. Oral administration of 3.6–8.0 g of curcumin in humans resulted in

peak plasma curcumin concentrations of 0.004–0.644 μg/ml. Similarly, peak plasma concentration of curcumin, C_{max} 1.35 μg/ml, was observed at 1 h, after oral administration of a single dose of 2 g/kg curcumin in rats (Goktas et al. 2020). To improve stability and bioavailability of curcumin, curcumin (C)-loaded nanomicelles (C-NMs) were prepared using pluronic® copolymers. Pluronics, triblock copolymers consisting of two poly(ethylene oxide) (PEO) chains and a central block of poly (propylene oxide) (PPO) block, have emulsifying and surfactant properties. These C-NMs have an average particle diameter of 333 nm, ZP of –26.1 mV, and EF of 87.8%. In vitro, these nanomicelles released curcumin (C) gradually with time up to 24 h, and then concentration of C remained constant up to 48 h. Both native C and C-NMs on oral treatment at the dose of 100 mg/kg C/day to STZ-induced diabetic rats for 14 days showed antidiabetic effect by reduction of serum glucose, TC, and TG levels and increased pancreatic SOD activity and reduced MDA level in diabetic rats. The effects of C-NMs were better compared to native C-treated group. Moreover, C-NMs increased the expression of Pdx1 and NKx6.1 genes in pancreatic tissue for protection of pancreatic β-cells from apoptosis. These findings demonstrate that micelle of curcumin improves the efficacy of curcumin in the protection of pancreatic islets and insulin secretion from β-cells and has hypoglycemic effect (El-far et al. 2017). Curcumin-loaded polymeric nanoparticles (C-PNs) were prepared using amphiphilic polymer, poly (ethylene glycol)-methacrylate-co-poly [2-(dimethylamino)-ethyl methacrylate]-methylaluminoxane (Poly-PEGMA-DMAEMA-MAO). C-PNs on oral treatment (16 mg/kg/day – actual dose of C was 4 mg/kg/day because drug loading capacity of C-PNs was 25%) to diabetic neuropathy in rats for 2 weeks reduced diabetic neuropathic pain by reduction of serum glucose level and the expression of P2Y12 receptor, inflammatory cytokines, IL-1β, and connexin 43 (Cx43) in dorsal root ganglia (DRG) in diabetic rats. Accumulating evidence indicates that hyperglycemia-induced Akt-dependent overexpression of purinergic 2 receptor (P2RY12) activates satellite glial cells (SGCs) in DRG to stimulate the production of inflammatory factors, IL-1β, and Cx43 for induction of mechanical or thermal hyperalgesia, which results in neuropathic pain by increasing sympathetic activity. Therefore, C-PNs of curcumin decrease neuropathic pain by suppression of Akt-dependent P2Y12 receptor in SGC activation (Jia et al. 2017). Curcumin-loaded block multi-polymer, poly (gamma-benzyl L-glutamate)-poly (ethylene glycol)-poly (gamma-benzyl L-glutamate) (PBLG-PEG-PBLG) nanoparticles (C-PNs), improves oral solubility and bioactivity of curcumin. C-PNs have particle size of 30 nm and loading capacity of 32.3% of curcumin. Pharmacokinetic study in rats revealed that after administration of C-PNs in rats, peak plasma curcumin concentration, C_{max}, was 19,860 ng/ml within 2 h after administration and remained at a low level (8 ng/ml) after 3 days, whereas after administration of native curcumin in rats, peak plasma curcumin concentration, C_{max}, was 28,300 ng/ml within 0.25 h and declined after 4 h (0 ng/ml). In vitro, C-PNs released about 9.9% of curcumin after 0.25 h, and about 99.1% of curcumin was released after 3 days. Treatment of both native curcumin (C) (20 mg/kg/day) and C-PNs (20 mg/kg/3 days) by hypodermic injection to STZ-induced diabetic rats for 8 weeks improved myocardial function by reduction

of myocardial apoptosis through upregulation of the expression of calcium-sensing receptor (CaSR), H_2S producing endogenous cystathionine-γ-lyase enzyme (CSE), calmodulin (CaM), Ca^{2+}, and H_2S in cardiomyocytes and reduction of insulin resistance in cardiomyocytes of diabetic rats, while the effects of C-PNs were higher than the C-treated group. Accumulating evidence demonstrates that increased H_2S production improves cardiac function and inhibits apoptosis of cardiomyocytes. CaSR regulates the production of H_2S by increasing the levels of intracellular Ca^{2+} in cardiomyocytes to enhance the activity of CaM and CSE. In diabetic cardiomyocytes, the expression of CaSR is decreased from oxidative stress and excess ROS accumulation. Therefore, nanopolymer carriers of curcumin improve bioactivity of curcumin by increasing its half-life and oral solubility (Tong et al. 2018). Curcumin-loaded polylactide-poly(ethylene glycol) (PLA-PEG) copolymer nanoparticles (C-PPNs) were more effective in suppression of hepatic inflammation in STZ-induced diabetic rats compared to free curcumin (C) treatment at the same dose. Both C-PPNs and free C reduced the levels of serum MDA, NO, NF-κB, COX2, AST, ALT, and hepatic COX2 and TGFβ1 levels and increased the expression of hepatic GSH and PPARγ for mitigation of hepatic inflammation in diabetic rats, but the effects of C-PPNs were better than that of free C-treated group (El-Naggar et al. 2019).

7.3.4 Capsaicinoids

Oleoresin capsicum (OC), an oily lipophilic extract of dried ripe red pepper (*Capsicum* spp.) and rich in capsaicinoids, capsaicin **49** and dihydrocapsaicin **144**, has been reported to exhibit anti-adipogenic activity. OC has been reported to have low solubility and poor bioavailability. To improve the bioavailability of OC, OC-loaded nanoemulsions (NE-OC) were prepared in 0.2% β-cyclodextrin solution. For both OC and NE-OC on oral supplementation in diet (0.01% of diet) to HFD-fed obese rats for 14 weeks, only NE-OC reduced body weight and adipose tissue mass and plasma TC level in obese rats, while OC did not. Moreover, NE-OC significantly decreased the activity of TG synthesis-related gene, glycerol 3-phosphate dehydrogenase (GPDH), in white adipose tissue (WAT), while OC did not. Furthermore, both OC and NE-OC significantly increased the expression of fatty acid oxidation and mitochondrial thermogenesis-related genes, PPARα, CPT1α, UCP2, and the activity of AMPK, and reduced the expression of lipogenesis-related genes, PPARγ, SREBP1c, and aP2 in adipose tissue of obese rats, while the effects of NE-OC were better than those of OC-treated diabetic rats. These findings indicate that possibly, NE-OC improves bioactivity of OC by increasing bioavailability of OC in adipose tissue (Kim et al. 2014). Accumulating evidence suggests that alginate-coated double-layered nanoemulsions have better stability and physiochemical properties compared to single-layered nanoemulsions. To substantiate the better anti-obesity efficacy of double-layered nanoemulsions compared to monolayered nanoemulsions a double-layered nanoemulsions, of OC (ANE-OC) and single-layered nanoemulsions of OC (SNE-OC) were prepared using Tween 80 and alginate, and

only Tween 80, respectively and treated with 3T3-L1 adipocytes. It was observed that in mature 3T3-L1 cells, the intracellular lipid content and TG content were lower in ANE-OC-treated cells compared to SNE-OC-treated cells. Moreover, the amount of FFAs and glycerol was significantly higher in ANE-OC-treated cells compared to SNE-OC-treated cells. In addition, ANE-OC downregulated the expression of lipogenesis genes, PPARγ, and aP2 and upregulated the expression of lipolytic genes, HSL, and CPT1α more efficiently compared to SNE-OC-treated 3T3-L1 adipocytes. These findings indicate that ANE-OC is more effective in the treatment of obesity (Lee et al. 2017).

7.3.5 Alkaloids

Berberine **48**, a major isoquinoline alkaloid of many plants of genus *Coptis, Hydrastis*, and *Berberis*, has antidiabetic, cardioprotective, nephroprotective, hypolipidemic, and hepatoprotective activities. Due to poor bioavailability (0.68% in rats), a high dose of berberine (100–250 mg/kg for animals, 900–1500 mg/kg for diabetic patients) is needed for achieving its therapeutic efficacy. Heavy dose (of berberine)-induced adverse effects, such as anorexia, stomach upset, diarrhea, and constipation, greatly hinder its clinical applications. Berberine (B)-loaded solid-lipid nanoparticles (B-SLNs) were synthesized using aqueous berberine solution in a mixture of soybean phospholipid and glycerol tripalmitate. Pharmacokinetic study in rats after oral administration of a single dose of native berberine and B-SLNs (50 mg/kg) showed an improved bioavailability of berberine from B-SLNs, as evidenced by significant increase in plasma berberine C_{max} 44.651 μg/ml against 11.057 μg/ml from native berberine and in plasma AUC_{0_t} value of 113.57 μg/l h against 56.478 μg/l h from native berberine. Both B-SLNs and native berberine on treatments (100 mg/kg/day, i.g.) to diabetic db/db mice for 4 weeks showed antidiabetic effect by suppressing body weight gain and FBG and improving glucose tolerance and insulin tolerance in diabetic mice. Moreover, B-SLNs and native B increased insulin secretion and pancreatic islet numbers. The B-SLNs showed better effects in improvement of glucose tolerance, insulin sensitivity, and islet regeneration compared to native B in db/db mice. Moreover, the carrier materials, lecithin and glycerol tripalmitate, were nontoxic in the experimental conditions. Therefore, encapsulation of berberine in SLNs improves antidiabetic activity of berberine through improvement of its bioavailability (Xue et al. 2013). Berberine-loaded anhydrous reverse micelles (B-ARMs) were prepared by lyophilization of W/O emulsions using soy phosphatidylcholine and medium-chain triglyceride oil. B-ARMs enhanced the oral bioavailability of berberine by 2.4-fold, and maximum plasma concentration of berberine was increased to 2.1-fold within 2 h after administration in rats, compared to that in free B-solution (BS) administration-treated rats. Oral treatment of B-ARMs at a dose of 100 mg/kg of B to diabetic mice reduced the level of FBG by 57% after 4 h of treatment, and this glucose reduction was continued for 12 h and returned to 87% after 16 h, while there was no significant reduction of FBG level in orally treated BS to diabetic mice at this dose (100 mg/kg). However,

intravenous treatment of free BS to diabetic mice at a dose of 2.5 mg/kg reduced the level of FBG by 22% after 4 h. Moreover, long-term treatment of B-ARMs (100 mg/kg/day) to type 1 diabetic mice for six consecutive days restored the blood glucose level to normal range (3–7 mM/l). Hence, ARM delivery system of berberine improves its antidiabetic efficacy (Wang et al. 2011). Berberine nanosuspension (B-NS) consisting of a mixture of berberine, D-α-tocopheryl polyethylene glycol 1000 succinate, and hypromellose in distilled water was prepared by high-pressure homogenization method. B-NS have an average PS of 73.1 nm, PDI of 0.302, and ZP of +6.99 mV. B-NS on chronic treatment (50 mg/kg/day, i.g.) to STZ-induced diabetic mice for 8 weeks showed better reduction of serum glucose and TC levels and body weight, compared to an equivalent dose of free BS and metformin (300 mg/kg). These results indicate that B-NS improves glucose and lipid metabolism of berberine in diabetic mice (Wang et al. 2015). Berberine-loaded cross-linked D-α-tocopheryl-polyethylene glycol-thiol-succinamide micelles (B-CTAMs) increased the accumulation of berberine in hepatocytes because the catabolized product of the micelles, and D-α-tocopheryl succinate inhibited the activity of hepatic cytochrome P450 isoenzymes (CYP450) and P-gp efflux pump and thereby reduced the metabolism and excretion of berberine. Tissue distribution analysis of berberine (B) from B-CTAMs after oral administration of a single dose of 50 mg/kg of B revealed that the accumulation of B in the liver was increased by +248.8% and was much higher than that in plasma (+99.1%) and other main organs (heart, spleen, lung, and kidney). B-CTAMs have an average particle size (PS) of 51.7 nm, PDI of 0.188, and ZP of –18.16 mV. In HFD-fed obese mice, B-CTAMs on i.g. treatment (50 mg/kg of B/day) for 8 weeks reduced aortic lesion areas, body weight gain, and liver and epididymal fat mass in adipose tissue in obese mice. Moreover, these B-micelles decreased the levels of plasma TG, TC, and LDL-C, hepatic TG content and hepatocyte size, and the levels of pro-inflammatory cytokines, TNFα, and IL6 in the plasma, liver and adipose tissue. In addition, these micelles enhanced the expression of LDLR, p-AMPK, InsR, and p-Akt in the liver of obese mice. Meanwhile, BS (berberine solution) on oral treatment (50 mg/kg/day) to obese mice for 8 weeks reduced hepatic lipid content and enhanced the expression levels of hepatic p-AMPK, p-InsR, and p-Akt to a lower magnitude compared to B-CTAM-treated obese mice. Therefore, liver target-specific B-nanomicelles are more effective in the treatment of hepatic steatosis through increased bioavailability of berberine in the liver (Guo et al. 2019).

7.3.6 Phenolic Acids

Trans-Ferulic acid **72**, the most common antioxidant phenolic acid constituent of cereals (rice, wheat, and oat), pineapple, coffee bean, peanut, and tomatoes, among others, has several health benefits against cancer, diabetes and diabetes-related disorders, heart diseases, and renal diseases. Its poor solubility in water results in low oral bioavailability (<1.0%) and restricted its biomedical applications. To improve its oral bioavailability, *t*-ferulic acid (FA) encapsulated polymeric

nanoparticles (FA-PNs) were synthesized using natural polymer, chitosan, and tripolyphosphate by ionic gelation method. These FA-PNs improved bioavailability of FA in rats. FA-PNs have an average PS of 213 nm, PDI of 0.343, ZP of +14.2mV, and EF of 54.49% of FA. In vitro, FA-PNs exhibited a slow release of FA at PH 5.0, 26.8% in initial 12 h, >50.0% in 24 h, and about 78.0% in 5 days. FA-PNs and native FA on oral treatments (10 mg/kg/day) to STZ-induced diabetic rats for 14 days reduced serum glucose and serum lipid profile (TC, LDL-C, VLDL-C, TG) and increased serum insulin and HDL levels and body weight in diabetic rats, while the effects of FA-PNs were better than those of native FA-treated diabetic group. Moreover, these nanocarriers have no toxicity in experimental conditions. Therefore, polymeric nanocarriers of FA improve hypoglycemic effect of FA through enhancement of its oral bioavailability (Panwar et al. 2018). The bioavailability of FA was also improved by preparation of FA-loaded nanostructured liquid carriers (FA-NLCs) using ethyl oleate as lipid component and glyceryl behenate as solid-lipid component in a microemulsion-based method. These FA-NLCs have PS of 102 nm and EF of 77.30% of FA and have greater stability than FA-S. Pharmacokinetic study revealed that FA-NLCs increased plasma FA concentration, C_{max}, AUC, half-life, and mean residence time (MRT) of FA by more than twofold, compared to that of free FA aqueous solution after oral administration at a dose of 80 mg/kg in rats. Possibly these FA-NLCs can improve the antidiabetic activity of FA (Zhang et al. 2016b).

7.3.7 Quinones

Rhein (RH) **126**, a major anthraquinone constituent of *Rheum palmatum* and *R. tanguticum* as well as found in other plants including *Cassia tora* and *Polygonum multiflorum*, has been widely used in Asian countries for the treatment of liver and kidney diseases, diabetes, and cancer. In China, the RH capsule has been approved for clinical trials in DN patients. Its low oral bioavailability hampers its bioactivity in clinical trials. To improve the bioavailability of RH in the kidney, kidney-targeted RH-loaded liposomal nanoparticles (RH-KLNs) were synthesized using lipid copolymer, polycaprolactone-polyethyleneimine (PCL-PCI)-based core and kidney-targeting peptide, lysine-cysteine-serine-alanine-valine-proline-isoleucine-cysteine (KCSAVPLC)-modified lipid layers. These RH-KLNs have an average PS of 59.5 nm, PDI of 0.1–0.2, ZP of –5.4 mV, EF of 90.22%, and RH loading capacity of 5.17%. These liposomal Ns (RH-KLNs) have rapid cellular uptake in human kidney 2 (HK2) cells by promoting endocytosis of renal cells. Accumulating evidence demonstrates that nanoparticles with sizes above 100 nm are seldom distributed in the kidney and are mostly trapped by the liver and spleen. Biodistribution analysis of RH-KLNs in DN mice after i.v. administration of a dose of 5 mg/kg of RH revealed that these RH-KLNs have concentration 2–4 times higher in the kidney than that of the liver, lung, and intestine and 7–20 times higher than that of the heart, spleen, and brain and have lower urinary excretion compared to free RH solution (RHS). In vitro, these RH-KLNs showed sustained

release behavior of RH without significant burst release, releasing about 25% and 61.8% of RH at 3 h and 48 h, respectively, whereas free RH solution showed about 90% release of RH within 4 h. For intravenous treatment of RH-KLNs and RHS at a dose of 5 mg/kg/day to DN mice for 20 days, both RH-KLNs and RHS significantly improved renal function by reduction of urinary protein level and levels of serum glucose, urea nitrogen, creatinine and kidney index, and increased urinary creatinine excretion as well as reduction of renal fibrosis by suppression of secretion and accumulation of fibronectin and TGFβ1 by reducing the p-level of Smad2/3 proteins in renal tissues of DN mice, while these effects of RH-KLNs in DN mice were better than those of RHS group. Therefore, these kidney target-specific nanoliposomes of RH improve bioactivity of RH in DN treatment (Wang et al. 2019).

Emodin (1,3,8-trihydroxy-6-methylanthraquinone, EM) **123**, a major bioactive anthraquinone of *Rheum palmatum* and *Polygonum cuspidatum*, has antidiabetic, antinociceptive, anti-inflammatory, and anticancer activities. This anthraquinone exhibits these pharmacological effects at high doses. High doses of emodin exhibit several adverse side effects including toxicity. Encapsulation of emodin in polymeric nanoparticles (EM-PNs) using amphiphilic polymer, poly-(ethylene glycol) methacrylate-(2-(dimethylamino)ethyl methacrylate)-methacrylamide (PEGMA-DMAEMA-MAM), improved bioavailability and bioactivity of emodin. Pretreatment of EM-PNs (5 mg/rat containing 1 mg of EM/3 doses in every alternative d, by sublingual vein injection) to STZ-induced diabetic neuropathic pain (DNP) in rats for 7 days decreased both mechanical and thermal hyperalgesia (pain) by increasing mechanical withdrawal threshold and thermal withdrawal latency values through suppression of the expression levels of inflammatory markers, TNFα and purin 2X3 (P2X3) receptor, and p-levels of ERK1/2 kinase in dorsal root ganglia (DRG) neurons of diabetic rats. Accumulating research results indicate that P2X3 receptors play the key role for transmission of neuropathic pain signal from periphery to central nervous system (CNS). The expression of P2X3 is upregulated from chronic constriction injury of the sciatic nerve (DRG neurons) from long-standing hyperglycemia-induced destruction of homeostasis of peripheral tissue. Hyperglycemia-induced TNFα production activates the receptor of TNFα, TNFR1, to release ATP, which in turn activates P2X3 receptor. P2X3 receptors increase the phosphorylation levels of ERK1/2 kinases for induction of pain in DRG neurons. Moreover, in vitro, EM-PNs (1.85 μM) in human embryonic kidney (HEK) 293 cells transfected with α,β-methylene ATP (α,β-meATP), an agonist of P2X3 receptors, inhibited α,β-me-ATP activated current by 50%, compared to that of free EM (30 μM) treatment. These findings suggested that nano-emodin improved the activity of emodin at low doses in the prevention of DNP (Li et al. 2017).

Thymoquinone **363**, main bioactive quinone constituent of the seeds of medicinal herb *Nigella sativa* (black cumin), has several health benefits including antidiabetic, hepatoprotective, antidepressant, antianxiety, and antitumor activities. It showed slow absorption and rapid elimination when administered orally in diabetic animals. To improve bioactivity of thymoquinone (TQ) in nanoparticulate drug delivery system, thymoquinone-loaded polymeric nanocarriers (TQ-PNs) were synthesized using nontoxic natural anionic polymer gum rosin (solid resin from pine tree,

containing mainly diterpenes, abietic acid, and isopimaric acid), lecithin, polyvinyl alcohol, polysorbate 80, and oleic acid by nanoprecipitation method. These TQ-PNs have an average PS of 70.21 nm, PDI of 0.251, and ZP of –45.3 mV. In vitro, TQ-PNs released TQ slowly, 2.07% and 14.23% at 1 h and 24 h, respectively, compared to the release of TQ of 32.29 and 59.60% at 1 h and 24 h, respectively, from free TQ solution (TQS). TQ-PNs and free TQS on oral treatment (40 or 80 mg/kg bw/day, p.o.) to STZ-NA-induced type 2 diabetic rats for 21 days significantly showed hypoglycemic and hypolipidemic effects by reduction of the levels of serum glucose, HbA1c, TC, TG, and LDL, and serum HDL level in diabetic rats compared to diabetic control group, but the effects of TQ-PNs were better than that of TQS at the same dose. Actually, the doses of 40 and 80 mg/kg of TQ-PNs contained 20 and 40 mg/kg of TQ, respectively. Therefore, nanoencapsulated TQ showed better antidiabetic effect than free TQS at the half-dose of TQS. Hence, TQ-PNs could be utilized in clinical trials of diabetes after further studies on tissue distribution, therapeutic targets, toxicity, pharmacokinetics, and pharmacodynamics (Rani et al. 2018).

7.3.8 Saponins

Glycyrrhizin **458a**, main sweet tasting triterpene glycoside (saponin) constituent of the roots of *Glycyrrhiza glabra* (liquorice), has antihyperglycemic, antihyperlipidemic, hepatoprotective, cardioprotective, antidepressant, and antitumor activities. Its poor bioavailability in rats due to slow and incomplete absorption in the GI tract hinders its clinical applications. To improve the bioavailability of glycyrrhizin, glycyrrhizin (GL)-loaded polymeric nanoparticles (GL-PNs) were synthesized using chitosan and gum arabic as basic polymers in ionotropic gelation method. These GL-PNs have an average PS of 181.4 nm, ZP of +31.4mV, EF of 99.84%, and loading capacity of 25%. In vitro, GL-PNs released GL slowly and released GL at 1 h of 14.32%, compared to release of GL of 25.79% at 1 h from free GL solution. For oral treatment of GL-PNs (40 mg/kg/day containing 8.4 mg/kg of GL) and free GL solution (GLS) (40 mg/kg/day) to STZ-NA-induced diabetic rats for 21 days, both GL-PNs and GLS showed hypoglycemic and hypolipidemic effects by reduction of the levels of serum glucose, HbA1c, TC, TG, LDL, and VLDL and increased HDL level in diabetic rats, while the effects of GL-PNs were better than that of GLS-treated diabetic rats. The effects of GL-PNs were comparable to that of metformin-loaded nanoparticle (40 mg/kg/day, containing 9.2 mg/kg of metformin)-treated diabetic rats. Metformin-loaded nanoparticles were prepared using the same polymers. Hence, GL-PNs of glycyrrhizin improved antidiabetic activity of glycyrrhizin by increasing its bioavailability (Rani et al. 2017).

7.3.9 Carotenoids

Lycopene **24**, major carotene pigment of ripe tomato (*Lycopersicum esculentum*), has various pharmacological activities against cardiovascular diseases, diabetes, cancer, and memory and cognitive disorders (Alzheimer's disease and Parkinson's disease). It has strong antioxidant potential, greater than that of β-carotene and vitamin E by 47 and 100 times, respectively. It is highly sensitive to heat and light and thereby creates difficulty in its clinical applications. Niosomes are nonionic surfactant-based lipid vesicles and have the ability to encapsulate both lipophilic and hydrophilic drugs and protect them from external factors and improve their lifetime and absorption in the GI tract. Lycopene (LYCO)-loaded nanoniosomes (LYCO-NNs) were prepared using span 60 as nonionic surfactant, cholesterol, and aqueous mannitol solution. LYCO-NNs have an average PS of 202 nm, ZP of –2.25mV, and EF of 62.8% and stability over a period of 3 months. In vitro, these LYCO-NNs released lycopene initially at a faster rate over a period of 10 h and then steadily up to 72 h, releasing 19%, 48%, and 67.3% of entrapped lycopene at 24-h, 48-h, and 72-h period, respectively. LYCO-NNs and free LYCO solution on oral administrations (200 mg/kg/day) to diabetic rats for 14 days reduced blood glucose level and the levels of serum TC, LDL, and VLDL, compared to diabetic control group, but the effects of LYCO-NNs were better than that of free LYCO-treated group. The effects of LYCO-NNs were similar to that of glibenclamide (5 mg/kg)-treated diabetic rats. Therefore, nanoniosomes are efficient delivery systems of lycopene in treatment of diabetes (Sharma et al. 2017).

7.3.10 Unsaturated Fatty Acids

Docosahexaenoic acid (DHA) **170**, main unsaturated fatty acid constituent of fish oil, has been found to improve insulin secretion and insulin action in diabetic animals. DHA-loaded solid state ZnO nanoparticles (DHA-ZnONs) were prepared using gum arabic, NaOH powder, and zinc acetate in a calcination process. These DHA-ZnONs showed better activity of DHA in insulin secretion from pancreatic β-cells and insulin sensitivity in skeletal muscle and adipose tissue in diabetic rats, compared to free DHA, on oral administration at a dose of 10 mg/kg/day for a period of 30 days. Moreover, DHA-ZnONs protected the pancreatic islets and liver tissues of diabetic rats more efficiently compared to free DHA-treated group by increasing the activity of SOD and reducing the MDA level. Furthermore, these DHA-ZnONs increased glucose uptake in the skeletal muscle more efficiently compared to free DHA group (Hussein et al. 2019a). DHA-loaded silver nanoparticles (DHA-AgNs) were prepared using silver nitrate, NaOH, benign polymers, soluble starch, and Tween 80 (polyethylene sorbitol ester). These DHA-AgNs on treatment in diabetic rats showed improvement of endothelial dysfunctions in arteries by enhancing the levels of serum antioxidant enzyme, paraoxonase 1 (PON1), nitric oxide (NO), and insulin and decreasing the levels of serum fasting glucose and lipid profile in diabetic rats, and these effects were better than that of free DHA-treated group. Accumulating

evidence demonstrates that PON1 improves arterial function by reduction of atherosclerotic plaque formation and NO improves relaxation process of endothelial cells of arteries. Both plasma PON1 and NO levels are decreased in diabetic animals and humans (Hussein et al. 2019b).

7.4 Nanoencapsulated Plant Extracts

Stevia rebaudiana Bertoni (SR) extract has been used for treatment of diabetes in many Asian countries. The active constituent of this plant, kaurane-type diterpene glycoside, stevioside **449** (4–15% of plant extract), increased insulin secretion from pancreatic beta cells to reduce hyperglycemia in diabetic rats and humans. In diabetic patients, long-term treatments of SR extract at high doses are required for normalization of blood glucose levels, because of poor bioavailability and short half-life of stevioside. To address this problem and to develop a controlled and prolonged release of stevioside from the plant extract in the target tissues, the SR extract-loaded titanium dioxide nanoparticles (SR-TiO_2Ns) were prepared using SR extracts containing 20 and 30 μM of stevioside, titanium-n-butoxide, and polyvinylpyrrolidone. These SR-TiO_2Ns containing 20 and 30 μM of stevioside on i.p. treatments to alloxan-induced diabetic rats significantly reduced plasma glucose and HbA1c levels at 4 h after administration and continued this hypoglycemic effect for 30 days. Moreover, these SR-TiO_2Ns decreased serum TC (62% and 64%, respectively) and TG (59% and 63%) and increased insulin secretion from the pancreas (80% and 100%, respectively) in diabetic rats. These results suggest that SR-TiO_2Ns improve both hypoglycemic and hypolipidemic effects of SR extract by controlled release of nanostevioside in blood circulation and distribution to insulin sensitive tissues (Langle et al. 2015). Stevioside (ST)-loaded polymeric nanoparticles (ST-PNs) were prepared using biodegradable copolymer pluronic F 68. These ST-PNs have PS of 110–130 nm and loading capacity of stevioside of 16.32%. In vitro, these ST-PNs showed a sustained release of stevioside with half-release and complete release at 25 h and 200 h, respectively. These polymeric nanosteviosides could be utilized in diabetes treatment (Barwal et al. 2013).

Costus speciosus Sm. syn. *Cheilocostus speciosus* has been used in treatment of diabetes. An ethanolic extract of the roots of this plant containing costunolide **10** as an active constituent, on treatment in diabetic rats, reduced hyperglycemia by increasing insulin secretion and insulin activity in the liver and skeletal muscle of diabetic rats. In the liver, this extract increased glucose uptake and glycogen synthesis by upregulation of the activity of the proteins, GLUT2, glucokinase (GCK) and glycogen synthase (GS) (Ali et al. 2014). An ethanolic extract of *C. speciosus* leaf (CSE)-loaded polymeric nanoparticles (CSE-PNs) was prepared using polymer polylactic-co-glycolic acid (PLGA). Both CSE-PNs and free CSF on oral treatments (100 and 150 mg/kg/day) to STZ-induced diabetic rats for 30 days reduced the levels of serum glucose, TC, TG, LDL, ALP, AST, and LDH and increased serum HDL-c in diabetic rats, while the effects of CSE-PNs were better than that of free CSE-treated diabetic rats at the same doses. Moreover, CSE-PNs

increased glucose uptake in skeletal muscle by upregulation of GLUT4 expression more effectively compared to free CSE (Alamoudi et al. 2014).

A herbal extract formulation containing the extract of mulberry leaf and *Pueraria lobata* rhizome (MPE) has been prescribed to treat diabetes in Asian countries. The major bioactive phytochemicals of this extract formulation are rutin **54** and puerarin **8**. To improve the antidiabetic efficacy of this extract at lower doses, MPE-loaded selenium nanoparticles (MPE-SeNs) were prepared using polymers PLGA-PEG, DoTAP (dioleoyl-3-trimethylammonium propane), poloxamer 188, Na_2SeO_3, and GSH in solvent diffusion/in situ reduction method. These MPE-SeNs have an average PS of 120 nm and EF of 89.38% for rutin and 90.59% for puerarin. Pharmacokinetic study after oral administration of MPE-SeNs in rats showed an enhanced availability of rutin and puerarin in plasma by more than twofold compared to that of rutin and puerarin from free MPE administration. MPE-SeNs on oral treatment (125 mg/kg/day) to diabetic Goto Kakizaki rats for 14 days significantly reduced BGL and improved pancreatic β-cell function and glucose utilization in adipocytes of diabetic rats, and these effects were better than that of free MPE-treated diabetic rats at the same dose. Therefore, encapsulation of MPE in SeNs enhanced the antidiabetic effects of phytochemicals present in the extract (Deng et al. 2019).

7.5 Summary and Future Perspectives

Many phytochemicals have been found as promising natural drugs in prevention and treatment of obesity and diabetes and their comorbidities. However, their low stability, aqueous solubility, and bioavailability as well as high rate of metabolism restrict their clinical applications in these fields. A considerable amount of studies has demonstrated that applications of biocompatible (nontoxic to humans) and biodegradable nanocarriers can effectively improve the delivery of these phytochemicals to the target disease tissues with increasing their bioavailability and bioactivity and even increasing the synergistic effects of some phytochemicals. A recent review article briefly discussed the nanoformulations of some phytochemicals, including resveratrol, curcumin, quercetin, naringenin, apigenin, luteolin, mangiferin, berberine, asiatic acid, emodin, gallic acid, gymnemic acid, thymoquinone, pelargonidin, and rosmarinic acid to increase their bioavailability and antidiabetic activities. Some of nanoformulated natural molecules have better antidiabetic effects compared to that of metformin (Dewanjee et al. 2020). It is an emerging dimension of natural products research.

Each nanocarrier system has its own characteristics, loading capacity, and releasing ability of drugs and other factors on the protection of drugs from the environmental enzymes in the body of the host. Proper selection of nanocarriers for delivery of a particular phytochemical is required by making a good match between the carrier and the natural drug to be loaded for the effective doses of the drug to the disease tissue and to get maximum benefits and minimum side effects and toxicity among others. Some of the nanocarriers may change their integrity and

characteristics due to digestion by gastrointestinal and hepatic enzymes, and hence, pharmacokinetic and pharmacodynamic studies of the nanocarriers are required prior to their applications in delivery systems of phytochemicals (Wang et al. 2014). Safety is the most important factor for the use of nanocarriers/nanoparticles in delivery of phytochemicals. The side effects of nanocarriers must be considered seriously compared to their benefits before selection for delivery of a phytochemical. Target ligands, surfactants, and emulsifiers used in the synthesis of nanocarriers may have hepatotoxic, nephrotoxic, and immunotoxic effects. Nanoencapsulation of phytochemicals provides only dose advantages, but the safe dose ranges of nanoencapsulated phytochemicals must be evaluated before their clinical trials. Moreover, both short- and long-term safety of nanocarriers and nanoencapsulated phytochemicals are to be assessed. Furthermore, the efficacy of nanoencapsulated phytochemicals in ordinary rat models may not reflect the similar efficacy in obese humans. Future research should be focused on the development of in vitro and in vivo safety tests and guidelines on the use of these nanocarriers in phytochemicals. Hence, safe dose-range efficacy and its short- and long-term effects and pharmacokinetics of any phytochemical-loaded nanoparticles are to be assessed rigorously in different mutant polygenic animal models having human phenotypes and approved by the FDA or other competent authority before clinical trials against obese and diabetic patients.

References

Ahangarpour A, Oroojan AA, Khorsandi L et al (2018) Solid lipid nanoparticles of myricitrin have antioxidant and antidiabetic effects on streptozotocin-nicotinamide-induced diabetic model and myotube cell of male mouse. Oxid Med Cell Longev 2018:7496936

Alamoudi EF, Khalil WKB, Ghaly IS et al (2014) Nanoparticles from *Costus speciosus* extract improves the antidiabetic and antilipidemic effects against STZ-induced diabetes mellitus in albino rats. Int J Pharm Rev Res 29:279–285

Ali HA, Almaghrabi OA, Afifi ME (2014) Molecular mechanisms of anti-hyperglycemic effects of *Costus specious* extract in streptozotocin-induced diabetic rats. Saudi Med J 35:1501–1506

Anton N, Vandamme TF (2011) Nano-emulsions and micro-emulsions: clarifications of the critical differences. Pharm Res 28:978–985

Barwal I, Sood A, Sharma M et al (2013) Development of stevioside pluronic-F-68 copolymer base PLA-nanoparticles as an antidiabetic nanomedicine. Colloids Surf B Biointerfaces 101:510–516

Beloqui A, Solinis MA, Rodriguez-Gascon A et al (2016) Nanostructured lipid carriers: promising drug delivery systems for future clinics. Nanotechnol Biol Med 12:143–161

Blanco E, Shen H, Ferrari M (2015) Principles of nanoparticle design for overcoming biological barriers to drug delivery. Nat Biotechnol 33:941

Bulboaca AE, Boarescu PM, Porfire AS et al (2020) The effect of nano-epigallocatechin- gallate on oxidative stress and matrix metalloproteinases in experimental diabetes mellitus. Antioxidants 9:172

Chang CY, Wang MC, Miyagawa T et al (2017) Preparation of arginine-glycine-aspartic acid-modified biopolymeric nanoparticles containing epigallocatechin-3-gallate for targeting vascular endothelial cells to inhibit corneal neovascularization. Int J Nanomed 12:279–294

Das S, Roy P, Pal R et al (2014) Engineered silybin nanoparticles educe efficient control in experimental diabetes. PLoS One 9:e101818

Deng W, Wang H, Wu B et al (2019) Selenium-layered nanoparticles serving for oral delivery of phytomedicines with hypoglycaemic activity to synergistically potentiate the antidiabetic effect. Acta Pharm Sin B 9:74–86

Dewanjee S, Chakraborty P, Mukherjee B et al (2020) Plant-based antidiabetic nanoformulations: the emerging paradigm for effective therapy. Int J Mol Sci 21:2217

Duan Y, Dhar A, Patel C et al (2020) A brief review on solid lipid nanoparticles: part and parcel of contemporary drug delivery systems. RSC Adv 10:26777–26791

El-far YM, Zakaria MM, Gabr MM et al (2017) Nanoformulated natural therapeutics for management of streptozotocin- induced diabetes: potential use of curcumin nanoformulation. Nanomedicine 12:1689–1711

El-Naggar ME, Al-Joufi F, Anwar M et al (2019) Curcumin-loaded PLA-PEG copolymer nanoparticles for treatment of liver inflammation in streptozotocin-induced diabetic rats. Colloids Surf B Biointerfaces 177:389–398

Goktas Z, Zu Y, Abbasi M et al (2020) Recent advances in nanoencapsulation of phytochemicals to combat obesity and its comorbidities. J Agric Food Chem 68:8119–8131

Guo HH, Feng CL, Zhang WX et al (2019) Liver-target nanotechnology facilitates berberine to ameliorate cardio-metabolic diseases. Nat Commun 10:1981

Hong Z, Xu Y, Yin JF et al (2014) Improving the effectiveness of (-)-epigallocatechin gallate (EGCG) against rabbit atherosclerosis by EGCG-loaded nanoparticles prepared from chitosan and polyaspartic acid. J Agric Food Chem 62:12603–12609

Hussein J, Attia MF, El Bana M et al (2019a) Solid state synthesis of docosahexaenoic acid-loaded zinc oxide nanoparticle as a potential antidiabetic agent in rats. Int J Biol Macromol 140:1305–1314

Hussein JS, Rasheed W, Ramzy T et al (2019b) Synthesis of docosahexaenoic acid-loaded silver nanoparticles for improving endothelial dysfunctions. Hum Exp Toxicol 38:962–973

Jaiswal M, Dudhe R, Sharma PK (2015) Nanoemulsion: an advanced mode of drug delivery system. 3 Biotech 5:123–127

Jia T, Rao J, Zou L et al (2017) Nanoparticle-encapsulated curcumin inhibits diabetic neuropathic pain involving the P2Y12 receptor in the dorsal root ganglia. Front Neurosci 11:755

Kim JY, Lee MS, Jung S et al (2014) Anti-obesity efficacy of nanoemulsion oleoresin capsicum in obese rats fed a high-fat diet. Int J Nanomed 9:301–310

Langle A, Gonzalez-Coronel MA, Carmona-Gutierrez G et al (2015) *Stevia rebaudiana* loaded titanium oxide nanomaterials as an antidiabetic agent in rats. Rev Bras Farmacogn 25:145–151

Lee MS, Jung S, Shin Y et al (2017) Lipolytic efficacy of alginate double-layer nanoemulsion containing oleoresin capsicum in differentiated 3T3-L1 adipocytes. Food Nutr Res 61(1): 1339553

Li L, Sheng X, Zhao S et al (2017) Nanoparticle-encapsulated emodin decreases diabetic neuropathic pain probably via a mechanism involving P2X3 receptor in the dorsal root ganglia. Purinergic Signal 13:559–568

Maity S, Mukhopadhyay P, Kundu PP et al (2017) Alginate-coated chitosan core-shell nanoparticles for efficient oral delivery of naringenin in diabetic animals—an in vitro and in vivo approach. Carbohydr Polym 170:124–132

Mohseni R, Arabsadeghabadi Z, Ziamajidi N et al (2019) Oral administration of resveratrol-loaded solid lipid nanoparticle improves insulin resistance through targeting expression of SNARE proteins in adipose and muscle tissue in rats with type 2 diabetes. Nanoscale Res Lett 14:227

Mozafari MR (2010) Nanoliposomes: preparation and analysis. In: Weissig V (ed) Methods in molecular biology, vol 605. Springer, pp 29–50

Mukhopadhyay P, Maity S, Mandal S et al (2018) Preparation, characterization and in vitro evaluation of pH sensitive, safe-quercetin-succinylated chitosan-alginate core-shell-corona nanoparticles for diabetes treatment. Carbohydr Polym 182:42–51

Panwar R, Raghuwanshi N, Srivastava AK et al (2018) In vitro-sustained release of nanoencapsulated ferulic acid and its impact in induced diabetes. Mater Sci Eng C 92:381–392

Peng Y, Meng Q, Zhou J et al (2018) Nanoemulsion delivery system of tea polyphenols enhanced the bioavailability of catechins in rats. Food Chem 242:527–532
Rani R, Dahiya S, Dhingra D et al (2017) Evaluation of anti-diabetic activity of glycyrrhizin-loaded nanoparticles in nicotinamide-streptozotocin-induced diabetic rats. Eur J Pharm Sci 106:220–230
Rani R, Dahiya S, Dhingra D et al (2018) Improvement of anti-hyperglycemic activity of nano-thymoquinone in rat model of type 2 diabetes. Chem Biol Interact 295:119–132
Reis CP, Neufeld RJ, Ribeiro AJ et al (2006) Nanocapsulation 1: methods for preparation of drug-loaded polymeric nanoparticles. Nanomedicine (Lond) 2:8–21
Reza Mozafari M, Johnson C, Hatziantoniou S et al (2008) Nanoliposomes and their applications in food nanotechnology. J Liposome Res 18:309–327
Sharma PK, Saxena P, Jaswanth A et al (2017) Anti-diabetic activity of lycopene niosomes: experimental observation. J Pharm Drug Devel 4:103
Shi F, Wei Z, Zhao Y et al (2016) Nanostructured lipid carriers loaded with baicalin: an efficient carrier for enhanced antidiabetic effects. Pharmacogn Mag 12:198–202
Singh J, Mittal P, Bonde GV et al (2018) Design, optimization, characterization and in vivo evaluation of quercetin enveloped Soluplus®/P407 micelles in diabetes treatment. Artif Cells Nanomed Biotechnol 46:5546–5555
Sun M, Nic S, Pan X et al (2014) Quercetin- nanostructured lipid carriers: characteristics and anti-breast cancer activities in vitro. Colloids Surf B Biointerfaces 113:15–24
Sur S, Rathore A, Dave V et al (2019) Recent developments in functionalized polymer nanoparticles for efficient drug delivery system. Nano Struct Nano Objects 20:100397
Tong F, Liu S, Yan B et al (2017) Quercetin nanoparticle complex attenuated diabetic nephropathy via regulating the expression level of ICAM 1 on endothelium. Int J Nanomed 12:7799–7813
Tong F, Chai R, Jiang H et al (2018) In vitro/vivo drug release and anti-diabetic cardiomyopathy properties of curcumin/PBLG-PEG-PBLG nanoparticles. Int J Nanomed 13:1945–1962
Torchilin VP (2007) Micellar nanocarriers: pharmaceutical perspectives. Pharm Res 24:1–16
Wan S, Zhang L, Quan Y et al (2018) Resveratrol-loaded PLGA nanoparticles: enhanced stability, solubility and bioactivity of resveratrol for non-alcoholic fatty liver disease therapy. R Soc Open Sci 5:181457
Wang T, Wang N, Song H et al (2011) Preparation of an anhydrous reverse micelle delivery system to enhance oral bioavailability and anti-diabetic efficacy of berberine. Eur J Pharm Sci 44:127–135
Wang S, Nie S, Sun M et al (2014) Application of nanotechnology in improving bioavailability and bioactivity of diet-derived phytochemicals. J Nutr Biochem 25:363–376
Wang Z, Wu J, Zhou Q et al (2015) Berberine nanosuspension enhances hypoglycaemic efficacy on streptozotocin induced diabetic C57BL/6 mice. Evid Based Complement Alternat Med 2015: 239749
Wang J, Tan J, Luo J et al (2017a) Enhancement of scutellarin oral delivery efficacy by vitamin B-12-modified amphiphilic chitosan derivatives to treat type II diabetes induced- retinopathy. J Nanobiotechnol 15:18
Wang Y, Wang S, Firempong CK et al (2017b) Enhanced solubility and bioavailability of naringenin via liposomal nanoformulation: preparation and in vitro and in vivo evaluations. AAPS PharmSciTech 18:586–594
Wang G, Li Q, Chen D et al (2019) Kidney-targeted rhein-loaded liponanoparticles for diabetic nephropathy via size control and enhancement of renal cellular uptake. Theranostics 9:6191–6208

Xue M, Yang MX, Zhang WX et al (2013) Characterization, pharmacokinetics, and hypoglycaemic effect of berberine loaded solid lipid nanoparticles. Int J Nanomed 8:4677–4687

Zhang J, Nie S, Martinez-Zaguilan R, Sennoune SR et al (2016a) Formulation, characteristics and anti-atherogenic bioactivities of CD36- targeted epigallocatechin gallate (EGCG)- loaded nanoparticles. J Nutr Biochem 30:14–23

Zhang Y, Li Z, Zhang K et al (2016b) Ethyl oleate containing nanostructured lipid carriers improve oral bioavailability of *trans*-ferulic acid as compared with conventional solid lipid nanoparticles. Int J Pharm 511:57–64

Zu Y, Overby H, Ren G et al (2018) Resveratrol liposomes and lipid nanocarriers: comparison of characteristics and inducing browning of white adipocytes. Colloids Surf B 164:414–423

8 Clinical Trials of Phytomedicines in the Management of Obesity and Diabetes

Biswanath Dinda

8.1 Introduction

Phytomedicines, also known as herbal medicines, have been used in different countries for the treatment and prevention of various diseases, including obesity and diabetes. Chronic hyperglycemia in uncontrolled diabetes leads to the development of vascular complications, including cardiovascular diseases, kidney diseases, eye diseases, and lower-limb amputations. Many herbal formulations have been commercially used in different countries in capsules or tablets as dietary food supplements as remedy for hyperglycemia. Most of these herbal formulations have insufficient scientific data about the bioactive phytochemicals, mode of actions in diabetic patients, and doses of optimum efficacy and toxicities on long-term use in high doses. The antidiabetic and anti-obesity activities of most of these herbal formulations have been tested in diabetic animal models. The antidiabetic and anti-obesity efficacies of some herbal and polyherbal formulations have been verified by clinical trials in type 2 diabetic and obese patients. There are many discrepancies in clinical results in antidiabetic efficacies in diabetic animal models and humans. This chapter summarizes the results of clinical trials of herbal and phytochemical formulations in humans and some major discrepancies in the results in clinical trials in rodents and humans.

B. Dinda (✉)
Department of Chemistry, Tripura University, Suryamaninagar, Agartala, Tripura, India

B. Dinda (ed.), *Natural Products in Obesity and Diabetes*,
https://doi.org/10.1007/978-3-030-92196-5_8

8.2 Clinical Trials on Phytomedicines

8.2.1 Herbal Formulations

The fruits of *Momordica charantia*, known as bitter melon, karela, or bitter gourd, are popular vegetable fruits for the treatment of diabetes and its comorbidities among the indigenous populations of Asia, South America, the Caribbean, and East Africa. The phytochemicals, namely, charantin **463a**, a cucurbitane-type triterpenoid, saponins, momordicine II and 3-hydroxy-cucurbita-5,24-dien-19-al-7, 23 di-*O*-β-D-glucopyranoside, peptide β, and vicine **339a**, a glycol alkaloid, have been found to have significant insulin secreting and hypoglycemic effect in diabetic animals. The processed bitter gourd in the form of capsules or tablets is marketed under the brand names Gourdin, Karela, and Glucobetic in Canada, India, the UK, the USA, and many Asian countries as natural antidiabetic agents. But, adequate scientific information on the active constituents, their concentrations, and modes of actions is not available. In a clinical trial, oral supplementation of *M. charantia* capsules (two capsules, three times a day after meals, each capsule containing 4.8 g lyophilized bitter gourd powder) to T2DM patients ($n = 40$) for 3 months reduced serum HbA1c, FBG,TC levels, and body weight to a less extent. For definite conclusions on its effectiveness, further study in more patients is required (Dans et al. 2007). In another clinical trial, treatment of *M. charantia* fruit extract in capsules (four capsules/day, containing 2 g of *M. charantia* fruit pulp in dried powder and 0.04–0.05% of charantin (a mixture of β-sitosterol 3-*O*-glucoside and stigmasterol 3-*O*-glucoside in 1:1 ratio)) **463a** to T2DM patients for 4 weeks showed modest hypoglycemic effect and significant reduction of plasma fructosamine levels, and this hypoglycemic effect was less than that of metformin-treated group (1 g/day). The lower doses of bitter melon (0.5 and 1.0 g/day) did not significantly decrease plasma fructosamine levels in diabetic patients (Fuangchan et al. 2011). In animal model, oral treatment of *M. charantia* fruit ethanolic extract (100–400 mg/kg/day) to HFD/STZ-diabetic rats for 4 weeks significantly reduced FBG levels (7.5 vs. 17.0 mM/l) (Ma et al. 2017).

In sweet potato (*Ipomoea batatas*), the tuberous roots are consumed as vegetables in subtropical and tropical countries and are used in traditional medicine in diabetes treatment. The tubers contain antioxidant phytochemicals, such as anthocyanins, complex carbohydrates, (1-3)-β-D-galactans, β-carotene, vitamin C, linoleic acid, and α-linolenic acid as major bioactive constituents. In three clinical trials, dietary supplementation of sweet potato (4 g/day in tablets) to T2DM patients ($n = 140$) for 3–5 months significantly reduced serum HbA1c levels (7.21–6.68%) (Ooi and Loke 2013). In another clinical trial, treatment of white sweet potato (WSP) (20 g in 70 g of formula level) to elderly T2DM patients ($n = 34$) for 60 days reduced serum HbA1c, FBG, and LDL-C levels and increased serum adiponectin, HDL-C, and vitamin A levels in WSP-treated group. 100 g of WSP contains 20 g protein, 12.9 g fat, 60.3 g carbohydrates, 13.5 g sugar, and 6.3 g dietary fiber (Chen et al. 2019). In animal model, oral treatment of WSP methanolic extract (4 g/kg bw/day) to alloxan-diabetic rats for 14 days significantly reduced blood glucose levels (7.7 vs. 10.1 mM/

l) in diabetic rats (Akhtar et al. 2018). These findings suggest that sweet potato could be useful as dietary supplement in the treatment of diabetes.

Ginseng (*Panax ginseng*) berry 70% ethanolic extract contains 19.99% of ginsenosides, having ginsenosides Rb1 **65**, Rb2 **459**, Rc **498**, Rd **499**, Re **64**, Rg1 **460**, and Rg2 **460a** of concentrations of 0.77%, 1.90%, 2.11%, 1.65%, 11.06%, 1.66%, and 0.84%, respectively. These ginsenosides have potential antidiabetic effect in animal models. In a clinical trial, treatment of ginseng berry extract in capsules (four capsules/day, two capsules at a single time before breakfast and dinner, each capsule containing 250 mg of ginseng berry extract) to T2DM patients ($n = 72$) with FBG levels of 110 mg/dl or higher for 12 weeks significantly reduced FBG (3.7%) and PPBG (10.7%). No adverse effects were reported. These findings suggest that ginseng berry extract could be used as an adjuvant antidiabetic agent for type 2 diabetic patients in prediabetic stage (Choi et al. 2018).

Delphinol, a standardized delphinidin anthocyanin-rich maqui berry (*Aristotella chilensis*) extract, containing 25% delphindin glycosides and 35% total anthocyanins, has been commercialized in capsules bearing 60, 120, and 180 mg Delphinol, as a dietary supplement for management of blood glucose and as an antioxidant agent by a Chile-based pharmaceutical industry. The major anthocyanins are delphinidin-3-sambioside-5-glucoside and delphinidin-3,5-diglucoside. Dietary supplementation of Delphinol in three different doses (60, 120, and 180 mg at a single dose in the morning 1 hour before glucose intake or before overnight fasting) to prediabetic subjects ($n = 36$) dose-dependently reduced both postprandial and fasting blood glucose and serum insulin levels after 30 min of glucose intake or in overnight fasting state. The lower dose (60 mg) is more effective and it contains 21 mg of maqui berry anthocyanins. Delphinol regulates glucose metabolism by three possible mechanisms: (1) by inhibition of the activity of intestinal glucose transporters, SGLT1, and SGLT2, (2) by increasing incretin-dependent insulin secretion, and (3) by increasing insulin sensitivity in target tissues (Alvarado et al. 2016).

The stem bark of cinnamon (*Cinnamomum cassia* and other *Cinnamomum* spp.) has long been used as spice in Asian countries. Cinnamon contains a variety of phytochemicals including cinnamaldehyde, cinnamic acid, eugenol **271**, β-caryophyllene **445**, E-nerolidol, and α-thujene, and many of them have hypoglycemic and insulin secreting effects in diabetic animals. In a clinical trial, oral intake of cinnamon (2 g/day) by T2DM patients ($n = 58$, among them, 25 male and 33 female) on their prescribed oral hypoglycemic drugs for 12 weeks significantly decreased serum HbA1c levels (8.22–7.86%) and both systolic and diastolic blood pressures (132.6–129.2 mmHg and 85.2–80.2 mmHg) compared to the placebo group (taking only oral hypoglycemic drugs), but no significant reduction in FBG and BMI was observed in diabetic patients compared to placebo group. No significant change in serum lipid profiles (TG, TC, HDL-C, and LDL-C) was found in cinnamon treated group (Akilen et al. 2010). In animal model, a 20% methanolic extract of cinnamon bark on oral treatment (500 mg/kg/day) to STZ-diabetic rats for 28 days significantly decreased serum FBG levels (8.1 vs. 15.7 mM/l) (Qusti et al.

2016). These results suggest that cinnamon supplementation may improve glycemic and blood pressure levels in diabetic patients.

Olive (*Olea europaea*) leaf extract in tablets has been consumed in many European countries as dietary supplement in glycemic control for diabetic patients. Olive leaf extract contains oleuropein **353**, oleuropein aglycone, hydroxytyrosol **354**, and tyrosol as major bioactive phytochemicals. In a controlled clinical trial, oral treatment of an alcoholic extract of olive leaf in tablets at a dose of 500 mg/day to T2DM adult patients ($n = 79$) for 14 weeks reduced serum HbA1c levels (8.0–1.5% vs. 8.9–2.75% in placebo group) and fasting insulin levels in the treatment group, but did not change postprandial plasma insulin levels in the treated group. In normal and STZ-diabetic rats, olive leaf extract treatment reduced postprandial glucose levels through suppression of the activity of starch digestive and absorption enzymes α-glucosidases and α-amylases. These findings suggest that olive leaf extract exhibits hypoglycemic effect in both diabetic humans and rats in different mechanisms (Wainstein et al. 2012).

Green cumin (*Cuminum cyminum*) essential oil in capsules (50 and 100 mg) has been commercialized in European countries as dietary supplement for glycemic control in diabetic patients. The major active components in the essential oil of green cumin are cuminaldehyde, γ-terpinine, α-sabinin, α-flandren, and α-kadinin, which have inhibitory effect of α-glucosidase and aldose reductase activity. In a clinical trial, treatment of cumin essential oil in capsules at two different doses (50 and 100 mg, one capsule/day) to T2DM patients ($n = 33$) for a period of 8 weeks significantly decreased FBG (114.4 vs. 170.3 mg/dl in 100 mg treated group and 163.6 vs. 169.9 mg/dl in 50 mg treated group), serum insulin, and HbA1c levels in treated group. In addition, cumin treatment significantly decreased serum levels of inflammatory factors TNF-α and hs-CRP and increased serum adiponectin levels in diabetic patients (Jafari et al. 2017).

Scoparia dulcis leaf extract on oral administration (200 mg/kg bw/day) to STZ-diabetic rats for 6 weeks showed significant hypolipidemic effect by reduction of serum and tissue lipid profile (TG, TC, FFAs, PLs, VLDL-C, and LDL-C) levels and HMGCR activity in the liver of diabetic rats. In addition, the extract reduced serum glucose levels via reduction of hepatic glucose production by suppression of gluconeogenic enzyme G6Pase activity and increased hepatic glycogen synthesis by increasing the activity of the enzymes HK, G6PD and GS, and glucose uptake in the skeletal muscle by increasing the expression and translocation of GLUT4 proteins to the plasma membrane in diabetic rats. The leaf extract of *S. dulcis* strongly inhibited the activity of intestinal α-glucosidases and mildly the activity of pancreatic α-amylase in diabetic rats. In Sri Lanka, *S. dulcis* leaf porridge (SDP), known as kola kenda, has been commercialized in airtight packet containing 40 g of SDP as food supplement in management of glycemic and lipid profiles for type 2 diabetic patients. In a clinical trial, oral supplementation of SDP (40 g, once a day for 3 days/week, containing 35 mg of *S. dulcis* leaf extract/kg bw) to T2DM patients ($n = 35$) for 3 months significantly reduced serum HbA1c (7.9–6.5%) and FBG (174–160 mg/dl) levels, but no significant changes in serum insulin and lipid profiles were observed. Each 40 g of SDP contains *S. dulcis* fresh leaf, red rice, and scraped

coconut kernel in a ratio of 13–15:25–30:10–13 (w/w/w). Phytochemicals, namely, apigenin **197**, luteolin **196**, hispidulin **201**, scutellarin **352a**, betulinic acid **207**, and β-sitosterol-3-β-D-glucoside, were present as major bioactive constituents in the leaf extract of *S. dulcis*. These findings justify the traditional practice of SDP as diet supplement in hyperglycemic control in diabetic patients (Pari and Latha 2006; Mishra et al. 2013; Senadheera et al. 2015).

Aloe vera (L.) Burm. F has long been used in traditional medicine in many countries as purgative and for the treatment of wounds in the skin, coughs, ulcers, gastritis, cancer, diabetes, arthritis, and immune system deficiencies. Its leaf gel has been reported to have hypoglycemic and hypolipidemic effect in STZ-diabetic rats. *Aloe vera* leaf gel consists of a variety of phytochemicals (about 75), including antioxidant vitamins C and E and β-carotene; mucilage-forming carbohydrates, aloeride, acylated glucomannans, and glucogalactomannan; protein lectins; anthraquinones, emodin **123**, and aloe-emodin **123a**; and β-sitosterol (Hamman 2008). In a clinical trial, *A. vera* leaf gel (one 300 mg capsule, twice in a day) on oral treatment to hyperlipidemic T2DM patients, aged 40–60 years ($n = 30$), along with their prescribed regular oral hypoglycemic drugs, two 5 mg glyburide tablets and two 500 mg metformin tablets/day for 2 months, reduced FBG, serum HbA1c, TC, and LDL-C levels, as compared to the placebo group ($n = 30$) taking only regular oral hypoglycemic drugs. No significant changes on other serum lipid levels and liver/kidney function tests were observed between aloe gel treatment and placebo groups. Moreover, no adverse effects were reported. These findings suggest that *Aloe vera* leaf gel may be a safe dietary supplement for the control of hyperglycemia and hyperlipidemia in diabetic patients (Huseini et al. 2012).

Fenugreek (*Trigonella foenum-graecum* L.) seeds (known as methi) are widely used spice in Indian kitchen and have been used in traditional medicine in diabetes treatment in Asia. In both diabetic animals and humans, fenugreek seeds showed significant hypoglycemic effects. The major active phytochemicals in fenugreek seeds are soluble fibers, saponins, diosgenin **87**, trigonelline **345b**, and 4-hydroxyisoleucine **345a**. A meta-analysis of ten clinical trials among 278 T2DM patients reported that oral intake of fenugreek seed powder in capsules or extract (1–100 g/day) by T2DM patients for a period of 1–3 months decreased FBG (up to –0.96 mM/l in ten trials), PPG (up to –2.19 mM/l, in seven trials), and HbA1c (up to –0.85%, in three trials) as compared with the placebo group. These findings suggest that fenugreek seeds may be a useful adjuvant in glycemic control of diabetic subjects (Neelakantan et al. 2014). An aqueous-alcoholic extract of fenugreek seeds on oral treatment at doses of 0.5–2.0 g/kg/day, p.o., to alloxan-diabetic rats for 30 days markedly reduced FBG (7.6 vs. 15.5 mM/l) and HbA1c levels and decreased the activity of serum α-glucosidase and lipase as well as hepatic inflammation in diabetic rats (Joshi et al. 2015).

Astragalus membranaceus roots (radix) (AMR) have long been used in traditional Chinese medicine for treatment of chronic phlegmatic disorders, intestinal inflammation, stomach ulcer, chronic diarrhea, and diabetes. Several phytochemicals, including flavonoids astragalin **66a**; formononetin **389**; calycosin **389a**; calycosin-7-*O*-glucoside; astraisoflavan-7-*O*-glucoside; cycloartane triterpene

glycosides (saponins) astragaloside I, II, and IV **332a**; and polysaccharides, are found as major bioactive constituents in AMR. In STZ-diabetic rats, AMR polysaccharides reduced serum glucose levels and increased pancreatic insulin secretion via upregulation of GLP-1 secretion from the small intestine. A meta-analysis of 13 clinical trials among 1054 T2DM subjects reported that oral treatment of AMR extract at different doses reduced FBG, PPG, and fasting insulin by –0.83%, –1.19%, and –0.33%, respectively, whereas i.p. injection of AMR extract reduced FBG and PPG to a less extent in diabetic subjects (Tian et al. 2016).

Urtica dioica L. (nettle) leaves have significant insulin secreting, PPARγ agonistic, and α-glucosidase inhibitory effects in diabetic animals and in vitro assays. HPLC analysis of nettle leaf extract revealed the presence of gallic acid, rutin, and quercetin as major active chemical constituents. In a randomized, double-blind placebo-controlled clinical trial, oral treatment of nettle leaf extract (one 500 mg capsule, three times a day) to advanced T2DM patients, aged 40–60 years ($n = 46$) on their oral hyperglycemic drugs and having FBG levels above 200 mg/dl and HbA1c levels above 8%, for a period of 3 months, reduced fasting and postprandial blood glucose levels, serum levels of HbA1c, creatinine, and liver enzymes SGOT and SGPT, and both systolic and diastolic blood pressures, as compared with the placebo group ($n = 46$). No adverse effects were reported by the treated diabetic patients. These results suggest that nettle leaf extract could be utilized as a safe food supplement for glycemic control in diabetic patients (Kianbakht et al. 2013a).

Mulberry (*Morus alba*) leaf aqueous extract has significant hypoglycemic effect in diabetic animals. 1-Deoxynojirimycin **108** present in the aqueous mulberry leaf extract has strong inhibitory effect against α-glucosidase. In a clinical trial, oral supplementation of mulberry leaf aqueous extract (5 g/day) to prediabetic patients ($n = 36$) for 4 weeks reduced postprandial blood glucose levels significantly after 30 and 60 min of drug administration and plasma insulin levels as compared to the placebo group (Kim et al. 2015). These findings suggest that mulberry leaf aqueous extract may be a useful diet supplement in glycemic control of diabetic patients.

The rhizomes of ginger (*Zingiber officinale*) are consumed as spice in many countries and are used in traditional medicine for treatment of cataract, rheumatism, asthma, stroke, constipation, and diabetes. In diabetic animals, oral treatment of ginger extract showed significant hypoglycemic effects via glucose uptake, insulin secretion, and inhibition of the activities of α-glucosidase and α-amylase. Several antioxidant phytochemicals, such as 6, 8, and 10-gingerols **154–154b**, 6-shogaol **153**, 6-paradol **152**, and zingerones, are found in ginger. In a double-blind, placebo-controlled trial, ginger rhizome extract on oral treatment in 500 mg capsules (2 g/day, two capsules before lunch and two capsules before dinner) to T2DM patients, aged 40–60 years ($n = 25$), for 10 weeks significantly reduced serum levels of FBG (–26.30 mg/dl vs. 11.91 mg/dl) and HbA1c (–0.38 vs. 0.32%) compared to the placebo group ($n = 25$). No significant changes in serum levels of TG, TC, LDL-C, and HDL-C were observed between the ginger- and placebo-treated groups (Arzati et al. 2017). In another trial, oral treatment of ginger powder in capsules of 800 mg (two capsules/day, one before lunch and another before dinner) to T2DM patients ($n = 33$) having HbA1c levels between 7 and 10% and BMI between 20 and

35 kg/m^2 and taking their prescribed OHAs for 12 weeks significantly reduced serum FBG, HbA1c, insulin, HOMA-IR, TG, TC, CRP, and PGE_2 levels by –9.1 vs. 16.0 mg/dl, –1.0 vs. 0.4%, –3.7 vs. 0.1 μU/ml, –1.7 vs. 0.2, –45.4 vs. 2.5 mg/dl, –15.4 vs. 5.8 mg/dl, –2.5 vs. –0.7 mg/dl, and –126.7 vs. –21.4 pg/ml, respectively, compared to the placebo group ($n = 30$). No significant differences in HDL, LDL, and TNFα were observed between the two groups (Arablou et al. 2014). An aqueous extract of ginger on i.p. administration (500 mg/kg/day) to STZ-diabetic rats for a period of 7 weeks significantly reduced serum FG (52%), TC (44%), and TG (41%) compared to the control group (Al-Amin et al. 2006). These findings suggest that ginger might be an effective diet supplement as adjuvant therapy in glycemic and dyslipidemia controls in diabetic complications.

An aqueous ethanol extract of Asian antidiabetic plant *Salacia oblonga* on oral treatment at a single dose of 480 mg/day in T2DM patients after a high-carbohydrate meal significantly decreased serum PPBG levels (6.7 mM/l vs. 8.9 mM/l in placebo group) and insulin levels (Williams et al. 2007). In an animal model, an aqueous extract of *S. oblonga* on oral treatment (100 mg/kg/day, p.o.) in Zucker obese rats for 6 weeks markedly reduced PPBG levels (13.9 vs. 20 mM/l in control) (Li et al. 2004). The phytochemicals thiosugars salacinol **452a** and kotalanol **452b** present in the extract have strong inhibitory effect against intestinal α-glucosidases. Thus, *S. oblonga* extract is useful in the control of serum postprandial glucose levels in diabetic patients.

An aqueous-alcoholic extract rich in anthocyanins from Caucasian antidiabetic fruit whortleberry (*Vaccinium arctostaphylos*) on oral treatment in 350 mg capsule, each capsule three times a day in aged 40–60 years T2DM patients ($n = 37$) having FPG levels of 200–250 mg/dl and HbA1c levels of 7–8% and taking their regular oral hypoglycemic agents for 3 months, significantly decreased serum FG (–16 vs. –4.7 mg/dl) and PPG (–13.5 vs. + 6.5 mg/dl) and HbA1c (6.9 vs. 7.4%), compared to the placebo group taking only oral hypoglycemic agents. No significant adverse effects on the liver/kidney function and other adverse effects were observed in the two groups (Kianbakht et al. 2013b).

Chinese wolfberry or Goji berry (*Lycium barbarum*) has been prescribed in traditional Chinese medicine for treatment of urinary disorders. Wolfberry fruits on extraction with water afforded polysaccharides (LBP) composed of arabinose, galactosamine, lactose, and glucose. In a clinical trial, oral treatment of LBP in capsules of 150 mg, two capsules/day after dinner, to T2DM patients ($n = 37$), having FBG levels above 7.0 mM/l, for a period of 3 months significantly decreased serum glucose (–7.86% vs. 1.61% in placebo group) and increased insulinogenic index (–0.98 to 0.04%) compared to placebo group ($n = 30$) without showing significant changes in serum lipid profiles (TC, TG, HDL, and ApoB) between the two groups. The hypoglycemic efficacy was more significant in diabetic patients taking no OHAs than in patients taking OHAs (Cai et al. 2015). In an animal model, oral treatment of LBP (25 mg/day, i.p.) to STZ-induced diabetic rats with high glucose-aggravated ischemic brain injury for 4 weeks significantly reduced serum glucose levels (20 vs. 28 mM/l) and glucotoxicity in the brain and improved neurogenic deficit function in the brain by upregulation of mitochondrial fusion-

related protein Optic atrophy-1 (Opa-1) and downregulating the expression of mitochondrial fission-related protein Dynamin-related protein-1 (Drp-1) in the brain for maintenance of normal mitochondrial function in the brain of diabetic rats. These findings suggest that LBP could be useful in hyperglycemia-induced neural disorders in the brain (Liu et al. 2017).

Silymarin, an extract of milk thistle (*Silybum marianum*) seeds, rich in flavonolignan silibinin, also known as silybin (A and B) **352b**, showed significant hypoglycemic effect in both diabetic cellular and animal models. In a clinical trial, silymarin on oral intake (140 mg, thrice daily) by T2DM patients ($n = 20$) for 45 days reduced FBG, serum insulin, HOMA-IR, TG, and TG/HDL-C ratio by 11.01, 14.35, 25.92, 23.7, and 27.67%, respectively, as compared to the placebo group ($n = 20$). Moreover, silymarin treated group showed increased levels of serum HDL-C and insulin sensitivity check index as compared to the placebo group. These findings suggest that silymarin supplementation in diet improves glycemic index and lipid profiles in T2DM patients (Ebrahimpour-Koujan et al. 2018).

Nigella sativa seeds, popularly known as black cumin, have been found with antidiabetic effects in diabetic animal models. A meta-analysis of clinical trials in T2DM patients reported that oral supplementation of *N. sativa* seed powder or seed oil (0.5–2.0 g/day) to T2DM patients ($n = 255$) for a period from 2 to 12 months significantly decreased FBG (–17.84 mg/dl), HbA1c (–0.71%), TC (–22.99 mg/dl), LDL-C (–22.38 mg/dl), and TG (–6.80 mg/dl) in diabetic patients. The antioxidant phytochemicals, namely, thymoquinone **126a**, dithymoquinone, linoleic acid, and oleic acid, have been identified in seed extracts of black cumin. These findings suggest that black cumin seeds or seed oil may be useful as dietary supplement in glycemic control for diabetic patients (Daryabeygi-Khotbehsara et al. 2017).

Juglans regia L. (walnut) leaf has been used in traditional medicine in diabetes treatment in Iran and other countries. The leaves of the plant contain phenolic compounds ferulic acid, vanillic acid, coumaric acid **19**, ellagic acid **320**, myricetin **22**, and juglone as major antioxidant compounds. In a randomized double-blind, placebo-controlled trial, oral treatment of 70% ethanol extract of *J. regia* leaf in 100 mg capsules (two capsules/day) to T2DM patients, aged 40–60 years ($n = 61$), having FBG levels between 150 and 200 mg/dl and HbA1c levels between 7 and 9%, for 3 months along with their OHAs, metformin and glibenclamide, and restricted diet significantly decreased FBG (–25 vs. + 2 mg/dl), HbA1c (–0.9 vs. 0.3%), TC (–12.47 vs. + 5.55 mg/dl), and TG (–16.15 vs. + 21.18 mg/dl) levels compared with the baseline and with the placebo group taking only OHAs. No liver and kidney disorders and other side effects were reported (Hosseini et al. 2014). In alloxan-induced diabetic rats, oral treatment of *J. regia* leaf ethanol extract (200 mg/kg/day) for 4 weeks significantly decreased FBG (5.3 mM/l vs. 33.2 mM/l) and HbA1c levels, as well as increased insulin secretion and regeneration of pancreatic β-cell mass as compared to the control group. The effects of the extract were similar to the glibenclamide treatment group (Asgary et al. 2008). These findings suggest that *J. regia* leaf extract could be an adjuvant in diabetes treatment.

Green tea (*Camellia sinensis*) is a popular soft drink consumed by the people in many countries. The flavanols, such as epigallocatechin gallate (EGCG) **35**, epigallocatechin **36**, epicatechin gallate **37**, and epicatechin **39**, are the most common catechins, and caffeine **41** are found in high concentrations in green tea. In a double-blind controlled trial, a continuous ingestion of green tea either with 582.8 mg of catechins in 340 ml of water (catechin group, $n = 23$) or 96.3 mg of catechins in 340 ml water (control group, $n = 20$) by T2DM patients having no nephropathy and hyperlipidemic problems and along with their prescribed oral insulinotropic agents for a period of 12 weeks significantly reduced waist circumference (–3.3 vs. 0.1 cm), serum glucose (–8.0 vs. 4.9 mg/dl), HbA1c (–0.37 vs. –0.01%), TG (–16.8 vs. –0.2 mg/dl), TC (–10.3 vs. 4.9 mg/dl), and FFAs (–130 vs. –69 μEq/l) levels and systolic blood pressure (–5.9 vs. –3.9 mmHg) and increased serum adiponectin (1.32 vs. 0.34 ng/ml) and insulin (1.78 vs. –0.55 μU/ml) levels in the catechin group than in the control group. In T2DM patients not taking oral insulinotropic agents, the catechin treatment group showed much reduction of serum glucose (–14.6 vs. 7.3 mg/dl) levels compared with the control group (Nagao et al. 2009). A meta-analysis of 17 clinical trials among 1133 type 2 diabetic and overweight/obese subjects suggested that green tea consumption (four or more cups/day) for a period of 2 weeks to 6 months significantly reduced FBG and HbA1c levels by –0.09 mM/l and –0.3%, respectively (Liu et al. 2013). These findings suggest that catechin-rich beverages might be a useful diet supplement in the management of obesity and glycemic and lipid profiles in newly diagnosed diabetic patients.

Herbal hepatoprotective drug-silymarin-based a polyherbal formulation in capsules of 600 mg, each capsule contains toasted powder of 200 mg *Silybium marianum* seeds, 200 mg *Boswellia serrata* (olibanum gum) and 200 mg nettle *(Urtica dioica*) leaves, has been recommended for treatment of type 2 diabetes in Iran. HPLC analysis of the extract of this polyherbal capsule reveals the presence of silibinin, α-pinene, and rutin **54** as major chemical constituents. In a placebo-controlled clinical trial, oral treatment of this polyherbal formulation (one capsule/day along with oral hypoglycemic drug) to T2DM patients ($n = 30$) having FBG levels between 150 and 180 mg/dl, and HbA1c levels between 7.5 and 8.5%, for 90 days significantly reduced FBG and serum HbA1c and TG levels as compared to the placebo group ($n = 30$, used only oral hypoglycemic drug), but no significant changes in serum TC and blood pressure levels were observed between the two groups. Further studies are required using more diabetic patients to confirm these observed findings (Khalili et al. 2017).

An Ayurvedic polyherbal combination, PDBT in capsules (each capsule contains 500 mg of combined extract), consisting of a mixture of the aqueous extracts of five herbs, *Tinospora cordifolia* stem, *Pterocarpus marsupium* bark, *Gymnema sylvestre* leaves, *Zingiber officinale* rhizome, and *Momordica charantia* fruits, has been commercialized in India for treatment of prediabetic patients (FBG levels between 100 and 125 mg/dl). In a clinical trial, PDBT on oral treatment at a dose of two capsules twice daily, after breakfast and before dinner, to prediabetic patients ($n = 57$) along with their lifestyle management (LSM) oral hypoglycemic drugs

for 6 months significantly decreased BG levels (fasting and PP), HbA1c, fasting insulin, and HOMA-IR values as compared to the placebo group ($n = 57$, used only LSM oral hypoglycemic drugs). But no significant change in BMI levels was observed. No adverse effects were reported (Nakanekar et al. 2019).

"GSPF-kwath," an Ayurvedic polyherbal formulation consisting of a mixture of the aqueous extracts of ten herbs, *Gymnema sylvestre* (gulmar) leaves, *Syzygium cumini* (jamun) seeds, *Phyllanthus emblica* (amla) fruits, *Curcuma longa* (haldi) rhizomes, *Pterocarpus marsupium* (vijaysaar) heartwood, *Terminalia chebula* (harad) fruits, *Cassia fistula* (amaltas) fruits, *Picrorhiza kurroa* (kutki) rhizomes, *Swertia chirata* (chirayita) seeds, and *Terminalia bellirica* (behala) fruits, has been commercialized by a pharmaceutical industry in India for treatment of type 2 diabetes. In a clinical trial, oral intake of "GSPF-kwath" (50 ml equivalent to 10 g of the kwath, in empty stomach/day) by T2DM patients ($n = 30$) for 6 months significantly reduced postprandial and fasting blood glucose levels and serum HbA1c, TC, TG, LDL-C, and VLDL-C levels and increased serum HDL-C levels in diabetic patients. No adverse effect was reported. These findings suggest that this polyherbal formulation could be utilized as a safe and effective diet supplement in the control of hyperglycemia and hyperlipidemia for diabetic patients (Mahajan et al. 2015). However, further studies in large number of patients and on the active constituents of this polyherbal formulation are necessary for its scientific confirmation and popularization in the market.

Another standardized polyherbal formulation (PHF) consisting of aqueous extracts (83.3 mg from each of six herbs, *Cyperus rotundus*, *Cedrus deodara*, *Berberis aristata*, *Emblica officinalis*, *Terminalia bellirica*, and *Terminalia chebula*), in capsules of 500 mg, has been commercialized in Indian market for treatment of type 2 diabetes. HPLC analysis of the PHF indicated the presence of berberine (1.27%), quercetin (0.01%), and gallic acid (3.09%) as major active components. In a clinical trial, oral treatment of the PHF (500 mg/day to a maximum of 3 g/day) to newly diagnosed T2DM patients ($n = 93$) for 6 months and a metformin treatment group (500 mg/day to a maximum of 2 g/day) for 6 months showed reduction of fasting and postprandial blood glucose levels by 25.52% and 24.22%, in PHF-treated group, and of 31.46% and 24.05%, respectively, in metformin-treated group. Moreover, PHF-treated group showed significant reduction of serum HbA1c levels (7.38–6.07% vs. 7.73–6.43%) similar to that in metformin-treated group but has much reduction of serum TC, TG, and LDL-C levels, compared to metformin-treated group. Other biochemical parameters on liver enzymes and renal functions were found toward the normal. Further studies on the mode of action of bioactive phytochemicals and in large-scale diabetic patients are needed for its scientific validation (Awasthi et al. 2015).

A polyherbal formulation under the trade name "Diabecon," consisting of extracts from specific parts of *Gymnema sylvestre*, *Balsamodendron mukul*, *Pterocarpus marsupium*, *Glycyrrhiza glabra, Casearia esculenta, Eugenia jambolana, Asperagus racemosus*, *Boerhavia diffusa, Tinospora cordifolia*, *Sphaeranthus indicus, Swertia chirata, Tribulus terrestris, Phyllanthus amarus,*

Gmelina arborea, Gossypium herbaceum, Berberis aristata, Aloe vera, Shilajeet, *Momordica charantia*, *Piper nigrum*, *Ocimum sanctum*, *Abutilon indicum*, *Curcuma longa*, *Rumex maritimus*, and Trikatu as main constituents, has been commercialized in tablets by the Himalaya Drug company, India, for the treatment of diabetes. In a meta-analysis of 15 clinical trials on diabetes patients, Diabecon on oral treatment (two tablets/day and one tablet/day) to T2DM patients in absence of other oral hypoglycemic drugs (OHDs) ($n = 320$) and along with their prescribed conventional OHDs/insulin ($n = 69$), respectively, for 12–60 weeks, significantly improved FBG, PPBG, serum levels of HbA1c, TC, insulin, and microalbuminuria, as compared to the placebo group. No adverse effects, except skin rashes and gastritis in a few patients, were reported. Possibly, the antioxidant activities of the plant extracts protected the diabetic pancreas from oxidative stress and inflammation-induced injury and apoptosis of pancreatic β-cells and improved pancreatic β-cell mass regeneration and insulin secretion and regulated lipid and glucose metabolism in peripheral tissues (Kundu and Chatterjee 2010). Future studies are necessary for identification of active constituents present in this polyherbal formulation and their concentrations and major targets of actions.

Two more polyherbal formulations under the trade names "Diabeta Plus" and "Glycoherb" have been commercialized in India for treatment of diabetes. Diabeta Plus is useful for suppression of stress and hepatic toxicity as well as for reduction of hyperglycemia in diabetic patients. Glycoherb has potential antioxidant and hypoglycemic effects (Choudhury et al. 2018).

8.2.2 Phytochemicals

Resveratrol **47**, a stilbenoid phytochemical present in grapes and other fruits, has significant antidiabetic effect in animal models. In a clinical trial, resveratrol on oral supplementation (250 mg/day) to T2DM patients along with their oral hypoglycemic agents (OHAs) for a period of 3 months significantly improved serum HbA1c levels (9.99 vs. 9.65%), systolic blood pressure (139.7 vs. 127.9 mmHg), TC (4.70 vs. 4.33 mM/l), and TPs (75.6 vs. 72.3 mg/dl) in diabetic patients compared to the placebo group (used only OHAs). No significant changes in body weight and HDL-C and LDL-C levels were observed. No adverse effects were reported. Hence, resveratrol may be used as an adjuvant drug in glycemic control of diabetic patients (Bhatt et al. 2012). In another clinical trial, resveratrol on oral supplementation (150 mg/day) to aged 52 years and above obese patients with BMI of 32 kg/m^2 and above, and FBG of 5.5 mM/l and above for 30 days significantly suppressed postprandial glucagon levels (4.4 vs. 3.9 min × nM/l, $p = 0.01$) without affecting fasting glucagon levels or fasting/postprandial plasma incretin hormone levels in obese patients (Knop et al. 2013).

Commercially available curcuminoids consist of curcumin **9** (36.06%), demethoxycurcumin **156** (18.85%), and bisdemethoxycurcumin **157** (42.58%) as

major constituents, and all these constituents have been found to possess significant hepatoprotective, antihyperlipidemic, and antihyperglycemic activities in diabetic animal models. A clinical trial of curcuminoids on oral treatment (300 mg/day) to overweight/obese type 2 diabetic patients ($n = 50$) with BMI > 24.0 kg/m^2, FBG > 7.0 mM/l, or PPG > 11.1 mM/l for 3 months as compared to the placebo group ($n = 50$). Curcuminoid treated group significantly decreased FBG ($p < 0.01$), HbA1c ($p = 0.031$), and insulin resistance index (HOMA-IR) ($p < 0.01$) in the diabetic patients. Curcuminoids also decreased serum total FFAs and TG levels and increased LPL activity but showed no change in BMI levels as compared to the placebo group. These findings suggest that dietary supplementation of curcuminoids may improve glycemic level in diabetic patients (Na et al. 2013). In another clinical trial, oral treatment of curcuminoids plus piperine (500 + 5 mg/day) to T2DM patients ($n = 100$, curcuminoid plus piperine treated group, $n = 50$, and placebo group, $n = 50$) for 3 months significantly decreased serum glucose (–9 vs. –3 mg/dl) and HbA1c (–0.9 vs. –0.12%), C-peptide (–0.6 vs. 0.02 ng/ml), and AST (–3 vs. –0.3 U/l) as compared to the placebo group, but no significant difference in hs-CRP levels was observed between the two groups. These findings suggest that piperine improves the bioavailability of curcuminoids, and curcuminoid plus piperine supplementation has beneficial effect on the control of glycemic and hepatic toxic biomarker levels in T2DM patients (Panahi et al. 2018).

Berberine **48** is an isoquinoline alkaloid, present as major constituent in *Coptis chinensis* French, an important herb in traditional Chinese medicine for treatment of diabetes and gastrointestinal disorders. The antidiabetic efficacy of berberine in diabetic animals has been reported by many groups. In a clinical trial, oral treatment of berberine (500 mg, three times a day before main meals) or metformin (500 mg, three times a day, after main meals) to newly diagnosed T2DM patients ($n = 36$), aged 25–75 years and with HbA1c levels > 7.0%, FBG levels > 7.0 mM/l, and BMI > 22 kg/m^2 for 3 months, significantly decreased FBG (10.6–6.9 mM/l), PPBG (19.8–11.1 mM/l), HbA1c (9.5–7.5%), and fasting insulin (29.1–24.0 μU/ml) levels, without significant changes in lipid profile in diabetic patients. The hypoglycemic effect of berberine was similar to that of metformin-treated group. During a trial with poorly controlled type 2 diabetic patients ($n = 48$), about 34.5% patients suffered from transient gastrointestinal adverse effect. Further study on the effective dose of berberine without any adverse effect is required for the treatment of diabetic patients (Yin et al. 2008).

8.3 Discrepancies in Glucose Lowering and Hypolipidemic Efficacy of Herbal Extracts in Diabetic Animal and Human Studies: Major Factors

There are several instances where the antidiabetic and antihyperlipidemic effects of herbal extracts in diabetic animal studies failed to translate the results in clinical trials in diabetic humans. For instance, an oral treatment of an aqueous-alcoholic extract of antidiabetic plant *Caralluma fimbriata* at a dose of 200 mg/kg/day in DIO rats for

90 days significantly reduced hyperglycemia and hypertriglyceridemia in obese rats (Sudhakara et al. 2014). Meanwhile, an extract of *C. fimbriata* on oral treatment in 500 mg capsules (one capsule/day) to overweight/obese subjects for 12 weeks showed no significant reduction of serum glucose and lipid profiles (Astell et al. 2013). An extract from antidiabetic plant *Ginkgo biloba* on oral treatment (300 mg/kg/day) in STZ-diabetic rats for 30 days almost normalized glycemic and hyperlipidemic levels in diabetic rats (Cheng et al. 2013). Meanwhile, the oral treatment of an active extract (EGb 761) from *G. biloba* at a dose of 120 mg/day in T2DM patients along with conventional hypoglycemic drug metformin for 3 months mildly reduced serum HbA1c level but showed no significant change in FBG level in diabetic patients compared to the placebo group (Kudolo et al. 2006). A similar discrepancy in antihyperglycemic results was observed on *Aralia taibaiensis* extracts. A root-bark extract rich in saponins from *A. taibaiensis* on oral treatment at a dose of 320 mg/kg/day in STZ-diabetic rats for 28 days markedly reduced serum glucose levels in treated diabetic rats (Weng et al. 2014). But oral treatment of an extract from the root-bark of *A. taibaiensis* in combination with oral hypoglycemic glipizide in T2DM patients mildly reduced serum HbA1c and LDL-C levels (Liu et al. 2015). About 49 plant extracts have been found to exhibit strong hypoglycemic effect in animal models but showed poor hypoglycemic effect in clinical trials in type 2 diabetic humans (Furman et al. 2020). Several factors play key roles in anomaly of antidiabetic effects of plant extracts in animal and human studies. Some of them are highlighted here.

1. **Variation in the concentrations and composition of antidiabetic constituents in plant extracts**
   The concentrations and composition of bioactive chemical constituents in anti-obesity and antidiabetic plants depend on several factors, including the plant parts used, season of collection, geographical location of the plant species, and the environmental conditions in growing period and harvesting time and season. For example, 1-deoxynojirimycin (DNJ) **108**, a potent inhibitor of α-glucosidase and present as major antidiabetic component in mulberry leaf extract, and its concentration in leaf depend on the harvest season and the age of the leaf. The young mulberry leaves collected from the top parts of branches in summer have high concentrations of DNJ (Kimura et al. 2007). Kaurenoic acid **108a**, a hypoglycemic kaurane diterpenoid, present in antidiabetic plant *Wedelia paludosa* (syn. *Acmela brasiliensis*), was found in different concentrations in leaves, stems, and roots of the plant in different growing seasons; the maximum concentrations were found in roots and stems (6.65 and 4.96 mg/g of dry plant, respectively) on collection in autumn (Bresciani et al. 2004).
2. **Applied doses of the plant extracts in animal and human studies**
   In experimental diabetic rats, mice, and other animals, the plant extracts at the doses 100–500 mg/kg bw/day are usually applied, whereas in diabetic and obese humans, the plant extracts at the doses 100 mg to 6000 mg/day, equivalent to 1.5–85 mg/kg for a 70 kg adult, have been applied in general. The antidiabetic efficacy of a plant extract depends on the concentration/s of the antidiabetic component/s present in the applied dose of the extract, and at certain low

concentrations, their antidiabetic effects were not found. Possibly, the requisite concentrations of antidiabetic constituents are not available in the tested doses in human studies. Most of the animal and human studies did not evaluate the concentrations of active constituents and their major therapeutic targets.

3. **Choice of appropriate animal models that are closely similar (mimics) to human obesity and diabetes**
   Accumulating evidence demonstrates that alloxan or a single large dose of STZ-induced diabetic rats/mice provides the face validity (mimic disease signs and symptoms of human type 1 diabetes) for human type 1 diabetes study (Wilcox et al. 2016). Another study reported that NOD mice, AKITA mice, or BB rats provide both face and construct validity (i.e., etiology of the disease, such that mechanisms of β-cell destructions in animals and diabetic humans are almost similar) and are highly suitable for type 1 diabetes study (Graham and Schuurman 2015). In humans, obesity and its closely associated diabetes and diabetic vascular complications are induced by multiple interactions of the environmental factors with different types of genes, and hence mutated polygenic animal models are superior than mutated monogenic animal models. Several studies suggest that inbred C57BL/6J DIO mouse, the New Zealand obese (NZO) mouse, and high-fat diet fed KK-Ay mouse are highly suitable for the study of insulin resistance, dyslipidemia, mitochondrial biogenesis, and pancreatic β-cell failure, in obesity and type 2 diabetes (Fang et al. 2019; Donath et al. 2013; Boni-Schnetzier and Meier 2019). Some groups suggested that chemically induced (STZ and HFD fed) type 2 diabetic rats were superior to spontaneously diabetic db/db mice in the study of predictive validity of glucose and HbA1c lowering effects in diabetic humans (Varga et al. 2015).
4. **Timing of drug administration at different stages of disease development**
   In diabetic animal experiments, the plant extracts are administered at the early stages and before development of the disease. In clinical trials in humans, the plant extracts are generally applied to the obese and type 2 diabetic patients, when the disease is well established in the patients and developed much earlier in the body. As a result, the plant extracts in humans are exposed to large amounts of mutant genes and proteins related to the disease pathogenesis.
5. **Impact of co-therapy in human studies**
   Only a few clinical trials in type 2 diabetic patients are reported, where plant extracts are the sole therapeutic intervention. In most of the cases, plant extracts are administered in type 2 diabetic patients along with their conventional oral hypoglycemic agents (OHAs)/insulin. In such cases, the antidiabetic effects of the tested extracts may be masked or diminished by the effects of OHAs.
6. **Duration of therapy**
   In animal models, particularly in rodents, most of the experiments were conducted in obese and diabetic mice/rats from 14 days to 16 weeks, whereas in clinical trials in diabetic humans, the experiments were carried out from 8 to 12 weeks. The average lifespan of mice and rats is 2 and 3 years, whereas the average expected lifespan of humans as per global scale is 80 years. It indicates that one human year is equivalent to nine mice days and one rat month is

equivalent to three human years (Dutta and Sengupta 2016; Sengupta 2013). These facts indicate that animal studies were conducted in longer duration compared to human studies. The Committee for Medicinal Plants for Human Use (CHMP), European Medicines Agency vide note CPMP/EWP/1080/00 Rev 2, January 2018, recommended that 8–12-week study is sufficient to identify the efficacy of the drug in lowering of blood glucose levels in type 2 diabetic patients, but for its confirmation, a minimum of 6 months' duration is necessary and in type 1 diabetic patients, 24–26 weeks or more duration is suitable in the study of confirmation in serum glucose and HbA1c lowering effects of natural drugs.

7. **Lack of information on the composition of major bioactive constituents and their modes of actions**
   Most of the animal and human studies on plant extracts did not identify the major bioactive constituents responsible in hypoglycemic and hypolipidemic effects and their major therapeutic targets and bioavailability in diabetic and obese animals and humans. The bioavailability of these bioactive phytochemicals in animal and human is different. Several studies have identified the important roles of gut microbes in the metabolism and bioavailability of dietary polyphenols and polysaccharides and in the development of obesity and diabetes in the host. The composition of these gut microbiota in obese, diabetic, and healthy humans and rodents is different, and these gut microbiota have different physiological functions on dietary natural polyphenols and their bioavailability in different tissues (Kawabata et al. 2019).

8.4 Summary and Future Perspectives

Antidiabetic and anti-obesity effects of plant and mushroom extracts in obese and diabetic animals have been reported by several studies, but only a limited number of double-blind, placebo-controlled trials in obese and diabetic humans have been reported. In many cases, hypoglycemic and hypolipidemic efficacy of plant extracts is relatively low compared to those in animal studies. Most of the studies in animals did not identify the active constituents present in the extracts and their major therapeutic targets in glucose and lipid lowering effects and failed to explain the predictive validity of the results. The antidiabetic and anti-obesity efficacy of a limited number of plant extracts and phytochemicals has been evaluated in clinical trials in humans. Several nanoformulated plant, mushroom, and seaweed extracts and phytochemicals have been found more effective against tumor cell growth and diabetes compared to their free forms (Bonferoni et al. 2017; Dewanjee et al. 2020). We have to pay our attention in future for the study of these nanoformulated anti-obesity and antidiabetic plant and marine seaweed and animal extracts and phytochemicals in animal and human studies. Anthocyanin-rich fruits and fruit juices/extracts have been found effective in reduction of fasting/postprandial glucose, glycated hemoglobin, and lipid levels in obese and diabetic animals and humans (Yang et al. 2017). Future study is necessary to explore their utility as dietary supplement in glycemic control for obese and diabetic patients.

For effective utilization of these natural products from plants, mushrooms, marine algae, and animals as potent anti-obesity and antidiabetic natural drugs, an international multidisciplinary teamwork is necessary, where the experts from clinical practitioners, experimental diabetologists, phytochemists, microbiologists, and multi-omics biotecnologists might be included, and major pharmaceutical industries have to take leading role for requisite fund and instrument facilities and for protection of intellectual property rights of the discovery. Pragmatic approach on standardized polyherbal formulations on symptom-specific treatment of obesity and diabetes as personalized medicine would be more effective in reduction of global burden on obesity and type 2 diabetes.

References

Akhtar N, Akram M, Daniyal M et al (2018) Evaluation of antidiabetic activity of *Ipomoea batatas* L. extract in alloxan-induced diabetic rats. Int J Immunopathol Pharmacol 32: 2058738418814678

Akilen R, Tsiami A, Devendra D et al (2010) Glycated haemoglobin and blood pressure-lowering effect of cinnamon in multi-ethnic type 2-diabetic patients in the UK: a randomized, placebo-controlled, double-blind clinical trial. Diabet Med 27:1159–1167

Al-Amin ZM, Thomson M, Al-Qattan KK et al (2006) Anti-diabetic and hypolipidemic properties of ginger (*Zingiber officinale)* in streptozotocin-induced diabetic rats. Br J Nutr 96:660–666

Alvarado JL, Leschot A, Olivera-Nappa A et al (2016) Delphinidin-rich maqui berry extract (Delphinol®) lowers fasting and postprandial glycemia and insulinemia in prediabetic individuals during oral glucose tolerance tests. Biomed Res Int 2016:9070537

Arablou T, Aryaeian N, Valizadeh M et al (2014) The effect of ginger consumption on glycemic status, lipid profile and some inflammatory markers in patients with type 2 diabetes mellitus. Int J Food Sci Nutr 65:515–520

Arzati MM, Honarvar NM, Saedisomeolia A et al (2017) The effects of ginger on fasting blood glucose, hemoglobin A1c, and lipid profiles in patients with type 2 diabetes. Int J Endocrinol Metab 15:e57927

Asgary S, Parkhideh S, Solhpour A et al (2008) Effect of ethanolic extract of *Juglans regia* L. on blood sugar in diabetes-induced rats. J Med Food 11:533–538

Astell KJ, Mathai ML, McAinch AJ et al (2013) A pilot study investigating the effect of *Caralluma fimbriata* extract on the risk factors of metabolic syndrome in overweight and obese subjects: a randomized controlled clinical trial. Complement Ther Med 21:180–189

Awasthi H, Nath R, Usman K et al (2015) Effects of a standardized Ayurvedic formulation on diabetes control in newly diagnosed type 2 diabetes; a randomized active controlled clinical study. Complement Ther Med 23:555–561

Bhatt JK, Thomas S, Nanjan MJ (2012) Resveratrol supplementation improves glycemic control in type 2 diabetes mellitus. Nutr Res 32:537–541

Bonferoni MC, Rossi S, Sandri G et al (2017) Nanoparticle formulations to enhance tumor targeting of poorly soluble polyphenols with potential anticancer properties. Semin Cancer Biol 46:205–214

Boni-Schnetzier M, Meier DT (2019) Islet inflammation in type 2 diabetes. Semin Immunopathol 41:501–513

Bresciani LF, Yunes RA, Burger C et al (2004) Seasonal variation of kaurenoic acid, a hypoglycemic diterpene present in *Wedelia paludosa* (*Acmela brasiliensis*) (Asteraceae). Z Naturforsch 59c:229–232

Cai H, Liu F, Zuo P et al (2015) Practical application of antidiabetic efficacy of *Lycium barbarum* polysaccharide in patients with type 2 diabetes. Med Chem 11:383–390

Chen CM, Shih CK, Su YJ et al (2019) Evaluation of sweet potato tube feeding formula in elderly diabetic patients: a randomized controlled trial. Nutr Metab 16:70

Cheng D, Liang B, Li Y (2013) Antihyperglycemic effect of *Ginkgo biloba* extract in streptozotocin-induced diabetes in rats. Biomed Res Int 2013:162724

Choi HK, Kim S, Kim MJ et al (2018) Efficacy and safety of *Panax ginseng* berry extract on glycemic control: a 12 wk randomized, double-blind, and placebo-controlled clinical trial. J Ginseng Res 42:90–97

Choudhury H, Pandey M, Hua CK et al (2018) An update on natural compounds in the remedy of diabetes mellitus: a systematic review. J Tradit Complement Med 8:361–376

Dans AML, Villarruz MVC, Jimeno CA et al (2007) The effect of *Momordica charantia* capsule preparation on glycemic control in type 2 diabetes mellitus needs further studies. J Clin Epidemiol 60:554–559

Daryabeygi-Khotbehsara R, Golzarand M, Ghaffari MP et al (2017) *Nigella sativa* improves glucose homeostasis and serum lipids in type 2 diabetes: a systematic review and meta-analysis. Complement Ther Med 35:6–13

Dewanjee S, Chakraborty P, Mukherjee B et al (2020) Plant-based antidiabetic nanoformulations: the emerging paradigm for effective therapy. Int J Mol Sci 21:2217

Donath MY, Dalmas E, Sauter NS et al (2013) Inflammation in obesity and diabetes: islet dysfunction and their therapeutic opportunity. Cell Metab 17:860–872

Dutta S, Sengupta P (2016) Men and mice : relating their ages. Life Sci 152:244–248

Ebrahimpour-Koujan S, Gargari BP, Mobasseri M et al (2018) Lower glycemic indices and lipid profile among type 2 diabetes mellitus patients who received novel dose of *Silybum marianum* (L.) Gaertn. (silymarin) extract supplement: a triple-blinded randomized controlled clinical trial. Phytomedicine 44:39–44

Fang JY, Lin CH, Huang TH et al (2019) In vivo rodent models of type 2 diabetes and their usefulness for evaluating flavonoid bioactivity. Nutrients 11:530

Fuangchan A, Sonthisombat P, Seubnukarn T et al (2011) Hypoglycemic effect of bitter melon compared with metformin in newly diagnosed type 2 diabetes patients. J Ethnopharmacol 134: 422–428

Furman BL, Candasamy M, Bhattamisra SK et al (2020) Reduction of blood glucose by plant extracts and their use in the treatment of diabetes mellitus; discrepancies in effectiveness between animal and human studies. J Ethnopharmacol 247:112264

Graham ML, Schuurman HJ (2015) Validity of animal models of type 1 diabetes, and strategies to enhance their utility in translational research. Eur J Pharmacol 759:221–230

Hamman JH (2008) Composition and applications of *Aloe vera* L. leaf gel. Molecules 13:1599–1616

Hosseini S, Jamshidi L, Mehrzadi S et al (2014) Effects of *Juglans regia* L. leaf extract on hyperglycemia and lipid profiles in type two diabetic patients: a randomized double-blind, placebo-controlled clinical trial. J Ethnopharmacol 152:451–456

Huseini HF, Kianbakht S, Hajiaghaee R et al (2012) Anti-hyperglycemic and anti-hypercholesterolemic effects of *Aloe vera* leaf gel in hyperlipidemic type 2 diabetic patients: a randomized double-blind placebo-controlled clinical trial. Planta Med 78:311–316

Jafari S, Sattari R, Ghavamzadeh S (2017) Evaluation the effect of 50 and 100 mg doses of *Cuminum cyminum* essential oil on glycemic indices, insulin resistance and serum inflammatory factors on patients with diabetes II: a double-blind randomized placebo-controlled clinical trial. J Tradit Complement Med 7:332–338

Joshi DV, Patil RR, Naik SR (2015) Hydroalcohol extract of *Trigonella foenum-graecum* seed attenuates markers of inflammation and oxidative stress while improving exocrine function in diabetic rats. Pharm Biol 53:201–211

Kawabata K, Yoshioka Y, Terao J (2019) Role of intestinal microbiota in the bioavailability and physiological functions of dietary polyphenols. Molecules 24:370

Khalili N, Fereydoonzadeh R, Mohtashami R et al (2017) Silymarin, olibanum, and nettle, a mixed herbal formulation in the treatment of type II diabetes: a randomized, double-blind, placebo-controlled clinical trial. J Evid Based Complement Alternat Med 22:603–608

Kianbakht S, Khalighi-Sigaroodi F, Dabaghian FH (2013a) Improved glycemic control in patients with advanced type 2 diabetes mellitus taking *Urtica dioica* leaf extract: a randomized double-blind placebo-controlled clinical trial. Clin Lab 59:1071–1076

Kianbakht S, Abasi B, Dabaghian FH (2013b) Anti-hyperglycemic effect of *Vaccinium arctostaphylos* in type 2 diabetic patients: a randomized controlled trial. Forsch Komplementmed 20:17–22

Kim JY, Ok HM, Kim J et al (2015) Mulberry leaf extract improves postprandial glucose response in prediabetic subjects: a randomized, double-blind placebo-controlled trial. J Med Food 18: 306–313

Kimura T, Nakagawa K, Kubota H et al (2007) Food-grade mulberry powder enriched with 1-deoxynojirimycin suppresses the elevation of postprandial blood glucose in humans. J Agric Food Chem 55:5869–5874

Knop FK, Konings E, Timmers S et al (2013) Thirty days of resveratrol supplementation does not affect postprandial incretin hormone responses, but suppresses postprandial glucagon in obese subjects. Diebet Med 30:1214–1218

Kudolo GB, Wang W, Javors M et al (2006) The effect of the ingestion of *Ginkgo biloba* extract (EGb 761) on the pharmacokinetics of metformin in non-diabetic and type 2 diabetic subjects—a double-blind placebo-controlled, crossover study. Clin Nutr 25:606–616

Kundu PK, Chatterjee PS (2010) Meta-analysis of diabecon tablets: efficacy and safety outcomes from 15 clinical trials in diabetes mellitus. Indian J Clin Pract 20:653–659

Li Y, Peng G, Li Q et al (2004) *Salacia oblonga* improves cardiac fibrosis and inhibits postprandial hyperglycemia in obese Zucker rats. Life Sci 75:1735–1746

Liu K, Zhou R, Wang B et al (2013) Effect of green tea on glucose control and insulin sensitivity; a meta-analysis of 17 randomized controlled trials. Am J Clin Nutr 98:340–348

Liu XH, Li XM, Han CC et al (2015) Effects of combined therapy with glipizide and Aralia root bark extract on glycemic control and lipid profiles in patients with type 2 diabetes mellitus. J Sci Food Agric 95:739–744

Liu WJ, Jiang HF, Rehman FUL et al (2017) *Lycium barbarum* polysaccharides decrease hyperglycemia-aggravated ischemic brain injury through maintaining mitochondrial fission and fusion balance. Int J Biol Sci 13:901–910

Ma C, Yu H, Xiao Y et al (2017) *Momordica charantia* extracts ameliorate insulin resistance by regulating the expression of SOCS-3 and JNK in type 2 diabetes mellitus rats. Pharm Biol 55: 2170–2177

Mahajan S, Chauhan P, Subramani SK et al (2015) Evaluation of "GSPF kwath": a *Gymnema sylvestre*-containing polyherbal formulation for the treatment of human type 2 diabetes mellitus. Eur J Integr Med 7:303–311

Mishra MR, Mishra A, Pradhan DK et al (2013) Antidiabetic and antioxidant activity of *Scoparia dulcis* Linn. Indian J Pharm Sci 75:610–614

Na LX, Li Y, Pan HZ et al (2013) Curcuminoids exert glucose-lowering effect in type 2 diabetes by decreasing serum free fatty acids: a double-blind, placebo-controlled trial. Mol Nutr Food Res 57:1569–1577

Nagao T, Meguro S, Hase T et al (2009) A catechin-rich beverage improves obesity and blood glucose control in patients with type 2 diabetes. Obesity 17:310–317

Nakanekar A, Kohli K, Tatke P (2019) Ayurvedic polyherbal combination (PDBT) for prediabetes: a randomized double blind placebo controlled study. J Ayurveda Integr Med 10:284–289

Neelakantan N, Narayanan M, de Souza RJ et al (2014) Effect of fenugreek (*Trigonella foenum-graecum* L.) intake on glycemia: a meta-analysis of clinical trials. Nutr J 13(7)

Ooi CP, Loke SC (2013) Sweet potato for type 2 diabetes mellitus. Cochrane Database Syst Rev 2013:CD009128

Panahi Y, Khalili N, Sahebi E et al (2018) Effects of curcuminoids plus piperine on glycemic, hepatic and inflammatory biomarkers in patients with type 2 diabetes mellitus: a randomized double-blind placebo-controlled trial. Drug Res 68:403–409

Pari L, Latha M (2006) Antihyperlipidemic effect of *Scoparia dulcis* (sweet broomweed) in streptozotocin diabetic rats. J Med Food 9:102–107

Qusti S, El Rabey HA, Balashram SA (2016) The hypoglycemic and antioxidant activity of cress seed and cinnamon on streptozotocin induced diabetes in male rats. Evid Based Complement Alternat Med 2016:5614564

Senadheera SPAS, Ekanayake S, Wanigatunge C (2015) Anti-hyperglycemic effects of herbal porridge made of *Scoparia dulcis* leaf extract in diabetes—a randomized crossover clinical trial. BMC Complement Altern Med 15:410

Sengupta P (2013) The laboratory rat; relating its age with humans. Int J Prev Med 4:624–630

Sudhakara G, Mallaiah P, Sreenivasulu N et al (2014) Beneficial effects of hydro-alcoholic extract of *Caralluma fimbriata* against high-fat diet-induced insulin resistance and oxidative stress in Wistar male rats. J Physiol Biochem 70:311–320

Tian H, Lu J, Zuo P et al (2016) The effect of *Astragalus* as an adjuvant treatment in type 2 diabetes mellitus: a (preliminary) meta-analysis. J Ethnopharmacol 191:206–215

Varga OE, Zsiros N, Olsson IAS (2015) Estimating the predictive validity of diabetic animal models in rosiglitazone studies. Obes Rev 16:498–507

Wainstein J, Ganz T, Boaz M et al (2012) Olive leaf extract as a hypoglycemic agent in both human diabetic subjects and in rats. J Med Food 15:605–610

Weng Y, Yu L, Cui J et al (2014) Antihyperglycemic, hypolipidemic and antioxidant activities of total saponins extracted from *Aralia taibaiensis* in experimental type 2 diabetic rats. J Ethnopharmacol 152:553–560

Wilcox NS, Rui J, Hebrok M et al (2016) Life and death of β-cells in Type 1 diabetes: a comprehensive review. J Autoimmun 71:51–58

Williams JA, Choe YS, Noss MJ et al (2007) Extract of *Salacia oblonga* lowers acute glycemia in patients with type 2 diabetes. Am J Clin Nutr 86:124–130

Yang L, Ling W, Du Z et al (2017) Effects of anthocyanins on cardiometabolic health: a systematic review and meta-analysis of randomized controlled trials. Adv Nutr 8:684–693

Yin J, Xing H, He J (2008) Efficacy of berberine in patients with type 2 diabetes mellitus. Metabolism 57:712–717